# AFFECTIVE PROCESSING AND NON-INVASIVE BRAIN STIMULATION

EDITED BY: Delin Sun, Wenbo Luo, Xiaochu Zhang and Nan Li
PUBLISHED IN: Frontiers in Human Neuroscience

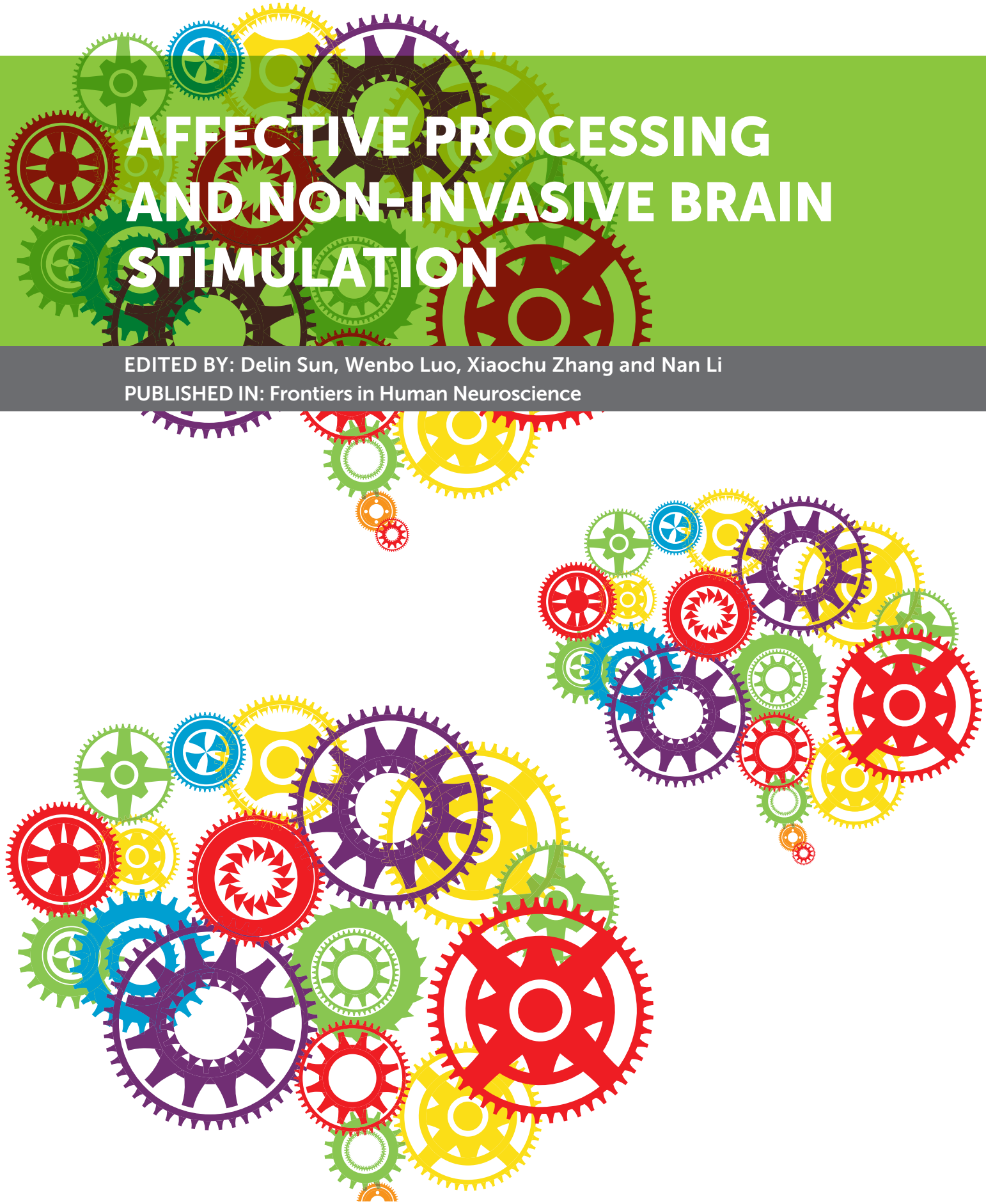

frontiers Research Topics

# frontiers



ISSN 1664-8714
ISBN 978-2-88974-299-8
DOI 10.3389/978-2-88974-299-8

## About Frontiers

Frontiers is more than just an open-access publisher of scholarly articles: it is a pioneering approach to the world of academia, radically improving the way scholarly research is managed. The grand vision of Frontiers is a world where all people have an equal opportunity to seek, share and generate knowledge. Frontiers provides immediate and permanent online open access to all its publications, but this alone is not enough to realize our grand goals.

## Frontiers Journal Series

The Frontiers Journal Series is a multi-tier and interdisciplinary set of open-access, online journals, promising a paradigm shift from the current review, selection and dissemination processes in academic publishing. All Frontiers journals are driven by researchers for researchers; therefore, they constitute a service to the scholarly community. At the same time, the Frontiers Journal Series operates on a revolutionary invention, the tiered publishing system, initially addressing specific communities of scholars, and gradually climbing up to broader public understanding, thus serving the interests of the lay society, too.

## Dedication to Quality

Each Frontiers article is a landmark of the highest quality, thanks to genuinely collaborative interactions between authors and review editors, who include some of the world's best academicians. Research must be certified by peers before entering a stream of knowledge that may eventually reach the public - and shape society; therefore, Frontiers only applies the most rigorous and unbiased reviews.
Frontiers revolutionizes research publishing by freely delivering the most outstanding research, evaluated with no bias from both the academic and social point of view. By applying the most advanced information technologies, Frontiers is catapulting scholarly publishing into a new generation.

## What are Frontiers Research Topics?

Frontiers Research Topics are very popular trademarks of the Frontiers Journals Series: they are collections of at least ten articles, all centered on a particular subject. With their unique mix of varied contributions from Original Research to Review Articles, Frontiers Research Topics unify the most influential researchers, the latest key findings and historical advances in a hot research area! Find out more on how to host your own Frontiers Research Topic or contribute to one as an author by contacting the Frontiers Editorial Office: frontiersin.org/about/contact

# AFFECTIVE PROCESSING AND NON-INVASIVE BRAIN STIMULATION

Topic Editors:
**Delin Sun,** Duke University, United States
**Wenbo Luo,** Liaoning Normal University, China
**Xiaochu Zhang,** University of Science and Technology of China, China
**Nan Li,** RIKEN, Japan

**Citation:** Sun, D., Luo, W., Zhang, X., Li, N., eds. (2022). Affective Processing and Non-invasive Brain Stimulation. Lausanne: Frontiers Media SA.
doi: 10.3389/978-2-88974-299-8

# Table of Contents

frontiers in Human Neuroscience

REVIEW
published: 04 September 2017
doi: 10.3389/fnhum.2017.00439

# Affective Processing in Non-invasive Brain Stimulation Over Prefrontal Cortex

*Wei Liu[1], Ya Shu Leng[2], Xiao Han Zou[1], Zi Qian Cheng[1], Wei Yang[1]* and Bing Jin Li[1]**

*[1] Jilin Provincial Key Laboratory on Molecular and Chemical Genetic, The Second Hospital of Jilin University, Changchun, China, [2] Department of Anesthesiology, The Third Hospital of Jilin University, Changchun, China*

The prefrontal cortex (PFC) is the most frequently targeted brain region by non-invasive brain stimulation (NBS) studies. Non-invasively stimulating the PFC has been shown to both modulate affective processing and improve the clinical symptoms of several psychiatric disorders, such as depression and schizophrenia. The magnitude of the modulation depends on several factors, including the stimulation frequency, the number of stimulation sessions, and the specific sub-region of the PFC that is stimulated. Although some of the potential underlying mechanisms have been identified, the exact mechanisms that underlie these cognitive and affective changes remain unclear. The present review aims to summarize recent advances in the study of affective processing using NBS over the PFC. We will provide a theoretical framework for better understanding how affective processing changes are induced by NBS, with the goal of providing testable hypotheses for future studies.

**Keywords: NBS, TMS, tDCS, tACS, affective processing, PFC**

OPEN ACCESS

***Edited by:***
*Wenbo Luo,*
*Liaoning Normal University, China*

***Reviewed by:***
*Bin Song,*
*McLean Hospital, United States*
*Tifei Yuan,*
*Nanjing Normal University, China*

****Correspondence:***
*Bing Jin Li*
*libingjin@jlu.edu.cn*
*Wei Yang*
*wyang2002@jlu.edu.cn*

***Received:*** *31 May 2017*
***Accepted:*** *16 August 2017*
***Published:*** *04 September 2017*

***Citation:***
*Liu W, Leng YS, Zou XH, Cheng ZQ, Yang W and Li BJ (2017) Affective Processing in Non-invasive Brain Stimulation Over Prefrontal Cortex. Front. Hum. Neurosci. 11:439. doi: 10.3389/fnhum.2017.00439*

## INTRODUCTION

Affective processing plays a significant role in survival and adaptation functions and often interacts with other cognitive processes such as memory, learning, decision making, motivation, and reactions to environmental circumstances (Davidson, 2002). Several biobehavioral scientists share the idea that there are two fundamental affective systems: those relating to positive and those relating to negative effects (Baker et al., 2014). Although the two systems rely on distinct neuroanatomical circuitry, increasing evidence suggests that the prefrontal cortex (PFC) and amygdala are involved in both systems (Pessoa and Adolphs, 2010; Li et al., 2017). Affective processing deficits are often a core factor in most psychiatric disorders such as depression, schizophrenia, phobia, anxiety disorder, bipolar disorder, and addiction. Non-invasive brain stimulation (NBS), which includes techniques such as transcranial magnetic stimulation (TMS) and transcranial direct/alternating current stimulation (tDCS/tACS), have been shown to be effective neuromodulating therapies for psychiatric disorders where impaired affective processing is a core feature, and have consequently shown great potential for future clinical applications. The PFC is the most frequently targeted region by NBS. To our knowledge, in contrast to the direct stimulation of the PFC, the effects of NBS on the amygdala are predominantly achieved through non-invasive stimulation of the PFC.

## AFFECTIVE PROCESSING OF TMS OVER THE PFC

Transcranial magnetic stimulation is developed on the basis of electromagnetic induction. The change of the extrinsic magnetic pulses on brain can produce an ionic current in the brain which can preferentially activate the pyramidal cells or at their axons and induce the change of neural excitability (Kobayashi and Pascual-Leone, 2003). Transcranial magnetic stimulation involves three modes: single pulse TMS, pair-pulse TMS, and repetitive TMS (rTMS). Repetitive TMS is the most mode in the therapy of depression and other psychiatric disorders. The Food and Drug Administration (FDA) has approved rTMS as an effective antidepressant treatment for medication-resistant patients with major depression. In clinical trials of psychiatric disorders, the PFC is the most studied brain regions with rTMS. The PFC is an important neural hub involved in mood and affective processing, in addition to playing an important role in the attentional control of affective information. The clinical effects of low-frequency (1 Hz) rTMS over the PFC are limited and significantly less than high-frequency (>1 Hz) rTMS (HF-rTMS) over the PFC (Alonso et al., 2001; Cohen et al., 2004). Therefore, most of the studies of rTMS are based on HF-rTMS. High-frequency rTMS is known to induce a depolarization of the neurons in the PFC (Guse et al., 2010). Its application over the dorsolateral PFC (dlPFC) was shown to produce a greater cognitive improvement in patients with psychiatric/neurological diseases than in healthy participants (Guse et al., 2010). The exact underlying neural mechanisms responsible for this improvement remain unknown. Besides, the number of stimulation sessions is likely to play a role, as a single session of HF-rTMS applied over the dlPFC was not sufficient to produce significant mood changes in either normal volunteers or depressed patients (Baeken et al., 2008; Leyman et al., 2011).

## AFFECTIVE PROCESSING OF TMS OVER THE PFC IN DEPRESSION

Affective processing of rTMS over the PFC has been shown in some affective disorders, such as depression, schizophrenia, and obsessive compulsive disorder. Depression is the most thoroughly studied in the clinical trials of rTMS. Repetitive TMS, as a typical mode of antidepressant treatment, has shown favorable effects on the depression. Although many studies have investigated the neural mechanisms of TMS over the PFC in depression, however, results are not always consistent and a clear picture has yet to emerge. High-frequency rTMS applied over the left dlPFC protects against the development of negative mood symptoms and increases the susceptibility to negative emotional stimuli (Möbius et al., 2016). High-frequency rTMS (10 Hz) over the left dlPFC of the depressed patients can improve the overall mood status, bias attentional processing toward negative information, and improve the Hamilton depression rating scale (Leyman et al., 2011). Although the first HF-rTMS stimulation session had no effect on the participants, there was a significant improvement following a 2-week treatment. However, no evidence showed the optimal treatment duration. The application of rTMS over the dlPFC also has effects on the cognitive control network and affects associated with cognitive control processes (Lantrip et al., 2017). However, measures of decision-making and impulse control were not affected by the application of rTMS over the left dlPFC, though measures of depression and anxiety both showed significant improvement (Tovar-Perdomo et al., 2017). This finding suggests that neurocognition may not be related to the psychopathological symptoms observed in these mood disorders. Furthermore, different rTMS stimulation frequency rates when applied over the dlPFC may have differential mood effects in depressed patients (Kimbrell et al., 1999; Speer et al., 2000; Speer et al., 2009). Although both low-frequency (1 Hz) and HF (20 Hz)-rTMS have shown to produce positive results, depressed patients who display therapeutic improvements for one stimulation frequency may actually get worse when using other stimulation frequencies (Kimbrell et al., 1999). After 2 days of rTMS treatment, a widespread increase in cerebral blood flow was observed following high-frequency (20 Hz) stimulation, whereas low-frequency (1 Hz) stimulation produced a decrease in cerebral blood flow (Speer et al., 2009). Moreover, depressed patients with lower baseline metabolism levels showed a better response to high-frequency (20 Hz) stimulation, whereas those with higher baseline levels showed a better response to low-frequency (1 Hz) stimulation (Speer et al., 2000, 2009). In contrast, other studies have reported that both 5 Hz-rTMS and 10 Hz-rTMS may produce similar clinical effects on patients with major depressive disorder (MDD; Philip et al., 2015).

Several studies have demonstrated that important dlPFC hemispheric differences exist in MDD: the left dlPFC tends to be hypoactive, whereas the right dlPFC is generally hyperactive (Maeda et al., 2000; Mayberg, 2003; Phillips et al., 2003; Fahim et al., 2004; Bermpohl et al., 2006; Grimm et al., 2008; Lally et al., 2015). This finding suggests that the left and right dlPFC might serve distinct functions and be differently affected in MDD. The hypoactivity in the left dlPFC is related to emotional judgment and the modulation of positive emotional valence in MDD, whereas the hyperactivity in the right dlPFC is associated with attention to emotional judgment and depression severity in MDD (Grimm et al., 2008). Hyperactivation of the right dlPFC can also induce a consistent attentional bias toward negative and aversive memories.

The activation of the left dlPFC caused by rTMS treatment can improve the memory retrieval of positive affective memories, whereas symptoms of anxiety can be induced by the stimulation of the right dlPFC (Balconi and Ferrari, 2012). The application of rTMS over the left dlPFC produces an increased neuronal excitability in the left dlPFC, and recovered the normal responsivity to emotional judgment. It may be a mechanism of recovery in MDD. Besides, the application of rTMS over the left dlPFC can also increase brain activity in the left dlPFC and the anterior cingulate gyrus, whereas it has been shown to decrease brain activity in the left fusiform gyrus, the left cerebellum, and the right dlPFC (Cardoso et al., 2008). It was also shown that rTMS produced a similar clinical improvement in depressed patients when compared with a fluoxetine treatment. Another common clinical symptom observed in depressed patients is

an inability to shift their attention focus, an impairment that is generally attributed to a dysfunction in the dlPFC. A single session of HF-rTMS over the left dlPFC can benefit task-switching performance and stabilize the patient's mood (Vanderhasselt et al., 2009). Although a single session of HF-rTMS over the left dlPFC is insufficient to produce subjective mood changes, it can significantly affect the hypothalamic–pituitary–adrenal (HPA)-axis by reducing salivary cortisol levels both immediately and 30 min after the stimulation (Baeken et al., 2009). These results indicate that changes involving the endocrine system may underlie the affective processing improvements.

The right dlPFC is related to symptoms of anxiety, depression, and panic. Chronic low-frequency rTMS over the right dlPFC showed a significant improvement in panic symptoms after 4 weeks of treatment, with the improvement peaking approximately after 8 weeks. However, the improvement of depressive symptoms required a longer treatment duration, where approximately only half the patients showed improvements after 8 weeks of treatment (Mantovani et al., 2013). The application of rTMS treatment to the right dlPFC can also increase subsequent event-related neural activity observed in bilateral, parietal, and temporal cortex; affect early stage affective visual processing; and enhance differential affective responses to fearful stimuli in individuals with anxiety (Zwanzger et al., 2014). Additionally, the right dlPFC may also be involved in the attentional processing of emotional information.

Multiple rTMS sessions applied to prefrontal regions may modulate the cortical excitability and improve the attentional control over emotional information. However, a single HF-rTMS session applied over the right dlPFC was shown to immediately impair the ability to inhibit negative information, whereas no significant changes were found when the left dlPFC was stimulated (Leyman et al., 2009). Such hemispheric stimulation differences were not observed for self-rated mood measures and emotionally induced facial expressions following dlPFC stimulation (Luo et al., 2010). Although both the left and right dlPFC play an important role in affective processing, sequential bilateral rTMS does not provide an added benefit compared with the application of HF-rTMS over the left dlPFC alone (Fitzgerald et al., 2012, 2016).

Besides the change of neural excitability, the alteration of various neurochemicals also contributes to neurobiological mechanisms of the antidepressant effect of rTMS. Repetitive TMS has been shown to change the endocrinological serum levels in the brain of healthy subjects (Evers et al., 2001). Infra-threshold stimulation only mildly decreased cortisol and thyroid stimulating hormone (TSH) serum levels in both the males and females. However, although this effect might stem from increased prolactin production in females, effects on other hormones were not observed. High-frequency rTMS (25 Hz) stimulations over the left dlPFC can decrease brain-derived neurotrophic factor (BDNF) serum levels in healthy men (Schaller et al., 2014). This effect can be further modulated by the smoking status of the male volunteers. It remains unknown whether sex is an additional modulating factor. However, the reported changes in BDNF levels have been inconsistent. Indeed, the findings of other studies have suggested that the use of acute rTMS over the PFC in healthy volunteers does not produce significant BDNF serum level changes (Lang et al., 2008). Moreover, rTMS applied over the dlPFC can also affect the cerebral glucose metabolism levels. In patients with medication-resistant depression, there are lower glucose metabolism that tends to be lower bilaterally in the dlPFC and in the anterior cingulum, whereas in contrast, several limbic and subcortical regions show increased glucose metabolism levels. After 2 weeks of rTMS treatment, however, glucose metabolism levels in the left middle temporal cortex and the fusiform gyrus significantly decreased in the patients who showed a better response; the general cerebral glucose metabolism pattern remained abnormal, however (Li et al., 2010). Finally, some animal studies and healthy human studies have shown that acute rTMS over the left dlPFC can transiently increase dopamine levels, whereas chronic rTMS does not produce the same effect (Kuroda et al., 2006).

The dorsomedial prefrontal cortex (dmPFC) is another important brain region that is affected by depression. Gray matter density of the dmPFC is reduced in depression, and the magnitude of this reduction correlates with the severity of depression (Koenigs et al., 2008; Koenigs and Grafman, 2009). Transcranial magnetic stimulation applied over the dmPFC can significantly improve the severity of clinical symptoms of depression by increasing the connectivity between the dmPFC and the thalamus, and also between the subgenual cingulate cortex and the caudate nucleus (Salomons et al., 2014; Dunlop et al., 2015; Schulze et al., 2016).

## AFFECTIVE PROCESSING OF TMS OVER THE PFC IN OTHER DISORDERS

Transcranial magnetic stimulation is also increasingly considered as a promising treatment for schizophrenia. Active HF-rTMS (10 Hz) applied to the left dlPFC can induce a significant improvement of the negative clinical symptoms of schizophrenia and associated emotional functioning (Prikryl et al., 2013). These effects may be attributed to both an increase in neuronal activity and an increase of neurotransmitters or receptors. Stimulation over the left dlPFC may also enhance the neural connectivity between the PFC and the amygdala. However, high-frequency bilateral rTMS did not result in any substantial benefit regarding the negative symptoms of schizophrenia (Fitzgerald et al., 2008). The mechanism remains unknown. Deep rTMS applied over bilateral PFC also can significantly reduce self-oriented anxiety during difficult and affective social situations in patients with autism spectrum disorder (Enticott et al., 2014). Furthermore, rTMS applied over the left dlPFC can improve impaired affective processing in patients with obsessive compulsive disorder (de Wit et al., 2015). Potential underlying mechanisms include a reduction in neural activity within the left dlPFC and an increase in connectivity between frontal areas and the amygdala. In addition, rTMS over PFC also significantly decreased drug cue craving in drug-addicted patients, including heroin and cocaine, and no significant adverse events were noted (Shen et al., 2016; Terraneo et al., 2016).

## AFFECTIVE PROCESSING OF tDCS OVER THE PFC

Transcranial direct current stimulation is another non-invasive brain neuromodulation technique that is receiving more attention within the research community. In tDCS, a constant and low intensity direct current (1–2 mA) is delivered to the brain area via electrodes on the scalp. Direct current can influence the frequency of neuronal spontaneous discharge. The frequency gets higher when the anode of tDCS closes to the soma and dendrite of neurons, while the cathode of tDCS makes it lower (Wagner et al., 2007). Besides, tDCS can only affect the active neurons.

Transcranial direct current stimulation may affect cortical neuronal activity in the dlPFC, and the tDCS polarity (cathodal or anodal) applied to the dlPFC modulates the performance of participants during a stimulus–response compatibility task (Morgan et al., 2014). Cathodal current inhibits cortical excitability, whereas anodal current enhances it (Da et al., 2013). Transcranial direct current stimulation applied over the dlPFC had no influence, however, on self-reported affective state measures in healthy individuals (Morgan et al., 2014). However, the result was not consistent with the other studies in healthy volunteers. Polarity of tDCS to the left dlPFC had shown converse results in affective processing. Although some studies found that anodal tDCS applied to the left dlPFC decreased negative mood valence both during and after stimulation in healthy participants, other studies reported the opposite finding (Boggio et al., 2009; Peña-Gómez et al., 2011; Maeoka et al., 2012). Cathodal tDCS applied to the left dlPFC has been shown to have no effects on negative mood (Peña-Gómez et al., 2011; Nitsche et al., 2012). Moreover, tDCS has been shown to produce different physiological effects when applied to the left compared with the right dlPFC. Anodal tDCS applied to the right dlPFC (or cathodal tDCS to the left dlPFC) can significantly regulate affective impulses, whereas the opposite stimulation conditions can promote risky decision-making behavior (Pripfl et al., 2013).

The effects of tDCS on depression, schizophrenia, substance use disorders, obsessive compulsive disorder, generalized anxiety disorder, and anorexia nervosa have been extensively studied (Khedr et al., 2014; Kekic et al., 2016; Lefaucheur et al., 2017). Although some studies have reported its effectiveness for psychiatric disorders, generalizations should be made with caution given that the tDCS technique is still in its infancy compared to other brain stimulation techniques.

## AFFECTIVE PROCESSING OF tDCS OVER THE PFC IN DEPRESSION

Transcranial direct current stimulation has been demonstrated as an effective, relatively safe and convenient treatment option for depression, which has been the most extensively studied clinical condition with this neuromodulation technique. The most studied brain region with tDCS in depression patients is the dlPFC, which plays a significant role in modulating emotions and motor cortex excitability. Cathodal stimulation current inhibits cortical excitability, whereas anodal current enhances it (Da et al., 2013; Brandão et al., 2015). The European Chapter of the International Federation of Clinical Neurophysiology produced guidelines that recommended the application of anodal tDCS over the left dlPFC (with a right orbitofrontal cathode) as a treatment option for patients with a MDD with (C level recommendation) and without drug resistance (B level recommendation) (Lefaucheur et al., 2017).

There are two neural networks involved in the neurobiology of depression. The first network underlies "hot" cognitive processes, is implicated in affective and reward processing, and is subserved by the limbic structures and the ventral PFC. The second network underlies "cold" cognitive processes; is related to non-emotional cognitive processing; and is subserved by the dorsal anterior cingulate cortex, the hippocampus, and the dlPFC (Drevets et al., 2008; Roiser and Sahakian, 2013; Nord et al., 2017). Cognitive deficits and executive dysfunctions are signature characteristics of major depression, and have been associated with the emotional dysregulation observed depression patients (Salehinejad et al., 2017). Ten sessions of tDCS applied over the dlPFC can significantly improve both the depressive symptoms and cognitive functions—such as working memory and attention—that are affected by depression. Working memory deficits are a common symptom associated with depression and other psychological conditions, such as schizophrenia. Working memory deficits can also be observed in healthy individuals exposed to situations producing acute stress. The application of anodal tDCS over the dlPFC can improve stress-induced working memory deficits in depression patients (Bogdanov and Schwabe, 2016). Furthermore, tDCS can enhance the improvement of working memory induced by neurocognitive training in depression patients (Vanderhasselt et al., 2015). Transcranial direct current stimulation can also modulate negative attentional bias measures in as little as a single tDCS session (Brunoni et al., 2014). The combined treatment of cognitive control training and tDCS applied over the dlPFC has been shown to produce a better improvement for depressed patients compared with tDCS alone (Segrave et al., 2014).

Transcranial direct current stimulation can enhance neuronal activation in the PFC, dorsal hippocampus, ventral tegmental area, and nucleus accumbens (Peanlikhit et al., 2017). Transcranial direct current stimulation also enhances vagal activation, inhibits the HPA activity, and decreases the salivary cortisol levels (Brunoni et al., 2013b). Unlike TMS, tDCS may have no significant influence on the BDNF levels in depression patients (Palm et al., 2013).

A recent study indicated that anodal tDCS stimulation of the left dlPFC (or cathodal stimulation of the right tDCS) reduced vigilance levels in response to threat-related affective stimuli in healthy individuals (Ironside et al., 2016). The authors of this study also put forward the idea that the processing of threat-related affective information was a sensitive evaluation criterion to determine treatment effectiveness in clinical settings (Ironside et al., 2016). Finally, it has also been shown that anodal tDCS reduces cortisol levels and enhances vagal activity, both of which are involved in stress regulation (Brunoni et al., 2013b).

Although there is no mechanism to reveal the interactions between tDCS with antipsychotics and nonbenzodiazepine anticonvulsants in depressed patients, some antipsychotics, such as SNRIs, SSRIs, and tricyclics, can significantly enhance the improvement of tDCS (Brunoni et al., 2013a). However, benzodiazepine can reduce the improvement associated with tDCS (Brunoni et al., 2013a). The use of a tDCS treatment after the administration of lorazepam (a GABAergic agonist) can initially reduce cortical excitability only to later increase excitability (Nitsche et al., 2004). Anodal stimulation has been shown to decrease local gamma-aminobutyric acid (GABA) levels, whereas cathodal stimulation inhibits glutamatergic activity (Stagg et al., 2009). GABA/glutamate levels are also modulated by benzodiazepine, which may explain the interaction effects observed when combining tDCS with benzodiazepines (Hasan et al., 2012).

## AFFECTIVE PROCESSING OF tDCS OVER THE PFC IN SCHIZOPHRENIA

Transcranial direct current stimulation applied to the PFC has been shown to be an effective and relatively safe therapeutic option for adults and children with schizophrenia (Mattai et al., 2011). Negative symptoms and cognitive dysfunction are important facets of schizophrenia and are under the regulation of the fronto–thalamic–parietal and frontal–striatal networks (Galderisi et al., 2015; Palm et al., 2016). The dlPFC is a central hub in both of these networks and is functionally impaired in schizophrenia, leading to important cognitive deficits (Galderisi et al., 2015; Sheffield et al., 2015). Negative symptoms include a flattening of the affect, alogia, avolition–apathy, anhedonia–asociality, and attention disorders (Palm et al., 2016). Furthermore, the currently available evidence suggests that negative symptoms and cognitive dysfunctions are both associated with the affective processing deficits observed in schizophrenia. The application of prefrontal tDCS combined with stable antipsychotic medication has been shown to improve negative symptoms in patients with severe schizophrenia (Palm et al., 2016).

Prefrontal tDCS has also been shown to improve working memory performance and affective identification performance in patients with schizophrenia, and to enhance connectivity between brain networks in healthy individuals as measured by resting-state functional connectivity magnetic resonance imaging (fcMRI) (Rassovsky et al., 2015; Orlov et al., 2017). Auditory verbal hallucinations constitute another important clinical symptom in schizophrenia and are believed to be related to abnormal hyperactivity in the left temporoparietal junction, in addition to abnormal connectivity between frontal and temporal brain areas. The application of tDCS over the left dlPFC can significantly reduce the occurrence of auditory verbal hallucinations through the regulation of resting-state functional connectivity between brain areas in the related network (Mulquiney et al., 2011; Andrade, 2013; Mondino et al., 2016).

## AFFECTIVE PROCESSING OF tDCS OVER THE PFC IN DRUG DEPENDENCE AND BULIMIA NERVOSA

The PFC also plays a critical role in developing addictions, particularly those related to drug use and smoking. Drug dependence has been associated with a reduction of brain activity within the PFC, which is believed to be subsequent to structural and functional damage to the PFC (Goldstein and Volkow, 2002; Da et al., 2013). Cravings are associated with enhanced drug cue-related prefrontal activation (Tapert et al., 2003; Wilson et al., 2004; McBride et al., 2006). The application of tDCS over the left dlPFC is reported to inhibit the neural activation within the PFC normally triggered by drug-related cues, and to reduce acute substance cravings in drug addicts (Da et al., 2013; Wang et al., 2016). Moreover, tDCS can improve the general mood status of drug addict patients (Da et al., 2013).

Bulimia nervosa is an abnormal and excessive food craving disorder that can lead to other health problems including obesity. Some studies have indicated that the application of tDCS over either the right or the left dlPFC can enhance inhibitory control while reducing food cravings and intake (Burgess et al., 2016; Ljubisavljevic et al., 2016; Macedo et al., 2016; Georgii et al., 2017; Kekic et al., 2017; Lowe et al., 2017). The specific underlying mechanisms may involve an increased regulation of the reward and decision-making neural networks (Fregni et al., 2008).

## AFFECTIVE PROCESSING OF tDCS OVER THE PFC IN OTHER DISORDERS

Posttraumatic stress disorder produces deficient fear extinction mechanisms and is associated with an abnormal activation of key brain regions that are part of the fear extinction network, which includes the ventromedial PFC, amygdala, and hippocampus (Marin et al., 2014). Furthermore, the integrity of this network is related to symptom severity in posttraumatic stress disorder. Transcranial direct current stimulation has been shown to enhance the recall of positive memories that improve fear extinction mechanism in posttraumatic stress disorder (Penolazzi et al., 2010; Asthana et al., 2013; Marin et al., 2014).

Pain is a multidimensional experience involving cognitive, attentional, and affective processes. Pain is often associated with negative emotions such as unpleasantness or anxiety, which can, in turn, modulate the pain experience. The application of tDCS over the left dlPFC can alleviate affective pain by increasing the neural activity in the left dlPFC, and also by down-regulating pain inhibitory systems (Maeoka et al., 2012). This mechanism may rely on a distinct and independent pathway from those regulating the somatosensory perception of pain (Boggio et al., 2009).

## AFFECTIVE PROCESSING IN tACS OVER THE PFC

There are only a few studies that have investigated the effects of tACS on affective processing. These studies focused primarily

on improving working memory functions in both healthy individuals and patients with schizophrenia (Meiron and Lavidor, 2014; Hoy et al., 2016). It has also been suggested that the bi-frontal application of tACS might improve functional connectivity between the different prefrontal regulatory components of working memory in humans. Furthermore, tACS applied to the left dlPFC can entrain endogenous cortical oscillations and produce working memory improvements in schizophrenia patients similar to those observed following tDCS.

## DISCUSSION

Affective processing plays a significant role in survival and adaptation functions. Disturbance of affective processing is a core factor for most psychiatric disorders, such as, anxiety, depression, schizophrenia, phobia, and addiction. Although NBS studies have provided tantalizing symptom improvement and affective processing in some psychiatric disorders, such as depression and schizophrenia, there are still lots of limits for clinical applications. As we reviewed, depression is the most thoroughly studied affective disorder in TMS and tDCS; however, there are no standardized treatment protocols in the clinical application of rTMS for depressived patients. Repetitive TMS over the left dlPFC can improve the overall mood status, bias attentional processing toward negative information, increase susceptibility to negative emotional stimuli, and improve the Hamilton depression rating scale in the patients with depression. Repetitive TMS applied over the right dlPFC produces significant improvement in panic and depressive symptoms. Repetitive TMS treatment on the right dlPFC can also affect early stage affective visual processing, and enhance differential affective responses to fearful stimuli in individuals with anxiety. Transcranial direct current stimulation applied over the dlPFC can significantly improve the depressive symptom, cognitive function, such as working memory and attention, and stress-induced working memory deficits, and modulate the negative attentional bias in patients with depression. In depression, complicated pathogenesis, diversified pathogenic factor, manifold clinical symptoms, and individual differences make it difficult for the treatment of depression. Therefore, high-quality multicenter randomized clinical trials are required to confirm the best optimal treatment for patients with depression, for instance, the frequency of rTMS, timing and course of the treatment, and evaluation of the therapeutic effect. In addition, some studies have indicated the changes of neural excitability and the alteration of various neurochemicals may be neurobiological mechanisms of the antidepressant effect of rTMS. Notwithstanding, there are also some potential mechanisms remaining to be revealed. In addition, the short- and long-term implications of NBS in patients with depression should get sufficient attention. Besides depression, other psychiatric disorders, for instance, schizophrenia, addiction, bulimia nervosa, and posttraumatic stress disorder, have exhibited favorable responses to NBS treatment. However, NBS also needs more evidence to verify the efficacy and explore physiological basis of affective processing in these psychiatric disorders.

## CONCLUSION

The PFC is the most frequently studied region with NBS. The application of NBS over the PFC can significantly modulate affective processing and improve the clinical symptoms of several psychiatric disorders, such as depression and schizophrenia. The effects of TMS over the PFC on affective processing depend on the exact stimulation frequency, the number of consecutive stimulation sessions, and the targeted sub-region of the PFC. Although some potential mechanisms have been identified, the overall picture is yet to be complete. The application of TMS over the left dlPFC can increase brain activity in the left dlPFC and the anterior cingulate gyrus, whereas it also decreases brain activity measured in the left fusiform gyrus, the left cerebellum, and the right dlPFC. Transcranial magnetic stimulation applied to the right dlPFC can increase event-related neural activity bilaterally in the parietal and temporal cortex, increase early stage affective visual processing, and enhance differential affective responses to fearful stimuli. Transcranial direct current stimulation can enhance neuronal activation in the PFC, dorsal hippocampus, ventral tegmental area, and nucleus accumbens. However, the exact mechanisms underlying the tDCS effects remain unclear. As more and more studies investigate the effects and underlying mechanisms of NBS, its clinical applications should continue to be scrutinized.

## AUTHOR CONTRIBUTIONS

WL, YL, XZ, ZC, and BL wrote the manuscript. WY and BL provided the critical revisions. All authors approved the final version of the manuscript for submission.

## FUNDING

This work was supported by the National Natural Science Foundation of China (Grant Nos. 31571126 and 31300850) and the Graduate Innovation Fund of Jilin University.

## REFERENCES

Alonso, P., Pujol, J., Cardoner, N., Benlloch, L., Deus, J., Menchón, J. M., et al. (2001). Right prefrontal repetitive transcranial magnetic stimulation in obsessive-compulsive disorder: a double-blind, placebo-controlled study. *Am. J. Psychiatry* 158, 1143–1145. doi: 10.1176/appi.ajp.158.7.1143

Andrade, C. (2013). Transcranial direct current stimulation for refractory auditory hallucinations in schizophrenia. *J. Clin. Psychiatry* 74:e1054-8. doi: 10.4088/JCP.13f08826

Asthana, M., Nueckel, K., Mühlberger, A., Neueder, D., Polak, T., Domschke, K., et al. (2013). Effects of transcranial direct current stimulation on consolidation of fear memory. *Front. Psychiatry* 4:107. doi: 10.3389/fpsyt.2013.00107

Baeken, C., De Raedt, R., Leyman, L., Schiettecatte, J., Kaufman, L., Poppe, K., et al. (2009). The impact of one HF-rTMS session on mood and salivary cortisol in treatment resistant unipolar melancholic depressed patients. *J. Affect. Disord.* 113, 100–108. doi: 10.1016/j.jad.2008.05.008

Baeken, C., Leyman, L., De Raedt, R., Vanderhasselt, M. A., and D'haenen, H. (2008). Left and right high frequency repetitive transcranial magnetic stimulation of the dorsolateral prefrontal cortex does not affect mood in female volunteers. *Clin. Neurophysiol.* 119, 568–575. doi: 10.1016/j.clinph.2007.11.044

Baker, J. T., Holmes, A. J., Masters, G. A., Yeo, B. T., Krienen, F., Buckner, R. L., et al. (2014). Disruption of cortical association networks in schizophrenia and psychotic bipolar disorder. *JAMA Psychiatry* 71, 109–118. doi: 10.1001/jamapsychiatry.2013.3469

Balconi, M., and Ferrari, C. (2012). rTMS stimulation on left DLPFC affects emotional cue retrieval as a function of anxiety level and gender. *Depress. Anxiety* 29, 976–982. doi: 10.1002/da.21968

Bermpohl, F., Fregni, F., Boggio, P. S., Thut, G., Northoff, G., Otachi, P. T., et al. (2006). Effect of low-frequency transcranial magnetic stimulation on an affective go/no-go task in patients with major depression: role of stimulation site and depression severity. *Psychiatry Res.* 141, 1–13. doi: 10.1016/j.psychres.2005.07.018

Bogdanov, M., and Schwabe, L. (2016). Transcranial stimulation of the dorsolateral prefrontal cortex prevents stress-induced working memory deficits. *J. Neurosci.* 36, 1429–1437. doi: 10.1523/JNEUROSCI.3687-15.2016

Boggio, P. S., Zaghi, S., and Fregni, F. (2009). Modulation of emotions associated with images of human pain using anodal transcranial direct current stimulation (tDCS). *Neuropsychologia* 47, 212–217. doi: 10.1016/j.neuropsychologia.2008.07.022

Brandão, F. R. A., Baptista, A. F., Brandão, R. A., Meneses, F. M., Okeson, J., and de Sena, E. P. (2015). Analgesic effect of cathodal transcranial current stimulation over right dorsolateral prefrontal cortex in subjects with muscular temporomandibular disorders: study protocol for a randomized controlled trial. *Trials* 16:415. doi: 10.1186/s13063-015-0938-0

Brunoni, A. R., Ferrucci, R., Bortolomasi, M., Scelzo, E., Boggio, P. S., Fregni, F., et al. (2013a). Interactions between transcranial direct current stimulation (tDCS) and pharmacological interventions in the Major Depressive Episode: findings from a naturalistic study. *Eur. Psychiatry* 28, 356–361. doi: 10.1016/j.eurpsy.2012.09.001

Brunoni, A. R., Vanderhasselt, M. A., Boggio, P. S., Fregni, F., Dantas, E. M., Mill, J. G., et al. (2013b). Polarity- and valence-dependent effects of prefrontal transcranial direct current stimulation on heart rate variability and salivary cortisol. *Psychoneuroendocrinology* 38, 58–66. doi: 10.1016/j.psyneuen.2012.04.020

Brunoni, A. R., Zanao, T. A., Vanderhasselt, M. A., Valiengo, L., de Oliveira, J. F., Boggio, P. S., et al. (2014). Enhancement of affective processing induced by bifrontal transcranial direct current stimulation in patients with major depression. *Neuromodulation* 17, 138–142. doi: 10.1111/ner.12080

Burgess, E. E., Sylvester, M. D., Morse, K. E., Amthor, F. R., Mrug, S., Lokken, K. L., et al. (2016). Effects of transcranial direct current stimulation (tDCS) on binge eating disorder. *Int. J. Eat Disord.* 49, 930–936. doi: 10.1002/eat.22554

Cardoso, E. F., Fregni, F., Martins, M. F., Boggio, P. S., Luis, M. M., Coracini, K., et al. (2008). rTMS treatment for depression in Parkinson's disease increases BOLD responses in the left prefrontal cortex. *Int. J. Neuropsychopharmacol.* 11, 173–183. doi: 10.1017/S1461145707007961

Cohen, H., Kaplan, Z., Kotler, M., Kouperman, I., Moisa, R., and Grisaru, N. (2004). Repetitive transcranial magnetic stimulation of the right dorsolateral prefrontal cortex in posttraumatic stress disorder: a double-blind, placebo-controlled study. *Am. J. Psychiatry* 161, 515–524. doi: 10.1176/appi.ajp.161.3.515

Da, S. M. C., Conti, C. L., Klauss, J., Alves, L. G., do, N. C. H. M., Fregni, F., et al. (2013). Behavioral effects of transcranial direct current stimulation (tDCS) induced dorsolateral prefrontal cortex plasticity in alcohol dependence. *J. Physiol. Paris* 107, 493–502. doi: 10.1016/j.jphysparis.2013.07.003

Davidson, R. J. (2002). Anxiety and affective style: role of prefrontal cortex and amygdala. *Biol. Psychiatry* 51, 68–80. doi: 10.1016/S0006-3223(01)01328-2

de Wit, S. J., van der Werf, Y. D., Mataix-Cols, D., Trujillo, J. P., van Oppen, P., Veltman, D. J., et al. (2015). Emotion regulation before and after transcranial magnetic stimulation in obsessive compulsive disorder. *Psychol. Med.* 45, 3059–3073. doi: 10.1017/S0033291715001026

Drevets, W. C., Price, J. L., and Furey, M. L. (2008). Brain structural and functional abnormalities in mood disorders: implications for neurocircuitry models of depression. *Brain Struct. Funct.* 213, 93–118. doi: 10.1007/s00429-008-0189-x

Dunlop, K., Gaprielian, P., Blumberger, D., Daskalakis, Z. J., Kennedy, S. H., Giacobbe, P., et al. (2015). MRI-guided dmPFC-rTMS as a treatment for treatment-resistant major depressive disorder. *J. Vis. Exp.* 102:e53129. doi: 10.3791/53129

Enticott, P. G., Fitzgibbon, B. M., Kennedy, H. A., Arnold, S. L., Elliot, D., Peachey, A., et al. (2014). A double-blind, randomized trial of deep repetitive transcranial magnetic stimulation (rTMS) for autism spectrum disorder. *Brain Stimul.* 7, 206–211. doi: 10.1016/j.brs.2013.10.004

Evers, S., Hengst, K., and Pecuch, P. W. (2001). The impact of repetitive transcranial magnetic stimulation on pituitary hormone levels and cortisol in healthy subjects. *J. Affect. Disord.* 66, 83–88. doi: 10.1016/S0165-0327(00)00289-5

Fahim, C., Stip, E., Mancini-Marie, A., Mensour, B., Leroux, J. M., Beaudoin, G., et al. (2004). Abnormal prefrontal and anterior cingulate activation in major depressive disorder during episodic memory encoding of sad stimuli. *Brain Cogn.* 54, 161–163.

Fitzgerald, P. B., Herring, S., Hoy, K., McQueen, S., Segrave, R., Kulkarni, J., et al. (2008). A study of the effectiveness of bilateral transcranial magnetic stimulation in the treatment of the negative symptoms of schizophrenia. *Brain Stimul.* 1, 27–32. doi: 10.1016/j.brs.2007.08.001

Fitzgerald, P. B., Hoy, K. E., Elliot, D., McQueen, S., Wambeek, L. E., and Daskalakis, Z. J. (2016). A negative double-blind controlled trial of sequential bilateral rTMS in the treatment of bipolar depression. *J. Affect. Disord.* 198, 158–162. doi: 10.1016/j.jad.2016.03.052

Fitzgerald, P. B., Hoy, K. E., Herring, S. E., McQueen, S., Peachey, A. V., Segrave, R. A., et al. (2012). A double blind randomized trial of unilateral left and bilateral prefrontal cortex transcranial magnetic stimulation in treatment resistant major depression. *J. Affect. Disord.* 139, 193–198. doi: 10.1016/j.jad.2012.02.017

Fregni, F., Orsati, F., Pedrosa, W., Fecteau, S., Tome, F. A., Nitsche, M. A., et al. (2008). Transcranial direct current stimulation of the prefrontal cortex modulates the desire for specific foods. *Appetite* 51, 34–41. doi: 10.1016/j.appet.2007.09.016

Galderisi, S., Merlotti, E., and Mucci, A. (2015). Neurobiological background of negative symptoms. *Eur. Arch. Psychiatry Clin. Neurosci.* 265, 543–558. doi: 10.1007/s00406-015-0590-4

Georgii, C., Goldhofer, P., Meule, A., Richard, A., and Blechert, J. (2017). Food craving, food choice and consumption: the role of impulsivity and sham-controlled tDCS stimulation of the right dlPFC. *Physiol. Behav.* 177, 20–26. doi: 10.1016/j.physbeh.2017.04.004

Goldstein, R. Z., and Volkow, N. D. (2002). Drug addiction and its underlying neurobiological basis: neuroimaging evidence for the involvement of the frontal cortex. *Am. J. Psychiatry* 159, 1642–1652. doi: 10.1176/appi.ajp.159.10.1642

Grimm, S., Beck, J., Schuepbach, D., Hell, D., Boesiger, P., Bermpohl, F., et al. (2008). Imbalance between left and right dorsolateral prefrontal cortex in major depression is linked to negative emotional judgment: an fMRI study in severe major depressive disorder. *Biol. Psychiatry* 63, 369–376. doi: 10.1016/j.biopsych.2007.05.033

Guse, B., Falkai, P., and Wobrock, T. (2010). Cognitive effects of high-frequency repetitive transcranial magnetic stimulation: a systematic review. *J. Neural Transm.* 117, 105–122. doi: 10.1007/s00702-009-0333-7

Hasan, A., Nitsche, M. A., Herrmann, M., Schneider-Axmann, T., Marshall, L., Gruber, O., et al. (2012). Impaired long-term depression in schizophrenia: a cathodal tDCS pilot study. *Brain Stimul.* 5, 475–483. doi: 10.1016/j.brs.2011.08.004

Hoy, K. E., Whitty, D., Bailey, N., and Fitzgerald, P. B. (2016). Preliminary investigation of the effects of γ-tACS on working memory in schizophrenia. *J Neural Transm.* 123, 1205–1212. doi: 10.1007/s00702-016-1554-1

Ironside, M., O'Shea, J., Cowen, P. J., and Harmer, C. J. (2016). Frontal cortex stimulation reduces vigilance to threat: implications for the treatment of depression and anxiety. *Biol. Psychiatry* 79, 823–830. doi: 10.1016/j.biopsych.2015.06.012

Kekic, M., Boysen, E., Campbell, I. C., and Schmidt, U. (2016). A systematic review of the clinical efficacy of transcranial direct current stimulation (tDCS) in psychiatric disorders. *J. Psychiatr. Res.* 74, 70–86. doi: 10.1016/j.jpsychires.2015.12.018

Kekic, M., McClelland, J., Bartholdy, S., Boysen, E., Musiat, P., Dalton, B., et al. (2017). Single-session transcranial direct current stimulation temporarily improves symptoms, mood, and self-regulatory control in bulimia nervosa: a randomised controlled trial. *PLoS ONE* 12:e0167606. doi: 10.1371/journal.pone.0167606

Khedr, E. M., Elfetoh, N. A., Ali, A. M., and Noamany, M. (2014). Anodal transcranial direct current stimulation over the dorsolateral prefrontal cortex improves anorexia nervosa: a pilot study. *Restor. Neurol. Neurosci.* 32, 789–797. doi: 10.3233/RNN-140392

Kimbrell, T. A., Little, J. T., Dunn, R. T., Frye, M. A., Greenberg, B. D., Wassermann, E. M., et al. (1999). Frequency dependence of antidepressant response to left prefrontal repetitive transcranial magnetic stimulation (rTMS) as a function of baseline cerebral glucose metabolism. *Biol. Psychiatry* 46, 1603–1613. doi: 10.1016/S0006-3223(99)00195-X

Kobayashi, M., and Pascual-Leone, A. (2003). Transcranial magnetic stimulation in neurology. *Lancet Neurol.* 2, 145–156. doi: 10.1016/S1474-4422(03)00321-1

Koenigs, M., and Grafman, J. (2009). Prefrontal asymmetry in depression? The long-term effect of unilateral brain lesions. *Neurosci. Lett.* 459, 88–90. doi: 10.1016/j.neulet.2009.04.063

Koenigs, M., Huey, E. D., Calamia, M., Raymont, V., Tranel, D., and Grafman, J. (2008). Distinct regions of prefrontal cortex mediate resistance and vulnerability to depression. *J. Neurosci.* 28, 12341–12348. doi: 10.1523/JNEUROSCI.2324-08.2008

Kuroda, Y., Motohashi, N., Ito, H., Ito, S., Takano, A., Nishikawa, T., et al. (2006). Effects of repetitive transcranial magnetic stimulation on [11C]raclopride binding and cognitive function in patients with depression. *J. Affect. Disord.* 95, 35–42. doi: 10.1016/j.jad.2006.03.029

Lally, N., Nugent, A. C., Luckenbaugh, D. A., Niciu, M. J., Roiser, J. P., and Zarate, C. A. (2015). Neural correlates of change in major depressive disorder anhedonia following open-label ketamine. *J. Psychopharmacol.* 29, 596–607. doi: 10.1177/0269881114568041

Lang, U. E., Hellweg, R., Gallinat, J., and Bajbouj, M. (2008). Acute prefrontal cortex transcranial magnetic stimulation in healthy volunteers: no effects on brain-derived neurotrophic factor (BDNF) concentrations in serum. *J. Affect. Disord.* 107, 255–258. doi: 10.1016/j.jad.2007.08.008

Lantrip, C., Gunning, F. M., Flashman, L., Roth, R. M., and Holtzheimer, P. E. (2017). Effects of transcranial magnetic stimulation on the cognitive control of emotion: potential antidepressant mechanisms. *J. ECT* 33, 73–80. doi: 10.1097/YCT.0000000000000386

Lefaucheur, J. P., Antal, A., Ayache, S. S., Benninger, D. H., Brunelin, J., Cogiamanian, F., et al. (2017). Evidence-based guidelines on the therapeutic use of transcranial direct current stimulation (tDCS). *Clin. Neurophysiol.* 128, 56–92. doi: 10.1016/j.clinph.2016.10.087

Leyman, L., De Raedt, R., Vanderhasselt, M. A., and Baeken, C. (2009). Influence of high-frequency repetitive transcranial magnetic stimulation over the dorsolateral prefrontal cortex on the inhibition of emotional information in healthy volunteers. *Psychol. Med.* 39, 1019–1028. doi: 10.1017/S0033291708004431

Leyman, L., De Raedt, R., Vanderhasselt, M. A., and Baeken, C. (2011). Effects of repetitive transcranial magnetic stimulation of the dorsolateral prefrontal cortex on the attentional processing of emotional information in major depression: a pilot study. *Psychiatry Res.* 185, 102–107. doi: 10.1016/j.psychres.2009.04.008

Li, B., Ge, T., and Cui, R. (2017). Long-term plasticity in amygdala circuits: implication of CB1-dependent LTD in stress. *Mol. Neurobiol.* doi: 10.1007/s12035-017-0643-y [Epub ahead of print].

Li, C. T., Wang, S. J., Hirvonen, J., Hsieh, J. C., Bai, Y. M., Hong, C. J., et al. (2010). Antidepressant mechanism of add-on repetitive transcranial magnetic stimulation in medication-resistant depression using cerebral glucose metabolism. *J. Affect. Disord.* 127, 219–229. doi: 10.1016/j.jad.2010.05.028

Ljubisavljevic, M., Maxood, K., Bjekic, J., Oommen, J., and Nagelkerke, N. (2016). Long-term effects of repeated prefrontal cortex transcranial direct current stimulation (tDCS) on food craving in normal and overweight young adults. *Brain Stimul.* 9, 826–833. doi: 10.1016/j.brs.2016.07.002

Lowe, C. J., Vincent, C., and Hall, P. A. (2017). Effects of noninvasive brain stimulation on food cravings and consumption: a meta-analytic review. *Psychosom. Med.* 79, 2–13. doi: 10.1097/PSY.0000000000000368

Luo, W., Feng, W., He, W., Wang, N. Y., and Luo, Y. J. (2010). Three stages of facial expression processing: ERP study with rapid serial visual presentation. *Neuroimage* 49, 1857–1867. doi: 10.1016/j.neuroimage.2009.09.018

Macedo, I. C., de Oliveira, C., Vercelino, R., Souza, A., Laste, G., Medeiros, L. F., et al. (2016). Repeated transcranial direct current stimulation reduces food craving in Wistar rats. *Appetite* 103, 29–37. doi: 10.1016/j.appet.2016.03.014

Maeda, F., Keenan, J. P., and Pascual-Leone, A. (2000). Interhemispheric asymmetry of motor cortical excitability in major depression as measured by transcranial magnetic stimulation. *Br. J. Psychiatry* 177, 169–173. doi: 10.1192/bjp.177.2.169

Maeoka, H., Matsuo, A., Hiyamizu, M., Morioka, S., and Ando, H. (2012). Influence of transcranial direct current stimulation of the dorsolateral prefrontal cortex on pain related emotions: a study using electroencephalographic power spectrum analysis. *Neurosci. Lett.* 512, 12–16. doi: 10.1016/j.neulet.2012.01.037

Mantovani, A., Aly, M., Dagan, Y., Allart, A., and Lisanby, S. H. (2013). Randomized sham controlled trial of repetitive transcranial magnetic stimulation to the dorsolateral prefrontal cortex for the treatment of panic disorder with comorbid major depression. *J. Affect. Disord.* 144, 153–159. doi: 10.1016/j.jad.2012.05.038

Marin, M. F., Camprodon, J. A., Dougherty, D. D., and Milad, M. R. (2014). Device-based brain stimulation to augment fear extinction: implications for PTSD treatment and beyond. *Depress. Anxiety* 31, 269–278. doi: 10.1002/da.22252

Mattai, A., Miller, R., Weisinger, B., Greenstein, D., Bakalar, J., Tossell, J., et al. (2011). Tolerability of transcranial direct current stimulation in childhood-onset schizophrenia. *Brain Stimul.* 4, 275–280. doi: 10.1016/j.brs.2011.01.001

Mayberg, H. S. (2003). Modulating dysfunctional limbic-cortical circuits in depression: towards development of brain-based algorithms for diagnosis and optimised treatment. *Br. Med. Bull.* 65, 193–207. doi: 10.1093/bmb/65.1.193

McBride, D., Barrett, S. P., Kelly, J. T., Aw, A., and Dagher, A. (2006). Effects of expectancy and abstinence on the neural response to smoking cues in cigarette smokers: an fMRI study. *Neuropsychopharmacology* 31, 2728–2738. doi: 10.1038/sj.npp.1301075

Meiron, O., and Lavidor, M. (2014). Prefrontal oscillatory stimulation modulates access to cognitive control references in retrospective metacognitive commentary. *Clin. Neurophysiol.* 125, 77–82. doi: 10.1016/j.clinph.2013.06.013

Möbius, M., Lacomblé, L., Meyer, T., Schutter, D. J., Gielkens, T., Becker, E. S., et al. (2016). Repetitive transcranial magnetic stimulation modulates the impact of a negative mood induction. *Soc. Cogn. Affect. Neurosci.* 12, 526–533. doi: 10.1093/scan/nsw180

Mondino, M., Jardri, R., Suaud-Chagny, M. F., Saoud, M., Poulet, E., and Brunelin, J. (2016). Effects of fronto-temporal transcranial direct current stimulation on auditory verbal hallucinations and resting-state functional connectivity of the left temporo-parietal junction in patients with schizophrenia. *Schizophr. Bull.* 42, 318–326.doi: 10.1093/schbul/sbv114

Morgan, H. M., Davis, N. J., and Bracewell, R. M. (2014). Does transcranial direct current stimulation to prefrontal cortex affect mood and emotional memory retrieval in healthy individuals. *PLoS ONE* 9:e92162. doi: 10.1371/journal.pone.0092162

Mulquiney, P. G., Hoy, K. E., Daskalakis, Z. J., and Fitzgerald, P. B. (2011). Improving working memory: exploring the effect of transcranial random noise stimulation and transcranial direct current stimulation on the dorsolateral prefrontal cortex. *Clin. Neurophysiol.* 122, 2384–2389. doi: 10.1016/j.clinph.2011.05.009

Nitsche, M. A., Koschack, J., Pohlers, H., Hullemann, S., Paulus, W., and Happe, S. (2012). Effects of frontal transcranial direct current stimulation on emotional state and processing in healthy humans. *Front. Psychiatry* 3:58. doi: 10.3389/fpsyt.2012.00058

Nitsche, M. A., Liebetanz, D., Schlitterlau, A., Henschke, U., Fricke, K., Frommann, K., et al. (2004). GABAergic modulation of DC stimulation-induced motor cortex excitability shifts in humans. *Eur. J. Neurosci.* 19, 2720–2726. doi: 10.1111/j.0953-816X.2004.03398.x

Nord, C. L., Forster, S., Halahakoon, D. C., Penton-Voak, I. S., Munafò, M. R., and Roiser, J. P. (2017). Prefrontal cortex stimulation does not affect emotional bias, but may slow emotion identification. *Soc. Cogn. Affect. Neurosci.* 12, 839–847. doi: 10.1093/scan/nsx007

Orlov, N. D., Tracy, D. K., Joyce, D., Patel, S., Rodzinka-Pasko, J., Dolan, H., et al. (2017). Stimulating cognition in schizophrenia: a controlled pilot study of the effects of prefrontal transcranial direct current stimulation upon memory and learning. *Brain Stimul.* 10, 560–566. doi: 10.1016/j.brs.2016.12.013

Palm, U., Fintescu, Z., Obermeier, M., Schiller, C., Reisinger, E., Keeser, D., et al. (2013). Serum levels of brain-derived neurotrophic factor are unchanged after transcranial direct current stimulation in treatment-resistant depression. *J. Affect. Disord.* 150, 659–663. doi: 10.1016/j.jad.2013.03.015

Palm, U., Keeser, D., Hasan, A., Kupka, M. J., Blautzik, J., Sarubin, N., et al. (2016). Prefrontal transcranial direct current stimulation for treatment of schizophrenia with predominant negative symptoms: a double-blind, sham-controlled proof-of-concept study. *Schizophr. Bull.* 42, 1253–1261. doi: 10.1093/schbul/sbw041

Peanlikhit, T., Van Waes, V., Pedron, S., Risold, P. Y., Haffen, E., Etiévant, A., et al. (2017). The antidepressant-like effect of tDCS in mice: a behavioral and neurobiological characterization. *Brain Stimul.* 10, 748–756. doi: 10.1016/j.brs.2017.03.012

Peña-Gómez, C., Vidal-Piñeiro, D., Clemente, I. C., Pascual-Leone, Á., and Bartrés-Faz, D. (2011). Down-regulation of negative emotional processing by transcranial direct current stimulation: effects of personality characteristics. *PLoS ONE* 6:e22812. doi: 10.1371/journal.pone.0022812

Penolazzi, B., Di, D. A., Marzoli, D., Mammarella, N., Fairfield, B., Franciotti, R., et al. (2010). Effects of transcranial direct current stimulation on episodic memory related to emotional visual stimuli. *PLoS ONE* 5:e10623. doi: 10.1371/journal.pone.0010623

Pessoa, L., and Adolphs, R. (2010). Emotion processing and the amygdala: from a 'low road' to 'many roads' of evaluating biological significance. *Nat. Rev. Neurosci.* 11, 773–783. doi: 10.1038/nrn2920

Philip, N. S., Carpenter, S. L., Ridout, S. J., Sanchez, G., Albright, S. E., Tyrka, A. R., et al. (2015). 5Hz repetitive transcranial magnetic stimulation to left prefrontal cortex for major depression. *J. Affect. Disord.* 186, 13–17. doi: 10.1016/j.jad.2014.12.024

Phillips, M. L., Drevets, W. C., Rauch, S. L., and Lane, R. (2003). Neurobiology of emotion perception II: implications for major psychiatric disorders. *Biol. Psychiatry* 54, 515–528. doi: 10.1016/S0006-3223(03)00171-9

Prikryl, R., Ustohal, L., Prikrylova, K. H., Kasparek, T., Venclikova, S., Vrzalova, M., et al. (2013). A detailed analysis of the effect of repetitive transcranial magnetic stimulation on negative symptoms of schizophrenia: a double-blind trial. *Schizophr. Res.* 149, 167–173. doi: 10.1016/j.schres.2013.06.015

Pripfl, J., Neumann, R., Köhler, U., and Lamm, C. (2013). Effects of transcranial direct current stimulation on risky decision making are mediated by 'hot' and 'cold' decisions, personality, and hemisphere. *Eur. J. Neurosci.* 38, 3778–3785. doi: 10.1111/ejn.12375

Rassovsky, Y., Dunn, W., Wynn, J., Wu, A. D., Iacoboni, M., Hellemann, G., et al. (2015). The effect of transcranial direct current stimulation on social cognition in schizophrenia: a preliminary study. *Schizophr. Res.* 165, 171–174. doi: 10.1016/j.schres.2015.04.016

Roiser, J. P., and Sahakian, B. J. (2013). Hot and cold cognition in depression. *CNS Spectr.* 18, 139–149. doi: 10.1017/S1092852913000072

Salehinejad, M. A., Ghanavai, E., Rostami, R., and Nejati, V. (2017). Cognitive control dysfunction in emotion dysregulation and psychopathology of major depression (MD): Evidence from transcranial brain stimulation of the dorsolateral prefrontal cortex (DLPFC). *J. Affect. Disord.* 210, 241–248. doi: 10.1016/j.jad.2016.12.036

Salomons, T. V., Dunlop, K., Kennedy, S. H., Flint, A., Geraci, J., Giacobbe, P., et al. (2014). Resting-state cortico-thalamic-striatal connectivity predicts response to dorsomedial prefrontal rTMS in major depressive disorder. *Neuropsychopharmacology* 39, 488–498. doi: 10.1038/npp.2013.222

Schaller, G., Sperling, W., Richter-Schmidinger, T., Mühle, C., Heberlein, A., Maihöfner, C., et al. (2014). Serial repetitive transcranial magnetic stimulation (rTMS) decreases BDNF serum levels in healthy male volunteers. *J. Neural Transm.* 121, 307–313. doi: 10.1007/s00702-013-1102-1

Schulze, L., Wheeler, S., McAndrews, M. P., Solomon, C. J., Giacobbe, P., and Downar, J. (2016). Cognitive safety of dorsomedial prefrontal repetitive transcranial magnetic stimulation in major depression. *Eur. Neuropsychopharmacol.* 26, 1213–1226. doi: 10.1016/j.euroneuro.2016.04.004

Segrave, R. A., Arnold, S., Hoy, K., and Fitzgerald, P. B. (2014). Concurrent cognitive control training augments the antidepressant efficacy of tDCS: a pilot study. *Brain Stimul.* 7, 325–331. doi: 10.1016/j.brs.2013.12.008

Sheffield, J. M., Repovs, G., Harms, M. P., Carter, C. S., Gold, J. M., MacDonald, A. W., et al. (2015). Fronto-parietal and cingulo-opercular network integrity and cognition in health and schizophrenia. *Neuropsychologia* 73, 82–93. doi: 10.1016/j.neuropsychologia.2015.05.006

Shen, Y., Cao, X., Tan, T., Shan, C., Wang, Y., Pan, J., et al. (2016). 10-Hz repetitive transcranial magnetic stimulation of the left dorsolateral prefrontal cortex reduces heroin cue craving in long-term addicts. *Biol. Psychiatry* 80, e13–e14. doi: 10.1016/j.biopsych.2016.02.006

Speer, A. M., Benson, B. E., Kimbrell, T. K., Wassermann, E. M., Willis, M. W., Herscovitch, P., et al. (2009). Opposite effects of high and low frequency rTMS on mood in depressed patients: relationship to baseline cerebral activity on PET. *J. Affect. Disord.* 115, 386–394. doi: 10.1016/j.jad.2008.10.006

Speer, A. M., Kimbrell, T. A., Wassermann, E. M., Repella, J. D., Willis, M. W., Herscovitch, P., et al. (2000). Opposite effects of high and low frequency rTMS on regional brain activity in depressed patients. *Biol. Psychiatry* 48, 1133–1141. doi: 10.1016/S0006-3223(00)01065-9

Stagg, C. J., Best, J. G., Stephenson, M. C., O'Shea, J., Wylezinska, M., Kincses, Z. T., et al. (2009). Polarity-sensitive modulation of cortical neurotransmitters by transcranial stimulation. *J. Neurosci.* 29, 5202–5206. doi: 10.1523/JNEUROSCI.4432-08.2009

Tapert, S. F., Cheung, E. H., Brown, G. G., Frank, L. R., Paulus, M. P., Schweinsburg, A. D., et al. (2003). Neural response to alcohol stimuli in adolescents with alcohol use disorder. *Arch. Gen. Psychiatry* 60, 727–735. doi: 10.1001/archpsyc.60.7.727

Terraneo, A., Leggio, L., Saladini, M., Ermani, M., Bonci, A., and Gallimberti, L. (2016). Transcranial magnetic stimulation of dorsolateral prefrontal cortex reduces cocaine use: a pilot study. *Eur. Neuropsychopharmacol.* 26, 37–44. doi: 10.1016/j.euroneuro.2015.11.011

Tovar-Perdomo, S., McGirr, A., Van den Eynde, F., Rodrigues, D. S. N., and Berlim, M. T. (2017). High frequency repetitive transcranial magnetic stimulation treatment for major depression: dissociated effects on psychopathology and neurocognition. *J. Affect. Disord.* 217, 112–117.doi: 10.1016/j.jad.2017.03.075

Vanderhasselt, M. A., De Raedt, R., Baeken, C., Leyman, L., and D'Haenen, H. (2009). A single session of rTMS over the left dorsolateral prefrontal cortex influences attentional control in depressed patients. *World J. Biol. Psychiatry* 10, 34–42. doi: 10.1080/15622970701816514

Vanderhasselt, M. A., De Raedt, R., Namur, V., Lotufo, P. A., Bensenor, I. M., Boggio, P. S., et al. (2015). Transcranial electric stimulation and neurocognitive training in clinically depressed patients: a pilot study of the effects on rumination. *Prog. Neuropsychopharmacol. Biol. Psychiatry* 57, 93–99. doi: 10.1016/j.pnpbp.2014.09.015

Wagner, T., Fregni, F., Fecteau, S., Grodzinsky, A., Zahn, M., and Pascual-Leone, A. (2007). Transcranial direct current stimulation: a computer-based human model study. *Neuroimage* 35, 1113–1124. doi: 10.1016/j.neuroimage.2007.01.027

Wang, Y., Shen, Y., Cao, X., Shan, C., Pan, J., He, H., et al. (2016). Transcranial direct current stimulation of the frontal-parietal-temporal area

attenuates cue-induced craving for heroin. *J. Psychiatr. Res.* 79, 1–3. doi: 10.1016/j.jpsychires.2016.04.001

Wilson, S. J., Sayette, M. A., and Fiez, J. A. (2004). Prefrontal responses to drug cues: a neurocognitive analysis. *Nat. Neurosci.* 7, 211–214.doi: 10.1038/nn1200

Zwanzger, P., Steinberg, C., Rehbein, M. A., Bröckelmann, A. K., Dobel, C., Zavorotnyy, M., et al. (2014). Inhibitory repetitive transcranial magnetic stimulation (rTMS) of the dorsolateral prefrontal cortex modulates early affective processing. *Neuroimage* 101, 193–203. doi: 10.1016/j.neuroimage.2014.07.003

**Conflict of Interest Statement:** The authors declare that the research was conducted in the absence of any commercial or financial relationships that could be construed as a potential conflict of interest.

frontiers in Human Neuroscience

ORIGINAL RESEARCH
published: 08 September 2017
doi: 10.3389/fnhum.2017.00451

# Self-Reference Emerges Earlier than Emotion during an Implicit Self-Referential Emotion Processing Task: Event-Related Potential Evidence

*Haiyan Zhou[1,2,3†], Jialiang Guo[1,4†], Xiaomeng Ma[1], Minghui Zhang[1], Liqing Liu[1], Lei Feng[5,6], Jie Yang[5,6], Zhijiang Wang[7,8,9], Gang Wang[5,6,10] and Ning Zhong[1,2,3,10,11]**

[1]*Faculty of Information Technology, Beijing University of Technology, Beijing, China,* [2]*Beijing International Collaboration Base on Brain Informatics and Wisdom Services, Beijing University of Technology, Beijing, China,* [3]*Beijing Key Laboratory of Magnetic Resonance Imaging and Brain Informatics, Beijing University of Technology, Beijing, China,* [4]*State Key Laboratory of Cognitive Neuroscience and Learning & IDG/McGovern Institute for Brain Research, Beijing Normal University, Beijing, China,* [5]*The National Clinical Research Center for Mental Disorders, Beijing Anding Hospital, Capital Medical University, Beijing, China,* [6]*Beijing Key Laboratory of Mental Disorders, Beijing Anding Hospital, Capital Medical University, Beijing, China,* [7]*Institute of Mental Health (Sixth Hospital), Peking University, Beijing, China,* [8]*National Clinical Research Center for Mental Disorders, Key Laboratory of Mental Health, Ministry of Health, Peking University, Beijing, China,* [9]*Beijing Municipal Key Laboratory for Translational Research on Diagnosis and Treatment of Dementia, Beijing, China,* [10]*Beijing Advanced Innovation Center for Future Internet Technology, Beijing University of Technology, Beijing, China,* [11]*Department of Life Science and Informatics, Maebashi Institute of Technology, Maebashi, Japan*

Self-referential emotion refers to the process of evaluating emotional stimuli with respect to the self. Processes indicative of a self-positivity bias are reflected in electroencephalogram (EEG) signals at ∼400 ms when the task does not require a discrimination of self from other. However, when distinguishing between self-referential and other-referential emotions is required, previous studies have shown inconsistent temporal dynamics of EEG signals in slightly different tasks. Based on the observation of early self–other discrimination, we hypothesized that self would be rapidly activated in the early stage to modulate emotional processing in the late stage during an implicit self-referential emotion. To test this hypothesis, we employed an implicit task in which participants were asked to judge the order of Chinese characters of trait adjectives preceded by a self ("I") or other pronoun ("He" or "She"). This study aimed to explore the difference of social-related emotional evaluation from self-reference; the other pronoun was not defined to a specific person, rather it referred to the general concept. Sixteen healthy Chinese subjects participated in the experiment. Event-related potentials (ERPs) showed that there were self-other discrimination effects in the N1 (80–110 ms) and P1 (170–200 ms) components in the anterior brain. The emotional valence was discriminated in the later component of N2 (220–250 ms). The interaction between self-reference and emotional valence occurred during the late positive potential (LPP; 400–500 ms). Moreover, there was a positive correlation between response time (RT) and N1 in the self-reference condition based on the positive-negative contrast, suggesting a modulatory effect of the self-positivity bias. The results indicate that self-reference emerges earlier than emotion and then combines with emotional processing in an implicit task. The findings extend the view that the self plays a highly integrated and modulated role in self-referential emotion processing.

**Keywords: emotion, self, self-reference, other-reference, ERP**

OPEN ACCESS

***Edited by:***
*Xiaochu Zhang,*
*University of Science and Technology of China, China*

***Reviewed by:***
*Christoph W. Korn,*
*University Medical Center Hamburg-Eppendorf, Germany*
*Irene Messina,*
*University of Padua, Italy*

****Correspondence:***
*Ning Zhong*
*zhongn@bjut.edu.cn*

*[†]These authors have contributed equally to this work.*

***Received:*** *02 May 2017*
***Accepted:*** *25 August 2017*
***Published:*** *08 September 2017*

***Citation:***
*Zhou H, Guo J, Ma X, Zhang M, Liu L, Feng L, Yang J, Wang Z, Wang G and Zhong N (2017) Self-Reference Emerges Earlier than Emotion during an Implicit Self-Referential Emotion Processing Task: Event-Related Potential Evidence. Front. Hum. Neurosci. 11:451. doi: 10.3389/fnhum.2017.00451*

## INTRODUCTION

Self-referential emotion refers to the process of evaluating emotional stimuli with respect to the self (Zinck, 2008). A self-referential task in which participants are asked to judge whether the emotional personality trait words describe themselves is widely used to investigate this issue. The medial prefrontal cortex is reportedly involved in self-representation (Macrae et al., 2004; Northoff and Bermpohl, 2004; Northoff et al., 2006; Moran et al., 2009; Rameson et al., 2010; Qin and Northoff, 2011). This self-related region cooperates with the emotional limbic and frontal-parietal systems to evaluate and modulate emotion and cognition (Han and Ma, 2014; Hu et al., 2016), suggesting a complex interaction of self, emotion and general cognition during self-referential emotion processing.

Event-related potentials (ERPs) can reveal dynamic temporal patterns and clarify how self-referential emotion is processed. Emotions are usually characterized as adaptive response patterns to the emotionally significant presence of events (Russell, 2003; Scherer, 2005), and there is early emotional discrimination in the stage of 200–300 ms (Schupp et al., 2006; 2007; Kissler et al., 2007, 2009; Citron, 2012; Citron et al., 2013; Imbir et al., 2015). Self-relevant emotional information often entails positively biased processing (Fields and Kuperberg, 2015). For example, when participants are asked to judge which emotional trait words describe the self from one's own perspective, a friend's perspective, or a stranger's perspective, the N400 (200–400 ms) amplitude is reduced by positive relative to negative words, both in the self-respective and friend-perspective conditions (Zhou et al., 2013; Li et al., 2016). The results from a cross-cultural study suggested that such self-positivity biases are similar in both Eastern Asian and Western populations in the late positive potential (LPP) component (350–850 ms; Cai et al., 2016). In addition, self-referential emotion could occur earlier depending on the self-esteem level (Zhang et al., 2013; Yang et al., 2014b).

However, one of the most important roles of self is to discriminate one's own from non-self or other-related stimuli. The widely reported self-prioritization effect in perception and memory suggests a social discrimination function of self (Macrae et al., 2004, 2017; Sui et al., 2012a,b, 2015; Schäfer et al., 2015, 2016). The components of N1 (50–150 ms), P2 (about 150–250 ms), and P300 (about 300–500 ms) have shown the advantage effect for self-relevant stimuli (Zhao et al., 2009, 2011; Fan et al., 2011; Yang et al., 2012; Chen et al., 2015; Liu et al., 2016). Interestingly, self-identification is highly sensitive to temporal processing, and there is a self-relevant degree effect where high self-relevant stimuli are preferentially processed relative to those low in self-relevance (Chen et al., 2011, 2015; Guan et al., 2014). The tasks and elicited ERP components vary among studies, but the findings consistently suggest that self- and other-relevant processes could be rapidly discriminated in the very early stage. Hence, automatic self-discrimination might modulate the time course of self-referential emotion.

In an implicit self-referential processing task, participants were instructed to silently read noun words preceded by either self-related pronoun word ("my") or non-self-related word (article word "the"). ERP analysis showed that emotion was rapidly discriminated in an early time window of early posterior negativity (EPN, 200–300 ms), regardless of whether the preceding words were self-referential or other-referential, while emotion was modulated by self-reference in the later stage of LPP (450–600 ms; Herbert et al., 2011b). The later interaction between self-reference and emotion is consistent with findings in the self-referential emotion task without discrimination of self- and other-relevant (Zhou et al., 2013; Cai et al., 2016; Li et al., 2016) and further suggest that self-reference interacts with emotion to categorize information, but after emotional discrimination. Nevertheless, the self-discrimination effect was not reported.

In addition, the time course is more complicated when self-referential emotion needs to be distinguished from other-reference emotion. In another implicit study conducted by Herbert et al. (2011a), participants were instructed to silently read unpleasant, pleasant and neutral pronoun-noun and article—noun expressions that were related to the participants themselves, related to an unknown third person, or had no self-other reference at all ("my", "his", or "the"). Self-related and other-related pronoun-noun pairs were differentiated at 250–350 ms, followed by the interaction between self and emotion at 350–550 ms in the anterior brain. In the posterior brain, the conditions of self and other pronouns were differentiated from the non-self-reference condition (article words) at 200–400 ms, accompanied by emotional discrimination. In another investigation with sentence reading and scenario comprehension, self and other discriminated almost automatically in the occipital (P1, 50–100 ms) and frontal (N1, 100–150 ms; P2, 200–300 ms) regions (Fields and Kuperberg, 2012). These findings demonstrate that when it is required by task demands to discriminate self from other, self-discrimination occurs earlier than the so-called adaptive emotional response, and then the self would integrate the emotional information. That means the self-referential emotion could be highly self-specialized in temporal dynamics.

Inconsistent findings were also reported. For example, when participants were asked to read two-sentence social vignettes that were either self- or other-relevant, only a self-positivity bias effect at 300–500 ms was reported (Fields and Kuperberg, 2015). In a study with Chinese participants (Chen et al., 2014), personality trait words were implicitly preceded by self or other pronouns, and participants were asked to judge word emotional valence. There was an advanced self-positivity bias in the early time window of N2 (100–200 ms), but there were no main effects of emotion or self–other discrimination. Another study using the go/no-go paradigm reported a similar interaction between self and emotion in the component of N270 (200–400 ms; Wu et al., 2014). All these studies showed a consistent interaction between self and emotion processing, while there were no main effects of self and emotion. The absence of emotion discrimination in these studies could not be explained by the task paradigms since the tasks emphasized more on emotional processing. However, the enhanced emotional processing in these tasks might facilitate the

interaction between emotional information and self-reference, decreasing the processing of self–other discrimination. There is therefore a need to clarify the time course of self and emotion processing using a more implicit self-reference emotion task paradigm.

In this study, we investigated the time course of self- and other-referential emotion using a modified implicit, self-referential task paradigm (Herbert et al., 2011a,b; Chen et al., 2014). In the task, an affective personality trait word was preceded by a pronoun word to indicate self- or other-relevance, and then the participants were asked to judge whether the following Chinese character was the first or the second character in the affective word. This task might involve less emotional or semantic activation of the trait word compared to silent reading (Herbert et al., 2011a,b) or emotion judgment (Chen et al., 2014), and would decrease the interaction between emotional information and self-reference. The processing of self-referential emotion in this task would therefore be more implicit since the judgment is unrelated to self-reference and emotion. Based on the rapid and automatic self-identification effect, we hypothesized that self-related processes would be rapidly activated in the early stage to modulate emotional processing in the late stage. Both early and late ERP components were analyzed.

# MATERIALS AND METHODS

## Ethics Statement

The study was approved by the Ethics Committee of Beijing Anding Hospital, Capital Medical University, Beijing, China, compliant with the ethical standards outlined in the Declaration of Helsinki. Written informed consent was obtained from each subject prior to their participation, after the nature and possible consequences of the studies were explained.

## Participants

Sixteen healthy, right-handed subjects (eight males and eight females) participated in this study. Their ages ranged from 21 to 60 (43.19 ± 13.03). The participants were all Han Chinese and lived in mainland China. All participants reported no history of neurological or psychiatric disorders.

## Materials and Procedure

A total of 96 two-character personality trait words were selected from the Chinese Affective Words System (Wang et al., 2008), and the words are listed in Supplementary Table S1. Half of the words were positive and half were negative (valence scores of 6.55 ± 0.41 and 3.29 ± 0.37, respectively; $t_{(94)} = -41.026$, $p < 0.00001$). The differences of arousal and familiarity were not significant (for arousal, positive = 4.72 ± 0.60, negative = 4.85 ± 0.60, $t_{(94)} = 1.062$, $p = 0.291$; for familiarity, positive = 5.45 ± 0.49, negative = 5.30 ± 0.41, $t_{(94)} = -1.540$, $p = 0.127$).

The selected affective personality words were combined with the self-referential factor to produce four experimental conditions: Self Positive (SP), Self Negative (SN), Other Positive (OP), and Other Negative (ON). To balance the combination effect, the positive and negative words were randomly divided into two lists and used in two experimental procedures. In the first procedure, personality word list A was only combined with the pronoun of self, and list B was only combined with the pronoun of other. In the second procedure, the combination was switched, with list A to other pronouns and list B to self pronouns. Only one of the two procedures was used for each participant. Within lists A and B, the only significant difference was for the dimension of emotional valence, not for arousal or familiarity. There were no differences between lists A and B in the three dimensions. Detailed information for the affective personality words in lists A and B is shown in **Table 1**.

The implicit self-referential task is depicted in **Figure 1A**. For each trial, after a white "+" appeared in the middle of the black screen for 500 ms, a personal pronoun word appeared on the screen for 1000 ms. For the self-referential condition, it was the Chinese character of "我" (means I), and for the other-referential condition, it was "他" (means He) for male participants and "她" (means She) for female participants. To compare our procedure, "the + noun" in Herbert et al.'s (2011b) study, does not make any reference to another person whereas "he/she + adjective" refers to some other person. After a "+" was shown on the screen for 500 ms, an affective personality trait word (for example, "充沛" means vigorous in the positive condition, and "悲观" means pessimistic in the negative condition) appeared for 1000 ms. Finally, after a "+" was on the screen for 500 ms, a Chinese character was shown for a maximum of 10,000 ms. The participants were asked to judge whether the character was the first or second character in the previous affective word, and they were instructed to press the response key with their index finger for the first character (for examples, "充" and "悲") or their middle finger for the second character (for examples, "沛" and "观"). The character disappeared once the participant responded. The inter-stimulus interval (ISI) was 1600–2000 ms.

**TABLE 1 |** Detailed information about the affective personality trait words used in the task.

| | List A | | | List B | | | *P* value (List A vs. List B) | |
|---|---|---|---|---|---|---|---|---|
| | **Positive** | **Negative** | ***P* value** | **Positive** | **Negative** | ***P* value** | **Positive** | **Negative** |
| Valence | 6.489 ± 0.461 | 3.221 ± 0.398 | <0.001 | 6.613 ± 0.349 | 3.359 ± 0.332 | <0.001 | 0.298 | 0.196 |
| Arousal | 4.849 ± 0.532 | 4.845 ± 0.511 | 0.991 | 4.594 ± 0.653 | 4.857 ± 0.689 | 0.182 | 0.146 | 0.955 |
| Familiarity | 5.402 ± 0.539 | 5.319 ± 0.442 | 0.561 | 5.489 ± 0.451 | 5.287 ± 0.382 | 0.102 | 0.547 | 0.794 |

*Self-/other-reference and affective words were divided between Lists A and B, which were balanced in the dimensions of valence, arousal and familiarity.*

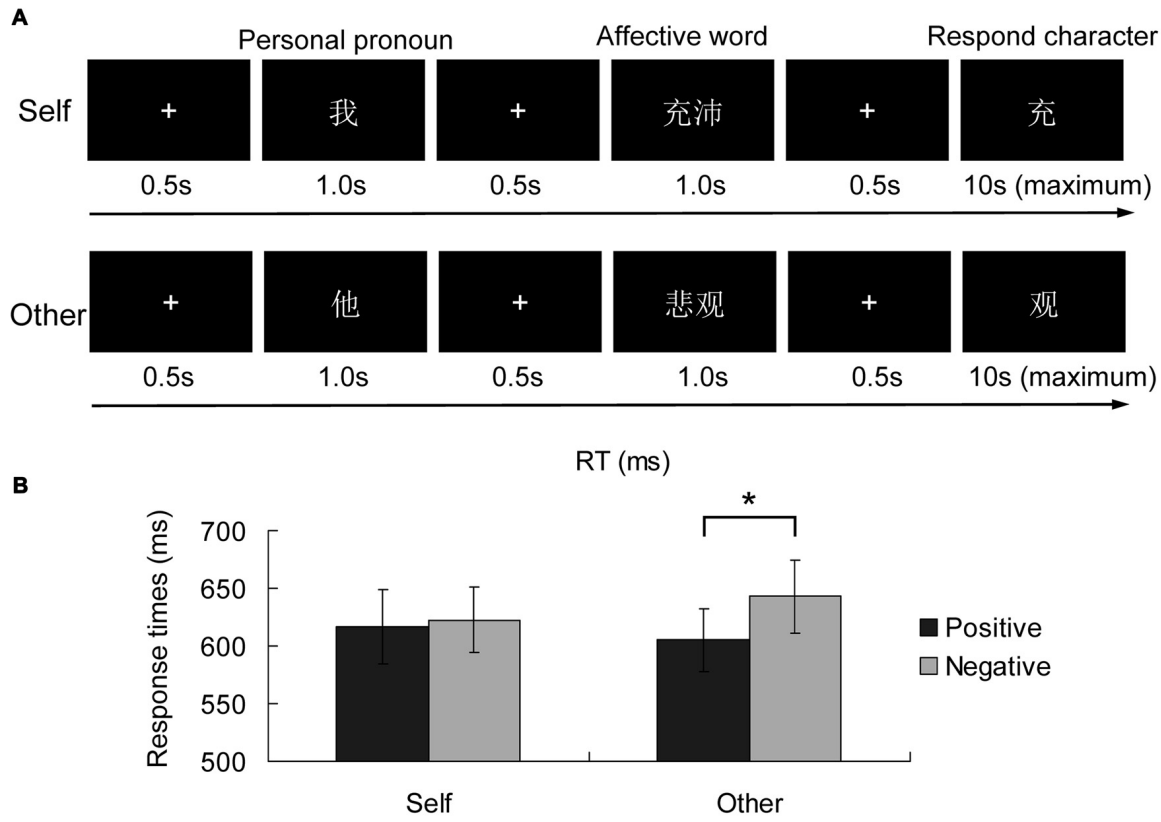


**FIGURE 1 |** Implicit self-referential emotion task procedure **(A)** and the response times (RTs) in the experimental conditions **(B)**. After a self-referential or non-self-referential pronoun word appeared, a positive or negative personality trait word was shown on the screen, and participants were asked to judge the order of the following character in the affective word. The black and gray bars indicate the self-reference and other-reference conditions respectively. The error bars are the standard errors in each condition. $^{*}p < 0.05$.

There were a total of four blocks, each including 24 trials with an equal number of trials in the SP, SN, OP and ON conditions. The numbers of the two kinds of response types were balanced in each block. Participants practiced to familiarize themselves with the task before the formal experiment. Both the accuracy and response time (RT) were recorded during the experiment.

## Behavioral Data Analysis

First, the errors and extreme responses with RTs out of the three standard deviations (SDs) in each condition for each participant were deleted, corresponding to ∼3% (41/1536) of data. Then both the accuracy and RTs in the four experimental conditions were calculated for each participant. Under each condition, the accuracy was calculated by the remaining number of data divided by the total number and RT was the average value of the remaining data. Finally, 2 (self-reference: self vs. other) × 2 (emotion: positive vs. negative) repeated measures analysis of variance (ANOVA) was performed using SPSS Statistics 20.0 (IBM, Armonk, NY, USA) to investigate the self-reference and emotional valence effects and their interaction for both accuracy and RT.

## ERP Recording and Analysis

The ERP data were recorded during the experiment in a quiet, softly lit room. Participants were instructed to sit comfortably in a seat. The distance from their eyes to the screen was about 80 cm, and the horizontal and vertical angles of view were ∼5°. Brain electrical activity was recorded with a 64-electrode cap (Brain Products, Gilching, Germany) placed according to the extended International 10/20-system and referenced to the frontocentral midline electrode (FCz). The horizontal electrooculogram (HEOG) was recorded at the outer canthi, about 1.5 cm from the left eye, and the vertical electrooculogram (VEOG) was recorded about 1.5 cm below the right eye. Both the electroencephalograms (EEGs) and electrooculograms (EOGs) were collected with the electrode impedances kept below 5 kΩ. EEG and EOG signals were amplified on-line with a band-pass filtering range of 0.01–30 Hz and sampled with 1000 Hz.

The EEG signals were processed with the Brain Vision Analyzer 2.0 software package (Brain Products). All data were re-referenced to the averaged left and right mastoids (TP9 and TP10) and resampled at 250 Hz. A high-pass Butterworth filter with 0.3 Hz was applied. The EEGs were corrected

for ocular artifacts using the independent component analysis (ICA) method, and both the EEG epoch for the artifacts and incorrect responses were excluded from the analysis. Event-locked ERPs were obtained by extracting an epoch beginning 200 ms before the affective words and ending 600 ms after the word's appearance. The data were baseline corrected with respect to the mean voltage over the 200 ms preceding personality word presentation. According to the ERP waves, we did analysis separately in the anterior and posterior brain. In the anterior region, we analyzed the average amplitudes of the N1 (80–110 ms), P1 (170–200 ms), N2 (220–250 ms) and LPP (400–500 ms) components in the left (AF7, AF3, F5, F3, FC5 and FC3), middle (F2, F1, Fz, FC1, FC2 and FCz), and right (AF8, AF4, F6, F4, FC6 and FC4) areas. A 3 (location: left vs. middle vs. right) × 2 (self-reference: self vs. other) × 2 (emotion: positive vs. negative) repeated ANOVA was performed to investigate the location effect, self-reference effect, emotional valence effect and their interactions. In the posterior region, we analyzed the average amplitudes of the P1 (100–130 ms), N1 (160–190 ms), and P2 (250–280 ms) components in the left (PO7, PO3 and O1), middle (POz and Pz), and right (PO8, PO4 and O2) areas. A 3 (location: left vs. middle vs. right) × 2 (self-reference: self vs. other) × 2 (emotion: positive vs. negative) repeated measures ANOVA was performed to investigate the location effect, self-reference effect, emotional valence effect, and their interactions.

# RESULTS

## Behavioral Results

For accuracy, there were no effects for self-reference, emotion, or the interaction between self and emotion (all $p > 0.05$). For RT, the effect of emotion was marginally significant ($F_{(1,15)} = 3.317$, $p = 0.089$), and the effect of self-reference did not reach the significance level ($p > 0.05$). However, as shown in **Figure 1B**, the interaction between self-reference and emotion reached the significance level ($F_{(1,15)} = 4.931$, $p = 0.042$). The simple effect analysis showed a significant emotional valence effect in the other-reference condition ($F_{(1,15)} = 6.74$, $p = 0.020$), while the emotional valence effect in the self-reference condition did not reach the significance level ($p > 0.05$).

## ERP Results

### Results in the Anterior Brain

For the N1 component, the main effect of location was significant ($F_{(2,30)} = 3.384$, $p = 0.047$), and LSD *post hoc* test showed that the amplitude in the left region was weaker than that in the right region ($p = 0.028$). There was a self-reference effect ($F_{(1,15)} = 6.167$, $p = 0.025$), with weaker amplitude in the self-reference condition. **Figure 2** shows the self-reference effect and **Figure 5A** shows the individual-subject effect.

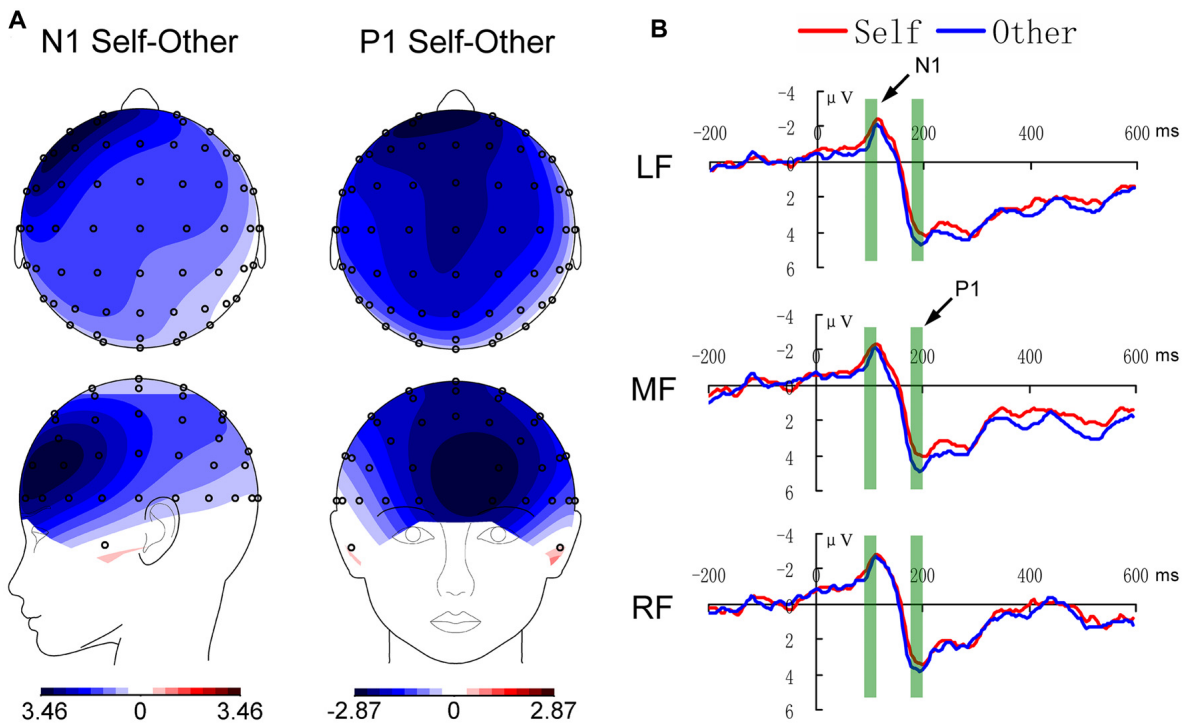


**FIGURE 2 |** The self–other discrimination effects in the N1 (80–110 ms) and P1 (170–200 ms) components in the anterior region. **(A)** Displays the topological maps, and **(B)** shows the waveforms. LF, MF and RF indicate the left, middle and right anterior brain regions, respectively.

For the component of P1, there was only a self-reference effect with weaker amplitude in the self-reference condition ($F_{(1,15)} = 5.678$, $p = 0.031$), as shown in **Figures 2**, **5B**.

For the component of N2, the effect of location was significant ($F_{(2,30)} = 7.723$, $p = 0.002$), and the LSD *post hoc* test showed that the amplitude in the right region was weaker than those in the left and middle regions (both $p < 0.01$). In addition, as shown in **Figures 3**, **5C**, the main effect of emotion was significant ($F_{(1,15)} = 5.560$, $p = 0.032$), with weaker amplitude in the positive condition.

For the component of LPP shown in **Figure 4**, the effect of location reached the significance level ($F_{(2,30)} = 23.303$,

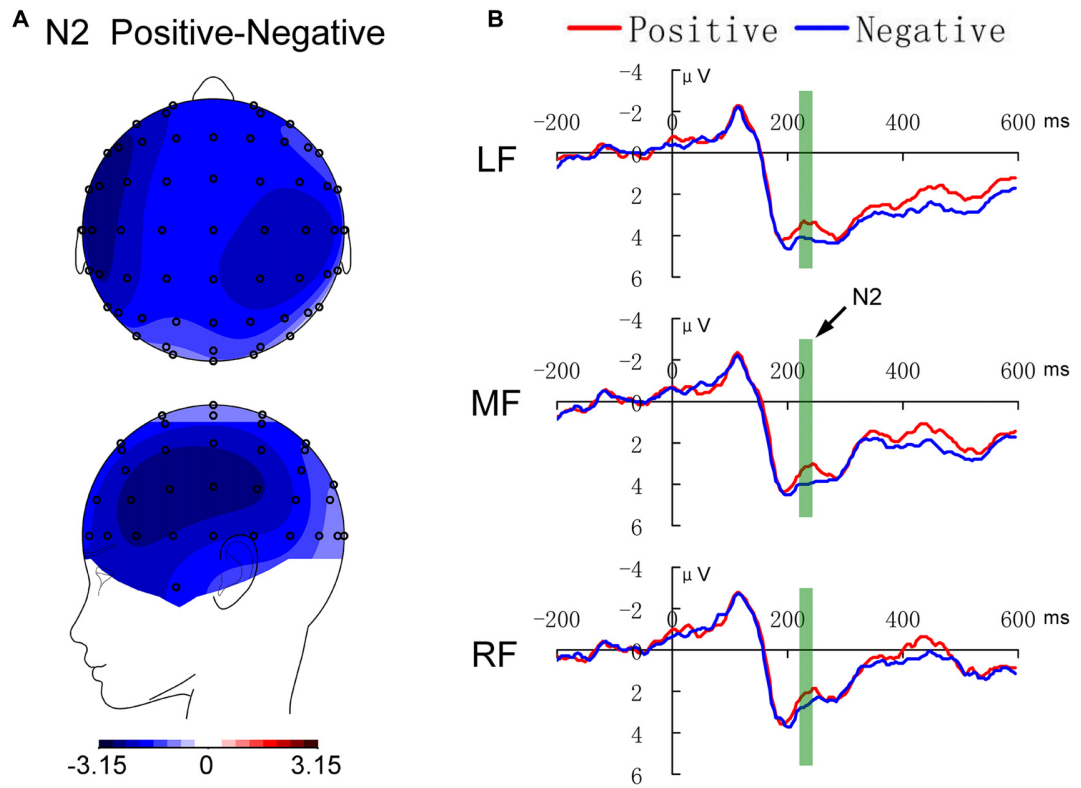


**FIGURE 3 |** The emotional valence effect in the P2 (230–260 ms) component in the anterior brain. **(A)** Displays the topological maps, and **(B)** shows the waveforms. LF, MF and RF indicate the left, middle and right anterior brain regions, respectively.

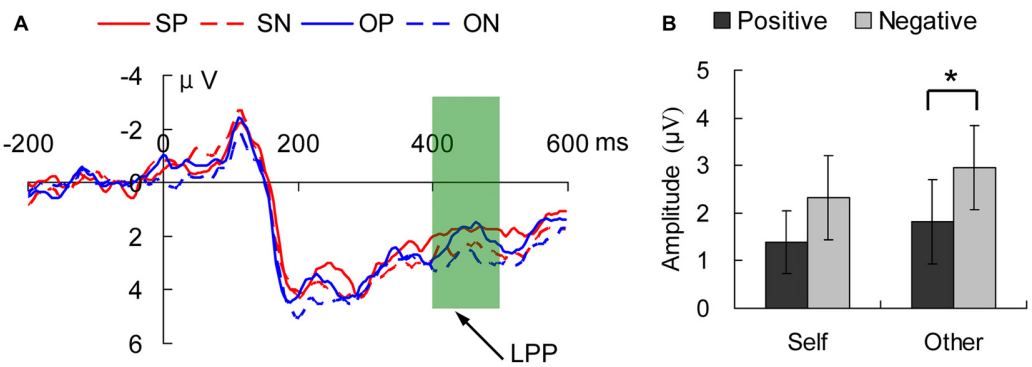


**FIGURE 4 |** The three-way interaction in the late positive potential (LPP; 400–500 ms) component in the anterior brain. **(A)** Displays the waveforms in the four conditions and **(B)** shows the average amplitudes in the LPP time-window. The solid lines show the positive emotion and the dashed lines show the negative emotion. self positive (SP), self negative (SN), other positive (OP), other negative (ON) indicate the conditions of self-referential positive emotion, self-referential negative emotion, other-referential positive emotion and other-referential negative emotion, respectively. The error bars are the standard errors in each condition. *$p < 0.05$.

$p$ = 0.000), and the LSD *post hoc* test showed that the amplitude in the right region was weaker than those in the left and middle regions (both $p < 0.01$). The three-way interaction was significant ($F_{(2,30)}$ = 4.399, $p$ = 0.021). The simple simple effect analysis showed that in the left region, there was a marginally significant emotional valence effect in the self-reference condition ($F_{(1,15)}$ = 3.54, $p$ = 0.080) and a significant emotional valence effect in the other-reference condition ($F_{(1,15)}$ = 4.94, $p$ = 0.042); no other interactions between factors were observed (all $p > 0.05$).

### Results in the Posterior Brain

There was no significant main effect or interaction for the P1 component in the posterior brain. For the component of N1, the only significant effect was the location ($F_{(2,30)}$ = 5.624, $p$ = 0.008), and the LSD *post hoc* test showed that the amplitude in the middle region was weaker than those in the left and right regions (both $p < 0.05$). For P2, there was a significant effect for location ($F_{(2,30)}$ = 3.589, $p$ = 0.040), and the LSD *post hoc* test showed that the amplitude in the middle region was stronger than that in the right regions ($p$ = 0.002). The three-way interaction reached the significance level ($F_{(2,30)}$ = 4.149, $p$ = 0.026), while the simple simple effect showed no significant effects (all $p > 0.05$).

## *Post Hoc* Correlation Analysis between ERPs and RT

According to the ANOVA results, self-other was discriminated in the early components of N1 and P1; however, there was no self-positivity bias effect on behavioral performance. To explore the self-modulated emotional effect during the processing, we conducted a *post hoc* Pearson correlation analysis between ERPs (N1 and P1) and log-transformed RT data. Separate correlation analyses were performed in the self-reference and other-reference conditions in the left anterior region, where the self-other discrimination effect was strongest. To adjust for the multiple comparisons, Bonferroni correction ($n$ = 4) was performed at an α value of 0.05. As shown in **Figure 6**, there was a positive correlation between RT and N1 in the

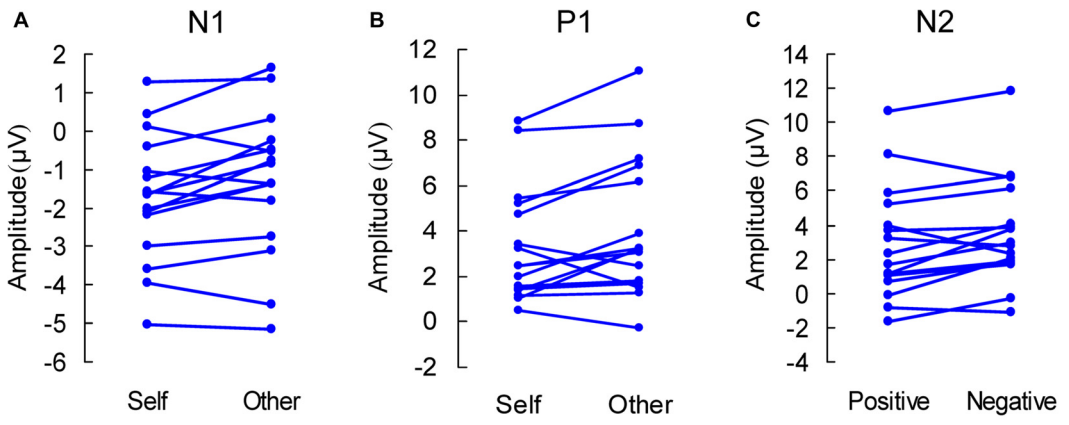


**FIGURE 5 |** Individual-subject experimental effects in the anterior brain. **(A,B)** Display the self-reference effect in the components of N1 and P1, respectively. **(C)** Displays the emotional valence effect.

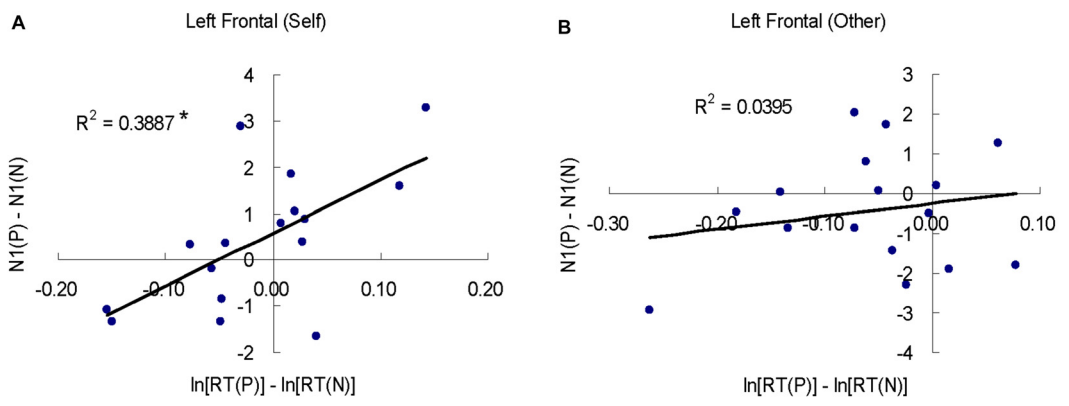


**FIGURE 6 |** The correlations between behavioral RT and N1. **(A,B)** Indicate the correlation between RT and N1 based on the emotional valence effect in the self- and other-referential conditions. P indicates the positive condition and N is for the negative condition. *$p < 0.05$, Bonferroni corrected.

self-reference condition ($r = 0.625$, $p < 0.05$, Bonferroni corrected), but no correlation in the other-reference condition ($p > 0.05$).

# DISCUSSION

In this study, the temporal dynamics of self-referential emotion were investigated using an implicit task. The ERP patterns showed an expected and distinct self–other discrimination effect in the very early stages, with the emotional valence effect activated lightly later. Self-modulated emotion processing occurred in a later time window.

## Automatic Self–Other Identification Processing in the Early Stage

We observed a strong self–other identification effect in the early automatic processing stage for both the components of N1 (80–110 ms) and P1 (170–200 ms) in the anterior brain. This effect could not simply be attributable to the priming effect of pre-presented pronoun words. Considering the task procedure and data pattern in this study, the waveforms were slow waves ∼500 ms after pronoun presentation. Before word presentation, there was an additional 500 ms of cross-presentation, which would decrease the priming effects of pronoun words to some degree. In addition, compared with results obtained using the similar "pronoun + emotional word" priming paradigms (Herbert et al., 2011b; Chen et al., 2014), neither group reported such an effect. The difference might be related to the experimental task and design. As mentioned before, enhanced emotional processing might have weakened the effect of discrimination self from other in a previous study (Chen et al., 2014); while our task paradigm is more implicit and does not emphasize self or emotional processing. In the study by Herbert et al. (2011b), the task required distinction between self- and none-self-related words ("my" vs. "the"), but there was no need to identify self-reference from other-reference. This experimental design might explain the absence of self-reference effect, because "the + noun" does not make any reference to another person. In another study conducted by the same group, where there was no priming of pronoun words but earlier self-other discrimination was observed with a contrast of self-reference and other-reference (Herbert et al., 2011a). It seems that the other-reference condition increases the social-related evaluation of emotional processing, while article words ("the") do not have such a socially defined effect.

Early self-related identification is usually found in Chinese populations for both explicit (Sui et al., 2012c; Zhang et al., 2013) and implicit (Sui et al., 2009; Fan et al., 2011, 2013; Yang et al., 2012; Liu et al., 2016) self-referential processing. There is even a temporal sensitivity to the self-relevant degree effect in Chinese individuals (Chen et al., 2011, 2015; Guan et al., 2014). Our finding of early self-discrimination is consistent with studies of Chinese subjects (Sui et al., 2009, 2012c; Chen et al., 2011, 2015; Fan et al., 2011, 2013; Yang et al., 2012; Zhang et al., 2013; Guan et al., 2014; Liu et al., 2016) and Western populations (Herbert et al., 2011a; Sui et al., 2012c; Tacikowski et al., 2014). Research suggests that automatic processing bias towards self might not reflect stimuli familiarity but could be related to perceptual salient processing with social self-relevance, termed the self-prioritization effect (Macrae et al., 2004, 2017; Sui et al., 2012a,b, 2015; Humphreys and Sui, 2015; Schäfer et al., 2015, 2016). The self could be a center to integrate different information types at various processing stages (Sui and Humphrey, 2015), and the self-modulation effect could happen automatically or intentionally (Humphreys and Sui, 2015). Our results illustrate that the self can be rapidly identified from others to further integrate processing in a relatively automatic way.

## Emotion and Self-Modulated Emotional Processing

Although emotional processing was not emphasized in this task, there were strong emotional valence effects in the ERP data. The early component of N2 was sensitive to emotion information, with weaker amplitude in the positive condition than in the negative condition. These results are consistent with findings using an implicit task paradigm (Herbert et al., 2011a). As previously mentioned, emotional discrimination at the stage of EPN is usually regarded as an automatic adaptive response according to the degree of arousal (Schupp et al., 2006; 2007; Kissler et al., 2007, 2009; Citron, 2012; Citron et al., 2013; Imbir et al., 2015). However, there is a difference between our findings and previous results. The early emotional valence effect was observed in the anterior frontal brain, especially in the left hemisphere, while the EPN was reported in the posterior occipital brain. Actually, there is another possible reason for the difference between negative and positive stimuli. Fields and Kuperberg (2012) observed a stronger activity in the negative condition during the time window of 500–800 ms. They argued that this kind of emotional discrimination might be related to the negative bias (Taylor, 1991; Ito et al., 1998; Baumeister et al., 2001; Rozin and Royzman, 2001; Holt et al., 2009), which was related to the frontal region, whereas the arousal effect was to the posterior brain. More investigations with specified experimental designs are needed to clarify the debate surrounding the arousal and negative bias hypothesis. However, the early occurring emotional valence effect observed here suggests that there might be a strong social affective evaluation in Chinese subjects.

There was an interaction between self-reference and emotion observed in both the behavioral RT and late LPP in the left anterior brain. The results are generally consistent with the findings in previous studies using an implicit paradigm (Herbert et al., 2011a,b; Chen et al., 2014; Wu et al., 2014), but the time courses are later than those with the explicit paradigm (Zhang et al., 2013; Zhou et al., 2013; Yang et al., 2014a; Cai et al., 2016; Li et al., 2016). These patterns indicate that the increased specificity of the self-reference would bring forward the combination of self-reference and emotion information. Moreover, the simple effect analysis showed that there was significant emotional

valence effect in the other-reference condition, but not the self-reference condition. Most previous studies showed the emotional effect in the self-related condition and suggested a self-positivity bias; however several others showed at least a tendency of larger emotional effects in the other-related or non-self-related conditions than in the self-related condition, but the tendency was not clearly reported or mentioned in those studies. For example, the numbers of correctly recalled items in Herbert and colleagues' studies (Figure 4 in Herbert et al., 2011a), and the LPP amplitudes in the studies of Field and Kuperberg (Figure 5 in Fields and Kuperberg, 2012; Figure 2 in Fields and Kuperberg, 2015). One of the commonalities within the studies is the relative implicit task that imposes no direct processing demands on the self or emotion. It was argued that the self-positivity bias would emerge when making a judgment or behavioral response with regard to the self (Chambers and Windschitl, 2004; Alicke and Govorun, 2005), while the implicit paradigms used by others and in our studies might reduce access to important aspects of self-concept and could not elicit a self-positivity bias effect (Fields and Kuperberg, 2015).

However, the absence of self-positivity bias in behavior or the late component of LPP could not mean there is no self-modulated emotion during the entire process. A *post hoc* correlation analysis showed that the brain could modulate the behavior response in the early stage of N1 in the self-reference condition. Because longer RTs and greater N1 negative amplitude usually indicate strengthened effortful processing, the increased positive-negative difference in N1 shows a promoting effect on the self-referential behavior response. The correlation pattern actually reflects the self-positivity bias, and our findings suggest that the early ERP effects would contribute to the behavioral response.

## Limitations and Future Directions

With an implicit self-referential emotion task, different ERPs showed the temporal effects of self-reference and emotion and their interaction. There are some notable limitations that should be addressed in future research. First, the age range is unusually large, and the sample is relatively small. Considering that the task was simple and the variation in the behavioral RTs was not large, this might decrease the age effect to some degree. However, a larger and more homogenous sample would increase the power of the findings. Second, results based on the pronoun priming paradigm need more consideration. One is about the self-reference effect. As discussed above, the influence of priming paradigm was weakened to some degree, and there is considerable evidence of early self–other discrimination. However, caution is needed when considering the priming effect. Another issue is the other-reference condition. It seems that the other-reference increased the social-related evaluation of emotional processing (Herbert et al., 2011a), while article words ("the") did not have such a socially defined effect (Herbert et al., 2011b). Our study mainly focused on the temporal dynamics on the self- and other-referential emotion. However, the other pronoun was not defined to a specific person such as a friend, a stranger or mother, which would affect the processing for self-referential emotion (Zhou et al., 2013; Li et al., 2016). Finally, some results seem to be related to specific culture-related features. For example, both self–other discrimination and emotional valence effects emerged earlier than in Western subjects. The Eastern Asian cultures foster interdependent self-construal, relying on how others perceive and evaluate the self (Ma et al., 2014), so it is more influenced by social context information (Kitayama and Uskul, 2011; de Greck et al., 2012; Sui et al., 2012c; Han and Ma, 2014, 2015; Ma et al., 2014; Park and Kitayama, 2014). The context-inference processing strategy would increase highly sensitive discrimination between self and others in Chinese individuals. Furthermore, Chinese subjects usually show higher sensitivity to public or social evaluation and are more anxious (Liew et al., 2011), which would increase their sensitivity to emotional processing. However, the general framework is emphasized in social neuroscience (Gaertner et al., 2012), such as with the hypothesis of interdependent vs. dependent (Markus and Kitayama, 1991). As mentioned before, similar self-referential processing was observed in both Eastern and Western populations (Fields and Kuperberg, 2012; Herbert et al., 2013; Schindler et al., 2014; Tacikowski et al., 2014; Cai et al., 2016). Further studies with cross-cultural paradigms are needed to examine temporal patterns during self-referential emotion processing, which would be helpful to further clarify the roles of related factors.

# CONCLUSION

An implicit self-referential emotion task was used to investigate the time-course of self and emotion processing in Chinese subjects. ERPs showed that self-reference effect occurred in the N1 and P1 components in the anterior brain, earlier than the emotional valence effect in the component of N2. Their interaction was in the LPP component. A correlation pattern was observed between N1 and RT. The findings suggest that self-modulated emotional processing occurs in a rapid and automatic way in the Chinese population.

# AUTHOR CONTRIBUTIONS

HZ, JG, LF, GW and NZ: conceived and designed the experiments. HZ, JG, XM, MZ, LL, LF and JY: performed the experiments. HZ, JG and ZW: analyzed the data. HZ, JG and NZ: wrote the article.

# ACKNOWLEDGMENTS

The authors are grateful to Professor Shihui Han who kindly discussed some issues regarding the methods and results. This work was supported by the National Basic Research Program of China (2014CB744600), International Science & Technology Cooperation Program of China (2013DFA32180), and National Natural Science Foundation of China (61272345), as well as the Beijing Advanced Innovation Center for Future

Internet Technology in Beijing University of Technology, Beijing Municipal Commission of Education, Beijing International Collaboration Base on Brain Informatics and Wisdom Services, and Beijing Key Laboratory of Magnetic Resonance Imaging and Brain Informatics.

## SUPPLEMENTARY MATERIAL

The Supplementary Material for this article can be found online at: http://journal.frontiersin.org/article/10.3389/fnhum.2017.00451/full#supplementary-material

## REFERENCES


Alicke, M. D., and Govorun, O. (2005). "The better-than-average effect," in *The Self and Social Judgement*, eds M. D. Alicke, D. A. Dunning, J. I. Krueger (New York, NY: Psychology Press), 85–106.

Baumeister, R., Bratslavsky, E., Finkenauer, C., and Vohs, K. (2001). Bad is stronger than good. *Rev. Gen. Psychol.* 5, 323–370. doi: 10.1037/1089-2680.5.4.323

Cai, H., Wu, L., Shi, Y., Gu, R., and Sedikides, C. (2016). Self-enhancement among westerners and easterners: a cultural neuroscience approach. *Soc. Cogn. Affect. Neurosci.* 11, 1569–1578. doi: 10.1093/scan/nsw072

Chambers, J. R., and Windschitl, P. D. (2004). Biases in social comparative judgments: the role of nonmotivated factors in above-average and comparative-optimism effects. *Psychol. Bull.* 130, 813–838. doi: 10.1037/0033-2909.130.5.813

Chen, J., Shui, Q., and Zhong, Y. (2015). Self-esteem modulates automatic attentional responses to self-relevant stimuli: evidence from event-related brain potentials. *Front. Hum. Neurosci.* 9:376. doi: 10.3389/fnhum.2015.00376

Chen, J., Yuan, J., Feng, T., Chen, A., Gu, B., and Li, H. (2011). Temporal features of the degree effect in self-relevance: neural correlates. *Biol. Psychol.* 87, 290–295. doi: 10.1016/j.biopsycho.2011.03.012

Chen, Y., Zhong, Y., Zhou, H., Zhang, S., Tan, Q., and Fan, W. (2014). Evidence for implicit self-positivity bias: an event-relate brain potential study. *Exp. Brain Res.* 232, 985–994. doi: 10.1007/s00221-013-3810-z

Citron, F. (2012). Neural correlates of written emotion word processing: a review of recent electrophysiological and hemodynamic neuroimaging studies. *Brain Lang.* 122, 211–226. doi: 10.1016/j.bandl.2011.12.007

Citron, F., Weekes, B., and Ferstl, E. (2013). Effects of valence and arousal on written word recognition: time course and ERP correlates. *Neurosci. Lett.* 533, 90–95. doi: 10.1016/j.neulet.2012.10.054

de Greck, M., Shi, Z., Wang, G., Zuo, X., Yang, X., Wang, X., et al. (2012). Culture modulates brain activity during empathy with anger. *Neuroimage* 59, 2871–2882. doi: 10.1016/j.neuroimage.2011.09.052

Fan, W., Chen, J., Wang, X.-Y., Cai, R., Tan, Q., Chen, Y., et al. (2013). Electrophysiological correlation of the degree of self-reference effect. *PLoS One* 8:e80289. doi: 10.1371/journal.pone.0080289

Fan, W., Zhang, Y., Wang, X., Zhang, X., and Zhong, Y. (2011). The temporal features of self-referential processing evoked by national flag. *Neurosci. Lett.* 505, 233–237. doi: 10.1016/j.neulet.2011.10.017

Fields, E., and Kuperberg, G. (2012). It's all about you: an ERP study of emotion and self-relevance in discourse. *Neuroimage* 62, 562–574. doi: 10.1016/j.neuroimage.2012.05.003

Fields, E., and Kuperberg, G. (2015). Loving yourself more than your neighbor: ERPs reveal online effects of a self-positivity bias. *Soc. Cogn. Affect. Neurosci.* 10, 1202–1209. doi: 10.1093/scan/nsv004

Gaertner, L., Sedikides, C., Luke, M., O'Mara, E. M., Iuzzini, J., Jackson, L. E., et al. (2012). A motivational hierarchy within: primacy of the individual self, relational self, or collective self? *J. Exp. Soc. Psychol.* 48, 997–1013. doi: 10.1016/j.jesp.2012.03.009

Guan, L., Qi, M., Zhang, Q., and Yang, J. (2014). The neural basis of self-face recognition after self-concept threat and comparison with important others. *Soc. Neurosci.* 9, 424–435. doi: 10.1080/17470919.2014.920417

Han, S., and Ma, Y. (2014). Cultural differences in human brain activity: a quantitative meta-analysis. *Neuroimage* 99, 293–300. doi: 10.1016/j.neuroimage.2014.05.062

Han, S., and Ma, Y. (2015). A culture-behavior-brain loop model of human development. *Trends Cogn. Sci.* 19, 666–676. doi: 10.1016/j.tics.2015.08.010

Herbert, C., Herbert, B., Ethofer, T., and Pauli, P. (2011a). His or mine? The timecourse of self-other identification in emotion processing. *Soc. Neurosci.* 6, 277–288. doi: 10.1080/17470919.2010.523543

Herbert, C., Pauli, P., and Herbert, B. (2011b). Self-reference modulates the processing of emotional stimuli in the absence of explicit self-referential appraisal instructions. *Soc. Cogn. Affect. Neurosci.* 6, 653–661. doi: 10.1093/scan/nsq082

Herbert, C., Sfärlea, A., and Blumenthal, T. (2013). Your emotion or mine: labeling feelings alters emotional face perception-an ERP study on automatic and intentional affect labeling. *Front. Hum. Neurosci.* 7:378. doi: 10.3389/fnhum.2013.00378

Holt, D., Lynn, S., and Kuperberg, G. (2009). Neurophysiological correlates of comprehending emotional meaning in context. *J. Cogn. Neurosci.* 21, 2245–2262. doi: 10.1162/jocn.2008.21151

Hu, C., Di, X., Eickhoff, S., Zhang, M., Peng, K., Guo, H., et al. (2016). Distinct and common aspects of physical and psychological self-representation in the brain: a meta-analysis of self-bias in facial and self-referential judgments. *Neurosci. Biobehav. Rev.* 61, 197–207. doi: 10.1016/j.neubiorev.2015.12.003

Humphreys, G. W., and Sui, J. (2015). The salient self: social saliency effects based on self-bias. *J. Cogn. Psychol.* 27, 129–140. doi: 10.1080/20445911.2014.996156

Imbir, K., Jarymowicz, M., Spustek, T., Kuś, R., and Żygierewicz, J. (2015). Origin of emotional valence effects on ERP correlates of emotional word processing: the emotion duality approach. *PLoS One* 10:e0126129. doi: 10.1371/journal.pone.0126129

Ito, T., Larsen, J., Smith, N., and Cacioppo, J. (1998). Negative information weighs more heavily on the brain: the negativity bias in evaluative categorizations. *J. Pers. Soc. Psychol.* 75, 887–900. doi: 10.1037/0022-3514.75.4.887

Kissler, J., Herbert, C., Peyk, P., and Junghofer, M. (2007). Buzzwords: early cortical responses to emotional words during reading. *Psychol. Sci.* 18, 475–480. doi: 10.1111/j.1467-9280.2007.01924.x

Kissler, J., Herbert, C., Winkler, I., and Junghofer, M. (2009). Emotion and attention in visual word processing: an ERP study. *Biol. Psychol.* 80, 75–83. doi: 10.1016/j.biopsycho.2008.03.004

Kitayama, S., and Uskul, K. (2011). Culture, mind, and the brain: current evidence and future directions. *Annu. Rev. Psychol.* 62, 419–449. doi: 10.1146/annurev-psych-120709-145357

Li, S., Xu, K., Xu, Q., Xia, R., Ren, D., and Zhou, A. (2016). Positive bias in self-appraisals from friend's perspective: an event-related potential study. *Neuroreport* 27, 694–698. doi: 10.1097/WNR.0000000000000599

Liew, S., Ma, Y., Han, S., and Aziz-Zadeh, L. (2011). Who's afraid of the boss: cultural differences in social hierarchies modulate self-face recognition in chinese and americans. *PLoS One* 6:e16901. doi: 10.1371/journal.pone.0016901

Liu, M., He, X., Roststhein, P., and Sui, J. (2016). Dynamically orienting your own face facilitates the automatic attraction of attention. *Cogn. Neurosci.* 7, 37–44. doi: 10.1080/17588928.2015.1044428

Ma, Y., Bang, D., Wang, C., Allen, M., Frith, C., Roepstorff, A., et al. (2014). Sociocultural patterning of neural activity during self-reflection. *Soc. Cogn. Affect. Neurosci.* 9, 73–80. doi: 10.1093/scan/nss103

Macrae, C., Moran, J., Heatherton, T., Banfield, J., and Kelley, W. (2004). Medial prefrontal activity predicts memory for self. *Cereb. Cortex* 14, 647–654. doi: 10.1093/cercor/bhh025

Macrae, C., Visokomogilski, A., Golubickis, M., Cuningham, W., and Sahraie, A. (2017). Self-relevance prioritizes access to visual awareness. *J. Exp. Psychol. Hum. Percept. Perform.* 43, 438–443. doi: 10.1037/xhp0000361

Markus, H. R., and Kitayama, S. (1991). Culture and the self: implications for cognition, emotion, and motivation. *Psychol. Rev.* 98, 224–253. doi: 10.1037/0033-295X.98.2.224

Moran, J. M., Heatherton, T. F., and Kelley, W. M. (2009). Modulation of cortical midline structures by implicit and explicit self-relevance evaluation. *Soc. Neurosci.* 4, 197–211. doi: 10.1080/17470910802250519

Northoff, G., and Bermpohl, F. (2004). Cortical midline structures and the self. *Trends Cogn. Sci.* 8, 102–107. doi: 10.1016/j.tics.2004.01.004

Northoff, G., Heinzel, A., de Greck, M., Bermpohl, F., Dobrowolny, H., and Panksepp, J. (2006). Self-referential processing in our brain—A meta-analysis of imaging studies on the self. *Neuroimage* 31, 440–457. doi: 10.1016/j.neuroimage.2005.12.002

Park, J., and Kitayama, S. (2014). Interdependent selves show face-induced facilitation of error processing: cultural neuroscience of self-threat. *Soc. Cogn. Affect. Neurosci.* 9, 201–208. doi: 10.1093/scan/nss125

Qin, P., and Northoff, G. (2011). How is our self related to midline regions and the default-mode network? *Neuroimage* 57, 1221–1233. doi: 10.1016/j.neuroimage.2011.05.028

Rameson, L. T., Satpute, A. B., and Lieberman, M. D. (2010). The neural correlates of implicit and explicit self-relevant processing. *Neuroimage* 50, 701–708. doi: 10.1016/j.neuroimage.2009.12.098

Rozin, P., and Royzman, E. (2001). Negativity bias, negativity dominance, and contagion. *Pers. Soc. Psychol. Rev.* 5, 296–320. doi: 10.1207/s15327957pspr0504_2

Russell, J. (2003). Core affect and the psychological construction of emotion. *Psychol. Rev.* 110, 145–172. doi: 10.1037/0033-295x.110.1.145

Schäfer, S., Wentura, D., and Frings, C. (2015). Self-prioritization beyond perception. *Exp. Psychol.* 62, 415–425. doi: 10.1027/1618-3169/a000307

Schäfer, S., Wesslein, A., Spence, C., Wentura, D., and Frings, C. (2016). Self-prioritization in vision andition and touch. *Exp. Brain Res.* 234, 2141–2150. doi: 10.1007/s00221-016-4616-6

Scherer, K. R. (2005). What are emotions? And how can they be measured? *Soc. Sci. Inform.* 44, 695–729. doi: 10.1177/0539018405058216

Schindler, S., Wegrzyn, M., Steppacher, I., and Kissler, J. (2014). It's all in your head—how anticipating evaluation affects the processing of emotional trait adjectives. *Front. Psychol.* 5:1292. doi: 10.3389/fpsyg.2014.01292

Schupp, H. T., Flaisch, T., Stockburger, J., and Junghöfer, M. (2006). Emotion and attention: event-related brain potential studies. *Prog. Brain Res.* 156, 31–51. doi: 10.1016/s0079-6123(06)56002-9

Schupp, H. T., Stockburger, J., Codispoti, M., Junghöfer, M., Weike, A. I., and Hamm, A. O. (2007). Selective visual attention to emotion. *J. Neurosci.* 27, 1082–1089. doi: 10.1523/JNEUROSCI.3223-06.2007

Sui, J., Chechlacz, M., and Humphreys, G. (2012a). Dividing the self: distinct neural substrates of task-based and automatic self-prioritization after brain damage. *Cognition* 122, 150–162. doi: 10.1016/j.cognition.2011.10.008

Sui, J., He, X., and Humphreys, G. (2012b). Perceptual effects of social salience: evidence from self-prioritization effects on perceptual matching. *J. Exp. Psychol. Hum. Percept. Perform.* 38, 1105–1117. doi: 10.1037/a0029792

Sui, J., Hong, Y., Hong Liu, C., Humphreys, G. W., and Han, S. (2012c). Dynamic cultural modulation of neural responses to one's own and friend's faces. *Soc. Cogn. Affect. Neurosci.* 8, 326–332. doi: 10.1093/scan/nss001

Sui, J., Chechlacz, M., Rotshtein, P., and Humphreys, G. (2015). Lesion-symptom mapping of self-prioritization in explicit face categorization: distinguishing hypo- and hyper-self-biases. *Cereb. Cortex* 25, 374–383. doi: 10.1093/cercor/bht233

Sui, J., and Humphrey, G. (2015). The integrative self: how self-reference integrates perception and memory. *Trends Cogn. Sci.* 19, 719–728. doi: 10.1016/j.tics.2015.08.015

Sui, J., Liu, C., and Han, S. (2009). Cultural difference in neural mechanisms of self-recognition. *Soc. Neurosci.* 4, 402–411. doi: 10.1080/17470910802674825

Tacikowski, P., Cygan, H., and Nowicka, A. (2014). Neural correlates of own and close-other's name recognition: ERP evidence. *Front. Hum. Neurosci.* 8:194. doi: 10.3389/fnhum.2014.00194

Taylor, S. (1991). Asymmetrical effects of positive and negative events: the mobilization-minimization hypothesis. *Psychol. Bull.* 110, 67–85. doi: 10.1037/0033-2909.110.1.67

Wang, Y., Zhou, L., and Luo, Y. (2008). The pilot establishment and evaluation of Chinese affective words system. *Chin. Ment. Health J.* 22, 608–612. doi: 10.3321/j.issn:1000-6729.2008.08.014

Wu, L. L., Gu, R. L., Cai, H. J., Luo, Y. L. L., and Zhang, J. X. (2014). The neural response to maternal stimuli: an ERP study. *PLoS One* 9:e111391. doi: 10.1371/journal.pone.0111391

Yang, J., Dedovic, K., Guan, L., Chen, Y., and Qi, M. (2014a). Self-esteem modulates dorsal medial prefrontal cortical response to self-positivity bias in implicit self-relevant processing. *Soc. Cogn. Affect. Neurosci.* 9, 1814–1818. doi: 10.1093/scan/nst181

Yang, J., Qi, M., and Guan, L. (2014b). Self-esteem modulates the latency of P2 component in implicit self-relevant processing. *Biol. Psychol.* 97, 22–26. doi: 10.1016/j.biopsycho.2014.01.004

Yang, J., Guan, L., Dedovic, K., Qi, M., and Zhang, Q. (2012). The neural correlates of implicit self-relevant processing in low self-esteem: An ERP study. *Brain Res.* 1471, 75–80. doi: 10.1016/j.brainres.2012.06.033

Zhang, H., Guan, L., Qi, M., and Yang, J. (2013). Self-esteem modulates the time course of self-positivity bias in explicit self-evaluation. *PLoS One* 8:e81169. doi: 10.1371/journal.pone.0081169

Zhao, K., Wu, Q., Zimmer, H., and Fu, X. (2011). Electrophysiological correlates of visually processing subject's own name. *Neurosci. Lett.* 491, 143–147. doi: 10.1016/j.neulet.2011.01.025

Zhao, K., Yuan, J., Zhong, Y., Peng, Y., Chen, J., Zhou, L., et al. (2009). Event-related potential correlates of the collective self-relevant effect. *Neurosci. Lett.* 464, 57–61. doi: 10.1016/j.neulet.2009.07.017

Zhou, A., Li, S., Herbert, C., Xia, R., Xu, K., Xu, Q., et al. (2013). Perspective taking modulates positivity bias in self-appraisals: behavioral and event-related potential evidence. *Soc. Neurosci.* 8, 326–333. doi: 10.1080/17470919.2013.807873

Zinck, A. (2008). Self-referential emotions. *Conscious. Cogn.* 17, 496–505. doi: 10.1016/j.concog.2008.03.014

**Conflict of Interest Statement**: The authors declare that the research was conducted in the absence of any commercial or financial relationships that could be construed as a potential conflict of interest.

frontiers in Human Neuroscience

ORIGINAL RESEARCH
published: 31 October 2017
doi: 10.3389/fnhum.2017.00516

# The Role of Motivation in Cognitive Reappraisal for Depressed Patients

*Xiaoxia Wang*[1], *Xiaoyan Zhou*[2], *Qin Dai*[3], *Bing Ji*[4] *and Zhengzhi Feng*[5]*

[1] *Department of Basic Psychology, School of Psychology, Third Military Medical University, Chongqing, China,* [2] *Department of Clinical Psychology, Chongqing City Mental Health Center, Chongqing, China,* [3] *Department of Psychological Nursing, School of Nursing, Third Military Medical University, Chongqing, China,* [4] *Department of Radiology, Southwest Hospital, Third Military Medical University, Chongqing, China,* [5] *Department of Behavioral Medicine, School of Psychology, Third Military Medical University, Chongqing, China*

**Background:** People engage in emotion regulation in service of motive goals (typically, to approach a desired emotional goal or avoid an undesired emotional goal). However, how motives (goals) in emotion regulation operate to shape the regulation of emotion is rarely known. Furthermore, the modulatory role of motivation in the impaired reappraisal capacity and neural abnormalities typical of depressed patients is not clear. Our hypothesis was that (1) approach and avoidance motivation may modulate emotion regulation and the underlying neural substrates; (2) approach/avoidance motivation may modulate emotion regulation neural abnormalities in depressed patients.

**Methods:** Twelve drug-free depressed patients and fifteen matched healthy controls reappraised emotional pictures with approach/avoidant strategies and self-rated their emotional intensities during fMRI scans. Approach/avoidance motivation was measured using Behavioral Inhibition System and Behavioral Activation System (BIS/BAS) Scale. We conducted whole-brain analyses and correlation analyses of regions of interest to identify alterations in regulatory prefrontal-amygdala circuits which were modulated by motivation.

**Results:** Depressed patients had a higher level of BIS and lower levels of BAS-reward responsiveness and BAS-drive. BIS scores were positively correlated with depressive severity. We found the main effect of motivation as well as the interactive effect of motivation and group on the neural correlates of emotion regulation. Specifically, hypoactivation of IFG underlying the group differences in the motivation-related neural correlates during reappraisal may be partially explained by the interaction between group and reappraisal. Consistent with our prediction, dlPFC and vmPFC was differentially between groups which were modulated by motivation. Specifically, the avoidance motivation of depressed patients could predict the right dlPFC activation during decreasing positive emotion, while the approach motivation of normal individuals could predict the right vmPFC activation during decreasing negative emotion. Notably, striatal regions were observed when examining the neural substrates underlying the main effect of motivation (lentiform nucleus) and the interactive effect between motivation and group (midbrain).

OPEN ACCESS

***Edited by:***
*Xiaochu Zhang,*
*University of Science and Technology of China, China*

***Reviewed by:***
*Yuejia Luo,*
*Shenzhen University, China*
*Xu Lei,*
*Southwest University, China*

***Correspondence:**
*Zhengzhi Feng*
*fzz@tmmu.edu.cn*

***Received:*** *31 July 2017*
***Accepted:*** *11 October 2017*
***Published:*** *31 October 2017*

***Citation:***
*Wang X, Zhou X, Dai Q, Ji B and Feng Z (2017) The Role of Motivation in Cognitive Reappraisal for Depressed Patients. Front. Hum. Neurosci. 11:516. doi: 10.3389/fnhum.2017.00516*

**Conclusions:** Our findings highlight the modulatory role of approach and avoidance motivation in cognitive reappraisal, which is dysfunctional in depressed patients. The results could enlighten the CBT directed at modifying the motivation deficits in cognitive regulation of emotion.

**Keywords: cognitive reappraisal, major depressive disorder, model of the cognitive control of emotion (MCCE), behavioral inhibition system (BIS), behavioral activation system (BAS)**

## INTRODUCTION

Emotional disturbance figures prominently in major depressive disorder (MDD), with anhedonia and negative affect as key psycho-pathological dimensions. Emotional dysfunction predicts the severity of symptoms, non-response to antidepressant treatment and non-remission in depression (Vrieze et al., 2013). Theoretically, it is posited that compromises in cognitive control of emotion may be central to the psychopathology of major depression (Ressler and Mayberg, 2007; Disner et al., 2011). According to the integrated model of cognitive control of emotion (MCCE) (Ochsner et al., 2012), the most commonly studied exemplar of cognitive control of emotion is reappraisal, which is typically steered toward weakening or changing the emotional response to a stimulus by reinterpreting its semantic meaning. Recent functional neuroimaging studies have mapped the brain systems that support reappraisal of emotional stimuli, which increases activation in executive control regions and decreases activation in subcortical regions such as the amygdala (Kanske et al., 2012; Perlman et al., 2012; Dillon and Pizzagalli, 2013; Smoski et al., 2013). In MDD, instructed reappraisal strategies instantiate hyper-/hypoactivation in the prefrontal cortex, such as diminished activation of the dorsal lateral prefrontal cortex (dlPFC) (Erk et al., 2010); enhanced activation of the anterior cingulate (Beauregard et al., 2006), lateral orbitalfrontal cortex (Kanske et al., 2012), and right ventral medial prefrontal cortex (vmPFC) (Johnstone et al., 2007); and/or deficit in suppressing activation in limbic structures such as the amygdala and insula (Beauregard et al., 2006; Johnstone et al., 2007; Erk et al., 2010; Kanske et al., 2012), while the self-reported regulation success of depressed patients remains intact (Johnstone et al., 2007; Erk et al., 2010; Wang et al., 2014).

One explanation for the inconsistent neural findings pertaining to depression-related differences may be the diversity of emotion regulation strategies. This explanation could be evidenced by the fact of the divergence of prefrontal activations for other emotion regulation strategies, such as expression suppression (LPFC), distraction (parietal regions) and mindfulness (dlPFC/dmPFC) (Livingston et al., 2015; Morawetz et al., 2016). Even when reappraisal was concerned, different strategies of reappraisal such as reinterpretation (vlPFC) and distancing (parietal regions) recruited different prefrontal regions (Dörfel et al., 2014). Taken together, the previous literature review suggested that different emotion regulation strategies recruit both convergent and divergent activations in prefrontal regions (Morawetz et al., 2016).

Another explanation might be the confounding effects of motivation in emotion regulation. Theoretically, emotion regulation involves the pursuit of desired emotional goals in the service of hedonic or instrumental motives (Tamir, 2016). Hedonic motives include approach motivation steering toward appetitive stimuli and avoidance motivation directing away from aversive stimuli, which depend on two independent neurobiological systems—the behavioral activation system (BAS) and the behavioral inhibition system (BIS) (Corr, 2008). Previous evidence has supported the modulatory role of motivation in emotion regulation. BAS/BIS could bias higher-order cognitive control toward context-dependent regulation of emotion (Gray and Braver, 2002). Drive and fun-seeking (sub-dimensions of BAS) have demonstrated unique positive associations with adaptive ER (Tull et al., 2010). By contrast, strong BIS sensitivity and weak BAS-reward may predispose for difficulties regulating emotions, which in turn resulted in greater depression and other mental symptoms (Markarian et al., 2013).

Furthermore, hedonic motives may modulate the group differences in neural substrates of emotion regulation processes. Previous study suggested that depressed patients with higher BIS scores less recruited left ventral lateral PFC (vlPFC), a cognitive control region which was implicated in reappraisal for both groups. Depressed patients with higher BAS scores exhibited less signal change in amygdala during down regulation of their negative emotion. However, the similar relationships were not observed in healthy controls (Johnstone et al., 2007). Collectively, these results suggested that besides the motivation disposition deficits (heightened BIS levels and dampened BAS levels), the involvement of motivation in emotion regulation may differentiate between depressed vs. non-depressed individuals.

However, it remained to be tested whether BAS/BIS modulated cognitive control and emotion generation neural regions during other emotion regulation processes (e.g., up-regulation of positive/negative emotion, down-regulation of positive emotion). Typically, the participants in the reappraisal study were instructed to either increase ("enhance") or decrease ("suppress") the elicited emotional response. However, valence but not hedonic motives (approach/avoidance) are manipulated in such experiment context (Rottenberg, 2017). We proposed that motivation could be manipulated by distinguishing between approach-oriented (immersion) and avoidance-oriented (detachment) reappraisal. Thus in service

**Abbreviations:** MDD, Major depressive disorder; BIS/BAS Scale, BBS, Behavioral Inhibition System and Behavioral Activation System Scale; PCC, Posterior cingulate cortex; PHG, Para-hippocampal Gyrus; MTG, Middle Temporal Gyrus; STG, Superior Temporal Gyrus; ER, Emotion Regulation; IFG, Inferior frontal gyrus; vmPFC, Ventral medial frontal cortex; vlPFC, Ventral lateral frontal cortex; MCCE, Model of the cognitive control of emotion; dlPFC, Dorsal lateral prefrontal cortex.

of instrumental goals, the participants may be instructed to be psychologically distanced from the emotion stimuli to calm down (avoidant strategy), or immersed in the emotion context without approaching a solution (approach strategy) (Ayduk and Kross, 2010; Kross and Ayduk, 2011). In the experiment context, behavior is not always oriented toward the hedonic goals of momentary experience of pleasure or pain, but sometimes steering toward avoiding the positive and approaching the negative stimuli. Likewise, in daily life, behavior may be motivated toward maximizing pleasure and minimizing pain in the future (Higgins, 2012). Therefore, our first hypothesis was that approach/avoidance motivation differentially modulates reappraisal in depressed patients vs. normal healthy controls.

Due to widespread and interdependence of the neural networks of motivation and emotion regulation (Ernst and Fudge, 2009; Ernst, 2014), we mainly focused on those prefrontal-limbic regions which reliably distinguish between approach- and avoidance-oriented reappraisal (immersion/detachment). First, avoidance-oriented reappraisal (distancing) seems to recruit parietal regions which involve changing the perspective from which stimuli are understood and experienced (Ochsner et al., 2012). Approach-oriented reappraisal (immersion) selectively recruited left rostral medial prefrontal cortex (BA9/10) and posterior cingulate cortices which involve generating words that describe the emotional events (Ochsner et al., 2004). Second, ample evidence has indicated that hedonic motivates (BAS/BIS) predicted specific cognitive control abilities (Prabhakaran et al., 2011), and moderated activation in frontal cortex (e.g., MFG, dlPFC) associated with cognitive control (Spielberg et al., 2011, 2012; Bahlmann et al., 2015). More evidence also indicated that BIS modulates the amygdala/insula response (Reuter et al., 2004; Cunningham et al., 2010) and BAS correlates with ventral PFC and striatum activity in reaction to positive stimuli (appetitive pictures, monetary reward) (Beaver et al., 2006; Locke and Braver, 2008; Simon et al., 2010). Therefore, our second hypothesis was that these regions of interest (PFC, amygdala and striatum) may be differentially recruited between groups when taking covariates of BAS/BIS into consideration. The biased modulatory role of motivation underlying emotion regulation of depressed patients may not only help clarify the mechanism of emotion dysregulation of major depression, but also guide more personalized psychological intervention by addressing specific motivation deficits in MDD.

# MATERIALS AND METHODS

## Participants

Twelve currently drug-free, major depressed outpatients and 15 normal controls (MDD: male/female = 5/7; HC: male/female = 7/8) were recruited and evaluated by structured clinical interview for DSM-IV-TR Axis I (SCID I) (Lowe et al., 2004). The patients were screened via diagnoses from an experienced psychiatric clinician according to DSM-IV-TR. The recruited participants have had a major depressive episode, without history of neurological disease or presence of axis I psychiatric disorders, with no use of psychiatric medicine for at least 2 weeks. The healthy control group had no current or past axis I disorders and no first-degree family history of MDD, bipolar disorder, or schizophrenia. This study was approved by Ethics Committee of Third Military Medical University. The written consent form of each participant was obtained before they conducted the experiment.

## Materials

### Emotion Stimuli

Pictures of stimuli were selected from the International Affective Picture System (IAPS) (Lang et al., 2008) based on normative ratings and were matched for content of scenes and people (Table S1). Valence and arousal ratings of pictures in each session and each condition were kept homogeneous, with non-significant differences in an ANOVA (emotion × reappraisal) ($Ps > 0.05$) (Wang et al., 2014). Twenty-four trials (12/positive; 12/negative) were included in the "detach/immerse" condition, and 36 trials (12/positive; 12/negative; 12/neutral) were included in the "attend" condition. Therefore, the neutral pictures were only presented under the "attend" condition. A different set of affect arousing images was selected for the practice blocks to avoid confounding effects.

### BIS/BAS Scale

We adopted a revised Chinese version of the Behavioral Inhibition System and Behavioral Activation System Scale (BBS) immediately after the scan. This scale was confirmed to be reliable and valid among Chinese populations. The Cronbach α of the total scale and the BIS, BASR, BASD, and BASF subscales were respectively 0.70, 0.59, 0.72, 0.66, and 0.55. The four-factor model of the Chinese revised version of BBS was selected because the four-factor model indicated a better model fit ($AIC_{two\text{-}factor} < AIC_{four\text{-}factor}$, RMESA < 0.05, GFI, AGFI, IFI, CFI > 0.90) than the two-factor model (BIS, BAS) (RMESA = 0.082, GFI = 0.847, AGFI = 0.805, IFI = 0.613, CFI = 0.600, AIC = 445.620) (Li et al., 2008).

### Beck Depression Inventory (BDI)

BDI is the most widely used self-rating scale which is the revised version of BDI according to the DSM-IV. BDI consists of 21 items of emotional, cognitive, motivational and somatic symptoms, which are scored from 0 (symptom not present) to 3 (symptom very intense). The BDI had a 1-week test–retest reliability of $r = 0.93$ and an internal consistency $\alpha = 0.91$. Scores with 0–4 indicates normal, 5–7 mild depression, 8–15 moderate depression, and 16–63 severe depression (Beck et al., 1996).

### Zung Self-Rated Depression Scale (SDS)

SDS consists of 20 items of psychological and somatic symptoms, which are scored from 1 (a little of the time) to 4 (most of the time). SDS has a split-half reliability of 0.73 and internal consistencies ranging from 0.68 to 0.82. Scores greater than 50 indicate mild depression, greater than 60 indicate moderate depression, and greater than 70 indicate severe depression (Zung, 1986).

### Hamilton Depression Rating Scale (HAMD-24)

HAMD-24 is the most widely used interview scale to measure severity of depression in an inpatient population. Scores of

0–7 are considered normal, and scores greater than or equal to 20 indicate moderately severe depression (Hamilton, 1960; Williams, 2001).

## Experimental Procedure

Prior to the experiment, the participants practiced the three conditions with a different set of emotional pictures to become familiar with the task and emotion regulation strategies.

The task was performed in three consecutive blocks ("ATTEND," "DETACH," and "IMMERSE"). Block design was utilized to avoid potential task-switching effects that might obscure differences between regulation and passive viewing conditions (Moser et al., 2010). During the ATTEND block (as baseline condition), the subjects responded naturally without trying to change the emotional state elicited by the stimuli. During the DETACH block (avoidance-oriented reappraisal), participants were asked to interpret the situation depicted as fake or unreal, as would someone with no personal attachment to the events. During the IMMERSE block (approach-oriented reappraisal), subjects were asked to perceive each picture as real by imagining themselves or a loved one in the scene. The distinction between strategies (detach/immerse) was orthogonal within valence such that immersion was "good" for positive pictures and "bad" for negative ones, while detachment was "good" for negative pictures and "bad" for positive ones. The order of the other two blocks (DETACH/IMMERSE) was counterbalanced across participants. Within each block, the order of trials contributing to that block's 2 (ER) × 2 (emotion) design was randomized (Moser et al., 2010).

At the start of each block, a cue instruction was presented for 10 s. After a fixation period of 2 s, one of the twelve pictures used for each valence condition (positive/negative/ neutral) appeared for 8 s on the screen. Then, the participants pressed four buttons (within 4 s) with two fMRI compatible joysticks (SA-9800 E, http://www.sinorad.com/) connected to an E-prime 2.0 system (Psychology Software Tools, Sharpsburg, PA, USA), which registered their self-reported ratings of emotional intensity on a 4-point Likert scale (1 = barely not; 2 = weak; 3 = relatively strong; 4 = very strong). There was an 8-second break before the next trial to commence. The protocol for the paradigm was administered using the commercial software package E-Prime 2.0 (standard version). After scanning, the participants were asked to elaborate on the strategies used to confirm the effectiveness of emotion regulation.

## MRI Data Acquisition

MRI data were collected on a Siemens 3T Tim Trio MRI system (Erlangen, Germany). Sessions included an auto-align localizer, a T1-weighted MPRAGE structural image (slice thickness = 4 mm, field of view (FOV) = 240 × 240 × 240 $mm^3$, matrix = 256 × 256 × 256) and three functional sessions. Functional sequence was obtained with a time repetition (TR) of 2,000 ms, a flip angle of 90°, a time echo of 30 ms, an FOV of 240 × 240 $mm^2$, a matrix of 64 × 64, a slice thickness of 4 mm, and a slice interval of 0.8 mm. During scanning, visual stimuli were presented to the participants through the goggles mounted on the head coil.

## Data Analysis

### Behavioral Data

The magnitude of the emotion regulation effect was measured by the change in subjective emotion ratings between the "detach/immerse" and "view" conditions for each valence of emotion. The present study was an extension of our prior study, based on the published dataset (Wang et al., 2014). We compared the BBS subscales scores between groups by performing two independent sample *t*-tests using SPSS software (Version 19, SPSS Inc., Chicago, IL, USA). To rule out the possibility that group differences in the BBS subscale scores would be partially explained by gender effects (Knyazev et al., 2004), we performed a multivariate analysis of variance (MANOVA) to test whether the motivational scores differed across the groups and/or genders. To optimize the homogeneity of the samples, outliers over 3 standard deviations away from the mean were diagnosed and excluded, and we used box-plot methods and Cook's distance to detect outliers in SPSS.

### Functional MRI Data

All functional and structural image processing and statistical analyses were conducted with SPM8 (http://www.fil.ion.ucl.ac.uk/spm/software/spm8/). The first trial of each block (attend/detach/immerse condition) was discarded to reach the magnetization equilibrium. The remaining volumes were corrected for slice timing, and then realigned to the mean volume to correct for head motion. None of the participants had head motion exceeding 3 mm translation or 3° of rotation across all volumes. Images were spatially normalized to the standard MNI space using a 12-parameter affine transformation, and smoothed by convolution with a standard 8-mm full-width at half-maximum (FWHM) isotropic Gaussian kernel. The whole-brain voxel-wise analysis based on multiple linear regression model was used. Each condition was modeled using a box-car function convolved with a canonical hemodynamic response function (HRF). The realignment parameters were also included in the models as covariates of no interest.

First, to examine the group-related differences in emotion regulation, we conducted a between-group comparison of whole-brain activations under each ER condition. Second, to test the hypothesis that motivation dispositions differentially modulated reappraisal-related brain responses in two groups, we conducted a voxel-wise analysis of covariance (ANCOVA) with group, emotion and ER as between-subject factors and BIS/BAS subscale scores as covariates. The interactive effects between group and motivation, as well as the main effect of group on emotion regulation were examined. In addition, to examine the group-related differences in motivation, we conducted a two-sample *t*-test with the BIS/BAS scores as covariates. Third, for each group and each contrast (reappraisal vs. attend), we conducted a one-sample *t*-test by entering the BIS/BAS scores as covariates of interest to identify clusters that show a linear relationship with BIS/BAS scores. Finally, we examined the correlations between BIS/BAS scores and the time courses of a priori regions of interest (ROIs) (PFC/amygdala). Those neural correlates of motivation by group interaction across ER conditions (striatum, e.g., midbrain and lentiform nucleus) were also examined.

### *Definition of ROIs*

Based on previous neuroimaging studies on emotion regulation (Beauregard et al., 2006; Johnstone et al., 2007; Abler et al., 2010; Erk et al., 2010; Kanske et al., 2012), the following ROI criteria were identified for further analysis: bilateral dlPFC (BA9,46) and bilateral vmPFC (BA10,11,32,25). To produce the ROIs, we used masks derived from WFU PickAtlas software (version 3.0; ANSIR Laboratory, WFU School of Medicine, Winston-Salem, North Carolina) with a threshold of $p < 0.05$ and an extent threshold of 5 voxels. ROI time courses were extracted within anatomically pre-defined ROIs by generating the first eigenvariate of 8 mm around the peak voxels using the MATLAB package REX (Response Exploration) (Duff et al., 2007). A corrected threshold of $P < 0.01$ (two-tailed) for multiple comparison was derived from a combined threshold of $P < 0.05$ for each voxel and a cluster size of greater than 54 voxels using the AlphaSim program embedded in the REST software program (http://www.restfmri.net/forum/REST_V1.5). The parameters were as follows: single voxel $p < 0.01$, 1,000 iterations, FWHM = 4 mm, and a gray matter mask. We adjusted for multiple comparisons between Pearson correlations using Bonferroni correction, with a corrected threshold of $P < 0.003$ (=0.05/15).

# RESULTS

## Group Differences in Demographic and Clinical Variables

The two groups were matched for age (average age; MDD: 29.50 ± 8.46 SD; HC: 25.80 ± 5.89 SD) and education (average years; MDD: 14.00 ± 3.77; HC: 14.80 ± 2.83) ($P > 0.05$). The patient and control groups did not differ in terms of age, education level or gender ratio ($Ps > 0.05$). Significant differences were found in BDI and SDS scores between the two groups ($Ps < 0.05$). Average scores of BASD and BASR for the patient group were lower than those for the control group ($P = 0.036$ and 0.002), and the BIS score for the patient group was higher than that of the control group ($P = 0.049$). No significant group difference was detected with respect to BASF scores ($P > 0.05$) (**Table 1**).

The results showed that BIS, BASD and BASR differed between groups. Multivariate analysis of variance (MANOVA) revealed that the main effects of gender (Wilks' Lambda $F = 1.297$, $P = 0.305$, $\eta^2 = 0.305$) and gender-by-group interaction were not statistically significant (Wilks' Lambda $F = 1.160$, $P = 0.358$, $\eta^2 = 0.188$), thus ruling out the possibility that group differences in motivation dispositions would be partially explained by gender effects (**Table 2**).

### Relationship between BIS/BAS Scores and Depressive Severity

For the MDD group, BIS scores were positively correlated with BDI ($r = 0.860$, $P < 0.001$, $n = 12$). No statistically significant correlations between BIS scores and depressive symptoms were found for the control group ($Ps > 0.05$). No statistically significant correlations between BAS scores and depressive severity for both groups.

**TABLE 1 |** Group comparison of demographic, clinical, and neuropsychological variables.

| Variables | HC ($n = 15$) | MDD ($n = 12$) | *P*-value |
|---|---|---|---|
| | Mean ± SD | Mean ± SD | |
| Age | 25.80 ± 5.89 | 29.50 ± 8.46 | 0.088 |
| Education (years) | 14.80 ± 2.83 | 14.00 ± 3.77 | 0.094 |
| Gender ratio (M: F) | 7/8 | 5/7 | 0.841 |
| BDI | 4.27 ± 4.23 | 26.17 ± 12.65 | <0.001** |
| SDS | 36.54 ± 5.74 | 64.08 ± 12.60 | <0.001** |
| HAMD-24 | NA | 25.17 ± 5.18 | |
| Number of previous episodes | NA | 1 in 9/12 patients<br>2 in 2/12 patients<br>3 in 1/12 patients | |
| BIS | 14.87 ± 2.13 | 16.67 ± 2.39 | 0.049* |
| BASD | 12.53 ± 2.59 | 10.42 ± 2.31 | 0.036* |
| BASR | 14.53 ± 1.19 | 12.50 ± 1.93 | 0.002** |
| BASF | 14.80 ± 2.18 | 14.08 ± 1.62 | 0.352 |

*$P < 0.05$. **$P < 0.01$; NA, not applicable.

### Relationship between BIS/BAS Scores and Emotion (Regulation)

The emotion regulation effects were comparable between the two groups, which result was reported in the previous study (Wang et al., 2014). The correlations between BIS/BAS scores and emotion responding/regulation effects were analyzed. Positive association was observed in the control group between BAS-drive and negative affect (attend/negative vs. attend/neutral) ($r = 0.614$, $P = 0.024$, $n = 13$). However, this association was not observed in the MDD group ($P > 0.05$). The correlations between BIS/BAS and positive emotion, as well as between BIS/BAS and the emotion regulation effects (positive/detach; negative/detach; positive/immerse; negative/immerse) were not significant for both groups ($Ps > 0.05$).

## Functional MRI Data

### Group Differences in Neural Activation under Each Emotion Regulation Condition

For "detach-attend" contrasts of positive and negative stimuli, lower activations in the posterior cingulate (PCC) and para-hippocampal gyrus (PHG) and greater activations in the middle and superior temporal gyrus (MTG, STG) were found in depressed patients. For "immerse-attend" contrasts of positive and negative stimuli, similar results were observed in depressed patients (**Table 3**). Collectively, these results demonstrated that weaker PCC/PHG and stronger MTG/STG activations could be generalized across ER conditions for the MDD group.

### Group Effects on Motivation-Related Brain Responses Underlying Emotion Regulation

ANCOVA analysis revealed the left midbrain activation (MNI coordinates: −6, −32, 0, $Z = 2.82$, cluster size: 3,967) underlying the interactive effect between group and motivation. As for the group differences in motivation-related neural substrates during reappraisal, in addition to those regions with group differences (PCC, PHG, STG, MTG) without adjusting for

**TABLE 2 |** Gender effects on motivation disposition profiles.

| Variables | Group | Male ($\underline{x} \pm SD$) | Female ($\underline{x} \pm SD$) | Levene' s test | Box's *M*-test | Mean difference | Std. error | *P*-value |
|---|---|---|---|---|---|---|---|---|
| | | | | *P*-value | | | | |
| BIS | MDD | 17.00 ± 2.23 | 16.43 ± 2.64 | 0.197 | $p = 0.28$[a] | −0.26 | 0.90 | 0.775 |
| | HC | 14.29 ± 1.11 | 15.38 ± 2.72 | | | | | |
| BASD | MDD | 11.60 ± 2.07 | 9.57 ± 2.23 | 0.616 | | 1.85 | 0.93 | 0.058 |
| | HC | 13.43 ± 1.99 | 11.75 ± 2.92 | | | | | |
| BASR | MDD | 12.40 ± 1.34 | 12.57 ± 2.37 | 0.293 | | 0.08 | 0.63 | 0.896 |
| | HC | 14.71 ± 1.38 | 14.38 ± 1.06 | | | | | |
| BASF | MDD | 15.40 ± 0.89 | 13.14 ± 1.35 | 0.014* | | 1.05 | 0.73 | 0.165 |
| | HC | 14.71 ± 2.06 | 14.88 ± 2.42 | | | | | |

*$P < 0.05$. [a]Box's M test confirmed the equivalence of covariance matrices across levels of the independent variables.

BIS/BAS covariates under each condition (**Table 3**), additional regions such as the bilateral inferior frontal gyrus (IFG, BA45) and lentiform nucleus were also observed (**Table 4**). These results suggested that the IFG and lentiform nucleus may play an essential role in approach/avoidance motivation which differentiated the MDD group from the HC group. Specifically, across the "detach" and "immerse" conditions for the depressed patients, lower IFG (BA45) activation was modulated by BASD, BASR, and BIS scores; lower right lentiform nucleus activation was modulated by BASD and BIS scores; and greater left lentiform nucleus activation was modulated by BASF scores (**Table 4**).

Next, we examined the neural substrates underlying the main effect of motivation (IFG, lentiform nucleus) as well as the interactive effect between motivation and group (midbrain) under each ER condition. (1) **IFG**. Comparison of motivation-related neural correlates between groups under each ER condition did not yield significant IFG activation. For each group, no IFG activation was found under each ER condition. (2) **Lentiform nucleus**. Normal individuals exhibited more activation in lentiform nucleus under positive/detach and negative/detach conditions, which was modulated by BAS (BASR/BASF). Depressed patients demonstrated more activation in lentiform nucleus under positive/immerse and negative/immerse conditions, which was modulated by BIS. (3) **Midbrain**. Normal individuals exhibited more activation in midbrain under positive/detach and negative/detach conditions, which was modulated by BASR. Depressed patients demonstrated more activation in midbrain under positive/immerse and negative/immerse conditions, which was modulated by BASF and BASF/BIS respectively (Table S2).

## Motivation Dispositions Modulate Neural Responses ER-Related Regions of Interest in Each Group

### *PFC*

(1) For normal individuals, bilateral dlPFC (BA9) and vmPFC (BA10) were activated under the *Positive (detach-attend)* and *Negative (detach-attend)* conditions, which were modulated by BIS and BASD respectively. Control subjects also exhibited increased ventral lateral PFC (vlPFC) (BA47) activation modulated by BASR under the *Negative (detach-attend)* condition. (2) For depressed patients, left dlPFC (BA9) was activated under the *Negative (immerse-attend)* condition which was modulated by BASD (**Table 5**).

### *Midbrain and lentiform nucleus*

(1) For normal individuals, midbrain was activated (a) under the *Positive (detach-attend)*, *Positive (immerse-attend)* and *Negative (detach-attend)* conditions, which was modulated by BASD/BASR, and (b) under the *Negative (immerse-attend)* condition which was modulated by BIS. (2) For depressed patients, midbrain was activated under the *Negative (detach-attend)* condition, which was modulated by BASR. Additionally, depressed patients demonstrated enhanced lentiform nucleus activation under the *Negative (immerse-attend)* condition, which was modulated by BASD (**Table 5**).

### *Amygdala*

Under the *Positive* (*immerse-attend)* condition, depressed patients exhibited heightened activations in the right amygdala modulated by BASF (**Table 5**). The result complemented with our previous observation of enhanced right amygdala activation in this contrast (Wang et al., 2014). Furthermore, the Pearson correlation between the self-reported emotion enhancement effect and the neuroimaging signal change in the right amygdala under this condition was significant ($r = 0.594$, $P = 0.042$, $n = 12$) for the MDD group.

To obtain complementary evidence, we also computed the intensity of peak activation derived from functional ROIs under each condition, as well as the correlations between brain activations and BIS/BAS scores. Only significant correlations were reported here. (1) For depressed patients, right dlPFC (BA9; peak MNI coordinates: $x = 42$, $y = 22$, $z = 26$) activation was negatively modulated by BIS scores when they detached from positive emotional stimuli, and when we entered BDI scores as a predictor into the GLM, BIS, and BDI scores jointly predicted right dlPFC activation, with additional variance derived from depressive symptoms (from 31.3% to 59.6%) (**Table 6**). (2) For healthy controls, right vmPFC (BA10; peak MNI coordinates: $x = 14$, $y = 54$, $z = 2$) activation was positively modulated

**TABLE 3 |** Group differences in contrasts of "reappraisal" vs. "attend" of emotion.

| Region of activation | Side | BA | MNI Coordinates | | | *Z* score |
|---|---|---|---|---|---|---|
| | | | *x* | *y* | *z* | |
| **A. POSITIVE(DETACH-ATTEND)** | | | | | | |
| **MDD < control** | | | | | | |
| Posterior cingulate | R | 30 | 22 | −64 | 10 | 2.33 |
| **MDD > control** | | | | | | |
| Middle temporal gyrus | R | 19 | 42 | −60 | 18 | 3.02 |
| Superior temporal gyrus | L | 41 | −42 | −36 | 4 | 2.42 |
| **B. NEGATIVE(DETACH-ATTEND)** | | | | | | |
| **MDD < control** | | | | | | |
| Posterior cingulate | L | 30 | −22 | −62 | 8 | 3.06 |
| Parahippocampal gyrus | L | 19 | −26 | −50 | 0 | 2.72 |
| Posterior cingulate | R | 30 | 20 | −66 | 16 | 2.52 |
| Parahippocampal gyrus | R | 30 | 32 | −52 | 6 | 2.51 |
| **MDD > control** | | | | | | |
| Middle temporal gyrus | L | 22 | −52 | −46 | 2 | 2.13 |
| **C. POSITIVE(IMMERSE-ATTEND)** | | | | | | |
| **MDD < control** | | | | | | |
| Parahippocampal gyrus | R | 36 | 32 | −40 | −10 | 2.00 |
| Lingual gyrus | R | 18 | 14 | −82 | 6 | 1.70 |
| **MDD > control** | | | | | | |
| Superior temporal gyrus | L | 41 | −54 | −28 | 18 | 3.06 |
| Insula | L | 13 | −50 | −6 | 12 | 2.79 |
| Inferior parietal lobule | R | 40 | 56 | −28 | 22 | 2.07 |
| Caudate | R | | 20 | 2 | 24 | 2.31 |
| **D. NEGATIVE(IMMERSE-ATTEND)** | | | | | | |
| **MDD < control** | | | | | | |
| Parahippocampal gyrus | L | 36 | −26 | −44 | −10 | 2.71 |
| Parahippocampal gyrus | R | 37 | 36 | −44 | −14 | 1.72 |
| Lingual gyrus | R | 19 | 22 | −62 | −2 | 2.00 |
| **MDD > control** | | | | | | |
| Middle temporal gyrus | R | | 50 | −38 | −6 | 2.38 |
| Superior temporal gyrus | R | 21 | 54 | −26 | −8 | 1.98 |

*All clusters were thresholded at $P < 0.05$ and AlphaSim-corrected with an extent of at least 54 voxels.*

**TABLE 4 |** Motivation effects on group-dependent brain activities during reappraisal.

| Region of activation | Side | BA | MNI coordinates | | | Cluster size | *Z* score |
|---|---|---|---|---|---|---|---|
| | | | *x* | *y* | *z* | | |
| **A. BASD** | | | | | | | |
| **Control > MDD** | | | | | | | |
| Inferior frontal gyrus | L | 45 | −28 | 34 | −4 | | 2.16 |
| Posterior cingulate | R | 23 | 12 | −34 | 18 | | 2.56 |
| Posterior cingulate | L | 29 | −12 | −44 | 18 | 695 | 2.39 |
| Lentiform nucleus | R | | 22 | −20 | 2 | 87 | 2.28 |
| Parahippocampal gyrus | L | 36 | −28 | −34 | −10 | 196 | 2.1 |
| Middle temporal gyrus | L | 39 | −40 | −66 | 20 | 105 | 2.01 |
| Superior temporal gyrus | L | 39 | −48 | −54 | 16 | | 1.82 |
| **B. BASR** | | | | | | | |
| **Control > MDD** | | | | | | | |
| Inferior frontal gyrus | R | 45 | 46 | 22 | 10 | 55 | 2.02 |
| Parahippocampal gyrus | R | 19 | 42 | −46 | −8 | | 2.93 |
| Posterior cingulate | R | 30 | 28 | −70 | 10 | 361 | |
| Anterior cingulate | R | 32 | 14 | 40 | 14 | 72 | |
| **C. BASF** | | | | | | | |
| **Control > MDD** | | | | | | | |
| Posterior cingulate | L | 29 | 0 | −36 | −20 | 64 | 2.25 |
| Superior temporal gyrus | L | 13 | −50 | −46 | 24 | | 1.82 |
| **MDD > Control** | | | | | | | |
| Lentiform nucleus | L | | −28 | −8 | −2 | 93 | 2.12 |
| Midbrain | L | | −2 | −20 | −4 | 52 | 2.05 |
| Lentiform nucleus | R | | 30 | −8 | 2 | 42 | 1.82 |
| **D. BIS** | | | | | | | |
| **Control > MDD** | | | | | | | |
| Inferior frontal gyrus | L | 45 | −36 | 34 | 218 | | 2.29 |
| Lentiform nucleus | R | | 28 | 8 | 4 | 939 | 2.32 |

*The group-by-motivation interaction identified regions where BIS/BAS scores modulated brain responses differently between the depressed patients and the control group regardless of reappraisal conditions. All clusters were thresholded at $P < 0.05$ and AlphaSim-corrected with an extent of at least 54 voxels.*

by BASR scores in healthy controls when they detached from negative emotional stimuli (**Table 6**).

For depressed patients, BIS scores negatively predicted right dlPFC (BA9; peak MNI coordinates: $x = 42$, $y = 22$, $z = 26$) activation when they detached from positive emotional stimuli. For healthy controls, BASR scores positively predicted right vmPFC (BA10; peak MNI coordinates: $x = 14$, $y = 54$, $z = 2$) activation when they detached from negative emotional stimuli (**Figure 1**).

## DISCUSSION

The present study demonstrated the modulatory role of motivational dispositions during cognitive regulation of emotion, and the dysfunctional motivated regulation of emotion for major depressive disorder. Behaviorally, our results confirmed the approach and avoidance motivation deficits of MDD, with lower levels of BAS-reward responsiveness and BAS-drive and higher levels of BIS. Furthermore, BIS levels were related to the severity of depressive symptoms of MDD group. These results support the claim of BAS and BIS sensitivities as stable markers of mood disorders (Henriques and Davidson, 2000; Fletcher et al., 2013; Quilty et al., 2014). Specifically, higher BIS sensitivity may increase the avoidance goals and behaviors and amplify affective reactions to negative events (Gable et al., 2000) and is responsible for the excessive negative emotion observed in MDD. In contrast, lower BAS functioning may be associated with approach deficits which limit the access to positive emotion and rewarding experiences (Trew, 2011) and in turn lead to sustained

**TABLE 5 |** BIS/BAS modulated regions during reappraisal in healthy and depressed groups.

| Region of activation | Side | BA | MNI Coordinates | | | Cluster size | *Z* score |
|---|---|---|---|---|---|---|---|
| | | | *x* | *y* | *z* | | |
| **A. POSITIVE (DETACH-ATTEND)** | | | | | | | |
| **Control** | | | | | | | |
| [BIS] | | | | | | | |
| Inferior frontal gyrus | R | 47 | 46 | 22 | −28 | 188 | 2.86 |
| Middle frontal gyrus | R | 10 | 32 | 54 | −12 | 56 | 2.11 |
| [BASR] | | | | | | | |
| Inferior frontal gyrus | R | 47 | 26 | 32 | −14 | | 3.56 |
| Midbrain | R | | 4 | −12 | −20 | | 3.44 |
| [BASD] | | | | | | | |
| Midbrain | R | | 0 | −30 | −12 | 104 | 2.04 |
| **MDD** | | | | | | | |
| [BIS] | | | | | | | |
| Posterior cingulate | R | 23 | 14 | −58 | 16 | 1460 | 2.93 |
| Middle frontal gyrus | R | 9 | 42 | 22 | 26 | | 2.02 |
| **B. NEGATIVE (DETACH-ATTEND)** | | | | | | | |
| **Control** | | | | | | | |
| [BASD] | | | | | | | |
| Medial frontal gyrus | R | 10 | 6 | 56 | −4 | 107 | 2.90 |
| Anterior cingulate | L | 32 | −22 | 36 | 14 | 86 | 2.74 |
| Midbrain | R | | 4 | −24 | −16 | 96 | 2.66 |
| [BASR] | | | | | | | |
| Hippocampus | L | | −26 | −46 | 8 | 385 | 2.45 |
| Medial frontal gyrus | R | 10 | 14 | 54 | 2 | 74 | 2.36 |
| **MDD** | | | | | | | |
| [BASD] | | | | | | | |
| Middle frontal gyrus | L | 9 | −40 | 20 | 20 | | 2.59 |
| Middle frontal gyrus | R | 9 | 42 | 28 | 22 | | 2.32 |
| [BASR] | | | | | | | |
| Midbrain | L | | 0 | −18 | −6 | | 2.23 |
| Posterior cingulate | L | 30 | 0 | −62 | 14 | 88 | 2.20 |
| **C. POSITIVE (IMMERSE-ATTEND)** | | | | | | | |
| **Control** | | | | | | | |
| [BASD] | | | | | | | |
| Midbrain | R | | 4 | −24 | −16 | 96 | 2.66 |
| [BASR] | | | | | | | |
| Midbrain | R | | 6 | −24 | −14 | | 2.53 |
| Middle frontal gyrus | R | 46 | 42 | 34 | 8 | 113 | 2.42 |
| Cingulate gyrus | L | 24 | −6 | 4 | 24 | 110 | 2.36 |
| Amygdala | L | | −26 | −4 | −20 | 59 | 2.25 |
| [BASF] | | | | | | | |
| Middle frontal gyrus | R | 10 | 40 | 40 | −2 | 165 | 3.51 |
| Medial frontal gyrus | R | 10 | 22 | 52 | 2 | 89 | 2.46 |
| Medial frontal gyrus | R | 10 | 18 | 40 | −18 | 84 | 2.41 |
| **MDD** | | | | | | | |
| [BASD] | | | | | | | |
| Cingulate gyrus | R | 24 | 2 | −2 | 42 | 659 | 3.03 |
| [BASF] | | | | | | | |
| Amygdala | R | | 32 | −12 | −18 | | 2.02 |
| [BIS] | | | | | | | |
| Medial frontal gyrus | L | 9 | −20 | 44 | 18 | 160 | 2.36 |
| **D. NEGATIVE (IMMERSE-ATTEND)** | | | | | | | |
| **Control** | | | | | | | |
| [BIS] | | | | | | | |
| Midbrain | L | | −4 | −8 | −12 | 58 | 2.76 |
| **MDD** | | | | | | | |
| [BASD] | | | | | | | |
| Middle frontal gyrus | L | 9 | −42 | 18 | 28 | 11,221 | 4.39 |
| Lentiform nucleus | L | | −26 | −4 | 8 | | 4.05 |
| Inferior parietal lobule | R | 40 | 44 | −24 | 44 | 532 | 3.14 |

*A one-sample t-test for each group and for each condition was performed, and BIS/BAS scores were entered as covariates of interest, which yielded whole-brain activation. All clusters were thresholded at P < 0.05 and AlphaSim-corrected with an extent of at least 54 voxels.*

negative affect. Consistent with this assumption, lower BAS-drive are positively related to greater negative affect (compared to viewing neutral stimuli) in the control group. However, we did not find any other correlation between the BAS/BIS and positive/negative affect. Moreover, we did not find any significant association between motivation and ER effects, which was also not observed in the relevant study which examined the modulatory role of motivation in emotion regulation (Johnstone et al., 2007). Therefore, we further examined the modulatory role of motivation in the neural correlates of emotion regulation. Before that, abnormal neural substrates of emotion regulation were examined in depressed patients.

## Abnormal Neural Correlates of Emotion Regulation in Depressed Patients

Although stronger MTG and STG were activated during emotion regulation for the MDD group, MTG and STG were less modulated by BAS across ER conditions. The hypoactivation of MTG for clinical depression is consistently activated in fMRI cognitive reappraisal studies (Pico-Perez et al., 2017). Greater MTG activation of depressed patients may represent more resources devoted to lexical representation and retrieval (Huang et al., 2012), and processing emotionally laden negative stimuli (Paquette et al., 2003; Jessen and Kotz, 2015). STG is involved in reinterpretation of emotion stimuli (Pico-Perez et al., 2017). Thus stronger STG activation observed in depressed patients may reflect novelty detection (Dominguez-Borras et al., 2009) to visual stimuli with medium to high arousal (Mather et al., 2006). Therefore, enhanced MTG/STG activations less modulated by BAS-drive for the MDD group may reflect dysfunction in the goal-directed system.

Moreover, less PHG and PCC were activated during emotion regulation for the MDD group, while PHG and PCC were less modulated by BAS across ER conditions. The PHG and PCC were critical to emotion regulation. The PHG is implicated in the early appraisal and encoding of emotional significance during regulation of behavioral responses (Almeida et al., 2009). The PHG showed decreased activation during down-

**TABLE 6 |** Motivational dispositions Predict Reappraisal-related Brain Activity in functional ROIs.

| Group | Contrast | Brain region | BBS Subscales | Significance | Standard coefficients | Adjusted $R^2$ (*P*) |
|---|---|---|---|---|---|---|
| MDD | Positive (detach-attend) | R_dlPFC | BIS | 0.045** | −0.789 | 0.313 (0.164) |
| | | R_dlPFC | BIS | 0.002** | 1.561 | 0.596 (0.007) |
| | | | BDI | 0.003** | −1.532 | |
| HC | Negative (detach-attend) | R_vmPFC | BASR | 0.031** | 0.713 | 0.434 (0.043) |

*BIS/BAS scores were entered into a generalized linear regression model to predict reappraisal-related brain activation. Functional ROI time courses (beta values) under each condition in each group were generated by extracting the first eigenvariate of 8 mm around the peak voxels of respective clusters with no scaling, using a Matlab package REX (Response Exploration). BBS, BIS/BAS scale; L, left hemisphere; R, right hemisphere. **P < 0.01.*

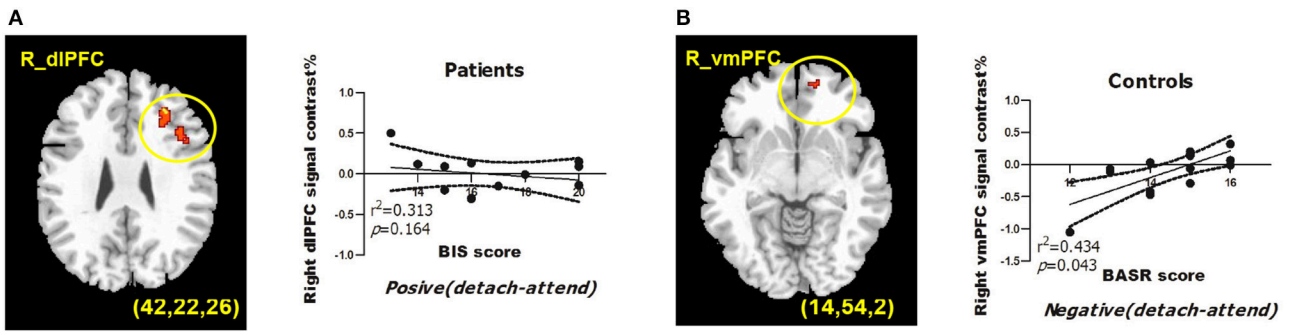


**FIGURE 1 |** BIS/BAS measures predict BOLD signals from regions of interests during reappraisal of emotions. **(A)** BIS scores predict right dlPFC activation under detach-positive condition for depressed patients. **(B)** BASR scores predict right vmPFC activation under detach-negative condition for healthy controls. MDD, depressed patient group; HC, healthy control group. The correlation coefficients and significance were indicated below each panel. All clusters survived the voxel-wise whole-brain analysis Alpha-sim corrected at $p < 0.05$ with an extent of at least 54 voxels.

and increased activation levels during upregulation of emotion (Frank et al., 2014). Our result was contradictory with previous observation of hyperactivation of the PHG during positive reappraisal (actively make a negative picture more positive) in depressed patients (Sheline et al., 2009). Hypoactivation of the PCC has been reliably reported in the cognitive reappraisal of depressed patients (Pico-Perez et al., 2017). PCC has strong reciprocal connections with parahippocampal cortices and plays an important role in successful retrieval of autobiographical memories (Maddock et al., 2001), which is critical to the deployment of successful self-focused reappraisal strategies. Therefore, the lack of recruitment of PCC may be related to deficits in approach motivation.

Overall, the approach motivation may be differentially involved in those neural regions implicated in different stages of emotion processing, which leads to biased early stage salience processing, semantic processing and self-relevant memory retrieval.

## Biased Modulatory Role of Motivation Underlying the Neural Correlates of Emotion Regulation

Both BAS and BIS sensitivity modulated the IFG (vlPFC, BA45) and lentiform nucleus differentially between groups during emotion regulation. Therefore, these two regions may be key regions implicated in the integration of motivation and emotion regulation.

### Prefrontal Regions

IFG hypoactivation of MDD group was observed for motivation-related neural correlates across ER conditions. First, our result supported the role of IFG in reappraisal, which region becomes more effective at supporting reappraisal with age (Belden et al., 2015). Abnormal function of IFG in reappraisal may exhibit in two ways: (1) less IFG activation was found in children with MDD history (Belden et al., 2015), which is aligned with our result. (2) Although comparable IFG activation was found in adult MDD patients, this region is not mediated by vmPFC to down regulate the amygdala activation (Johnstone et al., 2007). Second, our result did not yield the main effect of motivation (either across the ER conditions or under each ER condition) or the interactive effect between motivation and group on IFG activation. In contrast, our previous study support the role of the IFG as the interactive region of reappraisal and group (Wang et al., 2014).

Despite a higher level of avoidance motivation and its contradictory effect on right dlPFC activation, depressed patients still showed heightened right dlPFC activation during decreasing positive emotion. Our results echoed with the role of dlPFC as critical for distancing from emotions (Hutcherson et al., 2012) and modulating the vmPFC representation of the values assigned to stimuli. Therefore, the contradictory effect of avoidance motivation (increased BIS level and its negative correlation with dlPFC activation) and exaggerated activation in right dlPFC may explain the comparable self-reported ER effects between the two groups.

Heightened right vmPFC activation could partially be explained by greater appetitive motivation when healthy controls are detached from negative emotions. Previous evidence indicates the role of vmPFC in encoding emotional value during the experience and regulation of both positive and negative emotional stimuli (Winecoff et al., 2013) Heightened right vlPFC activation could partially be explained by biased approach and avoidance motivation when healthy controls are detached from positive emotions. The vlPFC plays an essential role in both increasing and decreasing emotion (Dörfel et al., 2014; Tupak et al., 2014). Our results extended previous findings that depressed patients with higher BIS tended to recruit the vlPFC to a less extent while decreasing negative emotion (Johnstone et al., 2007). Collectively, due to the evidence that prefrontally mediated cognitive control can either inhibit or augment reactions to achieve successful goal-directed behavior (Eippert et al., 2007), the altered prefrontal emotion regulatory network (dlPFC/vmPFC/vlPFC) in depressed patients demonstrated ineffective top-down modulation of emotion, as well as impaired modulatory role of approach/avoidance motivation in emotion regulation.

### Midbrain and Lentiform Nucleus

Striatal regions were observed when examining the neural substrates underlying the main effect of motivation (lentiform nucleus) and the interactive effect between motivation and group (midbrain). (1) Lentiform nucleus was differentially involved in emotion regulation process between HC and MDD group. Specifically, normal individuals recruited lentiform nucleus during the avoidance-oriented reappraisal which was modulated by BAS (BASR/BASF), while depressed patients recruited this region during approach-oriented reappraisal, which was modulated by BIS. Lentiform nucleus, part of the dorsal striatum, comprised of the globus pallidus and the putamen. Lentiform nucleus is involved in appetitive motivation and cognitive flexibility (Aarts et al., 2011; Fuentes-Claramonte et al., 2015), which function is intact in normal individuals even when they are required to be emotionally detached from the stimuli. In contrast, abnormal brain metabolism and gray matter volume of lentiform nucleus has been reported in MDD patients (Du et al., 2014; Su et al., 2014). Furthermore, heightened avoidance motivation of the MDD patients may hinder the effort to approach the stimuli and amplify the emotion responding. Accordingly, the hyperactivation of lentiform nucleus compared to normal controls during immersion was comprehensible because the lentiform nucleus is activated when MDD patients upregulated their negative emotion but not positive emotion. (2) The ventral tegmental area (VTA) which is the component of midbrain, play a role in receiving rewarding/aversive signals with motivation salience, and releasing dopamine into the ventral striatum, the amygdala and the prefrontal cortex.

### Amygdala

Under the immerse/positive condition, greater activation in the right amygdala was found in MDD patients, which was modulated by BAS-fun seeking. The right amygdala was activated when the individual was immersed in positive emotion (Wang et al., 2014), and the signal change of right amygdala reflected the regulation effect of positive emotion. Therefore, depressed patients might maintain relatively intact hedonic motivation (comparable BASF levels) and experiences (amygdala activation) of appetitive stimuli. This result extended previous evidence that patients with higher BAS failed to decrease amygdala activation (when down-regulating emotion) (Johnstone et al., 2007).

Collectively, these results suggest that aberrant motivational disposition is implicated in the emotion dysregulation model of depression. The current study has a few limitations. *First*, because of the small sample size, caution should be taken in drawing conclusions from the analyses of this sample. However, the agreement between the behavioral and neural patterns observed in this study and those reported in previous studies justify applying the results of this study to future research. *Second*, because the present study is correlational, a follow-up study is required to manipulate the approach/avoidance motivation underlying the neural substrates of emotion regulation. Nonetheless, the clinical implications of this study merit future exploration. The relationship between individual motivation disposition and emotion dysregulation of depressed patients may guide more personalized cognitive behavioral therapy (CBT) by addressing specific motivation deficits in MDD.

## AUTHOR CONTRIBUTIONS

XW conducted the experiment, analyzed the data and drafted the manuscript; QD revised the manuscript; XZ interpreted the data; BJ conducted the fMRI scanning; ZF designed the experiment.

## FUNDING

This research was financially supported by the Youth Cultivation Foundation of Medical Science (2016XPY08), National Natural Science Foundation of China (NSFC30970898, 31640036) and Key Project of the Applied Basic Research Programs for Military Mental Health (BWS14J029).

## ACKNOWLEDGMENTS

We gratefully acknowledge the invaluable assistance of Prof. Huaqing Meng (the First Affiliated Hospital of Chongqing Medical University, China) and Dr. Chenggang Jiang (Institute of Surgery Research of Daping Hospital, China) in patient recruitment. We would also like to thank Prof. Jinhui Wang for providing technical advice on fMRI data statistics and Chengju Liao, Yun Liu, and Liying Gan for their helpful comments regarding experimental design.

## SUPPLEMENTARY MATERIAL

The Supplementary Material for this article can be found online at: https://www.frontiersin.org/articles/10.3389/fnhum.2017.00516/full#supplementary-material

## REFERENCES


Aarts, E., van Holstein, M., and Cools, R. (2011). Striatal dopamine and the interface between motivation and cognition. *Front. Psychol.* 2:163. doi: 10.3389/fpsyg.2011.00163

Abler, B., Hofer, C., Walter, H., Erk, S., Hoffmann, H., Traue, H. C., et al. (2010). Habitual emotion regulation strategies and depressive symptoms in healthy subjects predict fMRI brain activation patterns related to major depression. *Psychiatry Res.* 183, 105–113. doi: 10.1016/j.pscychresns.2010.05.010

Almeida, J. R., Mechelli, A., Hassel, S., Versace, A., Kupfer, D. J., and Phillips, M. L. (2009). Abnormally increased effective connectivity between parahippocampal gyrus and ventromedial prefrontal regions during emotion labeling in bipolar disorder. *Psychiatry Res.* 174, 195–201. doi: 10.1016/j.pscychresns.2009.04.015

Ayduk, O., and Kross, E. (2010). From a distance: implications of spontaneous self-distancing for adaptive self-reflection. *J. Pers. Soc. Psychol.* 98, 809–829. doi: 10.1037/a0019205

Bahlmann, J., Aarts, E., and D'Esposito, M. (2015). Influence of motivation on control hierarchy in the human frontal cortex. *J. Neurosci.* 35, 3207–3217. doi: 10.1523/JNEUROSCI.2389-14.2015

Beauregard, M., Paquette, V., and Levesque, J. (2006). Dysfunction in the neural circuitry of emotional self-regulation in major depressive disorder. *Neuroreport* 17, 843–846. doi: 10.1097/01.wnr.0000220132.32091.9f

Beaver, J. D., Lawrence, A. D., van Ditzhuijzen, J., Davis, M. H., Woods, A., and Calder, A. J. (2006). Individual differences in reward drive predict neural responses to images of food. *J. Neurosci.* 26, 5160–5166. doi: 10.1523/JNEUROSCI.0350-06.2006

Beck, A. T., Steer, R. A., and Brown, G. K. (1996). *Manual of Beck Depression Inventory-II*. Washington, DC: American University.

Belden, A. C., Pagliaccio, D., Murphy, E. R., Luby, J. L., and Barch, D. M. (2015). Neural activation during cognitive emotion regulation in previously depressed compared to healthy children: evidence of specific alterations. *J. Am. Acad. Child Adolesc. Psychiatry* 54, 771–781. doi: 10.1016/j.jaac.2015.06.014

Corr, P. J. (2008). The reinforcement sensitivity theory of personality and psychopathology. *Int. J. Psychophysiol.* 69, 151–152. doi: 10.1016/j.ijpsycho.2008.05.377

Cunningham, W. A., Arbuckle, N. L., Jahn, A., Mowrer, S. M., and Abduljalil, A. M. (2010). Aspects of neuroticism and the amygdala: chronic tuning from motivational styles. *Neuropsychologia* 48, 3399–3404. doi: 10.1016/j.neuropsychologia.2010.06.026

Dillon, D. G., and Pizzagalli, D. A. (2013). Evidence of successful modulation of brain activation and subjective experience during reappraisal of negative emotion in unmedicated depression. *Psychiatry Res.* 212, 99–107. doi: 10.1016/j.pscychresns.2013.01.001

Disner, S. G., Beevers, C. G., Haigh, E. A., and Beck, A. T. (2011). Neural mechanisms of the cognitive model of depression. *Nat. Rev. Neurosci.* 12, 467–477. doi: 10.1038/nrn3027

Dominguez-Borras, J., Trautmann, S. A., Erhard, P., Fehr, T., Herrmann, M., and Escera, C. (2009). Emotional context enhances auditory novelty processing in superior temporal gyrus. *Cereb. Cortex* 19, 1521–1529. doi: 10.1093/cercor/bhn188

Dörfel, D., Lamke, J., Hummel, F., Wagner, U., Erk, S., and Walter, H. (2014). Common and differential neural networks of emotion regulation by detachment, reinterpretation, distraction, and expressive suppression: a comparative fMRI investigation. *NeuroImage* 101, 298–309. doi: 10.1016/j.neuroimage.2014.06.051

Du, M., Liu, J., Chen, Z., Huang, X., Li, J., Kuang, W., et al. (2014). Brain grey matter volume alterations in late-life depression. *J. Psychiatry Neurosci.* 39, 397–406. doi: 10.1503/jpn.130275

Duff, E. P., Cunnington, R., and Egan, G. F. (2007). REX: response exploration for neuroimaging datasets. *Neuroinformatics* 5, 223–234. doi: 10.1007/s12021-007-9001-y

Eippert, F., Veit, R., Weiskopf, N., Erb, M., Birbaumer, N., and Anders, S. (2007). Regulation of emotional responses elicited by threat-related stimuli. *Hum. Brain Mapp.* 28, 409–423. doi: 10.1002/hbm.20291

Erk, S., Mikschl, A., Stier, S., Ciaramidaro, A., Gapp, V., Weber, B., et al. (2010). Acute and sustained effects of cognitive emotion regulation in major depression. *J. Neurosci.* 30, 15726–15734. doi: 10.1523/JNEUROSCI.1856-10.2010

Ernst, M. (2014). The triadic model perspective for the study of adolescent motivated behavior. *Brain Cogn.* 89, 104–111. doi: 10.1016/j.bandc.2014.01.006

Ernst, M., and Fudge, J. L. (2009). A developmental neurobiological model of motivated behavior: anatomy, connectivity and ontogeny of the triadic nodes. *Neurosci. Biobehav. Rev.* 33, 367–382. doi: 10.1016/j.neubiorev.2008.10.009

Fletcher, K., Parker, G., and Manicavasagar, V. (2013). Behavioral Activation System (BAS) differences in bipolar I and II disorder. *J. Affect Disord.* 151, 121–128. doi: 10.1016/j.jad.2013.05.061

Frank, D. W., Dewitt, M., Hudgens-Haney, M., Schaeffer, D. J., Ball, B. H., Schwarz, N. F., et al. (2014). Emotion regulation: quantitative meta-analysis of functional activation and deactivation. *Neurosci. Biobehav. Rev.* 45, 202–211. doi: 10.1016/j.neubiorev.2014.06.010

Fuentes-Claramonte, P., Avila, C., Rodriguez-Pujadas, A., Ventura-Campos, N., Bustamante, J. C., Costumero, V., et al. (2015). Reward sensitivity modulates brain activity in the prefrontal cortex, ACC and striatum during task switching. *PLoS ONE* 10:e123073. doi: 10.1371/journal.pone.0123073

Gable, S. L., Reis, H. T., and Elliot, A. J. (2000). Behavioral activation and inhibition in everyday life. *J. Pers. Soc. Psychol.* 78, 1135–1149. doi: 10.1037/0022-3514.78.6.1135

Gray, J. R., and Braver, T. S. (2002). "Integration of emotion and cognitive control_A neurocomputational hypothesis of dynamic goal regulation," in *Emotional Cognition: From Brain to Behaviour. Advances in Consciousness Research*, eds S. C. Moore and M. Oaksford (Amsterdam: John Benjamins Publishing Company), 289–316. doi: 10.1075/aicr.44.12gra

Hamilton, M. (1960). A rating scale for depression. *J. Neurol. Neurosurg. Psychiatry* 23:56. doi: 10.1136/jnnp.23.1.56

Henriques, J. B., and Davidson, R. J. (2000). Decreased responsiveness to reward in depression. *Cogn. Emot.* 14, 711–724. doi: 10.1080/02699930050117684

Higgins, E. T. (2012). *Beyond Pleasure and Pain: How Motivation Works.* Oxford, UK: Oxford University Press.

Huang, J., Zhu, Z., Zhang, J. X., Wu, M., Chen, H., and Wang, S. (2012). The role of left inferior frontal gyrus in explicit and implicit semantic processing. *Brain Res.* 1440, 56–64. doi: 10.1016/j.brainres.2011.11.060

Hutcherson, C. A., Plassmann, H., Gross, J. J., and Rangel, A. (2012). Cognitive regulation during decision making shifts behavioral control between ventromedial and dorsolateral prefrontal value systems. *J. Neurosci.* 32, 13543–13554. doi: 10.1523/JNEUROSCI.6387-11.2012

Jessen, S., and Kotz, S. A. (2015). Affect differentially modulates brain activation in uni- and multisensory body-voice perception. *Neuropsychologia* 66, 134–143. doi: 10.1016/j.neuropsychologia.2014.10.038

Johnstone, T., van Reekum, C. M., Urry, H. L., Kalin, N. H., and Davidson, R. J. (2007). Failure to regulate: counterproductive recruitment of top-down prefrontal-subcortical circuitry in major depression. *J. Neurosci.* 27, 8877–8884. doi: 10.1523/JNEUROSCI.2063-07.2007

Kanske, P., Heissler, J., Schonfelder, S., and Wessa, M. (2012). Neural correlates of emotion regulation deficits in remitted depression: The influence of regulation strategy, habitual regulation use, and emotional valence. *Neuroimage* 61, 686–693. doi: 10.1016/j.neuroimage.2012.03.089

Knyazev, G. G., Slobodskaya, H. R., and Wilson, G. D. (2004). Comparison of the construct validity of the Gray–Wilson Personality Questionnaire and the BIS/BAS scales. *Pers. Individ. Diff.* 37, 1565–1582. doi: 10.1016/j.paid.2004.02.013

Kross, E., and Ayduk, O. (2011). Making meaning out of negative experiences by self-distancing. *Curr. Direct. Psychol. Sci.* 20, 187–191. doi: 10.1177/0963721411408883

Lang, P. J., Bradley, M. M., and Cuthbert, B. N. (2008). *International Affective Picture System (IAPS): Affective Ratings of Pictures and Instruction Manual.* Gainesville, FL: University of Florida.

Li, Y., Zhang, Y., Jiang, Y., Li, H., Mi, S., Yi, G., et al. (2008). The chinese version of the BIS/BAS scale: reliability and validity. *Chinese Mental Health J.* 22, 613–616. doi: 10.3321/j.issn:1000-6729.2008.08.015

Livingston, J. L., Kahn, L. E., and Berkman, E. T. (2015). *Motus Moderari: A Neuroscience-Informed Model for Self-Regulation of Emotion and Motivation.* New York, NY: Springer.

Locke, H. S., and Braver, T. S. (2008). Motivational influences on cognitive control: behavior, brain activation, and individual differences. *Cogn. Affect. Behav. Neurosci.* 8, 99–112. doi: 10.3758/CABN.8.1.99

Lowe, B., Spitzer, R. L., Grafe, K., Kroenke, K., Quenter, A., Zipfel, S., et al. (2004). Comparative validity of three screening questionnaires for DSM-IV depressive disorders and physicians' diagnoses. *J. Affect. Disord.* 78, 131–140. doi: 10.1016/S0165-0327(02)00237-9

Maddock, R. J., Garrett, A. S., and Buonocore, M. H. (2001). Remembering familiar people: the posterior cingulate cortex and autobiographical memory retrieval. *Neuroscience* 104, 667–676. doi: 10.1016/S0306-4522(01)00108-7

Markarian, S. A., Pickett, S. M., Deveson, D. F., and Kanona, B. B. (2013). A model of BIS/BAS sensitivity, emotion regulation difficulties, and depression, anxiety, and stress symptoms in relation to sleep quality. *Psychiatry Res.* 210, 281–286. doi: 10.1016/j.psychres.2013.06.004

Mather, M., Mitchell, K. J., Raye, C. L., Novak, D. L., Greene, E. J., and Johnson, M. K. (2006). Emotional arousal can impair feature binding in working memory. *J. Cogn. Neurosci.* 18, 614–625. doi: 10.1162/jocn.2006.18.4.614

Morawetz, C., Bode, S., Derntl, B., and Heekeren, H. R. (2016). The effect of strategies, goals and stimulus material on the neural mechanisms of emotion regulation: a meta-analysis of fMRI studies. *Neurosci. Biobehav. Rev.* 72, 111–128. doi: 10.1016/j.neubiorev.2016.11.014

Moser, J. S., Most, S. B., and Simons, R. F. (2010). Increasing negative emotions by reappraisal enhances subsequent cognitive control: a combined behavioral and electrophysiological study. *Cogn. Affect. Behav. Neurosci.* 10, 195–207. doi: 10.3758/CABN.10.2.195

Ochsner, K. N., Ray, R. D., Cooper, J. C., Robertson, E. R., Chopra, S., Gabrieli, J. D. E., et al. (2004). For better or for worse: neural systems supporting the cognitive down- and up-regulation of negative emotion. *NeuroImage* 53, 11–20. doi: 10.1016/j.neuroimage.2004.06.030

Ochsner, K. N., Silvers, J. A., and Buhle, J. T. (2012). Functional imaging studies of emotion regulation: a synthetic review and evolving model of the cognitive control of emotion. *Ann. N. Y. Acad. Sci.* 1251, E1–E24. doi: 10.1111/j.1749-6632.2012.06751.x

Paquette, V., Lévesque, J., Mensour, B., Leroux, J., Beaudoin, G., Bourgouin, P., et al. (2003). "Change the mind and you change the brain": effects of cognitive-behavioral therapy on the neural correlates of spider phobia. *NeuroImage* 18, 401–409. doi: 10.1016/S1053-8119(02)00030-7

Perlman, G., Simmons, A. N., Wu, J., Hahn, K. S., Tapert, S. F., Max, J. E., et al. (2012). Amygdala response and functional connectivity during emotion regulation: a study of 14 depressed adolescents. *J. Affect. Disord.* 139, 75–84. doi: 10.1016/j.jad.2012.01.044

Pico-Perez, M., Radua, J., Steward, T., Menchon, J. M., and Soriano-Mas, C. (2017). Emotion regulation in mood and anxiety disorders: A meta-analysis of fMRI cognitive reappraisal studies. *Prog. Neuropsychopharmacol. Biol. Psychiatry.* 79, 96–104. doi: 10.1016/j.pnpbp.2017.06.001

Prabhakaran, R., Kraemer, D. J. M., and Thompson-Schill, S. L. (2011). Approach, avoidance, and inhibition: personality traits predict cognitive control abilities. *Pers. Individ. Diff.* 51, 439–444. doi: 10.1016/j.paid.2011.04.009

Quilty, L. C., Mackew, L., and Bagby, R. M. (2014). Distinct profiles of behavioral inhibition and activation system sensitivity in unipolar vs. bipolar mood disorders. *Psychiatry Res.* 219, 228–231. doi: 10.1016/j.psychres.2014.05.007

Ressler, K. J., and Mayberg, H. S. (2007). Targeting abnormal neural circuits in mood and anxiety disorders: from the laboratory to the clinic. *Nat. Neurosci.* 10, 1116–1124. doi: 10.1038/nn1944

Reuter, M., Hennig, J., Stark, R., Walter, B., Kirsch, P., Schienle, A., et al. (2004). Personality and emotion: test of gray's personality theory by means of an fMRI study. *Behav. Neurosci.* 118, 462–469. doi: 10.1037/0735-7044.118.3.462

Rottenberg, J. (2017). Emotions in depression: what do we really know? *Annu. Rev. Clin. Psychol.* 13, 241–263. doi: 10.1146/annurev-clinpsy-032816-045252

Sheline, Y. I., Barch, D. M., Price, J. L., Rundle, M. M., Vaishnavi, S. N., Snyder, A. Z., et al. (2009). The default mode network and self-referential processes in depression. *Proc. Natl. Acad. Sci. U.S.A.* 106, 1942–1947. doi: 10.1073/pnas.0812686106

Simon, J. J., Walther, S., Fiebach, C. J., Friederich, H. C., Stippich, C., Weisbrod, M., et al. (2010). Neural reward processing is modulated by approach- and avoidance-related personality traits. *Neuroimage* 49, 1868–1874. doi: 10.1016/j.neuroimage.2009.09.016

Smoski, M. J., Keng, S. L., Schiller, C. E., Minkel, J., and Dichter, G. S. (2013). Neural mechanisms of cognitive reappraisal in remitted major depressive disorder. *J. Affect. Disord.* 151, 171–177. doi: 10.1016/j.jad.2013.05.073

Spielberg, J. M., Miller, G. A., Engels, A. S., Herrington, J. D., Sutton, B. P., Banich, M. T., et al. (2011). Trait approach and avoidance motivation: lateralized neural activity associated with executive function. *Neuroimage* 54, 661–670. doi: 10.1016/j.neuroimage.2010.08.037

Spielberg, J. M., Miller, G. A., Warren, S. L., Engels, A. S., Crocker, L. D., Banich, M. T., et al. (2012). A brain network instantiating approach and avoidance motivation. *Psychophysiology* 49, 1200–1214. doi: 10.1111/j.1469-8986.2012.01443.x

Su, L., Cai, Y., Xu, Y., Dutt, A., Shi, S., and Bramon, E. (2014). Cerebral metabolism in major depressive disorder: a voxel-based meta-analysis of positron emission tomography studies. *BMC Psychiatry* 14:321. doi: 10.1186/s12888-014-0321-9

Tamir, M. (2016). Why do people regulate their emotions? A taxonomy of motives in emotion regulation. *Pers. Soc. Psychol. Rev.* 20, 199–222. doi: 10.1177/1088868315586325

Trew, J. L. (2011). Exploring the roles of approach and avoidance in depression: an integrative model. *Clin. Psychol. Rev.* 31, 1156–1168. doi: 10.1016/j.cpr.2011.07.007

Tull, M. T., Gratz, K. L., Latzman, R. D., Kimbrel, N. A., and Lejuez, C. W. (2010). Reinforcement sensitivity theory and emotion regulation difficulties: a multimodal investigation. *Pers. Individ. Diff.* 49, 989–994. doi: 10.1016/j.paid.2010.08.010

Tupak, S. V., Dresler, T., Guhn, A., Ehlis, A., Fallgatter, A. J., Pauli, P., et al. (2014). Implicit emotion regulation in the presence of threat: Neural and autonomic correlates. *NeuroImage* 85, 372–379. doi: 10.1016/j.neuroimage.2013.09.066

Vrieze, E., Demyttenaere, K., Bruffaerts, R., Hermans, D., Pizzagalli, D. A., Sienaert, P., et al. (2013). Dimensions in major depressive disorder and their relevance for treatment outcome. *J. Affect. Disord.* 155, 35–41. doi: 10.1016/j.jad.2013.10.020

Wang, X., Feng, Z., Zhou, D., Lei, X., Liao, T., Zhang, L., et al. (2014). Dissociable self effects for emotion regulation: a study of chinese major depressive outpatients. *BioMed. Res. Int.* 2014, 1–11. doi: 10.1155/2014/408514

Williams, J. B. W. (2001). Standardizing the hamilton depression rating scale: past, present, and future. *Eur. Arch. Psychiatry Clin. Neurosci.* 251(Suppl. 2), I6. doi: 10.1007/BF03035120

Winecoff, A., Clithero, J. A., Carter, R. M., Bergman, S. R., Wang, L., and Huettel, S. A. (2013). Ventromedial prefrontal cortex encodes emotional value. *J. Neurosci.* 33, 11032–11039. doi: 10.1523/JNEUROSCI.4317-12.2013

Zung, W. W. K. (1986). *Zung Self-Rating Depression Scale and Depression Status Inventory*. Berlin; Heidelberg: Springer. doi: 10.1007/978-3-642-70486-4_21

**Conflict of Interest Statement:** The authors declare that the research was conducted in the absence of any commercial or financial relationships that could be construed as a potential conflict of interest.

frontiers in Human Neuroscience

REVIEW
published: 06 November 2017
doi: 10.3389/fnhum.2017.00526

# Recent Advances in Non-invasive Brain Stimulation for Major Depressive Disorder

*Shui Liu, Jiyao Sheng, Bingjin Li* and Xuewen Zhang**

*Jilin Provincial Key Laboratory on Molecular and Chemical Genetics, The Second Hospital of Jilin University, Changchun, China*

Non-invasive brain stimulation (NBS) is a promising treatment for major depressive disorder (MDD), which is an affective processing disorder involving abnormal emotional processing. Many studies have shown that repetitive transcranial magnetic stimulation (rTMS) and transcranial direct current stimulation (tDCS) over the prefrontal cortex can play a regulatory role in affective processing. Although the clinical efficacy of NBS in MDD has been demonstrated clinically, the precise mechanism of action remains unclear. Therefore, this review article summarizes the current status of NBS methods, including rTMS and tDCS, in the treatment of MDD. The article explores possible correlations between depressive symptoms and affective processing, highlighting the relevant affective processing mechanisms. Our review provides a reference for the safety and efficacy of NBS methods in the clinical treatment of MDD.

OPEN ACCESS

**Edited by:**
*Wenbo Luo,*
*Liaoning Normal University, China*

**Reviewed by:**
*Gianluca Serafini,*
*San Martino Hospital, University of Genoa, Italy*
*Yiqun Wang,*
*Fudan University, China*

***Correspondence:**
*Bingjin Li*
*libingjin@jlu.edu.cn*
*Xuewen Zhang*
*zhangxw@jlu.edu.cn*

**Received:** *19 August 2017*
**Accepted:** *18 October 2017*
**Published:** *06 November 2017*

**Citation:**
*Liu S, Sheng J, Li B and Zhang X (2017) Recent Advances in Non-invasive Brain Stimulation for Major Depressive Disorder. Front. Hum. Neurosci. 11:526. doi: 10.3389/fnhum.2017.00526*

**Keywords: non-invasive brain stimulation, repetitive transcranial magnetic stimulation, transcranial direct current stimulation, affective processing, major depressive disorder**

## INTRODUCTION

Major depressive disorder (MDD) is one of the most common and disabling mental disorders, and has become the second leading contributor to the global disease burden (Collins et al., 2011; Whiteford et al., 2013; Otte et al., 2016). MDD is characterized by maladaptive and persistent emotional responses to stressors (Groenewold et al., 2013). Because of its high incidence and common recurrence, MDD represents a serious challenge for world public health. Currently, approximately 1/3 of MDD patients globally exhibit treatment-resistant depression, because of invalid or ineffective antidepressant treatment (Rush et al., 2006).

Affective processing is crucial for the basic tasks of human survival and adaptation, involving many functions including perception, attention, learning, memory and responses to the environment (Narumoto et al., 2001; Garrett and Maddock, 2006; Del Piero et al., 2016). Dysfunctional affective processing is considered a key factor in the occurrence and development of many psychiatric disorders, including anxiety, schizophrenia and bipolar disorder (Anderson et al., 2017; Bocharov et al., 2017; Krakowski and Czobor, 2017; Wolkenstein et al., 2017). Previous studies have suggested that MDD is associated with dysfunctional processing in affective-related neural circuits (Clark et al., 2009). Meanwhile, cognitive abnormalities are also a core feature of depression, which involves many domains including attention, memory, executive functions and psychomotor speed (Gonda et al., 2015). Beck proposed a cognitive model of depression

**TABLE 1 |** Comparison between non-invasive brain stimulation (NBS) combined with antidepressants and individually NBS or antidepressants for major depressive disorder (MDD) in randomized controlled trials (RCTs).

| Experimental group | Control group | Sample size (N) | Subjects | Sessions duration and frequency (total sessions) | Stimulation site | Assessment | Main results | Reference |
|---|---|---|---|---|---|---|---|---|
| Active rTMS combined with paroxetine | Sham rTMS combined with paroxetine | 43 | Patients with first major depressive disorder | 10 Hz, 20 sessions for 4 weeks | left DLPFC | HAMD-24 | A significant improvement in the HAMD-24 after active rTMS combined with paroxetine vs. sham rTMS combined with paroxetine | Wang et al. (2017) |
| Active rTMS combined with escitalopram | Sham rTMS combined with escitalopram | 60 | Patients with first major depressive disorder | 10 Hz, 10 sessions for 2 weeks | DLPFC | HAMD-17, MADRS | A significant improvement in the HAMD-17 after active rTMS combined with escitalopram vs. other control groups | Huang et al. (2012) |
| Active tDCS combined with sertraline | Sham tDCS combined with sertraline; active tDCS combined with placebo; sham tDCS combined with placebo | 120 | Patients with major depressive disorder | 2 mA, 12 sessions for 6 weeks | DLPFC | HAMD-7, MADRS, BDI and CGI. | A significant improvement in the HAMD-7, MADRS, BDI and CGI after active rTMS combined with sertraline vs. other control groups | Brunoni et al. (2013) |
| Active rTMS combined with escitalopram | Sham-controlled rTMS combined with escitalopram | 45 | Patients with medication-resistant major depression | 8 Hz, 15 sessions for 3 weeks | Left DLPFC | HAMD-6, HAMD-17 and MES | A significant improvement in the HAMD-6 after active rTMS combined with escitalopram vs. the control group | Bretlau et al. (2008) |
| Active rTMS combination with amitriptyline | Sham-controlled rTMS combined with amitriptyline | 46 | Patients with non-psychotic depressive episode | 5 Hz, 20 sessions for 4 weeks | Left DLPFC | HAMD-17, MADRS, VAS and CGI | A significant improvement in the HAMD-17, MADRS, VAS and CGI after active rTMS combined with amitriptyline vs. the control group | Rumi et al. (2005) |
| Active rTMS combination with venlafaxine, sertraline or escitalopram | Sham rTMS combination with venlafaxine, sertraline or escitalopram | 99 | Patients with major depressive disorder | 15 Hz, 10 sessions for 2 weeks | Left DLPFC | HAMD | A significant improvement in the HAMD after active rTMS combined with antidepressants vs. other control groups | Rossini et al. (2005) |

*Abbreviation: HAM-D, Hamilton Depression Rating Scale; MES, Bech-Rafaelsen Melancholia scale; VAS, Visual Analog Scale; MARDS, Montgomery-Asberg depression rating scale; BDI, Beck Depression Inventory; CGI, Clinical Global Impression.*

**TABLE 2** | Comparison among rTMS, tDCS, ECT in the treatment of MDD.

| | Repetitive transcranial magnetic stimulation (rTMS) | Transcranial direct current stimulation (tDCS) | Modified electroconvulsive therapy (MECT) |
|---|---|---|---|
| Contraindications | Cochlear implants, brain stimulators or electrodes, aneurysm clips; implantable electronic devices (such as pacemakers, etc.), implantable defibrillator, a history of epilepsy, or the presence of a brain lesion (vascular, traumatic, neoplastic, infectious, or metabolic) | Implantable electronic devices (such as pacemakers, etc.), serious heart disease, acute large area of cerebral infarction, irritation area with hyperalgesia, increased intracranial pressure, pregnant women, vital signs instability, bleeding tendency patients | Implantable electronic devices (such as pacemakers, etc.), intracranial infections, intracranial tumors, intracranial metal, head trauma, serious heart disease, acute large area of cerebral infarction, irritation area with hyperalgesia, increased intracranial pressure, pregnant women, infants, vital signs instability, bleeding tendency of patients |
| Mechanism of action | The LTP-like and LTD-like effects of rTMS rely on NMDA receptor–mediated glutamatergic function | Modifying synaptic strength NMDA receptor-dependently or altering GABAergic activity (reduced) | Seizure induced changes in neurotransmitters, neuroplasticity and functional connectivity |
| Stimulation site and delivery parameters | High-frequency stimulation (10–20 Hz) over left DLPFC; low-frequency stimulation (≤1 Hz) over right DLPFC | Anodal stimulation over left DLPFC; cathodal stimulation over right DLPFC or right OFC (1–2 mA) | Bilateral treatments (both bitemporal and bifrontal) most often use 1.5–2.0 times seizure threshold (ST) and right unilateral 5–6 or even eight times ST |
| Side effects | Scalp pain during stimulation, transient headache, seizure induction, transient hearing loss | Redden of the skin, itching, burning, heat and tingling sensations at the stimulation site | Headache, muscle soreness, nausea and myalgia, cognitive impairment (such as retrograde amnesia) |
| Advantages | Non-invasive, lower cost | Non-invasive, portable, easy to use, long-acting, lowest cost | Most effective among three therapies |

in which negative stimuli in the environment can attract conscious or unconscious attention, and patients with depression tend to make negative evaluations of themselves and others, suggesting that depression might be caused by negative cognitive schemas (Disner et al., 2011). For example, hopelessness, manifested as overestimating the damage of a negative event and underestimating the positive outcome of the future, is thought to be an important cognitive risk factors of depression (Wang et al., 2015). Many behavioral studies have demonstrated that patients with MDD exhibit a negative emotional bias, manifesting as preferential processing of negative over positive stimuli, in accord with Beck's hypothesis (Erickson et al., 2005; Leyman et al., 2007; Yang et al., 2011). Strunk and Adler (2009) examined the relationship between depressive symptoms and bias, reporting that patients high in depressive symptoms exhibited significant pessimistic bias on three judgment tasks. The modern cognitive neuropsychological model of depression is a reformulation and expansion of Beck's cognitive model of depression, and the results are derived from pharmacological studies and concerning basic neurocognitive function. This model also proposes that patients with depression may develop an alteration in the bottom-up emotional stimulus processing, leading to negative perception (Roiser et al., 2012; Gonda et al., 2015).

Recent evidence suggests that negative affective and cognitive processing bias of MDD patients may originate from structural and functional abnormalities in specific brain regions, including the dorsolateral and ventral prefrontal cortex, hippocampus and amygdala, which are associated with affective processing (Campbell et al., 2004; Hamilton et al., 2008; Koenigs and Grafman, 2009). Numerous studies have demonstrated that the networks abnormality is one crucial mechanism in the occurrence and development of MDD, which underlies altered affective and cognitive processing, such as increased reactivity as well as increased attentional and cognitive bias towards negative stimuli in MDD (Hamilton et al., 2012; Groenewold et al., 2013). And the default mode network (DMN), the executive control network (ECN), and the salience network (SN) are three major networks in the recent studies of MDD. The DMN is involves in self-referential processing and episodic memory retrieval (Raichle et al., 2001). The ECN is involved in executive function and emotion regulation, with functional regions being the dorsolateral prefrontal cortex (DLPFC) and lateral posterior parietal regions (Miller and Cohen, 2001). The core regions in the SN include amygdala, and anterior hippocampus, which is involved in detection of, and direction of attention to, salient environmental stimuli (Chen and Etkin, 2013). Some studies revealed functional connectivity changes in the ECN and SN in depressed patients (Bonavita et al., 2017), which suggested the potential links between networks abnormality and depressive symptoms. Studies found that the enhancement of affective processing in MDD manifested excessive activation of the amygdala and supragenual cingulate of the brain (Matthews et al., 2008; Davey et al., 2011). In addition, the deficiency of cognitive control in MDD has demonstrated

the correlations with insufficient activity in the DLPFC and anterior cingulate gyrus (Holmes and Pizzagalli, 2008; McNeely et al., 2008). These findings suggest that during the affective processing of depressive individuals, networks abnormalities, manifested as enhanced affective processing and decreased cognitive control function, might result in a more intense experience of negative emotion, inducing depression.

Non-invasive brain stimulation (NBS) methods have been found to be effective for regulating human brain function, including transcranial magnetic stimulation (TMS), transcranial direct current stimulation (tDCS) and transcranial alternating current stimulation (tACS). In the past few decades, NBS techniques have been found to be useful for regulating healthy individual control of consciousness, and positive therapeutic effects have been reported for a range of psychiatric disorders, including depression, Alzheimer's disease, and epilepsy (Kuo et al., 2014; De Raedt et al., 2015). As NBS techniques develop, they have been applied in the clinical treatment of MDD, and the regulatory effects of NBS on affective processing have been consistently verified (Nitsche et al., 2012; Conson et al., 2015).

In the current review, we discuss the possible mechanisms by which NBS methods, including repetitive TMS (rTMS) and tDCS, improve depressive symptoms by modulating affective processing. Moreover, we examine research investigating the value of combining NBS with imaging techniques to improve antidepressant effects. Thus, this review article can provide a reference for the safety and efficacy of NBS methods in the clinical treatment of MDD.

# REPETITIVE TRANSCRANIAL MAGNETIC STIMULATION (rTMS)

## rTMS Overview

TMS is an NBS technique that was first created in 1985 by Brunoni et al. (Valero-Cabré et al., 2017). In TMS, electromagnetic induction is used to focus a current and modulate cortical function (Hallett, 2007). TMS devices consist of a capacitor to store charge and a stimulation coil to transfer energy. When the charge capacitor is rapidly released, the generated current passes through the stimulating coil to produce magnetic lines of flux with low resistance and no trauma, penetrating the skull to reach the cortex and reverse the current conduction in the cortex, thereby altering cortical excitability (Noda et al., 2015). rTMS is a new neurophysiological technique based on TMS, involving the delivery of repetitive stimuli at a specific cortical site. Previous studies have shown that low-frequency stimulation of rTMS ($\leq$1 Hz) can reduce the excitability of neurons and inhibit cortical activity, whereas high-frequency stimulation ($\geq$5 Hz) can increase the excitability of neurons and enhance cortical activity (Mitchell and Loo, 2006; Milev et al., 2016). To date, rTMS has been approved as a clinical therapy for MDD in several regions, including the USA, Canada the European Union (Tortella et al., 2014).

## Affective Processing-Related Mechanisms of rTMS in Antidepressant Treatment

Previous studies have indicated that multiple brain regions, including the amygdala, prefrontal cortex, parietal lobe and modality-specific sensory cortex regions, play distinct roles in regulating emotional processing (Dalgleish, 2004; Pessoa, 2017). The valence hypothesis proposes that affective processing exhibits hemispheric lateralization, with the right hemisphere specializing in negative emotion processing and the left hemisphere specializing in positive emotion processing (Prete et al., 2015). This hypothesis has been supported by neuroimaging studies (Grimm et al., 2008), and several previous studies have shown that the DLPFC influences emotional stimulus categorization, emotional evaluation, emotional memory, and emotional regulation (Brennan et al., 2017; Zilverstand et al., 2017). Thus, the DLPFC is thought to play a leading role in emotional control. Previous studies reported that activation of the left DLPFC is associated with processing positive emotions, whereas activation of the right DLPFC is thought to be responsible for processing negative emotions (Mondino et al., 2015). Schutter and van Honk (2005) found that, in patients with depression, left DLPFC responses were decreased and right DLPFC responses were increased.

rTMS is a relatively localized intervention, and several studies have examined its potential role in antidepressant treatment, with the DLPFC as a primary target (Lepping et al., 2014; Serafini et al., 2015; Carle et al., 2017; Carpenter et al., 2017). Two rTMS protocols are commonly used for treating MDD: high-frequency rTMS (10–20 Hz) targeting left DLPFC, and low-frequency rTMS ($\leq$1 Hz) targeting right DLPFC (Isenberg et al., 2005). Zwanzger et al. (2014) reported that inhibitory rTMS over the right DLPFC could improve and regulate affective processing, indicating that rTMS might exert an antidepressant role via affective processing-related mechanisms. A study of the role of frontal stimulation in emotional processing by Vanderhasselt et al. (2009) revealed that high-frequency rTMS applied to left DLPFC can improve task-switching abilities in depressed individuals. Moreover, clinical evidence has indicated that low-frequency rTMS over right DLPFC can increase response rates to monotherapy for MDD (Berlim et al., 2013b). These findings are consistent with the valence hypothesis, providing strong support for the notion that the antidepressant effects of rTMS involve the regulation of affective processing.

At the same time, some other brain regions associated with affective processing, including dorsomedial prefrontal cortex (DMPFC), frontopolar cortex (FPC), ventromedial prefrontal cortex (VMPFC), and ventrolateral prefrontal cortex (VLPFC), have been also considered as potential targets for clinical application of rTMS (Downar and Daskalakis, 2013; Junghofer et al., 2017). Of these, DMPFC received the most attention to date. Bakker et al. (2015) found that DMPFC-rTMS could show a similar antidepressant effect of DLPFC-rTMS in patients with MDD. Case series in MDD and bipolar disorder have provided initial evidence that DMPFC-rTMS may be safe, tolerable and effective in antidepressant treatment (Downar and Daskalakis, 2013; Downar et al., 2014). Nevertheless,

there is a need for more researches and clinical trials of DMPFC as a target for clinical application of rTMS in MDD.

## Combination of rTMS and Antidepressants in the Treatment of MDD

Previous studies have indicated that rTMS can lead to long-term and sustained remission of treatment-resistant MDD, significantly improving the quality of life and functional status of MDD patients (Galletly et al., 2016; Teng et al., 2017). Moreover, some studies have found that rTMS may improve antidepressant effect in combination with traditional antidepressants (**Table 1**). In a study by Wang et al. (2017), 43 patients with first-episode MDD were randomly divided into two groups. Subsequently, active or sham rTMS was applied to the left DLPFC, and a 4-week course of combination therapy with paroxetine was administered. The results indicated that patients in the active rTMS group had a higher response rate than those in the sham rTMS group at the end of the fourth week, and the remission rate in the experiment group was clearly elevated compared with the control group (Wang et al., 2017). These results suggest that rTMS might enhance the response of depressed patients to paroxetine, enhancing antidepressant efficacy. A double-blind clinical randomized controlled trial (RCT) by Huang et al. (2012) also confirmed the efficacy of rTMS in combination with conventional antidepressants in the treatment of depression. In their study, 60 patients with first-episode MDD were randomly categorized into two groups. In the first 2 weeks, patients in the two groups were treated with active or sham rTMS combined with escitalopram treatment, followed by another 2 weeks of escitalopram monotherapy. The results revealed that, compared with the control group, scores on the 17-item Hamilton Depression Rating Scale (HAMD-17) dropped more than 20% in the active rTMS group in the first 2 weeks. Furthermore, the active rTMS group exhibited a significantly faster score reduction compared with the sham group at 2 weeks, suggesting that rTMS had a synergistic effect in the treatment of MDD with traditional antidepressants.

## Comparison of rTMS and ECT in Antidepressant Treatment

Electroconvulsive therapy (ECT) has been used for the treatment of human diseases for more than 80 years, and is currently considered the most effective treatment for MDD (UK ECT Review Group, 2003). At present, the main technique used in clinical settings is modified ECT (MECT). This method involves the administration of anesthetics and muscle relaxants before treatment, so that the electrical stimulation does not cause convulsions, which in turn results in the elimination of muscle rigidity and tremor, as well as avoiding fracture, dislocation and other complications (Liu et al., 2016). Although ECT has been shown to be effective in the short term, its recurrence rate, particularly the high rate of early recurrence, and the cognitive side effects are important challenges in this form of antidepressant treatment (Jelovac et al., 2013; Fernie et al., 2014). A meta-analysis reported that despite continued drug treatment after ECT treatment, the relapse rates was 51.1% in the first year after treatment, peaking in the first 6 months, up to 37.7% (Jelovac et al., 2013).

There are clear differences in antidepressant mechanism, tolerance and acceptability between rTMS and ECT (**Table 2**). The antidepressant effects of rTMS and ECT in MDD have been compared in numerous studies (Möbius et al., 2017). Chen et al. (2017) conducted a meta-analysis including 25 clinical RCTs involving 1288 MDD patients. The findings revealed that the therapeutic effects of ECT were greater than those of rTMS, but right prefrontal-rTMS had the best tolerance. Jin et al. (2016) performed a retrospective study of 150 MDD patients receiving MECT and 150 MDD patients receiving rTMS, showing that in the short-term, the response rate in the MECT group was higher than that in the rTMS group, although there was no clear difference in long-term relapse-free survival between groups. Furthermore, the cost benefit of ECT was found to be higher than that of rTMS, and, because of its non-invasive and convenient features, as well as its minimal side effects relative to ECT, rTMS was favored by patients (Magnezi et al., 2016). Nevertheless, as an emerging treatment technology for antidepressant therapy, further in-depth clinical studies of rTMS are required before it becomes a widespread alternative to ECT.

## Disadvantages and Side Effects

The most common side effects of rTMS in clinical settings include headache (5%–23%) and discomfort at the stimulus site (20%–40%), and the most severe side effect is the induction of seizures (Machii et al., 2006; Maizey et al., 2013; Wall et al., 2014; Dobek et al., 2015; Boes et al., 2016). Prikryl and Kucerova (2005) reported a case of generalized tonic clonic seizure in a patient with MDD receiving rTMS. To date, fewer than 25 cases of rTMS-induced seizure have been reported worldwide. Therefore, high frequency rTMS is contraindicated in patients with a history of seizures, although the incidence rate is relatively low ($<$0.1%; Dobek et al., 2015).

# TRANSCRANIAL DIRECT CURRENT STIMULATION (tDCS)

## tDCS Overview

tDCS is an NBS method acting on specific cortical areas by producing a persistent, weak, direct current (usually 1–2 mA) through electrodes placed on the skull (Blumberger et al., 2015). The basic principle is that stimuli with different polarities can cause changes in the hyperpolarization or depolarization of the resting membrane potential. Anodic stimulation can improve the excitability of the cortex through the depolarization of the membrane potential, while cathodic stimulation can help reduce cortical excitability via hyperpolarization of neuronal membrane potentials (Stagg and Nitsche, 2011). Previous studies have indicated that the neurophysiological mechanisms of tDCS may involve subliminal regulation of the resting membrane potential of neurons inducing a polarity-dependent modification of

N-methyl-d-aspartate (NMDA) receptor function (Nitsche et al., 2003). Because NMDA receptor function is involved in synaptic plasticity formation, this can result in the production of neural remodeling and changes in the excitability of the cortex during stimulation (Nitsche et al., 2003). The stimulation of tDCS is weak, but it can also cause changes in cortical excitability, and the effect lasts longer after stimulation than that of rTMS. A previous study reported that following current stimulation of the body for several minutes, changes in cortical excitability can last for approximately 1 h after stimulation (Nitsche and Paulus, 2000). Meanwhile, compared with rTMS, tDCS has the advantages of portability, low equipment cost and minimal adverse reactions (Lefaucheur et al., 2017; **Table 2**).

## Affective Processing-Related Mechanisms of tDCS in Antidepressant Treatment

The DLPFC is one of the major brain areas involved in emotion regulation (Baeken et al., 2010), and various neuroimaging studies have indicated that it plays an important role in top-down regulation of affective processing (Disner et al., 2011). Some studies have suggested that DLPFC activity can be mediated by tDCS, thus playing a regulatory role in affective processing (Boggio et al., 2009; Sanchez et al., 2016). Single-session tDCS studies in healthy samples by Utz et al. (2010) revealed acute improvement in affective and cognitive processing. Further research has confirmed that the DLPFC plays an important role in the occurrence and development of depression (Schutter and van Honk, 2005). Imaging studies have also shown that left DLPFC cerebral blood flow and metabolism are decreased in patients with depression, while the right DLPFC exhibits increased metabolic activity (Shiozawa et al., 2015).

A number of studies have confirmed the role of tDCS in antidepressant treatment (Vigod et al., 2014; Al-Kaysi et al., 2017; Brennan et al., 2017). At present, the left and right DLPFC are typically used as anode and cathode stimulation sites for the majority of tDCS treatment methods, which can increase the excitability of the left DLPFC and inhibit the excitability of the right DLPFC to alleviate depressive symptoms (Meron et al., 2015). Through a double-blind RCT, Wolkenstein and Plewnia (2013) detected the effect of a single-session anodal tDCS targeting the left DLPFC in MDD patients, reporting a significant improvement in emotional cognitive control. This finding provided further evidence that tDCS might improve depressive symptoms by modulating emotional processing. Brunoni et al. (2011, 2013, 2014) conducted a double-blind RCT involving 24 depressive patients, and presented the emotional Stroop task, measuring response times (RTs) to positive-, negative-, and neutral-related words. The results revealed that active tDCS significantly modified negative attentional bias, abolishing the RT delay for negative words (Brunoni et al., 2014). This finding suggests that the regulatory effect of tDCS on affective processing might be an important mechanism underlying the antidepressant effects of the treatment method.

## Combination of tDCS and Antidepressants in the Treatment of MDD

Some studies have found that tDCS combined with traditional antidepressants might have a synergistic therapeutic effect (**Table 1**). Brunoni et al. (2011, 2013, 2014) conducted a double-blind RCT, dividing participants into four groups using pairwise combinations of sertraline/placebo and active/sham tDCS. When Montgomery-Asberg Depression Rating Scale (MADRS) scores were measured, the results revealed that combined treatment was significantly superior to placebo, tDCS only, and sertraline only. There was no significant difference in side effects between different modalities of intervention (Brunoni et al., 2013), indicating that the combination of tDCS and antidepressants in patients with MDD performed better than applying either treatment alone. These findings may provide a new direction for the widespread application of tDCS in MDD treatment.

## Disadvantages and Side Effects

According to the current safety guidelines of tDCS, the adverse effects are minimal for both healthy individuals and MDD patients, regardless of whether tDCS is applied to the motor areas or non-motor areas of the cortex. Reddening of the skin, heat, burning, itching, and tingling sensations at the stimulation site are the most common side effects of the treatment, and are reported by more than half of patients receiving tDCS (Brunoni et al., 2011; Shiozawa et al., 2014; Meron et al., 2015). Brunoni et al.'s (2011) systematic review of 117 studies conducted between 1998 and 2010 investigated the adverse effects of tDCS on the human brain, reporting that slight itching and tingling were the main adverse events, and that retention time was transient.

# PROSPECTS FOR NBS TECHNIQUES IN ANTIDEPRESSANT TREATMENT

The efficacy of NBS in treatment remains limited, even though its effectiveness in improving depressive symptoms in MDD patients has been consistently validated (McLoughlin et al., 2007; Berlim et al., 2013a; Lefaucheur et al., 2017). As a local brain stimulation technique, the therapeutic efficacy of NBS depends largely on the choice of stimulation sites and the accuracy of the location (Herbsman et al., 2009; Fox et al., 2012). Several previous studies have indicated that imaging-guided NBS could help to locate specific functional brain networks at a higher resolution. Using this approach, stimulation sites can be individually and accurately positioned according to anatomical differences of individual depressed patients, thereby improving the therapeutic effectiveness of NBS in antidepressant treatment, and supporting the extensive application of NBS approaches in the clinic (Mir-Moghtadaei et al., 2015; Luber et al., 2017).

Jha et al. (2016) examined the effects of a 4-week treatment regime in refractory MDD patients with single-photon emission computed tomography (SPECT) guided high-frequency rTMS and standard high-frequency rTMS. In

their experiment, subjects were assessed with the MADRS, the Beck Depression Inventory (BDI) and the Clinical Global Impression (CGI) scale. The response rate of the subjects in the brain SPECT guided group was found to be significantly higher than that in the standard group, on MADRS, BDI and CGI scores (Jha et al., 2016). These findings indicate that rTMS combined with brain SPECT targeting specific brain regions could improve antidepressant treatment in clinical settings.

An important topic for the future development of NBS is determining the combinations of imaging methods that provide optimal antidepressant treatment effects, to develop individualized treatment for MDD patients.

## LIMITATIONS

Several limits of this systematic review should be acknowledged. First, a common limitation to the research presented in this review is the widespread differences in measurement tools used to measure depressive symptoms and identify depression. A large number of different scales for measuring depressive symptoms were used across different studies, including the HAM-D, MES, VAS, MARDS, BDI and CGI, which may produce different amounts of measurement error in different samples depending on the population in which they are being used. Second, sample size of some RCTs in the review is relatively small. Finally, this review may be limited by reporting bias, the under-reporting of undesirable or non-significant experimental results. This may have leaded to lacking negative reports on the association between NBS and MDD, further weakening the evidence against a role of NBS in MDD.

## CONCLUSION

As an emerging non-invasive antidepressant treatment approach with few adverse reactions, NBS techniques have been extensively studied since their inception, and their clinical application in the treatment of MDD is increasing. Studies have indicated that the development of MDD may be closely related to abnormal affective processing (Harmer et al., 2009). Brunoni et al. (2014) found that one single active bi-frontal tDCS significantly modifies negative attentional bias in MDD. Other studies found that NBS including tDCS and rTMS can improved deficient cognitive control, further enhancing affective processing in MDD (Hoy et al., 2012; Wolkenstein and Plewnia, 2013). In a word, NBS may alleviate the symptoms of depression by regulating affective processing and enhancing cognitive control. As research progresses, it is likely that the antidepressant mechanisms of NBS will become more specific, the corresponding treatment effects will continue to improve, and its applications in MDD treatment will become more extensive.

## AUTHOR CONTRIBUTIONS

SL and JS wrote the manuscript. XZ and BL provided the critical revisions. All authors approved the final version of the manuscript for submission.

## ACKNOWLEDGMENTS

The work was supported by the Graduate Innovation Fund of Jilin University and Norman Bethune Program of Jilin University (2015212).

## REFERENCES

Al-Kaysi, A. M., Al-Ani, A., Loo, C. K., Powell, T. Y., Martin, D. M., Breakspear, M., et al. (2017). Predicting tDCS treatment outcomes of patients with major depressive disorder using automated EEG classification. *J. Affect. Disord.* 208, 597–603. doi: 10.1016/j.jad.2016.10.021

Anderson, N. E., Steele, V. R., Maurer, J. M., Rao, V., Koenigs, M. R., Decety, J., et al. (2017). Differentiating emotional processing and attention in psychopathy with functional neuroimaging. *Cogn. Affect. Behav. Neurosci.* 17, 491–515. doi: 10.3758/s13415-016-0493-5

Baeken, C., De Raedt, R., Van Schuerbeek, P., Vanderhasselt, M. A., De Mey, J., Bossuyt, A., et al. (2010). Right prefrontal HF-rTMS attenuates right amygdala processing of negatively valenced emotional stimuli in healthy females. *Behav. Brain Res.* 214, 450–455. doi: 10.1016/j.bbr.2010.06.029

Bakker, N., Shahab, S., Giacobbe, P., Blumberger, D. M., Daskalakis, Z. J., Kennedy, S. H., et al. (2015). rTMS of the dorsomedial prefrontal cortex for major depression: safety, tolerability, effectiveness, and outcome predictors for 10 Hz versus intermittent theta-burst stimulation. *Brain Stimul.* 8, 208–215. doi: 10.1016/j.brs.2014.11.002

Berlim, M. T., Van den Eynde, F., and Daskalakis, Z. J. (2013a). Efficacy and acceptability of high frequency repetitive transcranial magnetic stimulation (rTMS) versus electroconvulsive therapy (ECT) for major depression: a systematic review and meta-analysis of randomized trials. *Depress. Anxiety* 30, 614–623. doi: 10.1002/da.22060

Berlim, M. T., Van den Eynde, F., and Jeff Daskalakis, Z. (2013b). Clinically meaningful efficacy and acceptability of low-frequency repetitive transcranial magnetic stimulation (rTMS) for treating primary major depression: a meta-analysis of randomized, double-blind and sham-controlled trials. *Neuropsychopharmacology* 38, 543–551. doi: 10.1038/npp.2012.237

Blumberger, D. M., Hsu, J. H., and Daskalakis, Z. J. (2015). A review of brain stimulation treatments for late-life depression. *Curr. Treat. Options Psychiatry* 2, 413–421. doi: 10.1007/s40501-015-0059-0

Bocharov, A. V., Knyazev, G. G., and Savostyanov, A. N. (2017). Depression and implicit emotion processing: an EEG study. *Neurophysiol. Clin.* 47, 225–230. doi: 10.1016/j.neucli.2017.01.009

Boes, A. D., Stern, A. P., Bernstein, M., Hooker, J. E., Connor, A., Press, D. Z., et al. (2016). H-coil repetitive transcranial magnetic stimulation induced seizure in an adult with major depression: a case report. *Brain Stimul.* 9, 632–633. doi: 10.1016/j.brs.2016.04.013

Boggio, P. S., Zaghi, S., and Fregni, F. (2009). Modulation of emotions associated with images of human pain using anodal transcranial direct current stimulation (tDCS). *Neuropsychologia* 47, 212–217. doi: 10.1016/j.neuropsychologia.2008.07.022

Bonavita, S., Sacco, R., Esposito, S., d'Ambrosio, A., Della Corte, M., Corbo, D., et al. (2017). Default mode network changes in multiple sclerosis: a link between depression and cognitive impairment? *Eur. J. Neurol.* 24, 27–36. doi: 10.1111/ene.13112

Brennan, S., McLoughlin, D. M., O'Connell, R., Bogue, J., O'Connor, S., McHugh, C., et al. (2017). Anodal transcranial direct current stimulation of the left dorsolateral prefrontal cortex enhances emotion recognition in

depressed patients and controls. *J. Clin. Exp. Neuropsychol.* 39, 384–395. doi: 10.1080/13803395.2016.1230595

Bretlau, L. G., Lunde, M., Lindberg, L., Undén, M., Dissing, S., and Bech, P. (2008). Repetitive transcranial magnetic stimulation (rTMS) in combination with escitalopram in patients with treatment-resistant major depression: a double-blind, randomised, sham-controlled trial. *Pharmacopsychiatry* 41, 41–47. doi: 10.1055/s-2007-993210

Brunoni, A. R., Amadera, J., Berbel, B., Volz, M. S., Rizzerio, B. G., and Fregni, F. (2011). A systematic review on reporting and assessment of adverse effects associated with transcranial direct current stimulation. *Int. J. Neuropsychopharmacol.* 14, 1133–1145. doi: 10.1017/s1461145710001690

Brunoni, A. R., Valiengo, L., Baccaro, A., Zanão, T. A., de Oliveira, J. F., Goulart, A., et al. (2013). The sertraline vs. electrical current therapy for treating depression clinical study: results from a factorial, randomized, controlled trial. *JAMA Psychiatry* 70, 383–391. doi: 10.1001/2013.jamapsychiatry.32

Brunoni, A. R., Zanao, T. A., Vanderhasselt, M. A., Valiengo, L., de Oliveira, J. F., Boggio, P. S., et al. (2014). Enhancement of affective processing induced by bifrontal transcranial direct current stimulation in patients with major depression. *Neuromodulation* 17, 138–142. doi: 10.1111/ner.12080

Campbell, S., Marriott, M., Nahmias, C., and MacQueen, G. M. (2004). Lower hippocampal volume in patients suffering from depression: a meta-analysis. *Am. J. Psychiatry* 161, 598–607. doi: 10.1176/appi.ajp.161.4.598

Carle, G., Touat, M., Bruno, N., Galanaud, D., Peretti, C. S., Valero-Cabré, A., et al. (2017). Acute frontal lobe dysfunction following prefrontal low-frequency repetitive transcranial magnetic stimulation in a patient with treatment-resistant depression. *Front. Psychiatry* 8:96. doi: 10.3389/fpsyt.2017.00096

Carpenter, L. L., Aaronson, S. T., Clarke, G. N., Holtzheimer, P. E., Johnson, C. W., McDonald, W. M., et al. (2017). rTMS with a two-coil array: safety and efficacy for treatment resistant major depressive disorder. *Brain Stimul.* 10, 926–933. doi: 10.1016/j.brs.2017.06.003

Chen, A. C., and Etkin, A. (2013). Hippocampal network connectivity and activation differentiates post-traumatic stress disorder from generalized anxiety disorder. *Neuropsychopharmacology* 38, 1889–1898. doi: 10.1038/npp.2013.122

Chen, J. J., Zhao, L. B., Liu, Y. Y., Fan, S. H., and Xie, P. (2017). Comparative efficacy and acceptability of electroconvulsive therapy versus repetitive transcranial magnetic stimulation for major depression: a systematic review and multiple-treatments meta-analysis. *Behav. Brain Res.* 320, 30–36. doi: 10.1016/j.bbr.2016.11.028

Clark, L., Chamberlain, S. R., and Sahakian, B. J. (2009). Neurocognitive mechanisms in depression: implications for treatment. *Annu. Rev. Neurosci.* 32, 57–74. doi: 10.1146/annurev.neuro.31.060407.125618

Collins, P. Y., Patel, V., Joestl, S. S., March, D., Insel, T. R., Daar, A. S., et al. (2011). Grand challenges in global mental health. *Nature* 475, 27–30. doi: 10.1038/475027a

Conson, M., Errico, D., Mazzarella, E., Giordano, M., Grossi, D., and Trojano, L. (2015). Transcranial electrical stimulation over dorsolateral prefrontal cortex modulates processing of social cognitive and affective information. *PLoS One* 10:e0126448. doi: 10.1371/journal.pone.0126448

Dalgleish, T. (2004). The emotional brain. *Nat. Rev. Neurosci.* 5, 583–589. doi: 10.1038/nrn1432

Davey, C. G., Allen, N. B., Harrison, B. J., and Yücel, M. (2011). Increased amygdala response to positive social feedback in young people with major depressive disorder. *Biol. Psychiatry* 69, 734–741. doi: 10.1016/j.biopsych.2010.12.004

Del Piero, L. B., Saxbe, D. E., and Margolin, G. (2016). Basic emotion processing and the adolescent brain: task demands, analytic approaches, and trajectories of changes. *Dev. Cogn. Neurosci.* 19, 174–189. doi: 10.1016/j.dcn.2016.03.005

De Raedt, R., Vanderhasselt, M. A., and Baeken, C. (2015). Neurostimulation as an intervention for treatment resistant depression: from research on mechanisms towards targeted neurocognitive strategies. *Clin. Psychol. Rev.* 41, 61–69. doi: 10.1016/j.cpr.2014.10.006

Disner, S. G., Beevers, C. G., Haigh, E. A., and Beck, A. T. (2011). Neural mechanisms of the cognitive model of depression. *Nat. Rev. Neurosci.* 12, 467–477. doi: 10.1038/nrn3027

Dobek, C. E., Blumberger, D. M., Downar, J., Daskalakis, Z. J., and Vila-Rodriguez, F. (2015). Risk of seizures in transcranial magnetic stimulation: a clinical review to inform consent process focused on bupropion. *Neuropsychiatr. Dis. Treat.* 11, 2975–2987. doi: 10.2147/ndt.s91126

Downar, J., and Daskalakis, Z. J. (2013). New targets for rTMS in depression: a review of convergent evidence. *Brain Stimul.* 6, 231–240. doi: 10.1016/j.brs.2012.08.006

Downar, J., Geraci, J., Salomons, T. V., Dunlop, K., Wheeler, S., McAndrews, M. P., et al. (2014). Anhedonia and reward-circuit connectivity distinguish nonresponders from responders to dorsomedial prefrontal repetitive transcranial magnetic stimulation in major depression. *Biol. Psychiatry* 76, 176–185. doi: 10.1016/j.biopsych.2013.10.026

Erickson, K., Drevets, W. C., Clark, L., Cannon, D. M., Bain, E. E., Zarate, C. A., et al. (2005). Mood-congruent bias in affective go/no-go performance of unmedicated patients with major depressive disorder. *Am. J. Psychiatry* 162, 2171–2173. doi: 10.1176/appi.ajp.162.11.2171

Fernie, G., Bennett, D. M., Currie, J., Perrin, J. S., and Reid, I. C. (2014). Detecting objective and subjective cognitive effects of electroconvulsive therapy: intensity, duration and test utility in a large clinical sample. *Psychol. Med.* 44, 2985–2994. doi: 10.1017/s0033291714000658

Fox, M. D., Buckner, R. L., White, M. P., Greicius, M. D., and Pascual-Leone, A. (2012). Efficacy of transcranial magnetic stimulation targets for depression is related to intrinsic functional connectivity with the subgenual cingulate. *Biol. Psychiatry* 72, 595–603. doi: 10.1016/j.biopsych.2012.04.028

Galletly, C., Gill, S., Rigby, A., Carnell, B. L., and Clarke, P. (2016). Assessing the effects of repetitive transcranial magnetic stimulation on cognition in major depressive disorder using computerized cognitive testing. *J. ECT* 32, 169–173. doi: 10.1097/yct.0000000000000308

Garrett, A. S., and Maddock, R. J. (2006). Separating subjective emotion from the perception of emotion-inducing stimuli: an fMRI study. *Neuroimage* 33, 263–274. doi: 10.1016/j.neuroimage.2006.05.024

Gonda, X., Pompili, M., Serafini, G., Carvalho, A. F., Rihmer, Z., and Dome, P. (2015). The role of cognitive dysfunction in the symptoms and remission from depression. *Ann. Gen. Psychiatry* 14:27. doi: 10.1186/s12991-015-0068-9

Grimm, S., Beck, J., Schuepbach, D., Hell, D., Boesiger, P., Bermpohl, F., et al. (2008). Imbalance between left and right dorsolateral prefrontal cortex in major depression is linked to negative emotional judgment: an fMRI study in severe major depressive disorder. *Biol. Psychiatry* 63, 369–376. doi: 10.1016/j.biopsych.2007.05.033

Groenewold, N. A., Opmeer, E. M., de Jonge, P., Aleman, A., and Costafreda, S. G. (2013). Emotional valence modulates brain functional abnormalities in depression: evidence from a meta-analysis of fMRI studies. *Neurosci. Biobehav. Rev.* 37, 152–163. doi: 10.1016/j.neubiorev.2012.11.015

Hallett, M. (2007). Transcranial magnetic stimulation: a primer. *Neuron* 55, 187–199. doi: 10.1016/j.neuron.2007.06.026

Hamilton, J. P., Etkin, A., Furman, D. J., Lemus, M. G., Johnson, R. F., and Gotlib, I. H. (2012). Functional neuroimaging of major depressive disorder: a meta-analysis and new integration of base line activation and neural response data. *Am. J. Psychiatry* 169, 693–703. doi: 10.1176/appi.ajp.2012.11071105

Hamilton, J. P., Siemer, M., and Gotlib, I. H. (2008). Amygdala volume in major depressive disorder: a meta-analysis of magnetic resonance imaging studies. *Mol. Psychiatry* 13, 993–1000. doi: 10.1038/mp.2008.57

Harmer, C. J., Goodwin, G. M., and Cowen, P. J. (2009). Why do antidepressants take so long to work? A cognitive neuropsychological model of antidepressant drug action. *Br. J. Psychiatry* 195, 102–108. doi: 10.1192/bjp.bp.108.051193

Herbsman, T., Avery, D., Ramsey, D., Holtzheimer, P., Wadjik, C., Hardaway, F., et al. (2009). More lateral and anterior prefrontal coil location is associated with better repetitive transcranial magnetic stimulation antidepressant response. *Biol. Psychiatry* 66, 509–515. doi: 10.1016/j.biopsych.2009.04.034

Holmes, A. J., and Pizzagalli, D. A. (2008). Response conflict and frontocingulate dysfunction in unmedicated participants with major depression. *Neuropsychologia* 46, 2904–2913. doi: 10.1016/j.neuropsychologia.2008.05.028

Hoy, K. E., Segrave, R. A., Daskalakis, Z. J., and Fitzgerald, P. B. (2012). Investigating the relationship between cognitive change and antidepressant response following rTMS: a large scale retrospective study. *Brain Stimul.* 5, 539–546. doi: 10.1016/j.brs.2011.08.010

Huang, M. L., Luo, B. Y., Hu, J. B., Wang, S. S., Zhou, W. H., Wei, N., et al. (2012). Repetitive transcranial magnetic stimulation in combination with citalopram

in young patients with first-episode major depressive disorder: a double-blind, randomized, sham-controlled trial. *Aust. N Z J. Psychiatry* 46, 257–264. doi: 10.1177/0004867411433216

Isenberg, K., Downs, D., Pierce, K., Svarakic, D., Garcia, K., Jarvis, M., et al. (2005). Low frequency rTMS stimulation of the right frontal cortex is as effective as high frequency rTMS stimulation of the left frontal cortex for antidepressant-free, treatment-resistant depressed patients. *Ann. Clin. Psychiatry* 17, 153–159. doi: 10.1080/10401230591002110

Jelovac, A., Kolshus, E., and McLoughlin, D. M. (2013). Relapse following successful electroconvulsive therapy for major depression: a meta-analysis. *Neuropsychopharmacology* 38, 2467–2474. doi: 10.1038/npp.2013.149

Jha, S., Chadda, R. K., Kumar, N., and Bal, C. S. (2016). Brain SPECT guided repetitive transcranial magnetic stimulation (rTMS) in treatment resistant major depressive disorder. *Asian J. Psychiatr.* 21, 1–6. doi: 10.1016/j.ajp.2016.02.003

Jin, X. L., Xu, W. Q., Le, Y. J., and Dai, X. K. (2016). Long-term effectiveness of modified electroconvulsive therapy compared with repetitive transcranial magnetic stimulation for the treatment of recurrent major depressive disorder. *J. Nerv. Ment. Dis.* 204, 479–482. doi: 10.1097/nmd.0000000000000493

Junghofer, M., Winker, C., Rehbein, M. A., and Sabatinelli, D. (2017). Noninvasive stimulation of the ventromedial prefrontal cortex enhances pleasant scene processing. *Cereb. Cortex* 27, 3449–3456. doi: 10.1093/cercor/bhx073

Koenigs, M., and Grafman, J. (2009). The functional neuroanatomy of depression: distinct roles for ventromedial and dorsolateral prefrontal cortex. *Behav. Brain Res.* 201, 239–243. doi: 10.1016/j.bbr.2009.03.004

Krakowski, M. I., and Czobor, P. (2017). Proneness to aggression and its inhibition in schizophrenia: interconnections between personality traits, cognitive function and emotional processing. *Schizophr. Res.* 184, 82–87. doi: 10.1016/j.schres.2016.11.038

Kuo, M. F., Paulus, W., and Nitsche, M. A. (2014). Therapeutic effects of non-invasive brain stimulation with direct currents (tDCS) in neuropsychiatric diseases. *Neuroimage* 85, 948–960. doi: 10.1016/j.neuroimage.2013.05.117

Lefaucheur, J. P., Antal, A., Ayache, S. S., Benninger, D. H., Brunelin, J., Cogiamanian, F., et al. (2017). Evidence-based guidelines on the therapeutic use of transcranial direct current stimulation (tDCS). *Clin. Neurophysiol.* 128, 56–92. doi: 10.1016/j.clinph.2016.10.087

Lepping, P., Schönfeldt-Lecuona, C., Sambhi, R. S., Lanka, S. V., Lane, S., Whittington, R., et al. (2014). A systematic review of the clinical relevance of repetitive transcranial magnetic stimulation. *Acta Psychiatr. Scand.* 130, 326–341. doi: 10.1111/acps.12276

Leyman, L., De Raedt, R., Schacht, R., and Koster, E. H. (2007). Attentional biases for angry faces in unipolar depression. *Psychol. Med.* 37, 393–402. doi: 10.1017/s003329170600910x

Liu, C. C., Qian, X. Y., An, J. X., Yu, Z. L., Wu, J. P., Wen, H., et al. (2016). Electroconvulsive therapy under general anesthesia with cisatracurium, laryngeal mask airways, and bispectral index. *J. ECT* 32, 17–19. doi: 10.1097/yct.0000000000000251

Luber, B. M., Davis, S., Bernhardt, E., Neacsiu, A., Kwapil, L., Lisanby, S. H., et al. (2017). Using neuroimaging to individualize TMS treatment for depression: toward a new paradigm for imaging-guided intervention. *Neuroimage* 148, 1–7. doi: 10.1016/j.neuroimage.2016.12.083

Machii, K., Cohen, D., Ramos-Estebanez, C., and Pascual-Leone, A. (2006). Safety of rTMS to non-motor cortical areas in healthy participants and patients. *Clin. Neurophysiol.* 117, 455–471. doi: 10.1016/j.clinph.2005.10.014

Magnezi, R., Aminov, E., Shmuel, D., Dreifuss, M., and Dannon, P. (2016). Comparison between neurostimulation techniques repetitive transcranial magnetic stimulation vs. electroconvulsive therapy for the treatment of resistant depression: patient preference and cost-effectiveness. *Patient Prefer. Adherence* 10, 1481–1487. doi: 10.2147/ppa.s105654

Maizey, L., Allen, C. P., Dervinis, M., Verbruggen, F., Varnava, A., Kozlov, M., et al. (2013). Comparative incidence rates of mild adverse effects to transcranial magnetic stimulation. *Clin. Neurophysiol.* 124, 536–544. doi: 10.1016/j.clinph.2012.07.024

Matthews, S. C., Strigo, I. A., Simmons, A. N., Yang, T. T., and Paulus, M. P. (2008). Decreased functional coupling of the amygdala and supragenual cingulate is related to increased depression in unmedicated individuals with current major depressive disorder. *J. Affect. Disord.* 111, 13–20. doi: 10.1016/j.jad.2008.05.022

McLoughlin, D. M., Mogg, A., Eranti, S., Pluck, G., Purvis, R., Edwards, D., et al. (2007). The clinical effectiveness and cost of repetitive transcranial magnetic stimulation versus electroconvulsive therapy in severe depression: a multicentre pragmatic randomised controlled trial and economic analysis. *Health Technol. Assess.* 11, 1–54. doi: 10.3310/hta11240

McNeely, H. E., Lau, M. A., Christensen, B. K., and Alain, C. (2008). Neurophysiological evidence of cognitive inhibition anomalies in persons with major depressive disorder. *Clin. Neurophysiol.* 119, 1578–1589. doi: 10.1016/j.clinph.2008.03.031

Meron, D., Hedger, N., Garner, M., and Baldwin, D. S. (2015). Transcranial direct current stimulation (tDCS) in the treatment of depression: systematic review and meta-analysis of efficacy and tolerability. *Neurosci. Biobehav. Rev.* 57, 46–62. doi: 10.1016/j.neubiorev.2015.07.012

Milev, R. V., Giacobbe, P., Kennedy, S. H., Blumberger, D. M., Daskalakis, Z. J., Downar, J., et al. (2016). Canadian network for mood and anxiety treatments (CANMAT) 2016 Clinical guidelines for the management of adults with major depressive disorder: section 4. Neurostimulation treatments. *Can. J. Psychiatry* 61, 561–575. doi: 10.1177/0706743716660033

Miller, E. K., and Cohen, J. D. (2001). An integrative theory of prefrontal cortex function. *Annu. Rev. Neurosci.* 24, 167–202. doi: 10.1146/annurev.neuro.24.1.167

Mir-Moghtadaei, A., Caballero, R., Fried, P., Fox, M. D., Lee, K., Giacobbe, P., et al. (2015). Concordance between beamF3 and MRI-neuronavigated target sites for repetitive transcranial magnetic stimulation of the left dorsolateral prefrontal cortex. *Brain Stimul.* 8, 965–973. doi: 10.1016/j.brs.2015.05.008

Mitchell, P. B., and Loo, C. K. (2006). Transcranial magnetic stimulation for depression. *Aust. N Z J. Psychiatry* 40, 406–413. doi: 10.1080/j.1440-1614.2006.01816.x

Möbius, M., Lacomblé, L., Meyer, T., Schutter, D. J. L. G., Gielkens, T., Becker, E. S., et al. (2017). Repetitive transcranial magnetic stimulation modulates the impact of a negative mood induction. *Soc. Cogn. Affect. Neurosci.* 12, 526–533. doi: 10.1093/scan/nsw180

Mondino, M., Thiffault, F., and Fecteau, S. (2015). Does non-invasive brain stimulation applied over the dorsolateral prefrontal cortex non-specifically influence mood and emotional processing in healthy individuals? *Front. Cell. Neurosci.* 9:399. doi: 10.3389/fncel.2015.00399

Narumoto, J., Okada, T., Sadato, N., Fukui, K., and Yonekura, Y. (2001). Attention to emotion modulates fMRI activity in human right superior temporal sulcus. *Cogn. Brain Res.* 12, 225–231. doi: 10.1016/s0926-6410(01)00053-2

Nitsche, M. A., Fricke, K., Henschke, U., Schlitterlau, A., Liebetanz, D., Lang, N., et al. (2003). Pharmacological modulation of cortical excitability shifts induced by transcranial direct current stimulation in humans. *J. Physiol.* 553, 293–301. doi: 10.1113/jphysiol.2003.049916

Nitsche, M. A., Koschack, J., Pohlers, H., Hullemann, S., Paulus, W., and Happe, S. (2012). Effects of frontal transcranial direct current stimulation on emotional state and processing in healthy humans. *Front. Psychiatry* 3:58. doi: 10.3389/fpsyt.2012.00058

Nitsche, M. A., and Paulus, W. (2000). Excitability changes induced in the human motor cortex by weak transcranial direct current stimulation. *J. Physiol.* 527, 633–639. doi: 10.1111/j.1469-7793.2000.t01-1-00633.x

Noda, Y., Silverstein, W. K., Barr, M. S., Vila-Rodriguez, F., Downar, J., Rajji, T. K., et al. (2015). Neurobiological mechanisms of repetitive transcranial magnetic stimulation of the dorsolateral prefrontal cortex in depression: a systematic review. *Psychol. Med.* 45, 3411–3432. doi: 10.1017/s0033291715001609

Otte, C., Gold, S. M., Penninx, B. W., Pariante, C. M., Etkin, A., Fava, M., et al. (2016). Major depressive disorder. *Nat. Rev. Dis. Primers* 2:16065. doi: 10.1038/nrdp.2016.65

Pessoa, L. (2017). A network model of the emotional brain. *Trends Cogn. Sci.* 21, 357–371. doi: 10.1016/j.tics.2017.03.002

Prete, G., Laeng, B., Fabri, M., Foschi, N., and Tommasi, L. (2015). Right hemisphere or valence hypothesis, or both? The processing of hybrid faces in the intact and callosotomized brain. *Neuropsychologia* 68, 94–106. doi: 10.1016/j.neuropsychologia.2015.01.002

Prikryl, R., and Kucerova, H. (2005). Occurrence of epileptic paroxysm during repetitive transcranial magnetic stimulation treatment. *J. Psychopharmacol.* 19:313. doi: 10.1177/0269881105051545

Raichle, M. E., MacLeod, A. M., Snyder, A. Z., Powers, W. J., Gusnard, D. A., and Shulman, G. L. (2001). A default mode of brain function. *Proc. Natl. Acad. Sci. U S A* 98, 676–682. doi: 10.1073/pnas.98.2.676

Roiser, J. P., Elliott, R., and Sahakian, B. J. (2012). Cognitive mechanisms of treatment in depression. *Neuropsychopharmacology* 37, 117–136. doi: 10.1038/npp.2011.183

Rossini, D., Magri, L., Lucca, A., Giordani, S., Smeraldi, E., and Zanardi, R. (2005). Does rTMS hasten the response to escitalopram, sertraline, or venlafaxine in patients with major depressive disorder? A double-blind, randomized, sham-controlled trial. *J. Clin. Psychiatry* 66, 1569–1575. doi: 10.4088/jcp.v66n1212

Rumi, D. O., Gattaz, W. F., Rigonatti, S. P., Rosa, M. A., Fregni, F., Rosa, M. O., et al. (2005). Transcranial magnetic stimulation accelerates the antidepressant effect of amitriptyline in severe depression: a double-blind placebo-controlled study. *Biol. Psychiatry* 57, 162–166. doi: 10.1016/j.biopsych.2004.10.029

Rush, A. J., Kraemer, H. C., Sackeim, H. A., Fava, M., Trivedi, M. H., Frank, E., et al. (2006). Report by the ACNP Task Force on response and remission in major depressive disorder. *Neuropsychopharmacology* 31, 1841–1853. doi: 10.1038/sj.npp.1301131

Sanchez, A., Vanderhasselt, M. A., Baeken, C., and De Raedt, R. (2016). Effects of tDCS over the right DLPFC on attentional disengagement from positive and negative faces: an eye-tracking study. *Cogn. Affect. Behav. Neurosci.* 16, 1027–1038. doi: 10.3758/s13415-016-0450-3

Schutter, D. J., and van Honk, J. (2005). A framework for targeting alternative brain regions with repetitive transcranial magnetic stimulation in the treatment of depression. *J. Psychiatry Neurosci.* 30, 91–97.

Serafini, G., Pompili, M., Belvederi Murri, M., Respino, M., Ghio, L., Girardi, P., et al. (2015). The effects of repetitive transcranial magnetic stimulation on cognitive performance in treatment-resistant depression. A systematic review. *Neuropsychobiology* 71, 125–139. doi: 10.1159/000381351

Shiozawa, P., da Silva, M. E., and Cordeiro, Q. (2015). Transcranial direct current stimulation for treating depression in a patient with right hemispheric dominance: a case study. *J. ECT* 31, 201–202. doi: 10.1097/yct.0000000000000180

Shiozawa, P., Fregni, F., Bensenor, I. M., Lotufo, P. A., Berlim, M. T., Daskalakis, J. Z., et al. (2014). Transcranial direct current stimulation for major depression: an updated systematic review and meta-analysis. *Int. J. Neuropsychopharmacol.* 17, 1443–1452. doi: 10.1017/s1461145714000418

Stagg, C. J., and Nitsche, M. A. (2011). Physiological basis of transcranial direct current stimulation. *Neuroscientist* 17, 37–53. doi: 10.1177/1073858410386614

Strunk, D. R., and Adler, A. D. (2009). Cognitive biases in three prediction tasks: a test of the cognitive model of depression. *Behav. Res. Ther.* 47, 34–40. doi: 10.1016/j.brat.2008.10.008

Teng, S., Guo, Z., Peng, H., Xing, G., Chen, H., He, B., et al. (2017). High-frequency repetitive transcranial magnetic stimulation over the left DLPFC for major depression: session-dependent efficacy: a meta-analysis. *Eur. Psychiatry* 41, 75–84. doi: 10.1016/j.eurpsy.2016.11.002

Tortella, G., Selingardi, P. M., Moreno, M. L., Veronezi, B. P., and Brunoni, A. R. (2014). Does non-invasive brain stimulation improve cognition in major depressive disorder? A systematic review. *CNS Neurol. Disord. Drug Targets* 13, 1759–1769. doi: 10.2174/1871527313666141130224431

UK ECT Review Group. (2003). Efficacy and safety of electroconvulsive therapy in depressive disorders: a systematic review and meta-analysis. *Lancet* 361, 799–808. doi: 10.1016/s0140-6736(03)12705-5

Utz, K. S., Dimova, V., Oppenländer, K., and Kerkhoff, G. (2010). Electrified minds: transcranial direct current stimulation (tDCS) and galvanic vestibular stimulation (GVS) as methods of non-invasive brain stimulation in neuropsychology—a review of current data and future implications. *Neuropsychologia* 48, 2789–2810. doi: 10.1016/j.neuropsychologia.2010.06.002

Valero-Cabré, A., Amengual, J., Stengel, C., Pascual-Leone, A., and Coubard, O. A. (2017). Transcranial magnetic stimulation in basic and clinical neuroscience: a comprehensive review of fundamental principles and novel insights. *Neurosci. Biobehav. Rev*. doi: 10.1016/j.neubiorev.2017.10.006 [Epub ahead of print].

Vanderhasselt, M. A., De Raedt, R., Baeken, C., Leyman, L., and D'Haenen, H. (2009). A single session of rTMS over the left dorsolateral prefrontal cortex influences attentional control in depressed patients. *World J. Biol. Psychiatry* 10, 34–42. doi: 10.1080/15622970701816514

Vigod, S., Dennis, C. L., Daskalakis, Z., Murphy, K., Ray, J., Oberlander, T., et al. (2014). Transcranial direct current stimulation (tDCS) for treatment of major depression during pregnancy: study protocol for a pilot randomized controlled trial. *Trials* 15:366. doi: 10.1186/1745-6215-15-366

Wall, C., Croarkin, P., Bandel, L., and Schaefer, K. (2014). Response to repetitive transcranial magnetic stimulation induced seizures in an adolescent patient with major depression: a case report. *Brain Stimul.* 7, 337–338. doi: 10.1016/j.brs.2013.12.001

Wang, Y. Y., Jiang, N. Z., Cheung, E. F., Sun, H. W., and Chan, R. C. (2015). Role of depression severity and impulsivity in the relationship between hopelessness and suicidal ideation in patients with major depressive disorder. *J. Affect. Disord.* 183, 83–89. doi: 10.1016/j.jad.2015.05.001

Wang, Y. M., Li, N., Yang, L. L., Song, M., Shi, L., Chen, W. H., et al. (2017). Randomized controlled trial of repetitive transcranial magnetic stimulation combined with paroxetine for the treatment of patients with first-episode major depressive disorder. *Psychiatry Res.* 254, 18–23. doi: 10.1016/j.psychres.2017.04.005

Whiteford, H. A., Degenhardt, L., Rehm, J., Baxter, A. J., Ferrari, A. J., Erskine, H. E., et al. (2013). Global burden of disease attributable to mental and substance use disorders: findings from the Global Burden of Disease Study 2010. *Lancet* 382, 1575–1586. doi: 10.1016/S0140-6736(13)61611-6

Wolkenstein, L., and Plewnia, C. (2013). Amelioration of cognitive control in depression by transcranial direct current stimulation. *Biol. Psychiatry* 73, 646–651. doi: 10.1016/j.biopsych.2012.10.010

Wolkenstein, L., Kanske, P., Bailer, J., Wessa, M., Hautzinger, M., and Joormann, J. (2017). Impaired cognitive control over emotional material in euthymic bipolar disorder. *J. Affect. Disord.* 214, 108–114. doi: 10.1016/j.jad.2017.03.007

Yang, W., Zhu, X., Wang, X., Wu, D., and Yao, S. (2011). Time course of affective processing bias in major depression: an ERP study. *Neurosci. Lett.* 487, 372–377. doi: 10.1016/j.neulet.2010.10.059

Zilverstand, A., Parvaz, M. A., and Goldstein, R. Z. (2017). Neuroimaging cognitive reappraisal in clinical populations to define neural targets for enhancing emotion regulation. A systematic review. *Neuroimage* 151, 105–116. doi: 10.1016/j.neuroimage.2016.06.009

Zwanzger, P., Steinberg, C., Rehbein, M. A., Bröckelmann, A. K., Dobel, C., Zavorotnyy, M., et al. (2014). Inhibitory repetitive transcranial magnetic stimulation (rTMS) of the dorsolateral prefrontal cortex modulates early affective processing. *Neuroimage* 101, 193–203. doi: 10.1016/j.neuroimage.2014.07.003

**Conflict of Interest Statement**: The authors declare that the research was conducted in the absence of any commercial or financial relationships that could be construed as a potential conflict of interest.

frontiers in Human Neuroscience

ORIGINAL RESEARCH
published: 14 November 2017
doi: 10.3389/fnhum.2017.00551

# Attractiveness Modulates Neural Processing of Infant Faces Differently in Males and Females

*Lijun Yin[1,2], Mingxia Fan[3], Lijia Lin[1], Delin Sun[4] and Zhaoxin Wang[1,3]**

[1]*Shanghai Key Laboratory of Brain Functional Genomics (Ministry of Education), Institute of Cognitive Neuroscience, School of Psychology and Cognitive Science, East China Normal University, Shanghai, China,* [2]*Department of Psychology, Sun Yat-sen University, Guangzhou, China,* [3]*Shanghai Key Laboratory of MR, East China Normal University, Shanghai, China,* [4]*Brain Imaging and Analysis Center, Duke University Medical Center, Durham, NC, United States*

Consistent attention and proper processing of infant faces by adults are essential for infant survival. Previous behavioral studies showed gender differences in processing infant cues (e.g., crying, laughing or facial attractiveness) and more importantly, the efforts invested in nurturing offspring. The underlying neural mechanisms of processing unknown infant faces provide hints for understanding behavioral differences. This functional magnetic resonance imaging (fMRI) study recruited 32 unmarried adult (16 females and 16 males) participants to view unfamiliar infant faces and rate the attractiveness. Adult faces were also included. Behaviorally, despite that females and males showed no differences in attractiveness ratings of infant faces, a positive correlation was found between female's (but not male's) subjective liking for infants and attractiveness ratings of the infant faces. Functionally, brain activations to infant faces were modulated by attractiveness differently in males and females. Specifically, in female participants, activities in the ventromedial prefrontal cortex (vmPFC) and striatum/Nucleus Accumbens (NAcc) were positively modulated by infant facial attractiveness, and the modulation coefficients of these two regions were positively correlated. In male participants, infant facial attractiveness negatively modulated the activity in the dorsomedial prefrontal cortex (dmPFC). Our findings reveal that different neural mechanisms are involved in the processing of infant faces, which might lead to observed behavioral differences between males and females towards the baby.

**Keywords: infant, face, attractiveness, self, other, reward, gender difference**

OPEN ACCESS

***Edited by:***
*Muthuraman Muthuraman, Johannes-Gutenberg-University Hospital, Germany*

***Reviewed by:***
*Pinglei Bao, California Institute of Technology, United States*
*Topi Tanskanen, RIKEN, Japan*

****Correspondence:***
*Zhaoxin Wang*
*zxwang@nbic.ecnu.edu.cn*

***Received:*** *13 July 2017*
***Accepted:*** *31 October 2017*
***Published:*** *14 November 2017*

***Citation:***
*Yin L, Fan M, Lin L, Sun D and Wang Z (2017) Attractiveness Modulates Neural Processing of Infant Faces Differently in Males and Females. Front. Hum. Neurosci. 11:551. doi: 10.3389/fnhum.2017.00551*

## INTRODUCTION

Human babies are extremely vulnerable and completely dependent upon adults' care in order to survive (Senese et al., 2013). Despite the fact that both males and females take care of their infants to a certain extent, an intriguing fact is that women typically spend 2–3 times more with babies than men (Rossi, 1984; Mitchell et al., 2005; Bault et al., 2011). Besides, an overwhelming 97.7%–99.6% of prekindergarten and kindergarten teachers are female (e.g., U.S. Educational Statistics Yearbook of China, 2010; U.S. Bureau of the Census, 2011). Also, gender differences in the motivational processing of babies have been found in many behavioral studies (Doucet, 2009; Yamamoto et al., 2009; Hahn et al., 2013).

In a study about preference, females showed greater preference for infants than males, even at the age of 4 months (Maestripieri and Pelka, 2002). With regards to the neuroimaging studies, infant cues (e.g., crying, laughing, faces and etc.) have been found to elicit different neural patterns in males and females. Infant laughter and cries elicited activation in the amygdala and anterior cingulate of women, whereas the control stimuli elicited stronger activations in men (Sander et al., 2007). Independently of parental status, females but not males showed neural deactivation in the anterior cingulate cortex in response to both infant crying and laughing (Seifritz et al., 2003). In an EEG study, the baby-specific N1 response was much stronger in women than in men across the left hemisphere (Proverbio et al., 2011). When participants viewed faces of their own infants', rather than the faces of unfamiliar infants and adults, stronger neural activation in several regions, including the orbitofrontal cortex and anterior insula, have been found (Nitschke et al., 2004; Ranote et al., 2004; Kringelbach et al., 2008; Noriuchi et al., 2008; Strathearn et al., 2008).

Central to parental care is adults' ability to process infant cues (Parsons et al., 2014). One essential infant cue is facial attractiveness. An infant facial attractiveness or cuteness has been considered as an innate releasing mechanism for caretaking behaviors and affective orientation toward infants (Lorenz, 1943; Lobmaier et al., 2010; Hahn et al., 2013). Existing evidence suggests that there are consistent gender differences when it comes to processing infant attractiveness. Although both males and females show similar performance in detecting emotional valence and age (Parsons et al., 2011), compared to men, women were generally more perceptive and responsive to infant facial attractiveness (Parsons et al., 2011) and performed better in detecting attractive gradations of infant faces (Sprengelmeyer et al., 2009; Lobmaier et al., 2010). Moreover, infants who had relatively cuter faces elicited stronger caretaking motivation and higher activity in the striatum/nucleus accumbens (NAcc) in women (Glocker et al., 2009a,b). Thus understanding the underlying neural mechanisms of processing infant faces helps to understand established behavioral differences.

On one hand, the reward associated regions (e.g., the striatum/NAcc) might be the regions of interest in processing infant faces. On the other hand, self-resemblance, a putative cue of relatedness, might also play an important role in processing infant cues, especially in males. Both men and women are attracted to infant faces that look like their own (DeBruine, 2004). But men placed primary emphasis on cues of resemblance in a hypothetical adoption task (Volk and Quinsey, 2002) and in a task involved in making hypothetical parental investment decisions (Platek, 2002; Platek et al., 2003), while women mainly focused on cues of health and attractiveness (Volk and Quinsey, 2002). Therefore, self-other distinction associated regions such as the ventral medial prefrontal cortex (vmPFC) and dorsal medial prefrontal cortex (dmPFC) might be involved in the processing of infant faces (Mitchell et al., 2005; D'Argembeau et al., 2007).

Note that most of the functional imaging studies have focused on parental love, which limits the generalization of the findings to the non-parental care of infants. To further understand how gender influences the process of infant facial attractiveness, we conducted the present functional magnetic resonance imaging (fMRI) study investigating the neural mechanisms while males and females are viewing unknown infant faces. In the study, we manipulated the levels of infant facial attractiveness. To control general face-processing-related brain activations, we also included adult faces with average attractiveness. To reduce the confounding effects of age, marital status, as well as parenthood, only unmarried young female and male adults were recruited as participants. Based on previous findings, we expected to find different neural patterns while processing infant facial attractiveness in males and females, especially in the regions associated with reward processing, such as the striatum/NAcc and self-other distinction, such as vmPFC and dmPFC.

# MATERIALS AND METHODS

## Participants

Thirty-two Chinese students (16 females, aged from 20 to 25, mean age = 22.8 ± 1.5 (SD) years; 16 males, aged between 19 and 26, mean age = 22.3 ± 1.8 years) from East China Normal University took part in the current study. All participants were unmarried. They were right-handed with normal or corrected-to-normal vision and had a similar level of education. They did not report any psychiatric or neurological history, and female participants were with regular menstrual cycles between 25 and 35 days. An 11-point scale (−5 = strongly dislike, 0 = neutral, 5 = strongly like) was used to assess the participants' subjective feelings toward the infants before fMRI scanning. Female participants were arranged to take part in the experiment during the intervening period before and after the ovulation (i.e., 9 days before and 4 days after the ovulation). Female participants reported a mean of 3.1 days before the ovulation as calculated by their own menstrual phases. Written informed consents were obtained from all subjects, and the protocol was approved by the University Committee on Human Research Protection (UCHRP) at East China Normal University.

## Stimuli

One-hundred and eighty infant faces with neutral facial expression were selected from the Internet, an approach that has been used in previous studies (Brosch et al., 2007). The gender of the infant faces was not controlled as it was sometimes indistinguishable for babies (Proverbio et al., 2011). All pictures were transferred to gray-scale images with a black background of 640 × 480 resolution. The center between the two eyes was located at the same point to control for gaze (Nitschke et al., 2004). To make sure that the stimuli were suitable for testing our experimental hypotheses, all images were rated separately on a laptop by a separate group of 12 female participants for valence (with Self-Assessment Manikin, SAM), attractiveness (five-point scales ranging from 1 "not cute" to 5 "very cute"),

gender (male/female) and age (five-point scales for infant faces ranging from 0 to 4 years old; five-point scales for adult faces ranging from 1 "16–20 years old" to 5 "36–40 years old"). The attractiveness of infant faces were almost equally distributed between 2.4 and 4.2 out of five points. The mean attractiveness of the female and male adult faces were 2.3 (SD = 0.5) and 2.0 (0.4), respectively. Thirty-six adult faces (18 females and 18 males) with neutral facial expression were also adopted as to examine whether the process involved in viewing the infant faces can be differentiated from the adult faces. There were more infant faces to enable the manipulation of the attractiveness of infant faces. Note that adult faces and infant faces were from different individuals since babies' facial attractiveness cannot predict adult facial attractiveness of the same individuals (Harrison et al., 2011).

## Experimental Design

There were three functional runs. Each run lasted for 510 s and consisted of 10 blocks of infant faces and four blocks of adult faces (one for male and one for female, and each adult block was presented twice to increase signal-to-noise ratio). Each 18-s block consisted of six faces. Each face was presented for 3 s without inter-stimuli interval. During the 3-s of stimulus presentation, participants were asked to rate the attractiveness of the facial stimulus using a hand-shaped response box with their right hands, ranging from "1 = not attractive" to "5 = very attractive" with each rating was assigned to one finger. The inter-block fixation block lasted 18 s, with a fixation cross in the middle of the screen. The orders of these three kinds of block were pseudo-randomly mixed among three runs, and were counterbalanced between participants. This design was similar to Phan's study (Phan et al., 2003). Stimuli were presented through a goggles system (Invivo Co., Gainesville, FL, USA).

## MRI Data Acquisition

The scanning was conducted on a 3-Tesla Siemens Trio MR scanner. For functional images, 35 axial slices (FOV = 240 × 240 $mm^2$, matrix = 64 × 64, in-plane resolution = 3.75 × 3.75 $mm^2$, thickness = 4 mm, without gap) covering the whole brain were obtained using a T2*-weighted echo planar imaging (EPI) sequence (TR = 3000 ms, TE = 30 ms, flip angle = 90°), with 170 volumes. A high-resolution structural image was also acquired for each participant using 3D MRI sequences for anatomical co-registration and normalization (TR = 1900 ms, TE = 3.43 ms, flip angle = 7°, matrix = 256 × 256, FOV = 240 × 240 $mm^2$, slice thickness = 1 mm).

# DATA ANALYSIS

SPM8 was adopted for fMRI data analysis (Wellcome Department of Cognitive Neurology, London, UK)[1]. For each participant, the first two volumes of each run were discarded. EPI images were realigned to the first remaining volume of the first run to correct for head motions. Then the anatomical image was co-registered with the mean EPI image, segmented and then generated normalized parameters to MNI spaces. Next, all EPI data were projected to MNI template with a re-sampled voxel size of 2 × 2 × 2 $mm^3$. Finally, the functional images were spatially smoothed with a Gaussian kernel with a full width at half maximum (FWHM) of 8 mm. High-pass temporal filtering with a cut-off of 128 s was carried out to remove low-frequency drifts.

The statistical analyses of the fMRI data were based on two General Linear Models (i.e., GLM 1 and GLM 2). The canonical hemodynamic response function was used to model the fMRI signal.

## GLM 1

The first GLM model (GLM 1) was set up to investigate gender differences in the neural processing of infant faces and adult faces. Two regressors of interest, i.e., adult faces and infant faces, were included. For adult faces, a boxcar model was used and adult attractiveness was not considered due to its small variety (SD = 0.5 and 0.4 for females and males respectively). For infant faces, as there are individual differences in perceiving facial attractiveness, an event-related parametric statistical model was used as an event-related analysis can provide a more accurate model of the hemodynamic responses than an epoch-related analysis, even in a blocked design (Büchel et al., 1998; Mechelli et al., 2003; Phan et al., 2003). An orthogonal basis functions up to second order were used (Büchel et al., 1998). The zero-order term modeled the main effect of infant faces to the crosshair regardless of the attractiveness. The first-order term modeled a parametric linear increase in participants' subjective ratings of the attractiveness for each face, and a second-order term modeled a quadratic relationship. All these covariates were convolved with a canonical hemodynamic response function before including in the GLM model, and the six estimated head movement parameters were included in the design matrix to remove residual effects of head movements. The beta values of the adult face regressor, and the beta values of the zero-order term of the infant face regressors, were used as the interested indicators in the second level analysis.

For the second level analysis, a 2 × 2 flexible factorial model with the between-group factor (genders of the participants) and the within-subject factor (infant faces and adult faces) was built. Results were voxel-level height thresholded at $P < 0.001$ and survived after cluster-level family-wise error (FWE) correction, $P < 0.05$.

## GLM 2

A second GLM model (GLM 2) was set up to investigate the modulation of infant facial attractiveness on the neural activity in female and male participants. Infant faces were the regressor of interest. Participants' ratings of attractiveness were entered as the parametric modulator. The six estimated head movement

[1]http://www.fil.ion.ucl.ac.uk/spm/

**TABLE 1 |** Results of the flexible factorial analysis.

| Hem | Volume[a] | Maxima location | MNI coordinates | | | *T* |
|---|---|---|---|---|---|---|
| **Main effects of gender** | | | | | | |
| Female > Male | | | | | | |
| None | | | | | | |
| **Male > Female** | | | | | | |
| None | | | | | | |
| **Main effects of faces** | | | | | | |
| Infant > Adult | | | | | | |
| R | 6502 | Fusiform gyrus | 34 | −48 | −6 | 8.24 |
| R | 616 | Insula | 32 | 6 | 14 | 5.35 |
| L | 308 | Insula | −34 | 8 | 14 | 5.21 |
| **Adult > Infant** | | | | | | |
| R | 8942 | Middle frontal gyrus | 36 | 22 | 32 | 7.01 |
| R | 809 | Ventral lateral frontal gyrus | 30 | 62 | −2 | 6.95 |
| L | 2021 | Superior parietal lobule | −42 | −62 | 52 | 6.78 |
| R | 1954 | Superior parietal lobule | 36 | −68 | 50 | 6.38 |
| R | 424 | Middle temporal gyrus | 56 | −38 | −12 | 6.38 |
| L | 1157 | Ventral lateral frontal gyrus | −42 | 56 | −4 | 5.90 |
| M | 1252 | Precuneus | 0 | −58 | 24 | 5.53 |
| **Interactions** | | | | | | |
| Female (Infant-Adult) vs. Male (Infant-Adult) | | | | | | |
| R | 404 | Striatum/NAcc | 6 | 2 | 4 | 4.65 |
| Male (Infant-Adult) vs. Female (Infant-Adult) | | | | | | |
| None | | | | | | |

[a]*Volumes are given as number of 2.0 × 2.0 × 2.0 mm Voxels. Voxel-level height threshold P < 0.001, cluster-level P < 0.05, family-wise error (FWE) correction.*

parameters were included in the design matrix to remove residual effects of head movements.

For the second level analysis, one sample *t*-tests were used to estimate the effects of the parametric modulator (i.e., infant facial attractiveness) respectively in female and male participants. Based on the findings of previous studies (Mitchell et al., 2005; D'Argembeau et al., 2007; Glocker et al., 2009b), our regions of interest are the striatum/NAcc, the vmPFC and the dmPFC. The voxel-wised threshold was set at $p = 0.005$, with the spatial extent threshold setting at $k = 80$. A small volume correction (SVC) for FWE was used in a box with dimensions equaling of 8 mm in brain regions with prior hypotheses. Specifically, the coordinates of the striatum/NAcc were 10 12 −8 (in Talairach space), adopted from Glocker et al's (2009b) study, the coordinates of the vmPFC were −8 50 −2 (in MNI space; D'Argembeau et al., 2007), and the coordinates of the dmPFC were −9 51 36 (in MNI space; Mitchell et al., 2005). To investigate if the modulating effects differ between male and female participants, modulation coefficients were extracted from the aforementioned ROIs in males and females. Pair *t*-tests were used to compare modulation coefficients between males and females. The mean modulation coefficients of the vmPFC and striatum/NAcc for

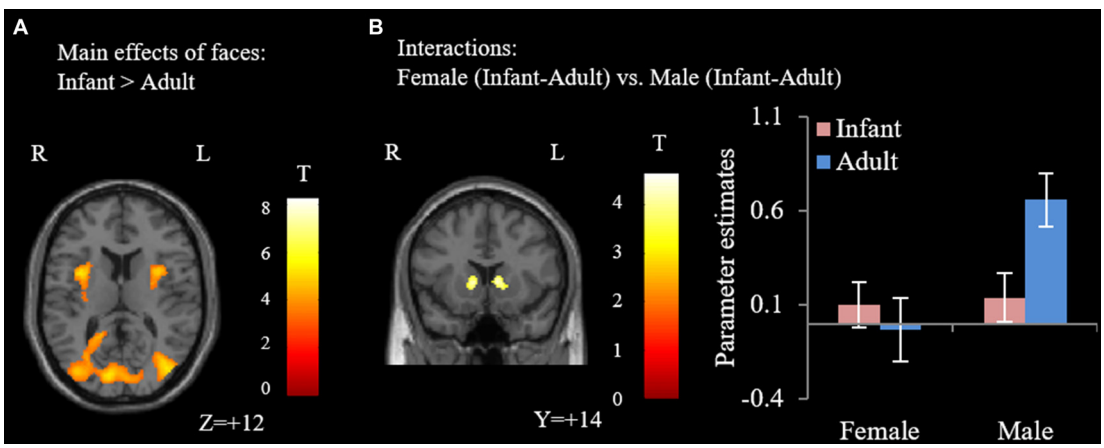


**FIGURE 1 |** Results of the flexible factorial analysis. **(A)** Infant faces elicited higher activation in the bilateral insula and fusiform gyrus. **(B)** The interaction effect of female participants (infant-adult) vs. male participants (infant-adult). Error bars denote standard error of the mean (SE). Parameter estimates were extracted from the peak voxel in the striatum/nucleus accumbens (NAcc; MNI: 6, 2, 4; voxel-wised threshold $P < 0.001$, cluster-level $P < 0.05$, family-wise error (FWE) correction).

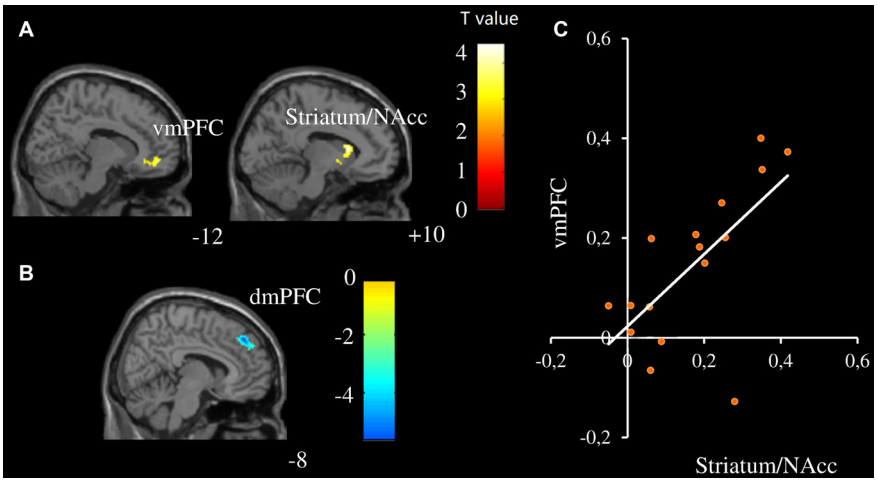


**FIGURE 2 |** Neural activity was modulated by infant facial attractiveness differently between males and females. **(A)** The ventromedial prefrontal cortex (vmPFC) and striatum/NAcc were positively modulated by infant facial attractiveness in female participants, while **(B)** dorsomedial prefrontal cortex (dmPFC) was negatively modulated by infant facial attractiveness in male participants ($N$ = 16, voxel-wised $p < 0.005$, uncorrected, $k$ = 80; Small Volume Corrected). **(C)** A significant correlation between modulation coefficients of striatum/NAcc (centered at 10, 16, 10; with 808 ml) and vmPFC (centered at −12, 50, −8; with 832 ml) was found in female participants ($r$ = 0.66, $p$ = 0.006).

each participant were then extracted and used for correlation analysis, with the threshold setting at $P < 0.05$ (two-tailed).

# RESULTS

## Behavioral Results

There was no significant gender difference in the ratings of liking for infants (women: 3.4 ± 1.5 (mean ± SD); men: 2.6 ± 1.7, $t_{(30)} = -1.5$, $p = 0.14$). Both groups gave significantly higher attractiveness ratings to infant faces than adult faces (females: 3.3 ± 0.6 vs. 2.4 ± 0.6, respectively, $t_{(15)} = 5.3$, $p < 0.001$; males: 3.1 ± 0.4 vs. 2.5 ± 0.5, respectively, $t_{(15)} = 4.1$, $p = 0.001$). We also found a significant correlation between subjective liking for infants and mean attractiveness of the infant faces in female participants ($r = 0.75$, $p = 0.001$) but not in male participants ($r = 0.15$, $p = 0.58$). No other effects were significant.

## Imaging Results

### GLM 1

Our major findings were listed in the **Table 1**. When we compare the neural activity in female and male participants, no significant activations were found. With regards to the effects of faces, compared with adult faces, infant faces significantly activated bilateral insula and fusiform gyri (**Figure 1A**). Adult faces elicited higher activation in the bilateral middle frontal gyri, bilateral ventral lateral frontal gyri, bilateral superior parietal lobules, right middle temporal gyrus and bilateral precuneus, compared with infant faces. In the comparison of infants' vs. adult faces, female participants showed higher activation in the striatum/NAcc (**Figure 1B**) compared with male participants. *Post hoc* analysis showed that adult faces elicited higher activity in male participants' striatum/NAcc ($ps \leq 0.003$). No significant differences were found in the other comparisons ($ps > 0.14$).

### GLM 2

Different modulation patterns were found between female and male participants, see **Table 2** for details. Specifically, the vmPFC and striatum/NAcc were positively modulated by infant facial attractiveness for female participants (**Figure 2A**), but not for male participants. Moreover, a positive correlation between the modulation coefficients of these two regions was found in female participants (**Figure 2C**). In male participants, the dmPFC was negatively modulated by infant facial attractiveness (**Figure 2B**), but not in female participants. The modulation coefficients in the

**TABLE 2 |** Brain regions that were modulated by infant facial attractiveness.

| Hem | Volume[a] | Maxima location | MNI coordinates | | | *T* |
|---|---|---|---|---|---|---|
| **Female (positive modulation)** | | | | | | |
| R | 101 | Striatum/NAcc | 10 | 16 | 10 | 4.52 |
| L | 104 | vmPFC | −12 | 50 | −8 | 3.96 |
| **Male (negative modulation)** | | | | | | |
| R | 209 | dmPFC | −8 | 44 | 40 | 5.53 |

[a]*Volumes are given as number of 2.0 × 2.0 × 2.0 mm voxels. Significant at p < 0.05 corrected for multiple comparisons at the cluster level with small volume correction (SVC).*

vmPFC and striatum/NAcc were significantly higher in females than in males (also significant from these ROIs, $ts_{(30)} > 1.7$, $ps < 0.05$). In the dmPFC, the modulation coefficients were significantly higher in males than in females ($t_{(30)} = 2.08$, $p = 0.023$).

## DISCUSSION

In the present study, we found significant gender differences in neural responses toward infant and adult faces in two aspects. The first aspect is associated with the general processing of faces. While no gender differences were found when we compared neural activity in female and male participants, a significant gender (male and female) by face (infant vs. adult) interaction was found in the striatum/NAcc. Contrary to our expectations, *post hoc* analysis revealed significantly higher activity when male participants viewed adult faces. The striatum/NAcc is the key structure of the reward system, which can be activated by the monetary reward (Delgado et al., 2000; Elliott et al., 2003; Ernst et al., 2005; Abler et al., 2006; Knutson et al., 2001a,b, 2003) and social reward (Izuma et al., 2008; Spreckelmeyer et al., 2009). It is also associated with discrimination between reward values (Galvan et al., 2005), with higher reward (monetary reward or social reward) value eliciting higher striatum/NAcc activity (Izuma et al., 2008; Spreckelmeyer et al., 2009). According to these previous findings, there might be a strong link between reward and the activation in the striatum/NAcc. Thus, it seems that male participants displayed lower reward-related neural responses to infant faces (compared to adult faces). As a matter of fact, in a previous study, as cited in the Introduction, infant laughing and crying elicited activation in the amygdala and anterior cingulate of women, whereas the control stimuli elicited stronger activations in men (Sander et al., 2007). Their results, together with our results, suggest that males, but not females, display lower motivational neural responses to infant cues than to adult cues.

The second aspect is related to the modulation of attractiveness on the neural responses toward infant faces. The activities of the striatum/NAcc and vmPFC in female participants were positively modulated by infant facial attractiveness, while in male participants the activity of dmPFC was negatively modulated by infant facial attractiveness. With regards to infant face processing, our results on the striatum/NAcc are in line with the findings from a previous study in which it was found that cuter baby schema elicited higher NACC activation for female participants (Glocker et al., 2009b). Previous studies showed that, as compared to males, females were slightly better at detecting gradations in the manipulated attractiveness of infant faces (Sprengelmeyer et al., 2009; Lobmaier et al., 2010). Women gave significantly higher "liking" ratings for infant faces (Radin, 1982; Parsons et al., 2011) and display approach behavior toward infants (Frodi and Lamb, 1978). Furthermore, we found that the modulator coefficient in the vmPFC was correlated with that in the striatum/NAcc for female participants. The ventral striatum/NAcc (including NAcc) receives extensive projections from VMPFC (Delgado, 2007). Enhanced brain activation in the vmPFC was also found while seeing one's own baby's neutral face or hearing one's own baby crying (Kringelbach et al., 2008; Noriuchi et al., 2008). The significant correlation between the vmPFC and striatum/NAcc suggests that these brain regions work together to initiate attractiveness induced likeness, especially in female participants. In females, the striatum/NAcc might be the key hub for initiating the attractiveness induced likeness.

A possible explanation is that self-other distinction is involved in the processing of infant facial attractiveness. Infant attractiveness was positively correlated with the activity of the vmPFC in female participants, but negatively correlated with the activity of the dmPFC in male participants. It was hypothesized that the vmPFC may be related to positive emotional evaluation. However, enhanced brain activation in the vmPFC was also found while seeing one's own baby's neutral face or hearing one's own baby crying (Kringelbach et al., 2008; Noriuchi et al., 2008). In a study on self/other similarity (Mitchell et al., 2005), the vmPFC was activated during judgments about similar people, whereas the dmPFC was activated in judgments about dissimilar individuals. Similarly, activation of the vmDFC was found for judgments targeting the self (vs. judgments targeting the other), whereas the activation in the dmPFC was found when taking a third-person perspective compared to a first-person one (D'Argembeau et al., 2007).

The evidence about maternal love (Bartels and Zeki, 2004; Nitschke et al., 2004; Noriuchi et al., 2008; Swain, 2008) was consistent with the argument that the vmPFC was related to self-involvement in the processing of infants. Viewing attractive infant faces might induce higher involvement of "similar/self" system in female participants, while less involvement, or "disengagement", of "dissimilar/other system" in male participants. Self might be the mediator of rewards (de Greck et al., 2008) in the processing of infant facial attractiveness. Through associating attractive babies with themselves, rather than others, women may feel more rewards toward cute infant faces. The explanation is in line with an evolutionary view that males have more evolutionary demands for this self-other distinction of babies because only males are susceptible to errors in identifying their offsprings (Platek et al., 2004). It has also been reported that young children were disproportionately at risk of homicide by step-parental males (Roach and Pease, 2011). Gender differences in caretaking behaviors show that women are more prone to physical care, either in families (Rossi, 1984; Baxter, 2002) or in social contexts other than family (Rossi, 1984). On the other hand, fathers act toward infants as if they are "things" rather than persons whom they can interact with; this is true even for egalitarian fathers (Rossi, 1984), in the sense that "others" are more likely to be treated as objects rather than human beings (Baars and Gage, 2010).

We also note that, behaviorally, participants of both genders considered infant faces to be more attractive than adult faces and we did not find significant differences between females' and males' ratings toward infant faces. Imaging results also showed that infant faces significantly activated bilateral insula

and fusiform gyri (vs. adult faces, **Figure 1A**) in both genders without significant interactions. Taken together, these results suggest that participants' ability to judge the attractiveness level of baby faces is comparable, while the striatum/NAcc and vmPFC/dmPFC motivational systems are differently involved in the processing of infant faces between males and females.

Our study bears several limitations. First, our study focused on unmarried adults. Therefore, it is unclear whether these differences are inherent or affected by culture. In addition, brain responses to infant facial attractiveness in other phases of the life cycle or in different marital/parental status (Proverbio et al., 2006) may differ. It is possible that reproductive hormones such as oxytocin may play a role in the evaluation of infant facial attractiveness (Sprengelmeyer et al., 2009), and parenthood may change the status of self-involvement as well as embodiment (Bault et al., 2011). Second, our sample size is relatively small (16 males and 16 females); further studies with larger sample sizes are desired. Third, the uneven number of trials corresponding to the infant and adult conditions respectively might influence statistical sensitivity. But we think that our findings are valid because our major conclusions are based on the findings from modulation analysis, in which adult faces were not included in the model.

In conclusion, we investigated the neural processing of infants' and adults' faces in females and males. Our major findings showed that: (1) females' (but not males) likeness toward infants are highly associated with facial attractiveness; and (2) the neural processing of infant faces differ for two genders, especially in the regions of the striatum/NAcc, vmPFC, and dmPFC. The regions might be associated with attractiveness induced likeness and self-other distinction. Our findings thus provide hints for understanding established gender differences in baby processing.

## AUTHOR CONTRIBUTIONS

LY, MF and ZW designed the study. LY and MF collected the data. LY and ZW analyzed the data. ZW, LY, LL and DS wrote the article.

## ACKNOWLEDGMENTS

This research was supported by the Natural Science Foundation of China (Nos. 30700235, 31070986). We are indebted to Ms. Natalie Leung of the Hong Kong University and Dr. Zhong Yuan Lai of Fudan University for correcting the English.

## REFERENCES

Abler, B., Walter, H., Erk, S., Kammerer, H., and Spitzer, M. (2006). Prediction error as a linear function of reward probability is coded in human nucleus accumbens. *Neuroimage* 31, 790–795. doi: 10.1016/j.neuroimage.2006.01.001

Baars, B. J., and Gage, N. M. (2010). *Cognition, Brain, and Consciousness: Introduction to Cognitive Neuroscience.* San Diego, CA: Academic Press.

Bartels, A., and Zeki, S. (2004). The neural correlates of maternal and romantic love. *Neuroimage* 21, 1155–1166. doi: 10.1016/j.neuroimage.2003.11.003

Bault, N., Joffily, M., Rustichini, A., and Coricelli, G. (2011). Medial prefrontal cortex and striatum mediate the influence of social comparison on the decision process. *Proc. Natl. Acad. Sci. U S A* 108, 16044–16049. doi: 10.1073/pnas.1100892108

Baxter, J. (2002). Patterns of change and stability in the gender division of household labour in Australia, 1986–1997. *J. Soc.* 38, 399–424. doi: 10.1177/144078302128756750

Brosch, T., Sander, D., and Scherer, K. (2007). That baby caught my eye... attention capture by infant faces. *Emotion* 7, 685–689. doi: 10.1037/1528-3542.7.3.685

Büchel, C., Holmes, A., Rees, G., and Friston, K. (1998). Characterizing stimulus-response functions using nonlinear regressors in parametric fMRI experiments. *Neuroimage* 8, 140–148. doi: 10.1006/nimg.1998.0351

D'Argembeau, A., Ruby, P., Collette, F., Degueldre, C., Balteau, E., Luxen, A., et al. (2007). Distinct regions of the medial prefrontal cortex are associated with self-referential processing and perspective taking. *J. Cogn. Neurosci.* 19, 935–944. doi: 10.1162/jocn.2007.19.6.935

DeBruine, L. M. (2004). Facial resemblance increases the attractiveness of same-sex faces more than other-sex faces. *Proc. Biol. Sci.* 271, 2085–2090. doi: 10.1098/rspb.2004.2824

de Greck, M., Rotte, M., Paus, R., Moritz, D., Thiemann, R., Proesch, U., et al. (2008). Is our self based on reward? Self-relatedness recruits neural activity in the reward system. *Neuroimage* 39, 2066–2075. doi: 10.1016/j.neuroimage.2007.11.006

Delgado, M. R. (2007). Reward-related responses in the human striatum. *Ann. N Y Acad. Sci.* 1104, 70–88. doi: 10.1196/annals.1390.002

Delgado, M. R., Nystrom, L. E., Fissell, C., Noll, D., and Fiez, J. A. (2000). Tracking the hemodynamic responses to reward and punishment in the striatum. *J. Neurophysiol.* 84, 3072–3077.

Doucet, A. (2009). Dad and baby in the first year: gendered responsibilities and embodiment. *Ann. Am. Acad. Pol. Soc. Sci* 624, 78–98. doi: 10.1177/0002716209334069

Elliott, R., Newman, J. L., Longe, O. A., and Deakin, J. (2003). Differential response patterns in the striatum and orbitofrontal cortex to financial reward in humans: a parametric functional magnetic resonance imaging study. *J. Neurosci.* 23, 303–307.

Ernst, M., Nelson, E. E., Jazbec, S., McClure, E. B., Monk, C. S., Leibenluft, E., et al. (2005). Amygdala and nucleus accumbens in responses to receipt and omission of gains in adults and adolescents. *Neuroimage* 25, 1279–1291. doi: 10.1016/j.neuroimage.2004.12.038

Frodi, A. M., and Lamb, M. E. (1978). Sex differences in responsiveness to infants: a developmental study of psychophysiological and behavioral responses. *Child Dev.* 49, 1182–1188. doi: 10.1111/j.1467-8624.1978.tb04087.x

Galvan, A., Hare, T. A., Davidson, M., Spicer, J., Glover, G., and Casey, B. (2005). The role of ventral frontostriatal circuitry in reward-based learning in humans. *J. Neurosci.* 25, 8650–8656. doi: 10.1523/JNEUROSCI.2431-05.2005

Glocker, M., Langleben, D., Ruparel, K., Loughead, J., Gur, R., and Sachser, N. (2009a). Baby schema in infant faces induces cuteness perception and motivation for caretaking in adults. *Ethology* 115, 257–263. doi: 10.1111/j.1439-0310.2008.01603.x

Glocker, M., Langleben, D., Ruparel, K., Loughead, J., Valdez, J., Griffin, M., et al. (2009b). Baby schema modulates the brain reward system in nulliparous women. *Proc. Natl. Acad. Sci. U S A* 106, 9115–9119. doi: 10.1073/pnas.0811620106

Hahn, A. C., Xiao, D., Sprengelmeyer, R., and Perrett, D. I. (2013). Gender differences in the incentive salience of adult and infant faces. *Q. J. Exp. Psychol. (Hove)* 66, 200–208. doi: 10.1080/17470218.2012.705860

Harrison, M. A., Shortall, J. C., Dispenza, F., and Gallup, G. G. Jr. (2011). You must have been a beautiful baby: ratings of infant facial attractiveness fail to predict ratings of adult attractiveness. *Infant Behav. Dev.* 34, 610–616. doi: 10.1016/j.infbeh.2011.06.003

Izuma, K., Saito, D. N., and Sadato, N. (2008). Processing of social and monetary rewards in the human striatum. *Neuron* 58, 284–294. doi: 10.1016/j.neuron.2008.03.020

Knutson, B., Adams, C. M., Fong, G. W., and Hommer, D. (2001a). Anticipation of increasing monetary reward selectively recruits nucleus accumbens. *J. Neurosci.* 21:RC159.

Knutson, B., Fong, G. W., Adams, C. M., Varner, J. L., and Hommer, D. (2001b). Dissociation of reward anticipation and outcome with event-related fMRI. *Neuroreport* 12, 3683–3687. doi: 10.1097/00001756-200112040-00016

Knutson, B., Fong, G. W., Bennett, S. M., Adams, C. M., and Hommer, D. (2003). A region of mesial prefrontal cortex tracks monetarily rewarding outcomes: characterization with rapid event-related fMRI. *Neuroimage* 18, 263–272. doi: 10.1016/s1053-8119(02)00057-5

Kringelbach, M., Lehtonen, A., Squire, S., Harvey, A., Craske, M., Holliday, I., et al. (2008). A specific and rapid neural signature for parental instinct. *PLoS One* 3:e1664. doi: 10.1371/journal.pone.0001664

Lobmaier, J. S., Sprengelmeyer, R., Wiffen, B., and Perrett, D. I. (2010). Female and male responses to cuteness, age and emotion in infant faces. *Evol. Hum. Behav.* 31, 16–21. doi: 10.1016/j.evolhumbehav.2009.05.004

Lorenz, K. (1943). Die angeborenen formen möglicher erfahrung. *Z. Tierpsychol.* 5, 235–409. doi: 10.1111/j.1439-0310.1943.tb00655.x

Maestripieri, D., and Pelka, S. (2002). Sex differences in interest in infants across the lifespan. *Hum. Nat.* 13, 327–344. doi: 10.1007/s12110-002-1018-1

Mechelli, A., Henson, R. N., Price, C. J., and Friston, K. J. (2003). Comparing event-related and epoch analysis in blocked design fMRI. *Neuroimage* 18, 806–810. doi: 10.1016/s1053-8119(02)00027-7

Mitchell, J. P., Banaji, M. R., and MacRae, C. N. (2005). The link between social cognition and self-referential thought in the medial prefrontal cortex. *J. Cogn. Neurosci.* 17, 1306–1315. doi: 10.1162/0898929055002418

Nitschke, J., Nelson, E., Rusch, B., Fox, A., Oakes, T., and Davidson, R. (2004). Orbitofrontal cortex tracks positive mood in mothers viewing pictures of their newborn infants. *Neuroimage* 21, 583–592. doi: 10.1016/j.neuroimage.2003.10.005

Noriuchi, M., Kikuchi, Y., and Senoo, A. (2008). The functional neuroanatomy of maternal love: mother's response to infant's attachment behaviors. *Biol. Psychiatry* 63, 415–423. doi: 10.1016/j.biopsych.2007.05.018

Parsons, C. E., Young, K. S., Joensson, M., Brattico, E., Hyam, J. A., Stein, A., et al. (2014). Ready for action: a role for the human midbrain in responding to infant vocalizations. *Soc. Cogn. Affect. Neurosci.* 9, 977–984. doi: 10.1093/scan/nst076

Parsons, C. E., Young, K. S., Kumari, N., Stein, A., and Kringelbach, M. L. (2011). The motivational salience of infant faces is similar for men and women. *PLoS One* 6:e20632. doi: 10.1371/journal.pone.0020632

Phan, K. L., Taylor, S. F., Welsh, R. C., Decker, L. R., Noll, D. C., Nichols, T. E., et al. (2003). Activation of the medial prefrontal cortex and extended amygdala by individual ratings of emotional arousal: a fMRI study. *Biol. Psychiatry* 53, 211–215. doi: 10.1016/s0006-3223(02)01485-3

Platek, S. M. (2002). Unconscious reactions to children's faces: the effect of resemblance. *Evol. Cogn.* 8, 207–214.

Platek, S. M., Critton, S. R., Burch, R. L., Frederick, D. A., Myers, T. E., and Gallup, G. G. (2003). How much paternal resemblance is enough? Sex differences in hypothetical investment decisions but not in the detection of resemblance. *Evol. Hum. Behav.* 24, 81–87. doi: 10.1016/s1090-5138(02)00117-4

Platek, S. M., Raines, D. M., Gallup, G. G. Jr., Mohamed, F. B., Thomson, J. W., Myers, T. E., et al. (2004). Reactions to children's faces: males are more affected by resemblance than females are, and so are their brains. *Evol. Hum. Behav.* 25, 394–405. doi: 10.1016/j.evolhumbehav.2004.08.007

Proverbio, A., Brignone, V., Matarazzo, S., Del Zotto, M., and Zani, A. (2006). Gender and parental status affect the visual cortical response to infant facial expression. *Neuropsychologia* 44, 2987–2999. doi: 10.1016/j.neuropsychologia.2006.06.015

Proverbio, A., Riva, F., Zani, A., and Martin, E. (2011). Is it a baby? Perceived age affects brain processing of faces differently in women and men. *J. Cogn. Neurosci.* 23, 3197–3208. doi: 10.1162/jocn_a_00041

Radin, N. (1982). "Primary caregiving and role-sharing fathers," in *Nontraditional Families: Parenting and Child Development,* ed. M. E. Lamb (Hillsdale, NJ: Erlbaum), 173–204.

Ranote, S., Elliott, R., Abel, K., Mitchell, R., Deakin, J., and Appleby, L. (2004). The neural basis of maternal responsiveness to infants: an fMRI study. *Neuroreport* 15, 1825–1829. doi: 10.1097/01.wnr.0000137078.64128.6a

Roach, J., and Pease, K. (2011). Evolution and the prevention of violent crime. *Psychology* 2, 393–404. doi: 10.4236/psych.2011.24062

Rossi, A. S. (1984). Gender and parenthood. *Am. Sociol. Rev.* 49, 1–19. doi: 10.2307/2095554

Sander, K., Frome, Y., and Scheich, H. (2007). FMRI activations of amygdala, cingulate cortex and auditory cortex by infant laughing and crying. *Hum. Brain Mapp.* 28, 1007–1022. doi: 10.1002/hbm.20333

Seifritz, E., Esposito, F., Neuhoff, J., Lüthi, A., Mustovic, H., Dammann, G., et al. (2003). Differential sex-independent amygdala response to infant crying and laughing in parents versus nonparents. *Biol. Psychiatry* 54, 1367–1375. doi: 10.1016/s0006-3223(03)00697-8

Senese, V. P., De Falco, S., Bornstein, M. H., Caria, A., Buffolino, S., and Venuti, P. (2013). Human infant faces provoke implicit positive affective responses in parents and non-parents alike. *PLoS One* 8:e80379. doi: 10.1371/journal.pone.0080379

Spreckelmeyer, K. N., Krach, S., Kohls, G., Rademacher, L., Irmak, A., Konrad, K., et al. (2009). Anticipation of monetary and social reward differently activates mesolimbic brain structures in men and women. *Soc. Cogn. Affect. Neurosci.* 4, 158–165. doi: 10.1093/scan/nsn051

Sprengelmeyer, R., Perrett, D., Fagan, E., Cornwell, R., Lobmaier, J., Sprengelmeyer, A., et al. (2009). The cutest little baby face a hormonal link to sensitivity to cuteness in infant faces. *Psychol. Sci.* 20, 149–154. doi: 10.1111/j.1467-9280.2009.02272.x

Strathearn, L., Li, J., Fonagy, P., and Montague, P. (2008). What's in a smile? Maternal brain responses to infant facial cues. *Pediatrics* 122, 40–51. doi: 10.1542/peds.2007-1566

Swain, J. E. (2008). Baby stimuli and the parent brain: functional neuroimaging of the neural substrates of parent-infant attachment. *Psychiatry* 5, 28–36.

Volk, A., and Quinsey, V. L. (2002). The influence of infant facial cues on adoption preferences. *Hum. Nat.* 13, 437–455. doi: 10.1007/s12110-002-1002-9

Yamamoto, R., Ariely, D., Chi, W., Langleben, D. D., and Elman, I. (2009). Gender differences in the motivational processing of babies are determined by their facial attractiveness. *PLoS One* 4:e6042. doi: 10.1371/journal.pone.0006042

**Conflict of Interest Statement**: The authors declare that the research was conducted in the absence of any commercial or financial relationships that could be construed as a potential conflict of interest.

The reviewer TT and handling Editor declared their shared affiliation, and the handling Editor states that the process nevertheless met the standards of a fair and objective review.

frontiers in Human Neuroscience

GENERAL COMMENTARY
published: 24 November 2017
doi: 10.3389/fnhum.2017.00562

# Commentary: Methamphetamine abuse impairs motor cortical plasticity and function

*Xiangju Du†, Chang Yu†, Zhen-Yu Hu* and Dong-Sheng Zhou**

*Ningbo Kangning Hospital, Ningbo, China*

**Keywords: addiction, schizophrenia, depression, TMS, NIBS**

**A commentary on**

**Methamphetamine abuse impairs motor cortical plasticity and function**
*by Huang, X., Chen, Y.Y., Shen, Y., Cao, X., Li, A., Liu, Q., et al. (2017). Mol. Psychiatry 22, 1274–1281. doi: 10.1038/mp.2017.143*

OPEN ACCESS

***Edited by:***
*Xiaochu Zhang,*
*University of Science and Technology of China, China*

***Reviewed by:***
*Yan-Xue Xue,*
*Peking University, China*
*Oscar Arias-Carrión,*
*Hospital General Dr. Manuel Gea Gonzalez, Mexico*
*Jijun Wang,*
*Shanghai Mental Health Center (SMHC), China*

****Correspondence:***
*Zhen-Yu Hu*
*hzy86690952@163.com*
*Dong-Sheng Zhou*
*wyzhouds@sina.com*

*† These authors have contributed equally to this work.*

***Received:*** *04 October 2017*
***Accepted:*** *07 November 2017*
***Published:*** *24 November 2017*

***Citation:***
*Du X, Yu C, Hu Z-Y and Zhou D-S (2017) Commentary: Methamphetamine abuse impairs motor cortical plasticity and function. Front. Hum. Neurosci. 11:562. doi: 10.3389/fnhum.2017.00562*

Psychiatric diseases demonstrate plasticity deficits in the brain. Animal studies have investigated the topic extensively. For instance, brain slice experiments with hippocampus/cortex preparations revealed plasticity changes in synaptic transmission of certain pathways, in a line with the learning and memory impairments in certain psychiatric diseases (Duman et al., 2016). Addiction is associated with synaptic transmission changes in mesolimbic and mesocortical pathways, with alterations of synaptic plasticity reported (Lüscher and Malenka, 2011). With an arsenal of animal reports on addiction evoked brain plasticity, surprisingly there were few studies translating such findings onto human subjects (Etkin, 2016). In a recent study published on the journal of *Molecular Psychiatry*, Huang et al. heroically investigated the cortical functional changes following methamphetamine abuse both in animal model and human addicts (Huang et al., 2017).

The authors firstly set up the animal model of methamphetamine self-administration and examined the synaptic plasticity on brain slices. The results showed that motor cortical, and dorsal-lateral rather than dorsal-medial striatal pathways exhibited impaired plasticity induction. Interestingly, molecular expression of GluN3A-containing NMDA receptors seems to be attributed for the altered plasticity. This is in a line with the previous finding that insertion of GluN3A-containing NMDA receptors at midbrain dopamine neurons resulted in anti-hebbian like plasticity (Mameli et al., 2011), given the fact that these NMDA receptors are less calcium permeable than canonical NMDA receptors.

To correlate the animal findings with human cortical plasticity, the authors employed a surrogate of synaptic plasticity in human—the plasticity of transcranial magnetic stimulation (TMS)-induced motor evoked potential (MEPs) (Huang et al., 2005), to dissect the potential impacts of methamphetamine on motor cortex. Notably, the Long-term potentiation (LTP) or Long-Term depression (LTD)-like changes of MEPs were both impaired in methamphetamine abusers, indicating that the cortical plasticity is impaired in human addicts. Interestingly, the plasticity deficits were in parallel with motor learning impairments, both in animal and human subjects (**Figure 1**).

Motor cortex is commonly a neglected region in addiction field. However, neuroimaging findings demonstrated that craving evoked by drug-associated cues involved motor and sensory regions (Yalachkov et al., 2010). In addition, animal studies detected drug cue-associated c-Fos expression in dorsal striatum (Willuhn and Steiner, 2006). Most importantly, the compulsive drug taking behavior could share certain neural pathways as obsessive compulsive disorder (OCD),

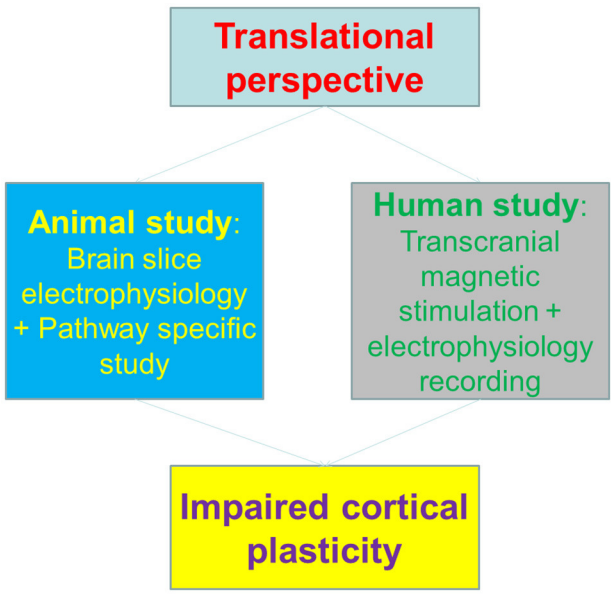


**FIGURE 1 |** The translational perspective and working scheme of Huang et al. paper.

therefore motor-striatal pathway might represent a new target in drug addiction (Everitt and Robbins, 2005). Indeed, exercise therapy is proved with efficacy in addiction rehabilitation, both in animal studies and human patients (Sanchez et al., 2015). Future studies are required to further elucidate if targeting motor cortex could bring benefits in addiction rehabilitation. Interesting, in addition to methamphetamine addiction, heroin addicts also exhibited cortical plasticity deficits (Shen et al., 2017).

Cortical plasticity is affected by a number of factors, such as genetic susceptibility to activity-dependent plasticity, trophic factor expression, neurotransmitters (Li Voti et al., 2011). Besides its applications on treatment of addiction or psychiatric diseases (Shen et al., 2016; Diana et al., 2017), TMS provides the unique chance to translate previous animal findings onto human subjects, the results of which could be taken for disease state diagnosis or prognosis for therapeutic treatments. In the future, TMS dependent measurements of EEG signals could provide functional cortex mapping non-invasively, but with much higher temporal resolution than brain imaging (e.g., fMRI; Miniussi and Thut, 2010). This will largely expand our understanding in addiction related brain functional changes, and to develop potential treatment against substance abuse.

Cortical plasticity impairment, however, is not limited to addiction. Previous studies reported that schizophrenia (Fitzgerald et al., 2004; Zhou et al., 2017), depression (Duman et al., 2016), and Alzheimer's disease (Di Lorenzo et al., 2016) patients also exhibited cortical function changes and plasticity deficits. This suggested that cortical functioning or ability of cortical modulation were blunted in these diseases. It is highly plausible that certain type of molecules (e.g., GluN3A) are involved in development and progression of these diseases (Pérez-Otaño et al., 2016); it is also possible that there are different factors altered in these diseases, though converged into the commonality of plasticity deficits. In addition, the circulating BDNF or neurotransmitter levels could be similar across different cortical areas, due to the diffusion with cerebrospinal fluid, resulting in changes of both motor cortex and other cortical areas simultaneously. These possibilities are worth of future investigation.

## AUTHOR CONTRIBUTIONS

All authors listed have made a substantial, direct and intellectual contribution to the work, and approved it for publication.

## FUNDING

The study was supported by the Major Science and Technology Projects in Ningbo, Zhejiang Province, China (2017C50063), and the Medical Science and Technology Project in Ningbo (2017A37).

## REFERENCES

Diana, M., Raij, T., Melis, M., Nummenmaa, A., Leggio, L., and Bonci, A. (2017). Rehabilitating the addicted brain with transcranial magnetic stimulation. *Nat. Rev. Neurosci.* 18, 685–693. doi: 10.1038/nrn.2017.113

Di Lorenzo, F., Ponzo, V., Bonnì, S., Motta, C., Negrao Serra, P. C., Bozzali, M., et al. (2016). Long-term potentiation-like cortical plasticity is disrupted in Alzheimer's disease patients independently from age of onset. *Ann. Neurol.* 80, 202–210. doi: 10.1002/ana.24695

Duman, R. S., Aghajanian, G. K., Sanacora, G., and Krystal, J. H. (2016). Synaptic plasticity and depression: new insights from stress and rapid-acting antidepressants. *Nat. Med.* 22, 238–249. doi: 10.1038/nm.4050

Etkin, A. (2016). Impaired cortical plasticity in drug abuse. *Sci. Transl. Med.* 8:ec113. doi: 10.1126/scitranslmed.aah3544

Everitt, B. J., and Robbins, T. W. (2005). Neural systems of reinforcement for drug addiction: from actions to habits to compulsion. *Nat. Neurosci.* 8, 1481–1489. doi: 10.1038/nn1579

Fitzgerald, P. B., Brown, T. L., Marston, N. A., Oxley, T., De Castella, A., Daskalakis, Z. J., et al. (2004). Reduced plastic brain responses in schizophrenia: a transcranial magnetic stimulation study. *Schizophr. Res.* 71, 17–26. doi: 10.1016/j.schres.2004.01.018

Huang, X., Chen, Y. Y., Shen, Y., Cao, X., Li, A., Liu, Q., et al. (2017). Methamphetamine abuse impairs motor cortical plasticity and function. *Mol. Psychiatry* 22, 1274–1281. doi: 10.1038/mp.2017.143

Huang, Y. Z., Edwards, M. J., Rounis, E., Bhatia, K. P., and Rothwell, J. C. (2005). Theta burst stimulation of the human motor cortex. *Neuron* 45, 201–206. doi: 10.1016/j.neuron.2004.12.033

Li Voti, P., Conte, A., Suppa, A., Iezzi, E., Bologna, M., Aniello, M. S., et al. (2011). Correlation between cortical plasticity, motor learning and BDNF genotype in healthy subjects. *Exp. Brain Res.* 212, 91–99. doi: 10.1007/s00221-011-2700-5

Lüscher, C., and Malenka, R. C. (2011). Drug-evoked synaptic plasticity in addiction: from molecular changes to circuit remodeling. *Neuron* 69, 650–663. doi: 10.1016/j.neuron.2011.01.017

Mameli, M., Bellone, C., Brown, M. T., and Lüscher, C. (2011). Cocaine inverts rules for synaptic plasticity of glutamate transmission in the ventral tegmental area. *Nat. Neurosci.* 14, 414–416. doi: 10.1038/nn.2763

Miniussi, C., and Thut, G. (2010). Combining TMS and EEG offers new prospects in cognitive neuroscience. *Brain Topogr.* 22, 249–256. doi: 10.1007/s10548-009-0083-8

Pérez-Otaño, I., Larsen, R. S., and Wesseling, J. F. (2016). Emerging roles of GluN3-containing NMDA receptors in the CNS. *Nat. Rev. Neurosci.* 17, 623–635. doi: 10.1038/nrn.2016.92

Sanchez, V., Lycas, M. D., Lynch, W. J., and Brunzell, D. H. (2015). Wheel running exercise attenuates vulnerability to self-administer nicotine in rats. *Drug Alcohol Depend.* 156, 193–198. doi: 10.1016/j.drugalcdep.2015.09.022

Shen, Y., Cao, X., Shan, C., Dai, W., and Yuan, T. F. (2017). Heroin Addiction impairs human cortical plasticity. *Biol. Psychiatry* 81, e49–e50. doi: 10.1016/j.biopsych.2016.06.013

Shen, Y., Cao, X., Tan, T., Shan, C., Wang, Y., Pan, J., et al. (2016). 10-Hz repetitive transcranial magnetic stimulation of the left dorsolateral prefrontal cortex reduces heroin cue craving in long-term addicts. *Biol. Psychiatry* 80, e13–e14. doi: 10.1016/j.biopsych.2016.02.006

Willuhn, I., and Steiner, H. (2006). Motor-skill learning-associated gene regulation in the striatum: effects of cocaine. *Neuropsychopharmacology* 31, 2669–2682. doi: 10.1038/sj.npp.1300995

Yalachkov, Y., Kaiser, J., and Naumer, M. J. (2010). Sensory and motor aspects of addiction. *Behav. Brain Res.* 207, 215–222. doi: 10.1016/j.bbr.2009.09.015

Zhou, D., Pang, F., Liu, S., Shen, Y., Liu, L., Fang, Z., et al. (2017). Altered motor-striatal plasticity and cortical functioning in patients with schizophrenia. *Neurosci. Bull.* 33, 307–311. doi: 10.1007/s12264-016-0079-9

**Conflict of Interest Statement:** The authors declare that the research was conducted in the absence of any commercial or financial relationships that could be construed as a potential conflict of interest.

frontiers in Human Neuroscience

ORIGINAL RESEARCH
published: 01 December 2017
doi: 10.3389/fnhum.2017.00579

# Psychopathy Moderates the Relationship between Orbitofrontal and Striatal Alterations and Violence: The Investigation of Individuals Accused of Homicide

*Bess Y. H. Lam[1]*, Yaling Yang[2], Robert A. Schug[3], Chenbo Han[4], Jianghong Liu[5] and Tatia M. C. Lee[6,7,8]**

*[1] Department of Rehabilitation Sciences, The Hong Kong Polytechnic University, Hung Hom, Hong Kong, [2] Department of Pediatrics, University of Southern California, Los Angeles, CA, United States, [3] School of Criminology and Criminal Justice, California State University, Long Beach, Long Beach, CA, United States, [4] Nanjing Brain Hospital, Nanjing Medical University, Nanjing, China, [5] School of Nursing, University of Pennsylvania, Philadelphia, PA, United States, [6] Laboratory of Neuropsychology, The University of Hong Kong, Pok Fu Lam, Hong Kong, [7] Laboratory of Cognitive Affective Neuroscience, The University of Hong Kong, Pok Fu Lam, Hong Kong, [8] The State Key Laboratory of Brain and Cognitive Sciences, The University of Hong Kong, Pok Fu Lam, Hong Kong*

OPEN ACCESS

**Edited by:**
*Xiaochu Zhang, University of Science and Technology of China, China*

**Reviewed by:**
*Juan Hou, Anhui University, China*
*Kai Wang, Anhui Medical University, China*
*Yat-Fan Nicolson Siu, Hong Kong Shue Yan University, Hong Kong*

***Correspondence:**
*Bess Y. H. Lam*
*bess0127@gmail.com*
*Tatia M. C. Lee*
*tmclee@hku.hk*

**Received:** *05 July 2017*
**Accepted:** *16 November 2017*
**Published:** *01 December 2017*

**Citation:**
*Lam BYH, Yang Y, Schug RA, Han C, Liu J and Lee TMC (2017) Psychopathy Moderates the Relationship between Orbitofrontal and Striatal Alterations and Violence: The Investigation of Individuals Accused of Homicide. Front. Hum. Neurosci. 11:579. doi: 10.3389/fnhum.2017.00579*

Brain structural abnormalities in the orbitofrontal cortex (OFC) and striatum (caudate and putamen) have been observed in violent individuals. However, a uni-modal neuroimaging perspective has been used and prior findings have been mixed. The present study takes the multimodal structural brain imaging approaches to investigate the differential gray matter volumes (GMV) and cortical thickness (CTh) in the OFC and striatum between violent (accused of homicide) and non-violent (not accused of any violent crimes) individuals with different levels of psychopathic traits (interpersonal and unemotional qualities, factor 1 psychopathy and the expressions of antisocial disposition and impulsivity, factor 2 psychopathy). Structural Magnetic Resonance Imaging data, psychopathy and demographic information were assessed in sixty seven non-violent or violent adults. The results showed that the relationship between violence and the GMV in the right lateral OFC varied across different levels of the factor 1 psychopathy. At the subcortical level, the psychopathy level (the factor 1 psychopathy) moderated the positive relationship of violence with both left and right putamen GMV as well as left caudate GMV. Although the CTh findings were not significant, overall findings suggested that psychopathic traits moderated the relationship between violence and the brain structural morphology in the OFC and striatum. In conclusion, psychopathy takes upon a significant role in moderating violent behavior which gives insight to design and implement prevention measures targeting violent acts, thereby possibly mitigating their occurrence within the society.

**Keywords: psychopathy, violence, orbitofrontal cortex, striatum, cortical thickness**

**Abbreviations:** CTh, cortical thickness; GMV, gray matter volumes; lOFC, lateral orbitofrontal cortex; mOFC, medial orbitofrontal cortex; OFC, orbitofrontal cortex; PCL-R, Psychopathy Checklist-Revised; ROI, region of interest; SES, socio-economic status.

## INTRODUCTION

Prior literature has shown that there is a link between brain alterations and antisocial behaviors (Raine and Yang, 2006; Yang and Raine, 2009). However, antisocial individuals itself is an inherently heterogeneous grouping which includes violent offenders, incarcerated and non-incarcerated adults with antisocial personality disorders, as well as individuals possessing different personality traits including psychopathic traits (Glenn and Yang, 2012). With reference to prior literature, offenders with various personality traits are likely to possess differential brain abnormalities (Soderstrom et al., 2002; Bertsch et al., 2013; Contreras-Rodríguez et al., 2015; Santana, 2016). For instance, Contreras-Rodríguez et al. (2015) found that psychopathic individuals had gray matter reduction involving prefrontal cortex, paralimbic, and limbic structures. On the other hand, Bertsch et al. (2013) detected alterations in orbitofrontal and ventromedial prefrontal cortex regions, and the temporal pole in antisocial individuals with borderline personality disorder while they found volumetric reductions in midline cortical areas (e.g., dorsomedial prefrontal cortex) in antisocial individuals with psychopathic traits. Therefore, by examining personality traits, specifically psychopathy in individuals who are violent, we can gain a better understanding of the future risks of antisocial behaviors (Hare, 1991).

Previous brain imaging studies (Yang and Raine, 2009) examined the OFC and striatum in psychopathic and antisocial individuals. For instance, a meta-analysis (Yang and Raine, 2009) had found reduced GMV, and activity in the right prefrontal cortex, including the OFC among antisocial individuals. Moreover, this OFC abnormality was associated with emotional deficits and poor decision-making in these individuals. Alongside with these findings, Blair (2007) also argued that the impairment in medial OFC (mOFC) might explain the dysfunction of flexible behavioral change found in psychopathy. Apart from the prefrontal cortex, the striatum, which is related to reward-seeking, is also a major brain region that is implicated in antisocial individuals (Raine and Yang, 2006). To be specific, dorsal striatum is related to habitual, or response-driven decision making while ventral striatum is generally known as a structure that is important in reward or goal-directed behaviors (O'Doherty et al., 2004; van der Meer et al., 2010). However, the striatum has received much less attention. Regarding the limited prior findings on the striatum, they were inconsistent. For instance, antisocial behaviors were associated with increased striatum GMV and activities (Tiihonen et al., 1995; Barkataki et al., 2006; Gatzke-Kopp et al., 2009; Ducharme et al., 2011; Schiffer et al., 2011). However, opposing results were found in other studies (Barros-Loscertales et al., 2006; Vollm et al., 2007). These inconsistent findings can be explained by the differences in the participants' characteristics (e.g., age) (Gogtay et al., 2004) and the varying definitions of antisocial behavior across studies as well as the variations in personality traits (e.g., Gregory et al., 2012)., Indeed, the literature regarding the OFC also suffered from the same limitation (Blair, 2010; Glenn and Yang, 2012) and most of the studies have focused on GMV which is only one dimension of structural brain characteristics. The present study examined the specific antisocial group-homicide for two major reasons. First, it is suggested that different types of violence have different underlying psychosocial mechanisms (Acierno et al., 1999). However, prior literature investigated homicide along with other types of violence (e.g., rape) (e.g., Gregory et al., 2012). Secondly, homicide causes high financial burden to the criminal justice and mental health system (DeLisi et al., 2010). Hence, the present study studied homicide specifically instead of a variety of violent offenses (e.g., physical assault and rape). Although it is important to study this specific type of violence, prior brain imaging studies pertaining to this group of people are scarce (Raine et al., 1998; Ermer et al., 2013). Specifically, Raine et al. (1998) found that affective murderers had lower left and right prefrontal functioning, higher right hemisphere subcortical functioning, and lower right hemisphere prefrontal/subcortical ratios when compared to the controls. A more recent study (Ermer et al., 2013) suggested that psychopathic traits were related to decreased GMV in diffuse paralimbic regions such as the OFC in incarcerated male adolescents. Taken these results together, regardless of inconsistent findings and the lack of multi-modal neuroimaging methods in prior literature, the OFC and striatum have been the regions of interest (ROIs) for the investigation of antisocial behaviors. To address the literature gap, the present study compared two types of structural brain characteristics (GMV and CTh) between a control group and a homogenous antisocial group with one specific type of antisocial behavior-homicide.

Psychopathy, a 2-factor (interpersonal & unemotional features, and antisocial & impulsive features) personality construct (Hare, 1991; Frick et al., 2003), is a potential moderator of the association between violence and the abnormalities in the striatum and the OFC. There is mounting evidence showing that psychopathy is associated with structural abnormalities in both the OFC (Blair, 2003) and the striatum (Buckholtz et al., 2010; Glenn et al., 2010), as well as with antisocial behaviors. However, prior studies mainly investigated GMV lacking empirical evidences related to CTh in psychopathy. One study (Gregory et al., 2012) revealed that psychopathy moderated the GMV in the anterior rostral prefrontal cortex among violent offenders. Yet, this study did not examine neural correlates other than the GMV. It also treated the construct of psychopathy as one, singular concept (global/total psychopathy score) (Miller et al., 2011). However, since prior findings suggested that OFC GMV was associated with emotion deficits and poor decision- making (Raine and Yang, 2006; Yang and Raine, 2009) and that striatum GMV was associated with antisocial behaviors (Tiihonen et al., 1995; Barkataki et al., 2006; Barros-Loscertales et al., 2006; Vollm et al., 2007; Gatzke-Kopp et al., 2009; Ducharme et al., 2011; Schiffer et al., 2011), each sub-factor of psychopathy should be associated with different neural correlates (Soderstrom et al., 2002; Glenn et al., 2010). In fact, not only that each sub-factor is related to different neural correlates, each is related to different psychosocial correlates (Benning et al., 2003). Given that there are differential neural and psychosocial correlates for the two subtypes of psychopathy, it is essential to investigate both

of them in relation to homicide, respectively, in the present study.

Despite the scarce studies, CTh, which is a structural characteristic of the brain independent from cortical surface or volume variance (Fischl and Dale, 2000), was found to be associated with violence (Narayan et al., 2007) and psychopathy (Ly et al., 2012; Wallace et al., 2014). For instance, right temporal cortical thinning was significantly related to severity of callous-unemotional traits in youths with conduct disorder (Wallace et al., 2014) while violence was related to cortical thinning in the right medial inferior frontal and right lateral sensory motor cortex (Narayan et al., 2007).

All these findings lead to the speculation that the interpersonal and unemotional features of psychopathy (factor 1 psychopathy) would a play a role in modulating the relationship between OFC GMV/CTh and violence while the antisocial and impulsive features (factor 2 psychopathy) would play a role in modulating the relationship between striatum GMV and violence. Hence, the present study aimed to go beyond prior literature by not only examining the global psychopathy (Miller et al., 2011) but also considering psychopathy as a 2-factor personality construct to investigate the relationship between psychopathy and the ROIs.

Taken together, the present study investigated the differential GMV and CTh in the OFC and striatum of violent and non-violent individuals with low and high psychopathy (global and the two psychopathic sub-factors), respectively. It was hypothesized that (1) the global psychopathy would moderate the GMV and CTh in the OFC, as well as the GMV in striatum in violent individuals; and (2) the interpersonal and unemotional features of psychopathy (factor 1 psychopathy) would moderate the GMV and CTh in the OFC, while the antisocial and impulsive features (factor 2 psychopathy) would moderate the GMV in the striatum in violent individuals.

# MATERIALS AND METHODS

## Participants

Sixty seven participants (23 accused of homicide and 44 not accused of any crimes; 56 males and 11 females) aged from 19 to 68 years (mean = 34.09 years) were recruited from Nanjing Brain Hospital in Nanjing, China. Accused murderers were detainees who were undergoing forensic psychiatric evaluation and were considered as violent participants in the present study. Those who were not accused of any crimes were considered as non-violent participants. Twenty eight of the participants were diagnosed with schizophrenia. The cross-tabulation of psychopathy against violence in the present study and more details of the demographic and neural correlates of the participants were shown in **Tables 1** and **2**. University Institutional Review Board (IRB) approval was obtained at the University of Southern California and the Human Research Ethics Committee for Non-clinical Faculties of The University of Hong Kong in accordance with the Declaration of Helsinki. Approval for the study was also obtained at Nanjing Brain Hospital. Informed and written consent was obtained from all participants.

**TABLE 1 |** Cross-tabulation of psychopathy against violence in the present study.

| | Psychopathy (median split) | | |
|---|---|---|---|
| | **Low** | **High** | **Total** |
| Non-violent | 29 | 15 | 44 |
| Violent | 5 | 18 | 23 |
| Total | 34 | 33 | 67 |

## Measures

### Clinical and Major Assessments

Each participant were assessed regarding the lifetime presence of Axis I and Axis II psychopathology using the Chinese Classification of Mental Disorders Version 3 (Chinese Society of Psychiatry, Chinese Medical Association, 2001) and the Diagnostic and Statistical Manual of Mental Disorders (DSM-IV) (American Psychiatric Association, 1994) by a psychiatrist at Nanjing Brain Hospital. The results collected from all participants showed negative regarding both lifetime and current abuse/dependence of substance. Given part of the participants were diagnosed with schizophrenia which may confound with current findings, schizophrenia diagnosis would be controlled for in the analyses of the present study. Moreover, only one participant reported using anti-anxiety medications or anti-depressants.

Psychopathic traits were assessed by PCL-R (Hare, 2003). PCL-R consists of two components: factor 1, which measures personality traits, such as superficial charm, shallow affect and lack of empathy; and factor 2, which measures impulsivity and antisocial behaviors. This 2-factor structure has been well validated across different populations such as female and male criminal offenders as well as male forensic psychiatric patients (Bolt et al., 2004). Also, PCL-R obtained good interrater reliability and internal consistency previously (Vitale et al., 2002) and in the present study ($r = 0.84$). The total/global psychopathy (the summation of factor 1 and factor 2 scores) and the two PCL-R $t$ subscores (factor 1 and factor 2) were computed for analyses in the present study. **Figures 1–3** show the distribution of the global psychopathy $t$ score, factor 1 psychopathy $t$ score and factor 2 psychopathy $t$ score, respectively. The expression of psychopathic traits varies across cultures (Neumann et al., 2012) which may explain why the PCL-R scores were much lower in the current sample when compared to the standard PCL-R cutoff. The full scale of IQ was measured using the Wechsler Adults Intelligence Scale: Revised in China (WAIS-RC) (Gong, 1992). SES was measured according to the scale devised by Hollingshead (Hollingshead, 1975).

### MRI Image Acquisition and Processing

All sMRI data was acquired using a 1.5T GE Signa scanner with a single-shot gradient echo MPRAGE sequence ($TR = 25$ ms, $TE = 6$ ms, field of view = 24 cm × 24 cm, matrix = 256 × 256, flip angle = 45°, thickness = 1.2 mm, 124 continuous sagittal slices without gap). CTh and volumetric segmentation were

**TABLE 2 |** Demographic and neural correlates as a function of violence in the present study.

| | Non-violent ($N = 44$) | Violent ($N = 23$) | Statistics | Total sample |
|---|---|---|---|---|
| **Demographics** | | | | |
| Age (years) | 32.61 (10.18) | 36.91 (14.36) | $t_{65} = -1.42$, $P = 0.16$ | 34.09 (11.85) |
| Gender (% males) | 84.09 | 82.61 | $\chi^2_{1,\ 67} = 0.024$, $P = 0.88$ | 83.6 |
| IQ | 98.45 (16.43) | 86.65 (13.39) | $t_{65} = 2.97$, $P = 0.004$** | 94.4 (16.36) |
| Schizophrenia diagnosis (% yes) | 31.82 | 60.87 | $\chi^2_{1,67} = 5.24$, $P = 0.02$* | 41.8 |
| Whole brain volumes ($\times$1000 mm$^3$) | 1465.78 (125.67) | 1426.12 (109.13) | $t_{65} = 1.28$, $P = 0.21$ | 1452.164 (120.907) |
| Socio-economic status (SES) | 52.16 (20.56) | 60.48 (18.39) | $t_{65} = -1.63$, $P = 0.11$ | 55.01 (20.10) |
| Violence (%yes) | – | – | – | 34.3 |
| **Neural correlates** | | | | |
| mOFC GMV (combined)[a] | 90.34 (10.56) | 86.38 (11.25) | $t_{65} = 1.42$, $P = 0.16$ | 88.98 (10.89) |
| Left[a] | 44.17 (6.24) | 42.37 (5.83) | $t_{65} = 1.15$, $P = 0.25$ | 43.55 (6.12) |
| Right[a] | 46.17 (5.46) | 44.02 (6.15) | $t_{65} = 1.47$, $P = 0.15$ | 45.43 (5.75) |
| lOFC GMV (combined)[a] | 60.29 (8.38) | 54.76 (80.16) | $t_{65} = 2.60$, $P = 0.01$* | 58.39 (8.62) |
| Left[a] | 28.88 (4.06) | 26.18 (4.31) | $t_{65} = 2.53$, $P = 0.01$** | 27.95 (4.31) |
| Right[a] | 31.42 (5.42) | 28.58 (4.32) | $t_{65} = 2.17$, $P = 0.03$* | 30.44 (5.22) |
| Caudate GMV (combined)[a] | 50.75 (8.92) | 48.24 (9.13) | $t_{65} = 1.08$, $P = 0.28$ | 49.89 (9.01) |
| Left[a] | 24.64 (5.73) | 24.28 (5.61) | $t_{65} = 0.25$, $P = 0.81$ | 24.51 (5.65) |
| Right[a] | 26.11 (5.03) | 23.97 (6.15) | $t_{65} = 1.53$, $P = 0.13$ | 25.38 (5.49) |
| Putamen GMV (combined)[a] | 69.51 (16.69) | 65.52 (18.13) | $t_{65} = 0.90$, $P = 0.37$ | 68.14 (17.16) |
| Left[a] | 35.68 (9.81) | 33.22 (8.28) | $t_{65} = 1.03$, $P = 0.31$ | 34.84 (9.33) |
| Right[a] | 33.83 (8.25) | 32.31 (11.81) | $t(65) = 0.61$, $P = 0.54$ | 33.30 (9.56) |
| mOFC CTh (combined)[b] | 5.36 (0.42) | 5.45 (0.35) | $t_{65} = -0.84$, $P = 0.41$ | 5.39 (0.40) |
| Left[b] | 2.75 (0.23) | 2.72 (0.20) | $t_{65} = 0.63$, $P = 0.53$ | 2.74 (0.22) |
| Right[b] | 2.61 (0.24) | 2.73 (0.20) | $t_{65} = -2.04$, $P = 0.05$* | 2.65 (0.24) |
| lOFC CTh (combined)[b] | 5.39 (0.43) | 5.43 (0.25) | $t_{65} = -0.41$, $P = 0.68$ | 5.40 (0.38) |
| Left[b] | 2.71 (0.21) | 2.72 (0.15) | $t_{65} = -0.23$, $P = 0.82$ | 2.72 (0.19) |
| Right[b] | 2.68 (0.25) | 2.71 (0.16) | $t_{65} = -0.49$, $P = 0.63$ | 2.69 (0.23) |

*Numbers in brackets represent the standard deviation (SD); lateral orbitofrontal cortex- lOFC; medial orbitofrontal cortex- mOFC; cortical thickness- CTh; gray matter volumes- GMV.* [a]*($\times$100 mm$^3$);* [b]*($\times$1 mm); *P < = 0.05, **P < = 0.01, ***P < = 0.001.*

estimated using the FreeSurfer software (FreeSurfer 4.0.5[1]) (Dale et al., 1999; Fischl et al., 1999, 2002), which is a widely documented and automated program for the analysis of brain structure (Fischl and Dale, 2000). Moreover, its validation was previously reaffirmed in studies regarding schizophrenia in contrast with manual measurements (Kuperberg et al., 2003).

In short, the FreeSurfer processing streams applied in the present study included three major functions: the removal of non-brain tissue, the segmentation of gray-white matter, and the transformation to a common space (i.e., the Montreal Neurological Institute space), respectively. In terms of volumetric estimation, after the FreeSurfer processing and estimation, GMV of subcortical brain ROIs in the present study including caudate and putamen were further traced manually using BrainSuite (Shattuck and Leahy, 2002), which would correct small errors. Regarding the estimation of CTh, after normalization of the intensity, gray-white tissue segmentation was used as the starting point for a deformable surface algorithm for the extraction of the pial and gray-white cortical surfaces (Dale et al., 1999). Then, the entire cortex of each participant was visually inspected for accuracies. Manual correction, if necessary, would be carried out using procedures that were established previously (Roussotte et al., 2011). After spatial normalization of the data, converting it to a cortical surface-based atlas, local CTh was estimated by calculating the shortest distance between a given point on the estimated pial surface and the gray/white matter boundary across the cortical mantle (Fischl and Dale, 2000). Maps were smoothed across the surface and averaged across participants with a 10-mm full-width at half-maximum Gaussian kernel using a non-rigid high-dimensional spherical averaging method. General linear model (GLM) was performed on the effects of each variable on thickness at each vertex for the statistical comparisons of surface maps (Fischl et al., 1999; Fischl and Dale, 2000).

## Statistical Analysis

The major aim of the present study was to investigate the moderation effect of psychopathic traits in the relationship between structural brain abnormalities (striatum and OFC) and violence. As such, the relationship between these structural brain abnormalities and violence was investigated as a function of psychopathic traits. To be specific, "structural brain abnormalities" refer to the relative differences in terms of the neural correlates between the non-violent group and the violent ones in the present study. By testing the moderation effect, we tested whether the effect of an independent variable (neural

[1]http://surfer.nmr.mgh.harvard.edu

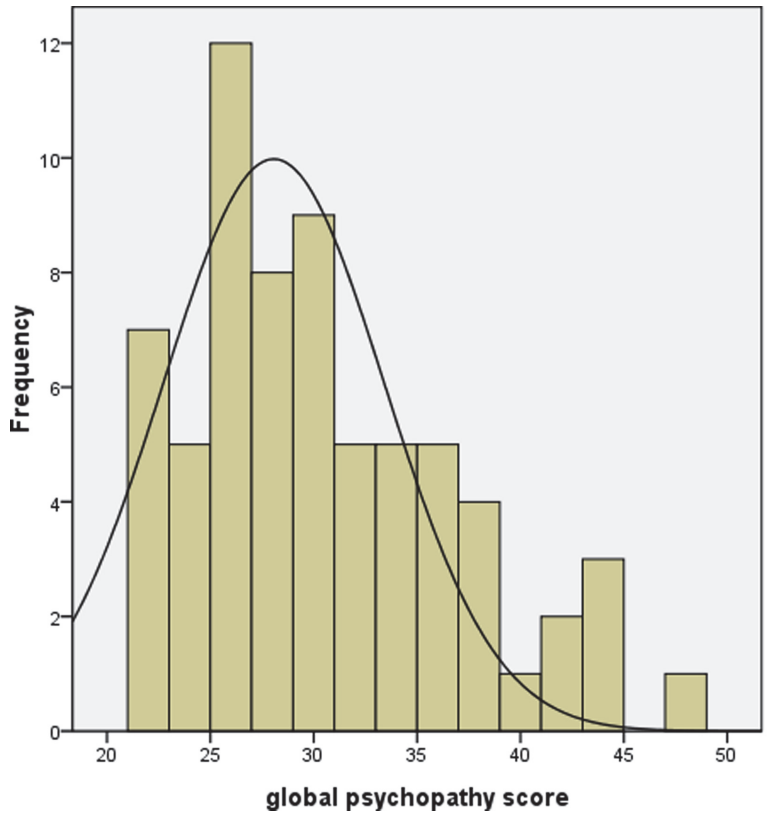


**FIGURE 1 |** The histogram of global psychopathy *t* score (mean = 30.04 (equivalent to 4 as in global psychopathy raw score), standard deviation = 6.36).

correlates) on a dependent variable (violence) varied across the level of a third variable/moderator variable (psychopathy), which interacted with the independent variable (Baron and Kenny, 1986; Edwards and Lambert, 2007). Specifically, we investigated whether the psychopathic personality traits influenced the strength of the relationship between neural correlates and violence. Therefore, the neural correlates were the independent variables and the binary variable (violence vs non-violence) was the outcome variable while the moderator was psychopathy in the present study. The ROIs (striatum and OFC) were chosen based on prior literature as well as the Qdec whole-brain findings in the present study. Based on the GMV/CTh in prior literature and the whole-brain findings devised by the vertex-based analysis using Qdec (a module of FreeSurfer developed to design and execute surface analysis), ROI analyses were performed for the lateral and mOFC (lOFC and mOFC), putamen, and caudate in the present study. The neural correlates of each ROI were computed: (1) total GMV/CTh by the summation of the left and the right hemispheric volumes/CTh; and (2) GMV/CTh by hemisphere. Correlations, between-group *t*-test and chi-square test were used to assess the association of demographic information with violence, psychopathy and neural correlates (**Tables 2**, **3**). Analyses of the ROI neural correlates were performed using SPSS (Chicago, IL, United States ) via employing logistic regressions. Logistic regressions were conducted for the outcome variable (violence), with the psychopathy scores and ROI neural correlates (lOFC, mOFC, caudate and putamen), and the interaction term of the two as the predictors. Significance was set based on a two-tailed alpha level of 0.05 for all tests. IQ and schizophrenia diagnosis were significantly associated with violence in the present study ($P < 0.05$) (**Table 2**) which is consistent with prior findings (Fazel et al., 2009; Diamond et al., 2012). In all analyses, the covariates (age, IQ, sex, SES, schizophrenia diagnosis and whole brain volumes) were controlled for.

# RESULTS

## Psychopathy Global Score

### Cortical Thickness

With the CTh of the lateral and mOFC (lOFC and mOFC) for both the left and the right hemispheres, psychopathy global score and the interaction terms (e.g., lOFC × psychopathy global score) as the dependent variables, the logistic regressions showed that all CTh neural correlates ($P > 0.05$), the psychopathy global score ($P = 0.22$) and all interaction terms ($P > 0.05$) were not significant. Similar results were found without controlling for the covariates of the present study ($P > 0.05$).

### Gray Matter Volumes

With the GMV of lOFC and mOFC, caudate and putamen in both the left and the right hemispheres, psychopathy global score

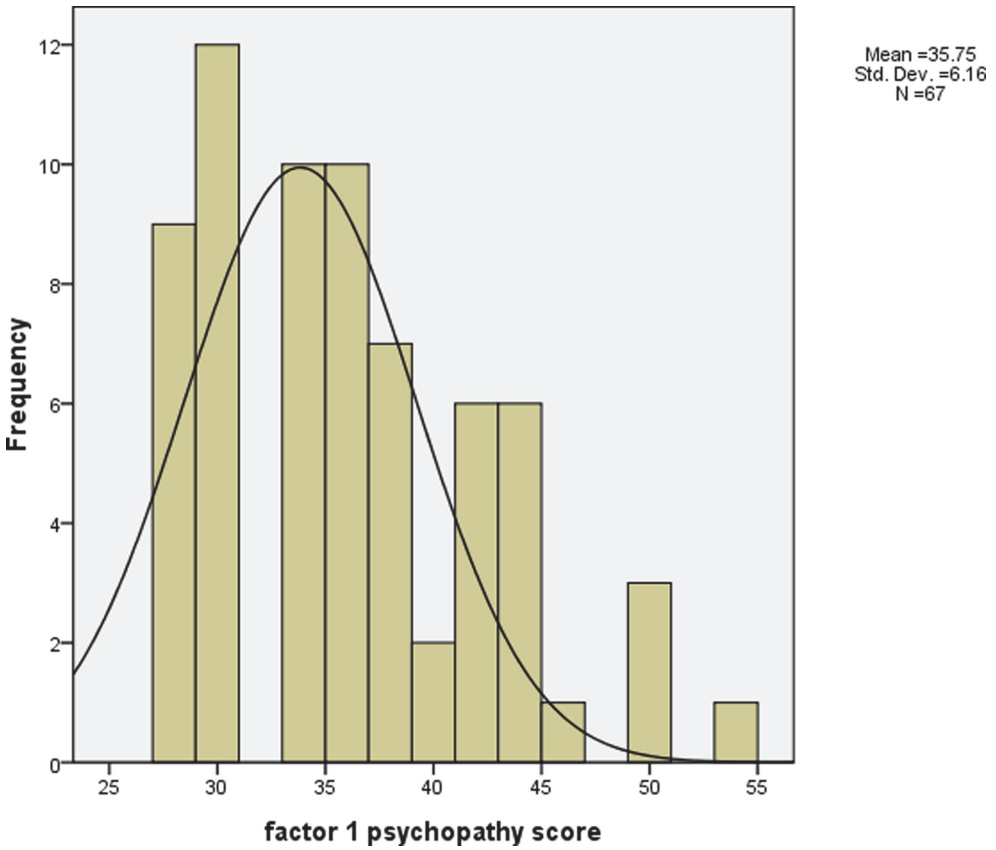


**FIGURE 2 |** The histogram of factor 1 psychopathy *t* score (mean = 35.75 (equivalent to 3 as in factor 1 psychopathy raw score), standard deviation = 6.16).

and the interaction terms (e.g., caudate GMV × psychopathy global score) as the predictors, the logistic regressions showed that all GMV neural correlates ($P > 0.05$), the psychopathy global score ($P = 0.22$) and all interaction terms ($P > 0.05$) were not significant.

## Psychopathy Subscores

### Cortical Thickness

With the CTh of the lateral and mOFC (lOFC and mOFC) for both the left and the right hemispheres, factor 1 psychopathy score and the interaction terms (e.g., lOFC × factor 1 psychopathy score) as the dependent variables, the logistic regressions showed that all CTh neural correlates ($P > 0.05$), the factor 1 psychopathy score ($P = 0.85$) and all interaction terms ($P > 0.05$) were not significant. Similar results were found for the factor 2 psychopathy model ($P > 0.05$).

### Gray Matter Volumes

In terms of the GMV, significant main effects of neural correlates and interaction effects of neural correlates × factor 1 psychopathy (PCL-F1) were found significant in predicting violence. Specifically, the GMV neural correlates (left caudate, left and right putamen; $P < = 0.05$) and interaction terms (left caudate × PCL-F1, left putamen × PCL-F1, right putamen × PCL-F1, and right lOFC × PCL-F1; $P < = 0.05$) were significant in predicting violence. **Table 4** shows the results of logistic regressions with covariates, neural correlates (GMV), factor 1 psychopathy score and the interaction terms predicting violence. These main and interaction effects were not significant for the factor 2 psychopathy model ($P > 0.05$).

# DISCUSSION

The present study undertook a multimodal perspective in the course of investigating the role of psychopathy within the relationship of violence and the OFC and striatum (caudate and putamen). In particular, the moderation effects of the global and sub-factors of psychopathy in the context of such association were investigated with reference to two groups of participants: violent and non-violent individuals. Major findings were only consistent with the second priori hypotheses, which suggested that psychopathic traits (particularly the factor 1 psychopathy) moderated the relationship between violence and the brain structural morphology in the OFC and the striatum. Moreover, the differential results between the GMV and CTh of the OFC suggested that the neural phenotype is more sensitive at the GMV level regarding the role of psychopathy in violence. These findings help us better understand the relationship between brain abnormalities (particularly the OFC and striatum), psychopathy

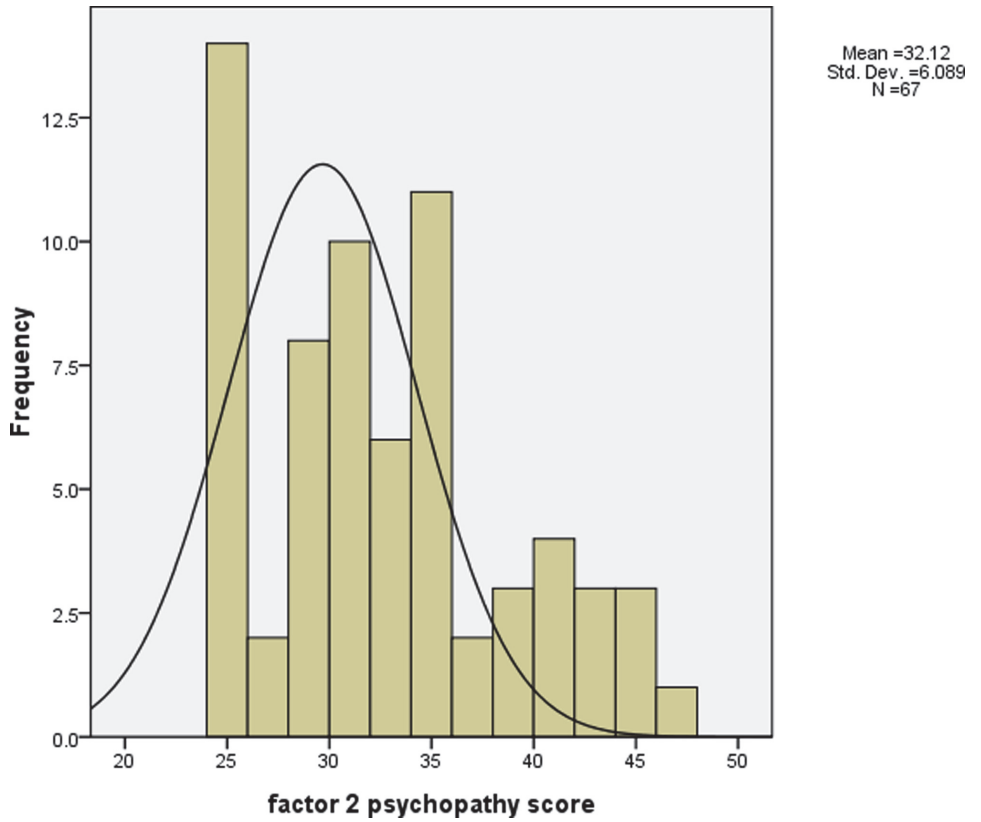


**FIGURE 3 |** The histogram of factor 2 psychopathy *t* score (mean = 32.12 (equivalent to 2 as in factor 2 psychopathy raw score), standard deviation = 6.09).

**TABLE 3 |** Correlations and *t*-values between demographics and total neural correlates.

| | mOFC GMV | lOFC GMV | Caudate GMV | Putamen GMV | mOFC CTh | lOFC CTh |
|---|---|---|---|---|---|---|
| Age (years) | −0.29* | −0.44*** | −0.02 | −0.30* | −0.37** | −0.32** |
| Whole brain volumes (×1000mm$^3$) | 0.61*** | 0.62*** | 0.29* | 0.40*** | 0.07 | −0.06 |
| Socio- economic status (SES) | −0.07 | −0.08 | −0.05 | −0.07 | 0.05 | −0.08 |
| IQ | 0.14 | 0.16 | −0.12 | 0.08 | 0.13 | 0.16 |
| Gender | $t(65) = 2.68$** | $t(65) = 3.08$** | $t(65) = 0.62$ | $t(65) = 1.96$ | $t(65) = 0.43$ | $t(65) = -0.71$ |
| Schizophrenia diagnosis | $t(65) = 1.40$ | $t(65) = 1.85$ | $t(65) = -3.12$** | $t(65) = 0.70$ | $t(65) = 1.47$ | $t(65) = 1.95$ |
| Psychopathy global score | −0.11 | −0.25* | 0.26* | 0.07 | −0.07 | −0.11 |
| Factor 1 psychopathy score | −0.14 | −0.26* | 0.19 | 0.07 | −0.10 | −0.06 |
| Factor 2 psychopathy score | −0.07 | −0.23 | 0.29* | 0.05 | −0.03 | −0.14 |

*Lateral orbitofrontal cortex- lOFC, medial orbitofrontal cortex- mOFC, cortical thickness- CTh, gray matter volumes- GMV. *P < = 0.05, **P < = 0.01, ***P < = 0.001.*

and violence, thus reduce the perpetration of violent crimes in the society potentially.

## Psychopathy as a Moderator

The key findings revealed that psychopathy was a moderator in the association of violence with the GMV in lateral OFC (lOFC) and striatum, its effects are particularly potent in the right hemisphere. This finding was consistent with prior findings suggesting that different personality traits played a significant role in structural brain abnormalities present within violent individuals (Soderstrom et al., 2002; Tiihonen et al., 2008; De Brito et al., 2009; Gregory et al., 2012; Bertsch et al., 2013). More specifically, the factor 1 psychopathy measuring the superficial charm, the shallow affect and the lack of empathy had moderated the association between the right lOFC GMV and violence significantly. These findings suggested that the effect of structural brain abnormality in the right lOFC on the perpetration of violent acts varied across the unemotional aspects of psychopathy. As such, the decrease of the level of unemotional aspects of psychopathy weakened the relationship between GMV in the right lOFC and the risk for the perpetration of violent acts. These findings are consistent with prior findings (Tiihonen et al., 2008; De Brito et al., 2009). Specifically, Tiihonen et al. (2008) found focal, symmetrical, bilateral areas of atrophy in GMV of

**TABLE 4 |** Logistic regressions with covariates (step 1), neural correlates (GMV), psychopathy scores (PCL-F1), and the interaction terms (step 2) predicting violence.

| | Factor 1 psychopathy score (PCL-F1) as the moderator | | | |
|---|---|---|---|---|
| | ***B*** | **Standard error** | **Wald test statistics** | ***P*** |
| **Step 1** | | | | |
| Gender | 0.97 | 0.94 | 1.06 | 0.30 |
| Schizophrenia diagnosis | 1.20 | 0.63 | 3.65 | 0.06 |
| Age | 0.001 | 0.03 | 0.003 | 0.96 |
| SES | 0.02 | 0.02 | 1.37 | 0.24 |
| IQ | −0.04 | 0.02 | 3.49 | 0.06 |
| Whole- brain volume | 0.00 | 0.00 | 1.62 | 0.20 |
| **Step 2** | | | | |
| Gender | 2.09 | 1.74 | 1.45 | 0.23 |
| Schizophrenia diagnosis | 4.35 | 2.51 | 3.02 | 0.08 |
| Age | 0.11 | 0.08 | 2.15 | 0.14 |
| SES | 0.10 | 0.06 | 2.61 | 0.11 |
| IQ | −0.06 | 0.07 | 0.86 | 0.35 |
| Whole- brain volume | 0.00 | 0.00 | 3.71 | 0.05* |
| Left caudate | 0.04 | 0.02 | 3.80 | 0.05* |
| Right caudate | 0.01 | 0.01 | 0.66 | 0.42 |
| Right putamen | −0.06 | 0.03 | 4.76 | 0.03* |
| Left putamen | 0.05 | 0.02 | 5.02 | 0.03* |
| Left mOFC | 0.04 | 0.02 | 2.87 | 0.09 |
| Right mOFC | 0.05 | 0.03 | 2.93 | 0.09 |
| Left lOFC | −0.09 | 0.05 | 3.64 | 0.06 |
| Right lOFC | −0.05 | 0.02 | 3.52 | 0.06 |
| PCL- F1/F2 | 3.54 | 2.02 | 3.08 | 0.08 |
| Left caudate × PCL-F1 | −0.001 | 0.001 | 4.05 | 0.04* |
| Right caudate × PCL- F1 | 0.00 | 0.00 | 0.76 | 0.38 |
| Right putamen × PCL- F1 | 0.00 | 0.00 | 4.82 | 0.03* |
| Left putamen × PCL- F1 | −0.001 | 0.001 | 5.01 | 0.03* |
| Left mOFC × PCL- F1 | 0.00 | 0.001 | 2.50 | 0.11 |
| Right mOFC × PCL- F1 | −0.001 | 0.001 | 2.86 | 0.09 |
| Left lOFC × PCL- F1 | 0.002 | 0.001 | 3.68 | 0.06 |
| Right lOFC × PCL- F1 | 0.001 | 0.001 | 3.73 | 0.05* |

*Lateral orbitofrontal cortex- lOFC, medial orbitofrontal cortex- mOFC, gray matter volumes- GMV. *P < = 0.05, **P < = 0.01, ***P < = 0.001.*

the post-central gyri, frontopolar cortex, and OFC among the offenders when compared with the healthy male counterparts. Along the same line, De Brito et al. (2009) found increased GMV in the OFC and anterior cingulate cortices, as well as increased GMV in the temporal lobes bilaterally among the boys with callous- unemotional conduct problems when compared with healthy boys. It was suggested that the abnormality in OFC GMV in psychopathy and violence was due to the delay in cortical maturation in these brain areas which are involved in decision making, morality and empathy (De Brito et al., 2009). However, there was no significant finding observed for the mOFC. This might be due to the fact that lOFC and mOFC serve different functions (Iversen and Mishkin, 1970). In terms of neuroanatomical functions, OFC as a whole is involved in monitoring reward values. Specifically, lOFC is responsible for the suppression of a response that is previously associated with reward as well as the mediation of the fight-flight response to threat (Elliott et al., 2000; Blair, 2001). The significant association between the lOFC GMV and violence found in the present study suggests the dysfunctions in lOFC lead to the inability to suppress the perpetration of violence. On the other hand, mOFC is related to instrumental learning (LaPierre et al., 1995), moral reasoning (Koenigs et al., 2007) and flexible behavioral change (Blair, 2007). The present study found no significant relationship between mOFC GMV and violence which may be because the perpetration of violence is not involved in the learning process subserved by mOFC.

As for the striatum, the results showed that the association of striatum (left and right putamen and left caudate) GMV with violence varied across psychopathy, which had already been anticipated (Glenn et al., 2010). To be specific, the association between the left caudate, left and right putamen GMV and violence varied across the level of psychopathy, especially the factor 1 psychopathy (unemotional aspects of psychopathy). This finding suggested that the level of unemotional aspects of psychopathy moderated the association between the right putamen GMV and the likelihood of perpetration of violent acts. This supported prior findings, in which it was the concurred

stance that psychopathy was the moderator in the relationship between brain abnormalities and violence (Soderstrom et al., 2002; Bertsch et al., 2013). However, the present finding regarding the striatum was inconsistent with a prior finding by Gregory et al. (2012). This might be because in the case of the precedent (e.g., Gregory et al., 2012), violent participants having committed a variety of violent offenses, including murder, rape and grievous bodily harm were examined; whereas the current study indexed violence by a homogenous group wherein participants who were accused only of homicide. Various types of violence have different underlying psychosocial mechanisms (Acierno et al., 1999) and these mechanisms may be reflecting different corresponding neural correlates. This may be the reason why no significant finding was found for striatum by Gregory et al. (2012) when a variety of violent acts were analyzed altogether while the present study found significant results in studying homicide alone. Taken all of the above findings together, the significant moderation effect of psychopathy on the relationship of structural abnormalities in the lOFC and striatum with violence suggested that reducing psychopathy could potentially protect against the perpetration of violent crimes. Future studies could perhaps look into this hypothesis, as it would likely facilitate the design of policies and measures of intervention and prevention in order to reduce the occurrence of violent activities in the society.

Nevertheless, how the cortical neural correlates (GMV/CTh of the OFC) related to violence did not vary according to the antisocial and impulsive psychopathic traits (factor 2). In addition to that, the antisocial and impulsive psychopathic trait (factor 2) was not a moderator in the relationship between the striatal neural correlates (GMV of the putamen/caudate) and violence. In short, these findings suggest that each sub-factor of psychopathy plays a specific role in the relationship of brain abnormalities and violence.

## Lateralization of the ROIs

It was observed that psychopathic traits moderated the OFC GMV in the right, but not the left hemisphere in the present study. This suggested that psychopathy might play a significant effect on the structure of the brain, particularly in the OFC GMV within violent individuals in the right hemisphere. This might be because antisocial behavior is related to the right-sided prefrontal pathology. Specifically, Tranel et al. (2002) opined that impairment in social conduct, decision-making, emotional processing and personality is only present in people with lesions to their right, but not the left OFC. However, the underlying mechanism of such a right-sided pathology in relation to antisocial behavior and psychopathy is yet to be investigated in future studies.

## Cortical Thickness and Gray Matter Volumes

The differential findings between the GMV and CTh of the OFC suggest that the role of psychopathy in violence might be more significant at the level of GMV when compared to the CTh. In fact, CTh is a structural characteristic of the brain, which is independent from cortical surface or volume variance (Fischl and Dale, 2000). More specifically, it is derived from a surface modeling (unfolding and flattening) (Fischl and Dale, 2000). There are a number of advantages in using this technique in comparison with the GMV measure. For instance, the measure of CTh was deemed more sensitive in neurodegenerative diseases such as in Parkinson's disease (Pereira et al., 2012). Also, the pre-processing steps for this technique enable a better inter-subject registration for matching homologous cortical regions (Fischl et al., 1999). However, it appears that the GMV is more sensitive in examining psychopathy and violence with the present findings. Future studies should further attest to this speculation.

## Limitations

Although this was the first study to investigate how psychopathy moderated the OFC/striatum in terms of their GMV and CTh regarding violence, this study suffered from a number of limitations. Firstly, the majority of the participants were males. There has been evidence showing the difference in gender may lead to alterations in the neurological functions within antisocial individuals (Raine et al., 2011). Although the genders of the test participants were controlled for in all the analyses in the present study, future studies should recruit an equal number of male and female participants. Secondly, the information of attempted homicide and history of violent assaults (not necessarily fatal) as well as convicted homicide was not recorded in the present study. Since it is possible that the "non-violent" participants attempted homicide and were never caught or charged, the non-violent group may include the "attempted but not accused" murderers. Also, the violent group may include the "innocent" murderers. Although the conviction rate of crime has remained high (∼99%) in China, future studies should address the concern regarding attempted and convicted homicide. Moreover, violence was indexed only by homicide accusation in the present study, the history of non-fatal violent assault may also be taken into consideration in future studies. Furthermore, current findings were based on cross-sectional data. However, we hypothesized this moderated relationship based on prior literature with longitudinal data (Raine and Yang, 2006; Yang and Raine, 2009). All in all, the moderated relationship found in the present study helps to set a good foundation for future studies to confirm such a relationship with longitudinal data. Last but not least, the current findings were based on a modest sample size. However, given that the results regarding CTh and GMV in the OFC did not converge, future studies with a bigger sample size should further analyze and investigate such a difference.

# CONCLUSION

In spite of the limitations, the present study should be credited for some of its strength. For instance, the participants were all free from current/lifetime substance abuse or dependence, which would have otherwise complicated the structural abnormalities in the brain in relation to antisocial behaviors (Glenn and Yang, 2012). Also, the authors had furthered the findings of prior literature with their study of both CTh and GMV in both cortical and subcortical brain regions. Most importantly,

the violent/non-violent individuals were stratified according to their level of psychopathy, specifically their global and sub-factors of psychopathy. This could have helped us better understand how different psychopathic traits were related to violence and specific brain regions. In summary, the present findings help us better understand the relationship between abnormalities in the brain (particularly in the OFC and striatum), psychopathy and violence, which is essential to the designing and development of intervention measures in order to mitigate the occurrence of crime. For example, since psychopathy is suggested to moderate the association among the abnormalities in the lOFC/striatum, implementing preventive programs such as the Violence Reduction Program (Wong and Gordon, 2013), which target psychopathy, may potentially reduce the incidence of violent crimes in the society.

## AUTHOR CONTRIBUTIONS

All authors designed the study. BL analyzed the data and wrote the first draft of the manuscript. TL and YY supervised the research project and critically revised the manuscript. All authors contributed to and have approved the final manuscript.

## ACKNOWLEDGMENTS

This work was supported by The University of Hong Kong Endowed Professorship in Neuropsychology; and a Zumberge Interdisciplinary Research Grant from the University of Southern California to Adrian Raine.

## REFERENCES

Acierno, R., Resnick, H., Kilpatrick, D. G., Saunders, B., and Best, C. L. (1999). Risk factors for rape, physical assault, and posttraumatic stress disorder in women: examination of differential multivariate relationships. *J. Anxiety Disord.* 13, 541–563. doi: 10.1016/S0887-6185(99)00030-4

American Psychiatric Association (1994). *Diagnostic and Statistical Manual of Mental Disorders*, 4th Edn. Washington, DC: American Psychiatric Press.

Barkataki, I., Kumari, V., Das, M., Taylor, P., and Sharma, T. (2006). Volumetric structural brain abnormalities in men with schizophrenia or antisocial personality disorder. *Behav. Brain Res.* 169, 239–247. doi: 10.1016/j.bbr.2006.01.009

Baron, R. M., and Kenny, D. A. (1986). The moderator–mediator variable distinction in social psychological research: conceptual, strategic, and statistical considerations. *J. Pers. Soc. Psychol.* 5, 1173–1182. doi: 10.1037/0022-3514.51.6.1173

Barros-Loscertales, A., Meseguer, V., Sanjuan, A., Belloch, V., Parcet, M. A., Torrubia, R., et al. (2006). Striatum gray matter reduction in males with an overactive behavioral activation system. *Eur. J. Neurosci.* 24, 2071–2074. doi: 10.1111/j.1460-9568.2006.05084.x

Benning, S. D., Patrick, C. J., Hicks, B. M., Blonigen, D. M., and Krueger, R. F. (2003). Factor structure of the psychopathic personality inventory: validity and implications for clinical assessment. *Psychol. Assess.* 15, 340–350. doi: 10.1037/1040-3590.15.3.340

Bertsch, K., Grothe, M., Prehn, K., Vohs, K., Berger, C., Hauenstein, K., et al. (2013). Brain volumes differ between diagnostic groups of violent criminal offenders. *Eur. Arch. Psychiatry Clin. Neurosci.* 263, 593–606. doi: 10.1007/s00406-013-0391-6

Blair, R. J. R. (2001). Neuro-cognitive models of aggression, the antisocial personality disorders and psychopathy. *J. Neurol. Neurosurg. Psychiatry* 71, 727–731. doi: 10.1136/jnnp.71.6.727

Blair, R. J. R. (2003). Neurobiological basis of psychopathy. *Br. J. Psychiatry* 182, 5–7. doi: 10.1192/bjp.182.1.5

Blair, R. J. R. (2007). Dysfunctions of medial and lateral orbitofrontal cortex in psychopathy. *Ann. N. Y. Acad. Sci.* 1121, 461–479. doi: 10.1196/annals.1401.017

Blair, R. J. R. (2010). Neuroimaging of psychopathy and antisocial behavior: a targeted review. *Curr. Psychiatry Rep.* 12, 76–82. doi: 10.1007/s11920-009-0086-x

Bolt, D. M., Hare, R. D., Vitale, J. E., and Newman, J. P. (2004) A multigroup item response theory analysis of the psychopathy checklist-revised. *Psychol. Assess.* 16, 155–168. doi: 10.1037/1040-3590.16.2.155

Buckholtz, J. W., Treadway, M. T., Cowan, R. L., Woodward, N. D., Benning, S. D., Li, R., et al. (2010). Mesolimbic dopamine reward system hypersensitivity in individuals with psychopathic traits. *Nat. Neurosci.* 13, 419–421. doi: 10.1038/nn.2510

Chinese Society of Psychiatry, Chinese Medical Association (2001). *Chinese Classification and Diagnostic Criteria of Mental Diseases (in Chinese)*, 3rd Edn. Jinan: Shandong Science and Technology Press.

Contreras-Rodríguez, O., Pujol, J., Batalla, I., Harrison, B. J., Soriano-Mas, C., Deus, J., et al. (2015). Functional connectivity bias in the prefrontal cortex of psychopaths. *Biol. Psychiatry* 78, 647–655. doi: 10.1016/j.biopsych.2014.03.007

Dale, A. M., Fischl, B., and Sereno, M. I. (1999). Cortical surface-based analysis – I.Segmentation and surface reconstruction. *Neuroimage* 9, 179–194. doi: 10.1006/nimg.1998.0395

De Brito, S. A., Mechelli, A., Wilke, M., Laurens, K. R., Jones, A. P., Barker, G. J., et al. (2009). Size matters: increased grey matter in boys with conduct problems and callous–unemotional traits. *Brain* 132, 843–852. doi: 10.1093/brain/awp011

DeLisi, M., Kosloski, A., Sween, M., Hachmeister, E., Moore, M., and Drury, A. (2010). Murder by numbers: monetary costs imposed by a sample of homicide offenders. *J. Forens. Psychiatry Psychol.* 21, 501–513. doi: 10.1080/14789940903564388

Diamond, B., Morris, R. G., and Barnes, J. C. (2012). Individual and group IQ predict inmate violence. *Intelligence* 40, 115–122. doi: 10.1016/j.intell.2012.01.010

Ducharme, S., Hudziak, J. J., Botteron, K. N., Ganjavi, H., Lepage, C., Collins, D. L., et al. (2011). Right anterior cingulate cortical thickness and bilateral striatal volume correlate with child behavior checklist aggressive behavior scores in healthy children. *Biol. Psychiatry* 70, 283–290. doi: 10.1016/j.biopsych.2011.03.015

Edwards, J. R., and Lambert, L. S. (2007). Methods for integrating moderation and mediation: a general analytical framework using moderated path analysis. *Psychol. Methods* 12, 1–22. doi: 10.1037/1082-989X.12.1.1

Elliott, R., Dolan, R. J., and Frith, C. D. (2000). Dissociable functions in the medial and lateral orbitofrontal cortex: evidence from human neuroimaging studies. *Cereb. Cortex* 10, 308–317. doi: 10.1093/cercor/10.3.308

Ermer, E., Cope, L. M., Nyalakanti, P. K., Calhoun, V. D., and Kiehl, K. A. (2013). Aberrant paralimbic gray matter in incarcerated male adolescents with psychopathic traits. *J. Am. Acad. Child Adolesc. Psychiatry* 52, 94–103. doi: 10.1016/j.jaac.2012.10.013

Fazel, S., Gulati, G., Linsell, L., Geddes, J. R., and Grann, M. (2009). Schizophrenia and violence: systematic review and meta-analysis. *PLOS Med.* 6:e1000120. doi: 10.1371/journal.pmed.1000120

Fischl, B., and Dale, A. M. (2000). Measuring the thickness of the human cerebral cortex from magnetic resonance images. *Proc. Natl. Acad. Sci. U.S.A.* 97, 11050–11055. doi: 10.1073/pnas.200033797

Fischl, B., Salat, D. H., Busa, E., Albert, M., Dieterich, M., Haselgrove, C., et al. (2002). Whole brain segmentation: automated labeling of neuroanatomical structures in the human brain. *Neuron* 33, 341–355. doi: 10.1016/S0896-6273(02)00569-X

Fischl, B., Sereno, M. I., and Dale, A. M. (1999). Cortical surface-based analysis. II: inflation, flattening, and a surface-based coordinate system. *Neuroimage* 9, 195–207. doi: 10.1006/nimg.1998.0396

Frick, P. J., Cornell, A. H., Barry, C. T., Bodin, S. D., and Dane, H. E. (2003). Callous-unemotional traits and conduct problems in the prediction of conduct

problem severity, aggression, and self-report of delinquency. *J. Abnorm. Child Psychol.* 31, 457–470. doi: 10.1023/A:1023899703866

Gatzke-Kopp, L. M., Beauchaine, T. P., Shannon, K. E., Chipman, J., Fleming, A. P., Crowell, S. E., et al. (2009). Neurological correlates of reward responding in adolescents with and without externalizing behavior disorders. *J. Abnorm. Child Psychol.* 118, 203–213. doi: 10.1037/a0014378

Glenn, A. L., Raine, A., Yaralian, P. S., and Yang, Y. (2010). Increased volume of the striatum in psychopathic individuals. *Biol. Psychiatry* 67, 52–58. doi: 10.1016/j.biopsych.2009.06.018

Glenn, A. L., and Yang, Y. (2012). The potential role of the striatum in antisocial behavior and psychopathy. *Biol. Psychiatry* 72, 817–822. doi: 10.1016/j.biopsych.2012.04.027

Gogtay, N., Giedd, J. N., Lusk, L., Hayashi, K. M., Greenstein, D., Vaituzis, A. C., et al.. (2004). Dynamic mapping of human cortical development during childhood through early adulthood. *Proc. Natl. Acad. Sci. U.S.A.* 101, 8174–8179. doi: 10.1073/pnas.0402680101

Gong, Y. X. (1992) *Manual for the Wechsler Adults Intelligence Scale: Revised in China*, 2nd Edn. Hunan Medical College, Changsha.

Gregory, S., Ffytche, D., Simmons, A., Kumari, V., Howard, M., Hodgins, S., et al. (2012). The antisocial brain: psychopathy matters. *Arch. Gen. Psychiatry* 69, 962–972. doi: 10.1001/archgenpsychiatry.2012.222

Hare, R. D. (1991). *The Hare Psychopathy Checklist-Revised*. Toronto: Multi-Health Systems.

Hare, R. D. (2003). *Hare Psychopathy Checklist- Revised. 2*. Multi-Health Systems, Toronto.

Hollingshead, A. B. (1975). *Four Factor Index of Social Status*. New Haven, CT: Yale University.

Iversen, S. D., and Mishkin, M. (1970). Perseverative interference in monkeys following selective lesions of the inferior prefrontal convexity. *Exp. Brain Res.* 11, 376–386. doi: 10.1007/BF00237911

Koenigs, M., Young, L., Adolphs, R., Tranel, D., Cushman, F., Hauser, M., et al. (2007). Damage to the prefrontal cortex increases utilitarian moral judgements. *Nature* 446, 908–911. doi: 10.1038/nature05631

Kuperberg, G. R., Broome, M. R., McGuire, P. K., David, A. S., Eddy, M., Ozawa, F., et al. (2003). Regionally localized thinning of the cerebral cortex in schizophrenia. *Arch. Gen. Psychiatry* 60, 878–888. doi: 10.1001/archpsyc.60.9.878

LaPierre, D., Braun, C. M. J., and Hodgins, S. (1995). Ventral frontal deficits in psychopathy: neuropsychological test findings. *Neuropsychologia* 33, 139–151. doi: 10.1016/0028-3932(94)00110-B

Ly, M., Motzkin, J. C., Philippi, C. L., Kirk, G. R., Newman, J. P., Kiehl, K. A., et al. (2012). Cortical thinning in psychopathy. *Am. J. Psychiatry* 169, 743–749. doi: 10.1176/appi.ajp.2012.11111627

Miller, J. D., Jones, S. E., and Lynam, D. R. (2011). Psychopathic traits from the perspective of self and informant reports: Is there evidence for a lack of insight? *J. Abnorm. Psychol.* 120, 758–764. doi: 10.1037/a0022477

Narayan, V. M., Narr, K. L., Kumari, V., Woods, R. P., Thompson, P. M., Toga, A. W., et al. (2007). Regional cortical thinning in subjects with violent antisocial personality disorder or schizophrenia. *Am. J. Psychiatry* 164, 1418–1427. doi: 10.1176/appi.ajp.2007.06101631

Neumann, C. S., Schmitt, D. S., Carter, R., Embley, I., and Hare, R. D. (2012). Psychopathic traits in females and males across the globe. *Behav. Sci. Law* 30, 557–574. doi: 10.1002/bsl.2038

O'Doherty, J., Dayan, P., Schultz, J., Deichmann, R., Friston, K., and Dolan, R. J. (2004). Dissociable roles of ventral and dorsal striatum in instrumental conditioning. *Science* 304, 452–454. doi: 10.1126/science.1094285

Pereira, J. B., Ibarretxe-Bilbao, N., Marti, M. J., Compta, Y., Junqué, C., Bargallo, N., et al. (2012). Assessment of cortical degeneration in patients with Parkinson's disease by voxel-based morphometry, cortical folding, and cortical thickness. *Hum. Brain Mapp.* 33, 2521–2534. doi: 10.1002/hbm.21378

Raine, A., Meloy, J. R., Bihrle, S., Stoddard, J., LaCasse, L., and Buchsbaum, M. S. (1998). Reduced prefrontal and increased subcortical brain functioning assessed using positron emission tomography in predatory and affective murderers. *Behav. Sci. Law* 16, 319–332. doi: 10.1002/(SICI)1099-0798(199822)16:3<319::AID-BSL311>3.0.CO;2-G

Raine, A., and Yang, Y. (2006). Neural foundations to moral reasoning and antisocial behavior. *Soc. Cogn. Affect. Neurosci.* 1, 203–213. doi: 10.1093/scan/nsl033

Raine, A., Yang, Y., Narr, K. L., and Toga, A. W. (2011). Sex differences in orbitofrontal gray as a partial explanation for sex differences in antisocial personality. *Mol. Psychiatry* 16, 227–236. doi: 10.1038/mp.2009.136

Roussotte, F. F., Sulik, K. K., Mattson, S. N., Riley, E. P., Jones, K. L., Adnams, C. M., et al. (2011). Regional brain volume reductions relate to facial dysmorphology and neurocognitive function in fetal alcohol spectrum disorders. *Hum. Brain Mapp.* 33, 920–937. doi: 10.1002/hbm.21260

Santana, E. J. (2016). The brain of the psychopath: a systematic review of structural neuroimaging studies. *Psychol. Neurosci.* 9, 420–443. doi: 10.1037/pne0000069

Schiffer, B., Muller, B. W., Scherbaum, N., Hodgins, S., Forsting, M., Wiltfang, J., Gizewski, E. R., et al. (2011). Disentangling structural brain alterations associated with violent behavior from those associated with substance use disorders. *Arch. Gen. Psychiatry* 68, 1039–1049. doi: 10.1001/archgenpsychiatry.2011.61

Shattuck, D. W., and Leahy, R. M. (2002) BrainSuite: an automated cortical surface identification tool. *Med. Image Anal.* 8, 129–142. doi: 10.1016/S1361-8415(02)00054-3

Soderstrom, H., Hultin, L., Tullberg, M., Wikkelso, C., Ekholm, S., and Forsman, A. (2002). Reduced frontotemporal perfusion in psychopathic personality. *Psychiatry Res.* 114, 81–94. doi: 10.1016/S0925-4927(02)00006-9

Tiihonen, J., Kuikka, J., Begström, K., Hakola, P., Karhu, J., Ryynänen, O. P. and Föhr, J. (1995). Altered striatal dopamine re-uptake sites in habitually violent and non-violent alcoholics. *Nat. Med.* 1, 654–657. doi: 10.1038/nm0795-654

Tiihonen, J., Rossi, R., Laakso, M. P., Hodgins, S., Testa, C., Perez, J., et al. (2008). Brain anatomy of persistent violent offenders: more rather than less. *Psychiatry Res.* 163, 201–212. doi: 10.1016/j.pscychresns.2007.08.012

Tranel, D., Bechara, A., and Denburg, N. L. (2002). Asymmetric functional roles of right and left ventromedial prefrontal cortices in social conduct, decision-making, and emotional processing. *Cortex* 38, 589–612. doi: 10.1016/S0010-9452(08)70024-8

van der Meer, M. A., Johnson, A., Schmitzer-Torbert, N. C., and Redish, A. D. (2010). Triple dissociation of information processing in dorsal striatum, ventral striatum, and hippocampus on a learned spatial decision task. *Neuron* 67, 25–32. doi: 10.1016/j.neuron.2010.06.023

Vitale, J. E., Smith, S. S., Brinkley, C. A., and Newman, J. P. (2002). The reliability and validity of the psychopathy checklist–revised in a sample of female offenders. *Crim. Justice Behav.* 29, 202–231. doi: 10.1177/0093854802029002005

Vollm, B., Richardson, P., McKie, S., Elliott, R., Dolan, M., and Deakin, B. (2007). Neuronal correlates of reward and loss in Cluster B personality disorders: a functional magnetic resonance imaging study. *Psychiatry Res.* 156, 151–167. doi: 10.1016/j.pscychresns.2007.04.008

Wallace, G. L., White, S. F., Robustelli, B., Sinclair, S., Hwang, S., Martin, A., et al. (2014). Cortical and subcortical abnormalities in youths with conduct disorder and elevated callous-unemotional traits. *J. Am. Acad. Child Adolesc. Psychiatry* 53, 456–465. doi: 10.1016/j.jaac.2013.12.008

Wong, S. C. P., and Gordon, A. (2013). The violence reduction programme: a treatment programme for violence-prone forensic clients. *Psychol. Crime Law* 19, 461–475. doi: 10.1080/1068316X.2013.758981

Yang, Y., and Raine, A. (2009). Prefrontal structural and functional brain imaging findings in antisocial, violent, and psychopathic individuals: a meta-analysis. *Psychiatry Res.* 174, 81–88. doi: 10.1016/j.pscychresns.2009.03.012

**Conflict of Interest Statement:** The authors declare that the research was conducted in the absence of any commercial or financial relationships that could be construed as a potential conflict of interest.

frontiers in Human Neuroscience

ORIGINAL RESEARCH
published: 04 January 2018
doi: 10.3389/fnhum.2017.00640

# Effects of Acute Alcohol Intoxication on Empathic Neural Responses for Pain

*Yang Hu*[1], *Zhuoya Cui*[1], *Mingxia Fan*[2], *Yilai Pei*[1] *and Zhaoxin Wang*[1,2]*

[1] Shanghai Key Laboratory of Brain Functional Genomics, Key Laboratory of Brain Functional Genomics, Ministry of Education, Institute of Cognitive Neuroscience, Shanghai, China, [2] Shanghai Key Laboratory of MRI, East China Normal University, Shanghai, China

The questions whether and how empathy for pain can be modulated by acute alcohol intoxication in the non-dependent population remain unanswered. To address these questions, a double-blind, placebo-controlled, within-subject study design was adopted in this study, in which healthy social drinkers were asked to complete a pain-judgment task using pictures depicting others' body parts in painful or non-painful situations during fMRI scanning, either under the influence of alcohol intoxication or placebo conditions. Empathic neural activity for pain was reduced by alcohol intoxication only in the dorsal anterior cingulate cortex (dACC). More interestingly, we observed that empathic neural activity for pain in the right anterior insula (rAI) was significantly correlated with trait empathy only after alcohol intoxication, along with impaired functional connectivity between the rAI and the fronto-parietal attention network. Our results reveal that alcohol intoxication not only inhibits empathic neural responses for pain but also leads to trait empathy inflation, possibly via impaired top-down attentional control. These findings help to explain the neural mechanism underlying alcohol-related social problems.

**Keywords: alcohol intoxication, pain empathy, fMRI, PPI, trait empathy**

OPEN ACCESS

***Edited by:***
*Xiaochu Zhang,*
*University of Science and Technology of China, China*

***Reviewed by:***
*Daniel Stjepanović,*
*Duke University, United States*
*Jie Zhuang,*
*Duke University, United States*

***Correspondence:**
*Zhaoxin Wang*
*zxwang@nbic.ecnu.edu.cn*

***Received:*** *13 July 2017*
***Accepted:*** *15 December 2017*
***Published:*** *04 January 2018*

***Citation:***
*Hu Y, Cui Z, Fan M, Pei Y and Wang Z (2018) Effects of Acute Alcohol Intoxication on Empathic Neural Responses for Pain. Front. Hum. Neurosci. 11:640. doi: 10.3389/fnhum.2017.00640*

## INTRODUCTION

Alcohol is favored for its acute ability to induce positive affect by activating neural reward systems (Fromme et al., 1999), as well as reduce stress and anxiety (Curtin and Lang, 2007). However, alcohol consumption, especially at high doses, is also associated with severely impaired social abilities, such as more aggressive behavior (Bushman and Cooper, 1990). Denson et al. (2008) has hypothesized that alcohol might increase aggression via a reduction in the ability to identify with and vicariously share the feeling, pain and thoughts of others, i.e., empathy (Denson et al., 2008), as the level of empathy is negatively correlated with the intensity and frequency of violence in sobriety (Miller and Eisenberg, 1988). Empathy is believed to be a key motivator and the proximate mechanism of altruistic and prosocial behavior (Preston and de Waal, 2002; Singer et al., 2006; Moriguchi et al., 2007). Thus, any change in empathy by alcohol consumption will have social implications.

In recent years considerable efforts have been made to investigate the neural correlates of human empathy. The majority of studies used experimental paradigms in which participants were exposed to stimuli depicting or indicating that other people were in pain. Recent imaging studies revealed that empathy for pain recruits a distributed network, including the anterior cingulate cortex (ACC) and bilateral anterior insula (AI), major components of self-pain related "affective

pain matrix" (Jackson et al., 2005; Hein and Singer, 2008; Singer and Lamm, 2009). Alcohol acts mainly as a central nervous system depressant. Previous neuroimaging studies indicated that alcohol dampened activity in the dorsal anterior cingulate cortex (dACC) (Ridderinkhof et al., 2002; Marinkovic et al., 2012) and the bilateral anterior insula (AI) (Padula et al., 2011) in tasks other than empathy. As these three regions that were affected by alcohol consumption are considered the core affective pain matrix of empathy (Lamm et al., 2010a; Fan et al., 2011), we hypothesized that empathic responses for pain in these regions may be reduced, and the three regions that affected by alcohol intoxication (dACC, bilateral AIs) were taken as regions of interest (ROI).

The second question we want to address is whether the effects of trait empathy on the empathic neural responses are altered by alcohol consumption. Interestingly, the majority of empathy studies with sober participants, if not all, have not found any correlation between trait empathy and the activity of the affective pain matrix (Decety, 2011). However, Giancola (2003) demonstrated that trait empathy, the tendency for people to imagine and experience the feelings and experiences of others, has moderating effects on alcohol-related aggression in men and women but not in men and women in sobriety (Giancola, 2003). These results suggest that the effects of trait empathy on behavior was affected by alcohol intoxication, as well as underlying neural correlates.

More important, attention plays an important role in empathy. Previous studies revealed that activity in the affective pain matrix is reduced, even absent, if attention was diverted away (Gu et al., 2010; Lamm et al., 2010b). Thus, activity in the affective pain matrix may be more affected by trait empathy if attention is impaired. The capacity to divide and sustain attention is indeed impaired by alcohol, even at blood-alcohol concentration (BAC) levels of 0.02–0.03% (Koelega, 1995). Therefore, in accordance with Giancola's finding, we predicted empathic neural responses were more affected by trait empathy in the intoxication condition instead of the placebo condition. Our results confirmed this prediction and found that brain activity in the rAI was correlated with trait empathy only in the alcohol condition.

Another intriguing point is that as the affective pain matrix, but not a single brain region, is involved in empathic processing of pain, there are likely interactions between these different brain regions. Noted that functional connection between brain regions that are engaged simultaneously in a task (Rogers et al., 2008) can be affected by task-related parameters (Friston et al., 1997), i.e., psychophysiological interactions (PPI). For example, Friston KJ et al provided an example of physiological interactions in the visual pathway were modulated by attention (Friston et al., 1997). As attention was also impaired by alcohol consumption (Steele and Josephs, 1990; Ridderinkhof et al., 2002; Calhoun et al., 2004; Van Horn et al., 2006; Marinkovic et al., 2012) and that empathic responses for pain were modulated by attention (Gu and Han, 2007), the functional connection between brain regions could be affected by alcohol consumption. To test this hypothesis, we further conducted a psychophysiological interactions (PPI) analysis (Friston et al., 1997) with rAI as the seed in both alcohol and placebo conditions.

# METHODS

## Participants

Twenty-one native Chinese students from East China Normal University (13 males; age = 23.4 ± 2.0 years old) volunteers attended the current study, 16 of them were available for final data analysis (10 males; age = 23.4 ± 2.1 years old). All participants were light or moderate social drinkers (once a week or less, with low quantity and no binging) (Lipton, 1994) and had scores on the Short Michigan Alcoholism Screening Test (SMAST) of <5 (Selzer et al., 1975). Other inclusion criteria were as follows: (1) right-handed with normal or corrected-to-normal vision, normal color perception; (2) no self-reported history of psychiatric or neurological disease, head injury, or drug abuse, and scores on the Beck Depression Index (BDI) were <13 (Beck et al., 1961); and (3) not allergic to orange juice. The participants were paid as compensation for their time. Written informed consent were obtained from all subjects, and the protocol was approved by the University committee on Human Research Protection (UCHRP) at East China Normal University. A power calculation based on the effect size of dACC (Hedges' unbiased d = 0.63 for left dACC and 0.56 for right dACC) reported in a previous study (Marinkovic et al., 2012) was performed using G*Power (Faul et al., 2009), resulting in about 12–16 participants with the power of 0.70. Note that in Marinkovic et al.'s study, the neural basis of alcohol's effects on cognitive control was investigated using a Siemens 3T scanner, we expected the alcohol's effects on the same brain regions using the same type of scanner and the same event-related design be similar.

## Materials

### Stimuli

One-hundred and sixty digital color pictures depicting right hands/feet in painful and non-painful everyday situations (80 each) from first-person perspective were used (e.g., **Figure 1**). The pictures were equally divided into two sets (each set consisted of 40 painful/non-painful pictures), one for the placebo condition and the other for the alcohol condition, and counterbalanced among participants. All pictures were presented twice to increase the signal-to-noise ratio. Among all stimuli, 104 pictures (52 painful pictures) were courtesy of Jackson and Decety (Jackson et al., 2005), and we created another 56 images (28 painful pictures) using a similar style. All pictures were resized to the same resolution (600 × 480 pixels).

### Beverage

Two types of beverages were used, containing either alcohol (0.85 g/kg, alcohol condition) or water (placebo condition) (Ridderinkhof et al., 2002). Body-weight dependent measures of ErGuoTou (one of the China's favorite liquor with a relatively high alcohol percentage, 55 or 56%) or an equal volume of water were dissolved in orange juice such that the total liquid volume

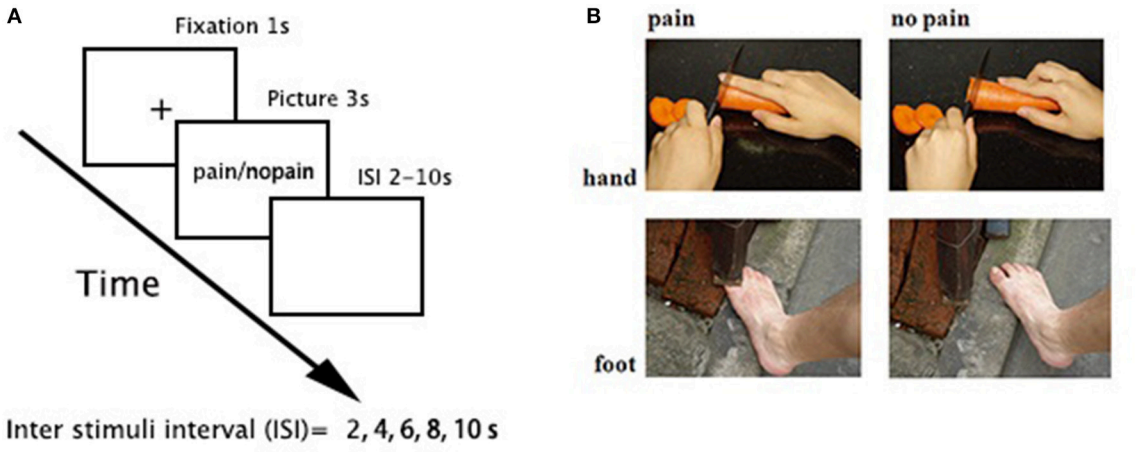


**FIGURE 1 |** Task paradigm. **(A)** a 3-s picture was presented in each trial, preceded by 1-s fixation and followed by a pseudorandom jittered inter stimuli interval (ISI, 2, 4, 6, 8, and 10 s, with a mean = 6 ± 2 s). The order of stimuli was pseudorandomly mixed in each run. **(B)** sample stimuli.

was 400 mL. A sip of ErGuoTou (about 1 mL, <0.015g/kg) was also added to the placebo condition as a taste mask.

## Procedure

A double-blind, placebo-controlled, within-subject design was used. There were two sessions scheduled at least 7 days apart, one for the alcohol condition and the other for the placebo condition. The order of the two sessions was counterbalanced between participants. The beverages were prepared by one of the authors (Z.X.W.). Neither the experimenters (Y.H., Z.Y.C., and M.X.F.) nor the data analyst (Y.H.) knew the beverage contents.

All participants were instructed to abstain from alcoholic beverages and recreational/psychoactive drugs for at least 48 h prior to each session, and were asked to eat only a light meal (avoiding fatty foods) 40–60 min prior to each fMRI session.

During each session, the participants first filled out the Interpersonal Reaction Index (IRI), an empathy trait scale (Davis, 1983), upon arrival. Then, they were asked to consume the beverage within 20–25 min. After a 25-min rest, their affect states were measured by the Positive Affect and Negative Affect Scale (PANAS) (Watson et al., 1988). Then, the participants were positioned in the scanner with foam padding around the head to minimize motion. The functional MRI runs commenced approximately 55 min after beverage ingestion, timed such that the upcoming cognitive task would concur with peak blood alcohol levels (Sripada et al., 2011).

An event-related fMRI design was applied (**Figure 1**). There were four functional runs. Each run consisted of 40 trials (20 painful). In each trial, a 3-s picture was presented, preceded by 1-s fixation and followed by a pseudorandom jittered inter stimuli interval (ISI, 2, 4, 6, 8, and 10 s, with a mean = 6 ± 2 s). The order of stimuli was pseudorandomly mixed in each run. Participants were instructed to judge whether the model in the stimuli was painful or not and responded with their right hand using a hand-shaped response box.

After scanning, the participants were again presented each picture and required to rate (1) the pain intensity felt by the model and the (2) subjective unpleasantness while watching, both on a 9-point Likert scale (1 = no pain/no unpleasantness, 9 = very painful/very unpleasant). Then, the participants were offered to be escorted back to their dorms and were advised to have a rest.

## Image Acquisition

The scanning was conducted using a 3-Tesla Siemens Trio MR scanner using a 12-channel head coil and included 4 functional runs and 1 anatomical run. For functional images, 35 axial slices (FOV = 240 × 240 $mm^2$, matrix = 64 × 64, in-plane resolution = 3.75 × 3.75 $mm^2$, thickness = 4 mm, without gap) covering the whole brain were obtained using a T2*-weighted echo planar imaging (EPI) sequences (TR = 2,000 ms, TE = 30 ms, flip angle = 90°). A high-resolution structural image for each participant was acquired using 3D MRI sequences for anatomical co-registration and normalization (TR = 1,900 ms, TE = 3.43 ms, flip angle = 7°, matrix = 256 × 256, FOV = 240 × 240 $mm^2$, slice thickness = 1 mm, without gap).

## Data Analysis

### Whole-Brain Analysis

Data from five participants was excluded because of poor behavioral performance (accuracy < 50%; $n = 2$), disruption of the inebriation procedure ($n = 2$), or quitting ($n = 1$). SPM8 was adopted for data analysis (Wellcome Department of Cognitive Neurology, London, UK; http://www.fil.ion.ucl.ac.uk/spm/). For each session of each participant, the EPI images were first realigned to the first volume to correct for head motions. Then, the anatomical image was co-registered with the mean EPI image, segmented and then generated normalized parameters to MNI space. Using these parameters, all EPI data were projected onto MNI space with a 2 × 2 × 2 $mm^3$ resolution and then smoothed using an 8-mm FWHM (full width half maximum)

isotropic Gaussian kernel. High-pass temporal filtering with a cut-off of 128 s was performed to remove low-frequency drifts.

For the first level analysis, a general linear model with two conditions (i.e., "pain" and "nopain") convolved with the canonical hemodynamic response function (HRF) was applied. The six estimated head movement parameters were included in the design matrix to remove the residual effects of head motion. Parameter estimates were then entered into the second level analysis using a 2 × 2 repeated measures ANOVA for exploration purpose, with stimuli type (painful vs. non-painful) and beverage type (alcohol vs. placebo) as independent factors. A voxel-wise threshold was set at $p < 0.001$ ($k = 40$) was adopted.

### ROI Analysis

Note that in pharmacological fMRI, prior hypotheses in functional brain imaging are often formulated by constraining the data analysis to ROIs, and this approach yields higher sensitivity than whole brain analyses (Mitsis et al., 2008). Thus, an ROI approach was performed to determine whether empathic responses for pain were reduced by alcohol intoxication using the AFNI software package (Cox, 1996). Three core regions of empathy were defined as ROIs, e.g., the dACC and bilateral AIs, with the following MNI (Montreal Neurological Institute) coordinates, adopted from a recent meta-analysis (Fan et al., 2011): dACC, x/y/z = −2/24/38; lAI/IFG, x/y/z = −42/18/0; and rAI/IFG, x/y/z = 38/24/−2. All ROIs were set as a sphere with a radius of 6 mm. For each ROI, the parameter estimates of 16 participants were extracted for further repeated measures ANOVA analysis and a paired *t*-test as post hoc analysis, with the threshold set to $p = 0.05$ (two tailed).

### Regression Analysis

A regression analysis was further applied to determine whether the empathic neural responses (i.e., pain > nopain) were mediated by trait empathy, using the following regressors: (1) the Empathic Concern subscale of the IRI (IRI-EC), i.e., the index of trait empathy, (2) mean behavioral index of pain intensity (contrast of pain vs. nopain), and (3) mean subjective rating of unpleasantness (contrast of pain vs. nopain), both in the placebo and alcohol conditions. A voxel-wise threshold was set at $p < 0.001$ within an inclusive mask (pain > nopain; $p < 0.05$, uncorrected; $k = 100$) was adopted and all brain regions survived FDR correction at cluster level.

### Psycho-Physiological Interaction (PPI) Analysis

The regression analysis revealed that activity in the rAI was modulated by trait empathy only in the intoxicated participants. A further PPI analysis (Friston et al., 1997) was then performed, with the rAI as seed. First, the source mask was defined as two 8-mm spheres centered at the peak voxel in the rAI (x/y/z = 40/16/−4) from main effect of empathy. The seed volume of interest (VOI) for each individual was then defined as a sphere with a 6-mm-radius centered at the peak voxel from the contrast of pain > nopain within these masks. The time series of each VOI was then extracted, and the PPI regressor was calculated as the element-by-element product of the mean-corrected activity of this VOI (the physiological regressor) and a vector coding for the differential stimuli effects of pain > nopain (the psychological regressor). These regressors were convolved with the canonical HRF and then entered into the regression model along with six head motion parameters. The individual contrast images were subsequently subjected to one-sample *t*-tests. Lastly, group analysis was applied to identify the brain regions displayed increased functional connectivity with the seed VOI (i.e., rAIs) during pain empathy both in the placebo and alcohol conditions. A voxel-wised threshold was set at $p < 0.001$ (uncorrected) and all brain regions survived FDR correction at cluster level.

# RESULTS

## Dispositional Measures

All scores of the dispositional measures were in the normal range (**Table 1**). The participants rated slightly higher in the positive affect after drinking in comparison with that in the placebo condition [PA-placebo: mean = 2.8 ($SD = 0.8$); PA-alcohol: 3.1(0.7); $t_{(15)} = 2.17$, $p = 0.046$], but not in negative affect [NA-placebo: 1.3(0.4); NA-alcohol: 1.4(0.4); $t_{(15)} = 1.16$, $p = 0.263$].

## Behavioral Results

As for reaction time (RT), both a main effect of the beverage and stimuli type was detected [$Fs_{(1,13)} > 8.1$, $ps < 0.014$, $\eta^2 > 0.38$], and the participants responded slower toward painful stimuli (v.s. non-painful stimuli) in both conditions [$ts_{(13)} > 2.2$, $ps < 0.045$] and that they displayed longer RT in the alcohol (vs. placebo) condition regardless of stimuli [$ts_{(13)} > 2.6$, $ps < 0.023$]. Neither a main effect nor a stimuli type×beverage interaction was found in accuracy [$Fs_{(1, 13)} < 4.2$, $ps > 0.06$, $\eta^2 < 0.23$]. Note behavioral data from two participants during scanning were lost because of technical reasons.

As for the post-scanning rating scores, a main effect of stimuli type was found in both pain intensity and unpleasantness [$F_{(1, 15)} > 97.0$, $p < 0.001$, $\eta^2 > 0.8$], whereas an interaction effect was only detected in unpleasantness [$F_{(1,15)} = 4.7$, $p = 0.046$, $\eta^2 = 0.24$]. The participants rated significantly higher on painful (vs. non-painful) stimuli regardless of beverage in both pain intensity [$ts_{(15)} > 15.3$, $p < 0.001$] and unpleasantness [$ts_{(15)} > 9.3$, $p < 0.001$]. Moreover, the unpleasantness rating difference between the painful stimuli and non-painful stimuli in the alcohol condition was larger than that in the placebo

**TABLE 1** | Scores on trait scales ($N = 16$).

| Scale | Scores (*SD*) |
|---|---|
| Interpersonal Reaction Index (IRI) | 64.2 (10.6) |
| Empathic concern subscale (EC) | 18.9 (3.1) |
| Fantasy subscale (FA) | 15.7 (4.8) |
| Perspective-taking subscale (PT) | 17.6 (3.2) |
| Personal distress subscale (PD) | 12.1 (3.4) |
| Short Michigan Alcoholism Screening Test (SMAST) | 0.4 (0.6) |
| Beck Depression Inventory (BDI) | 4.1 (3.2) |

condition [$t_{(15)} = 2.18$, $p = 0.046$]. The average values of these behavioral measurements are listed in **Table 2**.

## Imaging Results

### Whole-Brain Results

The main effects of empathy for pain (i.e., painful > non-painful) were found in the ACC/SMA (BA 6/8/24/32), bilateral AIs (BA 13) extending to IFG (BA 47), bilateral inferior parietal lobule (IPL, BA 7/39/40) and bilateral somatosensory cortex (BA 1/2/3), see **Table 3** and **Figure 2** for details. The beverage main effect (placebo > alcohol) was found in the mid-cingulate/SMA (BA 6/24), bilateral IPL extending to the supra-marginal gyrus (BA 7/40), left mid-insula (BA 13), and bilateral visual cortices (BA 19/37), along with several sub-cortical areas, including the hippocampus and thalamus, see **Table 4** and **Figure 3** for details. No significant interaction was found.

### ROI Results

In the three ROIs of the affective pain matrix, both main effects of stimuli type and beverage were observed [$Fs_{(1, 15)} > 6.52$, $ps < 0.022$, $\eta^2 > 0.3$; **Figure 4**]. However, a significant interaction was found only in the dACC [$F_{(1, 15)} = 4.99$, $p = 0.041$, $\eta^2 = 0.24$]. A post-hoc paired *t*-test indicated that increased empathic activity for pain (i.e., pain > nopain) in the dACC along with the rAI/IFG was found in the placebo condition [$ts_{(15)} > 2.71$, $ps < 0.016$] but not in the alcohol condition [$ts_{(15)} < 2.11$, $ps > 0.053$], whereas the left AI/IFG displayed enhanced activation from painful (vs. non-painful) stimuli regardless of the beverage type [$ts_{(15)} > 3.08$, $ps < 0.008$]. In addition, all ROIs displayed reduced activity to both types of stimuli after alcohol intoxication compared with the placebo condition [$ts_{(15)} < -2.17$, $ps < 0.045$]. No other main effect or interaction was detected.

### Regression Results

Within the core affective pain matrix, the voxel-wised regression analysis revealed that empathic activity for pain in the rAI was significantly positively related with the scores of the IRI-EC in the alcohol condition (**Figure 5A**) when the pain intensity

**TABLE 2 |** Average behavioral performance during and after fMRI scanning.

| Measurements | Condition | Accuracy (%; *SD*) | | | RT (ms; *SD*) | | |
|---|---|---|---|---|---|---|---|
| | | Painful | Non-painful | Total | Painful | Non-painful | Total |
| During Scanning | Placebo | 88.7 (7.6) | 93.8 (5.4) | 91.2 (7.0) | 1284 (279) | 1190.0 (235) | 1237.1 (257) |
| (*N* = 14) | Alcohol | 89.8 (6.5) | 91.4 (6.2) | 90.6 (6.3) | 1421 (192) | 1299.8 (198) | 1360.3 (201) |
| | | Intensity (*SD*) | | | Unpleasantness (*SD*) | | |
| | | Painful | Non-painful | Total | Painful | Non-painful | Total |
| After Scanning | Placebo | 7.5 (0.9) | 1.6 (0.3) | 4.5 (0.9) | 7.8 (0.6) | 4.0 (1.5) | 5.9 (0.8) |
| (*N* = 16) | Alcohol | 7.5 (1.0) | 1.7 (0.3) | 4.6 (0.8) | 7.9 (0.8) | 3.6 (1.6) | 4.7 (0.9) |

*Behavioral data from 2 participants during scanning were lost because of technical reasons.*

**TABLE 3 |** Main effects of empathy for pain.

| Contrasts | Regions | Side | Brodmann area (BA) | MNI coordinates | | | Cluster size | T score |
|---|---|---|---|---|---|---|---|---|
| | | | | x | y | z | | |
| Pain > nopain | dACC/MeFG | L/R | 9/32 | −6 | 31 | 32 | 407 | 4.92** |
| | AI/IFG | L | 13/47 | −40 | 19 | −1 | 1,330 | 5.55*** |
| | | R | 13/47 | 36 | 29 | −6 | 257 | 4.21* |
| | IPL | L | 7/40 | −55 | −31 | 37 | 1,089 | 7.68*** |
| Nopain > pain | MFG | L | 8 | −26 | 27 | 35 | 406 | 4.32** |
| | | R | 8 | 26 | 29 | 39 | 395 | 7.32** |
| | IPL/AG | L | 7/39 | −40 | −68 | 44 | 1,193 | 6.93*** |
| | SMG/AG | R | 39/40 | 55 | −55 | 30 | 2,034 | 6.63*** |
| | MTG | L | 21 | −53 | 0 | −8 | 632 | 6.39*** |
| | | R | 21 | 59 | 1 | −15 | 337 | 5.98* |
| | Precuneus/LG | L/R | 7/19 | 4 | −54 | 41 | 6,352 | 6.16*** |
| | ACC | R | 32 | 18 | 45 | 7 | 244 | 5.8* |

*L, left; R, right; dACC, dorsal anterior cingulate cortex; SMA, supplementary motor area; MeFG, medial frontal gyrus; CG, cingulated gyrus; MFG, middle frontal gyrus; IFG, inferior frontal gyrus; AI, anterior insula; PI, posterior insula; PCG, pre-central gyrus; PoCG, post-central gyrus; SMG, supramarginal gyrus; IPL, inferior parietal gyrus; AG, angular gyrus; MTG, middle temporal gyrus; LG, lingual gyrus;*p < 0.05,**p < 0.01, ***p < 0.001, FDR corrected at cluster-level.*

and unpleasant levels were controlled. The plot of the neural activity at the peak voxel vs. the score was displayed in **Figure 5B** (Pearson's correlation, $r = 0.86$, $p < 0.001$).

### PPI Results

Significant functional connectivity was observed between the rAI and the fronto-parietal areas, including the right dorso-lateral prefrontal cortex (BA 44) along with the bilateral IPL (BA 39), as well as the visual cortices during empathy for pain (i.e., pain > nopain) in the placebo condition but not in the alcohol condition (**Figure 6**), see **Table 5** for details.

## DISCUSSION

The present study was carried out to investigate the effects of alcohol consumption on empathy for pain. A significant interaction was found in the dACC. As the dACC is considered to be one of the core regions of the pain empathy-related network (Lamm et al., 2010a) to code the value of affective stimulus (Fan et al., 2011), our results suggest that the perceived affective value of empathic concern was impaired by alcohol intoxication (Steele and Josephs, 1990), which is in line with our hypothesis. Note that the dACC also plays a key and necessary role in voluntary and cognitive control (Shackman et al., 2011), such as resolving conflicts (Botvinick et al., 2001) or monitoring errors (Yeung et al., 2004; Marinkovic et al., 2012). Thus, reduced perceived affective value should result in an underestimation of others' pain as well as poor cognitive control, and then lead to poor control of aggressive behaviors (Steele and Josephs, 1990).

One of the most interesting findings was that the empathic responses in the rAI were positively correlated with trait

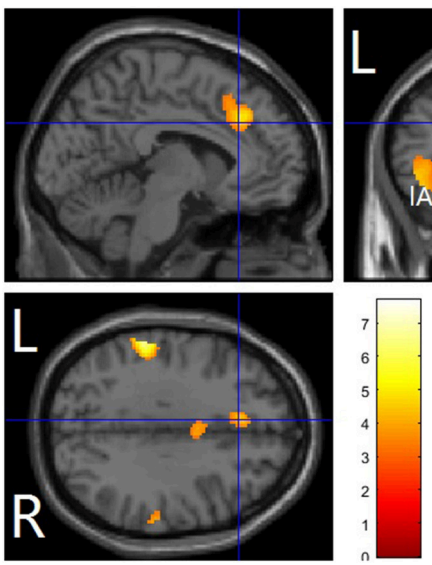


**FIGURE 2 |** Pain vs. nopain across sobriety /intoxication in a whole-brain analysis. The affective pain matrix was displayed. Voxel-wised threshold was set at $p = 0.001$, FDR corrected at cluster-level. L, left; R, right; ACC, anterior cingulate cortex/supplementary motor area; AI, anterior insula.

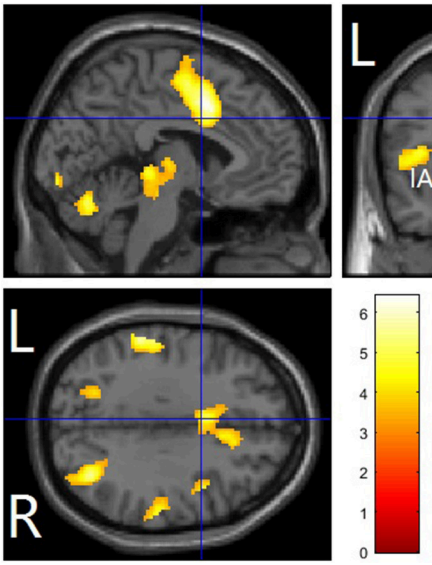


**FIGURE 3 |** Alcohol vs. placebo across pain and nopain conditions in a whole-brain analysis. The affective pain matrix was displayed. Voxel-wised threshold was set at $p = 0.001$. FDR corrected at cluster-level. L, left; R, right; ACC, anterior cingulate cortex/supplementary motor area; AI, anterior insula.

**TABLE 4 |** Main effects of beverage.

| Contrasts | Regions | Side | Brodmann area (BA) | MNI coordinates | | | Cluster size | T score |
|---|---|---|---|---|---|---|---|---|
| | | | | x | y | z | | |
| Placebo > alcohol | SMA/MCC/PCG | L/R | 6/24 | −6 | 10 | 38 | 2766 | 6.41*** |
| | IPL/PoCG/Precuneus | L | 2/40 | −59 | −32 | 27 | 2079 | 5.9*** |
| | Insula | L | 13 | −40 | 0 | 9 | 346 | 5.45** |
| | Midbrain/Thalamus | L | | −8 | −17 | 1 | 512 | 5.43*** |
| | Thalamus | R | | 10 | −25 | 0 | 593 | 5.06*** |
| Alcohol > placebo | AG/IPL | L | 39 | −51 | −60 | 42 | 256 | 4.75* |

*L, left; R, right; SMA, supplementary motor area; MCC, mid-cingulate gyrus; IFG, inferior frontal gyrus; PCG, pre-central gyrus; PoCG, post-central gyrus; IPL, inferior parietal gyrus; AG, angular gyrus; FG, fusiform gyrus; MOG, middle occipital gyrus; PhG, parahippocampal gyrus; *$p < 0.05$,**$p < 0.01$, ***$p < 0.001$, FDR corrected at cluster-level.*

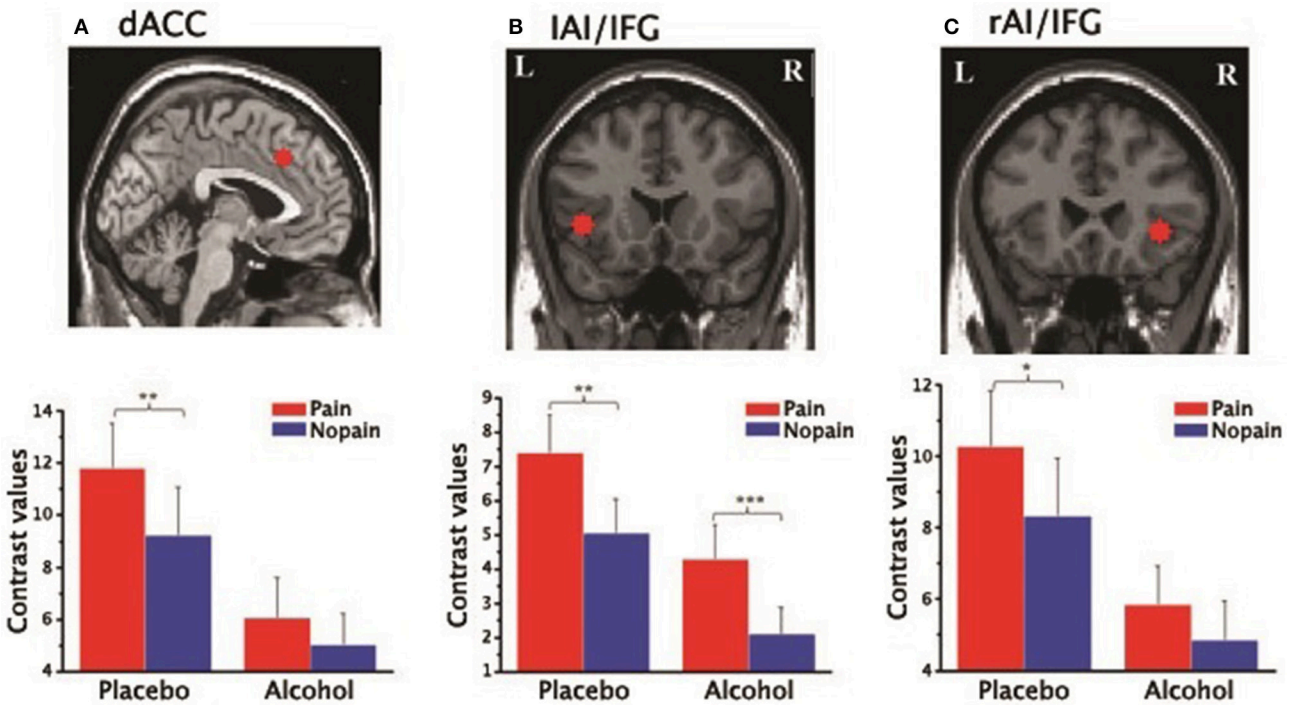


**FIGURE 4 |** Contrast values of the parameter estimates of the three ROIs of the affective pain matrix in the placebo and alcohol condition: **(A)** results for the dorsal anterior cingulate cortex (dACC); **(B)** results for the left anterior insula extending to the inferior frontal gyrus (lAI/IFG); **(C)** results for the right anterior insula extending to the inferior frontal gyrus (rAI/IFG). L, left; R, right; $^{*}p < 0.05$, $^{**}p < 0.01$, $^{***}p < 0.001$; The error bars represent the SEM.

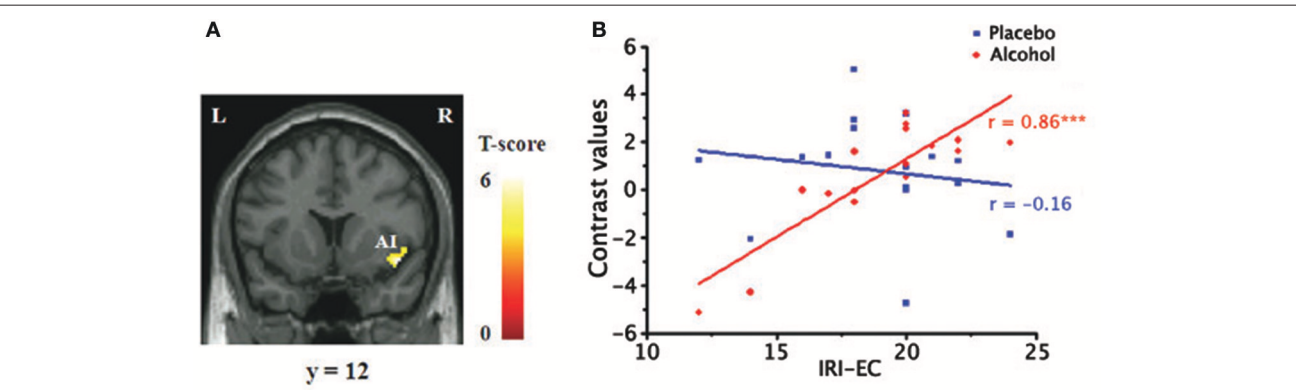


**FIGURE 5 |** Positive relationship between empathy concern subscale of Interpersonal Reaction Index (IRI-EC) scores and empathic neural responses for pain in the right AI. **(A)** A significant cluster superimposed onto a coronal section ($p < 0.001$, FDR corrected at cluster level), masked by the main effect of empathy (pain > nopain; $p < 0.05$); **(B)** A scatter plot of the positive correlation in the peak voxel for display purposes (x/y/z=44/12/-12, MNI coordinates). $^{***}p < 0.001$.

empathy in the alcohol condition, but not in the placebo condition. This finding is not due to changes of affective states or behavioral responses after drinking, as these confounding factors are ruled out in the regression analysis. The insula has long been considered one of the key regions that related with traits. For example, activation in insula was also found closely related to various trait measures, such as anxiety (Simmons et al., 2006) or intolerance (Simmons et al., 2008). Thus, our results indicate insula is also related with trait empathy, and intoxication leads to trait empathy inflation. These findings significantly extends the self-inflating phenomenon (i.e., enhancing feelings of self-appraisal) (Steele and Josephs, 1990) to the social cognition domain of trait empathy in intoxication.

Moreover, we found that the functional connectivity between the rAI and attention network, which occurred during empathy for pain in the placebo condition, was missing in the alcohol condition. It is believed that attention plays an

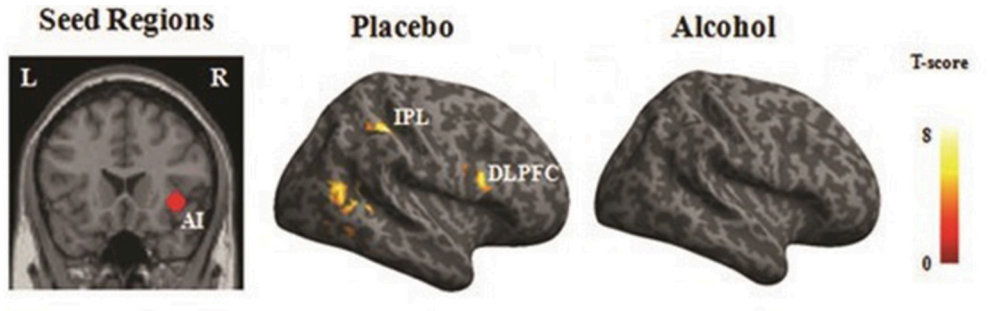


**FIGURE 6 |** PPI results. Regions that displayed increased functional connectivity with the right AI (rAI) during empathy for pain in the placebo and alcohol condition ($p < 0.001$). The right hemisphere is displayed. L, left; R, right; AI, anterior insula; DLPFC, dorsal lateral prefrontal cortex; IPL, inferior parietal gyrus.

**TABLE 5 |** Increased PPIs of the seed region during empathy for pain in the placebo and alcohol conditions ($p < 0.001$; $k = 100$).

| Condition | Seed region | Regions | Side | Brodmann area (BA) | MNI coordinates | | | *k* | T score |
|---|---|---|---|---|---|---|---|---|---|
| | | | | | x | y | z | | |
| Placebo | rAI | SMA | L/R | 6 | 4 | 6 | 52 | 101 | 5.5* |
| | | IPL | L | 40 | −42 | −42 | 44 | 410 | 6.67** |
| | | | R | 39 | 40 | −35 | 44 | 229 | 8.21** |
| | | PhG/MOG | L | 19/37 | −32 | −51 | −4 | 189 | 6.07** |
| | | DLPFC | R | 44 | 48 | 13 | 23 | 212 | 7.41** |
| | | STG/MTG | R | 22 | 48 | −57 | 18 | 373 | 8.14*** |
| | | FG | R | 20 | 40 | −40 | −13 | 159 | 5.8* |
| Alcohol | rAI | FG | R | 37 | 26 | −38 | −15 | 261 | 7.77*** |

*rAI, right anterior insula; SMA, supplementary motor area; DLPFC, dorso-lateral prefrontal cortex; IPL, inferior parietal gyrus; PhG, parahippocampal gyrus; TPJ, temporo-parietal junction; STG, superior temporal gyrus; MTG, middle temporal gyrus; FG, fusiform gyrus; LG, lingual gyrus; MOG, middle occipital gyrus; *p < 0.05,**p < 0.01, ***p < 0.001, FDR corrected at cluster-level.*

important role in empathy. For example, empathic responses in the AIs were significantly reduced when the participants were distracted (Gu and Han, 2007) or cognitively busy (Rameson et al., 2011). AIs activity during a pain perception task was also significantly reduced when higher activity was observed in the right dorsolateral prefrontal cortex (Lorenz et al., 2003). Considering that activities in the fronto-parietal attention/control network, including the SMA/ACC, bilateral dorsolateral frontal cortices (middle/inferior frontal gyri), and bilateral parietal areas, were significantly decreased by alcohol intoxication, we conclude that crosstalks between the rAI and attention network is impaired by alcohol consumption, resulting in impaired top-down modulation of the rAI.

Taken together, the most likely explanation is that empathy for pain is shaped by other factors (de Waal, 2007), such as social norm. Thus, people with both high and low trait empathy may display relatively normal empathy responses for pain in sobriety. However, as alcohol is a central nervous depressant, it seems that alcohol intoxication not only inhibits local neural activity, but also inhibits neural signal flow between brain regions. The communication between the attention network and rAI was downregulated, and influences of other factors on empathy were thus reduced, resulting in trait empathy inflation. These results provide a possible neural foundation for the finding that empathy plays a moderating role in alcohol-related aggression behaviors (Giancola, 2003).

Despite the fact that alcohol intoxication led to those neural changes, participants could still differentiate painful stimuli from non-painful stimuli correctly as well as their intensities after drinking. These findings not only undermine the possibility that participants were disengaged from our task after alcohol intoxication, they also suggest that there is disassociation between cognitive appraisal and neural empathic activation for pain after drinking. Preserved cognitive appraisal but impaired brain function in other domains such as affective information has been reported during alcohol intoxication (Padula et al., 2011). A recent lesion study revealed that only damage to the AIs rather than the dACC might be more necessary for affecting pain empathy and causing impaired behavioral empathic responses (Gu et al., 2012). Hence, the ability to correctly judge other's affective state may be preserved because of the relatively preserved empathic responses in the AIs. It is also possible that other factors (e.g., past knowledge) may be involved. These disassociations suggest that humans have an inability to

acknowledge their social dysfunction after drinking (Fromme et al., 1999).

There are two limitations. The first one is that although the double-blindness procedure used in our manuscript is widely used in previous studies such as Ridderinkhof et al. (2002), it remains possible that participants became aware of the experimental condition given the strong behavioral effects of alcohol over water placebo and our results can be affected by participant awareness. However, we think that our results are robust as the observed significant correlation between empathic neural activity in the right anterior insula (rAI) and trait empathy cannot be interpreted by participant awareness. Second, our sample size is relatively small (data from 16 participants were valid). We also note that a significant stimuli type×beverage interaction was only found in the ROI analysis, but not in the voxel-wised whole brain analysis, and no interaction was found in the AIs, possibly due to the small sample size. These results are in line with a previous suggestion that an ROI approach yields higher sensitivity than whole brain analyses in pharmacological fMRI with prior hypotheses (Mitsis et al., 2008). Further studies using a larger sample size are desired.

In summary, we provide the first piece of evidence that the empathic neural response for pain in the dACC is impaired by acute alcohol consumption in a group of healthy social drinkers. Moreover, we also show that alcohol intoxication leads to inflated trait empathy in the rAI. The neural correlates underlying trait empathy inflation are likely due to the impaired crosstalk between the rAI and attention neural network, i.e., impaired top-down modulation. Whether similar mechanisms are involved in other alcohol-related self-inflation deserves further investigation.

## AUTHOR CONTRIBUTIONS

YH, MF, ZW, and ZC: designed the study; YH, ZC, and MF: collected the data; YH: analyzed the data; YH, YP, and ZC: wrote the paper.

## FUNDING

This research was supported by the Natural Science Foundation of China (Nos. 30700235, 31070986). We are indebted to Dr. Lijia Lin for help on data analysis.

## REFERENCES

Beck, A. T., Ward, C. H., Mendelson, M., Mock, J., and Erbaugh, J. (1961). An inventory for measuring depression. *Arch. Gen. Psychiatry* 4, 561-571. doi: 10.1001/archpsyc.1961.01710120031004

Botvinick, M. M., Braver, T. S., Barch, D. M., Carter, C. S., and Cohen, J. D. (2001). Conflict monitoring and cognitive control. *Psychol. Rev.* 108, 624–652. doi: 10.1037/0033-295X.108.3.624

Bushman, B. J., and Cooper, H. M. (1990). Effects of alcohol on human aggression: an intergrative research review. *Psychol. Bull.* 107:341. doi: 10.1037/0033-2909.107.3.341

Calhoun, V. D., Pekar, J. J., and Pearlson, G. D. (2004). Alcohol intoxication effects on simulated driving: exploring alcohol-dose effects on brain activation using functional MRI. *Neuropsychopharmacology* 29, 2097-2117. doi: 10.1038/sj.npp.1300543

Cox, R. (1996). AFNI: software for analysis and visualization of functional magnetic resonance neuroimages. *Compu. Biomed. Res.* 29, 162–173. doi: 10.1006/cbmr.1996.0014

Curtin, J., and Lang, A. (2007). "Alcohol and emotion: insights and directives from affective science," in *Emotion and Psychopathology: Bridging Affective and Clinical Science,* eds J. Rottenberg and S. L. Johnson (Washington, DC: American Psychological Association).

Davis, M. (1983). Measuring individual differences in empathy: evidence for a multidimensional approach. *J. Pers. Soc. Psychol.* 44, 113–126. doi: 10.1037/0022-3514.44.1.113

Decety, J. (2011). Dissecting the neural mechanisms mediating empathy. *Emotion Rev.* 3:92. doi: 10.1177/1754073910374662

Denson, T. F., Aviles, F. E., Pollock, V. E., Earleywine, M., Vasquez, E. A., and Miller, N. (2008). The effects of alcohol and the salience of aggressive cues on triggered displaced aggression. *Aggress. Behav.* 34, 25–33. doi: 10.1002/ab.20177

de Waal, F. B. (2007). "The'Russian doll'model of empathy and imitation," in *On Being Moved: From Mirror Neuron Empathy,* ed S. Bråten (John Benjamins Publishing Company), 49–69.

Fan, Y., Duncan, N. W., de Greck, M., and Northoff, G. (2011). Is there a core neural network in empathy? An fMRI based quantitative meta-analysis. *Neurosci. Biobehav. Rev.* 35, 903–911. doi: 10.1016/j.neubiorev.2010.10.009

Faul, F., Erdfelder, E., Buchner, A., and Lang, A. G. (2009). Statistical power analyses using G*Power 3.1: tests for correlation and regression analyses. *Behav. Res. Methods* 41, 1149–1160. doi: 10.3758/BRM.41.4.1149

Friston, K. J., Buechel, C., Fink, G. R., Morris, J., Rolls, E., and Dolan, R. J. (1997). Psychophysiological and modulatory interactions in neuroimaging. *Neuroimage* 6, 218–229. doi: 10.1006/nimg.1997.0291

Fromme, K., D'Amico, E. J., and Katz, E. C. (1999). Intoxicated sexual risk taking: an expectancy or cognitive impairment explanation? *J. Stud. Alcohol* 60, 54–63. doi: 10.15288/jsa.1999.60.54

Giancola, P. R. (2003). The moderating effects of dispositional empathy on alcohol-related aggression in men and women. *J. Abnorm. Psychol.* 112, 275–281. doi: 10.1037/0021-843X.112.2.275

Gu, X., Gao, Z., Wang, X., Liu, X., Knight, R. T., and Hof, P. R., et al. (2012). Anterior insular cortex is necessary for empathetic pain perception. *Brain* 135, 2726–2735. doi: 10.1093/brain/aws199

Gu, X., and Han, S. (2007). Attention and reality constraints on the neural processes of empathy for pain. *Neuroimage* 36, 256–267. doi: 10.1016/j.neuroimage.2007.02.025

Gu, X., Liu, X., Guise, K. G., Naidich, T. P., Hof, P. R., and Fan, J. (2010). Functional dissociation of the frontoinsular and anterior cingulate cortices in empathy for pain. *J. Neurosci.* 30, 3739–3744. doi: 10.1523/JNEUROSCI.4844-09.2010

Hein, G., and Singer, T. (2008). I feel how you feel but not always: the empathic brain and its modulation. *Curr. Opin. Neurobiol.* 18, 153–158. doi: 10.1016/j.conb.2008.07.012

Jackson, P. L., Meltzoff, A. N., and Decety, J. (2005). How do we perceive the pain of others? A window into the neural processes involved in empathy. *Neuroimage* 24, 771–779. doi: 10.1016/j.neuroimage.2004.09.006

Koelega, H. (1995). Alcohol and vigilance performance: a review. *Psychopharmacology* 118, 233–249. doi: 10.1007/BF02245951

Lamm, C., Decety, J., and Singer, T. (2010a). Meta-analytic evidence for common and distinct neural networks associated with directly experienced pain and empathy for pain. *Neuroimage* 54, 2492-2502. doi: 10.1016/j.neuroimage.2010.10.014

Lamm, C., Meltzoff, A., and Decety, J. (2010b). How do we empathize with someone who is not like us? A functional magnetic resonance imaging study. *J. Cogn. Neurosci.* 22, 362–376. doi: 10.1162/jocn.2009.21186

Lipton, R. I. (1994). The effect of moderate alcohol use on the relationship between stress and depression. *Am. J. Public Health* 84, 1913–1917. doi: 10.2105/AJPH.84.12.1913

Lorenz, J., Minoshima, S., and Casey, K. (2003). Keeping pain out of mind: the role of the dorsolateral prefrontal cortex in pain modulation. *Brain* 126, 1079-1091. doi: 10.1093/brain/awg102

Marinkovic, K., Rickenbacher, E., Azma, S., and Artsy, E. (2012). Acute alcohol intoxication impairs top–down regulation of stroop incongruity as revealed by blood oxygen level-dependent functional magnetic resonance imaging. *Hum. Brain Mapp.* 33, 319–333. doi: 10.1002/hbm.21213

Miller, P. A., and Eisenberg, N. (1988). The relation of empathy to aggressive and externalizing/antisocial behavior. *Psychol. Bull.* 103, 324-344. doi: 10.1037/0033-2909.103.3.324

Mitsis, G. D., Iannetti, G. D., Smart, T. S., Tracey, I., and Wise, R. G. (2008). Regions of interest analysis in pharmacological fMRI: How do the definition criteria influence the inferred result? *Neuroimage* 40, 121–132. doi: 10.1016/j.neuroimage.2007.11.026

Moriguchi, Y., Decety, J., Ohnishi, T., Maeda, M., Mori, T., and Nemoto, K., et al. (2007). Empathy and judging other's pain: an fMRI study of alexithymia. *Cereb. Cortex* 17, 2223-2234. doi: 10.1093/cercor/bhl130

Padula, C. B., Simmons, A. N., Matthews, S. C., Robinson, S. K., Tapert, S. F., and Schuckit, M. A., et al. (2011). Alcohol attenuates activation in the bilateral anterior insula during an emotional processing task: a pilot study. *Alcohol Alcohol.* 46, 547–552. doi: 10.1093/alcalc/agr066

Preston, S. D., and de Waal, F. B. M. (2002). Empathy: its ultimate and proximate bases. *Behav. Brain Sci.* 25, 1–20. doi: 10.1017/S0140525X02000018

Rameson, L. T., Morelli, S. A., and Lieberman, M. D. (2011). The neural correlates of empathy: experience, automaticity, and prosocial behavior. *J. Cogn. Neurosci.* 24, 235–245. doi: 10.1162/jocn_a_00130

Ridderinkhof, K. R., de Vlugt, Y., Bramlage, A., Spaan, M., Elton, M., and Snel, J., et al. (2002). Alcohol consumption impairs detection of performance errors in mediofrontal cortex. *Science* 298, 2209-2211. doi: 10.1126/science.1076929

Rogers, B. P., Morgan, V. L., Newton, A. T., and Gore, J. C. (2008). Assessing functional connectivity in the human brain by fMRI. *Magn. Reson. Imaging* 26, 146–146. doi: 10.1016/j.mri.2007.06.002

Selzer, M. L., Vinokur, A., and van Rooijen, L. (1975). A self-administered short Michigan alcoholism screening test (SMAST). *J. Stud. Alcohol* 36, 117-126. doi: 10.15288/jsa.1975.36.117

Shackman, A. J., Salomons, T. V., Slagter, H. A., Fox, A. S., Winter, J. J., and Davidson, R. J. (2011). The integration of negative affect, pain and cognitive control in the cingulate cortex. *Nat. Rev. Neurosci.* 12, 154–167. doi: 10.1038/nrn2994

Simmons, A., Matthews, S. C., Paulus, M. P., and Stein, M. B. (2008). Intolerance of uncertainty correlates with insula activation during affective ambiguity. *Neurosci. Lett.* 430, 92–97. doi: 10.1016/j.neulet.2007.10.030

Simmons, A., Strigo, I., Matthews, S. C., Paulus, M. P., and Stein, M. B. (2006). Anticipation of aversive visual stimuli is associated with increased insula activation in anxiety-prone subjects. *Biol. Psychiatry* 60, 402–409. doi: 10.1016/j.biopsych.2006.04.038

Singer, T., and Lamm, C. (2009). The social neuroscience of empathy. *Ann. N. Y. Acad. Sci.* 1156, 81–96. doi: 10.1111/j.1749-6632.2009.04418.x

Singer, T., Seymour, B., O'Doherty, J. P., Stephan, K. E., Dolan, R. J., and Frith, C. D. (2006). Empathic neural responses are modulated by the perceived fairness of others. *Nature* 439, 466–469. doi: 10.1038/nature04271

Sripada, C. S., Angstadt, M., McNamara, P., King, A. C., and Phan, K. L. (2011). Effects of alcohol on brain responses to social signals of threat in humans. *Neuroimage* 55, 371–380. doi: 10.1016/j.neuroimage.2010.11.062

Steele, C. M., and Josephs, R. A. (1990). Alcohol myopia: its prized and dangerous effects. *Am. Psychol.* 45, 921-933. doi: 10.1037/0003-066X.45.8.921

Van Horn, J. D., Yanos, M., Schmitt, P. J., and Grafton, S. T. (2006). Alcohol-induced suppression of BOLD activity during goal-directed visuomotor performance. *Neuroimage* 31, 1209–1221. doi: 10.1016/j.neuroimage.2006.01.020

Watson, D., Clark, L. A., and Tellegen, A. (1988). Development and validation of brief measures of positive and negative affect: the PANAS scales. *J. Pers. Soc. Psychol.* 54, 1063-1070. doi: 10.1037/0022-3514.54.6.1063

Yeung, N., Botvinick, M. M., and Cohen, J. D. (2004). The neural basis of error detection: Conflict monitoring and the error-related negativity. *Psychol. Rev.* 111, 931–959. doi: 10.1037/0033-295X.111.4.931

**Conflict of Interest Statement:** The authors declare that the research was conducted in the absence of any commercial or financial relationships that could be construed as a potential conflict of interest.

frontiers in Human Neuroscience

ORIGINAL RESEARCH
published: 10 January 2018
doi: 10.3389/fnhum.2017.00653

# Linear Representation of Emotions in Whole Persons by Combining Facial and Bodily Expressions in the Extrastriate Body Area

*Xiaoli Yang[1†], Junhai Xu[1†], Linjing Cao[1], Xianglin Li[2], Peiyuan Wang[3], Bin Wang[2] and Baolin Liu[1,4*]*

[1] School of Computer Science and Technology, Tianjin Key Laboratory of Cognitive Computing and Applications, Tianjin University, Tianjin, China, [2] Medical Imaging Research Institute, Binzhou Medical University, Yantai, China, [3] Department of Radiology, Yantai Affiliated Hospital of Binzhou Medical University, Yantai, China, [4] Research State Key Laboratory of Intelligent Technology and Systems, National Laboratory for Information Science and Technology, Tsinghua University, Beijing, China

Our human brain can rapidly and effortlessly perceive a person's emotional state by integrating the isolated emotional faces and bodies into a whole. Behavioral studies have suggested that the human brain encodes whole persons in a holistic rather than part-based manner. Neuroimaging studies have also shown that body-selective areas prefer whole persons to the sum of their parts. The body-selective areas played a crucial role in representing the relationships between emotions expressed by different parts. However, it remains unclear in which regions the perception of whole persons is represented by a combination of faces and bodies, and to what extent the combination can be influenced by the whole person's emotions. In the present study, functional magnetic resonance imaging data were collected when participants performed an emotion distinction task. Multi-voxel pattern analysis was conducted to examine how the whole person-evoked responses were associated with the face- and body-evoked responses in several specific brain areas. We found that in the extrastriate body area (EBA), the whole person patterns were most closely correlated with weighted sums of face and body patterns, using different weights for happy expressions but equal weights for angry and fearful ones. These results were unique for the EBA. Our findings tentatively support the idea that the whole person patterns are represented in a part-based manner in the EBA, and modulated by emotions. These data will further our understanding of the neural mechanism underlying perceiving emotional persons.

**Keywords: emotion, extrastriate body area, pattern similarity analysis, MVPA, fMRI**

OPEN ACCESS

***Edited by:***
*Nan Li,*
*RIKEN, Japan*

***Reviewed by:***
*Daniel Stjepanović,*
*Duke University, United States*
*Xu Zhang,*
*Duke University, United States*

***Correspondence:**
*Baolin Liu*
*liubaolin@tsinghua.edu.cn*

*† These authors have contributed equally to this work.*

***Received:*** *22 May 2017*
***Accepted:*** *21 December 2017*
***Published:*** *10 January 2018*

***Citation:***
*Yang X, Xu J, Cao L, Li X, Wang P, Wang B and Liu B (2018) Linear Representation of Emotions in Whole Persons by Combining Facial and Bodily Expressions in the Extrastriate Body Area. Front. Hum. Neurosci. 11:653. doi: 10.3389/fnhum.2017.00653*

## INTRODUCTION

The ability to interpret emotions in other people is a crucial social skill in our daily lives. An emotion can be perceived by observing faces, hand gestures, bodies, whole persons, voices, and complex scenes. We know little about emotion perception in the human brain, especially the neural mechanism underlying human body perception. Previous studies have investigated the neural basis of integrating object parts into whole objects (Macevoy and Epstein, 2009), or the combining of two

associated objects into an object pair (Baeck et al., 2013). Behavioral studies have shown that the intact bodies can be visually perceived better than the body parts (Soria Bauser and Suchan, 2013). However, the use of static and neutral images in previous studies has limited the interpretation of the data (Liang et al., 2017). Thus, it remains unclear how the combination of faces and bodies is influenced by dynamic emotion information, which may activate just one specific network.

Neuroimaging studies have demonstrated that the stimuli of faces and bodies can activate regions in the ventral (VOTC) and lateral occipitotemporal cortices (LOTC). Faces are represented specifically in two subregions of the VOTC, the occipital face area (OFA) (Pitcher et al., 2007; Liu et al., 2010; Sormaz et al., 2016) and fusiform face area (FFA) (Zhang et al., 2012). Extensive behavioral studies have indicated that human faces are processed in a holistic manner, which means that the featural and configurable information is processed together as an integrated whole (McKone et al., 2001; Maurer et al., 2002). Further functional magnetic resonance imaging (fMRI) studies suggested that the FFA might be engaged in the holistic, non-part-based representation of faces (Zhang et al., 2012), whereas the OFA could process both the features and configurable information of faces (Calder and Young, 2005; Schiltz and Rossion, 2006).

Some similarities between the mechanism of processing bodies and faces (Minnebusch and Daum, 2009) have been confirmed, so the functional contributions of aforementioned face-sensitive areas allow for the understanding of the functional contributions of body-sensitive areas. The bodies or body parts have been found to be represented in the extrastriate body area (EBA) (Downing et al., 2006, 2007; Downing and Peelen, 2016) of the LOTC, and the fusiform body area (FBA) (Schwarzlose et al., 2005; Peelen et al., 2006; Downing and Peelen, 2016) of the VOTC. EBA is found in the posterior end of the inferior temporal sulcus and FBA which partly overlaps the FFA (Peelen and Downing, 2005; Schwarzlose et al., 2005; Peelen et al., 2006; de Gelder et al., 2010) is found in the lateral posterior fusiform gyrus (FG). There is functional similarity between OFA and EBA and between FFA and FBA in some way. By examining whether the perception of bodies was whole- or part-based, one study suggested that the response of the EBA increased linearly with the amount of body-related information (e.g., finger, hand, arm, torso), but in a step-like manner in the FBA, suggesting that the EBA shared a selective role for body parts and the FBA for whole persons or larger body parts (Taylor et al., 2007; Bracci et al., 2015). Furthermore, the FG, which includes the FFA and FBA, could represent the characteristics of the whole person (Kim and McCarthy, 2016). One previous study found that the synthetic patterns which are modeled by a linear combination of face- and body-evoked response patterns could precisely approximate the whole person-evoked response patterns in the right FG, implying a part-based manner of representation (Kaiser et al., 2014). Another recent study suggested that both the EBA and FBA preferred whole bodies to the sums of their scrambled parts (Brandman and Yovel, 2016), which indicated that bodies seemed to be represented in an integrated way, rather than in a part-based way in the EBA and FBA. Therefore, it remains controversial whether the EBA and FG represent the whole person in an integrated or part-based manner.

Some studies have found emotional effects on representations in the EBA (Grezes et al., 2007; Peelen and Downing, 2007) and FG (Fox et al., 2009; Morawetz et al., 2016). FG in the ventral visual stream was suggested to be capable of receiving top-down input signals from regions like the amygdala (AMG) for further detailed processing (Vuilleumier, 2005; Furl et al., 2013; Saarimaki et al., 2016). The superior temporal sulcus (STS) has been identified as playing a selective role in perceiving faces and bodies by fMRI techniques in macaque (Tsao et al., 2003; Pinsk et al., 2005) and human (Tsao et al., 2008; Pinsk et al., 2009) brain studies. Notably, the posterior STS (pSTS) was a crucial node, acting as a hub for processing social stimuli (Lahnakoski et al., 2012). Some studies have demonstrated that the pSTS was involved in the processing of movements, postures, and emotions of faces and bodies (Grezes et al., 2007; Candidi et al., 2011; Zhu et al., 2013; Baseler et al., 2014). In addition, the pSTS, together with the OFA and FFA, was found to comprise a core system of face perception (Fox et al., 2009). The core system for face perception was extended by including the AMG, inferior frontal gyrus (IFG), and insula, which were supposed to be recruited in processing emotional expressions (Ishai et al., 2005). However, emotion perception and experience do not show the 1:1 relationship within each brain region that the model suggests. The AMG, for example, is thought to underlie the decoding of facial expressions, but its activity may be present with other emotions and may at times be absent with fear (Sormaz et al., 2016; Zhang et al., 2016). Therefore, it remains unclear whether these areas could be modulated by emotion when representing the whole person in an integrated or part-based manner.

In this study, we considered two possible scenarios (**Figure 1**). In the first, whole person perception activates nothing but face- and body-selective neural populations, implying a part-based representation (**Figure 1A**). In the second, not only face- and body-selective neural populations, but also neurons specifically responsive to whole persons are activated; this reflects an integrated representation (Kaiser et al., 2014; **Figure 1B**). However, the coactivated patterns for multiple voxels can now be examined with the development of fMRI data analysis approaches. As compared with the traditional measure of the mean response magnitude, richer information on neural representations can be provided by the voxel-by-voxel activation patterns, and at a finer scale (Haynes and Rees, 2006; Norman et al., 2006; Liang et al., 2017). The two scenarios suggest different predictions for the pattern associations. In the first scenario, there is a strong correlation between the whole person-evoked response patterns and synthetic mean patterns (the average of face- and body-evoked activity patterns); this reflects a part-based representation (**Figure 1C**). In the second scenario, the whole person patterns cannot be modeled by a linear combination of two isolated face and body patterns, reflecting an integrated representation (**Figure 1D**; Kaiser et al., 2014). In the current study, we hypothesized that: (1) there were several specific areas (AMG, IFG, OFA, EBA, STS, FG, and insula) in which the whole person patterns could be modeled by means of face and body patterns, thus reflecting a part-based representation.

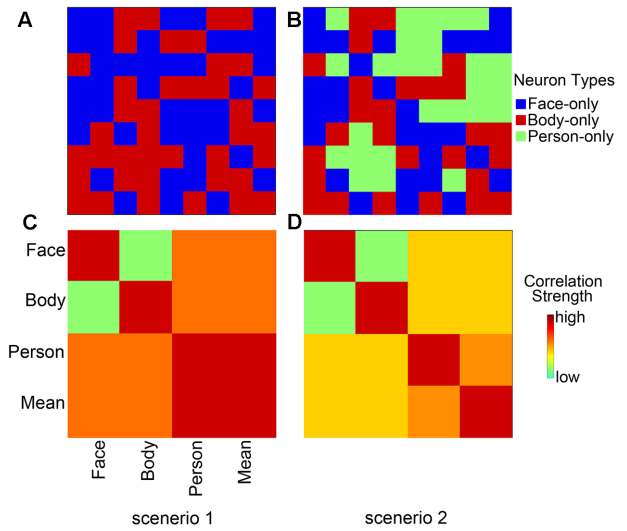


**FIGURE 1 |** Two hypothetical representation systems. **(A)** Scenario 1, part-based representations are shown as the activities of a population of neurons. Whole person perception activates only face- and body-selective neural populations. **(B)** Scenario 2, integrated representations are shown as the activities of a population of neurons that activate not only face- and body-selective neural populations, but also whole person-only neural populations. **(C)** Scenario 1, part-based representations shown as multi-voxel patterns. Whole person patterns are strongly correlated with the synthetic mean patterns, which were calculated as the average of, face and body patterns. **(D)** Scenario 2, integrated representations shown as multi-voxel patterns. The correlations between whole person patterns and the synthetic mean patterns were much weaker.

Furthermore, because these specific areas were suggested to be capable of processing emotional expressions (Haxby et al., 2000; Ishai et al., 2005), we also hypothesized that (2) emotions could modulate the relationship between the whole person and the synthetic mean person. That is to say the correlation value between the whole person and the synthetic mean person is different within each specific emotion. Therefore, we designed a block fMRI experiment in which images of nine conditions (body types: face, body, whole person; emotions: happiness, anger, fear) were presented to participants. Multi-voxel pattern analysis (MVPA) and pattern similarity analysis were conducted to examine how responses to the whole persons were associated with responses to the isolated faces and bodies in all regions of interest (ROIs) for each of the three emotions. Those regions for which encoding is part-based would demonstrate a good approximation between the whole person patterns and the linear combination of face and body patterns. Furthermore, we employed an optimization procedure to determine the optimal weights for combining the face and body patterns into the whole person pattern. In addition, we performed a multi-class classification analysis to quantify how well the activity patterns of face, body, synthetic mean person, and synthetic weighted mean person (the linear combination of face- and body-evoked response patterns, and the total weight of face and body patterns was 1) could be applied for decoding the emotions of whole person patterns.

# MATERIALS AND METHODS

## Participants

Twenty-four healthy participants were recruited in this study. All participants were right-handed, with normal or corrected-to-normal vision, and all declared having no history of neurological or psychiatric disorders. Four participants were excluded from further analysis due to movement artifacts, so we actually analyzed 20 participants (10 female; mean age 21.8 ± 1.83 years old, range from 19 to 25 years). This study was carried out in accordance with the recommendations of Institutional Review Board (IRB) of Tianjin Key Laboratory of Cognitive Computing and Application, Tianjin University with written informed consent from all subjects. All subjects gave written informed consent in accordance with the Declaration of Helsinki. The protocol was approved by the IRB of Tianjin Key Laboratory of Cognitive Computing and Application, Tianjin University.

## Experimental Stimuli

Three emotional materials (happiness, anger, and fear) (Grezes et al., 2007; de Gelder et al., 2012, 2015) were chosen from the GEneva Multimodal Emotion Portrayals (GEMEP) corpus (Banziger et al., 2012). Twenty-four video clips (four male and four female actors × three emotions) were selected and processed in grayscale using MATLAB (Kaiser et al., 2014; Soria Bauser and Suchan, 2015). Videos were edited to a duration of 2000 ms (25 frame/s) by trimming or combining longer- or shorter-length clips, respectively. Adobe Premiere Pro CC 2014 was used to generate the face and body videos by cutting out and masking the irrelevant aspect with Gaussian blur masks (Kret et al., 2011b); also, the face clips were magnified when necessary. The resulting clips were resized to 720 × 576 pixels and presented on the center of the screen. Representative stimuli for the main experiment were presented in **Figure 2A**.

Seventy-two video clips were included in the experiment. An initial validation study was conducted with another group of participants (8 female, mean age: 21.9 years; 10 male, mean age: 22.4 years). Raters were instructed to categorize the emotional materials with six labels (anger, surprise, happiness, sadness, fear, and disgust) and assess the emotional intensities according to a 9-point scale. All expressions were well-recognized (happy face: 97%, angry face: 86%, fearful face: 74%, happy body: 75%, angry body: 93%, fearful body: 82%, happy whole person: 95%, angry whole person: 95%, fearful whole person: 87%). There were no differences in intensity scores between the three emotional expressions [happiness versus anger: $t(17) = 0.73$, $p = 0.465$; happiness versus fear: $t(17) = 0.26$, $p = 0.796$; and anger versus fear: $t(17) = 1.07$, $p = 0.285$].

To examine the quantitative differences in movement in the videos, the movement per clip was estimated by quantifying the variation of light intensity (luminance) between two adjacent frames for each pixel (Grezes et al., 2007; Peelen and Downing, 2007). For each frame, the estimated movements were averaged across the pixels that scored (on a scale reaching a maximum of 255) higher than 10. Subsequently, these scores were averaged for each video. No significant differences were observed

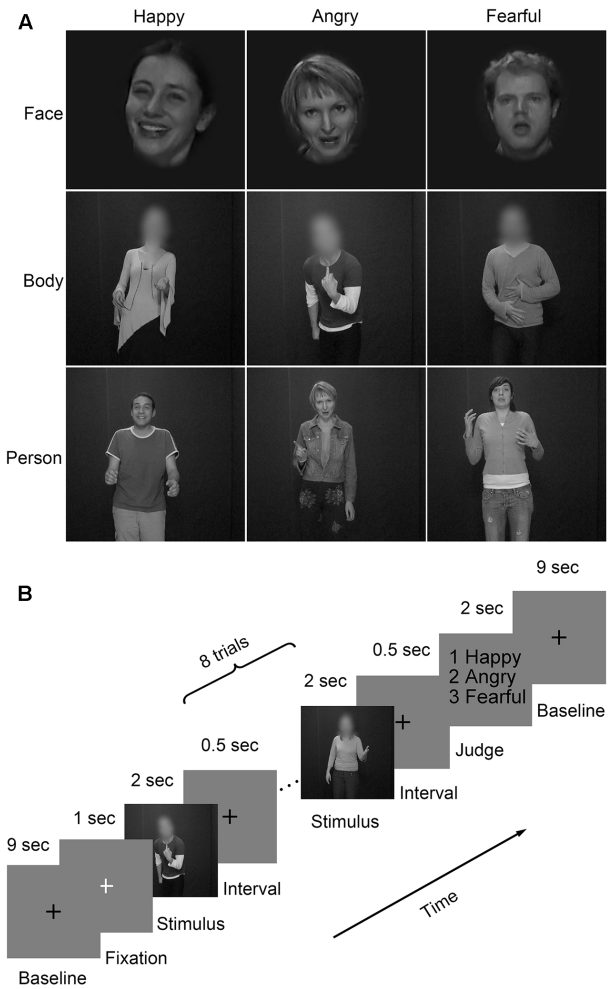


**FIGURE 2 |** Materials and paradigm of the main experiment. **(A)** Videos of faces, bodies, and whole persons showing three emotions (happiness, anger, and fear) were used in the main experiment. The faces or bodies were masked with Gaussian blur masks; **(B)** Subjects performed four runs of the emotion judgment task. Each of the first three runs consisted of face, body, and whole person conditions, while the last run was merely composed of whole person conditions. A black cross was displayed for 9 s and then a white cross for 1 s to control the attention of the subjects. They were presented between two adjacent blocks. Each block contained eight trials of the same category. Stimuli were presented for 2 s and separated by a 0.5-s interval. At the end of the block, subjects made an emotion judgment task by pressing the corresponding button within a 2-s time limit.

between the three emotional expressions [happiness versus anger: $t(23) = 0.833$, $p = 0.409$; happiness versus fear: $t(23) = 1.639$, $p = 0.108$; and anger versus fear: $t(23) = 2.045$, $p = 0.091$]. The low-level visual information of the stimuli, such as the contrast and luminance was also measured. For each frame, the estimated contrast corresponds to the standard deviation of luminance values across the pixels which score reaching a maximum of 255. The root mean square contrast has been shown to be the most reliable indicator of the visibility of broadband filtered images. Subsequently, these scores were averaged for each video. The mean contrast of 72 video clips was 18.89 ($SD = 7.30$). Similarly, the mean luminance of 72 video clips was 24.178 ($SD = 2.077$).

Furthermore, we have compared the luminance and contrast for different emotions and stimulus types. For the contrast, no significant differences were observed between three emotional expressions [happiness versus anger: $t(23) = 0.304$, $p = 0.763$; happiness versus fear: $t(23) = 0.384$, $p = 0.703$; and anger versus fear: $t(23) = 0.081$, $p = 0.936$]. And there were no significant differences for the luminance between three emotional expression [happiness versus anger: $t(23) = 1.188$, $p = 0.241$; happiness versus fear: $t(23) = 1.188$, $p = 0.241$; and anger versus fear: $t(23) = 0.322$, $p = 0.749$]. Statistical analyses for the luminance and contrast between different stimulus types, there was a significant difference between nine stimulus types for the contrast [$F(23) = 27.382$, $p < 0.001$], while no significant difference was observed for the luminance [$F(23) = 0.613$, $p = 0.764$].

## Procedure

There were four runs in the main experiment (**Figure 2B**). For each of the first three runs, three emotions (happiness, anger, and fear) expressed by three body types (face, body, and whole person) were presented. For the last run, only emotions expressed by the whole person were used. There was a 10,000 ms inter-block fixation interval (a black cross presented for 9000 ms and a white cross presented for 1000 ms to control subjects' attentions). Eighteen blocks of eight trials were pseudo-randomly presented each run. A trial consisted of a 2000 ms video and an inter-stimulus interval (ISI) of 500 ms. At the end of each block, participants were asked to make a choice between three emotions using a button press within a delay of 2000 ms.

The localizer run adopted a block design. Stimuli included four categories of dynamic or static face, body, person, and object. This run contained 16 blocks in total (4 categories × static/dynamic × repeat 2 times), and each type had two blocks, which included eight trials (1.5 s each) and a 10-s interval between blocks. The localizer run lasted for 362 s in total.

## Data Acquisition

Functional images were acquired by a 3.0 T Siemens scanner in Yantai Hospital Affiliated to Binzhou Medical University using an eight-channel head coil. Foam pads and earplugs were used to reduce the head motion and scanner noise. T2*-weighted images were acquired using an echo-planar image (EPI) sequence. In addition, T1-weighted images for an anatomical localization were acquired using a three-dimensional magnetization-prepared rapid-acquisition gradient echo (3D MPRAGE) sequence. The stimuli were displayed by high-resolution stereo 3D glasses within a VisualStim Digital MRI Compatible fMRI system. The imaging parameters of our experiment are provided in **Table 1**.

## Data Analysis

### Behavioral Measures

For each participant, the recognition accuracies and response times for the three emotions were calculated. Accuracies were tested using an analysis of variance (ANOVA) to examine the

**TABLE 1 |** Imaging parameters of T2*-weighted and T1-weighted images.

| Parameters | TR (ms) | TE (ms) | FOV | Voxel size ($mm^3$) | Matrix size | Slices | Thickness (mm) | Slices gap (mm) | FA |
|---|---|---|---|---|---|---|---|---|---|
| T2*-weighted images | 2000 | 30 | 224 × 224 | 3.1 × 3.1 × 4.0 | 64 × 64 | 33 | 4 | 0.6 | 90° |
| T1-weighted images | 1900 | 2.52 | 256 × 256 | 1 × 1 × 1 | 256 × 256 | 176 | 1 | 0 | 9° |

*TR, repetition time; TE, echo time; FOV, field of view; FA, flip angle.*

main effect and interactions between the factor Category and Emotion. Further paired *t*-tests were used to test the differences among the three emotions. SPSS 18 Software was used to perform the statistical analysis.

## Data Preprocessing

Data preprocessing was performed using the SPM8 software package[1]. The first five volumes of each run were discarded to allow for equilibration effects. The remaining 283 volumes of each run were slice-time corrected, spatially realigned to the first volume, subsampled at an isotropic voxel size of 3 mm, and normalized in the standard Montreal Neurological Institute (MNI) space. Especially for the functional images in the localization run, a 4-mm full-width at half-maximum (FWHM) isotropic Gaussian kernel was used for smoothing. The data in the first four runs were used without smoothing, as this was more suitable for the pattern similarity, weight, and pattern classification analyses. Then a general linear model (GLM) was constructed for each subject, and the subsequent analysis was conducted on each of the first three runs, generating nine activity patterns in total (happy face, happy body, happy whole person, angry face, angry body, angry whole person, fearful face, fearful body, and fearful whole person). Several sources of spurious variances along with their temporal derivatives were removed through the linear regression: six head motion parameters and averaged signals from white matter and cerebrospinal fluid (Power et al., 2015).

## Localization of Face- and Body-Selective Regions

The face-, body-, and both-selective regions were defined through a separate localizer run, in which participants performed a one-back task on face, body, whole-person, and object stimuli. The localizer scan consisted of 16 randomized blocks (four categories: face, body, whole person, and object; two statuses: static and dynamic, twice repeated for each condition) of eight trials. Each block was followed by a 10,000 ms fixation interval. Face, body, and whole person videos were the same as those in the main experiment. Object clips were selected from the materials used in a previous study (Fox et al., 2009). The middle static frames of video clips were used as the image stimulus. All stimuli were in grayscale and presented for1400 ms with an ISI of 100 ms on a gray background. Participants were required to indicate whether the present stimulus was the same as the previous one.

Through the GLM analysis, we identified the face-selective (AMG, IFG, and OFA), body-selective (EBA), and both-selective (STS, FG, and insula) areas by contrasting faces versus objects, bodies versus objects, and the average response to faces and bodies versus objects. The faces, bodies, and objects referred to the average responses to dynamic and static categories. The ROIs were generated with a liberal threshold ($p < 0.05$, with a minimum cluster extent of 10 voxels). The locations of the ROIs were shown in **Figure 3** and **Table 2**.

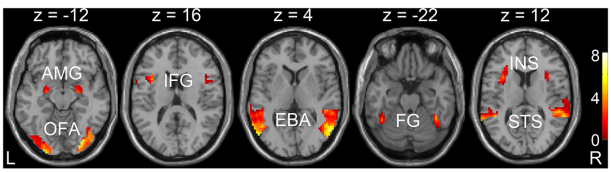


**FIGURE 3 |** Localizations of regions of interest (ROIs) at the group level. Localization was considered set for an ROI when $p < 0.05$, and with cluster corrections with a minimum extent of 10 voxels. AMG, amygdala; IFG, inferior frontal gyrus; OFA, occipital face area; EBA, extrastriate body area; STS, superior temporal sulcus; FG, fusiform gyrus; INS, insula.

## Multi-Voxel Pattern Analysis (MVPA)

The response pattern in each condition was calculated using MVPA and subsequently used to conduct the pattern similarity, weight, and pattern classification analyses. Specifically, two kinds of procedures for MVPA were included in this study (**Figure 4**). The first procedure utilized the activation patterns of each condition that were extracted from the beta values of the category regressors. These patterns were then used to perform the pattern similarity analysis and weight analysis (Kaiser et al., 2014). Pattern similarity analysis calculates the correlation coefficients between the face-, body-, whole person-evoked activity patterns, and the synthetic mean patterns (the average of face- and body-evoked activity patterns) in each ROI for the three emotions. The weight analysis can identify the weights of the face and body patterns for the case when the actual whole person patterns are maximally correlated with the synthetic mean patterns; thus, we initially evaluated the relative importance of face part and body part when people recognized a whole person. In the second MVPA step, the activation patterns of each ROI were drawn out from the normalized time series and 283 volumes were used per run. Subsequently, the activation patterns of each condition for every ROI were extracted from the time series and 20 volumes were used per condition per; these activation patterns were then used to perform the pattern classification analysis (Harry et al., 2013). The purpose of pattern classification analysis is to determine which category among the face, body, synthetic mean, and synthetic weighted mean patterns could best decode the emotions expressed by whole persons. It is important to note that only the functional data in the first three runs were used to conduct the pattern similarity analysis and weight analysis, because face, body, and whole person patterns have the same

[1]http://www.fil.ion.ucl.ac.uk/spm/software/spm8/

**TABLE 2 |** The peak coordinates, number of voxels, and peak intensities of functional ROIs.

| Hemisphere | Functional ROI | MNI coordinates | | | Voxel | Peak |
|---|---|---|---|---|---|---|
| | | *x* | *y* | *z* | number | intensity |
| R | Amygdala | 24 | −9 | −12 | 32 | 2.81 |
| L | | −24 | −9 | −15 | 35 | 4.10 |
| R | Inferior frontal gyrus | 39 | 6 | 33 | 227 | 3.56 |
| L | | −36 | 12 | 15 | 70 | 3.76 |
| R | Occipital face area | 24 | −93 | −3 | 190 | 5.88 |
| L | | −24 | −99 | −12 | 149 | 4.89 |
| R | Extrastriate body area | 51 | −72 | 0 | 879 | 7.33 |
| L | | −54 | −72 | 3 | 660 | 5.86 |
| R | Superior temporal sulcus | 54 | −36 | 9 | 429 | 5.74 |
| L | | −45 | −45 | 12 | 161 | 4.37 |
| R | Fusiform gyrus | 42 | −48 | −24 | 56 | 5.42 |
| L | | −42 | −51 | −21 | 40 | 2.92 |
| R | Insula | 36 | 21 | 3 | 176 | 2.45 |
| L | | −33 | 12 | 15 | 235 | 3.33 |

*Coordinates refer to the MNI coordinate system. $p < 0.05$, uncorrected, with a minimum cluster extent of 10 voxels. L, left. R, right.*

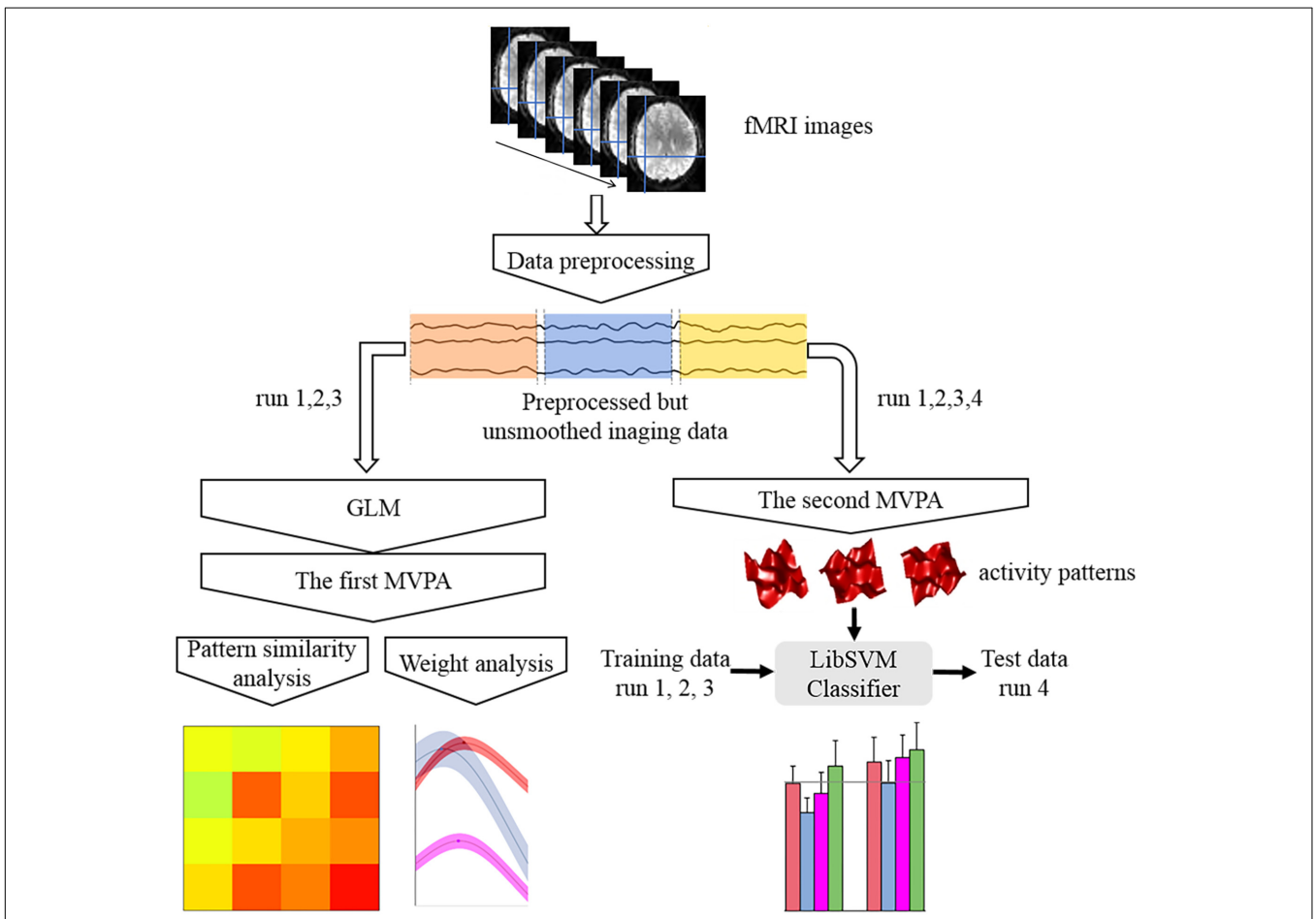


**FIGURE 4 |** Flow chart of the main analytical steps. There were two kinds of multi-voxel pattern analysis (MVPA) procedures. The results of the first MVPA were applied to pattern similarity analysis and weight analysis, while the results of the second one were used to perform classification analysis.

sampling points. However, we used all four runs to perform the category classification analysis to ensure that the training data (the first three runs) and test data (the fourth run) would be independent.

In the pattern similarity analysis, the average of face and body patterns across all voxels in a given ROI was calculated as a synthetic mean pattern, which was similar to the approach used in previous studies (Baeck et al., 2013; Kaiser et al., 2014). To estimate the pattern similarity of different categories, we computed the Pearson's linear correlations among the face, body, whole person, and synthetic mean patterns for every two out of three runs (three possible pairs altogether), and then a Fisher's $Z$ transformation was conducted. After that, a representational similarity matrix (RSM) was constructed for each individual subject. The RSMs were then averaged at the group level and $2 \times 3$ ANOVA analyses were performed to examine the main effect and significant interactions between the factors Category and Emotion.

To detect the optimal weights for face and body patterns within each emotion when modeling the whole person pattern, we designed a simple optimization procedure by our own to obtain the maximum value of the correlation between a linear combination of the face and body activation patterns with the whole person pattern, as was done in a previous study (Kaiser et al., 2014). For each subject, the data (the results of the first MVPA procedure) were first averaged across three runs. The optimization procedure was then conducted individually, and a Fisher's $Z$ transformation analysis was performed to transform the Pearson's correlation values to $z$-values. The total weight of face and body patterns was 1, given that the correlation magnitude was assumed to be related only to the face and body patterns. Hence, our approach represents the relative, rather than absolute, contributions of face and body patterns. We set the face coefficient to $\alpha$, and the body coefficient to $\beta$, such that it was constrained to be identical to $(1-\alpha)$. Thus the synthetic weighted mean pattern was approximately equal to $\alpha$ * face pattern + $\beta$ * body pattern. The correlation coefficients varied with the increase of $\alpha$ from 0 to 1 in 0.01 increments. The optimal weights of face and body patterns were obtained when the correlation between the synthetic mean patterns and whole person patterns reached its maximum value. Finally, statistical analyses were conducted on the correlations from the various alpha/beta values for each subject to examine the statistical significance.

If the whole person patterns could be represented by the face and body patterns, we inferred that the whole person patterns could be decoded using the combination of face and body patterns. So the pattern classification analysis using the multi-voxel patterns was carried out to assess the relationship between the whole person pattern and the single part ("face" and "body" pattern) and synthetic patterns ("mean" and "weighted mean" pattern). In MVPA[2], the functional imaging data were changed into activity patterns that were subsequently transformed to $z$-scores. Then significant feature extractions were conducted using ANOVA ($p = 0.05$) over all of the first three runs and all conditions, which were essential for reducing irrelevant features and achieving good performances (Pereira et al., 2009). By applying a linear support vector machine (LibSVM)[3] to perform the pattern classification analysis over emotions, we designed a "whole person" SVM predictor (from the fourth run) and four training models (from the first three runs). The models were trained by four patterns: a "face" and a "body" pattern, each evoked by face or body separately; a "mean" pattern that was represented by a combination of face and body patterns at the same weights, and a "weighted mean" at the individual optimal weights that were estimated in the above optimization procedure. It was worth noting that the pattern classifiers were trained or tested separately for each ROI. The classification results were tested against chance (33.33%) at the group level and corrected for multiple comparisons by analyzing the false-discovery rate (FDR) across 28 comparisons (seven ROIs and four classification accuracies for each).

# RESULTS

## Behavioral Performance

The mean recognition accuracy of face, body, and whole person expressions was 98.0% ($SD = 5.3$). The $3 \times 3$ ANOVA for accuracies with the factors Category (face, body, and whole person) and Emotion (happiness, anger, and fear) revealed no significant main effect for Category [$F(2,38) = 1.03$, $p = 0.367$] or Emotion [$F(2,38) = 2.98$, $p = 0.063$], nor a significant interaction [$F(4,76) = 0.69$, $p = 0.599$]. The statistical analysis by $3 \times 3$ ANOVA for the response time with the factors Category and Emotion showed a main effect for Emotion [$F(2,38) = 20.53$, $p < 0.001$] but not for Category [$F(2,38) = 1.91$, $p = 0.162$]; nor were any significant interactions observed [$F(4,76) = 1.91$, $p = 0.118$]. Additionally, paired comparisons among the three emotions irrespective of the factor Category showed that subjects' response times to happy expressions were shorter than those to anger [$t(19) = 3.98$, $p = 0.001$] or fear [$t(19) = 6.15$, $p < 0.001$]. In addition, they reacted significantly faster to the angry expressions than to the fearful ones [$t(19) = 2.75$, $p = 0.013$]. **Table 3** showed the descriptive statistics of behavioral data at the group level. The subjects' recognition accuracies and response times for the nine conditions in the emotion distinction task were shown, although only the means and standard deviations of correct responses were provided.

## Pattern Similarity Analysis

In order to examine the correlations between the face-evoked patterns, body-evoked patterns, whole person-evoked patterns, and synthetic mean patterns (an unweighted average of face- and body-evoked patterns), a pattern similarity analysis was conducted by calculating the RSM of each ROI. The whole person patterns and the synthetic mean patterns were highly correlated in the OFA, EBA, and FG ($r > 0.79$), and weakly correlated in the STS (happy: 0.48, angry: 0.55, fearful: 0.57). However, the whole person patterns were poorly correlated with the synthetic

[2]http://www.csbmb.princeton.edu/mvpa

[3]http://www.csie.ntu.edu.tw/~cjlin/libsvm/

**TABLE 3 |** Mean emotion identification accuracies and corresponding response times.

| Emotion | Category | Recognition rate (%) | | Response time (ms) | |
|---|---|---|---|---|---|
| | | Mean | *SD* | Mean | *SD* |
| Happy | Face | 100 | 0 | 713.74 | 163.39 |
| | Body | 97.50 | 6.11 | 669.36 | 160.87 |
| | Person | 100 | 0 | 675.25 | 155.35 |
| Angry | Face | 97.50 | 6.11 | 808.22 | 235.30 |
| | Body | 97.50 | 6.11 | 762.83 | 227.69 |
| | Person | 98.75 | 3.05 | 767.05 | 224.22 |
| Fearful | Face | 96.67 | 6.84 | 809.54 | 234.73 |
| | Body | 96.67 | 6.84 | 825.16 | 220.20 |
| | Person | 97.08 | 5.59 | 836.10 | 210.54 |

mean patterns ($r < 0.32$) in the ROIs including the AMG, IFG, and insula. **Figure 5** showed the results of the pattern similarity analyses for face-selective (AMG and OFA; **Figures 5A,B**), body-selective (EBA; **Figure 5C**), and both-selective (STS and FG; **Figures 5D,E**) areas for all three emotion conditions. We also tried to standardize the color scale, but the difference between the patterns of the brain regions became insignificant, as shown in **Supplementary Figure S1**.

Furthermore, we explored whether the whole person patterns were better approximated by the synthetic patterns than by the face or body patterns in the OFA, EBA, FG, and STS. Two 2 × 3 ANOVAs were conducted on the calculated $z$-values. Analysis with the factors Category (person-face and person-synthetic) and Emotion (happiness, anger, and fear) revealed a main effect in the EBA of Category [$F(1,19) = 20.88$, $p < 0.001$], in which the synthetic patterns approximated the person patterns significantly better than did face patterns; however, no significant main effect of Emotion [$F(2,38) = 1.96$, $p = 0.146$] nor significant interaction [$F(2,38) = 0.18$, $p = 0.834$] were identified. In the OFA, FG, and STS, no significant main effects or interactions were found. Analysis with the factors Category (person–body and person–synthetic) and Emotion (happiness, anger, and fear) identified significant main effects of Category in all four brain areas, indicating that the synthetic patterns better approximated the person patterns than did body patterns in all four areas. A main effect for Emotion was also observed in the EBA and STS [EBA: $F(2,38) = 3.93$, $p = 0.022$, STS: $F(2,38) = 3.56$, $p = 0.032$], but not the OFA or FG. No significant interactions were identified for any brain area. Taken together, these results show that only the EBA had greater person–synthetic correlations than both person–face and person–body correlations. In addition, this relationship in the EBA had been modulated by emotion. **Table 4** showed the differences between the person–synthetic correlation and the person–face correlations or the person–body correlations.

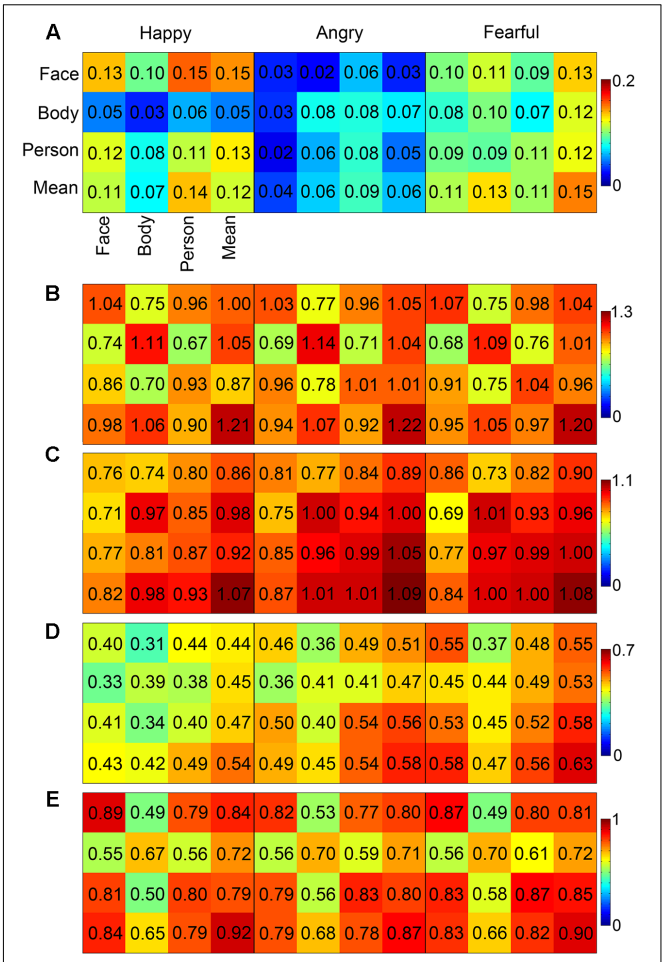


**FIGURE 5 |** MVPA results. The correlation matrices in the AMG, OFA, EBA, STS, and FG **(A–E)** for the three emotions that were calculated between each pair of the face patterns, body patterns, whole person patterns, and synthetic mean patterns (a simple average of face and body patterns). In the EBA, the whole person patterns can be precisely modeled by the synthetic mean patterns for each emotion.

## Weight Analysis

To investigate the relative contribution of the face patterns and body patterns in decoding the whole person patterns, an optimization procedure was applied to compute the optimal correlation coefficients. **Figure 6** showed the correlation curves and optimal values in the body-sensitive (EBA) and both-sensitive (FG and STS) areas. The maxima were above 1.55 in OFA, EBA, and FG for any emotion, ranging from 1.06 to 1.15 in the STS and below 0.80 in the other regions for any emotion. At the group level, we examined whether the optimal weights of the body patterns were different for the three emotions in the OFA, EBA, STS, and FG. A 3 × 4 ANOVA for body weighting with the factors Emotion and ROI revealed a significant main effect for Emotion [$F(2,38) = 10.02$, $p < 0.001$] and for ROI [$F(3,57) = 46.99$, $p < 0.001$], although no significant interaction between them was observed [$F(6,114) = 0.33$, $p = 0.923$]. Further paired comparisons showed greater weights of body patterns for fearful expressions than angry [$t(79) = 13.60$, $p < 0.001$] or happy [$t(79) = 13.80$, $p < 0.001$] expressions, while there was no significant difference between angry and

**TABLE 4 |** Differences between the person–synthetic correlation and the person–face correlations or the person–body correlations.

| Brain areas | The person–synthetic correlation versus the following correlations | | | | | | | | | | | |
|---|---|---|---|---|---|---|---|---|---|---|---|---|
| | Person–face | | | | | | Person–body | | | | | |
| | Main effect | | | | Interaction | | Main effect | | | | Interaction | |
| | Category | | Emotion | | | | Category | | Emotion | | | |
| | *F* | *p* | *F* | *p* | *F* | *p* | *F* | *P* | *F* | *p* | *F* | *p* |
| OFA | 0.02 | 0.880 | 1.13 | 0.328 | 0.19 | 0.826 | 30.24 | 0 | 1.78 | 0.174 | 0.01 | 0.992 |
| EBA | 20.88 | 0 | 1.96 | 0.146 | 0.18 | 0.834 | 4.71 | 0.032 | 3.93 | 0.022 | 0.12 | 0.887 |
| STS | 2.69 | 0.104 | 0.02 | 0.984 | 0.02 | 0.984 | 15.47 | 0 | 3.56 | 0.032 | 0.11 | 0.894 |
| FG | 0.03 | 0.871 | 0.31 | 0.733 | 0.05 | 0.952 | 34.37 | 0 | 0.65 | 0.522 | 0.05 | 0.949 |

*OFA, occipital face area; EBA, extrastriate body area; STS, superior temporal sulcus; FG, fusiform gyrus.*

happy emotions [$t(79) = 0.25$, $p = 0.802$]. We also discovered that body pattern weights in the EBA were significantly greater than those in the STS [$t(59) = 4.43$, $p < 0.001$], whereas those in the STS were notably higher than those in the FG [$t(59) = 4.71$, $p < 0.001$]. Those in the OFA were the lowest [significantly lower than those in the FG: $t(59) = 3.63$, $p = 0.001$].

Additionally, one-sample *t*-tests in the EBA found that the optimal weights for happy expressions were significantly lower than 0.5 [$t(19) = 2.99$, $p = 0.008$], indicating that more face than body information was needed when combining them to form the whole person pattern. No significant difference from 0.5 was found for the angry stimulus [$t(19) = 0.42$, $p = 0.676$], and only a weak trend toward significance for the fearful stimulus [$t(19) = 1.80$, $p = 0.088$], implying that the whole person patterns could be modeled by a linear combination of half of the face and body patterns in the EBA.

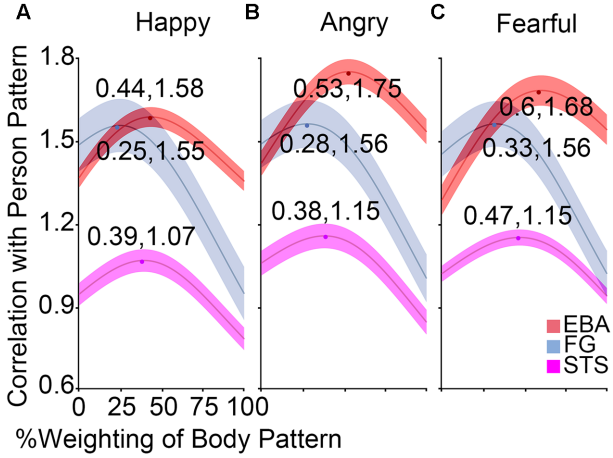


**FIGURE 6 |** Results of weight analysis. **(A–C)** The correlation curves at the group levels in the EBA, FG, and STS for happy, angry, and fearful emotions, which were computed by the correlations between the whole person pattern and the combination of face and body patterns according to variable weights. The middle line of every band represents the mean optimal estimate, while the half-width of every band represents SEM. The optimal weight of body patterns was lower than that of face patterns for happy expressions in the body-selective EBA, while it was almost the same as that of face patterns for angry and fearful expressions.

## Pattern Classification

If the whole person patterns could be represented by combining the face and body patterns, we inferred that the whole person patterns could also be decoded using the combination. Therefore, four kinds of classification analyzes based on the activated patterns were performed (between three emotions), whose models were trained by the face patterns, body patterns, synthetic mean patterns, and synthetic weighted mean patterns, respectively, and whose predictors were all activity patterns (which were subsequently transformed to *z*-scores) of the whole persons. After FDR corrections for multiple comparisons, none of the face and body patterns were successfully classified in all seven ROIs, which demonstrated that neither part alone could represent the emotional information conveyed by the whole person. Additionally, none of the average patterns or synthetic patterns were successfully classified in any area, while it was worth noting that the two classification accuracies (classifier were trained by the synthetic mean patterns and synthetic weighted mean patterns) in the EBA were relatively high. In total, this analysis was not very sensitive. Only in the EBA, could the whole person patterns successfully decode the synthetic mean patterns and synthetic weighted mean patterns. However, after FDR corrections for multiple comparisons, the result was no longer statistically significant. Only the results in the OFA, EBA, STS, and FG are shown in **Figure 7**, as accuracies in the other three ROIs were relatively small (see the detailed classification accuracies in **Supplementary Tables S1**, **S2**).

# DISCUSSION

In the present study, we explored how specific ROI responses to the whole persons were associated with the responses to the isolated faces and bodies. Our MVPA and pattern

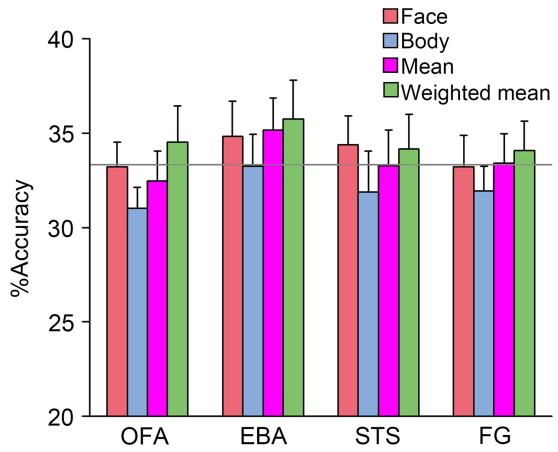


**FIGURE 7 |** Pattern classification performances. The accuracies of support vector machine (SVM) that were trained by "face," "body," "synthetic mean," and "synthetic weighted mean" and tested by the whole person predictor were not significantly greater than the chance level in all ROIs. Error bars indicate SEM.

similarity findings suggested that the whole person patterns approximated the combined weighted mean patterns of face and body in the EBA. Furthermore, the correlation coefficient of the body pattern was lower than that of the face pattern for happy expressions, although it was equal to that of the face patterns for the two threatening expressions (anger and fear).

## A Pattern Similarity between the Whole Person and Synthetic Person Was Shown in the EBA

In our study, the EBA and STS were the sole brain ROIs in which whole person–synthetic correlations were significantly greater than both whole person–face and whole person–body correlations irrespective of emotions. As a consequence, respective information from the face and body patterns contributed to the high similarity between the whole person patterns and the synthetic mean patterns in the EBA (Kaiser et al., 2014). The finding that the face and body patterns provided unique information to whole person patterns showed that the face and body were represented separately in the EBA. Developmental work has suggested that the response patterns of monkey inferior temporal neurons showed obvious clusters specific for faces, hands, and bodies (Kiani et al., 2007). Our findings were consistent with one functional imaging study that had proposed a distributed representation of faces, bodies, and objects in the human OTC, and highlighted category-specific modules in processing them at the same time (Caspari et al., 2014; Watson et al., 2016). Together with our findings, these results indicated that representations of faces and bodies in the EBA were likely to be quite distinct, supporting a part-based representation of whole persons therein.

Face and body patterns contribute equally in combination to form whole person patterns in the EBA for threatening expressions. In the EBA, the optimal weight of body patterns was lower than that of face patterns for happy expressions, but it was almost the same as that of face patterns for angry and fearful expressions. Faces and bodies are both familiar and salient in our daily life, and often convey some similar information, leading to many common points of processing even in affective neuroscience (de Gelder et al., 2010, 2015; Kim and McCarthy, 2016). Furthermore, unlike many studies using headless bodies, we employed bodies with blurred faces to avoid the confounder in which the headless bodies act as novel stimuli that attract more attention than normal. This ensured the contributions of faces and bodies combined to form the whole person would be compared fairly (Kret et al., 2011a,b). One previous study demonstrated that in the EBA, both faces and bodies produced more activations for threat than neutral expressions, and the difference in bodies versus faces was even larger (Kret et al., 2011b). Another study discovered that happy postures were less attended to than either angry or fearful postures by applying gaze measures (Kret et al., 2013). All the above findings were in accordance with our conclusions that body patterns might have a smaller weight than face patterns for happy expressions, but equal weights for angry and fearful expressions.

## Potential for Emotion Classification Performance by the Synthetic Weighted Mean Person in the EBA

In this study, we found that the responses to whole persons were potentially decoded by a weighted average of the responses to face and body, which was in line with previous studies mainly concerning object representations (Agam et al., 2010; Watson et al., 2016). Furthermore, other studies have found evidence for other forms of linear combinations (Zoccolan et al., 2005; Macevoy and Epstein, 2009) and for nonlinearities (Gawne and Martin, 2002; Heuer and Britten, 2002). Studies with monkeys can measure responses at the level of individual neurons, which is not practical in humans. A macaque study (Zoccolan et al., 2007) found that the exact relationship depended on how selective a neuron was for the given stimuli. For highly selective neurons, the relationship tended to be a simple average, as suggested in another experiment (Zoccolan et al., 2005) and which was in accordance with our study. Through a regression analysis, rather than MVPA, many studies of human subjects have found that a linear combination of the responses to two single objects could best decode the responses to the pair, supporting the most comprehensive model, the weighted mean of face and body patterns used in our experiment t (Macevoy and Epstein, 2009; Baeck et al., 2013).

Moreover, the body perception mechanism was directly explored in several studies (Droit-Volet and Gil, 2016; Borgomaneri et al., 2017). One previous study (Taylor et al., 2007) found a gradual activity increase in the EBA as more body

information was represented, suggesting, as we found, that the whole person might be represented in a part-based manner in the EBA. Another study (Liu et al., 2010) found that the OFA was sensitive to face parts. Given the previously proposed functional analogy between face- and body-sensitive areas of the VOTC (Minnebusch and Daum, 2009), we speculated that EBA might represent whole persons in a part-based manner, whereas the OFA preferred face parts. In addition, a recent study (Brandman and Yovel, 2016) pointed out that whole bodies were presented in a configurable rather than part-based manner in two body-selective areas, the EBA and FBA, by comparing the whole bodies and sums of their scrambled parts. Some aspects of this discrepancy may be explained. The preceding study mainly focused on the first-order configuration, so the presentation of stimuli was different from ours. That is, all of the body parts were presented simultaneously in a scrambled manner in the foregoing study, while parts were presented as isolated faces and bodies in our study. What's more, only signal changes and two-classification approaches were used in that study, resulting in a less comprehensive analysis to some extent. Furthermore, the emotion factor was not considered in any of the above studies. It is notable that some other studies, respectively, discovered that faces were represented in a holistic manner in the FFA (Zhang et al., 2012; Song et al., 2013), that configurable processing of headless bodies occurred in the right FBA (Soria Bauser and Suchan, 2015), and that a linear combination of face and headless body patterns was utilized in the FG (Kaiser et al., 2014). Our study showed no precise combination relationship in the FG, probably because not only face- and body-selective neurons, but also other neurons, were tuned uniquely to whole persons. This finding was confirmed in another study (Bernstein et al., 2014), which proposed that the integration of faces and bodies into whole persons was found in the FG at mid-level stages of object processing, but not in the lateral-occipital face and body areas at early stages. In our study, the face-selective areas (OFA and IFG) and emotion-sensitive areas (AMG and insula), as well as the STS, showed no part-based representation. The OFA has been reported to be capable of handling faces at the level of parts (Taylor et al., 2007; Liu et al., 2010). IFG, AMG, and insula could mainly process the information of emotional faces (Ishai et al., 2005; Fox et al., 2009). The results for the STS might originate from two sources. First, in our experiment, the STS may have lacked enough voxels sensitive to bodies; second, it may not have participated in the separate processing for faces and bodies, since it was reported to play a key role in integrating information from many channels (de Gelder et al., 2010; Candidi et al., 2015). To sum up, the current study is the first to apply pattern similarity analysis, weight analysis, and classification analysis to explore the linear relationship of emotion perception in faces, bodies, and whole persons in the AMG, IFG, OFA, EBA, STS, FG, and insula.

## Limitations

Several limitations should be addressed in this study. (1) Choice of the stimuli: in our study, we investigated whether there are brain regions that could be modulated by emotions when representing the whole person. However, as there is no neutral condition, our research is limited to a certain extent. Future work is needed to examine the differences within each brain region between positive emotional modulation and the modulation of relatively neutral emotions, in addition to the differences between negative emotional modulation and neutral emotional modulation, when neutral stimuli are included. (2) Sample of the study: to predetermine the sample size, *a priori* power analysis was conducted using the statistical software G * Power[4]. Based on the literatures we referred, we first calculated the effect sizes in these studies which ranged from 0.29 to 0.96. We assumed that our study had a moderate effect size (ranged from 0.65 to 0.79). The required sample size was then computed with *a priori* power analysis, when $\alpha$ error probability was 0.05, power ($1-\beta$ error probability) was 0.95, and the effect sizes changed from 0.65 to 0.79. The *a priori* power analysis suggested the required sample size was from 19 to 28 subjects. In our study, 20 subjects were included for further analyzes, which was not large enough. Although our sample size was similar to those reported in previous publications (Taylor et al., 2007; Prochnow et al., 2013; Kaiser et al., 2014; Brandman and Yovel, 2016) and one of our latest studies on the facial affective expression decoding (Liang et al., 2017), a larger group of participants was needed in the future studies. Moreover, when the sample size gets larger, a bigger statistical power can be obtained. And a larger number of participants can better prove the effectiveness of our findings, and separate truly significant results from apparent trends or false results related to having too few subjects. Furthermore, replicating this study with a larger number of participants, and examining the potential age-related differences between different age groups are also aspects of this issue worthy of study.

Several studies have shown that the body and face are processed separately in the early stages of processing (in the EBA and OFA, respectively), and then integrated into a representation in the FG. Therefore, each brain region may not be independent when perceiving the whole person, but instead may be somewhat dependent on each other. Our future work requires further exploration of the relationship between these brain regions associated with body perception and face perception, followed by construction of a larger brain area based on these relationships to reveal the underlying mechanisms when perceiving the whole person. Additional future work should identify whether there are brain regions representing whole person patterns in a more complex way, such as the second-order combination of faces and bodies. Furthermore, choosing weights for the synthetic weighted mean approach based on the similarity of the produced synthetic weighted mean patterns to the whole person patterns may introduce a bias in the classification. Future work is needed to develop the novel method of the weight analysis in calculating the synthetic weighted mean patterns to minimize the bias in the pattern classification analysis.

[4]http://www.gpower.hhu.de/

## CONCLUSION

This study provided tentative evidence that whole person patterns could be modeled by a linear combination of face and body patterns, and that there was emotional modulation in the EBA. Firstly, we found significant correlations between the whole person patterns and the synthetic mean patterns in the EBA for all three emotions. Secondly, the face and body patterns made equal contributions to integrating information when combining into whole person patterns for threatening expressions, while the face patterns shared a greater contribution for happy expressions. To summarize, we suggest that there are significant correlations in perceiving emotions expressed by dynamic faces, bodies, and whole persons. Furthermore, the human brain can perceive whole persons in a part-based manner in the EBA. Our study provided new evidence that emotions can modulate the correlations between different patterns. Future work is needed to examine the detailed functional interactions in representing emotions of whole persons in specific brain areas, and the differences between emotional modulation and the modulation of neutral conditions within each specific brain regions.

## AUTHOR CONTRIBUTIONS

BL designed the experiments. XY, JX, and PW performed the experiments. XY, JX, and LC analyzed the results. XY and JX wrote the manuscript. JX, XL, and BW contributed to manuscript revision. All authors contributed to discuss the results and have approved the final manuscript.

## FUNDING

This work was supported by the National Natural Science Foundation of China (Nos. 61271128, 61571327, and 61703302), Shandong Provincial Natural Science Foundation of China (No. ZR2015HM081), and Project of Shandong Province Higher Educational Science and Technology Program (J15LL01).

## ACKNOWLEDGMENT

We would like to thank Prof. Irene Rotondi (Campus Biotech, University of Geneva, Switzerland) for supplying the GEMEP Corpus.

## SUPPLEMENTARY MATERIAL

The Supplementary Material for this article can be found online at: https://www.frontiersin.org/articles/10.3389/fnhum.2017.00653/full#supplementary-material

**FIGURE S1 |** Results of multi-voxel pattern analysis in a standardized color scale. We also tried to standardize the color scale, but the difference between the patterns of the brain regions became insignificant.

**TABLE S1 |** Classification accuracies of the whole person predictor trained by the face, body, synthetic mean person and synthetic weighted mean person patterns. The chance level is 33.33%. AMG, amygdala; IFG, inferior frontal gyrus; OFA, occipital face area; EBA, extrastriate body area; STS, superior temporal sulcus; FG, fusiform gyrus; INS, insula.

**TABLE S2 |** FDR correction for multiple comparisons of the above table.

## REFERENCES

Agam, Y., Liu, H., Papanastassiou, A., Buia, C., Golby, A. J., Madsen, J. R., et al. (2010). Robust selectivity to two-object images in human visual cortex. *Curr. Biol.* 20, 872–879. doi: 10.1016/j.cub.2010.03.050

Baeck, A., Wagemans, J., and Op De Beeck, H. P. (2013). The distributed representation of random and meaningful object pairs in human occipitotemporal cortex: the weighted average as a general rule. *Neuroimage* 70, 37–47. doi: 10.1016/j.neuroimage.2012.12.023

Banziger, T., Mortillaro, M., and Scherer, K. R. (2012). Introducing the Geneva Multimodal expression corpus for experimental research on emotion perception. *Emotion* 12, 1161–1179. doi: 10.1037/a0025827

Baseler, H. A., Harris, R. J., Young, A. W., and Andrews, T. J. (2014). Neural responses to expression and gaze in the posterior superior temporal sulcus interact with facial identity. *Cereb. Cortex* 24, 737–744. doi: 10.1093/cercor/bhs360

Bernstein, M., Oron, J., Sadeh, B., and Yovel, G. (2014). An integrated face-body representation in the fusiform gyrus but not the lateral occipital cortex. *J. Cogn. Neurosci.* 26, 2469–2478. doi: 10.1162/jocn_a_00639

Borgomaneri, S., Vitale, F., and Avenanti, A. (2017). Behavioral inhibition system sensitivity enhances motor cortex suppression when watching fearful body expressions. *Brain Struct. Funct.* doi: 10.1007/s00429-017-1403-5 [Epub ahead of print].

Bracci, S., Caramazza, A., and Peelen, M. V. (2015). Representational similarity of body parts in human occipitotemporal cortex. *J. Neurosci.* 35, 12977–12985. doi: 10.1523/JNEUROSCI.4698-14.2015

Brandman, T., and Yovel, G. (2016). Bodies are represented as wholes rather than their sum of parts in the occipital-temporal cortex. *Cereb. Cortex* 26, 530–543. doi: 10.1093/cercor/bhu205

Calder, A. J., and Young, A. W. (2005). Understanding the recognition of facial identity and facial expression. *Nat. Rev. Neurosci.* 6, 641–651. doi: 10.1038/nrn1724

Candidi, M., Stienen, B. M., Aglioti, S. M., and De Gelder, B. (2011). Event-related repetitive transcranial magnetic stimulation of posterior superior temporal sulcus improves the detection of threatening postural changes in human bodies. *J. Neurosci.* 31, 17547–17554. doi: 10.1523/JNEUROSCI.0697-11.2011

Candidi, M., Stienen, B. M., Aglioti, S. M., and De Gelder, B. (2015). Virtual lesion of right posterior superior temporal sulcus modulates conscious visual perception of fearful expressions in faces and bodies. *Cortex* 65, 184–194. doi: 10.1016/j.cortex.2015.01.012

Caspari, N., Popivanov, I. D., De Maziere, P. A., Vanduffel, W., Vogels, R., Orban, G. A., et al. (2014). Fine-grained stimulus representations in body selective areas of human occipito-temporal cortex. *Neuroimage* 102(Pt 2), 484–497. doi: 10.1016/j.neuroimage.2014.07.066

de Gelder, B., De Borst, A. W., and Watson, R. (2015). The perception of emotion in body expressions. *Wiley Interdiscip. Rev. Cogn. Sci.* 6, 149–158. doi: 10.1002/wcs.1335

de Gelder, B., Hortensius, R., and Tamietto, M. (2012). Attention and awareness each influence amygdala activity for dynamic bodily expressions-a short review. *Front. Integr. Neurosci.* 6:54. doi: 10.3389/fnint.2012.00054

de Gelder, B., Van Den Stock, J., Meeren, H. K., Sinke, C. B., Kret, M. E., and Tamietto, M. (2010). Standing up for the body. Recent progress in uncovering the networks involved in the perception of bodies and bodily expressions. *Neurosci. Biobehav. Rev.* 34, 513–527. doi: 10.1016/j.neubiorev.2009.10.008

Downing, P. E., Chan, A. W., Peelen, M. V., Dodds, C. M., and Kanwisher, N. (2006). Domain specificity in visual cortex. *Cereb. Cortex* 16, 1453–1461. doi: 10.1093/cercor/bhj086

Downing, P. E., and Peelen, M. V. (2016). Body selectivity in occipitotemporal cortex: causal evidence. *Neuropsychologia* 83, 138–148. doi: 10.1016/j.neuropsychologia.2015.05.033

Downing, P. E., Wiggett, A. J., and Peelen, M. V. (2007). Functional magnetic resonance imaging investigation of overlapping lateral occipitotemporal activations using multi-voxel pattern analysis. *J. Neurosci.* 27, 226–233. doi: 10.1523/JNEUROSCI.3619-06.2007

Droit-Volet, S., and Gil, S. (2016). The emotional body and time perception. *Cogn. Emot.* 30, 687–699. doi: 10.1080/02699931.2015.1023180

Fox, C. J., Iaria, G., and Barton, J. J. (2009). Defining the face processing network: optimization of the functional localizer in fMRI. *Hum. Brain Mapp.* 30, 1637–1651. doi: 10.1002/hbm.20630

Furl, N., Henson, R. N., Friston, K. J., and Calder, A. J. (2013). Top-down control of visual responses to fear by the amygdala. *J. Neurosci.* 33, 17435–17443. doi: 10.1523/JNEUROSCI.2992-13.2013

Gawne, T. J., and Martin, J. M. (2002). Responses of primate visual cortical V4 neurons to simultaneously presented stimuli. *J. Neurophysiol.* 88, 1128–1135. doi: 10.1152/jn.2002.88.3.1128

Grezes, J., Pichon, S., and De Gelder, B. (2007). Perceiving fear in dynamic body expressions. *Neuroimage* 35, 959–967. doi: 10.1016/j.neuroimage.2006.11.030

Harry, B., Williams, M. A., Davis, C., and Kim, J. (2013). Emotional expressions evoke a differential response in the fusiform face area. *Front. Hum. Neurosci.* 7:692. doi: 10.3389/fnhum.2013.00692

Haxby, J. V., Hoffman, E. A., and Gobbini, M. I. (2000). The distributed human neural system for face perception. *Trends Cogn. Sci.* 4, 223–233. doi: 10.1016/S1364-6613(00)01482-0

Haynes, J. D., and Rees, G. (2006). Decoding mental states from brain activity in humans. *Nat. Rev. Neurosci.* 7, 523–534. doi: 10.1038/nrn1931

Heuer, H. W., and Britten, K. H. (2002). Contrast dependence of response normalization in area MT of the rhesus macaque. *J. Neurophysiol.* 88, 3398–3408. doi: 10.1152/jn.00255.2002

Ishai, A., Schmidt, C. F., and Boesiger, P. (2005). Face perception is mediated by a distributed cortical network. *Brain Res. Bull.* 67, 87–93. doi: 10.1016/j.brainresbull.2005.05.027

Kaiser, D., Strnad, L., Seidl, K. N., Kastner, S., and Peelen, M. V. (2014). Whole person-evoked fMRI activity patterns in human fusiform gyrus are accurately modeled by a linear combination of face- and body-evoked activity patterns. *J. Neurophysiol.* 111, 82–90. doi: 10.1152/jn.00371.2013

Kiani, R., Esteky, H., Mirpour, K., and Tanaka, K. (2007). Object category structure in response patterns of neuronal population in monkey inferior temporal cortex. *J. Neurophysiol.* 97, 4296–4309. doi: 10.1152/jn.00024.2007

Kim, N. Y., and McCarthy, G. (2016). Task influences pattern discriminability for faces and bodies in ventral occipitotemporal cortex. *Soc. Neurosci.* 11, 627–636. doi: 10.1080/17470919.2015.1131194

Kret, M. E., Pichon, S., Grezes, J., and De Gelder, B. (2011a). Men fear other men most: gender specific brain activations in perceiving threat from dynamic faces and bodies - an FMRI study. *Front. Psychol.* 2:3. doi: 10.3389/fpsyg.2011.00003

Kret, M. E., Pichon, S., Grezes, J., and De Gelder, B. (2011b). Similarities and differences in perceiving threat from dynamic faces and bodies. An fMRI study. *Neuroimage* 54, 1755–1762. doi: 10.1016/j.neuroimage.2010.08.012

Kret, M. E., Stekelenburg, J. J., Roelofs, K., and De Gelder, B. (2013). Perception of face and body expressions using electromyography, pupillometry and gaze measures. *Front. Psychol.* 4:28. doi: 10.3389/fpsyg.2013.00028

Lahnakoski, J. M., Glerean, E., Salmi, J., Jaaskelainen, I. P., Sams, M., Hari, R., et al. (2012). Naturalistic FMRI mapping reveals superior temporal sulcus as the hub for the distributed brain network for social perception. *Front. Hum. Neurosci.* 6:233. doi: 10.3389/fnhum.2012.00233

Liang, Y., Liu, B., Xu, J., Zhang, G., Li, X., Wang, P., et al. (2017). Decoding facial expressions based on face-selective and motion-sensitive areas. *Hum. Brain Mapp.* 38, 3113–3125. doi: 10.1002/hbm.23578

Liu, J., Harris, A., and Kanwisher, N. (2010). Perception of face parts and face configurations: an FMRI study. *J. Cogn. Neurosci.* 22, 203–211. doi: 10.1162/jocn.2009.21203

Macevoy, S. P., and Epstein, R. A. (2009). Decoding the representation of multiple simultaneous objects in human occipitotemporal cortex. *Curr. Biol.* 19, 943–947. doi: 10.1016/j.cub.2009.04.020

Maurer, D., Grand, R. L., and Mondloch, C. J. (2002). The many faces of configural processing. *Trends Cogn. Sci.* 6, 255–260. doi: 10.1016/S1364-6613(02)01903-4

McKone, E., Martini, P., and Nakayama, K. (2001). Categorical perception of face identity in noise isolates configural processing. *J. Exp. Psychol. Hum. Percept. Perform.* 27, 573–599. doi: 10.1037/0096-1523.27.3.573

Minnebusch, D. A., and Daum, I. (2009). Neuropsychological mechanisms of visual face and body perception. *Neurosci. Biobehav. Rev.* 33, 1133–1144. doi: 10.1016/j.neubiorev.2009.05.008

Morawetz, C., Bode, S., Baudewig, J., Jacobs, A. M., and Heekeren, H. R. (2016). Neural representation of emotion regulation goals. *Hum. Brain Mapp.* 37, 600–620. doi: 10.1002/hbm.23053

Norman, K. A., Polyn, S. M., Detre, G. J., and Haxby, J. V. (2006). Beyond mind-reading: multi-voxel pattern analysis of fMRI data. *Trends Cogn. Sci.* 10, 424–430. doi: 10.1016/j.tics.2006.07.005

Peelen, M. V., and Downing, P. E. (2005). Selectivity for the human body in the fusiform gyrus. *J. Neurophysiol.* 93, 603–608. doi: 10.1152/jn.00513.2004

Peelen, M. V., and Downing, P. E. (2007). The neural basis of visual body perception. *Nat. Rev. Neurosci.* 8, 636–648. doi: 10.1038/nrn2195

Peelen, M. V., Wiggett, A. J., and Downing, P. E. (2006). Patterns of fMRI activity dissociate overlapping functional brain areas that respond to biological motion. *Neuron* 49, 815–822. doi: 10.1016/j.neuron.2006.02.004

Pereira, F., Mitchell, T., and Botvinick, M. (2009). Machine learning classifiers and fMRI: A tutorial overview. *Neuroimage* 45, S199–S209. doi: 10.1016/j.neuroimage.2008.11.007

Pinsk, M. A., Arcaro, M., Weiner, K. S., Kalkus, J. F., Inati, S. J., Gross, C. G., et al. (2009). Neural representations of faces and body parts in macaque and human cortex: a comparative FMRI study. *J. Neurophysiol.* 101, 2581–2600. doi: 10.1152/jn.91198.2008

Pinsk, M. A., Desimone, K., Moore, T., Gross, C. G., and Kastner, S. (2005). Representations of faces and body parts in macaque temporal cortex: a functional MRI study. *Proc. Natl. Acad. Sci. U.S.A.* 102, 6996–7001. doi: 10.1073/pnas.0502605102

Pitcher, D., Walsh, V., Yovel, G., and Duchaine, B. (2007). TMS evidence for the involvement of the right occipital face area in early face processing. *Curr. Biol.* 17, 1568–1573. doi: 10.1016/j.cub.2007.07.063

Power, J. D., Schlaggar, B. L., and Petersen, S. E. (2015). Recent progress and outstanding issues in motion correction in resting state fMRI. *Neuroimage* 105, 536–551. doi: 10.1016/j.neuroimage.2014.10.044

Prochnow, D., Kossack, H., Brunheim, S., Muller, K., Wittsack, H. J., Markowitsch, H. J., et al. (2013). Processing of subliminal facial expressions of emotion: a behavioral and fMRI study. *Soc. Neurosci.* 8, 448–461. doi: 10.1080/17470919.2013.812536

Saarimaki, H., Gotsopoulos, A., Jaaskelainen, I. P., Lampinen, J., Vuilleumier, P., Hari, R., et al. (2016). Discrete neural signatures of basic emotions. *Cereb. Cortex* 26, 2563–2573. doi: 10.1093/cercor/bhv086

Schiltz, C., and Rossion, B. (2006). Faces are represented holistically in the human occipito-temporal cortex. *Neuroimage* 32, 1385–1394. doi: 10.1016/j.neuroimage.2006.05.037

Schwarzlose, R. F., Baker, C. I., and Kanwisher, N. (2005). Separate face and body selectivity on the fusiform gyrus. *J. Neurosci.* 25, 11055–11059. doi: 10.1523/JNEUROSCI.2621-05.2005

Song, Y., Luo, Y. L., Li, X., Xu, M., and Liu, J. (2013). Representation of contextually related multiple objects in the human ventral visual pathway. *J. Cogn. Neurosci.* 25, 1261–1269. doi: 10.1162/jocn_a_00406

Soria Bauser, D., and Suchan, B. (2015). Is the whole the sum of its parts? Configural processing of headless bodies in the right fusiform gyrus. *Behav. Brain Res.* 281, 102–110. doi: 10.1016/j.bbr.2014.12.015

Soria Bauser, D. A., and Suchan, B. (2013). Behavioral and electrophysiological correlates of intact and scrambled body perception. *Clin. Neurophysiol.* 124, 686–696. doi: 10.1016/j.clinph.2012.09.030

Sormaz, M., Watson, D. M., Smith, W. A., Young, A. W., and Andrews, T. J. (2016). Modelling the perceptual similarity of facial expressions from image statistics and neural responses. *Neuroimage* 129, 64–71. doi: 10.1016/j.neuroimage.2016.01.041

Taylor, J. C., Wiggett, A. J., and Downing, P. E. (2007). Functional MRI analysis of body and body part representations in the extrastriate and fusiform body areas. *J. Neurophysiol.* 98, 1626–1633. doi: 10.1152/jn.00012.2007

Tsao, D. Y., Freiwald, W. A., Knutsen, T. A., Mandeville, J. B., and Tootell, R. B. (2003). Faces and objects in macaque cerebral cortex. *Nat. Neurosci.* 6, 989–995. doi: 10.1038/nn1111

Tsao, D. Y., Moeller, S., and Freiwald, W. A. (2008). Comparing face patch systems in macaques and humans. *Proc. Natl. Acad. Sci. U.S.A.* 105, 19514–19519. doi: 10.1073/pnas.0809662105

Vuilleumier, P. (2005). How brains beware: neural mechanisms of emotional attention. *Trends Cogn. Sci.* 9, 585–594. doi: 10.1016/j.tics.2005.10.011

Watson, R., Huis in 't Veld, E. M., and de Gelder, B. (2016). The neural basis of individual face and object perception. *Front. Hum. Neurosci.* 10:66. doi: 10.3389/fnhum.2016.00066

Zhang, H., Japee, S., Nolan, R., Chu, C., Liu, N., and Ungerleider, L. G. (2016). Face-selective regions differ in their ability to classify facial expressions. *Neuroimage* 130, 77–90. doi: 10.1016/j.neuroimage.2016.01.045

Zhang, J., Li, X., Song, Y., and Liu, J. (2012). The fusiform face area is engaged in holistic, not parts-based, representation of faces. *PLOS ONE* 7:e40390. doi: 10.1371/journal.pone.0040390

Zhu, Q., Nelissen, K., Van Den Stock, J., De Winter, F. L., Pauwels, K., De Gelder, B., et al. (2013). Dissimilar processing of emotional facial expressions in human and monkey temporal cortex. *Neuroimage* 66, 402–411. doi: 10.1016/j.neuroimage.2012.10.083

Zoccolan, D., Cox, D. D., and Dicarlo, J. J. (2005). Multiple object response normalization in monkey inferotemporal cortex. *J. Neurosci.* 25, 8150–8164. doi: 10.1523/JNEUROSCI.2058-05.2005

Zoccolan, D., Kouh, M., Poggio, T., and Dicarlo, J. J. (2007). Trade-off between object selectivity and tolerance in monkey inferotemporal cortex. *J. Neurosci.* 27, 12292–12307. doi: 10.1523/JNEUROSCI.1897-07.2007

**Conflict of Interest Statement:** The authors declare that the research was conducted in the absence of any commercial or financial relationships that could be construed as a potential conflict of interest.

frontiers in Human Neuroscience

ORIGINAL RESEARCH
published: 11 January 2018
doi: 10.3389/fnhum.2017.00661

# Racial Bias in Neural Response for Pain Is Modulated by Minimal Group

*Fengtao Shen[1†], Yang Hu[1†], Mingxia Fan[2], Huimin Wang[1,3] and Zhaoxin Wang[1,2*]*

[1] Key Laboratory of Brain Functional Genomics, Ministry of Education, Shanghai Key Laboratory of Brain Functional Genomics, Institute of Cognitive Neuroscience, School of Psychology and Cognitive Science, East China Normal University, Shanghai, China, [2] Shanghai Key Laboratory of Magnetic Resonance, East China Normal University, Shanghai, China, [3] New York University-East China Normal University Institute of Brain and Cognitive Science, NYU Shanghai, Shanghai, China

Whether empathic racial bias could be modulated is a subject of intense interest. The present study was carried out to explore whether empathic racial bias for pain is modulated by minimal group. Chinese/Western faces with neutral expressions receiving painful (needle penetration) or non-painful (Q-tip touch) stimulation were presented. Participants were asked to rate the pain intensity felt by Chinese/Western models of ingroup/outgroup members. Their implicit racial bias were also measured. Two lines of evidence indicated that the anterior cingulate cortex (ACC) was modulated by racial bias: (1) Chinese models elicited stronger activity than Western did in the ACC, and (2) activity in the ACC was modulated by implicit racial bias. Whereas the right anterior insula (rAI) were modulated by ingroup bias, in which ingroup member elicited stronger activity than outgroup member did. Furthermore, activity in the ACC was modulated by activity of rAI (i.e., ingroup bias) in the pain condition, while activity in the rAI was modulated by activity of ACC (i.e., racial bias) in the nopain condition. Our results provide evidence that there are different neural correlates for racial bias and ingroup bias, and neural racial bias for pain can be modulated by minimal group.

**Keywords: racial bias, ingroup bias, minimal group, empathy, implicit racial bias**

OPEN ACCESS

***Edited by:***
*Nan Li,*
*RIKEN, Japan*

***Reviewed by:***
*Daniel Stjepanović,*
*Duke University, United States*
*Ying Wang,*
*University of Science and Technology of China, China*

****Correspondence:***
*Zhaoxin Wang*
*zxwang@nbic.ecnu.edu.cn*

*† These authors have contributed equally to this work.*

***Received:*** *15 July 2017*
***Accepted:*** *26 December 2017*
***Published:*** *11 January 2018*

***Citation:***
*Shen F, Hu Y, Fan M, Wang H and Wang Z (2018) Racial Bias in Neural Response for Pain Is Modulated by Minimal Group. Front. Hum. Neurosci. 11:661. doi: 10.3389/fnhum.2017.00661*

## INTRODUCTION

Empathy refers to the capacity to understand and respond to the unique affective experiences of other person (Decety and Jackson, 2006), which is believed to be a key motivator and the proximate mechanism of altruistic and prosocial behavior (Batson et al., 1991; Preston and de Waal, 2002; Singer et al., 2006; Moriguchi et al., 2007). The majority of studies using functional magnetic imaging (fMRI) to unveil the neural mechanisms of human empathy used paradigms in which participants were exposed to stimuli depicting or indicating that other people were in pain (vs. no pain), one of the most basic and universal human experiences (Lamm et al., 2011). A meta-analysis indicated that a core network consisting of bilateral anterior insular cortices and medial/anterior cingulate cortex is associated with empathy for pain (Lamm et al., 2011). Importantly, empathic neural responses for pain in this network predict individual differences in costly helping (Hein et al., 2010), which is in line with the suggestion that empathy is related to prosocial behavior. Interestingly, a number of recent studies on empathy for pain have provided evidence of an empathic bias toward own race members (Xu et al., 2009; Avenanti et al., 2010; Contreras-Huerta et al., 2013). It was also found that empathic sensorimotor responses for pain could be modulated by implicit racial bias (Avenanti et al., 2009, 2010). Indeed, racism often manifests itself as a lack of empathy for other-race (Bell, 1980). Whether racial empathic bias can be reduced by a simple way is an open question.

It has been recently demonstrated that response for pain depends on the social relationships between the observer and the individuals experiencing the outcome (Montalan et al., 2012). For example, Hein et al. (2010) reported that soccer fans display stronger empathic neural responses in the anterior insula (AI) while witnessing a fan of their favorite team (ingroup) experience pain (vs. a fan of a rival team, or outgroup). Following this idea, an ERP study showed that including other-race individuals in one's own team for competitions increases neural responses to facial pain expressions in other-race faces (Sheng and Han, 2012). It should be noted that the competition between groups can generate undesired negative social implications, such as hostility to outgroup (Gaertner and Dovidio, 2000). Tajfel reported that the mere categorization of individuals into two social groups on the basis of arbitrary criteria, i.e., a minimal group paradigm, is sufficient to produce ingroup bias as compared to natural groups without eliciting explicit negative affective factors (Tajfel, 1970). It has been found that a minimal group paradigm may diminish automatic racial bias (Kurzban et al., 2001; Van Bavel and Cunningham, 2009). Moreover, a behavioral experiment showed that the mere categorization of adults on the basis of minimal criteria is sufficient to elicit an ingroup bias in empathy for pain (Montalan et al., 2012). Similarly, children also display more empathy bias favoring their ingroup after a week's novel group merely based on color (Masten et al., 2010). Thus, a minimal group paradigm may be used to reduce empathic racial bias. However, to our knowledge, the only two imaging studies (one fMRI study and one ERP study) failed to detect any significant effect of intergroup relationships on racial bias in empathic neural responses for pain (Contreras-Huerta et al., 2013, 2014). These findings led to the first concern that the possible effects of minimal group on racial empathic bias, if exist, are very weak. Further study using a more sensitive approach is required to clarify this question. Regions of interest (ROI) approach yields higher sensitivity than whole brain analyses (Mitsis et al., 2008) and thus is used in the present study.

A second concern is that typically the contrast of pain and nopain conditions is considered neural empathic response for pain in most studies (Lamm et al., 2011). However, participants with stronger implicit racial bias show increased BOLD signal to other race's faces (i.e., a nopain condition) (Phelps et al., 2000). On the contrary, participants with stronger implicit racial bias show decreased empathic sensorimotor resonance (the contrast of pain vs. nopain conditions) to other race's hand model (Avenanti et al., 2010). Obviously, these opposite patterns suggest that neural responses to race might be different between nopain and pain conditions. If so, mathematically the decreased empathic responses (contrasts of pain vs. nopain) related to stronger racial bias might not necessarily reflect the decreased neural responses for other's pain, but just represent the increased neural responses in the nopain condition. Also, there the opposite patterns between nopain and pain conditions should lead to larger individual differences in the contrasts of pain vs. nopain, which makes it even harder to detect the possible weak effects of minimal group on racial bias. Thus, it would be helpful to analyze the data of pain and nopain conditions separately to address this concern.

In the present study, we investigated whether racial bias in neural response for pain is modulated by minimal group with a relative larger sample (29 participants). A non-competitive mix race minimal group paradigm was adopted, in which all participants were randomly assigned to a novel group. They were asked to memorize their in- and outgroup faces through several minutes' learning and memory (Kurzban et al., 2001; Van Bavel et al., 2008). Later, they were asked to rate the pain intensity of these faces with neutral expressions receiving painful (needle penetration) or non-painful (Q-tip touch) stimulation were presented during fMRI scanning (Xu et al., 2009). Novel Chinese and Western faces with matched attractiveness were used to rule out historical events as well as personal involvement that may confound the mechanism of simple group categorization. An ROI approach was applied, as this approach yields higher sensitivity than whole brain analyses (Mitsis et al., 2008). Participants' implicit and explicit attitudes toward Chinese and Westerns were also measured. We hypothesized that (1) neural responses can be modulated differently by minimal group and race, (2) neural responses are differently modulated by implicit racial bias, and (3) racial bias in neural response for pain can be modulated by minimal group.

# MATERIALS AND METHODS

## Participants

A total of 37 Chinese students from East China Normal University (6 males; mean age = 20.6 years, *SD* = 1.8) voluntarily attended the current study. Data from 8 participants attending the pilot study was not analyzed, and the remaining 29 participants were used for further analysis (4 males; 14 in Red Group and 15 in Green Group; mean age = 20.5 years, *SD* = 1.7). All were right-handed with normal or corrected-to-normal vision and normal color perception, and reported no psychiatric or neurological history. After completing all tasks, participants were debriefed and paid as compensation for their time. Written informed consents were obtained from all subjects, and the protocol was approved by the University Committee on Human Research Protection (UCHRP) at East China Normal University.

## Materials and Procedure

### Stimuli

A total of 16 novel colorful photographs of face with neural expression were used. They were divided into two groups: one was assigned as ingroup members and the other as outgroup members to participants pseudorandomly. Each group consisted of eight different faces including four Chinese faces (two males) and four Western faces (two males, all Caucasian), respectively. Facial attractiveness was matched according to subjective rating of a separate group of naïve participants ($n = 28$). Each participant was also asked to provide a standard digital photograph of his/her own face with neutral expression and the photo, after processed to fit experimental standard, was included in his/her learning task (but not in the MRI session) to enhance group identification (Van Bavel et al., 2008). These faces with neutral expressions receiving painful (needle penetration) or non-painful

(Q-tip touch) stimulation applied in the left/right cheeks were then used in the fMRI session (**Figure 1**). The mean luminance of the Western faces (85.4, $SD$ = 11.9) is higher than that of Chinese faces (70.3, $SD$ = 12.0, $t_{62}$ = 5, $p$ = 0.000004), while the contrast values are not significantly different between races (4.7 ± 0.6 for Western faces and 4.5 ± 0.7 for Chinese faces, $t_{62}$ = 1.1, $p$ = 0.28). The contrast is calculated by the following equation:

$$\text{Contrast Value} = \frac{\text{Face Luminance} - \text{Background Luminance}}{\text{Overall Luminance}}$$

## Pre-scanning Group Assignment

Having arrived at the imaging center, participants were informed that the current study aimed to explore whether they could integrate into a novel minimal group as soon as possible, in which members were with multi-cultural backgrounds. They were pseudorandomly assigned to a Red Group ($n$ = 19) or Green Group ($n$ = 18), and were told to distinguish their ingroup members from outgroup members through the following learning task. The whole learning task lasted for about 15 min.

During the first learning task, participants were instructed to memorize to which group these members belong. In each trial, a face was presented for 3 s, accompanied with a red or green frame to indicate group membership, with a 1-s inter-trial fixation cross. Faces from the same group were presented sequentially in a block manner and the order of group block was counterbalanced. Each face repeated four times during the whole phase.

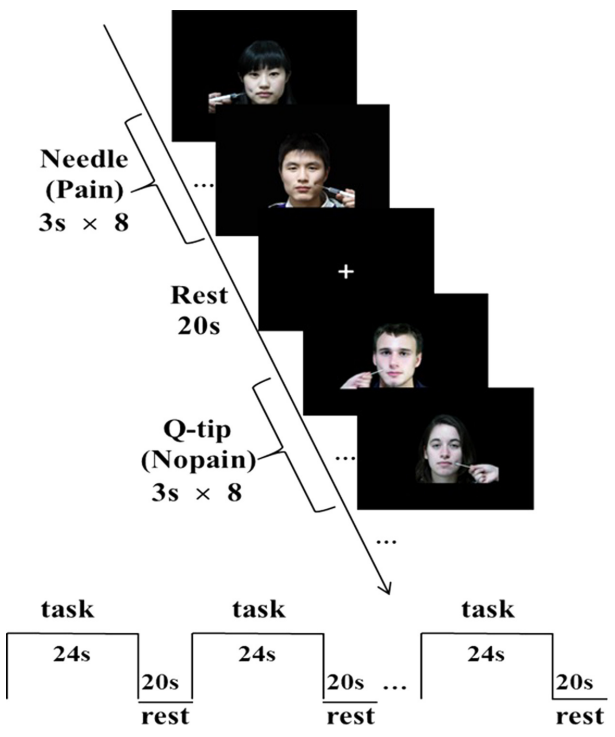


**FIGURE 1 |** Sample stimuli and fMRI experimental design. A block design was applied. Each block consisted of eight trials. Each 3-s trial depicted either ingroup or outgroup members from the same or difference race receiving painful (needle) or non-painful (Q-tip) stimulation, applied in either the left or the right cheeks.

The second learning task consisted of two blocks. In the first block, the procedure of each trial was the same as that of the first learning task except that participants were instructed to categorize each face in terms of their group membership within 3 s by pressing either "F" (ingroup members or him-/herself) or "J" (outgroup members). Then, a cartoon animation depicting either "pass a ball" or "hold a ball" for in-/outgroup members, respectively, was shown, to enhance participants' involvement. The second block was a category task, which was the same as the first block, with the exceptions as follows: (1) the color frame was removed, so that participants had to judge the group membership of each face relying on their memory; (2) each trial was followed by a feedback indicating whether the response was correct. A wrong response would lead to another judgment to the same stimuli again. A total of 30 participants with accuracy higher than 90% in this block were qualified to enter the MRI session.

## fMRI Task

A block design was applied. There were four functional runs in total. Each run consisted of eight blocks with a 2 × 2 × 2 design, each block depicted either ingroup or outgroup members from the same or difference race receiving painful or non-painful stimulation. Each block consisted of eight trials, with four different faces of the same race (four males) with neutral expression receiving painful or non-painful stimulation, applied in either the left or the right cheeks. In each trial, a stimulus without any cue of group membership was presented for 3 s, during which time participants were asked to rate the pain intensity felt by the model using a hand-shaped response box with their right hands, ranging from "1 = not painful at all" (with little finger) to "5 = severely painful" (with thumb) with each one corresponding to one finger. There was a 20-s inter-block interval, with a white fixation cross in the middle of the screen. The order of blocks within these four functional runs was counterbalanced. Stimuli were presented through goggles system (InVivo Co., United States).

## Post-scanning Procedure

Participants were first instructed to categorize each face again in terms of their group membership within 3 s to test whether they have memorized ingroup and outgroup members. Three questionnaires were used to assess (1) empathic ability, assessed by the Interpersonal Reactivity Index (IRI) (Davis, 1983), (2) attitudes of ethnic identity, measured by the Multigroup Ethnic Identity Measure (MEIM) (Phinney, 1992), and (3) the degree of agreement of individualistic and collectivistic values, detected by the Horizontal and Vertical Individualism and Collectivism (HVIC) scale (Triandis, 1996).

## Racial Attitudes Measurement

Participants' implicit and explicit attitude toward Chinese and Westerners were measured on a separate day after the fMRI session. The implicit racial attitude was measured by the Implicit Association Test (IAT) (Greenwald et al., 1998, 2003) using novel neutral Chinese and Western faces with matched attractiveness

(Avenanti et al., 2010). D-index of each participant was calculated (Greenwald et al., 2003). The explicit attitude was measured by a 5-point Likert scale (1–5) and a 11-point thermometer scale (0–10) on two racial groups (Greenwald et al., 2003).

## Image Acquisition

The scanning was conducted on a 3-Tesla Siemens Trio MR scanner, including four functional runs and one anatomical run in total. For functional images, 35 axial slices (FOV = 240 mm × 240 mm, matrix = 64 × 64, in-plane resolution = 3.75 mm × 3.75 mm, thickness = 4 mm, without gap) covering the whole brain were obtained using a T2*-weighted echo planar imaging (EPI) sequence (TR = 2000 ms, TE = 30 ms, flip angle = 90°). A high-resolution structural image was also acquired using 3D MRI sequences for anatomical co-registration and normalization (TR = 1900 ms, TE = 3.43 ms, flip angle = 7°, matrix = 256 × 256, FOV = 240 mm × 240 mm, slice thickness = 1 mm).

## Data Analysis

### Voxel-Wise Whole Brain Analysis

SPM8[1] was adopted for fMRI data analysis (Wellcome Department of Cognitive Neurology, London, United Kingdom). For each subject, EPI images were first realigned to the first volume to correct for head motion. One subject was excluded from further data analysis because of excessive inter-run head motion ( > 2 mm). Then, the anatomical image was co-registered with the mean EPI image, which was further segmented and then generated normalized parameters to MNI spaces. Next, all EPI data were projected to MNI template with a re-sampled voxel size of 2 mm × 2 mm × 2 mm. Finally, the functional images were spatially smoothed with a Gaussian kernel with a full width at half maximum (FWHM) of 8 mm. To remove low-frequency drifts, high-pass temporal filtering with a cutoff of 128 s was carried out.

Data from 29 participants were used for further analysis. For the first-level analysis, a boxcar model with eight conditions convolved with the canonical hemodynamic responses embedded in SPM (HRF) was applied. The six estimated head movement parameters were included in the design matrix to remove residual effects of head motion. Parameter estimates were then subject to a second-level analysis, a 2 × 2 × 2 ANOVA with condition (pain vs. nopain), race (Chinese vs. Western), and group (ingroup vs. outgroup) as factors with participants as dependent factors. The voxel-wise threshold was set at $p = 0.005$. To evaluate brain activations of empathy-related brain regions, the activation map was then masked by the contrasts between pain/nopain condition and rest as well as the contrast between pain condition and nopain condition ($p < 0.005$, uncorrected; $k = 30$). A Small Volume Correction was used in a sphere with radius = 8 mm.

### Region-of-Interest (ROI) Analysis

An ROI approach was then performed on regions survived in the voxel-wise analysis (Wang et al., 2010). Parameter estimates of signal intensity of 29 participants within each ROI were extracted using AFNI software package (Cox, 1996) for further repeated-measures ANOVA analysis, and paired *t*-test as *post hoc* analysis, threshold was set to $p = 0.05$ (one-tailed) for regions we have prior hypothesis, i.e., the AIs, in which ingroup members are expected to elicit stronger brain activity than outgroup members do.

We also calculated correlations between fMRI data of nopain/pain vs. rest and dispositional measures. We further assessed the relationship between the BOLD signals of the ACC and that of the rAI using correlation analysis. Bonferroni correction was used to correct for multiple comparison.

# RESULTS

## Dispositional Measures

Dispositional measures were listed as mean (SD). The mean score of IRI was 69.5 (9.3) with the mean of the empathic concern subscale was 19.0 (4.6). The mean score of MEIM was 56.7 (8.5). For the measurement of HVIC, no significant difference was found between the scores of Collectivism subscale and Individualism subscale [6.8 (1.0) and 6.5 (0.8), respectively; $t_{28} = 1.4$, $p = 0.18$]. All these scores were within the range of the norm values.

For the implicit racial attitude, the results of the IAT showed that D-index was significantly greater than zero ($t_{28} = 4.6$, $p < 0.001$), indicating an implicit preference for own-race to other-race group members. For the explicit racial attitude, participants preferred Chinese people to Western people [3.5 (0.8); $t_{28} = 3.1$, $p = 0.005$] and showed more positive attitudes toward own-race people than other-race people [Chinese: 7.6 (1.1); Western: 6.4 (1.2); $t_{28} = 3.7$, $p = 0.001$].

## Behavioral Results

Neither main effect nor interaction on response accuracy toward in- or outgroup Chinese/Western faces ($Fs_{1,28} < 1.2$, $ps > 0.1$) was found between pre- and post-scanning categorization tests. The average response accuracy of 29 participants in categorization task was shown in **Table 1**.

In the fMRI session, faces penetrated by a needle were rated more painful than those touched by a Q-tip ($F_{1,27} = 167$, $p < 0.001$). Furthermore, participants displayed higher rating scores toward Chinese faces in comparison with Western faces ($F_{1,27} = 49.0$, $p < 0.001$) both in the nopain and pain condition ($ts > 5.1$, $ps < 0.001$). Regarding the reaction time, both main race effect and race × condition interaction were found ($Fs > 25.9$, $ps < 0.001$), and these differences came from the Q-tip condition of the Western faces, which was much faster than any other conditions ($ts > 7.0$, $ps < 0.001$). No other main effect or interaction was found ($Fs_{1,27} < 3.9$, $ps > 0.06$). Please see **Table 2** for details.

## Imaging Results

The main effects of empathic responses for pain (i.e., contrast of pain vs. nopain) were found in the ACC and bilateral AIs, where participants showed stronger activity for the pain

[1]http://www.fil.ion.ucl.ac.uk/spm/

**TABLE 1 |** Mean response accuracy (SD) in pre- and post-scanning categorization test ($N$ = 29).

| | Chinese | | Western | | Total | |
|---|---|---|---|---|---|---|
| | Ingroup | Outgroup | Ingroup | Outgroup | Ingroup | Outgroup |
| Pre-scanning (%) | 97.7 (4.8) | 97.1 (4.4) | 98.7 (3.5) | 98.3 (4.0) | 98.1 (3.1) | 97.7 (3.0) |
| Post-scanning (%) | 99.0 (2.6) | 98.5 (3.9) | 98.5 (2.5) | 99.0 (4.2) | 98.6 (2.2) | 98.9 (2.4) |

**TABLE 2 |** Mean rating scores (SD) of pain intensity and reaction time (RT) during fMRI scanning ($N$ = 28).

| | Pain condition | | | | Nopain condition | | | |
|---|---|---|---|---|---|---|---|---|
| | Chinese | | Western | | Chinese | | Western | |
| | Ingroup | Outgroup | Ingroup | Outgroup | Ingroup | Outgroup | Ingroup | Outgroup |
| Rating | 2.9 (0.7) | 2.8 (0.7) | 2.7 (0.8) | 2.6 (0.7) | 0.8 (0.5) | 0.8 (0.5) | 0.4 (0.5) | 0.4 (0.3) |
| RT (ms) | 1251 (226) | 1244 (232) | 1287 (245) | 1311 (230) | 1234 (227) | 1248 (225) | 1103 (205) | 1097 (196) |

*Data from one subject was lost due to technical reasons.*

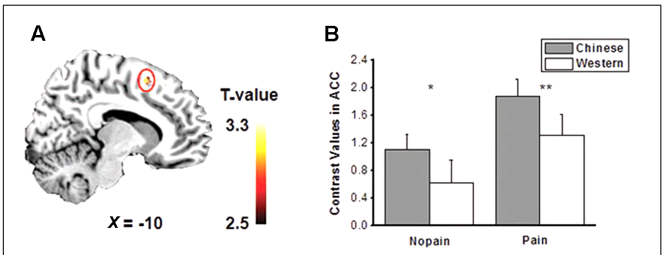


**FIGURE 2 | (A)** Activity of anterior cingulate cortex (ACC) was modulated by race ($p < 0.005$, small volume corrected). **(B)** Chinese models elicited stronger ACC activity than that of Western models both in the pain and nopain conditions (SE). *$p < 0.05$, **$p < 0.02$, one-tailed.

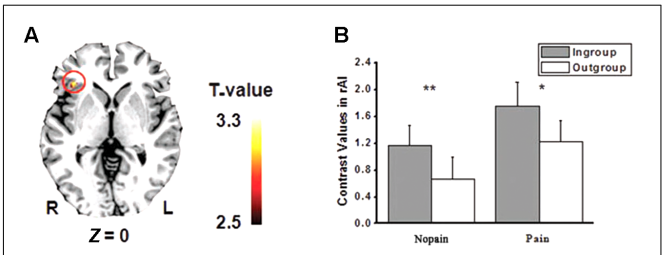


**FIGURE 3 | (A)** Activity of right anterior insula (rAI) was modulated by minimal group ($p < 0.005$, small volume corrected). **(B)** Ingroup models elicited stronger rAI activity than that of Outgroup models both in the pain and in the nopain conditions (SE). *$p = 0.05$, **$p < 0.02$, one-tailed.

condition than the nopain condition, in line with previous findings (Lamm et al., 2011). In these brain regions, the main effect of race was found in the ACC (**Figure 2A**), where participants displayed increased activity to Chinese members than Western members ($Fs_{1,28} > 7.9$, $ps < 0.01$) both in the nopain condition and in the pain condition ($ts_{28} > 2.2$, $ps < 0.05$, **Figure 2B**). The main effect of group was found in the right AI (**Figure 3A**), where participants showed increased responses toward ingroup members than outgroup members ($Fs_{1,28} > 7.9$, $ps < 0.01$) both in the nopain condition and in the pain condition ($ts_{28} > 1.7$, $ps \leq 0.05$, **Figure 3B**). Participants also displayed increased responses toward ingroup members than outgroup members in the orbitofrontal cortex (Small Volume Correction), whereas increased responses toward Western members than Chinese were observed in the visual cortices (FWE corrected). No significant interaction was found.

We calculated correlations between contrast values of nopain/pain vs. rest and dispositional measures, and found a negative correlation between D-index and racial bias (i.e., contrast of own-race vs. other-race) of ACC of non-painful stimuli vs. rest ($r = -0.47$, adjusted $p = 0.022$ after Bonferroni correction, **Figure 4A**) but a significant positive correlation between D-index and racial bias of ACC of painful stimuli vs. rest ($r = 0.46$, adjusted $p = 0.025$, **Figure 4B**). *Post hoc* $T$-test further showed a significant difference between the correlation coefficients in the pain condition and that in the nopain condition ($t_{26} = 4.54$, $p < 0.001$).

We further assessed the relationship between the BOLD signals of the ACC and that of the rAI. In the nopain condition, we found a significant positive correlation between the contrasts of own-race vs. other-race (i.e., racial bias; $r_{28} = 0.49$, adjusted $p = 0.028$ after Bonferroni correction) but not between the contrasts of ingroup vs. outgroup (i.e., ingroup bias; $r_{28} = 0.35$, $p = 0.07$,) in these two regions (**Figure 5A**), which was stood for both ingroup ($r_{28} = 0.67$, $p < 0.001$) and outgroup members ($r_{28} = 0.38$, $p = 0.04$, **Figure 5B**). In the pain condition, on the contrary, we found a significant correlation between the contrasts of ingroup vs. outgroup (i.e., ingroup bias; $r_{28} = 0.57$, adjusted $p = 0.004$) but not between the contrasts of own-race vs. other-race (i.e., racial bias; $r_{28} = 0.17$, $p = 0.39$) in these two regions (**Figure 6A**), and the correlations stood both for Chinese members ($r_{28} = 0.53$, $p = 0.003$) and Western members ($r_{28} = 0.76$, $p < 0.001$; **Figure 6B**).

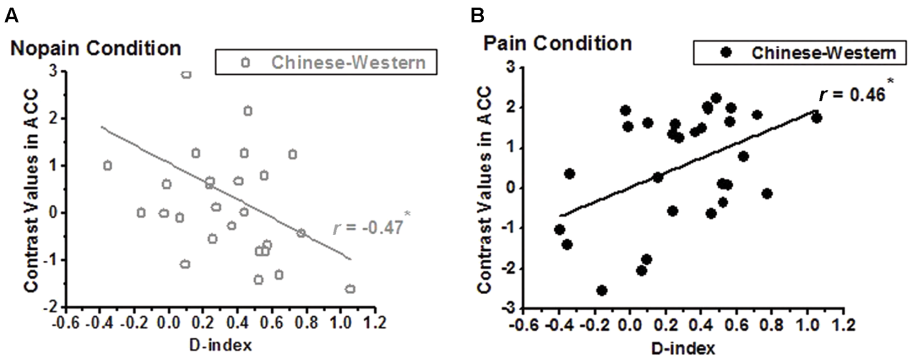


**FIGURE 4 |** Correlation between D-index and the contrasts of Chinese vs. Western of the ACC. **(A)** a significant negative correlation was found in the nopain condition (indexed by gray), but **(B)** a significant positive correlation was found in the pain condition (indexed by black), *adjusted $p < 0.05$.

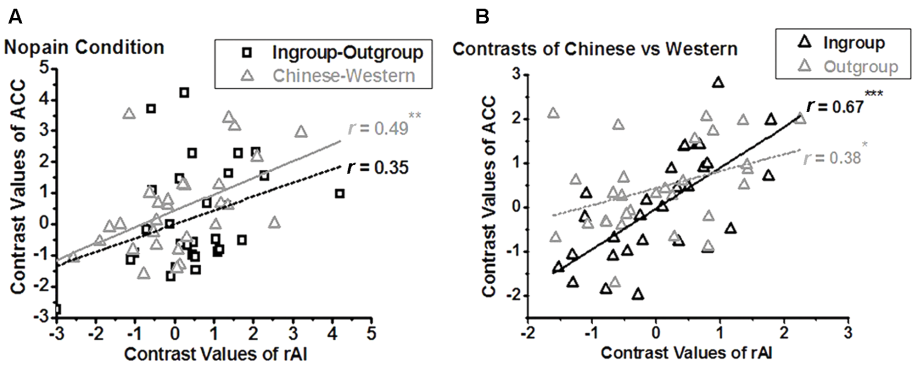


**FIGURE 5 |** Neural activity of the rAI is modulated by racial bias in nopain condition **(A)**, both for ingroup and outgroup **(B)**. In the nopain condition, a positive correlation is found between the contrasts of Chinese vs. Western (i.e., racial bias) of ACC and that of rAI (**A**, triangle; **adjusted $p < 0.05$), both for Ingroup and Outgroup members (**B**, *$p < 0.05$, ***$p < 0.001$, two tailed), but not between the contrasts of Ingroup vs. Outgroup (i.e., ingroup bias) of ACC and that of rAI (**A**, rectangle).

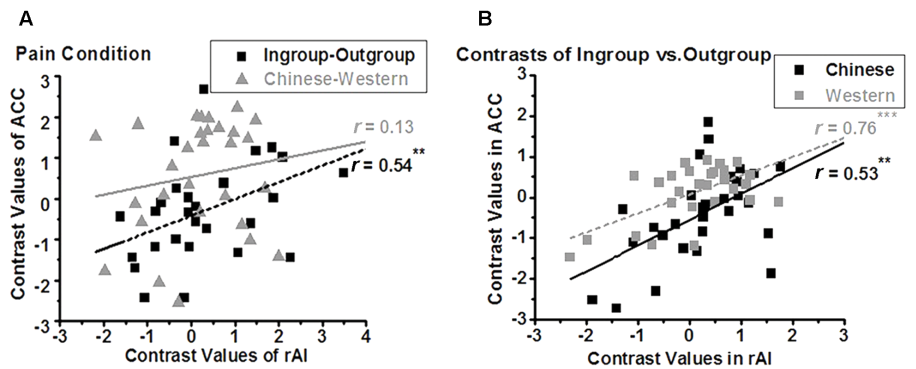


**FIGURE 6 |** Neural activity of ACC is modulated by ingroup bias in pain condition **(A)**, both for Chinese and Western **(B)**. In the pain condition, a positive correlation was found between the contrasts of Ingroup vs. Outgroup (i.e., ingroup bias) of rAI and that of ACC (**A**, rectangle, **adjusted $p < 0.01$), both for Chinese and Western pictures (**B**, **$p = 0.003$, ***$p < 0.001$, two tailed), but not between the contrasts of Chinese vs. Western (i.e., racial bias) of ACC and that of rAI (**A**, triangle).

## DISCUSSION

In the present study, we investigated whether racial bias in neural response for pain is modulated by minimal group. First, we found that different brain regions were modulated by racial bias and ingroup bias. To be specific, the ACC were more activated by the faces of own-race members than that of other-race members. Beyond previous studies (Xu et al., 2009), we further found that

activity of the ACC was modulated by implicit racial bias, but differently between nopain and pain conditions. Moreover, in line with our prior hypothesis, we found that the rAI was more activated by the faces of ingroup members than that of outgroup members. Second and critically, we found for the first time that neural responses of the ACC were modulated by ingroup bias in the pain condition, while neural responses of the rAI were modulated by racial bias in the nopain condition.

## Different Neural Correlates of Racial Bias and Ingroup Bias

We found that Chinese models elicited stronger activation than Western models did in the ACC, both for nopain and for pain conditions. Consistently, Xu et al. (2009) reported that the empathic neural response in the ACC decreased significantly when participants viewed faces of other races. Stanley et al. (2008) also suggest that the ACC is involved in the detection and regulation, respectively, of implicit attitudes. Our results confirmed Stanley's suggestion in that activity in the ACC was modulated by IAT. Moreover, we found that the activity of the ACC was modulated by implicit racial bias differently in the pain condition and nopain condition. To be specific, we found a positive correlation in the pain condition, but a negative correlation in the nopain condition, between racial contrasts of the ACC and D-index. Combined, these results suggest that the ACC is involved in empathic racial bias.

On the other hand, we found neural responses in the AI, but not the ACC, were modulated by minimal group, in line with a previous study (Lamm et al., 2007), as participants showed stronger BOLD signals to ingroup members than to outgroup members in the rAI. We assume that the difference between the BOLD signals is due to neither stimulus features nor affect, because all faces were neutral and were counterbalanced between participants. In addition, there was no explicit between-group affective or competitive difference during minimal group assignment. The difference between BOLD signals comes from minimal group assignment that is just a simple separation between 'us' and 'them.' Our results significantly extend previous studies about ingroup bias in face recognition/evaluation (Kurzban et al., 2001; Lebrecht et al., 2009; Hehman et al., 2010) and affective evaluation (Van Bavel and Cunningham, 2009).

## Racial Bias in Neural Response for Pain Is Modulated by Minimal Group

To further investigate whether racial bias in neural response for pain is modulated by minimal group, we calculated the correlations between neural responses of the rAI (which is related to ingroup bias as we have discussed) and the ACC (which is related to racial bias as we have discussed) in the pain condition. We found a positive correlation in the contrasts of ingroup vs. outgroup, but not in the contrasts of Chinese vs. Western, between the ACC and rAI in the pain condition, indicating that racial bias can be modulated by ingroup bias in the pain condition. Our results are in line with a previous ERP study that racial empathic bias can be affected by minimal group (Sheng and Han, 2012).

We also calculated the correlations between neural responses of the rAI (which is related to ingroup bias as we discussed) and the ACC (which is related to racial bias) in the nopain condition. Interestingly, we found a positive correlation in the contrasts of Chinese vs. Western, but not in the contrasts of ingroup vs. outgroup, between the ACC and rAI in the nopain condition, indicating that ingroup bias modulates racial bias in the nopain condition. We also note that neural responses of the ACC were modulated by implicit racial bias differently between nopain and pain conditions, i.e., a positive correlation between racial contrasts of the ACC and D-index in the nopain condition, but a negative correlation in the pain condition. It is high unlikely that the increased activity in the nopain condition reflects higher empathy in participants with higher racial bias. Instead, these results suggest that different mechanisms are underlying nopain and pain conditions. Further detailed study may tackle this question. Nevertheless, these differences could lead to larger individual differences and make it harder to detect possible effects of ingroup bias on racial bias in previous studies (Contreras-Huerta et al., 2013, 2014).

## Limitations

Our study bears several limitations. First, there was a large discrepancy in the gender of our participants (only four males). Stereotypically, females are portrayed as more nurturing and empathetic (Christov-Moore et al., 2014) and self-report data consistently indicates greater empathy in women (Baez et al., 2017). Despite experimental and neuropsychological measures show no consistent sex effect on empathy in most studies (Baez et al., 2017) but not all (Yang et al., 2009), it is possible that our results may be affected by gender discrepancy and further study is needed to address this question. The second issue is that no significant interaction was found in the voxel-wise analysis of imaging results. We note that the effects of minimal grouping on racial bias are very weak. Thus, this study may lack the power to detect such small difference. Further study using more participants is desired to address this issue. The third one is related to frequently reporting extremely high correlations between measures of emotion and BOLD signals of brain, or "Voodoo correlations" (Vul et al., 2009). Note that in this kind of study, typically, a voxel-wise approach was used and voxels were selected because they correlated highly with the behavioral measure of interest. However, Vul et al. (2009) also argued that the "Voodoo correlations" can be avoided by an ROI approach in which ROI is selected "blind" to the correlations of BOLD signals with the behavioral measure, as in the present study. Moreover, a sample correlation based on 25 subjects has an approximate 95% confidence interval of $\pm$ 0.4 (Nichols and Poline, 2009). In our case, data from 29 participants were used for the correlation analysis. Thus, we believe that our results are robust and the possibility of "Voodoo correlation" is very limited.

# CONCLUSION

In this study, we reported that there are different neural correlates of racial bias and ingroup bias, and moreover, racial bias in neural

response for pain is modulated by minimal group. Our findings indicate that even minimal group is sufficient to induce ingroup bias to reduce racial bias, especially in pain condition. Our findings provide important insights about racial bias, ingroup bias, as well as their dynamic relationship between nopain and pain conditions, and may have implications for understanding real-life social behaviors and provide a mechanism for a simple way to reduce racial bias.

## ETHICS STATEMENT

This study was carried out in accordance with the recommendations of the University of Committee on Human Research Protection of East China Normal University with written informed consent from all subjects. All subjects gave written informed consent in accordance with the Declaration of Helsinki.

## AUTHOR CONTRIBUTIONS

ZW and HW designed the study, analyzed the data, and wrote the paper. MF designed the study and collected the data. FS and YH collected the data, analyzed the data, and wrote the paper.

## FUNDING

This research was supported by the Natural Science Foundation of China (nos. 30700235, 31070986, and 31271134).

## ACKNOWLEDGMENTS

The authors thank the reviewers very much for their helpful comments.

## REFERENCES

Avenanti, A., Minio-Paluello, I., Bufalari, I., and Aglioti, S. M. (2009). The pain of a model in the personality of an onlooker: influence of state-reactivity and personality traits on embodied empathy for pain. *Neuroimage* 44, 275–283. doi: 10.1016/j.neuroimage.2008.08.001

Avenanti, A., Sirigu, A., and Aglioti, S. M. (2010). Racial bias reduces empathic sensorimotor resonance with other-race pain. *Curr. Biol.* 20, 1018–1022. doi: 10.1016/j.cub.2010.03.071

Baez, S., Flichtentrei, D., Prats, M., Mastandueno, R., Garcia, A. M., Cetkovich, M., et al. (2017). Men, women.who cares? A populationbased study on sex differences and gender roles in empathy and moral cognition. *PLOS ONE* 12:e0179336. doi: 10.1371/journal.pone.0179336

Batson, C. D., Batson, J. G., Slingsby, J. K., Harrell, K. L., Peekna, H. M., and Todd, R. M. (1991). Empathic joy and the empathy-altruism hypothesis. *J. Pers. Soc. Psychol.* 61, 413–426. doi: 10.1037/0022-3514.61.3.413

Bell, C. C. (1980). Racism: a symptom of the narcissistic personality. *J. Natl. Med. Assoc.* 72, 661–665.

Christov-Moore, L., Simpson, E. A., Coude, G., Grigaityte, K., Iacoboni, M., and Ferrari, P. F. (2014). Empathy: gender effects in brain and behavior. *Neurosci. Biobehav. Rev.* 46, 604–627. doi: 10.1016/j.neubiorev.2014.09.001

Contreras-Huerta, L. S., Baker, K. S., Reynolds, K. J., Batalha, L., and Cunnington, R. (2013). Racial bias in neural empathic responses to pain. *PLOS ONE* 8:e84001. doi: 10.1371/journal.pone.0084001

Contreras-Huerta, L. S., Hielscher, E., Sherwell, C. S., Rens, N., and Cunnington, R. (2014). Intergroup relationships do not reduce racial bias in empathic neural responses to pain. *Neuropsychologia* 64, 263–270. doi: 10.1016/j.neuropsychologia.2014.09.045

Cox, R. (1996). AFNI: software for analysis and visualization of functional magnetic resonance neuroimages. *Comput. Biomed. Res.* 29, 162–173. doi: 10.1006/cbmr.1996.0014

Davis, M. (1983). Measuring individual differences in empathy: evidence for a multidimensional approach. *J. Pers. Soc. Psychol.* 44, 113–126. doi: 10.1037/0022-3514.44.1.113

Decety, J., and Jackson, P. L. (2006). A social-neuroscience perspective on empathy. *Curr. Direct. Psychol. Sci.* 15, 54–58. doi: 10.1111/j.0963-7214.2006.00406.x

Gaertner, L., and Dovidio, J. F. (2000). *Reducing Intergroup Bias: The Common Ingroup Identity Model*. Philadelphia, PA: Psychology Press.

Greenwald, A., Nosek, B., and Banaji, M. (2003). Understanding and using the implicit association test: I. An improved scoring algorithm. *J. Pers. Soc. Psychol.* 85, 197–216. doi: 10.1037/0022-3514.85.2.197

Greenwald, A. G., McGhee, D. E., and Schwartz, J. L. K. (1998). Measuring individual differences in implicit cognition: the implicit association test. *J. Pers. Soc. Psychol.* 74, 1464–1480. doi: 10.1037/0022-3514.74.6.1464

Hehman, E., Mania, E. W., and Gaertner, S. L. (2010). Where the division lies: common ingroup identity moderates the cross-race facial-recognition effect. *J. Exp. Soc. Psychol.* 46, 445–448. doi: 10.1016/j.jesp.2009.11.008

Hein, G., Silani, G., Preuschoff, K., Batson, C. D., and Singer, T. (2010). Neural responses to ingroup and outgroup members' suffering predict individual differences in costly helping. *Neuron* 68, 149–160. doi: 10.1016/j.neuron.2010.09.003

Kurzban, R., Tooby, J., and Cosmides, L. (2001). Can race be erased? Coalitional computation and social categorization. *Proc. Natl. Acad. Sci. U.S.A.* 98, 15387–15392. doi: 10.1073/pnas.251541498

Lamm, C., Batson, C., and Decety, J. (2007). The neural substrate of human empathy: effects of perspective-taking and cognitive appraisal. *J. Cogn. Neurosci.* 19, 42–58. doi: 10.1162/jocn.2007.19.1.42

Lamm, C., Decety, J., and Singer, T. (2011). Meta-analytic evidence for common and distinct neural networks associated with directly experienced pain and empathy for pain. *Neuroimage* 54, 2492–2502. doi: 10.1016/j.neuroimage.2010.10.014

Lebrecht, S., Pierce, L. J., Tarr, M. J., and Tanaka, J. W. (2009). Perceptual other-race training reduces implicit racial bias. *PLOS ONE* 4:e4215. doi: 10.1371/journal.pone.0004215

Masten, C. L., Gillen-O'Neel, C., and Brown, C. S. (2010). Children's intergroup empathic processing: the roles of novel ingroup identification, situational distress, and social anxiety. *J. Exp. Child Psychol.* 106, 115–128. doi: 10.1016/j.jecp.2010.01.002

Mitsis, G. D., Iannetti, G. D., Smart, T. S., Tracey, I., and Wise, R. G. (2008). Regions of interest analysis in pharmacological fMRI: how do the definition criteria influence the inferred result? *Neuroimage* 40, 121–132. doi: 10.1016/j.neuroimage.2007.11.026

Montalan, B., Lelard, T., Godefroy, O., and Mouras, H. (2012). Behavioral investigation of the influence of social categorization on empathy for pain: a minimal group paradigm study. *Front. Psychol.* 3:389. doi: 10.3389/Fpsyg.2012.00389

Moriguchi, Y., Decety, J., Ohnishi, T., Maeda, M., Mori, T., Nemoto, K., et al. (2007). Empathy and judging other's pain: an fMRI study of alexithymia. *Cereb. Cortex* 17, 2223–2234. doi: 10.1093/cercor/bhl130

Nichols, T. E., and Poline, J. B. (2009). Commentary on Vul et al.'s (2009) "Puzzlingly High Correlations in fMRI Studies of Emotion, Personality, and Social Cognition". *Perspect. Psychol. Sci.* 4, 291–293. doi: 10.1111/j.1745-6924.2009.01126.x

Phelps, E. A., O'Connor, K. J., Cunningham, W. A., Funayama, E. S., Gatenby, J. C., Gore, J. C., et al. (2000). Performance on indirect measures of race evaluation predicts amygdala activation. *J. Cogn. Neurosci.* 12, 729–738. doi: 10.1162/089892900562552

Phinney, J. (1992). The multigroup ethnic identity measure: a new scale for use with diverse groups. *J. Adolesc. Res.* 7, 156–176. doi: 10.1177/074355489272003

Preston, S. D., and de Waal, F. B. (2002). Empathy: its ultimate and proximate bases. *Behav. Brain Sci.* 25, 515–526.

Sheng, F., and Han, S. H. (2012). Manipulations of cognitive strategies and intergroup relationships reduce the racial bias in empathic neural responses. *Neuroimage* 61, 786–797. doi: 10.1016/j.neuroimage.2012.04.028

Singer, T., Seymour, B., O'Doherty, J. P., Stephan, K. E., Dolan, R. J., and Frith, C. D. (2006). Empathic neural responses are modulated by the perceived fairness of others. *Nature* 439, 466–469. doi: 10.1038/nature04271

Stanley, D., Phelps, E., and Banaji, M. (2008). The neural basis of implicit attitudes. *Curr. Dir. Psychol. Sci.* 17, 164–170. doi: 10.1111/j.1467-8721.2008.00568.x

Tajfel, H. (1970). Experiments in intergroup discrimination. *Sci. Am.* 223, 96–102. doi: 10.1038/scientificamerican1170-96

Triandis, H. (1996). The psychological measurement of cultural syndromes. *Am. Psychol.* 51, 407–415. doi: 10.1037/0003-066X.51.4.407

Van Bavel, J., Packer, D., and Cunningham, W. (2008). The neural substrates of in-group bias: a functional magnetic resonance imaging investigation. *Psychol. Sci.* 11, 1131–1139. doi: 10.1111/j.1467-9280.2008.02214.x

Van Bavel, J. J., and Cunningham, W. A. (2009). Self-categorization with a novel mixed-race group moderates automatic social and racial biases. *Pers. Soc. Psychol. Bull.* 35, 321–335. doi: 10.1177/0146167208327743

Vul, E., Harris, C., Winkielman, P., and Pashler, H. (2009). Puzzlingly high correlations in fMRI studies of emotion, personality, and social cognition. *Perspect. Psychol. Sci.* 4, 274–290. doi: 10.1111/j.1745-6924.2009.01125.x

Wang, Z. X., Zhang, J. X., Wu, Q. L., Liu, N., Hu, X. P., Chan, R. C., et al. (2010). Alterations in the processing of non-drug-related affective stimuli in abstinent heroin addicts. *Neuroimage* 49, 971–976. doi: 10.1016/j.neuroimage.2009.08.020

Xu, X., Zuo, X., Wang, X., and Han, S. (2009). Do you feel my pain? Racial group membership modulates empathic neural responses. *J. Neurosci.* 29, 8525–8529. doi: 10.1523/JNEUROSCI.2418-09.2009

Yang, C. Y., Decety, J., Lee, S. Y., Chen, C. Y., and Cheng, Y. W. (2009). Gender differences in the mu rhythm during empathy for pain: an electroencephalographic study. *Brain Res.* 1251, 176–184. doi: 10.1016/j.brainres.2008.11.062

**Conflict of Interest Statement:** The authors declare that the research was conducted in the absence of any commercial or financial relationships that could be construed as a potential conflict of interest.

The handling editor declared a past co-authorship with the authors ZW and YH.

frontiers in Human Neuroscience

ORIGINAL RESEARCH
published: 25 January 2018
doi: 10.3389/fnhum.2018.00020

# Slow Is Also Fast: Feedback Delay Affects Anxiety and Outcome Evaluation

*Xukai Zhang*[1,2†], *Yi Lei*[1†], *Hang Yin*[1,2], *Peng Li*[1,3*] *and Hong Li*[1,3,4]

[1]*Brain Function and Psychological Science Research Center, Shenzhen University, Shenzhen, China,* [2]*Research Center of Brain and Cognitive Neuroscience, Liaoning Normal University, Dalian, China,* [3]*Shenzhen Key Laboratory of Affective and Social Cognitive Science, Shenzhen University, Shenzhen, China,* [4]*Center for Emotion and Brain, Shenzhen Institute of Neuroscience, Shenzhen, China*

Performance-related feedback plays an important role in improving human being's adaptive behavior. Using event-related potentials (ERPs), previous studies have associated a particular component, i.e., reward positivity (RewP), with outcome evaluation processing and found that this component was affected by waiting time before outcome evaluation. Prior research has also suggested that anxious individuals are more prone to detecting threats and susceptible to negative emotions, and show different patterns of brain activity in outcome evaluation. It is quite common that a decision-maker cannot receive feedback immediately; however, few studies have focused on the processing of delayed feedback, especially in subjects who exhibit trait anxiety. In this study, we recruited two groups of subjects with different trait anxiety levels and recorded ERPs when they conducted a time-estimation task with short (0.6–1 s) or long delayed (4–5 s) feedback. The ERP results during the cue phase showed that long waiting cues elicited more negative-going feedback-related negativity (FRN)-like component than short waiting cues in the high trait anxiety (HTA) group. More importantly, the two groups showed different patterns of ERP in the feedback condition. In the low trait anxiety (LTA) group, more positive-going RewP was found in the short-delayed than in the long-delayed condition. In contrast, no difference was found in the HTA group. This pattern may reflect the hyperactivity of the reward systems of HTA individuals in uncertain environments (e.g., the long-delay condition) compared with LTA individuals. Our results provide a direction for future research on the neural mechanisms of reinforcement learning and anxiety.

**Keywords: outcome evaluation, learning, anxiety, feedback delay, reward positivity**

OPEN ACCESS

***Edited by:***
*Xiaochu Zhang,*
*University of Science and Technology of China, China*

***Reviewed by:***
*Ruolei Gu,*
*Institute of Psychology (CAS), China*
*Li Hu,*
*Institute of Psychology (CAS), China*
*Rongjun Yu,*
*National University of Singapore, Singapore*

***Correspondence:**
*Peng Li*
*peng@szu.edu.cn*

†*Shared first author.*

***Received:*** *20 October 2017*
***Accepted:*** *15 January 2018*
***Published:*** *25 January 2018*

***Citation:***
*Zhang X, Lei Y, Yin H, Li P and Li H (2018) Slow Is Also Fast: Feedback Delay Affects Anxiety and Outcome Evaluation. Front. Hum. Neurosci. 12:20. doi: 10.3389/fnhum.2018.00020*

## INTRODUCTION

Learning from the environment can help people improve their behavior; performance-related feedback therefore plays a key role in adapting to a changing environment. Specially, according to the reinforcement learning theory, a decision-maker has a high chance to repeat behaviors which provided reward feedbacks and to avoid behaviors which lead to non-reward feedbacks before. The motivation of pursuing reward drives decision-makers select actions associated with high expectation of reward and feedback backward updates corresponding reward expectation of certain actions (Schultz et al., 1997). The so-called reward prediction error refers to the difference between current outcome and expected outcome (Schultz et al., 1997).

Researchers found that a particular event-related brain potential (ERP) component, feedback-related negativity (FRN), was highly related to reward prediction error during outcome processing (Holroyd and Coles, 2002). FRN is a frontocentral negativity deflection maximal at approximately 200–300 ms following the presentation of feedback (Miltner et al., 1997; Holroyd and Coles, 2002; Li et al., 2016). A more negative-going FRN is often observed in the processing of negative feedback, compared to that of positive feedback (Yeung and Sanfey, 2004; Ferdinand et al., 2012). A large body of research indicates that FRN reflects decreased phase of dopaminergic signal in the basal ganglia and that the generation of this potential occurs in the anterior cingulate cortex (ACC; Bellebaum and Daum, 2008; Holroyd et al., 2009; Hauser et al., 2014; Holroyd and Umemoto, 2016; but see Foti et al., 2011; Becker et al., 2014; Sambrook and Goslin, 2016).

Early on, the FRN was mainly associated with a large negative waveform elicited by losses (negative feedback) and absent for rewards (e.g., Holroyd and Coles, 2002; Hajcak et al., 2006). According to the influential reinforcement learning error-related negativity (RL_ERN) theory, the midbrain dopamine system is a key component for detecting and monitoring whether the actual outcomes match the expectations, then sending corresponding dopaminergic signals to the ACC, where a larger negative waveform is generated (Holroyd and Coles, 2002). However, this theory was not supported by several following studies. Oliveira et al. (2007) argued that the ACC activity was increased due to violations in expectancy, irrespective of outcome valence. This finding was confirmed by some other studies (Alexander and Brown, 2010; Ferdinand et al., 2012). With the development of the theory, Holroyd et al. (2008) proposed a new idea based on their original RL-ERN theory. They posited that the FRN was mainly driven by positive feedback: unexpected positive feedback increased the phase change in dopamine, which inhibited the conflict signal in ACC and thus canceled out the amplitude of the N200. Substantial evidence indicated greater modulation of FRN by correct feedback than by error feedback (Potts et al., 2006; Eppinger et al., 2008; Hewig et al., 2008; Holroyd and Coles, 2008; Heydari and Holroyd, 2016). The potential positive component elicited by reward feedback was renamed reward positivity (RewP) and was calculated by the difference wave of the positive feedback subtracted from the negative feedback (Baker and Holroyd, 2011).

Most recent studies have mainly focused on immediate feedback processing; however, in daily life, it is quite common that a person cannot receive feedback or reward immediately after decision-making. In recent years, many studies have investigated how delayed rewards influence decision-making (Green et al., 1994; Wittmann et al., 2007). Some researchers have conducted single-unit recording studies and indicated that the dopamine signal dynamically varied in different waiting time conditions, with stronger neuronal firing with an immediate reward compared to a delayed reward (Roesch et al., 2007). Subsequent studies have shown that the striatum and hippocampus have been involved in outcome processing for immediate and delayed rewards, respectively (Foerde and Shohamy, 2011). The variance in the activity of the reward system when the reward is delayed could be due to a shift from nondeclarative to declarative learning. Therefore, it would be interesting to know whether delayed feedback could also improve reinforcement learning in terms of behavioral adjustment.

Recently, several groups of researchers began to examine delayed feedback in EEG experiments. The purpose of the initial study was to explore whether temporal delay could affect RewP component elicited by monetary feedback in a gambling task (Weinberg et al., 2012). Their results showed that the RewP[1] was negligible when the delay was several seconds long. Subsequently, further research explored the linear effects of delayed time on outcome evaluation and tested whether the learning of optimal choice will be affected by different waiting time in a feedback learning task (Peterburs et al., 2016). Their results showed that the RewP decreased gradually with increased delay time, but no effect of time was found on behavioral learning. Moreover, Weismuller and Bellebaum (2016) used a probabilistic learning task to investigate whether the delayed feedback was sensitive to expectancy, and found the RewP was significantly more positive-going for unexpected compared to expected feedback in both of immediate and delayed feedback condition. More recently, Arbel et al. (2017) reported that the RewP component was only observed in immediate feedback condition. In our previous study, participants were asked to choose which balloon had money before making the selection; they would then see a cue that represented a long or short wait for the choice's outcome. Compared to the findings of other groups, we found that waiting time did not affect the FRN component (Wang et al., 2014). These inconsistent findings could be caused by two possible factors. First, most of these studies utilized random monetary feedback regardless of participants' actual performance. Although previous studies used a probabilistic learning task, the learning may only have happened in the beginning phase because participants could maintain the advantageous choice they learned before in the last phase. Second, none of these studies have looked at individual differences in the processing of waiting time. A longer waiting time could cause greater uncertainty, which in turn could influence participants' anxiety (Maner and Schmidt, 2006).

A large number of studies have shown that individual differences in factors such as stress, depression and anxiety influence the outcome evaluation process in decision-making (Foti and Hajcak, 2009; Gu et al., 2010a,b; Li et al., 2015). One study found that anxiety could enhance the perception of threats (Maner and Schmidt, 2006). High-anxiety individuals also showed more negative exception bias (Eisenberg et al., 1998; Wray and Stone, 2005; Maner and Schmidt, 2006). Notably, most of these findings came from self-reports data. Gu et al. (2010a) used ERP to investigate the relationship between anxiety and outcome evaluation; they found that the RewP in the high trait anxiety (HTA) group was more positive-going than that in low trait anxiety (LTA) groups in ambiguous conditions, and

[1]Note that the RewP component was originally named as FRN in these citations (Weinberg et al., 2012; Peterburs et al., 2016; Weismuller and Bellebaum, 2016; Arbel et al., 2017) in this paragraph.

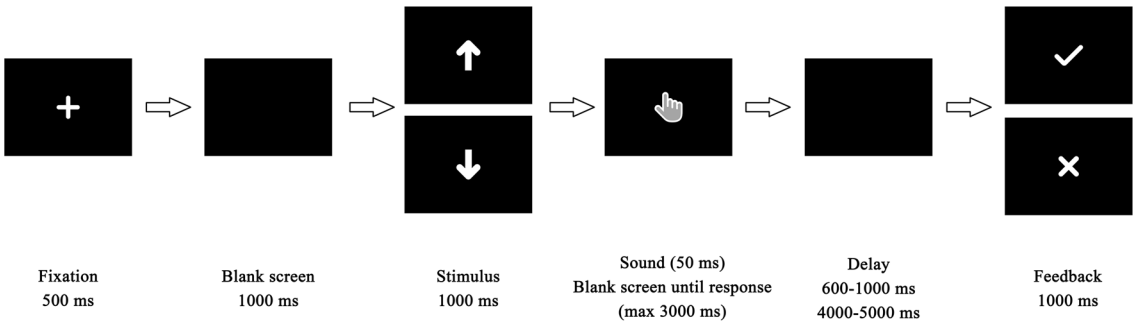


**FIGURE 1 |** Time course of stimulus presentation in the time estimation task.

they proposed that ambiguity makes feedback more threatening. The HTA individuals also showed less positive-going RewP than LTA individuals in negative conditions, confirming the negative bias of anxious individuals. While waiting for feedback can itself cause uncertainty, individual differences are a major cause of inconsistency in perceived uncertainty (Hirsh et al., 2012). Furthermore, neuroimaging studies have discussed the function of the hippocampus in anxiety and memory (for a review see Bannerman et al., 2004). Recent findings provide evidence that the dorsal hippocampus is not immune to anxiety and that trait anxiety shows more activity in the dorsal hippocampus than state anxiety, while the subregions may overlap with the memory function area (Satpute et al., 2012).

Based on the characteristics of anxious individuals described above, the purpose of this study was, first, to explore whether the length of waiting time for feedback in a trial-and-error task would affect learning, and second, to investigate whether the manipulation of waiting time would affect the outcome evaluation of trait anxiety individuals. Data analysis mainly focused on the behavioral adjustment data and the RewP amplitude. We hypothesized that more positive-going RewP would be observed in the short delay condition than that in the long delay condition in LTA individuals, but not in HTA individuals because the long waiting time would cause higher anxiety degrees for HTA than LTA groups (Hirsh et al., 2012). We also predicted that the adjustment of behavior after the long delay would be better than short delay due to the effect of waiting time on learning (Butler et al., 2007; Guzmán-Muñoz and Johnson, 2008; Metcalfe et al., 2009). Furthermore, we examined whether different brain activities could be observed in the HTA and LTA groups even in the cue phase when they first learn how long they will have to wait.

# MATERIALS AND METHODS

## Participants

A total of 739 undergraduate students were tested using the Chinese version of the State-Trait Anxiety Inventory (STAI; Spielberger et al., 1983). Seventeen students (13 females, age = 20.06 ± 1.09) whose scores were in the top 25% were randomly selected as the HTA subjects (pre-STAI scores = 57.35 ± 4.39), while another 17 students (13 females, age = 20.53 ± 1.70) whose scores were in the lowest 25% were randomly recruited as the LTA subjects (pre-STAI scores = 30.06 ± 2.05). The trait anxiety scores in the two groups were significantly different, $t_{(32)} = 23.11$, $p < 0.001$. This result was confirmed by a STAI retest a week later when the formal experiment was conducted, $t_{(32)} = 12.79$, $p < 0.001$. The post-STAI scores of HTA subjects (53.76 ± 6.68) was significantly larger than that of the LTA group (29.53 ± 4.06). All participants had normal or corrected-to-normal vision and normal audition, and none had a neurological or psychological history. Informed written consent was obtained before the experiment, which was approved by the Ethics Committee of Liaoning Normal University. Each subject received 38–42 yuan based on the accuracy of the experimental task.

## Experimental Procedure

Before the experiment, the participants were told they would complete a time estimation task (Miltner et al., 1997). The task was modified based on the classic time estimation task. Participants were to change or maintain current behavior in response to feedback to maintain the right perception of the duration of 1 s. In each trial (**Figure 1**), a fixation screen was shown for 500 ms, then replaced by a blank screen for 1000 ms. Afterward, an arrow indicating how long the participant would wait before final feedback was presented for 1000 ms. There were two different arrow cues with different orientations, which corresponded to long delay or short delay. The meanings of the two types of cues were counterbalanced between participants. Following the cue, the participants heard a sound (1500 Hz, 50 dB, lasting 50 ms) that indicated the beginning of the estimation. Participants were asked to estimate 1 s and to press the space button on the keyboard as soon as they believed that a second of time had passed. The duration between participants' responses and feedback stimuli was set randomly between 4000 ms and 5000 ms in the long-delay condition and between 600 ms and 1000 ms in the short-delay condition. Finally, feedback appeared in white on a black background and lasted for 1000 ms. If

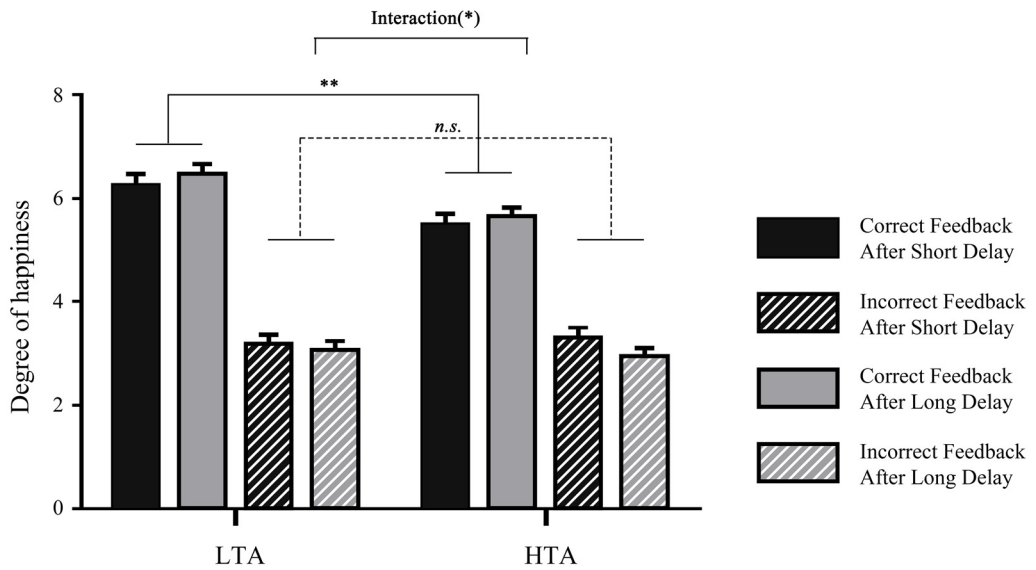


**FIGURE 2 |** Mean degree of happiness in each waiting time condition in the two groups. $^{**}p < 0.01$, $^{*}p < 0.05$.

participants' estimation was within the required time window (900–1100 ms), they received positive feedback indicated by a black "√" mark; otherwise, the feedback was an "X" mark. The inter-trial interval was set randomly between 1000 ms and 1500 ms.

The initial time window was set as 900 ms to 1100 ms. If a participant's reaction time (RT) was in this interval, their estimation was considered to be correct in that trial. Conversely, if their RT was not in this interval, they received the error feedback. The preset time window was adjusted according to the participants' performance trial by trial: 10 ms was added if they responded incorrectly and 10 ms was subtracted if they respond correctly. All of the participants received about 50% correct and 50% incorrect feedback overall based on the algorithm. The whole experiment consisted of 120 trials in the long-delay condition and 120 trials in short-delay condition.

The self-report questionnaire was completed when participants finished the experiment. In this questionnaire, the participants were asked to rate how much attention they paid to the outcome when the waiting time was long or short (1 = "ignored outcomes"; 7 = "paid close attention"), how they felt when they responded correctly in the long-delay condition and short-delay condition (1 = "very unhappy"; 7 = "very happy"), and how they felt when they responded incorrectly in the long-delay condition and short-delay condition (1 = "very unhappy"; 7 = "very happy").

## Data Recording and Analysis

The present study was a 2 (waiting time: long or short) × 2 (valence: correct or incorrect) × 2 (trait anxiety: HTA or LTA) design. In order to investigate the effect of valence and waiting time on behavior, we calculated the absolute changes in RT (ΔRT), meaning the absolute values of the different RTs between the current trial and the next trial (Holroyd and Krigolson, 2007; Li et al., 2016). Note that ΔRT is better than raw RT to indicate participants' behavioral adjustment because they could increase or decrease their RT after receiving negative feedback in such a time-estimation task. The ΔRT data was submitted to a 2 × 2 × 2 repeated measures analysis of variance (ANOVA) with trait anxiety (LTA or HTA) as the between-subject factor and with waiting time (long or short) and valence (correct or incorrect) as within-subject factors.

Continuous EEG data were recorded with a 64-channel system (eego, eemagine, Germany) and sampled at 500 Hz. The CPz was used as a reference online, and the left and right mastoids were digitally converted to average as re-references offline. Vertical electrooculograms were obtained via facial electrodes located above and below the left eye. Horizontal electrooculograms were obtained via facial electrodes placed at the outer canthi of the eyes. Impedances of all electrodes was kept under 15 kΩ. EEG data were analyzed by BrainVision Analyzer 2.0 software (Brain Products, Germany). A 0.1–20 Hz passband filter was applied to EEG data offline. Eye blink and ocular artifacts were corrected using independent component analysis (Lee et al., 1999). The segments ranged from −200 ms before the cue/feedback onset to 800 ms after the cue/feedback was presented. Before the cue/feedback stimulus onset, a −200 to 0 ms time range was used as a baseline. All of the periods in which the maximal amplitude was over ±80 μV were rejected as artifacts. Less than 5% of trials were rejected in each condition. Finally, the EEG data were averaged in each condition for further analysis in both the cue phase and feedback phase separately.

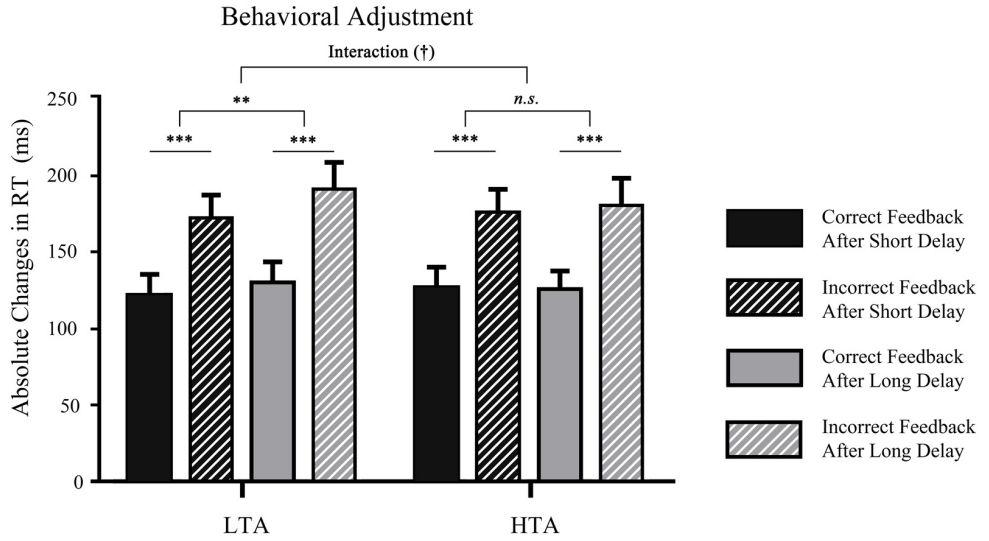


**FIGURE 3 |** Mean time estimation adjustment in each waiting time condition in the two groups. ***$p < 0.001$, **$p < 0.01$. †Means marginal significance.

The RewP amplitude was calculated by the difference waves at electrode Fz between negative feedback and positive feedback (Holroyd and Krigolson, 2007). The electrode Fz was selected because RewP reached the maximum peak at this site (Li et al., 2010, 2011; Wang et al., 2014). The RewP amplitude was measured by the mean amplitude in the 250–300 ms time window following feedback onset (Yeung et al., 2005; Yu and Zhou, 2006). The FRN-like in cue phase was measured by the mean amplitude in the 240–340 ms time window following cue onset. Additionally, the mean amplitudes of P300 were computed in a 340–440 ms time window at the electrode Pz where it peaks for feedback phase and cue phase respectively. The reason for analyzing this component is to investigate whether the amplitude of the FRN was confounded by P300 because of the general concern of component overlapping in this field (Gu et al., 2010a; Foti et al., 2011; Sambrook and Goslin, 2015). The FRN-like was submitted to a 2 (cue: short, long) × 2 (trait anxiety: high, low) repeated measures ANOVA for the cue phase and the RewP was submitted to 2 (waiting time: long, short) × 2 (trait anxiety: high, low) two-way ANOVA for the feedback phase. In addition, P300 amplitudes were submitted to a 2 (cue: short, long) × 2 (trait anxiety: high, low) repeated measures ANOVA for cue phase and 2 (waiting time: long, short) × 2 (valence: correct, incorrect) × 2 (trait anxiety: high, low) repeated measures ANOVA for the feedback phase. Greenhouse-Geisser corrections were used where necessary.

# RESULTS

## Behavioral Results

To examine whether attention was affected by the waiting time in two groups, the subjective ratings of attention in post-experiment questionnaire were submitted to a 2 (waiting time: long, short) × 2 (trait anxiety: high, low) repeated measures ANOVA. The results showed that the main effect of waiting time on attention did not reach significance, $F_{(1,32)} = 0.019$, $p = 0.891$, $\eta_p^2 = 0.001$. The interaction effect between waiting time and groups was not significant either, $F_{(1,32)} = 0.93$, $p = 0.342$, $\eta_p^2 = 0.03$. Moreover, the rating scores of feelings of happiness in the four different conditions: (a) waiting a long time for correct feedback; (b) waiting a long time for error feedback; (c) waiting a short time for correct feedback; and (d) waiting a short time for correct feedback, were submitted to a 2 (waiting time: long, short) × 2 (valence: correct, incorrect) × 2 (trait anxiety: high, low) repeated measures ANOVA, and the main effect feedback valence was significant, $F_{(1,32)} = 278.24$, $p < 0.001$, $\eta_p^2 = 0.90$, indicating that people felt happier when they received correct feedback than when they received incorrect feedback. Additionally, the interaction of trait anxiety and feedback valence was significant, $F_{(1,32)} = 5.45$, $p = 0.026$, $\eta_p^2 = 0.15$; pairwise comparison showed that the LTA group felt happier than the HTA group in the correct feedback condition ($p = 0.003$; **Figure 2**).

To determine whether the delay and feedback type influenced subsequent behavior in different trait anxiety groups, the ΔRT was analyzed by using a 2 (waiting time: long, short) × 2 (valence: correct, incorrect) × 2 (trait anxiety: high, low) three-way ANOVA (see **Figure 3**). The main effect of waiting time was significant, $F_{(1,32)} = 4.49$, $p < 0.05$, $\eta_p^2 = 0.12$. The ΔRT in the short-delay condition ($M = 155.92$, $SD = 10.73$) was smaller than that in the long-delay condition ($M = 148.87$, $SD = 9.87$). The main effect of outcome also reached significance, $F_{(1,32)} = 129.84$, $p < 0.001$, $\eta_p^2 = 0.80$; prior error outcomes promoted change for the next trials ($M = 179.46$, $SD = 11.32$) and led to a larger time adjustment than prior correct outcomes ($M = 125.33$, $SD = 9.50$). It is noteworthy that the interaction between trait anxiety and waiting time was marginally significant ($p = 0.072$). A larger absolute response time in the long-delay condition was found

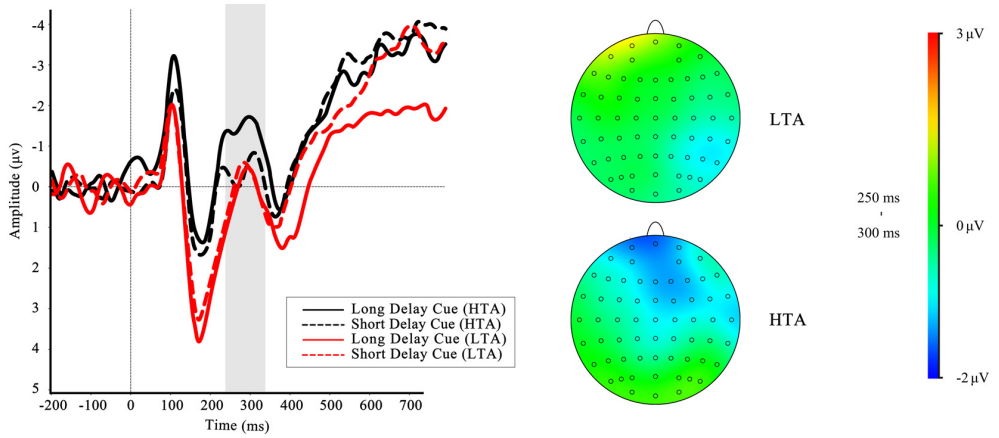


**FIGURE 4 |** Cue-locked event-related potential (ERP) waveforms at Fz comparing long- and short-delayed cues in high trait anxiety (HTA) and low trait anxiety (LTA) groups, along with different waveforms and topographic maps for long- and short-delayed cues in HTA and LTA groups in time range of feedback-related negativity (FRN). Gray shaded area shows the 240–340 ms analysis window in which the FRN-like was quantified.

only in LTA individuals ($p$ = 0.008), not in HTA individuals ($p$ = 0.855). No other significant effect was found (all $p > 0.05$).

## Electrophysiological Results

### Cue Phase

To investigate whether the brain activities of the HTA and LTA groups could differ even in the cue phase, we analyzed the FRN-like component according to one of our previous studies (Wang et al., 2016). The results showed a significant interaction effect between group and cue type on FRN-like amplitude, $F_{(1,32)}$ = 4.66, $p$ = 0.039, $\eta_p^2$ = 0.13. Simple effect analysis revealed that the effect of waiting time was significant in the HTA group, $F_{(1,32)}$ = 7.21, $p$ = 0.011, with more negative-going FRN-like amplitude for long-delay cues than short-delay cues in the HTA group, but not in the LTA group, $F_{(1,32)}$ = 0.13, $p$ = 0.717. The grand-average ERP waveforms for cues in the different trait anxiety groups are presented in **Figure 4**. The main effects of waiting time ($F_{(1,32)}$ = 2.69, $p$ = 0.111) and trait anxiety ($F_{(1,32)}$ = 0.29, $p$ = 0.60) were not significant. The same measures were used for P300, but no significant effects were found.

### Feedback Phase

The grand-average ERPs and RewP for short delay and long delay feedback at Fz are depicted in **Figure 5**. The main effect of waiting time was not significant, $F_{(1,32)}$ = 1.84, $p$ = 0.184. The ANOVA yielded significant interactions between trait anxiety group and waiting time, $F_{(1,32)}$ = 9.70, $p$ = 0.004, $\eta_p^2$ = 0.23. A simple effect analysis was performed to investigate the interaction, indicating a greater RewP amplitude in the LTA group when they waited a short time for outcome than when they waited a long time for outcome, $F_{(1,32)}$ = 10.0, $p$ = 0.003; however, this effect was not found in the HTA group, $F_{(1,32)}$ = 1.54, $p$ = 0.223. No other significant results were found (all $p > 0.05$).

The ANOVA on P300 amplitude found a reliable main effect of valence, suggesting that the P300 amplitude was greater when the feedback was correct than when the feedback was incorrect, $F_{(1,32)}$ = 67.93, $p < 0.001$, $\eta_p^2$ = 0.68. The interaction between valence and waiting time was significant, a more positive-going P300 was found when they waited a long time than a short time at the correct feedback condition. In addition, neither the main effect of the trait anxiety group ($F_{(1,32)}$ = 0.66, $p$ = 0.428) nor the interaction between the group and other factors reached significance: trait anxiety group × valence, $F_{(1,32)}$ = 0.39, $p$ = 0.538; anxiety group × waiting time, $F_{(1,32)}$ = 1.42, $p$ = 0.242; trait anxiety group × valence × waiting time, $F_{(1,32)}$ = 0.578, $p$ = 0.453. To sum up, we did not find any other significant interaction between trait anxiety group and other factors on P300 amplitude. Therefore, it was less likely that the amplitude of the FRN was confounded by P300 in the present results.

## DISCUSSION

In this study, we analyzed the RewP component as an indicator to investigate how waiting time affects outcome evaluation in individuals with high and LTA. To do so, we adopted a novel paradigm, in which a cue informed the participant how long he or she would wait before making a response, and the waiting time before final feedback was manipulated. The results showed that the HTA and LTA individuals had different brain responses to both the cue and feedback stimuli, as reflected by the FRN-like amplitudes and RewP amplitudes, respectively. Specifically, more negative-going FRN-like amplitudes were observed in the long-delay cue condition than in the short-delay cue condition, but only in the HTA group. More importantly, significant differences in RewP amplitude were found between the short- and long-delay conditions in the LTA group, but not in the HTA group.

ERP studies have previously reported some inconsistent findings in regard to feedback processing modulated by waiting time before feedback (Weinberg et al., 2012; Wang et al., 2014; Peterburs et al., 2016; Weismuller and Bellebaum, 2016; Arbel et al., 2017). As we mentioned before, different paradigms and

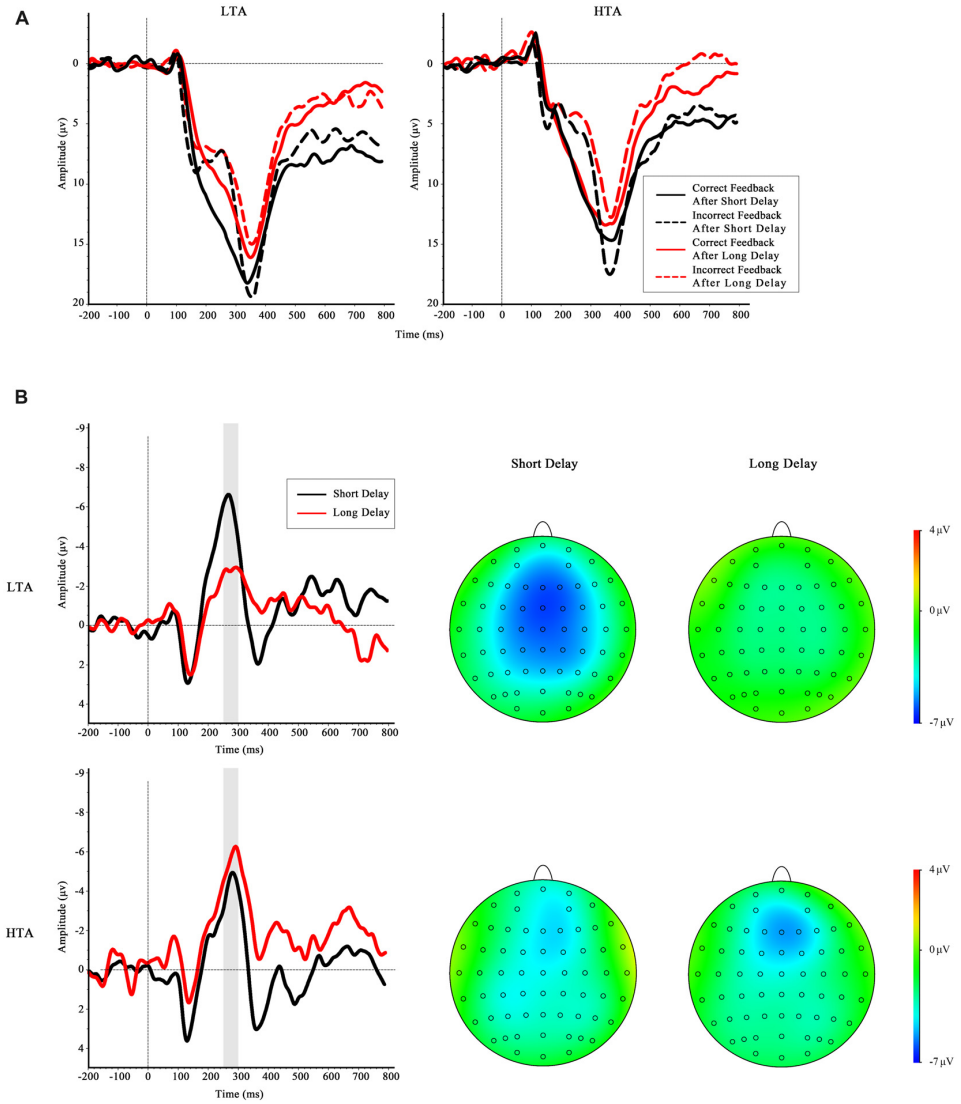


**FIGURE 5 | (A)** Feedback-locked grand-average ERP waveforms at Fz in four conditions for LTA group and HTA group. **(B)** The difference waves of HTA and LTA groups at the Fz. Gray shaded area shows the 250–300 ms analysis window in which the reward positivity (RewP) was quantified.

individual traits are two possible reasons for the incompatible results in these studies. Here, we used a modified time-estimation task in which feedback stimuli were mainly dependent on participants' performance. Compared to the gambling task that we used in our previous study, the present task could provide more information in terms of reinforcement learning.

First, by using a learnable task, the present study could test whether the long delay improved or hampered reinforcement learning efficiency. Consistent with our hypotheses, in a dynamic learning process, waiting time affected learning, which was shown in the absolute change of response time between two adjacent reactions. Several studies have reported better performance for delayed feedback than immediate feedback in scenarios such as vocabulary learning (Metcalfe et al., 2009), geographical representations learning (Guzmán-Muñoz and Johnson, 2008), and learning from a multiple-choice test (Butler et al., 2007). The larger time adjustment in our delayed feedback scenario indicate better performance in changing behavior. Furthermore, the marginal significant interaction of waiting time and group may support the above-mentioned explanations. Compared with the short delayed condition, the long delayed feedback could better promote the learning to adjust participants' estimation of 1 s only in LTA group. This observations requires further examination in future studies.

In line with previous studies, the waiting time also affected individuals' brain activities during outcome evaluation (Weinberg et al., 2012; Peterburs et al., 2016; Weismuller and Bellebaum, 2016; Arbel et al., 2017; but see Wang et al., 2014). Weinberg et al. (2012) only found a difference in gains and losses in a short-delay condition, not in a long-delay condition. In contrast, Peterburs et al. (2016) reported a linear effect trend of RewP by waiting time, reflected by gradually less positive-going

RewP amplitude with gradually increased waiting time. The observation that delay feedback reduced RewP amplitude were also replicated by two recent studies (Weismuller and Bellebaum, 2016; Arbel et al., 2017). Evidence from EEG and fMRI studies indicates a striatal source following reward and an association between reward feedback ERP signals and the blood oxygenation level dependent response in the ventral striatum (Carlson et al., 2011; Foti et al., 2011; Becker et al., 2014). Nevertheless, the striatum activity involved in feedback processing was reduced when the waiting time changed from short to long (Foerde and Shohamy, 2011). It has recently been proposed that the hippocampus bridges a temporal gap when the learning need to get information across time; with increasing waiting time, the striatum activity in feedback processing is gradually reduced and relies more on the hippocampus for declarative memory (Foerde and Shohamy, 2011). The results of the present study extended these findings by further showing that delay feedback dramatically reduced activity of reward system indexed by RewP amplitude, however, only in LTA group.

Based on the Spielberger (1972) theory, trait anxiety reflects a stable individual difference in the perception of anxiety from context and events. In the current study, HTA individuals exhibited a different processing pattern than the LTA individuals. In contrast to LTA individuals, HTA individuals showed similar RewP amplitudes in the two waiting time conditions. This was in line with attentional control theory, which holds that impaired attentional control makes individuals prioritize the processing of threat stimuli—and the anxiety can be affected not only by the external stimuli examined in most studies, but also by internal stimuli like worry (see review Eysenck et al., 2007). According to the subjective rating in our study, the long delay before feedback caused adverse effects. Psychological entropy theory indicates that individuals need to maintain a balance of entropy, and uncertainty results in high entropy and higher cognitive resource consumption to reach a goal (Hirsh et al., 2012). Thus, the different behavioral and brain response patterns between the two trait anxiety groups in our study may be due to HTA individuals being more sensitive to the imbalance of entropy caused by a long wait before final feedback. Furthermore, both non-human studies (Sapolsky et al., 1985; Uchida et al., 2008) and a human study (Satpute et al., 2012) have found that the distinct subregions of the hippocampus play an important role in mediating the different types of anxiety. Satpute et al. (2012) found that stress caused stronger activity in the dorsal hippocampus for trait anxiety individuals than for normal people. On the other hand, different from state anxiety, trait anxiety activates the posterior hippocampus and posterior cortical region to process the initial appraisal (Fanselow and Dong, 2010). The strong relationship between dorsal hippocampus and anxiety indicated that dorsal hippocampus is not only an important area of learning and memory but also has an association with anxiety. Thus, we speculate that the feedback processing relies more on the hippocampus when waiting time is longer (Arbel et al., 2017), but the trait anxiety individuals prioritize feelings of anxiety and therefore cannot call upon cognitive resources to improve performance through memories. In addition, the behavior results indicated that only the LTA group adjusted their performance differently in the two different waiting time conditions, which is consistent with our view that HTA individuals in the delayed feedback condition cannot effectively use feedback information across time.

In addition to the feedback stage, a larger negative wave was also elicited by the long-delayed cue than by the short-delayed cue. Importantly, this effect was only observed in HTA individuals. Although the cues did not provide feedback information, this FRN-like component appeared in a similar time window as classical FRN and had a similar scalp distribution as the FRN. A few recent studies focused on brain activity in cue and feedback phases, found that delta and theta activities reflected separate processes of these stimuli respectively in decision making (Wang et al., 2016). Not only can feedback modulate our behaviors, but advanced cues can also provide additional information for our subsequent actions. Furthermore, an fMRI study has shown that the anxious individuals exhibited significantly greater intolerance of uncertainty (IU) than the non-anxious individuals (Krain et al., 2008). In Krain et al.'s (2008) study, the anxiety disorders with high IU showed activation of frontal and limbic regions in response to uncertainty. The present finding in cue phase provided electrophysiological evidence that HTA group was more sensitive to the cue of uncertainty condition in terms of long waiting time than LTA group. The HTA individuals might treat long-delay cue as more threat signal, and showed more alertness at the beginning of a long-delay trial. Therefore, compared to the LTA group, HTA individuals maintained higher self-involvement throughout the trials. The relationship between cue-related brain activities and feedback-related activities must be investigated further in future studies.

## LIMITATION

One limitation of our study is that there was only 17 subjects in each group. Although this sample size is similar to the related published studies in this field (Moser et al., 2008; Dennis and Chen, 2009; Gu et al., 2010a), a relatively larger sample is necessary in future studies, considering the current concern of low replication rate in psychological studies (Button et al., 2013; Open Science Collaboration, 2015).

## CONCLUSION

In summary, our present study found that waiting time had different influences on the processing of feedback in LTA and HTA individuals. The LTA group reported more happiness in response to correct feedback than the HTA group. Moreover, a marginal interaction effect showed that the LTA group made more adjustments than HTA group. In line with these behavioral data, the present ERP data also found that different brain activity, as indexed by RewP, was observed in the two trait anxiety groups. These results suggested that the HTA group was more sensitive to the anxiety caused by a long delay

before feedback and showed similar brain responses during long and short delays. The hyperactivity during waiting time in HTA individuals may hamper flexible behavioral adjustment when they have more time to recall their performance before final feedback.

## AUTHOR CONTRIBUTIONS

XZ, PL, YL and HL designed this study. XZ and HY performed the study. XZ, HY and PL analyzed the data. YL, XZ, HL and PL wrote the article.

## ACKNOWLEDGMENTS

This study was supported by the National Natural Science Foundation of China (31671158 and 31671150), the (Key) Project of DEGP (2015WTSCX094 and 2015KCXTD009), Shenzhen Peacock Plan (grant no. KQTD2015033016104926) the Youth Project of Humanities and Social Sciences of Shenzhen University (16QNFC51), Natural Science Foundation of SZU (2017074) and Shenzhen Fundamental Research Projects (JCYJ20150729104249783). We thank LetPub (www.letpub.com) for its linguistic assistance during the preparation of this manuscript.

## REFERENCES

Alexander, W. H., and Brown, J. W. (2010). Computational models of performance monitoring and cognitive control. *Top. Cogn. Sci.* 2, 658–677. doi: 10.1111/j.1756-8765.2010.01085.x

Arbel, Y., Hong, L., Baker, T. E., and Holroyd, C. B. (2017). It's all about timing: an electrophysiological examination of feedback-based learning with immediate and delayed feedback. *Neuropsychologia* 99, 179–186. doi: 10.1016/j.neuropsychologia.2017.03.003

Baker, T. E., and Holroyd, C. B. (2011). Dissociated roles of the anterior cingulate cortex in reward and conflict processing as revealed by the feedback error-related negativity and N200. *Biol. Psychol.* 87, 25–34. doi: 10.1016/j.biopsycho.2011.01.010

Bannerman, D. M., Rawlins, J. N., Mchugh, S. B., Deacon, R. M., Yee, B. K., Bast, T., et al. (2004). Regional dissociations within the hippocampus--memory and anxiety. *Neurosci. Biobehav. Rev.* 28, 273–283. doi: 10.1016/j.neubiorev.2004.03.004

Becker, M. P., Nitsch, A. M., Miltner, W. H., and Straube, T. (2014). A single-trial estimation of the feedback-related negativity and its relation to BOLD responses in a time-estimation task. *J. Neurosci.* 34, 3005–3012. doi: 10.1523/jneurosci.3684-13.2014

Bellebaum, C., and Daum, I. (2008). Learning-related changes in reward expectancy are reflected in the feedback-related negativity. *Eur. J. Neurosci.* 27, 1823–1835. doi: 10.1111/j.1460-9568.2008.06138.x

Butler, A. C., Karpicke, J. D., and Roediger, H. L. III. (2007). The effect of type and timing of feedback on learning from multiple-choice tests. *J. Exp. Psychol. Appl.* 13, 273–281. doi: 10.1037/1076-898X.13.4.273

Button, K. S., Ioannidis, J. P., Mokrysz, C., Nosek, B. A., Flint, J., Robinson, E. S., et al. (2013). Power failure: why small sample size undermines the reliability of neuroscience. *Nat. Rev. Neurosci.* 14, 365–376. doi: 10.1038/nrn3475

Carlson, J. M., Foti, D., Mujica-Parodi, L. R., Harmon-Jones, E., and Hajcak, G. (2011). Ventral striatal and medial prefrontal BOLD activation is correlated with reward-related electrocortical activity: a combined ERP and fMRI study. *Neuroimage* 57, 1608–1616. doi: 10.1016/j.neuroimage.2011.05.037

Dennis, T. A., and Chen, C. C. (2009). Trait anxiety and conflict monitoring following threat: an ERP study. *Psychophysiology* 46, 122–131. doi: 10.1111/j.1469-8986.2008.00758.x

Eisenberg, A. E., Baron, J., and Seligman, M. E. (1998). Individual differences in risk aversion and anxiety. *Psychol. Bull.* 87, 245–251.

Eppinger, B., Kray, J., Mock, B., and Mecklinger, A. (2008). Better or worse than expected? Aging, learning, and the ERN. *Neuropsychologia* 46, 521–539. doi: 10.1016/j.neuropsychologia.2007.09.001

Eysenck, M. W., Derakshan, N., Santos, R., and Calvo, M. G. (2007). Anxiety and cognitive performance: attentional control theory. *Emotion* 7, 336–353. doi: 10.1037/1528-3542.7.2.336

Fanselow, M. S., and Dong, H. W. (2010). Are the dorsal and ventral hippocampus functionally distinct structures? *Neuron* 65, 7–19. doi: 10.1016/j.neuron.2009.11.031

Ferdinand, N. K., Mecklinger, A., Kray, J., and Gehring, W. J. (2012). The processing of unexpected positive response outcomes in the mediofrontal cortex. *J. Neurosci.* 32, 12087–12092. doi: 10.1523/jneurosci.1410-12.2012

Foerde, K., and Shohamy, D. (2011). Feedback timing modulates brain systems for learning in humans. *J. Neurosci.* 31, 13157–13167. doi: 10.1523/jneurosci.2701-11.2011

Foti, D., and Hajcak, G. (2009). Depression and reduced sensitivity to non-rewards versus rewards: evidence from event-related potentials. *Biol. Psychol.* 81, 1–8. doi: 10.1016/j.biopsycho.2008.12.004

Foti, D., Weinberg, A., Dien, J., and Hajcak, G. (2011). Event-related potential activity in the basal ganglia differentiates rewards from nonrewards: temporospatial principal components analysis and source localization of the feedback negativity. *Hum. Brain Mapp.* 32, 2207–2216. doi: 10.1002/hbm.21182

Green, L., Fry, A. F., and Myerson, J. (1994). Discounting of delayed rewards: a life-span comparison. *Psychol. Sci.* 5, 33–36. doi: 10.1111/j.1467-9280.1994.tb00610.x

Gu, R., Ge, Y., Jiang, Y., and Luo, Y. J. (2010a). Anxiety and outcome evaluation: the good, the bad and the ambiguous. *Biol. Psychol.* 85, 200–206. doi: 10.1016/j.biopsycho.2010.07.001

Gu, R., Huang, Y.-X., and Luo, Y.-J. (2010b). Anxiety and feedback negativity. *Psychophysiology* 47, 961–967. doi: 10.1111/j.1469-8986.2010.00997.x

Guzmán-Muñoz, F. J., and Johnson, A. (2008). Error feedback and the acquisition of geographical representations. *App. Cogn. Psychol.* 22, 979–995. doi: 10.1002/acp.1410

Hajcak, G., Moser, J. S., Holroyd, C. B., and Simons, R. F. (2006). The feedback-related negativity reflects the binary evaluation of good versus bad outcomes. *Biol. Psychol.* 71, 148–154. doi: 10.1016/j.biopsycho.2005.04.001

Hauser, T. U., Iannaccone, R., Stampfli, P., Drechsler, R., Brandeis, D., Walitza, S., et al. (2014). The feedback-related negativity (FRN) revisited: new insights into the localization, meaning and network organization. *Neuroimage* 84, 159–168. doi: 10.1016/j.neuroimage.2013.08.028

Hewig, J., Trippe, R. H., Hecht, H., Coles, M. G., Holroyd, C. B., and Miltner, W. H. (2008). An electrophysiological analysis of coaching in Blackjack. *Cortex* 44, 1197–1205. doi: 10.1016/j.cortex.2007.07.006

Heydari, S., and Holroyd, C. B. (2016). Reward positivity: reward prediction error or salience prediction error? *Int. J. Psychophysiol.* 53, 1185–1192. doi: 10.1111/psyp.12673

Hirsh, J. B., Mar, R. A., and Peterson, J. B. (2012). Psychological entropy: a framework for understanding uncertainty-related anxiety. *Psychol. Rev.* 119, 304–320. doi: 10.1037/a0026767

Holroyd, C. B., and Coles, M. G. H. (2002). The neural basis of human error processing: reinforcement learning, dopamine, and the error-related negativity. *Psychol. Rev.* 109, 679–709. doi: 10.1037/0033-295X.109.4.679

Holroyd, C. B., and Coles, M. G. (2008). Dorsal anterior cingulate cortex integrates reinforcement history to guide voluntary behavior. *Cortex* 44, 548–559. doi: 10.1016/j.cortex.2007.08.013

Holroyd, C. B., and Krigolson, O. E. (2007). Reward prediction error signals associated with a modified time estimation task. *Psychophysiology* 44, 913–917. doi: 10.1111/j.1469-8986.2007.00561.x

Holroyd, C. B., Krigolson, O. E., Baker, R., Lee, S., and Gibson, J. (2009). When is an error not a prediction error? An electrophysiological investigation. *Cogn. Affect. Behav. Neurosci.* 9, 59–70. doi: 10.3758/cabn.9.1.59

Holroyd, C. B., Pakzad-Vaezi, K. L., and Krigolson, O. E. (2008). The feedback correct-related positivity: sensitivity of the event-related brain potential to unexpected positive feedback. *Psychophysiology* 45, 688–697. doi: 10.1111/j.1469-8986.2008.00668.x

Holroyd, C. B., and Umemoto, A. (2016). The research domain criteria framework: the case for anterior cingulate cortex. *Neurosci. Biobehav. Rev.* 71, 418–443. doi: 10.1016/j.neubiorev.2016.09.021

Krain, A. L., Gotimer, K., Hefton, S., Ernst, M., Castellanos, F. X., Pine, D. S., et al. (2008). A functional magnetic resonance imaging investigation of uncertainty in adolescents with anxiety disorders. *Biol. Psychiatry* 63, 563–568. doi: 10.1016/j.biopsych.2007.06.011

Lee, T. W., Girolami, M., and Sejnowski, T. J. (1999). Independent component analysis using an extended infomax algorithm for mixed subgaussian and supergaussian sources. *Neural Comput.* 11, 417–441. doi: 10.1162/089976699300016719

Li, P., Baker, T. E., Warren, C., and Li, H. (2016). Oscillatory profiles of positive, negative and neutral feedback stimuli during adaptive decision making. *Int. J. Psychophysiol.* 107, 37–43. doi: 10.1016/j.ijpsycho.2016.06.018

Li, P., Han, C., Lei, Y., Holroyd, C. B., and Li, H. (2011). Responsibility modulates neural mechanisms of outcome processing: an ERP study. *Psychophysiology* 48, 1129–1133. doi: 10.1111/j.1469-8986.2011.01182.x

Li, P., Jia, S., Feng, T., Liu, Q., Suo, T., and Li, H. (2010). The influence of the diffusion of responsibility effect on outcome evaluations: electrophysiological evidence from an ERP study. *Neuroimage* 52, 1727–1733. doi: 10.1016/j.neuroimage.2010.04.275

Li, P., Song, X., Wang, J., Zhou, X., Li, J., Lin, F., et al. (2015). Reduced sensitivity to neutral feedback versus negative feedback in subjects with mild depression: evidence from event-related potentials study. *Brain Cogn.* 100, 15–20. doi: 10.1016/j.bandc.2015.08.004

Maner, J. K., and Schmidt, N. B. (2006). The role of risk avoidance in anxiety. *Behav. Ther.* 37, 181–189. doi: 10.1016/j.beth.2005.11.003

Metcalfe, J., Kornell, N., and Finn, B. (2009). Delayed versus immediate feedback in children's and adults' vocabulary learning. *Mem. Cognit.* 37, 1077–1087. doi: 10.3758/mc.37.8.1077

Miltner, W. H., Braun, C. H., and Coles, M. G. (1997). Event-related brain potentials following incorrect feedback in a time-estimation task: evidence for a "generic" neural system for error detection. *J. Cogn. Neurosci.* 9, 788–798. doi: 10.1162/jocn.1997.9.6.788

Moser, J. S., Hajcak, G., Huppert, J. D., Foa, E. B., and Simons, R. F. (2008). Interpretation bias in social anxiety as detected by event-related brain potentials. *Emotion* 8, 693–700. doi: 10.1037/a0013173

Oliveira, F. T., Mcdonald, J. J., and Goodman, D. (2007). Performance monitoring in the anterior cingulate is not all error related: expectancy deviation and the representation of action-outcome associations. *J. Cogn. Neurosci.* 19, 1994–2004. doi: 10.1162/jocn.2007.19.12.1994

Open Science Collaboration. (2015). Estimating the reproducibility of psychological science. *Science* 349:aac4716. doi: 10.1126/science.aac4716

Peterburs, J., Kobza, S., and Bellebaum, C. (2016). Feedback delay gradually affects amplitude and valence specificity of the feedback-related negativity (FRN). *Psychophysiology* 53, 209–215. doi: 10.1111/psyp.12560

Potts, G., Martin, L. E., Burton, P., and Montague, P. R. (2006). When things are better or worse than expected: the medial frontal cortex and the allocation of processing resources. *J. Cogn. Neurosci.* 17, 1112–1119. doi: 10.1162/jocn.2006.18.7.1112

Roesch, M. R., Calu, D. J., and Schoenbaum, G. (2007). Dopamine neurons encode the better option in rats deciding between differently delayed or sized rewards. *Nat. Neurosci.* 10, 1615–1624. doi: 10.1038/nn2013

Sambrook, T. D., and Goslin, J. (2015). A neural reward prediction error revealed by a meta-analysis of ERPs using great grand averages. *Psychol. Bull.* 141, 213–235. doi: 10.1037/bul0000006

Sambrook, T. D., and Goslin, J. (2016). Principal components analysis of reward prediction errors in a reinforcement learning task. *Neuroimage* 124, 276–286. doi: 10.1016/j.neuroimage.2015.07.032

Sapolsky, R. M., Krey, L. C., and Mcewen, B. S. (1985). Prolonged glucocorticoid exposure reduces hippocampal neuron number: implications for aging. *J. Neurosci.* 5, 1222–1227.

Satpute, A. B., Mumford, J. A., Naliboff, B. D., and Poldrack, R. A. (2012). Human anterior and posterior hippocampus respond distinctly to state and trait anxiety. *Emotion* 12, 58–68. doi: 10.1037/a0026517

Schultz, W., Dayan, P., and Montague, P. R. (1997). A neural substrate of prediction and reward. *Science* 275, 1593–1599. doi: 10.1126/science.275.5306.1593

Spielberger, C. D. (Ed.) (1972). "Anxiety as an emotional state," in *Anxiety Current Trends in Theory and Research* (New York, NY: Academic Press), 24–49.

Spielberger, C. D., Gorsuch, R. L., Lushene, R. E., and Vagg, P. R. (1983). *State-Trait Anxiety Inventory (STAI).* Palo Alto, CA: Consulting Psychologist Press.

Uchida, S., Nishida, A., Hara, K., Kamemoto, T., Suetsugi, M., Fujimoto, M., et al. (2008). Characterization of the vulnerability to repeated stress in Fischer 344 rats: possible involvement of microRNA-mediated down-regulation of the glucocorticoid receptor. *Eur. J. Neurosci.* 27, 2250–2261. doi: 10.1111/j.1460-9568.2008.06218.x

Wang, J., Chen, J., Lei, Y., and Li, P. (2014). P300, not feedback error-related negativity, manifests the waiting cost of receiving reward information. *Neuroreport* 25, 1044–1048. doi: 10.1097/wnr.0000000000000226

Wang, J., Chen, Z., Peng, X., Yang, T., Li, P., Cong, F., et al. (2016). To know or not to know? Theta and delta reflect complementary information about an advanced cue before feedback in decision-making. *Front. Psychol.* 7:1556. doi: 10.3389/fpsyg.2016.01556

Weinberg, A., Luhmann, C. C., Bress, J. N., and Hajcak, G. (2012). Better late than never? The effect of feedback delay on ERP indices of reward processing. *Cogn. Affect. Behav. Neurosci.* 12, 671–677. doi: 10.3758/s13415-012-0104-z

Weismuller, B., and Bellebaum, C. (2016). Expectancy affects the feedback-related negativity (FRN) for delayed feedback in probabilistic learning. *Psychophysiology* 53, 1739–1750. doi: 10.1111/psyp.12738

Wittmann, M., Leland, D. S., and Paulus, M. P. (2007). Time and decision making: differential contribution of the posterior insular cortex and the striatum during a delay discounting task. *Exp. Brain Res.* 179, 643–653. doi: 10.1007/s00221-006-0822-y

Wray, L. D., and Stone, E. R. (2005). The role of self-esteem and anxiety in decision making for self versus others in relationships. *J. Behav. Decis. Mak.* 18, 125–144. doi: 10.1002/bdm.490

Yeung, N., Holroyd, C. B., and Cohen, J. D. (2005). ERP correlates of feedback and reward processing in the presence and absence of response choice. *Cereb. Cortex* 15, 535–544. doi: 10.1093/cercor/bhh153

Yeung, N., and Sanfey, A. G. (2004). Independent coding of reward magnitude and valence in the human brain. *J. Neurosci.* 24, 6258–6264. doi: 10.1523/jneurosci.4537-03.2004

Yu, R., and Zhou, X. (2006). Brain responses to outcomes of one's own and other's performance in a gambling task. *Neuroreport* 17, 1747–1751. doi: 10.1097/01.wnr.0000239960.98813.50

**Conflict of Interest Statement**: The authors declare that the research was conducted in the absence of any commercial or financial relationships that could be construed as a potential conflict of interest.

frontiers in Human Neuroscience

ORIGINAL RESEARCH
published: 13 February 2018
doi: 10.3389/fnhum.2018.00052

# Perceived Gaze Direction Modulates Neural Processing of Prosocial Decision Making

*Delin Sun*[1,2,3,4], *Robin Shao*[1,2], *Zhaoxin Wang*[5] *and Tatia M. C. Lee*[1,2,6,7]*

[1]*Laboratory of Neuropsychology, The University of Hong Kong, Pokfulam, Hong Kong,* [2]*Laboratory of Cognitive Affective Neuroscience, The University of Hong Kong, Pokfulam, Hong Kong,* [3]*Duke-UNC Brain Imaging and Analysis Center, Duke University, Durham, NC, United States,* [4]*VA Mid-Atlantic Mental Illness Research, Education and Clinical Center (MIRECC), Durham, NC, United States,* [5]*Shanghai Key Laboratory of Brain Functional Genomics, Key Laboratory of Brain Functional Genomics, Ministry of Education, Institute of Cognitive Neuroscience, School of Psychology and Cognitive Science, East China Normal University, Shanghai, China,* [6]*The State Key Laboratory of Brain and Cognitive Sciences, The University of Hong Kong, Pokfulam, Hong Kong,* [7]*Institute of Clinical Neuropsychology, The University of Hong Kong, Pokfulam, Hong Kong*

Gaze direction is a common social cue implying potential interpersonal interaction. However, little is known about the neural processing of social decision making influenced by perceived gaze direction. Here, we employed functional magnetic resonance imaging (fMRI) method to investigate 27 females when they were engaging in an economic exchange game task during which photos of direct or averted eye gaze were shown. We found that, when averted but not direct gaze was presented, prosocial vs. selfish choices were associated with stronger activations in the right superior temporal gyrus (STG) as well as larger functional couplings between right STG and the posterior cingulate cortex (PCC). Moreover, stronger activations in right STG was associated with quicker actions for making prosocial choice accompanied with averted gaze. The findings suggest that, when the cue implying social contact is absent, the processing of understanding others' intention and the relationship between self and others is more involved for making prosocial than selfish decisions. These findings could advance our understanding of the roles of subtle cues in influencing prosocial decision making, as well as shedding lights on deficient social cue processing and functioning among individuals with autism spectrum disorder (ASD).

**Keywords: social decision making, eye gaze, fMRI, superior temporal gyrus, posterior cingulate cortex**

OPEN ACCESS

***Edited by:***
*Xiaolin Zhou,*
*Peking University, China*

***Reviewed by:***
*Maryam Ziaei,*
*The University of Queensland, Australia*
*Apoorva Rajiv Madipakkam,*
*Charité Universitätsmedizin Berlin, Germany*

***Correspondence:**
*Tatia M. C. Lee*
*tmclee@hku.hk*

***Received:*** *31 October 2017*
***Accepted:*** *31 January 2018*
***Published:*** *13 February 2018*

***Citation:***
*Sun D, Shao R, Wang Z and Lee TMC (2018) Perceived Gaze Direction Modulates Neural Processing of Prosocial Decision Making. Front. Hum. Neurosci. 12:52. doi: 10.3389/fnhum.2018.00052*

## INTRODUCTION

Prosocial behaviors are the cornerstone of a harmonic society (Keltner et al., 2014), and are associated with complex considerations of benefits and intentions of both self and others (Rilling and Sanfey, 2011). Recent work showed that prosocial actions can be promoted in the presence of eyes or eye-like stimuli (Haley and Fessler, 2005; Nettle et al., 2013), suggesting the role of the eyes in effectively biasing social decision making. Gaze is one of the most important conduits of information delivered by eyes, and plays significant roles in social interaction (Itier and Batty, 2009; Carlin and Calder, 2013). However, little is known about the neural processing of social decision making modulated by perceived gaze direction.

Compared to selfish actions, prosocial decisions are more associated with attributions of the intentions and desires of counterparts, the so-called Theory of Mind (ToM; Baron-Cohen et al., 1985). According to this theory, understanding others' needs and thoughts may promote the

engagement in prosocial actions (Dunfield, 2014), while benefiting others may in turn contribute to the development of better ToM (Weller and Lagattuta, 2014). Consistent with this, a recent meta-analysis showed that ToM and prosocial behaviors are positively related in children (Imuta et al., 2016). Evidence also suggests the ability of paying attention to or understanding the information delivered by gaze appears in very early stage of development (Farroni et al., 2002). Someone else's gaze informs us about the object or place he/she is looking at, and in turn how important or interesting such information is to him/her (Baron-Cohen, 1995; Shimojo et al., 2003; Frischen et al., 2007). Gaze direction has thus been proposed as a privileged stimulus for the attribution of mental state of others (Baron-Cohen, 1995). Direct gaze, usually accompanied with eye contact, indicates that someone is paying attention to us, while averted gaze implies the person is interested in people or objects other than us. On the other hand, Adams and Kleck (2003, 2005) found that direct gaze facilitates the processing of facial expressions indicating approach-oriented emotions (e.g., anger and joy), whereas averted gaze facilitates the processing of expressions implying avoidance-oriented emotions (e.g., fear and sadness). They thus proposed the "Shared Signal Hypothesis", which postulates that the perception of a specific emotion will be enhanced when gaze direction matches the underlying behavioral intent communicated by that emotion expression. Taken together, direct gaze implies potential social contact and enhances the perception of approach-oriented emotions while averted gaze does not, which could in turn influence how readily we process others' intentions and our subsequent social decision-making processes. However, no research has directly tested the effect of eye gaze direction on social decision making.

Brain regions related with ToM include the superior temporal gyrus (STG), posterior cingulate cortex (PCC), medial prefrontal cortex (mPFC), temporal-parietal junction (TPJ) and amygdala (Northoff and Bermpohl, 2004; Shaw et al., 2004; Schurz et al., 2014). These areas are widely implicated in social cognitive and decision-making processes (Moll et al., 2005, 2007; Rilling and Sanfey, 2011; Bastin et al., 2016). For example, Rilling et al. (2004) detected stronger activations in mPFC, PCC and TPJ when participants inferred the intent of human counterparts through their feedbacks during economic game tasks. Also, Moll and de Oliveira-Souza (2007) employed written statements describing action scenarios and found that prosocial emotions including guilt, embarrassment and compassion activated mPFC and bilateral STG. In a recent study, Morey et al. (2012) found that brief hypothetical scenarios in which the participants' actions lead to harmful consequences to others vs. to self were associated with more intense feelings of guilt as well as stronger activations in mPFC, right STG and PCC. Further, amygdala was reported to signal the interaction between gaze direction and perceived facial expression (N'Diaye et al., 2009; Cristinzio et al., 2010; Sato et al., 2010; Ziaei et al., 2016, 2017), suggesting its role in the appraisal of self-relevance. These findings disclosed a positive relationship between prosocial actions/emotions and activations in the ToM brain network, and supported the idea that prosocial behaviors are related with more considerations of others' thoughts and relationships between self and others.

Here, we were particularly interested in the STG. Existing imaging evidence indicates the right STG as being sensitive to gaze direction (Nummenmaa and Calder, 2009), suggesting its role as an eye direction detector (Baron-Cohen, 1995). Consistent with this, a patient with damage to the right STG showed difficulties in gaze discrimination and gaze-cued attention orientation (Akiyama et al., 2006). Stronger brain activations in right STG were also observed for direct than averted gaze (Calder et al., 2002; Pelphrey et al., 2004; but see Hardee et al., 2008). Previous studies have also found increased activations in the audience's right STG when an actor tried to deceive the audience about the weight of a box he was lifting (Grezes et al., 2004a), when an actor had a false belief about the weight of the box (Grezes et al., 2004b), and when an actor chose an object he did not like or rejected an object he preferred (Wyk et al., 2009), suggesting that the STG is involved in detecting other's intentions. Moreover, the STG may collaborate with other ToM areas to process gaze and social information, as it has both anatomical (Parvizi et al., 2006) and functional (Uddin et al., 2009) connections with the PCC. Stronger activations in bilateral STG, mPFC and PCC were reported in healthy participants when viewing direct than averted gaze (von dem Hagen et al., 2014), and greater mPFC-right STG functional connectivity was reported during social emotion, such as embarrassment and guilt, than basic emotion (Burnett and Blakemore, 2009).

In this study, we employed the functional magnetic resonance imaging (fMRI) method to investigate brain responses when participants were making either prosocial or selfish choices against anonymous counterparts in a novel economic exchanging game task (Sun et al., 2016). The effect of eye gaze direction was investigated by showing participants photos of counterparts' eyes with either direct or averted gaze. In line with existing findings, prosocial vs. selfish choices were proposed to be associated with more considerations of others' mental states as well as the relationship between self and others. In this context, prosocial choice was defined as behaviors that prioritize the benefit of other social, but not nonsocial (e.g., a robot), agents. We tested two types of relations between perceived gaze direction, social behaviors and the associated neural patterns. If prosocial choices were triggered by direct gaze that cues others' intentions of social contact, we hypothesized to find stronger activations in right STG and larger functional connectivity between right STG and other ToM areas during making prosocial vs. selfish choices when perceiving direct than averted gaze. On the other hand, averted gaze signals the lack of intentions for social contact, and the viewers may need to make more cognitive efforts to infer the counterpart's thoughts and to consider the relationship between self and others during making prosocial decisions. We then alternatively hypothesized to find stronger activations in right STG and larger functional connectivity between right STG and other ToM areas during making prosocial vs. selfish choices when detecting averted than direct gaze.

# MATERIALS AND METHODS

## Participants

Thirty Chinese female university students (age = 24 ± 2.4 years, range = 20–29 years) participated in this study. Only females were recruited to avoid confounding gender influence in social decision making (Lee et al., 2009; Zhang et al., 2012; Sun et al., 2015b, 2016). All participants were right-handed (Oldfield, 1971) and had normal or corrected-to-normal vision. No participant had metal or medical device implants or any history of neurological or mental disorders. All participants in this study provided written informed consent to participate in procedures reviewed and approved by the local ethical committees at the University of Hong Kong and the East China Normal University. Three participants were excluded due to data recording errors, thus 27 participants were included for final analyses.

## Eye Stimuli

There were three types of eye photos: human eyes with a direct gaze, human eyes with an averted gaze and robot's eyes (**Figure 1**). The photos of human eyes were collected from 24 volunteers (12 males and 12 females) prior to this study. Each volunteer gave two photos of his or her face with a front view and a neutral expression: one with a direct gaze and the other with an averted gaze (i.e., looking to the left). These photos were put into two sets, each containing six pictures of a male direct gaze, six pictures of a male averted gaze, six pictures of a female direct gaze, and six pictures of a female averted gaze. The two photos from the same volunteer never appeared in the same set to avoid the potential conflicts elicited by different gaze directions from the same volunteer. Half of the participants viewed the eyes in one set, while the other half viewed the other set of eyes. The photo of the robot's eyes was modified from a cartoon robot's eyes downloaded from Internet resources. All photos were of identical sizes and adapted to contain only the eye region before being changed into black and white through Adobe Photoshop software (San Jose, CA, USA).

## Task and Procedure

Each participant received the following instructions before experiment: "You are invited to interact with anonymous counterparts in an online game. You should treat each trial as a single-shot interaction since counterparts will vary across trials and players cannot recognize each other. A photo of either human eyes or a robot's eyes will be shown on a given trial to represent the counterpart type, i.e., human or robot, but not identity. In each trial, you will receive from a counterpart both a monetary investment as well as an offer on how to divide between you two the final amount, which is the appreciated investment through a computer-mimicked stock market. For simplicity, you will be shown just the final amount but not the initial investment. You can accept the offer or reject it by choosing an alternative plan that is more beneficial to you but less advantageous to the counterpart. After that, the counterpart will have 50-50 chance to know whether you have accepted or rejected his/her offer. If you reject an offer, your share in that trial will be transferred to the counterpart when he/she knows your choice. In the other conditions, you will keep your share. If you make no action, all benefits will be delivered to the counterpart in that trial. Your choices will influence the actual incomes of players. That is to say, both you and the counterpart will get the corresponding amount if you accept the offer. However, if the human counterpart does not know that you have chosen an alternative option, you will gain more than offered and he/she less than offered. All human players but not robot will finally receive real monetary bonuses proportional to the amounts earned during the task". Based on these instructions, the participant did not know that, in fact, computer programs mimicked all of the responses of human/robot counterparts. This approach was successful in our previous study utilizing similar task procedures (Sun et al., 2016). In order to reduce the influence of value calculation on participants' choices, expected utility (i.e., reward × probability) on a given trial was equal between accepting and rejecting an offer.

In each trial (**Figure 1**), following a jittered inter-trial-interval (ITI) of 3 s (Poisson-distributed), the amount of the increased investment was shown on the screen for 3 s (decision phase) during which the participant had to make her choice by pressing one of two buttons with the right index or middle finger. During the decision phase, four vertical bars were displayed on the screen, with the leftmost bar reflecting the counterpart's offer plan, the middle two bars reflecting the two available options for division to choose from, and the rightmost empty bar signaling the forthcoming outcome (yet to be revealed). One of the choice options corresponded to the counterpart's proposal, whereas the other option gave the participant a greater potential monetary reward, but carried a 50% risk of gaining nothing. In the option bars, the proportions of reward assigned to the counterpart was represented by the cyan-colored area, and the reward assigned to the participant was represented by the purple-colored area (**Figure 1**). The number above the option bars indicated the total amount of appreciated investment to be divided. The spatial positions of the two choice options were randomized across trials. Once the participant had made a choice, a black line appeared underneath the selected option bar. After a jittered inter-stimulus interval (ISI) of 3 s (Poisson-distributed), the participant was notified whether the real situation was detected and how much she gained in that trial in the following 3 s (outcome phase). A black line above the outcome bar indicated that the counterpart knew the participant's actual choice, while no such line was shown if the detection did not occur. When an action of rejecting the counterpart's offer was detected, the participant gained nothing in that trial and her share in the outcome bar became black. Under the other conditions, the participant kept the share for herself. If the participant failed to make a choice in that trial, or if the response exceeded the 3-s interval, all reward would be sent to the counterpart.

There were a total of 144 trials in the formal task. Photos of a direct gaze, an averted gaze, and a robot's eyes were each shown for 48 trials in randomized orders. The permutation of the offer—that is, the amount to be divided (a number randomly generated among 80, 100 and 150), the proposed portion of repayment to the counterpart (60%, 65%, 70%), and the location (left or right) of the bars representing two options were balanced

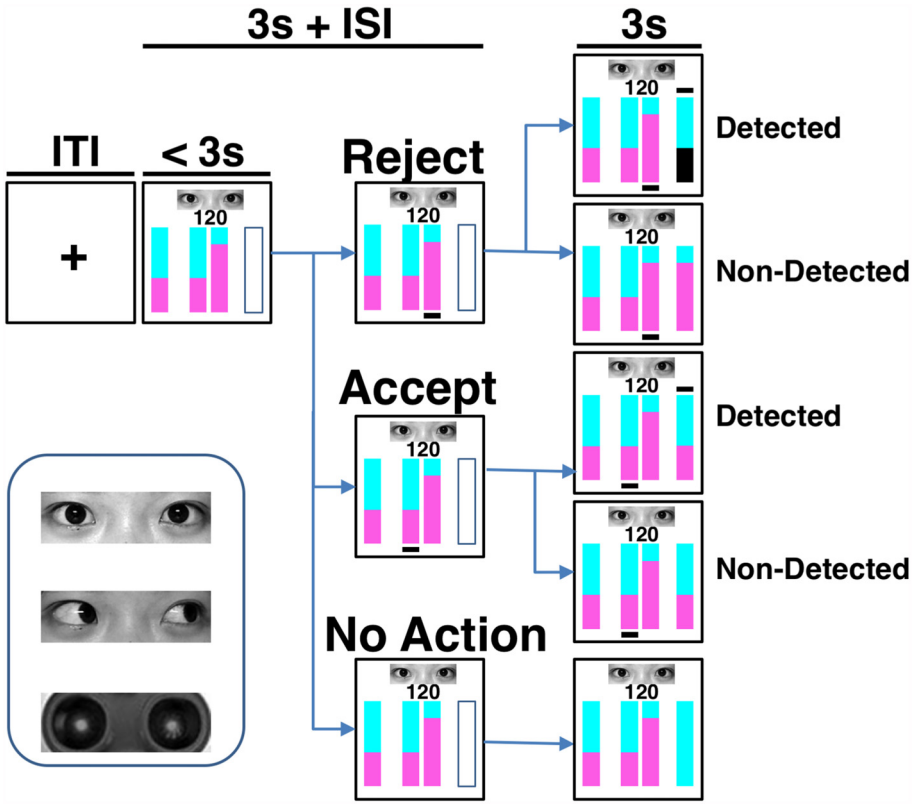


**FIGURE 1 |** Task paradigm and eye stimuli. The cyan and purple areas in the vertically stacked bars represented the proportions of reward assigned to the counterpart and the participant, respectively. In each trial, after knowing the total amount to be divided (i.e., the number in the screen) and the counterpart's offer (represented by the bar on the left-hand side), the participant could accept or reject the proposal by pressing one of two buttons corresponding to the bars in the middle of the screen within 3 s. To accept the counterpart's proposal is beneficial to both players, while to reject the proposal indicates a plan more advantageous to the participant. Immediately after the choice action, a black line was shown beneath the corresponding bar. The final reward distribution of a trial was presented by the outcome bar on the right-hand side at the last 3 s of the trial. A black line appeared above the outcome bar if the real situation was detected. On the contrary, no line was shown if the detection did not occur. When a rejection was detected, the participant gained nothing in that trial and her area in the outcome bar became black. Under the other conditions, the participant kept her share. If there was no response, or should the response exceed the 3-s decision-making phase, the reward of the trial was sent to the counterpart. Both inter-trial-interval (ITI) and inter-stimulus-interval (ISI) were on average 3 s. One of the three cues was presented during each trial. The cues are human eyes with direct or averted gaze and robot eyes.

across the different types of photos. Before getting into the scanner, each participant was given detailed instructions and completed a minimum of eight practice trials to ensure task comprehension. The photos used in the practice trials were different from those used in the formal task. All participants reported after the task that they believed they were playing with real human-being when the human eye stimuli were shown. The participants were debriefed after the experiment. Each participant was awarded 200 Chinese Yuan as compensation and also 0–100 Chinese Yuan (proportional to the task earnings) as a task bonus. The visual stimuli presentations and response collections were performed through the integrated functional imaging system (IFIS).

## Image Acquisition and Preprocessing

All images were acquired using a 3-Tesla Siemens Trio Tim MR scanner with a 12-channel head coil. T2*-weighted functional images were obtained using an EPI pulse sequence without inter-slice gap (33 axial slices parallel to the AC-PC line, TR = 2000 ms, TE = 30 ms, flip angle = 90°, Field of View (FOV) = 192 × 192 $mm^2$, voxel size = 3 × 3 × 4 $mm^3$). A high-resolution anatomical 3D T1-weighted MPRAGE image (192 slices, TR = 2530 ms, TE = 2.4 ms, flip angle = 7°, FOV = 224 × 256 $mm^2$, voxel size = 0.5 × 0.5 × 1 $mm^3$) was also acquired.

Images were preprocessed by using the CONN toolbox[1], which calls functions from SPM12 software (Wellcome Department of Imaging Neuroscience, UK), through slice-timing and motion correction, normalization to the MNI (Montreal Neurological Institute) space and, finally, smoothing with an 8-mm full-width half-maximum Gaussian kernel.

## Statistical Analyses

Participants made actions (either accept or reject) in more than 94% trials. For our research aims, conditions involving interactions with robot served as a control conditions

[1]https://sites.google.com/view/conn/

**TABLE 1 |** Frequency of action and reaction time (RT).

| Stimuli | Robot's eyes | | Human direct eyes | | Human averted eyes | |
|---|---|---|---|---|---|---|
| **Action** | **Accept** | **Reject** | **Accept** | **Reject** | **Accept** | **Reject** |
| **Frequency (%)** | | | | | | |
| Mean | 46.9 | 53.1 | 47.1 | 52.9 | 50.1 | 49.9 |
| Std | 13.5 | 13.5 | 12.9 | 12.9 | 12.1 | 12.1 |
| **Reaction time (ms)** | | | | | | |
| Mean | 1189.2 | 1143.1 | 1237.8 | 1217.9 | 1224.2 | 1223.4 |
| Std | 161.6 | 181.5 | 183.3 | 205.6 | 204.0 | 201.9 |

representing non-social-related processes such as general value-based decision making. We thus subtracted frequency of choice and mean reaction time (RT) related with robot counterpart from the corresponding data associated with human counterparts. No difference in choice frequencies was observed for human and robot counterpart trials ($p$s $> 0.287$). The four contrasts of interest were prosocial choice (i.e., accepting offer) accompanied with direct gaze, selfish choice (i.e., rejecting offer) accompanied with direct gaze, prosocial choice accompanied with averted gaze, and selfish choice accompanied with averted gaze. The frequency of choice and RTs were then respectively analyzed by a 2 (gaze direction: direct and averted) $\times$ 2 (choice: prosocial and selfish) repeated-measures ANOVA model.

Images were analyzed utilizing the SPM12 software. The general line model (GLM) was used to examine the experimental effects across task events within each participant. The onset of the decision phase was modeled by six regressors with 3-s duration which were combinations of eye stimuli (robot's eyes, direct human eyes and averted human eyes) and action (accept and reject offers). In addition, one regressor modeled the choice response, one modeled the onset of the outcome phase (3-s duration), and six extra regressors modeling residual head motions were included as nuisances. These regressors were convolved with the SPM canonical hemodynamic response function. High-pass temporal filtering with a cut-off of 128 s was employed to remove low-frequency drifts.

To form within-subject contrasts, consistent with the approach of behavioral data analyses, beta-weight images of regressors of robot counterpart were subtracted from the corresponding images associated with human players. This approach gave four contrast images per participant, i.e., prosocial choice accompanied with direct gaze, selfish choice accompanied with direct gaze, prosocial choice accompanied with averted gaze, and selfish choice accompanied with averted gaze. These contrasts were then entered into a group-level 2 (gaze direction: direct and averted) $\times$ 2 (choice: prosocial and selfish) flexible factorial model. Results were voxel-level height thresholded at $p < 0.001$ and survived family-wise error (FWE) cluster-level correction ($p < 0.05$) within the whole brain. To specifically test our *a priori* hypotheses, we also reported findings with voxel-level height threshold at $p < 0.001$ and survived FWE correction ($p < 0.05$) within regions of interests (ROIs) including the PCC (Brodmann's areas 23 and 31; Leech and Sharp, 2014), mPFC (Brodmann's areas 9, 10, 24, 25 and 32; Murray et al., 2016), and bilateral amygdala constructed using the WFU_PickAtlas toolbox[2]). We also investigated the findings in bilateral anterior TPJ (center coordinates: left, $x = -53$, $y = -30$, $z = 10$; right, $x = 47$, $y = -35$, $z = 12$) and posterior TPJ (center coordinates: left, $x = -53$, $y = -59$, $z = 20$; right, $x = 56$, $y = -56$, $z = 18$) in spheres with a radius of 8 mm (Schurz et al., 2014). All significant clusters contained more than 5 voxels. Mean beta values of fMRI contrasts were extracted for further analyses from the aforementioned ROIs showing significant task activations, using the MarsBaR toolbox[3]. Bonferroni method was employed to correct for multiple comparisons during *post hoc t* tests and fMRI-behavior correlation analyses.

We further investigated the functional coupling between the seed region and the rest of the brain, especially in the ROIs of ToM areas. The seed area was the region showing significant interaction between gaze direction and choice in the fMRI analyses. We performed a generalized psychophysiological interaction (gPPI) analysis through the gPPI toolbox[4]. Following fMRI analyses, four contrast images per participant were made reflecting the differences between playing against human vs. robot. These contrasts were also entered into a group-level 2 (gaze direction: direct and averted) $\times$ 2 (choice: prosocial and selfish) flexible factorial model. Results were voxel-level height thresholded at $p < 0.001$, FWE cluster-level corrected at $p < 0.05$, and contained more than 5 voxels. Mean beta values of gPPI contrasts were extracted for further analyses from the significant cluster through the MarsBaR toolbox. Bonferroni method was employed to correct for multiple comparisons during *post hoc t* tests and behavior-fMRI correlation analyses.

# RESULTS

## Behavioral Findings

Mean and standard deviations of behavioral measures were organized in **Table 1**. For our research purposes, behavioral data (i.e., frequency of choice and RT) and image contrasts related with robot counterpart were subtracted from the corresponding data associated with human counterparts. No significant gaze direction effects were found for either frequency of choice ($F$s $< 2.292$, $p$s $> 0.142$) or RT ($F$s $< 0.858$, $p$s $> 0.363$). Comparisons between human (including both direct and averted

[2]http://fmri.wfubmc.edu/software/pickatlas
[3]http://marsbar.sourceforge.net/
[4]http://www.nitrc.org/projects/gppi

gaze conditions) and computer counterparts were organized in the supplementary document.

## fMRI Findings

Averted gaze elicited stronger activations in right STG (Brodmann's area 22, cluster size = 293 voxels, T value = 4.18, peak MNI coordinates = [52, −46, 8], FWE-corrected cluster-level $p$ value = 0.018) than direct gaze, while there was no significantly stronger activation for direct than averted gaze. No main effect of choice was detected significant. Importantly, a significant interaction between gaze direction and choice was detected in the right STG (Brodmann's area 42/22, cluster size = 227 voxels, T value = 4.24, peak MNI coordinates = [70, −30, 16], FWE-corrected cluster-level $p$ value = 0.047, see **Figure 2A**), characterized by stronger activations during prosocial choices vs. selfish choices when presented with averted gaze than direct gaze. Mean beta values extracted from this right STG cluster were greater to prosocial choices than to selfish choices when averted ($t_{(26)}$ = 4.583, $p < 0.001$ corrected) but not direct ($t_{(26)}$ = −0.459, $p > 0.6$) gaze was presented (**Figure 2B**). No significant results were found in the other ROIs. Comparisons between human (including both direct and averted gaze conditions) and computer counterparts were organized in the Supplementary Table S1. Moreover, larger mean betas in the right STG cluster were accompanied with quicker actions (i.e., shorter mean RT) across participants for prosocial choice to averted gaze (Pearson's $R$ = −0.585, $p$ = 0.008 corrected, **Figure 2C**). No other correlation in right STG was found significant (all $p$s > 0.07 uncorrected), see Supplementary Table S2.

## gPPI Findings

We then investigated the functional couplings between the seed region and the rest of the brain, especially the ToM ROIs. The seed is the right STG cluster showing significant interaction between gaze direction and choice in the fMRI analyses. Prosocial choices vs. selfish choices were accompanied with larger gPPI values in PCC (surviving small-volume FWE correction; Brodmann's area 31, cluster size = 26 voxels, T value = 4.29, Z value = 4.11, peak MNI coordinates = [−4, −34, 48], FWE-corrected peak-level $p$ value = 0.009, **Figure 3A**) when averted gaze than direct gaze was shown. Mean beta values extracted from this PCC cluster showed that prosocial choices were accompanied with stronger functional couplings than selfish choices when averted ($t_{(26)}$ = 3.703, $p$ = 0.006 corrected) but not direct ($t_{(26)}$ = −0.672, $p > 0.5$) gaze was presented (**Figure 3B**). No significant gPPI results were found in the other ROIs.

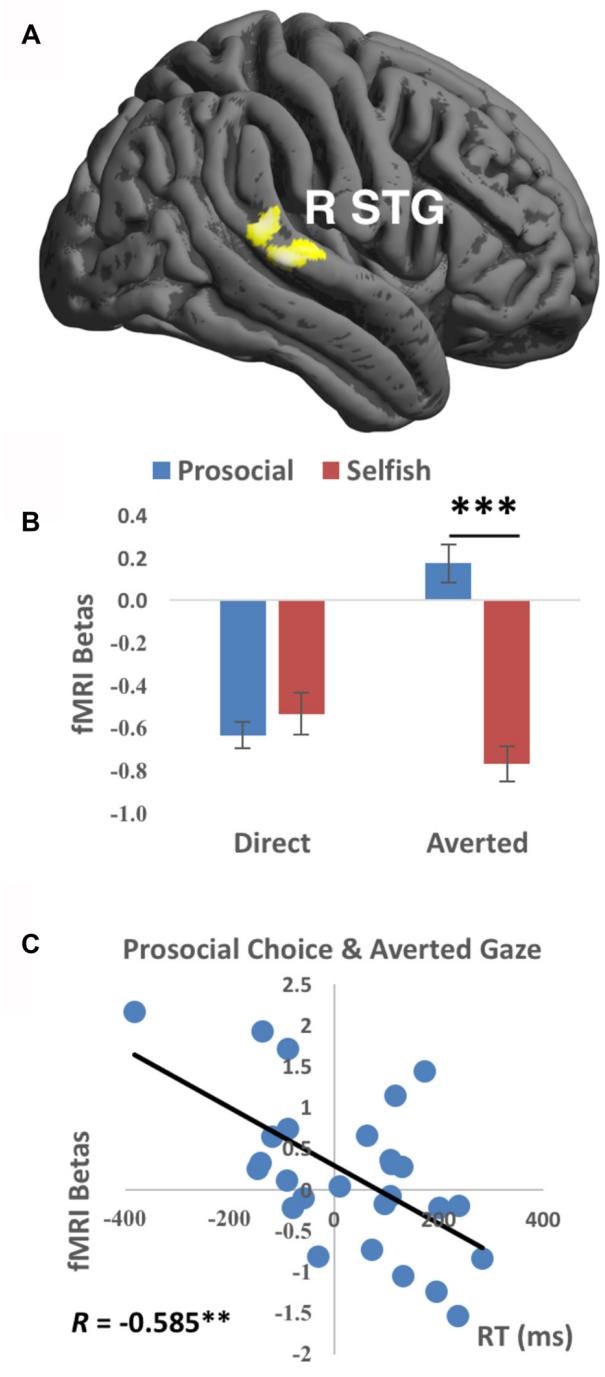


**FIGURE 2 |** Functional magnetic resonance imaging (fMRI) findings of the interaction between Gaze and Choice. **(A)** Prosocial vs. selfish choices were associated with stronger activations in right superior temporal gyrus (R STG) for averted than direct gaze. Imaging results were height-thresholded at $p < 0.001$ and survived $p < 0.05$ family-wise error (FWE) correction. **(B)** Larger fMRI beta values averaged within the cluster in R STG were found for prosocial choice than selfish choice when averted gaze was presented ($t_{(26)}$ = 4.583, $p$ = 0.006 corrected). Error bar denotes standard error mean. **(C)** Significant correlation (Pearson's $R$ = −0.585, $p$ = 0.008 corrected) was found between fMRI betas in R STG and reaction time (RT) for the condition of prosocial choice accompanied with averted gaze. $^{**}p < 0.01$, $^{***}p < 0.001$.

# DISCUSSION

Eye gaze plays vital roles in many social contexts (Itier and Batty, 2009). However, little is known about its influences on social decision making integral to everyday social functioning (Rilling and Sanfey, 2011). To the best of our knowledge, this is the first study investigating the neural processing of the interaction

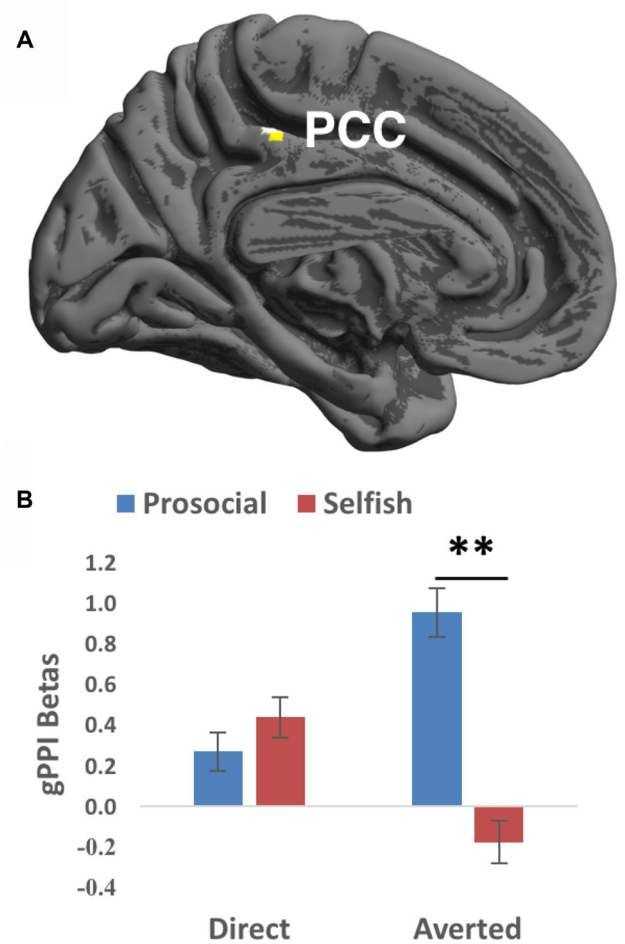


**FIGURE 3 |** Generalized psychophysiological interaction (gPPI) findings of the interaction between Gaze and Choice. **(A)** Prosocial vs. selfish choices were associated with larger gPPI values in posterior cingulate cortex (PCC) for averted than direct gaze. Imaging results were height-thresholded at $p < 0.001$ and survived $p < 0.05$ FWE correction within an anatomical mask of PCC consisting of Brodmann's area 23 and 31. **(B)** Larger gPPI beta values averaged within the cluster in PCC were found for prosocial choice than selfish choice when averted gaze was presented ($t_{(26)} = 4.583$, $p = 0.006$ corrected). Error bar denotes standard error mean. $^{**}p < 0.01$.

between social decisions and perceived gaze direction. Consistent with the second *a priori* hypothesis, we found that prosocial vs. selfish choice elicited stronger activations in right STG and larger right STG-PCC functional connectivity when averted rather than direct gaze was presented. Moreover, stronger activations in right STG was associated with quicker actions for making prosocial choice accompanied with averted gaze. Our findings suggest that both right STG and right STG-PCC functional connections are more involved for making prosocial choices than selfish decisions when the perceived subtle social cues signal a lack of intentions for social contact.

The right STG has been widely reported to play roles in responding to gaze direction (Itier and Batty, 2009), and in detecting, predicting and reasoning about actions and intentions of others (Allison et al., 2000). Importantly, our findings further demonstrate the role of right STG in social decision making. We found stronger activation in right STG for prosocial than selfish choice accompanied with averted gaze. This result suggests that, when the perceived subtle cue through others' gaze signals a lack of intentions for social contact, the right STG is more involved in inferring about the counterparts' intentions during making a decision to benefit them. This explanation is further supported by the negative correlation between right STG activation and RT during prosocial choice accompanied with averted gaze. By contrast, no significant differences were found between prosocial and selfish choices accompanied with direct gaze. It is possible that being observed by others' direct gaze is default in social interaction and carries a relatively constant level of processing about others' intention regardless of the choice made.

Perception of observations by others has been found to efficiently promote prosocial behaviors (Izuma et al., 2010). It is hypothesized that, when being observed by someone, people make prosocial actions in order to gain social approvals/reputations (Rege and Telle, 2004; Izuma, 2012) and/or to avoid the guilt of harming others (Morey et al., 2012). Consistent with this idea, Izuma (2012) detected more donations to charities and stronger activations in striatum when donating in the presence of observers than in their absence. Direct (vs. averted) gaze is proposed to cue the observations by others and may thus elicit stronger brain activations for prosocial than selfish choices. However, this hypothesis is inconsistent with our findings. It is thus difficult to explain the gaze effect on social decision making through social reputation or guilt.

Previous studies have also detected stronger STG activations in response to the mismatch between one's motion and the context (Grezes et al., 2004a,b; Wyk et al., 2009), and to moral judgments regarding the events that violate social norms (Prehn et al., 2008; Bahnemann et al., 2010). These findings suggest the roles of STG in reflecting the mismatch between observed actions and the context. If this theory also applies to the conflict between one's own actions and the context, we would hypothesize to find stronger STG activations for both prosocial decisions accompanied with averted gaze and selfish choices accompanied with direct gaze. The reasoning is that prosocial decision is suboptimal when not being observed by others (represented by averted gaze implying higher chance of "getting away with" potential punishment), and selfish decision is suboptimal when being observed by others (represented by direct gaze implying high risk of being caught and punished). However, we only detected stronger brain activations for the former but not the latter condition, suggesting that our results cannot be fully interpreted by the conflict between one's own actions and the context.

We also found larger functional couplings between right STG and PCC during making prosocial (vs. selfish) choices when perceiving averted gaze. The PCC has been widely reported in studies on self-referential processing (Lombardo et al., 2010; Brewer et al., 2013; Schurz et al., 2014). It is possible that more processing of others' intentions (represented by stronger right STG activations) is accompanied with more processing of the relationship between self and others. This thought is consistent with the previous findings that the PCC as well as the nearby

precuneus are associated with retrieval of episodic memory (Gobbini and Haxby, 2007; Sun et al., 2015c). In other words, during making prosocial decisions, when the perceived averted gaze implied lack of interpersonal interaction, participants need to recall their personal experiences in order to infer the others' intentions.

We did not find any significant results in the other ToM ROIs including mPFC, TPJ and amygdala. First, mPFC has been proposed to play central roles in ToM (Schurz et al., 2014). However, Krause et al. (2012) utilized repetitive transcranial magnetic stimulation (rTMS) to bilateral mPFC, and did not find significant effect on either cognitive or affective ToM performance. They further reported that deep rTMS disrupted affective ToM performance in participants with high empathy, but increased affective ToM performance in those with low empathy, suggesting that the roles of mPFC in affective ToM are modulated by the baseline empathic abilities. In our study, the interaction between perceived gaze direction and social decision making may also be influenced by the level of empathy in participants which we unfortunately did not measure. Second, studies have shown that TPJ is sensitive to prediction error, which means the degree to which current information is inconsistent with expectation, in various domains including social interaction (Behrens et al., 2008; Simon et al., 2017). People in multiple-rounds social interactions may employ TPJ to guide behaviors based on previous experiences. However, participants in our task paradigm were instructed to treat each trial as a single-shot interaction, and they could not utilize the experiences with a previous counterpart to influence the current interaction. Third, amygdala has been widely reported to play a central role in response to the interaction between perceived gaze direction and facial expression (Cristinzio et al., 2010; Sato et al., 2010; Ziaei et al., 2016). Facial expression is delivered by not only eyes but also other parts of the face such as the mouth (Ekman, 2003; Sun et al., 2015a). In this study, however, the photos of humans were taken merely in neutral expression, and only the eye region was displayed. These might have minimized the roles of mPFC, TPJ and amygdala in our task paradigm. Future studies should further investigate the brain activation and functional connectivity in the ToM ROIs utilizing alternative task paradigms and stimuli, taking into account individual differences in social traits.

We failed to find any significant behavioral result related with either gaze or interaction between gaze and choice in this study. The presence of eye-like stimuli has been repeatedly reported to increases prosocial behaviors such as greater investments (Bente et al., 2014), greater charitable donations (Powell et al., 2012), theft prevention (Bateson et al., 2013) and higher voting rate (Panagopoulos, 2014), the so-called "watching eyes effect" (Nettle et al., 2013). There are two possible explanations for our insignificant findings. First, most of previous laboratory and field studies on the "watching eyes effect" employed procedures in which a participant makes decisions for only one or just a few trials (Haley and Fessler, 2005; Nettle et al., 2013). By contrast, participants in our task made choices in 144 trials. Second, the "watching eyes effect" were observed when eyes or eye-like stimuli were present vs. absent, while eye stimuli were always present in our study. The behavioral and neural mechanisms of gaze direction influence on social decision making may be different from those of the "watching eyes effect". These need to be tested in future studies.

Our findings also have clinical implications, especially for people with autism spectrum disorders (ASDs) who exhibit impairments in reciprocal social interactions (Baron-Cohen et al., 1997). ASD has been found to relate to ToM impairments (Baron-Cohen et al., 2001). ASD patients show deficits in paying attention to the eye region (Spezio et al., 2007), extracting useful information from the eyes (Nation and Penny, 2008), and understanding others' mental states (Campbell et al., 2006). A later diagnosis of autism was found to be predicted at 18 months of age by an absence of joint attention (Baron-Cohen et al., 1996), which is a precursor to ToM and reflects the ability of attending to the object cued by another person's gaze direction (Emery, 2000). Our findings imply that ASD patients have deficits in processing subtle social cues in the environment such as eye gaze direction and/or in utilizing such information for making social decisions. Future work needs to clarify the neural underpinnings of social decision making in ASD patients when perceiving social cues. Further, previous studies suggested that brain stimulation techniques, such as TMS (Oberman et al., 2015) and Transcranial direct current stimulation (tDCS; Amatachaya et al., 2014, 2015), are promising methods of clinical treatment for ASD. These non-invasive brain stimulation techniques influence the activations in a small population of neurons in a targeted brain region. Our findings suggest that the right STG is a potential target for clinical intervention. Furthermore, the brain activation in the right STG and the right STG-PCC functional connections may also be employed to reflect the outputs of clinical treatment.

Our study have several limitations. First, our participants were all Chinese females. Caucasian and East Asian participants were found to fixate on the internal features (especially the eyes) and the center of faces (Blais et al., 2008), respectively, suggesting culture influences on face processing. People in western cultures may thus be more influenced by gaze direction while making social decisions. Future studies are needed for comparing the gaze-orienting effects across cultures and in different gender groups. Second, direct and averted gazes in this study were all shown in photos containing front-view faces, and were restricted within the eye region for simplicity. Previous studies have shown that head orientation (Itier et al., 2007) and dynamic gaze presentation (Putman et al., 2006) influenced the effects of gaze. Future studies should investigate the influence of gaze direction on social decision making in different head orientations and/or using a dynamic gaze (e.g., movies of gaze motion or real human eyes). Third, only left-oriented eyes were employed to represent the averted gaze in this study. Different directions of averted gaze may confer different social meanings and recruited different STG subregions in Calder et al. (2007). Future studies should separately investigate the effects of different averted gaze directions.

In conclusion, our study provides the first evidence that the neural processing of social decision making is influenced

by perceived gaze direction. Our findings suggest that, when the perceived gaze direction signals lack of social contact, making prosocial vs. selfish decisions is associated with greater neural processing of inferring others' intention and understanding the relationship between self and others. These findings also shed light on the deficiencies in processing subtle social cues and social functioning in ASD individuals.

## AUTHOR CONTRIBUTIONS

DS, RS, ZW and TMCL made substantial contributions to the conception or design of the work or the acquisition, analysis, or interpretation of data for the work; drafted the work or revised it critically for important intellectual content; approved the final version to be published; agreed to be accountable for all aspects of the work in ensuring that questions related to the accuracy or integrity of any part of the work are appropriately investigated and resolved.

## FUNDING

This work was supported by the Research Grant Council Humanities and Social Sciences Prestigious Fellowship (Ref: HKU703-HSS-13) and the National Natural Science Fund of China (Ref: 31070986). The fund agency has no role in study design, data collection and analysis, decision to publish, or preparation of the manuscript.

## SUPPLEMENTARY MATERIAL

The Supplementary Material for this article can be found online at: https://www.frontiersin.org/articles/10.3389/fnhum.2018.00052/full#supplementary-material

## REFERENCES

Adams, R. B. Jr., and Kleck, R. E. (2003). Perceived gaze direction and the processing of facial displays of emotion. *Psychol. Sci.* 14, 644–647. doi: 10.1046/j.0956-7976.2003.psci_1479.x

Adams, R. B. Jr., and Kleck, R. E. (2005). Effects of direct and averted gaze on the perception of facially communicated emotion. *Emotion* 5, 3–11. doi: 10.1037/1528-3542.5.1.3

Akiyama, T., Kato, M., Muramatsu, T., Saito, F., Umeda, S., and Kashima, H. (2006). Gaze but not arrows: a dissociative impairment after right superior temporal gyrus damage. *Neuropsychologia* 44, 1804–1810. doi: 10.1016/j.neuropsychologia.2006.03.007

Allison, T., Puce, A., and McCarthy, G. (2000). Social perception from visual cues: role of the STS region. *Trends Cogn. Sci.* 4, 267–278. doi: 10.1016/s1364-6613(00)01501-1

Amatachaya, A., Auvichayapat, N., Patjanasoontorn, N., Suphakunpinyo, C., Ngernyam, N., Aree-Uea, B., et al. (2014). Effect of anodal transcranial direct current stimulation on autism: a randomized double-blind crossover trial. *Behav. Neurol.* 2014:173073. doi: 10.1155/2014/173073

Amatachaya, A., Jensen, M. P., Patjanasoontorn, N., Auvichayapat, N., Suphakunpinyo, C., Janjarasjitt, S., et al. (2015). The short-term effects of transcranial direct current stimulation on electroencephalography in children with autism: a randomized crossover controlled trial. *Behav. Neurol.* 2015:928631. doi: 10.1155/2015/928631

Bahnemann, M., Dziobek, I., Prehn, K., Wolf, I., and Heekeren, H. R. (2010). Sociotopy in the temporoparietal cortex: common versus distinct processes. *Soc. Cogn. Affect. Neurosci.* 5, 48–58. doi: 10.1093/scan/nsp045

Baron-Cohen, S. (1995). *Mindblindness: An Essay on Autism and Theory of Mind.* Cambridge, MA: MIT Press.

Baron-Cohen, S., Cox, A., Baird, G., Swettenham, J., Nightingale, N., Morgan, K., et al. (1996). Psychological markers in the detection of autism in infancy in a large population. *Br. J. Psychiatry* 168, 158–163. doi: 10.1192/bjp.168.2.158

Baron-Cohen, S., Leslie, A. M., and Frith, U. (1985). Does the autistic-child have a "theory of mind"? *Cognition* 21, 37–46. doi: 10.1016/0010-0277(85)90022-8

Baron-Cohen, S., Wheelwright, S., Hill, J., Raste, Y., and Plumb, I. (2001). The "Reading the Mind in the Eyes" test revised version: a study with normal adults, and adults with Asperger syndrome or high-functioning autism. *J. Child Psychol. Psychiatry* 42, 241–251. doi: 10.1111/1469-7610.00715

Baron-Cohen, S., Wheelwright, S., and Jolliffe, T. (1997). Is there a "language of the eyes"? Evidence from normal adults and adults with autism or Asperger Syndrome. *Autism Res.* 4, 311–331. doi: 10.1080/713756761

Bastin, C., Harrison, B. J., Davey, C. G., Moll, J., and Whittle, S. (2016). Feelings of shame, embarrassment and guilt and their neural correlates: a systematic review. *Neurosci. Biobehav. Rev.* 71, 455–471. doi: 10.1016/j.neubiorev.2016.09.019

Bateson, M., Callow, L., Holmes, J. R., Redmond Roche, M. L., and Nettle, D. (2013). Do images of 'watching eyes' induce behaviour that is more pro-social or more normative? A field experiment on littering. *PLoS One* 8:e82055. doi: 10.1371/journal.pone.0082055

Behrens, T. E. J., Hunt, L. T., Woolrich, M. W., and Rushworth, M. F. S. (2008). Associative learning of social value. *Nature* 456, 245–249. doi: 10.1038/nature07538

Bente, G., Dratsch, T., Kaspar, K., Häβler, T., Bungard, O., and Al-Issa, A. (2014). Cultures of trust: effects of avatar faces and reputation scores on german and arab players in an online trust-game. *PLoS One* 9:e98297. doi: 10.1371/journal.pone.0098297

Blais, C., Jack, R. E., Scheepers, C., Fiset, D., and Caldara, R. (2008). Culture shapes how we look at faces. *PLoS One* 3:e3022. doi: 10.1371/journal.pone.0003022

Brewer, J. A., Garrison, K. A., and Whitfield-Gabrieli, S. (2013). What about the "self" is processed in the posterior cingulate cortex? *Front. Hum. Neurosci.* 7:647. doi: 10.3389/fnhum.2013.00647

Burnett, S., and Blakemore, S. J. (2009). Functional connectivity during a social emotion task in adolescents and in adults. *Eur. J. Neurosci.* 29, 1294–1301. doi: 10.1111/j.1460-9568.2009.06674.x

Calder, A. J., Beaver, J. D., Winston, J. S., Dolan, R. J., Jenkins, R., Eger, E., et al. (2007). Separate coding of different gaze directions in the superior temporal sulcus and inferior parietal lobule. *Curr. Biol.* 17, 20–25. doi: 10.1016/j.cub.2006.10.052

Calder, A. J., Lawrence, A. D., Keane, J., Scott, S. K., Owen, A. M., Christoffels, I., et al. (2002). Reading the mind from eye gaze. *Neuropsychologia* 40, 1129–1138. doi: 10.1016/s0028-3932(02)00008-8

Campbell, R., Lawrence, K., Mandy, W., Mitra, C., Jeyakuma, L., and Skuse, D. (2006). Meanings in motion and faces: developmental associations between the processing of intention from geometrical animations and gaze detection accuracy. *Dev. Psychopathol.* 18, 99–118. doi: 10.1017/s0954579406060068

Carlin, J. D., and Calder, A. J. (2013). The neural basis of eye gaze processing. *Curr. Opin. Neurobiol.* 23, 450–455. doi: 10.1016/j.conb.2012.11.014

Cristinzio, C., N'Diaye, K., Seeck, M., Vuilleumier, P., and Sander, D. (2010). Integration of gaze direction and facial expression in patients with unilateral amygdala damage. *Brain* 133, 248–261. doi: 10.1093/brain/awp255

Dunfield, K. A. (2014). A construct divided: prosocial behavior as helping, sharing, and comforting subtypes. *Front. Psychol.* 5:958. doi: 10.3389/fpsyg.2014.00958

Ekman, P. (2003). *Emotions Revealed: Recognizing Faces and Feelings to Improve Communication and Emotional Life.* New York, NY: Times Books.

Emery, N. J. (2000). The eyes have it: the neuroethology, function and evolution of social gaze. *Neurosci. Biobehav. Rev.* 24, 581–604. doi: 10.1016/s0149-7634(00)00025-7

Farroni, T., Csibra, G., Simion, G., and Johnson, M. H. (2002). Eye contact detection in humans from birth. *Proc. Natl. Acad. Sci. U S A* 99, 9602–9605. doi: 10.1073/pnas.152159999

Frischen, A., Bayliss, A. P., and Tipper, S. P. (2007). Gaze cueing of attention: visual attention, social cognition, and individual differences. *Psychol. Bull.* 133, 694–724. doi: 10.1037/0033-2909.133.4.694

Gobbini, M. I., and Haxby, J. V. (2007). Neural systems for recognition of familiar faces. *Neuropsychologia* 45, 32–41. doi: 10.1016/j.neuropsychologia.2006.04.015

Grezes, J., Frith, C., and Passingham, R. E. (2004a). Brain mechanisms for inferring deceit in the actions of others. *J. Neurosci.* 24, 5500–5505. doi: 10.1523/JNEUROSCI.0219-04.2004

Grezes, J., Frith, C. D., and Passingham, R. E. (2004b). Inferring false beliefs from the actions of oneself and others: an fMRI study. *Neuroimage* 21, 744–750. doi: 10.1016/s1053-8119(03)00665-7

Haley, K. J., and Fessler, D. M. T. (2005). Nobody's watching? Subtle cues affect generosity in an anonymous economic game. *Evol. Hum. Behav.* 26, 245–256. doi: 10.1016/j.evolhumbehav.2005.01.002

Hardee, J. E., Thompson, J. C., and Puce, A. (2008). The left amygdala knows fear: laterality in the amygdala response to fearful eyes. *Soc. Cogn. Affect. Neurosci.* 3, 47–54. doi: 10.1093/scan/nsn001

Imuta, K., Henry, J. D., Slaughter, V., Selcuk, B., and Ruffman, T. (2016). Theory of mind and prosocial behavior in childhood: a meta-analytic review. *Dev. Psychol.* 52, 1192–1205. doi: 10.1037/dev0000140

Itier, R. J., and Batty, M. (2009). Neural bases of eye and gaze processing: the core of social cognition. *Neurosci. Biobehav. Rev.* 33, 843–863. doi: 10.1016/j.neubiorev.2009.02.004

Itier, R. J., Villate, C., and Ryan, J. D. (2007). Eyes always attract attention but gaze orienting is task-dependent: evidence from eye movement monitoring. *Neuropsychologia* 45, 1019–1028. doi: 10.1016/j.neuropsychologia.2006.09.004

Izuma, K. (2012). The social neuroscience of reputation. *Neurosci. Res.* 72, 283–288. doi: 10.1016/j.neures.2012.01.003

Izuma, K., Saito, D. N., and Sadato, N. (2010). Processing of the incentive for social approval in the ventral striatum during charitable donation. *J. Cogn. Neurosci.* 22, 621–631. doi: 10.1162/jocn.2009.21228

Keltner, D., Kogan, A., Piff, P. K., and Saturn, S. R. (2014). The sociocultural appraisals, values, and emotions (SAVE) framework of prosociality: core processes from gene to meme. *Annu. Rev. Psychol.* 65, 425–460. doi: 10.1146/annurev-psych-010213-115054

Krause, L., Enticott, P. G., Zangen, A., and Fitzgerald, P. B. (2012). The role of medial prefrontal cortex in theory of mind: a deep rTMS study. *Behav. Brain Res.* 228, 87–90. doi: 10.1016/j.bbr.2011.11.037

Lee, T. M., Chan, C. C., Leung, A. W., Fox, P. T., and Gao, J. H. (2009). Sex-related differences in neural activity during risk taking: an fMRI study. *Cereb. Cortex* 19, 1303–1312. doi: 10.1093/cercor/bhn172

Leech, R., and Sharp, D. J. (2014). The role of the posterior cingulate cortex in cognition and disease. *Brain* 137, 12–32. doi: 10.1093/brain/awt162

Lombardo, M. V., Chakrabarti, B., Bullmore, E. T., Wheelwright, S. J., Sadek, S. A., Suckling, J., et al. (2010). Shared neural circuits for mentalizing about the self and others. *J. Cogn. Neurosci.* 22, 1623–1635. doi: 10.1162/jocn.2009.21287

Moll, J., and de Oliveira-Souza, R. (2007). Moral judgments, emotions and the utilitarian brain. *Trends Cogn. Sci.* 11, 319–321. doi: 10.1016/j.tics.2007.06.001

Moll, J., de Oliveira-Souza, R., Garrido, G. J., Bramati, I. E., Caparelli-Daquer, E. M. A., Paiva, M. L. M. F., et al. (2007). The self as a moral agent: link-ling the neural bases of social agency and moral sensitivity. *Soc. Neurosci.* 2, 336–352. doi: 10.1080/17470910701392024

Moll, J., Zahn, R., de Oliveira-Souza, R., Krueger, F., and Grafman, J. (2005). The neural basis of human moral cognition. *Nat. Rev. Neurosci.* 6, 799–809. doi: 10.1038/nrn1768

Morey, R. A., McCarthy, G., Selgrade, E. S., Seth, S., Nasser, J. D., and LaBar, K. S. (2012). Neural systems for guilt from actions affecting self versus others. *Neuroimage* 60, 683–692. doi: 10.1016/j.neuroimage.2011.12.069

Murray, E. A., Wise, S. P., and Graham, K. S. (2016). "Chapter 1: the history of memory systems," in *The Evolution of Memory Systems: Ancestors, Anatomy, and Adaptations*, eds M. Baum, C. Greene and M. Butler (Oxford: Oxford University Press), 22–24.

Nation, K., and Penny, S. (2008). Sensitivity to eye gaze in autism: is it normal? Is it automatic? Is it social? *Dev. Psychopathol.* 20, 79–97. doi: 10.1017/S0954579408000047

N'Diaye, K., Sander, D., and Vuilleumier, P. (2009). Self-relevance processing in the human amygdala: gaze direction, facial expression, and emotion intensity. *Emotion* 9, 798–806. doi: 10.1037/a0017845

Nettle, D., Harper, Z., Kidson, A., Stone, R., Penton-Voak, I. S., and Bateson, M. (2013). The watching eyes effect in the Dictator Game: it's not how much you give, it's being seen to give something. *Evol. Hum. Behav.* 34, 35–40. doi: 10.1016/j.evolhumbehav.2012.08.004

Northoff, G., and Bermpohl, F. (2004). Cortical midline structures and the self. *Trends Cogn. Sci.* 8, 102–107. doi: 10.1016/j.tics.2004.01.004

Nummenmaa, L., and Calder, A. J. (2009). Neural mechanisms of social attention. *Trends Cogn. Sci.* 13, 135–143. doi: 10.1016/j.tics.2008.12.006

Oberman, L. M., Rotenberg, A., and Pascual-Leone, A. (2015). Use of transcranial magnetic stimulation in autism spectrum disorders. *J. Autism Dev. Disord.* 45, 524–536. doi: 10.1007/s10803-013-1960-2

Oldfield, R. C. (1971). The assessment and analysis of handedness: the Edinburgh inventory. *Neuropsychologia* 9, 97–113. doi: 10.1016/0028-3932(71)90067-4

Panagopoulos, C. (2014). Watchful eyes: implicit observability cues and voting. *Evol. Hum. Behav.* 35, 279–284. doi: 10.1016/j.evolhumbehav.2014.02.008

Parvizi, J., Van Hoesen, G. W., Buckwalter, J., and Damasio, A. (2006). Neural connections of the posteromedial cortex in the macaque. *Proc. Natl. Acad. Sci. U S A* 103, 1563–1568. doi: 10.1073/pnas.0507729103

Pelphrey, K. A., Viola, R. J., and Mccarthy, G. (2004). When strangers pass—processing of mutual and averted social gaze in the superior temporal sulcus. *Psychol. Sci.* 15, 598–603. doi: 10.1111/j.0956-7976.2004.00726.x

Powell, K. L., Roberts, G., and Nettle, D. (2012). Eye images increase charitable donations: evidence from an opportunistic field experiment in a supermarket. *Ethology* 118, 1096–1101. doi: 10.1111/eth.12011

Prehn, K., Wartenburger, I., Mériau, K., Scheibe, C., Goodenough, O. R., Villringer, A., et al. (2008). Individual differences in moral judgment competence influence neural correlates of socio-normative judgments. *Soc. Cogn. Affect. Neurosci.* 3, 33–46. doi: 10.1093/scan/nsm037

Putman, P., Hermans, E., and Van Honk, J. (2006). Anxiety meets fear in perception of dynamic expressive gaze. *Emotion* 6, 94–102. doi: 10.1037/1528-3542.6.1.94

Rege, M., and Telle, K. (2004). The impact of social approval and framing on cooperation in public good situations. *J. Public Econ.* 88, 1625–1644. doi: 10.1016/s0047-2727(03)00021-5

Rilling, J. K., and Sanfey, A. G. (2011). The neuroscience of social decision-making. *Annu. Rev. Psychol.* 62, 23–48. doi: 10.1146/annurev.psych.121208.131647

Rilling, J. K., Sanfey, A. G., Aronson, J. A., Nystrom, L. E., and Cohen, J. D. (2004). The neural correlates of theory of mind within interpersonal interactions. *Neuroimage* 22, 1694–1703. doi: 10.1016/j.neuroimage.2004.04.015

Sato, W., Kochiyama, T., Uono, S., and Yoshikawa, S. (2010). Amygdala integrates emotional expression and gaze direction in response to dynamic facial expressions. *Neuroimage* 50, 1658–1665. doi: 10.1016/j.neuroimage.2010.01.049

Schurz, M., Radua, J., Aichhorn, M., Richlan, F., and Perner, J. (2014). Fractionating theory of mind: a meta-analysis of functional brain imaging studies. *Neurosci. Biobehav. Rev.* 42, 9–34. doi: 10.1016/j.neubiorev.2014.01.009

Shaw, P., Lawrence, E. J., Radbourne, C., Bramham, J., Polkey, C. E., and David, A. S. (2004). The impact of early and late damage to the human amygdala on 'theory of mind' reasoning. *Brain* 127, 1535–1548. doi: 10.1093/brain/awh168

Shimojo, S., Simion, C., Shimojo, E., and Scheier, C. (2003). Gaze bias both reflects and influences preference. *Nat. Neurosci.* 6, 1317–1322. doi: 10.1038/nn1150

Simon, K. C. N. S., Gómez, R. L., Nadel, L., and Scalf, P. E. (2017). Brain correlates of memory reconsolidation: a role for the TPJ. *Neurobiol. Learn. Mem.* 142, 154–161. doi: 10.1016/j.nlm.2017.03.003

Spezio, M. L., Huang, P. Y. S., Castelli, F., and Adolphs, R. (2007). Amygdala damage impairs eye contact during conversations with real people. *J. Neurosci.* 27, 3994–3997. doi: 10.1523/jneurosci.3789-06.2007

Sun, D., Chan, C. C. H., Fan, J. T., Wu, Y., and Lee, T. M. C. (2015a). Are happy faces attractive? The roles of early vs. late processing. *Front. Psychol.* 6:1812. doi: 10.3389/fpsyg.2015.01812

Sun, D., Chan, C. C. H., Hu, Y., Wang, Z., and Lee, T. M. C. (2015b). Neural correlates of outcome processing post dishonest choice: an fMRI and ERP study. *Neuropsychologia* 68, 148–157. doi: 10.1016/j.neuropsychologia.2015.01.013

Sun, D., Lee, T. M. C., and Chan, C. C. H. (2015c). Unfolding the spatial and temporal neural processing of lying about face familiarity. *Cereb. Cortex* 25, 927–936. doi: 10.1093/cercor/bht284

Sun, D., Lee, T. M. C., Wang, Z. X., and Chan, C. C. H. (2016). Unfolding the spatial and temporal neural processing of making dishonest choices. *PLoS One* 11:e0153660. doi: 10.1371/journal.pone.0153660

Uddin, L. Q., Kelly, A. M. C., Biswal, B. B., Castellanos, F. X., and Milham, M. P. (2009). Functional connectivity of default mode network components: correlation, anticorrelation, and causality. *Hum. Brain Mapp.* 30, 625–637. doi: 10.1002/hbm.20531

von dem Hagen, E. A. H., Stoyanova, R. S., Rowe, J. B., Baron-Cohen, S., and Calder, A. J. (2014). Direct gaze elicits atypical activation of the theory-of-mind network in autism spectrum conditions. *Cereb. Cortex* 24, 1485–1492. doi: 10.1093/cercor/bht003

Weller, D., and Lagattuta, K. H. (2014). Children's judgments about prosocial decisions and emotions: gender of the helper and recipient matters. *Child Dev.* 85, 2011–2028. doi: 10.1111/cdev.12238

Wyk, B. C. V., Hudac, C. M., Carter, E. J., Sobel, D. M., and Pelphrey, K. A. (2009). Action understanding in the superior temporal sulcus region. *Psychol. Sci.* 20, 771–777. doi: 10.1111/j.1467-9280.2009.02359.x

Zhang, H. J., Sun, D., and Lee, T. M. (2012). Impaired social decision making in patients with major depressive disorder. *Brain Behav.* 2, 415–423. doi: 10.1002/brb3.62

Ziaei, M., Burianová, H., Von Hippel, W., Ebner, N. C., Phillips, L. H., and Henry, J. D. (2016). The impact of aging on the neural networks involved in gaze and emotional processing. *Neurobiol. Aging* 48, 182–194. doi: 10.1016/j.neurobiolaging.2016.08.026

Ziaei, M., Ebner, N. C., and Burianová, H. (2017). Functional brain networks involved in gaze and emotional processing. *Eur. J. Neurosci.* 45, 312–320. doi: 10.1111/ejn.13464

**Conflict of Interest Statement**: The authors declare that the research was conducted in the absence of any commercial or financial relationships that could be construed as a potential conflict of interest.

frontiers in Human Neuroscience

ORIGINAL RESEARCH
published: 16 March 2018
doi: 10.3389/fnhum.2018.00070

# Emotion Regulation and Complex Brain Networks: Association Between Expressive Suppression and Efficiency in the Fronto-Parietal Network and Default-Mode Network

*Junhao Pan†, Liying Zhan†, ChuanLin Hu†, Junkai Yang, Cong Wang, Li Gu, Shengqi Zhong, Yingyu Huang, Qian Wu, Xiaolin Xie, Qijin Chen, Hui Zhou, Miner Huang* and Xiang Wu**

*Department of Psychology, Sun Yat-sen University, Guangzhou, China*

Emotion regulation (ER) refers to the "implementation of a conscious or non-conscious goal to start, stop or otherwise modulate the trajectory of an emotion" (Etkin et al., 2015). Whereas multiple brain areas have been found to be involved in ER, relatively little is known about whether and how ER is associated with the global functioning of brain networks. Recent advances in brain connectivity research using graph-theory based analysis have shown that the brain can be organized into complex networks composed of functionally or structurally connected brain areas. Global efficiency is one graphic metric indicating the efficiency of information exchange among brain areas and is utilized to measure global functioning of brain networks. The present study examined the relationship between trait measures of ER (expressive suppression (ES) and cognitive reappraisal (CR)) and global efficiency in resting-state functional brain networks (the whole brain network and ten predefined networks) using structural equation modeling (SEM). The results showed that ES was reliably associated with efficiency in the fronto-parietal network and default-mode network. The finding advances the understanding of neural substrates of ER, revealing the relationship between ES and efficient organization of brain networks.

**Keywords: DMN, emotion regulation, FPN, graph theory, resting-state fMRI**

OPEN ACCESS

***Edited by:***
*Delin Sun,*
*Duke University, United States*

***Reviewed by:***
*Zhen Yuan,*
*University of Macau, China*
*Junling Gao,*
*University of Hong Kong, Hong Kong*

****Correspondence:***
*Miner Huang*
*edshme@mail.sysu.edu.cn*
*Xiang Wu*
*rwfwuwx@gmail.com*

*†These authors have contributed equally to this work.*

***Received:*** *05 December 2017*
***Accepted:*** *07 February 2018*
***Published:*** *16 March 2018*

***Citation:***
*Pan J, Zhan L, Hu C, Yang J, Wang C, Gu L, Zhong S, Huang Y, Wu Q, Xie X, Chen Q, Zhou H, Huang M and Wu X (2018) Emotion Regulation and Complex Brain Networks: Association Between Expressive Suppression and Efficiency in the Fronto-Parietal Network and Default-Mode Network. Front. Hum. Neurosci. 12:70. doi: 10.3389/fnhum.2018.00070*

## INTRODUCTION

Emotion regulation (ER) refers to "the processes that influence which emotions we have, when we have them, and how we experience and express them" (Gross, 1998). People adopt a wide variety of ER strategies, such as situation selection, situation modification, attentional deployment, cognitive change and response modulation (Gross, 1998). In face of the complexity of ER, Gross and John (2003) suggested to focus on a smaller number of well-defined strategies: "Our focus on two specific, well-defined processes is predicated on the belief that our understanding of complex emotion regulatory processes is best advanced if we focus intensively on one or two processes at a time". The two major ER strategies or forms as suggested by Gross and John (2003) are expressive suppression (ES) and cognitive reappraisal (CR).

ES refers to the alteration of one's response to an emotional incident, while CR refers to the change of how one views the emotional incident in order to alter one's feelings. For example, when feeling sad after a heart-broken breakup, one could withhold any sad expression in order to control the intense feelings (i.e., ES); or he/she could persuade himself into thinking that the finished relationship is perhaps actually good for both (i.e., CR). Using ER tasks that typically instruct participants to use the ES or CR strategy when presented with emotionally negative stimuli or adopting the ER questionnaire (ERQ) that was specifically developed to assess the habitual ES and CR usage (Gross and John, 2003), CR has been shown to produce affective, cognitive and social consequences that are more beneficial, whereas ES has been consistently linked to more detrimental consequences such as depressive symptoms (Gross, 2002; Gross and John, 2003; Goldin et al., 2008).

Neural mechanisms of ER have been under investigation using brain-imaging approaches. Task-based functional magnetic resonance imaging (fMRI) studies have shown the involvement of the ventrolateral prefrontal cortex (vlPFC), inferior frontal gyrus (IFG), insula and amygdala in ES (Goldin et al., 2008; Lee et al., 2008) and the engagement of the dorsomedial PFC (dmPFC), dorsolateral PFC (dlPFC), vlPFC, insula, temporal cortex, parietal cortex and amygdala in CR (Kalisch, 2009; Diekhof et al., 2011; Buhle et al., 2014; Gross, 2015). Using the ERQ, studies analyzing gray matter volume and surface thickness have shown that brain structural variations in the ventromedial PFC (vmPFC), dorsal anterior cingulate cortex (dACC), dmPFC, superior frontal gyrus (SFG) and insula are associated with ES (Welborn et al., 2009; Giuliani et al., 2011a; Hermann et al., 2014; Wang et al., 2017), and CR is related to structural variations in the superior frontal cortex (SFC), vmPFC, dACC and amygdala (Welborn et al., 2009; Giuliani et al., 2011b; Hermann et al., 2014; Moore et al., 2016). Moreover, using the ERQ and resting-based fMRI, Wang et al. (2017) found that functional connections between the SFG and regions including the medial PFC (mPFC), precuneus and parahippocampal gyrus were related to ES gender difference.

Previous brain-imaging findings thus suggest the involvement of multiple brain areas in ER and indicate that ER may be related to the functioning of brain networks, which are composed of structurally or functionally connected brain regions (van den Heuvel and Hulshoff Pol, 2010; Smith et al., 2013). Whereas prior studies have investigated functions of individual brain regions in ER, it remains unknown whether and how ER is supported by global functioning of brain networks. To this end, we used global efficiency, one of the graph theory's global metrics, to assess the role of global functioning of brain networks in ER. There has been a growing interest to investigate the structural and functional organization of the brain by graph-theory based analyses, which consider the brain as organized into complex networks consisting of nodes (brain regions) and edges (structural or functional connectivity between regions; Rubinov and Sporns, 2010; De Vico Fallani et al., 2014; Mears and Pollard, 2016). The topological properties of complex networks can be assessed by a variety of measures (for reviews, see Bullmore and Sporns, 2009; Rubinov and Sporns, 2010; Wang et al., 2010; De Vico Fallani et al., 2014), among which network efficiency is considered to be a "more biologically relevant metric" describing networks in terms of information exchange among brain regions (Wang et al., 2010). Network efficiency can be measured by global efficiency and local efficiency at the global and local level, respectively (Wang et al., 2010; De Vico Fallani et al., 2014; Stanley et al., 2015). Note that global efficiency is inversely related to path length and is suggested to be "easier to estimate than path length when studying sparse networks" (Bullmore and Sporns, 2009); and local efficiency is positively associated with clustering coefficient. Given the purpose of investigating global functioning of brain networks, the present study focused on the metric of global efficiency, which is defined as the average inverse shortest path length in the network (Beaty et al., 2016). Global efficiency has been found to be related to cognitive (e.g., intelligence (Li et al., 2009; van den Heuvel et al., 2009), working memory (Alavash et al., 2015; Stanley et al., 2015)) and social (e.g., personality trait (Beaty et al., 2016) functions, as well as mental disorders (e.g., major depressive disorder (Meng et al., 2014), bipolar disorder (Collin et al., 2016), attention deficit/hyperactivity disorder (Wang et al., 2009)).

Global efficiency can be analyzed for the whole brain network (Li et al., 2009; Wang et al., 2009; Meng et al., 2014; Stanley et al., 2015) or subnetworks (Sheffield et al., 2015; Beaty et al., 2016). For subnetworks, research of resting-state functional connectivity has shown that the brain can be organized into networks composed of functionally connected brain regions (van den Heuvel and Hulshoff Pol, 2010; Power et al., 2011; Raichle, 2011; Cole et al., 2013; Smith et al., 2013). In brain connectivity research the brain is usually divided into a set of non-overlapping regions and the definition of brain networks is related to the brain parcellation (note that a validated parcellation strategy is still lacking; Power et al., 2011; Wig et al., 2011). Power et al. (2011) divided the brain into 264 putative regions and showed that 13 networks based on the 264 regions are in good agreement with major functional systems of the brain. Cole et al. (2013) further reduced the 13 networks into 10 networks by excluding two networks with less clear functionality and combing the "hand" and "face" networks based on consensus of a unified primary motor system. The 10 networks based on the 264-region parcellation were the somato-motor network (SMN), cingulo-opercular network (CON), auditory network (Aud.), default mode network (DMN), visual network (Vis.), fronto-parietal network (FPN), salience network (SAN), subcortical network (Sub.), ventral attention network (VAN) and dorsal attention network (DAN); and have been widely adopted in studies investigating relationships between network properties and cognitive functions (Cole et al., 2014b; Thompson and Fransson, 2015; Uddin, 2015; Vatansever et al., 2015; Long et al., 2016). For the major brain areas that have been found to be involved in ER, the lateral PFC is a core region of the FPN (Cole et al., 2013), the media PFC is a key region of the DMN (Buckner et al., 2008; Broyd et al., 2009), and the ACC is an important component of the CON (Power et al., 2011; Sadaghiani and D'Esposito, 2015). Based on the relationships between individual brain areas and ER and the relationships between individual brain areas and networks, it could be indicated that global efficiency in the

FPN, DMN and CON is more likely to be associated with ER. This inference, however, remains to be verified by experimental data and would be difficult to be considered as a strong prior hypothesis. For example, a study examining the Big Five personality traits showed that extraversion and agreeableness were correlated with activities in the midline regions of the DMN and neuroticism, openness and conscientiousness were correlated with activities in the parietal regions of the DMN (Sampaio et al., 2014). However, Beaty et al. (2016) found that only openness was associated with global efficiency in the DMN and suggested that the involvement of a brain region in a cognitive process does not necessarily imply the engagement of global functioning of the network to which that brain region belongs, because individual regions "are related to a wide range of cognitive, behavioral and emotional variables".

Taken together, the present study aimed to examine the relationship between ER and global functioning of brain networks. The ERQ was used to assess trait measures of the two ER strategies, ES and CR (Gross and John, 2003; Wang et al., 2007). Graph theory-based methods were applied to resting-state fMRI data (Bullmore and Sporns, 2009), and global functioning of the whole brain network and the 10 predefined networks (Cole et al., 2013) was examined by analyzing global efficiency. The association between the ER strategies and global efficiency in the brain networks was evaluated using structural equation modeling (SEM) that models error variance separately from true measurement variance (Beaty et al., 2016). We hypothesized that ER would be associated with global functioning of brain networks as indexed by global efficiency. More specifically, we inferred that global efficiency in the FPN, DMN and CON is likely to be associated with ER. In addition to the FPN, DMN and CON, the whole brain network and other networks in the 10 predefined networks were also analyzed, with the purpose of a more comprehensive understanding of the relationship between global efficiency in networks and ER.

# MATERIALS AND METHODS

## Participants

The present study recruited 54 participants from Sun Yat-sen University. Two participants were excluded for excessive motion in the MRI scan and four participants were excluded for missing behavioral data, and finally 48 participants (all right-handed, 13 male, mean age ± SD 22.77 ± 1.59) were included in the subsequent analyses. All participants were healthy and reported no history of neurological or psychiatric disorders, or cognitive or affective impairments. This study was carried out in accordance with the recommendations of research protocol approved by the Institutional Review Board of Psychology Department of Sun Yat-sen University with written informed consent from all subjects. All subjects gave written informed consent in accordance with the Declaration of Helsinki. The protocol was approved by the Institutional Review Board of Psychology Department of Sun Yat-sen University.

## MRI Data Acquisition and Preprocessing

The participants were scanned using a Siemens 3.0 Tesla MRI scanner (Siemens, Erlangen, Germany) located at South China Normal University (Guangzhou, China). Whole brain T2*-weighted resting-state functional images were acquired for 8 min as participants relaxed (stayed awake without thinking anything) with eyes closed, using an echo-planar imaging (EPI) sequence: repetition time (TR) = 2000 ms, echo time (TE) = 30 ms, flip angle (FA) = 90°, field of view (FOV) = 224 × 224 $mm^2$, slices = 32, matrix = 64 × 64, slice thickness = 3.5 mm, voxel size = 3.5 × 3.5 × 3.5 $mm^3$, 240 volumes, and interleaved slice ordering. Whole brain T1-weighted structural images were obtained in a sagittal orientation using the magnetization-prepared rapid gradient-echo (MPRAGE) sequence: TR = 2300 ms, TE = 3.24 ms, FA = 9°, FOV = 256 × 256 $mm^2$, inversion time = 900 ms, matrix = 256 × 256, slices = 176, slice thickness = 1 mm, and voxel size = 1 × 1 × 1 $mm^3$.

The data were preprocessed using Statistical Parametric Mapping (SPM12[1]) and Data Processing Assistant for Resting-State fMRI (DPARSF; Yang and Zang, 2010). Preprocessing consisted of standard resting-state functional connectivity preprocessing procedures as implemented in DPARSF, including removing the first 10 volumes of functional images, slice timing correction, motion correction (data of two participants were excluded under the criterion of 2 mm displacement or 2° rotation in any direction), coregistration of structure images to functional images, segmentation with the DARTEL method (Ashburner, 2007), normalization to the standard MNI space with the DARTEL method and resampling functional images at a voxel size of 3 × 3 × 3 $mm^3$, removing linear trends, regressing out nuisance variables (head motion parameters, white matter signals, and cerebrospinal fluid signals), filtering (0.01–0.1 Hz), and spatial smoothing (4-mm FHWM). Following previous work analyzing functional connectivity using graphic approaches (Zhao et al., 2012; Cole et al., 2013; Arnold et al., 2014; Santarnecchi et al., 2014; Beaty et al., 2016), in the present study whole brain signal was not regressed out as a nuisance variable because of the current controversy over global signal regression (Murphy et al., 2009) and the potential impact of global signal removal on topological properties of brain networks (Santarnecchi et al., 2014).

## Network Construction and Graphic Analyses

Graph analyses were conducted using graph theoretical network analysis (GRETNA; Wang et al., 2015). The present study adopted the 10 predefined networks based on the parcellation of the brain with 264 cortical and subcortical 10-mm diameter spherical regions (for detailed information, see Power et al., 2011; Cole et al., 2013). For each of the 10 networks in each participant's dataset, regional time series were calculated by averaging voxel time series in each of the N regions in that network, and a N × N functional connectivity matrix

[1]http://www.fil.ion.ucl.ac.uk/spm

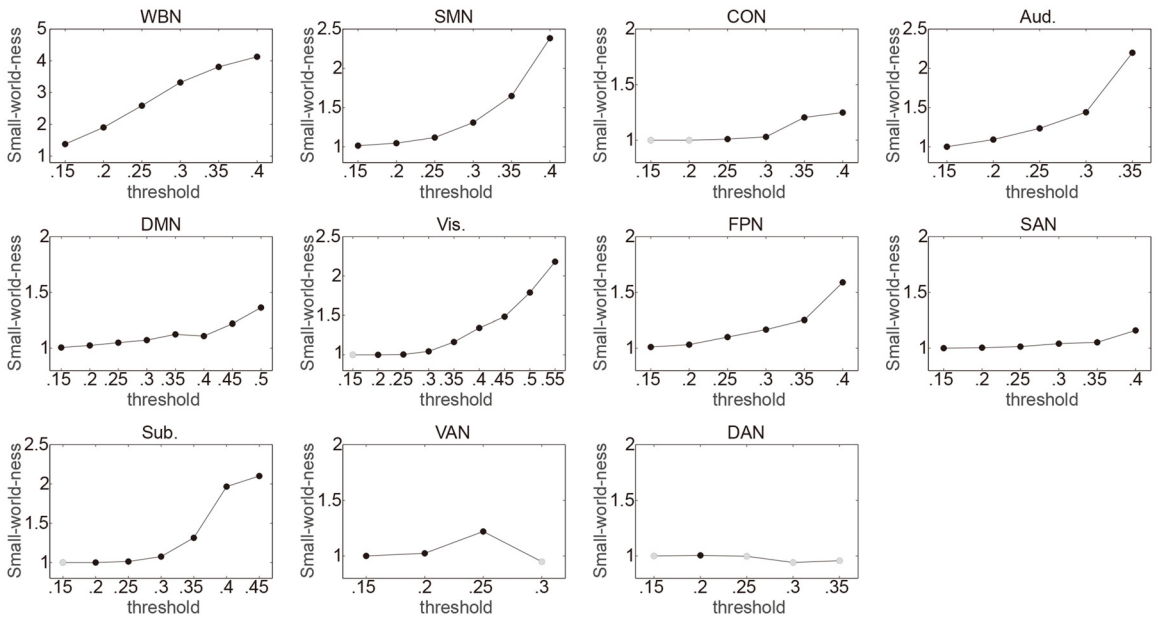


**FIGURE 1 |** Illustrating the small-world-ness of networks under different thresholds. Whole brain network (WBN), somato-motor network (SMN), cingulo-opercular network (CON), auditory network (Aud.), default mode network (DMN), visual network (Vis.), frontoparietal network (FPN), salience network (SAN), subcortical network (Sub.), ventral attention network (VAN) and dorsal attention network (DAN) represent the WBN, SMN, CON, Aud., DMN, Vis., FPN, SAN, Sub., VAN and DAN, respectively. For each threshold (Fisher transformed *r* ranging from 0.15 to 0.85 in 0.05 steps; totally 15 thresholds), it was first evaluated whether small word property of a network was estimable. The thresholds at which small word property of the network was not estimable were not included in following analyses and are not presented in the figure. The small-word-ness (σ) was then calculated with $\sigma > 1$ indicating that a network exhibits small-world property. The thresholds at which $\sigma > 1$ are indicated by black circles, and the thresholds at which $\sigma \leq 1$ are indicated by gray circles and were not included in following analyses.

was constructed by computing the Pearson correlation (with Fisher transformation) between each pair of regional time series of the N regions. The brain regions represented network nodes and the correlations between nodes represented network edges. The adjacency matrix was then computed from the correlation matrix by applying a threshold, which resulted in the binary undirected graph. Note that different thresholds would generate graphs of different connection density or sparsity, and network properties are suggested to be examined over a wide range of thresholds since currently there is no "good" threshold for graphic analysis (Bullmore and Sporns, 2009; Langer et al., 2012; Power et al., 2013). Therefore network

**TABLE 1 |** Connection density.

| Threshold | WBN (264) | SMN (35) | CON (14) | Aud. (13) | DMN (58) | Vis. (31) | FPN (25) | SAN (18) | Sub. (13) | VAN (9) | DAN (11) |
|---|---|---|---|---|---|---|---|---|---|---|---|
| 0.15 | 52.97 | 67.67 | N\A | 70.25 | 72.10 | N\A | 72.10 | 73.76 | N\A | 70.66 | N\A |
| 0.2 | 40.60 | 57.90 | N\A | 59.56 | 63.06 | 75.23 | 63.03 | 64.50 | 78.90 | 61.81 | 65.19 |
| 0.25 | 30.43 | 49.04 | 61.77 | 50.40 | 54.42 | 68.01 | 54.40 | 55.07 | 70.14 | 51.56 | N\A |
| 0.3 | 22.40 | 41.11 | 53.64 | 41.03 | 46.13 | 60.77 | 46.02 | 46.53 | 60.92 | N\A | N\A |
| 0.35 | 16.25 | 34.07 | 45.26 | 33.31 | 38.59 | 53.04 | 38.30 | 38.45 | 51.47 | N\A | N\A |
| 0.4 | 11.61 | 27.80 | 37.29 | N\A | 31.53 | 45.30 | 30.85 | 31.37 | 42.52 | N\A | N\A |
| 0.45 | N\A | N\A | N\A | N\A | 25.24 | 37.86 | N\A | N\A | 33.79 | N\A | N\A |
| 0.5 | N\A | N\A | N\A | N\A | 19.93 | 31.25 | N\A | N\A | N\A | N\A | N\A |
| 0.55 | N\A | N\A | N\A | N\A | N\A | 25.66 | N\A | N\A | N\A | N\A | N\A |
| 0.6 | N\A | N\A | N\A | N\A | N\A | N\A | N\A | N\A | N\A | N\A | N\A |
| 0.65 | N\A | N\A | N\A | N\A | N\A | N\A | N\A | N\A | N\A | N\A | N\A |
| 0.7 | N\A | N\A | N\A | N\A | N\A | N\A | N\A | N\A | N\A | N\A | N\A |
| 0.75 | N\A | N\A | N\A | N\A | N\A | N\A | N\A | N\A | N\A | N\A | N\A |
| 0.8 | N\A | N\A | N\A | N\A | N\A | N\A | N\A | N\A | N\A | N\A | N\A |
| 0.85 | N\A | N\A | N\A | N\A | N\A | N\A | N\A | N\A | N\A | N\A | N\A |

*Average connection density (%; i.e., actual number of edges in a graph relative to the total number of possible edges) across participants is listed for all networks at all thresholds (Fisher transformed r). The number of regions in a network is indicated below each network name. Note that the thresholds at which small word property of a network was not estimable and was not presented were not included in the following analyses and are marked by N\A (see* ***Figure 1****). Other conventions are as in* ***Figure 1****.*

thresholding in the present study used Fisher transformed $r$ values ranging from 0.15 to 0.85 (Achard et al., 2006; He et al., 2007; Langer et al., 2012; Arnold et al., 2014; Santarnecchi et al., 2014), with the aim of a more comprehensive analysis. Moreover, whether a network would have the property of the small world was evaluated for each threshold. The small-world topology is characterized through the characteristic path length $L$ and clustering coefficient $C$ (Watts and Strogatz, 1998). The characteristic path length is defined as the average of the shortest path lengths between any pair of nodes in the network. The clustering coefficient is defined as the average of the clustering coefficients over all nodes, where the clustering coefficient of a node is defined as the proportion of possible connections that actually exist between the nearest neighbors of a node. Compared with random networks that have the same number of nodes, same mean degree and same degree distribution as the real network (e.g., brain network) of interest, if the real network has higher clustering coefficient and similar characteristic path length (i.e., $\gamma = C_{net}/C_{ran} > 1$, $\lambda = L_{net}/L_{ran} \sim 1$, with $C_{net}$ and $L_{net}$ indicating the clustering coefficient and characteristic path length of the real network, respectively, and $C_{ran}$ and $L_{ran}$ indicating the clustering coefficient and characteristic path length of the random network, respectively), the real network would be considered as a small world (Watts and Strogatz, 1998). The ratio between the two parameters $\gamma$ and $\lambda$ ($\gamma/\lambda$) can be defined as a parameter $\sigma$ to measure the small-word-ness, with $\sigma > 1$ indicating that a network exhibits small-world property (Humphries et al., 2006). Moreover, before calculating the small-world-ness, it is recommended to first evaluate whether small word property of a network is estimable, which is indicated when the mean degree (k) of the network is larger than the log of the number (n) of the network's nodes (i.e., $k > \log(n)$; Watts and Strogatz, 1998). Note that small-world property tends to be not estimable for higher thresholds. This is because as the threshold increases, more weak connections will be removed from the network and the network will become sparser. As a result, the mean degree will decrease and is more likely to be less than the log of the number of the network's nodes (Watts and Strogatz, 1998; Achard et al., 2006; He et al., 2007). In the present study investigating brain networks, for each of the whole brain network and the 10 predefined networks, following the procedure described by Jäncke and Langer (2011) and Langer et al. (2012), the correlation matrices of all participants were first averaged to obtain an average correlation matrix and the corresponding adjacency matrix was calculated. Then for each threshold, whether small word property of a network is estimable was evaluated, and the small-word-ness ($\sigma$) was calculated. Note that the following analyses only included the thresholds at which small word property of a network was estimable (i.e., $k > \log(n)$) and

**TABLE 2 |** Association between expressive suppression (ES) and network global efficiency.

| Threshold | WBN (264) | SMN (35) | CON (14) | Aud.(13) | DMN (58) | Vis. (31) | FPN (25) | SAN (18) | Sub. (13) | VAN (9) | DAN (11) |
|---|---|---|---|---|---|---|---|---|---|---|---|
| 0.15 | −0.257 | 0.110 | N\A | −0.343 | −0.427 | N\A | −0.357 | −0.269 | N\A | −0.229 | N\A |
| | 0.09 | >0.50 | N\A | 0.03 | 0.05 | N\A | 0.04 | >0.50 | N\A | >0.50 | N\A |
| 0.2 | −0.249 | 0.008 | N\A | −0.349 | −0.436 | −0.127 | −0.342 | −0.293 | −0.067 | −0.129 | 0.128 |
| | 0.09 | >0.50 | N\A | 0.06 | 0.04 | >0.50 | 0.06 | >0.50 | >0.50 | >0.50 | >0.50 |
| 0.25 | −0.241 | 0.058 | −0.223 | −0.350 | −0.418 | −0.141 | −0.395 | −0.253 | −0.066 | −0.061 | N\A |
| | 0.10 | >0.50 | >0.50 | 0.11 | 0.06 | >0.50 | 0.01 | >0.50 | >0.50 | >0.50 | N\A |
| 0.3 | −0.235 | 0.072 | −0.278 | −0.369 | −0.423 | −0.134 | −0.355 | −0.335 | −0.106 | N\A | N\A |
| | 0.11 | >0.50 | >0.50 | 0.06 | 0.07 | >0.50 | 0.03 | 0.17 | >0.50 | N\A | N\A |
| 0.35 | −0.233 | 0.114 | −0.277 | −0.265 | −0.404 | −0.155 | −0.421 | −0.302 | −0.239 | N\A | N\A |
| | 0.13 | >0.50 | >0.50 | 0.34 | 0.12 | >0.50 | 0.00 | 0.38 | >0.50 | N\A | N\A |
| 0.4 | −0.228 | 0.065 | −0.255 | N\A | −0.399 | −0.127 | −0.467 | −0.325 | −0.189 | N\A | N\A |
| | 0.14 | >0.50 | >0.50 | N\A | 0.14 | >0.50 | 0.00 | 0.28 | >0.50 | N\A | N\A |
| 0.45 | N\A | N\A | N\A | N\A | −0.357 | −0.144 | N\A | N\A | −0.196 | N\A | N\A |
| | N\A | N\A | N\A | N\A | 0.29 | >0.50 | N\A | N\A | >0.50 | N\A | N\A |
| 0.5 | N\A | N\A | N\A | N\A | −0.348 | −0.147 | N\A | N\A | N\A | N\A | N\A |
| | N\A | N\A | N\A | N\A | >0.50 | >0.50 | N\A | N\A | N\A | N\A | N\A |
| 0.55 | N\A | N\A | N\A | N\A | N\A | −0.141 | N\A | N\A | N\A | N\A | N\A |
| | N\A | N\A | N\A | N\A | N\A | >0.50 | N\A | N\A | N\A | N\A | N\A |
| 0.6 | N\A | N\A | N\A | N\A | N\A | N\A | N\A | N\A | N\A | N\A | N\A |
| | N\A | N\A | N\A | N\A | N\A | N\A | N\A | N\A | N\A | N\A | N\A |
| 0.65 | N\A | N\A | N\A | N\A | N\A | N\A | N\A | N\A | N\A | N\A | N\A |
| | N\A | N\A | N\A | N\A | N\A | N\A | N\A | N\A | N\A | N\A | N\A |
| 0.7 | N\A | N\A | N\A | N\A | N\A | N\A | N\A | N\A | N\A | N\A | N\A |
| | N\A | N\A | N\A | N\A | N\A | N\A | N\A | N\A | N\A | N\A | N\A |
| 0.75 | N\A | N\A | N\A | N\A | N\A | N\A | N\A | N\A | N\A | N\A | N\A |
| | N\A | N\A | N\A | N\A | N\A | N\A | N\A | N\A | N\A | N\A | N\A |
| 0.8 | N\A | N\A | N\A | N\A | N\A | N\A | N\A | N\A | N\A | N\A | N\A |
| | N\A | N\A | N\A | N\A | N\A | N\A | N\A | N\A | N\A | N\A | N\A |
| 0.85 | N\A | N\A | N\A | N\A | N\A | N\A | N\A | N\A | N\A | N\A | N\A |
| | N\A | N\A | N\A | N\A | N\A | N\A | N\A | N\A | N\A | N\A | N\A |

*For each network at each threshold, association $\beta$ value (up row in a data cell) and corrected p value (Bonferroni corrected for the 10 networks, bottom row in a data cell) are presented. Associations with $p_{corrected}$ values $\leq 0.05$ are marked with the red color and associations with $p_{corrected}$ values $\leq 0.1$ are marked with the orange color. Other conventions are as in* ***Table 1****.*

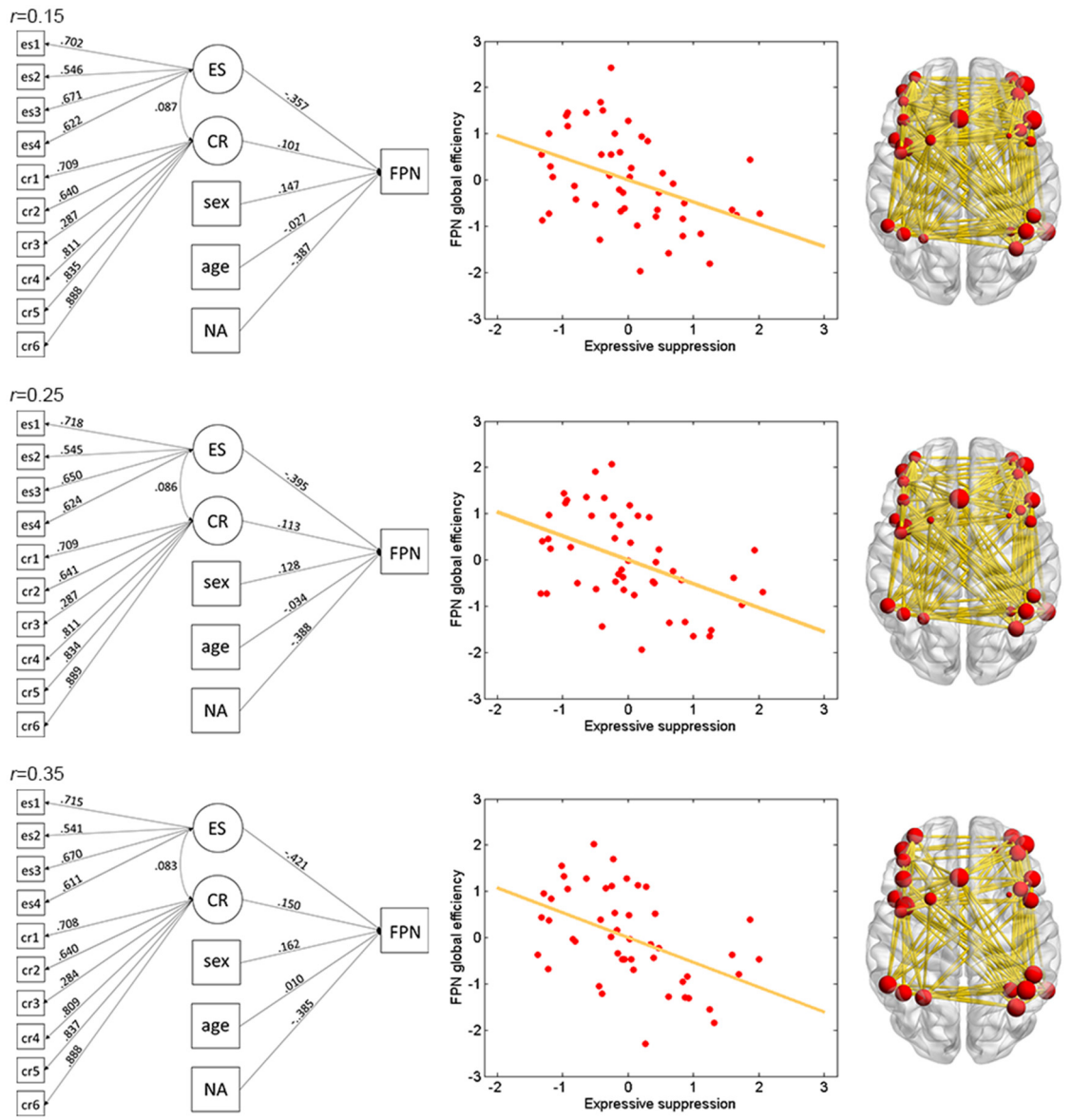


**FIGURE 2 |** Illustration of association between expressive suppression (ES) and global efficiency in the FPN. Shown are the results for thresholds 0.15 (top row), 0.25 (middle row) and 0.35 (bottom row). For each threshold, structural equation modeling (SEM) is presented on the left, which shows effects of the latent emotion regulation (ER) variables on FPN efficiency. es1–4 refer to the four questionnaire items for ES and cr1–6 refer to the six questionnaire items for cognitive reappraisal (CR). The paths are standardized coefficients. NA indicates negative affect. Scatter plot of the association between latent ES and FPN efficiency is presented in the middle. Note that all variables were standardized by Z-transformation. Nodes and edges that were used to define FPN are presented on the right for a representative participant (the size of nodes represents the degree). Other conventions are as in **Table 2**.

existed ($\sigma > 1$). After that, global efficiency was calculated for each network at each threshold for each participant, which was mathematically expressed as the inverse of the average shortest path length in the network (Wang et al., 2010; Beaty et al., 2016).

## Behavioral Assessment

Participants completed a Chinese version of the ERQ (Gross and John, 2003; Wang et al., 2007). The Chinese version of ERQ has satisfactory internal consistency and test-retest reliability (Wang et al., 2007). The ERQ had 10 items, with four items measuring ES and the other six items measuring CR. An example item for ES was: "I control my emotions by not expressing them"; and an example item for CR was "When I want to feel more positive emotion (such as joy or amusement), I change what I'm thinking about". Participants answered to these items on a 1-to-7 Linkert scale ("1" = "strongly disagree"; "7" = "strongly agree"), to indicate their habitual

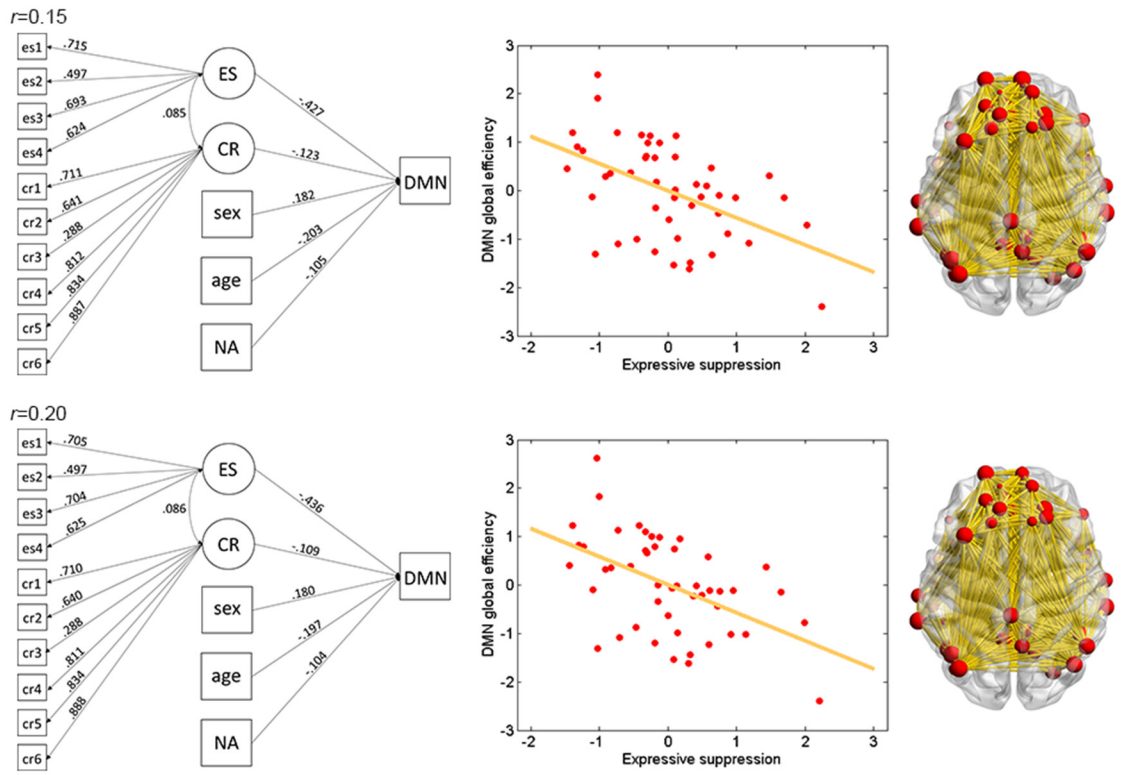


**FIGURE 3 |** Illustration of association between ES and global efficiency in the DMN. Results for thresholds 0.15 (top row) and 0.2 (bottom row) are shown. Other conventions are as in **Figure 2**.

use of these two ER strategies. Participants further completed a Chinese version of negative affect (NA) subscale of the Positive and NA Schedule (PANAS; Watson et al., 1988; Qiu et al., 2008). The Chinese version of NA subscale had nine items, and participants indicated their general frequency of negative mood states on a 1-to-5 Likert scale ("1" = "not at all", "5" = "extremely").

## Structural Equation Modeling (SEM)

The relationship between trait measures of ER (ES/CR) and global efficiency of a network was examined using SEM, which used latent variables to model error variance separately from true measurement variance (Skrondal and Rabe-Hesketh, 2004; Beaty et al., 2016; Figure 1A). ES and CR were formed as latent variables by specifying their corresponding questionnaire items (four items for ES and six items for CR) as indicators. Age and gender were modeled as observed variables. Note that in order to control for NA, the NA score was also modeled as an observed variable (Giuliani et al., 2011a,b). The analyses without controlling for the NA score are presented in the Supplementary Materials (see "Analyses without modeling the NA score as an observed variable", Supplementary Tables S1, S2). Standardized regression coefficients were reported. SEM analyses were conducted with Mplus 8 using maximum likelihood robust estimation.

# RESULTS

The mean scores of the two subscales of ERQ were: 2.92 (SD = 1.02) for ES and 4.99 (SD = 0.89) for CR. Consistent with previous results, the ES and CR scores did not statistically correlate with each other ($r = 0.037$, $p > 0.05$), and the internal consistency was acceptable (Cronbach's α was 0.73 and 0.86 for ES and CR, respectively; Gross and John, 2003; Kühn et al., 2011; Picó-Pérez et al., 2017). The mean score of the NA subscale was 19.88 (SD = 5.28). Consistent with previous reports (Giuliani et al., 2011a,b), the NA score did not correlate with the ES score ($r = 0.14$, $p = 0.32$) or the CR score ($r = 0.018$, $p = 0.90$), and no NA outlier (>3 SD) was found.

The relationship between ES/CR and global efficiency of each of the whole brain network and the 10 networks was examined using SEM over the 15 network thresholds. In sum, the data fit the model well regarding the model fit indices, e.g., comparative fit index (CFI), Tucker–Lewis index (TLI), root mean square error of approximation (RMSEA) and standardized root mean square residual (SRMR; Hu and Bentler, 1998; Brown, 2006; see "Supplementary description of SEM" in the Supplementary Materials for further details of the SEM method), providing support for the proposed theoretical models. Whether a network would have small world property was first evaluated for each threshold, and the following analyses only included

the thresholds at which small word property of the network was estimable (i.e., $k > \log(n)$) and was presented ($\sigma > 1$; see the "Materials and Methods" section for details). In general, consistent with previous findings (Watts and Strogatz, 1998; Achard et al., 2006; He et al., 2007), networks lacked small word property for higher thresholds (**Figure 1**). Connection density was assessed and listed in **Table 1**. Global efficiency distributions under different thresholds are listed for all networks in Supplementary Figure S1.

The results of ES are listed in **Table 2**. Note that it has been suggested to examine network properties over a wide range of thresholds since currently there is no "good" threshold for graphic analysis, and findings observed across a range of thresholds (in contrast to those occasionally observed at only a single or a few thresholds) would be considered more reliable (Stam et al., 2006; Bullmore and Sporns, 2009; van den Heuvel et al., 2009; Langer et al., 2012; Power et al., 2013; Xu et al., 2015). In the present results the most reliable association was found between ES and FPN, which was statistically significant ($p_{corrected} < 0.05$, corrected for 10 networks using Bonferroni correction) for thresholds from 0.15 to 0.4 (although marginally significant at threshold 0.2; **Table 2** and **Figure 2**). The association between ES and DMN would also be considered reliable, which was statistically significant ($p_{corrected} < 0.05$) for thresholds 0.15 and 0.2 and was marginally significant for thresholds 0.25 and 0.3 (**Table 2** and **Figure 3**). Moreover, ES was statistically ($p_{corrected} < 0.05$) associated with Aud. at threshold 0.15 (the association was marginally significant for thresholds 0.2 and 0.3) and was marginally associated with the whole brain network at thresholds 0.15, 0.2 and 0.25; which may not be as reliable as the associations between ES and FPN and between ES and DMN.

The results of CR are listed in **Table 3**. In contrast to ES results in which reliable associations across thresholds were found for the FPN and DMN (and less reliable associations for the Aud. and the whole brain network), CR was not statistically associated with efficiency in any network at any threshold.

## DISCUSSION

The present study examined the relationship between trait measures of ER (ES and CR) and global efficiency in resting-state brain networks (the whole brain network and 10 predefined networks) using SEM over 15 network thresholds (although in general networks lacked small word property for higher thresholds). The results showed that ES was reliably associated with efficiency in the fronto-parietal network (FPN) and default-mode network (DMN).

The FPN includes primarily portions of the frontal cortex and parietal cortex, in which the lateral PFC is a core region (Vincent et al., 2008; Dodds et al., 2011; Cole et al., 2013; Smith et al., 2013). The lateral PFC is an essential brain area for flexible control of

**TABLE 3 |** Association between cognitive reappraisal (CR) and network global efficiency.

| Threshold | WBN (264) | SMN (35) | CON (14) | Aud. (13) | DMN (58) | Vis. (31) | FPN (25) | SAN (18) | Sub. (13) | VAN (9) | DAN (11) |
|---|---|---|---|---|---|---|---|---|---|---|---|
| 0.15 | −0.090 | −0.236 | N\A | −0.225 | −0.123 | N\A | 0.101 | 0.058 | N\A | −0.116 | N\A |
| | >0.50 | >0.50 | N\A | >0.50 | >0.50 | N\A | >0.50 | >0.50 | N\A | >0.50 | N\A |
| 0.2 | −0.098 | −0.021 | N\A | −0.185 | −0.109 | −0.001 | 0.090 | 0.077 | 0.053 | −0.125 | 0.173 |
| | >0.50 | >0.50 | N\A | >0.50 | >0.50 | >0.50 | >0.50 | >0.50 | >0.50 | >0.50 | >0.50 |
| 0.25 | −0.110 | −0.239 | 0.013 | −0.117 | −0.134 | −0.017 | 0.113 | 0.007 | 0.100 | −0.198 | N\A |
| | 0.48 | 0.44 | >0.50 | >0.50 | >0.50 | >0.50 | >0.50 | >0.50 | >0.50 | >0.50 | N\A |
| 0.3 | −0.110 | −0.276 | 0.014 | −0.064 | −0.156 | −0.031 | 0.158 | −0.027 | 0.025 | N\A | N\A |
| | 0.47 | 0.23 | >0.50 | >0.50 | >0.50 | >0.50 | >0.50 | >0.50 | >0.50 | N\A | N\A |
| 0.35 | −0.114 | −0.231 | −0.004 | −0.144 | −0.190 | −0.041 | 0.150 | 0.015 | −0.060 | N\A | N\A |
| | 0.43 | 0.48 | >0.50 | >0.50 | >0.50 | >0.50 | >0.50 | >0.50 | >0.50 | N\A | N\A |
| 0.4 | −0.120 | −0.271 | 0.014 | N\A | −0.179 | −0.043 | 0.144 | 0.072 | 0.022 | N\A | N\A |
| | 0.39 | 0.22 | >0.50 | N\A | >0.50 | >0.50 | >0.50 | >0.50 | >0.50 | N\A | N\A |
| 0.45 | N\A | N\A | N\A | N\A | −0.217 | −0.055 | N\A | N\A | −0.056 | N\A | N\A |
| | N\A | N\A | N\A | N\A | 0.50 | >0.50 | N\A | N\A | >0.50 | N\A | N\A |
| 0.5 | N\A | N\A | N\A | N\A | −0.193 | −0.041 | N\A | N\A | N\A | N\A | N\A |
| | N\A | N\A | N\A | N\A | >0.50 | >0.50 | N\A | N\A | N\A | N\A | N\A |
| 0.55 | N\A | N\A | N\A | N\A | N\A | −0.052 | N\A | N\A | N\A | N\A | N\A |
| | N\A | N\A | N\A | N\A | N\A | >0.50 | N\A | N\A | N\A | N\A | N\A |
| 0.6 | N\A | N\A | N\A | N\A | N\A | N\A | N\A | N\A | N\A | N\A | N\A |
| | N\A | N\A | N\A | N\A | N\A | N\A | N\A | N\A | N\A | N\A | N\A |
| 0.65 | N\A | N\A | N\A | N\A | N\A | N\A | N\A | N\A | N\A | N\A | N\A |
| | N\A | N\A | N\A | N\A | N\A | N\A | N\A | N\A | N\A | N\A | N\A |
| 0.7 | N\A | N\A | N\A | N\A | N\A | N\A | N\A | N\A | N\A | N\A | N\A |
| | N\A | N\A | N\A | N\A | N\A | N\A | N\A | N\A | N\A | N\A | N\A |
| 0.75 | N\A | N\A | N\A | N\A | N\A | N\A | N\A | N\A | N\A | N\A | N\A |
| | N\A | N\A | N\A | N\A | N\A | N\A | N\A | N\A | N\A | N\A | N\A |
| 0.8 | N\A | N\A | N\A | N\A | N\A | N\A | N\A | N\A | N\A | N\A | N\A |
| | N\A | N\A | N\A | N\A | N\A | N\A | N\A | N\A | N\A | N\A | N\A |
| 0.85 | N\A | N\A | N\A | N\A | N\A | N\A | N\A | N\A | N\A | N\A | N\A |
| | N\A | N\A | N\A | N\A | N\A | N\A | N\A | N\A | N\A | N\A | N\A |

*Conventions are as in* ***Table 2****.*

thoughts and actions (MacDonald et al., 2000; Kerns et al., 2004; Egner and Hirsch, 2005) and is involved in various cognitive control tasks (for reviews, see Matsumoto and Tanaka, 2004; Badre and D'Esposito, 2009). The FPN has been shown to be related to task control processes (Dodds et al., 2011; Power et al., 2011; Cole et al., 2013, 2014b). The involvement of the lateral PFC in ES as shown in previous studies (Goldin et al., 2008) would be in line with the current finding of the association between ES and efficiency in the FPN. The DMN comprises majorly the media PFC, posterior cingulate cortex (PCC) and inferior parietal cortex (Buckner et al., 2008; Broyd et al., 2009; Power et al., 2011). The DMN was initially observed when participants are not focused on an specific task (e.g., in a resting state) and following studies have suggested that the DMN is related to a wide range of spontaneous and self-generated processes, such as episodic future thinking, autobiographical memory processing, mind wandering and thinking about others (Anticevic et al., 2012; Andrews-Hanna et al., 2014; Fox et al., 2015; Hamilton et al., 2015; Stawarczyk and D'Argembeau, 2015). Note that it has been suggested that the DMN is associated with reflecting about one's own emotional state, and understanding others' emotions (Andrews-Hanna, 2012; Andrews-Hanna et al., 2014). As a key region of the DMN, the media PFC has been found to be engaged in ES (Goldin et al., 2008; Welborn et al., 2009), which would be in agreement with the present finding of the association between ES and efficiency in the DMN. Combining these findings, it could be possible that for ES, efficiency in the DMN is related to emotional processing of an incident and efficiency in the FPN is associated with control of emotional responses. Furthermore, it was worth noting that an association between ES and efficiency in the CON was not observed, given dACC volume has been found to be related to ES (Dosenbach et al., 2007; Power et al., 2011; Hermann et al., 2014). This, in line with previous results (Sampaio et al., 2014; Beaty et al., 2016), could indicate that global functioning of a brain network may not be engaged in a cognitive process even when a brain region within the network is related to the process. Moreover, the present study systematically explored the whole brain network and 10 predefined networks and ES showed less reliable association with the Aud., which would require further investigation.

The ERQ assesses the habitual ES and CR usage: the more frequent one utilizes ES/CR to regulate his/her emotions, the higher this person will score on the ES/CR scale; and vice versa (Gross and John, 2003). In previous brain structural studies using the ERQ, positive relationships between ES and brain region volumes were often reported (Giuliani et al., 2011a; Kühn et al., 2011; Hermann et al., 2014; Wang et al., 2017); whereas Welborn et al. (2009) did not observe such positive associations but rather found a negative relationship between the vmPFC volume and ES. It has been suggested that the discrepancies among results of different studies could be due to different methodological factors such as whole-brain vs. ROI analysis (Hermann et al., 2014) and voxel- vs. surface-based analysis (Moore et al., 2016). For the current analyses of global functioning of brain networks, ES was negatively associated with efficiency in the FPN and DMN (the association with the Aud. was less reliable). Global efficiency in the whole brain networks has been found negatively associated with some mental disorders (Wang et al., 2009; Meng et al., 2014; Collin et al., 2016), such as major depressive disorder (Meng et al., 2014); and notably, ES has been consistently connected to negative affective and social consequences, including depressive symptoms (Gross, 2002). This could be one plausible clue for the currently observed negative association between ES and network efficiency.

Moreover, association between CR and efficiency in a network was not observed. While the lack of CR association was unexpected, it appeared to be in agreement with a report showing that CR usage as measured with the ERQ was associated with fewer brain regions as compared to ES usage; while ES was found to be related to multiple brain regions including the vmPFC, dmPFC and dACC, CR was only associated with the amygdala (Hermann et al., 2014). The discrepancies in structural (Hermann et al., 2014) and functional network (as in the present study) properties between ES and CR usages require to be further clarified.

The present study would be considered as a preliminary attempt to investigate the relationship between ER and complex brain networks and has many limitations. Besides the limitations as discussed above, the topological properties of complex networks can be assessed by a wide variety of measures (Bullmore and Sporns, 2009; Rubinov and Sporns, 2010; Wang et al., 2010; De Vico Fallani et al., 2014). While the present study focused on the global metric of global efficiency, the topological properties of complex networks would be investigated comprehensively in future ER studies. In particular, roles of individual nodes (regions) in ER remain to be addressed by using metrics such as centrality. Accordingly, the currently adopted 10 predefined brain networks were defined based on 264 putative brain regions. While the 264-region parcellation and the 10 networks are helpful for investigation of network properties in general, investigation of emotion-related functions would require further work. Particularly, an emotion-related network is not defined and amygdala -a key area in emotion processing- is not specifically defined (Power et al., 2011; Cole et al., 2013). Future research could define the region of interest (ROI) of the amygdala structurally or functionally (Poldrack, 2007) and define an emotion-related network by calculating correlation between the amygdala ROI with all other voxels in the brain (van den Heuvel and Hulshoff Pol, 2010). Then topological properties of the emotion-related network could be calculated and their relationships with ER could be examined.

In sum, ER is essential for human adaptive functioning (Gross, 1998; Ochsner and Gross, 2005). Whereas previous brain-imaging studies have investigated functions of individual brain areas in ER, the role of global functioning of brain networks remains unknown. The present finding of the association of ES with global efficiency in the FPN and DMN suggests that efficient organization of specific brain networks is a fundamental neural mechanism for ER. Meanwhile, whereas the results of current graphic analyses of resting-state functional networks showed consistency with the regional results from previous task-based fMRI and structural MRI studies (e.g., association between ES and areas in the FPN and DMN), discrepancies in the results were also revealed and would be addressed in future research (e.g.,

lack of association between ES and efficiency in the CON, lack of association between CR and network efficiency). Therefore, while the present findings suggest the important role of global functioning of brain networks in ER, it is also indicated that combining different research approaches is required for a better understanding of neural mechanisms underlying ER.

## DATA AVAILABILITY

The data generated during and/or analyzed during the current study are available from the corresponding author on reasonable request.

## AUTHOR CONTRIBUTIONS

LZ, CH, MH and XW designed the research. SZ, LG, JY and YH collected MRI data. LZ, CW, JY and QW analyzed MRI data. CH, XX, QC and HZ collected questionnaire data. CH analyzed questionnaire data. JP and LZ performed SEM analysis. JP, LZ, CH, MH and XW wrote the manuscript. All authors commented on the manuscript.

## ACKNOWLEDGMENTS

This work was supported by National Natural Science Foundation of China (31371129) and Research Project of Sun Yat-sen University (26000-31620003). We thank Zhengjia Dai for the discussion of MRI data acquisition and analysis.

## SUPPLEMENTARY MATERIAL

The Supplementary Material for this article can be found online at: https://www.frontiersin.org/articles/10.3389/fnhum.2018.00070/full#supplementary-material

## REFERENCES

Achard, S., Salvador, R., Whitcher, B., Suckling, J., and Bullmore, E. (2006). A resilient, low-frequency, small-world human brain functional network with highly connected association cortical hubs. *J. Neurosci.* 26, 63–72. doi: 10.1523/JNEUROSCI.3874-05.2006

Alavash, M., Doebler, P., Holling, H., Thiel, C. M., and Gießing, C. (2015). Is functional integration of resting state brain networks an unspecific biomarker for working memory performance? *Neuroimage* 108, 182–193. doi: 10.1016/j.neuroimage.2014.12.046

Andrews-Hanna, J. R. (2012). The brain's default network and its adaptive role in internal mentation. *Neuroscientist* 18, 251–270. doi: 10.1177/1073858411403316

Andrews-Hanna, J. R., Smallwood, J., and Spreng, R. N. (2014). The default network and self-generated thought: component processes, dynamic control, and clinical relevance: the brain's default network. *Ann. N Y Acad. Sci.* 1316, 29–52. doi: 10.1111/nyas.12360

Anticevic, A., Cole, M. W., Murray, J. D., Corlett, P. R., Wang, X.-J., and Krystal, J. H. (2012). The role of default network deactivation in cognition and disease. *Trends Cogn. Sci.* 16, 584–592. doi: 10.1016/j.tics.2012.10.008

Arnold, A. E. G. F., Protzner, A. B., Bray, S., Levy, R. M., and Iaria, G. (2014). Neural network configuration and efficiency underlies individual differences in spatial orientation ability. *J. Cogn. Neurosci.* 26, 380–394. doi: 10.1162/jocn_a_00491

Ashburner, J. (2007). A fast diffeomorphic image registration algorithm. *Neuroimage* 38, 95–113. doi: 10.1016/j.neuroimage.2007.07.007

Badre, D., and D'Esposito, M. (2009). Is the rostro-caudal axis of the frontal lobe hierarchical? *Nat. Rev. Neurosci.* 10, 659–669. doi: 10.1038/nrn2667

Beaty, R. E., Kaufman, S. B., Benedek, M., Jung, R. E., Kenett, Y. N., Jauk, E., et al. (2016). Personality and complex brain networks: the role of openness to experience in default network efficiency: openness and the default network. *Hum. Brain Mapp.* 37, 773–779. doi: 10.1002/hbm.23065

Brown, T. A. (2006). *Confirmatory Factor Analysis for Applied Research*. New York, NY: The Guildford Press.

Broyd, S. J., Demanuele, C., Debener, S., Helps, S. K., James, C. J., and Sonuga-Barke, E. J. S. (2009). Default-mode brain dysfunction in mental disorders: a systematic review. *Neurosci. Biobehav. Rev.* 33, 279–296. doi: 10.1016/j.neubiorev.2008.09.002

Buckner, R. L., Andrews-Hanna, J. R., and Schacter, D. L. (2008). The brain's default network: anatomy, function, and relevance to disease. *Ann. N Y Acad. Sci.* 1124, 1–38. doi: 10.1196/annals.1440.011

Buhle, J. T., Silvers, J. A., Wager, T. D., Lopez, R., Onyemekwu, C., Kober, H., et al. (2014). Cognitive reappraisal of emotion: a meta-analysis of human neuroimaging studies. *Cereb. Cortex* 24, 2981–2990. doi: 10.1093/cercor/bht154

Bullmore, E., and Sporns, O. (2009). Complex brain networks: graph theoretical analysis of structural and functional systems. *Nat. Rev. Neurosci.* 10, 186–198. doi: 10.1038/nrn2575

Cole, M. W., Bassett, D. S., Power, J. D., Braver, T. S., and Petersen, S. E. (2014a). Intrinsic and task-evoked network architectures of the human brain. *Neuron* 83, 238–251. doi: 10.1016/j.neuron.2014.05.014

Cole, M. W., Repovš, G., and Anticevic, A. (2014b). The frontoparietal control system: a central role in mental health. *Neuroscientist* 20, 652–664. doi: 10.1177/1073858414525995

Cole, M. W., Reynolds, J. R., Power, J. D., Repovs, G., Anticevic, A., and Braver, T. S. (2013). Multi-task connectivity reveals flexible hubs for adaptive task control. *Nat. Neurosci.* 16, 1348–1355. doi: 10.1038/nn.3470

Collin, G., van den Heuvel, M. P., Abramovic, L., Vreeker, A., de Reus, M. A., van Haren, N. E. M., et al. (2016). Brain network analysis reveals affected connectome structure in bipolar I disorder. *Hum. Brain Mapp.* 37, 122–134. doi: 10.1002/hbm.23017

De Vico Fallani, F., Richiardi, J., Chavez, M., and Achard, S. (2014). Graph analysis of functional brain networks: practical issues in translational neuroscience. *Philos. Trans. R. Soc. Lond. B Biol. Sci.* 369:20130521. doi: 10.1098/rstb.2013.0521

Diekhof, E. K., Geier, K., Falkai, P., and Gruber, O. (2011). Fear is only as deep as the mind allows. *Neuroimage* 58, 275–285. doi: 10.1016/j.neuroimage.2011.05.073

Dodds, C. M., Morein-Zamir, S., and Robbins, T. W. (2011). Dissociating inhibition, attention, and response control in the frontoparietal network using functional magnetic resonance imaging. *Cereb. Cortex* 21, 1155–1165. doi: 10.1093/cercor/bhq187

Dosenbach, N. U. F., Fair, D. A., Miezin, F. M., Cohen, A. L., Wenger, K. K., Dosenbach, R. A. T., et al. (2007). Distinct brain networks for adaptive and stable task control in humans. *Proc. Natl. Acad. Sci. U S A* 104, 11073–11078. doi: 10.1073/pnas.0704320104

Egner, T., and Hirsch, J. (2005). Cognitive control mechanisms resolve conflict through cortical amplification of task-relevant information. *Nat. Neurosci.* 8, 1784–1790. doi: 10.1038/nn1594

Etkin, A., Büchel, C., and Gross, J. J. (2015). The neural bases of emotion regulation. *Nat. Rev. Neurosci.* 16, 693–700. doi: 10.1038/nrn4044

Fox, K. C. R., Spreng, R. N., Ellamil, M., Andrews-Hanna, J. R., and Christoff, K. (2015). The wandering brain: meta-analysis of functional neuroimaging studies of mind-wandering and related spontaneous thought processes. *Neuroimage* 111, 611–621. doi: 10.1016/j.neuroimage.2015.02.039

Giuliani, N. R., Drabant, E. M., Bhatnagar, R., and Gross, J. J. (2011a). Emotion regulation and brain plasticity: expressive suppression use predicts anterior insula volume. *Neuroimage* 58, 10–15. doi: 10.1016/j.neuroimage.2011.06.028

Giuliani, N. R., Drabant, E. M., and Gross, J. J. (2011b). Anterior cingulate cortex volume and emotion regulation: is bigger better? *Biol. Psychol.* 86, 379–382. doi: 10.1016/j.biopsycho.2010.11.010

Goldin, P. R., McRae, K., Ramel, W., and Gross, J. J. (2008). The neural bases of emotion regulation: reappraisal and suppression of negative emotion. *Biol. Psychiatry* 63, 577–586. doi: 10.1016/j.biopsych.2007.05.031

Gross, J. J. (1998). The emerging field of emotion regulation: an integrative review. *Rev. Gen. Psychol.* 2, 271–299. doi: 10.1037//1089-2680.2.3.271

Gross, J. J. (2002). Emotion regulation: affective, cognitive, and social consequences. *Psychophysiology* 39, 281–291. doi: 10.1017/s0048577201393198

Gross, J. J. (2015). Emotion regulation: current status and future prospects. *Psychol. Inq.* 26, 1–26. doi: 10.1080/1047840x.2014.940781

Gross, J. J., and John, O. P. (2003). Individual differences in two emotion regulation processes: implications for affect, relationships, and well-being. *J. Pers. Soc. Psychol.* 85, 348–362. doi: 10.1037/0022-3514.85.2.348

Hamilton, J. P., Farmer, M., Fogelman, P., and Gotlib, I. H. (2015). Depressive rumination, the default-mode network and the dark matter of clinical neuroscience. *Biol. Psychiatry* 78, 224–230. doi: 10.1016/j.biopsych.2015.02.020

He, Y., Chen, Z. J., and Evans, A. C. (2007). Small-world anatomical networks in the human brain revealed by cortical thickness from MRI. *Cereb. Cortex* 17, 2407–2419. doi: 10.1093/cercor/bhl149

Hermann, A., Bieber, A., Keck, T., Vaitl, D., and Stark, R. (2014). Brain structural basis of cognitive reappraisal and expressive suppression. *Soc. Cogn. Affect. Neurosci.* 9, 1435–1442. doi: 10.1093/scan/nst130

Hu, L., and Bentler, P. M. (1998). Fit indices in covariance structure modeling: sensitivity to under parameterized model misspecification. *Psychol. Methods* 3, 424–453. doi: 10.1037//1082-989x.3.4.424

Humphries, M. D., Gurney, K., and Prescott, T. (2006). The brainstem reticular formation is a small-world, not scale-free, network. *Proc. Biol. Sci.* 273, 503–511. doi: 10.1098/rspb.2005.3354

Jäncke, L., and Langer, N. (2011). A strong parietal hub in the small-world network of coloured-hearing synaesthetes during resting state EEG: small-world network of coloured-hearing synaesthetes. *J. Neuropsychol.* 5, 178–202. doi: 10.1111/j.1748-6653.2011.02004.x

Kalisch, R. (2009). The functional neuroanatomy of reappraisal: time matters. *Neurosci. Biobehav. Rev.* 33, 1215–1226. doi: 10.1016/j.neubiorev.2009.06.003

Kerns, J. G., Cohen, J. D., MacDonald, A. W. III., Cho, R. Y., Stenger, V. A., and Carter, C. S. (2004). Anterior cingulate conflict monitoring and adjustments in control. *Science* 303, 1023–1026. doi: 10.1126/science.1089910

Kühn, S., Gallinat, J., and Brass, M. (2011). "Keep calm and carry on": structural correlates of expressive suppression of emotions. *PLoS One* 6:e16569. doi: 10.1371/journal.pone.0016569

Langer, N., Pedroni, A., Gianotti, L. R. R., Hänggi, J., Knoch, D., and Jäncke, L. (2012). Functional brain network efficiency predicts intelligence. *Hum. Brain Mapp.* 33, 1393–1406. doi: 10.1002/hbm.21297

Lee, T.-W., Dolan, R. J., and Critchley, H. D. (2008). Controlling emotional expression: behavioral and neural correlates of nonimitative emotional responses. *Cereb. Cortex* 18, 104–113. doi: 10.1093/cercor/bhm035

Li, Y., Liu, Y., Li, J., Qin, W., Li, K., Yu, C., et al. (2009). Brain anatomical network and intelligence. *PLoS Comput. Biol.* 5:e1000395. doi: 10.1371/journal.pcbi.1000395

Long, J., Xie, Q., Ma, Q., Urbin, M. A., Liu, L., Weng, L., et al. (2016). Distinct interactions between fronto-parietal and default mode networks in impaired consciousness. *Sci. Rep.* 6:38866. doi: 10.1038/srep38866

MacDonald, A. W. III., Cohen, J. D., Stenger, V. A., and Carter, C. S. (2000). Dissociating the role of the dorsolateral prefrontal and anterior cingulate cortex in cognitive control. *Science* 288, 1835–1838. doi: 10.1126/science.288.5472.1835

Matsumoto, K., and Tanaka, K. (2004). Conflict and cognitive control. *Science* 303, 969–970. doi: 10.1126/science.1094733

Mears, D., and Pollard, H. B. (2016). Network science and the human brain: using graph theory to understand the brain and one of its hubs, the amygdala, in health and disease. *J. Neurosci. Res.* 94, 590–605. doi: 10.1002/jnr.23705

Meng, C., Brandl, F., Tahmasian, M., Shao, J., Manoliu, A., Scherr, M., et al. (2014). Aberrant topology of striatum's connectivity is associated with the number of episodes in depression. *Brain* 137, 598–609. doi: 10.1093/brain/awt290

Moore, M., Iordan, A. D., Hu, Y., Kragel, J. E., Dolcos, S., and Dolcos, F. (2016). Localized or diffuse: the link between prefrontal cortex volume and cognitive reappraisal. *Soc. Cogn. Affect. Neurosci.* 11, 1317–1325. doi: 10.1093/scan/nsw043

Murphy, K., Birn, R. M., Handwerker, D. A., Jones, T. B., and Bandettini, P. A. (2009). The impact of global signal regression on resting state correlations: are anti-correlated networks introduced? *Neuroimage* 44, 893–905. doi: 10.1016/j.neuroimage.2008.09.036

Ochsner, K., and Gross, J. (2005). The cognitive control of emotion. *Trends Cogn. Sci.* 9, 242–249. doi: 10.1016/j.tics.2005.03.010

Picó-Pérez, M., Alonso, P., Contreras-Rodríguez, O., Martínez-Zalacaín, I., López-Solà, C., Jiménez-Murcia, S., et al. (2017). Dispositional use of emotion regulation strategies and resting-state cortico-limbic functional connectivity. *Brain Imaging Behav.* doi: 10.1007/s11682-017-9762-3 [Epub ahead of print].

Poldrack, R. A. (2007). Region of interest analysis for fMRI. *Soc. Cogn. Affect. Neurosci.* 2, 67–70. doi: 10.1093/scan/nsm006

Power, J. D., Cohen, A. L., Nelson, S. M., Wig, G. S., Barnes, K. A., Church, J. A., et al. (2011). Functional network organization of the human brain. *Neuron* 72, 665–678. doi: 10.1016/j.neuron.2011.09.006

Power, J. D., Schlaggar, B. L., Lessov-Schlaggar, C. N., and Petersen, S. E. (2013). Evidence for hubs in human functional brain networks. *Neuron* 79, 798–813. doi: 10.1016/j.neuron.2013.07.035

Qiu, L., Zheng, X., and Wang, Y. F. (2008). Revision of the positive affect and negative affect scale. *Chin. J. Appl. Psychol.* 14, 249–254.

Raichle, M. E. (2011). The restless brain. *Brain Connect.* 1, 3–12. doi: 10.1089/brain.2011.0019

Rubinov, M., and Sporns, O. (2010). Complex network measures of brain connectivity: uses and interpretations. *Neuroimage* 52, 1059–1069. doi: 10.1016/j.neuroimage.2009.10.003

Sadaghiani, S., and D'Esposito, M. (2015). Functional characterization of the cingulo-opercular network in the maintenance of tonic alertness. *Cereb. Cortex* 25, 2763–2773. doi: 10.1093/cercor/bhu072

Sampaio, A., Soares, J. M., Coutinho, J., Sousa, N., and Gonçalves, Ó. F. (2014). The big five default brain: functional evidence. *Brain Struct. Funct.* 219, 1913—1922. doi: 10.1007/s00429-013-0610-y

Santarnecchi, E., Galli, G., Polizzotto, N. R., Rossi, A., and Rossi, S. (2014). Efficiency of weak brain connections support general cognitive functioning. *Hum. Brain Mapp.* 35, 4566–4582. doi: 10.1002/hbm.22495

Sheffield, J. M., Repovs, G., Harms, M. P., Carter, C. S., Gold, J. M., MacDonald III, A. W., et al. (2015). Fronto-parietal and cingulo-opercular network integrity and cognition in health and schizophrenia. *Neuropsychologia* 73, 82–93. doi: 10.1016/j.neuropsychologia.2015.05.006

Skrondal, A., and Rabe-Hesketh, S. (2004). *Generalized Latent Variable Modeling: Multilevel, Longitudinal and Structural Equation Models*. Boca Raton, FL: CRC Press.

Smith, S. M., Vidaurre, D., Beckmann, C. F., Glasser, M. F., Jenkinson, M., Miller, K. L., et al. (2013). Functional connectomics from resting-state fMRI. *Trends Cogn. Sci.* 17, 666–682. doi: 10.1016/j.tics.2013.09.016

Stam, C. J., Jones, B. F., Nolte, G., Breakspear, M., and Scheltens, P. (2006). Small-world networks and functional connectivity in Alzheimer's disease. *Cereb. Cortex* 17, 92–99. doi: 10.1093/cercor/bhj127

Stanley, M. L., Simpson, S. L., Dagenbach, D., Lyday, R. G., Burdette, J. H., and Laurienti, P. J. (2015). Changes in brain network efficiency and working memory performance in aging. *PLoS One* 10:e0123950. doi: 10.1371/journal.pone.0123950

Stawarczyk, D., and D'Argembeau, A. (2015). Neural correlates of personal goal processing during episodic future thinking and mind-wandering: an ALE meta-analysis. *Hum. Brain Mapp.* 36, 2928–2947. doi: 10.1002/hbm.22818

Thompson, W. H., and Fransson, P. (2015). The frequency dimension of fMRI dynamic connectivity: network connectivity, functional hubs and integration in the resting brain. *Neuroimage* 121, 227–242. doi: 10.1016/j.neuroimage.2015.07.022

Uddin, L. Q. (2015). Salience processing and insular cortical function and dysfunction. *Nat. Rev. Neurosci.* 16, 55–61. doi: 10.1038/nrn3857

van den Heuvel, M. P., and Hulshoff Pol, H. E. (2010). Exploring the brain network: a review on resting-state fMRI functional connectivity. *Eur. Neuropsychopharmacol.* 8, 519–534. doi: 10.1016/j.euroneuro.2010.03.008

van den Heuvel, M. P., Stam, C. J., Kahn, R. S., and Hulshoff Pol, H. E. (2009). Efficiency of functional brain networks and intellectual performance. *J. Neurosci.* 29, 7619–7624. doi: 10.1523/jneurosci.1443-09.2009

Vatansever, D., Menon, D. K., Manktelow, A. E., Sahakian, B. J., and Stamatakis, E. A. (2015). Default mode dynamics for global functional integration. *J. Neurosci.* 35, 15254–15262. doi: 10.1523/jneurosci.2135-15.2015

Vincent, J. L., Kahn, I., Snyder, A. Z., Raichle, M. E., and Buckner, R. L. (2008). Evidence for a frontoparietal control system revealed by intrinsic functional connectivity. *J. Neurophysiol.* 100, 3328–3342. doi: 10.1152/jn.90355.2008

Wang, K., Huang, H., Chen, L., Hou, X., Zhang, Y., Yang, J., et al. (2017). MRI correlates of interaction between gender and expressive suppression among the Chinese population. *Neuroscience* 347, 76–84. doi: 10.1016/j.neuroscience.2017.01.042

Wang, L., Liu, H., Li, Z., and Du, W. (2007). Reliability and validity of emotion regulation questionnaire Chinese revised version. *China J. Health Psychol.* 15, 503–504.

Wang, J., Wang, X., Xia, M., Liao, X., Evans, A., and He, Y. (2015). Corrigendum: GRETNA: a graph theoretical network analysis toolbox for imaging connectomics. *Front. Hum. Neurosci.* 9:458. doi: 10.3389/fnhum.2015.00458

Wang, J., Zuo, X., and He, Y. (2010). Graph-based network analysis of resting-state functional MRI. *Front. Syst. Neurosci.* 4:16. doi: 10.3389/fnsys.2010.00016

Wang, L., Zhu, C., He, Y., Zang, Y., Cao, Q., Zhang, H., et al. (2009). Altered small-world brain functional networks in children with attention-deficit/hyperactivity disorder. *Hum. Brain Mapp.* 30, 638–649. doi: 10.1002/hbm.20530

Watson, D., Clark, L., and Tellegen, A. (1988). Development and validation of brief measures of positive and negative affect: the PANAS scales. *J. Pers. Soc. Psychol.* 54, 1063—1070. doi: 10.1037//0022-3514.54.6.1063

Watts, D. J., and Strogatz, S. H. (1998). Collective dynamics of "small-world" networks. *Nature* 393, 440–442. doi: 10.1038/30918

Welborn, B. L., Papademetris, X., Reis, D. L., Rajeevan, N., Bloise, S. M., and Gray, J. R. (2009). Variation in orbitofrontal cortex volume: relation to sex, emotion regulation and affect. *Soc. Cogn. Affect. Neurosci.* 4, 328–339. doi: 10.1093/scan/nsp028

Wig, G. S., Schlaggar, B. L., and Petersen, S. E. (2011). Concepts and principles in the analysis of brain networks. *Ann. N Y Acad. Sci.* 1224, 126–146. doi: 10.1111/j.1749-6632.2010.05947.x

Xu, J., Yin, X., Ge, H., Han, Y., Pang, Z., Tang, Y., et al. (2015). Attentional performance is correlated with the local regional efficiency of intrinsic brain networks. *Front. Behav. Neurosci.* 9:200. doi: 10.3389/fnbeh.2015.00200

Yang, C. G., and Zang, Y. F. (2010). DPARSF: a MATLAB toolbox for "pipeline" data analysis of resting-state fMRI. *Front. Syst. Neurosci.* 4:13. doi: 10.3389/fnsys.2010.00013

Zhao, X., Liu, Y., Wang, X., Liu, B., Xi, Q., Guo, Q., et al. (2012). Disrupted small-world brain networks in moderate Alzheimer's disease: a resting-state fMRI study. *PLoS One* 7:e33540. doi: 10.1371/journal.pone.0033540

**Conflict of Interest Statement**: The authors declare that the research was conducted in the absence of any commercial or financial relationships that could be construed as a potential conflict of interest.

frontiers in Human Neuroscience

ORIGINAL RESEARCH
published: 19 March 2018
doi: 10.3389/fnhum.2018.00094

# Multivariate Pattern Classification of Facial Expressions Based on Large-Scale Functional Connectivity

*Yin Liang[1], Baolin Liu[1,2]*, Xianglin Li[3] and Peiyuan Wang[4]*

*[1] School of Computer Science and Technology, Tianjin Key Laboratory of Cognitive Computing and Application, Tianjin University, Tianjin, China, [2] State Key Laboratory of Intelligent Technology and Systems, National Laboratory for Information Science and Technology, Tsinghua University, Beijing, China, [3] Medical Imaging Research Institute, Binzhou Medical University, Yantai, China, [4] Department of Radiology, Yantai Affiliated Hospital of Binzhou Medical University, Yantai, China*

It is an important question how human beings achieve efficient recognition of others' facial expressions in cognitive neuroscience, and it has been identified that specific cortical regions show preferential activation to facial expressions in previous studies. However, the potential contributions of the connectivity patterns in the processing of facial expressions remained unclear. The present functional magnetic resonance imaging (fMRI) study explored whether facial expressions could be decoded from the functional connectivity (FC) patterns using multivariate pattern analysis combined with machine learning algorithms (fcMVPA). We employed a block design experiment and collected neural activities while participants viewed facial expressions of six basic emotions (anger, disgust, fear, joy, sadness, and surprise). Both static and dynamic expression stimuli were included in our study. A behavioral experiment after scanning confirmed the validity of the facial stimuli presented during the fMRI experiment with classification accuracies and emotional intensities. We obtained whole-brain FC patterns for each facial expression and found that both static and dynamic facial expressions could be successfully decoded from the FC patterns. Moreover, we identified the expression-discriminative networks for the static and dynamic facial expressions, which span beyond the conventional face-selective areas. Overall, these results reveal that large-scale FC patterns may also contain rich expression information to accurately decode facial expressions, suggesting a novel mechanism, which includes general interactions between distributed brain regions, and that contributes to the human facial expression recognition.

**Keywords: facial expressions, fMRI, functional connectivity, multivariate pattern analysis, machine learning algorithm**

OPEN ACCESS

***Edited by:***
*Xiaochu Zhang,*
*University of Science and Technology of China, China*

***Reviewed by:***
*Jing Jin,*
*East China University of Science and Technology, China*
*Maria Clotilde Henriques Tavares,*
*University of Brasília, Brazil*

****Correspondence:***
*Baolin Liu*
*liubaolin@tsinghua.edu.cn*

***Received:*** *11 November 2017*
***Accepted:*** *27 February 2018*
***Published:*** *19 March 2018*

***Citation:***
*Liang Y, Liu B, Li X and Wang P (2018) Multivariate Pattern Classification of Facial Expressions Based on Large-Scale Functional Connectivity. Front. Hum. Neurosci. 12:94. doi: 10.3389/fnhum.2018.00094*

## INTRODUCTION

Facial expression is an important medium for social communication as it conveys information about others' emotion. Humans can quickly and effortlessly decode emotion expressions from faces and perceive them in a categorical manner. The mechanism under which enables human brain achieving the efficient recognition of facial expressions is intensively studied.

The usual way in exploring facial expression perception is recoding the brain activity patterns while participants are presented with facial stimuli. Jin et al. (2012, 2014a,b) have made a

lot of efforts on the stimulus presentation approaches with face stimuli. In order to accurately locate the increased neural activity in brain areas, functional magnetic resonance imaging (fMRI) technology is widely used. Using fMRI, earlier model for face perception is proposed by Haxby et al. (2000), in which they found a "core" and an "extended system" that participated in the processing of facial signals. Subsequently, the core face network, which contained the fusiform face area (FFA), the occipital face area (OFA) and the face-selective area in the posterior superior temporal sulcus (pSTS) have been widely discussed in facial expression perception studies and are considered as key regions (Haxby et al., 2000; Grill-Spector et al., 2004; Winston et al., 2004; Yovel and Kanwisher, 2004; Ishai et al., 2005; Rotshtein et al., 2005; Lee et al., 2010; Gobbini et al., 2011). Previous fMRI studies on facial expression perception mainly employed static expression images as stimuli (Gur et al., 2002; Murphy et al., 2003; Andrews and Ewbank, 2004). Because natural expressions include action, recent studies have suggested that dynamic stimuli are more ecologically valid than the static stimuli and the use of dynamic stimuli may be more appropriate to investigate the "authentic" mechanism of human facial expression recognition (Trautmann et al., 2009; Johnston et al., 2013). Recent studies with dynamic stimuli have found enhanced brain activation patterns compared with static stimuli and found that in addition to the conventional face-selective areas, motion-sensitive areas also significantly responded to facial expressions (Furl et al., 2012, 2013, 2015).

Most of the past fMRI studies on facial expression perception employed univariate statistics to analyze expression stimuli induced increments of neural activity in specific brain areas. Due to the expected existence of interactions between different brain areas, the analyses of functional connectivity (FC) attracted more and more attention, which is measured as the temporal correlations in the fMRI activity between distinct brain areas (Smith, 2012; Wang et al., 2016). Analysis of FC patterns has been applied in the recent studies of various objects categorization (He et al., 2013; Hutchison et al., 2014; Stevens et al., 2015; Wang et al., 2016), and it was generally observed that distinct brain regions are intrinsically interconnected. Considering these, FC patterns may also contribute to the facial expression recognition. A recent fMRI study on face perception employed FC patterns analysis to construct the hierarchical structure of the face-processing network (Zhen et al., 2013). However, it only focused on the FC patterns among the face-selective areas, the general FC interactions for facial expression recognition remained unclear. Consequently, exploring the whole-brain FC patterns during the processing of different expression information would be meaningful.

Machine learning techniques make use of the multivariate nature of the fMRI data and are being increasingly applied to decode cognitive processes (Pereira et al., 2009). Previous studies of facial expression decoding combined machine learning with multi-voxel activation patterns to examine the decoding performance in the specific brain areas. In these studies, Said et al. (2010) and Harry et al. (2013) respectively, highlighted the roles of STS and FFA in the facial expression decoding, and Wegrzyn et al. (2015) directly compared classification rates across the brain areas proposed by Haxby's model (Haxby et al., 2000). Additionally, Furl et al. (2012) and Liang et al. (2017) showed that both face-selective and motion-sensitive areas contributed to the facial expression decoding. Considerable attention has been paid to activation-based facial expression decoding in individual brain areas; however, the potential mechanisms of expression information representation through the FC patterns remained unclear. Recently, a study by Wang et al. (2016) showed the successful decoding of various object categories based on the FC patterns. Their study motivated us to explore whether facial expression information can also be robust decoded from the FC patterns.

The present fMRI study explored the role of the FC patterns in the facial expression recognition. We hypothesized that expression information may also be represented in the FC patterns. To address this issue, we collected neural activities while participants viewed facial expressions of six basic emotions (anger, disgust, fear, joy, sadness, and surprise) in a block design experiment. Both static and dynamic expression stimuli were included in our experiment. After scanning, we conducted a behavioral experiment in accordance to previous study to assess the validity of the facial stimuli, in which we recorded the classification accuracy, the emotional intensity the participants perceived and the corresponding reaction times for each facial stimulus (Furl et al., 2013, 2015). A standard anatomical atlas [Harvard-Oxford atlas, FSL, Oxford University, Meng et al. (2014)] was employed to define the anatomical regions in the brain. We obtained the whole-brain FC patterns for each facial expression and then applied multivariate pattern analyses with machine learning algorithms (fcMVPA) to examine the decoding performance for facial expressions based on the FC patterns.

# MATERIALS AND METHODS

## Participants

The data used in this study were collected in our previous study (Liang et al., 2017). Eighteen healthy, right-handed participants (nine females; range 20–24 years old) took part in our experiment. They were Chinese students who were recruited from the Binzhou Medical University. All participants were with no history of neurological or psychiatric disorders and had normal or corrected-to-normal vision. Participants signed informed consent before the experiment. This study was approved by the Institutional Review Board (IRB) of Tianjin Key Laboratory of Cognitive Computing and Application, Tianjin University.

## fMRI Data Acquisition

All the participants were scanned using a 3.0-T Siemens scanner with an eight-channel head coil in Yantai Affiliated Hospital of Binzhou Medical University. Foam pads and earplugs were used to reduce the head motion and scanner noise. Functional images were obtained using a gradient echo-planar imaging (EPI) sequence (TR = 2000 ms, TE = 30 ms, voxel size = 3.1 mm × 3.1 mm × 4.0 mm, matrix

size = 64 × 64, slices = 33, slices thickness = 4 mm, slice gap = 0.6 mm). In addition, a three-dimensional magnetization-prepared rapid-acquisition gradient echo (3D MPRAGE) sequence (TR = 1900 ms, TE = 2.52 ms, TI = 1100 ms, voxel size = 1 mm × 1 mm × 1 mm, matrix size = 256 × 256) was used to acquire the T1-weighted anatomical images. The stimuli were displayed by high-resolution stereo 3D glasses within a VisualStim Digital MRI Compatible fMRI system (Choubey et al., 2009; Liang et al., 2017; Yang et al., 2018).

## Procedure

All facial expression stimuli were taken from the Amsterdam Dynamic Facial Expression Set (ADFES), which is a standard facial expression database containing both images and videos of basic emotions (van der Schalk et al., 2011). Video clips of 12 different identities (six males andsix females) displayed six basic emotions (anger, disgust, fear, joy, sadness, and surprise) were chosen. The exemplar stimuli for the six basic emotions are shown in **Figure 1A**. We created the dynamic expression stimuli by cropping all videos to 1520 ms to retain the transition from a neutral expression to the expression apex, and the apex expression image was used as the static stimuli (Furl et al., 2013, 2015).

The experiment employed a block design, with four runs. There were three conditions in our experiment: static facial expressions, dynamic facial expressions and dynamic expressions with obscured eye-region. Each condition included all six basic expressions: anger, disgust, fear, joy, sadness, and surprise. Data from the obscured condition were not analyzed in the current study but were included for the purpose of another study (Liang et al., 2017). In each run, there were 18 blocks (6 expressions × 3 conditions), each expression and condition appearing once. The 18 blocks were presented in a pseudo-random order to ensure that the same emotion or condition were not presented consecutively (Axelrod and Yovel, 2012; Furl et al., 2013, 2015). **Figure 1B** shows the schematic representation of the employed paradigm. At the beginning of each run, there was a 10 s fixation cross, which was followed by a 24 s stimulus block (the same condition and expression) and then a 4 s button task. Successive stimulus blocks were separated by the presentation of a fixation cross for 10 s. In each stimulus block, 12 expression stimuli were presented (each for 1520 ms) with an interstimulus interval (ISI) of 480 ms. During the course of each stimulus block, participants were instructed to carefully watch the facial stimuli, and after the block, a screen appeared with six emotion categories and corresponding button indexes to instruct the participants to press a button to indicate the facial expression they had seen in the previous block (Liang et al., 2017; Yang et al., 2018). Participants were provided with one response pad per hand with three buttons each in the fMRI experiment (Ihme et al., 2014), and they were pre-trained to familiarize the button pad before scanning. The total duration of the experiment was 45.6 min, with each run lasting 11.4 min. Stimulus presentation was performed using

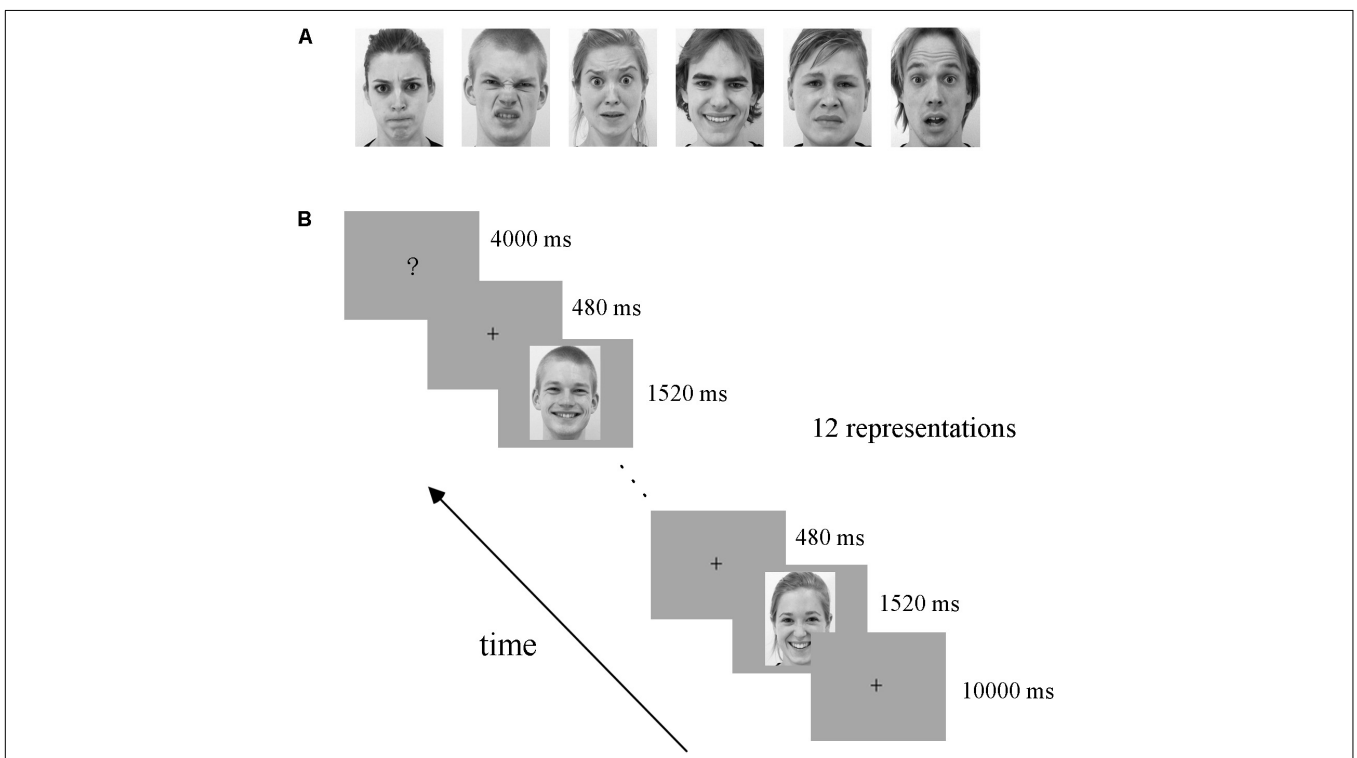


**FIGURE 1 |** Exemplar facial stimuli **(A)** and schematic representation of the experimental paradigm **(B)**. All facial expression stimuli were taken from the ADFES database. The experiment employed a block design, including four runs. There was a fixation cross (10 s) before each block, and then 12 expression stimuli appeared. Subsequently, the participants completed a button task after each block to indicate their discrimination of the expression they had seen.

E-Prime 2.0 Professional (Psychology Software Tools, Pittsburgh, PA, United States).

After scanning, participants were required to complete a behavioral experiment outside the scanner in accordance to the previous studies (Furl et al., 2013, 2015). During it, we recorded their classification of emotion category, emotional intensity rating and the corresponding reaction times for each stimulus used in the fMRI experiment. The emotional intensity for each stimulus was rated on a 1–9 scale with 1 refers to the lowest and 9 refers to the highest emotional intensity (Furl et al., 2013). Each stimulus was presented once in a random order, with the same duration as in the fMRI experiment.

## Data Preprocessing

Functional image preprocessing was conducted using SPM8 software[1]. For each run, the first five volumes were discarded to allow for T1 equilibration effects. The remaining functional images were corrected for the slice-time and head motion. Next, the functional data were normalized by using the structural image unified segmentation. The high-resolution structural image was co-registered with the functional images and was subsequently segmented into gray matter, white matter and cerebrospinal fluid. And the spatial normalization parameters estimated during unified segmentation were applied to normalize the functional images into the standard Montreal Neurological Institute (MNI) space, with a re-sampled voxel size of 3 mm × 3 mm × 3 mm. Finally, the functional data were spatially smoothed with a 4-mm full-width at half-maximum Gaussian kernel.

## Construction of Whole-Brain FC Patterns

Estimation of the task-related whole-brain FC was carried out using the CONN toolbox[2] (Whitfield-Gabrieli and Nieto-Castanon, 2012) in MATLAB. For each participant, the normalized anatomical volume and the preprocessed functional data were submitted to CONN. We employed the Harvard-Oxford atlas[3] (FSL, Oxford University, Meng et al., 2014) as network nodes, which contained 112 cortical and subcortical regions. Time series of functional MRI signal were extracted from each voxel and averaged within each ROI for each condition. CONN implemented a component-based (CompCor) strategy to remove the non-neural sources of confounders. Principle components associated with white matter (WM) and cerebrospinal fluid (CSF) were regressed out along with the six head movement parameters, and the data were temporally filtered with band-pass filter 0.01 – 0.1 HZ as previously used for task-induced connectivity analysis (Wang et al., 2016). We conducted ROI-to-ROI analysis to assess pairwise correlations between the ROIs. For both static and dynamic facial expressions, we obtained six FC matrices (112 × 112) for each participant, one per emotion category. Second-level analysis was performed for each facial expression for the group comparisons of the differences in expression-related FC between ROIs ($p < 0.001$, FDR corrected for connection-level, two-sides).

## Across-Subject Expression Classification Based on the FC Patterns

We employed multivariate pattern analysis and machine learning to examine whether facial expression information could be decoded from the FC patterns (fcMVPA). **Figure 2** represents the framework overview of our fcMVPA classification. We performed a six-way expression classification separately for the static and dynamic facial expressions. Due to some evidence showed that the interpretation of the negative FCs remained controversial (Fox M.D. et al., 2009; Weissenbacher et al., 2009; Wang et al., 2016), we also focused mainly on the positive FCs in current study. For each category, we obtained 6216 [(112 × 111)/2] connections in total. We performed the procedure adopted in Wang et al. (2016) to obtain the positive FCs. For each category, we conducted a one-sample *t*-test across participants for each of the 6216 connections and retained FCs that had values significantly greater than zero. *P*-values were corrected for multiple comparisons with the false discovery rate (FDR) $q = 0.01$. This procedure identified 1540 positive FCs for anger, 1792 positive FCs for disgust, 1466 positive FCs for fear, 1838 positive FCs for joy, 1799 positive FCs for sadness and 1726 positive FCs for surprise for the static expressions, while for the dynamic expressions, it correspondingly identified 1944, 1798, 1696, 1703, 1608, and 1822 positive FCs for each of the six basic expressions. Pooling the positive FCs together separately for static and dynamic conditions, we obtained a total of 3014 (for static) and 2986 (for dynamic) FCs that were significantly positive for at least one expression (Wang et al., 2016). For classification, we employed a linear support vector machine (SVM) classifier as implemented in the LIBSVM[4]. A leave-one-subject-out cross-validation scheme (LOOCV) was used to evaluate the performance (Liu et al., 2015; Wang et al., 2016; Jang et al., 2017). For multi-class classification, this implementation used a one-against-one voting strategy. In each iteration of LOOCV, we trained the classifier in all but one participant and the remaining one was used as the testing set. During the classifier training, we first obtained 15 classifiers for each pair of expressions and then added these pairwise classifiers to yield the linear ensemble classifier for each expression. Feature selection was executed using ANOVA ($p < 0.05$), which was only performed on the training data of each LOOCV fold to avoid peeking. The statistical significance of the decoding performance was evaluated with permutation test, in which the same cross-validation procedure was carried out for 1000 random shuffles of class labels (Liu et al., 2015; Wang et al., 2016; Fernandes et al., 2017). The *p*-value for the decoding accuracy was calculated as the fraction of the number of accuracies from 1000 permutation tests that were equal to or larger than the accuracy obtained with the correct labels. If no more than 5% ($p < 0.05$) of the accuracies from all permutation tests exceeded the actual accuracy using correct labels, the results was thought to be significant.

[1] http://www.fil.ion.ucl.ac.uk/spm/software/spm8/

[2] http://www.nitrc.org/projects/conn

[3] http://www.cma.mgh.harvard.edu/fsl_atlas.html

[4] http://www.csie.ntu.edu.tw/~cjlin/libsvm/

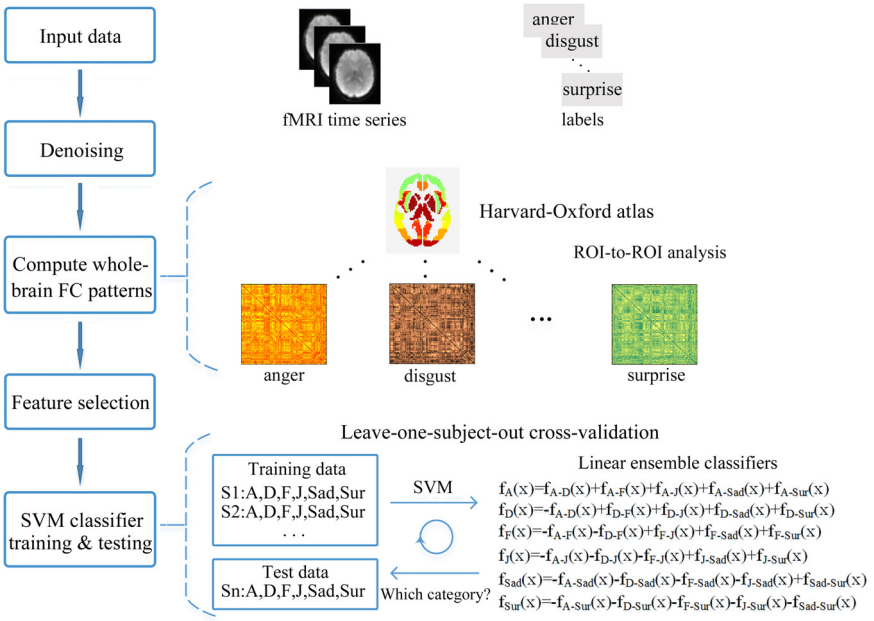


**FIGURE 2 |** Framework overview of the fcMVPA. The pairs of preprocessed functional images and the corresponding labels of expression categories were used as the input data. Estimation of the FC patterns was performed using CONN toolbox. Denoising was used to remove unwanted motion, physiological and other artifactual effects from the BOLD signals before the connectivity measured. Then, the whole-brain FC patterns for each of the six facial expressions were computed using ROI-to-ROI analysis with the 112 nodes defined by the Harvard-Oxford atlas. Feature selection was performed with ANOVA only using the training data. Finally, the FC pattern classification of six facial expressions was carried out in a leave-one-subject-out cross-validation scheme with a SVM classifier.

# RESULTS

## Behavioral Results

Participants completed a behavioral experiment in which they classified the emotional categories and rated the perceived emotional intensities for each facial stimulus after scanning. **Figure 3** shows the behavioral results. These results verified the validity of the facial stimuli used in our experiment as both static and dynamic facial expression stimuli could be successfully classified with high accuracies (**Figure 3A**). A further comparison of the classification accuracies, intensity ratings and the corresponding reaction times between static and dynamic facial expressions, we found that participants showed higher classification accuracies for dynamic compared with static facial expressions [one-tailed paired $t$-test, $t(17) = 3.265$, $p = 0.002$]. For the emotional intensity and the reaction times, there were no significant differences.

## Whole-Brain FC Patterns for Each Facial Expression in Static and Dynamic Conditions

We constructed the whole-brain FC patterns for each facial expression separately for the static and dynamic stimuli. For each participant, we got 12 FC matrices with each contained 6216 [(112 × 111)/2] connections between the pre-defined 112 brain notes. Second-level analysis was performed for each facial expression for the group comparisons of the differences in these ROI-to-ROI functional connections. **Figures 4**, **5** show the results of group-level analysis of the FC patterns for each facial expression ($p < 0.001$, FDR corrected for connection-level, two-sides).

## Facial Expression Decoding Based on fcMVPA

In this section, we explored whether facial expressions could be decoded from the FC patterns using fcMVPA. Since the interpretation of the negative FCs remained controversial (Fox M.D. et al., 2009; Weissenbacher et al., 2009; Wang et al., 2016), we focused on the positive FCs in the fcMVPA classification. Separately for the static and dynamic conditions, we obtained the positive FCs for each facial expression using one-sample $t$-test across participants with multiple comparisons (FDR $q = 0.01$) and by pooling the positive FCs together, we obtained 3014 (for static) and 2986 (for dynamic) FCs for the classification of static and dynamic facial expressions (Wang et al., 2016). In the main results below, we used these positive FCs. For the multiclass facial expression classification, the performance was evaluated with the LOOCV strategy. As shown in **Figure 6** (left columns), we found that classification accuracies based on the FC patterns were significantly above the chance level for both static and dynamic facial expressions ($p = 0.003$ for static facial expressions and $p < 0.001$ for dynamic facial expressions, 1000 permutations), indicating that expression information could be successfully decoded from the FC patterns.

Furthermore, we identified the expression-discriminative networks for the static and dynamic facial expressions, defined

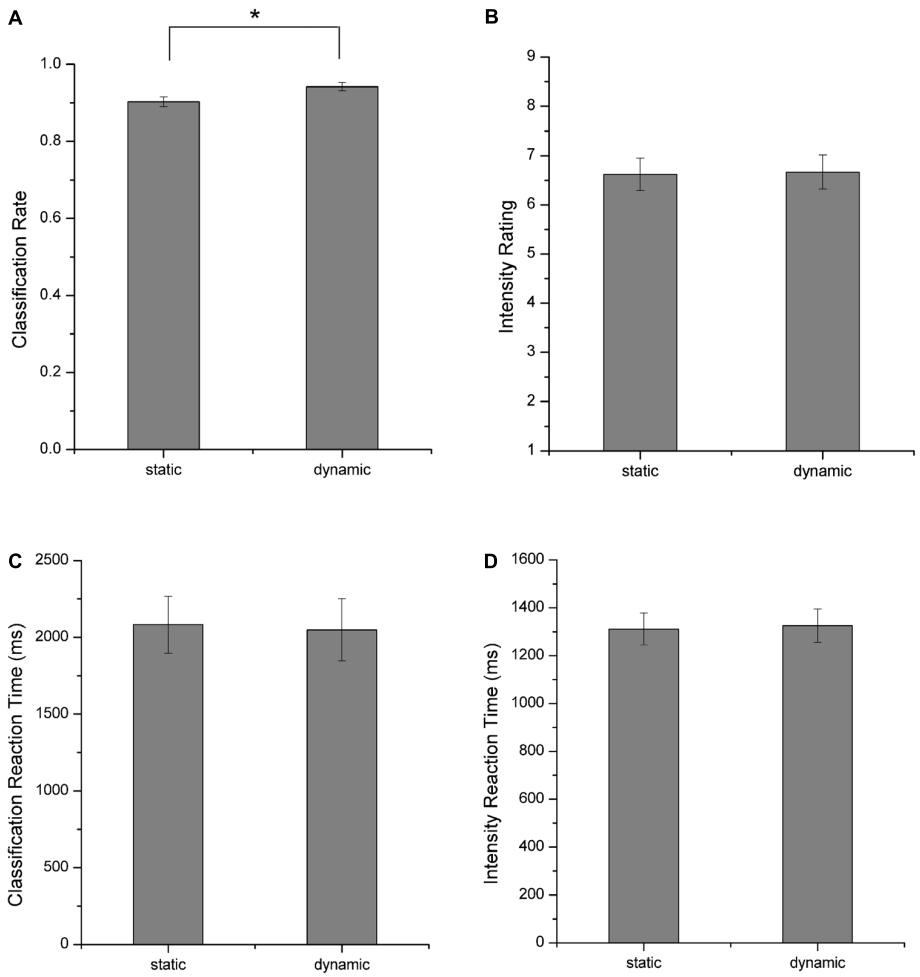


**FIGURE 3 |** Behavioral results. **(A)** Classification rates, **(B)** perceived emotional intensities, **(C)** reaction times for facial expression classification, and **(D)** reaction times for emotional intensity rating. All error bars indicate the SEM. *Indicates statistical significance with paired *t*-test, $p < 0.05$.

as FCs that contributed significantly in discriminating between different expression categories. Connections that were selected over all iterations of LOOCV feature selection (consensus features, ANOVA $p < 0.05$) composed the expression-discriminative networks. **Figure 7** shows the expression-discriminative networks for the static and dynamic facial expressions, all of which were widely distributed in both hemispheres. We summarized the brain regions that were involved in both static and dynamic expression-discriminative networks in **Table 1**. We found conventional face-selective areas, including the insula, inferior frontal gyrus, superior temporal gyrus, lateral occipital cortex (inferior occipital gyrus); temporal fusiform cortex (fusiform gyrus) and amygdala, which were commonly studied in previous fMRI studies on facial expression perception (Fox C.J. et al., 2009; Trautmann et al., 2009; Furl et al., 2013, 2015; Johnston et al., 2013; Harris et al., 2014). Moreover, we found the expression-discriminative networks contained brain regions far beyond these conventional face-selective areas. For instance, the middle temporal gyrus, which was reported sensitive to facial motion (Furl et al., 2012; Liang et al., 2017), was also included. Other regions that were not classically considered in previous fMRI studies on facial expression perception with activation measure were also included, such as the supramarginal gyrus, the lingual gyrus and the parahippocampal gyrus.

## DISCUSSION

The main purpose of this study was to explore whether the FC patterns effectively contributed to human facial expression recognition. To address this issue, we employed a block design experiment and conducted fcMVPA. We obtained the whole-brain FC patterns for each facial expression separately for static and dynamic stimuli and found that both static and dynamic facial expressions could be successfully decoded from the FC patterns. We also identified the expression-discriminative networks for the static and dynamic facial expressions, composed of FCs that significantly contributed to the classification between different facial expressions.

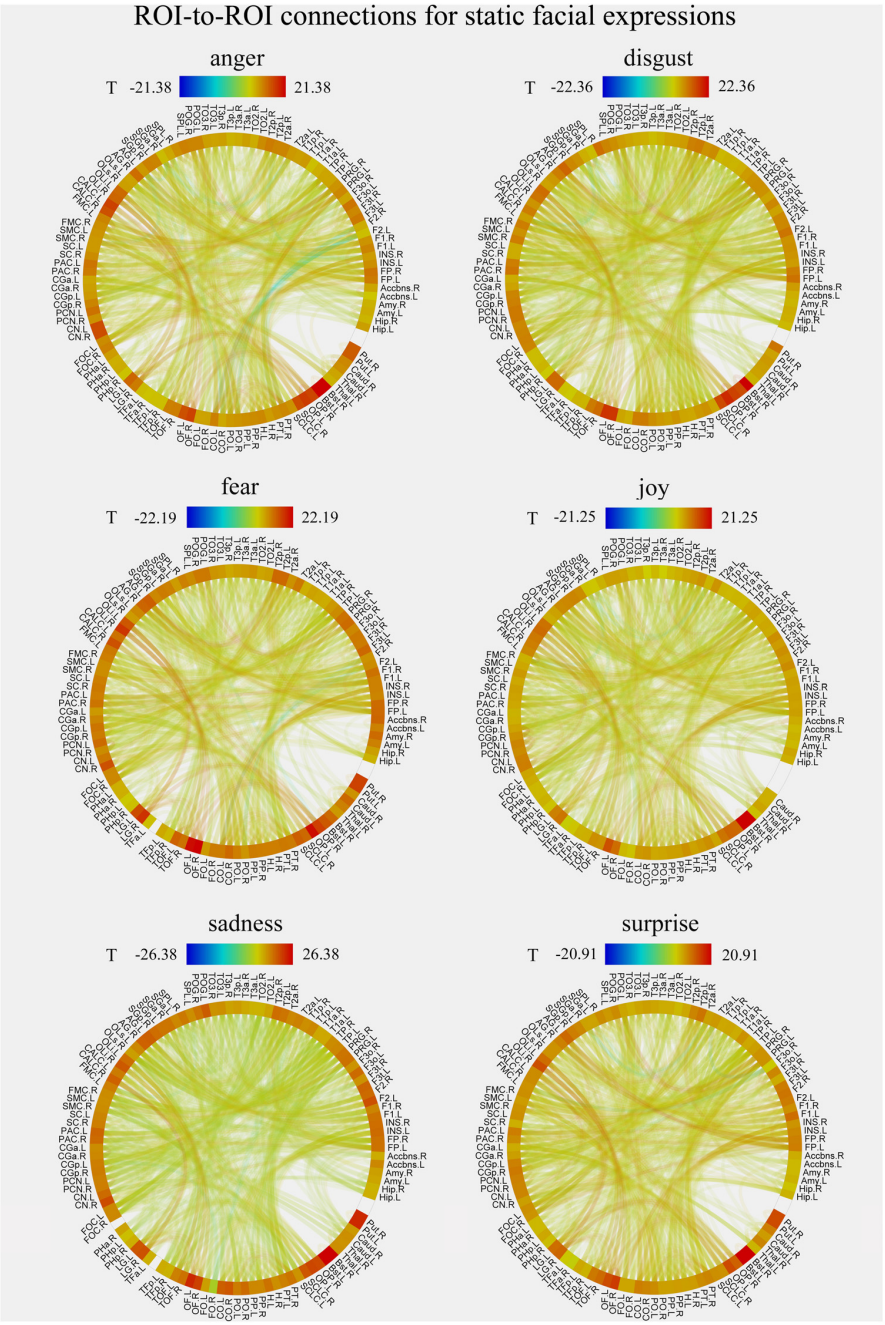


**FIGURE 4 |** Group-level results of ROI-to-ROI connections for each facial expression (anger, disgust, fear, joy, sadness, and surprise) in static condition ($p < 0.001$, FDR corrected at the connection-level, two-sided). All ROIs are deriving from the Harvard-Oxford brain atlas and are labeled with the abbreviations for clarity.

## Facial Expressions Are Decoded From the FC Patterns

Using multivariate connectivity pattern analysis and machine learning algorithm, we found the successful decoding of both static and dynamic facial expressions based on the FC patterns.

Previous studies on facial expression recognition are dominated by identifying cortical regions showing preferential activation to facial expressions (Gur et al., 2002; Winston et al., 2004; Trautmann et al., 2009; Furl et al., 2013, 2015; Johnston et al., 2013; Harris et al., 2014). Although a few recent studies have started to explore the decoding of facial expressions, they only conducted activation-based classification analyses on individual brain regions (Said et al., 2010; Furl et al., 2012; Harry et al., 2013; Wegrzyn et al., 2015; Liang et al., 2017). The potential effects of the FC patterns on the facial expression decoding still

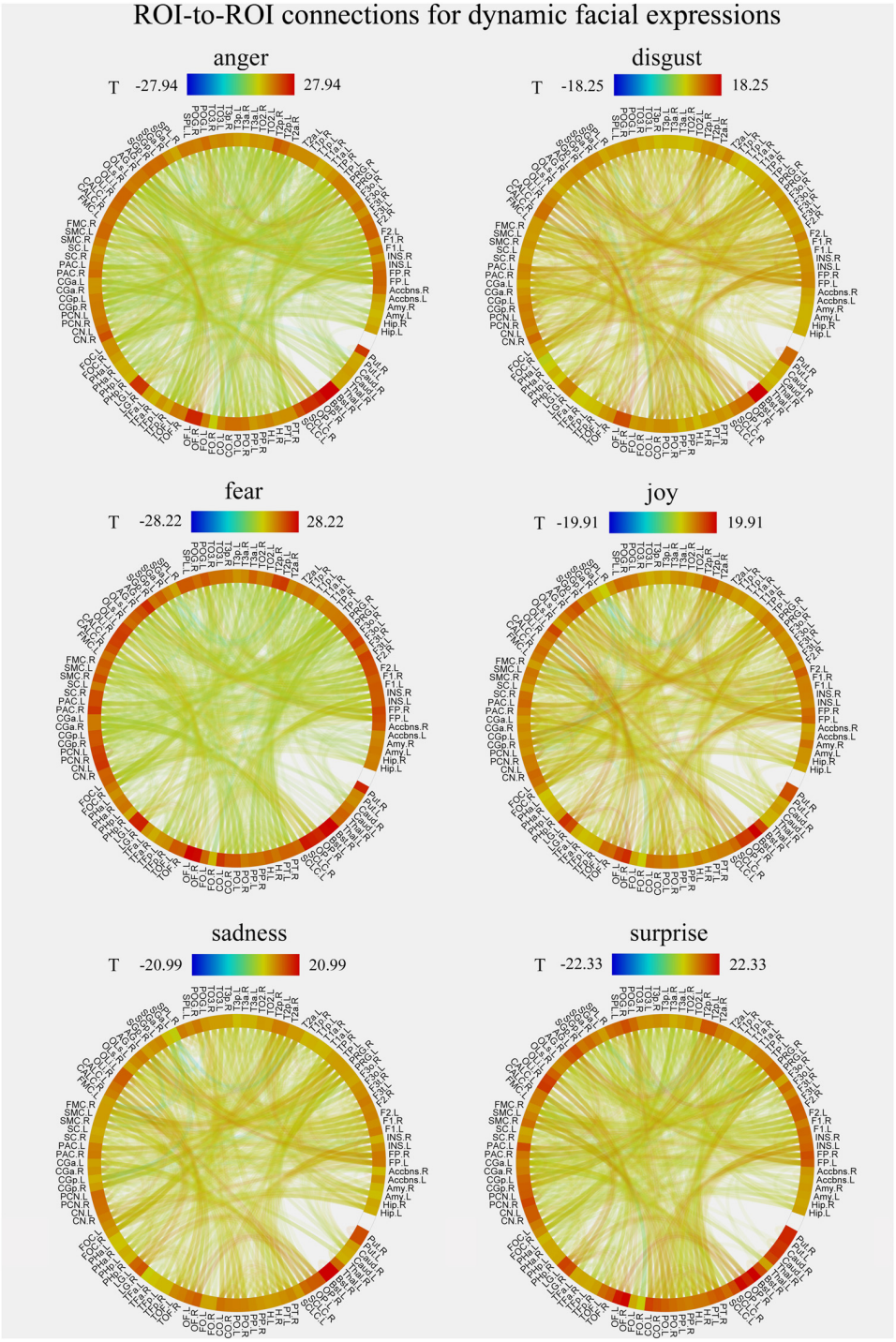


**FIGURE 5 |** Group-level results of ROI-to-ROI connections for each facial expression (anger, disgust, fear, joy, sadness, and surprise) in dynamic condition ($p < 0.001$, FDR corrected at the connection-level, two-sided). All ROIs are deriving from the Harvard-Oxford brain atlas and are labeled with the abbreviations for clarity.

undetected. Our study obtained the whole-brain FC patterns for each of the six basic expressions. Using fcMVPA, we found that expression information could be successfully decoded from the FC patterns. These results reveal that facial expression information may also be represented in the FC patterns, which add to the recently growing body of evidence for the large amount of information that the FC patterns contain for the decoding of individual brain maturity (Dosenbach et al., 2010),

object categories (Wang et al., 2016), tasks (Cole et al., 2013) and mental states (Pantazatos et al., 2012; Shirer et al., 2012). Our study further provides new evidence for the potential of the FC patterns in the facial expression decoding. To summarize, our results suggest that the FC patterns may also contain rich expression information and effectively contribute to the recognition of facial expressions.

## Expression-Discriminative Networks Contain Brain Areas Far Beyond Conventional Face-Selective Areas

Neuroscience studies on facial expressions have paid considerable attention to the face-selective areas which exhibited selectivity to facial stimuli based on traditional activation analyses. Previous fMRI studies have indicated that face-selective areas are involved in the processing of facial expressions (Fox C.J. et al., 2009; Fox M.D. et al., 2009; Trautmann et al., 2009; Foley et al., 2011; Furl et al., 2013, 2015; Johnston et al., 2013; Harris et al., 2014). In our study, we obtained compatible results. We found the involvement of the face-selective areas in both static and dynamic expression-discriminative networks. In particular, the lateral occipital cortex (inferior occipital gyrus) for the early face perception (Rotshtein et al., 2005); the temporal fusiform cortex (fusiform gyrus) for the processing of facial features and identity (Fox M.D. et al., 2009) and the superior temporal gyrus for the processing of transient facial signals (Hoffman and Haxby, 2000; Harris et al., 2014) which together constitute the "core face network," as well as a subset of brain areas in the extended face system including the amygdala, the insula and the inferior frontal gyrus that support the core system regions (Haxby et al., 2000; Fox C.J. et al., 2009; Trautmann et al., 2009; Johnston et al., 2013; Wegrzyn et al., 2015). Together, our results provide additional support for the importance of face-selective areas in the facial expression recognition with evidence from fcMVPA.

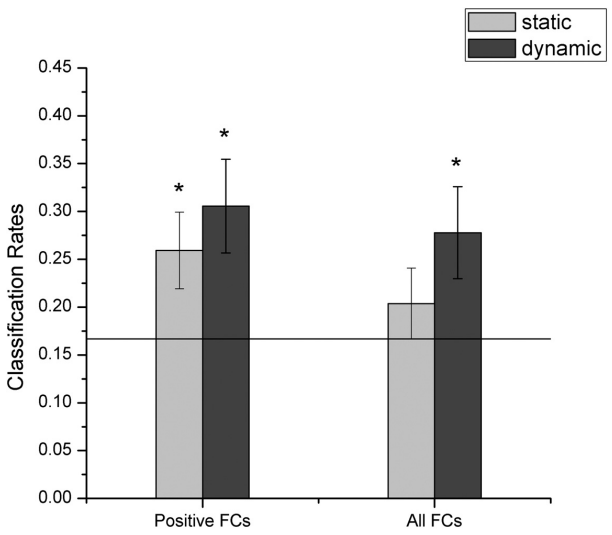


**FIGURE 6 |** Accuracies of decoding static and dynamic facial expressions using fcMVPA. The black line indicates the chance level, and all error bars indicate the SEM. *Represents statistical significance over 1000 permutation tests.

In addition, we found brain regions beyond these conventional face-selective areas participated in the expression-discriminative networks. The middle temporal gyrus, which was unanimously found sensitive to facial motion in the previous studies (Schultz and Pilz, 2009; Trautmann et al., 2009; Foley et al., 2011; Pitcher et al., 2011; Grosbras et al., 2012; Furl et al., 2013, 2015; Johnston et al., 2013; Schultz et al., 2013), was also included in our discriminative networks. Our results suggest the important role of the motion-sensitive areas in the processing of facial expressions. This is consistent with the previous evidence, which showed that motion-sensitive areas also represented expression information and contributed to the facial expression recognition (Furl et al., 2012; Liang et al., 2017). Moreover, other brain areas, which were found related to face or emotion perception in previous studies, were also included. For instance, the inferior

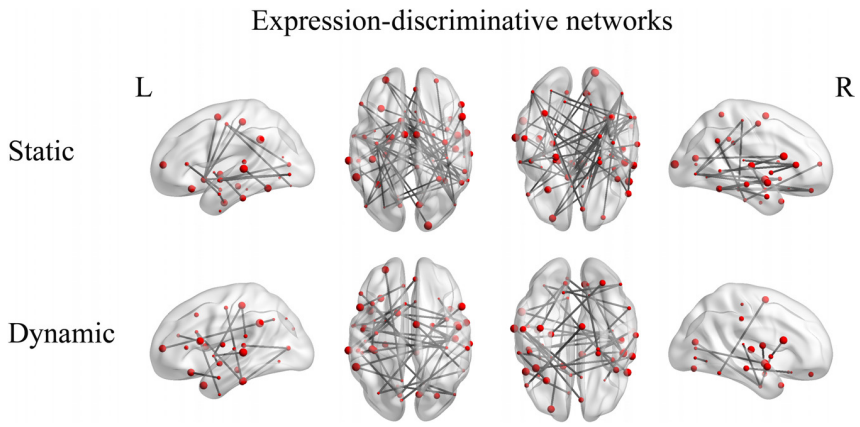


**FIGURE 7 |** Expression-discriminative networks for the static and dynamic facial expressions. The coordinates of each node are according to the Harvard-Oxford brain atlas. The brain regions are scaled by the number of their connections and the results are mapped on the cortical surfaces using BrainNet Viewer.

**TABLE 1 |** Overlapping regions across static and dynamic expression-discriminative networks.

| | Label | x | y | z |
|---|---|---|---|---|
| L | Frontal pole | −25 | 53 | 8 |
| L | Insular cortex | −36 | 1 | 0 |
| R | Insular cortex | 38 | 3 | 0 |
| L | Inferior frontal gyrus, pars triangularis | −50 | 29 | 9 |
| R | Inferior frontal gyrus, pars opercularis | 52 | 15 | 16 |
| L | Precentral gyrus | −34 | −12 | 49 |
| R | Temporal pole | 41 | 13 | −29 |
| L | Superior temporal gyrus, anterior division | −56 | −4 | −8 |
| R | Superior temporal gyrus, anterior division | 57 | −1 | −10 |
| L | Superior temporal gyrus, posterior division | −62 | −29 | 4 |
| L | Middle temporal gyrus, anterior division | −58 | −4 | −22 |
| R | Middle temporal gyrus, posterior division | 61 | −22 | −12 |
| L | Inferior temporal gyrus, anterior division | −48 | −5 | −39 |
| L | Inferior temporal gyrus, posterior division | −53 | −28 | −26 |
| R | Inferior temporal gyrus, temporooccipital part | 54 | −50 | −17 |
| L | Postcentral gyrus | −39 | −28 | 52 |
| R | Postcentral gyrus | 37 | −27 | 53 |
| L | Supramarginal gyrus, posterior division | −55 | −46 | 34 |
| R | Lateral occipital cortex, inferior division | 45 | −74 | −2 |
| L | Intracalcarine cortex | −10 | −75 | 8 |
| R | Intracalcarine cortex | 12 | −74 | 8 |
| R | Frontal medial cortex | −5 | 44 | −18 |
| R | Juxtapositional lobule cortex (formerly supplementary motor cortex) | 6 | −3 | 58 |
| R | Subcallosal cortex | 6 | 20 | −16 |
| L | Frontal orbital cortex | −30 | 24 | −16 |
| R | Parahippocampal gyrus, anterior division | 23 | −8 | −31 |
| L | Lingual gyrus | −13 | −66 | −5 |
| R | Lingual Gyrus | 14 | −63 | −5 |
| R | Temporal fusiform cortex, posterior division | −36 | −24 | −28 |
| L | Planum polare | −47 | −5 | −8 |
| R | Planum polare | 48 | −4 | −7 |
| R | Heschl's gyrus (includes H1 and H2) | 46 | −17 | 7 |
| L | Planum temporale | −53 | −30 | 11 |
| R | Planum temporale | 55 | −25 | 12 |
| R | Supracalcarine cortex | 9 | −74 | 14 |
| L | Hippocampus | −25 | −23 | −14 |
| R | Amygdala | 23 | −4 | −18 |

*The label and coordinates of each node are according to the Harvard-Oxford cortical and subcortical structural atlas.*

temporal gyrus was related to emotional processing of faces in the study of effectivity connectivity on face perception (Fairhall and Ishai, 2007); the supramarginal gyrus and parahippocampal gyrus were found preference to face category by the fcMVPA (Wang et al., 2016); the lingual gyrus was reported in response to face stimuli, independent of emotional valence (Fusar-Poli et al., 2009) and the hippocampus was conventionally considered as an emotion-related region which was involved in emotion processing, learning and memory (Amunts et al., 2005; Xia et al., 2017). Furthermore, our study showed that brain regions, such as the postcentral gyrus and the Heschl's gyrus, which were not classically considered in previous studies on facial expression perception with activation measure, were also included in the expression-discriminative networks. Together, these results suggest the potential effects of the activation-defined face-neutral regions in the recognition of facial expressions. To sum, our study showed the involvement of widespread brain regions beyond the conventional face-selective areas in the expression-discriminative networks, suggesting a potential mechanism which supports general interactive nature between distributed brain regions for the human facial expression recognition.

Moreover, it has been demonstrated a common neural substrate underlying the processing of static and dynamic facial expressions (Johnston et al., 2013). Our results support this idea with the analysis of FC, showing that a majority of common brain regions, which were involved in facial expression perception, are shared in the discriminative networks for both static and dynamic facial expressions.

In our present study, we employed comparable sample size as the previous fMRI studies on facial expression perception and MVPA-based analyses (Furl et al., 2012; Harry et al., 2013; Wegrzyn et al., 2015; Wang et al., 2016). Future studies with more samples may further improve the implementation of the classification scheme and boost the accuracy. Additionally, including of both Eastern and Western emotional expressions as stimuli in future studies could further investigate the potential cultural effect on facial expression recognition. In addition to the emotion information perceives from faces, body parts also convey emotion information (Kret et al., 2011, 2013). Therefore, further studies with comprehensive exploration of the FC patterns for both face and body emotions, investigating their similarities and differences may help to better understand human emotion perception.

## CONCLUSION

In summary, we show that expression information can be successfully decoded from the FC patterns and the expression-discriminative networks include brain regions far beyond the conventional face-selective areas identified in previous studies. Our results highlighted the important role of the FC patterns in the facial expression decoding, providing new evidence that the large-scale FC patterns may also contain rich expression

information and effectively contribute to the facial expression recognition. Our study extends the traditional research on facial expression recognition and may further the understanding of the potential mechanisms under which human brain achieve quick and accurate recognition of facial expressions.

## AUTHOR CONTRIBUTIONS

BL designed the study. YL, XL, and PW performed the experiments. YL analyzed the results and wrote the manuscript. YL and BL contributed to manuscript revision. All authors have approved the final manuscript.

## FUNDING

This work was supported by the National Natural Science Foundation of China (Nos. U1736219 and 61571327), Shandong Provincial Natural Science Foundation of China (No. ZR2015HM081), and Project of Shandong Province Higher Educational Science and Technology Program (J15LL01).

## REFERENCES

Amunts, K., Kedo, O., Kindler, M., Pieperhoff, P., Mohlberg, H., Shah, N. J., et al. (2005). Cytoarchitectonic mapping of the human amygdala, hippocampal region and entorhinal cortex: intersubject variability and probability maps. *Anat. Embryol.* 210, 343–352. doi: 10.1007/s00429-005-0025-5

Andrews, T. J., and Ewbank, M. P. (2004). Distinct representations for facial identity and changeable aspects of faces in the human temporal lobe. *Neuroimage* 23, 905–913. doi: 10.1016/j.neuroimage.2004.07.060

Axelrod, V., and Yovel, G. (2012). Hierarchical processing of face viewpoint in human visual cortex. *J. Neurosci.* 32, 2442–2452. doi: 10.1523/JNEUROSCI.4770-11.2012

Choubey, B., Jurcoane, A., Muckli, L., and Sireteanu, R. (2009). Methods for dichoptic stimulus presentation in functional magnetic resonance imaging - a review. *Open Neuroimag. J.* 3, 17–25. doi: 10.2174/1874440000903010017

Cole, M. W., Reynolds, J. R., Power, J. D., Repovs, G., Anticevic, A., and Braver, T. S. (2013). Multi-task connectivity reveals flexible hubs for adaptive task control. *Nat. Neurosci.* 16, 1348–1355. doi: 10.1038/nn.3470

Dosenbach, N. U. F., Nardos, B., Cohen, A. L., Fair, D. A., Power, J. D., Church, J. A., et al. (2010). Prediction of individual brain maturity using fMRI. *Science* 329, 1358–1361. doi: 10.1126/science.1194144

Fairhall, S. L., and Ishai, A. (2007). Effective connectivity within the distributed cortical network for face perception. *Cereb. Cortex* 17, 2400–2406. doi: 10.1093/cercor/bhl148

Fernandes, O., Portugal, L. C. L., Alves, R. C. S., Arruda-Sanchez, T., Rao, A., and Volchan, E. (2017). Decoding negative affect personality trait from patterns of brain activation to threat stimuli. *Neuroimage* 145(Pt B), 337–345. doi: 10.1016/j.neuroimage.2015.12.050

Foley, E., Rippon, G., Thai, N. J., Longe, O., and Senior, C. (2011). Dynamic facial expressions evoke distinct activation in the face perception network: a connectivity analysis study. *J. Cogn. Neurosci.* 24, 507–520. doi: 10.1162/jocn_a_00120

Fox, C. J., Iaria, G., and Barton, J. J. S. (2009). Defining the face processing network: optimization of the functional localizer in fMRI. *Hum. Brain Mapp.* 30, 1637–1651. doi: 10.1002/hbm.20630

Fox, M. D., Zhang, D., Snyder, A. Z., and Raichle, M. E. (2009). The global signal and observed anticorrelated resting state brain networks. *J. Neurophysiol.* 101, 3270–3283. doi: 10.1152/jn.90777.2008

Furl, N., Hadj-Bouziane, F., Liu, N., Averbeck, B. B., and Ungerleider, L. G. (2012). Dynamic and static facial expressions decoded from motion-sensitive areas in the macaque monkey. *J. Neurosci.* 32, 15952–15962. doi: 10.1523/JNEUROSCI.1992-12.2012

Furl, N., Henson, R. N., Friston, K. J., and Calder, A. J. (2013). Top-down control of visual responses to fear by the amygdala. *J. Neurosci.* 33, 17435–17443. doi: 10.1523/JNEUROSCI.2992-13.2013

Furl, N., Henson, R. N., Friston, K. J., and Calder, A. J. (2015). Network interactions explain sensitivity to dynamic faces in the superior temporal sulcus. *Cereb. Cortex* 25, 2876–2882. doi: 10.1093/cercor/bhu083

Fusar-Poli, P., Placentino, A., Carletti, F., Landi, P., Allen, P., Surguladze, S., et al. (2009). Functional atlas of emotional faces processing: a voxel-based meta-analysis of 105 functional magnetic resonance imaging studies. *J. Psychiatry Neurosci.* 34, 418–432.

Gobbini, M. I., Gentili, C., Ricciardi, E., Bellucci, C., Salvini, P., Laschi, C., et al. (2011). Distinct neural systems involved in agency and animacy detection. *J. Cogn. Neurosci.* 23, 1911–1920. doi: 10.1162/jocn.2010.21574

Grill-Spector, K., Knouf, N., and Kanwisher, N. (2004). The fusiform face area subserves face perception, not generic within-category identification. *Nat. Neurosci.* 7, 555–562. doi: 10.1038/nn1224

Grosbras, M.-H., Beaton, S., and Eickhoff, S. B. (2012). Brain regions involved in human movement perception: a quantitative voxel-based meta-analysis. *Hum. Brain Mapp.* 33, 431–454. doi: 10.1002/hbm.21222

Gur, R. C., Schroeder, L., Turner, T., McGrath, C., Chan, R. M., Turetsky, B. I., et al. (2002). Brain activation during facial emotion processing. *Neuroimage* 16(3 Pt 1), 651–662. doi: 10.1006/nimg.2002.1097

Harris, R. J., Young, A. W., and Andrews, T. J. (2014). Dynamic stimuli demonstrate a categorical representation of facial expression in the amygdala. *Neuropsychologia* 56, 47–52. doi: 10.1016/j.neuropsychologia.2014.01.005

Harry, B., Williams, M. A., Davis, C., and Kim, J. (2013). Emotional expressions evoke a differential response in the fusiform face area. *Front. Hum. Neurosci.* 7:692. doi: 10.3389/fnhum.2013.00692

Haxby, J. V., Hoffman, E. A., and Gobbini, M. I. (2000). The distributed human neural system for face perception. *Trends Cogn. Sci.* 4, 223–233. doi: 10.1016/S1364-6613(00)01482-0

He, C., Peelen, M. V., Han, Z., Lin, N., Caramazza, A., and Bi, Y. (2013). Selectivity for large nonmanipulable objects in scene-selective visual cortex does not require visual experience. *Neuroimage* 79, 1–9. doi: 10.1016/j.neuroimage.2013.04.051

Hoffman, E. A., and Haxby, J. V. (2000). Distinct representations of eye gaze and identity in the distributed human neural system for face perception. *Nat. Neurosci.* 3, 80–84. doi: 10.1038/71152

Hutchison, R. M., Culham, J. C., Everling, S., Flanagan, J. R., and Gallivan, J. P. (2014). Distinct and distributed functional connectivity patterns across cortex reflect the domain-specific constraints of object, face, scene, body, and tool category-selective modules in the ventral visual pathway. *Neuroimage* 96, 216–236. doi: 10.1016/j.neuroimage.2014.03.068

Ihme, K., Sacher, J., Lichev, V., Rosenberg, N., Kugel, H., Rufer, M., et al. (2014). Alexithymic features and the labeling of brief emotional facial expressions–An fMRI study. *Neuropsychologia* 64, 289–299. doi: 10.1016/j.neuropsychologia.2014.09.044

Ishai, A., Schmidt, C. F., and Boesiger, P. (2005). Face perception is mediated by a distributed cortical network. *Brain Res. Bull.* 67, 87–93. doi: 10.1016/j.brainresbull.2005.05.027

Jang, H., Plis, S. M., Calhoun, V. D., and Lee, J.-H. (2017). Task-specific feature extraction and classification of fMRI volumes using a deep neural network initialized with a deep belief network: evaluation using sensorimotor tasks. *Neuroimage* 145(Pt B), 314–328. doi: 10.1016/j.neuroimage.2016.04.003

Jin, J., Allison, B. Z., Kaufmann, T., Kűbler, A., Zhang, Y., Wang, X., et al. (2012). The changing face of P300 BCIs: a comparison of stimulus changes in a p300 BCI involving faces, emotion, and movement. *PLoS One* 7:e49688. doi: 10.1371/journal.pone.0049688

Jin, J., Allison, B. Z., Zhang, Y., Wang, X., and Cichocki, A. (2014a). An ERP-based BCI using an oddball paradigm with different faces and reduced errors in critical functions. *Int. J. Neural Syst.* 24:1450027. doi: 10.1142/S0129065714500270

Jin, J., Daly, I., Zhang, Y., Wang, X., and Cichocki, A. (2014b). An optimized ERP brain-computer interface based on facial expression changes. *J. Neural Eng.* 11:036004. doi: 10.1088/1741-2560/11/3/036004

Johnston, P., Mayes, A., Hughes, M., and Young, A. W. (2013). Brain networks subserving the evaluation of static and dynamic facial expressions. *Cortex* 49, 2462–2472. doi: 10.1016/j.cortex.2013.01.002

Kret, M. E., Pichon, S., Grèzes, J., and Gelder, B. D. (2011). Similarities and differences in perceiving threat from dynamic faces and bodies. An fMRI study. *Neuroimage* 54, 1755–1762. doi: 10.1016/j.neuroimage.2010.08.012

Kret, M. E., Stekelenburg, J. J., Roelofs, K., and de Gelder, B. (2013). Perception of face and body expressions using electromyography, pupillometry and gaze measures. *Front. Psychol.* 4:28. doi: 10.3389/fpsyg.2013.00028

Lee, L. C., Andrews, T. J., Johnson, S. J., Woods, W., Gouws, A., Green, G. G. R., et al. (2010). Neural responses to rigidly moving faces displaying shifts in social attention investigated with fMRI and MEG. *Neuropsychologia* 48, 477–490. doi: 10.1016/j.neuropsychologia.2009.10.005

Liang, Y., Liu, B., Xu, J., Zhang, G., Li, X., Wang, P., et al. (2017). Decoding facial expressions based on face-selective and motion-sensitive areas. *Hum. Brain Mapp.* 38, 3113–3125. doi: 10.1002/hbm.23578

Liu, F., Guo, W., Fouche, J.-P., Wang, Y., Wang, W., Ding, J., et al. (2015). Multivariate classification of social anxiety disorder using whole brain functional connectivity. *Brain Struct. Funct.* 220, 101–115. doi: 10.1007/s00429-013-0641-4

Meng, C., Brandl, F., Tahmasian, M., Shao, J., Manoliu, A., Scherr, M., et al. (2014). Aberrant topology of striatum's connectivity is associated with the number of episodes in depression. *Brain* 137(Pt 2), 598–609. doi: 10.1093/brain/awt290

Murphy, F. C., Nimmo-Smith, I., and Lawrence, A. D. (2003). Functional neuroanatomy of emotions: a meta-analysis. *Cogn. Affect. Behav. Neurosci.* 3, 207–233. doi: 10.3758/CABN.3.3.207

Pantazatos, S. P., Talati, A., Pavlidis, P., and Hirsch, J. (2012). Decoding unattended fearful faces with whole-brain correlations: an approach to identify condition-dependent large-scale functional connectivity. *PLoS Comput. Biol.* 8:e1002441. doi: 10.1371/journal.pcbi.1002441

Pereira, F., Mitchell, T., and Botvinick, M. (2009). Machine learning classifiers and fMRI: a tutorial overview. *Neuroimage* 45(Suppl. 1), S199–S209. doi: 10.1016/j.neuroimage.2008.11.007

Pitcher, D., Dilks, D. D., Saxe, R. R., Triantafyllou, C., and Kanwisher, N. (2011). Differential selectivity for dynamic versus static information in face-selective cortical regions. *Neuroimage* 56, 2356–2363. doi: 10.1016/j.neuroimage.2011.03.067

Rotshtein, P., Henson, R. N. A., Treves, A., Driver, J., and Dolan, R. J. (2005). Morphing Marilyn into Maggie dissociates physical and identity face representations in the brain. *Nat. Neurosci.* 8, 107–113. doi: 10.1038/nn1370

Said, C. P., Moore, C. D., Engell, A. D., Todorov, A., and Haxby, J. V. (2010). Distributed representations of dynamic facial expressions in the superior temporal sulcus. *J. Vis.* 10:11. doi: 10.1167/10.5.11

Schultz, J., Brockhaus, M., Bülthoff, H. H., and Pilz, K. S. (2013). What the human brain likes about facial motion. *Cereb. Cortex* 23, 1167–1178. doi: 10.1093/cercor/bhs106

Schultz, J., and Pilz, K. S. (2009). Natural facial motion enhances cortical responses to faces. *Exp. Brain Res.* 194, 465–475. doi: 10.1007/s00221-009-1721-9

Shirer, W. R., Ryali, S., Rykhlevskaia, E., Menon, V., and Greicius, M. D. (2012). Decoding subject-driven cognitive states with whole-brain connectivity patterns. *Cereb. Cortex* 22, 158–165. doi: 10.1093/cercor/bhr099

Smith, S. M. (2012). The future of FMRI connectivity. *Neuroimage* 62, 1257–1266. doi: 10.1016/j.neuroimage.2012.01.022

Stevens, W. D., Tessler, M. H., Peng, C. S., and Martin, A. (2015). Functional connectivity constrains the category-related organization of human ventral occipitotemporal cortex. *Hum. Brain Mapp.* 36, 2187–2206. doi: 10.1002/hbm.22764

Trautmann, S. A., Fehr, T., and Herrmann, M. (2009). Emotions in motion: dynamic compared to static facial expressions of disgust and happiness reveal more widespread emotion-specific activations. *Brain Res.* 1284, 100–115. doi: 10.1016/j.brainres.2009.05.075

van der Schalk, J., Hawk, S. T., Fischer, A. H., and Doosje, B. (2011). Moving faces, looking places: validation of the Amsterdam dynamic facial expression set (ADFES). *Emotion* 11, 907–920. doi: 10.1037/a0023853

Wang, X. S., Fang, Y. X., Cui, Z. X., Xu, Y. W., He, Y., Guo, Q. H., et al. ( (2016). Representing object categories by connections: evidence from a mutivariate connectivity pattern classification approach. *Hum. Brain Mapp.* 37, 3685–3697. doi: 10.1002/hbm.23268

Wegrzyn, M., Riehle, M., Labudda, K., Woermann, F., Baumgartner, F., Pollmann, S., et al. (2015). Investigating the brain basis of facial expression perception using multi-voxel pattern analysis. *Cortex* 69, 131–140. doi: 10.1016/j.cortex.2015.05.003

Weissenbacher, A., Kasess, C., Gerstl, F., Lanzenberger, R., Moser, E., and Windischberger, C. (2009). Correlations and anticorrelations in resting-state functional connectivity MRI: a quantitative comparison of preprocessing strategies. *Neuroimage* 47, 1408–1416. doi: 10.1016/j.neuroimage.2009.05.005

Whitfield-Gabrieli, S., and Nieto-Castanon, A. (2012). Conn: a functional connectivity toolbox for correlated and anticorrelated brain networks. *Brain Connect.* 2, 125–141. doi: 10.1089/brain.2012.0073

Winston, J. S., Henson, R. N. A., Fine-Goulden, M. R., and Dolan, R. J. (2004). fMRI-Adaptation reveals dissociable neural representations of identity and expression in face perception. *J. Neurophysiol.* 92, 1830–1839. doi: 10.1152/jn.00155.2004

Xia, Y., Zhuang, K., Sun, J., Chen, Q., Wei, D., Yang, W., et al. (2017). Emotion-related brain structures associated with trait creativity in middle children. *Neurosci. Lett.* 658, 182–188. doi: 10.1016/j.neulet.2017.08.008

Yang, X., Xu, J., Cao, L., Li, X., Wang, P., Wang, B., et al. (2018). Linear representation of emotions in whole persons by combining facial and bodily expressions in the extrastriate body area. *Front. Hum. Neurosci.* 11:653. doi: 10.3389/fnhum.2017.00653

Yovel, G., and Kanwisher, N. (2004). Face perception: domain specific, not process specific. *Neuron* 44, 889–898. doi: 10.1016/j.neuron.2004.11.018

Zhen, Z., Fang, H., and Liu, J. (2013). The hierarchical brain network for face recognition. *PLoS One* 8:e59886. doi: 10.1371/journal.pone.0059886

**Conflict of Interest Statement:** The authors declare that the research was conducted in the absence of any commercial or financial relationships that could be construed as a potential conflict of interest.

frontiers in Human Neuroscience

ORIGINAL RESEARCH
published: 19 April 2018
doi: 10.3389/fnhum.2018.00146

# Female Advantage in Automatic Change Detection of Facial Expressions During a Happy-Neutral Context: An ERP Study

*Qi Li*[1,2], *Shiyu Zhou*[3], *Ya Zheng*[3]* *and Xun Liu*[1,2]

[1]CAS Key Laboratory of Behavioral Science, Institute of Psychology, Chinese Academy of Sciences, Beijing, China, [2]Department of Psychology, University of Chinese Academy of Sciences, Beijing, China, [3]Department of Psychology, Dalian Medical University, Dalian, China

Sex differences in conscious emotional processing represent a well-known phenomenon. The present event-related potential (ERP) study examined sex differences in the automatic change detection of facial expressions, as indexed by the visual mismatch negativity (vMMN). As paid volunteers, 19 females and 19 males were presented peripherally with a passive emotional oddball sequence in a happy-neutral context and a fearful-neutral context while they performed a visual detection task in the center of the visual field. Both females and males showed comparable accuracy rates and reaction times in the primary detection task. Females relative to males showed a larger P1 for all facial expressions, as well as a more negative N170 and a less positive P2 for deviants vs. standards. During the early stage (100–200 ms), females displayed more negative vMMN responses to both happy and neutral faces than males over the occipito-temporal and fronto-central regions. During the late stage (250–350 ms), females relative to males exhibited more negative vMMN responses to both happy and neutral faces over the fronto-central and right occipito-temporal regions, but only more negative vMMN responses to happy faces over the left occipito-temporal region. In contrast, no sex differences were found for vMMN responses in the fearful-neutral context. These findings indicated a female advantage dynamically in the automatic neural processing of facial expressions during a happy-neutral context.

**Keywords: sex difference, automatic change detection, facial expression, visual mismatch negativity, pre-attentive processing**

OPEN ACCESS

***Edited by:***
*Xiaochu Zhang,*
*University of Science and Technology of China, China*

***Reviewed by:***
*Giulia Prete,*
*Università degli Studi "G. d'Annunzio" Chieti e Pescara, Italy*
*Jiang Zhongqing,*
*Liaoning Normal University, China*
*Rong Liu,*
*Capital Normal University, China*

***Correspondence:**
*Ya Zheng*
*zhengya@dmu.edu.cn*

***Received:*** *08 December 2017*
***Accepted:*** *03 April 2018*
***Published:*** *19 April 2018*

***Citation:***
*Li Q, Zhou S, Zheng Y and Liu X (2018) Female Advantage in Automatic Change Detection of Facial Expressions During a Happy-Neutral Context: An ERP Study. Front. Hum. Neurosci. 12:146. doi: 10.3389/fnhum.2018.00146*

## INTRODUCTION

Sex differences in emotional processing constitute one of well-known sex stereotypes (Grossman and Wood, 1993; Timmers et al., 2003). For example, females relative to males are more emotionally perceptive, more reactive to emotional stimuli, experience emotions with greater intensity, but are less efficient in emotion regulation (for a review, see Whittle et al., 2011). Sex differences in various aspects of emotional processing are associated with the prevalence of various emotional disorders (Gater et al., 1998; Bao and Swaab, 2010). It is vital to understand the sex difference in brain functions associated with emotional processing (Cahill, 2006; Grabowska, 2017).

Facial expression is an important tool for conveying social-emotional information, and rapid perception and interpretation of facial expression are critical for survival. The perceptual processing of facial expression has been indexed by several event-related potential (ERP) components.

The first ERP component is the P1, peaking at approximately 100 ms post stimulus onset at occipital sites. Despite inconsistencies, the effect of emotional facial expression begins as early as the P1, as reflected by larger P1 amplitudes for fearful relative to neutral or happy facial expression (for a review, see Vuilleumier and Pourtois, 2007). Following the P1 is a face-sensitive component called the N170, which is recorded about 130–200 ms post stimulus onset with an occipito-temporal distribution (Bentin et al., 1996). The N170 is enhanced for emotional relative to neutral facial expressions, including anger, fear and happy faces, and this modulation appears to be enhanced during emotion-irrelevant compared to emotion-relevant tasks (for a recent review, see Hinojosa et al., 2015). In addition, another component called the early posterior negativity (EPN) is also sensitive to emotional facial expressions. The EPN is a *relative* negativity with a posterior distribution occurring between 200–300 ms following stimulus onset and appears to reflect early automatic attention capture (Schupp et al., 2003). Recent research has demonstrated that the EPN is more negative for emotional compared to neutral faces (Marinkovic and Halgren, 1998; Rellecke et al., 2011; Itier and Neath-Tavares, 2017; Langeslag and van Strien, 2018).

In electrophysiological studies, several previous studies have demonstrated sex differences in neural responses to emotional facial expressions. For example, using an emotional oddball task, Campanella et al. (2004) found that N2b latency was delayed for happy faces compared to fearful faces in males but not in females. Another study found an enhanced P1 in response to fearful faces over the right hemisphere for female relative to male schizophrenia individuals (Lee et al., 2010). These studies indicate that sex differences in neural responses to emotional facial expressions can be reflected in the early processing stage. However, whereas almost previous studies have focused on the conscious processing of facial expressions, few studies, if any, paid attention to sex differences in the unconscious processing of facial expressions (Donges et al., 2012; Lee et al., 2017). Using a subliminal affective priming paradigm, a previous study found that females relative to males were more perceptive and responsive to happy, instead of sad, facial emotion despite the lack of conscious awareness (Donges et al., 2012). Recently, an ERP study employing a visual backward masking paradigm found that females exhibited larger P1 responses to subthreshold fearful faces than males (Lee et al., 2017). Here, we focus on one specific aspect of the unconscious processing of facial expression: the automatic change detection of facial expressions. We investigate whether females differed from males when facial expressions appeared outside of the focus of visual attention.

The automatic change detection of facial expression is associated with an ERP component called visual mismatch negativity (vMMN). As a counterpart of the auditory MNN (Näätänen et al., 2007), the vMMN is a negative-going wave with a posterior distribution that is maximal between 200–400 ms after stimulus onset (Czigler, 2007). This component is typically elicited by infrequency (deviant) stimuli embedded in a stream of frequency (standard) stimuli with differences in visual features, while participants are performing a primary task unrelated to the oddball task in order to draw their attention. Recent theories propose that the vMMN reflects a prediction error signal, i.e., the difference between a sensory input and the prediction generated by the representation of the repeated standard stimuli in transient memory (Kimura, 2012; Stefanics et al., 2014). This prediction error account has been supported not only by low-level visual features, such as color, orientation, movement, contrast and spatial frequency, but also by high-level visual properties such as facial expressions (for reviews, see Czigler, 2007; Kimura, 2012; Stefanics et al., 2014). Previous research has demonstrated that expression-related vMMN can be observed in multiple time windows (100–400 ms) over bilateral posterior occipito-temporal areas (Zhao and Li, 2006; Astikainen and Hietanen, 2009; Chang et al., 2010; Kovarski et al., 2017), together with frontal areas (Kimura et al., 2012; Stefanics et al., 2012; Liu et al., 2016). According to the prediction error model, the system that produces the expression-related vMMN automatically registers regularities in the emotional expression of unattended faces appearing outside of the focus of attention and then uses them as predictive memory representations, whereby sudden changes in emotional expressions, that is, the violation of these predictive memory representations, would orient attention to such changes for behavioral adaptation (Kimura et al., 2012; Stefanics et al., 2012).

To the best of our knowledge, only one study has investigated sex differences in the automatic change detection of facial expressions (Xu et al., 2013). Adopting schematic emotional faces, Xu et al. (2013) used an oddball task unrelated to participants' primary task (a visual detection task) and reported that females elicited a larger vMMN for sad faces than for happy faces during the early time window (120–230 ms) over the right hemisphere but not the left hemisphere. By contrast, males failed to exhibit this emotional modulation of the vMMN over both hemispheres. However, there were two limitations in that study. First, facial expressions in that study were manipulated by the direction of the mouth of schematic faces, thus preventing the conclusion of the sex differences in the automatic change detection of facial expressions from generalization. More importantly, although neutral faces were included in that study, vMMN responses to neutral facial expression were not analyzed. It thus remains unclear whether the observed sex differences were associated with emotional facial expressions specifically or facial expressions generally.

Here, this study aimed to address sex differences in the automatic change detection of facial expressions. We compared females' and males' vMMN responses to unattended rare (deviants) facial expressions delivered in a stream of frequent (standards) facial expressions (a passive emotional oddball sequence) in the visual periphery while participants were performing a primary change detection task in the center of the visual field. The primary task was employed to draw participants' attention and was independent of the passive oddball sequence. The oddball sequence included a happy-neutral context during which happy and neutral faces were used as deviants and standards in different blocks, and a fearful-neutral context during which fearful and neutral faces were used as deviants and standards in different blocks. In contrast to Xu et al. (2013) who

used schematic sad faces in their study, we employed fearful faces here since they are more representative in previous emotional vMMN studies (for a recent review, see Kovarski et al., 2017). Similar to a previous study (Stefanics et al., 2012), each stimulus screen consisted of four faces of different identity but displaying the same emotion, which were shuffled randomly around four locations in the visual periphery. This protocol allows for subtle control for low-level visual features and only high-level features, that is, the common emotional valence (happy, sad and neutral) across the four faces, can be extracted to establish and maintain predictive memory representations.

Based on previous research (Xu et al., 2013), we hypothesized that females relative to males would be more sensitive to automatic changes in emotional facial expressions, as reflected by enhanced vMMN responses. Given previous evidence of cerebral lateralization for positive and negative emotions (Prete et al., 2015a,b), sex differences in the emotional vMMN responses would possibly show a hemispheric asymmetry. No predictions were made for sex differences in neutral vMMN responses because of the lack of previous findings.

# MATERIALS AND METHODS

## Participants

As paid volunteers, 19 females ($M$ = 33.32 years, $SD$ = 7.06) and 19 males ($M$ = 31.57 years, $SD$ = 7.76) participated in the experiment. All participants were right-handed as determined by self-report. All had normal or corrected-to-normal vision and were free from psychological or neurological disorders. This study was carried out in accordance with the recommendations of the Dalian Medical University Institutional Review Board with written informed consent from all subjects. All subjects gave written informed consent in accordance with the Declaration of Helsinki. The protocol was approved by "the Dalian Medical University Institutional Review Board".

## Materials and Procedure

Emotional stimuli were images of facial expressions from 18 Chinese models (9 females and 9 males) in three expressions: happy, neutral and fearful, which were taken from the native Chinese Facial Affective Picture System (CFAPS; Gong et al., 2011). Each stimulus screen consisted of four images of faces (2 females and 2 males) expressing the same emotion (**Figure 1**). The four faces were selected from the 18 models randomly with the restriction that the face of the same individual was not presented on the next stimulus screen. The four faces were presented in the upper-left, upper-right, lower-left and lower-right part of the stimulus screen, each viewed from a distance of 0.5 m subtending a visual angle of approximately 5.73 × 8.02°. The distance of the center of each face picture from the center of the screen was 7.67° visual angle horizontally and 4.58° visual angle vertically. All faces, cropped into the shape of an ellipse, were presented with only interior characteristics being retained and were similar to one another in size, background, brightness, spatial frequency and contrast grade. Normative valence (1 = negative and 9 = positive) and arousal (1 = low intensity and 9 = high intensity) ratings from the CFAPS were assessed with separate one-way analysis of variance (ANOVA) with emotion (happy, neutral and fearful) as a within-subjects factor. For the valence ratings, there was a significant main effect, $F_{(2,34)}$ = 121.77, $p$ < 0.000001, $\eta_p^2$ = 0.88. *Post hoc* comparisons revealed that the valence-rating scores decreased as a gradient from happy ($M$ = 5.69, $SD$ = 0.88) to neutral ($M$ = 4.15, $SD$ = 0.51), and to fearful ($M$ = 2.84, $SD$ = 0.37) faces ($p$s < 0.0001). Similarly, there was a significant main effect for the arousal ratings, $F_{(2,34)}$ = 9.14, $p$ = 0.002, $\eta_p^2$ = 0.35. *Post hoc* comparisons indicated that the arousal-rating scores were higher for both happy ($M$ = 5.56, $SD$ = 0.26) and fearful ($M$ = 5.65, $SD$ = 0.58) faces than for neutral ($M$ = 5.09, $SD$ = 0.32) faces ($p$s < 0.005), with no differences between happy and fearful faces ($p$ > 0.9).

Each stimulus screen was displayed for 200 ms, following by an inter-stimulus interval of 450–650 ms. Experimental task consisted of two standard-deviant conditions (i.e., a happy-deviant-neutral-standard condition and a fearful-deviant-neutral-standard condition) and two reverse-standard-deviant conditions (i.e., a happy-standard-neutral-deviant condition and a fearful-standard-neutral-deviant condition). The presentation orders of the experimental conditions were counterbalanced across participants. Each condition included three blocks with a rest provided between blocks. In each block, ten standards were presented at the very beginning to establish sensory memory trace, and 30 deviants ($P$ = 0.18) were then delivered among 138 standards ($P$ = 0.82) in a pseudorandom way such that no less than two standards were delivered between consecutive deviants. Participants were asked to ignore the facial stimuli and to detect unpredictable changes in size of a fixation cross (0.80 × 0.80°) appearing in the center of the screen. The fixation cross became either larger (1.03 × 1.03°, 8 times) or smaller (0.57 × 0.57°, 8 times) from time to time, which never occurred simultaneously with facial stimuli. Participants were instructed to press one button when the fixation cross became larger and the other when it became smaller, with their left or right index finger as accurately and rapidly as possible. Buttons were reversed for half of the participants. This primary detection task was run to prevent participants from attending to facial stimuli. Several practice trials were provided prior to the experimental task for familiarization.

## Recording and Analysis

The EEG was recorded at 30 scalp locations using Ag/AgCl electrodes according to the extended 10–20 system (FP1, FP2, F7, F3, Fz, F4, F8, FT7, FC3, FCz, FC4, FT8, T7, C3, Cz, C4, T8, TP7, CP3, CPz, CP4, TP8, P7, P3, Pz, P4, P8, O1, Oz, O2). The EEG signals were referenced to the tip of the nose. The horizontal EOG was recorded via a pair of electrodes placed at the external canthi of each eye to monitor horizontal eye movements. The vertical EOG was recorded via a pair of electrodes placed above and below the left eye to detect vertical eye movements and blinks. The EEG and EOG were amplified and digitalized via a Neuroscan NuAmps amplifier with a band-pass of 0.1–100 Hz and a sampling rate of 500 Hz. Electrode impedance was kept under 5 KΩ throughout the experiment.

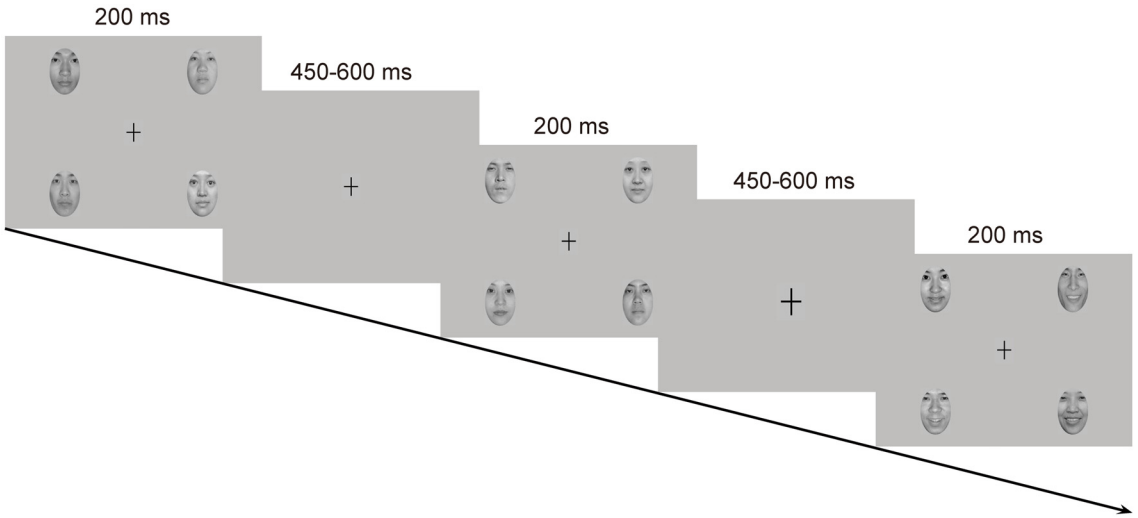


**FIGURE 1 |** Schematic representation of the passive emotional oddball sequence and the cross-change detection task.

The EEG data were analyzed using EEGLAB toolbox (Delorme and Makeig, 2004) and in-house codes under MATLAB environment (MathWorks, Natick, MA, USA). The EEG was filtered with a low-pass of 30 Hz (roll-off 6 dB/octave) and then was segmented into epochs from 100 ms pre-stimulus to 600 ms post-stimulus with the pre-stimulus activity serving as the baseline. The epoched data were screened manually for artifacts (e.g., spikes, drifts and non-biological signals) and then were entered into an informax independent component analysis (runica; Jung et al., 2001; Delorme and Makeig, 2004). Individual components were inspected and blink components were removed. The blink components in all datasets had a large EOG contribution and a frontal scalp distribution. To remove additional artifacts, a semiautomated procedure (Foti et al., 2011) was applied with artifacts defined as follows: a step more than 50 μV between sample points, a voltage difference exceeding 200 μV within a trial, or a maximum voltage difference less than 0.5 μV within 100-ms intervals. Moreover, we utilized an algorithm to remove the trials during which participants blinked while the facial stimuli were still on the screen and thus failed to process the stimuli (Lopez-Calderon and Luck, 2014). Finally, the cleaned data were averaged across trials for each condition and for each participant. Preliminary analysis on the number of the accepted ERP trials revealed no significant effects associated with sex ($ps > 0.05$) for both the happy-neutral context (happy deviants: 78 ± 6 for females and 85 ± 5 for males; happy standards: 277 ± 16 for females and 288 ± 18 for males; neutral deviants: 82 ± 5 for females and 81 ± 9 for males; neutral standards: 280 ± 14 for females and 273 ± 33 for males) and the fearful-neutral context (fearful deviants: 80 ± 8 for females and 79 ± 7 for males; fearful standards: 273 ± 20 for females and 269 ± 26 for males; neutral deviants: 82 ± 6 females and 79 ± 14 males; neutral standards: 280 ± 15 for females and 270 ± 50 for males).

Three ERP components were scored using the local-peak approach (i.e., searching for the largest point that is surrounded on both sides by smaller points) in different time windows over the occipito-temporal regions (i.e., P7 and P8): the P1 (60–130 ms), the N170 (100–200 ms), and the P2 (200–300 ms). vMMNs were created by subtracting the ERPs to standards from those to deviants, separately for the four experimental conditions. Due to the reverse manipulations, the subtractions were performed for the physically identical stimuli and thus resulted in four types of vMMNs (a happy vMMN: happy deviants minus happy standards, a neutral vMMN in the happy context: neutral deviants minus neutral standards, a fearful vMMN: fearful deviants minus fearful standards, and a neutral vMMN in the fearful context: neutral deviants minus neutral standards). Based on previous vMMN literature and the visual inspection of current waveforms, two subcomponents for each type of vMMN were scored as the mean amplitude of two time windows over the occipito-temporal (P7 and P8) and fronto-central (FCz and Cz) regions: the early vMMN (100–200 ms) and the late vMMN (250–350 ms).

Repeated measures ANOVAs were used for all statistical tests and were performed for the happy-neutral context and the fearful-neutral context, respectively. Peak amplitudes of each ERP component were analyzed using sex (male vs. female) as a between-subjects factor and type (deviant vs. standard), emotion (happy vs. neutral for the happy-neutral context; fearful vs. neutral for the fearful-neutral context), and hemisphere (left vs. right) as within-subjects factors. Peak latency results were not reported as they were less theoretically relevant to the present study. Mean amplitudes of each vMMN at occipito-temporal sites were analyzed with a Sex × Emotion × Hemisphere ANOVA. Mean amplitudes of each vMMN at fronto-central sites were analyzed with a Sex × Emotion × Site (FCz vs. Cz) ANOVA. Greenhouse-Geisser epsilon (G-GE) correction

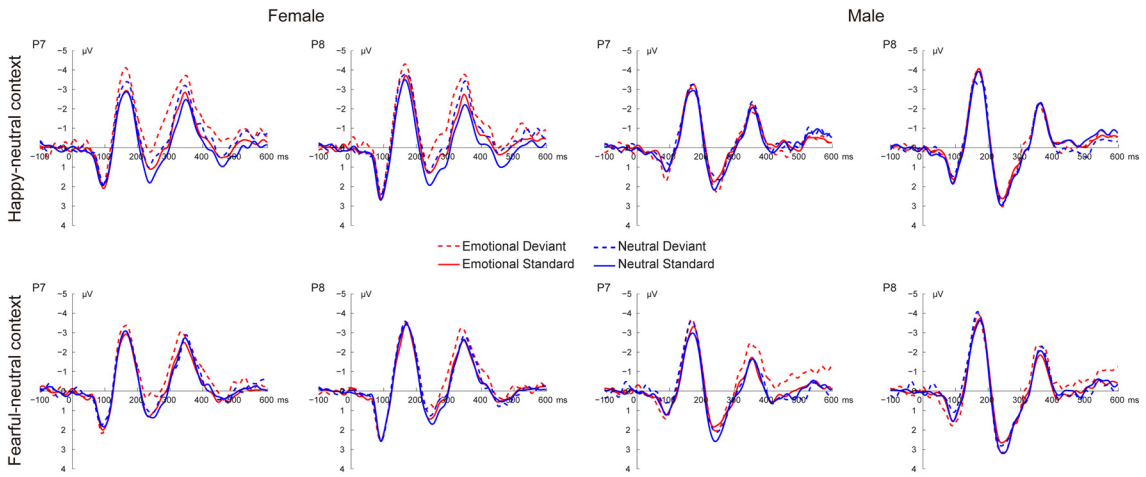


**FIGURE 2 |** Grand average event-related potential (ERP) waveforms elicited by deviant and standard facial expressions at P7 and P8 for females and males in the happy-neutral and the fearful-neutral contexts.

was applied for the violation of sphericity when necessary and Bonferroni correction was used for *post hoc* comparisons.

# RESULTS

## Behavioral Performance

Reaction times and accuracy rates for the detection of occasional changes of the fixation cross were compared between female and male groups using an independent-sample *t*-test. Both groups exhibited high accuracy rates for the change detection of the fixation cross (females: $M = 99.43\%$, $SD = 0.64$, males: $M = 99.51\%$, $SD = 0.72$), $t_{(36)} = -0.36$, $p = 0.742$. Although average reaction times were longer for female group ($M = 476.65$ ms, $SD = 56.93$) compared to male group ($M = 440.99$ ms, $SD = 64.22$), it failed to reach significance, $t_{(36)} = 1.81$, $p = 0.078$.

## Electrophysiological Data

### P1, N170 and P2 Components

**Figure 2** shows the grand average ERP waveforms at occipito-temporal sites (P7 and P8) elicited by standard and deviant stimuli for both females and males, respectively. As shown in **Figure 2**, all facial stimuli elicited the canonical P1, N170 and P2 components even when presented outside the focus of attention.

#### *The P1*

For the happy-neutral context, there was a significant main effect of sex, $F_{(1,36)} = 4.58$, $p = 0.039$, $\eta_p^2 = 0.11$, with a larger P1 for females than for males. Moreover, the P1 was enhanced over the right relative to the left hemisphere, as revealed by a significant main effect of hemisphere, $F_{(1,36)} = 7.90$, $p = 0.008$, $\eta_p^2 = 0.18$. For the fearful-neutral context, fearful faces elicited an increased P1 relative to neutral faces, $F_{(1,36)} = 4.20$, $p = 0.048$, $\eta_p^2 = 0.10$. Similarly, the main effect of sex was significant, $F_{(1,36)} = 6.24$, $p = 0.017$, $\eta_p^2 = 0.15$, due to a larger P1 for females than for males. Moreover, the P1 was larger over the right vs. the left hemisphere, $F_{(1,36)} = 7.70$, $p = 0.009$, $\eta_p^2 = 0.18$.

#### *The N170*

During the happy-neutral context, deviants elicited a larger N170 compared to standards, as revealed by a significant main effect of type, $F_{(1,36)} = 26.03$, $p < 0.0001$, $\eta_p^2 = 0.42$. This type effect was qualified by a significant two-way interaction between type and sex, $F_{(1,36)} = 8.29$, $p = 0.007$, $\eta_p^2 = 0.19$, mainly due to a larger N170 for deviants vs. standards among females ($p < 0.0001$) but not males ($p = 0.125$). With regard to the fearful-neutral context, only a significant main effect of type was obtained, $F_{(1,36)} = 12.58$, $p = 0.001$, $\eta_p^2 = 0.26$, with a larger N170 for deviants compared to standards.

#### *The P2*

For the happy-neutral context, happy relative to neutral faces elicited a less positive P2, $F_{(1,36)} = 5.73$, $p = 0.022$, $\eta_p^2 = 0.14$. Moreover, the P2 was less positive over the left compared to the right hemisphere, $F_{(1,36)} = 10.54$, $p = 0.003$, $\eta_p^2 = 0.23$. Importantly, there was a significant two-way interaction between type and sex, $F_{(1,36)} = 4.87$, $p = 0.034$, $\eta_p^2 = 0.12$. *Post hoc* comparisons revealed that deviants elicited a less positive P2 compared to standards among females ($p = 0.022$) but not males ($p = 0.477$). For the fearful-neutral context, the P2 was less positive over the left hemisphere than over the right hemisphere, $F_{(1,36)} = 7.65$, $p = 0.009$, $\eta_p^2 = 0.18$. This hemisphere effect seemed to be more pronounced for fearful faces ($p = 0.003$) relative to neutral faces ($p = 0.044$), resulting in a significant two-way interaction between emotion and hemisphere, $F_{(1,36)} = 5.95$, $p = 0.020$, $\eta_p^2 = 0.14$.

### vMMN Components

**Figures 3**, **4** present the grand average vMMNs, calculated as deviants minus standards, elicited by the physically identical

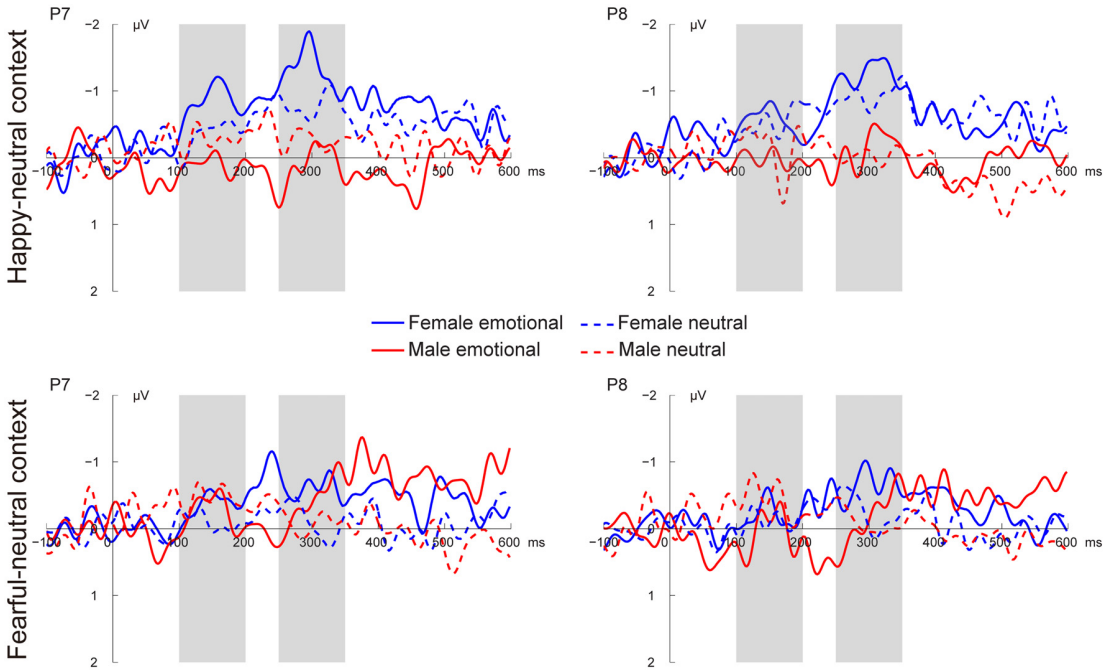


**FIGURE 3 |** Grand average visual mismatch negativity (vMMN) at occipito-temporal sites (P7 and P8) elicited by emotional and neutral facial expressions for females and males in the happy-neutral and the fearful-neutral contexts.

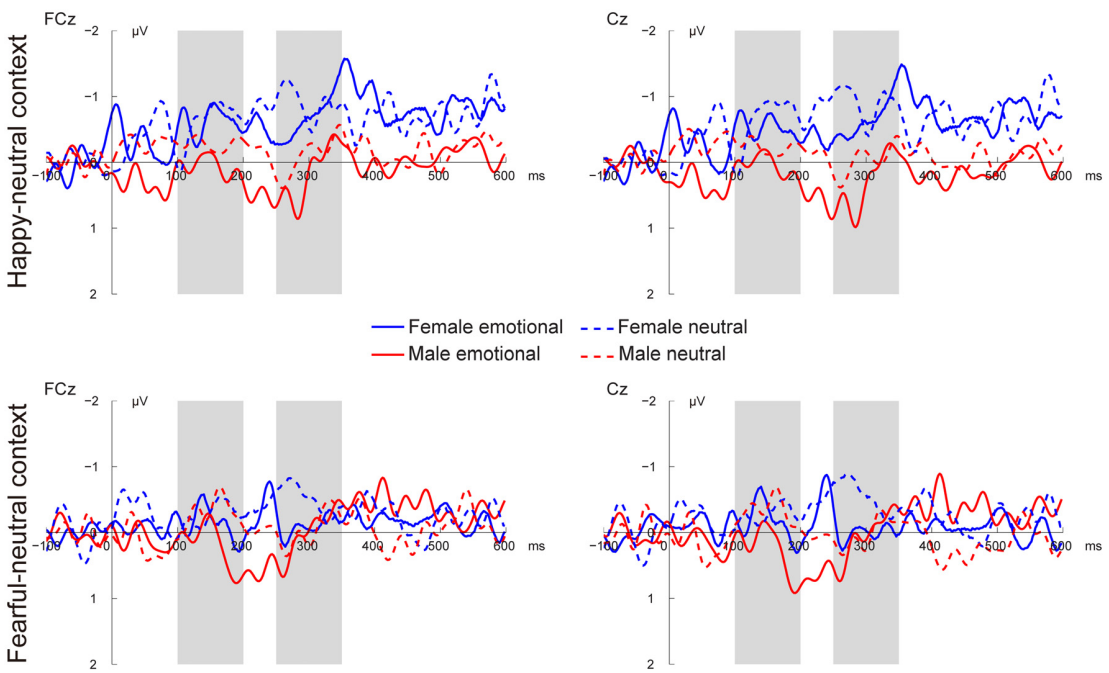


**FIGURE 4 |** Grand average vMMN at fronto-central sites (FCz and Cz) elicited by emotional and neutral facial expressions for females and males in the happy-neutral and the fearful-neutral contexts.

stimuli in the happy-neutral and fear-neutral contexts for both females and males. The topographic maps for the vMMNs are displayed in **Figure 5**, showing an occipito-temporal distribution and a fronto-central distribution in two different intervals (100–200 ms and 250–350 ms), which are consistent with previous research.

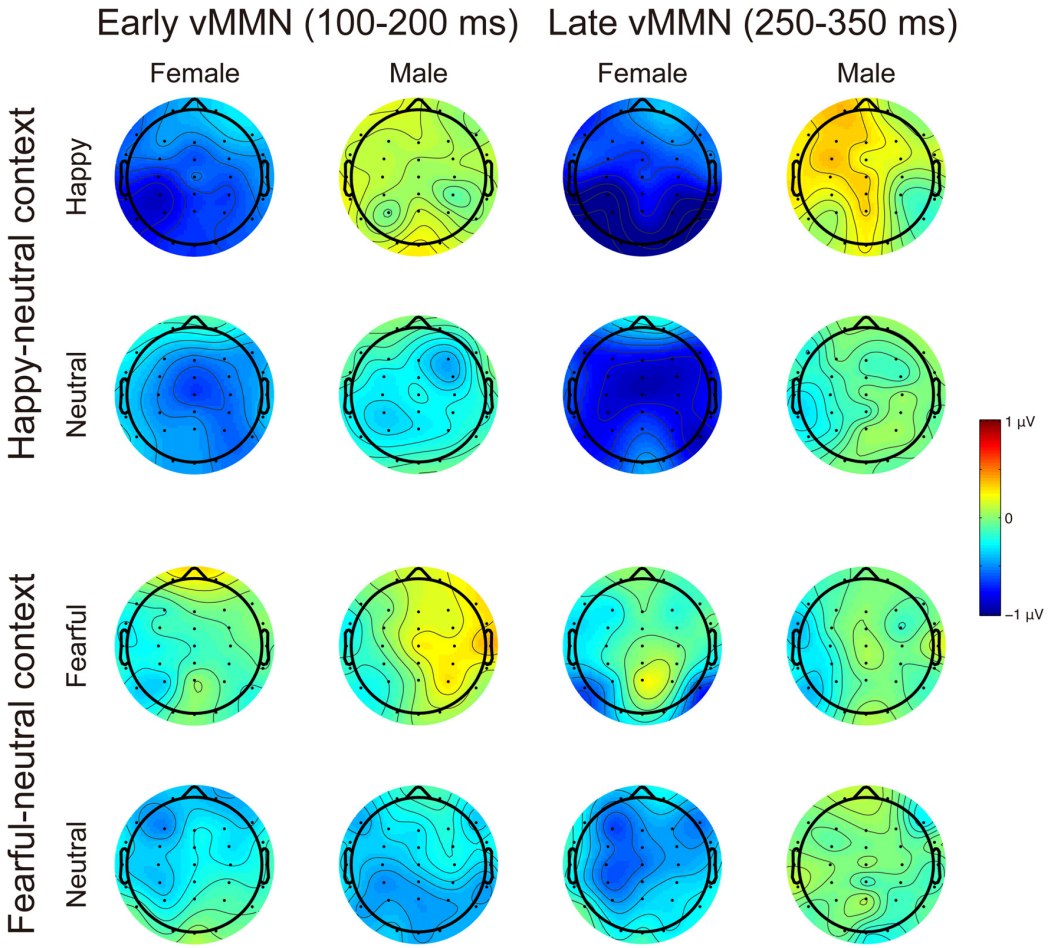


**FIGURE 5 |** Scalp topographic maps for the early (100–200 ms) and late (250–350 ms) vMMNs in response to emotional and neutral facial expressions for females and males in the happy-neutral and the fearful-neutral contexts.

### *The early vMMN*

For the happy-neutral context, females exhibited a larger vMMN than males over both the occipito-temporal regions, $F_{(1,36)} = 4.45$, $p = 0.042$, $\eta_p^2 = 0.11$, and the frontocentral regions, $F_{(1,36)} = 4.18$, $p = 0.048$, $\eta_p^2 = 0.10$. For the fearful-neutral context, no significant effects were found ($ps > 0.05$).

### *The late vMMN*

For the happy-neutral context, the main effect of sex was significant over both the occipito-temporal regions, $F_{(1,36)} = 7.59$, $p = 0.009$, $\eta_p^2 = 0.17$, and the frontal-central regions, $F_{(1,36)} = 5.94$, $p = 0.020$, $\eta_p^2 = 0.14$, with an enhanced vMMN for females compared to males. Critically, there was a significant three-way interaction of Sex × Emotion × Hemisphere over the occipito-temporal regions (**Figure 6**), $F_{(1,36)} = 4.34$, $p = 0.044$, $\eta_p^2 = 0.11$. *Post hoc* comparisons revealed that females showed more negative vMMN amplitudes compared to males over both the left ($p = 0.019$) and the right ($p = 0.032$) hemispheres for happy faces. For neutral faces, however, the sex effect was present over the right hemisphere ($p = 0.038$), but not the left hemisphere ($p = 0.194$). During the fearful-neutral context, no significant effects were found ($ps > 0.2$).

## DISCUSSION

Using a reverse-standard-deviant paradigm, the present study compared the vMMN, an index of automatic change detection, in response to unattended facial expressions between females and males. Both females and males showed comparable accuracy rates and reaction times for the detection of the unpredictable changes of the size of a fixation cross, indicating that the two groups did not differ in their overall task engagement. We found a larger P1 for females compared to males for all facial expressions. Moreover, females relative to males were more sensitive to the differences between deviants and standards in the happy-neutral context, as revealed by a more negative N170 and a less positive P2 for deviants vs. standards in females but not males. This greater sensitivity in females was further supported by vMMN findings. During the early stage (100–200 ms), females displayed more negative vMMN responses to both happy and neutral

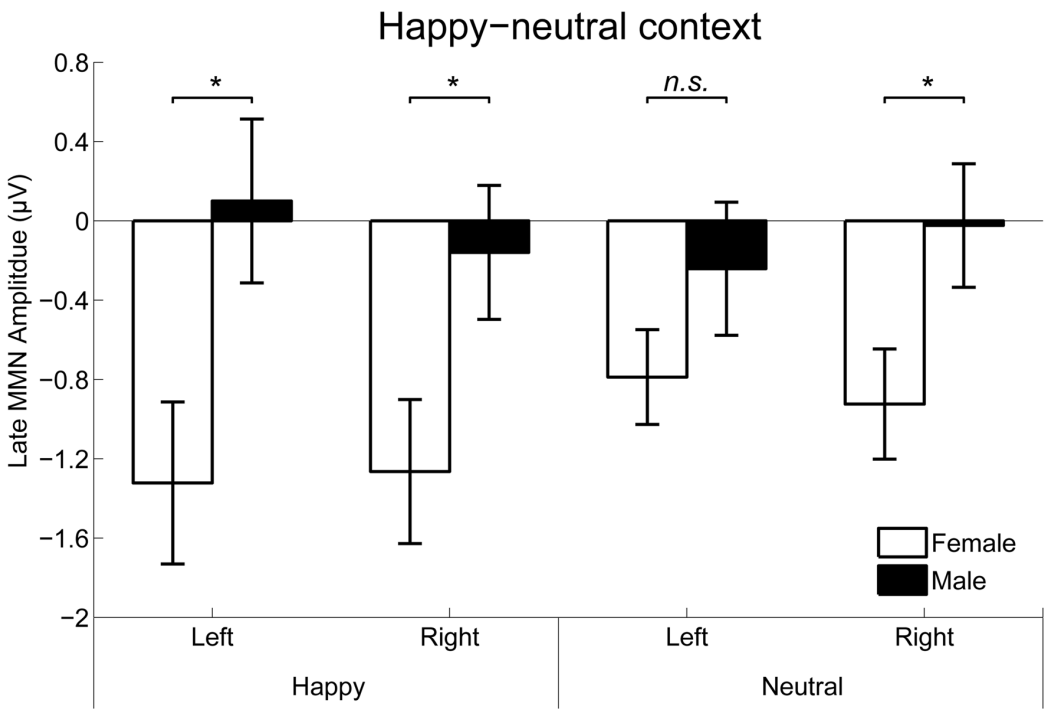


**FIGURE 6 |** The Sex × Emotion × Hemisphere interaction for the mean amplitude of the late vMMN over the occipito-temporal areas. Error bars represent standard error. $^*p < 0.05$, n.s., non-significant.

faces than males over the occipito-temporal and fronto-central regions. During the late stage (250–350 ms), females relative to males exhibited more negative vMMN responses to both happy and neutral faces over the fronto-central and right occipito-temporal regions, but only more negative vMMN responses to happy faces over the left occipito-temporal region. In contrast, no sex differences were found for vMMN responses in the fearful-neutral context.

A number of studies have demonstrated that females are more emotionally perceptive than females (Whittle et al., 2011). In the current study, we found a larger P1 for females than males for both emotional (happy and fearful) and neutral faces appearing in the visual periphery when their attention was engaged in a visual detection task in the center of the visual field. These findings are consistent with previous studies reporting a larger P1 for females vs. males (Lee et al., 2010) but extend these studies to show that sex differences could occur during non-attentional conditions. Furthermore, we found a more negative N170 and a less positive P2 for deviant facial expressions than for standard facial expressions in females but not males, which are in line with previous research (Xu et al., 2013). Moreover, the sex differences in both the N170 and P2 time windows were observed in the happy-neutral context, but not the fearful-neutral context, indicating a female advantage for processing positive emotions during non-attentional conditions.

The vMMN is thought to reflect the automatic detection of mismatches between a sensory input and the predictive memory representation generated by repeated standard stimuli (Czigler, 2007). Whereas most previous studies focused on sex differences in facial expressions on the conscious level (Whittle et al., 2011), the unconscious processing of facial expressions between females and males has been largely ignored. Given that sex differences have been reported in the early stage of facial expression processing (Campanella et al., 2004; Lee et al., 2010), it is possible that sex differences in facial expressions can occur during the pre-attentive stage. Using schematic faces, a previous study reported a larger vMMN (120–230 ms) in response to sad vs. happy faces over the right hemisphere for females, but not for males (Xu et al., 2013). In line with this study, we found that the pre-attentive processing of facial expressions was modulated by sex during the similar time window (100–200 ms). Specifically, females exhibited a greater level of vMMN responses compared to males in the occipito-temporal regions during the early processing stage, which appeared for both happy and neutral faces during the happy-neutral context. These findings suggest that females relative to males are more sensitive to the changes of both happy and neutral facial expressions during this stage. This early vMMN finding corresponded with the latency (peaking around 165 ms) and scalp topography (the occipito-temporal region) of the well-known face-sensitive N170 component, wherein females relative to males displayed larger N170 amplitudes for deviant vs. standard facial expressions during the happy-neutral context. The N170 reflects the structure encoding of faces (Bentin et al., 1996) as well as is sensitive to emotional expressions (Eimer and Holmes, 2007). It is thus possible that the early vMMN represents the visual processing of deviant and standard stimuli reflected by the N170, but these two processes cannot be differentiated in the current study.

Whereas the early vMMN findings revealed a female advantage in the automatic change detection of facial expressions, the late (250–350 ms) vMMN findings were more supportive of a female advantage in the automatic change detection of happy facial expression, rather than general facial expressions. Specifically, females compared to males exhibited a larger vMMN for both happy and neutral expressions over the fronto-central and right occipito-temporal regions, as the early vMMN did. Over the left hemisphere, however, females relative to males showed an enhanced late vMMN for happy facial expressions, with no sex differences for neutral facial expressions. Our late vMMN findings suggest that the left occipito-temporal region plays an important role in the female advantage in the automatic change detection of happy facial expressions. Supporting this idea, a well-known theory of emotional processing, the valence hypothesis, proposes that the left hemisphere is dominant for positive emotion processing whereas the right hemisphere is specialized in processing negative emotion processing (Davidson et al., 1990; Prete et al., 2015b). Indeed, using happy and fearful faces in a reverse-standard-deviant design, a previous study reported more negative vMMN responses to happy vs. fearful facial expressions over left temporal areas (Stefanics et al., 2012).

Surprisingly, we failed to find any sex differences in vMMN responses during the fearful-neutral context. There are several possible explanations about this finding. In order to elicit the vMMN, a predictive memory representation should be established by repeated standard stimuli and a violation of the predictive representation should occur. It is thus possible that the predictive memory representation failed to be generated in the fearful-neutral context. In our task, each stimulus screen consisted of two female faces and two male faces with the same expression and were shuffled randomly around four locations in the visual periphery. To generate a prediction error signal, the visual system has to extract the common feature across the four faces, that is, the emotional valence, and then establish a predictive memory representation. On the one hand, fearful faces might be more different from each other than happy faces and thus it was more difficult for participants to extract the common fearful facial expression. In consistent with this explanation, a recent theory has proposed that negative information is less similar than positive information (Alves et al., 2017). In this regards, the fearful faces might consist of more heterogeneous exemplars than the happy faces in the current study and thus were more difficult to be integrated. On the other hand, females relative to males might be more capable to discriminate fearful faces, as demonstrated in previous research (Whittle et al., 2011), such that these fearful faces were categorized on a more subtle level than happy faces in females. This appears to make it more difficult to generate a predictive memory representation in females compared to males, resulting in no sex differences observed during the fearful-neutral context. Both possibilities could be responsible for no sex differences in the fearful-neutral context. Unfortunately, they cannot be discriminated in the current study, which warrants further studies. A third possibility is linked to the possible subcortical involvement for fearful facial expressions. Specifically, convergent evidence highlights a subcortical face-detection pathway involving the superior colliculus, pulvinar and amygdala, which is especially sensitive to fearful facial expressions (for a review, see Johnson, 2005). Unfortunately, neural generators from the subcortical route are difficult, if not possible, to be detected by the scalp-recorded EEG (Luck, 2014).

## CONCLUSION

The current study investigated sex differences in the automatic detection of changes in facial expressions during a happy-neutral context and a fearful-neutral context. Females relative to males demonstrated stronger automatic processes of general facial expressions in early processing stage. During the late stage, despite a female advantage for general facial expressions over the fronto-central and right occipito-temporal regions, females exhibited a greater sensitivity to detecting pre-attentively the changes of happy facial expressions over the left occipito-temporal region than males. In addition, these sex differences were limited to the happy-neutral context, instead of the fearful-neutral context. Together, our findings revealed dynamic differences in the automatic neural processing of facial expressions between females and males in the happy-neutral context.

## AUTHOR CONTRIBUTIONS

YZ, QL and XL: conceived and designed the study. YX and SZ: data collection and analysis. QL and YZ: wrote the article.

## FUNDING

This work was supported by the National Natural Science Foundation of China (Grants 31500872 and 31571161), the National Social Science Foundation of China (Grant 14ZDB161), the Fundamental Research Program of Liaoning Higher Education Institutions (Grant LQ2017050), and CAS Key Laboratory of Behavioral Science, Institute of Psychology.

## REFERENCES

Alves, H., Koch, A., and Unkelbach, C. (2017). Why good is more alike than bad: processing implications. *Trends Cogn. Sci.* 21, 69–79. doi: 10.1016/j.tics.2016.12.006

Astikainen, P., and Hietanen, J. K. (2009). Event-related potentials to task-irrelevant changes in facial expressions. *Behav. Brain Funct.* 5:30. doi: 10.1186/1744-9081-5-30

Bao, A. M., and Swaab, D. F. (2010). Sex differences in the brain, behavior and neuropsychiatric disorders. *Neuroscientist* 16, 550–565. doi: 10.1177/1073858410377005

Bentin, S., Allison, T., Puce, A., Perez, E., and McCarthy, G. (1996). Electrophysiological studies of face perception in humans. *J. Cogn. Neurosci.* 8, 551–565. doi: 10.1162/jocn.1996.8.6.551

Cahill, L. (2006). Why sex matters for neuroscience. *Nat. Rev. Neurosci.* 7, 477–484. doi: 10.1038/nrn1909

Campanella, S., Rossignol, M., Mejias, S., Joassin, F., Maurage, P., Debatisse, D., et al. (2004). Human gender differences in an emotional visual oddball task: an event-related potentials study. *Neurosci. Lett.* 367, 14–18. doi: 10.1016/j.neulet.2004.05.097

Chang, Y., Xu, J., Shi, N., Zhang, B., and Zhao, L. (2010). Dysfunction of processing task-irrelevant emotional faces in major depressive disorder patients revealed by expression-related visual MMN. *Neurosci. Lett.* 472, 33–37. doi: 10.1016/j.neulet.2010.01.050

Czigler, I. (2007). Visual mismatch negativity: violation of nonattended environmental regularities. *J. Psychophysiol.* 21, 224–230. doi: 10.1027/0269-8803.21.34.224

Davidson, R. J., Ekman, P., Saron, C. D., Senulis, J. A., and Friesen, W. V. (1990). Approach-withdrawal and cerebral asymmetry: emotional expression and brain physiology. I. *J. Pers. Soc. Psychol.* 58, 330–341. doi: 10.1037/0022-3514.58.2.330

Delorme, A., and Makeig, S. (2004). EEGLAB: an open source toolbox for analysis of single-trial EEG dynamics including independent component analysis. *J. Neurosci. Methods* 134, 9–21. doi: 10.1016/j.jneumeth.2003.10.009

Donges, U. S., Kersting, A., and Suslow, T. (2012). Women's greater ability to perceive happy facial emotion automatically: gender differences in affective priming. *PLoS One* 7:e41745. doi: 10.1371/journal.pone.0041745

Eimer, M., and Holmes, A. (2007). Event-related brain potential correlates of emotional face processing. *Neuropsychologia* 45, 15–31. doi: 10.1016/j.neuropsychologia.2006.04.022

Foti, D., Weinberg, A., Dien, J., and Hajcak, G. (2011). Event-related potential activity in the basal ganglia differentiates rewards from nonrewards: temporospatial principal components analysis and source localization of the feedback negativity. *Hum. Brain Mapp.* 32, 2207–2216. doi: 10.1002/hbm.21182

Gater, R., Tansella, M., Korten, A., Tiemens, B. G., Mavreas, V. G., and Olatawura, M. O. (1998). Sex differences in the prevalence and detection of depressive and anxiety disorders in general health care settings: report from the World Health Organization Collaborative Study on Psychological Problems in General Health Care. *Arch. Gen. Psychiatry* 55, 405–413. doi: 10.1001/archpsyc.55.5.405

Gong, X., Huang, Y. X., Wang, Y., and Luo, Y. J. (2011). Revision of the Chinese facial affective picture system. *Chin. Ment. Health J.* 25, 40–46. doi: 10.3969/j.issn.1000-6729.2011.01.011

Grabowska, A. (2017). Sex on the brain: are gender-dependent structural and functional differences associated with behavior? *J. Neurosci. Res.* 95, 200–212. doi: 10.1002/jnr.23953

Grossman, M., and Wood, W. (1993). Sex differences in intensity of emotional experience: a social role interpretation. *J. Pers. Soc. Psychol.* 65, 1010–1022. doi: 10.1037/0022-3514.65.5.1010

Hinojosa, J. A., Mercado, F., and Carretié, L. (2015). N170 sensitivity to facial expression: a meta-analysis. *Neurosci. Biobehav. Rev.* 55, 498–509. doi: 10.1016/j.neubiorev.2015.06.002

Itier, R. J., and Neath-Tavares, K. N. (2017). Effects of task demands on the early neural processing of fearful and happy facial expressions. *Brain Res.* 1663, 38–50. doi: 10.1016/j.brainres.2017.03.013

Johnson, M. H. (2005). Subcortical face processing. *Nat. Rev. Neurosci.* 6, 766–774. doi: 10.1038/nrn1766

Jung, T. P., Makeig, S., Westerfield, M., Townsend, J., Courchesne, E., and Sejnowski, T. J. (2001). Analysis and visualization of single-trial event-related potentials. *Hum. Brain Mapp.* 14, 166–185. doi: 10.1002/hbm.1050

Kimura, M. (2012). Visual mismatch negativity and unintentional temporal-context-based prediction in vision. *Int. J. Psychophysiol.* 83, 144–155. doi: 10.1016/j.ijpsycho.2011.11.010

Kimura, M., Kondo, H., Ohira, H., and Schröger, E. (2012). Unintentional temporal context-based prediction of emotional faces: an electrophysiological study. *Cereb. Cortex* 22, 1774–1785. doi: 10.1093/cercor/bhr244

Kovarski, K., Latinus, M., Charpentier, J., Cléry, H., Roux, S., Houy-Durand, E., et al. (2017). Facial expression related vMMN: disentangling emotional from neutral change detection. *Front. Hum. Neurosci.* 11:18. doi: 10.3389/fnhum.2017.00018

Langeslag, S. J. E., and van Strien, J. W. (2018). Early visual processing of snakes and angry faces: an ERP study. *Brain Res.* 1678, 297–303. doi: 10.1016/j.brainres.2017.10.031

Lee, S. H., Kim, E. Y., Kim, S., and Bae, S. M. (2010). Event-related potential patterns and gender effects underlying facial affect processing in schizophrenia patients. *Neurosci. Res.* 67, 172–180. doi: 10.1016/j.neures.2010.03.001

Lee, S. A., Kim, C. Y., Shim, M., and Lee, S. H. (2017). Gender differences in neural responses to perceptually invisible fearful face-an ERP study. *Front. Behav. Neurosci.* 11:6. doi: 10.3389/fnbeh.2017.00006

Liu, T., Xiao, T., and Shi, J. (2016). Automatic change detection to facial expressions in adolescents: evidence from visual mismatch negativity responses. *Front. Psychol.* 7:462. doi: 10.3389/fpsyg.2016.00462

Lopez-Calderon, J., and Luck, S. J. (2014). ERPLAB: an open-source toolbox for the analysis of event-related potentials. *Front. Hum. Neurosci.* 8:213. doi: 10.3389/fnhum.2014.00213

Luck, S. J. (2014). *An Introduction to the Event-Related Potential Technique.* 2nd Edn. Cambridge, MA: MIT Press.

Marinkovic, K., and Halgren, E. (1998). Human brain potentials related to the emotional expression, repetition and gender of faces. *Psychobiology* 26, 348–356.

Näätänen, R., Paavilainen, P., Rinne, T., and Alho, K. (2007). The mismatch negativity (MMN) in basic research of central auditory processing: a review. *Clin. Neurophysiol.* 118, 2544–2590. doi: 10.1016/j.clinph.2007.04.026

Prete, G., Capotosto, P., Zappasodi, F., Laeng, B., and Tommasi, L. (2015a). The cerebral correlates of subliminal emotions: an eleoencephalographic study with emotional hybrid faces. *Eur. J. Neurosci.* 42, 2952–2962. doi: 10.1111/ejn.13078

Prete, G., Laeng, B., Fabri, M., Foschi, N., and Tommasi, L. (2015b). Right hemisphere or valence hypothesis, or both? The processing of hybrid faces in the intact and callosotomized brain. *Neuropsychologia* 68, 94–106. doi: 10.1016/j.neuropsychologia.2015.01.002

Rellecke, J., Palazova, M., Sommer, W., and Schacht, A. (2011). On the automaticity of emotion processing in words and faces: event-related brain potentials evidence from a superficial task. *Brain Cogn.* 77, 23–32. doi: 10.1016/j.bandc.2011.07.001

Schupp, H. T., Junghofer, M., Weike, A. I., and Hamm, A. O. (2003). Emotional facilitation of sensory processing in the visual cortex. *Psychol. Sci.* 14, 7–13. doi: 10.1111/1467-9280.01411

Stefanics, G., Csukly, G., Komlósi, S., Czobor, P., and Czigler, I. (2012). Processing of unattended facial emotions: a visual mismatch negativity study. *Neuroimage* 59, 3042–3049. doi: 10.1016/j.neuroimage.2011.10.041

Stefanics, G., Kremláček, J., and Czigler, I. (2014). Visual mismatch negativity: a predictive coding view. *Front. Hum. Neurosci.* 8:666. doi: 10.3389/fnhum.2014.00666

Timmers, M., Fischer, A., and Manstead, A. (2003). Ability versus vulnerability: beliefs about men's and women's emotional behaviour. *Cogn. Emot.* 17, 41–63. doi: 10.1080/02699930302277

Vuilleumier, P., and Pourtois, G. (2007). Distributed and interactive brain mechanisms during emotion face perception: evidence from functional neuroimaging. *Neuropsychologia* 45, 174–194. doi: 10.1016/j.neuropsychologia.2006.06.003

Whittle, S., Yücel, M., Yap, M. B. H., and Allen, N. B. (2011). Sex differences in the neural correlates of emotion: evidence from neuroimaging. *Biol. Psychol.* 87, 319–333. doi: 10.1016/j.biopsycho.2011.05.003

Xu, Q., Yang, Y., Wang, P., Sun, G., and Zhao, L. (2013). Gender differences in preattentive processing of facial expressions: an ERP study. *Brain Topogr.* 26, 488–500. doi: 10.1007/s10548-013-0275-0

Zhao, L., and Li, J. (2006). Visual mismatch negativity elicited by facial expressions under non-attentional condition. *Neurosci. Lett.* 410, 126–131. doi: 10.1016/j.neulet.2006.09.081

**Conflict of Interest Statement**: The authors declare that the research was conducted in the absence of any commercial or financial relationships that could be construed as a potential conflict of interest.

frontiers in Human Neuroscience

ORIGINAL RESEARCH
published: 14 May 2018
doi: 10.3389/fnhum.2018.00184

# Diagnosis of Autism Spectrum Disorders Using Multi-Level High-Order Functional Networks Derived From Resting-State Functional MRI

*Feng Zhao*[1], *Han Zhang*[2], *Islem Rekik*[3], *Zhiyong An*[1] *and Dinggang Shen*[2,4]*

[1] School of Computer Science and Technology, Shandong Technology and Business University, Yantai, China, [2] Department of Radiology and BRIC, University of North Carolina, Chapel Hill, NC, United States, [3] BASIRA Lab, CVIP Group, Computing, School of Science and Engineering, University of Dundee, Dundee, United Kingdom, [4] Department of Brain and Cognitive Engineering, Korea University, Seoul, South Korea

Functional brain networks derived from resting-state functional magnetic resonance imaging (rs-fMRI) have been widely used for Autism Spectrum Disorder (ASD) diagnosis. Typically, these networks are constructed by calculating functional connectivity (FC) between any pair of brain regions of interest (ROIs), i.e., using Pearson's correlation between rs-fMRI time series. However, this can only be called as a *low-order* representation of the functional interaction, because the relationship is investigated just between two ROIs. Brain disorders might not only affect low-order FC, but also *high-order* FC, i.e., the higher-level relationship among multiple brain regions, which might be more crucial for diagnosis. To comprehensively characterize such relationship for better diagnosis of ASD, we propose a multi-level, high-order FC network representation that can nicely capture complex interactions among brain regions. Then, we design a feature selection method to identify those discriminative multi-level, high-order FC features for ASD diagnosis. Finally, we design an ensemble classifier with multiple linear SVMs, each trained on a specific level of FC networks, for boosting the final classification accuracy. Experimental results show that the integration of both low-order and first-level high-order FC networks achieves the best ASD diagnostic accuracy (81%). We further investigated those selected discriminative low-order and high-order FC features and found that the high-order FC features can provide complementary information to the low-order FC features in the ASD diagnosis.

**Keywords: autism spectrum disorder, high-order functional connectivity, brain network, resting-state fMRI, learning-based classification**

OPEN ACCESS

***Edited by:***
*Nan Li,*
*RIKEN, Japan*

***Reviewed by:***
*Kelly Anne Barnes,*
*Baylor College of Medicine, United States*
*Xiaobo Chen,*
*Jiangsu University, China*
*Xiaosong He,*
*Thomas Jefferson University, United States*

***Correspondence:**
*Dinggang Shen*
*dgshen@med.unc.edu*

***Received:*** *18 February 2018*
***Accepted:*** *17 April 2018*
***Published:*** *14 May 2018*

***Citation:***
*Zhao F, Zhang H, Rekik I, An Z and Shen D (2018) Diagnosis of Autism Spectrum Disorders Using Multi-Level High-Order Functional Networks Derived From Resting-State Functional MRI. Front. Hum. Neurosci. 12:184. doi: 10.3389/fnhum.2018.00184*

## INTRODUCTION

Autism spectrum disorder (ASD) is a prevalent and highly heterogeneous childhood neurodevelopmental disease. It impairs children's social interaction, communication, and many other behavioral and cognitive functions in varying degrees (Ecker et al., 2010). According to the latest report released by the Centers for Disease Control and

Prevention[1], one out of 68 American children was affected by some form of ASD, an increase of 78% compared with the past decade. Accurate early diagnosis and timely intervention, especially for the infants under 12-month-old, may tremendously improve the outcome (Wolff et al., 2012; Jin et al., 2015; Zwaigenbaum et al., 2015). However, ASD is a very complex and highly heterogeneous disorder, involving many higher-level brain functions and even whole-brain structures and functions, which makes the diagnosis very challenging. To help tackle this challenge, several neuroimaging studies have used different non-invasive brain imaging modalities (Anagnostou and Taylor, 2011; Zhao et al., 2017), including structural magnetic resonance imaging (sMRI) (Wee et al., 2014a), electroencephalogram (EEG) (Duffy and Als, 2012), and diffusion tensor imaging (DTI) (Ingalhalikar et al., 2011; Gopikrishna et al., 2013), for developing computer-aided ASD diagnosis tools.

Recently, resting-state functional magnetic resonance imaging (rs-fMRI), which uses blood-oxygenation-level-dependent (BOLD) signals as a neurophysiological index to probe brain activity, has been applied to the diagnosis of ASD (Plitt et al., 2014; Price et al., 2014; Ha et al., 2015). Sensitive to the spontaneous and intrinsic neural activity, the BOLD signals can be used as effective and non-invasive measures to investigate neuropathological substrates of many neurological and psychiatric disorders at a whole-brain system level (Asghar et al., 2011; Keith et al., 2015). In particular, functional connectivity (FC), defined as the temporal correlation of the BOLD signals of different brain regions, reflect the close interactions of multiple brain regions that could be structurally segregated. In previous studies, many FC modeling methods have been proposed to construct brain functional networks, including Pearson's correlation, partial correlation, and sparse representation (Dijk et al., 2010; Wee et al., 2014b; Biao et al., 2016). However, most existing studies used Pearson's correlation for measuring FC due to its simplicity (Wee et al., 2012; Jie et al., 2014). However, the Pearson's correlation based FC networks can only capture the low-order functional relationship between two brain regions. This type of low-order FC networks may overlook more complex, high-order relationship that could be also altered in ASD children; thus, the use of additional high-order relationship may further help ASD diagnosis. Note that the high-order FC could capture the interaction among multiple brain regions, rather than simple pair-wise relationship. To date, several methods for constructing high-order FC networks have been developed (Chen et al., 2016; Wee et al., 2016; Zhang et al., 2016, 2017a,b; Zhou et al., 2018). For example, Chen et al. (2016) used sliding window approach to derive dynamic FC (time-varying FC) and then conducted additional round of Pearson's correlations ("correlation's correlation") between each pair of dynamic FC time series to build a high-order FC network. A more neurobiologically intuitive high-order FC method was proposed by Zhang et al. (2016) for more sensitive early Alzheimer's disease detection and has been adopted in other studies (Zhang et al., 2017a,b; Zhou et al., 2018). This method also uses "correlation's correlation," where the first round of correlation analysis generates regional FC topographical profiles (the FCs between one region to all other regions), which are further correlated between each pair of regions. In this way, the high-order FC represents similarity of FC topographical profiles, which supplements the traditional, BOLD-signal-synchronization-based low-order FC (Zhang et al., 2016). For more details, please refer to some previous methodological papers and clinical application papers (Chen et al., 2016; Wee et al., 2016; Zhang et al., 2016, 2017a,b; Zhou et al., 2018).

To the best of our knowledge, very few studies have used high-order FC for ASD children diagnosis. We hypothesize that brain networks in ASD children could be altered due to miswiring during abnormal development. Such miswiring could affect both low-order FC and high-order FC. Similar to the hypothesis behind Alzheimer's disease studies using high-order FC (Chen et al., 2016; Wee et al., 2016; Zhang et al., 2016, 2017b; Zhou et al., 2018), we propose that the high-order FC could be also affected in ASD and thus can be used as effective biomarkers for ASD diagnosis. There are two types of high-order FC methods previously proposed (Hansen et al., 2015; Chen et al., 2016; Wee et al., 2016; Zhang et al., 2016, 2017a,b; Glomb et al., 2017; Zhou et al., 2018). The first type of methods applied a second round of Pearson's correlation on the dynamic FC time series (Chen et al., 2016; Wee et al., 2016), but the neurological significance of the time-varying FC is still unclear and it could cause dramatically increased feature dimensionality (Zhang et al., 2016, 2017a), which could affect the robustness of classification model. The second type of methods is more straightforward (Zhang et al., 2016, 2017a,b; Zhou et al., 2018), by first calculating regional low-order FC topographical profiles (each characterizing the FC between one brain region and all other brain regions) and then using them as regional features to further compute another level of Pearson's correlation between any pair of brain regions (i.e., "correlation of correlations"). This kind of high-order FC networks could carry complementary information to the traditional low-order FC networks, and could be jointly used for improving ASD diagnosis. Theoretically, by repeating such a "correlation of correlations" analysis iteratively, one can generate many *higher-order* FC networks, each of which is derived from a precedent level of high-order FC network by computing the next higher level of correlations. Thus, it is of scientific and clinical importance to investigate (1) whether ASD diagnosis can benefit from high-order functional networks, and (2) to what extend integrating different levels of FC networks could improve the accuracy of ASD diagnosis.

To explore these hypotheses, we extend our previous works on high-order FC by proposing high(er)-order brain functional network representations at multiple levels. We then use these multi-level FC networks (with different levels of functional interactions) for a joint and better ASD diagnosis. Furthermore, we devise a generalized, multi-level high(er)-order brain networks based classification framework, which includes an ensemble of multiple classifiers, each trained using a specific level of high(er)-order FC network to capture level-specific diagnostic information. We apply our new framework to the Autism Brain Imaging Data Exchange (ABIDE) database for individual-based classification between ASD children and normal controls

[1]https://www.cdc.gov/ncbddd/autism/data.html.

(NC). **Figure 1** shows the pipeline of the proposed classification framework, which mainly includes the following four steps:

(1) Low-order FC network (*LON*) construction. We first estimate low-order FC network from the raw rs-fMRI time series. Each low-order network is represented as a correlation matrix.
(2) Multi-level high-order FC network construction. We construct the first-level of high-order FC network (represented by an "*HON-1*" matrix), with each element as the Pearson's correlation coefficient between two associated low-order FC profiles from two corresponding brain regions. We iteratively derive the second-, third- and higher-levels of higher-order networks (i.e., *HON-2*, *HON-3*, and so on) by using their respective previous level of high(er)-order FC profiles.
(3) LASSO-based feature selection. We treat the elements in the networks derived from Steps (1–2) as features for each subject. Then, LASSO algorithm (Tibshirani, 1996) is used to select multi-level high(er)-order FC features that are most relevant to the classification task.
(4) Ensemble classification. We construct an ensemble classifier with multiple linear SVM (support vector machine) classifiers (Cortes and Vapnik, 1995); each is trained using a specific level of FC features. The classification scores by all SVM classifiers are fused by weighted averaging to produce the final classification result.

The main contribution of this paper is devising a multi-level higher-order FC representation strategy to capture the interactions among brain regions at multiple levels. As such, the features generated in different levels can contain supplementary information for joint classification.

## MATERIALS AND DATA PREPROCESSING

The rs-fMRI dataset used in this study are obtained from the ABIDE database (Martino et al., 2014), which was created as a data repository for facilitating collaboration across laboratories to help accelerate scientific discovery in the autism research. To alleviate data heterogeneity, we randomly retrieved the rs-fMRI images from 54 ASD patients (47 male and 7 female) and 46 normal controls (40 male and 6 female) under 15 years of age, scanned at New York University Langone Medical Center. The detailed demographic information of the two groups, including age, gender, full-scale intelligence quotient (FIQ), and head motion (characterized by frame-wise displacement (FD)), were analyzed in **Table 1**. As we can see from **Table 1**, there were no significant differences ($p > 0.05$) in age, gender, FIQ, and FD between the normal control and ASD groups. ASD subjects were diagnosed based on the autism criteria in Diagnostic and Statistical Manual of Mental Disorders, 4th Edition, Text Revision (DSM-IV-TR) (American Psychiatric Association, 2000). More details on data collection, exclusion criteria, and scan parameters are available on the ABIDE website[2]

The subjects were scanned on a 3-Tesla Siemens Allegra scanner over 6 min, producing 180 time points at a repetition time of 2 s. In **Table 2**, we summarize main scanning parameters used in this study. The children taking psychostimulants were required to withhold the medication at least 24 h prior to the scan and subject to physician approval. During the rs-fMRI scan, most individuals were asked to relax with their eyes open, while a white cross-hair against a black background was projected on a screen. Their eye status was monitored by an eye tracker. The mean frame-wise displacement was computed to describe head motion for each individual. The individuals were excluded if their mean FD is larger than 1 mm (Lin et al., 2015; Ray et al., 2015). On the other hand, head motion effect was further corrected with the Friston 24-parameter model in the following process.

For rs-fMRI data preprocessing, we used a widely adopted Data Processing Assistant for rs-fMRI (DPARSF) toolbox (Yan and Zang, 2010). Specifically, the first 20-s data were discarded to ensure magnetization stabilization. Slice acquisition timing was

[2]http://fcon_1000.projects.nitrc.org/indi/abide/abide_I.html.

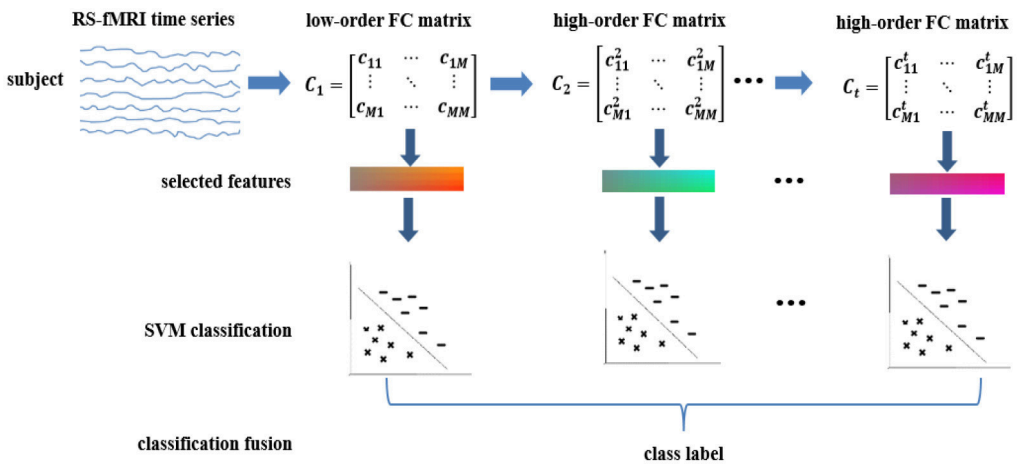


**FIGURE 1 |** Overview of the proposed multi-level high-order functional connectivity classification framework for ASD diagnosis.

**TABLE 1 |** The demographic information for ASD group and NC group.

| | Gender(M/F) | Age(years) (mean±sd) | FIQ(mean±sd) | FD(mm) (mean±sd) |
|---|---|---|---|---|
| ASD | 47/7 | 10.7 ± 2.28 | 109.41 ± 18.78 | 0.15 ± 0.07 |
| NC | 40/6 | 11.22 ± 2.34 | 114.20 ± 12.73 | 0.14 ± 0.05 |
| *p* | 0.99[a] | 0.27[b] | 0.078[b] | 0.36[b] |

*ASD, autism spectrum disorder; NC, normal control; M, male; F, female; FIQ, full scale intelligence quotient; FD, frame-wise displacement; p[a]: Statistical significance level was calculated using the $\chi^2$-test; p[b]: Statistical significance level was computed using the two-tailed two-sample t-test.)*

**TABLE 2 |** The rs-fMRI acquisition parameters.

| Parameter | Make(model) | Voxel Size | Flip Angle | TR/TE |
|---|---|---|---|---|
| **Value** | Siemens Magnetom (Allegra) | 3.0 × 3.0 × 4.0 ($mm^3$) | 90 (deg) | 2,000/15 (ms) |
| **Parameter** | **FOV read** | **Slice thickness** | **Bandwidth** | **# of Slices** |
| **Value** | 240 (mm) | 4.0 (mm) | 3906 (Hz/Px) | 33 |

corrected for each volume, followed by head motion correction (i.e., realignment) with rigid-body transformation. Then, all rs-fMRI volumes were normalized to the Montreal Neurological Institute (MNI) space and resampled to a resolution of 3 × 3 × 3 $mm^3$. Data scrubbing was further carried out to reduce the negative effect of head motion, and the volumes with FD larger than 0.5 mm were removed (Power et al., 2012), along with the preceding two time points and the following two time points. We further performed the two-tailed two-sample *t*-test on the number of volumes left after scrubbing to investigate if there exist significant difference between ASD group and NC group. We got a *p*-value of 0.19. Thus, this indicated there was no significant difference ($p > 0.05$) between the two groups in term of the number of volumes. Then, white matter, cerebral spinal fluid (CSF), global signals were regressed out as nuisance covariates. Head motion was corrected with the Friston 24-parameter model (i.e., 6 head motion parameters, 6 head motion parameters from the previous time point and the 12 corresponding squared items) to regress out head motion effects from the realigned data (Satterthwaite et al., 2013; Yan et al., 2013). Next, we parcellated the brain space into 116 regions-of-interest (ROIs) by applying the Automatic Anatomical Labeling (AAL) atlas (Tzourio-Mazoyer et al., 2002) to each image. For each ROI, we computed its mean time series and performed the band-pass filtering (0.01–0.08 Hz) for trading-off between avoiding physiological noise (Cordes et al., 2001), measurement error (Achard et al., 2008), and magnetic field drifts of the scanner (Tomasi and Volkow, 2010).

# METHODS

Because each FC network is represented as a fully-connected graph in a matrix format, we will mainly introduce how the corresponding matrices of the low-order and high-order FC networks are constructed in this section. Specifically, we first introduce how we derived the low-order FC network (*LON*) from the rs-fMRI time-series of a subject. Next, we introduce the construction strategy of *multi-level* high-order FC networks (*HON*s). Finally, the multi-level brain FC feature extraction, selection, and classification framework is described.

## Conventional Low-Order FC Network Construction

For each subject, we define $x_i \in R^M$ as the average rs-fMRI signal of all BOLD time-series signals in the voxels belonging to the *i*-th ROI. Here, *M* denotes the total number of temporal image volumes. We compute the Pearson's correlation between the *i*-th and the *j*-th ROIs as follows:

$$c_{ij} = corr(x_i, x_j) \tag{1}$$

Then, a conventional correlation-based FC network (i.e., *low-order* FC network) is generated by a corresponding symmetric matrix $C_{LON}$, as defined below:

$$C_{LON} = \left(c_{ij}\right)_{1 \le i,j \le M} \tag{2}$$

where each row or column of $C_{LON}$ denotes the Pearson correlation series between a specific ROI and all other ROIs. Each element in $C_{LON}$ is the Pearson correlation between the average time-series of a pair of ROIs *i* and *j*. Notably, $C_{LON}$ encodes low-order interactions between any pair of ROIs.

## Multi-Level High-Order FC Networks Construction

To fully capture high-order functional interactions across brain regions, we adopt a method proposed in (Zhang et al., 2016, 2017a) to generate the high-order FC networks based on "correlation's correlation." Specifically, let $c_i = (c_{i1}, c_{i2}, \cdots, c_{iM})$ denote a vector containing the correlations between the *i*-th ROI and all other ROIs. Mathematically, $c_i$ denotes the *i*-th row or column of the symmetric matrix $C_{LON}$ in Equation 2. We compute the "correlation's correlation" between the *i*-th ROI and the *j*-th ROI as follows:

$$c_{ij}^2 = corr(c_i, c_j) \tag{3}$$

where $c_i = \left(c_{i1}, \cdots, c_{i(i-1)}, c_{i(i+1)}, \cdots, c_{i(j-1)}, c_{i(j+1)}, \cdots, c_{iM}\right)$ and $c_j = \left(c_{j1}, \cdots, c_{j(i-1)}, c_{j(i+1)}, \cdots, c_{j(j-1)}, c_{j(j+1)}, \cdots, c_{iM}\right)$. $c_{ij}^2$ indicates how the FC profiles between the *i*-th ROI and all other ROIs *resemble* the FC profiles between the *j*-th ROI and all other ROIs, which can reveal more complex relationship between the FC profiles (or the vectors $\{c_i\}$), not just the original rs-fMRI time series $x_i$. As a result, the correlation $c_{ij}^2$ in Equation 3 can extract interaction information from all different ROIs, whereas the correlation $c_{ij}$ in Equation 1 involves just the two different ROIs. In other words, the correlation coefficient $c_{ij}^2$ is able to characterize more complex and abstract interaction among multiple brain regions. Thus, the corresponding matrix

$C_{HON-1}$ of the first-level of high-order FC network (*HON-1*) can be defined as follows:

$$C_{HON-1} = \left(c_{ij}^2\right)_{1\le i,j\le M} \tag{4}$$

Furthermore, for a specific subject, we can obtain multi-level FC networks by their corresponding matrix series, i.e., $\{C_{LON}, C_{HON-1}, \cdots, C_{HON-t}\}$, in a subsequent level-by-level manner, in which each matrix $C_{HON-i}$ ( $i \geq 2$) is derived from the previous-level matrix $C_{HON-(i-1)}$. In this way, higher-level connectivity features can be obtained from the low-level connectivity features, and thus form hierarchical representations of functional interactions across multiple brain regions.

## Multi-Level FC Feature Extraction, Selection and Classification

For the $l$-th subject, we use its corresponding set of multi-level FC matrices $\{C_{LON}^{(l)}, C_{HON-1}^{(l)}, \cdots, C_{HON-t}^{(l)}\}$ as raw features. Noting the symmetry of each FC matrix, we only vectorize its lower off-diagonal triangular part to define the feature vectors, i.e., $\{y_0^{(l)}, y_1^{(l)}, \cdots, y_t^{(l)}\}$, for representing the $l$-th subject. The dimensionality of $y_i^{(l)}$ $(0 \le i \le t)$ is $\frac{M(M-1)}{2}$, where $M$ denotes the number of ROIs as mentioned above.

The feature vectors $\{y_0^{(l)}, y_1^{(l)}, \cdots, y_t^{(l)}\}$ extracted from multi-level FC networks might include irrelevant or redundant features for ASD diagnosis. Therefore, feature selection is necessary. In order to select a small subset of features that are most relevant to ASD pathology, we adopt $L_1$-norm regularized least squares regression, known as LASSO (Least Absolute Shrinkage and Selection Operator) (Tibshirani, 1996), due to its simplicity and efficiency (Wee et al., 2012, 2016; Jin et al., 2015; Biao et al., 2016). Specifically, let $\omega_i = (w_{i1}, w_{i2}, \cdots, w_{id})^T$ represent the weight vector for the feature selection task and $K = \left(k_1, k_2, \cdots, k_N\right)^T$ is the class labels of $N$ training data (from $N$ training subjects). Here, $d$ is the number of features. Mathematically, the LASSO model can be described as follows:

$$\frac{1}{2}\sum_{l=1}^{N}\left\|k_l - \left(y_i^{(l)}\right)^T \omega_i\right\|_2^2 + \lambda\left\|\omega_i\right\|_1 \tag{5}$$

where $\lambda$ is a parameter for controlling the strength of $L_1$-norm regularization. The first term in Equation 5 is the empirical loss on the training data, and the second term is the $L_1 - norm$ regularization term that is used to enforce some elements of $\omega_i$ to be zero (i.e., corresponding to non-discriminative features in our classification task). In this way, we can jointly achieve classification error minimization and sparse feature selection. Let$\{\tilde{y}_0^{(l)}, \tilde{y}_1^{(l)}, \cdots, \tilde{y}_t^{(l)}\}$ denote selected features from the original feature vectors $\{y_0^{(l)}, y_1^{(l)}, \cdots, y_t^{(l)}\}$.

After selecting the most important features by LASSO, we use SVM with a linear kernel for ASD classification (Cortes and Vapnik, 1995). SVM seeks a maximum margin hyperplane to separate the samples of one class from another class. The empirical risk on training data and the complexity of the model can be balanced by the hyper-parameter $\gamma$, thus ensuring good generalization ability on the unseen data. Herein, we train an ensemble of $L$ SVM classifiers, each trained on a specific feature set $\left\{\tilde{y}_i^{(l)}\right\}_{l=1}^{L}$ $(i = 0, 1, \cdots, t)$, where $L$ denotes the number of levels used for computing different levels of functional connectivity. Then, the decision scores from all SVM models are fused linearly (by a weighting parameter $\alpha$ tuned for each SVM, $\alpha$ was selected from 0.1 to 0.9 with step 0.1) to produce the final label for the target subject. Note that we use 10-fold cross validation on the training data to evaluate the performance $\alpha$ of our algorithm for fair comparison. Hence, the value of $\alpha$ might change across cross-validated folds.

# EXPERIMENTS

For evaluation, we tested our proposed method for classifying ASD and NC subjects. We also performed feature weight analysis to identify multi-level brain connections that are most discriminative for classifying ASD and NC.

## Comparison of ASD Diagnosis Using Different Feature Types

For comparison, we used connectional brain features extracted from different orders of FC networks, including the matrix $C_{LON}$ from *LON*, $C_{HON-1}$ from *HON-1*, $C_{HON-2}$ from *HON-2*, and their combinations. We trained a set of linear SVMs based on the LIBSVM toolbox[3], each using a set of specific-level connectional features. For the case using specific-level connectional features, the output of each SVM is regarded as the final classification result. For the case of using the combination of different levels of connectional features, the final classification result is obtained by fusing decision scores from all SVMs.

In this study, we adopted a 10-fold cross-validation strategy to evaluate the generalization performance of our proposed method. Basically, all training subjects were partitioned into 10 subsets (each subset with a roughly equal sample size), and each time the samples within one subset are selected as the testing dataset, while the remaining samples in the other 9 subsets are combined together as the training dataset for feature selection and classification. Finally, we report the average accuracy of classification results across all 10 cross-validation folds.

As the performance of our method depends on a few hyper-parameters, such as $\lambda$ in the feature selection step (see Equation 5), $\gamma$ in SVM model, and $\alpha$ in the decision fusion step, it is important to fine-tune these hyper-parameters. Hence, we used a nested cross-validation on the training data to automatically identify the optimal values for these hyper-parameters within the following ranges: $\lambda \in [\mathbf{0.1}, \mathbf{0.2}, \cdots, \mathbf{0.6}]$, $\gamma \in \left[\mathbf{2^{-5}}, \mathbf{2^{-4}}, \cdots, \mathbf{2^5}\right]$, and $\alpha \in [\mathbf{0.1}, \mathbf{0.2}, \cdots, \mathbf{0.9}]$. Specifically, we further split the training set into the training subset and the validation subset and further performed another cross-validation. That is, for each combination of values for hyper-parameters, the validation subset from the training set is used for testing and the remaining training subset is used for training. This procedure was repeated

[3]https://www.csie.ntu.edu.tw/~cjlin/libsvm/.

10 times, which produced a classification accuracy under a specific combination of hyper-parameter values. Then, the hyper-parameter values with the best classification accuracy on the validation data were chosen and used to construct the optimal model based on all the training samples. The constructed model with optimized parameters was applied to the testing data.

For comprehensive evaluations, we used six different statistical measures, namely classification accuracy (ACC), sensitivity or true positive rate (TPR), specificity or true negative rate (TNR), precision or positive predictive value (PPV), negative predictive value (NPV), and F1 score[4] Higher values for these scores indicate better performance.

To avoid biased results due to the fold selection, the entire 10-fold cross-validation process was further repeated 20 times, each with a different partition of subjects. The average statistics of the 20 repetitions were finally reported. **Table 3** shows the mean classification performance for each compared feature type, where $C_{LON}$ denotes the feature derived from the low-order FC networks (*LON*) and $C_{LON} + C_{HON-1}$ denotes the combination of *LON* and *HON-1*. The meaning of the other symbols is similar. We also use the bold font to highlight the best results in the **Table 3**. At the same time, each feature type was also given a serial number for simplifying its description in the following. In order to investigate if there is any significant difference in ASD classification when different feature types were used, we performed the pair-wise *t*-test based on the 10-fold cross-validation accuracies. The *p* values at the 5% significance level are reported in **Table 4**, where each serial number denotes a different model using corresponding feature type in **Table 3**. The *p* values between the feature derived from $C_{LON} + C_{HON-1}$ and any other feature type are highlighted in bold.

As we can see from **Table 4**, there were significant differences ($p < 0.05$) in classification performance between any two different feature types. It indicates that the $C_{LON} + C_{HON-1}$ method significantly outperforms all other methods. From the results shown in **Table 3**, we can draw the following conclusions. (1) Compared with the single feature types, the combination of functional features with different orders can achieve better diagnostic accuracy. This indicates that different feature types can provide complementary information for diagnosis. (2) The combination of $C_{LON}$ and $C_{HON-1}$ achieves the best performance for all metrics, which might indicate that there exists more strongly complementary information between *LON* and $HON-1$. In contrast, other combinations of different feature types possibly include more irrelevant or redundant information, thus affecting their discriminative performance in classification.

In addition to the above ensemble learning for integrating low-order and high-order networks, we also evaluate another widely adopted strategy by firstly concatenating the features from different FC networks and then performing feature selection with LASSO and constructing a single linear SVM classification. The experimental results are shown in **Table 5**, where $\oplus$ denotes simple feature concatenation. For example, $C_{LON} \oplus C_{HON-1}$ denotes the concatenated features from the *LON* and *HON-1*. As we can see, simply concatenating the features from different types of networks only slightly improves the classification performance when compared to those using single type of brain networks (using either *LON* or *HON-1*), but is inferior to the ensemble classification (**Table 3**). The possible reason of such results is that considering different FC networks may contain information at different levels, leading to different distributions of their corresponding features. Simply concatenating the features can make the feature correlation and distribution more complex, making it difficult to capture by the traditional feature selection methods. In contrast, constructing two classifiers in respective feature space is able to avoid this problem and thus provide more reliable results.

[4]https://en.wikipedia.org/wiki/Sensitivity_and_specificity.

## The Most Discriminative Features for ASD Diagnosis

Based on the results of LASSO regression, we identified the most discriminative low-order and high-order functional features as those with the highest selection frequency across all 10-fold cross-validation runs. Note here we used the frequency of a feature to be selected in all cross-validation runs to reflect the contribution of the feature to the classification. Higher frequency indicates a larger contribution of the corresponding feature.

**Figure 2** displays the connectogram of the 10 most discriminative connections, where each connection denotes

**TABLE 3 |** ASD classification using different feature types.

| | Feature type | ACC | TPR | TNR | PPV | NPV | F1 |
|---|---|---|---|---|---|---|---|
| 1 | $C_{LON}$ | 0.73 | 0.75 | 0.70 | 0.74 | 0.72 | 0.75 |
| 2 | $C_{HON-1}$ | 0.70 | 0.73 | 0.67 | 0.70 | 0.70 | 0.71 |
| 3 | $C_{HON-2}$ | 0.67 | 0.74 | 0.64 | 0.65 | 0.74 | 0.69 |
| 4 | $C_{LON} + C_{HON-1}$ | **0.81** | **0.82** | **0.80** | **0.83** | **0.78** | **0.83** |
| 5 | $C_{LON} + C_{HON-2}$ | 0.76 | 0.77 | 0.75 | 0.80 | 0.72 | 0.78 |
| 6 | $C_{HON-1} + C_{HON-2}$ | 0.72 | 0.77 | 0.67 | 0.69 | 0.76 | 0.73 |
| 7 | $C_{LON} + C_{HON-1} + C_{HON-2}$ | 0.78 | 0.81 | 0.75 | 0.78 | **0.78** | 0.79 |

**TABLE 4 |** Significance test between different pair of feature types.

| | 2 | 3 | 4 | 5 | 6 | 7 |
|---|---|---|---|---|---|---|
| **1** | 0.044 | 0.037 | **0.018** | 0.047 | 0.049 | 0.040 |
| **2** | | 0.042 | **0.003** | 0.025 | 0.042 | 0.024 |
| **3** | | | **0.001** | 0.034 | 0.046 | 0.03 |
| **4** | | | | **0.036** | **0.024** | **0.047** |
| **5** | | | | | 0.034 | 0.049 |
| **6** | | | | | | 0.045 |

**TABLE 5 |** Classification accuracy based on simple feature concatenation.

| Feature type | ACC | TPR | TNR | PPV | NPV | F1 |
|---|---|---|---|---|---|---|
| $C_{LON} \oplus C_{HON-1}$ | 0.79 | 0.81 | 0.77 | 0.80 | 0.77 | 0.80 |
| $C_{LON} \oplus C_{HON-2}$ | 0.74 | 0.79 | 0.69 | 0.70 | 0.78 | 0.75 |
| $C_{HON-1} \oplus C_{HON-2}$ | 0.72 | 0.74 | 0.70 | 0.74 | 0.70 | 0.74 |
| $C_{LON} \oplus C_{HON-1} \oplus C_{HON-2}$ | 0.77 | 0.79 | 0.74 | 0.78 | 0.76 | 0.79 |

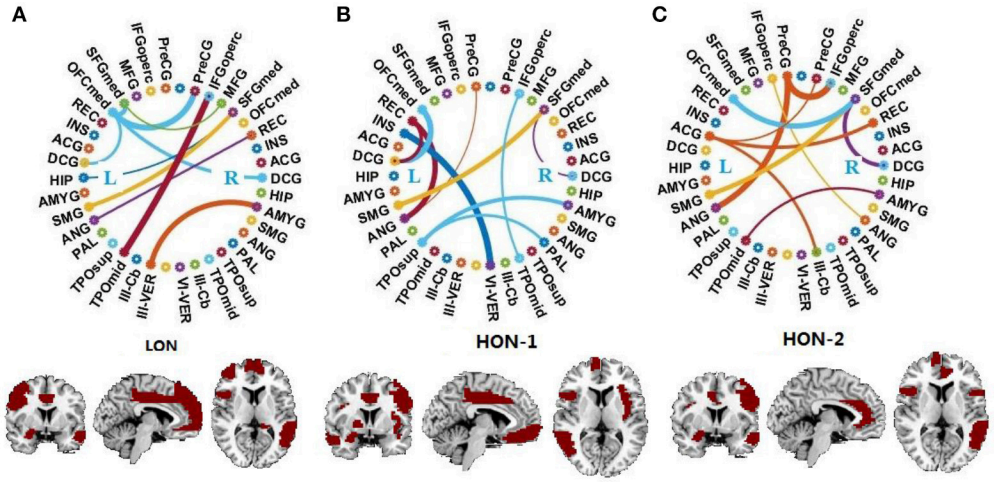


**FIGURE 2 |** Connectogram and involved brain regions of the top 10 discriminative connections selected by our framework in **(A)** the low-order FC network (*LON*), **(B)** the first-level high-order FC network *(HON-1)* and **(C)** the second-level high-order FC network *(HON-2)*, respectively. The thickness of each line reflects its selection frequency, i.e., thicker lines indicate higher selection frequency. The brain slice view shows the involved brain regions (or ROIs). The brain slices were located at (−5, 4, 9) in the standard Montreal Neurological Institute (MNI) space. For the abbreviations of brain regions, please refer to **Table 6**.

the correlation between two brain regions (Krzywinski et al., 2009). The thickness of each line reflects the frequency of being selected for the respective feature, i.e., a thicker line indicating higher frequency of being selected in all cross-validation runs. We also list the abbreviations of the selected ROIs in **Table 6**, and use the bold font to highlight the ROIs that are related to the perception of emotion, the interpretation of sensory information, language performance, and sports coordination (Herbert et al., 2005; Krzywinski et al., 2009; Ha et al., 2015).

From the results shown in **Figure 2** and **Table 6**, we derive the following conclusions. (1) It can be clearly observed that the discriminative connections and brain regions are distributed across both hemispheres and different lobes, indicating the distributed pattern of functional abnormalities over the whole brains of ASD patients. (2) The majority of brain regions with top selection frequencies, such as inferior frontal gyrus, amygdala, angular gyrus, and hippocampus, are related to social communication, emotion expression, language comprehension, and action coordination (Herbert et al., 2005; Ecker et al., 2015; Ha et al., 2015). These findings are in agreement with the behavioral phenotype of ASD (Geschwind and Levitt, 2007; American Psychiatric Association, 2013). (3) The selected features from the high-order network are largely different from those from the low-order network, indicating that different functional networks may provide complementary discriminative information for diagnosis.

**TABLE 6 |** ROIs selected from *LON*, *HON-1,* and *HON-2*.

| Abbreviation | ROI name | Abbreviation | ROI name |
|---|---|---|---|
| PreCG | Precentral gyrus | **IFGoperc** | **Inferior frontal gyrus (opercula)** |
| **MFG** | **Middle frontal gyrus** | SFGmed | Superior frontal gyrus (medial) |
| **OFCmed** | **Orbitofrontal cortex (medial)** | REC | Rectus gyrus |
| **INS** | **Insula** | **ACG** | **Anterior cingulate gyrus** |
| DCG | Middle cingulate gyrus | **HIP** | **Hippocampus** |
| **AMYG** | **Amygdala** | **SMG** | **Supramarginal gyrus** |
| **ANG** | **Angular gyrus** | **PAL** | **Pallidum** |
| **TPOsup** | **Temporal pole (superior)** | TPOmid | Temporal pole (middle) |
| VI-VER | Lobule VI of vermis | III-VER | Lobule III of vermis |
| III-Cb | Lobule III of cerebellar hemisphere | | |

## CONCLUSION

In this article, we proposed extracting multi-level high-order FC networks, derived from rs-fMRI, to capture the high-order correlation across different brain regions for ASD diagnosis. This is based on our hypothesis that different pairs of brain regions could influence each other, and their high-order correlations could contain more important discriminative information for ASD diagnosis, which is actually consistent with previous works, i.e., in Chen et al. (2016), Wee et al. (2016), Zhang et al. (2016, 2017a,b), Zhou et al. (2018). This important high-order connectivity information is overlooked in most existing methods for ASD diagnosis, which simply focused on low-order correlations between pairs of brain regions.

Experimental results have shown that (1) high-order FC networks indeed include crucial discriminant information for ASD diagnosis, and (2) the combination of different order FC networks, especially *LON* and *HON-1*, can significantly improve ASD diagnostic performance. Furthermore, we found that the most discriminative brain regions are related to episodic memory, social cognition and emotion processing.

These findings are in line with the behavioral phenotype of ASD, which is associated with several impairments of interaction, language, behavior, and cognitive functions.

Lastly, it should be noted that we used a simple feature selection method, thus the selected features may still include redundant information, which could affect our classification accuracy. Accordingly, the strategies for discriminative feature selection and fusion need further investigation, which will be investigated in our future work. In addition, it should be noted that LASSO regression tends to select only one feature from multiple highly correlated features. In the context of diagnosis, this means that, although these features could be also essentially valuable for discrimination, they might be discarded after feature selection due to the multi-collinearity in the data matrix. In this work, we mainly followed the lead of previous studies (Jin et al., 2015; Biao et al., 2016; Wee et al., 2016) and applied LASSO to select features since it has shown many merits in reducing model dimensionality and ameliorating overfitting problem. In our future work, the other features that might have been discarded but are highly correlated with those selected ones deserve dedicated investigation.

## AUTHOR CONTRIBUTIONS

All authors listed have made a substantial, direct and intellectual contribution to the work, and approved it for publication.

## ACKNOWLEDGMENTS

This work was supported in part by the National Natural Science Foundation of China (61773244, 61373079, 61672327, 61771230), the Provincial Natural Science Foundation of Shandong in China (ZR2015FL019, ZR2016FM40), Shandong Provincial Key Research and Development Program of China (2017CXGC0701), and the National Institutes of Health in USA (EB022880).

## REFERENCES

Achard, S., Bassett, D. S., Meyer-Lindenberg, A., and Bullmore, E. (2008). Fractal connectivity of long-memory networks. *Phys. Rev. E Stat. Nonlin. Soft Matter. Phys.* 77:036104. doi: 10.1103/PhysRevE.77.036104

American Psychiatric Association (2000). *Diagnostic and Statistical Manual of Mental Disorders, 4th Edn-text revision (DSMIV-TR)*. Washington, DC: American Psychiatric Association.

Anagnostou, E., and Taylor, M. J. (2011). Review of neuroimaging in autism spectrum disorders: what have we learned and where we go from here. *Mol. Autism* 2:4. doi: 10.1186/2040-2392-2-4

American Psychiatric Association (2013). *Diagnostic, and Statistical Manual of Mental Disorders, 5th Edn. (DSM-5). 2013, Text Revision.* Washington, DC: American Psychiatric Association.

Asghar, M. S., Hansen, A. E., Pedersen, S., Larsson, H. B., and Ashina, M. (2011). Pharmacological modulation of the BOLD response: a study of acetazolamide and glyceryl trinitrate in humans. *J. Magn. Resonance Imag.* 34, 921–927. doi: 10.1002/jmri.22659

Biao, J., Wee, C. Y., Shen, D. G., and Zhang, D. Q. (2016). Hyper-connectivity of functional networks for brain disease diagnosis. *Med. Image Analysis* 32, 84–100. doi: 10.1016/j.media.2016.03.003

Chen, X. B., Zhang, H., Gao, Y.,Wee, C. Y., Li, G., and Shen, D. G. (2016). High-order resting-state functional connectivity network for MCI classification. *Hum. Brain Mapp.* 37, 3282–3296. doi: 10.1002/hbm.23240

Cordes, D., Haughton, V. M., Arfanakis, K., Carew, J. D., Turski, P. A., Moritz, C. H., et al. (2001). Frequencies contributing to functional connectivity in the cerebral cortex in "resting-state" data. *Am. J. Neuroradiol.* 22, 1326–1333.

Cortes, C., and Vapnik, V. (1995). Support-vector networks. *Machine Learn.* 20, 273–297. doi: 10.1007/BF00994018

Dijk, K. V., Hedden, T., Venkataraman, A., Evans, K. C., Lazar, S. W., Buckner, R. L., et.al. (2010). Intrinsic functional connectivity as a tool for human connectomics: theory, properties, and optimization. *J. Neurophysiol.* 103, 297–321. doi: 10.1152/jn.00783.2009

Duffy, F. H., and Als, H. (2012). A stable pattern of EEG spectral coherence distinguishes children with autism from neuro-typical controls-a large case-control study. *BMC Med.* 10:64. doi: 10.1186/1741-7015-10-64

Ecker, C., Bookheimer, S. Y., and Murphy, D. G. (2015). Neuroimaging in autism spectrum disorder: brain structure and function across the lifespan. *Lancet Neurol.* 14:1211. doi: 10.1016/S1474-4422(15)00050-2

Ecker, C., Marquand, A., Mourão-Miranda, J., Johnston, P., Daly, E. M., Brammer, M. J., et al. (2010). Describing the brain in autism in five dimensions—magnetic resonance imaging-assisted diagnosis of autism spectrum disorder using a multiparameter classification approach. *J. Neurosci.* 30, 10612–10623. doi: 10.1523/JNEUROSCI.5413-09.2010

Geschwind, D. H., and Levitt, P. (2007). Autism spectrum disorders: developmental disconnection syndromes. *Curr. Opin. Neurobiol.* 17, 103–111. doi: 10.1016/j.conb.2007.01.009

Glomb, K., Ponce-Alvarez, A., Gilson, M., Ritter, P., and Deco, G. (2017). Resting state networks in empirical and simulated dynamic functional connectivity. *Neuroimage* 2017, 159–388. doi: 10.1016/j.neuroimage.2017.07.065

Gopikrishna, D., Libero, L. E., Sreenivasan, K. R., Deshpande, H. D., and Kana, R. K. (2013). Identification of neural connectivity signatures of autism using machine learning. *Front. Hum. Neurosci.* 7:670. doi: 10.3389/fnhum.2013.00670

Hansen, E., Battaglia, D., Spiegler, A., Deco, G., and Jirsa, V. K. (2015). Functional connectivity dynamics: modeling the switching behavior of the resting state. *Neuroimage* 2015, 105–525. doi: 10.1016/j.neuroimage.2014.11.001

Ha, S., Sohn, I. J., Kim, N., Sim, H. J., and Cheon, K. A. (2015). Characteristics of brains in autism spectrum disorder: structure, function and connectivity across the lifespan. *Exp. Neurobiol.* 24, 273–284. doi: 10.5607/en.2015.24.4.273

Herbert, M. R., Ziegler, D. A., Deutsch, C. K., et al. (2005). Brain asymmetries in autism and developmental language disorder: a nested whole-brain analysis. *Brain* 128, 213–226. doi: 10.1093/brain/awh330

Ingalhalikar, M., Parker, D., Bloy, L., Roberts, T. P., and Verma, R. (2011). Diffusion-based abnormality markers of pathology: toward learned diagnostic prediction of ASD. *Neuroimage* 57, 918–927. doi: 10.1016/j.neuroimage.2011.05.023

Jie, B., Zhang, D. Q., Gao, W., Wang, Q., Wee, C. Y., and Shen, D. G. (2014). Integration of network topological and connectivity properties for neuroimaging classification. *IEEE Trans. Biomed. Eng.* 61, 576–589. doi: 10.1109/TBME.2013.2284195

Jin, Y., Wee, C. Y., Shi, F., Thung, K. H., Ni, D., Yap, P. T., et al. (2015). Identification of infants at high-risk for autism spectrum disorder using multiparameter multiscale white matter connectivity networks. *Hum. Brain Mapp.* 36, 4880–4896. doi: 10.1002/hbm.22957

Keith, B., Josh, C., Jiang, B., Gokce, H., and Onder, H. (2015). Improving the precision of fMRI BOLD signal deconvolution with implications for connectivity analysis. *Magn. Resonan. Imag.* 33, 1314–1323. doi: 10.1016/j.mri.2015.07.007

Krzywinski, M., Schein, J., Birol, I., Connors, J., Gascoyne, R., Horsman, D., et al. (2009). Circos: an information aesthetic for comparative genomics. *Genome Res.* 19, 1639–1645. doi: 10.1101/gr.092759.109

Lin, H. Y., Tseng, W. Y., Lai, M. C., Matsuo, K., and Gau, S. S. (2015). Altered resting-state frontoparietal control network in children with

attention-deficit/hyperactivity disorder. *J. Int. Neuropsychol. Soc.* 21, 271–284. doi: 10.1017/S135561771500020X

Martino, A. D., Yan, C. G., Li, Q., Denio, E., Castellanos, F. X., Alaerts, K., et. al. (2014). The autism brain imaging data exchange: towards a large-scale evaluation of the intrinsic brain architecture in autism. *Mol. Psychiatry* 19, 659–667. doi: 10.1038/mp.2013.78

Plitt, M., Barnes, K. A., and Martin, A. (2014). Functional connectivity classification of autism identifies highly predictive brain features but falls short of biomarker standards. *Neuroimage Clin.* 7, 359–366. doi: 10.1016/j.nicl.2014.12.013

Power, J. D., Barnes, K. A., Snyder, A. Z., Schlaggar, B. L., and Petersen, S. E. (2012). Spurious but systematic correlations in functional connectivity MRI networks arise from subject motion. *Neuroimage* 63, 2142–2154. doi: 10.1016/j.neuroimage.2011.10.018

Price, T. C., Wee, Y., Gao, W., and Shen, D. (2014). "Multiple-network Classification of childhood autism using functional connectivity dynamics," in *International Conference on Medical Image Computing and Computer-Assisted Intervention –MICCAI* (Cambridge: Springer), 177–184.

Ray, S., Gohel, S., and Biswal, B. B. (2015). Altered functional connectivity strength in abstinent chronic cocaine smokers compared to healthy controls. *Brain Connect.* 5, 476–486. doi: 10.1089/brain.2014.0240

Satterthwaite, T. D., Elliott, M. A., Gerraty, R. T., Ruparel, K., Loughead, J., Calkins, M. E., et al. (2013). An improved framework for confound regression and filtering for control of motion artifact in the preprocessing of resting-state functional connectivity data. *Neuroimage* 64, 240–256. doi: 10.1016/j.neuroimage.2012.08.052

Tibshirani, R. (1996). Regression shrinkage and selection via the LASSO. *J. R. Stat. Soc. B* 58, 267–288.

Tomasi, D., and Volkow, N. D. (2010). Functional connectivity density mapping. *Proc. Natl. Acad. Sci. U.S.A.* 107, 9885–9890. doi: 10.1073/pnas.1001414107

Tzourio-Mazoyer, N., Landeau, B., and Papathanassiou, D., et.al (2002). Automated anatomical labeling of activations in SPM using a macroscopic anatomical parcellation of the MNI MRI single-subject brain. *Neuroimage* 15, 273–289. doi: 10.1006/nimg.2001.0978

Wee, C. Y., Wang, L., Shi, F. P.,Yap, T., and Shen, D. (2014a). Diagnosis of autism spectrum disorders using regional and interregional morphological features. *Hum. Brain Mapp.* 35, 3414–3430. doi: 10.1002/hbm.22411

Wee, C. Y., Yang, S., Yap, P. T., and Shen, D. G. (2016). Alzheimer's disease neuroimaging initiative: sparse temporally dynamic resting-state functional connectivity networks for early MCI identification. *Brain Imag. Behav.* 10, 342–356. doi: 10.1007/s11682-015-9408-2

Wee, C. Y., Yap, P. T., Zhang, D. Q., Wang, L. D., and Shen, G. (2012). "Constrained sparse functional connectivity networks for MCI classification," in *Medical Image Computing and Computer Assisted Intervention–MICCAI* (Nice: Springer), 212–219.

Wee, C. Y., Yap, P. T., Zhang, D. Q., Wang, L., and Shen, D. G. (2014b). Group-constrained sparse fMRI connectivity modeling for mild cognitive impairment identification. *Brain Struct. Funct.* 219, 641–656. doi: 10.1007/s00429-013-0524-8

Wolff, J. J., Gu, H., Gerig, G., Elison, J. T., Styner, J. T., Gouttard, S., et al. (2012). Differences in white matter fiber tract development present from 6 to 24 months in infants with autism. *Am. J. Psychiatry* 169, 589–600. doi: 10.1176/appi.ajp.2011.11091447

Yan, C. G., Cheung, B., Kelly, C., Colcombe, S., Craddock, R. C., et al. (2013). A comprehensive assessment of regional variation in the impact of head micromovements on functional connectomics. *Neuroimage* 76, 183–201. doi: 10.1016/j.neuroimage.2013.03.004

Yan, C. G., and Zang, Y. F. (2010). DPARSF: a MATLAB toolbox for "pipeline" data analysis of resting-state fMRI. *Front. Syst. Neurosci.* 4:13. doi: 10.3389/fnsys.2010.00013

Zhang, H., Chen, X. B., Shi, F., Li, G., and Kim, M. (2016). Topographical information-based high-order functional connectivity and its application in abnormality detection for mild cognitive impairment. *J. Alzheimer's Dis.* 54, 1095–1112. doi: 10.3233/JAD-160092

Zhang, H., Chen, X. B., Zhang, Y., and Shen, D. G. (2017a). Test-retest reliability of "high-order" functional connectivity in young healthy adults. *Front. Neurosci.* 11:439. doi: 10.3389/fnins.2017.00439

Zhang, Y., Zhang, H., Chen, X. B., Lee, S. W., and Shen, D. G. (2017b). Hybrid high-order functional connectivity networks using resting-state functional MRI for mild cognitive impairment diagnosis. *Sci. Rep.* 7:6530. doi: 10.1038/s41598-017-06509-0

Zhao, F. L.,Qiao, S., Shi, F., Yap, P. T., and Shen, D. G. (2017). Feature fusion via hierarchical supervised local CCA for diagnosis of autism spectrum disorder. *Brain Imag. Behav.* 11, 1050–1060. doi: 10.1007/s11682-016-9587-5

Zhou, Y. Y., Qiao, L. S., Li, W. K., Zhang, L. M., and Shen, D. G. (2018). Simultaneous estimation of low- and high-order functional connectivity for identifying mild cognitive impairment. *Front. Neuroinformat.* 12:3. doi: 10.3389/ fninf. 2018. 00003

Zwaigenbaum, L., Bauman, M. L., Stone, W. L., Yirmiya, N., Estes, A., Hansen, R. L., et al. (2015). Early Identification of autism spectrum disorder: recommendations for practice and research. *Pediatrics* 136, 41–49. doi: 10.1542/peds.2014-3667C

**Conflict of Interest Statement:** The authors declare that the research was conducted in the absence of any commercial or financial relationships that could be construed as a potential conflict of interest.

frontiers in Human Neuroscience

ORIGINAL RESEARCH
published: 15 May 2018
doi: 10.3389/fnhum.2018.00198

# Emotion-Related Consciousness Detection in Patients With Disorders of Consciousness Through an EEG-Based BCI System

*Jiahui Pan[1], Qiuyou Xie[2], Haiyun Huang[3,4], Yanbin He[2], Yuping Sun[3,4], Ronghao Yu[2] and Yuanqing Li[3,4]**

[1] School of Software, South China Normal University, Guangzhou, China, [2] Centre for Hyperbaric Oxygen and Neurorehabilitation, General Hospital of Guangzhou Military Command, Guangzhou, China, [3] School of Automation Science and Engineering, South China University of Technology, Guangzhou, China, [4] Guangzhou Key Laboratory of Brain Computer Interaction and Applications, Guangzhou, China

For patients with disorders of consciousness (DOC), such as vegetative state (VS) and minimally conscious state (MCS), detecting and assessing the residual cognitive functions of the brain remain challenging. Emotion-related cognitive functions are difficult to detect in patients with DOC using motor response-based clinical assessment scales such as the Coma Recovery Scale-Revised (CRS-R) because DOC patients have motor impairments and are unable to provide sufficient motor responses for emotion-related communication. In this study, we proposed an EEG-based brain-computer interface (BCI) system for emotion recognition in patients with DOC. Eight patients with DOC (5 VS and 3 MCS) and eight healthy controls participated in the BCI-based experiment. During the experiment, two movie clips flashed (appearing and disappearing) eight times with a random interstimulus interval between flashes to evoke P300 potentials. The subjects were instructed to focus on the crying or laughing movie clip and to count the flashes of the corresponding movie clip cued by instruction. The BCI system performed online P300 detection to determine which movie clip the patients responsed to and presented the result as feedback. Three of the eight patients and all eight healthy controls achieved online accuracies based on P300 detection that were significantly greater than chance level. P300 potentials were observed in the EEG signals from the three patients. These results indicated the three patients had abilities of emotion recognition and command following. Through spectral analysis, common spatial pattern (CSP) and differential entropy (DE) features in the delta, theta, alpha, beta, and gamma frequency bands were employed to classify the EEG signals during the crying and laughing movie clips. Two patients and all eight healthy controls achieved offline accuracies significantly greater than chance levels in the spectral analysis. Furthermore, stable topographic distribution patterns of CSP and DE features were observed in both the healthy subjects and these two patients. Our results suggest that cognitive experiments may be conducted using BCI systems in patients with DOC despite the inability of such patients to provide sufficient behavioral responses.

**Keywords: emotion recognition, disorders of consciousness (DOC), brain computer interface (BCI), P300, consciousness detection**

OPEN ACCESS

***Edited by:***
*Xiaochu Zhang, University of Science and Technology of China, China*

***Reviewed by:***
*Peng Xu, University of Electronic Science and Technology of China, China*
*Sara L. Gonzalez Andino, Geneva University Hospitals (HUG), Switzerland*

***Correspondence:**
*Yuanqing Li*
*auyqli@scut.edu.cn*

***Received:*** *26 February 2018*
***Accepted:*** *25 April 2018*
***Published:*** *15 May 2018*

***Citation:***
*Pan J, Xie Q, Huang H, He Y, Sun Y, Yu R and Li Y (2018) Emotion-Related Consciousness Detection in Patients With Disorders of Consciousness Through an EEG-Based BCI System. Front. Hum. Neurosci. 12:198. doi: 10.3389/fnhum.2018.00198*

## 1. INTRODUCTION

Patients with severe brain injury may suffer from disorders of consciousness (DOC), including coma, vegetative state (VS) and minimally conscious state (MCS). Keystones in diagnosing these disorders are the acquisition of voluntary responses, such as command following and functional communication, which indicate emergence from VS and MCS, respectively (Noirhomme et al., 2013). Currently, the clinical diagnosis of DOC patients is generally based on behavioral scales, such as the Coma Recovery Scale-Revised (CRS-R), which rely on overt motor responses to external stimuli at the time of observation (Seel et al., 2010). However, motor responses may be difficult to discern or inconsistent in this patient group, and it is becoming increasingly clear that relying on an overt behavioral response may result in misdiagnosis of a patients level of consciousness (Cruse and Owen, 2010; Coyle et al., 2017). In recent years, researchers have employed electroencephalography (EEG) and functional magnetic resonance imaging (fMRI) techniques (Owen et al., 2002; Laureys et al., 2004; Di et al., 2007; Monti et al., 2010; Cruse et al., 2012a; Li et al., 2015b; Wang et al., 2017) to detect residual brain functions and provide motor-independent evidence of consciousness in certain patients with DOC (see Noirhomme et al., 2013; Kotchoubey, 2017; Lancioni et al., 2017 for reviews).

Emotion recognition is an important brain function associated with many cognitive functions, including selective attention, working memory, language abilities, and decision making (Kohler et al., 2000; Molina et al., 2009). Several neuroimaging and electrophysiological studies have proposed probing the neural machanism of emotion recognition. For instance, fMRI findings have suggested that the amygdala and the orbitofrontal cortex are key areas in the brains emotion recognition system. Two important mechanisms for emotion recognition are constructing a simulation of the emotion observed in the perceiver and modulating sensory cortices through top-down influences (Adolphs, 2002). Many studies have also reported that injury sites in neurological patients could result in deficits in emotion recognition. For instance, some patients who suffer from stroke have shown difficulties in emotion recognition, that are more frequently observed in individuals with right brain damage than in those with left brain damage (Yuvaraj et al., 2013). Several studies have also reported emotion recognition deficits in patients with schizophrenia (Kohler et al., 2000; Taylor and Iii, 2012; Kayser et al., 2014; Corcoran et al., 2015; Bilgi et al., 2017), and the results have suggested that impairments in auditory, olfactory, or visual function may lead to deficits in emotion recognition. Furthermore, emotion recognition tasks have been included in the Functional Emotional Assessment Scale (FEAS), the Development Neuropsychological Assessment-II (NEPSY-II) and the Montreal Cognitive Assessment (MoCA), which are commonly used to evaluate cognitive impairments in patients with schizophrenia, attention deficit hyperactivity disorder (ADHD), and Parkinsons disease (Solomon et al., 2007; Marneweck and Hammond, 2014; Pitzianti et al., 2017). However, emotion recognition tasks do not include in the clinical behavioral scales such as the CRS-R for patients with DOC. Thus far, whether patients with DOC can recognize emotion remains unknown. One possible reason is that these DOC patients who are severely lack of motor ability cannot provide sufficient motor responses for emotion recognition-based behavioral experiments. By exploring emotion recognition in patients with DOC, we may be able to more thoroughly evaluate residual cognitive functions and determine the extent to which the multiple brain functions associated with emotion recognition are impaired after severe brain injury.

Brain-computer interfaces (BCIs) allow non-muscular communication and control by directly translating brain activities into computer control signals, thereby enabling users with motor disabilities to convey their intent to the external world (McFarland and Wolpaw, 2004). Therefore, BCIs may allow the exploration of residual cognition functions, such as emotion recognition, in patients with DOC. Recently, several BCI paradigms have been proposed for patients with DOC (Coyle et al., 2012; Lulé et al., 2012; Müller-Putz et al., 2012, 2013; Gibson et al., 2016; Wang et al., 2017). Lulé et al. (2012) used a 4-choice auditory P300-based BCI system to detect consciousness in 13 MCS, 3 VS and 2 locked-in syndrome (LIS) patients. Among the 18 DOC patients, one LIS patient presented significant accuracy 60%. Coyle and his colleagues (Coyle et al., 2015) developed a motor imagery-based BCI with auditory or visual feedback to detect consciousness in 4 MCS patients. The results indicated that all four patients had the capacity to use a simple BCI system with a peak mean classification accuracy above 70%. In our previous study (Pan et al., 2014), a visual hybrid P300 and steady-state visual evoked potentials (SSVEPs) BCI was developed to detect consciousness in eight patients with DOC (4 VS, 3 MCS, and 1 LIS), and three of them (1 VS, 1 MCS, and 1 LIS) achieved BCI accuracies significantly higher than the chance level. However, BCI-based consciousness detection systems for use by patients with DOC remain in their infancy. The performance of BCIs designed for DOC patients is generally poor due to their limited cognitive levels. Furthermore, because patients with DOC have suffered from severe brain injuries, large differences in EEG signals exist between these patients and healthy individuals. Thus, researchers strive to develop novel BCIs to improve the performance of consciousness detection.

Recent studies have validated that the accuracy and speed of BCIs can be improved by the emotion elicitation techniques and emotion-related processing (see Molina et al., 2009 for review). For instance, it has been shown that stimuli containing an affective component elicit latency and amplitude differences in the characteristic peaks of event-related potentials (ERPs), which can enhance the electrophysiological sources of control used in BCI systems (Kayser et al., 2000). To date, mirror neuron system (MNS)-based emotion elicitation techniques have been widely used. According to MNS mechanism, simple observation of emotional facial expressions done by another individuals might evoked the same brain activity as if they experienced the corresponding emotion themselves (Petrantonakis and Hadjileontiadis, 2011). Furthermore, many studies have focused on the EEG-based emotion recognition in healthy individuals. The power spectra of EEGs have also been assessed in different

frequency bands to examine their relationships with emotional states (Wang et al., 2014). Previous studies have reported several spectral power changes in various brain regions that have been associated with emotional responses; these changes have included theta (4–7 Hz) power changes at the right parietal lobe (Aftanas et al., 2004), alpha (8–13 Hz) power asymmetry at anterior areas of the brain (Allen et al., 2004), beta (14–30 Hz) power asymmetry at the parietal region (Schutter et al., 2001), and gamma (31–50 Hz) power changes at the right parietal regions (Li and Lu, 2009). Lin et al. reported an offline accuracy of 82.29% by using spectral power asymmetries across multiple frequency bands as features and a support vector machine (SVM) classifier to characterize EEG signals into four emotional states during music listening (Lin et al., 2010). Lv and colleagues investigated stable EEG patterns for emotion recognition using a graph regularized extreme learning machine (GELM) (Zheng et al., 2016). They found that the GELM with differential entropy (DE) features obtained average classification accuracies of 69.67% for the DEAP dataset and 91.07% for their SEED dataset based on 5-fold cross-validations. In our previous study (Pan et al., 2016), we employed facial expression pictures to develop an EEG-based BCI system for emotion recognition of happiness and sadness, and we achieved an average online accuracy of 87.5% using an SVM with common spatial pattern (CSP) features. To the best of our knowledge, emotion recognition, which is expected to be impaired to a certain degree, has not been studied in patients with DOC.

Considering the abovementioned factors, we proposed an EEG-based BCI system for the detection of consciousness in patients with DOC. Eight patients with DOC (3 VS and 5 MCS patients) and eight healthy controls participated in the BCI-based experiment. During the experiment, two movie clips flashed (appearing and disappearing) eight times with a random interstimulus interval to evoke P300 potentials. As the movie clip flashed, the corresponding spoken sound was simultaneously played. The subjects were instructed to focus on the crying or laughing movie clip and to count the flashes of the corresponding movie clip cued by the delivered instruction. The BCI system performed online P300 detection to determine which movie clip the patients attended to and presented the result as feedback. Three of the eight patients achieved online accuracies based on P300 detection that were significantly greater than chance level. Emotion recognition and the ability to follow commands were demonstrated in these three patients. Through the spectral analysis, CSP and DE features in the delta, theta, alpha, beta, and gamma frequency bands were employed to classify the EEG signals during the crying and laughing movie clips. Two patients and all eight healthy controls achieved offline accuracies significantly greater than chance level in the offline spectral analysis. Additionally, stable topographic distribution patterns of CSP and DE features were observed in both the healthy subjects and these two patients. Our results suggest that cognitive experiments may be conducted using BCI systems in patients with DOC despite the inability of such patients to provide sufficient behavioral responses.

# 2. METHODS

## 2.1. Subjects

Eight severely brain-damaged patients (four males; three with VS and five with MCS; mean age ± SD, 33.3 ± 14.8 years old; see **Table 1**) from a local hospital participated in this experiment. All of the patients included in this study were recruited according to predefined inclusion criteria. Inclusion criteria were as follows: (a) no centrally acting drugs; (b) no sedation within the prior 48 h; (c) periods of eye opening; (d) no history of impaired visual or auditory acuity before brain injury; and (e) diagnosis of VS or MCS after a traumatic brain injury (TBI), anoxic brain injury, or cerebrovascular accident. This study was approved by the Ethical Committee of the General Hospital of Guangzhou Military Command of the Peoples Liberation Army in Guangzhou, and complies with the Code of Ethics of the World Medical Association (Declaration of Helsinki). These patients or their legal surrogates provided written informed consent for participation in the BCI experiments and publication of their individual details in this manuscript.

The diagnoses of VS or MCS were based on the CRS-R, which contains 23 items organized in 6 subscales addressing auditory, visual, motor, oromotor, communication, and arousal processes. Scoring on each subscale is based on the specific operational criteria. The eight patients attended two CRS-R assessments: one during the week before the experiment and another at 1 month after the experiment. The CRS-R scores for each patient are presented in **Table 1**. Additionally, eight healthy subjects (HC1, HC2, HC3, HC4, HC5, HC6, HC7, and HC8) (seven males; mean age ± SD, 29.2 ± 3.3 years old) participated in the experiment as a control group.

## 2.2. Stimuli and Graphic User Interface (GUI)

Movie clips of emotional facial expression were used as stimuli. Eighty movie clips including video and audio recordings of 1,400 ms in duration, which were used in our previous study (Li et al., 2015a) , were selected as stimuli. These audiovisual stimuli consisted of two sets of emotional movie clips: 40 laughing movie clips and 40 crying movie clips, corresponding to happy and sad emotional states, respectively. All the movie clips were edited using Premiere Pro software, version CS6 (Adobe, San Jose, CA, USA) to ensure identical overall luminance levels on a gray scale. In addition, they were edited using Adobe Audition software, version CS6 (Adobe, San Jose, CA, USA) to ensure that the audio recordings had identical power levels. Note that after the experiments, each healthy subject was asked to rate the emotional content of each movie clip using the self-assessment manikin (SAM, Bradley and Lang, 1994). The SAM evaluation rating of the valence-arousal scales were (7.09 ± 0.91, 5.21 ± 1.67) and (2.41 ± 0.81, 4.27 ± 1.21) for laughing and crying movie clips, respectively.

The GUI used in this study is illustrated in **Figure 1**. Two movie clips, a crying movie clip and a laughing movie clip, were pseudorandomly chosen from the two sets of movie clips and were displayed on the left and right sides of the GUI. The size (area) of each movie clip was 9 cm × 7.2 cm, and the

**TABLE 1 |** Summary of patients' clinical status.

| Patient | Age | Gender | Clinical diagnosis | Etiology | Time since injury (months) | CRS-R score (subscores) | |
|---|---|---|---|---|---|---|---|
| | | | | | | Before experiment | After 1 month |
| P1 | 33 | F | VS | NTBI | 2 | 7 (1-1-2-1-0-2) | 7 (1-1-2-1-0-2) |
| P2 | 49 | F | MCS | NTBI | 6 | 9 (1-3-2-1-0-2) | 11 (3-3-2-1-0-2) |
| P3 | 26 | M | VS | TBI | 2 | 5 (1-1-1-0-0-2) | 13 (3-3-3-1-1-2) |
| P4 | 23 | M | MCS | TBI | 3 | 10 (2-3-2-1-0-2) | 10 (2-3-2-1-0-2) |
| P5 | 37 | M | MCS | TBI | 2 | 9 (1-3-2-1-0-2) | 9 (1-3-2-1-0-2) |
| P6 | 18 | F | MCS | TBI | 2 | 8 (1-1-3-1-0-2) | 8 (1-1-3-1-0-2) |
| P7 | 60 | F | VS | TBI | 4 | 7 (1-1-2-1-0-2) | 7 (1-1-2-1-0-2) |
| P8 | 20 | M | MCS | TBI | 2 | 8 (1-1-3-1-0-2) | 8 (1-1-3-1-0-2) |

*CRS-R, coma recovery scale-revised; NTBI, non-traumatic brain injury; and TBI, traumatic brain injury; CRS-R subscales: Auditory, visual, motor, oromotor, communication, and arousal functions.*

**FIGURE 1 |** GUI of the BCI, in which a crying movie clip and a laughing movie clip are arranged on the left and right sides, respectively. The two movie clips flashed (appearing and disappearing) on the black background with a random inter-stimulus interval.

horizontal distance between the two movie clips in the GUI was 6 cm. The ratio of the movie clip size to the GUI size was set at 0.12:1. Two loudspeakers were placed behind the monitor to present the auditory stimuli. The two videos clips flashed (appearing and disappearing), with each clip appearing for 1,400 ms. When the video clip appeared, the corresponding audio clip was simultaneously played from the speaker. Specifically, one movie clip (e.g., the crying movie clip in **Figure 1**) was flashed eight times, and then the other movie clip (e.g., the laughing movie clip in **Figure 1**) was flashed eight times. The interval between two consecutive movie clips was randomly chosen from among 500, 600, 700, 800, 900, 1,000, 1,100, and 1,200 ms. The patients were instructed to focus on one movie clip (e.g., the crying or laughing movie clip) and to count the flashes of the corresponding movie clip.

## 2.3. Data Acquisition

A NuAmps amplifier (Neuroscan Compumedics, USA) and an EEG cap (LT 37) were used to record 30-electrode scalp EEG signals for data acquisition. The EEG signals were amplified, sampled at 250 Hz, bandpass filtered between 0.1 and 60 Hz, and referenced to the right mastoid. The impedances of all electrodes were kept below 5$k\Omega$. In order to remove ocular movement artifacts from the EEG signal, an electrooculogram (EOG) was captured from two pairs of electrodes ("HEOR" and "HEOL";"VEOU" and "VEOL").

## 2.4. Experimental Procedures

During the experiment, patients were seated on a comfortable wheelchair and repeatedly instructed to avoid blinking or moving their body. Before the experiment, preliminary screening was conducted to explain the procedure to patients.

In this experiment, two experimental runs were conducted: one for calibration and the other for online evaluation. Each subject first performed a calibration run of 20 trials with the GUI in **Figure 1** to collect training data. In this study, we collected a small training dataset for each subject, because the BCI system was designed mainly for patients with DOC who are easily fatigued during experiments. We trained the initial SVM classifier using the EEG data from the calibration run. Each subject subsequently performed an evaluation run of 50 trials.

The online evaluation run contained five blocks, each of which was composed of 10 trials and was conducted on separate days because the patients were easily fatigued. The experimental procedure of one trial in this experiment is illustrated as follows. Two pairs of audiovisual stimuli were first constructed, for which one pair of audiovisual stimuli corresponded to a laughing movie clip and the other pair corresponded to a crying movie clip. These audiovisual stimuli were pseudorandomly chosen from two sets of emotional movie clips, which consisted of 40 laughing movie clips and 40 crying movie clips corresponding to happy and sad emotional states, respectively. Each trial began by presenting audiovisual instructions, which lasted 10 s. The subject was instructed to "Pay attention to the happy/sad movie clips and to count the flashes of the happy/sad movie clips." Note that the two emotional states appeared in a pseudo-random order, with half the trials containing the happy movie clip and the other half containing the sad movie clip. Following presentation of the instructions, the two pairs of audiovisual stimuli, constructed as described above, were presented. The two video clips flashed (appearing and disappearing), with each appearing for 1,400 ms. When the video clip appeared, the corresponding audio clip was simultaneously played from the speakers. The interval between two consecutive audiovisual stimuli was randomly chosen from among 500, 600, 700, 800, 900, 1,000, 1,100, and 1,200 ms. After the 36 s audiovisual presentation, the BCI algorithm determined

the target movie clip. If the detection result was correct, positive feedback consisting of the laughing or crying facial expression in the given trial and auditory applause was delivered for 4 s; otherwise, no feedback was given. Before the next trial beginning, there was a break of at least 10 s depending on the patient's level of fatigue. If the patient showed continuous body movements (e.g., coughing) or decreased arousal (i.e., closed eyes for a period of 5 s) in a trial, the trial was rejected to reduce artifacts, and the next trial began after the patient re-awakened and re-stabilized.

## 2.5. Data Processing and Algorithm

The P300 detection algorithms and spectral analysis methods were designed separately. The former was used to detect whether the subject responsed to the target movie clip in real-time, and the latter was used to detect whether the EEG signals during the crying and laughing movie clips could be classified using emotion-related CSP and DE features. The algorithms and analysis methods used in this study are described in the following sections.

### 2.5.1. Online P300 Detection

First, the EEG signals were filtered between 0.1 and 10 Hz. Then, we extracted a segment of the EEG signal from each channel (0–600 ms from the start of the movie clip) for each flash of a movie clip. This segment was down-sampled by a factor of 5 to obtain a data vector (with a length of 30) from each channel. Next, we concatenated the vectors from all channels to obtain a new data vector (with a length of 900) corresponding to the movie clip flashes. In order to improve signal-to-noise ratio, we constructed a feature vector corresponding to each movie clip by averaging the data vectors across the eight flashes in a trial. Finally, we applied the SVM classifier to the two feature vectors corresponding to the two types of movie clips, and two SVM scores were obtained for each trial. Specifically, the SVM classifier was first trained using the training data, in which the feature vectors corresponding to the target and non-target movie clips were labeled +1 and -1, respectively. For each test trial, the trained SVM was applied to the two feature vectors corresponding to the two movie clips, and the predicted target movie clip was the movie clip corresponding to the higher score.

### 2.5.2. Offline Spectral Analysis

In the offline analysis, we performed spectral analysis by stimulating the online training and testing. The EEG data were first bandpass filtered over the five frequency bands: delta (1–3 Hz), theta (4–7 Hz), alpha (8–13 Hz), beta (14–30 Hz), and gamma (31–50 Hz). After bandpass filtering, we extracted two segments (one for the laughing movie clip and one for the crying movie clip) of EEG data over an 18 s period (4,500 data points) for each channel and each frequency band. For each segment, we extracted the CSP feature and the DE feature, as described below.

First, a CSP spatial filter, $\mathbf{W}$, was learned in a subject-specific manner to enhance the separability between the two emotion classes (i.e., happiness and sadness) in the training data. Specifically, a training dataset was collected for each subject during a calibration run, in which 20 trials of the instructed emotion recognition task were performed. The spatial filter matrix $\mathbf{W}$ was constructed by the well-known joint diagonalization method (Blanchard and Blankertz, 2004). For each trial, the CSP features were then extracted using the following filter:

$$\mathbf{fm} = \log_{10}(diag(\overline{\mathbf{W}}\mathbf{E}\mathbf{E}^T\overline{\mathbf{W}}^T))$$

where $\mathbf{fm}$ denotes the CSP feature vector, $\overline{\mathbf{W}}$ is a submatrix composed of the first and last three rows of $\mathbf{W}$ , and $\mathbf{E}$ is an EEG data matrix corresponding to one trial. In Eq. (1), $diag(\overline{\mathbf{W}}\mathbf{E}\mathbf{E}^T\overline{\mathbf{W}}^T)$ is a vector composed of all entries on the diagonal line of the matrix $\overline{\mathbf{W}}\mathbf{E}\mathbf{E}^T\overline{\mathbf{W}}^T$ , and the operator $\log_{10}(.)$ is used to calculate the logarithm of each entry of the vector. In this study, we selected the top and bottom three components from $\mathbf{W}$ that best separated the two emotion classes. Furthermore, their logarithm variances were calculated, and a 6-D CSP feature vector was constructed for each frequency band.

We then used the discrete Fourier transform to calculate the power spectral density for each segment. The DE was defined as the logarithmic power spectral density for a fixed-length EEG sequence. For each frequency band, we constructed the DE feature vector by concatenating the differential entropies from all of the channels.

Two feature vectors of a trial corresponding to the two segments (one for the laughing movie clip and one for the crying movie clip) were then obtained by concatenating all of the CSP and DE feature vectors of all frequency bands. An SVM classifier was first trained using the training data, in which the feature vectors corresponding to the laughing and crying movie clips were labeled +1 and -1, respectively. For a test EEG trial, two feature vectors were first obtained, as described above, and then were fed into the SVM classifier to obtain two SVM scores. If both the SVM score corresponding to the laughing movie clip and the sum of the two SVM scores were positive, the predicted emotional state is happiness. If both the SVM score corresponding to the crying movie clip and the sum of the two SVM scores are negative, the predicted emotional state was sadness.

### 2.5.3. Performance Measures

For each subject, the ratio of trials with correct responses (hits) to the total number of trials was calculated as the accuracy rate. To obtain the significance level of the accuracy, the $\chi^2$ statistical test was performed. Specifically, the $\chi^2$ statistic was calculated as follows (Kübler and Birbaumer, 2008; Pan et al., 2014):

$$\chi^2 = \sum_{i=1}^{k} \frac{(fo_i - fe_i)^2}{fe_i} \quad (1)$$

where $fo_i$ and $fe_i$ were the observed and expected frequencies of the $i$th class ($i = 1, 2, ..., k$) (degree of freedom: 1). In this study, the observations fell into two classes (hit and miss). Therefore, the chance level that the target was selected was 0.5, whereas the chance level for selecting a non-target was 0.5. Considering that

50 trials of the BCI evaluation were conducted for each subject, the expected $fo_1$ and $fo_2$ were 25 and 25, respectively. Specifically, $fo_1$ and $fo_2$ was the number of times that the target (i=1) or a non-target (i=2) was determined in the BCI evaluation. We obtained a value of 3.84 for $\chi^2$ test with a significance level of $p = 0.05$, corresponding to 32 hits in 50 trials or an accuracy of 64%.

## 3. RESULTS

**Table 2** summarizes the accuracy rates of the P300 detection (online) and the spectral analysis (offline) for the experiment. For the P300 detection, three of the eight patients (patients P2, P3, and P6) achieved the significant accuracies (66–78%), corresponding to a significance level of 0.05. For patients P1, P4, P5, P7, and P8, the accuracies of the P300 detection were not significant. For spectral analysis, two of the eight patients (patients P2 and P3) achieved accuracies ranging from 66 to 68%, whereas patients P1, P4, P5, P6, P7, and P8 achieved accuracies lower than 64% (ranging from 48 to 60%). Furthermore, all eight healthy subjects (HC1, HC2, HC3, HC4, HC5, HC6, HC7, and HC8) achieved the significant accuracies (ranging from 78 to 100%) for both P300 detection and spectral analysis.

For the three patients (P2, P3, and P6) and two healthy controls (HC1 and HC2) whose accuracies of the P300 detection were significant, we calculated ERP waveforms from 0 to 800 ms after stimulus onset by averaging the EEG channel signals across 50 trials in the online experiment. **Figure 2** shows the ERP waveforms of the "Fz," "Cz," and "Pz" electrodes for the three patients and two healthy controls. A highly similar P300 component elicited in all of the target curves.

**TABLE 2 |** Accuracy rates of the P300 detection (online) and the spectral analysis (offline) for the subjects.

| Subjects | Online accuracy (P300 detection) | *p*-value | Offline accuracy (spectral analysis) | *p*-value |
|---|---|---|---|---|
| P1 | 52 | 0.778 | 52 | 0.778 |
| P2 | **78** | <0.001 | **68** | 0.011 |
| P3 | **68** | 0.011 | **66** | 0.047 |
| P4 | 54 | 0.572 | 50 | 1.000 |
| P5 | 56 | 0.396 | 48 | 0.778 |
| P6 | **66** | 0.047 | 60 | 0.157 |
| P7 | 50 | 1.000 | 54 | 0.572 |
| P8 | 58 | 0.258 | 58 | 0.258 |
| HC1 | **100** | <0.001 | **90** | <0.001 |
| HC2 | **100** | <0.001 | **76** | <0.001 |
| HC3 | **96** | <0.001 | **90** | <0.001 |
| HC4 | **100** | <0.001 | **76** | <0.001 |
| HC5 | **94** | <0.001 | **70** | 0.005 |
| HC6 | **78** | <0.001 | **68** | 0.011 |
| HC7 | **96** | <0.001 | **76** | <0.001 |
| HC8 | **98** | <0.001 | **82** | <0.001 |

*The accuracies significantly higher than the chance level 50% (accuracy ≥64% or p≤0.05) are highlighted in bold.*

To illustrate the influence of happy and sad movie clips on different brain regions, we projected the DE and CSP features onto the scalp to obtain the brain patterns of the five selected frequency bands across all trials with happy or sad movie clips. Here, brain patterns are considered neural activities in critical brain areas and frequency bands that share commonalities across trials during the happy and sad movie clips. Specifically, the DE features of each trial were calculated as the logarithmic power spectral density using the 18-s EEG signals of the target movie clip from each electrode. **Figure 3** shows the topographical maps of the average DE features of the happy and sad emotions for the two healthy controls (HC1 and HC2) and the two patients (P2 and P3) who achieved accuracies higher than the significance level of 64% in spectral analysis. As shown in **Figure 3**, patients P2 and P3 had neural patterns that were similar to those of healthy controls HC1 and HC2: (1) In the delta band, the prefrontal area exhibited greater activation for sad emotions than happy emotions; (2) in the theta and alpha bands, the parietal area exhibited enhanced energy for sad emotions compared with happy emotions; and (3) in the beta and gamma bands, the lateral temporal and occipital areas exhibited greater activation for happy emotions than sad emotions.

Furthermore, the CSP filters were trained using the 50 trials obtained in the online experiment, which were used to project the original signals represented the weights of the original signals for achieving optimally discriminative projection (Yu et al., 2015). For two healthy controls (HC1 and HC2) and two patients (P2 and P3), we plotted the two spatial filters (the first and the last rows of $\mathbf{W}$) and the corresponding spatial patterns (the first and the last rows of $\mathbf{A}$, where $\mathbf{A} = (\mathbf{W}^{-1})^T$ in **Figure 4** as scalp maps for two frequency bands (alpha and gamma bands). The spatial filters/patterns are scaled by their maximum absolute values such that the values at each electrode position are normalized to the range of [-1,1]. Temporal and occipital asymmetries in the alpha and gamma bands can be observed from the CSP spatial patterns shown in **Figure 4** for happy and sad emotion recognition. Specifically, the first filter/pattern was associated with more power over the right sensory cortical areas, because it was obtained by maximizing the variance of the first class (i.e., happy emotion). Accordingly, the last filter/pattern, corresponding to the second class (sad emotion), was associated with greater activation of the left sensory cortical areas. Such associations were clearly observed in both the healthy controls (HC1 and HC2) and the two patients (P2 and P3).

Among the three VS patients, one patient (P3) progressed to MCS 1 month after the experiment. More interestingly, the two patients (patients P2 and P3) with significant accuracies in both online P300 detection and offline spectral analysis improved their consciousness levels to a large degree 1 month after the experiment, while the other patients remained clinically unchanged. Specifically, their CRS-R scores improved from 9 and 5 (before the experiment) to 11 and 13 (1 month after the experiment), respectively. The CRS-R scores for each patient

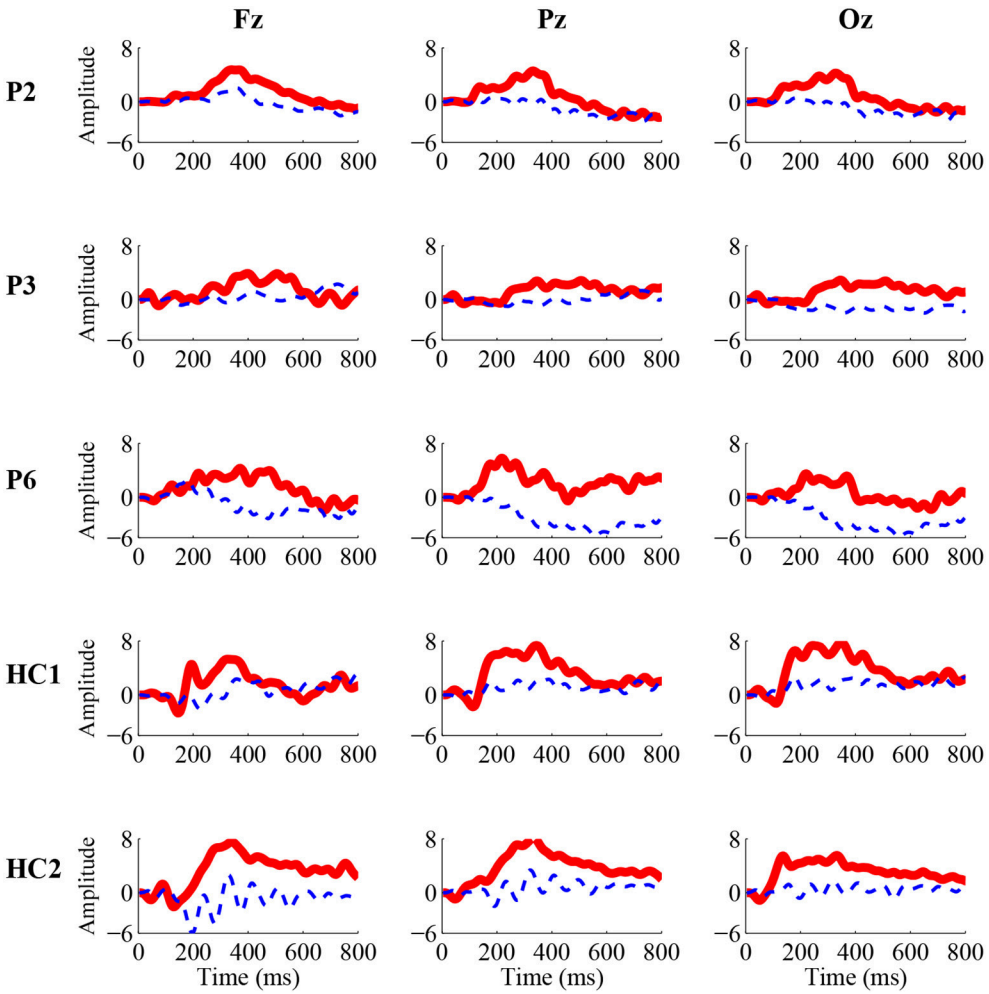


**FIGURE 2 |** Grand-average P300 ERP waveforms from the "Fz" (left), "Cz" (middle), and "Pz" (right) electrodes in the online experiment for three patients (P2, P3, and P6) and two healthy controls (HC1 and HC2). The solid red curves containing the P300 component correspond to the target movie clip, while the dashed blue curves without the P300 component correspond to the non-target movie clip.

before and 1 month after the experiment were shown in **Table 1**.

## 4. DISCUSSION

The detection of consciousness as well as residual cognitive function in patients with DOC is highly challenging but crucial for providing accurate diagnoses, selecting the optimal nursing strategies and ensuring overall quality of life. In this study, we used an EEG-based BCI to detect consciousness in patients with DOC. In this novel BCI paradigm, two movie chips, a crying movie clip and a laughing movie clip, were displayed on the left and right sides of the GUI, respectively, and flashed (appearing and disappearing) with a random interstimulus interval to evoke P300 potentials. When the movie clip was displayed, the corresponding audio clip was simultaneously played. Through the online P300 detection, the BCI system determined which movie clip the subjects attended to (i.e., responding to the instructions). Eight patients and eight healthy controls were involved in the experiment using our BCI system. They were instructed to focus on the crying or laughing movie clip and to count the flashes of the corresponding movie clip indicated by the instruction. Three of these patients (patients P2, P3, and P6) achieved online accuracies of greater than 64% (66–78%), which were considered significant. Furthermore, P300 responses (**Figure 2**) could be observed in these three patients. These three patients thus demonstrated the abilities to recognize emotion and follow commands.

It should be stressed that to perform the experimental tasks, many cognitive functions are required, such as language comprehension (i.e., understanding the task instructions), emotion processing (i.e., recognizing the emotional stimuli), and object selection (i.e., attending to the target movie clip). The absence of any of these cognitive functions could lead to failure of performing the task. Furthermore, negative results could not be used as evidence for a lack of consciousness, because

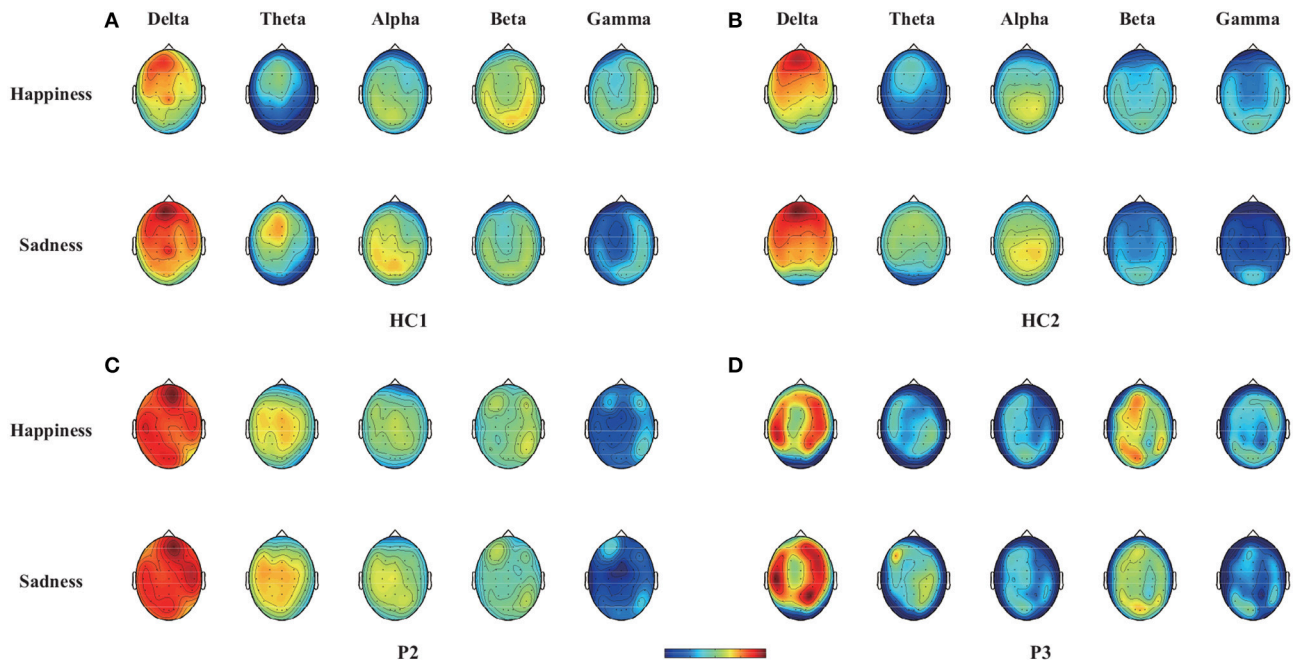


**FIGURE 3 |** Topographical maps of the average DE features across trials with happy or sad emotional states in the five bands (delta, theta, alpha, beta, and gamma bands) for two healthy controls (HC1 and HC2) and two patients (P2 and P3). Note that the two healthy controls HC1 and HC2 and the two patients P2 and P3 achieved accuracies greater than 64% in offline spectral analysis. **(A)** Healthy subject HC1, **(B)** Healthy subject HC2, **(C)** Patient P2, **(D)** Patient P3.

false-negative findings in BCI studies are possible, even in healthy subjects. However, our positive results did indicate that such cognitive functions and residual consciousness existed in these patients.

Through the offline analysis, CSP and DE features in the delta, theta, alpha, beta, and gamma frequency bands were employed to classify the EEG signals recorded while the subjects watched the crying and laughing movie clips, corresponding to sad and happy emotions, respectively. Two patients (patients P2 and P3) achieved offline accuracies of the spectral analysis (66–68%) that were significantly greater than chance level. Furthermore, we projected the DE and CSP features of the happy and sad emotions onto the scalp in different frequency bands for two healthy controls (HC1 and HC2) and these two patients. To further illustrate the influence of happy and sad movie clips on different brain regions, we projected the DE and CSP features onto the scalp to obtain the brain patterns of the five selected frequency bands in **Figures 3**, **4**. For or the sad emotion, the neural patterns had significantly higher delta responses at prefrontal sites and significantly higher theta and alpha responses at parietal sites. For the happy emotion, the neural patterns had stronger beta and gamma responses at the lateral temporal and occipital sites. Our results are partially consistent with the findings of previous works (Mühl et al., 2014; Zheng et al., 2016). For instance, studies (Onton and Makeig, 2009; Hadjidimitriou and Hadjileontiadis, 2012) have found that during positive emotion processing (e.g., emotion recognition of happy facial expressions), the energy of beta and gamma responses is enhanced. Increased delta band power was reported over parietal regions for negative stimuli compared with positive stimuli (Zheng et al., 2016). In addition, the experimental results in **Figure 4** show that some of the asymmetric spatial patterns extracted by CSP were consistent with recent neurophysiological findings. For example, the event-related desynchronization in the alpha band (decreased alpha power) in response to stimulation is believed to represent increased sensory processing and, hence, has been associated with activation of task-relevant sensory cortical regions (Klimesch et al., 2007). Increases of gamma band activity have been observed over temporal regions in response to positive emotion, compared to negative emotion (Onton and Makeig, 2009). Taken together, stable brain patterns of the DE and CSP features associated with happy and sad emotions were observed in the two patients and the two healthy controls. Whether the happy and sad emotional responses were evoked using our BCI paradigm needs to be further confirmed in future studies.

For patients with brain damage, assessing emotion recognition ability is of substantial importance. First, emotion recognition is an important aspect of the cognition function of the human brain. Studies of the neural basis of emotion recognition (Adolphs, 2002) have suggested that somatosensory-related cortices in the right hemisphere play a critical role in emotion recognition. Areas of the amygdala, orbitofrontal and insular cortices are activated when subjects are engaged in emotion recognition (Adolphs, 2002). Second, basic emotional ability is relevant to the level of consciousness. Emotion and consciousness emerge as the result of neuronal activity

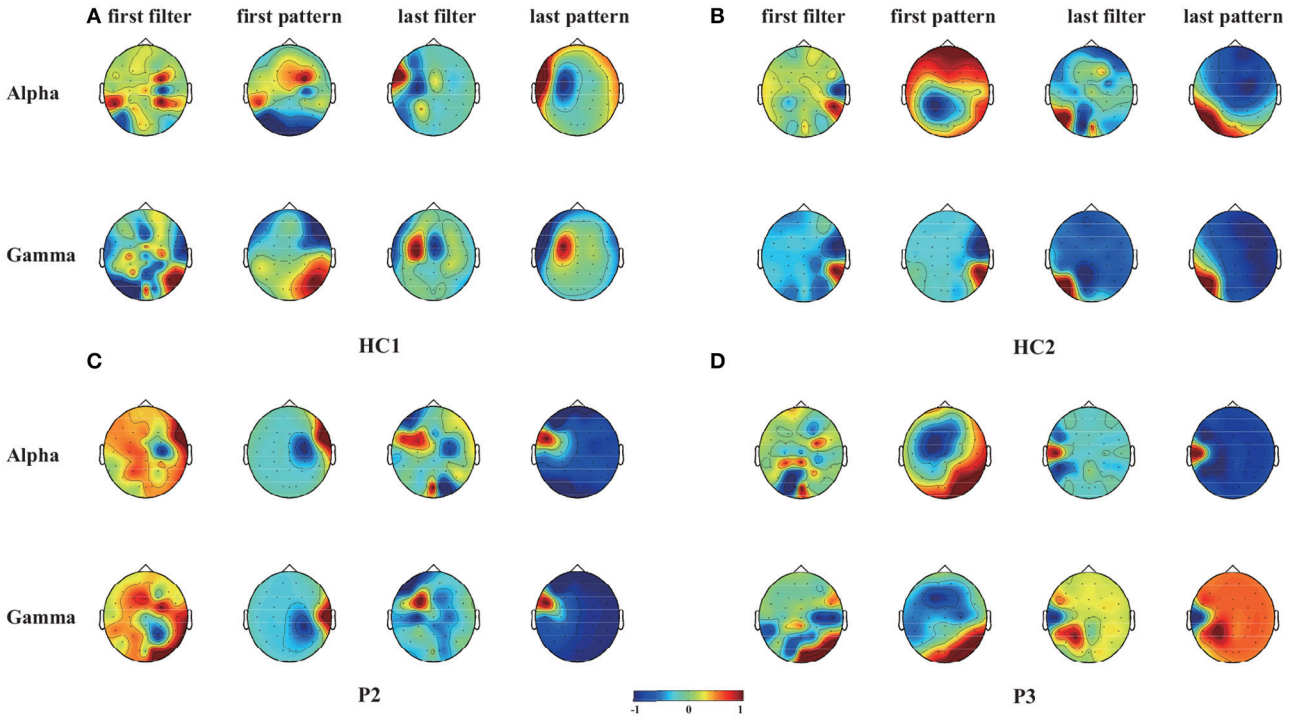


**FIGURE 4 |** Scalp maps of two spatial filters (the first and the last rows of $W$) and the corresponding spatial patterns (the first and the last rows of $A$, where $A = (W^{-1})^T$) for each of the alpha and gamma bands and for two healthy controls (HC1 and HC2) and two patients (P2 and P3). These CSP filters were trained using 50 trials gathered from the online evaluation. **(A)** Healthy subject HC1, **(B)** Healthy subject HC2, **(C)** Patient P2, **(D)** Patient P3.

in the brain (Damasio, 1999, 2003). Some studies have suggested that emotion is a possible facet of consciousness (Balconi and Lucchiari, 2007; Tsuchiya and Adolphs, 2007). Third, assessing emotion recognition ability may help us better understand other cognitive functions (e.g., language comprehension, working memory, and executive function) in patients with DOC. Several behavioral scales, including the FEAS, NEPSY-II, and MoCA, contain emotion recognition-based indices that are commonly used to evaluate the mental states of patients with schizophrenia, ADHD and Parkinson's diseases (Solomon et al., 2007; Marneweck and Hammond, 2014; Pitzianti et al., 2017). For patients with DOC, clinical assessment scales such as the CRS-R do not contain emotion recognition tasks. BCIs can provide both experimenters and patients with real-time feedback independent of motor responses, making detection and assessment of the emotion recognition abilities of patients with DOC possible, as demonstrated in this study. Using an EEG-based BCI, emotion recognition-related cognitive functions were successfully detected in 3 of 8 patients with DOC. Our results showed that the emotion recognition systems (including somatosensory related cortices in the right hemisphere) were at least partially effective for these three patients.

As previously discussed, misdiagnoses can occur based on behavioral observation scales such as the CRS-R. Therefore, BCIs can be used as a supportive bedside tool to assess patients residual cognitive ability. For instance, our experiment results showed that one VS patient (P3) was able to perform the BCI experimental task with an accuracy significantly higher than chance level. This result is consistent with previous fMRI (Monti et al., 2010) and EEG (Cruse et al., 2012b) data showing that some VS patients who are diagnosed based on the behavioral ceiteria might have residual cognitive function and even some level of consciousness. In fact, according to follow-up behavioral CRS-R assessments, this VS patient progressed to MCS 1 month after the experiment, thus supporting our BCI assessment result for this VS patient.

Notably, in our experiment, several patients achieved online accuracies (approximately 70%) that were significantly higher than chance level but much lower than the performance of the healthy subjects (which was generally higher than 90%). This discrepancy may be explained by two key factors. First, because the patients became easily fatigued, we could not collect sufficient training data before each online test block. Therefore, the performance of the classifier may have been affected by the insufficient amount of training data. Second, the patients with DOC had much lower levels of consciousness than the healthy subjects. Further studies are required to determine how to improve BCI accuracies for patients with DOC. A more elaborate preprocessing method could be employed to reduce the artifacts of the EEG signals, and the feature selection algorithms could be designed to adapt to these patients. Furthermore, our present offline

results suggest that EEG signals recorded while the subjects watched the crying and laughing movie clips could be classified using emotion-related features. In future work, we may further integrate the P300 and emotion-related features to improve the ability to identify consciousness in patients with DOC.

## 5. CONCLUSION

In summary, BCIs can help patients with DOC who are very lack of motor responses to show emotion recognition. BCIs were thus verificated as an effective tool for the detection of related abilities. Given our focus on consciousness detection, we did not consider neutral stimuli in this study. Whether patients with DOC are able to differentiate their happy and sad emotions from neutral stimuli still remains unknown. This needs to be further confirmed in a future study.

## AUTHOR CONTRIBUTIONS

YL, JP, QX, and RY: designed this study; YL: designed the BCI systems, experiments and paradigms; JP: implemented the BCI systems; RY, QX, and YH: conducted the clinical assessments of participants; JP, HH, and YS: collected the BCI data; JP: analyzed the data; JP and YL: wrote the manuscript.

## ACKNOWLEDGMENTS

This work was supported by the National Key Basic Research Program of China (973 Program) under Grant 2015CB351703; the National Natural Science Foundation under Grants 61633010, and 61503143; the Guangdong Natural Science Foundation under Grants 2014A030312005, 2015A030313609, and 2017A030310364; and the Pearl River S&T Nova Program of Guangzhou under Grant 201710010038.

## REFERENCES

Adolphs, R. (2002). Neural systems for recognizing emotion. *Curr. Opin. Neurobiol.* 12, 169–177. doi: 10.1016/S0959-4388(02)00301-X

Aftanas, L. I., Reva, N., Varlamov, A., Pavlov, S., and Makhnev, V. (2004). Analysis of evoked EEG synchronization and desynchronization in conditions of emotional activation in humans: temporal and topographic characteristics. *Neurosci. Behav. Physiol.* 34, 859–867. doi: 10.1023/B:NEAB.0000038139.39812.eb

Allen, J. J., Coan, J. A., and Nazarian, M. (2004). Issues and assumptions on the road from raw signals to metrics of frontal EEG asymmetry in emotion. *Biol. Psychol.* 67, 183–218. doi: 10.1016/j.biopsycho.2004.03.007

Balconi, M., and Lucchiari, C. (2007). Consciousness and emotional facial expression recognition: subliminal/supraliminal stimulation effect on n200 and p300 erps. *J. Psychophysiol.* 21, 100–108. doi: 10.1027/0269-8803.21.2.100

Bilgi, M. M., Taspinar, S., Aksoy, B., Oguz, K., Coburn, K., and Gonul, A. S. (2017). The relationship between childhood trauma, emotion recognition, and irritability in schizophrenia patients. *Psychiatry Res.* 251, 90–96. doi: 10.1016/j.psychres.2017.01.091

Blanchard, G., and Blankertz, B. (2004). BCI competition 2003: Data set iia - spatial patterns of self-controlled brain rhythm modulations. *IEEE Trans. Biomed. Eng.* 51, 1062–1066. doi: 10.1109/TBME.2004.826691

Bradley, M. M., and Lang, P. J. (1994). Measuring emotion: the self-assessment manikin and the semantic differential. *J. Behav. Ther. Exp. Psychiatry* 25, 49–59. doi: 10.1016/0005-7916(94)90063-9

Corcoran, C. M., Keilp, J. G., Kayser, J., Klim, C., Butler, P. D., Bruder, G. E., et al. (2015). Emotion recognition deficits as predictors of transition in individuals at clinical high risk for schizophrenia: a neurodevelopmental perspective. *Psychol. Med.* 45:2959. doi: 10.1017/S0033291715000902

Coyle, D., Carroll, A., Stow, J., McCann, A., Ally, A., and McElligott, J. (2012). "Enabling control in the minimally conscious state in a single session with a three channel BCI," in *The 1st International DECODER Workshop* (Paris), 25–28.

Coyle, D., Stow, J., McCreadie, K., McElligott, J., and Carroll, . (2015). Sensorimotor modulation assessment and brain-computer interface training in disorders of consciousness. *Arch. Phys. Med. Rehabil.* 96, 62–70. doi: 10.1016/j.apmr.2014.08.024

Coyle, D., Stow, J., McCreadie, K., Sciacca, N., McElligott, J., and ine Carroll (2017). *Motor Imagery BCI with Auditory Feedback as a Mechanism for Assessment and Communication in Disorders of Consciousness*. Cham: Springer International Publishing.

Cruse, D., Chennu, S., Chatelle, C., Bekinschtein, T. A., Fernández-Espejo, D., Pickard, J. D., et al. (2012a). Bedside detection of awareness in the vegetative state: a cohort study. *Lancet* 378, 2088–2094. doi: 10.1016/S0140-6736(11)61224-5

Cruse, D., Chennu, S., Fernández-Espejo, D., Payne, W. L., Young, G. B., and Owen, A. M. (2012b). Detecting awareness in the vegetative state: electroencephalographic evidence for attempted movements to command. *PLoS ONE* 7:e49933. doi: 10.1371/journal.pone.0049933

Cruse, D., and Owen, A. M. (2010). Consciousness revealed: new insights into the vegetative and minimally conscious states. *Curr. Opin. Neurol.* 23, 656–60. doi: 10.1097/WCO.0b013e32833fd4e7

Damasio, A. (1999). The feeling of what happens: body and emotion in the making of consciousness. *Q. Rev. Biol.* 51, 1579–1579.

Damasio, A. (2003). Feelings of emotion and the self. *Ann. N.Y. Acad. Sci.* 1001, 253–261. doi: 10.1196/annals.1279.014

Di, H. B., Yu, S. M., Weng, X. C., Laureys, S., Yu, D., Li, J. Q. et al. (2007). Cerebral response to patient's own name in the vegetative and minimally conscious states. *Neurology* 68, 895–899. doi: 10.1212/01.wnl.0000258544.79024.d0

Gibson, R. M., Chennu, S., Fernndez-Espejo, D., Naci, L., Owen, A. M., and Cruse, D. (2016). Somatosensory attention identifies both overt and covert awareness in disorders of consciousness. *Ann. Neurol.* 80:412. doi: 10.1002/ana.24726

Hadjidimitriou, S. K., and Hadjileontiadis, L. J. (2012). Toward an EEG-based recognition of music liking using time-frequency analysis. *IEEE Trans. Biomed. Eng.* 59:3498. doi: 10.1109/TBME.2012.2217495

Kayser, J., Bruder, G. E., Tenke, C. E., Stewart, J. E., and Quitkin, F. M. (2000). Event-related potentials (erps) to hemifield presentations of emotional stimuli: differences between depressed patients and healthy adults in p3 amplitude and asymmetry. *Int. J. Psychophysiol.* 36, 211–236. doi: 10.1016/S0167-8760(00)00078-7

Kayser, J., Tenke, C. E., Kroppmann, C. J., Alschuler, D. M., Fekri, S., Bendavid, S., et al. (2014). Auditory event-related potentials and alpha oscillations in the psychosis prodrome: neuronal generator patterns during a novelty oddball task. *Int. J. Psychophysiol.* 91, 104–120. doi: 10.1016/j.ijpsycho.2013.12.003

Klimesch, W., Sauseng, P., and Hanslmayr, S. (2007). EEG alpha oscillations: the inhibition-timing hypothesis. *Brain Res. Rev.* 53:63. doi: 10.1016/j.brainresrev.2006.06.003

Kohler, C. G., Bilker, W., Hagendoorn, M., Gur, R. E., and Gur, R. C. (2000). Emotion recognition deficit in schizophrenia: association with symptomatology and cognition. *Biol. Psychiatry* 48, 127–136. doi: 10.1016/S0006-3223(00)00847-7

Kotchoubey, B. (2017). Evoked and event-related potentials in disorders of consciousness: a quantitative review. *Consciousn. Cogn.* 54, 155–167. doi: 10.1016/j.concog.2017.05.002

Kübler, A., and Birbaumer, N. (2008). Brain-computer interfaces and communication in paralysis: extinction of goal directed thinking in

completely paralysed patients? *Clin. Neurophysiol.* 119, 2658–2666. doi: 10.1016/j.clinph.2008.06.019

Lancioni, G. E., Bosco, A., OReilly, M. F., Sigafoos, J., and Belardinelli, M. O. (2017). Assessment and intervention with patients with severe disorders of consciousness. *Adv. Neurodev. Disord.* 1, 1–7. doi: 10.1007/s41252-017-0025-5

Laureys, S., Perrin, F., Faymonville, M.-E., Schnakers, C., Boly, M., Bartsch, V., et al. (2004). Cerebral processing in the minimally conscious state. *Neurology* 63, 916–918. doi: 10.1212/01.WNL.0000137421.30792.9B

Li, M., and Lu, B.-L. (2009). "Emotion classification based on gamma-band EEG," in *Engineering in Medicine and Biology Society, 2009. EMBC 2009. Annual International Conference of the IEEE* (Minneapolis, MN: IEEE), 1223–1226.

Li, Y., Long, J., Huang, B., Yu, T., Wu, W., Liu, Y., et al. (2015a). Crossmodal integration enhances neural representation of task-relevant features in audiovisual face perception. *Cereb. Cortex* 25, 384–395. doi: 10.1093/cercor/bht228

Li, Y., Pan, J., He, Y., Fei, W., Laureys, S., Xie, Q., et al. (2015b). Detecting number processing and mental calculation in patients with disorders of consciousness using a hybrid brain-computer interface system. *BMC Neurol.* 15:259. doi: 10.1186/s12883-015-0521-z

Lin, Y.-P., Wang, C.-H., Jung, T.-P., Wu, T.-L., Jeng, S.-K., Duann, J.-R., et al. (2010). EEG-based emotion recognition in music listening. *Biomed. Eng. IEEE Trans.* 57, 1798–1806. doi: 10.1109/TBME.2010.2048568

Lulé, D., Noirhomme, Q., Kleih, S. C., Chatelle, C., Halder, S., Demertzi, A., et al. (2012). Probing command following in patients with disorders of consciousness using a brain–computer interface. *Clin. Neurophysiol.* 124, 101–106. doi: 10.1016/j.clinph.2012.04.030

Marneweck, M., and Hammond, G. (2014). Discriminating facial expressions of emotion and its link with perceiving visual form in parkinson's disease. *J. Neurol. Sci.* 346, 149–155. doi: 10.1016/j.jns.2014.08.014

McFarland, D. J., and Wolpaw, J. R. (2004). Brain-computer interfaces for communication and control. *Suppl. Clin. Neurophysiol.* 57:607. doi: 10.1016/S1567-424X(09)70400-3

Molina, G. G., Tsoneva, T., and Nijholt, A. (2009). "Emotional brain-computer interfaces," in *International Conference on Affective Computing and Intelligent Interaction and Workshops* (Amsterdam), 1–9.

Monti, M. M., Vanhaudenhuyse, A., Coleman, M. R., Boly, M., Pickard, J. D., Tshibanda, L., et al. (2010). Willful modulation of brain activity in disorders of consciousness. *New Engl. J. Med.* 362, 579–589. doi: 10.1056/NEJMoa0905370

Mühi, C., Allison, B., Nijholt, A., and Chanel, G. (2014). A survey of affective brain computer interfaces: principles, state-of-the-art, and challenges. *Brain Comput. Interfaces* 1, 66–84. doi: 10.1080/2326263X.2014.912881

Müller-Putz, G., Klobassa, D., Pokorny, C., Pichler, G., Erlbeck, H., Real, R., et al. (2012). "The auditory p300-based SSBCI: a door to minimally conscious patients?" in *Engineering in Medicine and Biology Society (EMBC), 2012 Annual International Conference of the IEEE* (San Diego, CA: IEEE), 4672–4675.

Müller-Putz, G. R., Pokorny, C., Klobassa, D. S., and Horki, P. (2013). A single-switch BCI based on passive and imagined movements: toward restoring communication in minimally conscious patients. *Int. J. Neural Syst.* 23:1250037. doi: 10.1142/S0129065712500372

Noirhomme, Q., Lesenfants, D., Lehembre, R., Lugo, Z., Chatelle, C., Vanhaudenhuyse, A., et al. (2013). "Detecting consciousness with a brain-computer interface," in *Converging Clinical and Engineering Research on Neurorehabilitation,* eds J. L. Pons, D. Torricelli, and M. Pajaro (Berlin; Heidelberg: Springer), 1261–1264.

Onton, J., and Makeig, S. (2009). High-frequency broadband modulations of electroencephalographic spectra. *Front. Hum. Neurosci.* 3:61. doi: 10.3389/neuro.09.061.2009

Owen, A. M., Menon, D. K., Johnsrude, I. S., Bor, D., Scott, S. K., Manly, T., et al. (2002). Detecting residual cognitive function in persistent vegetative state. *Neurocase* 8, 394–403. doi: 10.1076/neur.8.4.394.16184

Pan, J., Li, Y., and Wang, J. (2016). "An EEG-based brain-computer interface for emotion recognition," in *International Joint Conference on Neural Networks* (Vancouver, BC), 2063–2067.

Pan, J., Xie, Q., He, Y., Wang, F., Di, H., Laureys, S., et al. (2014). Detecting awareness in patients with disorders of consciousness using a hybrid brain-computer interface. *J. Neural Eng.* 11:056007. doi: 10.1088/1741-2560/11/5/056007

Petrantonakis, P. C., and Hadjileontiadis, L. J. (2011). Emotion recognition from brain signals using hybrid adaptive filtering and higher order crossings analysis. *IEEE Trans. Affect. Comput.* 1, 81–97. doi: 10.1109/T-AFFC.2010.7

Pitzianti, M., Grelloni, C., Casarelli, L., D'Agati, E., Spiridigliozzi, S., Curatolo, P., et al. (2017). Neurological soft signs, but not theory of mind and emotion recognition deficit distinguished children with adhd from healthy control. *Psychiatry Res.* 256, 96–101. doi: 10.1016/j.psychres.2017.06.029

Schutter, D. J., Putman, P., Hermans, E., and van Honk, J. (2001). Parietal electroencephalogram beta asymmetry and selective attention to angry facial expressions in healthy human subjects. *Neurosci. Lett.* 314, 13–16. doi: 10.1016/S0304-3940(01)02246-7

Seel, R. T., Sherer, M., Whyte, J., Katz, D. I., Giacino, J. T., Rosenbaum, A. M., et al. (2010). Assessment scales for disorders of consciousness: evidence-based recommendations for clinical practice and research. *Arch. Phys. Med. Rehabilit.* 91, 1795–1813. doi: 10.1016/j.apmr.2010.07.218

Solomon, R., Necheles, J., Ferch, C., and Bruckman, D. (2007). Pilot study of a parent training program for young children with autism: the play project home consultation program. *Autism Int. J. Res. Pract.* 11:205. doi: 10.1177/1362361307076842

Taylor, S. F., and Iii, M. D. (2012). Brain mapping biomarkers of socio-emotional processing in schizophrenia. *Schizophrenia Bull.* 38:73. doi: 10.1093/schbul/sbr105

Tsuchiya, N., and Adolphs, R. (2007). Emotion and consciousness. *Trends Cogn. Sci.* 11, 158–167. doi: 10.1016/j.tics.2007.01.005

Wang, F., He, Y., Qu, J., Xie, Q., Lin, Q., Ni, X., et al. (2017). Enhancing clinical communication assessments using an audiovisual BCI for patients with disorders of consciousness. *J. Neural Eng.* 14:046024. doi: 10.1088/1741-2552/aa6c31

Wang, X.-W., Nie, D., and Lu, B.-L. (2014). Emotional state classification from EEG data using machine learning approach. *Neurocomputing* 129, 94–106. doi: 10.1016/j.neucom.2013.06.046

Yu, T., Xiao, J., Wang, F., Zhang, R., Gu, Z., Cichocki, A., et al. (2015). Enhanced motor imagery training using a hybrid BCI with feedback. *IEEE Trans. Biomed. Eng.* 62, 1706–1717. doi: 10.1109/TBME.2015.2402283

Yuvaraj, R., Murugappan, M., Norlinah, M. I., Sundaraj, K., and Khairiyah, M. (2013). Review of emotion recognition in stroke patients. *Dementia Geriatric Cogn. Disord.* 36, 179–196. doi: 10.1159/000353440

Zheng, W. L., Zhu, J. Y., and Lu, B. L. (2016). Identifying stable patterns over time for emotion recognition from EDG. *IEEE Trans. Affect. Comput.* 99:1. doi: 10.1109/TAFFC.2017.2712143

**Conflict of Interest Statement:** The authors declare that the research was conducted in the absence of any commercial or financial relationships that could be construed as a potential conflict of interest.

frontiers in Human Neuroscience

ORIGINAL RESEARCH
published: 29 May 2018
doi: 10.3389/fnhum.2018.00214

# Neural Basis of the Emotional Conflict Processing in Major Depression: ERPs and Source Localization Analysis on the N450 and P300 Components

*Jing Zhu[1], Jianxiu Li[1]*, Xiaowei Li[1]*, Juan Rao[1], Yanrong Hao[1], Zhijie Ding[2] and Gangping Wang[2]*

*[1] Gansu Provincial Key Laboratory of Wearable Computing, School of Information Science and Engineering, Lanzhou University, Lanzhou, China, [2] The Third People's Hospital of Tianshui City, Tianshui, China*

**Objects:** Effective psychological function requires that cognition is not affected by task-irrelevant emotional stimuli in emotional conflict. Depression is mainly characterized as an emotional disorder. The object of this study is to reveal the behavioral and electrophysiological signature of emotional conflict processing in major depressive disorder (MDD) using event-related potentials (ERPs) and standardized low-resolution brain electromagnetic tomography (sLORETA) analysis.

**Method:** We used a face–word Stroop task involving emotional faces while recording EEG (electroencephalography) in 20 patients with MDD and 20 healthy controls (HCs). And then ERPs were extracted and the corresponding brain sources were reconstructed using sLORETA.

**Results:** Behaviorally, subjects with MDDs manifested significantly increased Stroop effect when examining the RT difference between happy incongruent trials and happy congruent trials, compared with HC subjects. ERP results exhibited that MDDs were characterized by the attenuated difference between P300 amplitude to sad congruent stimuli and sad incongruent stimuli, as electrophysiological evidence of impaired conflict processing in subjects with MDD. The sLORETA results showed that MDD patients had a higher current density in rostral anterior cingulate cortex (rostral ACC) within N450 time window in response to happy incongruent trials than happy congruent stimuli. Moreover, HC subjects had stronger activity in right inferior frontal gyrus (rIFG) region in response to incongruent stimuli than congruent stimuli, revealing successful inhibition of emotional distraction in HCs, which was absent in MDDs.

**Conclusion:** Our results indicated that rostral ACC was implicated in the processing of negative emotional distraction in MDDs, as well as impaired inhibition of task-irrelevant emotional stimuli, relative to HCs. This work furnishes novel behavioral and neurophysiological evidence that are closely related to emotional conflict among MDD patients.

**Keywords: major depressive disorder, emotional conflict, event-related potentials, source localization, standardized low-resolution brain electromagnetic tomography, N450, P300**

OPEN ACCESS

***Edited by:***
*Xiaochu Zhang, University of Science and Technology of China, China*

***Reviewed by:***
*Ruolei Gu, Institute of Psychology (CAS), China*
*Wenhai Zhang, Yancheng Institute of Technology, China*

***Correspondence:**
*Jianxiu Li*
*jxli2015@lzu.edu.cn*
*Xiaowei Li*
*lixwei@lzu.edu.cn*

***Received:*** *28 December 2017*
***Accepted:*** *08 May 2018*
***Published:*** *29 May 2018*

***Citation:***
*Zhu J, Li J, Li X, Rao J, Hao Y, Ding Z and Wang G (2018) Neural Basis of the Emotional Conflict Processing in Major Depression: ERPs and Source Localization Analysis on the N450 and P300 Components. Front. Hum. Neurosci. 12:214. doi: 10.3389/fnhum.2018.00214*

## INTRODUCTION

Depression is among the most prevalent of all psychiatric disorders (First, 2013). Major depression disorder (MDD) has become a serious mental health issue, which always accompanies by severe symptom[1]. The cardinal features of depressive disorder are the impaired inhibition of task-irrelevant stimuli, especially to negative emotional information (Gotlib and Joormann, 2010). Typically, depressed individuals have difficulty in disengaging attention from negative thoughts, memories, and events in order to sustain attention toward on-going cognitive tasks (Siegle et al., 2002; Disner et al., 2011). In turn, susceptibility to emotional distraction adversely affects the ability of patients to respond to daily life needs. Activation abnormalities in brain areas implicated in emotional processing have been confirmed (Groenewold et al., 2013). However, the influence of negative emotions on depression in emotional conflict processing is still unclear.

Emotional Stroop tasks were commonly used to investigate the emotional conflict of depression in previous studies (Mcneely et al., 2008; Epp et al., 2012). In the research of Epp, subjects are instructed to identify the ink color of words that are either emotionally neutral (such as "apple") or emotionally salient (such as "sad"), depressed subjects usually show longer reaction times (RTs) when naming the ink color of sad than neutral words in comparison to healthy controls (HCs) (Epp et al., 2012). However, the conventional emotional Stroop task does not directly reflect the conflict of emotional processing, since the emotional words and task-related information (ink color) are not in a lexical competition. Remarkably, report of face–word Stroop paradigm (Etkin et al., 2006) provides a feasible way to assess more directly the effects of emotional conflict in major depression. In this task, faces with happy and fearful expressions were presented with the words "happy" or "fear" shown above the facial expression, which yield emotional conflict. The face–word Stroop task is described in the previous literature and has been used in both healthy subjects and diseased subjects to investigate the emotional conflict (Etkin et al., 2006; Egner et al., 2008; Shen et al., 2013; Xue et al., 2017), but relatively few studies were found in major depression using this task.

Except for the researches of experimental paradigm, some researches of conflict control focus on the structural and functional aspects of brain. Here, we exploit some of the methodological insights gained from the study of cognitive conflict and apply them to emotional conflict. Literatures on cognitive conflict indicate that the anterior cingulate cortex (ACC) plays an important role in conflict monitoring (Botvinick et al., 2004; Holmes and Pizzagalli, 2008a) and response selection (Turken and Swick, 1999), similar findings have been reported in tasks involving conflict monitoring (Mansouri et al., 2009). Examination of a broad range of functional imaging, electrophysiological, as well as anatomical data in support of functional segregation has led some authors to divide the ACC into dorsal division for "cognitive" processes and ventral division for "affective" processes (Devinsky et al., 1995; Bush et al., 2000; Steele and Lawrie, 2004). The ventral division composed of rostral and subgenual components (Van Hoesen et al., 1993). Key regions such as the left rostral ACC and right precuneus have been proved to play a paramount role in emotion regulation of depression (Mitterschiffthaler et al., 2008). Furthermore, patients with frontal lobe injury that include the right inferior frontal gyrus (rIFG) are often impaired on inhibitory control tasks (Aron et al., 2003; Rubia et al., 2010). Dolcos and Mccarthy (2006) revealed a role of the IFG in inhibition of emotional distraction in healthy adults. Subjects with great activity in the IFG to emotional distracters tended to rate emotional distracters as less distracting, suggesting that activity in the IFG indexed successful inhibition of emotional distraction. Most of the above studies focused on the brain activation used the functional magnetic resonance imaging (fMRI) with high spatial resolution, but suffer from relatively low temporal resolution. On the other hand, event-related potential (ERP) has a higher temporal resolution, is inexpensive. Combination of high time resolution ERP and standardized low-resolution brain electromagnetic tomography (sLORETA) (Pascual-Marqui, 2002) can effectively solve the inverse source imaging.

The ERP is an impactful technique to explore brain activities (Shen et al., 2013; Zhao et al., 2017a) and has been used to investigate conflict control. So far, researchers observed that two ERP components were related to conflict processing: N450 and P300. N450 component is defined as a negative voltage deflection peaking approximately 450 milliseconds after stimulus presentation with origins in a frontocentral scalp distribution. The N450 component is often assumed to be an index of conflict detection and conflict monitoring, most likely in the response stage (West, 2003) and showed greater N450 amplitude following incongruent stimuli than following congruent stimuli. The P300 is a positive-going potential at parietal electrode sites which peaks around 300–600 ms window following the stimulus onset (Zhao et al., 2017b). P300 component reflects the conflict resolution process because the component is considered to index the stimulus assessment and reflect the sensitivity to the response selection process (Duncan, 1981; Xue et al., 2017). MDDs exhibited abnormal conflict processing in cognitive conflict tasks. As an example, Holmes and Pizzagalli (2008b) found a greater Stroop effect on the RT in depressive patients, and the Stroop effect for N450 component was absent in patients with depression relative to healthy subjects. Another research reported that both the overall N450 amplitude and N450 congruent effect were attenuated in low-performing depression (Holmes and Pizzagalli, 2008a). Moreover, a study of patients with MDD by Dai and Feng (2011) found a smaller P300 amplitude at parietal sites relative to HC subjects using emotional Stroop paradigm. These findings supported that P300 and N450 are all involved with conflict processing. Combined with ERP source imaging, we were interested in exploring the neural mechanisms underlying the emotional conflict processing in MDDs during a face–word Stroop task.

In the current study, we used a face–word Stroop task to examine how the MDD influences the neural process during emotional conflict. In this task, we used emotional faces as our experimental materials. The components of P300 and N450

[1]https://www.nimh.nih.gov/health/topics/depression/index.shtml

associated with conflict processing were extracted for further analysis. On the behavioral level, compared with HCs, we hypothesized that MDD patients would have increased RT Stroop effect in response to happy incongruent stimuli with negative distraction word and happy congruent stimuli with positive distraction. In addition, on the neurological level, we expected MDD patients would demonstrate certain abnormal neurophysiological indicators, which might be manifested as (i) attenuated difference between P300 component to sad congruent stimuli and sad incongruent stimuli; (ii) enhanced rostral ACC activity to happy incongruent stimuli compared with happy congruent stimuli. Further, we hypothesized the rIFG would be recruited under successful suppression of interference in HCs.

# MATERIALS AND METHODS

## Participants

Twenty patients with MDD (aged 32.65 ± 9.6 years; 11 females and 10 males; education level 10.70 ± 3.40 years) and 20 HCs (aged 30.85 ± 9.82 years; 10 females and 10 males; education level 12.10 ± 2.35 years) participated in the experiment. All participants were right-handed, with normal or corrected-to-normal visual acuity. The diagnosis of MDD was determined by a psychiatrist using the Mini International Neuropsychiatric Interview (MINI) (Lecrubier et al., 1997), which was based on the Diagnostic and Statistical Manual of Mental Disorders-IV (DMS-IV) (O'Shea, 1989) and the International Classification of Diseases-10. The HC individuals were free of brain illness history, psychiatric disorders, or medications. Meanwhile, the Patient Health Questionnaire-9 (PHQ-9) was used to assess the severity of depressive symptoms in both groups. Independent *t*-tests were performed to test the difference between two groups, in terms of the age, education, and PHQ-9 scores, respectively, while group difference in the gender was examined by using the Chi-squared test. There are no significant differences between MDD patients and HCs in age ($t_{38} = -0.95$, $p = 0.56$), gender ($\chi^2 = 0.75$, $p = 0.50$), and education level (MDD, 10.70 ± 3.40 years; HC, 12.10 ± 2.35 years; $t_{38} = 1.51$, $p = 0.15$). The PHQ-9 scores from MDD patients were significantly higher than those from HCs (18.75 ± 4.34 for MDD patients; 0.62 ± 1.90 for HC individuals; $t_{38} = 17.09$, $p < 0.0005$). Moreover, the comorbidity anxiety was assessed by psychiatrists using the MINI and the Generalized Anxiety Disorder Scale-7 (GAD-7). The depressive participants with high generalized anxiety symptom were excluded. All participants provided written informed consent before enrolment in the study, which was approved by The Third People's Hospital of Tianshui City's ethics committee. Each subject would receive 100 China Yuan for the participation after experiment.

## Design and Implementation of the Face–Word Stroop Task

Forty happy and 40 sad faces were selected from the international affective pictures systems (IAPSs) (Lang et al., 1997) for use during this study. The faces measured 10.84 cm × 8.13 cm, 240 pixels/inch, and all non-facial features were trimmed (i.e., no hair or clothing). We used Matlab to equate mean pixel luminance, contrast, center-spatial frequency of all faces. The happy facial expression with "高兴" and sad facial expression with "悲伤" were defined as happy congruent condition and sad congruent condition, respectively, whereas the happy facial expression with "悲伤" and sad facial expression with "高兴" were defined as happy incongruent and sad incongruent conditions, respectively. An example of stimuli materials for each condition is shown in **Figure 1A**. Gender and facial expression were balanced across responses and trial type.

The experimental protocol is shown in **Figure 1B**. In each trial, stimulus is displayed for 1000 ms in the center of the black screen, and then a central-fixation cross is presented with a varying inter-stimulus interval (ISI) for 3000–5000 ms (mean ISI = 4000 ms). Participants are instructed to press keys as quickly and accurately as possible to identify the emotion of the presented facial expression, while ignoring emotionally congruent or incongruent words, by pressing button "left" and "right" corresponding to the happy (right middle finger) and sad (right index finger) facial expressions, respectively.

The task consisted of 160 trials of happy or sad facial expressions with the red letters "高兴" (which means "happy") or "悲伤" (which means "sad") shown above the facial expression. The number of trials for each condition is equal (40 trials), with a pseudo-random order. IBM compatible computers and DELL 17-I were used to present this task which was programmed with E-Prime version 2.0 software (Psychology Software Tools Inc., Pittsburgh, PA, United States). Participants were asked to complete four practice trials and reach an accuracy rate (AR) of over 75% before the real experiment. The experiment took place in sound attenuation, light dark down, and air conditioning room.

## EEG Data Acquisition and Preprocessing

EEG was recorded by Net Station software (version 4.5.4) using a 128-channel HydroCel Geodesic Sensor Net site. Impedance of each electrode was kept below 60 kΩ. The sampling rate was 250 Hz. The Cz electrode was used as the reference, and then EEG data were re-referenced offline to average reference (Liu et al., 2015). EEGLAB (Delorme and Makeig, 2004) toolbox and ERPLAB (Lopezcalderon and Luck, 2014) toolbox in Matlab were used to process and analyze the continuous EEG data. Specifically, the EEG data were filtered by high-pass filter with a cutoff frequency of 0.1 Hz and low-pass filter with a cutoff frequency of 30 Hz. We removed the section of EEG data with large muscle noise or extreme voltage offset by visual inspection, such as swallowing and coughing. Components that associated with eye movements and eye blinking activities were identified and removed by performing independent component analysis (ICA) for each participant (Jung et al., 2000).

## Analysis of Behavioral Data

For behavioral data, we mainly focused on analyzing behavioral adjustments related to the occurrence of conflict responses. According to previous studies (Holmes and Pizzagalli, 2008b; Epp et al., 2012; Schmidt, 2013), we calculated the Stroop effect and Gratton effect. The Stroop effect is a measurement of interference caused by incongruent stimuli compared with congruent

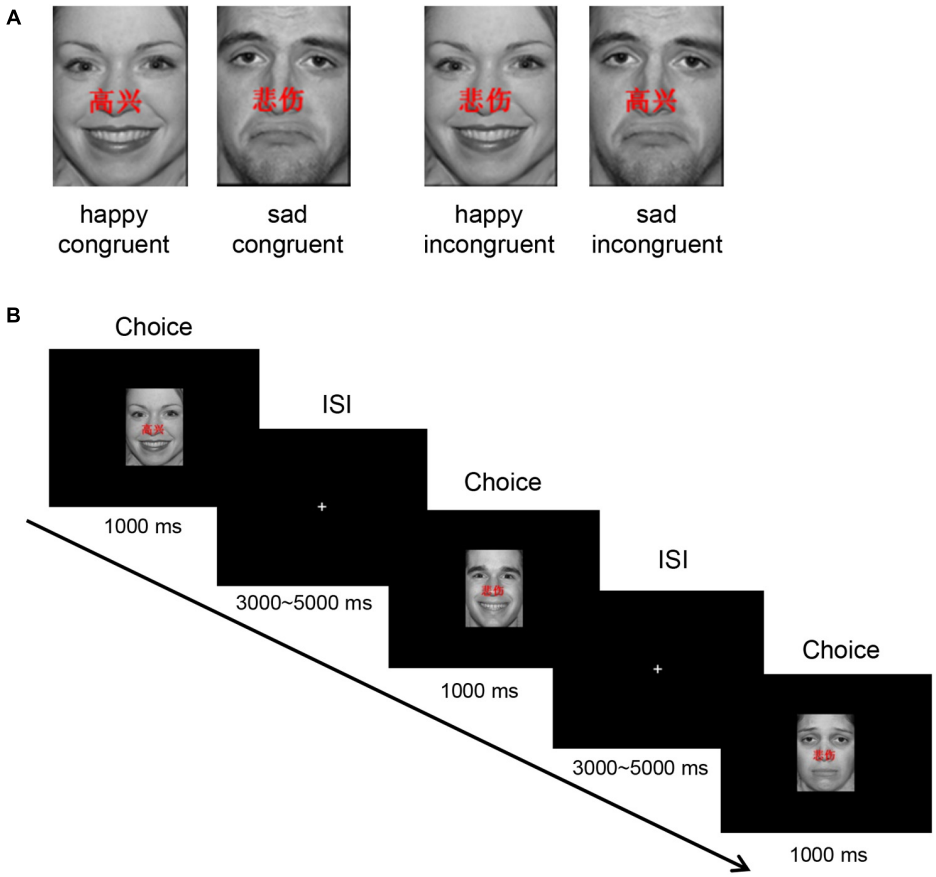


**FIGURE 1 |** Experimental protocol. **(A)** An example of stimuli materials for each condition. **(B)** Example timelines used in the face–word Stroop task. Participants needed to complete the identification of facial affect with happy or sad expressions that had either "高兴" (which means "happy") or "悲伤" (which means "sad") word written across them.

stimuli. It is calculated as: ($RT_{incongruent\ trials} - RT_{congruent\ trials}$) and ($Accuracy_{congruent\ trials} - Accuracy_{incongruent\ trials}$). As a result, the larger scores are indicative of increased Stroop interference effect (Holmes and Pizzagalli, 2008b). The Gratton effect is a demonstration of post-conflict behavior adjustment. It is calculated as: ($RT_{incongruent\ trials\ following\ incongruent\ trial} - RT_{incongruent\ trials\ following\ congruent\ trial}$) and ($Accuracy_{incongruent\ trials\ following\ incongruent\ trial} - Accuracy_{incongruent\ trials\ following\ congruent\ trial}$). The higher scores are indicative of increased cognitive control (Epp et al., 2012). For Gratton effect, we only examined the trials with the correct response for analysis of post-conflict adjustment, in order to distinguish the post-conflict and post-error adjustment effects (Pizzagalli et al., 2006). The number of trials with high conflict trials and low conflict trials in each group was about 40. Numbers of trials remaining for each trial type were balanced.

## Analysis of ERP Components

In order to measure the ERP waveforms, ICA-corrected EEG data were segmented into epochs starting at 200 ms prior to stimuli onset until 1000 ms after the stimuli appeared, and baseline corrected using −200 to −100 ms pre-stimuli. Approximately 7% of all trails (the signal exceeded ±100 μV) for each emotional face in congruent and incongruent conditions were excluded. Statistical results manifested that numbers of trials remaining for each trial type had no significant difference ($p > 0.05$).

Event-related potential analyses mainly focused on components of N450 and P300. Based on the previously reported literature (Krompinger and Simons, 2011; Xue et al., 2017) and scalp topographies, in the present study, the mean amplitude and latency of the N450 were measured between 350 and 700 ms following the stimuli onset at average electrodes of AF3, AF4, FP1, FP2, F5, and F6. The P300 was defined at average electrodes of CPz and Pz with a time window between 300 and 600 ms after stimuli presentation.

## Standardized Low-Resolution Brain Electromagnetic Tomography

To identify neural generators involved in emotional conflict of major depression and their corresponding functional roles in the emotional conflict control, the brain sources of each ERP component were reconstructed using sLORETA (Pascual-Marqui, 2002). The sLORETA is a functional source imaging

method based on a three-shell spherical model registered to the Talairach human brain atlas, available as a digitized MRI from provided the Brain Imaging Centre, Montreal Neurological Institute (MNI, Talairach and Tournoux, 1988). The spatial extent of the current density includes cortical gray matter and hippocampal area, a total of 6239 voxels at 5 mm spatial resolution. At each voxel, the dipole moment of three directions was estimated. The sLORETA uses the minimum norm criterion to estimate the current density, positioning according to the local maximum current density. According to our previous research (Li et al., 2015), 69 scalp electrodes were used in source localization analysis to answer two questions, i.e., "When" and "where." The "When" question tries to position the difference temporally and the "Where" question tries to position these differences in the three-dimensional space within the brain.

In order to answer the "When" problem, paired and independent *t*-tests were calculated for all 300 time-samples of each epoch (4 ms each per sample, i.e., 1200 ms) to examine the differences between conditions and between groups, respectively. For each comparison, we selected separately about 10 significant time-samples ($p < 0.05$, two-tailed) within the time ranges of P300 and N450 components for further analysis. The significance level was corrected for multiple comparisons and false positives (Nichols and Holmes, 2002). Afterward, in order to answer the "Where" question, sLORETA values were created from these time-samples for each condition and group. Paired and independent *t*-tests were calculated to identify the differences between the conditions and between the groups. For each comparison, source localization results of ERP data of each trial type were compared voxel-by-voxel using an independent log-F-ratio statistic test, and found significant activation of brain areas at $p < 0.05$.

## Statistical Analyses

### Behavioral Data

Only trials in which participants made responses were considered. We also excluded the trials with RT that exceeded the individual mean ± 2 standard deviation (SD) for each trial type.

For the Stroop effect, mixed 2 × 2 ANOVA with group (MDDs vs. HCs) as a between-subjects factor and $face_{score}$ (Stroop scores for emotional faces, $happy_{stroop}$ vs. $sad_{stroop}$) as a within-subject factor was conducted on RT and AR. For the Gratton effect of RT and AR, independent *t*-tests were performed to test the difference between MDDs and HCs. As described above, merely the trials after the correct trial were considered.

### ERP Data

To evaluate the characteristics of emotional conflict in MDDs, we compared ERP components between MDDs and HCs. In particular, the analyses mainly focused on N450 component associated with conflict monitoring and P300 associated with conflict resolution processing. Repeated-measure ANOVAs with face (happy vs. sad) and congruency (congruent vs. incongruent) as within-subjects factors and group (MDDs vs. HCs) as between-subjects factor were conducted for the mean amplitude and latency of P300 and N450, respectively. Greenhouse–Geisser corrections were applied. In these analyses, we corrected for multiple comparisons with the Bonferroni method.

# RESULTS

## Behavioral Measures

The average RT and AR scores of two groups for the Stroop effect and the Gratton effect are described in **Table 1**.

### Stroop Effect

Statistical analysis on the RT did reveal a significant interaction effect of $face_{score}$ × group ($F_{1,38} = 4.06$, $p = 0.05$). No other significant effects emerged. To further explore this interaction of between $face_{score}$ and group, *post hoc* Newman-Keuls tests were performed. Results revealed that the difference between groups was significant in responding to happy facial expression ($F_{1,38} = 6.12$, $p < 0.02$), indicating that the Stroop score between happy incongruent trials and happy congruent trials in MDDs was significantly higher than those of HC group.

ARs revealed a significant main effect of $face_{score}$ ($F_{1,38} = 6.00$, $p < 0.02$), with higher Stroop scores to identify happy facial expression than to identify sad facial expression in participants. No other main effects or interactions obtained significance.

**TABLE 1 |** Summary of behavioral, the ERP average of channels AF3, AF4, FP1, FP2, F5, and F6 for the N450 component and the ERP average of channels CPz and Pz for the P300 component in the MDDs and HCs.

| | | MDDs | HCs |
|---|---|---|---|
| *A. Behavioral performance* | | | |
| Stroop scores RT | Happy face | 27.42 (18.87) | 10.36 (24.58) |
| | Sad faces | 11.67 (24.29) | 15.52 (26.63) |
| Stroop scores AR | Happy face | 5.00 (9.17) | 5.62 (6.00) |
| | Sad faces | 0.37 (5.63) | 2.37 (6.04) |
| Gratton scores RT | | 6.4 (26.56) | 14.61 (27.19) |
| Gratton scores AR | | 3.4 (7.97) | 2.93 (5.24) |
| *B. Scalp ERP data* | | | |
| N450 amplitude (μV) | Happy congruent | −0.70 (4.25) | −0.4861 (9.76) |
| | Happy incongruent | −1.25 (6.29) | −1.03 (9.41) |
| | Sad congruent | −1.05 (4.92) | −0.99 (7.27) |
| | Sad incongruent | −1.65 (4.89) | −1.57 (9.42) |
| N450 latency (ms) | Happy congruent | 620.07 (78.19) | 487.27 (42.52) |
| | Happy incongruent | 590.80 (59.81) | 498.37 (44.62) |
| | Sad congruent | 621.13 (76.61) | 596.467 (88.62) |
| | Sad incongruent | 615.37 (95.69) | 489.07 (54.33) |
| P300 amplitude (μV) | Happy congruent | 4.51 (2.72) | 3.10 (3.96) |
| | Happy incongruent | 4.34 (3.23) | 2.63 (3.60) |
| | Sad congruent | 4.47 (2.78) | 2.00 (3.42) |
| | Sad incongruent | 4.78 (3.25) | 3.11 (3.65) |
| P300 latency (ms) | Happy congruent | 497.60 (56.53) | 514.40 (53.53) |
| | Happy incongruent | 502.00 (45.84) | 504.60 (66.63) |
| | Sad congruent | 494.50 (58.48) | 471.80 (58.80) |
| | Sad incongruent | 498.10 (54.69) | 490.90 (53.31) |

### Conflict-Adaptation (Gratton) Effects

For both RT and AR, independent *t*-tests result showed that there are no significant differences between MDD patients and HCs.

## ERP Waveforms of Two Groups in Face–Word Stroop Task

For amplitude of N450, no significant main or interaction effect was found. For latency of N450, there was a significant difference between two groups (**Figure 2**, $F_{1,38} = 28.72$, $p < 0.0005$). Furthermore, the results of statistical analysis revealed significant main effects of face ($F_{1,38} = 9.94$, $p < 0.01$) and congruency ($F_{1,38} = 14.14$, $p < 0.01$), and a two-way interaction of face × congruency ($F_{1,38} = 8.54$, $p < 0.01$, and a three-way interaction of face × congruency × group ($F_{1,38} = 19.07$, $p < 0.0005$) were significant. To further examine the three-way interaction, a simple effect test was performed. It showed a significant effect of congruency for happy facial expression in MDD group ($F_{1,38} = 5.30$, $p < 0.02$), and a significant effect of congruency for sad facial expression in HC group ($F_{1,38} = 28.13$, $p < 0.0005$). The HC individuals manifested shorter N450 latency at sad incongruent trials than at sad congruent trials. However, MDD group had shorter N450 latency at happy incongruent trials than at happy congruent trials.

We found significant differences in P300 amplitude between two groups (**Figure 3**, $F_{1,38} = 4.75$, $p < 0.05$). A significant interaction of face × congruency ($F_{1,38} = 6.23$, $p < 0.02$) and a three-way marginal interaction of face × congruency × group ($F_{1,38} = 4.04$, $p = 0.052$) were observed. No significant main or interaction effect was found. To further examine the three-way marginal interaction, a simple effect test was performed. It showed a significant effect of congruency for sad facial expression in HC group ($F_{1,38} = 6.96$, $p < 0.02$), such that P300 latency following sad incongruent stimuli was significantly higher than sad congruent stimuli in HCs. For P300 latency, no significant main or interactions effects were found. The detailed amplitude and latency of P300 and N450 were summarized in **Table 1**.

## sLORETA: Between Groups and Conditions Differences for ERP Components

The sLORETA statistical non-parametric maps from within-subject comparison and between-subject comparison within N450 and P300 time windows were shown in **Figure 4**. Note that these maps represent log-F-ratio statistic results for each comparison. HC group exhibited a significant difference between current densities of congruent trials and incongruent trials with activation during incongruent trials being higher (**Figure 4**). As illustrated in **Table 2**, the differences revealed significantly increased inferior frontal gyrus [IFG: Brodmann area (BA) 47] activation to happy incongruent stimuli than happy congruent stimuli, as well as enhanced IFG, superior or medial frontal gyrus (SFG/MFG: BA 6/8/9) activation to sad incongruent stimuli relative to sad congruent stimuli at the N450 time window. However, MDD patients demonstrated a pattern of significantly increased current density in rostral ACC (BA 24/32/33), posterior cingulate cortex (PCC: BA 23/30/31), cingulate gyrus (BA 23/24), and insula (BA13) activation to the happy incongruent stimuli than happy congruent stimuli at N450 time window.

Groups differed was significant solely on the current density of incongruent stimuli. As we demonstrated in **Supplementary Figure S1**, for happy incongruent trials, sLORETA analysis suggested that MDD patients had lower activity in precentral gyrus (BA 6) within the N450 time window relative to HC individuals. For sad incongruent trials, a higher estimated current density in precuneus (BA 7/19), as well as superior and inferior parietal lobule (SPL/IPL: BA 7/40) were observed in MDD patients for P300 component compared with HCs. The difference of congruent conditions was not significant between groups. The summary of the results is presented in **Table 2**.

## Correlations

To examine the relationship between behavior and electrophysiological signature, we correlated the RT Stroop score and AR Stroop score separately with the difference in amplitudes of the P300 and N450 on emotion-incongruent and emotion-congruent trials. Pearson's correlation test was used to assess the correlation between variables. A negative relationship of RT Stroop score with the difference in P300 amplitude between sad incongruent and sad congruent trials was observed in HCs ($p = 0.002$, $r = -0.64$). This negative correlation was lost in MDDs. The difference in P300 amplitude as a function of each of the RT measure is shown in **Supplementary Figure S2**.

# DISCUSSION

The goal of present study was to examine the impact of sad and happy emotions on major depression in response to emotional deficit, with a face–word Stroop task in which emotional faces as experimental materials. The following findings emerged. Firstly, for Stroop effect, MDD subjects were characterized by significantly increased scores between RT of happy congruent trials and RT of happy incongruent trials, relative to HC subjects. Since the Stroop effect is a measurement of interference elicited by the incongruent trials, relative to congruent (Holmes and Pizzagalli, 2008b; Schmidt, 2013; Braverman and Meiran, 2015), higher Stroop scores indicated increased interference effects. This finding manifested that MDDs had increased RT interference effects to happy incongruent trials in comparison to HCs. For both sad congruent trials and sad incongruent trials, no group differences for Stroop scores emerged in our study. The models of Beck et al. (1979) and Bower (1981) predict that depression associated with an attentional bias for mood-congruent stimuli. This result suggests that the emotional conflict processing in major depression was characterized by an attentional bias for negative distractive stimuli and need enhanced cognitive control. Moreover, participants showed higher Stroop scores to identify happy facial expression than to identify sad facial expression in AR, indicating that happy congruent trials than sad incongruent trials induced enhanced interference effects. However, for Gratton effect, comparison of post-conflict behavior adjustment in two groups had no significant difference in RT and AR.

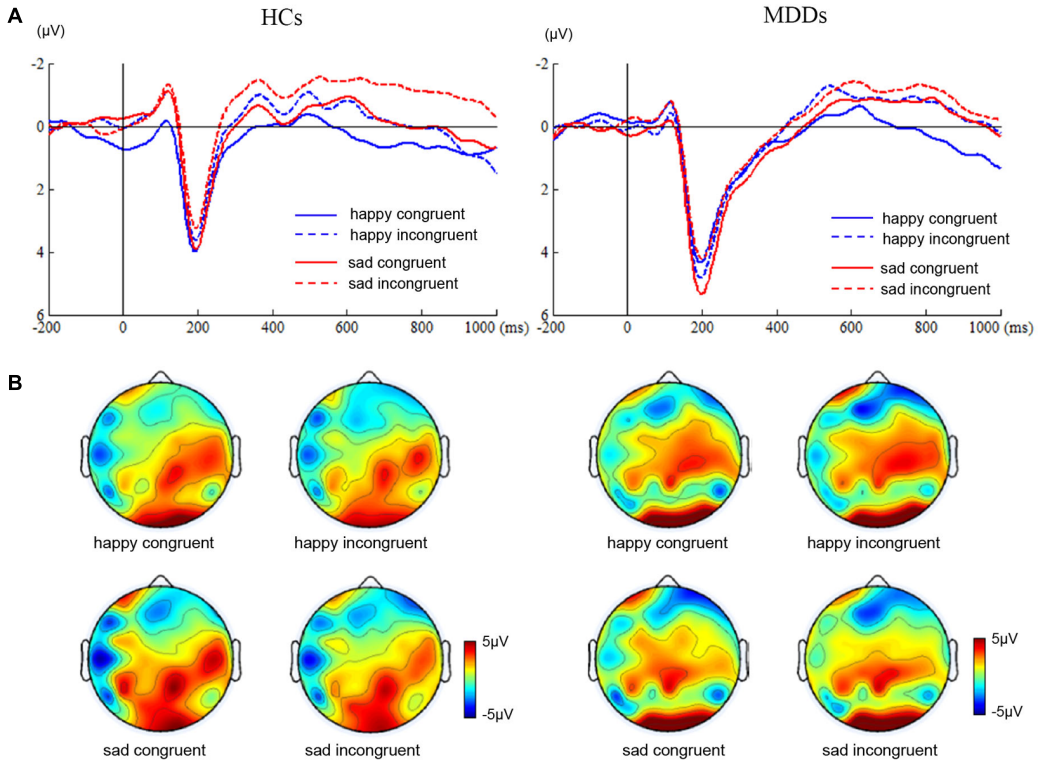


**FIGURE 2 |** ERP waveforms and scalp topographies of N450. The waveforms were averaged across AF3, AF4, FP1, FP2, F5, and F6 to reflect the N450 ANOVA findings **(A)**. The corresponding scalp topographies elicited by the target congruent stimuli and incongruent stimuli were obtained for a 20-ms long time interval around the latencies of the N450 peaks **(B)**.

Secondly, patients with MDD failed to show obvious Stroop interference effects for N450 amplitude (**Figure 2**). However, significantly shorter latency of the N450 to happy incongruent stimuli than happy congruent stimuli was found in MDDs. Previous studies have shown that the N450 was attenuated in folks with impaired ability to suppress competitive lexical information in incongruent trials (Mayes et al., 2005). Contrary to these findings, this study manifested that MDDs were characterized by significantly shorter N450 latency in response to happy incongruent stimuli than happy congruent stimuli. The finding may suggest that MDDs require early evaluation processes during incongruent stimuli with negative distractive word compared with congruent stimuli with positive distractive word, so as to perform the task at a normative level. Although the HCs failed to observe Stroop effect at N450 time window between congruent and incongruent stimuli during the Stroop task, a slice of examines have manifested that the effect is usually more robust when trials frequency is manipulated (Vanderhasselt and De, 2009).

With regard to P300, P300 amplitude of HC individuals was significantly greater when following sad incongruent stimuli relative to following sad congruent stimuli, and was maximal at central-parietal recording sites (**Figure 3**). The larger P300 amplitude indicates the stronger inhibition capability to incongruent stimulus, which is consistent with previous studies (Ramautar et al., 2006; Smith et al., 2010). Pearson's correlations showed that a significant negative relationship between RT Stroop score and the difference in P300 amplitude for sad faces had emerged in the present study in HCs (**Supplementary Figure S2A**), which indicated that larger P300 amplitude difference between sad incongruent and sad congruent trials reflects greater inhibition capability and is corresponding to lower Stroop interference effect in RT. Unlike HCs, this pattern was absent in MDDs. The previous study has reported that patients with depression have diverse attention to emotional information relative to HCs, which is characterized by a higher degree of participation in emotional information (Liu et al., 2007). The finding may imply that the processing of depression on the sad face affects the handling of emotional conflicts of patients with MDD.

Thirdly, source localization analyses indicated that MDD subjects had significantly enhanced activity in rostral ACC (BA 24/32/33), PCC (BA 23/30/31), and insula (BA 13) within N450 time window in response to happy incongruent stimuli than happy congruent stimuli (**Figure 4A** and **Table 2**). Previous studies have shown that rostral ACC integrates emotions and conflicts (Kanske and Kotz, 2011), and are activated for conflict when stimuli are emotional (Egner et al., 2008). The current results indicated that response to conflict from negative distractive word was associated with activation in the rostral ACC. These results offer support for the longstanding view that the rostral ACC is involved in

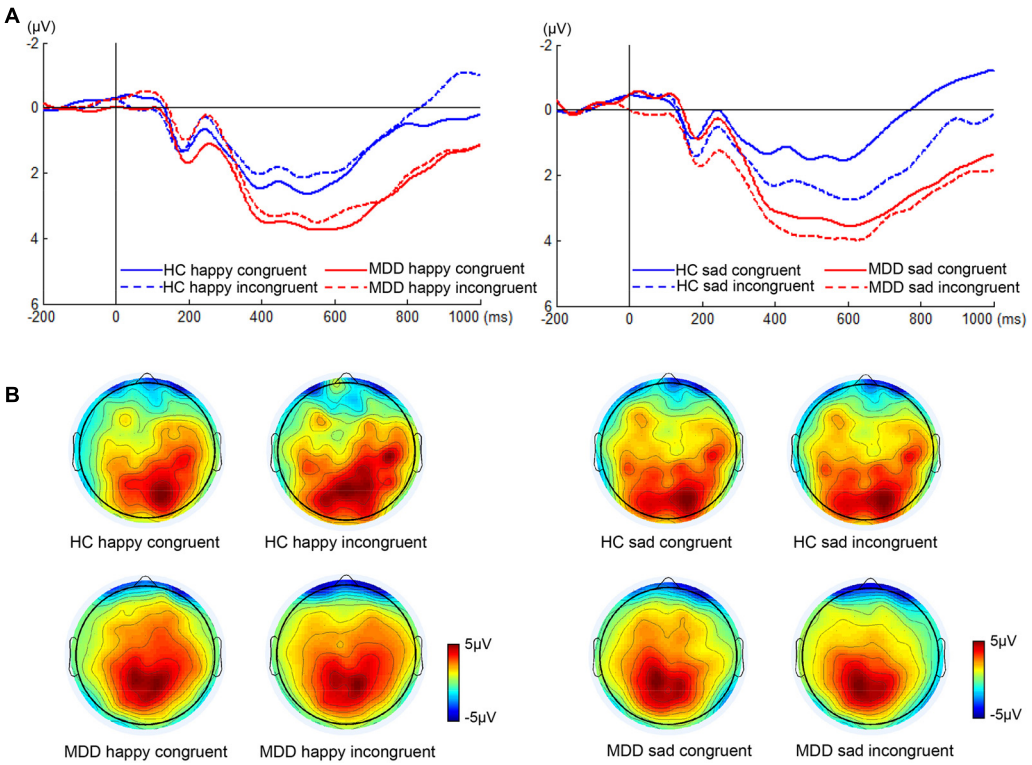


**FIGURE 3 |** ERP waveforms and scalp topographies of P300. The waveforms were averaged across electrodes CPz and Pz to reflect the P300 ANOVA findings **(A)**. The corresponding scalp topographies elicited by the target congruent stimuli and incongruent stimuli were obtained for a 20-ms long time interval around the latencies of the P300 peaks **(B)**.

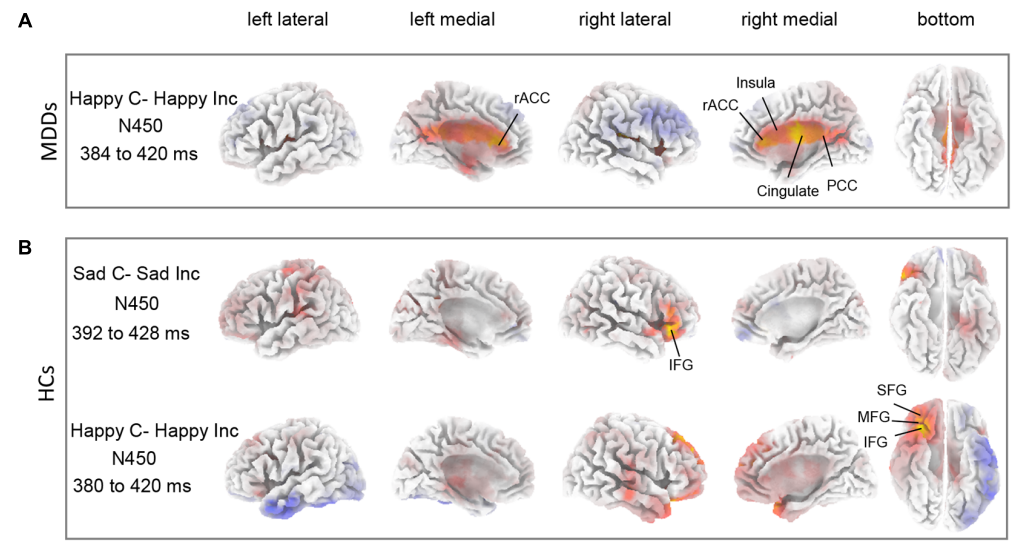


**FIGURE 4 |** Differences between task conditions. The statistical differences between congruent and incongruent task conditions are shown for HC **(A)** and for MDD **(B)** groups within N450 time window. Yellow color indicates significantly higher estimated current density of incongruent trials compared with congruent trials. The time periods for different components are also shown in **Table 2**.

affective processing (Devinsky et al., 1995; Bush et al., 2000). Furthermore, substantiate previous data indicating that the rostral ACC is involved in processing task-irrelevant emotional stimuli (Bishop et al., 2004; Egner et al., 2008), and that its processing may be exclusive to the affective domain (Mohanty et al., 2007). Besides, similar work using fMRI on an emotional

**TABLE 2 |** Comparison of congruent and incongruent tasks as well as HCs and MDD individuals in the time ranges of P300 and N450 components in sLORETA.

| Lobe | Structure | OBA | Activity | MNI |
|---|---|---|---|---|
| *A. Differences between task conditions in HCs* | | | | |
| (a) N450 sad congruent trials < sad incongruent trials (392–428 ms) | | | | |
| Frontal lobe | Inferior frontal gyrus | 47R | ↑ | 30, 30, −20 |
| Frontal lobe | Middle frontal gyrus | 11R | ↑ | 30, 35, −20 |
| Frontal lobe | Superior frontal gyrus | 9R | ↑ | 20, 50, 40 |
| (b) N450 happy congruent trials < happy incongruent trials (380–420 ms) | | | | |
| Frontal lobe | Inferior frontal gyrus | 47R | ↑ | 45, 30, −5 |
| *B. Differences between task conditions in MDDs* | | | | |
| (a) N450 happy congruent trials < happy incongruent trials (384–420 ms) | | | | |
| Sub-lobar | Insula | 13R | ↑ | 35, −20, 20 |
| Limbic lobe | Cingulate gyrus | 23/24R | ↑ | 5, −10, 30 |
| Limbic lobe | Cingulate gyrus | 24/31L | ↑ | −5, −5, 30 |
| Limbic lobe | Anterior cingulate | 24/33L | ↑ | −5, 25, 15 |
| Limbic lobe | Anterior cingulate | 24/32/33R | ↑ | 5, 30, 15 |
| Sub-lobar | Insula | 13L | ↑ | −35, −15, 20 |
| Limbic lobe | Posterior cingulate | 23R | ↑ | 5, −30, 25 |
| Limbic lobe | Posterior cingulate | 23L | ↑ | −5, −45, 25 |
| Limbic lobe | Posterior cingulate | 23/30M | ↑ | 0, −50, 20 |
| *C. Differences between groups* | | | | |
| (a) N450 for happy incongruent trials (360–400 ms) MDDs < HCs | | | | |
| Frontal lobe | Precentral gyrus | 6R | ↓ | 45, −5, 55 |
| (b) P300 for sad incongruent trials (480–520 ms) MDDs > HCs | | | | |
| Parietal lobe | Inferior parietal lobule | 40R | ↑ | 40, −55, 50 |
| Parietal lobe | Superior parietal lobule | 7R | ↑ | 40, −60, 50 |

*OBA, orientation Brodmann area; R, right; L, left; M, medial; ↑, significantly increased neural activity; ↓, significantly decreased neural activity; MNI, Montreal Neurological Institute.*

Stroop task manifested that severity of depressive symptoms was positively correlated with PCC activity in processing negative distractors (Kaiser et al., 2015), which was also considered indicative of evidence of impaired conflict processing that MDD patients processed increased internally directed attention to negative emotional stimuli. These findings suggested that negative emotional distraction leads to greater conflict in the high depressive symptoms of individuals and rostral ACC is involved in processing task-irrelevant emotional stimuli.

Finally, incongruent stimuli in HC subjects induced higher activity in IFG (BA 47) region at N450 time window compared with sad congruent stimuli (**Figure 4B** and **Table 2**). The defect of inhibition may undermine the adaptive emotional regulation strategy, this requires an individual to overcome and replace the initial negative interpretation of emotional induction. In fact, the deficiencies of inhibition have been confirmed in depression (Gotlib and Joormann, 2010). Saunders and Jentzsch (2014) found that participants with a high-depression symptom score processed difficulty with inhibition on an emotional-face Stroop task. In particular, a slice of studies have reported that the IFG is associated with successful cognitive function and executive function in the inhibition process (Whalen et al., 1998; Chiu et al., 2008; Morein-Zamir et al., 2014). Chiu et al. (2008) revealed enhanced activity in the region of right IFG to affective response inhibition. As Morein-Zamir et al. (2014) detected a significantly reduced activation when controlling for attentional processing, it indicated that low activation of the right IFC in ADHD was connected with the impaired response inhibition. HCs demonstrated increased right IFG activity to incongruent stimuli relative to congruent stimuli, which was suggesting of successful inhibition of emotional distraction. MDD patients lack this inhibitory effect on processing of emotional distraction. Furthermore, a significant effect of increased activity was found in region of the MFG for sad incongruent stimuli in HC group implies that attention may reorient to relevant targets from unrelated emotional distraction. This finding is in line with previous studies by Japee et al. (2015) which was suggestive of a crucial role of right MFG in reorienting of attention.

The statistical differences between groups for the sad incongruent task condition are illustrated in **Supplementary Figure S1**. The differences manifested an increase of activity in SPL and IPL (BA 7/40) within P300 time window (**Table 2**). Activation of the SPL can be caused when the subjects have to disengage their attention from fixation and move it to a cued location (Liu et al., 2003; Serences et al., 2004; Shomstein and Yantis, 2004). In the current work, the change in the SPL and IPL was interpreted as shift of attention from happy emotional distraction to location of sad facial expression in MDD individuals. We speculate that the higher activation in SPL in MDDs may reflect top-down attentional control.

From a clinical perspective, impairment of emotional conflict control is a major characteristic of MDD patients. The results of this study support the notion that depressive participants displayed dysfunction in the executive process and dysfunction of both emotional conflict monitoring and cognitive control processes. The major limitation of the present work is that relatively few electrodes are used in source localization. As emphasized in the previous study (Liu et al., 2017, 2018), high-density EEG can furnish both high spatial sampling density and large head coverage. Furthermore, there are many advanced tools for an effective network study (Yao et al., 2016; Hu et al., 2017), the introduction of which to them into major depression research would be meaningful. Finally, the research of functional and structural integrity of frontal pathways which are closely connected with emotional conflict among MDD patients should remain an important area for future study using high-density EEG.

## CONCLUSION

The present study investigated the differences in behavior and neural response to the emotional conflict in major depressive subjects and HCs, using a face–word Stroop task. Compared with HCs, abnormalities in MDDs in emotional conflict have been demonstrated through novel behavioral and neurophysiological

evidence. As an example, MDD patients exhibited significant Stroop effects during the processing of happy incongruent and happy congruent trials, as well as the attenuated difference between P300 component to sad congruent stimuli and sad incongruent stimuli, relative to HCs. Source localization analyses indicated that MDDs had enhanced rostral ACC activity to happy incongruent stimuli than congruent stimuli, indicating that the rostral ACC is involved in processing task-irrelevant emotional stimuli. Furthermore, a higher activation in the region of right IFG was found in HCs for incongruent stimuli than for congruent stimuli. The increased activation in the right IFG was indicative of successful suppression of the emotional distraction in HCs, which was absent in MDD patients. These findings not only improve our understanding of the inhibition of MDD patients, but also pave the way for cognitive neuropsychological disorders modeling.

## AUTHOR CONTRIBUTIONS

JL and XL conceived and designed the study. JZ, JL, and ZD acquired the data. JZ, JL, and XL analyzed and interpreted the data. All authors wrote the manuscript.

## FUNDING

This study was funded by the National Basic Research Program of China (973 Program) (No. 2014CB744600); the National Natural Science Foundation of China (Nos. 61632014 and 61210010); the International Cooperation Project of Ministry of Science and Technology (No. 2013DFA11140); and the Program of Beijing Municipal Commission of Science and Technology (No. Z171100000117005).

## ACKNOWLEDGMENTS

We thank Dr. Quanying Liu for her great help in analyzing data and drafting manuscript.

## SUPPLEMENTARY MATERIAL

The Supplementary Material for this article can be found online at: https://www.frontiersin.org/articles/10.3389/fnhum.2018.00214/full#supplementary-material

**FIGURE S1 |** Differences between groups. The statistical differences between MDDs and HCs for happy incongruent trials within N450 time window **(A)** and for sad incongruent trials within P300 time windows **(B)**, respectively. Yellow color indicates MDDs > HCs. Blue color indicates MDDs < HCs. The time periods for different components are shown in **Table 2**.

**FIGURE S2 |** Relationship between difference in P300 amplitude and RT Stroop score. The difference in P300 amplitude between sad incongruent and sad congruent trials is significantly correlated with RT Stroop score for HCs **(A)**. However, it was not correlated with RT Stroop score for MDDs **(B)**. *X*-axis: RT Stroop score; *Y*-axis: Difference amplitude represents the difference in amplitude of the P300 on emotion-incongruent and emotion-congruent trials.

## REFERENCES

Aron, A. R., Fletcher, P. C., Bullmore, E. T., Sahakian, B. J., and Robbins, T. W. (2003). Stop-signal inhibition disrupted by damage to right inferior frontal gyrus in humans. *Nat. Neurosci.* 6, 115–116. doi: 10.1038/nn1003

Beck, A. T., Rush, J. A., Shaw, B. F., and Emery, G. (1979). *The Cognitive Therapy of Depression*. New York, NY: The Guilford Press.

Bishop, S., Duncan, J., Brett, M., and Lawrence, A. D. (2004). Prefrontal cortical function and anxiety: controlling attention to threat-related stimuli. *Nat. Neurosci.* 7, 184–188. doi: 10.1038/nn1173

Botvinick, M. M., Cohen, J. D., and Carter, C. S. (2004). Conflict monitoring and anterior cingulate cortex: an update. *Trends Cogn. Sci.* 8, 539–546. doi: 10.1016/j.tics.2004.10.003

Bower, G. H. (1981). Mood and memory. *Am. Psychol.* 36, 129–148. doi: 10.1037/0003-066X.36.2.129

Braverman, A., and Meiran, N. (2015). Conflict control in task conflict and response conflict. *Psychol. Res.* 79, 238–248. doi: 10.1007/s00426-014-0565-5

Bush, G., Luu, P., and Posner, M. I. (2000). Cognitive and emotional influences in anterior cingulate cortex. *Trends Cogn. Sci.* 4, 215–222. doi: 10.1016/S1364-6613(00)01483-2

Chiu, P. H., Holmes, A. J., and Pizzagalli, D. A. (2008). Dissociable recruitment of rostral anterior cingulate and inferior frontal cortex in emotional response inhibition. *Neuroimage* 42, 988–997. doi: 10.1016/j.neuroimage.2008.04.248

Dai, Q., and Feng, Z. (2011). Deficient interference inhibition for negative stimuli in depression: an event-related potential study. *Clin. Neurophysiol.* 122, 52–61. doi: 10.1016/j.clinph.2010.05.025

Delorme, A., and Makeig, S. (2004). EEGLAB: an open source toolbox for analysis of single-trial EEG dynamics including independent component analysis. *J. Neurosci. Methods* 134, 9–21. doi: 10.1016/j.jneumeth.2003.10.009

Devinsky, O., Morrell, M. J., and Vogt, B. A. (1995). Contributions of anterior cingulate cortex to behaviour. *Brain* 118(Pt 1), 279–306. doi: 10.1093/brain/118.1.279

Disner, S. G., Beevers, C. G., Haigh, E. A. P., and Beck, A. T. (2011). Neural mechanisms of the cognitive model of depression. *Nat. Rev. Neurosci.* 12, 467–477. doi: 10.1038/nrn3027

Dolcos, F., and Mccarthy, G. (2006). Brain systems mediating cognitive interference by emotional distraction. *J. Neurosci.* 26, 2072–2079. doi: 10.1523/JNEUROSCI.5042-05.2006

Duncan, C. C. (1981). The Stroop effect: brain potentials localize the source of interference. *Science* 214, 938–940. doi: 10.1126/science.7302571

Egner, T., Etkin, A., Gale, S., and Hirsch, J. (2008). Dissociable neural systems resolve conflict from emotional versus nonemotional distracters. *Cereb. Cortex* 18, 1475–1484. doi: 10.1093/cercor/bhm179

Epp, A. M., Dobson, K. S., Dozois, D. J. A., and Frewen, P. A. (2012). A systematic meta-analysis of the Stroop task in depression. *Clin. Psychol. Rev.* 32, 316–328. doi: 10.1016/j.cpr.2012.02.005

Etkin, A., Egner, T., Peraza, D. M., Kandel, E. R., and Hirsch, J. (2006). Resolving emotional conflict: a role for the rostral anterior cingulate cortex in modulating activity in the amygdala. *Neuron* 51, 871–882. doi: 10.1016/j.neuron.2006.07.029

First, M. B. (2013). Diagnostic and statistical manual of mental disorders, 5th edition, and clinical utility. *J. Nerv. Ment. Dis.* 201, 727–729. doi: 10.1017/S1092852913000710

Gotlib, I. H., and Joormann, J. (2010). Cognition and depression: current status and future directions. *Annu. Rev. Clin. Psychol.* 6, 285–312. doi: 10.1146/annurev.clinpsy.121208.131305

Groenewold, N. A., Opmeer, E. M., De, J. P., Aleman, A., and Costafreda, S. G. (2013). Emotional valence modulates brain functional abnormalities in depression: evidence from a meta-analysis of fMRI studies. *Neurosci. Biobehav. Rev.* 37, 152–163. doi: 10.1016/j.neubiorev.2012.11.015

Holmes, A. J., and Pizzagalli, D. (2008a). Spatiotemporal dynamics of error processing dysfunctions in major depressive disorder. *Arch. Gen. Psychiatry* 65, 179–188. doi: 10.1001/archgenpsychiatry.2007.19

Holmes, A. J., and Pizzagalli, D. A. (2008b). Response conflict and frontocingulate dysfunction in unmedicated participants with major depression. *Neuropsychologia* 46, 2904–2913. doi: 10.1016/j.neuropsychologia.2008.05.028

Hu, B., Dong, Q., Hao, Y., Zhao, Q., Shen, J., and Zheng, F. (2017). Effective brain network analysis with resting-state EEG data: a comparison between heroin abstinent and non-addicted subjects. *J. Neural Eng.* 14:046002. doi: 10.1088/1741-2552/aa6c6f

Japee, S., Holiday, K., Satyshur, M. D., Mukai, I., and Ungerleider, L. G. (2015). A role of right middle frontal gyrus in reorienting of attention: a case study. *Front. Syst. Neurosci.* 9:23. doi: 10.3389/fnsys.2015.00023

Jung, T. P., Makeig, S., Humphries, C., Lee, T. W., Mckeown, M. J., Iragui, V., et al. (2000). Removing electroencephalographic artifacts by blind source separation. *Psychophysiology* 37, 163–178. doi: 10.1111/1469-8986.3720163

Kaiser, R. H., Andrews-Hanna, J. R., Spielberg, J. M., Warren, S. L., Sutton, B. P., Miller, G. A., et al. (2015). Distracted and down: neural mechanisms of affective interference in subclinical depression. *Soc. Cogn. Affect. Neurosci.* 10, 654–663. doi: 10.1093/scan/nsu100

Kanske, P., and Kotz, S. A. (2011). Emotion triggers executive attention: anterior cingulate cortex and amygdala responses to emotional words in a conflict task. *Hum. Brain Mapp.* 32, 198–208. doi: 10.1002/hbm.21012

Krompinger, J. W., and Simons, R. F. (2011). Cognitive inefficiency in depressive undergraduates: Stroop processing and ERPs. *Biol. Psychol.* 86, 239–246. doi: 10.1016/j.biopsycho.2010.12.004

Lang, P. J., Bradley, M. M., and Cuthbert, B. N. (1997). *International Affective Picture System (IAPS): Technical Manual And Affective Ratings*. NIMH Center for the Study of Emotion and Attention, Technical Report, No A-6. Gainesville, FL: University of Florida.

Lecrubier, Y., Sheehan, D. V., Weiller, E., Amorim, P., Bonora, I., Sheehan, K. H., et al. (1997). The mini international neuropsychiatric interview (MINI). A short diagnostic structured interview: reliability and validity according to the CIDI. *Eur. Psychiatry* 12, 224–231. doi: 10.1016/S0924-9338(97)83296-8

Li, X. W., Hu, B., Xu, T. T., Shen, J., and Ratcliffe, M. (2015). A study on EEG-based brain electrical source of mild depressed subjects. *Comput. Methods Programs Biomed.* 120, 135–141. doi: 10.1016/j.cmpb.2015.04.009

Liu, M., Yao, S., Yang, H., and Xiang, H. (2007). A study on the distractor inhibition mechanism of depressed individuals in affective evaluation task. *Psychol. Sci.* 30, 613–616.

Liu, Q., Balsters, J. H., Baechinger, M., van der Groen, O., Wenderoth, N., and Mantini, D. (2015). Estimating a neutral reference for electroencephalographic recordings: the importance of using a high-density montage and a realistic head model. *J. Neural Eng.* 12:056012. doi: 10.1088/1741-2560/12/5/056012

Liu, Q., Farahibozorg, S., Porcaro, C., Wenderoth, N., and Mantini, D. (2017). Detecting large-scale networks in the human brain using high-density electroencephalography. *Hum. Brain Mapp.* 38, 4631–4643. doi: 10.1002/hbm.23688

Liu, Q., Ganzetti, M., Wenderoth, N., and Mantini, D. (2018). Detecting large-scale brain networks using EEG: impact of electrode density, head modeling and source localization. *Front. Neuroinform.* 12:4. doi: 10.3389/fninf.2018.00004

Liu, T., Slotnick, S. D., Serences, J. T., and Yantis, S. (2003). Cortical mechanisms of feature-based attentional control. *Cereb. Cortex* 13, 1334–1343. doi: 10.1093/cercor/bhg080

Lopezcalderon, J., and Luck, S. J. (2014). ERPLAB: an open-source toolbox for the analysis of event-related potentials. *Front. Hum. Neurosci.* 8:213. doi: 10.3389/fnhum.2014.00213

Mansouri, F. A., Tanaka, K., and Buckley, M. J. (2009). Conflict-induced behavioural adjustment: a clue to the executive functions of the prefrontal cortex. *Nat. Rev. Neurosci.* 10, 141–152. doi: 10.1038/nrn2538

Mayes, L. C., Molfese, D. L., Key, A. P., and Hunter, N. C. (2005). Event-related potentials in cocaine-exposed children during a Stroop task. *Neurotoxicol. Teratol.* 27, 797–813. doi: 10.1016/j.ntt.2005.05.011

Mcneely, H. E., Lau, M. A., Christensen, B. K., and Alain, C. (2008). Neurophysiological evidence of cognitive inhibition anomalies in persons with major depressive disorder. *Clin. Neurophysiol.* 119, 1578–1589. doi: 10.1016/j.clinph.2008.03.031

Mitterschiffthaler, M. T., Williams, S. C., Walsh, N. D., Cleare, A. J., Donaldson, C., Scott, J., et al. (2008). Neural basis of the emotional Stroop interference effect in major depression. *Psychol. Med.* 38, 247–256. doi: 10.1017/S0033291707001523

Mohanty, A., Engels, A. S., Herrington, J. D., Heller, W., Ho, M. H., Banich, M. T., et al. (2007). Differential engagement of anterior cingulate cortex subdivisions for cognitive and emotional function. *Psychophysiology* 44, 343–351. doi: 10.1111/j.1469-8986.2007.00515.x

Morein-Zamir, S., Dodds, C., van Hartevelt, T. J., Schwarzkopf, W., Sahakian, B., Müller, U., et al. (2014). Hypoactivation in right inferior frontal cortex is specifically associated with motor response inhibition in adult ADHD. *Hum. Brain Mapp.* 35, 5141–5152. doi: 10.1002/hbm.22539

Nichols, T. E., and Holmes, A. P. (2002). Nonparametric permutation tests for functional neuroimaging: a primer with examples. *Hum. Brain Mapp.* 15, 1–25. doi: 10.1002/hbm.1058

O'Shea, B. (1989). *Diagnostic and Statistical Manual of Mental Disorders*, 3rd Edn. Washington, DC: American Psychiatric Association, 54–54.

Pascual-Marqui, R. D. (2002). Standardized low-resolution brain electromagnetic tomography (sLORETA): technical details. *Methods Find. Exp. Clin. Pharmacol.* 24, 5–12.

Pizzagalli, D. A., Peccoralo, L. A., Davidson, R. J., and Cohen, J. D. (2006). Resting anterior cingulate activity and abnormal responses to errors in subjects with elevated depressive symptoms: a 128-channel EEG study. *Hum. Brain Mapp.* 27, 185–201. doi: 10.1002/hbm.20172

Ramautar, J. R., Kok, A., and Ridderinkhof, K. R. (2006). Effects of stop-signal modality on the N2/P3 complex elicited in the stop-signal paradigm. *Biol. Psychol.* 72, 96–109. doi: 10.1016/j.biopsycho.2005.08.001

Rubia, K., Cubillo, A., Smith, A. B., Woolley, J., Heyman, I., and Brammer, M. J. (2010). Disorder-specific dysfunction in right inferior prefrontal cortex during two inhibition tasks in boys with attention-deficit hyperactivity disorder compared to boys with obsessive-compulsive disorder. *Hum. Brain Mapp.* 31, 287–299. doi: 10.1002/hbm.20864

Saunders, B., and Jentzsch, I. (2014). Reactive and proactive control adjustments under increased depressive symptoms: insights from the classic and emotional-face Stroop task. *Q. J. Exp. Psychol.* 67, 884–898. doi: 10.1080/17470218.2013.836235

Schmidt, J. R. (2013). Questioning conflict adaptation: proportion congruent and Gratton effects reconsidered. *Psychon. Bull. Rev.* 20, 615–630. doi: 10.3758/s13423-012-0373-0

Serences, J. T., Yantis, S., Culberson, A., and Awh, E. (2004). Preparatory activity in visual cortex indexes distractor suppression during covert spatial orienting. *J. Neurophysiol.* 92, 3538–3545. doi: 10.1152/jn.00435.2004

Shen, Y., Xue, S., Wang, K., and Qiu, J. (2013). Neural time course of emotional conflict control: an ERP study. *Neurosci. Lett.* 541, 34–38. doi: 10.1016/j.neulet.2013.02.032

Shomstein, S., and Yantis, S. (2004). Control of attention shifts between vision and audition in human cortex. *J. Neurosci.* 24, 10702–10706. doi: 10.1523/JNEUROSCI.2939-04.2004

Siegle, G. J., Steinhauer, S. R., Thase, M. E., Stenger, V. A., and Carter, C. S. (2002). Can't shake that feeling: event-related fMRI assessment of sustained amygdala activity in response to emotional information in depressed individuals. *Biol. Psychiatry* 51, 693–707. doi: 10.1016/S0006-3223(02)01314-8

Smith, J. L., Smith, E. A., Provost, A. L., and Heathcote, A. (2010). Sequence effects support the conflict theory of N2 and P3 in the Go/NoGo task. *Int. J. Psychophysiol.* 75, 217–226. doi: 10.1016/j.ijpsycho.2009.11.002

Steele, J. D., and Lawrie, S. (2004). Segregation of cognitive and emotional function in the prefrontal cortex: a stereotactic meta-analysis. *Neuroimage* 21, 868–875. doi: 10.1016/j.neuroimage.2003.09.066

Talairach, J., and Tournoux, P. (1988). *Co-Planar Stereotaxic Atlas of the Human Brain: 3-Dimensional Proportional System : An Approach to Cerebral Imaging*. New York, NY: Georg Thieme Verlag.

Turken, A. U., and Swick, D. (1999). Response selection in the human anterior cingulate cortex. *Nat. Neurosci.* 2, 920–924. doi: 10.1038/13224

Van Hoesen, G. W., Morecraft, R. J., and Vogt, B. A. (1993). "Connections of the monkey cingulate cortex," in *Neurobiology of Cingulate Cortex and Limbic Thalamus*, eds B. A. Vogt, and M.Gabriel (Boston, MA: Birkhäuser), 249–284. doi: 10.1007/978-1-4899-6704-6_9

Vanderhasselt, M. A., and De, R. R. (2009). Impairments in cognitive control persist during remission from depression and are related to the number of past episodes: an event related potentials study. *Biol. Psychol.* 81, 169–176. doi: 10.1016/j.biopsycho.2009.03.009

West, R. (2003). Neural correlates of cognitive control and conflict detection in the Stroop and digit-location tasks. *Neuropsychologia* 41, 1122–1135. doi: 10.1016/S0028-3932(02)00297-X

Whalen, P. J., Bush, G., McNally, R. J., Wilhelm, S., McInerney, S. C., Jenike, M. A., et al. (1998). The emotional counting Stroop paradigm: a functional magnetic resonance imaging probe of the anterior cingulate affective division. *Biol. Psychiatry* 44, 1219–1228. doi: 10.1016/S0006-3223(98)00251-0

Xue, S., Wang, S., Kong, X., and Qiu, J. (2017). Abnormal neural basis of emotional conflict control in treatment-resistant depression. *Clin. EEG Neurosci.* 48, 103–110. doi: 10.1177/1550059416631658

Yao, Z., Hu, B., Xie, Y., Zheng, F., Liu, G., Chen, X., et al. (2016). Resting-state time-varying analysis reveals aberrant variations of functional connectivity in autism. *Front. Hum. Neurosci.* 10:463. doi: 10.3389/fnhum.2016.00463

Zhao, Q., Li, H., Hu, B., Li, Y., Gillebert, C. R., Mantini, D., et al. (2017a). Neural correlates of drug-related attentional bias in heroin dependence. *Front. Hum. Neurosci.* 11:646. doi: 10.3389/fnhum.2017.00646

Zhao, Q., Li, H., Hu, B., Wu, H., and Liu, Q. (2017b). Abstinent heroin addicts tend to take risks: ERP and source localization. *Front. Neurosci.* 11:681. doi: 10.3389/fnins.2017.00681

**Conflict of Interest Statement:** The authors declare that the research was conducted in the absence of any commercial or financial relationships that could be construed as a potential conflict of interest.

frontiers in Human Neuroscience

REVIEW
published: 30 May 2018
doi: 10.3389/fnhum.2018.00215

# Mechanisms of Transcranial Magnetic Stimulation Treating on Post-stroke Depression

*Xiaoqin Duan, Gang Yao, Zhongliang Liu, Ranji Cui and Wei Yang**

*Jilin Provincial Key Laboratory on Molecular and Chemical Genetics, The Second Hospital of Jilin University, Changchun, China*

Post-stroke depression (PSD) is a neuropsychiatric affective disorder that can develop after stroke. Patients with PSD show poorer functional and recovery outcomes than patients with stroke who do not suffer from depression. The risk of suicide is also higher in patients with PSD. PSD appears to be associated with complex pathophysiological mechanisms involving both psychological and psychiatric problems that are associated with functional deficits and neurochemical changes secondary to brain damage. Transcranial magnetic stimulation (TMS) is a non-invasive way to investigate cortical excitability via magnetic stimulation of the brain. TMS is currently a valuable tool that can help us understand the pathophysiology of PSD. Although repetitive TMS (rTMS) is an effective treatment for patients with PSD, its mechanism of action remains unknown. Here, we review the known mechanisms underlying rTMS as a tool for better understanding PSD pathophysiology. It should be helpful when considering using rTMS as a therapeutic strategy for PSD.

**Keywords: noninvasive brain stimulation, transcranial magnetic stimulation, post-stroke depression, mechanism, BDNF**

OPEN ACCESS

***Edited by:***
*Wenbo Luo,*
*Liaoning Normal University, China*

***Reviewed by:***
*Filippo Brighina,*
*Università degli Studi di Palermo, Italy*
*Bin Song,*
*McLean Hospital, United States*

****Correspondence:***
*Wei Yang*
*wyang2002@jlu.edu.cn*

***Received:*** *06 November 2017*
***Accepted:*** *08 May 2018*
***Published:*** *30 May 2018*

***Citation:***
*Duan X, Yao G, Liu Z, Cui R and Yang W (2018) Mechanisms of Transcranial Magnetic Stimulation Treating on Post-stroke Depression. Front. Hum. Neurosci. 12:215. doi: 10.3389/fnhum.2018.00215*

## INTRODUCTION

Stroke is the most common cause of adult disability in developing countries (Kaadan and Larson, 2017) and has both physical and economic repercussions for patients. Post-stroke depression (PSD) is a severe and fearful complication that occurs in nearly one third of patients who suffer stroke and can even occur in patients who have suffered only a minor stroke or transient ischemic attack (TIA; Carnes-Vendrell et al., 2016). PSD can affect functional ability, rehabilitation outcome, and quality of life, and is related to a higher mortality rate of stroke patients (Miranda et al., 2018). Additionally, stroke severity is an important risk factor for PSD, as is the mental history of the patient. Preventing PSD requires participation from family members and society (Shi et al., 2017). It appears to be associated with complex pathophysiological mechanisms involving both psychological and psychiatric problems that are associated with functional deficits and neurochemical changes secondary to brain damage. Although antidepressants are considered the treatment of choice for PSD, the benefits are not perfect. Indeed, whether pharmacological treatment is needed to prevent PSD or improve neurological outcomes after stroke is uncertain (Kim, 2016; Xu et al., 2016). Fortunately, studies suggest that transcranial magnetic stimulation (TMS) is beneficial for patients with PSD (Gu and Chang, 2017; Shen et al., 2017).

TMS is an important technique for noninvasive brain stimulation (NIBS; Edwards et al., 2017). NIBS, using electromagnetic waves and direct electrical current, is a new frontier in treating

neuropsychiatric illnesses or psychiatric maladies (Gupta and Adnan, 2018). Several types of NIBS have been developed over the years, including electroconvulsive therapy (ECT), transcranial alternating current stimulation (tACS), magnetic seizure therapy (MST), TMS and transcranial direct current stimulation (tDCS). Among them, ECT is the best at reducing depression and has unparalleled efficacy even in older populations. However, the risk of amnesia is a severely limiting factor. While tACS has several advantages including biphasic and sinusoidal currents, the ability to entrain large neuronal populations, and subtle control over somatic effects, its best practices remain unclear and further study is required (Tavakoli and Yun, 2017). MST is a proposed form of electrotherapy using magnetic brain stimulation. It preserves the efficacy of ECT while reducing the risk of amnesia through the more precise localization offered by magnetic stimulation (Luber et al., 2013). However, its clinical effects still need to be studied. The most commonly used NIBS are TMS and tDCS. tDCS modulates membrane potential via electrical currents (Rektorová and Anderková, 2017). It does not directly induce action potentials in neurons, but instead is believed to influence spontaneous activity of targeted brain networks. TMS can be directed more specifically than tDCS. Additionally, it can exert a causal influence on brain networks and its clinical efficacy has already been established in the treatment of mental disorders (Hendrikse et al., 2017). Among all the types of NIBS, TMS—especially repetitive TMS (rTMS)—is the best at controlling the frequency and the location of stimulation. This advantage, in addition to others, has opened up new possibilities for clinical exploration and treatment of neuropsychiatric conditions. Meta-analysis of the literature shows that rTMS can combat PSD and that it is actively used in therapy (Klein et al., 2015). However, its exact mechanism of action is still unknown. Here, we explore what we know about the mechanisms underlying rTMS treatment of PSD.

## MECHANISMS THROUGH WHICH TMS IMPROVES PSD

In 2008, rTMS on the left dorsolateral prefrontal cortex (DLPFC) was approved for the treatment of major depression in the USA (Saitoh et al., 2012). Since then, rTMS has been widely used in cases of treatment-resistant depression (TRD) that do not respond adequately to adequate courses of at least two antidepressants (Xie et al., 2013; Lucas et al., 2017). Moreover, application of high frequency rTMS over the dorsal anterior cingulate cortex (dACC) and medial prefrontal cortex (mPFC) has been reported to be a useful intervention for apathy resulting from stroke (Sasaki et al., 2017). A few related studies have examined the mechanism through which rTMS lessens depression in PSD. TMS is known to influence neuronal plasticity in the brain by originating the long-term potentiation (LTP) and long-term depression (LTD). Low-intensity TMS primarily stimulates low-threshold inhibitory neurons, while high-intensity TMS excites projection neurons. Although detailed mechanisms have not yet been characterized very well, several theories have been proposed.

### Increased Concentration of Brain-Derived Neurotrophic Factor (BDNF)

Brain-Derived Neurotrophic Factor (BDNF) is an important neurotrophic factor that is distributed extensively in the central nervous system. BDNF is crucial for the survival, growth and maintenance of neurons within brain circuits that control emotion and cognition (Kowiański et al., 2018). Phillips (2017) has suggested that neuroplasticity that takes place in major depressive disorder (MDD) is related to BDNF levels. BDNF is crucial for exercise learning and systemic rehabilitation after stroke. BDNF concentration in patients with acute ischemic stroke has been reported to be lower than that in healthy controls. Additionally, low levels of BDNF are associated with increased risk of stroke, worsening of functional outcome, and increased stroke-related mortality. Recently, single nucleotide polymorphisms of the BDNF gene were studied in patients with stroke. Mizui et al. (2017) found that the BDNF pro-peptide can facilitate hippocampal LTD and that the BDNF polymorphism Val66Met impacted the biological activity of the BDNF pro-peptide. Further, Kotlęga et al. (2017) reported that the Met allele is associated with adverse consequences and prognosis after stroke. Thus, BDNF and BDNF polymorphisms play important roles in brain plasticity, especially in changes of function and morphology.

PSD has been correlated with low BDNF expression levels (Chen et al., 2015). Low levels of BDNF can lead to mood dysregulation and loss of hippocampal function. A variety of biological, environmental and pharmacological factors can affect mood by modulating BDNF expression (Phillips, 2017). Additionally, studies have shown that high-frequency rTMS enhances BDNF expression levels. BDNF is a key factor in the increased hippocampal cell proliferation and neuronal differentiation after application of rTMS. Further, reports show that in several brain areas in rats, including the hippocampal CA1 and CA3 subfields, high-frequency rTMS (20 Hz) triggers BDNF expression. Aside from increasing BDNF levels, rTMS might also activate the BDNF/ERK signaling pathway to upregulate cell proliferation in the hippocampus (Cui et al., 2017).

### Increased Glucose Metabolism in the Cortex and in Specific Neural Networks

In a seminal experiment, Siebner et al. (1998) measured the relative changes in the regional cerebral metabolic rate of glucose (rCMRglc) during 2 Hz rTMS of the left sensorimotor cortex and during imitation of rTMS-induced arm movements using positron emission tomography (PET). Since then, combining rTMS and PET has been used to visualize rTMS-related net brain activation and to analyze functional networks (Li et al., 2013; Val-Laillet et al., 2015; Heiss, 2016).

More recently, Parthoens et al. (2014) combined the neurostimulation with positron emission tomography (microPET) in small animals to quantify regional 2-Deoxy-2-[$^{18}$F] fluoro-D-glucose $^{18}$F-FDG uptake in the rat brain in response to low- (1 Hz) or high- (50 Hz) frequency paradigms. This method is now often used to visualize neuronal activation of the cortex and cortical networks during different types of

stimulation (Akman et al., 2015; Adriaanse et al., 2016; Malpetti et al., 2017). rTMS at differing frequencies has been shown to decrease $^{18}$F-FDG-uptake in dorsal cortical regions while increasing it in ventral regions (Parthoens et al., 2016). Baeken et al. (2015) examined the clinical effects of high-frequency rTMS on glucose metabolism in the subgenual anterior cingulate cortex (sgACC) by stimulating left DLPFC. The results show that sgACC is a specific region whose treatment with high frequency rTMS leads to an antidepressant response. Another study demonstrated that the clinical response to high frequency-rTMS treatment in patients with TRD might depend on the metabolic state of the cerebellum. It implied that other localized brain regions might be warranted for stimulation, especially the cerebellum when patients do not respond to DLPFC high-frequency rTMS (Wu and Baeken, 2017). In a related $^{18}$F-FDG-PET study, an increase in glucose metabolism of the rat cerebellar cortex was observed after high-frequency rTMS, along with reduced synthesis of neural plasticity-related proteins such as metabotrophic glutamate receptor (mGluR), protein kinase C (PKC) and glutamate receptor 2 (GluR2). These findings suggested that rTMS could act on the rat cerebellar cortex to induce LTD-related neuroplasticity (Lee et al., 2014). Another study suggests that manipulating pre-rTMS neural activity in patients with MDD could predict and augment the antidepressant effects of rTMS treatment, including increased frontal θ and glucose uptake (Li et al., 2016). Some scholars have used rTMS with $^{18}$F-FDG-PET to study the neurophysiological and spatial dynamics induced by repetitive 1-Hz rTMS in the temporal cortex. One study found that rTMS can cause a reduction in glucose metabolism of the temporal lobe and an increase in glucose metabolism of the mPFC and ipsilateral cortex. Further, statistical parametric mapping of FDG-PET data revealed a focal reduction of glucose metabolism in the stimulated temporal area and an increase in the bilateral precentral, ipsilateral superior and middle frontal, prefrontal, and cingulate gyri. This suggests that 1-Hz rTMS in the temporal cortex can cause cortico-cortical modulation and induce extensive functional changes in neural networks via long-range neuronal connections (Lee et al., 2013). Hayashi et al. (2004) showed statistically robust changes in FDG uptake in the macaque brain after the rTMS. Specifically, they found a reduction in the motor/premotor cortices and an increase in orbitofrontal cortices and the limbic-associated areas involving the anterior/posterior cingulate. Impressively, these changes in uptake continued for at least 8 days after treatment. These results demonstrate that functional connections allow motor rTMS to have long-lasting effects on motor-related regions and distant limbic-related areas.

Glucose metabolism is known to decrease in the ischemic hemisphere, especially in patients with PSD. Using $^{18}$F-FDG micro-PET imaging, Gao et al. (2010) reported that glucose uptake in rat cortex and striatum was larger in an rTMS group than in a control group. Meanwhile, the number of caspase3-positive cells was significantly lower, and the ratio of Bcl-2/Bax was higher in the rTMS group. Thus, rTMS treatment increased glucose metabolism and inhibited apoptosis in the ischemic brain. Additionally, rTMS has emerged as a promising therapeutic intervention in the treatment of affective disorders. Preliminary evidence from PET scans suggests that high-frequency (20 Hz) stimulation might increase brain glucose metabolism in a transsynaptic fashion, whereas low-frequency (1 Hz) stimulation might do the opposite (Post et al., 1999). Another study has shown that glucose levels decreased after tDCS (Sampaio et al., 2012). No study has reported a change in glucose levels after non-repeated TMS. In the future, our team intends to explore glucose levels in patients with PSD who have diabetes.

## Increased Neurogenesis

Neuroplasticity is a natural property of the nervous system that allows functional changes and reorganization after lesions or environmental changes. PSD has been shown to be linked to basal ganglia and frontal lobe lesions, white matter degeneration, and interruption of brain network connectivity. TMS has been reported to increase white matter fractional anisotropy (FA) values and increase left frontal lobe activation (Hallett et al., 2017). Also, TMS can induce electro-magnetic currents in the related cortical neurons. Varying frequencies and intensities of TMS can directly increase or decrease excitability in the cortical area (Ambriz-Tututi et al., 2012) so as to promote the functional reconstruction of the damaged neural network and repair neuronal structure. Thus TMS can contribute to brain-network research including the study of cortical-cerebellar and cortical-basal ganglia relationships. Furthermore, it was reported that rTMS is conductive to the proliferation, differentiation and migration of neural stem cells (NSCs) and inhibits their apoptosis (Cui et al., 2017). Different magnitudes and numbers of pulses can induce different effects on NSCs, meanwhile, several neurotransmitter systems, such as the γ-aminobutyric acid (GABA) system, could be activated by rTMS to modulate the niche of NSCs in the subventricular zone (or other region with NSCs) to cause an increase in cell proliferation (Lozeron et al., 2016; Cui et al., 2017). Indeed, when rats with post-traumatic brain injury received rTMS, they exhibited significantly greater proliferation in the subventricular zone, significantly higher rates of neuron survival, and significantly reduced rates of apoptosis than similarly injured control rats (Lu et al., 2017). These findings suggest that high-frequency rTMS could promote neurogenesis.

## Modulation of Neurobiochemical Effects

Stroke can lead to abnormalities in the expression of biogenic amine neurotransmitters and cytokines. Additionally, reactive oxygen species generated during stroke can cause oxidative stress, lipid peroxidation and protein oxidation in nerve tissue. PSD could be related to any of these pathophysiological processes (Nabavi et al., 2015).

Experimental evidence in rodents indicate that rTMS produces complex neurobiochemical effects such as induction of immediate early genes, changes in how neurotransmitters release is modulated, changes in glutamate α-amino-3-hydroxy-5-methyl-4-isoxazolepropionic acid (AMPA) receptor/N-methyl-D-aspartate (NMDA) receptor expression (influencing calcium ion dynamics), actions on the neuroendocrine system, neuroprotection via reduced oxidative stress and inflammation, and changes in neurotrophin expression. These molecular effects

may modify the intrinsic and extrinsic electrophysiological properties of neurons and reprogram the expression of excitatory and inhibitory neurotransmitters and their cognate receptors, which lead to long-lasting synaptic plasticity-related changes similar to LTP and LTD (Di Lazzaro et al., 2010; Soundara Rajan et al., 2017).

EI Arfani et al. (2017) found that total striatal 5-hydroxyindolacetic acid (a metabolite of serotonin) levels were reduced after accelerated high-frequency rTMS, and motor activity in rats increased as a result. In addition to its clinical antidepressant effect, serotonin can improve motor function and assist learning and memory functions. Studies have shown that serotonin can induce neural plasticity by modulating paired co-stimuli, which may help explain the mechanism by which serotonin plays a positive role in learning and as a medical treatment for depression and stroke (Batsikadze et al., 2013).

In addition, applying rTMS to the motor cortex increases dopamine in the striatum (Kulishova and Shinkorenko, 2014), and improved motor performance in PD may be related to an elevation of serum dopamine concentration after rTMS (Khedr et al., 2007). Strafella et al. (2003) also measured changes in extracellular dopamine concentration following rTMS of the motor cortex and found that it led to focal dopamine release in the ipsilateral caudate nucleus. Further, rTMS is capable of inducing lasting alterations in cortical excitability (Liebetanz et al., 2003). Thus, rTMS can increase cortical excitability via dopamine release. It is worthy to be studied in future.

### Regulation of Emotion Through LTD-Like and LTP-Like Plasticity

rTMS can regulate emotion through both inhibition and excitation. A newer form of rTMS protocol, known as theta-burst stimulation (TBS), has been shown to produce similar if not greater effects on brain activity than standard rTMS (Chung et al., 2015). Inhibitory rTMS is thought to act via LTD and require low-frequency (1 Hz) stimulation and continuous theta burst stimulation (cTBS). In contrast, excitatory rTMS is thought to act via LTP, require high-frequency (5–20 Hz) stimulation and intermittent theta burst stimulation (iTBS). One study suggests that rTMS may be able to effectively and selectively modulate psychiatric symptomatology in which the orbitofrontal cortex (OFC) is implicated (Fettes et al., 2017). Depressed patients have hypometabolism of the left DLPFC, which is ameliorated by rTMS. rTMS regulates mood by acting on the cortical-subcortical network (Shen et al., 2017). Casula et al. (2016) found that the DLPFC has the potential to generate robust spike-timing dependent plasticity (STDP). Pellicciari et al. (2017) reported that bilateral TBS treatment induced a remarkable rearrangement of bilateral DLPFC oscillatory activity, which parallels clinical advances. Specifically, left DLPFC iTBS decreased θ- and α-band oscillations and increased higher frequencies, while right DLPFC cTBS increased α-oscillatory activity evoked by TMS. These results highlighted that idea that iTBS is able to modulate cortical excitability and increase spontaneous neuronal activity in the higher frequency ranges. Additionally, priming TBS of rTMS is ineffective in modifying motor cortex (M1) plasticity in older adults because the neuroplastic potential of primary motor cortex in older adults is low (Opie et al., 2017). Research on younger individuals suggests that neuroplastic responses can be enhanced via rTMS, with larger responses observed following both LTP and LTD-like protocols. In this sense, the effect of rTMS on neuroplasticity is related to age. Thus, rTMS can improve cortical excitation in patients with PSD, which can improve their emotion.

## CONCLUSIONS AND FUTURE DIRECTIONS

Although the mechanisms underlying the effect of rTMS on PSD are unknown, its effectiveness cannot be denied. In our clinical work, we generally use 1000 rTMS pulses (5–10 Hz at 80%–100% of resting motor threshold [rMT]) over the left DLPFC and 1000 rTMS pulses (1 Hz at 80%–100% of rMT) over the right DLPFC for 10 days to treat depression after stroke. Understanding the how rTMS affects PSD should help the development of new and more effective treatments, and the mechanism should be further studied to provide a strong theoretical basis for clinical application.

Recently, researchers have explored the mechanisms underlying rTMS therapy using a variety of methods. Neuroimaging, including PET and functional magnetic resonance imaging, have been used to learn about the remote effects of TMS on the brain (Hallett et al., 2017). Also, TMS-induced electromyographic (EMG) and electroencephalographic responses to drugs can help us understand excitability, connectivity and plasticity in brain (Ziemann et al., 2015). Based on the thinking that motor-evoked potentials elicited by TMS in a target muscle are variable, and that the source of variable muscle responses may not be apparent using conventional bipolar EMG (particularly over areas with several distinct neighboring muscles), Neva et al. (2017) suggest that high-density surface EMG (HDsEMG) provides a useful way to differentiate which wrist extensor muscles are activated by TMS. In future studies, a record of event-related potentials combined with machine learning and applied statistics could be used to build models of neural activity (Holdgraf et al., 2017) that will reveal more details regarding the underlying mechanisms of rTMS-related improvement in PSD.

## AUTHOR CONTRIBUTIONS

XD and GY wrote the manuscript. ZL, WY and RC provided the critical revisions. All authors approved the final version of the manuscript for submission.

## FUNDING

This work was supported by the National Natural Science Foundation of China (Grant No. 31471120).

## ACKNOWLEDGMENTS

We thank Adam Phillips, PhD, from Liwen Bianji, Edanz Editing China (www.liwenbianji.cn/ac), for editing the English text of a draft of this manuscript.

## REFERENCES


Adriaanse, S. M., Wink, A. M., Tijms, B. M., Ossenkoppele, R., Verfaillie, S. C., Lammertsma, A. A., et al. (2016). The association of glucose metabolism and eigenvector centrality in Alzheimer's disease. *Brain Connect.* 6, 1–8. doi: 10.1089/brain.2014.0320

Akman, C. I., Provenzano, F., Wang, D., Engelstad, K., Hinton, V., Yu, J., et al. (2015). Topography of brain glucose hypometabolism and epileptic network in glucose transporter 1 deficiency. *Epilepsy Res.* 110, 206–215. doi: 10.1016/j.eplepsyres.2014.11.007

Ambriz-Tututi, M., Sánchez-González, V., and Drucker-Colín, R. (2012). Transcranial magnetic stimulation reduces nociceptive threshold in rats. *J. Neurosci. Res.* 90, 1085–1095. doi: 10.1002/jnr.22785

Baeken, C., Marinazzo, D., Everaert, H., Wu, G. R., Van Hove, C., Audenaert, K., et al. (2015). The impact of accelerated HF-rTMS on the subgenual anterior cingulate cortex in refractory unipolar major depression: insights from 18FDG PET brain imaging. *Brain Stimul.* 8, 808–815. doi: 10.1016/j.brs.2015.01.415

Batsikadze, G., Paulus, W., Kuo, M. F., and Nitsche, M. A. (2013). Effect of serotonin on paired associative stimulation-induced plasticity in the human motor cortex. *Neuropsychopharmacology* 38, 2260–2267. doi: 10.1038/npp.2013.127

Carnes-Vendrell, A., Deus-Yela, J., Molina-Seguin, J., Pifarre-Paredero, J., and Purroy, F. (2016). Update on post-stroke depression: posing new challenges in patients with a minor stroke or transient ischaemic attack. *Rev. Neurol.* 62, 460–467.

Casula, E. P., Pellicciari, M. C., Picazio, S., Caltagirone, C., and Koch, G. (2016). Spike-timing-dependent plasticity in the human dorso-lateral prefrontal cortex. *Neuroimage* 143, 204–213. doi: 10.1016/j.neuroimage.2016.08.060

Chen, H. H., Zhang, N., Li, W. Y., Fang, M. R., Zhang, H., Fang, Y. S., et al. (2015). Overexpression of brain-derived neurotrophic factor in the hippocampus protects against post-stroke depression. *Neural Regen. Res.* 10, 1427–1432. doi: 10.4103/1673-5374.165510

Chung, S. W., Hoy, K. E., and Fitzgerald, P. B. (2015). Theta-burst stimulation: a new form of TMS treatment for depression? *Depress. Anxiety* 32, 182–192. doi: 10.1002/da.22335

Cui, M., Ge, H., Zhao, H., Zou, Y., Chen, Y., and Feng, H. (2017). Electromagnetic fields for the regulation of neural stem cells. *Stem Cells Int.* 2017:9898439. doi: 10.1155/2017/9898439

Di Lazzaro, V., Profice, P., Pilato, F., Capone, F., Ranieri, F., Pasqualetti, P., et al. (2010). Motor cortex plasticity predicts recovery in acute stroke. *Cereb. Cortex* 20, 1523–1528. doi: 10.1093/cercor/bhp216

Edwards, C. A., Kouzani, A., Lee, K. H., and Ross, E. K. (2017). Neurostimulation devices for the treatment of neurologic disorders. *Mayo Clin. Proc.* 92, 1427–1444. doi: 10.1016/j.mayocp.2017.05.005

EI Arfani, A., Parthoens, J., Demuyser, T., Servaes, S., and De Coninck, M. (2017). Accelerated high-frequency repetitive transcranial magnetic stimulation enhances motor activity in rats. *Neuroscience* 347, 103–110. doi: 10.1016/j.neuroscience.2017.01.045

Fettes, P., Schulze, L., and Downar, J. (2017). Cortico-striatal-thalamic loop circuits of the orbitofrontal cortex: promising therapeutic targets in psychiatric illness. *Front. Syst. Neurosci.* 11:25. doi: 10.3389/fnsys.2017.00025

Gao, F., Wang, S., Guo, Y., Wang, J., Lou, M., Wu, J., et al. (2010). Protective effects of repetitive transcranial magnetic stimulation in a rat model of transient cerebral ischaemia: a microPET study. *Eur. J. Nucl. Med. Mol. Imaging* 37, 954–961. doi: 10.1007/s00259-009-1342-3

Gu, S. Y., and Chang, M. C. (2017). The effects of 10-Hz repetitive transcranial magnetic stimulation on depression in chronicstroke patients. *Brain Stimul.* 10, 270–274. doi: 10.1016/j.brs.2016.10.010

Gupta, A., and Adnan, M. (2018). Hypomania risk in noninvasive brain stimulation. *Cureus* 10:e2204. doi: 10.7759/cureus.2204

Hallett, M., Di Iorio, R., Rossini, P. M., Park, J. E., Chen, R., Celnik, P., et al. (2017). Contribution of transcranial magnetic stimulation to assessment of brain connectivity and networks. *Clin. Neurophysiol.* 128, 2125–2139. doi: 10.1016/j.clinph.2017.08.007

Hayashi, T., Ohnishi, T., Okabe, S., Teramoto, N., Nonaka, Y., Watabe, H., et al. (2004). Long-term effect of motor cortical repetitive transcranial magnetic stimulation [correction]. *Ann. Neurol.* 56, 77–85. doi: 10.1002/ana.20151

Heiss, W. D. (2016). Imaging effects related to language improvements by rTMS. *Restor. Neurol. Neurosci.* 34, 531–536. doi: 10.3233/RNN-150631

Hendrikse, J., Kandola, A., Coxon, J., Rogasch, N., and Yücel, M. (2017). Combining aerobic exercise and repetitive transcranial magnetic stimulation to improve brainfunction in health and disease. *Neurosci. Biobehav. Rev.* 83, 11–20. doi: 10.1016/j.neubiorev.2017.09.023

Holdgraf, C. R., Rieger, J. W., Micheli, C., Martin, S., Knight, R. T., and Theunissen, F. E. (2017). Encoding and decoding models in cognitive electrophysiology. *Front. Syst. Neurosci.* 11:61. doi: 10.3389/fnsys.2017.00061

Kaadan, M. I., and Larson, M. J. (2017). Management of post-stroke depression in the middle east and north africa: too little is known. *J. Neurol. Sci.* 378, 220–224. doi: 10.1016/j.jns.2017.05.026

Khedr, E. M., Rothwell, J. C., Shawky, O. A., Ahmed, M. A., Foly, N., and Hamdy, A. (2007). Dopamine levels after repetitive transcranial magnetic stimulation of motor cortex in patients with Parkinson's disease: preliminary results. *Mov. Disord.* 22, 1046–1050. doi: 10.1002/mds.21460

Kim, J. S. (2016). Post-stroke mood and emotional disturbances: pharmacological therapy based on mechanisms. *J. Stroke* 18, 244–255. doi: 10.5853/jos.2016.01144

Klein, M. M., Treister, R., Raij, T., Pascual-Leone, A., Park, L., Nurmikko, T., et al. (2015). Transcranial magnetic stimulation of the brain: guidelines for pain treatment research. *Pain* 156, 1601–1614. doi: 10.1097/j.pain.0000000000000210

Kotlęga, D., Peda, B., Zembroń-Łacny, A., Gołąb-Janowska, M., and Nowacki, P. (2017). The role of brain-derived neurotrophic factor and its single nucleotide polymorphisms in stroke patients. *Neurol. Neurochir. Pol.* 51, 240–246. doi: 10.1016/j.pjnns.2017.02.008

Kowiański, P., Lietzau, G., Czuba, E., Waśkow, M., Steliga, A., and Moryś, J. (2018). BDNF: a key factor with multipotent impact on brain signaling and synaptic plasticity. *Cell. Mol. Neurobiol.* 38, 579–593. doi: 10.1007/s10571-017-0510-4

Kulishova, T. V., and Shinkorenko, O. V. (2014). The effectiveness of early rehabilitation of the patients presenting with ischemic stroke. *Vopr. Kurortol. Fizioter. Lech. Fiz. Kult.* 6, 9–12.

Lee, M., Kim, S. E., Kim, W. S., Han, J., Kim, H. J., Kim, B. S., et al. (2013). Cortico-cortical modulation induced by 1-Hz repetitive transcranial magnetic stimulation of the temporal cortex. *J. Clin. Neurol.* 9, 75–82. doi: 10.3988/jcn.2013.9.2.75

Lee, S. A., Oh, B. M., Kim, S. J., and Paik, N. J. (2014). The molecular evidence of neural plasticity induced by cerebellar repetitive transcranial magnetic stimulation in the rat brain: a preliminary report. *Neurosci. Lett.* 575, 47–52. doi: 10.1016/j.neulet.2014.05.029

Li, C. T., Chen, L. F., Tu, P. C., Wang, S. J., Chen, M. H., Su, T. P., et al. (2013). Impaired prefronto-thalamic functional connectivity as a key feature of treatment-resistant depression: a combined MEG, PET and rTMS study. *PLoS One* 8:e70089. doi: 10.1371/journal.pone.0070089

Li, C. T., Hsieh, J. C., Huang, H. H., Chen, M. H., Juan, C. H., Tu, P. C., et al. (2016). Cognition-modulated frontal activity in prediction and augmentation of antidepressant efficacy: a randomized controlled pilot study. *Cereb. Cortex* 26, 202–210. doi: 10.1093/cercor/bhu191

Liebetanz, D., Fauser, S., Michaelis, T., Czéh, B., Watanabe, T., Paulus, W., et al. (2003). Safety aspects of chronic low-frequency transcranial magnetic stimulation based on localized proton magnetic resonance spectroscopy and histology of the rat brain. *J. Psychiatr. Res.* 37, 277–286. doi: 10.1016/s0022-3956(03)00017-7

Lozeron, P., Poujois, A., Richard, A., Masmoudi, S., Meppiel, E., Woimant, F., et al. (2016). Contribution of TMS and rTMS in the understanding of the pathophysiology and in the treatment of dystonia. *Front. Neural Circuits* 10:90. doi: 10.3389/fncir.2016.00090

Lu, X., Bao, X., Li, J., Zhang, G., Guan, J., Gao, Y., et al. (2017). High-frequency repetitive transcranial magnetic stimulation for treating moderate traumatic brain injury in rats: a pilot study. *Exp. Ther. Med.* 13, 2247–2254. doi: 10.3892/etm.2017.4283

Luber, B., McClintock, S. M., and Lisanby, S. H. (2013). Applications of transcranial magnetic stimulation and magnetic seizure therapy in the study and treatment of disorders related to cerebral aging. *Dialogues Clin. Neurosci.* 15, 87–98.

Lucas, N., Hubain, P., Loas, G., and Jurysta, F. (2017). Treatment resistant depression: actuality and perspectives in 2017. *Rev. Med. Brux.* 38, 16–25.

Malpetti, M., Ballarini, T., Presotto, L., Garibotto, V., Tettamanti, M., and Perani, D. (2017). Gender differences in healthy aging and Alzheimer's dementia: a $^{18}$F-FDG-PET study of brain and cognitive reserve. *Hum. Brain Mapp.* 38, 4212–4227. doi: 10.1002/hbm.23659

Miranda, J. J., Moscoso, M. G., Toyama, M., Cavero, V., Diez-Canseco, F., and Ovbiagele, B. (2018). Role of mHealth in overcoming the occurrence of post-stroke depression. *Acta Neurol. Scand.* 137, 12–19. doi: 10.1111/ane.12832

Mizui, T., Ohira, K., and Kojima, M. (2017). BDNF pro-peptide: a novel synaptic modulator generated as an N-terminal fragment from the BDNF precursor by proteolytic processing. *Neural Regen. Res.* 12, 1024–1027. doi: 10.4103/1673-5374.211173

Nabavi, S. F., Dean, O. M., Turner, A., Sureda, A., Daglia, M., and Nabavi, S. M. (2015). Oxidative stress and post-stroke depression: possible therapeutic role of polyphenols? *Curr. Med. Chem.* 22, 343–351. doi: 10.2174/0929867321666141106122319

Neva, J. L., Gallina, A., Peters, S., Garland, S. J., and Boyd, L. A. (2017). Differentiation of motor evoked potentials elicited from multiple forearm muscles: an investigation with high-density surface electromyography. *Brain Res.* 1676, 91–99. doi: 10.1016/j.brainres.2017.09.017

Opie, G. M., Vosnakis, E., Ridding, M. C., Ziemann, U., and Semmler, J. G. (2017). Priming theta burst stimulation enhances motor cortex plasticity in young but not old adults. *Brain Stimul.* 10, 298–304. doi: 10.1016/j.brs.2017.01.003

Parthoens, J., Verhaeghe, J., Servaes, S., Miranda, A., Stroobants, S., and Staelens, S. (2016). Performance characterization of an actively cooled repetitive transcranial magnetic stimulation coil for the rat. *Neuromodulation* 19, 459–468. doi: 10.1111/ner.12387

Parthoens, J., Verhaeghe, J., Wyckhuys, T., Stroobants, S., and Staelens, S. (2014). Small-animal repetitive transcranial magnetic stimulation combined with [$^{18}$F]-FDG microPET to quantify the neuromodulation effect in the rat brain. *Neuroscience* 275, 436–443. doi: 10.1016/j.neuroscience.2014.06.042

Pellicciari, M. C., Ponzo, V., Caltagirone, C., and Koch, G. (2017). Restored asymmetry of prefrontal cortical oscillatory activity after bilateral theta burststimulation treatment in a patient with major depressive disorder: a TMS-EEG study. *Brain Stimul.* 10, 147–149. doi: 10.1016/j.brs.2016.09.006

Phillips, C. (2017). Brain-derived neurotrophic factor, depression, and physical activity: making the neuroplastic connection. *Neural Plast.* 2017:7260130. doi: 10.1155/2017/7260130

Post, R. M., Kimbrell, T. A., McCann, U. D., Dunn, R. T., Osuch, E. A., Speer, A. M., et al. (1999). Repetitive transcranial magnetic stimulation as a neuropsychiatric tool: present status and future potential. *J. ECT* 15, 39–59. doi: 10.1097/00124509-199903000-00005

Rektorová, I., and Anderková, Ľ. (2017). Noninvasive brain stimulation and implications for nonmotor symptoms in Parkinson's disease. *Int. Rev. Neurobiol.* 134, 1091–1110. doi: 10.1016/bs.irn.2017.05.009

Saitoh, Y., Hosomi, K., and Maruo, T. (2012). Stimulation of primary motor cortex and reorganization of cortical function. *Rinsho Shinkeigaku* 52, 1182–1184. doi: 10.5692/clinicalneurol.52.1182

Sampaio, L. A., Fraguas, R., Lotufo, P. A., Benseñor, I. M., and Brunoni, A. R. (2012). A systematic review of non-invasive brain stimulation therapies and cardiovascular risk: implications for the treatment of major depressive disorder. *Front. Psychiatry* 3:87. doi: 10.3389/fpsyt.2012.00087

Sasaki, N., Hara, T., Yamada, N., Niimi, M., Kakuda, W., and Abo, M. (2017). The efficacy of high-frequency repetitive transcranial magnetic stimulation for improving apathy in chronic stroke patients. *Eur. Neurol.* 78, 28–32. doi: 10.1159/000477440

Shen, X., Liu, M., Cheng, Y., Jia, C., Pan, X., Gou, Q., et al. (2017). Repetitive transcranial magnetic stimulation for the treatment of post-stroke depression: a systematic review and meta-analysis of randomized controlled clinical trials. *J. Affect. Disord.* 211, 65–74. doi: 10.1016/j.jad.2016.12.058

Shi, Y., Yang, D., Zeng, Y., and Wu, W. (2017). Risk factors for post-stroke depression: a meta-analysis. *Front. Aging Neurosci.* 9:218. doi: 10.3389/fnagi.2017.00218

Siebner, H. R., Willoch, F., Peller, M., Auer, C., Boecker, H., Conrad, B., et al. (1998). Imaging brain activation induced by long trains of repetitive transcranial magnetic stimulation. *Neuroreport* 9, 943–948. doi: 10.1097/00001756-199803300-00033

Soundara Rajan, T., Ghilardi, M. F. M., Wang, H. Y., Mazzon, E., Bramanti, P., Restivo, D., et al. (2017). Mechanism of action for rTMS: a working hypothesis based on animal studies. *Front. Physiol.* 8:457. doi: 10.3389/fphys.2017.00457

Strafella, A. P., Paus, T., Fraraccio, M., and Dagher, A. (2003). Striatal dopamine release induced by repetitive transcranial magnetic stimulation of the human motor cortex. *Brain* 126, 2609–2615. doi: 10.1093/brain/awg268

Tavakoli, A. V., and Yun, K. (2017). Transcranial alternating current stimulation (tACS) mechanisms and protocols. *Front. Cell. Neurosci.* 11:214. doi: 10.3389/fncel.2017.00214

Val-Laillet, D., Aarts, E., Weber, B., Ferrari, M., Quaresima, V., Stoeckel, L. E., et al. (2015). Neuroimaging and neuromodulation approaches to study eating behavior and prevent and treat eating disorders and obesity. *Neuroimage Clin.* 8, 1–31. doi: 10.1016/j.nicl.2015.03.016

Wu, G. R., and Baeken, C. (2017). Longer depressive episode duration negatively influences HF-rTMS treatment response: a cerebellar metabolic deficiency? *Brain Imaging Behav.* 11, 8–16. doi: 10.1007/s11682-016-9510-0

Xie, J., Chen, J., and Wei, Q. (2013). Repetitive transcranial magnetic stimulation versus electroconvulsive therapy for major depression: a meta-analysis of stimulus parameter effects. *Neurol. Res.* 35, 1084–1091. doi: 10.1179/1743132813Y.0000000245

Xu, X. M., Zou, D. Z., Shen, L. Y., Liu, Y., Zhou, X. Y., Pu, J. C., et al. (2016). Efficacy and feasibility of antidepressant treatment in patients with post-stroke depression. *Medicine* 95:e5349. doi: 10.1097/md.0000000000005349

Ziemann, U., Reis, J., Schwenkreis, P., Rosanova, M., Strafella, A., Badawy, R., et al. (2015). TMS and drugs revisited 2014. *Clin. Neurophysiol.* 126, 1847–1868. doi: 10.1016/j.clinph.2014.08.028

**Conflict of Interest Statement**: The authors declare that the research was conducted in the absence of any commercial or financial relationships that could be construed as a potential conflict of interest.

frontiers in Human Neuroscience

ORIGINAL RESEARCH
published: 31 May 2018
doi: 10.3389/fnhum.2018.00104

# Altered Brain Regional Homogeneity Following Electro-Acupuncture Stimulation at *Sanyinjiao* (SP6) in Women With Premenstrual Syndrome

*Yong Pang[1†], Huimei Liu[1†], Gaoxiong Duan[2†], Hai Liao[2†], Yanfei Liu[2], Zhuo Feng[1], Jien Tao[1], Zhuocheng Zou[1], Guoxiang Du[2], Rongchao Wan[2], Peng Liu[3] and Demao Deng[2]**

[1]Department of Acupuncture, First Affiliated Hospital, Guangxi University of Chinese Medicine, Nanning, China, [2]Department of Radiology, First Affiliated Hospital, Guangxi University of Chinese Medicine, Nanning, China, [3]Life Science Research Center, School of Life Science and Technology, Xidian University, Xi'an, China

**Background**: Premenstrual syndrome (PMS) is a menstrual cycle-related disorder which causes physical and mood changes prior to menstruation and is associated with the functional dysregulation of the brain. Acupuncture is an effective alternative therapy for treating PMS, and sanyinjiao (SP6) is one of the most common acupoints used for improving the symptoms of PMS. However, the mechanism behind acupuncture's efficacy for relieving PMS symptoms remains unclear. The aim of this study was to identify the brain response patterns induced by acupuncture at acupoint SP6 in patients with PMS.

**Materials and Methods**: Twenty-three females with PMS were enrolled in this study. All patients underwent resting-state fMRI data collection before and after 6 min of electroacupuncture stimulation (EAS) at SP6. A regional homogeneity (ReHo) approach was used to compare patients' brain responses before and after EAS at SP6 using REST software. The present study was registered at http://www.chictr.org.cn, and the Clinical Trial Registration Number is ChiCTR-OPC-15005918.

**Results**: EAS at SP6 elicited decreased ReHo value at the bilateral precuneus, right inferior frontal cortex (IFC) and left middle frontal cortex (MFC). In contrast, increased ReHo value was found at the bilateral thalamus, bilateral insula, left putamen and right primary somatosensory cortex (S1).

**Conclusions**: Our study provides an underlying neuroimaging evidence that the aberrant neural activity of PMS patients could be regulated by acupuncture at SP6.

**Keywords: premenstrual syndrome, acupuncture, sanyinjiao, ReHo, fMRI**

OPEN ACCESS

***Edited by:***
*Nan Li,*
*RIKEN, Japan*

***Reviewed by:***
*Xiaosong He,*
*Thomas Jefferson University, United States*
*Ying Wang,*
*University of Science and Technology of China, China*

****Correspondence:***
*Demao Deng*
*demaodeng@163.com*

*[†]These authors have contributed equally to this work.*

***Received:*** *17 October 2017*
***Accepted:*** *05 March 2018*
***Published:*** *31 May 2018*

***Citation:***
*Pang Y, Liu H, Duan G, Liao H, Liu Y, Feng Z, Tao J, Zou Z, Du G, Wan R, Liu P and Deng D (2018) Altered Brain Regional Homogeneity Following Electro-Acupuncture Stimulation at Sanyinjiao (SP6) in Women With Premenstrual Syndrome. Front. Hum. Neurosci. 12:104. doi: 10.3389/fnhum.2018.00104*

## INTRODUCTION

Premenstrual syndrome (PMS) is a well-known gynecological disorder in fertile women involving a series of psychological, behavioral and physical symptoms, which periodically appear during the luteal phase of the menstrual cycle and relieve soon after the occurrence of menstruation (Yonkers et al., 2008). Approximately 30%–40% of menstruating females suffer from PMS which

significantly impacts their daily lives, and 3%–8% of women meet strict DSM-IV diagnosis criteria for premenstrual dysphoric disorder (PMDD), which is a more serious and disabling form of PMS (Ryu and Kim, 2015). Substantial studies have suggested that the etiology of PMS is associated with the functional dysregulation of the central nervous system (CNS) during the luteal phase (Brooks et al., 2002; Amin et al., 2006; Rapkin and Akopians, 2012; Barth et al., 2014; Gao X. et al., 2014). In addition, many neuroimaging studies have also indicated abnormal neural activity in PMS individuals. For example, previous fMRI studies indicated that PMS patients exhibited aberrant neural activity of the default mode network (DMN), which is a region responsible for self-referential activities, such as evaluating characteristics of external and internal cues, planning the future and remembering the past (De Bondt et al., 2015; Liu et al., 2015), suggesting that the abnormal modulation of the DMN might play a crucial role in the pathology of PMS. Consistent with this finding, our most recent study found that PMS patients have abnormal spontaneous neural activity in the DMN and emotion-related brain regions during the luteal phase of the menstrual cycle (Liao et al., 2017). Therefore, a CNS-related intervention modality might be an important therapeutic approach for relieving symptoms of PMS.

As an important therapeutic modality in complementary and alternative medicine (CAM), acupuncture has demonstrated its effectiveness in relieving the physical and psychological symptoms of PMS (Jang et al., 2014). It has been widely and increasingly applied for relieving symptoms of obstetrics and gynecological conditions, including PMS (Kim et al., 2011). According to traditional Chinese medicine (TCM), *sanyinjiao* (SP6), located 3 cun (1 cun = 3.33 cm) directly above the tip of the medial malleoulus on the posterior border of the tibia, has been shown to ameliorate menstrual-related disorders, including primary dysmenorrhea and PMS (Stux and Bruce Pomeranz, 1996; Chae et al., 2007). SP6 is commonly selected as the acupoint of choice for improving the physical and psychological symptoms of PMS in clinical settings (Cho and Kim, 2010). Previous studies have shown that the modulatory effects of acupuncture on patients are mainly mediated via the CNS (Fang et al., 2009). More specifically, acupuncture treatment may work to alleviate symptoms of PMS by modulating abnormal brain responses of the CNS. However, studies attempting to elucidate the modulatory mechanism of acupuncture on PMS are unclear and insufficient. Therefore, more studies on this topic are needed.

fMRI is an important technique to investigate the functions of human brain (Bifone and Gozzi, 2011; Branco et al., 2016). Additionally, fMRI has the ability to monitor acupuncture-related neural response patterns in humans and provides an opportunity for exploring the neural mechanisms of acupuncture. Numerous fMRI studies on acupuncture have found specific activation patterns in the brain elicited by acupuncture (Hui et al., 2000; Wu et al., 2002; Yoo et al., 2004). Regional homogeneity (ReHo), a widely used method, can detect the similarity of synchrony between the time series of a specific voxel with its nearest neighboring voxels and with the report the intensity of regional spontaneous activity in brain (Zang et al., 2004). fMRI combined with ReHo analysis has been widely and successfully used to investigate the mechanisms of a variety of neuropsychiatric diseases (Liu et al., 2006; Wu et al., 2009; Guo et al., 2011). More specifically, our most recent work demonstrated the feasibility of using ReHo to detect the abnormal patterns of spontaneous neural activity in PMS patients (Liao et al., 2017).

In this study we collected fMRI data before and after electro-acupuncture stimulation (EAS) at acupoint SP6 in females with PMS to investigate whether EAS at SP6 could regulate the aberrant brain activity in PMS patients using ReHo analysis. We further hypothesized that the abnormal neural activity in PMS patients could be regulated through EAS at SP6.

# MATERIALS AND METHODS

## Ethics Statement

This study conforms to the Declaration of Helsinki and was approved by the Medicine Ethics Committee of First Affiliated Hospital, Guangxi University of Chinese Medicine. Every subject was informed of the experimental procedures and asked to sign an informed consent. This study was registered on http://www.chictr.org.cn, the Clinical Trial Registration Number is ChiCTR-OPC-15005918, and the registration number was obtained on 29/01/2015.

## Participants

This study was a follow-up study based on the results of our previous studies, and used the same patient samples as in our previously published manuscript (Liao et al., 2017). Twenty-three female PMS patients were recruited via advertisements posted at the Guangxi University of Chinese Medicine. Each participant was prospectively screened for two consecutive months and asked to complete a daily rating of severity of problems (DRSP) questionnaire in order to quantify the severity of her premenstrual symptoms (Endicott et al., 2006). Diagnostic criteria for PMS were based on the recommendations and guidelines for PMS (Halbreich et al., 2007), while the Diagnostic and Statistical Manual of Mental Disorders-5th Edition (DSM-5; American Psychiatric Association, 2013) was used to exclude participants with PMDD. An experienced gynecologist diagnosed each patient.

The inclusion criteria were as follows: (1) 18–45 years old, right-handed; (2) regular menstrual cycle separated by 24–35 days; (3) premenstrual symptoms occurring 2 weeks before menses in most menstrual cycles; (4) symptoms disappear shortly following the onset of menses; (5) symptoms interfere with daily functioning and/or relationships and/or cause emotional or physical distress or suffering; (6) symptoms periodically appear in the late luteal phase of menstrual cycle and relieve soon after the middle-follicular phase; and (7) symptoms do not worsen due to another physical or mental chronic disorder. The exclusion criteria were: (1) a history of other diseases, including menopausal syndrome, dysmenorrhea, thyroid disease, mastopathy, gynecological inflammation, hysterectomy or bilateral oophorectomy, cancer, or diabetes; (2) a history of psychiatric disorders, such as schizophrenia, schizoaffective disorder, delusional

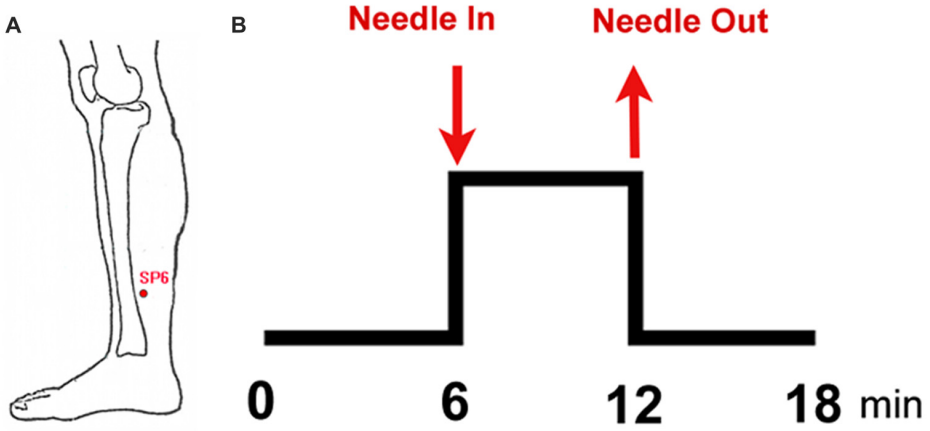


**FIGURE 1 |** Experimental paradigm. **(A)** Location of sanyinjiao (SP6); **(B)** electroacupuncture stimulation (EAS) paradigm.

mental disorder, organic mental disorder, psychotic features coordinated or uncoordinated with mood or bipolar disorder; (3) use of benzodiazepines, steroid compound, or other psychotropic drugs; (4) is lactating or pregnant; (5) has any MRI or acupuncture contraindication; and (6) a history of alcohol or drug abuse or is a smoker.

## Experimental Paradigm

This study adopted the non-repeated event-related (NRER) paradigm designed by Qin et al. (2008; **Figure 1**). Every participant underwent two 6-min fMRI scans, which included a 6-min resting state scan before and after EAS. Acupuncture manipulation was completed by an experienced and licensed acupuncturist (device type: HuaTuo-brand, SDZ-V-type, Shanghai, China). EAS was executed by inserting a stainless-steel disposable needle (specifications: 0.30 mm × 45 mm; Huatuo-brand, Suzhou, Jiangsu, China) into the left leg at acupoint SP6. Another electrode was connected to the acupuncture needle, which was superficially inserted into a point 1.0 cm away from SP6. Due to the physical characteristics of women and sex hormone levels, the test date was arranged during the late luteal phase of the menstrual cycle. All of the tests were performed between 20:00 and 22:00 to ensure a relatively stable and low level of endogenous cortisol and estradiol (Bao et al., 2004). Each subject was informed to "keep their eyes closed, but to stay awake" during the fMRI scan. After the fMRI scan, all subjects were asked to recall Deqi sensations, which are thought to have therapeutic effects in clinical practice, and to complete the visual analog scale (VAS, includes sensations of soreness, numbness, fullness, heaviness, tingling, coolness, warmth, sharp pain, dull pain, aching and pressure; Hui et al., 2005, 2007).

## fMRI Data Collection

fMRI data was collected with a 3.0 tesla MRI system (Magnetom Verio, Siemens Medical, Erlangen, Germany) at the First Affiliated Hospital of Guangxi University of Chinese Medicine. Data was acquired with a single-shot gradient-recalled echo planar imaging (EPI) sequence. The related parameters were as follows: time repetition (TR) = 2000 ms, time echo (TE) = 30 ms, flip angle = 90°, matrix size = 64 × 64, field of view (FOV) = 240 mm × 240 mm, slice thickness = 5 mm and number of slices = 31. High-resolution T1-weighted structural images were collected by a volumetric three-dimensional spoiled gradient recall sequence using the following parameters: TR = 1900 ms, TE = 2.22 ms, flip angle = 9°, matrix size = 250 × 250, FOV = 250 mm × 250 mm, slice thickness = 1 mm and 176 slices.

## Data Preprocessing

The procedures of data preprocessing were identical to our previous work (Liao et al., 2017). Data preprocessing was performed using SPM8 (SPM8)[1]. To ensure the stability of the initial fMRI signal, the first 10 volumes of each time series were removed. Then the remaining functional data was corrected for time delay signals between different slices and realigned to the first volume. Head motion parameters were calculated by assessing the translation in each direction and the angular rotation on every axis for each volume. If the translation/rotation was more than 1.5 mm/1.5°, the data was discarded. The realigned fMRI data was spatially normalized to the montreal neurological institute (MNI) space using the normalization parameters estimated by T1 structural image unified segmentation and was re-sampled to 3 mm × 3 mm × 3 mm voxels. Several sources of spurious variance, such as the estimated motion parameters, average BOLD signals in ventricular and white matter regions, were filtered from the functional images. To abate the effect of low-frequency drifts and high-frequency noise, linear drift was removed and temporal filtering (0.01–0.08 Hz) was applied to the time series of each volume.

## ReHo Analysis

Data preprocessing details can be found in our previous study (Liao et al., 2017). This study used Kendall's coefficient of

[1]http://www.fil.ion.ucl.ac.uk/spm/

concordance (KCC) to measure the synchronization of the time series of a given voxel to its 26 nearest voxels in a voxel-wise way based on the hypothesis that a voxel was temporally similar to the ones of its neighbors. Individual ReHo maps were constructed by calculating the KCC within a gray matter mask in a voxel-wise manner using REST software[2]. The KCC maps were then spatially smoothed via a Gaussian kernel of 6 mm full-width at half-maximum.

## Statistical Analysis

Paired *t*-tests were used to measure patterns of neural activity (ReHo maps) in PMS patients before and after acupuncture at SP6. The contrast threshold was set at $p < 0.05$ (false discovery rate [FDR] corrected) and cluster size >30.

# RESULTS

## Demographic and Clinical Results

Due to obvious head motion, three participants were excluded. Twenty PMS patients were included in the final analysis. The detailed results are shown in **Table 1**.

## Deqi Sensations

The main Deqi sensations included soreness, numbness, fullness, heaviness and tingling. Deqi sensations of participants induced by SP6 were expressed as intensity (**Figure 2**).

## Functional Imaging Results

Compared to pre-EAS, EAS at SP6 elicited decreased ReHo values at the bilateral precuneus, right inferior frontal cortex (IFC), and left middle frontal cortex (MFC), and increased ReHo values at the bilateral thalamus, bilateral insula, left putamen and right primary somatosensory cortex (S1; **Figure 3** and **Table 2**).

# DISCUSSION

In the present study, we employed fMRI and ReHo analysis to explore EAS induced brain alternations in PMS patients. Our results indicate that EAS at SP6 elicited specific patterns of brain changes during the luteal phase in PMS patients. Our findings provide neuroimaging evidence to better understand the modulatory mechanisms of acupuncture in PMS patients.

[2]http://restfmri.net/forum/index.php

**TABLE 1 |** Demographic and clinical characteristics of the study.

| Variable | PMS |
|---|---|
| Number | 20 |
| Age (years) | 21.85 ± 1.72 |
| BMI | 18.60 ± 1.71 |
| DRSP, follicular | 39.16 ± 4.15 |
| DRSP, luteal | 73.47 ± 7.84 |
| ΔDRSP | 34.31 ± 3.69 |
| Menophania (years) | 13.75 ± 1.44 |
| Length of menstrual cycle (days) | 29.95 ± 1.76 |
| Menstruation (days) | 5.60 ± 1.09 |

*Data are presented as mean ± SD. PMS, premenstrual syndrome; BMI, body mass index; DRSP, daily record of severity of problems; ΔDRSP, difference betweem follicular and luteal phases.*

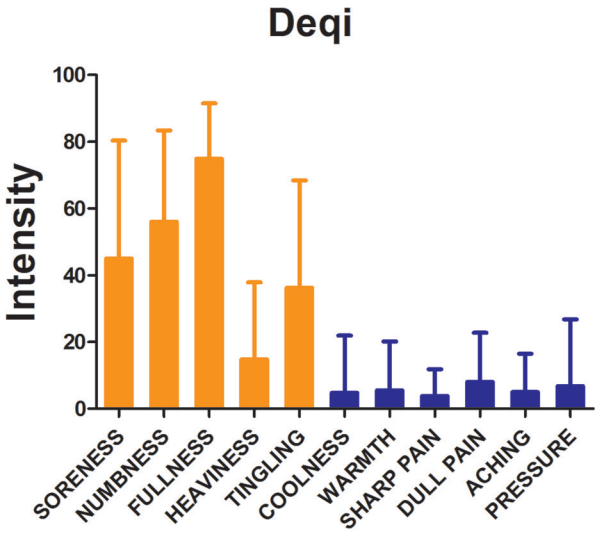


**FIGURE 2 |** Results of psychophysical analysis. Soreness, numbness, fullness, heaviness and tingling were the most commonly reported Deqi sensations. The error bar stands for standard deviation (SD) of the Deqi sensations.

As a therapeutic modality in East Asia, acupuncture needles are used to stimulate acupoints on the human body to produce modulation effects. Previous acupuncture neuroimaging studies have shown brain changes in the sensorimotor cortical network (e.g., insula, thalamus, as well as the primary and secondary somatosensory cortex) and the limbic-paralimbic-neocortical network (LPNN; e.g., medial prefrontal cortex, caudate, amygdala, posterior cingulate cortex, precuneus and parahippocampus) induced by acupuncture stimulation (Dhond et al., 2007; Fang et al., 2009; Chae et al., 2013). Our results are consistent with these previous findings. In the present study we elaborated upon this research and investigated changes in neural activity (decreased and increased) using ReHo analysis to illuminate the modulatory effects of acupuncture at SP6 in PMS patients.

## Decreased ReHo Value in the DMN

We found decreased ReHo values in some areas of the DMN, a network that is involved in self-referential activities, such as remembering the past and planning for the future (Raichle and Snyder, 2007; Buckner et al., 2008). The precuneus, a key node of the DMN, is significantly involved in a distributed network with cortical and sub-cortical regions to integrate both self-generated and external information (Cavanna and Trimble, 2006), and is associated with emotion processing (Tanaka and Kirino, 2016). The precuneus appears to induce significant neural changes in response to incongruent stimuli information rather than to congruent stimuli (Kitada et al., 2014). The CNS of PMS patients usually faces incongruent stimuli due to fluctuations in sex hormones (Halbreich et al., 2003). Thus, we conjecture that the decreased ReHo in the precuneus

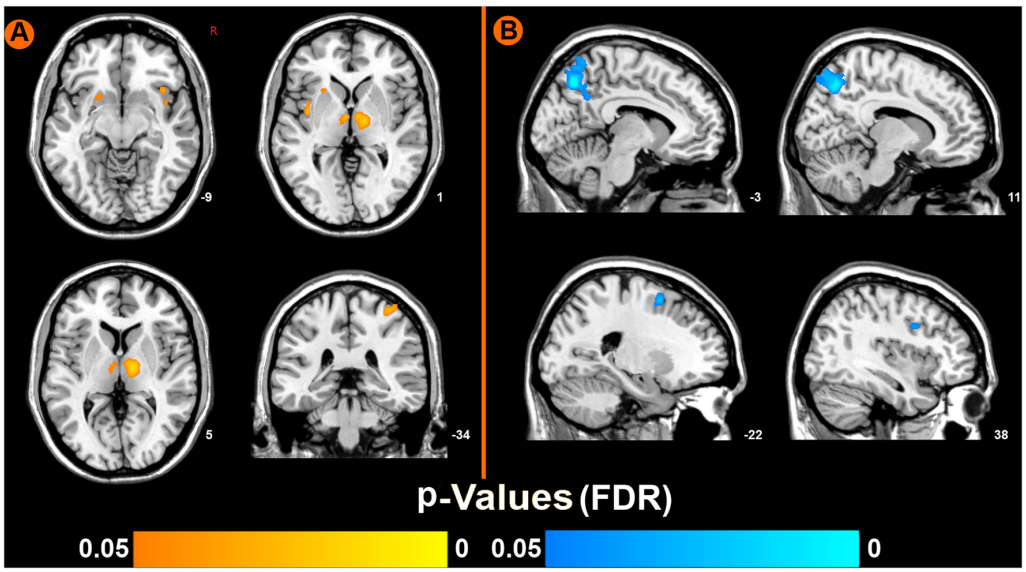


**FIGURE 3 |** Brain regions showing increased or decreased regional homogeneity (ReHo) values induced by EAS at SP6, compared to pre-acupuncture ($p < 0.05$, false discovery rate corrected). **(A)** Increased ReHo values regions after EAS at SP6. **(B)** Decreased ReHo values regions after EAS at SP6.

**TABLE 2 |** Main localization of brain maps by comparing electro-acupuncture stimulation (EAS) with resting state in premenstrual syndrome (PMS) patients.

| Regions | BA | MNI | | | *T*-Value | Vol |
|---|---|---|---|---|---|---|
| | | *X* | *Y* | *Z* | | |
| Right S1 | 3/1 | 42 | −33 | 66 | 5.92 | 59 |
| Left insula | 48 | −39 | 0 | −3 | 4.78 | 54 |
| Right insula | 48 | 39 | 18 | −9 | 3.95 | 43 |
| Left thalamus | | −3 | −9 | 0 | 4.13 | 39 |
| Right thalamus | | 12 | −12 | 3 | 4.74 | 88 |
| Left putamen | | −24 | 18 | 0 | 3.82 | 47 |
| Left middle frontal cortex | 6 | −21 | 9 | 57 | −3.89 | 64 |
| Right inferior frontal cortex | 6/9 | 39 | 6 | 33 | −5.16 | 53 |
| Left precuneus | 31 | −9 | −69 | 57 | −5.89 | 126 |
| Right precuneus | 31 | 12 | −72 | 48 | −4.66 | 112 |

*Abbreviation: BA, Brodmann area; MNI, montreal neurological institute; Vol, voxels; S1, primary somatosensory cortex; PMS, premenstrual syndrome. The highlighted data in gray background are the related brain regions showing decreased ReHo values, and the unhighlighted part are the related brain regions showing increased ReHo values.*

is related to sex hormone fluctuations. In addition, the IFC and MFC, major components of the prefrontal cortex (PFC), are mainly associated with the integration of emotional and cognitive functions (Gusnard et al., 2001; Simpson et al., 2001). In a previous study, investigators found that the function of the PFC in emotional response inhibition was susceptible to changes in the female menstrual cycle (Amin et al., 2006), and that the PFC was more likely to have abnormal neural activity in response to negative emotional stimuli. Our previous study found increased ReHo values in the bilateral precuneus, right IFC, and left MFC, which we refer to as the DMN (Liao et al., 2017), and these results are consistent with other studies (De Bondt et al., 2015; Liu et al., 2015). We speculate that the negative psychological symptoms (e.g., mood swings, anger, impatience and depression) or incongruent stimuli from fluctuations in the menstrual cycle in PMS are due to abnormal DMN activity. Therefore, insights into the modulation of the DMN by invention methods are necessary to understand the therapeutic modulatory mechanisms for PMS. Fortunately, previous studies have suggested that ReHo can be used to measure spontaneous neural activity during a task and thus can measure task activations (Yuan et al., 2013). Moreover, many western medicine studies have suggested that ReHo analysis can provide critical information to better understand CNS-related functional neural synchrony alterations induced by some treatment methods, such as hemodialysis and equine-assisted activities and therapy, and the decreased ReHo values in the DMN have been suggested to be significantly associated with medication modulatory effects on patient's brain (Chen et al., 2015; Yoo et al., 2016). It is worth noting that in the current study the majority of the decreased ReHo values elicited by acupuncture at SP6 were located in the DMN, including the right IFC, left MFC and bilateral precuneus. These findings indicate that the abnormal neural activity of the DMN was modulated by SP6 in PMS patients and might

have helped reestablish normal function to the DMN and thus have rehabilitation implications. The modulation effects of acupuncture and its clinical efficacy also suggests that acupuncture serves a role in maintaining the body's homeostatic balance (Mayer, 2000). Thus, we speculate that the underlying mechanism of acupuncture on PMS might be attributed to acupuncture intervention effects on re-establishing the normal neural activity of the DMN.

### Increased ReHo Value in Sensorimotor Cortical Network

This study also found increased ReHo values in some brain regions of the sensorimotor cortical network, such as the bilateral thalamus, bilateral insula, left putamen and right S1. The thalamus plays an important role in controlling the flow of information to the cortex (Sherman and Guillery, 2002). It relays motor, sensory, and spatial information to the cortex (Sherman, 2007) and mediates the interaction of attention and arousal (Portas et al., 1998). The spinothalamic tract projects to the thalamus, from which information is transmitted to the S1 and insula, respectively (Anand et al., 2007). The insula receives afferent information from the thalamus, and forms anatomical interconnections with extensive cortical and sub-cortical structures related to higher-order brain functions, including pain perception, memory, and decision-making (Craig et al., 2000; Craig, 2011; Nieuwenhuys, 2012; Zhuo, 2016). The putamen is an important component of the striato–thalamo–cortical circuitry and is related to habitual behavior, action initiation and motivational processing (Graybiel, 2008). Prior studies indicate that pain stimuli are not only in core areas of the afferent neuraxis, including the thalamus, S1 and insula (Coghill et al., 2001; Brooks et al., 2002; Bingel et al., 2003), but also in the motor output system (e.g., putamen), which is responsible for producing spatially guided defensive behavior (Bingel et al., 2002). Moreover, fMRI studies on acupuncture have revealed that brain changes in the sensorimotor cortical network are induced by acupuncture (e.g., insula, thalamus, putamen, as well as S1 (Fang et al., 2009). Davis et al. (1998) demonstrated that the changes in the somatosensory cortex together with the thalamus occurred following somatosensory stimulation at various acupoints. Furthermore, fMRI studies revealed that acupuncture at SP6 could induce changes in neural activity in the sensorimotor cortical network of a sleep-deprived brain (Gao L. et al., 2014). Interestingly, our study also revealed that there was a trend between Deqi sensations and ReHo changes in certain brain regions using a correlation analysis (see the Supplementary Table S1). Several Deqi sensations (Coolness, Warmth, Pressure and Sharp pain) were positively correlated with ReHo changes at the bilateral precuneus, bilateral insula and left putamen. Meanwhile, tingling and numbness were negatively correlated with ReHo changes at the precuneus and insula. To our knowledge, Deqi sensations are complex subjective experiences associated with the sensorimotor cortex. Based on these findings, we speculate that acupuncture at SP6 might have modulatory effects on the sensorimotor cortical network. According to our current results of increased ReHo at the bilateral insula, bilateral thalamus, left putamen, and right S1 following acupuncture at SP6 in PMS patients, we speculate that the widely increased synchronization of neuronal activity in the sensorimotor cortical network may be due to altered sensory transduction pathways in the brain induced by SP6.

There are several limitations in this study. First, the present study only demonstrated increased/decreased ReHo values in the brain of PMS patients modulated by acupuncture at SP6 but did not show that these ReHo values were "PMS specific," as there were no healthy controls or sham conditions. In the future, the use of a control condition would be advised. Second, although our study indicated that there was a trend between Deqi sensations and ReHo changes of certain brain regions, we were unable to extract any meaningful results from these complicated correlations. Finally, our sample size of PMS patients was not very big; therefore, the present findings should be retested with a larger sample size in the future.

In conclusion, we elaborated on our previous study and used ReHo analysis to investigate the specific fMRI brain response patterns to acupuncture at SP6 in PMS patients during the late luteal phase. Our findings indicate that the abnormal neural activity of the DMN and sensorimotor cortical network in PMS patients could be modulated by acupuncture at SP6. These results provide neuroimaging evidence to better understand the underlying mechanisms of acupuncture at SP6 in PMS patients.

## AUTHOR CONTRIBUTIONS

DD and YP proposed the theory and designed the experiment, made substantial contributions to the present study, revised and handled the manuscript. HLiu, GDuan and HLiao mainly were mainly responsible for recruiting and evaluating PMS patients. ZF, JT and ZZ mainly for recruiting the PMS patients and treating with acupuncture. GDu and RW performed the MR scan protocols and acquired and stored MRI data. YL and PL conducted the data processing and analysis, interpreted the conceptions of data processing. All of the authors consented the final version to be published.

## FUNDING

The current study was supported by the National Natural Science Foundation of China (Grant Nos. 81760886, 81771918, 81471811, 81471738) and the Guangxi Natural Science Foundation (Grant Nos. 2017GXNSFBA198095, 2016GXNSFAA380086, 2011GXNSFA018176).

## ACKNOWLEDGMENTS

Thanks to all PMS patients who participated in the experiment.

## SUPPLEMENTARY MATERIAL

The Supplementary Material for this article can be found online at: https://www.frontiersin.org/articles/10.3389/fnhum.2018.00104/full#supplementary-material

## REFERENCES


American Psychiatric Association (2013). *Diagnostic and Statistical Manual of Mental Disorders: DSM-5$^{TM}$*. 5th Edn. Arlington, VA: American Psychiatric Publishing, Inc.

Amin, Z., Epperson, C. N., Constable, R. T., and Canli, T. (2006). Effects of estrogen variation on neural correlates of emotional response inhibition. *Neuroimage* 32, 457–464. doi: 10.1016/j.neuroimage.2006.03.013

Anand, P., Aziz, Q., Willert, R., and van Oudenhove, L. (2007). Peripheral and central mechanisms of visceral sensitization in man. *Neurogastroenterol. Motil.* 19, 29–46. doi: 10.1111/j.1365-2982.2006.00873.x

Bao, A. M., Ji, Y. F., Van Someren, E. J. W., Hofman, M. A., Liu, R. Y., and Zhou, J. N. (2004). Diurnal rhythms of free estradiol and cortisol during the normal menstrual cycle in women with major depression. *Horm. Behav.* 45, 93–102. doi: 10.1016/j.yhbeh.2003.09.004

Barth, A. M. I., Ferando, I., and Mody, I. (2014). Ovarian cycle-linked plasticity of δ-GABAA receptor subunits in hippocampal interneurons affects γ oscillations *in vivo*. *Front. Cell. Neurosci.* 8:222. doi: 10.3389/fncel.2014.00222

Bifone, A., and Gozzi, A. (2011). *Functional and Pharmacological MRI in Understanding Brain Function at a Systems Level.* Berlin Heidelberg: Springer.

Bingel, U., Quante, M., Knab, R., Bromm, B., Weiller, C., and Buchel, C. (2002). Subcortical structures involved in pain processing: evidence from single-trial fMRI. *Pain* 99, 313–321. doi: 10.1016/s0304-3959(02)00157-4

Bingel, U., Quante, M., Knab, R., Bromm, B., Weiller, C., and Büchel, C. (2003). Single trial fMRI reveals significant contralateral bias in responses to laser pain within thalamus and somatosensory cortices. *Neuroimage* 18, 740–748. doi: 10.1016/s1053-8119(02)00033-2

Branco, P., Seixas, D., Deprez, S., Kovacs, S., Peeters, R., Castro, S. L., et al. (2016). Resting-state functional magnetic resonance imaging for language preoperative planning. *Front. Hum. Neurosci.* 10:11. doi: 10.3389/fnhum.2016.00011

Brooks, J. C. W., Nurmikko, T. J., Bimson, W. E., Singh, K. D., and Roberts, N. (2002). fMRI of thermal pain: effects of stimulus laterality and attention. *Neuroimage* 15, 293–301. doi: 10.1006/nimg.2001.0974

Buckner, R. L., Andrews-Hanna, J. R., and Schacter, D. L. (2008). The brain's default network: anatomy, function, and relevance to disease. *Ann. N Y Acad. Sci.* 1124, 1–38. doi: 10.1196/annals.1440.011

Cavanna, A. E., and Trimble, M. R. (2006). The precuneus: a review of its functional anatomy and behavioural correlates. *Brain* 129, 564–583. doi: 10.1093/brain/awl004

Chae, Y., Chang, D. S., Lee, S. H., Jung, W. M., Lee, I. S., Jackson, S., et al. (2013). Inserting needles into the body: a meta-analysis of brain activity associated with acupuncture needle stimulation. *J. Pain* 14, 215–222. doi: 10.1016/j.jpain.2012.11.011

Chae, Y., Kim, H. Y., Lee, H. J., Park, H. J., Hahm, D. H., An, K., et al. (2007). The alteration of pain sensitivity at disease-specific acupuncture points in premenstrual syndrome. *J. Physiol. Sci.* 57, 115–119. doi: 10.2170/physiolsci.rp012706

Chen, H. J., Qi, R., Kong, X., Wen, J., Liang, X., Zhang, Z., et al. (2015). The impact of hemodialysis on cognitive dysfunction in patients with end-stage renal disease: a resting-state functional MRI study. *Metab. Brain Dis.* 30, 1247–1256. doi: 10.1007/s11011-015-9702-0

Cho, S. H., and Kim, J. (2010). Efficacy of acupuncture in management of premenstrual syndrome: a systematic review. *Complement. Ther. Med.* 18, 104–111. doi: 10.1016/j.ctim.2009.12.001

Coghill, R. C., Gilron, I., and Iadarola, M. J. (2001). Hemispheric lateralization of somatosensory processing. *J. Neurophysiol.* 85, 2602–2612. doi: 10.1152/jn.2001.85.6.2602

Craig, A. D. (2011). Significance of the insula for the evolution of human awareness of feelings from the body. *Ann. N Y Acad. Sci.* 1225, 72–82. doi: 10.1111/j.1749-6632.2011.05990.x

Craig, A. D., Chen, K., Bandy, D., and Reiman, E. M. (2000). Thermosensory activation of insular cortex. *Nat. Neurosci.* 3, 184–190. doi: 10.1038/72131

Davis, K. D., Kwan, C. L., Crawley, A. P., and Mikulis, D. J. (1998). Functional MRI study of thalamic and cortical activations evoked by cutaneous heat, cold and tactile stimuli. *J. Neurophysiol.* 80, 1533–1546. doi: 10.1152/jn.1998.80.3.1533

De Bondt, T., De Belder, F., Vanhevel, F., Jacquemyn, Y., and Parizel, P. M. (2015). Prefrontal GABA concentration changes in women-Influence of menstrual cycle phase, hormonal contraceptive use, and correlation with premenstrual symptoms. *Brain Res.* 1597, 129–138. doi: 10.1016/j.brainres.2014.11.051

Dhond, R. P., Kettner, N., and Napadow, V. (2007). Neuroimaging acupuncture effects in the human brain. *J. Altern. Complement. Med.* 13, 603–616. doi: 10.1089/acm.2007.7040

Endicott, J., Nee, J., and Harrison, W. (2006). Daily Record of Severity of Problems (DRSP): reliability and validity. *Arch. Womens Ment. Health* 9, 41–49. doi: 10.1007/s00737-005-0103-y

Fang, J., Jin, Z., Wang, Y., Li, K., Kong, J., Nixon, E. E., et al. (2009). The salient characteristics of the central effects of acupuncture needling: limbic-paralimbic-neocortical network modulation. *Hum. Brain Mapp.* 30, 1196–1206. doi: 10.1002/hbm.20583

Gao, X., Sun, P., Qiao, M., Wei, S., Xue, L., and Zhang, H. (2014). Shu-Yu capsule, a Traditional Chinese Medicine formulation, attenuates premenstrual syndrome depression induced by chronic stress constraint. *Mol. Med. Rep.* 10, 2942–2948. doi: 10.3892/mmr.2014.2599

Gao, L., Zhang, M., Gong, H., Bai, L., Dai, X. J., Min, Y., et al. (2014). Differential activation patterns of FMRI in sleep-deprived brain: restoring effects of acupuncture. *Evid. Based Complement. Alternat. Med.* 2014:465760. doi: 10.1155/2014/465760

Graybiel, A. M. (2008). Habits, rituals, and the evaluative brain. *Annu. Rev. Neurosci.* 31, 359–387. doi: 10.1146/annurev.neuro.29.051605.112851

Guo, W. B., Liu, F., Xue, Z. M., Yu, Y., Ma, C. Q., Tan, C. L., et al. (2011). Abnormal neural activities in first-episode, treatment-naive, short-illness-duration, and treatment-response patients with major depressive disorder: a resting-state fMRI study. *J. Affect. Disord.* 135, 326–331. doi: 10.1016/j.jad.2011.06.048

Gusnard, D. A., Akbudak, E., Shulman, G. L., and Raichle, M. E. (2001). Medial prefrontal cortex and self-referential mental activity: relation to a default mode of brain function. *Proc. Natl. Acad. Sci. U S A* 98, 4259–4264. doi: 10.1073/pnas.071043098

Halbreich, U., Backstrom, T., Eriksson, E., O'Brien, S., Calil, H., Ceskova, E., et al. (2007). Clinical diagnostic criteria for premenstrual syndrome and guidelines for their quantification for research studies. *Gynecol. Endocrinol.* 23, 123–130. doi: 10.1080/09513590601167969

Halbreich, U., Borenstein, J., Pearlstein, T., and Kahn, L. S. (2003). The prevalence, impairment, impact, and burden of premenstrual dysphoric disorder (PMS/PMDD). *Psychoneuroendocrinology* 28, 1–23. doi: 10.1016/s0306-4530(03)00098-2

Hui, K. K., Liu, J., Makris, N., Gollub, R. L., Chen, A. J., Moore, C. I., et al. (2000). Acupuncture modulates the limbic system and subcortical gray structures of the human brain: evidence from fMRI studies in normal subjects. *Hum. Brain Mapp.* 9, 13–25. doi: 10.1002/(sici)1097-0193(2000)9:1<13::aid-hbm2>3.0.co;2-f

Hui, K. K., Liu, J., Marina, O., Napadow, V., Haselgrove, C., Kwong, K. K., et al. (2005). The integrated response of the human cerebro-cerebellar and limbic systems to acupuncture stimulation at ST 36 as evidenced by fMRI. *Neuroimage* 27, 479–496. doi: 10.1016/j.neuroimage.2005.04.037

Hui, K. K., Nixon, E. E., Vangel, M. G., Liu, J., Marina, O., Napadow, V., et al. (2007). Characterization of the "deqi" response in acupuncture. *BMC Complement. Altern. Med.* 7:33. doi: 10.1186/1472-6882-7-33

Jang, S. H., Kim, D. I., and Choi, M. S. (2014). Effects and treatment methods of acupuncture and herbal medicine for premenstrual syndrome/premenstrual dysphoric disorder: systematic review. *BMC Complement. Altern. Med.* 14:11. doi: 10.1186/1472-6882-14-11

Kim, S. Y., Park, H. J., Lee, H., and Lee, H. (2011). Acupuncture for premenstrual syndrome: a systematic review and meta-analysis of randomised controlled trials. *BJOG* 118, 899–915. doi: 10.1111/j.1471-0528.2011.02994.x

Kitada, R., Sasaki, A. T., Okamoto, Y., Kochiyama, T., and Sadato, N. (2014). Role of the precuneus in the detection of incongruency between tactile and visual texture information: a functional MRI study. *Neuropsychologia* 64, 252–262. doi: 10.1016/j.neuropsychologia.2014.09.028

Liao, H., Pang, Y., Liu, P., Liu, H., Duan, G., Liu, Y., et al. (2017). Abnormal spontaneous brain activity in women with premenstrual syndrome revealed by regional homogeneity. *Front. Hum. Neurosci.* 11:62. doi: 10.3389/fnhum.2017.00062

Liu, H., Liu, Z., Liang, M., Hao, Y., Tan, L., Kuang, F., et al. (2006). Decreased regional homogeneity in schizophrenia: a resting state fMRI study. *Neuroreport* 17, 19–22. doi: 10.1097/01.wnr.0000195666.22714.35

Liu, Q., Li, R., Zhou, R., Li, J., and Gu, Q. (2015). Abnormal resting-state connectivity at functional MRI in women with premenstrual syndrome. *PLoS One* 10:e0136029. doi: 10.1371/journal.pone.0136029

Mayer, D. J. (2000). Acupuncture: an evidence-based review of the clinical literature. *Annu. Rev. Med.* 51, 49–63. doi: 10.1146/annurev.med.51.1.49

Nieuwenhuys, R. (2012). The insular cortex: a review. *Prog. Brain Res.* 195, 123–163. doi: 10.1016/B978-0-444-53860-4.00007-6

Portas, C. M., Rees, G., Howseman, A. M., Josephs, O., Turner, R., and Frith, C. D. (1998). A specific role for the thalamus in mediating the interaction of attention and arousal in humans. *J. Neurosci.* 18, 8979–8989. doi: 10.1523/JNEUROSCI.18-21-08979.1998

Qin, W., Tian, J., Bai, L., Pan, X., Yang, L., Chen, P., et al. (2008). FMRI connectivity analysis of acupuncture effects on an amygdala-associated brain network. *Mol. Pain* 4:55. doi: 10.1186/1744-8069-4-55

Raichle, M. E., and Snyder, A. Z. (2007). A default mode of brain function: a brief history of an evolving idea. *Neuroimage* 37, 1083–1090; discussion 1097–1089. doi: 10.1016/j.neuroimage.2007.02.041

Rapkin, A. J., and Akopians, A. L. (2012). Pathophysiology of premenstrual syndrome and premenstrual dysphoric disorder. *Menopause Int.* 18, 52–59. doi: 10.1258/mi.2012.012014

Ryu, A., and Kim, T. H. (2015). Premenstrual syndrome: a mini review. *Maturitas* 82, 436–440. doi: 10.1016/j.maturitas.2015.08.010

Sherman, S. M. (2007). The thalamus is more than just a relay. *Curr. Opin. Neurobiol.* 17, 417–422. doi: 10.1016/j.conb.2007.07.003

Sherman, S. M., and Guillery, R. W. (2002). The role of the thalamus in the flow of information to the cortex. *Philos. Trans. R. Soc. Lond. B Biol. Sci.* 357, 1695–1708. doi: 10.1098/rstb.2002.1161

Simpson, J. R. Jr., Snyder, A. Z., Gusnard, D. A., and Raichle, M. E. (2001). Emotion-induced changes in human medial prefrontal cortex: I. During cognitive task performance. *Proc. Natl. Acad. Sci. U S A* 98, 683–687. doi: 10.1073/pnas.98.2.683

Stux, M. G., and Bruce Pomeranz, P. D. (1996). *Basics of Acupuncture.* Berlin: Springer Berlin.

Tanaka, S., and Kirino, E. (2016). Functional connectivity of the precuneus in female university students with long-term musical training. *Front. Hum. Neurosci.* 10:328. doi: 10.3389/fnhum.2016.00328

Wu, M. T., Sheen, J. M., Chuang, K. H., Yang, P., Chin, S. L., Tsai, C. Y., et al. (2002). Neuronal specificity of acupuncture response: a fMRI study with electroacupuncture. *Neuroimage* 16, 1028–1037. doi: 10.1006/nimg.2002.1145

Wu, T., Long, X., Zang, Y., Wang, L., Hallett, M., Li, K., et al. (2009). Regional homogeneity changes in patients with Parkinson's disease. *Hum. Brain Mapp.* 30, 1502–1510. doi: 10.1002/hbm.20622

Yonkers, K. A., O'Brien, P. M., and Eriksson, E. (2008). Premenstrual syndrome. *Lancet* 371, 1200–1210. doi: 10.1016/S0140-6736(08)60527-9

Yoo, J. H., Oh, Y., Jang, B., Song, J., Kim, J., Kim, S., et al. (2016). The effects of equine-assisted activities and therapy on resting-state brain function in attention-deficit/hyperactivity disorder: a pilot study. *Clin. Psychopharmacol. Neurosci.* 14, 357–364. doi: 10.9758/cpn.2016.14.4.357

Yoo, S. S., Teh, E. K., Blinder, R. A., and Jolesz, F. A. (2004). Modulation of cerebellar activities by acupuncture stimulation: evidence from fMRI study. *Neuroimage* 22, 932–940. doi: 10.1016/j.neuroimage.2004.02.017

Yuan, R., Di, X., Kim, E. H., Barik, S., Rypma, B., and Biswal, B. B. (2013). Regional homogeneity of resting-state fMRI contributes to both neurovascular and task activation variations. *Magn. Reson. Imaging* 31, 1492–1500. doi: 10.1016/j.mri.2013.07.005

Zang, Y., Jiang, T., Lu, Y., He, Y., and Tian, L. (2004). Regional homogeneity approach to fMRI data analysis. *Neuroimage* 22, 394–400. doi: 10.1016/j.neuroimage.2003.12.030

Zhuo, M. (2016). Contribution of synaptic plasticity in the insular cortex to chronic pain. *Neuroscience* 338, 220–229. doi: 10.1016/j.neuroscience.2016.08.014

**Conflict of Interest Statement**: The authors declare that the research was conducted in the absence of any commercial or financial relationships that could be construed as a potential conflict of interest.

frontiers in Human Neuroscience

ORIGINAL RESEARCH
published: 05 June 2018
doi: 10.3389/fnhum.2018.00230

# Identification of the Features of Emotional Dysfunction in Female Individuals With Methamphetamine Use Disorder Measured by Musical Stimuli Modulated Startle Reflex

*Xi-Jing Chen*[1,2], *Chun-Guang Wang*[3], *Wang Liu*[1,2], *Monika Gorowska*[2], *Dong-Mei Wang*[1,2]* *and Yong-Hui Li*[1,2]

[1]CAS Key Laboratory of Mental Health, Institute of Psychology, Beijing, China, [2]Department of Psychology, University of Chinese Academy of Sciences, Beijing, China, [3]Beijing Municipal Bureau of Drug Rehabilitation Administration, Beijing, China

Emotional dysregulation contributes to the development of substance use disorders (SUDs) and is highly associated with drug abuse and relapse. Music as a contextual auditory stimulus can effectively stimulate the reward circuitry, modulate memory associated with drug taking, and enhance emotional experiences during drug taking. However, the studies of the emotional responses to music in individuals with SUDs are scarce. Using startle reflex and self-reports, this study assessed the psychophysiological and cognitive emotional responses (i.e., valence, arousal and proximity) to happy, peaceful, and fearful music stimuli in 30 females with methamphetamine use disorder (MUD) and 30 healthy females. The results found that participants with MUD showed an inhibited startle response to fearful music compared to normal controls ($t$ = 3.7, $p < 0.01$), and no significant differences were found in the startle responses to happy and peaceful music between the two groups. For the self-reported ratings, participants with MUD showed a decreased arousal in the response to fearful ($t$ = 4.1, $p < 0.01$) and happy music ($t$ = 3.8, $p < 0.01$), an increased valence in the response to fearful music ($t$ = 4.4, $p < 0.01$), and a higher level of proximity in the response to fearful ($t$ = 3.8, $p < 0.01$) and happy music ($t$ = 2.2, $p$ = 0.03). No significant differences were found in the rating of arousal to peaceful music, the valence to happy and peaceful music, as well as the proximity to peaceful music between the two groups. The females with MUD showed attenuated psychophysiological response and potentiated cognitive response (i.e., valence, arousal) to fearful music, as well as a high proximity to musical stimuli with high arousal regardless of its valence. These results have important implications for promoting the effectiveness of assessment and therapy selections for female MUD patients with impaired emotion regulation.

**Keywords: substance use disorders, methamphetamine, music stimuli, startle reflex, females**

**Abbreviations:** MUD, methamphetamine use disorder; SUDs, substance use disorders.

OPEN ACCESS

***Edited by:***
*Xiaochu Zhang,*
*University of Science and Technology of China, China*

***Reviewed by:***
*Lingdan Wu,*
*Universität Konstanz, Germany*
*Annie Lynne Heiderscheit,*
*Augsburg College, United States*

***Correspondence:**
*Dong-Mei Wang*
*wangdm@psych.ac.cn*

***Received:*** *28 February 2018*
***Accepted:*** *18 May 2018*
***Published:*** *05 June 2018*

***Citation:***
*Chen X-J, Wang C-G, Liu W, Gorowska M, Wang D-M and Li Y-H (2018) Identification of the Features of Emotional Dysfunction in Female Individuals With Methamphetamine Use Disorder Measured by Musical Stimuli Modulated Startle Reflex. Front. Hum. Neurosci. 12:230. doi: 10.3389/fnhum.2018.00230*

## INTRODUCTION

Substance use disorders (SUDs) is featured as "a cluster of cognitive, behavioral and physiological symptoms indicating that the individual continues using the substance despite significant substance-related problems" in Diagnostic and Statistical Manual of Mental Disorders Fifth Edition ([DSM-5], p. 483, American Psychiatric Association, 2013). Emotional dysregulation is an important problem that contributes to the development of SUDs (London et al., 2004, 2015). Chronic drug abuse involves the plastic change in the neural circuits mediating the reward system and anti-reward system (Koob and Moal, 2005). With the prolongation of drug use, the reward system increases its threshold (i.e., decrease neurotransmitter function) as a neuroadaptive change to make abusers become more difficult to experience pleasure feelings, and the anti-reward system including corticotrophin-releasing factor, norepinephrine and dynorphin are activated to produce negative or stress states. Consequently, depression and anxiety become the two most prevalent negative emotions in methamphetamine abusers (London et al., 2004). Moreover, research found the hypoactivation of the ventromedial prefrontal cortex/anterior cingulate cortex (vmPFC/rACC) and abnormal (i.e., no activation, hypoactivation, or hyperactivation) activation of amygdala and insula in individuals with SUDs (Salloum et al., 2007; Gilman and Hommer, 2008; O'Daly et al., 2012; Wilcox et al., 2016). These findings indicate the dysfunctional emotion regulation in people with SUDs, including dampened cognitive function for inhibiting intense affect, and abnormal emotion processing and reactivity.

Emotional reactivity has been commonly applied as one dimension for assessing the impairment of emotional regulation in people with SUDs (Blanchart et al., 2008; Smoski et al., 2011; Savvas et al., 2012). Previous studies that utilized visual emotional stimuli (i.e., pictures, facial expressions, videos) for eliciting emotional responses found inconsistent findings across the different types of drug users. Stimulant substance users (e.g., cocaine) demonstrated a more sensitive perception to the pleasant to unpleasant stimuli, and depressant users (e.g., heroin) tended to neutralize the rating on both unpleasant and pleasant stimuli (Kornreich et al., 2003; Aguilar de Arcos et al., 2005). These results suggest that there are different characteristics of emotional experience across drug types depending on the various clinical impact of drugs. In addition, research found the gender differences in emotion regulation between female and male with SUDs (Potenza et al., 2012). Compared to male cocaine dependents, female dependents showed an increased activation in amygdala and insula during a personalized stressful narrative, indicating that female with SUDs may be more vulnerable and experience more emotion regulation difficulties when facing stress. These findings suggest that gender should be taken into consideration in the assessment and therapy selection for treating people with SUDs.

The emotional reactivity can be measured using self-reports and psychophysiological measurements. The self-reported valence, arousal and proximity of emotions assess the cognitive aspect of emotion regulation (i.e., emotion recognition, perception). Valence refers to the nature of the emotional stimulus (i.e., positive vs. negative, or pleasurable vs. unpleasant); arousal refers to the intensity of the stimulus (i.e., low or high intensity); and proximity refers to the motivational reaction toward the emotional stimulus (i.e., approach or avoidance). Valence and arousal reflect the nature and intensity of motivational activation respectively (Bradley et al., 2001). The research found that individuals with SUDs reported high arousal (i.e., increase of anxiety, heart rate and salivary cortisol levels), negative valence (increased negative emotion), and avoidance motivation in the response to stressful stimuli, which often lead to drug craving and abuse (Sinha et al., 2000; Baker et al., 2004). Psychophysiological measurements mainly focus on assessing the implicit physiological responses to emotions with or without consciousness. Startle reflex is an effective measure that has been extensively used for probing emotional reactivity (Lang et al., 1990; Cook et al., 1992). As a response of the defensive emotional system, it can record the automatic defensive reaction (i.e., the amplitude of the eye link) in response to a loud white noise. The startle reflex is enhanced in response to negative emotional stimuli and is inhibited in response to positive emotional stimuli in normal people (Lang et al., 1998; Bradley and Lang, 2000).

Music as auditory stimuli can effectively modulate emotional experience. Music reward involves the brain regions that highly overlap with the regions of drug reward (Salimpoor et al., 2011; Zatorre and Salimpoor, 2013). A fMRI study (Menon and Levitin, 2005) found that music mediated the activity of mesolimbic reward circuitry including nucleus accumbens (NAcc), ventral tegmental area (VTA), hypothalamus and insula. Pleasant music significantly activated the interaction between the NAcc and hypothalamus, as well as insula and orbitofrontal cortex (Blum et al., 2010). The quality of musical elements (e.g., rhythm, harmony, timbre, musical structure, speed, power and melody) is associated with the valence and arousal of emotional experiences (Zhou, 1999). It is important to note the distinct characteristics of music as an emotional stimulus comparing to other kinds of emotional stimuli (e.g., picture, video, script). For example, people normally withdraw or avoid from the negative emotional stimuli, yet some listeners have an approach motivation toward sad music that match their affect state for improving mood (Garrido and Schubert, 2013).

Moreover, musical experience and training can change the plasticity of brain regions related to emotion regulation. Musicians and people with musical training exhibited a higher level of musical rewarding experience than people with no musical background (Mas-Herrero et al., 2013). A EEG study revealed that after 3 months of improvisational music therapy for depressed clients, significant increased absolute power was found at left fronto-temporal alpha and theta, indicating the impact of music intervention on reducing depression and anxiety symptoms (Fachner et al., 2013). Gender effect was found when use music for emotion regulation. The activation of medial prefrontal cortex (mPFC) decreases in males and increases in females during music listening (Carlson et al., 2015).

In the context of SUDs, animal study demonstrated that after repeatedly associated with methamphetamine, music as a contextual conditioned stimulus can significantly increase

extracellular dopamine levels in the nucleus accumbens and basolateral amygdala, as well as locomotor activity in rats (Polston et al., 2011), suggesting that music can effectively stimulate the dopamine circuitry and modulate associated memory of drug taking. An investigation of 143 substance abusers found that music was a common contextual stimulus during drug using. Seventy percent of the substance abusers listened to music for more than 1 h each day, and reported that music enhanced their emotional experience during drug taking (Dingle et al., 2015).

Despite the powerful impact of music on emotion regulation, the studies of emotional responses to music in people with SUDs are scarce. Given the different neurotoxicity of drugs and gender effect, the aim of this study is to explore the emotional perception and responses to music stimuli in females with methamphetamine use disorder (MUD). We hypothesize that female individuals with MUD will have a biased emotional perception and response to pleasant and unpleasant musical stimuli compared to normal controls.

# MATERIALS AND METHODS

## Participants

Thirty female participants with MUD were recruited from the Xin-He Drug Rehabilitation Center, and 30 healthy female participants as controls were recruited from a manufacture factory in Beijing, China. Two psychologists interviewed all participants for gathering demographic information and screening, and then participants filled out the State-Trait Anxiety Inventory, Beck Depression, and Barcelona Music Reward Questionnaire for assessing anxiety, depression and musical reward sensitivity.

For the MUD participants, the inclusion criteria are: (1) aged 18–55 years; (2) a history of using methamphetamine and fulfilled the diagnosis of stimulant use disorder in the Chinese version of DSM-5 (pp. 232–238, American Psychiatric Association, 2014). Stimulant use disorder refers to the clinically significant impairment or distress caused by the use of amphetamine-type substance, cocaine, or other kinds of stimulant, such as amphetamine, dextroamphetamine, methamphetamine, cocaine and methylphenidate.

Exclusion criteria: (1) a history of brain damage or a coma over 30 min; (2) a history of using other kind of drugs (e.g., heroin, cocaine); (3) illiteracy; (4) a history or a family history of mental illness; and (5) hearing problems. All participants had no musical training history. The study was carried out in accordance with the recommendation of the Declaration of Helsinki. The protocol was approved by the Ethics Committee of Institute of Psychology, CAS (H17001). All subjects gave a written informed consent in accordance with the Declaration of Helsinki.

## Musical Excerpts

Three musical excerpts presenting three emotions (i.e., happy, fearful, peaceful) were adapted from a previous study (Vieillard et al., 2008). Five excerpts of each emotion were selected out of a pool of 42 excerpts based on the assessment of 30 music majored colleague students. They evaluated the valence (0 = pleasant, 9 = unpleasant) and arousal (0 = relaxing, 9 = stimulating) of each musical excerpt using a Likert scale. The happy excerpts were selected based on the high arousal and valence, the fearful excerpts were selected based on the high arousal and low valence, and the peaceful excerpts were selected based on the low arousal and high valence. Then the top five excerpts of each emotion were selected for the study (see Supplementary Table S1 for the list of the music excerpts).

Fifteen chosen music excerpts were further evaluated and validated by 46 college students with no musical training on the dimensions of valence, arousal and proximity (0 = approach, 9 = withdraw). In terms of valence, happy excerpts was higher than peaceful excerpts ($t = 5.6$, $p < 0.01$) and fearful excerpts ($t = 16.95$, $p < 0.01$), and peaceful excerpts was higher than fearful excerpts ($t = 12.25$, $p < 0.01$); in terms of arousal, peaceful excerpts was lower than happy excerpts ($t = -7.59$, $p < 0.01$) and fearful excerpts ($t = -5.45$, $p < 0.01$), and there was no significant difference between happy and fearful excerpts; in terms of proximity, fearful excerpts was lower than peaceful excerpts ($t = -16.69$, $p < 0.01$) and happy excerpts ($t = -14.02$, $p < 0.01$), and no significant difference was found between happy and peaceful excerpts. The results indicated that the selected music excerpts elicited differentiated emotions corresponding with their valence, arousal, and proximity. All music excerpts were piano melodic music produced by a digital synthesizer with a duration from 10 s to 14 s. Each excerpt was normalized to equate loudness using the normalization function of the *Audition 3* software.

## Measurements

### Startle Reflex

White noise of 100 dB, 50 ms burst was presented over Sony MDR-XB500AP head-phones to elicit startle responses. Five white noise probes were presented during the first minute with a randomized interval before the presentation of music stimuli. Then three types of music excerpts were presented with a 3 s interval between each excerpt, and each type of music was presented with three randomly placed startle probes (**Figure 1**).

For startle data recording, the Eye-blink Electromyographic (EMG) data were collected from the orbicularis oculi using two mini-electrodes placed below the left eye (Larson et al., 2005). After each white noise, EMG activity (μv) was automatically recorded. EMG signals pass through bandpass filtered at 10 and 500 Hz and were amplified by 1000. The sampling rate was set at 1000 Hz. The maximum amplitude of each response between 20 ms and 120 ms after startle probe onset was considered as valid data and included for analysis (Balaban et al., 1986). To reduce individual variability in the raw startle reflex data, the raw data were standardized within in each participant, In the light of a previous study (Roy et al., 2009), the standardized score was expressed as T scores (50 + 10 Hz), which led to a mean of 50 and a standard deviation of 10 for each participant.

### Self-Reported Emotional Responses

Self-reported emotional responses to music excerpt were measured using a Likert scale scored from 0 to 9. After each music

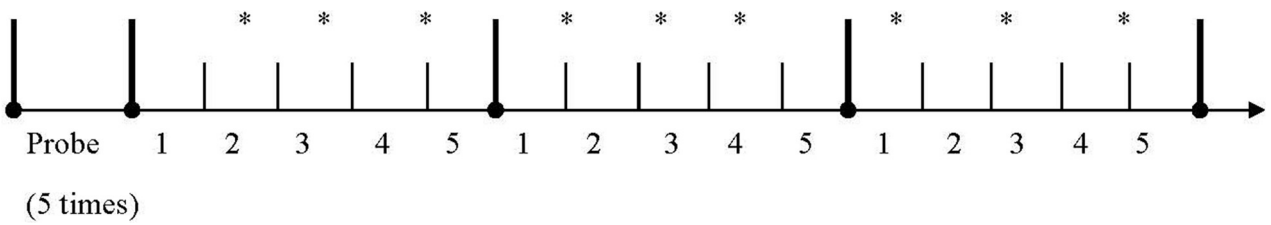


**FIGURE 1 |** Distribution of probes during the presentation of three types of music excerpts. *Note*: *White noise probe.

excerpt, the participants assess it on the dimension of valence (0: unpleasant, 9: pleasant), arousal (0: relaxing, 9: stimulating), and proximity (0: withdraw, 9: approach).

### Anxiety

Anxiety was measured using the Chinese version of State-trait Anxiety Inventory. It consists of 20 items and ranged from 20 to 80. Higher scores indicate higher level of anxiety.

### Depression

Depression was measured using the Chinese version of Beck Depression Inventory. It consists of 13 items and ranged from 0 to 63 (4–7: mild depression, 8–15: moderated depression, 16 or higher: severe depression). Higher scores indicate higher level of depression.

### Musical Reward Sensitivity

Barcelona Musical Reward Questionnaire was developed by Mas-Herrero and his colleagues (Mas-Herrero et al., 2013) for assessing music reward sensitivity. It evaluates the sensitivity to music from the dimensions of emotional evocation, sensory-motor, mood regulation, musical seeking and social reward. It consists of 20 items and scored from 1 (completely disagree) to 5 (completely agree). A higher score indicates a higher level of musical reward sensitivity (0–40: low, 40–60: standard, 60 or higher: high).

## Procedure

The researcher helped the participants to put on headphones and affix the electrodes for startle reflex. The participants sat comfortably in a quiet room and watched natural scenes (i.e., the sea life aquarium) on a computer screen for 1 min to relax. Before the presentation of the music stimuli, five white noise probes were played randomly during 1 min. Then, three types emotional music excerpts were presented in a counterbalanced order across subjects. The startle reflex responses were recorded during the listening process. After each music excerpt, the participants rated the valence, arousal and proximity of the excerpt.

## Data Analysis

Data analysis was performed using the Statistical Product and Service Solutions (SPSS) 17.0. The comparison of demographic information, anxiety, depression, music reward, self-reported ratings and startle reflex between two groups were analyzed using independent sample *t*-test.

# RESULTS

The two groups were matched in age, anxiety, depression and musical reward sensitivity (**Table 1**). The control group had more years of education than the methamphetamine (MA) group.

## Startle Reflex

Compared to the normal control, the MA group showed a lower level of startle response to fearful music (MA: 49.08, Control: 53.66, $t = 3.7$, $p < 0.01$). There was no significant difference in the response to peaceful and happy music between the two groups, although the startle reflex

**TABLE 1 |** The comparison between the two groups in demographic information and clinical characteristics.

| | Methamphetamine group ($n$ = 30) | Control group ($n$ = 30) | Difference $p$ |
|---|---|---|---|
| **Outcome** | **M (*SD*)** | **M (*SD*)** | |
| Age (year) | 30.97 (7.41) | 29.58 (7.17) | 0.09 |
| Education (year) | 9.21 (3.12) | 12.30 (2.14) | 0.01** |
| BMRQ | 76.21 (9.08) | 75.83 (7.31) | 0.07 |
| BDI | 12.63 (9.69) | 12.35 (9.35) | 0.08 |
| TSAI (state) | 37 (10.38) | 36.67 (9.56) | 0.07 |
| TSAI (trait) | 39.64 (7.93) | 40.21 (8.22) | 0.06 |
| Abstinent period (month) | 8.68 (3.64) | - | - |
| Total time of drug use (month) | 35.23 (22.41) | - | - |
| Total drug use amount in a year (gram) | 82.35 (124.53) | - | - |

*Note. BMRQ, Barcelona Musical Reward Questionnaire; BDI, Beck Depression Inventory; STAI, State and Trait Anxiety Inventory; **$p \leq 0.01$.*

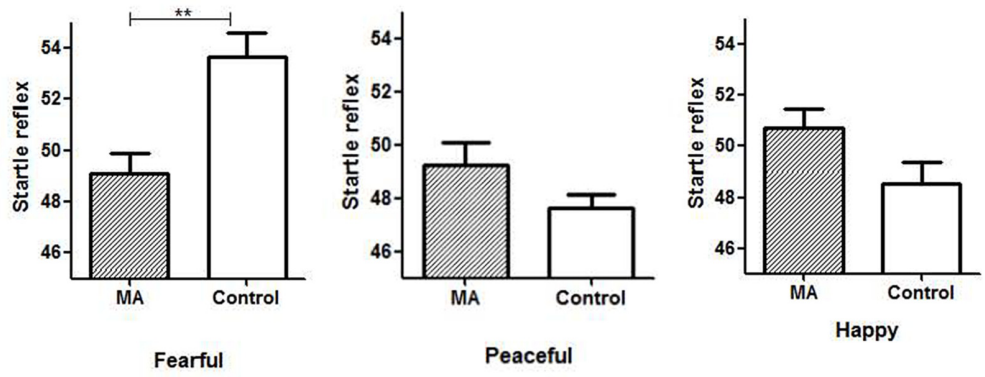


**FIGURE 2 |** Startle reflex amplitudes in response to three emotional music excerpts in the two groups. *Note*: MA, methamphetamine group; Control, healthy control group; $^{**}p \leq 0.01$.

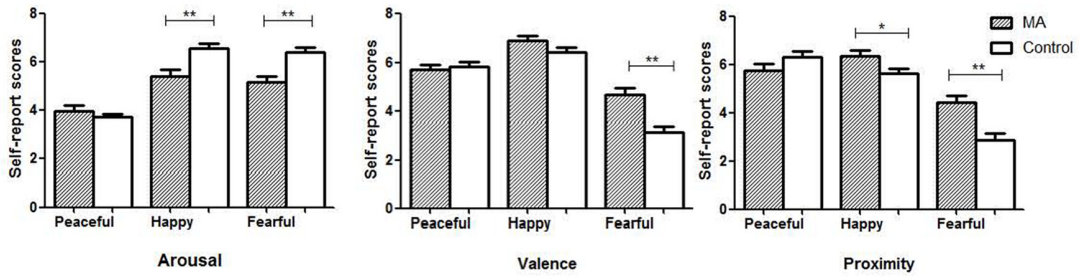


**FIGURE 3 |** The self-reported emotions of arousal, valence and proximity in the two groups. *Note*: MA, methamphetamine group; Control, healthy control group; $^{*}p \leq 0.05$, $^{**}p \leq 0.01$.

amplitudes to both music stimuli in the MA group were higher (**Figure 2**).

## Self-Reported Emotions

Compared to the control group, the MA group showed a lower level of arousal in response to happy music ($t = 3.8$, $p < 0.01$) and fearful music ($t = 4.1$, $p < 0.01$), a higher valence (i.e., more pleasant) in response to fearful music ($t = 4.4$, $p < 0.01$), and a higher proximity (i.e., approach motive) in response to happy ($t = 2.2$, $p = 0.03$) and fearful music ($t = 3.8$, $p < 0.01$; **Figure 3**).

# DISCUSSION

The female participants with MUD showed an inhibited startle response to negative (i.e., fearful) music, and a tendency of potentiated startle response to positive music (i.e., happy, peaceful). These reactivities that opposite to the reactions in normal people may indicate the impaired emotional processing and emotional regulation (Lang et al., 1998; Bradley and Lang, 2000). Moreover, the increased self-reported valence to fearful music, and decreased self-reported arousal of MUD participants to both positive and negative music accords with their dysfunctional startle reflex response, which reflects the dampened emotional perception on the emotional valence and arousal. These findings are in line with previous studies (Carrico et al., 2013; May et al., 2013) that people with SUDs show attenuated response to emotional stimuli.

The participants with MUD showed a higher level of valence and lower level of arousal, as well as a decreased startle response to fearful music than the normal controls suggesting their biased emotional perception and psychophysiological reactivity to music. Tempo and harmony influence the arousal and valence of music emotional experience respectively (Gomez and Danuser, 2007; Hodges, 2010). The fearful music excerpts used in the study feature fast tempo and dissonant melodies, which may create intense and stimulating feelings. The MUD participants also showed a higher level of proximity to both positive and negative music with high arousal. Given the chronic drug use impairs the reward system, individuals with dampened reward function may seek for the strong stimulant feature of high arousal music to acquire pleasurable feelings. Huron (2011) pointed out that the brain can distinguish "fake" negative emotions in music from real threat in life, therefore it is "safe" for people to enjoy music that conveys negative emotions. Drug abusers tend to use drugs to decrease or avoid negative feelings (Otto et al., 2004). To be open and experience "negative" music and may help them to face their negative feelings and deal with their problems instead of taking drugs. For music therapy, music with high arousal may be used to

attract the attention and increase the motivation of patients with SUDs.

It is noteworthy that there was no significant difference in the cognitive responses including valence, arousal, and proximity to peaceful music between the two groups. Given depression and anxiety are the two most prominent negative emotions in methamphetamine users (London et al., 2004), this result may suggest the suitability of using peaceful music for relaxation in treating patients with MUD as they may respond well to peaceful music. In addition to music listening, active musical activities such as improvisation can help people to explore and express various feelings, facilitate meaningful communicate, gain public recognition and bring a sense of achievement (Soshensky, 2001; Baker et al., 2007; Silverman, 2009).

The study has several limitations. Only female subjects with MUD participated in this study, there is a lack of the comparison between two genders. The educations years in participants with MUD are less than the healthy controls. However, the music listening task did not require a high level of cognitive function, therefore we suppose this difference did not affect the task. The future study will add male participants, improve the comparability of the two groups, and supply more psychophysiological measurements, such as ERP, EEG, skin conductance.

In summary, the study utilized emotional music stimuli to elicit emotional responses of female individuals with MUD, and assessed them with cognitive and psychophysiological measurements. The results found that the females with MUD showed inhibited psychophysiological and cognitive emotional responses to fearful music, and a high proximity to musical stimuli with high arousal regardless of its valence. These results have important implications for promoting the effectiveness of assessment and therapy for female MUD patients with impaired emotion regulation.

## DATASETS ARE AVAILABLE ON REQUEST

The raw data supporting the conclusions of this manuscript will be made available by the authors, without undue reservation, to any qualified researcher.

## AUTHOR CONTRIBUTIONS

X-JC designed and implemented the experiment, analyzed the data and drafted the manuscript. C-GW and WL conducted the interview for the participants. MG helped with the data collection process. D-MW and Y-HL guided the study design and directed the experiment implementation.

## FUNDING

This work was supported by the National Key Research and Development Program of China (2017YFC1310405, 2016YFC0800907), the National Natural Science Foundation of China (U1736124, 31371035), and the CAS Key Lab of Mental Health (Y7CX424007).

## SUPPLEMENTARY MATERIAL

The Supplementary Material for this article can be found online at: https://www.frontiersin.org/articles/10.3389/fnhum.2018.00230/full#supplementary-material

## REFERENCES

Aguilar de Arcos, F., Verdejo-García, A., Peralta-Ramírez, M. I., Sánchez-Barrera, M., and Pérez-García, M. (2005). Experience of emotions in substance abusers exposed to images containing neutral, positive, and negative affective stimuli. *Drug Alcohol Depend.* 78, 159–167. doi: 10.1016/j.drugalcdep.2004.10.010

American Psychiatric Association. (2013). *Diagnostic and Statistical Manual of Mental Disorders.* 5th Edn. Arlington, VA: American Psychiatric Publishing.

American Psychiatric Association. (2014). *Diagnostic and Statistical Manual of Mental Disorders.* 5th Edn. Beijing: Peking University Press.

Baker, F. A., Gleadhill, L., and Dingle, G. A. (2007). Music therapy and emotional exploration: exposing substance abuse clients to the experiences of non-drug-induced emotions. *Arts Psychother.* 34, 321–330. doi: 10.1016/j.aip.2007.04.005

Baker, T. B., Piper, M. E., McCarthy, D. E., Majeskie, M. R., and Fiore, M. C. (2004). Addiction motivation reformulated: an affective processing model of negative reinforcement. *Psychol. Rev.* 111, 33–51. doi: 10.1037/0033-295x.111.1.33

Balaban, M. T., Losito, B. D. G., Simons, R. F., and Graham, F. K. (1986). Off-line latency and amplitude scoring of the human reflex eye blink with Fortran IV. *Psychophysiology* 23, 612–621.

Blanchart, K., Roose, A., Claes, L., and Bijttebier, P. (2008). "Emotional reactivity and effortful control as predictors of substance use and antisocial behavior in adolescence" in *Paper presented at the 14th European Conference on Personality Tartu* (Estonia), 283–287.

Blum, K., Chen, T. J., Chen, A. L., Madigan, M., Downs, B. W., Waite, R. L., et al. (2010). Do dopaminergic gene polymorphisms affect mesolimbic reward activation of music listening response? Therapeutic impact on Reward Deficiency Syndrome (RDS). *Med. Hypotheses* 74, 513–520. doi: 10.1016/j.mehy.2009.10.008

Bradley, M. M., Codispoti, M., Cuthbert, B. N., and Lang, P. J. (2001). Emotion and motivation I: defensive and appetitive reactions in picture processing. *Emotion* 1, 276–298. doi: 10.1037/1528-3542.1.3.276

Bradley, M. M., and Lang, P. J. (2000). Affective reactions to acoustic stimuli. *Psychophysiology* 37, 204–215. doi: 10.1111/1469-8986.3720204

Carlson, E., Saarikallio, S., Toiviainen, P., Bogert, B., Kliuchko, M., and Brattico, E. (2015). Maladaptive and adaptive emotion regulation through music: a behavioral and neuroimaging study of males and females. *Front. Hum. Neurosci.* 9:466. doi: 10.3389/fnhum.2015.00466

Carrico, A. W., Woods, W. J., Siever, M. D., Discepola, M. V., Dilworth, S. E., Neilands, T. B., et al. (2013). Positive affect and processes of recovery among treatment-seeking methamphetamine users. *Drug Alcohol Depend.* 132, 624–629. doi: 10.1016/j.drugalcdep.2013.04.018

Cook, E. W. III., Davis, T. L., Hawk, L. W., Spence, E. L., and Gautier, C. H. (1992). Fearfulness and startle potentiation during aversive visual stimuli. *Psychophysiology* 29, 633–645. doi: 10.1111/j.1469-8986.1992.tb02038.x

Dingle, G. A., Kelly, P. J., Flynn, L. M., and Baker, F. A. (2015). The influence of music on emotions and cravings in clients in addiction treatment: a study of two clinical samples. *Arts Psychother.* 45, 18–25. doi: 10.1016/j.aip.2015.05.005

Fachner, J., Gold, C., and Erkkilä, J. (2013). Music therapy modulates fronto-temporal activity in rest-eeg in depressed clients. *Brain Topogr.* 26, 338–354. doi: 10.1007/s10548-012-0254-x

Garrido, S., and Schubert, E. (2013). Moody melodies: do they cheer us up? a study of the effect of sad music on mood. *Psychol. Music* 43, 244–260. doi: 10.1177/0305735613501938

Gilman, J. M., and Hommer, D. W. (2008). Modulation of brain response to emotional images by alcohol cues in alcohol-dependent patients. *Addict. Biol.* 13, 423–434. doi: 10.1111/j.1369-1600.2008.00111.x

Gomez, P., and Danuser, B. (2007). Relationships between musical structure and psychophysiological measures of emotion. *Emotion* 7, 377–387. doi: 10.1037/1528-3542.7.2.377

Hodges, D. A. (2010). "Psychophysiological measures," in *Music and Emotion: Theory and Research*, eds P. N. Juslinand and J. Sloboda (New York, NY: Oxford University Press), 279–312.

Huron, D. (2011). Why is sad music pleasurable? A possible role for prolactin. *Music. Sci.* 15, 146–158. doi: 10.1177/102986491101500202

Lang, P. J., Bradley, M. M., and Cuthbert, B. N. (1990). Emotion, attention, and the startle reflex. *Psychol. Rev.* 97, 377–395. doi: 10.1037/0033-295x.97.3.377

Koob, G. F., and Moal, M. L. (2005). Plasticity of reward neurocircuitry and the 'dark side' of drug addiction. *Nat. Neurosci.* 8, 1442–1444. doi: 10.1038/nn1105-1442

Kornreich, C., Foisy, M. L., Philippot, P., Dan, B., Tecco, J., Noël, X., et al. (2003). Impaired emotional facial expression recognition in alcoholics, opiate dependence subjects, methadone maintained subjects and mixed alcohol-opiate antecedents subjects compared with normal controls. *Psychiatry Res.* 119, 251–260. doi: 10.1016/S0165-1781(03)00130-6

Lang, P. J., Bradley, M. M., and Cuthbert, B. N. (1998). Emotion, motivation, and anxiety: brain mechanisms and psychophysiology. *Biol. Psychiatry* 44, 1248–1263. doi: 10.1016/s0006-3223(98)00275-3

Larson, C. L., Ruffalo, D., Nietert, J. Y., and Davidson, R. J. (2005). Stability of emotion-modulated startle during short and long picture presentation. *Psychophysiology* 42, 604–610. doi: 10.1111/j.1469-8986.2005.00345.x

London, E. D., Kohno, M., Morales, A. M., and Ballard, M. E. (2015). Chronic methamphetamine abuse and corticostriatal deficits revealed by neuroimaging. *Brain Res.* 1628, 174–185. doi: 10.1016/j.brainres.2014.10.044

London, E. D., Simon, S. L., Berman, S. M., Mandelkern, M. A., Lichtman, A. M., Bramen, J., et al. (2004). Mood disturbances and regional cerebral metabolic abnormalities in recently abstinent methamphetamine abusers. *Arch. Gen. Psychiatry* 61, 73–84. doi: 10.1001/archpsyc.61.1.73

Mas-Herrero, E., Marco-Pallares, J., Lorenzo-Seva, U., Zatorre, R., and Rodriguez-Fornells, A. (2013). Individual differences in music reward experiences. *Music Percept.* 31, 118–138. doi: 10.1525/mp.2013.31.2.118

May, A. C., Stewart, J. L., Migliorini, R., Tapert, S. F., and Paulus, M. P. (2013). Methamphetamine dependent individuals show attenuated brain response to pleasant interoceptive stimuli. *Drug Alcohol Depend.* 131, 238–246. doi: 10.1016/j.drugalcdep.2013.05.029

Menon, V., and Levitin, D. (2005). The rewards of music listening: response and physiological connectivity of the mesolimbic system. *Neuroimage* 28, 175–184. doi: 10.1016/j.neuroimage.2005.05.053

O'Daly, O. G., Trick, L., Scaife, J., Marshall, J., Ball, D., Phillips, M. L., et al. (2012). Withdrawal-associated increases and decreases in functional neural connectivity associated with altered emotional regulation in alcoholism. *Neuropsychopharmacology* 37, 2267–2276. doi: 10.1038/npp.2012.77

Otto, M. W., Safren, S. A., and Pollack, M. H. (2004). Internal cue exposure and the treatment of substance use disorders: lessons from the treatment of panic disorder. *J. Anxiety Disord.* 18, 69–87. doi: 10.1016/j.janxdis.2003.07.007

Polston, J. E., Rubbinaccio, H. Y., Morra, J. T., Sell, E. M., and Glick, S. D. (2011). Music and methamphetamine: conditioned cue-induced increases in locomotor activity and dopamine release in rats. *Pharmacol. Biochem. Behav.* 98, 54–61. doi: 10.1016/j.pbb.2010.11.024

Potenza, M. N., Hong, K. I., Lacadie, C. M., Fulbright, R. K., Tuit, K. L., and Sinha, R. (2012). Neural correlates of stress-induced and cue-induced drug craving: influences of sex and cocaine dependence. *Am. J. Psychiatry* 169, 406–414. doi: 10.1176/appi.ajp.2011.11020289

Roy, M., Mailhot, J. P., Gosselin, N., Paquette, S., and Peretz, I. (2009). Modulation of the startle reflex by pleasant and unpleasant music. *Int. J. Psychophysiol.* 71, 37–42. doi: 10.1016/j.ijpsycho.2008.07.010

Salimpoor, V. N., Benovoy, M., Larcher, K., Dagher, A., and Zatorre, R. J. (2011). Anatomically distinct dopamine release during anticipation and experience of peak emotion to music. *Nat. Neurosci.* 14, 257–262. doi: 10.1038/nn.2726

Salloum, J. B., Ramchandani, V. A., Bodurka, J., Rawlings, R., Momenan, R., George, D., et al. (2007). Blunted rostral anterior cingulate response during a simplified decoding task of negative emotional facial expressions in alcoholic patients. *Alcohol. Clin. Exp. Res.* 31, 1490–1504. doi: 10.1111/j.1530-0277.2007.00447.x

Savvas, S. M., Somogyi, A. A., and White, J. M. (2012). The effect of methadone on emotional reactivity. *Addiction* 107, 388–392. doi: 10.1111/j.1360-0443.2011.03634.x

Silverman, M. J. (2009). A descriptive analysis of music therapists working with consumers in substance abuse rehabilitation: current clinical practice to guide future research. *Arts Psychother.* 36, 123–130. doi: 10.1016/j.aip.2008.10.005

Sinha, R., Fuse, T., Aubin, L. R., and O'Malley, S. S. (2000). Psychological stress, drug-related cues and cocaine craving. *Psychopharmacology* 152, 140–148. doi: 10.1007/s002130000499

Smoski, M. J., Salsman, N., Wang, L., Smith, V., Lynch, T. R., Dager, S. R., et al. (2011). Functional imaging of emotion reactivity in opiate-dependent borderline personality disorder. *Personal. Disord.* 2, 230–241. doi: 10.1037/a0022228

Soshensky, R. (2001). Music therapy and addiction. *Music Ther. Perspect.* 19, 45–52. doi: 10.1093/mtp/19.1.45

Vieillard, S., Peretz, I., Cosselin, N., Khalfa, S., Gagnon, L., and Bouchard, B. (2008). Happy, sad, scary and peaceful musical excerpts for research on emotions. *Cogn. Emot.* 22, 720–752. doi: 10.1080/02699930701503567

Wilcox, C. E., Pommy, J. M., and Adinoff, B. (2016). Neural circuitry of impaired emotion regulation in substance use disorders. *Am. J. Psychiatry* 173, 344–361. doi: 10.1176/appi.ajp.2015.15060710

Zatorre, R. J., and Salimpoor, V. N. (2013). From perception to pleasure: music and its neural substrates. *Proc. Natl. Acad. Sci. U S A* 110, 10430–10437. doi: 10.1073/pnas.1301228110

Zhou, H. (1999). Homogeneous joint perception—the basic link between music sound and its performance object. *Journal of Central Conservatory of Music* 2, 59–64.

**Conflict of Interest Statement**: The authors declare that the research was conducted in the absence of any commercial or financial relationships that could be construed as a potential conflict of interest.

frontiers in Human Neuroscience

GENERAL COMMENTARY
published: 25 June 2018
doi: 10.3389/fnhum.2018.00255

# Commentary: Effectiveness of theta burst vs. high-frequency repetitive transcranial magnetic stimulation in patients with depression (THREE-D): a randomized non-inferiority trial

*Cuilan Han, Zhongming Chen* and Lin Liu**

*Department of Psychiatry, Ningbo Kangning Hospital, Ningbo, China*

**Keywords: brain stimulation, depression, treatment, iTBS, TMS, tDCS**

**A commentary on**

**Effectiveness of theta burst vs. high-frequency repetitive transcranial magnetic stimulation in patients with depression (THREE-D): a randomized non-inferiority trial**
*by Blumberger, D. M., Vila-Rodriguez, F., Thorpe, K. E., Feffer, K., Noda, Y., Giacoble, P., et al. (2018). Lancet 391, 1683–1692. doi: 10.1016/S0140-6736(18)30295-2*

OPEN ACCESS

***Edited by:***
*Xiaochu Zhang,*
*University of Science and Technology of China, China*

***Reviewed by:***
*Yingying Tang,*
*Shanghai Mental Health Center (SMHC), China*
*Ranji Cui,*
*Second Affiliated Hospital of Jilin University, China*

****Correspondence:***
*Zhongming Chen*
*hancuilannb@163.com*
*Lin Liu*
*104797809@qq.com*

***Received:*** *30 April 2018*
***Accepted:*** *04 June 2018*
***Published:*** *25 June 2018*

***Citation:***
*Han C, Chen Z and Liu L (2018) Commentary: Effectiveness of theta burst vs. high-frequency repetitive transcranial magnetic stimulation in patients with depression (THREE-D): a randomized non-inferiority trial. Front. Hum. Neurosci. 12:255. doi: 10.3389/fnhum.2018.00255*

Transcranial magnetic stimulation (TMS) has been widely adopted for clinical treatments for depression and many other psychiatric disorders (Brunoni et al., 2017). Previous clinical trials demonstrated numerous benefits of TMS therapy over pharmacological treatments, in terms of minor side effects, well tolerated for most patients, and the comparable effectiveness (Fitzgerald and Daskalakis, 2012). However, in clinical practices, a half-hour TMS therapy could be slow and cost weeks to be fully effective; the patients need to 5 days per week during the periods, which is time consuming and much less convenient than taking pills. Should a faster and more concentrated TMS protocol be effective for depression or other psychiatric disorders, it might reduce the treatment time length during the whole treatment period (Fitzgerald et al., 2018). A recent study by Blumberger et al. demonstrated the possibility to perform theta burst stimulation protocol on depression patients and achieve similar antidepressant effects than classical high frequency ones (Blumberger et al., 2018).

The pulse concentration of TMS protocol determines the amount of neural excitation generated in the targeted cortex (Walsh and Cowey, 2000). It is conceivable that some non-responders could turn into responders with increased amount of pulses, and/or more adverse effects as well. The question remains to which extent should TMS pulses be increased, to reach maximum effects. In previous efforts treating depression patients, high frequency stimulation protocol ranging from 10 to 20 Hz for 20 to 30 min (2000–3000 pulses) were commonly adopted over the left dorsal lateral prefrontal cortex, based on the hypothesis that high frequency stimulation could induce "potentiation" like effect on neural transmission and enhance blood flow into the region.

Since 2005, theta burst stimulation (TBS) has been developed as a novel approach in controlling neural activity, with proved efficacy on motor evoked potentials (MEPs) (Huang et al., 2005). The intermittent theta burst stimulation (iTBS) induces potentiation at the given cortical region, while continuous theta burst stimulation (cTBS) suppresses the local brain activity (Martin et al., 2006; Ishikawa et al., 2007). iTBS consists of 3 pulses at 50 Hz and repeated at 5 Hz, 2 s on and 8 s off, leading to 600 pulses at around 3 min. Surprisingly, this short protocol generates similar extent in the excitatory effects on cortex, measured both electrophysiological responses and functional

imaging (Huang et al., 2005). Limited studies argued for the use of iTBS in depression treatments (Duprat et al., 2017; Li et al., 2018), including treatment resistant depression.

The questions remain if the short protocol will be as effective when adopted as treatment procedures, or if the procedure is well tolerable in daily application. Blumberger et al. set out to initiate the "THREE-D" trial to compare the effectiveness between iTBS and 10 Hz rTMS in clinical treatments of depression in more than 400 patients (Blumberger et al., 2018). The primary outcome, 17-item Hamilton Rating Scale for Depression, demonstrated clear changes in both groups of patients following 4 weeks of 5 days magnetic stimulation treatment. Notably, the two groups did not show any inter-group differences, suggesting that iTBS is non-inferior to the classical rTMS procedures. While on the other hand, iTBS is much faster and practicable to treat more patients in a day.

In terms of adverse effects, the two groups were similar–more than half subjects reported headache, the most common adverse effects following TMS therapy. The occurrence rates for nausea, dizziness, fatigue, etc. were comparable between the two groups as well. The study also reported more "painful" experience in iTBS group, along with a higher self-reported pain score, but not with more dropout rate in these patients (Blumberger et al., 2018). This suggested that the iTBS is tolerable in daily session treatment and does not accompany more adverse effects. However, in future practices the painful feeling still worth more evaluation for other types of patients.

Cortical plasticity studies demonstrated comparable effects between iTBS and 10 Hz rTMS, even with 600 pulses or 2000–3000 pulses, respectively. Indeed, the treatment effects were similar between the two groups as well. Doubling the dosage of iTBS is not recommended, since this might even lead to inhibitory effects. On the other hand, most previous iTBS studies were performed at the intensity of 80% active motor threshold (AMT), which is around 50–60% of resting motor threshold (RMT). In current study, Blumberger et al. employed 120% of RMT at prefrontal cortex, which could boost the excitatory effects, yet the exact extent still requires further physiological evidences.

In conclusion, the demonstration of new protocol effectiveness, in addition to the classical standard, has largely expanded the possibility to treat more patients per TMS machine per day, and might facilitate the access of patients to treatments. It is also important to consider if the individual variability in treatment effect is due to the different inter-individual plasticity induction responses (Lopez-Alonso et al., 2014). In future, other TBS based treatment protocols would prove their usefulness in clinical treatments for different psychiatric diseases, such as schizophrenia or insomnia (Brunelin et al., 2011; Mensen et al., 2014).

## AUTHOR CONTRIBUTIONS

All authors designed the study together. CH, ZC, and LL wrote the paper together and approved the final version.

## FUNDING

The authors were supported by the hospital.

## REFERENCES

Blumberger, D. M., Vila-Rodriguez, F., Thorpe, K. E., Feffer, K., Noda, Y., Giacoble, P., et al. (2018). Effectiveness of theta burst versus high-frequency repetitive transcranial magnetic stimulation in patients with depression (THREE-D): a randomised non-inferiority trial. *Lancet* 391, 1683–1692. doi: 10.1016/S0140-6736(18)30295-2

Brunelin, J., Szekely, D., Costes, N., Mondino, M., Bougerol, T., Saoud, M., et al. (2011). Theta burst stimulation in the negative symptoms of schizophrenia and striatal dopamine release. An iTBS-[11C]raclopride PET case study. *Schizophr. Res.* 131, 264–265. doi: 10.1016/j.schres.2011.05.019

Brunoni, A. R., Chaimani, A., Moffa, A. H., Razza, L. B., Gattaz, W. F., Daskalakis, Z. J., et al. (2017). Repetitive transcranial magnetic stimulation for the acute treatment of major depressive episodes: a systematic review with network meta-analysis. *JAMA Psychiatry* 74, 143–152. doi: 10.1001/jamapsychiatry.2016.3644

Duprat, R., Wu, G. R., De Raedt, R., and Baeken, C. (2017). Accelerated iTBS treatment in depressed patients differentially modulates reward system activity based on anhedonia. *World J. Biol. Psychiatry* 9, 1–12. doi: 10.1080/15622975.2017.1355472

Fitzgerald, P. B., and Daskalakis, Z. J. (2012). A practical guide to the use of repetitive transcranial magnetic stimulation in the treatment of depression. *Brain Stimul.* 5, 287–296. doi: 10.1016/j.brs.2011.03.006

Fitzgerald, P. B., Hoy, K. E., Elliot, D., Susan Mcqueen, R. N., Wambeek, L. E., and Daskalakis, Z. J. (2018). Accelerated repetitive transcranial magnetic stimulation in the treatment of depression. *Neuropsychopharmacology*. 43, 1565–1572. doi: 10.1038/s41386-018-0009-9

Huang, Y. Z., Edwards, M. J., Rounis, E., Bhatia, K. P., and Rothwell, J. C. (2005). Theta burst stimulation of the human motor cortex. *Neuron* 45, 201–206. doi: 10.1016/j.neuron.2004.12.033

Ishikawa, S., Matsunaga, K., Nakanishi, R., Kawahira, K., Murayama, N., Tsuji, S., et al. (2007). Effect of theta burst stimulation over the human sensorimotor cortex on motor and somatosensory evoked potentials. *Clin. Neurophysiol.* 118, 1033–1043. doi: 10.1016/j.clinph.2007.02.003

Li, C. T., Chen, M. H., Juan, C. H., Liu, R. S., Lin, W. C., Bai, Y. M., et al. (2018). Effects of prefrontal theta-burst stimulation on brain function in treatment-resistant depression: a randomized sham-controlled neuroimaging study. *Brain Stimul*. doi: 10.1016/j.brs.2018.04.014. [Epub ahead of print].

López-Alonso, V., Cheeran, B., Río-Rodriguez, D., and Fernández-Del-Olmo, M. (2014). Inter-individual variability in response to non-invasive brain stimulation paradigms. *Brain Stimul.* 7, 372–380. doi: 10.1016/j.brs.2014.02.004

Martin, P. G., Gandevia, S. C., and Taylor, J. L. (2006). Theta burst stimulation does not reliably depress all regions of the human motor cortex. *Clin. Neurophysiol.* 117, 2684–2690. doi: 10.1016/j.clinph.2006.08.008

Mensen, A., Gorban, C., Niklaus, M., Kuske, E., and Khatami, R. (2014). The effects of theta-burst stimulation on sleep and vigilance in humans. *Front. Hum. Neurosci.* 8:420. doi: 10.3389/fnhum.2014.00420

Walsh, V., and Cowey, A. (2000). Transcranial magnetic stimulation and cognitive neuroscience. *Nat. Rev. Neurosci.* 1, 73–79. doi: 10.1038/35036239

**Conflict of Interest Statement:** The authors declare that the research was conducted in the absence of any commercial or financial relationships that could be construed as a potential conflict of interest.

frontiers in Human Neuroscience

ORIGINAL RESEARCH
published: 26 June 2018
doi: 10.3389/fnhum.2018.00257

# The Diagnosis of Autism Spectrum Disorder Based on the Random Neural Network Cluster

*Xia-an Bi *, Yingchao Liu, Qin Jiang, Qing Shu, Qi Sun and Jianhua Dai*

*College of Information Science and Engineering, Hunan Normal University, Changsha, China*

As the autism spectrum disorder (ASD) is highly heritable, pervasive and prevalent, the clinical diagnosis of ASD is vital. In the existing literature, a single neural network (NN) is generally used to classify ASD patients from typical controls (TC) based on functional MRI data and the accuracy is not very high. Thus, the new method named as the random NN cluster, which consists of multiple NNs was proposed to classify ASD patients and TC in this article. Fifty ASD patients and 42 TC were selected from autism brain imaging data exchange (ABIDE) database. First, five different NNs were applied to build five types of random NN clusters. Second, the accuracies of the five types of random NN clusters were compared to select the highest one. The random Elman NN cluster had the highest accuracy, thus Elman NN was selected as the best base classifier. Then, we used the significant features between ASD patients and TC to find out abnormal brain regions which include the supplementary motor area, the median cingulate and paracingulate gyri, the fusiform gyrus (FG) and the insula (INS). The proposed method provides a new perspective to improve classification performance and it is meaningful for the diagnosis of ASD.

**Keywords: fMRI, random elman neural network cluster, autism spectrum disorder, neural network, classification**

OPEN ACCESS

***Edited by:***
*Wenbo Luo,*
*Liaoning Normal University, China*

***Reviewed by:***
*Rifai Chai,*
*University of Technology Sydney, Australia*
*Da-Hui Wang,*
*Beijing Normal University, China*

****Correspondence:***
*Xia-an Bi*
*bixiaan@hnu.edu.cn*

***Received:*** *06 February 2018*
***Accepted:*** *05 June 2018*
***Published:*** *26 June 2018*

***Citation:***
*Bi X, Liu Y, Jiang Q, Shu Q, Sun Q and Dai J (2018) The Diagnosis of Autism Spectrum Disorder Based on the Random Neural Network Cluster. Front. Hum. Neurosci. 12:257. doi: 10.3389/fnhum.2018.00257*

## INTRODUCTION

Autism spectrum disorder (ASD) characterized by impairments in social deficits and communication (Knaus et al., 2008) is a typically neurological disease with high heredity (Baird et al., 2006) and prevalence (Chakrabarti and Fombonne, 2001). It is reported that the prevalence of ASD has increased from 0.67% in 2000 to 1.47% in 2010 (Xu et al., 2018). Thus, the early diagnosis of ASD is meaningful. However, the traditional diagnostic methods are mainly based on clinical interviews and behavior observation, which makes the diagnosis inaccurate. There are two ways that could be applied to improve the diagnostic accuracy of ASD. One of the ways is the usage of the neuroimaging technique, such as Electroencephalogram (EEG; Peters et al., 2013), positron emission tomography (PET; Pagani et al., 2017), structural magnetic resonance imaging (sMRI; Sato et al., 2013) and functional magnetic resonance imaging (fMRI; Ren et al., 2014). The specific properties of fMRI make it widely used (Bennett et al., 2017). Another way is the usage of machine learning which could automatically improve the algorithm performance based on the previous experiences (Jordan and Mitchell, 2015). The neural network (NN) belongs to a branch of machine learning, which is inspired by human brain and has the function of effective pattern recognition. The NN has been successfully employed in the automated classification related to ASD. For instance, Iidaka (2015) applied probabilistic neural

network (PNN) to classify ASD patients and typical controls (TC), and the accuracy is close to 90%. Guo et al. (2017) proposed a new feature extraction based on the deep neural network (DNN) to classify the ASD patients and TC, and the accuracy is 86.36%. Heinsfeld et al. (2018) used the deep learning to diagnose ASD, and the accuracy is 70%. Heinsfeld et al. (2018) adopted deep learning to classify the ASD patients and TC, and the accuracy is 70%. These studies fully show that the accuracy of a single NN is not high and unstable in the diagnosis of some diseases.

As the single NN has the advantages of dealing with the imperfect data and solving the problem of complex nonlinear systems, the combination of multiple NNs would combine their differences and also improve classification performance. Therefore, we combine multiple NNs into a model which is named as the random NN cluster in this article. The new method could achieve better feature extraction and classification performance. Specifically, five different NNs are applied to build five types of random NN clusters which are able to classify ASD patients and TC. Then, we compare the accuracies of the five types of random NN clusters. The random Elman NN cluster has the highest accuracy which is approximately close to 100%, thus the Elman NN is selected as the best base classifier. Next, the random Elman NN cluster is used to find the significant features which are able to reflect the difference between ASD patients and TC. Finally, the abnormal brain regions are found out, including the supplementary motor area, the median cingulate and paracingulate gyri, the fusiform gyrus (FG) and the insula (INS). In conclusion, the random NN cluster is an effective method for classification and it could provide a new perspective to improve classification performance in the diagnosis of ASD.

# MATERIALS AND METHODS

## Demographic Information

In this article, the original imaging data was selected from autism brain imaging data exchange (ABIDE) database[1]), which includes the neuroimaging data of ASD patients and TC. The ASD patients should meet the criteria of childhood autism and the TC should meet the criteria of healthy control. The fMRI data was acquired on 3.0-T Siemens MRI scanner. The sequence parameters include: TR = 3000 ms, TE = 28 ms, matrix = $64 * 64$, slice thickness = 0.0 mm, pixel spacing $X$ = 3.0 mm, pixel spacing $Y$ = 3.0 mm, flip angle = 90°, no slice gap, axial slices = 34, time points = 120. In the scanning process, all participants are expected to lie still and stay awake. Finally, 92 participants that consist of 50 ASD patients and 42 TC were selected out in this article.

The differences of sex and age between the ASD group and TC group were tested by chi-square test and examined by two-sample $t$-test respectively. The results are shown in **Table 1**. It is referred that there are two groups which have no statistical significance between the sex and the age.

[1]http://fcon_1000.projects.nitrc.org/indi/abide/

**TABLE 1** | Basic information of ASD and TC.

| Variables (Mean ± SD) | ASD ($n$ = 50) | TC ($n$ = 42) | $P$ value |
|---|---|---|---|
| Sex (M/F) | 5/45 | 6/36 | 0.528 |
| Age (years) | 13.34 ± 2.41 | 13.05 ± 1.82 | 0.520 |

*Abbreviations: ASD, autism spectrum disorder; TC, typical controls.*

## Data Preprocessing

In order to lower the signal-to-noise ratio of fMRI images, all fMRI images need to be preprocessed. In this article, we used the Data Processing Assistant for Resting-State fMRI (DPARSF[2]) software (Chao-Gan and Yu-Feng, 2010). The data preprocessing includes the following eight steps: (a) converting DICOM format to NIFTI format; (b) removing the first 10 time points; (c) slicing timing (Kiebel et al., 2007); (d) realigning with the aim of reducing head motion (Grootoonk et al., 2000); (e) normalizing (Misaki et al., 2010); (f) smoothing with the aim of removing the noise caused by breathing, heartbeat and high frequency signal (Challis et al., 2015); (g) temporal filtering with the aim of regressing out movement vectors by high-pass temporal filtering (Kasper et al., 2014); and (h) removing covariates, such as the whole brain signal, white matter, cerebrospinal fluid signal regression treatment (Lund and Hanson, 2001).

## Basic Theory of the Neural Network

The operation of the human brain always attracts many researchers' attention. The artificial neural network (ANN) is evolved from the human brain which could achieve an effective nonlinear mapping function. In addition, it has excellent classification performance in different fields such as the field of medicine (Beheshti et al., 2014), economics (Wang et al., 2015) and business (Tkác and Verner, 2016). The following introduces five types of NNs.

### Backpropagation Neural Network

The Backpropagation (BP) NN is the core of the forward NN and it is able to realize the non-linear mapping (Ren et al., 2014). However, there is no effective method to determine parameters of BP NN, and the network could not be repeated because the initial weights are random numbers.

**Figure 1A** shows the structure of the BP NN. $x$ represents the neuron of the input layer, the $mth$ output $t_M^m(n)$ is defined as $x(n)$ in the input layer, where $n$ is the number of iteration and $M$ is the number of total inputs. $k$ represents the neuron of the hidden layer. $y$ represents the neuron of the output layer. $w_{mi}$ represents the weight from the $mth$ input layer to the $ith$ hidden layer, and $w_{ij}$ represents the weight from the $ith$ hidden layer to the $jth$ output layer. $c(n)$ represents the target output. The $ith$ input $s_I^i(n)$ is denoted as $\sum_{m=1}^{M} w_{mi}(n)t_M^m(n)$ in the hidden layer, where $I$ is the number of neurons in the hidden layer. The output $t_I^i(n)$ is denoted as $f\left(s_I^i(n)\right)$ in the hidden layer, where $f(\cdot)$ represents the sigmoid function. The $jth$ output $t_J^j(n)$ is denoted as $g\left(\left(s_J^j(n)\right)\right)$ in the output layer, where $J$ is the number of the output layer

[2]http://d.rnet.co/DPABI/DPABI_V2.3_170105.zip

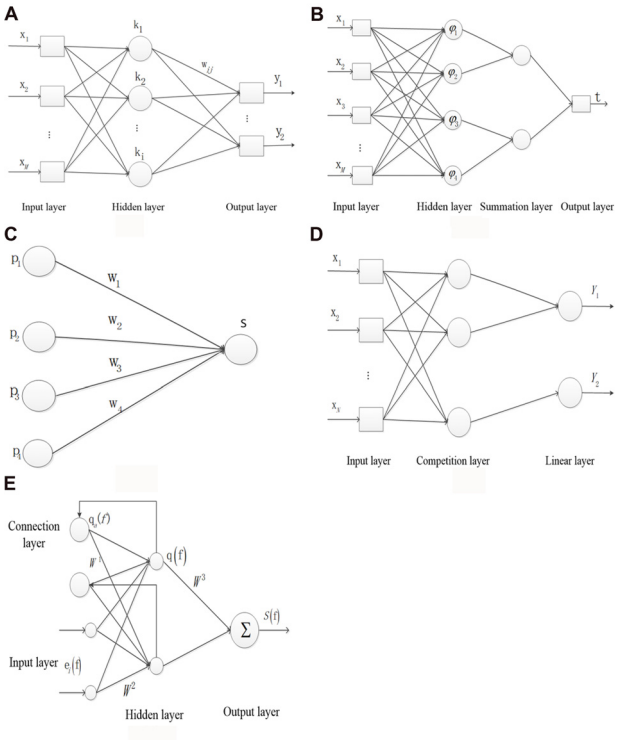


**FIGURE 1 |** The structure of the five types of neural networks (NNs). **(A)** Backpropagtion neural network. **(B)** Probabilistic neural network. **(C)** Competition neural network. **(D)** Learning vector quantization neural network. **(E)** Elman neural network.

and $g(\cdot)$ represents the linear function. The error $E_j(n)$ is denoted as $c_j(n) - t_j^j(n)$ in each layer. The total error $E$(n) is denoted as $\sum_{j=1}^{J} E_j^2(n)/2$.

### Probabilistic Neural Network

The PNN is used to classify based on the Bayesian decision theory (Khan et al., 2015). PNN has the advantages of short duration, and the basis function has a little influence on the classification result.

**Figure 1B** shows the structure of the PNN. $x$ represents the neuron of input layer. The neuron $\phi_{ij}$ in the hidden layer is denoted as $\exp\left[-(s-s_{ij})(s-s_{ij})^T/\sigma^2\right]/(2\pi)^{\frac{1}{2}}\sigma^d$, where $s_{ij}$ represents the *jth* core of *ith* sample, $\sigma$ represents the smoothing factor and $d$ represents the sample dimension. $v_i$ represents the relationship of the input and output sample in the hidden layer and is denoted as $\sum_{j=1}^{L}\varphi_{ij}/L$, where $L$ represents the neuron number in the summation layer. $t$ is denoted as $argmax\ (v_i)$ which represents the relationship of the input and output sample in the output layer.

### Competition Neural Network

In the competition NN, the output neurons compete with each other at the same time and only a winning neuron is finally selected. The learning rule is developed from the inner star rule.

**Figure 1C** shows the structure of the inner star model. $p_i$ represents the neuron of input layer. $w_i$ represents the connection weight. The output neuron $S$ is denoted as $X_w$ in the core layer. The adjustable weight $\Delta w_i$ is denoted as $\eta(p_i - w_i)\ S$. $\eta$ represents the learning rate.

### Learning Vector Quantization Neural Network

The learning vector quantization (LVQ) NN was proposed by Kohonen (Hung et al., 2011). LVQ originated from the competition NN and each sample has its corresponding classified label.

**Figure 1D** shows the structure of LVQ network. $x$ represents the neuron of input layer and $N$ is the number of neuron. The first and second neurons correspond to the output label of $Y_1$ and the third neuron corresponds to the output label of $Y_2$ in the competition layer. $p_i$ represents the *ith* input sample. $w_1$ represents the weight between the input layer and the competition layer. The output $b$ is denoted as $p_i w_1$.

### Elman Neural Network

The Elman NN has the function of the local memory and feedback which helps to deal with the vary time series, thus this type of NN has high stability. Specifically, the memory function is reflected in the connection layer remembering the output of the layer hidden in the previous step (Wang et al., 2014).

**Figure 1E** shows the structure of Elman NN. $e_i(f)$ represents the *ith* input vector of the input layer at time *f*. The output at $f$ time $q_a(f)$ in the connection layer is denoted as $\alpha q(f-1)$, where α represents the delay at time $f-1$. $q(f)$ represents the output of hidden layer. $S(f)$ represents the output of the output layer. $W^1$ represents the weight between the connection layer and the hidden layer. $W^2$ represents the weight between the input layer and the hidden layer. $W^3$ represents the weight between the hidden layer and the input layer. The error $M$ is denoted as $[S_d(f) - S(f)]^T[S_d(f) - S(f)]/2$, where $S_d$ and $S$ represents the output and the actual output, respectively.

## The Application of Graph Theory

The human brain could be denoted by a complex network. Graph theory belonging to a branch of mathematics is used for analyzing the complex system. Therefore, the human brain network could be analyzed by graph theory. Graph theory has two important elements: nodes and edges.

The brain of each subject is divided into 90 regions (45 in each hemisphere) using anatomical automatic labeling (AAL) template (Plitt et al., 2015), which is regarded as the node of the brain network. The average time series of all voxels in a region are regarded as the time series of the region. The time series of two separated brain regions could be transformed into the Pearson correlation coefficient which forms a features matrix, and then the 90 diagonal elements are removed. These Pearson correlation coefficients are taken as the edge of the brain network. Thus there are 4005 ($90 * 89/2$) weighted edges. Then we used the absolute value of the correlation coefficient and set a fit threshold for the feature matrix to obtain an adjacency matrix. The threshold equals to 0.25 in this article.

The functional connectivity is usually selected as features between two brain regions (Plitt et al., 2015). There are also

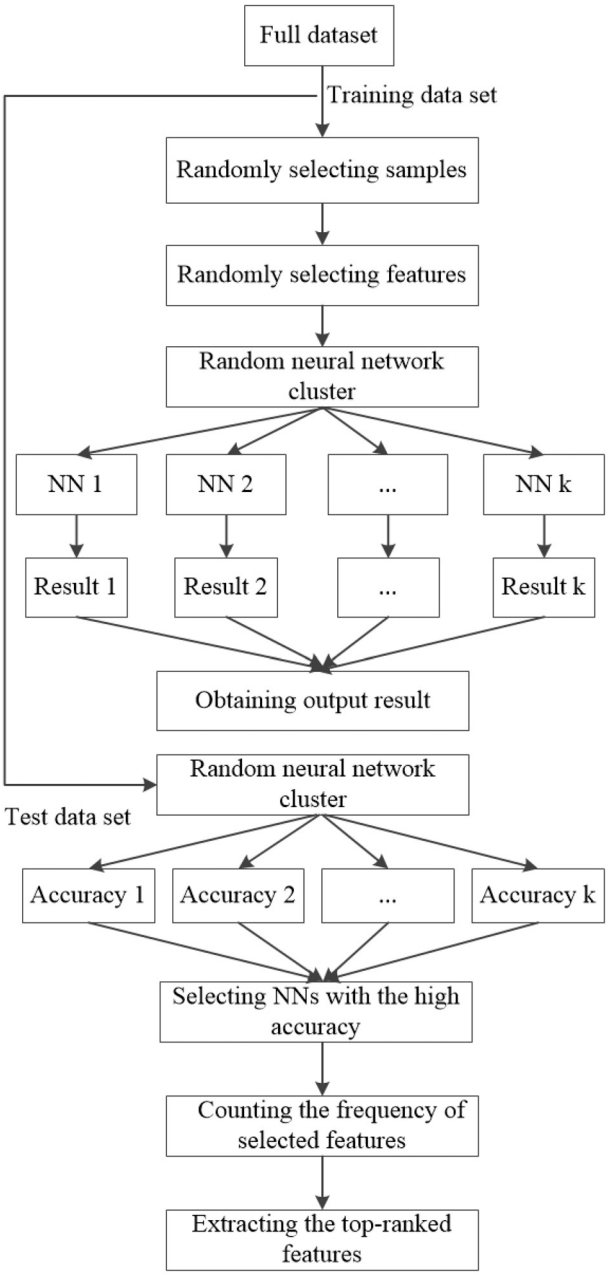


**FIGURE 2 |** The formation of the random NN cluster.

other indicators in graph theory analysis that could be selected as features such as the degree, clustering coefficient, shortest path and local efficiency of brain regions.

The degree of node represents the number of the directly linked edges. Shortest path is used for measuring the shortest path from a node to another node. The local efficiency reflects the capability of local information communication between one node and its neighbor nodes. It is assumed that $N_i$ represents the degree of node $i$, $d_{ij}$ represents the distance of node $i$ and node $j$, $V_i$ represents a node set in which all nodes directly connected to the node $i$. The local efficiency of node $i$ is measured as $E(i) = \frac{1}{N_i(N_i-1)} \sum_{i \neq j \in V_i} \frac{1}{d_{ij}}$. Clustering coefficient reflects the degree of local cohesion between a node and its neighbor nodes. The clustering coefficient of node $i$ measures as $C_i = \frac{e}{C_{N_i}^2} = \frac{2e}{N_i(N_i-1)}$, where $e$ is the sum of adjacent edges. The number of degree, shortest path, clustering coefficient and local efficiency in each subject's brain is 90, 4005, 90 and 90, respectively. Then the four indicators are integrated as the sample features of subsequent experiments.

## The Random Neural Network Cluster

### The Design of the Random Neural Network Cluster

As a single NN has the advantages of dealing with the imperfect data and solving the problem of complex nonlinear systems, it is usually used for classification. However, the classification performance is not high and unstable. In this article, the random NN cluster is proposed by combining multiple NNs and it is an effective method to improve classification performance. The design of the random NN cluster is generated by the following steps.

Given a full dataset $D = (\boldsymbol{X}_1, Y_1), (\boldsymbol{X}_2, Y_2), \ldots, (\boldsymbol{X}_N, Y_N)$, it contains $N$ samples. $Y_i$ represents the *ith* class label. $\boldsymbol{X}_i$ represents the *ith* input sample which includes $M$ features and it could be expressed as $\boldsymbol{X}_i = (x_{i1}, x_{i2}, \ldots, x_{iM})$, where $x_{ij}$ represents the *jth* feature of the *ith* sample.

The classification and feature extraction are carried out by using the random NN cluster. First, the full dataset $D$ is divided into the training set $N_1$ and the test set $N_2$ and the proportion is 8:2. Second, $n$ samples are randomly selected from ($N_1$ ($N_1 \gg n$)) and $m$ features are randomly selected from $M$ ($M \gg m$) to form a single NN. The process is repeated for $k$ times. When there is a new sample entering into the random NN cluster, $k$ NNs would have $k$ classification results. Third, the majority of class labels are selected as the classification result of the random NN cluster. Fourth, the correctly predictive proportion of all the test samples $N_2$ is regarded as the accuracy of the random NN cluster. Then, the NNs with the highest accuracy are selected out and the corresponding frequency of the selected features is counted. Finally, the features with top-ranked frequency are regarded as the significant features. The formation of the random NN cluster is shown in **Figure 2**.

### The Classification of the Random Neural Network Cluster

In our experiment, there are 50 ASD patients and 42 TC. It is assumed that the class labels of TC and ASD patients are $h_1$ and $h_2$, respectively. As we use 90°, 90 clustering coefficients, 4005 shortest paths and 90 local efficiencies as the features, there are 4275 features for each subject. Thus, the sample feature could be defined as $X_i = (x_{i1}, x_{i2}, \ldots, x_{i4275})$, where $x_i$ represents the *jth* feature of the *ith* subject. The classification method of the random NN cluster is described as the following.

First, 92 subjects are divided into a training set and a test set, and the proportion is 8:2. Thus the training set has 73 subjects and the test set has 19 subjects. Second, 70 subjects

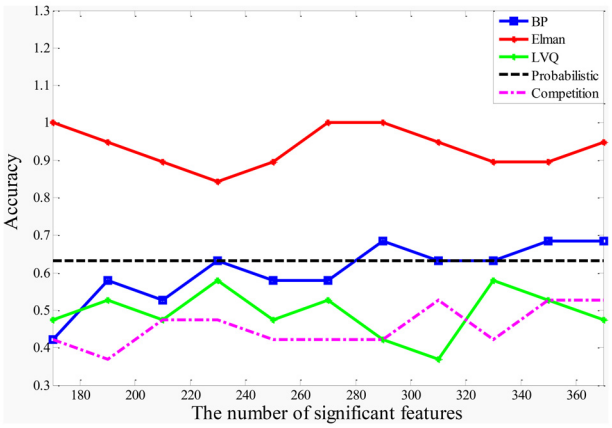


**FIGURE 3 |** The accuracies of the five types of random NN clusters.

are randomly selected from 73 subjects and 120 features are randomly selected from 4275 features to establish a single NN, and this process is repeated for 1000 times to construct a random NN cluster. We calculate the accuracy of the NN using the toolbox of NN in the Matlab and the parameters of each NN are appropriate adjusted to get better classification results. Third, we apply five types of NNs (BP) NN, Elman NN, Probabilistic NN, LVQ NN and Competitive NN) to construct the five types of random NN clusters, which are the random BP NN cluster, the random Elman NN cluster, the random Probabilistic NN cluster, the random LVQ NN cluster and the random Competition NN cluster. In the five types of random NN clusters, the base classifier of the random NN cluster with highest accuracy is regarded as the best base classifier.

Finally, 19 samples enter into the random NN cluster, and 1000 NNs make decisions at the same time to obtain the classification result of each sample. The majority of class labels are regarded as the predictive label of each sample. When the predictive class label is the same as the real class label, the label is called as consistent label. The accuracy of the random NN cluster equals to the number of consistent label divided by 19.

In the 1000 NNs, not every NN contributes to the random NN cluster. Thus, it is important to find out the significant NNs which contribute greatly to the random NN cluster. In this article, we select the NNs from 1000 NNs whose accuracies are greater than 0.6 as the significant NNs.

### Extracting Features From the Random Neural Network Cluster

As each NN has different characteristics, the selected features would make different contributions to NN and the random NN cluster. Therefore, it is necessary to select the significant features which could reflect the classification performance between the ASD patients and TC based on fMRI data. The process of extracting features is as follows.

First, the samples and features are randomly selected from the training set to construct the random NN cluster. Second, the samples of the test set enter into each NN of the random NN cluster to get the accuracies of 1000 NNs. Third, the NNs whose accuracies are greater than 0.6 are selected from 1000 NNs, and we call these NNs as the significant NNs. Fourth, we select the features of significant NNs from the total 4275 features, and these features are sorted in a descending order according to their frequencies. Next, the features with high frequency are considered as the significant features which could be used to distinguish between ASD patients and TC. Then, we select a part of significant features as the sample features to construct a random NN cluster and calculate their accuracies. Finally, the number of significant features corresponding to the random NN cluster with the highest accuracy is the optimal number.

After completing the features extraction in the whole brain, we use the significant features to find out the abnormal brain regions between ASD patients and TC. In order to estimate the abnormal degree of a brain region, the number of features which are related to the brain region is regarded as the criteria. If the brain region is not related to any significant feature, the weight of the brain region is 0. The greater the number of features is, the higher the abnormal degree is.

## RESULTS

### The Performances of the Random Neural Network Cluster

In this article, the five different types of NNs (BP NN, Elman NN, Probabilistic NN, LVQ NN and Competitive NN) are applied to construct the five types of random NN clusters. The classification performances of the five types of random NN clusters are shown in **Figure 3**. It is referred that the accuracies of the random Competition NN cluster and the accuracies of the random LVQ NN cluster are not high; the accuracies of the random Elman NN cluster fluctuate around 95%, even nearly reach to 100%; the accuracies of the random BP NN cluster and the random Probabilistic NN cluster are higher than the random Competition NN cluster and the random LVQ NN cluster. Thus, we finally select the Elman NN as the best base classifier and the subsequent results are acquired based on the random Elman NN cluster.

The training errors and the test errors of the five types of random NN clusters are shown in **Table 2**. **Figure 4** shows the accuracies of 1000 NNs in four types of random NN clusters. As the accuracies of 1000 NNs in the random probabilistic NN cluster are the same values, **Figure 4** does not show the accuracies of probabilistic NNs. From the **Table 2** and **Figure 4** we could

**TABLE 2 |** The errors of the five types of random neural network (NN) clusters.

| Variables (Mean ± SD) | Training errors | Test errors |
|---|---|---|
| Random BP neural network cluster | 0.60 ± 0.09 | 0.60 ± 0.08 |
| Random probabilistic neural network cluster | 0.63 ± 0.00 | 0.63 ± 0.00 |
| Random Elman neural network cluster | 0.93 ± 0.04 | 0.93 ± 0.05 |
| Random LVQ neural network cluster | 0.50 ± 0.06 | 0.49 ± 0.06 |
| Random competition neural network cluster | 0.46 ± 0.07 | 0.45 ± 0.05 |

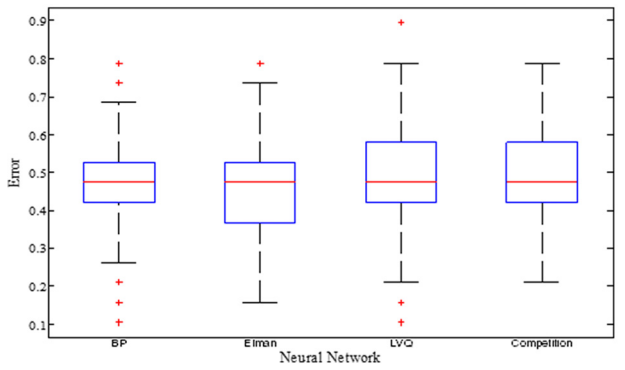


**FIGURE 4 |** The accuracies of 1000 NNs in four types of random NN clusters.

learn that the error is higher in a single NN and is lower in a random NN cluster.

In order to show the performance of the random NN cluster, we compared the non-NN variant of the classifiers (the support vector machine (SVM) and the decision-making tree) with the NN. When the decision-making tree is made as the classifier, the highest classification accuracy is 87%. When the SVM is made as the classifier, the highest classification accuracy is 84%. These are lower than the highest classification accuracy of the random NN cluster.

In our experimental results, when the number of the classifier is 270 which could be discussed in the following part, the accuracy of the random Elman NN cluster is the highest. Therefore, we fix the number of base classifiers on 270. Then, we repeat the experiments for 50 times, and obtain the results of their classifiers' accuracies. The differences between the base classifier of Elman NN and the base classifier of the decision-making tree are tested by the two-sample *t*-test. *P* value is close to 0.015, which refers that these two groups have statistical significance. The differences between the base classifier of Elman NN and the base classifier of the SVM are tested by the two-sample *t*-test. *P* value equals to 0.000, which refers that these two groups have statistical significance. **Table 3** shows the result of statistical significance between the three methods.

## The Significant Neural Networks and Features

When the samples of the test set enter into the random Elman NN cluster, we could obtain the accuracies of 1000 Elman NNs. We select the Elman NN whose accuracy is greater than 0.6 as the significant Elman NNs, and the result indicates that the number of significant Elman NNs is 270. These significant Elman NNs make great contributions to distinguish between ASD and TC in the random Elman NN cluster.

After determining the significant Elman NNs, we could select significant features with higher accuracy from these NNs. In order to determine the optimal number of the significant features, we make the accuracy of the random Elman NN cluster as the criteria. **Figure 3** shows the accuracies of the random Elman NN cluster with different numbers of significant features. It is referred that when the number of significant features is 170, 260, 270 and 280, the accuracies of the random Elman NN cluster fluctuate around 95%, even nearly reach to 100%. But when the number of features is 170, the accuracies of the random Elman NN cluster are not stable. We choose the 270 as the optimal number of significant features because the accuracies of the random Elman NN cluster are highest and stable.

## The Abnormal Brain Regions

In this article, we focus on the brain regions of which the weights are higher than 11. They are the Supp_Motor_Area (SMA), the Cingulum_Mid (DCG), the Fusiform (FFG), the Insula (INS), the Frontal_Inf_Oper (IFGoperc), the Cingulum_Post (PCG), the Calcarine (CAL), the Occipital_Sup (SOG).

**Table 4** shows the regions whose weights are higher than 11 and their corresponding volumes. **Figure 5** shows the distribution of 90 brain regions using Brain-NetViewer[3]. The red nodes indicate the brain regions, and the size of the nodes indicates the abnormal degree of the brain regions. The greater the node is, the higher the abnormal degree is.

# DISCUSSION

## Classification Performance

In recent years, there are some researchers trying to classify and diagnose ASD patients from TC. Wang et al. (2012) used fMRI data to classify ASD patients and TC with the classification sensitivity of 82.8% and the specificity of 82.8%. Ecker et al. (2010) applied SVM to classify ASD patients and TC and the sensitivity and specificity of classification was 90% and 80% respectively. Uddin et al. (2013) employed functional connectivity to classify ASD patients and TC, and the classification accuracy was 78%. As the classification accuracy is not high in most existing studies, the random NN cluster is proposed to improve the classification performance in the diagnosis of ASD. In this article, five different NNs were applied to construct the five types of random NN clusters. The highest accuracy of the random BP NN cluster and the random

[3]http://www.nitrc.org/projects/bnv/

**TABLE 3 |** The result of statistical significance between the three methods.

| Base classifier (Mean ± SD) | SVM | Elman NN | Decision tree | *P* value |
|---|---|---|---|---|
| Accuracy (%) | 0.773 ± 0.034 | 0.847 ± 0.032 | 0.834 ± 0.016 | 0.000[a]/0.015[b] |

[a]*the p value of the two-sample t-test between SVM and NN.* [b]*the p value of the two-sample t-test between decision tree and NN.*

**TABLE 4 |** The regions with higher weight.

| Regions | The volume of region | Weight |
|---|---|---|
| SMA.R | [9 062] | 18 |
| DCG.R | [8 −9 40] | 15 |
| FFG.L | [−31 40 −20] | |
| INS.L | [−3 5 73] | 14 |
| IFGoperc.R | [5015 21] | 13 |
| INS.R | [3962] | |
| DCG.L | [−5 −15 42] | 12 |
| PCG.R | [7 −42 22] | |
| CAL.L | [−7 −79 6] | |
| SOG.L | [−17 84 28] | |
| PreCG.L | [−39–651] | 11 |
| SFGdor.R | [22 31 44] | |
| MFG.L | [−33 33 35] | |
| ROL.L | [−47 −8 14] | |
| SFGmed.R | [9 51 30] | |
| PCG.L | [−5 43 25] | |
| PCL.L | [−8 25 70] | |

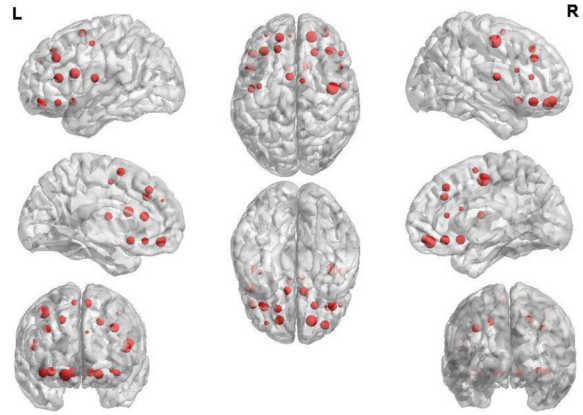


**FIGURE 5 |** The distribution of 90 brain regions.

Probabilistic NN cluster are 68.4% and 63.2% respectively. The highest accuracy of the random LVQ NN cluster and the accuracy of random Competitive NN cluster are only 57.8% and 52.6%. We ultimately selected the Elman NN as the best base classifier and the high accuracy of the random Elman NN cluster nearly reaches to 100%. The experimental results show that the performance of the random NN cluster is very good.

The Elman NN is able to deal with the dynamic data, thus it is suitable for the fMRI data which changes in a period of time. In general, the random Elman NN cluster could be applied to the rapid and accurate detection of the abnormal brain regions in ASD patients.

## Additional Discussion of the Random Neural Network Cluster

In this part, we discuss the additional issues including the parameters, complexity, errors, weight and the overfitting of the random NN cluster.

In the random NN cluster, the parameters are decided by the accuracy of the random NN cluster. Besides, the importance of parameters in bad classifier could be reduced by the randomness of the random NN cluster. In a single NN, the parameters are adaptive and they are under the control of NN toolbox. Generally, after a series of strict process of parameters selection, the performance of the random NN cluster improves.

The random NN cluster is complicated which is reflected in the following two points. On the one hand, the process of constructing a random NN cluster is complex because the number of base classifiers is 1000. On the other hand, the process of finding the optimal number of base classifiers is complex because we need to select the optimal number of base classifiers based on the accuracy of the random NN cluster constructed by different number of base classifiers.

In terms of the weight, there are two kinds of weights in our method. When the accuracy of the random NN cluster is calculated, the percentage of voting for each base classifier (NN) is the same. In the interior structure of a single NN, the weight is set by the NN toolbox.

The subjects have been divided into a training set and a test set. The training set is used for building the random NN cluster, and the test set is used for testing the performance of the random NN cluster. Our experimental results show that the random NN cluster works well on the test set, thereby there is no overfitting. In addition, a random NN cluster was composed of many NNs and each NN is unique due to the random samples and random features, which also ensures that there is no overfitting.

## Analysis of the Significant Neural Networks and Features

To classify ASD patients from TC correctly, we selected the significant NNs and features. In this article, we used five different types of NNs to construct five types of random NN clusters and the process of establishing a single NN repeated for 1000 times to construct a random NN cluster. The accuracies of the five types of random NN clusters were compared, and then the corresponding NN in the random NN cluster with the highest accuracy was selected as the best base classifier. When the number of NNs is large, it is more difficult to calculate. But the classification result is more consistent with the actual result in this situation. Thus, it is important to select an appropriate number of NNs. In this article, we used 1000 NNs to construct the random NN cluster. As each NN has its own characteristics, the NNs make different contributions to the random NN cluster. The greater the accuracy of NN is, the higher the contribution is. If the accuracy is more than 0.5, the classification is good in machine learning (Krishnan and Westhead, 2003). The accuracy of threshold is generally artificially set, and we selected the Elman NNs whose accuracies were greater than 0.6 as the significant Elman NNs. To select these significant features, we firstly made a preliminary filtration from the 4275 sample features to select a part of features. These features were sorted in a descending order according to their frequencies and the features with higher frequency are considered as the significant features. It is the above process of

feature extraction that makes our method different from other methods. Our method is able to make full use of all features and select out appropriate significant features at higher speed.

## Analysis of the Brain Regions With the Greater Weight

In this article, the random NN cluster has been applied to classify ASD patients from TC and find out the abnormal brain regions. Some abnormal brain regions were found out corresponding to AAL template in ASD patients such as the supplementary motor area (SMA.R), the median cingulate and paracingulate gyri (DCG), the fusiform gyrus (FFG.L), the insula (INS), the inferior frontal gyrus (IFGoperc.R), the posterior cingulate gyrus (PCG), the calcarine fissure and surrounding cortex (CAL.L), the superior occipital gyrus (SOG.L), the precentral gyrus (PreCG.L), the superior frontal gyrus (SFGdor.R), the middle frontal gyrus (MFG.L), the rolandic operculum (ROL.L), the medial of superior frontal gyrus (SFGmed.R) and the paracentral lobule (PCG.L). In many studies, some abnormal regions were found out in ASD patients. For instance, Murdaugh et al. (2012) concluded that ASD patients had less deactivation in DMN regions including medial prefrontal cortex, anterior cingulate cortex and posterior cingulate gyrus. Itahashi et al. (2015) discovered local functional disruptions in the right superior frontal gyrus and middle frontal gyrus in ASD patients. Choi et al. (2015) found out abnormal regions of ASD patients in the right dorsolateral prefrontal cortex, the right parietal lobe, the right orbitofrontal cortex and the superior temporal gyrus. Subbaraju et al. (2017) concluded that the prefrontal cortex, the posterior and medial portions were abnormal in ASD patients.

Our experimental results are consistent with these findings. In this article, we focused on some abnormal regions which had larger frequency such as the supplementary motor area, the cingulate gyrus, the FG and the INS.

### The Supplementary Motor Area (SMA.R)

The SMA.R had the greatest frequency in the abnormal brain regions in ASD patients. It is referred that the SMA.R makes a great contribution to classify ASD and TC in the random Elman NN cluster. The SMA is linked to the function of movement observation, preparation and execution (Enticott et al., 2009). It is responsible for planning and executing motor tasks (Hupfeld et al., 2017).

Our experimental results are consistent with many previous studies. Chen et al. (2015) found that intrinsic functional connectivity was related to the somatosensory default mode and visual regions in ASD patients. Kestemont et al. (2016) explored that there were more activation differences between ASD patients and TC concentrating in the SMA, the left precentral gyrus and so on. Fournier et al. (2010) observed that the motor dysfunction in SMA could be a feature of diagnosing ASD. Ewen et al. (2016) detected the abnormal regions of ASD patients locating in the motor network which includes the SMA.

The abnormal SMA may lead to the physical movement deficits in ASD patients. The above results reveal that SMA may be a clinical and pervasive feature to diagnose ASD in the future.

### The Cingulate Gyrus

The cingulate gyrus had the higher frequency in the abnormal brain regions. It is referred that the cingulate gyrus makes a great contribution to classify ASD and TC in the random Elman NN cluster. The cingulate gyrus is associated with the neurocognitive function (Calabrese et al., 2008), the somatosensory function (Nair et al., 2015) and the behaviors and cognitive processes (Apps et al., 2016).

Our experimental results are consistent with many previous studies. Cascio et al. (2014) discovered that the INS and the anterior cingulate cortex were abnormal regions in ASD patients. Thakkar et al. (2008) concluded that the abnormalities of the anterior cingulate cortex in ASD could make contributions to repetitive behavior. Apps et al. (2016) found out the abnormal regions such as the left orbitofrontal cortex and left posterior cingulate gyrus in ASD patients.

The abnormal cingulate gyrus may lead to the cognitive processes deficits in ASD patients. The above results reveal that the cingulate gyrus may be a clinical and pervasive feature to diagnose ASD in the future.

### The Fusiform Gyrus (FG)

The FG had the higher frequency in the abnormal brain regions in ASD patients. It is referred that the FG makes a great contribution to classify ASD patients and TC in the random Elman NN cluster. The FG is associated with the social-emotional and face recognition (Oblak et al., 2010; Hernandez et al., 2015).

Our experimental results are consistent with many previous studies. Yucel et al. (2014) found the difference between ASD patients and TC involved in the amygdala and the FG. Apps et al. (2016) discovered that the amygdala and the FG were abnormal in ASD patients. Kaiser et al. (2016) found out some abnormal regions such as the FG.R, the right amygdala and the bilateral ventrolateral prefrontal cortex in ASD patients.

The abnormal FG may lead to the face recognition deficits in ASD patients. This founding reveal that the FG may be regarded as a new biomarker to further test the disease of ASD and provide convenience for clinical diagnosis of ASD.

### The Insula (INS)

The INS had a relatively higher frequency in the abnormal regions, thus it is referred that the INS makes a great contribution to classify ASD and TC in the random Elman NN cluster. The INS are relevant to the cognition mechanism (Uddin and Menon, 2009).

Our experimental results are consistent with many previous studies. Murdaugh et al. (2012) found out some abnormal regions of ASD patients including the posterior cingulate gyrus, the INS and the SMA. Plitt et al. (2015) explored that the inferior frontal gyrus and the INS were abnormal in ASD patients. Keehn et al. (2016) detected that the occipital cortex, the dorsolateral prefrontal cortex and the INS were abnormal in ASD patients.

The abnormal INS may lead to the simulation mechanism deficits in ASD patients. These results reveal that the INS may be regarded as a new biomarker to further test the disease of ASD and provide convenience for clinical diagnosis of ASD.

In this article, the random NN cluster was proposed to classify ASD patients from TC and found out the abnormal brain regions in ASD patients based on the fMRI data. The new method has some advantages. On the one hand, we selected the random Elman NN cluster from five types of random NN clusters and its highest accuracy even could nearly reach to 100%. On the other hand, we used the random Elman NN cluster could find the significant features which are the most differences between ASD patients and TC. Therefore, the random NN cluster might be an appropriate approach for diagnosing ASD. There are some limitations. First, our experimental sample size is not large. In this article, 92 participants were selected from ABIDE which was the maximum number of samples that we could obtain. In the future studies, the new method can be applied to the larger sample size. Second, this article integrated the four indicators as the features of subjects. In the future studies, we could also integrate other indicators as features.

## ETHICS STATEMENT

This study was carried out in accordance with the recommendations of National Institute of Aging-Alzheimer's Association (NIA-AA) workgroup guidelines, Institutional Review Board (IRB). The study was approved by Institutional Review Board (IRB) of each participating site, including the Banner Alzheimer's Institute, and was conducted in accordance with Federal Regulations, the Internal Conference on Harmonization (ICH) and Good Clinical Practices (GCP).

## AUTHOR CONTRIBUTIONS

X-aB proposed the design of the work and revised it critically for important intellectual content. QSun and QJ carried out the experiment for the work and drafted part of the work. YL, QShu and JD collected, interpreted the data and drafted part of the work. All the authors approved the final version to be published and agreed to be accountable for all aspects of the work in ensuring that questions related to the accuracy or integrity of any part of the work are appropriately investigated and resolved.

## FUNDING

This work is supported by the National Natural Science Foundation of China (Grant Nos. 61502167, 61473259).

## REFERENCES

Apps, M. A., Rushworth, M. F., and Chang, S. W. (2016). The anterior cingulate gyrus and social cognition: tracking the motivation of others. *Neuron* 90, 692–707. doi: 10.1016/j.neuron.2016.04.018

Baird, G., Simonoff, E., Pickles, A., Chandler, S., Loucas, T., Meldrum, D., et al. (2006). Prevalence of disorders of the autism spectrum in a population cohort of children in South Thames: the special needs and autism project (SNAP). *Lancet* 368, 210–215. doi: 10.1016/S0140-6736(06)69041-7

Beheshti, Z., Shamsuddin, S. M. H., Beheshti, E., and Yuhaniz, S. S. (2014). Enhancement of artificial neural network learning using centripetal accelerated particle swarm optimization for medical diseases diagnosis. *Soft Comput.* 18, 2253–2270. doi: 10.1007/s00500-013-1198-0

Bennett, R. H., Somandapalli, K., Roy, A. K., and Di Martino, A. (2017). The neural correlates of emotional lability in children with Autism spectrum disorder. *Brain Connect.* 7:281. doi: 10.1089/brain.2016.0472

Calabrese, D. R., Wang, L., Harms, M. P., Ratnanather, J. T., Barch, D. M., Cloninger, C. R., et al. (2008). Cingulate gyrus neuroanatomy in schizophrenia subjects and their non-psychotic siblings. *Schizophr. Res.* 104, 61–70. doi: 10.1016/j.schres.2008.06.014

Cascio, C. J., Foss-Feig, J. H., Heacock, J., Schauder, K. B., Loring, W. A., Rogers, B. P., et al. (2014). Affective neural response to restricted interests in autism spectrum disorders. *J. Child Psychol. Psychiatry* 55, 162–171. doi: 10.1111/jcpp.12147

Chakrabarti, S., and Fombonne, E. (2001). Pervasive developmental disorders in preschool children. *JAMA* 285, 3093–3099. doi: 10.1001/jama.285.24.3093

Challis, E., Hurley, P., Serra, L., Bozzali, M., Oliver, S., and Cercignani, M. (2015). Gaussian process classification of Alzheimer's disease and mild cognitive impairment from resting-state fMRI. *Neuroimage* 112, 232–243. doi: 10.1016/j.neuroimage.2015.02.037

Chao-Gan, Y., and Yu-Feng, Z. (2010). DPARSF: a MATLAB toolbox for "Pipeline" data analysis of resting-state fMRI. *Front. Syst. Neurosci.* 4:13. doi: 10.3389/fnsys.2010.00013

Chen, C. P., Keown, C. L., Jahedi, A., Nair, A., Pflieger, M. E., Bailey, B. A., et al. (2015). Diagnostic classification of intrinsic functional connectivity highlights somatosensory, default mode, and visual regions in autism. *Neuroimage Clin.* 8, 238–245. doi: 10.1016/j.nicl.2015.04.002

Choi, U.-S., Kim, S.-Y., Sim, H.-J., Lee, S.-Y., Park, S.-Y., Jeong, J.-S., et al. (2015). Abnormal brain activity in social reward learning in children with autism spectrum disorder: an fMRI study. *Yonsei Med. J.* 56, 705–711. doi: 10.3349/ymj.2015.56.3.705

Ecker, C., Marquand, A., Mourão-Miranda, J., Johnston, P., Daly, E. M., Brammer, M. J., et al. (2010). Describing the brain in autism in five dimensions—magnetic resonance imaging-assisted diagnosis of autism spectrum disorder using a multiparameter classification approach. *J. Neurosci.* 30, 10612–10623. doi: 10.1523/jneurosci.5413-09.2010

Enticott, P. G., Bradshaw, J. L., Iansek, R., Tonge, B. J., and Rinehart, N. J. (2009). Electrophysiological signs of supplementary-motor-area deficits in high-functioning autism but not Asperger syndrome: an examination of internally cued movement-related potentials. *Dev. Med. Child Neurol.* 51, 787–791. doi: 10.1111/j.1469-8749.2009.03270.x

Ewen, J. B., Lakshmanan, B. M., Pillai, A. S., McAuliffe, D., Nettles, C., Hallett, M., et al. (2016). Decreased modulation of EEG oscillations in high-functioning autism during a motor control task. *Front. Hum. Neurosci.* 10:198. doi: 10.3389/fnhum.2016.00198

Fournier, K. A., Hass, C. J., Naik, S. K., Lodha, N., and Cauraugh, J. H. (2010). Motor coordination in autism spectrum disorders: a synthesis and meta-analysis. *J. Autism Dev. Disord.* 40, 1227–1240. doi: 10.1007/s10803-010-0981-3

Grootoonk, S., Hutton, C., Ashburner, J., Howseman, A. M., Josephs, O., Rees, G., et al. (2000). Characterization and correction of interpolation effects in the realignment of fMRI time series. *Neuroimage* 11, 49–57. doi: 10.1006/nimg.1999.0515

Guo, X., Dominick, K. C., Minai, A. A., Li, H., Erickson, C. A., and Lu, L. J. (2017). Diagnosing autism spectrum disorder from brain resting-state functional connectivity patterns using a deep neural network with a novel feature selection method. *Front. Neurosci.* 11:460. doi: 10.3389/fnins.2017.00460

Heinsfeld, A. S., Franco, A. R., Craddock, R. C., Buchweitz, A., and Meneguzzi, F. (2018). Identification of autism spectrum disorder using deep learning and the ABIDE dataset. *Neuroimage Clin.* 17, 16–23. doi: 10.1016/j.nicl.2017.08.017

Hernandez, L. M., Rudie, J. D., Green, S. A., Bookheimer, S., and Dapretto, M. (2015). Neural signatures of autism spectrum disorders: insights into brain network dynamics. *Neuropsychopharmacology* 40, 171–189. doi: 10.1038/npp.2014.172

Hung, W.-L., Chen, D.-H., and Yang, M.-S. (2011). Suppressed fuzzy-soft learning vector quantization for MRI segmentation. *Artif. Intell. Med.* 52, 33–43. doi: 10.1016/j.artmed.2011.01.004

Hupfeld, K. E., Ketcham, C. J., and Schneider, H. D. (2017). Transcranial direct current stimulation (tDCS) to the supplementary motor area (SMA) influences performance on motor tasks. *Exp. Brain Res.* 235, 851–859. doi: 10.1007/s00221-016-4848-5

Iidaka, T. (2015). Resting state functional magnetic resonance imaging and neural network classified autism and control. *Cortex* 63, 55–67. doi: 10.1016/j.cortex.2014.08.011

Itahashi, T., Yamada, T., Watanabe, H., Nakamura, M., Ohta, H., Kanai, C., et al. (2015). Alterations of local spontaneous brain activity and connectivity in adults with high-functioning autism spectrum disorder. *Mol. Autism* 6:30. doi: 10.1186/s13229-015-0026-z

Jordan, M. I., and Mitchell, T. M. (2015). Machine learning: trends, perspectives, and prospects. *Science* 349, 255–260. doi: 10.1126/science.aaa8415

Kaiser, M. D., Yang, D. Y. J., Voos, A. C., Bennett, R. H., Gordon, I., Pretzsch, C., et al. (2016). Brain mechanisms for processing affective (and nonaffective) touch are atypical in autism. *Cereb. Cortex* 26, 2705–2714. doi: 10.1093/cercor/bhv125

Kasper, L., Haeberlin, M., Dietrich, B. E., Gross, S., Barmet, C., Wilm, B. J., et al. (2014). Matched-filter acquisition for BOLD fMRI. *Neuroimage* 100, 145–160. doi: 10.1016/j.neuroimage.2014.05.024

Keehn, B., Nair, A., Lincoln, A. J., Townsend, J., and Müller, R.-A. (2016). Under-reactive but easily distracted: an fMRI investigation of attentional capture in autism spectrum disorder. *Dev. Cogn. Neurosci.* 17, 46–56. doi: 10.1016/j.dcn.2015.12.002

Kestemont, J., Vandekerckhove, M., Bulnes, L. C., Matthys, F., and Van Overwalle, F. (2016). Causal attribution in individuals with subclinical and clinical autism spectrum disorder: an fMRI study. *Soc. Neurosci.* 11, 264–276. doi: 10.1080/17470919.2015.1074104

Khan, Z. U., Hayat, M., and Khan, M. A. (2015). Discrimination of acidic and alkaline enzyme using Chou's pseudo amino acid composition in conjunction with probabilistic neural network model. *J. Theor. Biol.* 365, 197–203. doi: 10.1016/j.jtbi.2014.10.014

Kiebel, S. J., Klöppel, S., Weiskopf, N., and Friston, K. J. (2007). Dynamic causal modeling: a generative model of slice timing in fMRI. *Neuroimage* 34, 1487–1496. doi: 10.1016/j.neuroimage.2006.10.026

Knaus, T. A., Silver, A. M., Lindgren, K. A., Hadjikhani, N., and Tagerflusberg, H. (2008). fMRI activation during a language task in adolescents with ASD. *J. Int. Neuropsychol. Soc.* 14, 967–979. doi: 10.1017/s1355617708081216

Krishnan, V. G., and Westhead, D. R. (2003). A comparative study of machine-learning methods to predict the effects of single nucleotide polymorphisms on protein function. *Bioinformatics* 19, 2199–2209. doi: 10.1093/bioinformatics/btg297

Lund, T. E., and Hanson, L. G. (2001). Physiological noise reduction in fMRI using vessel time-series as covariates in a general linear model. *Neuroimage* 13:191. doi: 10.1016/s1053-8119(01)91534-4

Misaki, M., Kim, Y., Bandettini, P. A., and Kriegeskorte, N. (2010). Comparison of multivariate classifiers and response normalizations for pattern-information fMRI. *Neuroimage* 53, 103–118. doi: 10.1016/j.neuroimage.2010.05.051

Murdaugh, D. L., Shinkareva, S. V., Deshpande, H. R., Wang, J., Pennick, M. R., and Kana, R. K. (2012). Differential deactivation during mentalizing and classification of autism based on default mode network connectivity. *PLoS One* 7:e50064. doi: 10.1371/journal.pone.0050064

Nair, A., Carper, R. A., Abbott, A. E., Chen, C. P., Solders, S., Nakutin, S., et al. (2015). Regional specificity of aberrant thalamocortical connectivity in autism. *Hum. Brain Mapp.* 36, 4497–4511. doi: 10.1002/hbm.22938

Oblak, A. L., Gibbs, T. T., and Blatt, G. J. (2010). Decreased GABA(B) receptors in the cingulate cortex and fusiform gyrus in autism. *J. Neurochem.* 114, 1414–1423. doi: 10.1111/j.1471-4159.2010.06858.x

Pagani, M., Nobili, F., Morbelli, S., Arnaldi, D., Giuliani, A., Öberg, J., et al. (2017). Early identification of MCI converting to AD: a FDG PET study. *Eur. J. Nucl. Med. Mol. Imaging* 44, 2042–2052. doi: 10.1007/s00259-017-3761-x

Peters, J. M., Taquet, M., Vega, C., Jeste, S. S., Fernández, I. S., Tan, J., et al. (2013). Brain functional networks in syndromic and non-syndromic autism: a graph theoretical study of EEG connectivity. *BMC Med.* 11:54. doi: 10.1186/1741-7015-11-54

Plitt, M., Barnes, K. A., and Martin, A. (2015). Functional connectivity classification of autism identifies highly predictive brain features but falls short of biomarker standards. *Neuroimage Clin.* 7, 359–366. doi: 10.1016/j.nicl.2014.12.013

Ren, C., An, N., Wang, J., Li, L., Hu, B., and Shang, D. (2014). Optimal parameters selection for BP neural network based on particle swarm optimization: a case study of wind speed forecasting. *Knowl. Based Syst.* 56, 226–239. doi: 10.1016/j.knosys.2013.11.015

Sato, J. R., Hoexter, M. Q., Oliveira, P. P. Jr., Brammer, M. J., MRC AIMS Consortium, Murphy, D., et al. (2013). Inter-regional cortical thickness correlations are associated with autistic symptoms: a machine-learning approach. *J. Psychiatr. Res.* 47, 453–459. doi: 10.1016/j.jpsychires.2012.11.017

Subbaraju, V., Suresh, M. B., Sundaram, S., and Narasimhan, S. (2017). Identifying differences in brain activities and an accurate detection of autism spectrum disorder using resting state functional-magnetic resonance imaging: a spatial filtering approach. *Med. Image Anal.* 35, 375–389. doi: 10.1016/j.media.2016.08.003

Thakkar, K. N., Polli, F. E., Joseph, R. M., Tuch, D. S., Hadjikhani, N., Barton, J. J. S., et al. (2008). Response monitoring, repetitive behaviour and anterior cingulate abnormalities in autism spectrum disorders (ASD). *Brain* 131, 2464–2478. doi: 10.1093/brain/awn099

Tkác, M., and Verner, R. (2016). Artificial neural networks in business: two decades of research. *Appl. Soft. Comput.* 38, 788–804. doi: 10.1016/j.asoc.2015.09.040

Uddin, L. Q., and Menon, V. (2009). The anterior insula in autism: under-connected and under-examined. *Neurosci. Biobehav. Rev.* 33, 1198–1203. doi: 10.1016/j.neubiorev.2009.06.002

Uddin, L. Q., Supekar, K., Lynch, C. J., Khouzam, A., Phillips, J., Feinstein, C., et al. (2013). Salience network-based classification and prediction of symptom severity in children with autism. *JAMA Psychiatry* 70, 869–879. doi: 10.1001/jamapsychiatry.2013.104

Wang, H., Chen, C., and Fushing, H. (2012). Extracting multiscale pattern information of fMRI based functional brain connectivity with application on classification of autism spectrum disorders. *PLoS One* 7:e45502. doi: 10.1371/journal.pone.0045502

Wang, L., Zeng, Y., and Chen, T. (2015). Back propagation neural network with adaptive differential evolution algorithm for time series forecasting. *Expert. Syst. Appl.* 42, 855–863. doi: 10.1016/j.eswa.2014.08.018

Wang, J., Zhang, W., Li, Y., Wang, J., and Dang, Z. (2014). Forecasting wind speed using empirical mode decomposition and Elman neural network. *Appl. Soft. Comput.* 23, 452–459. doi: 10.1016/j.asoc.2014.06.027

Xu, G., Strathearn, L., Liu, B., and Bao, W. (2018). Prevalence of autism spectrum disorder among US children and adolescents, 2014–2016. *JAMA* 319, 81–82. doi: 10.1001/jama.2017.17812

Yucel, G. H., Belger, A., Bizzell, J., Parlier, M., Adolphs, R., and Piven, J. (2014). Abnormal neural activation to faces in the parents of children with autism. *Cereb. Cortex* 25, 4653–4666. doi: 10.1093/cercor/bhu147

**Conflict of Interest Statement**: The authors declare that the research was conducted in the absence of any commercial or financial relationships that could be construed as a potential conflict of interest.

frontiers in Human Neuroscience

ORIGINAL RESEARCH
published: 29 June 2018
doi: 10.3389/fnhum.2018.00267

# Incorporation of Multiple-Days Information to Improve the Generalization of EEG-Based Emotion Recognition Over Time

*Shuang Liu[1,2†], Long Chen[1†], Dongyue Guo[1], Xiaoya Liu[1], Yue Sheng[1], Yufeng Ke[2], Minpeng Xu[1], Xingwei An[2], Jiajia Yang[1] and Dong Ming[1,2*]*

[1] Neural Engineering & Rehabilitation Lab, Department of Biomedical Engineering, College of Precision Instruments and Optoelectronics Engineering, Tianjin University, Tianjin, China, [2] Academy of Medical Engineering and Translational Medicine, Tianjin University, Tianjin, China

Current studies have got a series of satisfying accuracies in EEG-based emotion classification, but most of the classifiers used in previous studies are totally time-limited. To produce generalizable results, the emotion classifier should be stable over days, in which the day-to-day variations of EEG should be appropriately handled. To improve the generalization of EEG-based emotion recognition over time by learning multiple-days information which embraces the day-to-day variations, in this paper, 17 subjects were recruited to view several video clips to experience different emotion states, and each subject was required to perform five sessions in 5 days distributed over 1 month. Support vector machine was built to perform a classification, in which the training samples may come from 1, 2, 3, or 4 days' sessions but have a same number, termed learning 1-days information (L1DI), learning 2-days information (L2DI), learning 3-days information (L3DI), and learning 4-days information (L4DI) conditions, respectively. The results revealed that the EEG variability could impair the performance of emotion classifier dramatically, and learning more days' information to construct a classifier could significantly improve the generalization of EEG-based emotion recognition over time. Mean accuracies were 62.78, 67.92, 70.75, and 72.50% at L1DI, L2DI, L3DI, and L4DI conditions, respectively. Features at L4DI condition were ranked by modified RFE, and features providing better contribution were applied to obtain the performances of all conditions, results showed that the performance of SVMs trained and tested with the feature subset were all improved for L1DI, L2DI ($*p < 0.05$), L3DI ($**p < 0.01$), and L4DI ($*p < 0.05$) conditions. It could be a substantial step forward in the development of emotion recognition from EEG signals because it may enable a classifier trained on one time to handle another.

**Keywords: emotion, electroencephalogram (EEG), generalization, emotion recognition, day-to-day variations**

OPEN ACCESS

***Edited by:***
*Xiaochu Zhang,*
*University of Science and Technology of China, China*

***Reviewed by:***
*Xin Zhu,*
*University of Aizu, Japan*
*Zhipeng Liu,*
*Institute of Biomedical Engineering, Japan*

***Correspondence:**
*Dong Ming*
*richardming@tju.edu.cn*

*[†] These authors have contributed equally to this work.*

***Received:*** *28 February 2018*
***Accepted:*** *08 June 2018*
***Published:*** *29 June 2018*

***Citation:***
*Liu S, Chen L, Guo D, Liu X, Sheng Y, Ke Y, Xu M, An X, Yang J and Ming D (2018) Incorporation of Multiple-Days Information to Improve the Generalization of EEG-Based Emotion Recognition Over Time. Front. Hum. Neurosci. 12:267. doi: 10.3389/fnhum.2018.00267*

## INTRODUCTION

Emotion is a psycho-physiological process triggered by the conscious and/or unconscious perception of an object or a situation, which is often associated with mood, temperament, personality disposition, and motivation (Koelstra et al., 2012). It plays a key role in non-verbal communication, and it is essential to understand human behavior. Emotion recognition has

recently received an increasing amount of attention in human-computer interface and affective disorder diagnosis (Acharya et al., 2015; Atkinson and Campos, 2015; Yin et al., 2017). Through measuring the human signals, operators could recognize the current emotion state just by the automatic emotion recognition system. So it could also be used to many other applications such as driving safety, entertainment, e-learning, and telemedicine (Nasoz et al., 2004; Liu et al., 2010). Though emotion recognition has been traditionally done from facial expressions, speech or gesture, these signals have a critical limitation in that these could be deliberately changed to hide the true emotion (Yoon and Chung, 2013). Physiological measures, such as electroencephalogram (EEG), electrocardiogram (ECG), electromyogram signal, respiratory volume, and skin conductance, have been widely used recently because of its objective (Khalili and Moradi, 2008; Kim and André, 2008; Koelstra et al., 2012; Yoon and Chung, 2013). Among these, non-invasively measured EEG has been a growing popular tool with the advantages of high time resolution as well as simple and affordable recording requirement (Xu et al., 2016).

A variety of EEG features have been employed in emotion recognition so far. EEG power spectrum distributions has been repeatedly reported to be a discriminable marker of emotions. Specifically, frontal asymmetry in the alpha band has been used as a predictor of valence (Lee et al., 2014). More recently, nonlinear features have been proposed to recognize emotions, such as fractal dimensions (Sourina et al., 2009; Liu et al., 2010; Ahmadlou et al., 2012), Hurst exponent (Wang et al., 2014; Acharya et al., 2015) and entropy (Duan et al., 2013; Wang et al., 2014), wavelet-chaos methodology (Ahmadlou et al., 2012). Furthermore, phase synchronization and coherence (Miskovic and Schmidt, 2010; Martini et al., 2012) have also been considered as emotional features.Regarding the classification, there have been lots of machine learning methods producing excellent performance, such as the support vector machine (SVM) (Brown et al., 2011; Nie et al., 2011; Soleymani et al., 2012; Duan et al., 2013; Hidalgo-Muñoz A. et al., 2013; Hidalgo-Muñoz A. R. et al., 2013), k-nearest neighbor (Guyon and Elisseeff, 2003) multilayer perceptron (Yoon and Chung, 2013), linear discriminant analysis (Murugappan et al., 2010) and Bayesian network (Hidalgo-Muñoz A. et al., 2013; Hidalgo-Muñoz A. R. et al., 2013), and so on. Current studies got a series of satisfying accuracies in emotion classification from EEG signals, but most of the classifiers are time-limited. It is however impossible that an emotion classifier trained on the data at specific time can only recognize emotion state at the same time in practical application.

As we know, a person' EEG patterns may appear differently at different time even when he is under the same emotion due to some external factors such as temperature, humidity, or a diet, and also some uncontrollable internal factors such as the hormones or baseline mood that can cause variations in physiology (Chueh et al., 2012). The reliability of resting EEGs over time has already been studied for decades. The correlation coefficients were reported to decrease with the test-retest interval increasing, and power spectral parameters were proved to be more stable than others such as entropy and coherence features (Gasser et al., 1985; Salinsky et al., 1991; Kondacs and Szabó, 1999; Gudmundsson et al., 2007). It seems that the stability of emotional EEG features has not been substantially addressed until very recently. Liu et al. (Lan et al., 2014) used the Intra-class Correlation Coefficient (ICC) to quantified the stability of four feature parameters regarding emotion recognition, respectively, but it did not present a way to solve the day-to-day variations of EEG. An emotion classifier does not generalize over days if the day-to-day variations is not appropriately handled. If a classifier is built by the data drawn from just 1 day, the input features may carry the information unique to that day which the classifier would learn. Once the testing set was independently from another day, the performance of the classifier was undermined. Up to now, researchers have not yet reported the effort to handle this issue in EEG-based emotion recognition.

This study aims to investigate the influence of EEG's day-to-day variations on the performance of an emotion classifier, and the benefit of the multiple-days information to constructing a classifier generalizing over time. This paper is organized as follows. Section Materials and Methods addresses the methodology including the experiment and data processing. Section Results shows the results. The discussion and conclusion are stated in section Discussion and Conclusion.

# MATERIALS AND METHODS

## Materials

### Participants

The experiment was performed with 17 healthy participants (12 female, 5 male, age range 20–28). All participants had normal or corrected-to-normal vision and normal hearing, and none of them had a history of severe medical treatment, psychological or neurological disorders. A signed consent was obtained from each subject before the experiment was carried out.

### Stimuli and Experimental Procedure

A group of emotional movie clips were used to evoke subject's neutral, positive, and negative states. To evaluate the effectiveness of these clips, 30 subjects took part in a questionnaire survey and the final 45 movie clips with strongest ratings and a small variation were selected for use in the experiment. The spoken language of the clips is Chinese or dubbed into Chinese with the length of from 5 to 20 min.

Before the experiment, each subject was informed of the experimental procedure and the meaning of valence and arousal used for self-assessment. The subjects were required to perform five sessions in 5 days distributed over 1 month, with 6–9 video clips in each recording session. Recording sessions for two representative subjects are depicted in **Figure 1**. The number of days between consecutive sessions was in a random order of four intervals: 1 day apart, 3 days apart, 1 week apart and 2 weeks apart intervals. This randomization was intended to reduce the effect of strategic changes. The participants were invited to the listening room between 18:00 p.m. and 20:00 p.m. and presented 6–9 clips for every recording session, ensuring there were 2 clips successfully eliciting positive, neutral and negative emotion states, respectively. After watching a video, the participants were required to score their feelings on a 9-point

scale in terms of emotional valence and arousal, and then had a short break. Subjects were informed to report what they actually felt during watching movie clips, not what they thought they should feel.

### EEG Recording and Preprocessing

During watching the clips, EEG data were recorded continuously using 60 sites using a NeuroScan SynAmps$^{2TM}$, positioned following the international 10–20 system (Tytell, 1961). **Figure 2** shows 60-channels EEG cap layout used in this study. Right mastoid was used as reference, and the central region was used as the grounding site. The EEGs were digitized at 1,000 Hz and filtered at 0.1–100 Hz.

A preprocessing step was performed for the raw EEG signals. All channels were re-referenced to bilateral mastoid, and down-sampled to 500 Hz. EOG artifacts were removed using independent component analysis (ICA) (Li et al., 2006). Data were segmented according to the subjects' self-report about which period of time they felt a strong emotional experience.

| | MON | TUE | WED | THU | FRI | SAT | SUN |
|---|---|---|---|---|---|---|---|
| **Week1** | | day1 | | | day2 | day1 | day2 |
| **Week2** | | | day3 | | day3 | day4 | |
| **Week3** | | | day4 | | | | |
| **Week4** | | | | | | day5 | |
| **Week5** | | | day5 | | | | |

**FIGURE 1 |** Data collection days for two representative subjects.

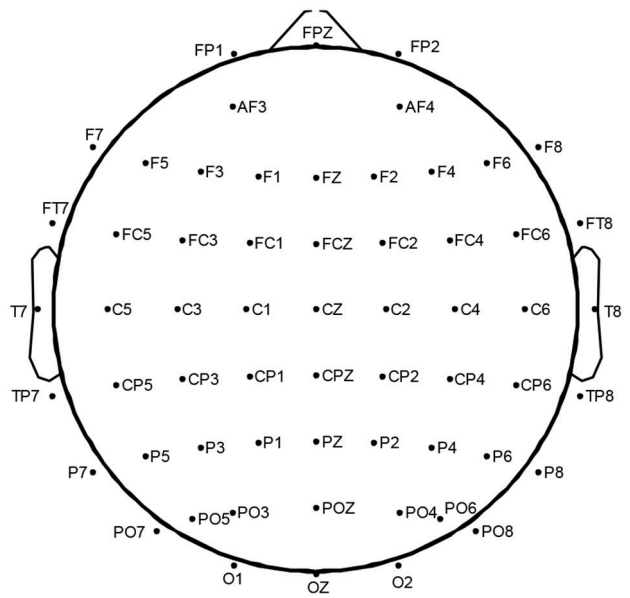


**FIGURE 2 |** International 10–20 system for 60 electrodes.

## Methods

### Feature Extraction

EEG power spectrum distributions in various frequency bands have been repeatedly reported to be a discriminable marker of emotions (Balconi and Lucchiari, 2006; Lee et al., 2014; Verma and Tiwary, 2014). In this paper, all of the 60-channel data were spectrally analyzed using Welch's method with a hamming widow of 500 ms with 50% overlap. Then the spectral powers in delta band (0.5–4 Hz), theta band (4–8 Hz), alpha band (8–13 Hz), beta band (13–30 Hz), low gamma band (30–44 Hz), and high gamma band (44–100 Hz), were computed, resulting in 360 total features (6 per channel × 60 channels), and 5-s epoch was extracted as a sample. The number of extracted samples depended on the feedback data of the subject, but equal numbers of samples were used to train the classifier, this would be described in detail below.

### Different Strategies of Classifier Calibration

This work tried to investigate the influence of EEG's day-to-day variations on the performance of an emotion classifier firstly. To this end, two different methods, within-day classification (WDC), the standard cross-day classification (SCDC) were compared.

(1) WDC: The training and the testing data were all from the same day. Eighty percent of the data samples from test day were randomly selected and used for classifier training, while the remaining 20% were sent to the testing set. To obtain a robust result, this procedure was repeated 5 times, and the classification rates were got by averaging all the 5 accuracies. Each day was treated as the test day once.

(2) SCDC: The training and testing data were from two independent days. Eighty percent of the data samples from 1 day were randomly selected as the training data, and the data from remaining 4 days were sent to test the classifier, respectively. Each day was used to train a classifier once. The number of training samples in both WDC and SCDC was equal to ensure fair and valid comparisons.

### Learning Multiple-Days Information for Classifier Calibration

In order to verify the benefit of the multiple-days information to constructing a classifier generalizing over time, the classifiers were built by learning N-days information ($N = 1, 2, 3, 4$) and compared, termed as L1DI, L2DI, L3DI, and L4DI, respectively. For LNDI, the classifier learned N-days information, and data samples from the remaining 5-N days were sent to the testing set. **Figure 3** shows the flow charts of LNDI.

Take L3DI as an example, the procedure was as follows:

The feature vector of the i*th* day was obtained by Welch's method (see section Feature Extraction) and represented by vector of $Y^i_{M_i}$ in form,

$$Y^i_{M_i} = [y(1); y(2); \ldots; y(M_i)] \quad (1)$$

Where $M_i$ denotes the number of samples extracted from the ith day. The superscript refers the ith day and the subscript is the number of the vector.

$$M_{min} = floor\left(\frac{\min(M_1, M_2, M_3, M_4, M_5)}{12}\right) * 12 \quad (2)$$

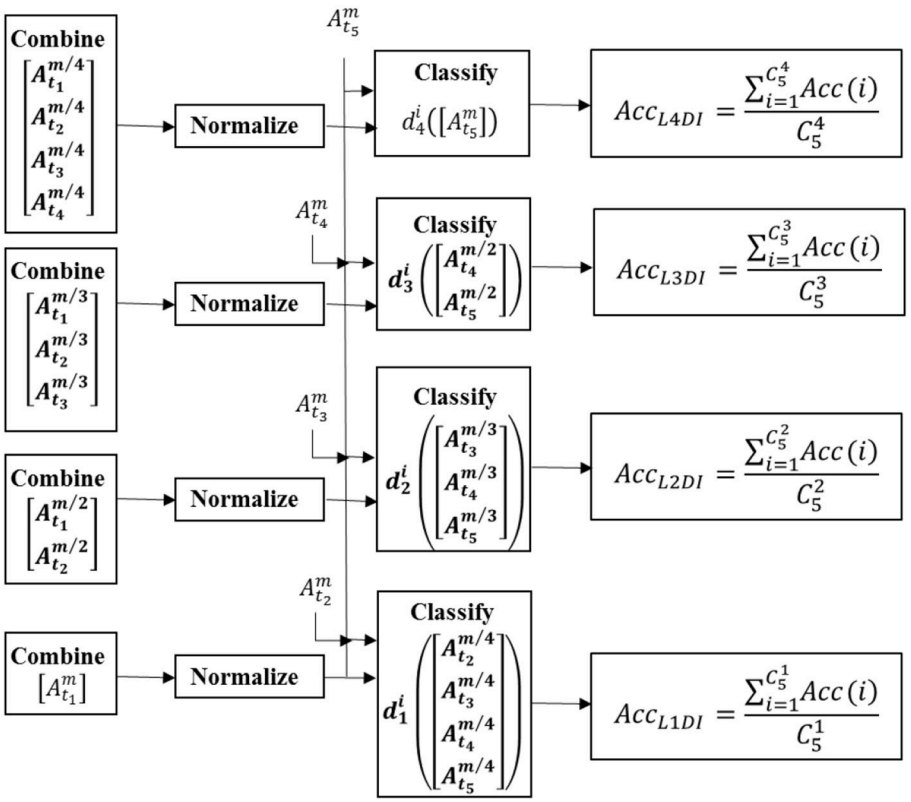


**FIGURE 3 |** The flow charts of LNDI.

Where $M_{min}$ is the minimum number of data samples among these 5 days. Then 3 of 5 days to train a classifier and all possible combinations of training and testing days were taken into consideration to get a robust result and reduce the impact of any 1 day being an outlier. For the k*th* possible combination, the training set and testing set were constructed as follows:

$$Y^k = [Y^{t_1}_{M_{min}/3}; Y^{t_2}_{M_{min}/3}; Y^{t_3}_{M_{min}/3}] \quad (3)$$

$$T^k = [Y^{t_4}_{M_{min}/2}; Y^{t_5}_{M_{min}/2}] \quad (4)$$

Where $Y^k$ is the training set and $T^k$ is the testing set for the k*th* possible combination, $t_1$, $t_2$, and $t_3$ refer to the selected number of days to train a classifier, and $t_4$, $t_5$ were the number of days to test. The number of data samples were set to $M_{min}$ both in training and testing set, and the same for L1DI, L2DI, L3DI, and L4DI.

$$\mathrm{Acc}\,(\mathrm{k}) = \mathrm{SVM}(Y^k, T^k) \quad (5)$$

The accuracy of the k*th* possible combination was obtained by SVM (Chang and Lin, 2006).

The accuracy of L3DI was obtained by averaging all possible combinations,

$$Acc_{L3DI} = \frac{\sum_{k=1}^{C_5^3} Acc(k)}{C_5^3} \quad (6)$$

To increase the reliability of the accuracy results, ten repetitions of abovementioned procedure were performed, and these ten classification rates were averaged to get the accuracy.

## The Specifically-Designed Recursive Feature Elimination (RFE)

To evaluate if learning multiple-days information (LMDI) could make the classifier easier to pick out the emotion-related features and discard day-specific ones, a specifically designed RFE was used for feature selection under L4DI condition. The method could rank all the features and then obtain the robust subset. The data samples were provided to the SVMs, split into training, testing, and validation sets. Fifty percent of the data samples from each day were randomly selected for feature selection, and the remaining 50% were held back as a validation set to control overfitting, as shown in **Figure 4**. The procedure can be summarized as follows:

(1) Fifty percent of the data samples from each day were randomly selected to construct the feature selection set, based on which 4 of 5 days were sent to train a classifier, the remaining 1 day were testing set. The number of training and testing samples followed the section Learning Multiple-Days Information for Classifier Calibration.
(2) To get the contribution ranking of features, firstly, one feature in N-dimension feature set was removed and then

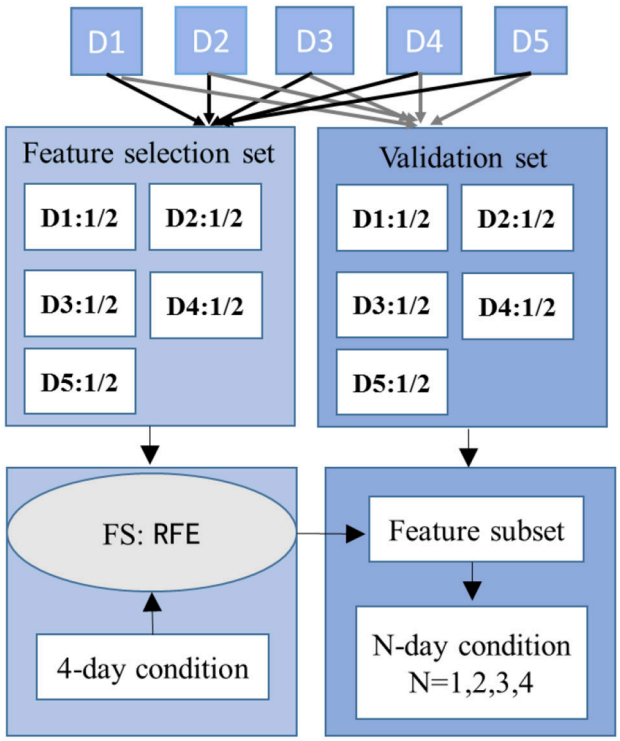


**FIGURE 4 |** The illustration depicts a fold of the feature selection procedure.

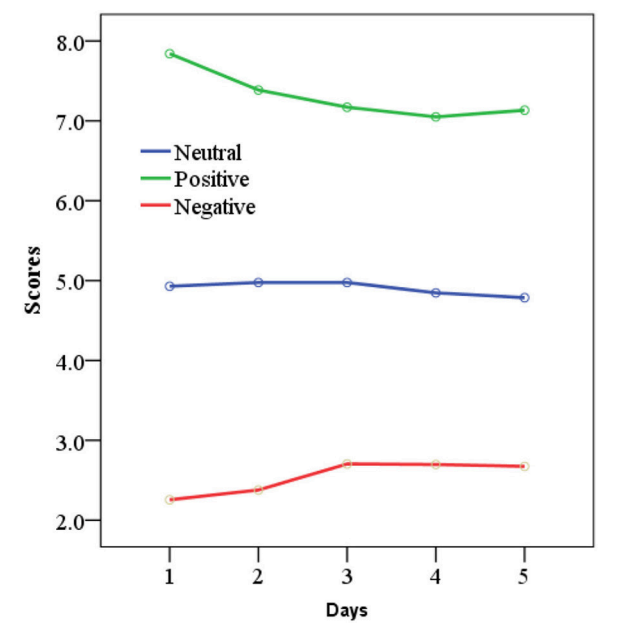


**FIGURE 5 |** Valance ratings of neutral, positive, and negative states in 5-day experiment.

we computed the performances with remaining N-1 features; secondly, we removed each other feature once and then computed the performance with remaining N-1 features; Thirdly, we ranked the N performances got from the above two steps, and the feature owns the least contribution in the case that the corresponding performance has the minimum loss of accuracy.

(3) The top M of the feature ranking were considered as the robust features since these M features could achieve a relatively stable and high accuracy. As there were 5 combinations, so there were 5 feature lists with M features. Those selected 5, 4, and 3 times were considered features with better contribution and those with 2, 1, and 0 times were termed features with bad contribution. Salient feature subset was constructed by these features providing better contribution.

(4) The validation sets with the feature subset were then taken as input of the SVM to validate the feature subset under L1DI, L2DI, L3DI, and L4DI conditions, respectively.

# RESULTS

## The EEG Inter-Day Variability on Emotion Classification

All the participants completed the 5-day experiment. All the rating scores (valence and arousal ratings) were collected, but we just concerned the valence dimension in subsequent analysis. Valance ratings of neutral, positive, and negative states were presented in **Figure 5**. To check our valence manipulation, 3 emotions by 5 days repeated-measure ANOVAs for valence ratings were performed. A main effect for three-class emotions on valence ratings was found, $F = 1353.5$, $p < 0.001$. The main effect for time (5 days) on valence ratings had no significance, $F = 0.524$, $p = 0.718$. This illustrated that the video clips have evoked the target emotions successfully, and there was no significant difference in valence ratings of 5 days.

## The EEG Inter-Day Variability on Emotion Classification

We computed three-class (positive, neutral, and negative) accuracies of WDC and SCDC, shown in **Figure 6**. WDC is labeled when trained and tested on the same day, while SCDC is labeled when trained and tested on the different days, which is detailed in section Different Strategies of Classifier Calibration. As shown in **Figure 6A**, WDC returned the averaged accuracy of above 98%, which was impressive. **Figure 6B** shows the SCDC results using SVM, collapsed to about 60%, which presumably suffered from day-to-day variability. All classifiers are also well above chance performance.

We calculated accuracies with different window width to further dissect the effect of EEG's day-to-day variations on the performance of emotion classification, shown in **Figure 7**. The data was split into several parts with a certain particular window width in each day, one part was sent to the training set, and the next part was to testing set in sequence, as depicted in **Figure 7A**. Window width were set to 5 s, 1 min, 5 min, and more than 5 min. More than 5 min was the condition that data at a certain emotional state in each day was split into two halves, one half was to the training set and the other half was to the testing set. Window width was from 5 to 20 min

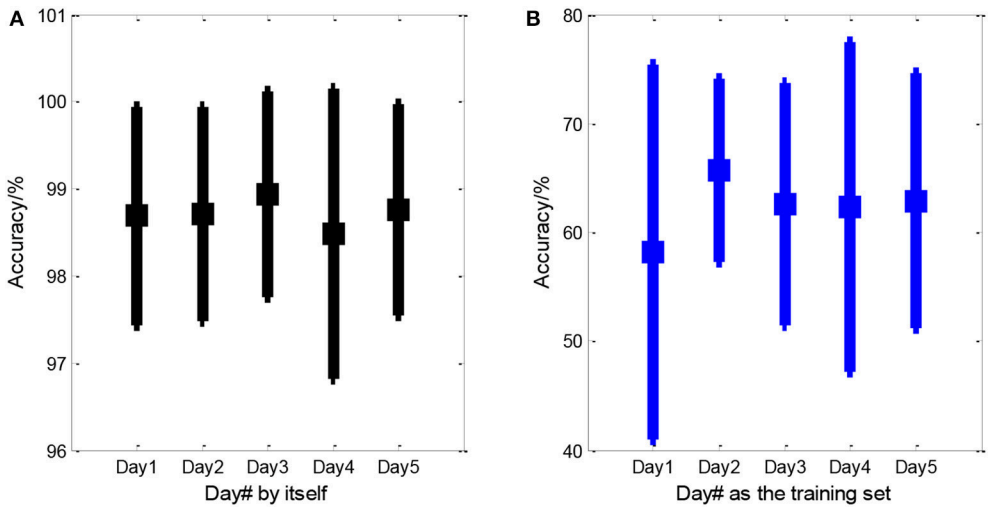


**FIGURE 6 |** Averaged accuracies of within- and standard cross-day emotion classification. **(A)** Within-day classification and **(B)** the standard cross-day scenario that accounted for inter-day EEG variability. The spot indicates the mean value and the line is the standard deviation. In **(A)**, Day# presented the day that training samples and testing samples were both from. In **(B)**, Day# indicated the training day, and remaining 4 days were hold as the testing days.

in this condition. As depicted in **Figure 7B**, the performance tends to decrease with larger window width. Paired *T*-test was performed on the accuracies between each two window width, we verified that all accuracies differ significantly ($p < 0.05$). These results underpinned that the EEG variability can deteriorate the performance of emotion classifier dramatically.

## Classification Accuracies With Different Number of Days in the Training Set

So we computed the accuracies of 4 conditions: L1DI, L2DI, L3DI, and L4DI conditions. **Figure 8** shows the performance in 17 subjects, and the bottom right panel shows the mean accuracies across all subjects. As can be seen from **Figure 8**, the accuracies tended to increase with more days in the training set for all the subjects, the mean accuracies were 62.78, 67.92, 70.75, and 72.50% at L1DI, L2DI, L3DI, and L4DI conditions, respectively. Paired T- test revealed that the accuracy at L1DI condition was significantly lower than that of L2DI ($p < 0.01$), L3DI ($p < 0.01$), and L4DI conditions ($p < 0.01$). This confirmed the prediction that learning multiple-days information would improve the cross-day accuracies was correct.

## Performance With the Feature Subset Applied to Other Conditions

Using data from more days to retrain a classifier could improve the accuracies over days, partly because it embraces the day-to-day changes incrementally. Thus the classifier trained by more days might weight emotion-related features heavily and inversely weaken the day-dependent features. The feature rank was obtained by modified RFE which detailed in the above.

To check whether these feature subsets picked out by RFE at L4DI condition are emotion-related, and thus could benefit the performances of all conditions (L1DI, L2DI, L3DI, and L4DI conditions), the performances were computed on validation sets with all 360 features and the feature subset (mean number of the features was 174 across 17 subjects), respectively. As shown in **Figure 9**, compared with the performance of cross-day SVMs trained and tested with all the 360 features, the performance of SVMs trained and tested with the feature subset were all improved for L1DI, L2DI ($^{*}p < 0.05$), L3DI ($^{**}p < 0.01$), and L4DI ($^{*}p < 0.05$) conditions, confirming the benefit of adding more days in training set for a classifier to weight emotional features heavily.

Another issue that should be discussed is about the most emotion-relevant EEG frequency ranges. **Figure 10** presents the distribution of the salient features averaged over 17 subjects. Contribution rate (CR) was computed for 64 channels in delta, theta, alpha, beta, low gamma, and high gamma bands, and depicted in **Figure 10**. It is obvious that the gamma band dominates a great proportion of the salient features, indicating gamma ranges might be importantly discriminable ranges for recognize the emotions.

## The Sensitivity of the Positive, Negative and Neutral Valence

The confusion matrices in **Table 1** provided a closer look at the sensitivity of the positive, negative and neutral valence. The row is the predicted label and the column is the real label. It could be found that positive, neutral and negative emotions were accurately recognized as 71.5, 76.9, and 59%, respectively. Moreover, there were a relatively higher proportion for negative valence that falsely classified as the neutral valence.

# DISCUSSION AND CONCLUSION

Results of this study demonstrated that classifiers that are trained and tested on EEG data from the same day can very accurately

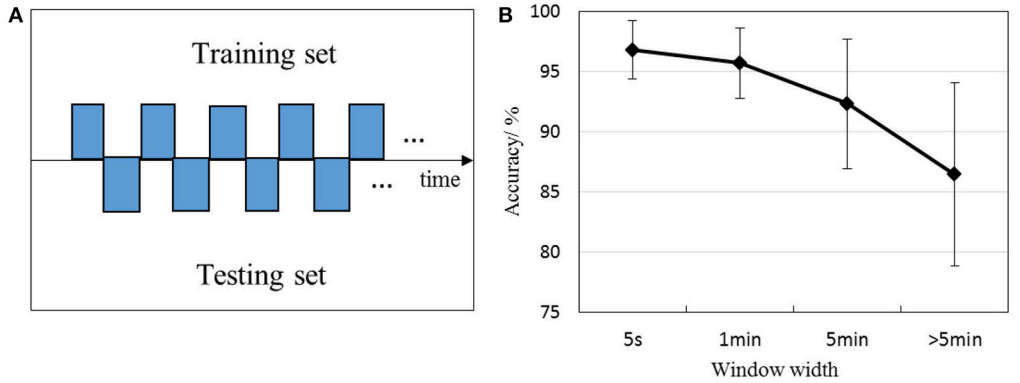


**FIGURE 7 |** Classification rates with different window width. For example, 1 min represents the first 12 samples were sent to the training set, and the next 12 samples to the testing set in sequence, then the third 12 samples were to the training set. **(A)** Illustrates the sample partitioning method with a certain particular window width, **(B)** depicts the performance with different window width.

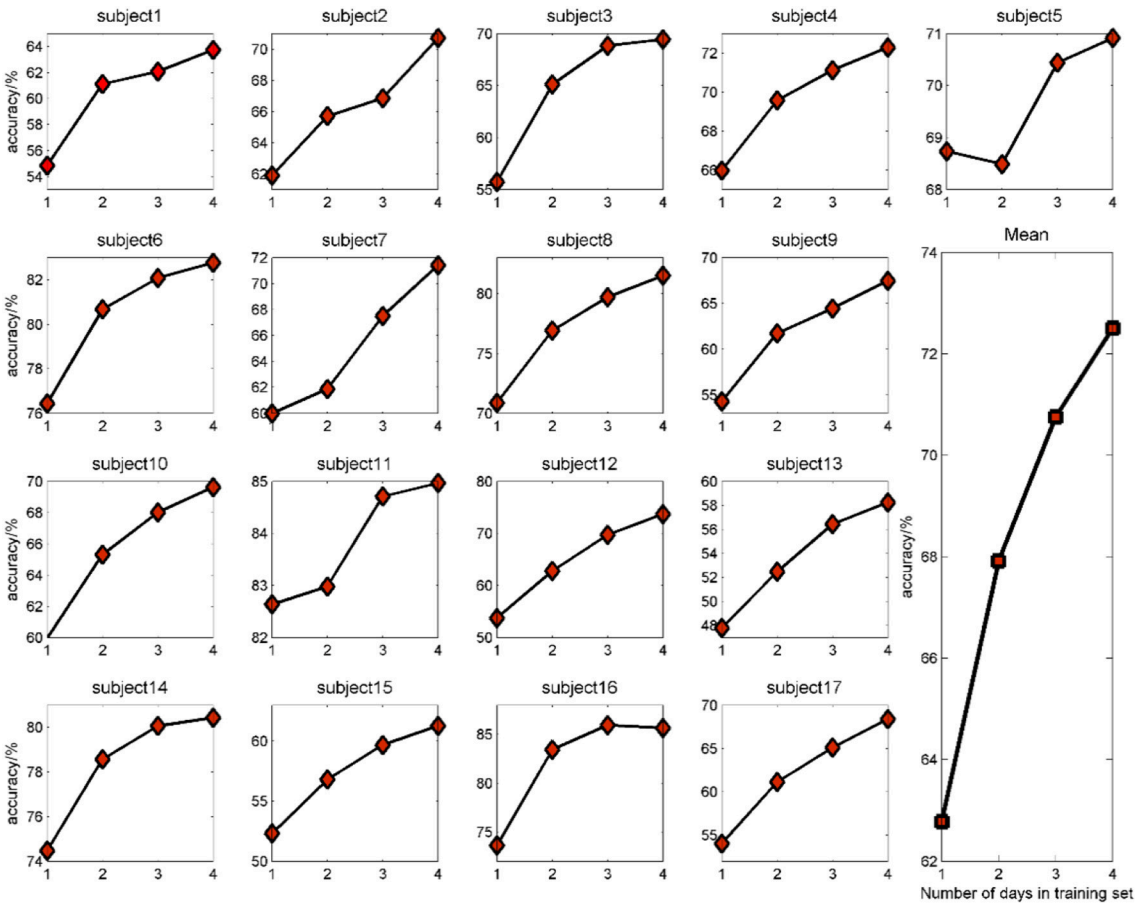


**FIGURE 8 |** Classification accuracy with different number of days in the training set for all the subjects.

determine which emotion state produced the data. However the performance would be undermined by the day-dependent features when the testing samples were completely from an independent day, which was ignored by the existing studies. Prior work handling the day-dependent effect mainly focused on the feature selection. They often tried to find some robust feature which obtained better classification rates from a mass of features, but it did not solve the issue of the day-dependent effect

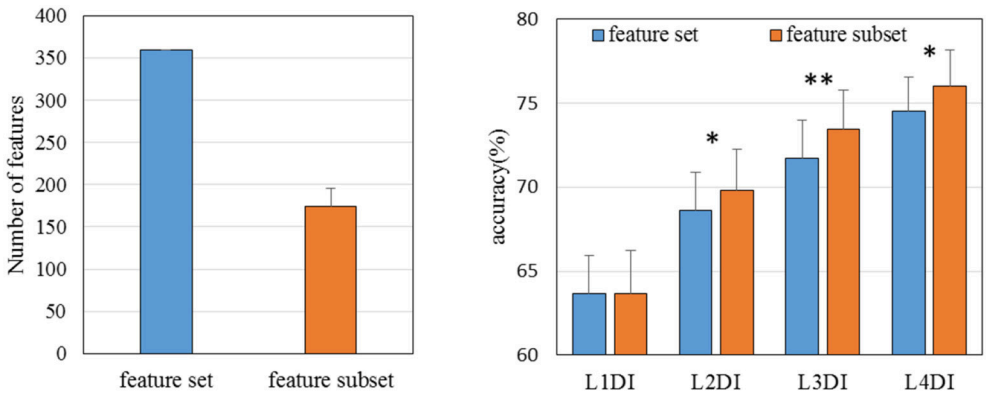


**FIGURE 9 |** The performances of SVMs trained and tested with all 360 features and the feature subset (mean feature numbers was 174 across 17 subjects), respectively. *$P < 0.05$; **$P < 0.01$.

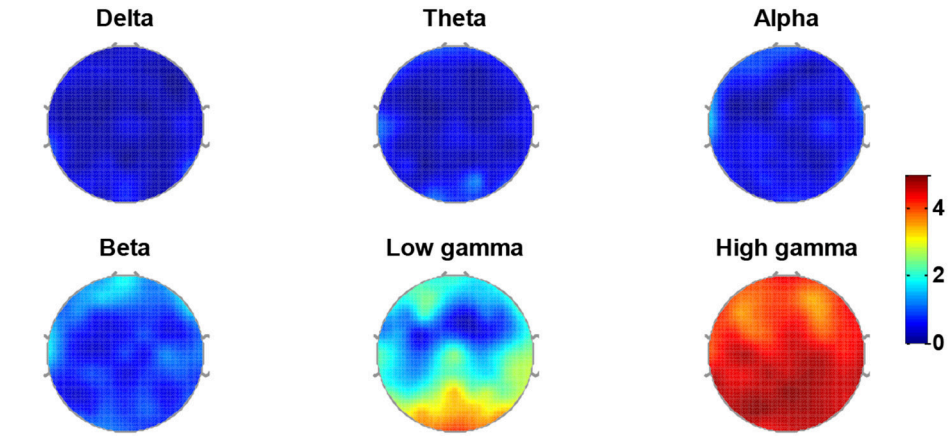


**FIGURE 10 |** Topographic mapping of the quantified feature contributions averaged across 17 subjects for delta, theta, alpha, beta, low gamma, and high gamma bands.

**TABLE 1 |** Confusion Matrices under L4DI condition.

| Real label \ Predicted label | Positive | Neutral | Negative |
|---|---|---|---|
| Positive | 0.715 | 0.144 | 0.1141 |
| Neutral | 0.077 | 0.769 | 0.154 |
| Negative | 0.128 | 0.282 | 0.590 |

thoroughly because the testing data took part in the procedure of feature selection. This study worked on emotion classification improvement by adding the day-to-day variability information into the emotion classifier. A novel classifier strategy, LMDI, was developed to include emotional EEG patterns from different days, which could improve the generalization of a classifier over time.

To avoid overfitting, the data were divided into two equal parts, one part for feature selection and the other for validation. Feature ranking was obtained under L4DI by RFE, and the top 100 features were considered to construct the robust feature subset. It has fortunately been found that accuracies could be significantly improved for all conditions (L1DI, L2DI, L3DI, and L4DI) with the relative low-dimension robust feature subset. These results showed that LMDI indeed improved the generalization of a classifier over time. It could be a substantial step forward in the development of emotion recognition from EEG signals because it may enable a classifier trained on one time to handle another.

All possible combinations of training and testing days were taken into consideration to avoid the impact of any 1 day being an outlier. An issue that should be discussed is whether the day-to-day variation of 1 day apart is smaller than more days apart. Take Day3 as the testing set for example, we obtained average accuracies of 60.8, 67.8, 61.4, and 68.5%, respectively for Day1, Day2, Day4, and Day5 as the training set. This implied the day-to-day variation is not gradually varied with the time, because the variation was caused by the change of EEG baseline, as well as the

external condition such as electrode placements. The influence of day combinations on the recognition accuracies was also discussed here. Take Day 3 as the testing set for example as before, the results showed that there was no significant difference among the classification rates of different combinations respectively for L2DI ($p > 0.1$) and L3DI ($p > 0.1$).

In addition to their importance in emotion studies, day-dependent effect studies may also be indispensable in other fields such as mental workload, and other BCI systems. Therefore, more attention must be paid to day-dependence studies at both basic and applied levels. There are still challenges for future studies. A more generalized study protocol capable of handling different tasks, subjects and days should be a must.

## ETHICS STATEMENT

This study was carried out in accordance with the recommendations of the ethical committee of Tianjin University. The protocol was approved by the ethical committee of Tianjin University. All subjects gave written informed consent in accordance with the Declaration of Helsinki.

## AUTHOR CONTRIBUTIONS

SL: conceptualization, planning, data collection, data analysis, and writing the manuscript. LC: conceptualization, data collection, and proofreading. DG: data collection and supporting data analysis. XL: data collection and proofreading. YS: supporting data collection. YK: conceptualization and supporting data analysis. MX: conceptualization, supporting data analysis. XA: supporting data analysis and proofreading. JY: proofreading. DM: conceptualization, planning, supporting data analysis, and proofreading.

## ACKNOWLEDGMENTS

Supported by National Natural Science Foundation of China (No.81630051, 91520205, 61603269, and 81601565), and Tianjin Key Technology R&D Program (No. 15ZCZDSY00930).

## REFERENCES

Acharya, U. R., Sudarshan, V. K., Adeli, H., Santhosh, J., Koh, J. E. W., Puthankatti, S. D., et al. (2015). A novel depression diagnosis index using nonlinear features in EEG signals. *Eur. Neurol.* 74, 79–83. doi: 10.1159/000438457

Ahmadlou, M., Adeli, H., and Adeli, A. (2012). Fractality analysis of frontal brain in major depressive disorder. *Int. J. Psychophysiol.* 85, 206–211. doi: 10.1016/j.ijpsycho.2012.05.001

Atkinson, J., and Campos, D. (2015). Improving BCI-based emotion recognition by combining EEG feature selection and kernel classifiers? *Expert Syst. Appl.* 47, 35–41. doi: 10.1016/j.eswa.2015.10.049

Balconi, M., and Lucchiari, C. (2006). EEG correlates (event-related desynchronization) of emotional face elaboration: a temporal analysis. *Neurosci. Lett.* 392, 118–123. doi: 10.1016/j.neulet.2005.09.004

Brown, L., Grundlehner, B., and Penders, J. (2011). "Towards wireless emotional valence detection from EEG," in *Paper Presented at the Conference: International Conference of the IEEE Engineering in Medicine & Biology Society IEEE Engineering in Medicine & Biology Society Conference* (Boston, MA).

Chang, C. C., and Lin, C. J. (2006). LIBSVM: a library for support vector machines. *ACM Trans. Intell. Syst. Technol.* 2, 389–396. doi: 10.1145/1961189.1961199

Chueh, T., chen, T., Lu, H. H., Ju, S., Tao, T., and Shaw, J. (2012). Statistical prediction of emotional states by physiological signals with manova and machine learning. *Int. J. Patt. Recogn. Artif. Intell.* 26:1250008. doi: 10.1142/S0218001412500085

Duan, R. N., Zhu, J. Y., and Lu, B. L. (2013). "Differential entropy feature for EEG-based emotion classification," in *Paper presented at the International IEEE/EMBS Conference on Neural Engineering* (San Diego, CA).

Gasser, T., Bächer, P., and Steinberg, H. (1985). Test-retest reliability of spectral parameters of the EEG. *Electroencephalogr. Clin. Neurophysiol.* 60, 312–319. doi: 10.1016/0013-4694(85)90005-7

Gudmundsson, S., Runarsson, T. P., Sigurdsson, S., Eiriksdottir, G., and Johnsen, K. (2007). Reliability of quantitative EEG features. *Clin. Neurophysiol.* 118, 2162–2171. doi: 10.1016/j.clinph.2007.06.018

Guyon, I., and Elisseeff, A. (2003). An introduction to variable feature selection. *J. Mach. Learn. Res.* 3, 1157–1182.

Hidalgo-Muñoz, A., López, M., Pereira, A., Santos, I., and Tomé, A. (2013). Spectral turbulence measuring as feature extraction method from EEG on affective computing. *Biomed. Signal Process. Control* 8, 945–950. doi: 10.1016/j.bspc.2013.09.006

Hidalgo-Muñoz, A. R., López, M. M., Santos, I. M., Pereira, A. T., Vázquez-Marrufo, M., Galvao-Carmona, A., et al. (2013). Application of SVM-RFE on EEG signals for detecting the most relevant scalp regions linked to affective valence processing. *Expert Syst. Appl.* 40, 2102–2108. doi: 10.1016/j.eswa.2012.10.013

Khalili, Z., and Moradi, M. (2008). "Emotion detection using brain and peripheral signals," *Paper Presented at the Biomedical Engineering Conference, CIBEC 2008, Cairo International* (Cairo).

Kim, J., and André, E. (2008). Emotion recognition based on physiological changes in music listening. *IEEE Trans. Patt. Anal. Mach. Intell.* 30, 2067–2083. doi: 10.1109/TPAMI.2008.26

Koelstra, S., Muhl, C., Soleymani, M., Lee, J.-S., Yazdani, A., Ebrahimi, T., et al. (2012). Deap: a database for emotion analysis; using physiological signals. *IEEE Trans. Affect. Comput.* 3, 18–31. doi: 10.1109/T-AFFC.2011.15

Kondacs, A., and Szabó, M. (1999). Long-term intra-individual variability of the background EEG in normals. *Clin. Neurophysiol.* 110, 1708–1716. doi: 10.1016/S1388-2457(99)00122-4

Lan, Z., Sourina, O., Wang, L., and Liu, Y. (2014). "Stability of features in real-time EEG-based Emotion Recognition Algorithm," in *Paper Presented at the International Conference on Cyberworlds* (Santander).

Lee, G., Kwon, M., Sri, S. K., and Lee, M. (2014). Emotion recognition based on 3D fuzzy visual and EEG features in movie clips. *Neurocomputing* 144, 560–568. doi: 10.1016/j.neucom.2014.04.008

Li, Y., Ma, Z., Lu, W., and Li, Y. (2006). Automatic removal of the eye blink artifact from EEG using an ICA-based template matching approach. *Physiol. Meas.* 27, 425–436. doi: 10.1088/0967-3334/27/4/008

Liu, Y., Sourina, O., and Nguyen, M. K. (2010). "Real-time EEG-based human emotion recognition and visualization," in *Paper Presented at the International Conference on Cyberworlds* (Singapore).

Martini, N., Menicucci, D., Sebastiani, L., Bedini, R., Pingitore, A., Vanello, N., et al. (2012). The dynamics of EEG gamma responses to unpleasant visual stimuli: from local activity to functional connectivity. *Neuroimage* 60, 922–932. doi: 10.1016/j.neuroimage.2012.01.060

Miskovic, V., and Schmidt, L. A. (2010). Cross-regional cortical synchronization during affective image viewing. *Brain Res.* 1362, 102–111. doi: 10.1016/j.brainres.2010.09.102

Murugappan, M., Nagarajan, R., and Yaacob, S. (2010). Combining spatial filtering and wavelet transform for classifying human emotions using EEG signals. *J. Med. Biol. Eng.* 31, 45–51. doi: 10.5405/jmbe.710

Nasoz, F., Alvarez, K., Lisetti, C. L., and Finkelstein, N. (2004). Emotion recognition from physiological signals using wireless sensors for presence technologies. *Cogn. Technol. Work* 6, 4–14. doi: 10.1007/s10111-003-0143-x+

Nie, D., Wang, X. W., Shi, L. C., and Lu, B. L. (2011). "EEG-based emotion recognition during watching movies," in *Paper Presented at the International IEEE/EMBS Conference on Neural Engineering* (Cancun).

Salinsky, M. C., Oken, B. S., and Morehead, L. (1991). Test-retest reliability in EEG frequency analysis. *Electroencephalogr. Clin. Neurophysiol.* 79, 382–392. doi: 10.1016/0013-4694(91)90203-G

Soleymani, M., Pantic, M., and Pun, T. (2012). Multimodal emotion recognition in response to videos. *IEEE Trans Affect. Comput.* 3, 211–223. doi: 10.1109/T-AFFC.2011.37

Sourina, O., Sourin, A., and Kulish, V. (2009). "EEG data driven animation and its application," in *Paper presented at the International Conference on Computer Vision/computer Graphics Collaboration Techniques* (Rocquencourt).

Tytell, D. (1961). The ten twenty electrode system: international federation of societies for electroencephalography and clinical neurophysiology. *Am. J. EEG Technol.* 110, 13–19.

Verma, G. K., and Tiwary, U. S. (2014). Multimodal fusion framework: a multiresolution approach for emotion classification and recognition from physiological signals. *Neuroimage* 102, 162–172. doi: 10.1016/j.neuroimage.2013.11.007

Wang, X.-W., Nie, D., and Lu, B.-L. (2014). Emotional state classification from EEG data using machine learning approach. *Neurocomputing* 129, 94–106. doi: 10.1016/j.neucom.2013.06.046

Xu, M., Liu, J., Chen, L., Qi, H., He, F., Zhou, P., et al. (2016). Incorporation of inter-subject information to improve the accuracy of subject-specific P300 classifiers. *Int. J. Neural Syst.* 26:1650010. doi: 10.1142/S0129065716500106

Yin, Z., Zhao, M., Wang, Y., Yang, J., and Zhang, J. (2017). Recognition of emotions using multimodal physiological signals and an ensemble deep learning model. *Comput. Methods Programs Biomed.* 140, 93–110. doi: 10.1016/j.cmpb.2016.12.005

Yoon, H. J., and Chung, S. Y. (2013). EEG-based emotion estimation using Bayesian weighted-log-posterior function and perceptron convergence algorithm. *Comput. Biol. Med.* 43, 2230–2237. doi: 10.1016/j.compbiomed.2013.10.017

**Conflict of Interest Statement:** The authors declare that the research was conducted in the absence of any commercial or financial relationships that could be construed as a potential conflict of interest.

frontiers in Human Neuroscience

ORIGINAL RESEARCH
published: 03 August 2018
doi: 10.3389/fnhum.2018.00317

# Anodal Transcranial Direct Current Stimulation Over the Supplementary Motor Area Improves Anticipatory Postural Adjustments in Older Adults

*Tomonori Nomura[1]* and Hikari Kirimoto[2]*

*[1] Faculty of Rehabilitation, Niigata University of Health and Welfare, Niigata, Japan, [2] Department of Sensorimotor Neuroscience, Graduate School of Biomedical and Health Sciences, Hiroshima University, Hiroshima, Japan*

We examined the influence of anodal transcranial direct current stimulation (tDCS) over the supplementary motor area (SMA) on anticipatory postural adjustments (APAs) and center of pressure (COP) sway in older adults. The study enrolled 12 healthy older adult volunteers. Subjects received anodal tDCS (2 mA) or sham stimulation over the SMA for 15 min and performed a self-paced rapid upward arm movement task on a force plate before, immediately after, and 15 min after the stimulation condition. APAs were measured as the temporal difference between activation onset in the deltoid anterior (AD) and biceps femoris (BF) muscles. The root mean square (RMS) area of COP sway, sway path length, medio-lateral mean velocity, and antero-posterior mean velocity of standing posture were also measured before and after the stimulation condition during the task. Anodal tDCS of the SMA extended APAs and decreased COP sway path length immediately after and 15 min after stimulation compared to baseline. These findings suggest that anodal tDCS over the SMA enhanced APAs function and improved postural sway during rapid upward arm movement in older adults.

**Keywords: anticipatory postural adjustments, center of pressure sway, motor deficit, supplementary motor area, transcranial direct current stimulation**

OPEN ACCESS

***Edited by:***
*Delin Sun,*
*Duke University, United States*

***Reviewed by:***
*Rahul Goel,*
*Baylor College of Medicine, United States*
*Wei Peng Teo,*
*Deakin University, Australia*

****Correspondence:***
*Tomonori Nomura*
*nomura@nuhw.ac.jp*

***Received:*** *06 April 2018*
***Accepted:*** *18 July 2018*
***Published:*** *03 August 2018*

***Citation:***
*Nomura T and Kirimoto H (2018) Anodal Transcranial Direct Current Stimulation Over the Supplementary Motor Area Improves Anticipatory Postural Adjustments in Older Adults. Front. Hum. Neurosci. 12:317. doi: 10.3389/fnhum.2018.00317*

## INTRODUCTION

Nitsche and Paulus (2000) were the first to report modulation of the primary motor cortex (M1) by anodal transcranial direct current stimulation (tDCS) in human subjects. Since this discovery, numerous studies have described anodal tDCS as a useful tool for improving motor performance in healthy subjects and patients with neurological disorders such as stroke hemiplegia (see review, Hashemirad et al., 2016; Kang et al., 2016). The direction of current flow determines the effects on the underlying tissue. When tDCS is applied over the primary motor cortex (M1), anodal tDCS (using the anodal electrode over M1 and the cathodal electrode over the contralateral orbit) enhances cortical excitability, which increases the amplitude of motor evoked potentials (MEPs). On the other hand, cathodal tDCS (using the cathodal electrode over M1) shows the opposite effect (Nitsche and Paulus, 2000). Yet, most previous studies applied tDCS over M1 rather than the motor association cortex. A recent study demonstrated that anodal tDCS over the supplementary motor area (SMA) promotes short-term visuomotor learning (Vollmann et al., 2013) and improves reaction times in the balance task, which is a task that requires complex planning (Hupfeld et al., 2017). In addition, anodal tDCS over SMA modulates anticipatory postural adjustments

(APAs) in index finger flection tasks (Bolzoni et al., 2015) while cathodal stimulation has an inhibitory effect on APAs in rapid upward arm movements while standing (Kirimoto et al., 2013). Accordingly, anodal tDCS over the SMA may have important therapeutic utility for older adults with deteriorated balance function.

The SMA plays an important role in motor planning prior to the initiation of movement (Stephan et al., 1995; Taube et al., 2015). APAs are a representative function of the SMA. In the first report to describe APAs, it was found that activation of the postural muscles of the legs and trunk that control standing posture preceded the activation of muscles directly involved in rapid upward arm movements while standing (Belen'kii et al., 1967). APAs function is markedly reduced in patients with Parkinson's disease; as such, the basal ganglia–subthalamic nucleus–SMA loop is thought to be involved in APAs generation (Jacobs et al., 2009). Additionally, brain function imaging studies combining functional magnetic resonance imaging (fMRI) or magnetoencephalography (MEG) and electroencephalography (EEG) have described increased excitability in the SMA, globus pallidus, putamen, and thalamus during bimanual load-lifting tasks involving APAs with healthy subjects (Ng et al., 2011).

Older adults without lesions in the basal ganglia–subthalamic nucleus–SMA loop have lower APAs than young adults (Kanekar and Aruin, 2014), and the functional degradation of APAs is associated with an increased risk of falls in older adults (Overstall et al., 1977; Hass et al., 2008). While balance is not just purely controlled via central motor processes, but also involves an interaction with cognitive function, a decrease in the connectivity of SMA – basal ganglia – thalamus, which play an important role in postural adjustment, may be considered as one cause for the reduction of APAs function. Hence, anodal tDCS over the SMA is one possible approach to restoring APA function as a fall prevention measure in aging individuals. Two previous reports have described an effect of tDCS over the SMA on APAs in healthy young adults (Kirimoto et al., 2013; Bolzoni et al., 2015), however, to our knowledge, no study has described effects on APAs function and postural regulation in older adults. If tDCS over SMA for older adults promotes the start of activation of postural muscle preceding the prime mover muscle in rapid upward arm movement tasks, it is expected to have the effect of preventing falls due to an individual's posture change.

The aim of this study was to compare APAs and center of pressure (COP) sway at the time of a rapid upward arm movement before and after tDCS over the SMA in older adults, and to inform the potential utility of this intervention for fall prevention.

# MATERIALS AND METHODS

## Subjects

We studied 12 healthy older adults [4 men and 8 women, 72.3 ± 5.3 years, mean ± standard deviation (SD)] who were able to understand and follow instructions and were without neurologic, sensory, motor, vision, or cognitive impairment. We also used a brief assessment of cognitive status, the Mini Mental Status Examination (MMSE) which patients scored on average, 29.7 ± 0.5 (mean ± SD). All subjects were strongly right-handed as determined by an Oldfield inventory score of 0.9–1.0 (Oldfield, 1971). All subjects provided written informed consent prior to the experiment. The study was conducted in accordance with the Declaration of Helsinki and the experimental protocol was approved by the ethics committee of Niigata University of Health and Welfare (approval no. 17789–170303).

## Experimental Procedures

All subjects received anodal tDCS (2 mA) or sham stimulation for 15 min in a counter-balanced order. To avoid carryover effects, each volunteer completed 2 sessions of 10 trials each on separate days that were each at least 14 days apart. Subjects performed self-paced rapid upward arm movements 10 times on a force plate before, immediately after, and 15 min after tDCS. Throughout the experiment, subjects were asked to make upward arm movements as fast as they could, and to maintain a constant COP. Prior to the start of the experiment, each subject performed the task of holding a 30 s resting standing position on the COP measurement force plate, 3 times, which was measured and the average coordinates were calculated. Subjects stood on the force plate and confirmed that their own COP position was within the average coordinate on a monitor. They were then instructed to move the right arm upward and forward to shoulder level at full speed, then hold this position for 3 s. Subjects gazed at their own COP position during the task execution and we instructed them to constantly raise their arm at a maximum effort speed in the same forward direction and to take care not to change the COP position during the task execution. In order to reduce the learning effect of the assignment, the experiment was started after sufficient training before each test session. During the task, electromyography (EMG) activity was recorded from the deltoid anterior (AD) as the prime mover muscle and the biceps femoris (BF) as a postural muscle, according to previous APAs studies (Kanekar and Aruin, 2014; Kubicki et al., 2016). Additionally, an accelerometer taped to right wrist was used to evaluate movement of the arm.

## tDCS

Transcranial direct current stimulation was delivered using a direct current stimulator (Eldith; NeuroConn GmbH, Ilmenau, Germany) through a pair of saline-soaked surface sponge electrodes (anodal, 3 cm × 3 cm; cathodal, 5 cm × 7 cm). The anodal electrode was placed to cover FC1 and FC3, which corresponds to the left SMA based on the international 10–20 extended system for electrode placement, as previously reported (Vollmann et al., 2013; Hupfeld et al., 2017). This landmark was identified by measuring and marking the skull prior to electrode placement, similar to previous studies (Cui et al., 1999; Oostenveld and Praamstra, 2001; Stock et al., 2013). The cathode electrode was placed above the right supraorbital region in order to be functionally inefficient as previously shown (Nitsche and Paulus, 2000; Nitsche et al., 2007). The current intensity of tDCS was 2 mA and the duration of stimulation was 15 min with a 30 s fade-in/fade-out time. In the sham experiment, tDCS was turned off after 30 s (Gandiga et al., 2006).

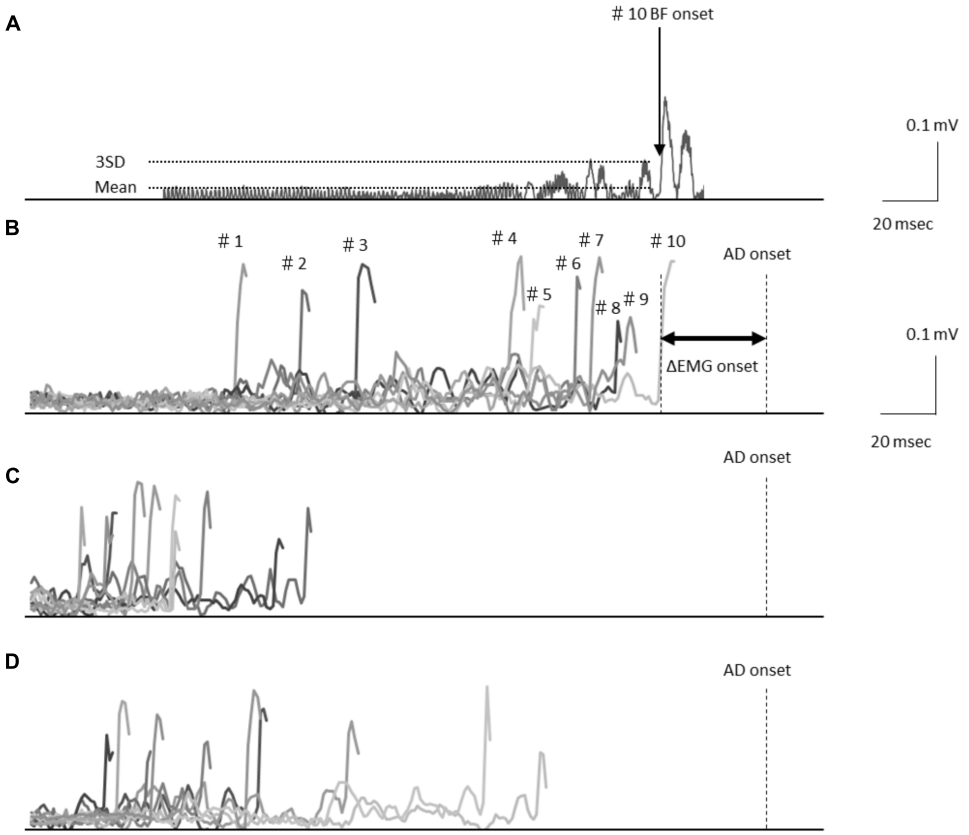


**FIGURE 1 | (A)** Electromyography waveforms in the biceps femoris (BF) during a self-paced rapid shoulder flexion task for a representative case. BF onset was defined as the point at which the EMG signal reached at least 3 standard deviations above the mean baseline. Data are shown representing the baseline stimulation condition **(B)**, immediately after stimulation **(C)**, and 15 min after stimulation **(D)** recorded from the representative subject. Electromyography waveforms were presented for the baseline stimulation condition in 10 trials of BF onset. Latency differences (ΔEMG onset) were calculated by subtracting the time of EMG burst onset of the BF (BF onset) from that of the activation onset of the deltoid anterior muscle (AD) (AD onset).

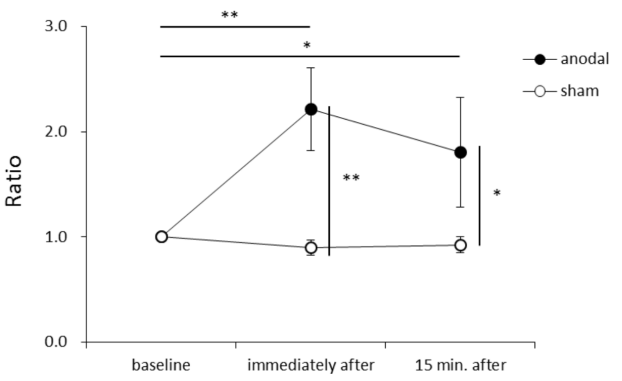


**FIGURE 2 |** Serial changes in ΔEMG onset before, immediately after, and 15 min after anodal or sham transcranial direct current stimulation (tDCS) over the supplementary motor area (SMA). ΔEMG onset was calculated by subtracting the time of EMG burst onset of the biceps femoris from that of the activation onset of the deltoid anterior muscle. Data were normalized to average value at baseline (mean ± standard error of the mean). $*p < 0.05$, $**p < 0.01$.

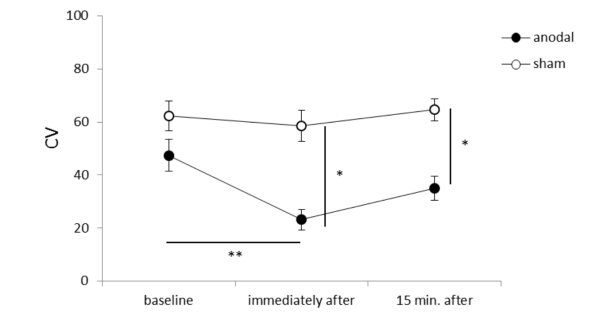


**FIGURE 3 |** Serial changes in the percentage coefficient of variation (CV) before, immediately after, and 15 min after anodal or sham tDCS over the SMA (mean ± standard error of the mean). $*p < 0.05$, $**p < 0.01$.

## COP Recording

Subjects stood upright on a force plate (CFP400PA102RS, Leptrino, Japan) with equal weight on each foot and their eyes open. COP visual feedback was provided on a monitor 1.5 m in

front of participants with a height parallel to the line of sight. On the force plate, the distance between the feet was equal to the distance between the shoulder peaks, and the bottom outside of both fifth proximal phalanges was adjusted to the same distance. Subjects were instructed to look at and maintain the displayed COP position during the rapid upward right arm movement task. Ground reaction signals were recorded at 100 Hz and low-pass filtered (20 Hz). Data were recorded and stored on a personal computer for off-line analysis (BSMLGR, Leptrino, Japan). The average COP RMS area, sway path length, medio-lateral (ML) mean velocity, and antero-posterior (AP) mean velocity were calculated for analysis.

## EMG and Acceleration Recording

Surface EMG was recorded from the right AD and BF muscles using double differential active electrodes (FSE-DEMG1, 4Assist, Japan). The skin was cleaned with alcohol and the recording and reference electrodes were placed over the center of each muscle. A ground electrode was attached to the anterior aspect of the leg over the left tibia. EMG signals were amplified (×500) and band-pass filtered (5–1,000 Hz) with an EMG amplifier system (FA-DL-140, 4assist, Japan) and digitized at 10 KHz (PowerLab, AD Instruments, Bella Vista, NSW, Australia). Data were also recorded form 3-axis acceleration sensors (FA-DL-110, 4Assist, Japan) attached to the subject's right wrist and stored on a personal computer for off-line analysis (Chart 7, AD Instruments, Bella Vista, NSW, Australia).

## Statistical Analysis

The EMG signal baseline for each muscle was sampled over a period of 100 ms while the participant stood quietly prior to beginning any movement. The activity onset in each muscle was defined as the point at which the EMG signal reached at least 3 SD above the mean baseline for a period of at least 20 ms (Nana-Ibrahim et al., 2008). APAs were measured by computing their timing (APAt) as previously reported (Fujiwara et al., 2003). APAt was defined as the temporal difference between activation onset in the AD and BF muscles (ΔEMG onset). The coefficient of variations (CV) was calculated to confirm the stability of the change of ΔEMG onset. The calculated average value ($\overline{X}$) and SD (σ) of ΔEMG onset for each session ($CV = \sigma/\overline{X}$) was then determined. A decreasing CV with a ΔEMG onset indicated a stable ΔEMG onset. Acceleration onset was measured using the same calculation method as EMG onset based on the 1,000 ms before and after movement onset; these values were used to compute the interval of acceleration and COP. The average acceleration and maximum acceleration on the y axis were measured, and the accuracy of the upward arm movement was evaluated. ΔEMG onset, average acceleration, maximum acceleration, RMS area, sway path length, ML mean velocity, and AP mean velocity were calculated the average data of the 10 trials each stimulation condition and normalized by the average values obtained before the stimulation condition. Parameter values taken before tDCS, immediately after tDCS, and 15 min after tDCS were compared with a two-way repeated-measures analysis of variance (ANOVA) (intervention [sham, anodal]) × (time [before tDCS, immediately after tDCS, 15 min after tDCS]). Significant differences were further analyzed with Bonferroni *post hoc* tests. All analyses were performed with IBM SPSS Statistics software version 20 (SPSS; IBM, Armonk, NY, United States) and the significance level was set at 5%.

# RESULTS

## EMG Activity After tDCS Over the SMA

**Figure 1** shows representative EMG waveforms in the BF during the self-paced rapid shoulder flexion task before, immediately after, and 15 min after anodal tDCS over the SMA. ΔEMG onset was extended after anodal tDCS compared to baseline. A two-way repeated measures ANOVA of ΔEMG onset revealed significant main effects of intervention [$F_{(1,11)} = 10.267$, $p = 0.008$, $\eta^2 = 0.483$, $1–\beta = 0.83$], time [$F_{(2,22)} = 6.595$, $p = 0.006$, $\eta^2 = 0.375$, $1–\beta = 0.74$], and the intervention × time interaction term [$F_{(2,22)} = 11.293$, $p = 0.002$, $\eta^2 = 0.432$, $1–\beta = 0.81$] (**Figure 2**). A *post hoc* analysis revealed significant differences between anodal and sham tDCS both immediately after ($p = 0.005$) and 15 min after stimulation ($p = 0.020$). There were also significant differences between baseline and immediately after stimulation ($p = 0.006$) and between baseline and 15 min after stimulation for anodal tDCS ($p = 0.025$). **Figure 3** shows percentages of the coefficients of variation (CVs) in ΔEMG onset. An ANOVA of *CV*-values revealed significant main effects of intervention [$F_{(1,11)} = 6.187$, $p = 0.032$, $\eta^2 = 0.382$, $1–\beta = 0.62$] and time [$F_{(2,22)} = 3.982$, $p = 0.035$, $\eta^2 = 0.285$, $1–\beta = 0.65$]. A *post hoc* analysis showed significant differences between anodal and sham tDCS both immediately after ($p = 0.022$) and 15 min after stimulation ($p = 0.017$). There was also a significant difference between baseline and immediately after stimulation for anodal tDCS ($p = 0.002$).

## Upward Arm Movement Acceleration

**Figure 4** shows the average acceleration (A) and maximum acceleration (B) of rapid upward arm movements in the y-axis for each time-point in each stimulation condition. There were no significant between-group or within-group differences.

## COP Sway After tDCS Over the SMA

**Figure 5** shows the RMS area, sway path length, ML mean velocity, and AP mean velocity for each time-point in each stimulation condition. An ANOVA of sway path length revealed significant main effects of intervention [$F_{(1,11)} = 6.449$, $p = 0.028$, $\eta^2 = 0.370$, $1–\beta = 0.74$], time [$F_{(2,22)} = 7.085$, $p = 0.004$, $\eta^2 = 0.392$, $1–\beta = 0.82$], and the intervention × time interaction term [$F_{(2,22)} = 4.197$, $p = 0.029$, $\eta^2 = 0.276$, $1–\beta = 0.60$]. A *post hoc* analysis showed significant differences between anodal and sham tDCS immediately after stimulation ($p = 0.022$), between baseline and immediately after stimulation for anodal tDCS ($p < 0.001$), and between baseline and 15 min after stimulation for anodal tDCS ($p < 0.001$). An ANOVA of AP mean velocity revealed a significant main effect of time [$F_{(2,22)} = 5.713$, $p = 0.010$, $\eta^2 = 0.342$, $1–\beta = 0.60$]. A *post hoc* analysis showed significant differences between baseline and immediately after stimulation for anodal tDCS ($p = 0.004$), and between baseline and 15 min

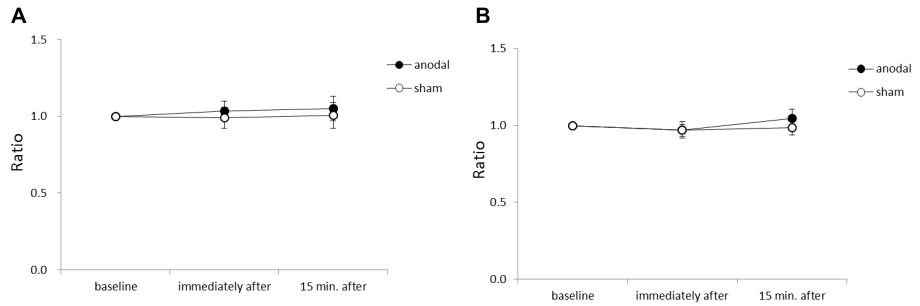


**FIGURE 4 |** Serial changes in average acceleration and maximum acceleration in the *y*-axis before, immediately after, and 15 min after anodal or sham tDCS over the SMA. **(A)** Normalized values of average acceleration in the *y*-axis. **(B)** Normalized values of maximum acceleration in the *y*-axis. All data reflect the mean ± standard error of the mean.

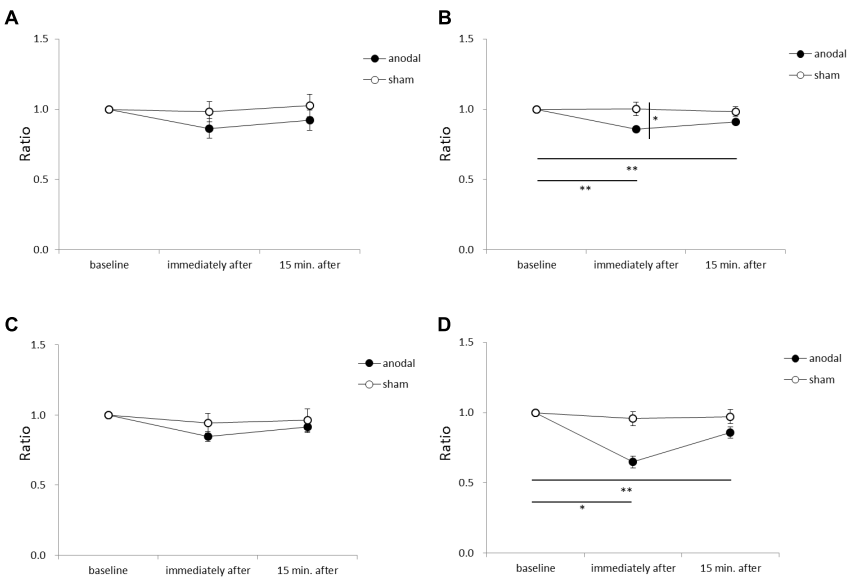


**FIGURE 5 |** Serial changes in root mean square (RMS) area, sway path length, medio-lateral (ML) mean velocity, and antero-posterior (AP) mean velocity before, immediately after, and 15 min after anodal or sham tDCS over the SMA. **(A)** Normalized RMS area values. **(B)** Normalized sway path length values. **(C)** Normalized ML mean velocity values. **(D)** Normalized AP mean velocity values. All data reflect the mean ± standard error of the mean. $^{*}p < 0.05$, $^{**}p < 0.01$.

after stimulation for anodal tDCS ($p = 0.012$). There were no significant between-group or within-group differences in RMS area or ML mean velocity.

## DISCUSSION

The present study demonstrated that anodal tDCS over the SMA extended ΔEMG onset time for the AD and BF muscles during a rapid upward arm movement task in healthy older adults. Additionally, the CV of ΔEMG onset was decreased after anodal tDCS compared to sham stimulation. Further, COP sway path length was decreased immediately after and 15 min after tDCS compared to baseline. These findings suggest that tDCS over the SMA enhanced the timing of postural regulator muscle activity preceding rapid upward arm movements and strengthened stable execution of the APAs function in healthy older individuals.

Previous studies have reported that APAs are changed by the COP position before the start of motion (Fujiwara et al., 2003) and by acceleration in the upward arm movement task (Lee et al., 1987). When upward arm movements are made slowly with backward positioning of the body's center of gravity, forward movement of the body center of gravity is estimated to be small, and thus APAs time is shortened. In this study, subjects were asked to execute upward arm movements as fast as they could while maintaining a constant COP. Importantly, average acceleration of the rapid upward arm movement did not vary between before and after tDCS. Therefore, changes in ΔEMG onset and its CV as well as COP sway path length can be attributed to anodal tDCS over the SMA rather than confounding factors such as changes in COP position and decreased acceleration of upward arm movements over time.

As described in other postural control tasks, older adults exhibit delays in the onset of anticipatory postural EMG activity

compared to young adults (Kanekar and Aruin, 2014). In our previous study, the APAs time of young adults was 60 ms in a self-paced rapid upward arm movement task (Kirimoto et al., 2013). In this study of older subjects, the APAs time was extended from 36 ms pre-stimulation to 81 ms immediately after stimulation. This result shows that APAs time of older subjects pre-stimulation is delayed more than in the young subjects and approaches APA time of young subjects immediately after stimulation. Studies of young healthy adults suggest that anodal tDCS over the SMA is associated with improvements in motor skill (Vollmann et al., 2013). Further, SMA activation appears to be highly correlated with motor skill learning, suggesting an important role of the SMA in the acquisition of new motor skills (Lefebvre et al., 2012). Our results are consistent with these studies and suggest that anodal tDCS improved the stability of the postural control during rapid upward arm movement. The stability of posture control is meaningful for older adults, as many activities of daily living are conventionally performed in a stable standing position.

Our results also showed positive effects of anodal tDCS on the COP sway path length, corresponding to improved motor performance in postural control. The COP sway path length is increased in older adults compared to young adults (Benjuya et al., 2004). Additionally, fallers show a significantly higher COP sway path length compared to non-fallers (Melzer et al., 2004), and the COP sway path length is an independent factor predicting falls in older adults (Johansson et al., 2017). Taken together, improvements in the COP sway path length by anodal tDCS over the SMA may decrease the likelihood of falling in older adults.

Transcranial direct current stimulation is a non-invasive technique that allows the modulation of cortical excitability in humans (Nitsche and Paulus, 2000; Priori, 2003). It is thought that neuronal cell membranes below the anode are depolarized while those below the cathode are hyperpolarized, leading to increases and decreases in cortical excitability, respectively (Nitsche and Paulus, 2000; Antal et al., 2017; Lefaucheur et al., 2017). The cathode electrode is most effective when placed on the forehead on the contralateral side (Nitsche and Paulus, 2000). However, in any place it may affect the cortex beneath the cathode electrode (Schambra et al., 2011). It may also be necessary to consider placing the reference electrode outside the head. Numerous studies have reported the improvement of various motor functions by tDCS over M1 in healthy subjects and patients on the premise of this hypothesis (Hashemirad et al., 2016; Kang et al., 2016). In this study, we selected the SMA stimuli position by using tDCS on the scalp in conformity with a previous study of SMA tDCS in young adults by Hupfeld et al. (2017). Anode tDCS can lead to improved connectivity of the SMA pathway, connectivity between SMA and M1, SMA- cerebellar connectivity (Hamada et al., 2009; Polanía et al., 2012; Hupfeld et al., 2017). We hypothesize that tDCS promoted connectivity of the SMA modulated within the APAs processing network, consistent with the implications of previous research. It is possible that reinforcement of mutual connectivity of the SMA may have a positive effect on posture adjustment improvement. In our previous study, we also reported stimulatory effects of simultaneous tDCS over the SMA and dorsal premotor cortex on distant sites including M1 and the somatosensory cortex (Kirimoto et al., 2011). Accordingly, it is possible that the modulation of areas other than the SMA responsible for generating and outputting APAs (e.g., M1) was in part responsible for the observed changes in EMG and COP parameters in older adults. Further studies are needed to elucidate the neurophysiological effects of tDCS. In particular, it is necessary to verify whether there is an effect of tDCS over the SMA on posture control and risk of falling in older adults using electrophysiological methods.

### Limitations

The sample size was small in this study which was one of the major limitations. However, in our study, we were able to examine whether the anodal tDCS can contribute to posture control for APAs functional changes due to aging of healthy older adults. These results have the potential to inform the development of anodal tDCS enhanced protocols in training. The effects of promotion of APAs function may be expected using the anodal tDCS as a condition stimulus before training. We will continue to consider protocols for older adults with balance disabilities. The findings in this study may assist with the development of enhanced protocols involving the combination of anode tDCS with exercise training and other rehabilitation protocols.

## CONCLUSION

The present study demonstrates that anodal tDCS over the SMA extended ΔEMG onset time, decreased the CV of ΔEMG onset time, and reduced the COP sway path length during a rapid upward arm movement task. We suggest that anodal tDCS over the SMA is an effective method for improving APAs function in older adults.

## AUTHOR CONTRIBUTIONS

HK conceived the study and designed the experiment. TN conducted the experiments. TN and HK performed the statistical analysis and interpreted the data, wrote and approved the manuscript.

## FUNDING

This work was supported by JSPS KAKENHI grant numbers JP17K01533 and JP16K01522 and by a Grant-in-Aid for Challenging Exploratory Research from Niigata University of Health and Welfare, 2016 (H28B16).

## ACKNOWLEDGMENTS

We thank all the study volunteers for their time and patience during experiments.

## REFERENCES


Antal, A., Alekseichuk, I., Bikson, M., Brockmoller, J., Brunoni, A. R., Chen, R., et al. (2017). Low intensity transcranial electric stimulation: safety, ethical, legal regulatory and application guidelines. *Clin. Neurophysiol.* 128, 1774–1809. doi: 10.1016/j.clinph.2017.06.001

Belen'kii, V. E., Gurfinkel, V. S., and Pal'tsev, E. I. (1967). Control elements of voluntary movements. *Biofizika* 12, 135–141.

Benjuya, N., Melzer, I., and Kaplanski, J. (2004). Aging-induced shifts from a reliance on sensory input to muscle cocontraction during balanced standing. *J. Gerontol. A Biol. Sci. Med. Sci.* 59, 166–171. doi: 10.1093/gerona/59.2.M166

Bolzoni, F., Bruttini, C., Esposti, R., Castellani, C., and Cavallari, P. (2015). Transcranial direct current stimulation of SMA modulates anticipatory postural adjustments without affecting the primary movement. *Behav. Brain Res.* 291, 407–413. doi: 10.1016/j.bbr.2015.05.044

Cui, R. Q., Huter, D., Lang, W., and Deecke, L. (1999). Neuroimage of voluntary movement: topography of the Bereitschaftspotential, a 64-channel DC current source density study. *Neuroimage* 9, 124–134. doi: 10.1006/nimg.1998.0388

Fujiwara, K., Maeda, K., and Toyama, H. (2003). Influences of illusionary position perception on anticipatory postural control associated with arm flexion. *J. Electromyogr. Kinesiol.* 13, 509–517. doi: 10.1016/S1050-6411(03)00083-X

Gandiga, P. C., Hummel, F. C., and Cohen, L. G. (2006). Transcranial DC stimulation (tDCS): a tool for double-blind sham-controlled clinical studies in brain stimulation. *Clin. Neurophysiol.* 117, 845–850. doi: 10.1016/j.clinph.2005.12.003

Hamada, M., Hanajma, R., Terao, Y., Okabe, S., Nakatani-Enomoto, S., Furubayashi, T., et al. (2009). Primary motor cortical metaplasticity induced by priming over the supplementary motor area. *J. Physiol.* 587, 4845–4862. doi: 10.1113/jphysiol.2009.179101

Hashemirad, F., Zoghi, M., Fitzgerald, P. B., and Jaberzadeh, S. (2016). The effect of anodal transcranial direct current stimulation on motor sequence learning in healthy individuals: a systematic review and meta-analysis. *Brain Cogn.* 102, 1–12. doi: 10.1016/j.bandc.2015.11.005

Hass, C. J., Waddell, D. E., Wolf, S. L., Juncos, J. L., and Gregor, R. J. (2008). Gait initiation in older adults with postural instability. *Clin. Biomech.* 23, 743–753. doi: 10.1016/j.clinbiomech.2008.02.012

Hupfeld, K. E., Ketcham, C. J., and Schneider, H. D. (2017). Transcranial direct current stimulation (tDCS) to the supplementary motor area (SMA) influences performance on motor tasks. *Exp. Brain Res.* 235, 851–859. doi: 10.1007/s00221-016-4848-5

Jacobs, J. V., Lou, J. S., Kraakevik, J. A., and Horak, F. B. (2009). The supplementary motor area contributes to the timing of the anticipatory postural adjustment during step initiation in participants with and without Parkinson's disease. *Neuroscience* 164, 877–885. doi: 10.1016/j.neuroscience.2009.08.002

Johansson, J., Nordstrom, A., Gustafson, Y., Westling, G., and Nordstrom, P. (2017). Increased postural sway during quiet stance as a risk factor for prospective falls in community-dwelling elderly individuals. *Age Ageing* 46, 964–970. doi: 10.1093/ageing/afx083

Kanekar, N., and Aruin, A. S. (2014). The effect of aging on anticipatory postural control. *Exp. Brain Res.* 232, 1127–1136. doi: 10.1007/s00221-014-3822-3

Kang, N., Summers, J. J., and Cauraugh, J. H. (2016). Transcranial direct current stimulation facilitates motor learning post-stroke: a systematic review and meta-analysis. *J. Neurol. Neurosurg. Psychiatry* 87, 345–355. doi: 10.1136/jnnp-2015-311242

Kirimoto, H., Ogata, K., Onishi, H., Oyama, M., Goto, Y., and Tobimatsu, S. (2011). Transcranial direct current stimulation over the motor association cortex induces plastic changes in ipsilateral primary motor and somatosensory cortices. *Clin. Neurophysiol.* 122, 777–783. doi: 10.1016/j.clinph.2010.09.025

Kirimoto, H., Yoshida, S., Matsumoto, T., Kojima, S., Suzuki, M., Onishi, H., et al. (2013). P 71. The effects of cathodal transcranial direct current stimulation of the supplementary motor area on the function of anticipatory postural adjustments. *Clin. Neurophysiol.* 124, e98–e99. doi: 10.1016/j.clinph.2013.04.149

Kubicki, A., Fautrelle, L., Bourrelier, J., Rouaud, O., and Mourey, F. (2016). The early indicators of functional decrease in mild cognitive impairment. *Front. Aging Neurosci.* 8:193. doi: 10.3389/fnagi.2016.00193

Lee, W. A., Buchanan, T. S., and Rogers, M. W. (1987). Effects of arm acceleration and behavioral conditions on the organization of postural adjustments during arm flexion. *Exp. Brain Res.* 66, 257–270. doi: 10.1007/BF00243303

Lefaucheur, J.-P., Antal, A., Ayache, S. S., Benninger, D. H., Brunelin, J., Cogiamanian, F., et al. (2017). Evidence-based guidelines on the therapeutic use of transcranial direct current stimulation (tDCS). *Clin. Neurophysiol.* 128, 56–92. doi: 10.1016/j.clinph.2016.10.087

Lefebvre, S., Dricot, L., Gradkowski, W., Laloux, P., and Vandermeeren, Y. (2012). Brain activations underlying different patterns of performance improvement during early motor skill learning. *Neuroimage* 62, 290–299. doi: 10.1016/j.neuroimage.2012.04.052

Melzer, I., Benjuya, N., and Kaplanski, J. (2004). Postural stability in the elderly: a comparison between fallers and non-fallers. *Age Ageing* 33, 602–607. doi: 10.1093/ageing/afh218

Nana-Ibrahim, S., Vieilledent, S., Leroyer, P., Viale, F., and Zattara, M. (2008). Target size modifies anticipatory postural adjustments and subsequent elementary arm pointing. *Exp. Brain Res.* 184, 255–260. doi: 10.1007/s00221-007-1178-7

Ng, T. H., Sowman, P. F., Brock, J., and Johnson, B. W. (2011). Premovement brain activity in a bimanual load-lifting task. *Exp. Brain Res.* 208, 189–201. doi: 10.1007/s00221-010-2470-5

Nitsche, M. A., Doemkes, S., Karakose, T., Antal, A., Liebetanz, D., Lang, N., et al. (2007). Shaping the effects of transcranial direct current stimulation of the human motor cortex. *J. Neurophysiol.* 97, 3109–3117. doi: 10.1152/jn.01312.2006

Nitsche, M. A., and Paulus, W. (2000). Excitability changes induced in the human motor cortex by weak transcranial direct current stimulation. *J. Physiol.* 527(Pt 3), 633–639. doi: 10.1111/j.1469-7793.2000.t01-1-00633.x

Oldfield, R. C. (1971). The assessment and analysis of handedness: the Edinburgh inventory. *Neuropsychologia* 9, 97–113. doi: 10.1016/0028-3932(71)90067-4

Oostenveld, R., and Praamstra, P. (2001). The five percent electrode system for high-resolution EEG and ERP measurements. *Clin. Neurophysiol.* 112, 713–719. doi: 10.1016/S1388-2457(00)00527-7

Overstall, P. W., Exton-Smith, A. N., Imms, F. J., and Johnson, A. L. (1977). Falls in the elderly related to postural imbalance. *Br. Med. J.* 1, 261–264. doi: 10.1136/bmj.1.6056.261

Polanía, R., Paulus, W., and Nitsche, M. A. (2012). Modulating cortico-striatal and thalamo-cortical functional connectivity with transcranial direct current stimulation. *Hum. Brain Mapp.* 33, 2499–2508. doi: 10.1002/hbm.21380

Priori, A. (2003). Brain polarization in humans: a reappraisal of an old tool for prolonged non-invasive modulation of brain excitability. *Clin. Neurophysiol.* 114, 589–595. doi: 10.1016/S1388-2457(02)00437-6

Schambra, H. M., Abe, M., Luckenbaugh, D. A., Reis, J., Krakauer, J. W., and Cohen, L. G. (2011). Probing for hemispheric specialization for motor skill learning: a transcranial direct current stimulation study. *J. Neurophysiol.* 106, 652–661. doi: 10.1152/jn.00210.2011

Stephan, K. M., Fink, G. R., Passingham, R. E., Silbersweig, D., Ceballos-Baumann, A. O., Frith, C. D., et al. (1995). Functional anatomy of the mental representation of upper extremity movements in healthy subjects. *J. Neurophysiol.* 73, 373–386. doi: 10.1152/jn.1995.73.1.373

Stock, A. K., Wascher, E., and Beste, C. (2013). Differential effects of motor efference copies and proprioceptive information on response evaluation processes. *PLoS One* 8:e62335. doi: 10.1371/journal.pone.0062335

Taube, W., Mouthon, M., Leukel, C., Hoogewoud, H. M., Annoni, J. M., and Keller, M. (2015). Brain activity during observation and motor imagery of different balance tasks: an fMRI study. *Cortex* 64, 102–114. doi: 10.1016/j.cortex.2014.09.022

Vollmann, H., Conde, V., Sewerin, S., Taubert, M., Sehm, B., Witte, O. W., et al. (2013). Anodal transcranial direct current stimulation (tDCS) over supplementary motor area (SMA) but not pre-SMA promotes short-term visuomotor learning. *Brain Stimul.* 6, 101–107. doi: 10.1016/j.brs.2012.03.018


**Conflict of Interest Statement:** The authors declare that the research was conducted in the absence of any commercial or financial relationships that could be construed as a potential conflict of interest.

frontiers in Human Neuroscience

ORIGINAL RESEARCH
published: 07 August 2018
doi: 10.3389/fnhum.2018.00313

# A Functional Near-Infrared Spectroscopy Study of State Anxiety and Auditory Working Memory Load

*Yi-Li Tseng[1]*, Chia-Feng Lu[2], Shih-Min Wu[1], Sotaro Shimada[3], Ting Huang[1] and Guan-Yi Lu[1]*

*[1] Department of Electrical Engineering, Fu Jen Catholic University, New Taipei City, Taiwan, [2] Department of Biomedical Imaging and Radiological Sciences, National Yang-Ming University, Taipei, Taiwan, [3] Department of Electronics and Bioinformatics, School of Science and Technology, Meiji University, Tokyo, Japan*

Cognitive studies have suggested that anxiety is correlated with cognitive performance. Previous research has focused on the relationship between anxiety level and the perceptual load within the frontal region, such as the dorsolateral prefrontal and anterior cingulate cortices. High-anxious individuals are predicted to have worse performance on cognitively-demanding tasks requiring efficient cognitive processing. A few functional magnetic resonance imaging studies have specifically discussed the performance and brain activity involving working memory for high-anxious individuals. This topic has been further explored with electroencephalography, although these studies have mostly provided results involving visual face-related stimuli. In this study, we used auditory stimulation to manipulate the working memory load and attempted to interpret the deficiency of cognitive function in high-anxious participants or patients using functional near infrared spectroscopy (fNIRS). The fNIRS signals of 30 participants were measured while they were performing an auditory working memory task. For the auditory *n*-back task, there were three experimental conditions, including two *n*-back task conditions of stimuli memorization with different memory load and a condition of passive listening to the stimuli. Hemodynamic responses from frontal brain regions were recorded using a wireless fNIRS device. Brain activation from the ventrolateral and orbital prefrontal cortex were measured with signals filtered and artifacts removed. The fNIRS signals were then standardized with statistical testing and group analysis was performed. The results revealed that there were significantly stronger hemodynamic responses in the right ventrolateral and orbital prefrontal cortex when subjects were attending to the auditory working memory task with higher load. Furthermore, the right lateralization of the prefrontal cortex was negatively correlated with the level of state anxiety. This study revealed the possibility of incorporating fNIRS signals as an index to evaluate cognitive performance and mood states given its flexibility regarding portable applications compared to other neuroimaging techniques.

**Keywords: functional near-infrared spectroscopy (fNIRS), auditory working memory, memory load, state anxiety, prefrontal cortex (PFC)**

OPEN ACCESS

***Edited by:***
*Delin Sun,*
*Duke University, United States*

***Reviewed by:***
*Noman Naseer,*
*Air University, Pakistan*
*Ning Ma,*
*RIKEN Brain Science Institute (BSI), Japan*
*Huijun Zhang,*
*Guangdong University of Technology, China*

****Correspondence:***
*Yi-Li Tseng*
*yltseng@mail.fju.edu.tw*

***Received:*** *28 April 2018*
***Accepted:*** *16 July 2018*
***Published:*** *07 August 2018*

***Citation:***
*Tseng Y-L, Lu C-F, Wu S-M, Shimada S, Huang T and Lu G-Y (2018) A Functional Near-Infrared Spectroscopy Study of State Anxiety and Auditory Working Memory Load. Front. Hum. Neurosci. 12:313. doi: 10.3389/fnhum.2018.00313*

# INTRODUCTION

## Anxiety Disorder and Cognitive Function

Neurophysiological studies have suggested that anxiety is highly correlated with cognitive performance (Eysenck et al., 2007; Osinsky et al., 2012). The level of anxiety in these studies was assessed by trait anxiety as measured by, for instance, the State-Trait Anxiety Inventory (STAI) (Spielberger et al., 1970). State anxiety is conceptualized as a transient emotional state during which an individual is unable to respond to events that are threatening an existing goal (Eysenck and Calvo, 1992; Eysenck et al., 2007; Power and Dalgleish, 2015), whereas trait anxiety is a relatively stable personality characteristic (Horwitz, 2001; Schmukle and Egloff, 2004). Investigations have focused on prefrontal mechanisms and top-down selective attention to threatening events (Bishop et al., 2004; Ohman, 2005). In highly anxious subjects, attentional control is more likely to be influenced by emotional stimuli, particularly concerning tasks engaging conflict stimuli with low working memory load (Osinsky et al., 2012; Pacheco-Unguetti et al., 2012; Vytal et al., 2012). Moreover, cognitive processes are also affected in high-anxious subjects in the absence of threat-related stimuli (Basten et al., 2012). These studies have mainly focused on the relationship between the anxiety level and working memory or perceptual load in the frontal region, especially in the prefrontal cortex (Bishop, 2009; Basten et al., 2012).

These recent studies have claimed that there is interference of trait anxiety in inhibition and attentional shift in working memory. The ease of "overload" in anxious subjects resulting in diluting cognitive resources particularly affects the processes associated with inhibition and attentional shift (Berggren and Derakshan, 2013), and can be observed when there is lower cognitive load (Berggren et al., 2013). There is no doubt that high-anxious subjects are predicted to have worse performance on cognitively demanding tasks requiring more efficient cognitive processes, and the examination of compensatory strategy will be the future direction of research (Ansari and Derakshan, 2011a; Berggren and Derakshan, 2013).

## Neuroimaging Evidence for Anxiety and Cognitive Impairment

Recent functional magnetic resonance imaging (fMRI) studies have reported varying brain activities in frontal regions for subjects with distinct anxiety levels (Bishop et al., 2004; Bishop, 2009; Basten et al., 2011, 2012). Basten et al. reported that there is stronger task-relevant activation in high-anxious subjects in the dorsal lateral prefrontal cortex (DLPFC) and left inferior frontal sulcus (Basten et al., 2011, 2012). Stronger deactivation was found in the rostral-ventral anterior cingulate cortex (ACC), which is one of the main regions in the default-mode network (Basten et al., 2012). Higher levels of anxiety were associated with stronger task-related activation in the ACC but with reduced functional connectivity between the ACC and lateral prefrontal cortex (LPFC) (Comte et al., 2015). In addition, there is reduced functional connectivity of the DLPFC with posterior lateral frontal regions, the dorsal ACC, and a word-sensitive area in the left fusiform gyrus (Basten et al., 2011), whereas stronger connectivity is found for the right DLPFC with the ventrolateral PFC in high-anxious subjects (Basten et al., 2012). Some of these recent studies have found stronger or compensatory activation in certain brain regions for high-anxious participants with comparable levels of performance accuracy (Ansari and Derakshan, 2011a; Basten et al., 2011). However, other studies have found weaker activation in high-anxious subjects with slower performance (Bishop, 2009; Ansari and Derakshan, 2011b). Altered neurophysiological signals including electroencephalography (EEG) and magnetoencephalography (MEG) have also been reported for subjects with different mental illness and anxiety levels. High-anxious subjects may show atypical event-related potential/field (ERP/ERF) and event-related spectral perturbations (ERSPs). Recent EEG studies have shown that there is altered activation in subjects showing high anxiety in cognitive tasks such as attention (Osinsky et al., 2012), working memory, and emotional stimuli (Dennis and Hajcak, 2009; MacNamara and Hajcak, 2009, 2010; Ansari and Derakshan, 2011a,b; MacNamara et al., 2011; Hajcak et al., 2013; Stout et al., 2013). Lower ERP is found in high-anxious participants especially in the frontal and central regions (Ansari and Derakshan, 2011a,b). Recently in time-frequency ERSPs studies, Cavanagh and colleagues found that frontal-midline theta signals, reflecting midcingulate cortex activity, are moderated by anxiety and may predict adaptive behavioral adjustments (Cavanagh and Shackman, 2014). These findings emphasize the importance of brain activation in anxiety regulation especially in the frontal and central regions.

Although neurophysiological techniques, such as EEG and MEG, provide good temporal resolution during the execution of tasks, these methods do not offer sufficient spatial resolution. In comparison, fMRI provides better spatial resolution without the influence of electrooculography and motion artifacts. Several critical brain regions related to anxiety and cognitive functions, including the DLPFC and ACC, are constantly reported in fMRI studies. Nevertheless, it is somewhat impossible to measure fMRI signals in a natural and real-life situation for further diagnosis or applications of mental training. This study intended to incorporate a portable functional near-infrared spectroscopy (fNIRS) system in order to provide a more flexible solution to measuring the performance on cognitive tasks from subjects with different anxiety levels. Compared with fMRI, an fNIRS system is able to record hemodynamic responses with a higher sampling rate under real-life environmental conditions.

## Functional NIRS as a Highly Flexible Device to Study Mental Diseases and Cognitive Functions

In the past decade, fNIRS has been proposed as a flexible and portable device to record brain hemodynamic responses during the performance of cognitive tasks such as learning, memory, and motor reactions (Shimada and Hiraki, 2006; Shimada and Oki, 2012; Noah et al., 2015). In several studies of memory function, the hemodynamic responses recorded by a fNIRS system from the PFC have been found to correlate highly with gray-matter fMRI activities during a working memory

task (Sato et al., 2013; Noah et al., 2015). Consistent with the previous findings with fMRI, LPFC activation of the fNIRS signal is also reportedly associated with working memory in adults and even preschool children (Hoshi et al., 2003; Tsujimoto et al., 2004; Schreppel et al., 2008; Sanefuji et al., 2011). Hoshi and colleagues found that there are hemodynamic changes in the human LPFC during visual working memory tasks (Hoshi et al., 2003). Later, in 2008, Schreppel and colleagues used a 52-channel fNIRS system to claim that prefrontal activities reflect both maintenance and attentional monitoring processes during a visual *n*-back task (Schreppel et al., 2008). Sanefuji and colleagues provided further supporting evidence with preschool children and proposed that there is a correlation between memory ability and activation in the left ventrolateral prefrontal cortex (VLPFC) (Sanefuji et al., 2011). In line with previous results, Ogawa and colleagues highlighted that there is correlation between working memory performance and the neural activation measured using an fNIRS system. Participants with better working memory performance had higher levels of oxyhemoglobin activation (Ogawa et al., 2014). In addition, activation in the bilateral LPFC depends on memory load (Tsujimoto et al., 2004). This evidence suggests that fNIRS is useful and convenient for measuring working memory performance.

The prefrontal hemodynamic response recorded by an fNIRS system has also become an important marker in the study of emotion regulation and mental diseases. Aoki and colleagues demonstrated that fNIRS signals can be used to investigate neural processing during emotional control of negative mood. Correlation analysis has shown that the level of negative mood is inversely associated with PFC activity during verbal working memory tasks (Aoki et al., 2011, 2013; Sato et al., 2014). In contrast, the emotional valence of the pictures positively affected the level oxygenated hemoglobin in anterior parts of the medial prefrontal cortex (MPFC) and left inferior frontal gyrus during a facial emotional *n*-back task (Ozawa et al., 2014). Although Lai and colleagues reported that a normal intensity level of psycho-physiological stress can benefit working memory performance at high load (Lai et al., 2014), other fNIRS studies have claimed that there is altered prefrontal brain activities in patients with mental diseases and problems in emotional regulation. Ehlis and colleagues found reduced VLPFC activation in patients with attention-deficit/hyperactivity disorder (ADHD) during a visual working memory task (Ehlis et al., 2008). In contrast, patients with major depressive disorder (MDD) have shown different patterns with increased activations in the LPFC and superior temporal cortex during the two-back visual task and associated with poorer task performance than healthy controls (Pu et al., 2011). Furthermore, other studies have focused on altered prefrontal activation after drug treatment. Ramasubbu and colleagues reported that there are reduced prefrontal hemodynamic responses but improved cognitive performance after treatment with methylphenidate (Ramasubbu et al., 2012). These previous findings suggest that there are complicated interactions between emotional regulation, cognitive performance, and drug treatment.

In the past few years, the prefrontal region has been highlighted as critical in auditory connections that are involved in the processing of key pieces of information for auditory memory recognition in primates (Plakke et al., 2013; Plakke and Romanski, 2014). Although the existing literature on working memory has emphasized visual processes rather than auditory modalities, more studies have started to focus on the pathway of non-verbal or auditory memory (Huang et al., 2013; Plakke et al., 2013; Plakke and Romanski, 2014; Muñoz-López et al., 2015). It has also been reported that the frontal lobe may be involved in auditory detection, discrimination, and working memory in humans (Plakke and Romanski, 2014). In 2013, Huang et al. claimed that the subregions of the anterior DLPFC are selectively associated with auditory working memory, and areas in more inferior lateral aspects of the PFC and inferior frontal cortex are associated with auditory attention and not working memory (Huang et al., 2013). These studies emphasized the importance of the frontal cortex for information processing during auditory working memory. However, there remains discrepancy between the existing experimental designs of auditory memory and real-world conditions, as most previous studies focused on the primary auditory cortex with simple tones as stimuli (Weinberger, 2014).

In this study, we investigated whether changes in prefrontal activation correlated with working memory load and trait anxiety level. We recorded hemodynamic responses from an fNIRS system while participants were performing a musical *n*-back working memory task (Pallesen et al., 2010). Four-channel fNIRS signals were recorded by a portable system to address the following hypotheses: (1) the hemodynamic responses of the lateral PFC would increase with auditory working memory load, and (2) compared to the subjects with low anxiety level, high-anxious participants would have alterations in hemodynamic responses during auditory working memory, especially in the prefrontal regions. It is worth noting that this work was an extension from our proof-of-concept study (Wu et al., 2017) with considerable improvement in two aspects. First, this work proposed the correlation between anxiety level, cognitive load, and fNIRS responses. Second, advanced fNIRS signals processing methods were incorporated to improve the signal quality from portable fNIRS devices. To the best of our knowledge, this study is the first to explore the correlation between anxiety level and cognitive load incorporating fNIRS signals during a musical working memory task, with music chords serving as stimuli.

# MATERIALS AND METHODS

## Participants

Thirty volunteers without neurological disorders were recruited for the experiment. Prior to the experiment, all were asked to provide informed consent in accordance with the procedure of the human subject research ethics committee/Institutional Review Board at the Fu Jen Catholic University, Taiwan, and then completed a rating scale to estimate their familiarity to distinct types of music. To avoid introducing bias pertaining to differing musical skill levels, a music-familiarity scare was administered.

## STAI

The STAI was used for measuring the participants' anxiety level (Spielberger et al., 1970). The STAI measures the state anxiety (STAI-S) and trait anxiety levels (STAI-T). Both parts of the STAI include 20 questions each, which are scored on a 4-point Likert-type scale. Specifically, the STAI-S is based on the temporary and present emotional situation of the participants, while the STAI-T can evaluate the state of pressure or anxiety during a period of time. In this study, we used the Chinese version of the STAI (cSTAI), which is validated with its psychometric characteristics found in the study by Savostyanov et al. (2009) and Shek (1993). Scores range between 20 and 80 for both the STAI-S and STAI-T, with higher scores associated with high state or trait anxiety level.

## Experimental Paradigm

The subjects participated in an auditory *n*-back working memory task. The proposed auditory *n*-back WM task was modified by the paradigm developed by Pallesen et al (Pallesen et al., 2010). The paradigm is useful in studying emotion regulation during cognitive tasks by manipulating the memory load and the emotional type of the stimuli. There were three experimental conditions, including two *n*-back task conditions of memorizing the stimuli, an easy 1-back task (1B) and a difficult 2-back task (2B), and a condition of passive listening to the stimuli (PL). The stimuli were 12 sound combinations of major, minor, and dissonant chords, each spanning three frequency levels separated by an octave. The chords were produced and presented using the Overture 4.0 software, and were programed to have the same duration (1,000 ms) and loudness level. The major chords consisted of A, C#, E, A, and C#. The minor chords consisted of of A, C, E, A, and C and are considered in music theory as imperfect consonance. The dissonant chords were composed of A, Bb, G, Ab, and C, which are considered as the most dissonant intervals. After each stimulus, participants were requested to press the left button in the 1B task when the chord matched that of the previous trial, and in the 2B task when the chord matched that presented two trials back. In all other trials and the PL condition, participants pressed the right button with their right hands.

The experimental design is illustrated in **Figure 1**. There were two sessions separated by a break of 2 min in the experiment. Each session consisted of 18 blocks with different combinations of task conditions (PL, 1B, or 2B) and chord category (major, minor, or dissonant). Each type of block was presented four times during the experiment. An instruction screen was shown for 12 s between the blocks to prepare the subject for the following task. Twenty trials were presented with each trial constructed of a sound presentation (1,000 ms), followed by a brief silence (1,500 ms) before the next trial. The fNIRS signals were recorded during the two sessions, and the participants were instructed to remain calm with their eyes open while fixating on a central cross on the screen.

## fNIRS Recording

The participants were recruited in the experiment with their fNIRS data recorded in a shielded room. The fNIRS signals were recorded with a sampling rate of 2 Hz using a wireless and portable system, BRAIN-NIRS Hb13 (ASTEM Co. Ltd., Kawasaki, Japan), as shown in **Figure 2A**. Light-emitting diodes with operating wavelengths of 770 and 830 nm are used. The concentration of oxygenated hemoglobin (oxy-Hb) and deoxygenated hemoglobin (deoxy-Hb) were recorded from four locations on the scalp. The center of the probe was placed on the frontal area (Fpz), and four sensors were set on F7, F8, Fp1, and Fp2 according to the international 10–20 system for electroencephalography, as illustrated in **Figure 2B** (Jasper, 1958). These four positions corresponded to the left/right VLPFC and orbital prefrontal cortex (OPFC), based on anatomical cranio-cerebral correlation studies (Okamoto et al., 2004; Sanefuji et al., 2011). The concentration change in oxy-Hb was used for further analysis, since it is more sensitive to changes in cerebral blood flow.

## fNIRS Signals Analysis

The HOMER2 toolbox was used for the preprocessing of oxy-Hb and deoxy-Hb (Huppert et al., 2009). Since the quality of fNIRS signals are often affected by artifacts such as respiration, eye blinking, motion, and cardiac cycle effects (Izzetoglu et al., 2005; Ayaz et al., 2010; McKendrick et al., 2014), two methods were incorporate for artifact rejection. First, the wavelet-based artifact removal algorithm (Molavi and Dumont, 2012; Brigadoi et al., 2014) was applied to the raw fNIRS signals to correct spike artifacts. Second, a band-pass filter was used to remove baseline wandering. Finally, the correlation-based signal improvement method (Cui et al., 2010) was used to eliminate the effect of motion artifacts.

The spike artifacts produced by head or body movement (Robertson et al., 2010) were removed using discrete wavelet transformation (Molavi and Dumont, 2012) modified based on the function hmrMotionCorrectWavelet.m in the HOMER2 toolbox (Huppert et al., 2009). The method calculates the difference between artifacts and fNIRS signals in terms of duration and amplitude (Brigadoi et al., 2014). The fNIRS signal, $x(t)$, from a single channel can be expanded using the discrete wavelet transform as:

$$x(t) = \sum_{k} v_{j_0 k}\phi_{j_0 k}(t) + \sum_{j=j_0}^{\infty}\sum_{k} w_{jk}\psi_{jk}(t),$$

where $\phi(t)$ and $\psi(t)$ are the mother wavelet and scaling functions, with $j$ and $k$ the dilation and translation parameters, and $j_0$ the coarsest scale in the decomposition. The wavelet coefficients are denoted as $v_{jk}$ and $w_{jk}$. According to the fast wavelet transform algorithm (Mallat, 1989), the wavelet coefficients, $w_{jk}$, are composed of the wavelet filter bank high-pass filters. The normal cumulative distribution function of $w_{jk}$ and the variance of the distribution can be estimated. If the probability of the values is larger than $w_{jk}$, less than a probability $\alpha$, the coefficient could be classified as one produced by artifacts and should be removed (Molavi and Dumont, 2012). By reconstructing the fNIRS signals, the spike artifacts could be removed.

The fNIRS signals were then band-pass filtered (0.0015–0.02 Hz) to attenuate the high frequency noise, respiration, and cardiac cycle effects. Since the block frequency of this

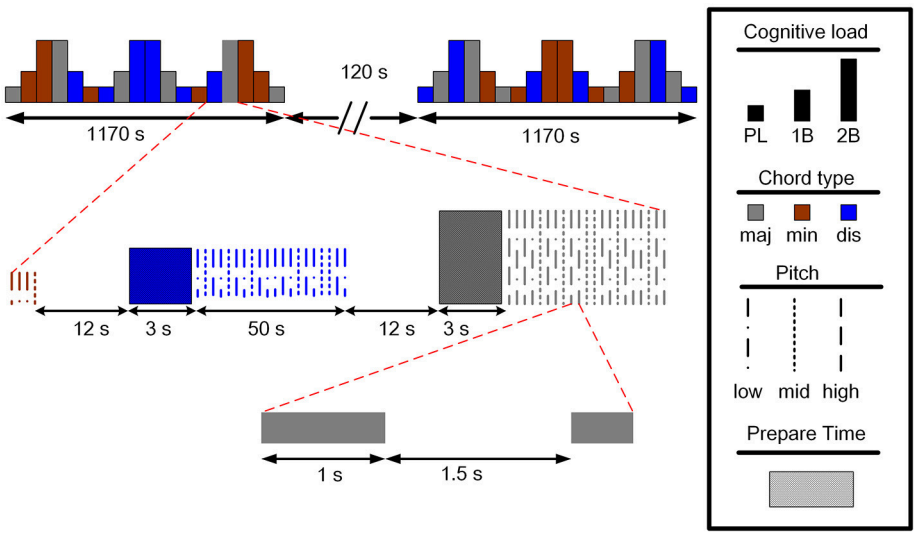


**FIGURE 1 |** The experimental paradigm of the auditory *n*-back working memory task (maj: major, min: minor, dis: dissonant).

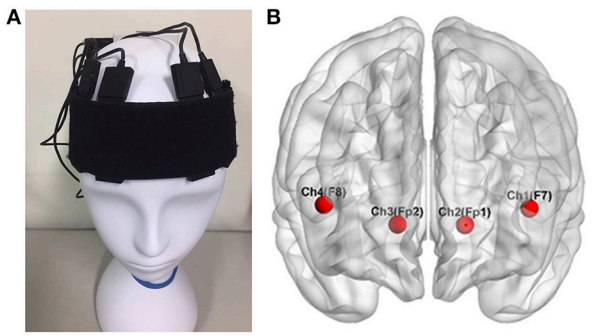


**FIGURE 2 |** The four locations of functional near infrared spectroscopy sensors on the subject's scalp **(A)**. These electrodes corresponded to F7, F8, Fp1, and Fp2 in the 10–20 system **(B)**, located over the left and right ventrolateral prefrontal cortex and the orbital prefrontal cortex Wu et al. (2017).

experimental design is close to 0.002 Hz, the low frequency of the band-pass filter was set to 0.0015 Hz to eliminate the low-frequency baseline wandering.

In the last step of signal preprocessing, the quality of the fNIRS signals was improved based on the negative correlation between oxygenated and deoxygenated hemoglobin dynamics (Cui et al., 2010). Let $x_0$ and $y_0$ be the true oxy- and deoxy-Hb, the recorded oxy- and deoxy-Hb, $x$ and $y$, can be written as:

$$\begin{cases} x = x_0 + \beta F + Noise \\ y = y_0 + F + Noise, \end{cases}$$

where $F$ is the noise with identical effects on oxy- and deoxy-Hb and is subject to a constant factor $\beta$. Since the concentration of oxy-Hb and deoxy-Hb are assumed to be negative correlated, the relationship of $x_0$ and $y_0$ can be expressed as:

$$x_0 = -\gamma y_0,$$

where $\gamma$ is a parameter concerning the amplitude difference between oxy and deoxy-Hb. By the assumption that (1) the amplitude of deoxy-Hb is usually lower than that of oxy-Hb, and (2) the amplitude of the noise ($F$) and true oxy-Hb are minimally correlated (Cui et al., 2010), the true amplitude of oxy- and deoxy-Hb can thus be obtained with negative correlation as:

$$\begin{cases} x_0 = \frac{1}{2}(x - \beta y) \\ y_0 = -\frac{1}{\beta} x_0. \end{cases}$$

The negative correlation based signal improvement used in this study was modified from the function hmrMotionCorrectCbsi.m in the HOMER2 toolbox (Huppert et al., 2009). An index of lateralized hemodynamic responses is also proposed by subtracting the hemodynamic responses of the right VLPFC (F8) by the left VLPFC (F7). Group analysis and statistical testing were then performed after signal preprocessing.

## Statistical Analysis

Statistical analysis were performed using MATLAB R2016a (The MathWorks, Inc., Natick, MA). The fNIRS signals were segmented and normalized using the average of the hemodynamic responses in 3 s before the onset of each session as a baseline. For individual analysis, the averages of the oxy-Hb change in all blocks were calculated and compared between conditions (PL, 1B, and 2B) with student's paired $t$-test. Group analyses of all participants were performed by calculating the Pearson's linear correlation coefficients between the state and trait anxiety scores with the mean oxy-Hb changes and lateralized hemodynamic responses of the data.

# RESULTS

## Subjective Rating on Music Familiarity, Anxiety, and Behavioral Performance in the Auditory *n*-Back Task

From all 30 participants recruited to the study, two were rejected due to low task accuracy (i.e., average accuracy <60%) which is close to the chance level. Consequently, a total of 28 participants (14 women) with a mean age of 21.5 ± 1.4 years were included into the data sample. Among the 28 participants, the behavior results in the auditory *n*-back task revealed that the average correctness of the 1-back task was 84.8 ± 9.6%, which is 15.5% higher than that of the 2-back task (69.3 ± 10.4%). The overall task accuracy or correctness averaged between the two conditions of the auditory working memory task was 77.0 ± 9.4%. Trait anxiety raw scores ranged from 34 to 57 with the average score of 45.8 ± 5.8, and the raw scores of state anxiety ranged from 24 to 56 with the average score of 35.9 ± 8.6. No significant correlation was found between task performance and anxiety levels. None of the participants were music experts, but most of them had systematically studied at least one instrument for no more than 5 years. In addition, most of the participants reported the habit of listening to music for at least 1 h per week. The average reaction time of the three conditions of passive listening, 1-back, and 2-back are 807 ± 257 ms, 1,149 ± 142 ms, and 1,252 ± 147 ms, respectively.

## Hemodynamic Responses

The concentration of oxy- and deoxy-Hb was calculated from the fNIRS signals and is shown in **Figure 3**. The hemodynamic responses at F8 were recorded from a single subject when the participant was attending to the *n*-back auditory working memory task. As illustrated in **Figure 3**, the amplitudes of oxy-Hb signal (red line) after the removal of spike artifacts and band-pass filtering increased with the increment of task loads (gray bars). In addition, the oxy-Hb signals were negatively correlated with the amplitudes of the deoxy-Hb signal (blue line) after the removal of motion artifacts using the negative correlation-based signal improvement algorithm.

The fNIRS signals of oxy- and deoxy-Hb were then averaged over the time points in each block and normalized according the mean value of their baseline. As illustrated in **Figure 4**, the hemodynamic responses recorded from the four channels of the fNIRS system were standardized and averaged across the three conditions. Stronger activations were observed from all four channels under higher auditory working memory load. The average amplitudes of oxy-Hb signals were most pronounced when the participants were attending to the two-back task. In the right VLPFC (F8), a significant difference was found between PL and 2B ($p = 0.040$), and also 1B and 2B ($p = 0.021$). The difference was also pronounced in the right OPFC (Fp2) with significance between PL and 2B ($p = 0.009$), and also 1B and 2B ($p = 0.045$). The results revealed that there are significantly stronger hemodynamic responses in the right VLPFC and OPFC when participants were attending to the auditory working memory task with high memory load.

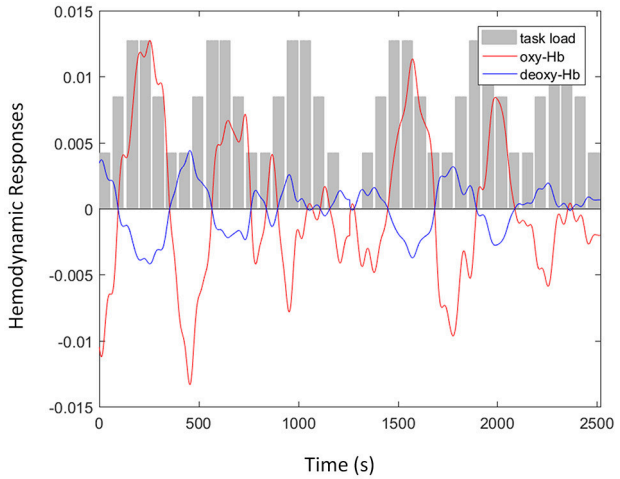


**FIGURE 3 |** An example of functional near infrared spectroscopy signals with oxyhemoglobin (oxy-Hb) (red line) and deoxy-Hb (blue line) signals recorded at F8 from a single subject when the participant was attending to the *n*-back auditory working memory tasks including three levels of task load (gray bars): passive listening, one-back, and two-back.

## Correlation Between Anxiety Scores and Auditory Working Memory Load

Group analysis of all participants were performed by calculating the Pearson's linear correlation between anxiety scores and hemodynamic responses of the fNIRS signals. The association between state and trait anxiety with the mean oxy-Hb amplitudes and lateralized hemodynamic responses were evaluated in all of the four channels in the PFC. The significance between state anxiety and lateralized hemodynamic responses was found under higher working memory load during the 2B condition ($r = -0.575$; $p = 0.0033$), as shown in **Figure 5**. A negative correlation was observed between state anxiety and right lateralized hemodynamic responses, which is the activation difference between the right and left VLPFC (F7 and F8). The negative correlation between state anxiety and the lateralization index was observed to be slightly more pronounced in the female group ($r = -0.642$; $p = 0.0243$) than in the male group ($r = -0.548$; $p = 0.0652$) but did not reach the significant level. There was no pronounced correlation found between anxiety levels and the lateralization index under low working memory load conditions during 1B and passive listening conditions. We also examined the correlations between task performance and the oxy-Hb signal changes, and no significant difference was found.

In summary, increased hemodynamic responses in the right PFC were observed under higher auditory working memory load. The results also indicated that there was no obvious correlation between task performance and prefrontal hemodynamic responses of fNIRS signals. In contrast, the prefrontal right lateralization of the PFC was negative correlated with the level of state anxiety.

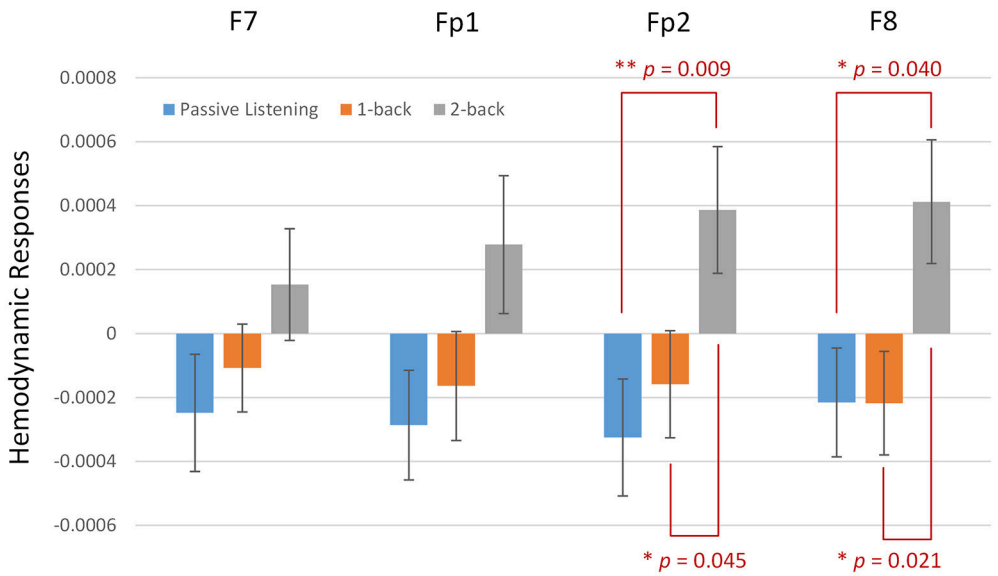


**FIGURE 4 |** Hemodynamic responses recorded by the functional near infrared spectroscopy system when subjects were attending to the *n*-back auditory working memory tasks including three conditions: passive listening, one-back, and two-back. Stronger activations were observed from Fp2 and F8, which are localized over the right ventrolateral and orbital prefrontal cortex. Activations were more pronounced under higher working memory load. (** and * denote the significant level at the 1 and 5 per cent levels, respectively).

## DISCUSSION

The aim of this study was to explore the effect of anxiety on auditory working memory with a portable four-channel fNIRS device. We report the following findings. First, there were increased changes in hemodynamic responses in the right orbital and ventral PFC under higher auditory working memory load during the two-back task. Second, a negative correlation was found between state anxiety and the right lateralization index of the ventral PFC. However, the correlation was not observed between trait anxiety and hemodynamic responses. This suggests that the level of fNIRS signals is correlated to the anxiety scales observed during the experiment instead of the personality of the participants. Third, the results of this study showed the feasibility of using a portable and flexible four-channel fNIRS system to evaluate the effect of anxiety on working memory performance rather than other complex neuroimaging techniques. Detailed findings and their connections with previous studies are discussed in the following subsections, with the aim of drawing a precise picture of the prefrontal hemodynamic responses underlying anxiety levels and auditory working memory.

### Increased Hemodynamic Reponses in the Right Prefrontal Areas Under High Task Load

Our results showed that there is a pronounced increment of hemodynamic responses in the right VLPFC and OPFC under high auditory working memory load. Although the increment was observed in all four channels located in the prefrontal regions, only the channels located at Fp2 and F8 showed significance. Prefrontal activation has long been reported to be correlated with working memory processes in fMRI studies (Manoach et al., 1997; D'Esposito, 2007; Barbey et al., 2013; Lara and Wallis, 2015; Riley and Constantinidis, 2016). Recently, the prefrontal region has been further emphasized as critical in auditory connections that represent key pieces of information for auditory memory recognition in primates and humans (Huang et al., 2013; Plakke et al., 2013; Plakke and Romanski, 2014; Muñoz-López et al., 2015). Consistent with the previous fMRI findings, fNIRS signals are also reportedly associated with visual working memory in adults and children (Hoshi et al., 2003; Tsujimoto et al., 2004; Schreppel et al., 2008; Sanefuji et al., 2011). Previous fNIRS studies have found that hemodynamic responses in the bilateral LPFC increased during visual *n*-back tasks (Hoshi et al., 2003; Schreppel et al., 2008), an item-recognition task (Tsujimoto et al., 2004), verbal and spatial working memory tasks (Aoki et al., 2011; Ogawa et al., 2014; Sato et al., 2014), and visual and auditory working memory tasks (Sanefuji et al., 2011). For higher visual working memory load during the *n*-back tasks using materials such as digits (Hoshi et al., 2003) or faces (Schreppel et al., 2008), previous studies have also reported the increment of the bilateral VLPFC or the anterior parts of the medial frontal cortex (Ozawa et al., 2014). Although a significant difference was only found in the right OPFC and VLPFC in this study, the increment of fNIRS signals was observed at all four channels located over the PFC (**Figure 4**), which is in line with previous results. Our findings were in line with those of previous studies on visual working memory. The increased hemodynamic responses in the right VLPFC and OPFC observed in the present study may reflect the involvement of retrieval processes during auditory working memory under different levels of task load.

In contrast, we observed no correlation between overall correctness and oxy-Hb activation. In previous studies, the levels

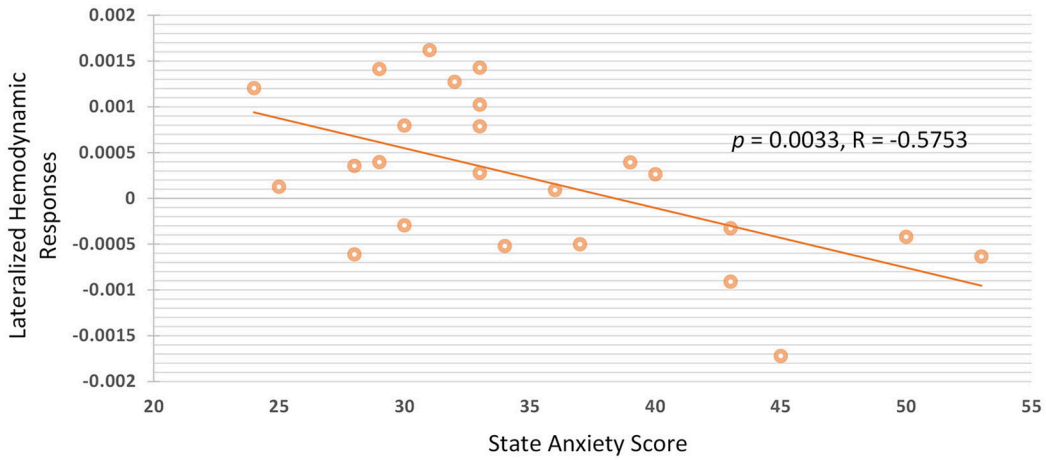


**FIGURE 5 |** There is negative correlation between state anxiety and lateralized hemodynamic responses under higher working memory load.

of oxy-Hb activation in the VLPFC have been reported to be correlated with working memory performance. Sanefuji and colleagues demonstrated that activation in the left VLPFC of preschool children was positively correlated with the memory ability measured by the Wechsler Intelligence Scale (Sanefuji et al., 2011). Ogawa and colleagues also provided evidence to this end and proposed that there is a positive correlation between the activation of the LPFC and visual working memory performance (Ogawa et al., 2014). These previous findings suggest that there exist complicated interactions between memory load, task performance, and the prefrontal hemodynamic responses.

## Negative Correlation Between State Anxiety and Right Lateralization in the PFC

Following the findings of altered hemodynamic responses during auditory working memory processes, we further identified a correlation between anxiety and the level of oxy-Hb in the PFC under high memory load. Our results showed that there is a negative correlation between state anxiety and the right lateralization index in the VLPFC. Consistent with previous findings, the correlation analysis showed that the level of negative mood, which can be measured by a profile of mood states questionnaire, is inversely associated with PFC activity during a verbal working memory task (Aoki et al., 2011, 2013; Sato et al., 2014). Furthermore, mood-cognition interaction was found in the PFC in participants of different ethnicities and language backgrounds (Sato et al., 2014). In contrast, some studies have observed a positive correlation between negative emotion and hemodynamic responses in the MPFC using a facial emotional expression of an *n*-back task, which alters the emotional states of the participants by external stimuli (Ozawa et al., 2014). The map of the relationship between mental disorders and prefrontal hemodynamic responses of fNIRS signals is still under construction, especially of mental diseases with deficits in emotional regulation. Previous studies have also reported that the lateral PFC shows reduced fNIRS signals during working memory tasks in patients with ADHD (Ehlis et al., 2008), MDD (Pu et al., 2011), and attention deficits after traumatic brain injury. Furthermore, altered prefrontal activation has also been reported after methylphenidate treatment, which is a drug used in the treatment of ADHD and depression (Ramasubbu et al., 2012). In line with these previous findings, we suggest that there are complicated interactions between emotional regulation and cognitive performance.

# LIMITATIONS

The restricted range of anxiety scores may be a limitation. Hence, we have compared the anxiety scores in this study with some previous results in different countries and culture. Two Russian studies (Knyazev et al., 2004) reported trait anxiety scores with the average of 41.3 ± 9.6 and 41.8 ± 9.9. In an US study (Blackhart et al., 2006), the trait anxiety scores were reported with the average of 40.93 ± 7.43 and 36.43 ± 6.72. In two German studies (Sehlmeyer et al., 2010; Basten et al., 2011), the trait anxiety scores were reported with the average of 33.9 ± 8.36 and 33.3 ± 5.7 and was claimed to be comparable to the values of the German normative sample with the average of 34.7 ± 8.4. In this study, trait anxiety raw scores ranged from 34 to 57 with the average score of 45.8 ± 5.8, and the raw scores of state anxiety ranged from 24 to 56 with the average score of 35.9 ± 8.6. According to these previous results, we compared the range and cultural difference of anxiety scores. First, the range of the observed anxiety scores are typically not that large in a group of healthy participants, and the standard deviations calculated are often lower than ten. The standard deviations (or ranges) of the state and trait anxiety reported in this study are comparable and consistent with those reported in the previous studies (Knyazev et al., 2004, 2016; Blackhart et al., 2006; Sehlmeyer et al., 2010; Basten et al., 2011). Second, although some previous studies have also focused on the cultural difference and anxiety level (Baloğlu et al., 2011), they used other scores to evaluate the anxiety level rather than the STAI. In addition, the age and background may not be matched for

the participants recruited with anxiety scores reported in the previous studies (Knyazev et al., 2004, 2016; Blackhart et al., 2006; Sehlmeyer et al., 2010; Basten et al., 2011). Therefore, more evidence is demanded to claim if cultural difference could be a factor to affect the conclusion, and we discussed the correlation between anxiety level and prefrontal hemodynamic responses based on the range of anxiety scores reported in this study.

The accuracy of the auditory *n*-back task is observed to be lower than the study using a similar paradigm proposed by Pallesen et al. (2010). The lower accuracy of our behavioral results may due to three reasons. First, the experimental design is slightly different from the previous study. The time for response in our study is only 1,500 ms. The shorter time for response may result in worse task performance. Second, thirty participants were recruited in this study, which were more than those recruited in the previous study (Pallesen et al., 2010). The lack of experience in music and the larger number of recruited participants may also result in lower accuracy. Third, the stimuli used in this experiment was music chords, which is more complex than traditional auditory single task. Several previous studies have discussed about the accuracy of visual and auditory *n*-back task in a larger group of participants (Jaeggi et al., 2010). For visual or auditory single task, the accuracy has been reported to be higher than 90% under both 1- and 2-back conditions. However, the correctness decreases when task complexity increased. Hence, the accuracy were observed to be lower than 90% in this study. There is often an inverse relationship between the performance and task difficulty (e.g., shorter time for reaction and increased complexity of stimuli). Although the performance may be improved by decreasing the task difficulty, the effect of anxiety may be more obvious when task difficulty is increased. The task designed in this study was intended to increase the task difficulty and observe the anxiety-induced effect on prefrontal hemodynamic responses. However, there might be a quick drop in performance after task overload. Therefore, we increased the task difficulty but set a lower and reasonable threshold to the task accuracy in order to achieve the maximum effect on hemodynamic responses induced by anxiety.

### Monitoring of Brain States and Cognitive Evaluations Using Portable fNIRS Solutions

By validating the high correlation between fNIRS signals and gray-matter fMRI activities in the PFC (Sato et al., 2013; Noah et al., 2015), fNIRS has been proposed as a flexible tool to observe brain hemodynamic responses for cognitive evaluations (Shimada and Hiraki, 2006; Shimada and Oki, 2012; Noah et al., 2015). Most of the previous studies have incorporated high-density fNIRS systems with up to 52 channels to record hemodynamic responses during cognitive experiments (Schreppel et al., 2008; Aoki et al., 2011, 2013; Pu et al., 2011; Sato et al., 2014), and the activation of different brain regions is identified by channels/regions of interests. Unlike the high-density and expensive fNIRS solutions, we demonstrated the possibility of using only four channels of fNIRS signals located on the scalp of the prefrontal regions to evaluate the cognitive process affected by emotion regulation. Incorporating the fNIRS devices with a lower number of channels has become a growing trend (Ehlis et al., 2008; Sanefuji et al., 2011; Ramasubbu et al., 2012; Ogawa et al., 2014; Ozawa et al., 2014), especially when conducting cognitive experiments with children as participants or when recruiting patients with mental disorders. For experiments using two- or four-channel fNIRS systems (Sanefuji et al., 2011; Ramasubbu et al., 2012), the setup time would be shorter with lower complexity of experimental preparation. In comparison with other neuroimaging modalities such as fMRI, an fNIRS system is a compact solution to observe hemodynamic responses from the prefrontal regions, and it can be more flexibly applied in vulnerable participants. To our knowledge, this study is the first to show that the working memory processes affected by emotion regulation can be observed using a four-channel portable fNIRS device. The performance of cognitive processes or mental training can therefore be quantitatively evaluated by accommodating a compact fNIRS system.

## CONCLUSIONS

We proposed an experimental paradigm of auditory working memory to evaluate the correlation between anxiety and memory load. The results revealed that there were significantly stronger hemodynamic responses in the right ventrolateral and orbital PFC when subjects were attending to the auditory working memory task with higher load. In addition, the right lateralization index of the VLPFC was negative correlated with the level of state anxiety. This study showed the flexibility of incorporating fNIRS as an index to evaluate cognitive performance. Furthermore, fNIRS can potentially be applied to functional mapping in children or patients with mental disorders (Tsujimoto et al., 2004). Since it imposes fewer constraints on behavior than fMRI, fNIRS appears to be more practical than fMRI for cognitive neuroscience investigations involving the primate cortex (Fuster et al., 2005). In addition to studies on brain functions, fNIRS may also be a useful tool for the development of brain-computer interfaces (Coyle et al., 2004; Fazli et al., 2012; Kaiser et al., 2014) or the validation of drugs for mental diseases that can cause reduction in lateral prefrontal activities accompanied by improved cognitive performance (Ramasubbu et al., 2012). In summary, we suggest that it is possible to incorporate fNIRS signals as an index of cognitive evaluation given its flexibility regarding portable applications compared to other neuroimaging techniques.

## AUTHOR CONTRIBUTIONS

Y-LT, C-FL, and S-MW conceived analytical hypothesis, performed data analysis and interpretation, and drafted, revised the work. SS, TH, and G-YL performed data analysis

and interpretation. All authors approved the work for publication.

## FUNDING

This work was supported by grant 106-2221-E-030-004- from the Ministry of Science and Technology, Taiwan.

## ACKNOWLEDGMENTS

The authors would like to thank Prof. Alexander N. Savostyanov, Psychology Department, Tomsk State Research University, Tomsk, Russia, and Prof. Michelle Liou, Institute of Statistical Science, Academia Sinica, Taiwan, for their support in verifying the Chinese version of the State-Trait Anxiety Inventory and editorial suggestions.

## REFERENCES

Ansari, T. L., and Derakshan, N. (2011a). The neural correlates of cognitive effort in anxiety: effects on processing efficiency. *Biol. Psychol.* 86, 337–348. doi: 10.1016/j.biopsycho.2010.12.013

Ansari, T. L., and Derakshan, N. (2011b). The neural correlates of impaired inhibitory control in anxiety. *Neuropsychologia* 49, 1146–1153. doi: 10.1016/j.neuropsychologia.2011.01.019

Aoki, R., Sato, H., Katura, T., Matsuda, R., and Koizumi, H. (2013). Correlation between prefrontal cortex activity during working memory tasks and natural mood independent of personality effects: an optical topography study. *Psychiat. Res. Neuroimag.* 212, 79–87. doi: 10.1016/j.pscychresns.2012.10.009

Aoki, R., Sato, H., Katura, T., Utsugi, K., Koizumi, H., Matsuda, R., et al. (2011). Relationship of negative mood with prefrontal cortex activity during working memory tasks: an optical topography study. *Neurosci. Res.* 70, 189–196. doi: 10.1016/j.neures.2011.02.011

Ayaz, H., Izzetoglu, M., Shewokis, P. A., and Onaral, B. (2010). "Sliding-window motion artifact rejection for Functional Near-Infrared Spectroscopy," in *Annual International Conference of the IEEE Engineering in Medicine and Biology Society*, (Buenos Aires), 6567–6570.

Baloğlu, M., Deniz, M. E., and Kesici, Ş. (2011). A descriptive study of individual and cross-cultural differences in statistics anxiety. *Learn. Individ. Diff.* 21, 387–391. doi: 10.1016/j.lindif.2011.03.003

Barbey, A. K., Koenigs, M., and Grafman, J. (2013). Dorsolateral prefrontal contributions to human working memory. *Cortex* 49, 1195–1205. doi: 10.1016/j.cortex.2012.05.022

Basten, U., Stelzel, C., and Fiebach, C. J. (2011). Trait anxiety modulates the neural efficiency of inhibitory control. *J. Cogn. Neurosci.* 23, 3132–3145. doi: 10.1162/jocn_a_00003

Basten, U., Stelzel, C., and Fiebach, C. J. (2012). Trait anxiety and the neural efficiency of manipulation in working memory. *Cogn. Affect. Behav. Neurosci.* 12, 571–588. doi: 10.3758/s13415-012-0100-3

Berggren, N., and Derakshan, N. (2013). Attentional control deficits in trait anxiety: why you see them and why you don't. *Biol. Psychol.* 92, 440–446. doi: 10.1016/j.biopsycho.2012.03.007

Berggren, N., Richards, A., Taylor, J., and Derakshan, N. (2013). Affective attention under cognitive load: reduced emotional biases but emergent anxiety-related costs to inhibitory control. *Front. Hum. Neurosci.* 7:188. doi: 10.3389/fnhum.2013.00188

Bishop, S. J. (2009). Trait anxiety and impoverished prefrontal control of attention. *Nat. Neurosci.* 12, 92–98. doi: 10.1038/nn.2242

Bishop, S., Duncan, J., Brett, M., and Lawrence, A. D. (2004). Prefrontal cortical function and anxiety: controlling attention to threat-related stimuli. *Nat. Neurosci.* 7, 184–188. doi: 10.1038/nn1173

Blackhart, G. C., Minnix, J. A., and Kline, J. P. (2006). Can EEG asymmetry patterns predict future development of anxiety and depression? A preliminary study. *Biol. Psychol.* 72, 46–50. doi: 10.1016/j.biopsycho.2005.06.010

Brigadoi, S., Ceccherini, L., Cutini, S., Scarpa, F., Scatturin, P., Selb, J., et al. (2014). Motion artifacts in functional near-infrared spectroscopy: a comparison of motion correction techniques applied to real cognitive data. *Neuroimage* 85, 181–191. doi: 10.1016/j.neuroimage.2013.04.082

Cavanagh, J. F., and Shackman, A. J. (2014). Frontal midline theta reflects anxiety and cognitive control: meta-analytic evidence. *J. Physiol. Paris* 109, 3–15. doi: 10.1016/j.jphysparis.2014.04.003

Comte, M., Cancel, A., Coull, J. T., Schön, D., Reynaud, E., Boukezzi, S., et al. (2015). Effect of trait anxiety on prefrontal control mechanisms during emotional conflict. *Hum. Brain Mapp.* 36, 2207–2214. doi: 10.1002/hbm.22765

Coyle, S., Ward, T., Markham, C., and McDarby, G. (2004). On the suitability of near-infrared (NIR) systems for next-generation brain–computer interfaces. *Physiol. Meas.* 25, 815–822. doi: 10.1088/0967-3334/25/4/003

Cui, X., Bray, S., and Reiss, A. L. (2010). Functional near infrared spectroscopy (NIRS) signal improvement based on negative correlation between oxygenated and deoxygenated hemoglobin dynamics. *Neuroimage* 49, 3039–3046. doi: 10.1016/j.neuroimage.2009.11.050

D'Esposito, M. (2007). From cognitive to neural models of working memory. *Philos. Trans. R. Soc. B Biol. Sc.* 362, 761–772. doi: 10.1098/rstb.2007.2086

Dennis, T. A., and Hajcak, G. (2009). The late positive potential: a neurophysiological marker for emotion regulation in children. *J. Child Psychol. Psychiatry* 50, 1373–1383. doi: 10.1111/j.1469-7610.2009.02168.x

Ehlis, A. C., Bähne, C. G., Jacob, C. P., Herrmann, M. J., and Fallgatter, A. J. (2008). Reduced lateral prefrontal activation in adult patients with attention-deficit/hyperactivity disorder (ADHD) during a working memory task: a functional near-infrared spectroscopy (fNIRS) study. *J. Psychiatr. Res.* 42, 1060–1067. doi: 10.1016/j.jpsychires.2007.11.011

Eysenck, M. W., and Calvo, M. G. (1992). Anxiety and performance: the processing efficiency theory. *Cogn. Emot.* 6, 409–434. doi: 10.1080/02699939208409696

Eysenck, M. W., Derakshan, N., Santos, R., and Calvo, M. G. (2007). Anxiety and cognitive performance: attentional control theory. *Emotion* 7, 336–353. doi: 10.1037/1528-3542.7.2.336

Fazli, S., Mehnert, J., Steinbrink, J., Curio, G., Villringer, A., Müller, K.-R., et al. (2012). Enhanced performance by a hybrid NIRS–EEG brain computer interface. *Neuroimage* 59, 519–529. doi: 10.1016/j.neuroimage.2011.07.084

Fuster, J., Guiou, M., Ardestani, A., Cannestra, A., Sheth, S., Zhou, Y. D., et al. (2005). Near-infrared spectroscopy (NIRS) in cognitive neuroscience of the primate brain. *Neuroimage* 26, 215–220. doi: 10.1016/j.neuroimage.2005.01.055

Hajcak, G., MacNamara, A., Foti, D., Ferri, J., and Keil, A. (2013). The dynamic allocation of attention to emotion: simultaneous and independent evidence from the late positive potential and steady state visual evoked potentials. *Biol. Psychol.* 92, 447–455. doi: 10.1016/j.biopsycho.2011.11.012

Horwitz, E. (2001). Language anxiety and achievement. *Annu. Rev. Appl. Linguist.* 21, 112–126. doi: 10.1017/S0267190501000071

Hoshi, Y., Tsou, B. H., Billock, V. A., Tanosaki, M., Iguchi, Y., Shimada, M., et al. (2003). Spatiotemporal characteristics of hemodynamic changes in the human lateral prefrontal cortex during working memory tasks. *Neuroimage* 20, 1493–1504. doi: 10.1016/S1053-8119(03)00412-9

Huang, S., Seidman, L. J., Rossi, S., and Ahveninen, J. (2013). Distinct cortical networks activated by auditory attention and working memory load. *Neuroimage* 83, 1098–1108. doi: 10.1016/j.neuroimage.2013.07.074

Huppert, T. J., Diamond, S. G., Franceschini, M. A., and Boas, D. A. (2009). HomER: a review of time-series analysis methods for near-infrared spectroscopy of the brain. *Appl. Opt.* 48, D280–D298. doi: 10.1364/AO.48.00D280

Izzetoglu, M., Izzetoglu, K., Bunce, S., Ayaz, H., Devaraj, A., Onaral, B., et al. (2005). Functional near-infrared neuroimaging. *IEEE Trans. Neural Syst. Rehabil. Eng.* 13, 153–159. doi: 10.1109/TNSRE.2005.847377

Jaeggi, S. M., Buschkuehl, M., Perrig, W. J., and Meier, B. (2010). The concurrent validity of the N-back task as a working memory measure. *Memory* 18, 394–412. doi: 10.1080/09658211003702171

Jasper, H. H. (1958). The ten twenty electrode system of the international federation. *Electroencephalogr. Clin. Neurophysiol.* 10, 371–375.

Kaiser, V., Bauernfeind, G., Kreilinger, A., Kaufmann, T., Kübler, A., Neuper, C., et al. (2014). Cortical effects of user training in a motor imagery based brain–computer interface measured by fNIRS and EEG. *Neuroimage* 85, 432–444. doi: 10.1016/j.neuroimage.2013.04.097

Knyazev, G. G., Savostyanov, A. N., Bocharov, A. V., and Rimareva, J. M. (2016). Anxiety, depression, and oscillatory dynamics in a social interaction model. *Brain Res.* 1644, 62–69. doi: 10.1016/j.brainres.2016.04.075

Knyazev, G. G., Savostyanov, A. N., and Levin, E. A. (2004). Alpha oscillations as a correlate of trait anxiety. *Int. J. Psychophysiol.* 53, 147–160. doi: 10.1016/j.ijpsycho.2004.03.001

Lai, V., Theppitak, C., Makizuka, T., Higuchi, Y., Movahed, M., Kumudini, G., et al. (2014). A normal intensity level of psycho-physiological stress can benefit working memory performance at high load. *Int. J. Ind. Ergon.* 44, 362–367. doi: 10.1016/j.ergon.2013.11.015

Lara, A. H., and Wallis, J. D. (2015). The role of prefrontal cortex in working memory: a mini review. *Front. Syst. Neurosci.* 9:173. doi: 10.3389/fnsys.2015.00173

MacNamara, A., Ferri, J., and Hajcak, G. (2011). Working memory load reduces the late positive potential and this effect is attenuated with increasing anxiety. *Cogn. Affect. Behav. Neurosci.* 11, 321–331. doi: 10.3758/s13415-011-0036-z

MacNamara, A., and Hajcak, G. (2009). Anxiety and spatial attention moderate the electrocortical response to aversive pictures. *Neuropsychologia* 47, 2975–2980. doi: 10.1016/j.neuropsychologia.2009.06.026

MacNamara, A., and Hajcak, G. (2010). Distinct electrocortical and behavioral evidence for increased attention to threat in generalized anxiety disorder. *Depress. Anxiety* 27, 234–243. doi: 10.1002/da.20679

Mallat, S. G. (1989). A theory for multiresolution signal decomposition: the wavelet representation. *IEEE Trans. Pattern Anal. Mach. Intell.* 11, 674–693. doi: 10.1109/34.192463

Manoach, D. S., Schlaug, G., Siewert, B., Darby, D. G., Bly, B. M., Benfield, A., et al. (1997). Prefrontal cortex fMRI signal changes are correlated with working memory load. *Neuroreport* 8, 545–549. doi: 10.1097/00001756-199701200-00033

McKendrick, R., Ayaz, H., Olmstead, R., and Parasuraman, R. (2014). Enhancing dual-task performance with verbal and spatial working memory training: continuous monitoring of cerebral hemodynamics with NIRS. *NeuroImage* 85(Pt 3), 1014–1026. doi: 10.1016/j.neuroimage.2013.05.103

Molavi, B., and Dumont, G. A. (2012). Wavelet-based motion artifact removal for functional near-infrared spectroscopy. *Physiol. Meas.* 33:259. doi: 10.1088/0967-3334/33/2/259

Muñoz-López, M., Insausti, R., Mohedano-Moriano, A., Mishkin, M., and Saunders, R. (2015). Anatomical pathways for auditory memory II: information from rostral superior temporal gyrus to dorsolateral temporal pole and medial temporal cortex. *Front. Neurosci.* 9:158. doi: 10.3389/fnins.2015.00158

Noah, J. A., Ono, Y., Nomoto, Y., Shimada, S., Tachibana, A., Zhang, X., et al. (2015). fMRI Validation of fNIRS Measurements During a Naturalistic Task. *J. Vis. Exp.* 100:52116. doi: 10.3791/52116

Ogawa, Y., Kotani, K., and Jimbo, Y. (2014). Relationship between working memory performance and neural activation measured using near-infrared spectroscopy. *Brain Behav.* 4, 544–551. doi: 10.1002/brb3.238

Ohman, A. (2005). The role of the amygdala in human fear: automatic detection of threat. *Psychoneuroendocrinology* 30, 953–958. doi: 10.1016/j.psyneuen.2005.03.019

Okamoto, M., Dan, H., Sakamoto, K., Takeo, K., Shimizu, K., Kohno, S., et al. (2004). Three-dimensional probabilistic anatomical cranio-cerebral correlation via the international 10–20 system oriented for transcranial functional brain mapping. *Neuroimage* 21, 99–111. doi: 10.1016/j.neuroimage.2003.08.026

Osinsky, R., Gebhardt, H., Alexander, N., and Hennig, J. (2012). Trait anxiety and the dynamics of attentional control. *Biol. Psychol.* 89, 252–259. doi: 10.1016/j.biopsycho.2011.10.016

Ozawa, S., Matsuda, G., and Hiraki, K. (2014). Negative emotion modulates prefrontal cortex activity during a working memory task: a NIRS study. *Front. Hum. Neurosci.* 8:46. doi: 10.3389/fnhum.2014.00046

Pacheco-Unguetti, A. P., Acosta, A., Lupiá-ez, J., Román, N., and Derakshan, N. (2012). Response inhibition and attentional control in anxiety. *Q. J. Exp. Psychol. (Hove).* 65, 646–660. doi: 10.1080/17470218.2011.637114

Pallesen, K. J., Brattico, E., Bailey, C. J., Korvenoja, A., Koivisto, J., Gjedde, A., et al. (2010). Cognitive control in auditory working memory is enhanced in musicians. *PLoS ONE* 5:e11120. doi: 10.1371/journal.pone.0011120

Plakke, B., Ng, C. W., and Poremba, A. (2013). Neural correlates of auditory recognition memory in primate lateral prefrontal cortex. *Neuroscience* 244, 62–76. doi: 10.1016/j.neuroscience.2013.04.002

Plakke, B., and Romanski, L. M. (2014). Auditory connections and functions of prefrontal cortex. *Front. Neurosci.* 8:199. doi: 10.3389/fnins.2014.00199

Power, M., and Dalgleish, T. (2015). *Cognition and Emotion: From Order to Disorder*. London: Psychology press.

Pu, S., Yamada, T., Yokoyama, K., Matsumura, H., Kobayashi, H., Sasaki, N., et al. (2011). A multi-channel near-infrared spectroscopy study of prefrontal cortex activation during working memory task in major depressive disorder. *Neurosci. Res.* 70, 91–97. doi: 10.1016/j.neures.2011.01.001

Ramasubbu, R., Singh, H., Zhu, H., and Dunn, J. F. (2012). Methylphenidate-mediated reduction in prefrontal hemodynamic responses to working memory task: a functional near-infrared spectroscopy study. *Hum. Psychopharmacol. Clin. Exp.* 27, 615–621. doi: 10.1002/hup.2258

Riley, M. R., and Constantinidis, C. (2016). Role of prefrontal persistent activity in working memory. *Front. Syst. Neurosci.* 9:181. doi: 10.3389/fnsys.2015.00181

Robertson, F. C., Douglas, T. S., and Meintjes, E. M. (2010). Motion artifact removal for functional near infrared spectroscopy: a comparison of methods. *IEEE Trans. Biomed. Eng.* 57, 1377–1387. doi: 10.1109/TBME.2009.2038667

Sanefuji, M., Takada, Y., Kimura, N., Torisu, H., Kira, R., Ishizaki, Y., et al. (2011). Strategy in short-term memory for pictures in childhood: a near-infrared spectroscopy study. *Neuroimage* 54, 2394–2400. doi: 10.1016/j.neuroimage.2010.09.090

Sato, H., Dresler, T., Haeussinger, F. B., Fallgatter, A. J., and Ehlis, A. C. (2014). Replication of the correlation between natural mood states and working memory-related prefrontal activity measured by near-infrared spectroscopy in a German sample. *Front. Hum. Neurosci.* 8:37. doi: 10.3389/fnhum.2014.00037

Sato, H., Yahata, N., Funane, T., Takizawa, R., Katura, T., Atsumori, H., et al. (2013). A NIRS–fMRI investigation of prefrontal cortex activity during a working memory task. *Neuroimage* 83, 158–173. doi: 10.1016/j.neuroimage.2013.06.043

Savostyanov, A. N., Tsai, A. C., Liou, M., Levin, E. A., Lee, J. D., Yurganov, A. V., et al. (2009). EEG-correlates of trait anxiety in the stop-signal paradigm. *Neurosci. Lett.* 449, 112–116. doi: 10.1016/j.neulet.2008.10.084

Schmukle, S. C., and Egloff, B. (2004). Does the Implicit Association Test for assessing anxiety measure trait and state variance? *Eur. J. Pers.* 18, 483–494. doi: 10.1002/per.525

Schreppel, T., Egetemeir, J., Schecklmann, M., Plichta, M. M., Pauli, P., Ellgring, H., et al. (2008). Activation of the prefrontal cortex in working memory and interference resolution processes assessed with near-infrared spectroscopy. *Neuropsychobiology* 57, 188–193. doi: 10.1159/000147473

Sehlmeyer, C., Konrad, C., Zwitserlood, P., Arolt, V., Falkenstein, M., and Beste, C. (2010). ERP indices for response inhibition are related to anxiety-related personality traits. *Neuropsychologia* 48, 2488–2495. doi: 10.1016/j.neuropsychologia.2010.04.022

Shek, D. T. (1993). The Chinese version of the State-Trait Anxiety Inventory: its relationship to different measures of psychological well-being. *J. Clin. Psychol.* 49, 349–358. doi: 10.1002/1097-4679(199305)49:3<349::AID-JCLP2270490308>3.0.CO;2-J

Shimada, S., and Hiraki, K. (2006). Infant's brain responses to live and televised action. *Neuroimage* 32, 930–939. doi: 10.1016/j.neuroimage.2006.03.044

Shimada, S., and Oki, K. (2012). Modulation of motor area activity during observation of unnatural body movements. *Brain Cogn.* 80, 1–6. doi: 10.1016/j.bandc.2012.04.006

Spielberger, C. D., Gorsuch, R. L., and Lushene, R. E. (1970). *Manual for the State-Trait Anxiety Inventory*. Palo Alto, CA: Consulting Psychologists Press.

Stout, D. M., Shackman, A. J., and Larson, C. L. (2013). Failure to filter: anxious individuals show inefficient gating of threat from working memory. *Front. Hum. Neurosci.* 7:58. doi: 10.3389/fnhum.2013.00058

Tsujimoto, S., Yamamoto, T., Kawaguchi, H., Koizumi, H., and Sawaguchi, T. (2004). Prefrontal cortical activation associated with working memory in adults and preschool children: an event-related optical topography study. *Cereb. Cortex* 14, 703–712. doi: 10.1093/cercor/bhh030

Vytal, K., Cornwell, B., Arkin, N., and Grillon, C. (2012). Describing the interplay between anxiety and cognition: from impaired performance under low cognitive load to reduced anxiety under high load. *Psychophysiology* 49, 842–852. doi: 10.1111/j.1469-8986.2012.01358.x

Weinberger, N. M. (2014). Neuromusic research: some benefits of incorporating basic research on the neurobiology of auditory learning and memory. *Front. Syst. Neurosci.* 7:128. doi: 10.3389/fnsys.2013.00128

Wu, S.-M., Ding, H.-M., and Tseng, Y.-L. (2017). "A functional near-infrared spectroscopy study of auditory working memory load," in *International Conference on Human-Computer Interaction* (Vancouver, BC: Springer), 273–277.

**Conflict of Interest Statement:** The authors declare that the research was conducted in the absence of any commercial or financial relationships that could be construed as a potential conflict of interest.

frontiers in Human Neuroscience

ORIGINAL RESEARCH
published: 14 August 2018
doi: 10.3389/fnhum.2018.00324

# The Neuroanatomical Basis of Two Subcomponents of Rumination: A VBM Study

*Emily L. L. Sin*[1,2†], *R. Shao*[1,2†], *Xiujuan Geng*[1,2], *Valda Cho*[2] *and Tatia M. C. Lee*[1,2,3*]

[1]*State Key Laboratory of Brain and Cognitive Sciences, The University of Hong Kong, Pokfulam, Hong Kong,* [2]*Laboratory of Neuropsychology, The University of Hong Kong, Pokfulam, Hong Kong,* [3]*Institute of Clinical Neuropsychology, The University of Hong Kong, Pokfulam, Hong Kong*

Rumination is a trait that includes two subcomponents, namely brooding and reflective pondering, respectively construed as maladaptive and adaptive response styles to negative experiences. Existing evidence indicates that rumination in general is associated with structural and functional differences in the anterior cingulate cortex (ACC) and the dorsal lateral prefrontal cortex (DLPFC). However, conclusive evidence on the specific neural structural basis of each of the two subcomponents is lacking. In this voxel-based morphometry study, we investigated the independent and specific neural structural basis of brooding and reflective pondering in 30 healthy young adults, who belonged to high or low brooding or reflective pondering groups. Consistent with past research, modest but significant positive correlation was found between brooding and reflective pondering. When controlling for reflective pondering, high-brooding group showed increased gray matter volumes in the left DLPFC and ACC. Further analysis on extracted gray matter values showed that gray matter of the same DLPFC and ACC regions also showed significant negative effects of reflective pondering. Taken together, our findings indicate that the two subcomponents of rumination might share some common processes yet also have distinct neural basis. In view of the significant roles of the left DLPFC and ACC in attention and self-related emotional processing/regulation, our findings provide insight into how the potentially shared and distinct cognitive, affective and neural processes of brooding and reflective pondering can be extended to clinical populations to further elucidate the neurobehavioral relationships between rumination and prefrontal abnormality.

**Keywords: voxel-based morphometry, MRI, rumination, brooding, reflective pondering**

OPEN ACCESS

***Edited by:***
*Nan Li,*
*RIKEN, Japan*

***Reviewed by:***
*Haijiang Li,*
*Shanghai Normal University, China*
*Xiaosong He,*
*University of Pennsylvania, United States*

***Correspondence:**
*Tatia M. C. Lee*
*tmclee@hku.hk*

*[†]These authors have contributed equally to this work*

***Received:*** *15 May 2018*
***Accepted:*** *25 July 2018*
***Published:*** *14 August 2018*

***Citation:***
*Sin ELL, Shao R, Geng X, Cho V and Lee TMC (2018) The Neuroanatomical Basis of Two Subcomponents of Rumination: A VBM Study. Front. Hum. Neurosci. 12:324. doi: 10.3389/fnhum.2018.00324*

## INTRODUCTION

Rumination refers to a person indulging in passive and repetitive thinking on symptoms of distress and the possible causes and consequences of those symptoms (Nolen-Hoeksema and Morrow, 1993). Rumination is considered to be a trait-like construct and is present as a spectrum in the general population, with some individuals manifesting more prominent ruminative characteristics than others (Nolen-Hoeksema and Morrow, 1991; Just and Alloy, 1997; Spasojević and Alloy, 2001; Moberly and Watkins, 2008; Smith et al., 2009). Previous studies found that rumination is positively related to other personality traits such as neuroticism (Muris et al., 2005), and high ruminative level is associated with affective disorders such as depression and anxiety (Berman et al., 2011; Hamilton et al., 2011;

Vanhalst et al., 2012). In essence, rumination characterizes individuals' response and coping styles when faced with life distresses. According to the Response Style Theory, there are two subcomponents in rumination, namely brooding and reflective pondering, both of which can be quantitatively measured using the Response Style Scale (RSS).

Previous research has revealed a positive correlation between the two RSS subcomponents (Treynor et al., 2003; Nolen-Hoeksema et al., 2008). However, there are various differences between the two subcomponents in terms of their psychometric properties. First, brooding and reflective pondering were identified as two distinctive factors through factor analysis (Treynor et al., 2003). Moreover, brooding is positively and moderately associated with depression both concurrently and longitudinally, while reflective pondering is only associated with depression concurrently (Treynor et al., 2003). Conceptually, they may have some overlapping in initial processing of negative events but differ markedly in the characteristics of subsequent cognitive-affective processes. Specifically, brooding refers to the tendency to reflect on the (potential) negative impact of a current situation without devising a constructive solution (Treynor et al., 2003). Reflective pondering, on the other hand, is a tendency to contemplate the current situation with a constructive solution in mind and intentionally ponder one's mind with a focus on problem solving (Treynor et al., 2003; Whitmer and Gotlib, 2013). In other words, during the brooding process, one is usually trapped in the affective loop and cannot move on to cognitive problem-solving, while during reflective pondering, one can successfully proceed to constructive cognitive processes directed at the problem at hand. Thus, brooding and reflective pondering were suggested to have different clinical implications, with brooding being considered a maladaptive form of coping strategy, while reflective pondering was suggested to be adaptive (Treynor et al., 2003).

A body of cross-sectional and longitudinal research has identified effects of personality traits such as neuroticism on gray matter volume (Blankstein et al., 2009; DeYoung et al., 2010; Taki et al., 2013). These studies show that it is valuable to understand the neuroanatomical basis of individual differences in personally traits. However, existing research on the neural basis of rumination trait is limited. One recent study found that gray matter volume of the dorsolateral prefrontal cortex (DLPFC) positively predicted rumination in non-depressed individuals, which was interpreted as potentially reflecting functional inefficiency and overloading (Wang et al., 2015). In another study, self-reported rumination was positively predicted by resting-state functional connectivity between the DLPFC and the rostral anterior cingulate cortex (ACC) in depressed patients, which in turn was positively correlated with the DLPFC cortical thickness (Späti et al., 2015). Collectively, existing evidence suggests that the DLPFC and ACC gray matter structures are most commonly associated with self-reported rumination (Pizzagalli, 2011; Ghaznavi and Deckersbach, 2012; Kühn et al., 2012; Wang et al., 2015). Indeed, the total score of rumination showed negative correlation with left ACC gray matter volume among healthy participants even after controlling for depressive symptomology (Kühn et al., 2012), underscoring the integral role of the ACC in ruminative processes (Pizzagalli, 2011). However, brooding and reflective pondering were not separately investigated in Kühn et al. (2012), hence the relationship between ACC or DLPFC gray matter volume and each of the two subcomponents of rumination remains unclear.

The DLPFC was proposed to perform memory and attention functions, as well as cognitive manipulation of incoming information (Dixon et al., 2017). Consistent with this, depressive patients show both DLPFC structural abnormalities and functional hypoactivity in resting-state and task-based fMRI (Gotlib and Hamilton, 2008; Koenigs and Grafman, 2009). Among healthy participants, in task-based fMRI, healthy subjects with high brooding tendency showed more DLPFC activations when trying to disengage from negative information compared to those with low brooding tendency (Vanderhasselt et al., 2011, 2013). Similarly, among major depressive patients, rumination induction elicited greater activations in the DLPFC than a distraction task (Cooney et al., 2010). The ACC is important for encoding affective value as well as in emotion regulation and cognitive control (Mohanty et al., 2007). Greater activations in the rostral ACC (rACC) were found while participants were performing an emotional rather than cognitive stroop task (Mohanty et al., 2007). Further, when performing an emotion contrast task, dorsal ACC activity predicted individual differences in brooding score (Vanderhasselt et al., 2013).

Our study specifically investigated the independent neuroanatomical (gray matter volume) basis of the two rumination subcomponents to elucidate the underlying common and distinct cognitive and affective mechanisms of brooding and reflective pondering. Based on existing literature on important roles of the DLPFC and the ACC on cognitive executive control and affect processing/regulation, we focused on those two areas as regions of interest (ROI). We hypothesized: (1) a positive relationship between scores on brooding and reflective pondering; (2) gray matter volumes in the DLPFC and ACC would be larger for high than low brooders. Given previous evidence suggesting opposite clinical implications for brooding (maladaptive) and reflective pondering (adaptive), we tentatively hypothesized that; and (3) reflective pondering would show opposite (i.e., negative) relations with DLPFC and ACC gray matter volume to brooding.

# MATERIALS AND METHODS

## Participants, Measures and Procedure

Thirty healthy, right-handed, Chinese adults (11 males and 19 females) aged between 20 years and 48 years old (Mean = 31.77 years; SD = 6.84 years) participated in this study. These participants were recruited from the community. Participants did not have any current or prior history of neurological or psychiatric disorders that might affect their cognitive functioning. The current study was approved by the Institutional Review Board of The University of Hong Kong. All participants signed informed consents prior to participation.

The Ruminative Response Scale (RRS; Nolen-Hoeksema and Morrow, 1991) is a 22-item self-rating scale designed to assess an

individual's propensity to ruminate. It consists of two subscales that purport to measure the two subcomponents of rumination, namely brooding and reflective pondering. The items are mainly self-relevant and focus on the possible antecedents and consequences of one's depressed mood state, which can be used to ascertain how an individual generally feels, thinks, and reacts when feeling down or depressed.

The Chinese version of the 14-item Hospital Anxiety and Depression Scale (HADS; Leung et al., 1999) was used to measure the severity of depression (HADS-D) and anxiety (HADS-A) in the participants. The HADS is a widely used scale in measuring the severity of depression and anxiety symptoms in both psychological and neuropsychiatric studies. There are two subscales, anxiety and depression, containing seven questions in each. Scores range from 0 to 21 and are categorized as follows: normal 0–7, mild 8–10, moderate 11–14 and severe 15–21 (Whelan-Goodinson et al., 2009). The Chinese version of HADS has good internal consistency (Cronbach alpha = 0.86; Leung et al., 1999).

Through employing a median split procedure on the Brooding and Reflective subscales of the RRS, all participants were assigned to either High Brooding Group (HBG) or Low Brooding Group (LBG) and either High Reflective Pondering Group (HRG) or Low Reflective Pondering Group (LRG). The Brooding and Reflective scores showed modest but significant correlation ($r = 0.394$; $p = 0.031$).

In total, 14 participants (five males; mean age = 30.57 years) were assigned to the LBG (brooding score $\leq$9; Mean = 7.86; SD = 1.02), whereas the remaining 16 participants were assigned to the HBG (six males; mean age = 32.81 years; brooding score >9; Mean = 12.81; SD = 2.43). The high and LBGs only differed in terms of the brooding levels ($t = -7.44$, $p < 0.001$), but not in age ($t = -0.90$, $p = 0.644$), gender composition ($X^2 = 0.010$, $p = 0.919$), self-reported level of depression or anxiety ($|t| < 1.17$, $p$s $> 0.25$), or reflective pondering score ($t = -1.820$, $p = 0.080$).

In a similar vein, the same 30 participants were divided into LRG (reflective pondering score $\leq$9; 15 subjects with three males; mean age = 30.87 years) and HRG (reflective pondering score >9; 15 subjects with eight males; mean age = 32.67 years) based on their scores on the Reflective Pondering subscale of the RRS. Again, no significant between-group difference was identified in demographic characteristics (age: $t = -0.714$, $p = 0.481$; gender composition: $X^2 = 3.589$, $p = 0.128$), self-reported level of depression or anxiety ($|t| < 0.44$, $p$s $> 0.66$). Also, the HRG scored significantly higher than the LRG group only on the Reflective Pondering subscale of the RRS ($t = -8.735$, $p < 0.001$), but not on the Brooding subscale ($t = -1.614$, $p = 0.118$).

On the study day, each participant was instructed to complete the self-reported questionnaires including the RRS and HADS, before entering the MRI scanner.

## Image Acquisition

High-resolution anatomical images were acquired via a 3.0 Tesla Philips Medical Systems Achieva scanner with an eight-channel SENSE head coil. A three-dimensional, T1-weighted, magnetization-prepared rapid acquisition gradient-echo sequence was used with 164 contiguous sagittal slices (time to repetition = 7 ms; time to echo = 3.2 ms; acquisition matrix = 240 × 230; sagittal field of view = 164 mm; flip angle = 8°; voxel size = 1 × 1 × 1 $mm^3$).

## Structural Brain Image Pre-processing and Analysis

The CAT12 toolbox[1] within SPM12 (FIL, London, UK) in MATLAB 7.12.0 environment (Mathworks Inc., Natick, MA, USA) was used to preprocess the MRI images. The T1 images were manually reoriented and centered on the anterior commissure as the point of origin. Each T1 image was then visually inspected in SPM12 to check for any artifacts or gross anatomical abnormalities. Next, the T1 images were segmented into six tissue types and normalized to the standard MNI template through the DARTEL procedure using customized template. Segmentation and normalization quality was manually inspected for all participants. Finally, the resulted modulated normalized gray matter images were smoothed with a standard Gaussian kernel of 8-mm FWHM.

The smoothed gray matter images were then used for subsequent imaging analyses in SPM12. Two general linear models (independent-samples *t*-tests) were used to examine the respective effect of brooding group (LBG vs. HBG) and reflective pondering group (LRG vs. HRG), while controlling for the other component (reflective pondering score in the former case and brooding score in the latter case). As presented above, the brooding and reflective pondering continuous scores significantly correlated with each other ($r = 0.394$; $p < 0.05$), meaning that the analysis power for detecting the effect of either variable would be markedly reduced if both were included simultaneously in the model. However, the correlations between brooding group and reflective pondering score, and between reflective pondering group and brooding score, were not significant ($p$s $\geq 0.08$). Thus, for the whole-brain imaging analysis with relatively stringent statistical correction thresholds and limited power, we decided to use the dichotomous brooding (and reflective pondering) group variable when investigating their effects, while keeping them as continuous when they entered the model as nuisance variables, in order to achieve a balance of analysis power and complete control of nuisance effects. For completeness, a multiple regression analysis was also performed on the T1 images in which both the brooding and reflective pondering scores were entered as continuous variables, and results of this analysis were compared to those of the group-based analyses outlined above. Age, gender and total intracranial volume (TIV) were also entered as additional nuisance variables. We primarily focused on two *a priori* ROIs, namely the DLPFC and ACC, which were constructed using WFU_Pickatlas software based on Talairach Daemon atlas. Both masks were bilateral. Within those ROIs, small-volume correction tests were conducted. Through conducting the ROI-based analyses, we ensured that any DLPFC or ACC clusters that we observed were anatomically confined to the respective structure. Complementary whole-brain analyses were

[1] http://dbm.neuro.uni-jena.de/vbm

also performed. To account for Type-I errors, the results threshold were set at uncorrected $p < 0.001$ at voxel level, and FWE-corrected $p < 0.05$ at cluster level, within the searching space of either the ROIs or across the whole brain.

## Statistical Analyses

Correlation analysis was conducted in SPSS 20.0 (IBM, Armonk, NY, USA) to examine the relationship between brooding and reflective pondering scores. To further characterize the independent associations between the two subcomponents of RRS and gray matter volume, we extracted the average gray matter values from the significant clusters resulted from the independent-samples *t*-tests, and conducted a set of univariate ANOVA assessing the effects of brooding and/or reflective pondering groups while controlling for age, gender, TIV and the alternative RRS subscale score. For completeness, we also replicated the significant results with both brooding and reflective pondering scores as continuous independent variables in multiple-regression analyses. Notably, the ANOVA analyses are not independent from the whole-brain analyses, but it rather served the function of checking whether the regional gray matter volume that was significantly affected by brooding (or reflective pondering) at the whole-brain level would also show some levels of relation with the alternative subscale. All statistical results were evaluated at $p < 0.05$, two-tailed.

# RESULTS

## Psychometric Analysis

The two subcomponents of the RRS were significantly and positively correlated ($r = 0.394$, $p = 0.031$; **Figure 1**). Participants' HADS-D (mean = 3.46, SD = 2.12) and HADS-A scores (mean = 4.21, SD = 2.69) were significantly and marginally correlated with their brooding scores ($r = 0.402$ and 0.342, $p = 0.038$ and 0.081, respectively) after controlling for reflective pondering scores (**Figure 1**). In contrast, neither HADS-D nor HADS-A scores correlated with reflective pondering scores after controlling for brooding scores ($|r| < 0.11$, $ps > 0.58$).

## Imaging Analysis

ROI analysis revealed a significant main effect of brooding group on both DLPFC and ACC gray matter volumes, with the HBG showing increased gray matter than the LBG (DLPFC: peak coordinate = −48, 15, 50, max $t = 5.73$, cluster size = 762 voxels, FWE-corrected $p = 0.005$; ACC: peak coordinate = −9, 39, 20, max $t = 4.69$, cluster size = 915 voxels, FWE-corrected $p < 0.001$; **Figure 2**). The ACC cluster remained significant in the multiple regression analyses in which both brooding and reflective pondering scores were entered as continuous variables (max $t = 4.54$, cluster size = 247, FWE-corrected $p = 0.017$), while the DLPFC cluster no longer survived cluster-based FWE correction. However, the DLPFC cluster survived peak-level FWE correction in the multiple regression analysis (max $t = 5.11$, FWE-corrected $p = 0.031$, cluster size = 53). Whole-brain analysis revealed no significant cluster. We also found no cluster that survived correction at whole-brain or ROI-level for the effect of reflective pondering group.

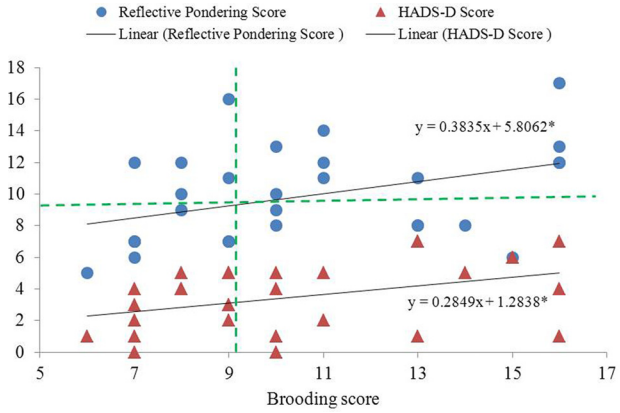


**FIGURE 1 |** Significant inter-correlation between the brooding and reflective pondering subscales of the rumination response scale (RRS) questionnaire, and between brooding and HADS-D. Brooding score showed significant and positive correlation with both reflective pondering and HADS-D scores (controlling for reflective pondering score). The two dashed lines indicate cut-off points for dividing low- and high-brooding (vertical line) and reflective pondering (horizontal line) groups. *Significant at $p < 0.05$, 2-tailed.

The mean gray matter values of the significant DLPFC and ACC clusters were extracted and subjected to further complementary ANOVA analyses in SPSS. As expected, significant effects of brooding group were observed for both clusters (DLPFC: $F_{(1,24)} = 30.68$, $p < 0.001$; ACC: $F_{(1,24)} = 23.538$, $p < 0.001$). However, reflective pondering also showed significant, albeit quantitatively smaller, effects on both clusters (DLPFC: $F_{(1,24)} = 5.671$, $p = 0.026$; ACC: $F_{(1,24)} = 8.972$, $p = 0.006$). Thus, the two rumination subcomponents showed opposite relations with the gray matter volumes of the same ACC and DLPFC regions, with the effect of reflective pondering being smaller in magnitude and undetected at the whole brain/ROI level. Quantitatively similar results were obtained if both brooding and reflective pondering scores were entered as continuous variables in a multiple-regression analysis (for brooding: $ts \geq 2.64$, $ps \leq 0.014$; for reflective pondering: $ts \leq -2.34$, $ps \leq 0.028$). No significant interactive effect of the two RSS subscale scores was observed on either DLPFC or ACC gray matter volume ($p > 0.9$). Further *post hoc* analyses revealed that while the HBG showed increased gray matter in both DLPFC and ACC than the LBG (DLPFC: $t_{(25)} = 5.405$, $p < 0.001$; ACC: $t_{(25)} = 4.852$, $p < 0.001$), the HRG showed gray matter reductions in both DLPFC and ACC than the LRG (DLPFC: $t_{(25)} = -2.332$, $p = 0.029$; ACC: $t_{(25)} = -2.923$, $p = 0.008$; **Figure 2**).

# DISCUSSION

In this study, we confirmed that in healthy individuals, brooding and reflective pondering showed modest positive

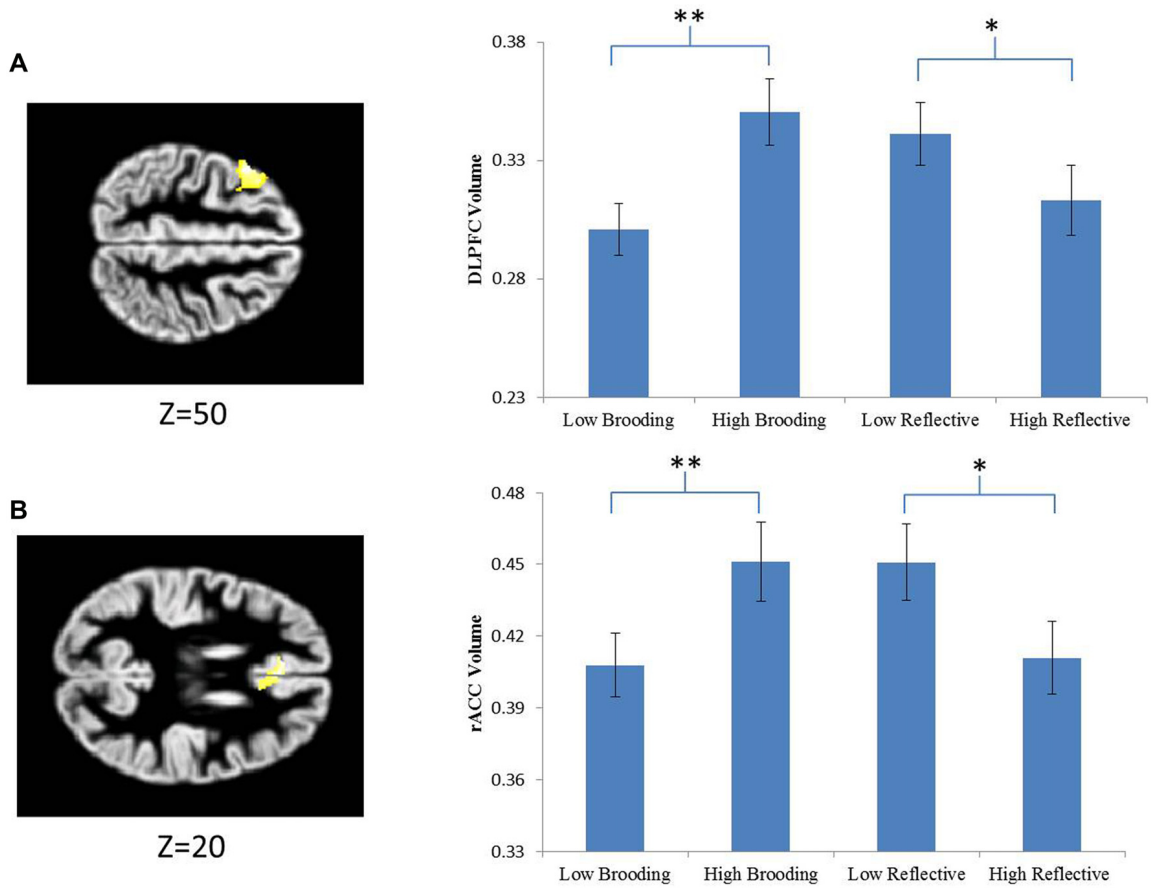


**FIGURE 2 |** Extracted parameter estimates of significant clusters to the effect of brooding. Signals were extracted from two *a priori* regions of interests (ROIs). **(A)** The dorsal lateral prefrontal cortex (DLPFC) and **(B)** the anterior cingulate cortex (ACC). The significant clusters (DLPFC and rostral ACC) are overlaid on standard anatomical templates. MNI z coordinates are provided below the axial slices. *Indicates statistically significant effects at $p < 0.05$, **indicates statistically significant effects at $p < 0.001$.

correlation with each other. However, while brooding showed independent positive effect on gray matter volumes of the left DLPFC and rostral ACC, reflective pondering showed independent negative effect on those structures. Thus, our results suggest that while the two subcomponents of rumination might share some common processes, they appear to have distinct and potentially even opposite underlying neural mechanisms.

## Conceptual Overlapping of Brooding and Reflective Pondering

We found a positive correlation between the scores of the two subcomponents of RSS. Consistent with previous studies, positive relationship between the two subcomponents may reflect the conceptual overlapping between them (Nolen-Hoeksema and Morrow, 1993; Treynor et al., 2003). As explained in the introduction, brooding refers to the process that one focuses on the cause and consequence of his/her negative experiences without engaging in constructive problem-solving, while reflective pondering is a tendency to contemplate the current situation with a constructive solution in mind. Conceptually, both types of ruminative processes start with attending closely to the negative events. Thus, the positive correlation found likely reflects the common initial attentive processes to negative stimuli (Nolen-Hoeksema and Morrow, 1991, 1993). However, brooding and reflective pondering styles diverge in subsequent cognitive and emotional processes, as discussed below.

## Brooding, DLPFC and ACC

Our findings indicate that participants with higher brooding tendency also showed larger left DLPFC gray matter volume. The DLPFC is strongly implicated in working memory and attention processes, as well as in manipulation of incoming information (Miller and Cohen, 2001; Dixon et al., 2017). Reduction of DLPFC volume has been found in patients with major depressive disorder (Grieve et al., 2013; Lai, 2013). More specifically, the left DLPFC was proposed to be specifically involved in responding to positively-valenced stimuli (Pizzagalli et al., 2005; Balconi and Ferrari, 2012a,Balconi

and Ferrari, 2012b), and reduced left vs. right lateral PFC activation may underlie the affect regulation deficits in depressed individuals (Mathersul et al., 2008; Briceño et al., 2013). Given brooding refers to a tendency to maintain attention to negative stimuli (Joormann et al., 2006), high-brooders would tend to experience greater difficulties in disengaging from negative information, possibly due to lower efficiency of DLPFC functioning. Thus, among high-brooders, the left DLPFC may be recruited to greater extents to compensate for this inefficiency (Vanderhasselt et al., 2011, 2013; Wang et al., 2015), possibly through upregulating positive affective processing, which then gradually lead to increase in DLPFC structural volume (Draganski et al., 2004; Scholz et al., 2009; Wang et al., 2015). Failure to engage in this compensatory process could lead to greater affective dysregulation and more negative affective states, coupled with reduced DLPFC volume as observed in major depressive patients (Grieve et al., 2013; Lai, 2013). In our study, brooding and affective symptomology were positively correlated, suggesting that high brooding tendency constitutes core characteristics of affective dysregulation. Furthermore, the association between brooding and depressive scores appeared quantitatively stronger than that between brooding and anxiety scores, consistent with existing research that while rumination may be specifically associated with depression, anxiety may exhibit a stronger relationship with worry (Hong, 2007; Yook et al., 2010). Such associations need to be further tested in clinical/subclinical samples. Since our high-brooding participants were still free of clinical affective disorders, increased left DLPFC volume might be a key adaptive mechanism that protected those individuals from developing clinically significant affective conditions. It is worth noting that subtle difference in the brooding effect on DLPFC volume was observed depending on whether brooding score was dichotomized or entered as continuous variable, such that the effect survived the predefined cluster-level correction in the former case but only survived peak-level correction in the latter case. The lack of statistical power due to modest inter-correlation between the brooding and reflective pondering scores may partly contribute to this discrepancy. Alternatively, there could be inter-participant heterogeneities within the high-brooding group in engagement of compensatory processes for the dysregulated cognitive-affective system. Moreover, it may be that the relationship between brooding score and DLPFC gray matter is not entirely linear across the full spectrum of brooding tendency. These possibilities need to be tested in future research involving larger participant samples.

We also found a positive association between high brooding tendency and ACC gray matter volume, regardless of whether brooding score was dichotomized or assessed as a continuous variable. The rostral ACC is considered to be responsible for assessment of emotional information and regulation of emotional responses (Mohanty et al., 2007). As part of the default mode network, the rostral ACC is also heavily involved in self-referential processing (Nejad et al., 2013), which is an integral component of rumination. Specifically, brooding was suggested to be similar to analytic self-focusing processes that are associated with clinical affective symptoms and poor problem-solving skills (Nejad et al., 2013). Thus, the increased ACC volume in high-brooders may be a long-term consequence of heightened engagement in self-referential affective processing (Pizzagalli, 2011). Moreover, brooding is associated with negative attention biases, and the increased in ACC volume may reflect a shift towards general hypervigilance and reactivity to negative affective stimuli (Boes et al., 2008). On the other hand, gray matter volume of the ACC was found to be significantly reduced in both major depression and bipolar disorder (Drevets et al., 1997, 2008; Grieve et al., 2013; Lai, 2013). In this regard, the increased ACC structural volume, which could be a long-term consequence of greater recruitment of this region in performing affect regulatory functions (Draganski et al., 2004; Scholz et al., 2009), could be an adaptive mechanism that protected the high-brooding participants from developing clinical affective disorders.

## Reflective Pondering, DLPFC and ACC

Although we did not find significant gray matter volume differences between high- and low-reflective pondering groups at the whole-brain level, we observed negative effects of reflective pondering on both left DLPFC and ACC gray matter volumes which showed positive effects of brooding. These results indicate that reflective pondering has distinct and opposite neural basis to brooding. As discussed above, during the initial stage of information processing, both high-brooders and high-reflective ponderers may show heightened attention towards negative stimuli (Vanderhasselt et al., 2013; Whitmer and Gotlib, 2013). However, during subsequent cognitive and affective processing, high-reflective pondering individuals may show better ability in disengaging from negative self-focused affective processing towards problem-focused cognitive processing. In this regard, high-reflective ponderers can be considered as manifesting relatively high levels of early-stage negative affective bias *as well as* high later-stage negative affect regulatory capacity, which might explain why the DLPFC and ACC volumetric difference between the high- and low-reflective pondering groups was not as prominent as that between high- and low-brooding groups. Consistent with this reasoning, existing evidence indicates that reflective pondering is unrelated to cognitive biases after controlling for brooding and depressive scores in healthy subjects, suggesting that unlike the maladaptive style of brooding, reflective pondering encompasses certain adaptive mechanisms that reduce the prolonging affective impact of negative stimuli (Joormann et al., 2006). In this vein, individuals scoring higher on reflective pondering might be considered to have greater efficiencies in cognitive and affect regulatory functions performed by the DLPFC, which would explain the relatively lower DLPFC volumes in those individuals. Such speculation needs to be formally tested by future functional network connectivity studies to clarify the intricate relationships between DLPFC structural volume and functional connectivity/efficiency, rumination and affect regulatory functioning.

Likewise, reflective pondering showed a negative relationship with rostral ACC volume. The rostral ACC is important in regulating self-referential affective processes. As individuals scoring higher in reflective pondering tend to more quickly disengage from negative self-focused processing, there is less need for those individuals to recruit the rostral ACC, leading to the long-term consequence of relatively lower ACC structural volume. A related possibility is that high-reflective ponderers are more efficient in affect regulatory functions performed by the rostral ACC; therefore, the structural volumes of the ACC are relatively small in those individuals. These speculations again need to be formally tested in future functional activation and connectivity studies.

## LIMITATIONS

Our study has several limitations. First, the current study adopted a cross-sectional design, which precluded us from determining the directionality of the brain-emotion relationship. It remains unknown whether the changes in brain structures preceded or followed the development of rumination response style. Second, in view of our modest sample sizes, the current results should be interpreted with caution and replicated on larger samples. Third, we did not include complementary questionnaires (other than the HADS) to establish the external construct validity of the rumination subscales. Future study could include other trait scales like the Neuroticism scale from NEO Personality Inventory. Last but not the least, future studies may include patients with affective disorders to further advance our understanding on the emotional, cognitive and neural mechanisms of brooding and reflective pondering during the course of clinical conditions. These insights are critical to the development of comprehensive intervention programs.

## CONCLUSION

This study provides important evidence that among healthy adults, the two subcomponents of rumination, namely brooding and reflective pondering, respectively showed independent positive and negative effect on gray matter volumes of the left DLPFC and ACC, areas that have been implicated in attention, affect reactivity/regulation, and self-referential processes. Based on these results, we propose that while brooding and reflective pondering might share some initial attentional processes to negative stimuli, these two different rumination styles show distinct subsequent cognitive and affect regulatory processes, as reflected by their distinct neural structural basis, which in turn have different clinical significances. These findings provide new and important insights into the neurocognitive processes of the rumination sub-processes, which can be extended to clinical populations to further elucidate the neurobehavioral and potential adaptive effects of rumination styles and prefrontal abnormality.

## AUTHOR CONTRIBUTIONS

VC and TL conceptualized the study. VC collected the data. ES, RS and XG analyzed the data. ES, RS, XG and TL wrote the manuscript. All authors read and approved the final version of the manuscript and agreed with its submission to Frontiers in Human Neuroscience.

## FUNDING

This work was supported by The University of Hong Kong May Endowed Professorship in Neuropsychology to TL.

## REFERENCES

Balconi, M., and Ferrari, C. (2012a). Emotional memory retrieval. rTMS stimulation on left DLPFC increases the positive memories. *Brain Imaging Behav.* 6, 454–461. doi: 10.1007/s11682-012-9163-6

Balconi, M., and Ferrari, C. (2012b). rTMS stimulation on left DLPFC affects emotional cue retrieval as a function of anxiety level and gender. *Depress. Anxiety* 29, 976–982. doi: 10.1002/da.21968

Berman, M. G., Peltier, S., Nee, D. E., Kross, E., Deldin, P. J., and Jonides, J. (2011). Depression, rumination and the default network. *Soc. Cogn. Affect. Neurosci.* 6, 548–555. doi: 10.1093/scan/nsq080

Blankstein, U., Chen, J. Y. W., Mincic, A. M., McGrath, P. A., and Davis, K. D. (2009). The complex minds of teenagers: neuroanatomy of personality differs between sexes. *Neuropsychologia* 47, 599–603. doi: 10.1016/j.neuropsychologia.2008.10.014

Boes, A. D., McCormick, L. M., Coryell, W. H., and Nopoulos, P. (2008). Rostral anterior cingulate cortex volume correlates with depressed mood in normal healthy children. *Biol. Psychiatry* 63, 391–397. doi: 10.1016/j.biopsych.2007.07.018

Briceño, E. M., Weisenbach, S. L., Rapport, L. J., Hazlett, K. E., Bieliauskas, L. A., Haase, B. D., et al. (2013). Shifted inferior frontal laterality in women with major depressive disorder is related to emotion processing deficits. *Psychol. Med.* 43, 1433–1445. doi: 10.1017/S0033291712002176

Cooney, R. E., Joormann, J., Eugène, F., Dennis, E. L., and Gotlib, I. H. (2010). Neural correlates of rumination in depression. *Cogn. Affect. Behav. Neurosci.* 10, 470–478. doi: 10.3758/CABN.10.4.470

DeYoung, C. G., Hirsh, J. B., Shane, M. S., Papademetris, X., Rajeevan, N., and Gray, J. R. (2010). Testing predictions from personality neuroscience: brain structure and the big five. *Psychol. Sci.* 21, 820–828. doi: 10.1177/0956797610370159

Dixon, M. L., Thiruchselvam, R., Todd, R., and Christoff, K. (2017). Emotion and the prefrontal cortex: an integrative review. *Psychol. Bull.* 143, 1033–1081. doi: 10.1037/bul0000096

Draganski, B., Gaser, C., Busch, V., Schuierer, G., Bogdahn, U., and May, A. (2004). Neuroplasticity: changes in gray matter induced by training. *Nature* 427, 311–312. doi: 10.1038/427311a

Drevets, W. C., Price, J. L., Simpson, J. R. Jr., Todd, R. D., Reich, T., Vannier, M., et al. (1997). Subgenual prefrontal cortex abnormalities in mood disorders. *Nature* 386, 824–827. doi: 10.1038/386824a0

Drevets, W. C., Savitz, J., and Trimble, M. (2008). The subgenual anterior cingulate cortex in mood disorders. *CNS Spectr.* 13, 663–681. doi: 10.1017/s1092852900013754

Ghaznavi, S., and Deckersbach, T. (2012). Rumination in bipolar disorder: evidence for an unquiet mind. *Biol. Mood Anxiety Disord.* 2:2. doi: 10.1186/2045-5380-2-2

Gotlib, I. H., and Hamilton, J. P. (2008). Neuroimaging and depression: current status and unresolved issues. *Curr. Dir. Psychol. Sci.* 17, 159–163. doi: 10.1111/j.1467-8721.2008.00567.x

Grieve, S. M., Korgaonkar, M. S., Koslow, S. H., Gordon, E., and Williams, L. M. (2013). Widespread reductions in gray matter volume in depression. *Neuroimage Clin.* 3, 332–339. doi: 10.1016/j.nicl.2013.08.016

Hamilton, J. P., Furman, D. J., Chang, C., Thomason, M. E., Dennis, E., and Gotlib, I. H. (2011). Default-mode and task-positive network activity in Major

Depressive Disorder: implications for adaptive and maladaptive rumination. *Biol. Psychiatry* 70, 327–333. doi: 10.1016/j.biopsych.2011.02.003

Hong, R. Y. (2007). Worry and rumination: differential associations with anxious and depressive symptoms and coping behavior. *Behav. Res. Ther.* 45, 277–290. doi: 10.1016/j.brat.2006.03.006

Joormann, J., Dkane, M., and Gotlib, I. H. (2006). Adaptive and maladaptive components of rumination? Diagnostic specificity and relation to depressive biases. *Behav. Ther.* 37, 269–280. doi: 10.1016/j.beth.2006.01.002

Just, N., and Alloy, L. B. (1997). The response styles theory of depression: tests and an extension of the theory. *J. Abnorm. Psychol.* 106, 221–229. doi: 10.1037/0021-843x.106.2.221

Koenigs, M., and Grafman, J. (2009). The functional neuroanatomy of depression: distinct roles for ventromedial and dorsolateral prefrontal cortex. *Behav. Brain Res.* 201, 239–243. doi: 10.1016/j.bbr.2009.03.004

Kühn, S., Vanderhasselt, M.-A., De Raedt, R., and Gallinat, J. (2012). Why ruminators won't stop: the structural and resting state correlates of rumination and its relation to depression. *J. Affect. Disord.* 141, 352–360. doi: 10.1016/j.jad.2012.03.024

Lai, C.-H. (2013). Gray matter volume in major depressive disorder: a meta-analysis of voxel-based morphometry studies. *Psychiatry Res.* 211, 37–46. doi: 10.1016/j.pscychresns.2012.06.006

Leung, C. M., Wing, Y. K., Kwong, P. K., and Shum, A. L. K. (1999). Validation of the chinese-cantonese version of the hospital anxiety and depression scale and comparison with the hamilton rating scale of depression. *Acta Psychiatr. Scand.* 100, 456–461. doi: 10.1111/j.1600-0447.1999.tb10897.x

Mathersul, D., Williams, L. M., Hopkinson, P. J., and Kemp, A. H. (2008). Investigating models of affect: relationships among EEG α asymmetry, depression and anxiety. *Emotion* 8, 560–572. doi: 10.1037/a0012811

Miller, E. K., and Cohen, J. D. (2001). An integrative theory of prefrontal cortex function. *Annu. Rev. Neurosci.* 24, 167–202. doi: 10.1146/annurev.neuro.24.1.167

Moberly, N. J., and Watkins, E. R. (2008). Ruminative self-focus and negative affect: an experience sampling study. *J. Abnorm. Psychol.* 117, 314–323. doi: 10.1037/0021-843x.117.2.314

Mohanty, A., Engels, A. S., Herrington, J. D., Heller, W., Ho, M.-H. R., Banich, M. T., et al. (2007). Differential engagement of anterior cingulate cortex subdivisions for cognitive and emotional function. *Psychophysiology* 44, 343–351. doi: 10.1111/j.1469-8986.2007.00515.x

Muris, P., Roelofs, J., Rassin, E., Franken, I., and Mayer, B. (2005). Mediating effects of rumination and worry on the links between neuroticism, anxiety and depression. *Personal. Individ. Differ.* 39, 1105–1111. doi: 10.1016/j.paid.2005.04.005

Nejad, A. B., Fossati, P., and Lemogne, C. (2013). Self-referential processing, rumination, and cortical midline structures in major depression. *Front. Hum. Neurosci.* 7:666. doi: 10.3389/fnhum.2013.00666

Nolen-Hoeksema, S., and Morrow, J. (1991). A prospective study of depression and posttraumatic stress symptoms after a natural disaster: the 1989 Loma Prieta Earthquake. *J. Pers. Soc. Psychol.* 61, 115–121. doi: 10.1037/0022-3514.61.1.115

Nolen-Hoeksema, S., and Morrow, J. (1993). Effects of rumination and distraction on naturally occurring depressed mood. *Cogn. Emot.* 7, 561–570. doi: 10.1080/02699939308409206

Nolen-Hoeksema, S., Wisco, B. E., and Lyubomirsky, S. (2008). Rethinking rumination. *Perspect. Psychol. Sci.* 3, 400–424. doi: 10.1111/j.1745-6924.2008.00088.x

Pizzagalli, D. A. (2011). Frontocingulate dysfunction in depression: toward biomarkers of treatment response. *Neuropsychopharmacology* 36, 183–206. doi: 10.1038/npp.2010.166

Pizzagalli, D. A., Sherwood, R. J., Henriques, J. B., and Davidson, R. J. (2005). Frontal brain asymmetry and reward responsiveness: a source-localization study. *Psychol. Sci.* 16, 805–813. doi: 10.1111/j.1467-9280.2005.01618.x

Scholz, J., Klein, M. C., Behrens, T. E. J., and Johansen-Berg, H. (2009). Training induces changes in white-matter architecture. *Nat. Neurosci.* 12, 1370–1371. doi: 10.1038/nn.2412

Smith, S. M., Fox, P. T., Miller, K. L., Glahn, D. C., Fox, P. M., Mackay, C. E., et al. (2009). Correspondence of the brain's functional architecture during activation and rest. *Proc. Natl. Acad. Sci. U S A* 106, 13040–13045. doi: 10.1073/pnas.0905267106

Spasojević, J., and Alloy, L. B. (2001). Rumination as a common mechanism relating depressive risk factors to depression. *Emotion* 1, 25–37. doi: 10.1037/1528-3542.1.1.25

Späti, J., Hänggi, J., Doerig, N., Ernst, J., Sambataro, F., Brakowski, J., et al. (2015). Prefrontal thinning affects functional connectivity and regional homogeneity of the anterior cingulate cortex in depression. *Neuropsychopharmacology* 40, 1640–1648. doi: 10.1038/npp.2015.8

Taki, Y., Thyreau, B., Kinomura, S., Sato, K., Goto, R., Wu, K., et al. (2013). A longitudinal study of the relationship between personality traits and the annual rate of volume changes in regional gray matter in healthy adults. *Hum. Brain Mapp.* 34, 3347–3353. doi: 10.1002/hbm.22145

Treynor, W., Gonzalez, R., and Nolen-Hoeksema, S. (2003). Rumination reconsidered: a psychometric analysis. *Cogn. Ther. Res.* 27, 247–259. doi: 10.1023/A:1023910315561

Vanderhasselt, M.-A., Baeken, C., Van Schuerbeek, P., Luypaert, R., De Mey, J., and De Raedt, R. (2013). How brooding minds inhibit negative material: an event-related fMRI study. *Brain Cogn.* 81, 352–359. doi: 10.1016/j.bandc.2013.01.007

Vanderhasselt, M.-A., Kühn, S., and De Raedt, R. (2011). Healthy brooders employ more attentional resources when disengaging from the negative: an event-related fMRI study. *Cogn. Affect. Behav. Neurosci.* 11, 207–216. doi: 10.3758/s13415-011-0022-5

Vanhalst, J., Luyckx, K., Raes, F., and Goossens, L. (2012). Loneliness and depressive symptoms: the mediating and moderating role of uncontrollable ruminative thoughts. *J. Psychol.* 146, 259–276. doi: 10.1080/00223980.2011.555433

Wang, K., Wei, D., Yang, J., Xie, P., Hao, X., and Qiu, J. (2015). Individual differences in rumination in healthy and depressive samples: association with brain structure, functional connectivity and depression. *Psychol. Med.* 45, 2999–3008. doi: 10.1017/s0033291715000938

Whelan-Goodinson, R., Ponsford, J., and Schönberger, M. (2009). Validity of the hospital anxiety and depression scale to assess depression and anxiety following traumatic brain injury as compared with the structured clinical interview for DSM-IV. *J. Affect. Disord.* 114, 94–102. doi: 10.1016/j.jad.2008.06.007

Whitmer, A. J., and Gotlib, I. H. (2013). An attentional scope model of rumination. *Psychol. Bull.* 139, 1036–1061. doi: 10.1037/a0030923

Yook, K., Kim, K. H., Suh, S. Y., and Lee, K. S. (2010). Intolerance of uncertainty, worry, and rumination in major depressive disorder and generalized anxiety disorder. *J. Anxiety Disord.* 24, 623–628. doi: 10.1016/j.janxdis.2010.04.003

**Conflict of Interest Statement**: The authors declare that the research was conducted in the absence of any commercial or financial relationships that could be construed as a potential conflict of interest.

frontiers in Human Neuroscience

ORIGINAL RESEARCH
published: 21 August 2018
doi: 10.3389/fnhum.2018.00325

# Effect of Modulating Activity of DLPFC and Gender on Search Behavior: A tDCS Experiment

*Xiaolan Yang[1,2], Yiyang Lin[3], Mei Gao[3] and Xuejun Jin[3]**

[1]School of Business and Management, Shanghai International Studies University, Shanghai, China, [2]Academy of Financial Research, Zhejiang University, Hangzhou, China, [3]College of Economics, Zhejiang University, Hangzhou, China

Studies of search behavior have shown that individuals stop searching earlier and accept a lower point than predicted by the optimal, risk-neutral stopping rule. This behavior may be related to individual risk preferences. Studies have also found correlativity between risk preferences and the dorsolateral prefrontal cortex (DLPFC). As risk attitude plays a crucial role in search behavior, we studied whether modulating the activity of DLPFC, by using a transcranial direct current stimulation (tDCS) device, can change individual search behavior. We performed a sequential search task in which subjects decided when to accept a point randomly drawn from a uniform distribution. A total of 49 subjects (23 females, mean age = 21.84 ± 2.09 years, all right-handed) were recruited at Zhejiang University from May 2017 to September 2017. They repeated the task in 80 trials and received the stimulation at the end of the 40th trial. The results showed that after receiving right anodal/left cathodal stimulation, subjects increased their searching duration, which led to an increase in their accepted point from 778.17 to 826.12. That is, the subjects may have changed their risk attitude to search for a higher acceptable point and received a higher benefit. In addition, the effect of stimulation on search behavior was mainly driven by the female subjects rather than by the male subjects: the female subjects significantly increased their accepted point from 764.15 to 809.17 after right anodal/left cathodal stimulation, while the male subjects increased their accepted point from 794.18 to 845.49, but the change was not significant.

**Keywords: search behavior, dorsolateral prefrontal cortex, transcranial direct current stimulation, risk attitude, gender difference**

OPEN ACCESS

***Edited by:***
*Xiaochu Zhang,*
*University of Science and Technology of China, China*

***Reviewed by:***
*Ali Yadollahpour,*
*Ahvaz Jundishapur University of Medical Sciences, Iran*
*Filippo Brighina,*
*Università degli Studi di Palermo, Italy*

****Correspondence:***
*Xuejun Jin*
*cec_jxj@zju.edu.cn*

***Received:*** *04 March 2018*
***Accepted:*** *25 July 2018*
***Published:*** *21 August 2018*

***Citation:***
*Yang X, Lin Y, Gao M and Jin X (2018) Effect of Modulating Activity of DLPFC and Gender on Search Behavior: A tDCS Experiment. Front. Hum. Neurosci. 12:325. doi: 10.3389/fnhum.2018.00325*

## INTRODUCTION

Search behavior is evident in many areas, such as job searches (Cox and Oaxaca, 1989, 2000), shopping choices and investment decisions. The literature suggests that search behavior plays a crucial role in international trade (Besedes, 2008), mutual fund flows (Sirri and Tufano, 1998) and house prices (Ihlanfeldt and Mayock, 2012).

Studies have examined search behavior under different experimental designs. For example, Holt (2005) designed a search game where the point distribution was known and the search cost was constant. In another study, Cox and Oaxaca (2008) analyzed changes in optimal behavior along with changes in interest rates, subsidy, risk, cost, probability and horizon in the experiment. Viefers (2012) added uncertainty to the point distribution.

Many studies on search behavior have focused on search duration and the reservation point. For search duration, experimental studies have shown that individuals stop searching earlier than the duration predicted by the optimal and risk-neutral assumption (Schunk and Winter, 2009). The average search duration is also shorter when there is ambiguity about the point distribution than when the point distribution is known (Asano et al., 2011). However, subjects normally change their own reservation point under different conditions. For example, the reservation point tends to be lower when the true point distribution is unknown to subjects than when the point distribution is clear (Asano et al., 2015). Especially in the labor market, subjects lower their reservation wages if they have to wait an uncertain amount of time for offers to arrive (Brown et al., 2011).

Risk attitude is one of the major factors affecting search behavior. Holt (2005) studied search behavior based on the assumption of risk neutrality. Cox and Oaxaca (2008) found that the assumption of risk aversion better explained search behavior. Evidence has shown that heterogeneity in search behavior is linked to heterogeneity in individual preferences (Schunk and Winter, 2009). For example, ambiguity can notably affect the search behavior of risk-averse subjects but not of risk-neutral or risk-prone subjects (Asano et al., 2011). Additionally, research has observed gender differences in risk attitude, with women tending to be more risk averse than men in both gain and loss frames (Croson and Gneezy, 2009).

To predict search behavior with precision, different search models have been constructed, such as the real options model (Maart et al., 2011) and the reference point updating model (Schunk and Winter, 2009). However, the search duration suggested by the real options model is shorter than its actual duration (Maart et al., 2011), and the reference point updating model is still unable to explain how people form and update reference points in dynamic choice situations (Schunk and Winter, 2009). Because of individual heterogeneity, no model can explain individual search behavior and perfectly predict actual search decisions. As a result, the decision-making process in search behavior remains uncertain. Specifically, studies have found correlativity between search behavior and risk preference (Holt, 2005; Cox and Oaxaca, 2008; Schunk and Winter, 2009; Asano et al., 2011), while the causal relationship remains unclear.

Noninvasive brain stimulation (NIBS) techniques have been widely used for studying the physiology of the central nervous system and identifying the functional role of specific brain structures (Dayan et al., 2013). These techniques can reveal the causal relationship between brain activity and individual behavior. Transcranial direct current stimulation (tDCS) and transcranial magnetic stimulation (TMS) are the two most commonly used forms of NIBS. Both of them can identify causal links between specific brain structures supporting cognitive, affective, sensory and motor functions (Dayan et al., 2013). Therefore, it is necessary to conduct further research on brain activity during search behavior by using a tDCS or TMS device, which can reveal the causal relationship between search behavior and individual heterogeneities, including the heterogeneity of risk preferences and gender differences.

Search behavior involves many decision-making processes, which are determined by the activity of the cerebral cortex, especially the prefrontal cortex. Neuroimaging studies have shown evidence of a relationship between the decision-making process and the dorsolateral prefrontal cortex (DLPFC). For example, Fleck et al. (2006) used a functional magnetic resonance imaging (fMRI) device and found that right DLPFC activity was greater for low-confidence than for high-confidence decisions in episodic retrieval and visual perception tasks. More recently, brain stimulation techniques have been increasingly used to investigate how modulating the activity of the DLPFC may affect individual decision-making processes and risk attitudes. Some researchers have found that both right anodal/left cathodal and left anodal/right cathodal tDCS over the DLPFC can reduce the participants' degree of risk aversion (Ye et al., 2015b) and increase the propensity for risk-taking among marijuana users (Boggio et al., 2010). However, Fecteau et al. (2007a) indicated that participants receiving bilateral DLPFC tDCS adopted a risk-averse response style during ambiguous decision making. Ye et al. (2015a) found that the participants tended to be risk seeking in the gain frame and risk averse in the loss frame after the right anodal/left cathodal tDCS over the DLPFC. For the TMS study, Knoch et al. (2006) found that subjects were more risk-taking after receiving 1 Hz rTMS over the right DLPFC when facing a complex risk task involving calculation of the level of risk and balance of benefit and risk. Subjects performing self-control behaviors in making intertemporal choices became more impatient after receiving 1 Hz rTMS over the left DLPFC (Figner et al., 2010). In short, NIBS can induce more cautious or riskier behaviors (Levasseur-Moreau and Fecteau, 2012). Because modulating the activity of the DLPFC by tDCS or TMS could change subjects' risk preference, and risk preference plays an important role in search behavior, it is meaningful to investigate whether DLPFC could affect risky decision-making behaviors under uncertainty in the search game. This could allow us to better understand individual search behavior from a neuroscience perspective.

Gender differences have been widely discussed in the tDCS research on different prefrontal cortexes. For example, after anodal tDCS over the medial prefrontal cortex (mPFC), the ability to explain and predict other people's mental states is enhanced in female subjects but not in males (Adenzato et al., 2017). Additionally, after receiving anodal tDCS over the ventral prefrontal cortex (VPC), female subjects tended to significantly increase utilitarian responses in tasks involving moral judgment, while males showed no significant difference (Fumagalli et al., 2010). Research on DLPFC has found that females improve their accuracy in verbal working memory (WM) after active right DLPFC anodal stimulation in the highest WM load condition, while males benefit more from left DLPFC stimulation (Meiron and Lavidor, 2013). Therefore, this study takes into account gender-related differences.

In this study, we investigated the casual relationship between DLPFC activity and search behavior. We performed a sequential search task. In the task, subjects decided when to accept the point at which a distribution was certain. Once subjects accepted the point, that trial was concluded, and the accepted point

was converted into a payment; otherwise, subjects had to pay a constant cost for waiting for the next new point. Each trial continued indefinitely until a given point was accepted. We adopted a pre–post design and compared the subjects' average search duration, average accepted point and average search income before and after different stimulation treatments. We aimed to test whether any types of stimulation could change subjects' search behavior and to find causal relationships between DLPFC activity and search behavior. Gender differences were considered in our study.

# MATERIALS AND METHODS

## Subjects

A total of 52 subjects (27 males, mean age = 22.30 ± 2.21; 25 females, mean age = 21.44 ± 1.88 years; 50 right-handed) were recruited at Zhejiang University from different majors via an advertisement posted on the school's bulletin board system. The subjects were excluded if: (i) they did not understand the procedure; or (ii) they were left-handed or were left-handed before correction but now are right-handed. Based on these criteria, three subjects were excluded and 49 subjects (26 males, mean age = 22.31 ± 2.30; 23 females, mean age = 21.30 ± 1.72 years; all right-handed) remained. The subjects were randomly assigned to receive right anodal/left cathodal tDCS ($n$ = 15, eight females), left anodal/right cathodal tDCS ($n$ = 17, seven females), or sham stimulation ($n$ = 17, eight females). The experiment lasted approximately 70 min and the average payment to the subjects was 49.19 CNY (approximately 7.81 USD)[1]. This study was carried out in accordance with the recommendations of the Zhejiang University ethics committee. The protocol was approved by the Zhejiang University ethics committee. All subjects gave written informed consent in accordance with the Declaration of Helsinki. None of the subjects reported any adverse side effects regarding pain on the scalp or headaches after the experiment.

## Transcranial Direct Current Stimulation (tDCS)

tDCS is a NIBS technique delivered by a battery-driven stimulator (multichannel noninvasive wireless tDCS neurostimulator, Starlab, Spain). A pair of saline-soaked sponge electrodes (5 cm × 7 cm) were fixed on the scalp of the participant using a rubber belt. We then applied a constant 2 mA current flow lasting for 20 min with 30 s of ramp up and down via the electrodes (Boggio et al., 2008; Fregni et al., 2008; Nitsche et al., 2008; Vanderhasselt et al., 2013). There were no physiological injuries to any of the participants. The tDCS technique facilitates neural excitability depending on electrode polarity. The anodal electrode enhances cortical excitability while the cathodal electrode weakens it (Nitsche and Paulus, 2000). As in a previous study (Gandiga et al., 2006), the current delivered in the sham stimulation only lasted for 30 s once it reached 2 mA. This constant but perceptible stimulation makes the subjects equate it with a regular process of stimulation.

[1]We used the exchange rate of 6.2962 CNY to 1 USD on February 5, 2018.

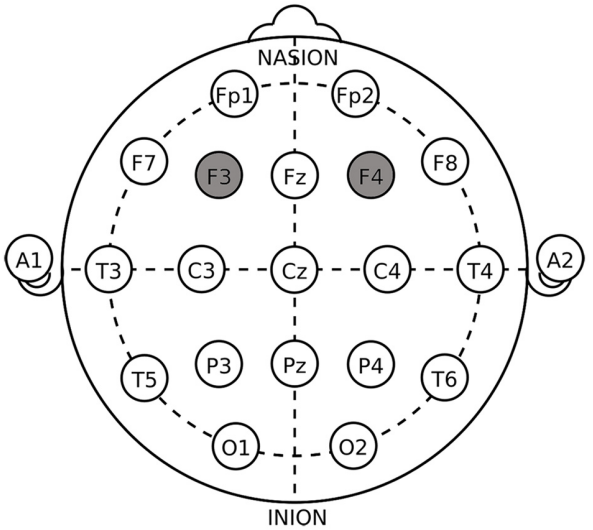


**FIGURE 1 |** Electrode placements in dorsolateral prefrontal cortex (DLPFC) stimulations.

Electrodes placed over F3 and F4 affect the DLPFC area (Fecteau et al., 2007a,b; Boggio et al., 2009). **Figure 1** shows that the anodal (cathodal) electrode was placed over the right F4 and the cathodal (anodal) electrode was placed over the left F3, following the right anodal/left cathodal (left anodal/right cathodal) treatment based on the International 10-20 System for electrode placement.

## Experimental Design

### The Search Game

The search game (**Figure 2**) was based on the experimental design of Holt (2005) and Asano et al. (2015). The game consisted of two parts, part A and part B. The subjects made decisions in each part. In each part, the subject faced 40 trials including unlimited rounds. In the first round of each trial, a point was drawn randomly from a uniform distribution with a lower bound of 0 and an upper bound of 1,000 by a computer[2]. The subject was expected to choose to click either the "accept" or "reject" button after observing the given point on the screen. Once the subject accepted the point, the trial was concluded and the accepted point was converted into a payment. Otherwise, he or she had to pay a constant cost and moved on to the next round in which a point was again drawn from the same point distribution. The subject continued to search in this manner until a given point was accepted. Recall was not allowed. In the game, 100 experimental points could be converted to 1.50 CNY and the constant cost was 20 points. For example, in one trial, a subject rejected the given points in the first three rounds and accepted the point of 852 in the fourth round. The search duration was four rounds, the total

[2]Before the experiment, we used the computer to generate 40 realizations for 40 trials from the uniform distribution (0, 1,000) and presented the same realization to all of the subjects in the experiment. Adopting the above method, sampling error was controlled and the subjects' decisions were compared with one other.

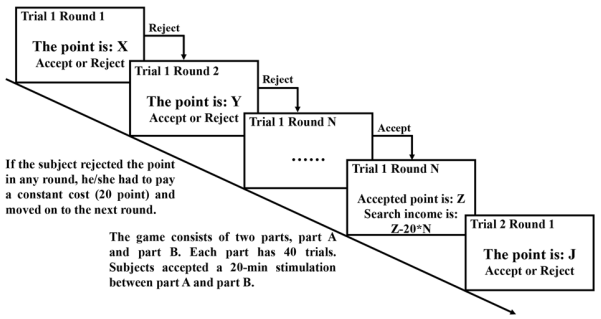


**FIGURE 2 |** Schematic representation of the experimental design. In part A, we used the computer to generate 40 realizations for 40 trials from the uniform distribution (0, 1,000) before the game and presented the same realization to all of the subjects in the game. In part B, the same realizations of points as part A were used in 30 trials in a different order and 10 new realizations of points from the same uniform distribution (0, 1,000) were generated before the game and used in the remaining 10 trials.

search cost was 80 points, and the search income (payment) was 11.58 CNY. The decision task in part B was similar to part A[3]. Part B used the same realizations of points as part A in 30 trials in a different order and used 10 new realizations in the remaining 10 trials.

The subjects then received a 20-min stimulation before part B. When the 40 trials in part B were concluded, one trial in part A and another trial in part B were randomly selected. Then, we calculated the payoffs of the two trials to determine the total payment for each subject.

### Procedure

The experiment was conducted with the software z-Tree (Fischbacher, 2007). At the beginning of the experiment, each subject was provided with instructions. The subjects were informed that: (i) they would not incur any losses from the search task; (ii) they would earn an attendance fee of 20.00 CNY (3.18 USD); and (iii) other payoffs were determined by their decisions made in the experiment. After a public reading of the instructions, three pilot trials were conducted to facilitate subjects to practice the task. Then, part A, including 40 trials, was started. The trials were conducted one at a time. After the 40 trials in part A were concluded, the experimenters placed tDCS devices on the subjects' heads for the 20-min stimulation. The subjects were reminded to sit comfortably and relax. When the stimulation ended, the devices were removed. New experimental instructions were provided in another public reading, and part B of the experiment commenced, again with z-Tree software. When the 40 trials in part B were concluded, one trial in part A and another trial in part B were randomly selected by the computer to determine the subjects' payoffs. The final payment was a combination of the show-up fee and the payoffs from the two parts. Finally, each subject completed a questionnaire before finally receiving their payment. This questionnaire contained 15 questions regarding personal information such as gender, age, major, place of origin, household income, consumption expenditures and the experimental process. The questionnaire information is summarized in **Supplementary Table S1**.

### Data Analysis

We aimed to test whether the subjects' search behavior would be changed after the stimulation between part A and part B. We randomly selected 30 trials out of total 40 trials in part A and repeated them in different orders in part B. Data analysis was only focused on these selected 30 trials both in part A and part B. To investigate the subjects' search behavior, we measured the subjects' average search duration, average accepted point, and average search income, and compared them before and after the right anodal/left cathodal stimulation, the left anodal/right cathodal stimulation, and the sham stimulation. Statistical analyses were performed using SPSS statistical software (version 20).

Repeated-measures analysis of variance (ANOVA) and a paired *t*-test were used in statistical analysis. Repeated-measures ANOVA with parameters (search duration, accepted point, and search income) and time (before and after stimulation) were used as with-subject factors, while stimulation types (right anodal/left cathodal, left anodal/right cathodal and sham) served as between-subject factors and were used to test the influence of stimulation. The sample was divided into male and female groups and a paired *t*-test was used to examine differences in single variables (search duration, accepted point and search income) before and after stimulations in each group. By comparing the effect of stimulation in the two groups, we could test the influence of gender differences on search behavior. **Supplementary Table S1** shows all the experimental data.

## RESULTS

## The Optimal Reservation Point in Search Behavior

In our experiment, each point was drawn randomly from a uniform distribution (0, 1,000) and the search cost was 20 points. Following Holt (2005), we used an expected value to find the optimal reservation point on the assumption of risk neutrality. The optimal reservation point can be found by locating the point at which the expected benefit of another search is equal to the search cost (Holt, 2005).

Suppose the current draw is 800 in our experiment and we consider the expected gains from searching. There is a 4/5 chance that the next draw is 800 or below, in which case the net gain is 0 and the expected value of the gain is (4/5)0 = 0. There is a 1/5 chance that the next draw is more than 800 and the net gain on average is half of the distance from 800 to 1,000, i.e., 100. Then, the expected

[3]Among those trials in part B, the same realizations of points as part A were used in 30 trials in a different order. This controlled for sampling error and, hence, facilitated the comparison between the subjects' decisions in the two parts. No subject was informed about the relationship between the two parts. Ten new realizations of points from the same uniform distribution (0, 1000) were used in the remaining 10 trials to prevent subjects from discovering the relationship between the two parts. After the experiment, the 30 trials used both in part A and part B were selected as the required experimental data.

value of the gain is (1/5)*(100) = 20 points. Therefore, the total expected benefit of another search is 20 points. Any lower current draw produces an expected benefit from a further search that is above 20 points, and any higher current draw produces a lower expected benefit. Obviously, 800 is the optimal reservation point with the assumption of risk neutrality in which the expected benefit of another search equals the search cost. For a risk-averse person, the optimal reservation point is lower than 800 because he or she prefers to stop at 800, which represents a sure thing and does not involve the uncertainty of searching for a new point. For a risk-seeking person, the optimal reservation point is higher than 800. Finally, for any risk-neutral subject, the optimal search strategy is simply to keep searching until a draw of more than 800 appears.

The means of the average accepted point before and after stimulation in the experiment are summarized in **Table 1**. The means of the average accepted point before the three types of stimulation were lower than predicted by the optimal, risk-neutral stopping rule, which is consistent with Schunk and Winter (2009). In addition, the mean of the average accepted point after the right anodal/left cathodal stimulation was higher than the means after the other two types of stimulation. This result indicates that the subjects who received the right anodal/left cathodal stimulation may have been more risk seeking and tended to accept a higher point than other subjects. This is consistent with Ye et al. (2015a), who found that subjects tended to be risk seeking in the gain frame after the right anodal/left cathodal tDCS over the DLPFC.

## Effect of tDCS on Search Behavior

There was no significant difference in the subjects' average search duration, average accepted point, or average search income in different treatments before the stimulation (one-way ANOVA; search duration: $F_{(2,46)} = 0.023$, $p = 0.977$; accepted point: $F_{(2,46)} = 0.104$, $p = 0.902$; search income: $F_{(2,46)} = 0.162$, $p = 0.851$). This demonstrated that the subjects' search behavior was not different across the treatments before stimulations.

To test whether the stimulation of tDCS changed the subjects' search behavior in different treatments, we applied repeated-measures ANOVA with parameters (average search duration, average accepted point, and average search income) and time (before and after stimulation) as with-subject factors, while stimulation types served as between-subject factors. We found a significant effect of the interaction between time and parameter ($F_{(1,46)} = 14.180$, $p < 0.001$). Simple main effect tests showed diverse effects of different treatments on different parameters (**Figure 3**). The subjects' average search duration showed no significant difference before and after the stimulation (sham: $F_{(1,46)} = 1.200$, $p = 0.279$; left anodal/right cathodal: $F_{(1,46)} = 0.450$, $p = 0.506$; right anodal/left cathodal: $F_{(1,46)} = 1.945$, $p = 0.170$). The subjects' average accepted point and average search income were significantly higher after the right anodal/left cathodal stimulation (accepted point: $F_{(1,46)} = 7.795$, $p = 0.008$; search income: $F_{(1,46)} = 10.598$, $p = 0.002$), but there was no significant difference after the left anodal/right cathodal stimulation (accepted point: $F_{(1,46)} = 2.137$, $p = 0.151$; search income: $F_{(1,46)} = 2.983$, $p = 0.091$) or the sham stimulation (accepted point: $F_{(1,46)} = 1.858$, $p = 0.179$; search income: $F_{(1,46)} = 2.020$, $p = 0.162$). These results indicated that subjects tended to increase the accepted point and obtained a higher search income after receiving right anodal/left cathodal stimulation.

To make our conclusion more robust, we used the experimental data and calculated the medians of search duration, accepted point and search income before and after the stimulation. Then, we compared them by repeated-measures ANOVA again. A significant effect of the interaction between time and parameter was again found ($F_{(1,46)} = 10.018$, $p = 0.003$). Similar effects of different treatments on the accepted point and search income were observed. After receiving the right anodal/left cathodal treatment, the subjects' median of accepted point and median of search income were significantly higher (accepted point: $F_{(1,46)} = 7.435$, $p = 0.009$; search income: $F_{(1,46)} = 9.566$, $p = 0.003$), but there was no significant difference in the subjects' accepted point and search income before and after the left anodal/right cathodal stimulation (accepted point: $F_{(1,46)} = 1.211$, $p = 0.277$; search income: $F_{(1,46)} = 1.375$, $p = 0.247$) or the sham stimulation (accepted point: $F_{(1,46)} = 1.221$, $p = 0.275$; search income: $F_{(1,46)} = 1.303$, $p = 0.260$). The results of medians were consistent with the results of the means, which strongly verified our conclusion.

In conclusion, we found that the accepted point was significantly higher after the right anodal/left cathodal stimulation. More specifically, the subjects' accepted point was slightly lower than the optimal reservation point before the stimulation but exceeded the optimal reservation point after the right anodal/left cathodal stimulation. This significant difference in the accepted point before and after the stimulation may be

**TABLE 1 |** The means of average accepted point before and after three types of stimulation.

| | Treatment | Mean (point) | Distance (point) |
|---|---|---|---|
| Before stimulation | Sham | 792.80 | −7.20 |
| | L+/R− | 788.57 | −11.43 |
| | R+/L− | 778.17 | −21.83 |
| After stimulation | Sham | 814.79 | 14.79 |
| | L+/R− | 812.15 | 12.15 |
| | R+/L− | 826.12 | 26.12 |

*L+/R−, Left anodal/Right cathodal; R+/L−, Right anodal/Left cathodal; Distance equals the mean of average accepted point minus the optimal reservation point 800. Average accepted points before and after stimulation were calculated based on the experimental data, where there were 30 trials before and after stimulation.*

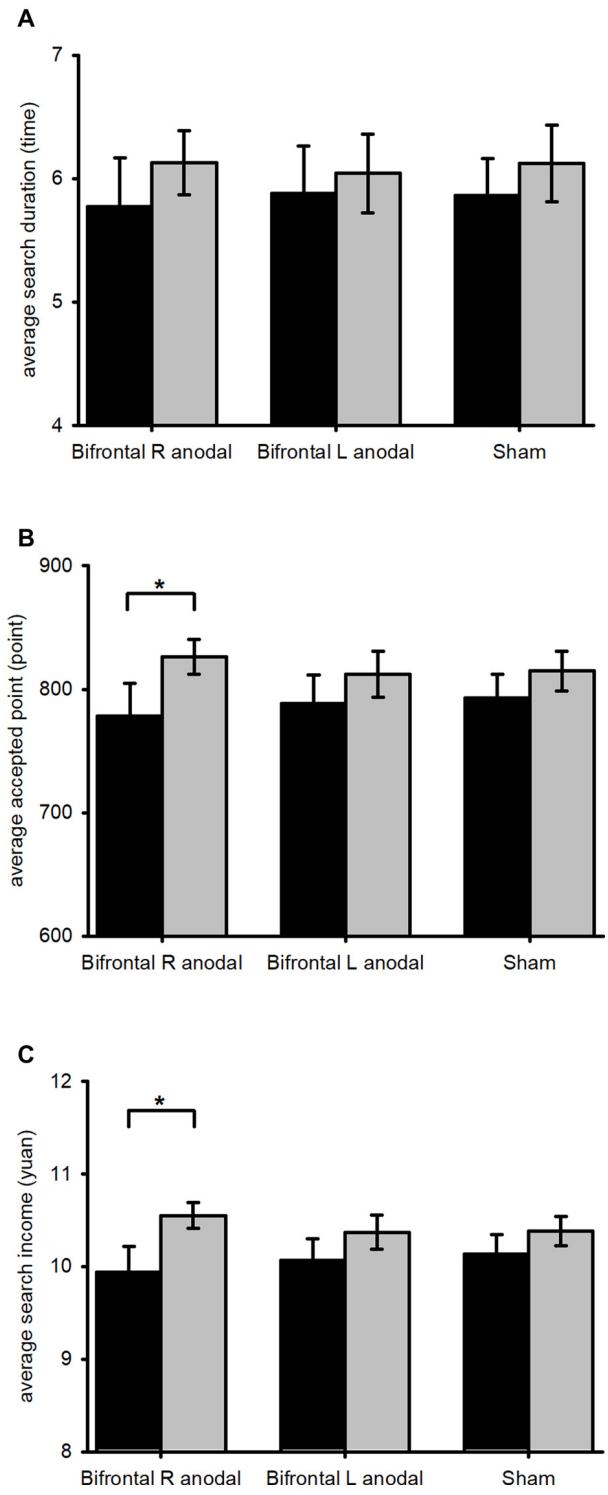


**FIGURE 3 |** The average values of search duration, accepted income and search income before and after stimulation. Black bars, pre-transcranial direct current stimulation (pre-tDCS); gray bars, post-tDCS. Error bars indicate 95% confidence intervals. Subjects' average search duration showed no significant difference after any types of stimulation **(A)**. Subjects' average accepted point and average search income were significantly higher after right anodal/left cathodal tDCS **(B,C)**. $^*P < 0.05$.

related to a change in risk attitude. After receiving the right anodal/left cathodal tDCS over the DLPFC, subjects tended to be risk seeking (Ye et al., 2015a), and increased their reservation point in the game. As the accepted point significantly increased after the stimulation, search income also increased significantly.

## Gender Differences

Finally, we tested whether the gender of subjects affected search behavior. One-way ANOVAs showed no significant effect of gender on search duration ($F_{(1,47)} = 1.603$, $p = 0.212$), accepted point ($F_{(1,47)} = 2.433$, $p = 0.126$), or search income ($F_{(1,47)} = 2.759$, $p = 0.103$) before the stimulation, but found a significant effect of gender on accepted point ($F_{(1,47)} = 2.975$, $p = 0.091$) and search income ($F_{(1,47)} = 3.657$, $p = 0.062$) after the stimulation at the level of 10% significance. Additionally, we added gender to the repeated-measures ANOVA and a main effect of gender ($F_{(1,43)} = 3.349$, $p = 0.074$) was observed.

To further test the relationship between gender differences and stimulation types in search behavior, we divided the entire sample into two groups: males ($n = 26$) and females ($n = 23$). We applied a paired $t$-test to distinguish the differences between the two groups (**Figure 4**). There was no significant difference in the male subjects' search behavior before or after the three types of stimulation. There was no significant difference in the female subjects' search behavior after the left anodal/right cathodal stimulation or the sham stimulation. After receiving right anodal/left cathodal stimulation, the female subjects significantly increased their average accepted point ($t_{(1,7)} = -2.793$, $p = 0.027$) and average search income ($t_{(1,7)} = -3.443$, $p = 0.011$), but the average search duration showed no significant difference ($t_{(1,7)} = -0.878$, $p = 0.409$). These results demonstrated that the female subjects tended to significantly increase their accepted point and gain higher search income after the right anodal/left cathodal tDCS, while the male subjects showed no significant difference. This suggests that the significant differences of accepted point and search income in the total sample before and after the right anodal/left cathodal stimulation were mainly attributable to the female subjects.

In addition, a gender difference in risk preference was observed before the stimulation. The mean of the average accepted point in the female group was 765.60, which was lower than the optimal reservation point, while the mean of the average accepted point in the male group was 805.65, which was higher than predicted by the optimal rule. This difference suggests that even before the stimulation the female subjects were risk averse and the male subjects were risk seeking, consistent with Croson and Gneezy (2009) and Ye et al. (2015a). In our experiment, we found that gender differences were also significant after the right anodal/left cathodal stimulation. The female subjects were more sensitive to the stimulation and became risk seeking after the right anodal/left cathodal stimulation, while the male subjects showed no significant difference in risk attitude after the same stimulation. As a result, after the right anodal/left cathodal stimulation, the female subjects significantly increased their accepted point and gained higher search income, while the male subjects showed no significant difference.

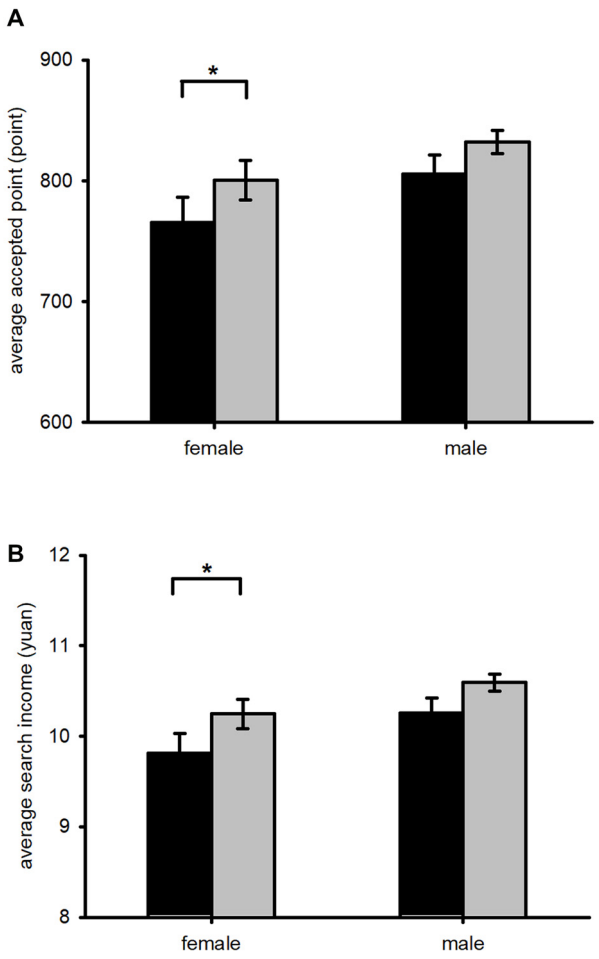


**FIGURE 4 |** The gender difference before and after receiving right anodal/left cathodal tDCS over DLPFC. Black bars, pre-tDCS; gray bars, post-tDCS. Error bars indicate 95% confidence intervals. Female subjects significantly increased accepted points and search income after the right anodal/left cathodal stimulation, while male subjects showed no significant difference after the same stimulation. $^*P < 0.05$.

## DISCUSSION

In this study, we tested the effect of modulating the activity of DLPFC on search behavior. By comparing the average values of search duration, accepted point, and search income before and after the stimulation, we found that using the right anodal/left cathodal tDCS over DLPFC significantly increased the subjects' accepted point and search income. Furthermore, this study demonstrated that there was a gender difference after the stimulation. The accepted point and search income were significantly higher after the right anodal/left cathodal stimulation in the female group, while there was no significant difference in the male group. This revealed that the effect of tDCS on search behavior was mainly driven by the female subjects rather than by the male subjects.

Previous tDCS research has studied individual decision-making behavior involving risk attitudes. We further constructed a sequential search task with uncertainty and incorporated tDCS devices into the task to analyze subjects' search behavior. We aimed to reveal the causal relationship between DLPFC activity and search behavior and find the exact effect of different types of stimulation on the subjects' behavior. The between-subjects design normally lacks statistical power because there is heterogeneity among different subjects. Hence, we adopted a within-subject design to avoid heterogeneity among subjects and compared search behavior before and after the stimulation. However, the learning effect may be significant. Thus, we added three pilot trials to facilitate subjects to become familiarized with the task. This can stabilize the baseline performance thus reducing learning effects. We also randomized the order of the trials. Our results showed that there was a significant difference after the right anodal/left cathodal stimulation but not after the left anodal/right cathodal stimulation or the sham stimulation. Therefore, the learning effect might have been reduced in our search game.

In our experiment, the subjects significantly increased their accepted point and obtained higher search income after receiving right anodal/left cathodal stimulation. Considerable literature has shown that people normally stop searching earlier than predicted by the optimal, risk-neutral stopping rule (Schunk and Winter, 2009). The risk aversion assumption is more consistent with individual search behavior than the risk neutral assumption (Cox and Oaxaca, 2008). In fact, risk attitude does play an important role in search behavior (Cox and Oaxaca, 1989; Asano et al., 2011). Previous tDCS studies have shown that subjects tend to choose more risky options after right anodal/left cathodal tDCS in the gain frame (Ye et al., 2015a). Subjects' degrees of risk aversion may be reduced after both right anodal/left cathodal and left anodal/right cathodal tDCS over DLPFC (Ye et al., 2015b). Combined with the results from the literature, one possible explanation for our results is that subjects receiving right anodal/left cathodal stimulation were more risk seeking and had a higher reservation point, so they chose to stop searching late and significantly increased their accepted point, which was larger than the optimal reservation point. As a result, they also gained a significantly higher search income.

Studies in experimental economics have indicated that there are substantial gender differences regarding risk aversion (Croson and Gneezy, 2009; Ye et al., 2015a). These studies are consistent with our results indicating that males tended to be more risk seeking than females before the stimulation. Several possible reasons can explain the gender difference in risk taking. First, previous research shows that both men and women are overconfident, but men are more overconfident in their success in uncertain situations than women (Deaux and Farris, 1977; Lichtenstein et al., 1982; Lundeberg et al., 1994). Generally, men are more confident to gain a higher point in the next search and more risk seeking to spend more time searching for an acceptable point. Second, men are more likely to regard a risky situation as a challenge that calls for participation, while women treat it as a threat that encourages avoidance (Arch, 1993). Thus, when facing uncertainty in the search game, men tended to search for a longer time than women.

Moreover, we found that there were significant gender differences in search behavior after the stimulation. The female subjects significantly increased their accepted point and gained higher search income after the right anodal/left cathodal tDCS, while the male subjects showed no significant difference. Recent studies have found that bilateral tDCS stimulation over DLPFC altered individuals' risk attitude (Ye et al., 2015a,b; Zheng et al., 2016). We may infer from our results that the female subjects became more risk seeking after increasing right DLPFC activity and decreasing left DLPFC involvement in search behavior, while the male subjects showed no significant difference in risk attitude after the same stimulation. This supports the idea that there are different brain activation patterns elicited in response to cognitive tasks between males and females (Bell et al., 2006). These results also suggest that females were responsible for the changes in the accepted points and search incomes before and after the right anodal/left cathodal tDCS over DLPFC.

In addition, executive functions have been widely studied in neuroscience and they can effortfully guide behavior towards a goal (Banich, 2009). Some studies have found that the DLPFC is important for executive function (Wagner et al., 2001; Forbes et al., 2014). A number of researchers have studied gender differences in executive function. Several researchers have found that women outperform men on tests of verbal memory (Weiss et al., 2003) and information processing (Majeres, 1990). Wanless et al. (2013) and Gestsdottir et al. (2014) found that girls tended to exhibit more inhibitory control than boys during childhood. Search behavior reflects a role of executive functions, which are a set of mental skills that help you get things done. The present study provides new evidence for gender differences in executive functions. Our findings also support the view that DLPFC plays an important role in execution function.

The limitations in our study primarily concern the focality of tDCS. Since electrode montage could favor current spread across the stimulated cortices, it remains unclear whether the stimulation effects of tDCS were the result of selective modulation of the target area or the result of the inevitable widespread and nonselective modulation over the cortex (Sellaro et al., 2016). Unilateral stimulation is necessary to make our results more robust in future research.

## DATA AVAILABILITY

All datasets (generated/analyzed) for this study are included in the manuscript and the supplementary files.

## AUTHOR CONTRIBUTIONS

XY, YL, MG and XJ designed the experiment, wrote the manuscript, revised the manuscript and finally approved the version to be published. YL and MG performed the experiment and drew the figures. XY and YL analyzed the data.

## FUNDING

This work was supported by National Natural Science Foundation of China (Grant number: 71673249), and the Fundamental Research Funds for the Central Universities of China.

## SUPPLEMENTARY MATERIAL

The Supplementary Material for this article can be found online at: https://www.frontiersin.org/articles/10.3389/fnhum.2018.00325/full#supplementary-material

**TABLE S1 |** Experimental data and questionnaire information. The means and medians of search duration, accepted point and search income before and after the stimulation are listed in the table. The data from Q2 column to Q13 column correspond to the questions on the questionnaire.

## REFERENCES

Adenzato, M., Brambilla, M., Manenti, R., De Lucia, L., Trojano, L., Garofalo, S., et al. (2017). Gender differences in cognitive Theory of Mind revealed by transcranial direct current stimulation on medial prefrontal cortex. *Sci. Rep.* 7:41219. doi: 10.1038/srep41219

Arch, E. C. (1993). Risk-taking: a motivational basis for sex differences. *Psychol. Rep.* 73, 3–11. doi: 10.2466/pr0.1993.73.1.3

Asano, T., Okudaira, H., and Sasaki, M. (2011). An experimental test of a search model under knightian uncertainty. *Discussion Papers in Economics and Business*. 11-05, Osaka University, Graduate School of Economics and Osaka School of International Public Policy (OSIPP). Available online at: https://ideas.repec.org/p/osk/wpaper/1105.html

Asano, T., Okudaira, H., and Sasaki, M. (2015). An experimental test of a search model under ambiguity. *Theory Dec.* 79, 627–637. doi: 10.1007/s11238-015-9488-x

Banich, M. T. (2009). Executive function: the search for an integrated account. *Curr. Dir. Psychol. Sci.* 18, 89–94. doi: 10.1111/j.1467-8721.2009.01615.x

Bell, E. C., Willson, M. C., Wilman, A. H., Dave, S., and Silverstone, P. H. (2006). Males and females differ in brain activation during cognitive tasks. *Neuroimage* 30, 529–538. doi: 10.1016/j.neuroimage.2005.09.049

Besedes, T. (2008). A search cost perspective on formation and duration of trade. *Rev. Int. Econ.* 16, 835–849. doi: 10.1111/j.1467-9396.2008.00752.x

Boggio, P. S., Sultani, N., Fecteau, S., Merabet, L. B., Mecca, T. P., Pascual-Leone, A., et al. (2008). Prefrontal cortex modulation using transcranial DC stimulation reduces alcohol craving: a double-blind, sham-controlled study. *Drug Alcohol Depend.* 92, 55–60. doi: 10.1016/j.drugalcdep.2007.06.011

Boggio, P. S., Zaghi, S., and Fregni, F. (2009). Modulation of emotions associated with images of human pain using anodal transcranial direct current stimulation (tDCS). *Neuropsychologia* 47, 212–217. doi: 10.1016/j.neuropsychologia.2008.07.022

Boggio, P. S., Zaghi, S., Villani, A. B., Fecteau, S., Pascual-Leone, A., and Fregni, F. (2010). Modulation of risk-taking in marijuana users by transcranial direct current stimulation (tDCS) of the dorsolateral prefrontal cortex (DLPFC). *Drug Alcohol Depend.* 112, 220–225. doi: 10.1016/j.drugalcdep.2010.06.019

Brown, M., Flinn, C. J., and Schotter, A. (2011). Real-time search in the laboratory and the market. *Am. Econ. Rev.* 101, 948–974. doi: 10.1257/aer.101.2.948

Cox, J. C., and Oaxaca, R. L. (1989). Laboratory experiments with a finite-horizon job-search model. *J. Risk Uncertainty* 2, 301–329. doi: 10.1007/bf00209391

Cox, J. C., and Oaxaca, R. L. (2000). Good news and bad news: search from unknown wage offer distributions. *Exp. Econ.* 2, 197–225. doi: 10.1007/bf01669196

Cox, J. C., and Oaxaca, R. L. (2008). "Laboratory tests of job search models," in *Handbook Of Experimental Economics Results*, eds C. R. Rlott and V. L. Smith (Amsterdam: North-Holland), 311–318.

Croson, R., and Gneezy, U. (2009). Gender differences in preferences. *J. Econ. Lit.* 47, 448–474. doi: 10.1257/jel.47.2.448

Dayan, E., Censor, N., Buch, E. R., Sandrini, M., and Cohen, L. G. (2013). Noninvasive brain stimulation: from physiology to network dynamics and back. *Nat. Neurosci.* 16, 838–844. doi: 10.1038/nn.3422

Deaux, K., and Farris, E. (1977). Attributing causes for one's own performance: the effects of sex, norms, and outcome. *J. Res. Pers.* 11, 59–72. doi: 10.1016/0092-6566(77)90029-0

Fecteau, S., Knoch, D., Fregni, F., Sultani, N., Boggio, P. S., and Pascual-Leone, A. (2007a). Diminishing risk-taking behavior by modulating activity in the prefrontal cortex: a direct current stimulation study. *J. Neurosci.* 27, 12500–12505. doi: 10.1523/JNEUROSCI.3283-07.2007

Fecteau, S., Pascualleone, A., Zald, D. H., Liguori, P., Théoret, H., Boggio, P. S., et al. (2007b). Activation of prefrontal cortex by transcranial direct current stimulation reduces appetite for risk during ambiguous decision making. *J. Neurosci.* 27, 6212–6218. doi: 10.1523/JNEUROSCI.0314-07.2007

Figner, B., Knoch, D., Johnson, E. J., Krosch, A. R., Lisanby, S. H., Fehr, E., et al. (2010). Lateral prefrontal cortex and self-control in intertemporal choice. *Nat. Neurosci.* 13, 538–539. doi: 10.1038/nn.2516

Fischbacher, U. (2007). Z-Tree. Zurich toolbox for readymade economic experiments. *Exp. Econ.* 10, 171–178. doi: 10.1007/s10683-006-9159-4

Fleck, M. S., Daselaar, S. M., Dobbins, I. G., and Cabeza, R. (2006). Role of prefrontal and anterior cingulate regions in decision-making processes shared by memory and nonmemory tasks. *Cereb. Cortex* 16, 1623–1630. doi: 10.1093/cercor/bhj097

Forbes, C. E., Poore, J. C., Krueger, F., Barbey, A. K., Solomon, J., and Grafman, J. (2014). The role of executive function and the dorsolateral prefrontal cortex in the expression of neuroticism and conscientiousness. *Soc. Neurosci.* 9, 139–151. doi: 10.1080/17470919.2013.871333

Fregni, F., Orsati, T. O., Pedrosa, W., Fecteau, S., Tome, F. A. M. F., Nitsche, M. A., et al. (2008). Transcranial direct current stimulation of the prefrontal cortex modulates the desire for specific foods. *Appetite* 51, 34–41. doi: 10.1016/j.appet.2007.09.016

Fumagalli, M., Vergari, M., Pasqualetti, P., Marceglia, S., Mameli, F., Ferrucci, R., et al. (2010). Brain switches utilitarian behavior: does gender make the difference? *PLoS One* 5:e8865. doi: 10.1371/journal.pone.0008865

Gandiga, P. C., Hummel, F. C., and Cohen, L. G. (2006). Transcranial DC stimulation (tDCS): a tool for double-blind sham-controlled clinical studies in brain stimulation. *Clin. Neurophysiol.* 117, 845–850. doi: 10.1016/j.clinph.2005.12.003

Gestsdottir, S., Suchodoletz, A. V., Wanless, S. B., Hubert, B., Guimard, P., Birgisdottir, F., et al. (2014). Early behavioral self-regulation, academic achievement, and gender: longitudinal findings from france, germany, and iceland. *Appl. Dev. Sci.* 18, 90–109. doi: 10.1080/10888691.2014.894870

Holt, C. A. (2005). "ISO," in *Markers, Games, and Strategic Behavior: Recipes for Interactive Learning*, ed. A. D'Ambrosio (Boston, NJ: Addison Wesley), 97–105.

Ihlanfeldt, K., and Mayock, T. (2012). Information, search, and house prices: revisited. *J. Real Estate Financ. Econ.* 44, 90–115. doi: 10.1007/s11146-010-9282-z

Knoch, D., Gianotti, L. R., Pascual-Leone, A., Treyer, V., Regard, M., Hohmann, M., et al. (2006). Disruption of right prefrontal cortex by low-frequency repetitive transcranial magnetic stimulation induces risk-taking behavior. *J. Neurosci.* 26, 6469–6472. doi: 10.1523/JNEUROSCI.0804-06.2006

Levasseur-Moreau, J., and Fecteau, S. (2012). Translational application of neuromodulation of decision-making. *Brain Stimul.* 5, 77–83. doi: 10.1016/j.brs.2012.03.009

Lichtenstein, S., Fischhoff, B., and Phillips, L. D. (1982). "Calibration of probabilities: the state of the art to 1980," in *Judgment Under Uncertainty: Heuristics and Biases*, eds D. Kahneman, P. Slovic and A. Tversky (Cambrige, NJ: Cambridge University Press), 306–334.

Lundeberg, M. A., Fox, P. W., and Punćcohaŕ, J. (1994). Highly confident, but wrong: gender differences and similarities in confidence judgments. *J. Educ. Psychol.* 86, 114–121. doi: 10.1037/0022-0663.86.1.114

Maart, S. C., Mubhoff, O., Odening, M., and Schade, C. (2011). "Closing down the farm: an experimental analysis of disinvestment timing," in *13th EAAE 2011 Congress Change and Uncertainty*, Zurich, Switzerland.

Majeres, R. L. (1990). Sex differences in comparison and decision processes when matching strings of symbols. *Intelligence* 14, 357–370. doi: 10.1016/0160-2896(90)90023-m

Meiron, O., and Lavidor, M. (2013). Unilateral prefrontal direct current stimulation effects are modulated by working memory load and gender. *Brain Stimul.* 6, 440–447. doi: 10.1016/j.brs.2012.05.014

Nitsche, M. A., Cohen, L. G., Wassermann, E. M., Priori, A., Lang, N., Andrea, A., et al. (2008). Transcranial direct current stimulation: state of the art 2008. *Brain Stimul.* 1, 206–223. doi: 10.1016/j.brs.2008.06.004

Nitsche, M. A., and Paulus, W. (2000). Excitability changes induced in the human motor cortex by weak transcranial direct current stimulation. *J. Physiol.* 527, 633–639. doi: 10.1111/j.1469-7793.2000.t01-1-00633.x

Schunk, D., and Winter, J. (2009). The relationship between risk attitudes and heuristics in search tasks: a laboratory experiment. *J. Econ. Behav. Organ.* 71, 347–360. doi: 10.1016/j.jebo.2008.12.010

Sellaro, R., Nitsche, M. A., and Colzato, L. S. (2016). The stimulated social brain: effects of transcranial direct current stimulation on social cognition. *Ann. N Y Acad. Sci.* 1369, 218–239. doi: 10.1111/nyas.13098

Sirri, E. R., and Tufano, P. (1998). Costly search and mutual fund flows. *J. Financ* 53, 1589–1622. doi: 10.1111/0022-1082.00066

Vanderhasselt, M. A., De Raedt, R., Brunoni, A. R., Campanhã, C., Baeken, C., Remue, J., et al. (2013). tDCS over the left prefrontal cortex enhances cognitive control for positive affective stimuli. *PLoS One* 8:e62219. doi: 10.1371/journal.pone.0062219

Viefers, P. (2012). Should I stay or should I go? A laboratory analysis of investment opportunities under ambiguity. Available online at: https://www.ssrn.com/abstract=2622163

Wagner, A. D., Maril, A., Bjork, R. A., and Schacter, D. L. (2001). Prefrontal contributions to executive control: fMRI evidence for functional distinctions within lateral prefrontal cortex. *Neuroimage* 14, 1337–1347. doi: 10.1006/nimg.2001.0936

Wanless, S. B., McCleland, M. M., Lan, X., Son, S. H., Cameron, C. E., Morrison, F. J., et al. (2013). Gender differences in behavioral regulation in four societies: the United States, Taiwan, South Korea, and China. *Early Child. Res. Q.* 28, 621–633. doi: 10.1016/j.ecresq.2013.04.002

Weiss, E. M., Kemmler, G., Deisenhammer, E. A., Fleischhacker, W. W., and Delazer, M. (2003). Sex differences in cognitive functions. *Pers. Indiv. Differ.* 35, 863–875. doi: 10.1016/s0191-8869(02)00288-x

Ye, H., Chen, S., Huang, D., Wang, S., Jia, Y., and Luo, J. (2015a). Transcranial direct current stimulation over prefrontal cortex diminishes degree of risk aversion. *Neurosci. Lett.* 598, 18–22. doi: 10.1016/j.neulet.2015.04.050

Ye, H., Chen, S., Huang, D., Wang, S., and Luo, J. (2015b). Modulating activity in the prefrontal cortex changes decision-making for risky gains and losses: a transcranial direct current stimulation study. *Behav. Brain. Res.* 286, 17–21. doi: 10.1016/j.bbr.2015.02.037

Zheng, H., Huang, D., Chen, S., Wang, S., Guo, W., Luo, J., et al. (2016). Modulating the activity of ventromedial prefrontal cortex by anodal tDCS enhances the trustee's repayment through altruism. *Front. Psychol.* 7:1437. doi: 10.3389/fpsyg.2016.01437

**Conflict of Interest Statement**: The authors declare that the research was conducted in the absence of any commercial or financial relationships that could be construed as a potential conflict of interest.

frontiers in Human Neuroscience

ORIGINAL RESEARCH
published: 31 August 2018
doi: 10.3389/fnhum.2018.00347

# Impulsiveness in Reactive Dieters: Evidence From Delay Discounting in Orthodontic Patients

*Wu Zhang*[1,2†], *Chunmiao Mai*[3,4†], *Hongmin Chen*[5*] and *Huijun Zhang*[3,4*]

[1]*The First Affiliated Hospital of Jinan University, Jinan University, Guangzhou, China,* [2]*School of Stomatology of Jinan University, Jinan University, Guangzhou, China,* [3]*School of Management, Guangdong University of Technology, Guangzhou, China,* [4]*Center for Studies of Psychological Application, Guangdong Provincial Key Laboratory of Mental Health and Cognitive Science, School of Psychology, South China Normal University, Guangzhou, China,* [5]*Mental Quality Education Center, Beijing Technology and Business University, Beijing, China*

**Introduction**: Researchers have made efforts to distinguish the behavioral differences and underlying mechanisms that explain the various possible outcomes of dieting (success, failure and relapse). Although extensive research has demonstrated that eating behavior and individual impulsiveness are closely related to subjective appetite and decision making, very few studies have investigated how subjective and appetite impulsiveness is affected by reactive dieting.

**Methods**: In the present study, we utilized the power of food scale (PFS) and the intertemporal choice task and to examine subjective appetite and impulsivity of decision making in orthodontic patients. As a result of their orthodontic devices and the subsequent pain and discomfort caused by eating, these patients become reactive dieters. In order to explore the dynamic influence of orthodontic treatment on appetite and impulsiveness, we collected data for both patients and control participants across three testing sections. We also computed a regression model for further exploration in explaining how potential factors contributed to different choices.

**Results**: We found that the orthodontic group scored significantly lower in PFS than the control group, which indicated a suppression in appetite. Besides, reward and waiting time were significant factors in computational perspective. Moreover, although patients showed a bias in choosing smaller, immediate reward options, they exhibited a decrease in the delay discounting rate as treatment progressed. These findings confirm that subjective appetite and impulsiveness were inhibited due to reactive dieting.

**Keywords: orthodontic patients, reactive dieters, impulsiveness, intertemporal choice, subjective appetite**

OPEN ACCESS

***Edited by:***
*Delin Sun,*
*Duke University, United States*

***Reviewed by:***
*Ning Ma,*
*RIKEN Brain Science Institute (BSI), Japan*
*Ying Wang,*
*University of Science and Technology of China, China*

***Correspondence:**
*Hongmin Chen*
*chenhm@btbu.edu.cn*
*Huijun Zhang*
*zhanghuijun@gmail.com*

*†These authors have contributed equally to this work*

***Received:*** *28 February 2018*
***Accepted:*** *13 August 2018*
***Published:*** *31 August 2018*

***Citation:***
*Zhang W, Mai C, Chen H and Zhang H (2018) Impulsiveness in Reactive Dieters: Evidence From Delay Discounting in Orthodontic Patients. Front. Hum. Neurosci. 12:347. doi: 10.3389/fnhum.2018.00347*

## INTRODUCTION

People proactively control their diet for a variety of reasons, such as weight control, keeping fit, reducing blood glucose and lipids, religious fasting. During the dieting process, one has to overcome food temptation or even ignore nutritional needs to achieve a healthy balance between subjective desires and objective goals. For dieting to be successful, previous eating habits need to be changed

by inhibiting dietary needs. Consequently, the inhibition capacity of each individual plays a key role in whether they will succeed in dieting or not.

Eating habits are also closely related to individual impulsiveness. Generally, impulsive individuals find it difficult to manage their diet and develop good eating habits. This phenomenon has been observed in a variety of diverse groups (Nederkoorn et al., 2006a,b; van den Berg et al., 2011; Weafer and Fillmore, 2012). More specifically it has been found that impulsiveness is closely related to inhibition capacity. Extensive research had demonstrated that bingeing individuals show lower inhibition capacity in comparison to healthy controls towards food stimuli in response inhibition tasks (Volkow and Wise, 2005; Grosshans et al., 2011; Lyu et al., 2016). Personal body mass index (BMI) has been seen to be positively associated with reaction time in a stop-signal task among impulsive individuals (Mühlberg et al., 2016), demonstrating that people with high trait impulsivity and poor control in weight have the difficulty in inhibiting responses. Individuals with relatively low inhibition capacity have been shown to consume much more high-calorie foods than those with a higher inhibition capacity (Houben, 2011; Houben and Jansen, 2011). In a recent study, dieters passively viewed food cues while activity in the inferior frontal gyrus, a brain region associated with inhibitory control, was measured (Lopez et al., 2016). Results showed reduced activation in this region in dieters with high desire to food compared to the dieters with low desire. This suggests that more cognitive resources were required to inhibit food stimuli-related impulsivity in order to balance the cognitive conflict between food temptation and dietary needs (Keller and Hartmann, 2016). These results suggest that top-down regulation of appetite plays a key role in determining whether dieters were able to diet successfully. This is consistent with the notion that regulation ability determines whether people can control eating behavior effectively (Papies et al., 2008; Werthmann et al., 2011).

Therefore, the training to improve regulation ability has been used as an approach to inhibit appetite for specific foods in individuals (Houben and Jansen, 2011; Houben, 2011; Veling et al., 2011a; Forman et al., 2016; Adams et al., 2017). This training was particularly effective for long-term dieters (Veling et al., 2011b). Results showed that foods related to nogo-signals were rated lowly while foods related to go-signals were rated more highly.

The above studies demonstrate that appetite control and the ability to behaviorally inhibit food-related stimuli are closely related. In addition to this line of research, the relationship between appetite and inhibition within the context of decision making has also been examined (Bartholdy et al., 2016). For instance, a study has found that the ability of overweight women to choose to delay gratification is positively correlated to their ability to inhibit food. Indeed, this correlation was more significant when they were shown food-related stimuli compared to when they were shown non-food stimuli, indicating that impulsiveness on decision making tasks can be influenced by inhibition capacity of food-related stimuli (Yeomans and Brace, 2015). Overall, these results offer some suggestion that eating and appetite do not only involve behavioral inhibition of food stimuli, but are also likely to engage more complex processes of impulsivity inhibition relating to goal-based decision making.

However, the aforementioned studies only focused on the participants with obesity or eating disorder, and thereafter have difficulty in distinguishing the effect of dietary habits from the effect of inherent factors, e.g., metabolic capability. In addition, the motivation of proactive dieter who changes his or her eating habits intentionally is associated with inhibiting behavior. Given the scarcity of relevant studies, we aimed to explore more fully the question of whether dietary habits or appetite influence impulsiveness in normal individuals.

Orthodontic treatment has a great impact on both the eating habits and appetite of patients especially in the early stage of the procedure. During this stage, arch wire attachments are used to apply direct force to irregular teeth. This inflicts pain and discomfort on patients, which in turn causes dietary restriction. This leads to an alteration in the eating habits of orthodontic patients such that they become more restricted. Thus, the application of orthodontic devices triggers a conflict between the desire to eat food and the oral pain and discomfort that they experience as a consequence of trying to satisfy this desire. In this way it is similar to individuals who proactively overcome food temptation in order to lose weight. That is, orthodontic patients have to overcome eating difficulties and various forms of discomfort caused by orthodontic treatment in the short term in order to achieve future improvement in oral aesthetics and functionality. But they have no specific motivation on diet. Given the notion that orthodontic devices cause patients to modulate their diet in a reactive manner, we can argue that changes in eating habits may affect their ability to balance short-term difficulties with long-term improvements. Through studies of orthodontic patients, it will be possible to develop a deeper understanding about how individual eating habits and appetite influence impulsivity in decision making.

Such a conflict between immediate discomfort and future interests lends itself to intertemporal choice (Frederick et al., 2002). This refers to choices in which individuals must make a tradeoff between costs and benefits occurring at different times (Liang and Liu, 2011). The classic example of such a tradeoff involves smaller sooner (SS) rewards and larger longer (LL) rewards. From the perspective of a rational economist, people should choose larger delayed rewards to maximize their interest. However, people are generally biased towards more immediate rewards. This is especially true for individuals who are highly impulsive (Thaler, 1981; O'Donoghue and Rabin, 1999). Mazur (1984) proposed that people tend to discount the subjective value of money as a function of delays in time. He explained this choice pattern mathematically using a hyperbolic function: $SV = R/(1 + kT)$, where $SV$ represents the subjective value of the delayed reward $R$ associated with waiting time $T$, and $k$ was the delay discounting rate. The first goal of this study was to explore whether appetitive changes brought about by orthodontic devices impact impulsivity in decision making during treatment. Impulsivity in this case

refers to an increased preference for immediate rewards. More specifically this can be described as an increase in the delay discounting rate.

The classic intertemporal choice paradigm modulates two dimensions, available reward and waiting time. Traditionally a bias for immediate rewards has been explained as the result of subjective devaluation as a function of delayed time, as described by the hyperbolic discounting model (Mazur, 1984; Laibson, 1997). But other studies have put forward different perspectives. Hariri et al. (2006) found that high discounters exhibited greater ventral striatal activation in comparison to low discounters when they were faced with immediate rewards, demonstrating that high discounters overestimate immediate rewards rather than underestimate future rewards. Another ERP study has drawn similar conclusions that high discounters overvalue immediate rewards (Cherniawsky and Holroyd, 2013). However, some researchers consider that the bias to immediate rewards in high discounters is generated by amplified subjective temporal perception (Zauberman et al., 2009). Thus, the second goal of this study was to examine the delay discounting rate of orthodontic patients in more detail by determining the influence of appetitive changes on both the reward sensitivity and time sensitivity during intertemporal choice.

In this study, we utilized the power of food scale (PFS; Cappelleri et al., 2009) to evaluate subjective appetite and an intertemporal choice task to explore individual impulsiveness on decision making. We measured the performance of a group of orthodontic patients on these two tasks and compared it with a group of normal controls. In orthodontics, the treatment process is divided into various temporal periods (Brown and Moerenhout, 1991): early treatment (2 weeks after applying devices), middle adaptation (4 weeks later), and subsequent adaptation period (4 months later). In order to explore the dynamic effects of eating habits and appetite on impulsivity in decision making, we tracked behavior changes across three distinct sections: the first, before treatment; the second, early treatment; and the third, adaptation to treatment. Previous studies have observed that inhibition training in behavioral responding to food stimuli can lead to a subsequent devaluation in the attractiveness of those food items. Given this finding, we hypothesized that a reduction in appetite caused by orthodontic-related difficulties in eating would lead to a reduction in impulsive responding of patients. More specifically, patients would choose less SS options in the intertemporal task and show a related reduction in their delay discounting rate after the application of an orthodontic device. Meanwhile, the orthodontic devices led to restraint on patients' daily diet instead of their monetary rewards. Therefore, we predicted that the time sensitivity of patients, rather than reward sensitivity, would change significantly as a result of orthodontic treatment. This prediction is driven by the assumption that, during treatment, patients would have had to overcome conflicts between long time-consuming treatment and urgent desires of improving appearance. A consequently weakened sensitivity to time as well an underestimation of subjective time perception would bring about a decrease in choices for SS options.

# MATERIALS AND METHODS

## Participants

The orthodontic patients were recruited from the dental department of a public hospital and were devoted to the treatment of orthodontics. They had never received orthodontic treatment before our recruitment. Thirty-three of them finished all measures in three test sections. Participants who performed absolute choice preference in the task were excluded. After exclusion, the orthodontics group consisted of 30 patients who would undergo orthodontic treatment (11 males, 19 females; mean age = 23.40, SD = 5.78; education = 14.00, SD = 1.92). The control group consisted of 31 adults (7 males, 24 females; mean age = 22.42, SD = 2.29; education = 15.13, SD = 1.80). They were recruited from local community and campus. Groups were matched on sex ($\chi^2 = 1.45$, $p = 0.23$) and age ($t_{(59)} = 0.88$, $p = 0.38$). But the orthodontics group had shorter education years than the control group ($t_{(59)} = -2.37$, $p = 0.02$). All participants were right-handed, had normal or corrected-to-normal vision, were not color-blind, had no psychiatric illness and had not experienced dieting or suffered from eating disorders.

All orthodontic patients wore Self-brackets (Demon Q) and Demon CuNiTi Round 0.014 from KaVo-Sybron Dental Co., Ltd (Shanghai).

This study was carried out in accordance with the recommendations of Ethics Guideline, the Human Research Ethics Committee for Non-Clinical Faculties in South China Normal University. The protocol was approved by the Human Research Ethics Committee for Non-Clinical Faculties in South China Normal University. All subjects gave written informed consent in accordance with the Declaration of Helsinki. They could gain 50 RMB as reward after finishing all the three tests.

## Measurement Scale

The PFS was developed to assess the psychological impact of food and as a measure of subjective appetite for palatable food (Cappelleri et al., 2009). It has since been revised into an Asian version (Yoshikawa et al., 2012). The scale consists of 15 items, involving three levels of food proximity: food available indicates the degree of the desire to eat when palatable food is available in the environment but not physically present, food present indicates the degree of the desire when palatable food is present at hand, food tasted indicates the degree of the desire when we taste palatable food but not consume it (Cappelleri et al., 2009). Each item is rated from one to five points. Higher total scores indicate a greater influence of palatable food in the three contexts with different food proximity, referred to participant's decreased ability to resist food temptation and increasing odds of being obese.

## Task

The intertemporal choice task required participants to select one of two monetary reward choices. One choice represented an immediate but smaller reward, the other one represented a larger but delayed reward. Participants were instructed that aim of the task was to assess how people make decisions about

different monetary rewards. Each trial consisted of one option with a relatively smaller monetary reward (5, 10, 20, 30, 40, 50, 60, 70, 80, 90 yuan) obtainable right now (SS option), and one option with a relatively larger monetary reward (100 yuan) obtainable after a longer delay (LL option). Participants were asked to choose by pressing a key corresponding to the laterality of their preferred option I left or right). Reward sensitivity was calculated as the difference between every combination of LL and SS presented during the task (Δ Reward: 10, 20, 30, 40, 50, 60, 70, 80, 90, 95 yuan). Waiting time was calculated as the difference between the waiting time associated with LL and SS options (Δ Time: 1 day, 1 week, 1 month, 6 months, 1 year and 2 years). Each trial ran as follows: a fixation point ("+") appeared in the screen center for 1,000 ms. Then reward options were presented for 5,000 ms or disappeared once an option had been selected. Following this, feedback on the participant's choices was presented for 1,000 ms (see **Figure 1**). Pairs of stimuli were displayed randomly and counterbalanced across the left and right side of the screen. Each amount (from ¥5 to ¥ 95) and delay duration were repeated twice (one time per left and right side). The computerized task consisted of 120 trials.

## Procedure

All participants were required to participant in the behavioral tasks and fill all measurement scales involved in three separate sections. Experimental tasks and conditions were maintained the same for each section. The orthodontics group participated in the first section before they adopted the orthodontic treatment. This represented a baseline measure. The second section was conducted 2 weeks after the orthodontic devices have been put in place. This section aimed to probe how the orthodontic treatment had affected patient performance. The third and last section was conducted 6 weeks after the treatment. This represented the adaption phase for orthodontic patients at which point, according to customary orthodontic wisdom, patients will have gotten used to the treatment. Control participants completed all three sections in accordance with the time intervals of the patient group.

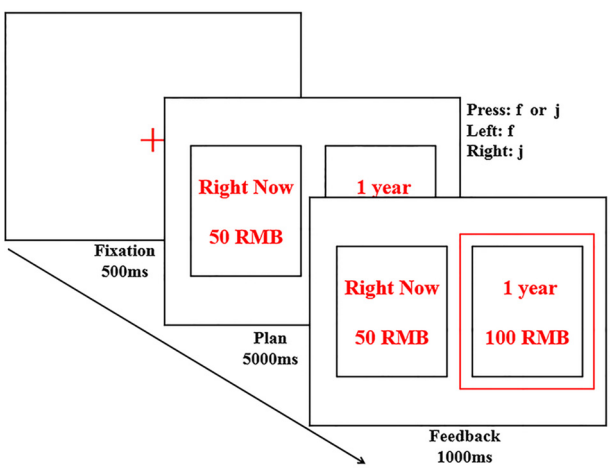


**FIGURE 1 |** Illustration of the procedure in the intertemporal choice task. Subjects were asked to choose one of the options by pressing "f" or "j" key and shown feedback in red frame. In this trial, the participant chose an option with Δ Time of 1 year and Δ Reward of 50 yuan. In the actual experiment, options were presented in Chinese.

All data were collected in the behavioral lab affiliated with South China Normal University. Once participants arrived at the lab, they were given instructions about what was required from them during the experiment. All stimuli were presented on a 14-inch computer screen which was positioned 23 inches away from participant. Each experimental section consisted of two parts: the PFS scale and the intertemporal choice task. Sufficient practice was provided prior to the main tasks to ensure that participants were familiar with what was required of them. The whole procedure lasted 20 min and included breaks.

## Statistical Analysis

The data of subjects who performed absolute choice preference (always chose most of the SS or LL in three tasks) were eliminated from further analysis. Three patients who always chose SS options in all the three tests and two controls who always selected LL options were excluded. Reaction trials too fast (RT <500 ms) or too slow (RT >4,000 ms) were further eliminated. Over the three sections, 1%, 1% and 4% of trials in the orthodontics group respectively were removed as a consequence. The control group had 2%, 0.4% and 1% of trials removed.

This study aimed to explore the dynamic impact of orthodontic treatment on decision-making. We measured reward sensitivity (Δ Reward), time sensitivity (Δ Time), the percentage of SS choice, reaction time and delay discounting rate ($k$ value) to quantify decision-making behavior. We conducted a 2 (group: orthodontics and controls) × 10 (Δ Reward: 10, 20, 30, 40, 50, 60, 70, 80, 90, 95 yuan) × 6 (Δ Time: 1 day, 1 week, 1 month, 6 months, 1 year and 2 years) × 3 (test time: first, second and third test) mixed design.

Data analyses were performed using SPSS 17.0 including $\chi^2$ test, independent $T$-test, repeated measures ANOVA, *post hoc* comparisons and logistics regression. Behavioral performances of the two groups were compared across the three research sections.

# RESULTS

## Measurement Scale

Scores for PFS of all participants were calculated (see **Figure 2**). We computed a mixed ANOVA with group as a between-subjects factor, test time as a within-subject factor and PFS scores as dependent variable. We found that the main effects for both group ($F_{(1,59)}$ = 13.07, $p$ = 0.001, $\eta_p^2$ = 0.18, *power* = 0.95) and time ($F_{(2,118)}$ = 11.75, $p$ < 0.001, $\eta_p^2$ = 0.17, *power* = 0.99) were significant. Multiple comparisons (LSD, Least Significant Difference; same as follows) showed differences between PFS scores taken from the first and second sections and between the first and third sections ($p$ = 0.001 and $p$ < 0.001 respectively). The interaction effect was also statistically significant ($F_{(2,118)}$ = 7.13,

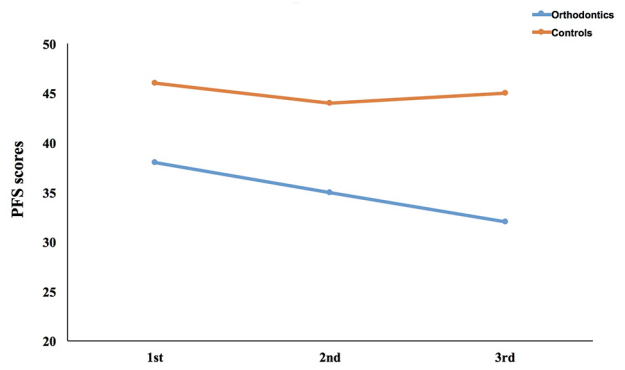


**FIGURE 2 |** Results of power of food scale (PFS) across three sections. We calculated the PFS scores in all the three sections between the orthodontics group and the control group.

$p = 0.001$, $\eta_p^2 = 0.11$, *power* = 0.93). A simple effects test showed that there were significant differences in PFS scores for the two groups across all three sections (all *p*s < 0.02). PFS scores for the orthodontics group were generally lower than those of the control group. More importantly, they showed a decrease over testing sections, which suggests that appetite declined with time.

## Reaction Time

We calculated a mixed ANOVA with reaction time as a dependent variable, group as a between-subjects factor (see **Table 1**). Choice (SS, LL) and test time were used as within-subject factors. The main effect of group was marginally significant ($F_{(1,59)} = 3.42$, $p = 0.07$, $\eta_p^2 = 0.06$, *power* = 0.44), while that of choice was not significant ($F_{(1,59)} = 0.87$, $p = 0.36$, $\eta_p^2 = 0.02$, *power* = 0.15). As the test time yielded a main effect ($F_{(2,118)} = 42.29$, $p < 0.001$, $\eta_p^2 = 0.42$, *power* = 1.00), *post hoc* tests were conducted and showed that the reaction time decreased significantly with testing sections (all *p*s < 0.001). Although the interaction effect between group and choice yielded a clearly significant difference ($F_{(1,59)} = 6.94$, $p = 0.01$, $\eta_p^2 = 0.11$, *power* = 0.74), none of the interaction effects reached the point of statistical significance (all *p*s > 0.6). A simple effects test indicated that participants from the orthodontics group were faster than those in the control group across all the three sections when selecting SS options (all *p*s < 0.05), however this was not evident when considering the LL option.

**TABLE 2 |** Performance of choice preference.

| | Group | | | | | |
|---|---|---|---|---|---|---|
| | Orthodontics group | | | Controls group | | |
| Choice (%) | 1st | 2nd | 3rd | 1st | 2nd | 3rd |
| SS | 0.71 | 0.64 | 0.65 | 0.44 | 0.43 | 0.43 |
| SD | 0.18 | 0.28 | 0.29 | 0.19 | 0.22 | 0.22 |

## Choice Preference

To evaluate preference in choice between the two groups, we calculated a mixed ANOVA with percentage of SS options as a dependent variable (see **Table 2**). Only the main effect of group was evident ($F_{(1,59)} = 20.70$, $p < 0.001$, $\eta_p^2 = 0.26$, *power* = 0.99), revealing that participants from the orthodontics group showed a much stronger bias to SS option than those from the control group. Results from reaction time performance and choice preference confirm that orthodontics patients preferred to choose smaller and sooner rewards with greater impulsivity than control participants.

## Reward Sensitivity

Reward amount and waiting time were dominant factors affecting decision making. People would balance these two indices when considering SS and LL options. We quantified how monetary reward sensitivity and time sensitivity influenced decision behavior.

The index of Δ Reward was grouped into three values: small Δ ($10 \leq \Delta \leq 30$), medium Δ ($40 \leq \Delta \leq 60$), large Δ ($70 \leq \Delta \leq 95$). To examine the impact of reward sensitivity on choice performance between the two groups across different sections (see **Figure 3**), we conducted a mixed variance analysis using group as a between-subjects factor, Δ Reward and test time as within-subject factors and percentage of SS options chosen as the dependent variable. We found that the main effect of group was highly significant ($F_{(1,59)} = 20.76$, $p < 0.001$, $\eta_p^2 = 0.26$, *power* = 0.99), suggesting that participants from the orthodontics group performed with higher levels of impulsivity toward immediate rewards. The factor Δ Reward was also found to be significant ($F_{(2,118)} = 134.88$, $p < 0.001$, $\eta_p^2 = 0.70$, *power* = 1.00). Multiple comparisons revealed that participants chose a significantly higher percentage of SS options for small Δ compared to both medium Δ ($p < 0.001$) and large Δ ($p < 0.001$). They also chose a higher percentage of SS options for medium Δ compared to large Δ ($p < 0.001$). However, neither the main effect of test time, nor the interaction of two factors and three

**TABLE 1 |** Performance of reaction time.

| RT (ms) | | Orthodontics group | | Controls group | | Difference | | | |
|---|---|---|---|---|---|---|---|---|---|
| | | *M* | *SD* | *M* | *SD* | *F* | Significance | $\eta_p^2$ | Power |
| 1st | SS | 1491 | 425 | 1753 | 414 | 5.95 | 0.02 | 0.09 | 0.67 |
| | LL | 1632 | 448 | 1700 | 328 | 0.45 | 0.50 | 0.01 | 0.10 |
| 2nd | SS | 1312 | 451 | 1546 | 390 | 4.70 | 0.03 | 0.07 | 0.57 |
| | LL | 1415 | 470 | 1511 | 334 | 0.86 | 0.36 | 0.01 | 0.15 |
| 3rd | SS | 1211 | 409 | 1432 | 363 | 4.99 | 0.03 | 0.08 | 0.59 |
| | LL | 1285 | 451 | 1370 | 306 | 0.75 | 0.39 | 0.01 | 0.14 |

*Note: M indicates averaged reaction time of each group at each time point; SD indicates the standard deviation of reaction time of each group at each time point.*

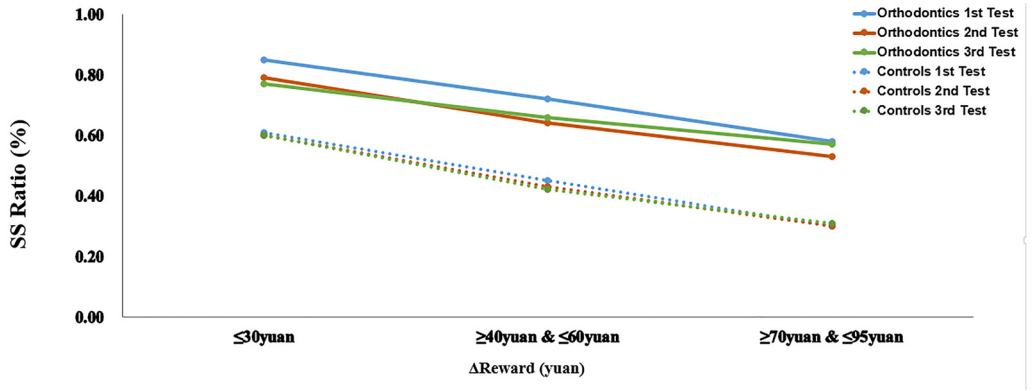


**FIGURE 3 |** Performance as a function of Δ Reward. The percentage of smaller sooner (SS) choices are presented separately according to the increasing differences in reward magnitude between two groups across three testing sections.

factors were significant. The two groups performed similarly with respect to their patterns of SS options as a function of Δ Reward.

## Time Sensitivity

In the following calculation, units of time were represented uniformly as days. The index of Δ Time was divided into six levels: 1 day, 7, 30, 183, 365 and 730 days. The performance of SS selection was calculated between the two groups across the three sections (see **Figure 4**). A mixed analysis of variance was fit to the data using percentage of SS options as the dependent variable, group was a between-subjects factor and Δ Time as a within-subject factor. We found that main effects for both groups ($F_{(1,59)} = 20.94$, $p < 0.001$, $\eta_p^2 = 0.26$, *power* = 0.99) and waiting time ($F_{(5,295)} = 165.19$, $p < 0.001$, $\eta_p^2 = 0.74$, *power* = 1.00] to be significantly different. Multiple comparisons showed that the two groups differed in every pairwise comparisons ($p < 0.001$). The interaction effect between groups and waiting time was clearly significant ($F_{(5,295)} = 4.22$, $p = 0.001$, $\eta_p^2 = 0.07$, *power* = 0.96) while all other interaction effects were not significant. A simple effects results showed that two groups differed in all Δ Time conditions (all $ps < 0.01$) in the first section. The similar patterns were observed in both the second and third test (all $ps < 0.05$) except in the condition of waiting for 1 day, in which participants did not exhibit different time sensitivity. These results confirm

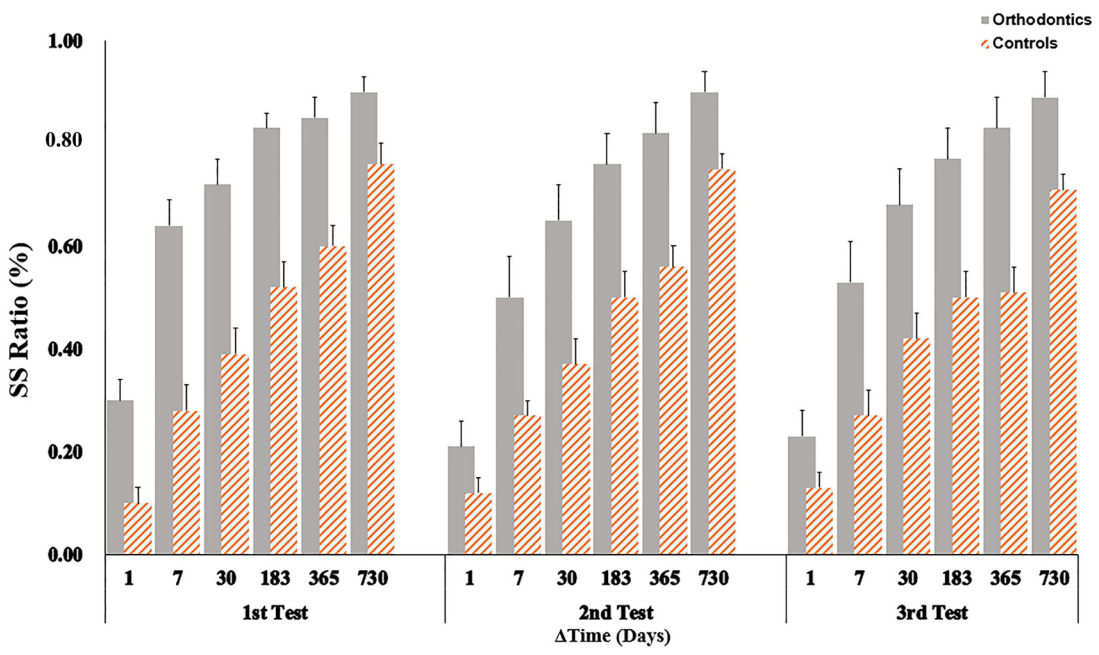


**FIGURE 4 |** Performance as function of Δ Time. The percentage of SS choices were shown for six different time intervals. Orthodontic patients were biased to choose SS options in each waiting time condition for each section. Error bars showed one standard error.

**TABLE 3 |** Overall model of Δ Reward and Δ Time in choice.

| | Regression coefficients β | *SD* | Wald $\chi^2$ | Odds ratio (OR) | 95% CI | Significance |
|---|---|---|---|---|---|---|
| ΔReward | −2.35 | 0.03 | 4979.39 | 0.10 | 0.09–0.10 | <0.001 |
| ΔTime | 2.65 | 0.04 | 5025.24 | 14.18 | 13.17–15.25 | <0.001 |
| Constant | 0.27 | 0.02 | 194.14 | 1.30 | | <0.001 |

that participants from the orthodontics group showed a greater bias for more impatient choices. A covariate analysis that took education into account did not make a difference to this pattern of results.

## Binary Logistic Regression in Choice

We computed multivariate unconditional logistics regression to assess how reward and waiting time contributed to the subjects' choices in trial-by-trial levels. The possible independent variables were considered as Δ Reward and Δ Time. They were z-scored normalized before regression. The dependent variable was the choice (SS = 1, LL = 0). We measured regression coefficients β, odds ratio, 95% confidence interval as well as significance (in the level of $p < 0.05$), using forward stepwise regression based on maximum likelihood estimation. The overall results were reported in the following table (see **Table 3**).

Results showed that two factors were significant in explaining the choice (respectively, $\beta_{\Delta Reward} = -2.35$, $OR_{\Delta Reward} = 0.10$, $p_{\Delta Reward} < 0.001$; $\beta_{\Delta Time} = 2.65$, $OR_{\Delta Time} = 14.18$, $p_{\Delta Time} < 0.001$). The constant was also significant in the model (β = 0.27, OR = 1.30, $p < 0.001$). These results confirmed the meaningful relation between reward, waiting time and choice.

To further estimate the contribution of Δ Reward and Δ Time between two group in each test, we calculated the Regression coefficients β values respectively (see **Table 4**). The independent variables were group, β type and test time while the dependent variable was coefficient β value. We measured a three-factor mixed analysis of variance. However, no significant effect was found in either main effect or interaction effect.

## Delay Discounting Function

To examine how subjects discounted rewards according to waiting time before and after orthodontic treatment, we calculated the discount factor for each testing section. Delayed discounts predicted the degree of how people devalued rewards over time. The discount rate is conventionally described through the hyperbolic function (Grossbard and Mazur, 1986; Mazur, 1987). In this study, the hyperbolic function was:

$$SV = R/(1 + kW) \quad (1)$$

In order to derive the discount rate of each participant ($k$ parameter) when SS option was selected, Grecucci et al. (2014) had transformed equation 1 into formula as follows:

$$k = (\mathrm{RLL} - \mathrm{RSS}) / \left[(\mathrm{RSS} * \mathrm{WLL}) - (\mathrm{RSS} * \mathrm{WSS})\right] \quad (2)$$

In this formula, RLL represented the reward linked to LL option (RLL = 100), RSS represented the reward linked to SS option, WLL was the waiting time related to LL option and WSS was the waiting time related to SS option (WSS = 0). In this study, the formula could be simplified into: $k = \Delta\mathrm{Reward}/(\mathrm{RSS}^*\Delta\mathrm{Time})$.

To compare the discounting rates between two groups over time, we used group and test time as independent variables with $k$ value as the dependent variable and entered them into a mixed variance analysis (see **Table 5**). Results showed that the main effect of group was significant ($F_{(1,59)} = 13.52$, $p = 0.001$, $\eta_p^2 = 0.19$, *power* = 0.95) although test time was not significant ($F_{(2,118)} = 0.87$, $p = 0.42$, $\eta_p^2 = 0.01$, *power* = 0.20). A significant interaction effect was evident ($F_{(2,118)} = 3.20$, $p = 0.04$, $\eta_p^2 = 0.05$, *power* = 0.60), with a simple effects test indicating differences in pairwise comparisons (all $p$s $< 0.05$). The tendency to discount reward with time of orthodontics patients was greater than that of control participants across all three sections. *Post hoc* comparison of $k$ value in the orthodontics group showed that there was an obvious difference between the first and second section ($p = 0.04$), while a significant difference was not observed between the second and third test ($p = 0.84$). This result demonstrated a remarkable decrease in the discounting rate of orthodontics in the second section.

Some research (Appelhans et al., 2012; Grecucci et al., 2014) had estimated "indifference points," a balanced index between

**TABLE 4 |** Contribution of Δ Reward and Δ Time between two group.

| Regression coefficients β | | Orthodontics group | | Controls group | | Difference | | | |
|---|---|---|---|---|---|---|---|---|---|
| | | *M* | *SD* | *M* | *SD* | *F* | Significance | $\eta_p^2$ | Power |
| 1st | ΔReward | −2.64 | 0.10 | −2.95 | 0.10 | 1.03 | 0.31 | 0.02 | 0.17 |
| | ΔTime | 3.05 | 0.12 | 3.17 | 0.11 | 0.97 | 0.33 | 0.02 | 0.16 |
| | Constant | 1.34 | 0.06 | −0.70 | 0.06 | 0.53 | 0.47 | 0.01 | 0.11 |
| 2nd | ΔReward | −2.32 | 0.09 | −2.67 | 0.09 | 1.03 | 0.31 | 0.02 | 0.17 |
| | ΔTime | 2.98 | 0.11 | 2.88 | 0.09 | 0.97 | 0.33 | 0.02 | 0.16 |
| | Constant | 0.99 | 0.05 | −0.60 | 0.05 | 1.97 | 0.17 | 0.03 | 0.28 |
| 3rd | ΔReward | −2.10 | 0.08 | −2.60 | 0.09 | 1.03 | 0.31 | 0.02 | 0.16 |
| | ΔTime | 2.65 | 0.10 | 2.71 | 0.09 | 0.97 | 0.33 | 0.02 | 0.16 |
| | Constant | 1.04 | 0.05 | −0.57 | 0.05 | 1.87 | 0.18 | 0.03 | 0.27 |

**TABLE 5 |** Discounting rate (*k* value) of both groups.

| *k* value | Orthodontics group | | Controls group | | Difference | | | |
|---|---|---|---|---|---|---|---|---|
| | *M* | *SD* | *M* | *SD* | *F* | Significance | $\eta_p^2$ | Power |
| 1st Test | 0.30 | 0.29 | 0.05 | 0.07 | 21.67 | <0.001 | 0.27 | 0.996 |
| 2nd Test | 0.20 | 0.26 | 0.07 | 0.15 | 5.82 | 0.019 | 0.09 | 0.660 |
| 3rd Test | 0.23 | 0.29 | 0.08 | 0.19 | 5.27 | 0.025 | 0.08 | 0.617 |

instant reward and delayed reward in the intertemporal task. It was supposed the point in which people selected 50% equally in SS option (or LL option). In this point, people valued equally in the two options. According to the equation transformation (Grecucci et al., 2014), the computation formula could be as follows:

$$\mathrm{RSS}/\left[1+\left(k^{*}\,\mathrm{WSS}\right)\right] = \mathrm{RLL}/[1+\left(k^{*}\,\mathrm{WLL}\right) \quad (3)$$

These points were measured by converting the subjective values. In this study, the formula could be simplified into: WLL = (RLL − RSS)/($k$*RSS). To devalue 100 RMB to 50 RMB in the 3rd section, the patients needed 4 days while the controls needed 13 days.

$$\mathrm{WLL}_{\mathrm{patients}} = (100-50)/(0.23^{*}\,50) = 4$$
$$\mathrm{WLL}_{\mathrm{controls}} = (100-50)/(0.08^{*}\,50) = 13$$

Hyperbolic function graphs were plotted in GraphPad Prism 5 in accordance with the degree of discount in two groups respectively across the three sections (as shown in **Figure 5**). These show that steepness of the discount curve was greater for the orthodontics group compared to the control group. We also calculated the area under the hyperbolic curve (AUC) for each participant in each section (see **Table 6**). We performed a mixed ANOVA on groups and test sections as independent variables and AUC as the dependent variable. The main effect of groups was markedly significant ($F_{(1,59)} = 25.57$, $p < 0.001$, $\eta_p^2 = 0.30$, *power* = 0.99) while that of test time was only marginally significant ($F_{(2,118)} = 2.88$, $p = 0.06$, $\eta_p^2 = 0.05$, *power* = 0.55). The interaction effect was also significant ($F_{(2,118)} = 4.46$, $p = 0.01$, $\eta_p^2 = 0.07$, *power* = 0.76). A further simple effects test revealed that AUC of orthodontics patients was clearly larger than controls across all three sections (all $p$s < 0.002). Consistent with patterns derived from $k$ values, *post hoc* comparisons showed that the AUC increased significantly in the second test compared to the first test ($p = 0.003$) but it was similar to the third test ($p = 0.65$).

## Task Difficulty

To verify whether the task difficulty made a difference in the reaction time, we measure general linear regression to explore the effects of group and Δutility on reaction time. The choice utility was calculated according to the hyperbolic function:

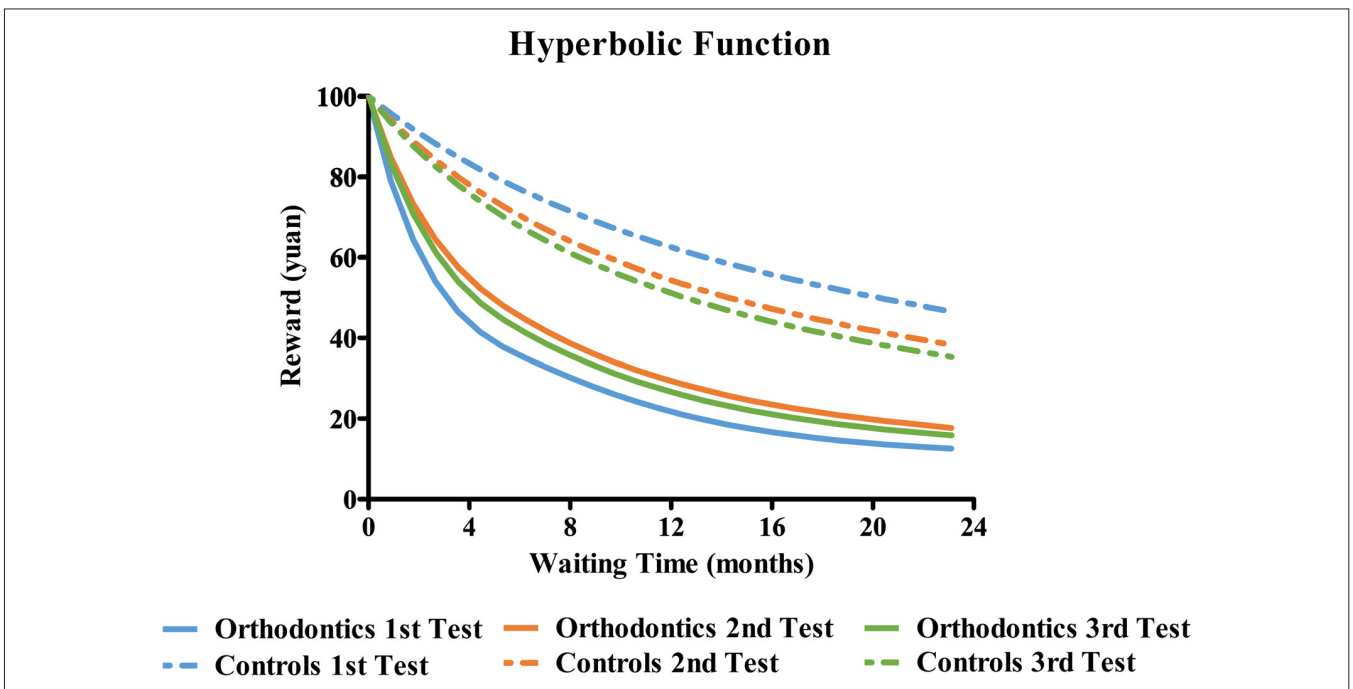


**FIGURE 5 |** Waiting time and Hyperbolic Function. Fitted hyperbolic functions were plotted for a fixed reward of 100 yuan for both groups according to their *k* values across three sections. For the purposes of graphical presentation, the unit of waiting time was converted from "days" to "months". As is illustrated, the orthodontic patients showed steeper discount function compared to control participants across all the three sections.

**TABLE 6 |** Area behind the curve of two groups (Area).

| Area | Orthodontics group | | Controls group | | Difference | | | |
|---|---|---|---|---|---|---|---|---|
| | *M* | *SD* | *M* | *SD* | *F* | Significance | $\eta_p^2$ | Power |
| 1st Test | 1037 | 522 | 1887 | 464 | 45.26 | <0.001 | 0.43 | 1.000 |
| 2nd Test | 1329 | 627 | 1849 | 568 | 11.52 | 0.001 | 0.16 | 0.916 |
| 3rd Test | 1301 | 640 | 1866 | 562 | 13.43 | 0.001 | 0.19 | 0.950 |

$SV = R/(1 + kT)$. The utility of SS choice was the SS reward while the utility of LL choice was the subjective value after devaluation of LL reward. The Δutility was the result of the difference between LL utility and SS utility.

The results showed that the regression model was significant ($F = 217.28$, $p < 0.01$). The factor of group was remarkable in the regression model ($t = 85.53$, $p < 0.01$) while the factor of Δutility was excluded to the model ($t = 1.38$, $p = 0.17$). 10% of the variation of the reaction time can be explained by changes in the group (corrected $R^2 = 0.01$). These results revealed that reaction time was the result of the difference between two groups rather than the task difficulty.

## Individual Appetite and Delay Discounting

In order to explore the relationship between food sensitivity and impulsiveness of decision making in the intertemporal choice task, we computed Pearson correlation analyses between PFS scores (and three PFS subscale scores), as well as SS ratio, RTs of SS choice, and *k* value for the three sections. Results indicated that individual appetite and task performance were not significantly correlated (all *p*s > 0.1).

# DISCUSSION

This study examined whether appetitive changes caused by difficulties in eating affected impulsivity in decision making. We did this by comparing performance in an intertemporal choice task before and after orthodontic treatment with a group who did not undergone this treatment. The results confirmed our hypothesis that the appetite of orthodontic patients would be suppressed after installation of orthodontic devices, and that there would be a subsequent decrease in impulsiveness as measured by the intertemporal choice task.

There has been a great deal of research on the relationship between individual impulsivity and dietary inhibition, as well as behavioral inhibition. Impulsivity and dietary inhibition may engage a common neural mechanism. For example, the intensity of activity in the brain region of known as the dorso-lateral prefrontal cortex (DLPFC) is generally regarded as an indicator of behavior inhibition capacity. It is closely related to biases in preference for SS options as well as the delay discounting rate in the intertemporal choice task (He et al., 2016; Wesley and Bickel, 2014), and is thought to predict the success rate of individuals in their endeavor to diet or inhibit eating (Weygandt et al., 2015). A serial study has found that the activation intensity of DLPFC during intertemporal choice was positively correlated with dietary inhibition (Dong et al., 2016). Spontaneous neuronal activity of DLPFC in the resting state has also been found to be negatively correlated with dietary inhibition (Dong et al., 2015). These results suggest that these two processes share common neural mechanism. As such, difficulties in eating or dietary inhibition are likely to affect individual impulsivity. Recent studies have illustrated that inhibition training of specific foods contributes to the suppression of food sensitivity and evaluation (Chen Z. et al., 2016; Chen et al., 2017). The researchers manipulated go-nogo training on participants by using food pictures as stimuli, as well as requiring them to evaluate the attractiveness of food pictures related to go-signal and nogo-signal before and after the training. This study supported the arguments that the evaluation to food was affected by individual's inhibition tendency and that the effect of inhibition training might further affect subjective appetite. Our study was consistent with this notion. Thus, we interpret a persistent reduction in impulsiveness as indexed by the intertemporal choice task is a consequence of eating difficulties experienced by patients as a result of their orthodontics devices through the common neural circuit of behavioral inhibition and impulsivity (Chen S. et al., 2016). Our findings build on this evidence by suggesting that the impact of eating inhibition on behavior not only affect food-related behavior, but also can also be extended to general decision making tasks. In respect to decision making, some previous studies had computed regression analysis in intertemporal choice paradigm to explore the possible factors to the final choice (Appelhans et al., 2012; Grecucci et al., 2014). In our study, the results of regression model have demonstrated the significant contribution of reward factor and waiting time factor to the choice performance.

We found that patients' subjective appetite for food changed dynamically as the course of the orthodontic treatment progressed. However, previous research in which proactive dieters were more strongly influenced by food after dieting over time suggests the opposite conclusion (Forman et al., 2007). We can put forward two possibilities for this discrepancy. One possibility is that self-report measures are unlikely to accurately reflect the subjective state of participants because of measurement bias and social commitment bias (Sayette et al., 2000). Usually obese individuals tend to underreport subjective appetite or hunger state because of social pressures or feelings of shame (Stunkard, 1959). Indeed, eating tasks have been found to be more effective than self-report measures for subjective appetite (Nijs et al., 2010). The second possibility might be that the orthodontics patients, as reactive dieters, inhibited appetite in order to eat less and to avoid pain and discomfort. This type of appetite inhibition can be described as a more reactive when compared to the more proactive response exhibited by individuals who choose to diet. Besides, this result didn't

support the assumption of the correlation between appetite and impulsiveness. Further studies would benefit from making use of more accurate and objective measures to explain subjective appetite.

In the present study, we observed a significant reduction in subjective appetite in reactive dieters. These were patients faced with pain and discomfort in eating due to the application of orthodontic devices. In addition, we found an associated decrease in impulsive monetary choices over time. According to the hyperbolic function, the smaller this delay discounting rate, the slower the individual discounted subjective value and the less impulsive they were in their decision making (Myerson et al., 2013). This finding demonstrated that the inhibition of eating behaviors regulated impulsivity inhibition in decision making, suggesting the presence of a common physiological mechanism.

It was revealed that the patients had shown a highly impulsive level at the beginning as compared to the controls. One possible explanation was due to their personality of impulsiveness. Wittmann and Paulus (2008) argued that individual differences in temporal perception were likely to affect the delay discounting rate in intertemporal choices to some extent. They observed that an overestimation of time led to an SS bias while underestimation of time led to more LL options. Orthodontic treatment is a medical procedure that carries patients with pain and eating difficulty. Most adult patients make a decision to undertake orthodontic treatment because they are unhappy with their facial appearance and the associated negative impact it has on their daily life. The strong conflict between eager to become good-looking and having to wait patiently are likely to drive them overestimate the time and result in a high impulsivity level.

## LIMITATION

A general limitation of the current study is the significantly higher impulsiveness level in patients as compared to controls in each test section, which make doubts in the generalization of findings about the inhibition effect of reactive dieting in impulsiveness. It is hard to explain this always highly impulsive level in patients at the behavioral perspective. Two groups were categorized based upon whether adopting orthodontic treatment rather than scale measurement. We didn't control the initial level of impulsivity between two groups. However, it is notable that two groups were balanced in demographics and the grouping criteria was the orthodontic treatment. All the dynamic changes in patients were in result of the treatment effect, more specifically were due to reactive dieting. To control for potential confounding effects in impulsivity, it would be better to utilize the Barratt Impulsiveness Scale (Hollander et al., 1998) as the pre-inclusion standard. A longer tracking examination is helpful to reveal whether the impulsiveness level in patients will continuously decrease along with the treatment.

In respect of reward sensitivity and time sensitivity, they were not significantly affected by orthodontic treatment. The lack of such effects suggests that changes in task performance from patients across sections were related to the interaction of variation between reward magnitude and delay, rather than one specific factor.

An additional limitation is subjective appetite and impulsivity did not differ after a long-term adaptation of orthodontic treatment. Patients exhibited similar levels of food sensitivity and decision-making performance from one stage of treatment to the next. This implies that changes in behavioral and psychological aspects were not affected by the adaptation in 6 weeks after the orthodontic treatment. Whether there is a significant adaptive effect in subsequent treatment periods remains to be seen and would require further, longitudinal study. It would be beneficial to consider whether or not patients remained in a state of reactive dieting and experienced associated difficulties in eating when they are in the late stage of treatment.

## CONCLUSION

This novel study explored the subjective appetite and impulsiveness of decision making in reactive dieters. We found that both of these factors were affected by the restricted diet brought about by the application of orthodontic devices. Reactive dieting suppressed subjective appetite as well as individual impulsivity. This study adds to our understanding of how reactive dieting influences aspects of physiology and behavior.

## AUTHOR CONTRIBUTIONS

WZ and HZ designed the study. CM and WZ collected research data. All four authors finished the manuscript.

## FUNDING

This work was supported by the National Natural Science Foundation of China (No. 31600931) and Guangdong Medical Research Foundation (No. A2017260).

## REFERENCES

Adams, R. C., Lawrence, N. S., Verbruggen, F., and Chambers, C. D. (2017). Training response inhibition to reduce food consumption: mechanisms, stimulus specificity and appropriate training protocols. *Appetite* 109, 11–23. doi: 10.1016/j.appet.2016.11.014

Appelhans, B. M., Woolf, K., Pagoto, S. L., Schneider, K. L., Whited, M. C., and Liebman, R. (2012). Inhibiting food reward: delay discounting, food reward sensitivity, and palatable food intake in overweight and obese women. *Obesity* 19, 2175–2182. doi: 10.1038/oby.2011.57

Bartholdy, S., Dalton, B., O'Daly, O. G., Campbell, I. C., and Schmidt, U. (2016). A systematic review of the relationship between eating, weight and inhibitory control using the stop signal task. *Neurosci. Biobehav. Rev.* 64, 35–62. doi: 10.1016/j.neubiorev.2016.02.010

Brown, D. F., and Moerenhout, R. G. (1991). The pain experience and psychological adjustment to orthodontic treatment of preadolescents,

adolescents, and adults. *Am. J. Orthod. Dentofacial Orthop.* 100, 349–356. doi: 10.1016/0889-5406(91)70073-6

Cappelleri, J. C., Bushmakin, A. G., Gerber, R. A., Leidy, N. K., Sexton, C. C., Karlsson, J., et al. (2009). Evaluating the power of food scale in obese subjects and a general sample of individuals: development and measurement properties. *Int. J. Obes.* 33, 913–922. doi: 10.1038/ijo.2009.107

Chen, S., Dong, D., Jackson, T., Su, Y., and Chen, H. (2016). Altered frontal interhemispheric resting state functional connectivity is associated with bulimic symptoms among restrained eaters. *Neuropsychologia* 81, 22–30. doi: 10.1016/j.neuropsychologia.2015.06.036

Chen, Z., Veling, H., Dijksterhuis, A., and Holland, R. W. (2016). How does not responding to appetitive stimuli cause devaluation: evaluative conditioning or response inhibition? *Mol. Cell. Endocrinol.* 145, 1687–1701. doi: 10.1037/xge0000236

Chen, Z., Veling, H., Dijksterhuis, A., and Holland, R. W. (2017). Do impulsive individuals benefit more from food go/no-go training? Testing the role of inhibition capacity in the no-go devaluation effect. *Appetite* 124, 99–110. doi: 10.1016/j.appet.2017.04.024

Cherniawsky, A. S., and Holroyd, C. B. (2013). High temporal discounters overvalue immediate rewards rather than undervalue future rewards: an event-related brain potential study. *Cogn. Affect. Behav. Neurosci.* 13, 36–45. doi: 10.3758/s13415-012-0122-x

Dong, D., Jackson, T., Wang, Y., and Chen, H. (2015). Spontaneous regional brain activity links restrained eating to later weight gain among young women. *Biol. Psychol.* 109, 176–183. doi: 10.1016/j.biopsycho.2015.05.003

Dong, D., Wang, Y., Jackson, T., Chen, S., Wang, Y., Zhou, F., et al. (2016). Impulse control and restrained eating among young women: evidence for compensatory cortical activation during a chocolate-specific delayed discounting task. *Appetite* 105, 477–486. doi: 10.1016/j.appet.2016.05.017

Forman, E. M., Hoffman, K. L., McGrath, K. B., Herbert, J. D., Brandsma, L. L., and Lowea, M. R. (2007). The power of food scale predicts chocolate cravings and consumption and response to a cravings intervention. *Appetite* 49:291. doi: 10.1016/j.appet.2007.03.071

Forman, E. M., Shaw, J. A., Goldstein, S. P., Butryn, M. L., Martin, L. M., Meiran, N., et al. (2016). Mindful decision making and inhibitory control training as complementary means to decrease snack consumption. *Appetite* 103, 176–183. doi: 10.1016/j.appet.2016.04.014

Frederick, S., Loewenstein, G., and O'Donoghue, T. (2002). Time discounting and time preference: a critical review. *J. Econ. Lit.* 40, 351–401. doi: 10.1257/jel.40.2.351

Grecucci, A., Giorgetta, C., Rattin, A., Guerreschi, C., Sanfey, A. G., and Bonini, N. (2014). Time devours things: how impulsivity and time affect temporal decisions in pathological gamblers. *PLoS One* 9:e109197. doi: 10.1371/journal.pone.0109197

Grossbard, C. L., and Mazur, J. E. (1986). A comparison of delays and ratio requirements in self-control choice. *J. Exp. Anal. Behav.* 45, 305–315. doi: 10.1901/jeab.1986.45-305

Grosshans, M., Loeber, S., and Kiefer, F. (2011). Implications from addiction research towards the understanding and treatment of obesity. *Addict. Biol.* 16, 189–198. doi: 10.1111/j.1369-1600.2010.00300.x

Hariri, A. R., Brown, S. M., Williamson, D. E., Flory, J. D., de Wit, H., and Manuck, S. B. (2006). Preference for immediate over delayed rewards is associated with magnitude of ventral striatal activity. *J. Neurosci.* 26, 13213–13217. doi: 10.1523/JNEUROSCI.3446-06.2006

He, Q., Chen, M., Chen, C., Xue, G., Feng, T., and Bechara, A. (2016). Anodal stimulation of the left DLPFC increases IGT scores and decreases delay discounting rate in healthy males. *Front. Psychol.* 7:1421. doi: 10.3389/fpsyg.2016.01421

Hollander, E., DeCaria, C. M., Mari, E., Wong, C. M., Mosovich, S., Grossman, R., et al. (1998). Short-time single-blind fluvoxamine treatment of pathological gambling. *Am. J. Psychiatry* 155, 1781–1783. doi: 10.1176/ajp.155.12.1781

Houben, K. (2011). Overcoming the urge to splurge: influencing eating behavior by manipulating inhibitory control. *J. Behav. Ther. Exp. Psychiatry* 42, 384–388. doi: 10.1016/j.jbtep.2011.02.008

Houben, K., and Jansen, A. (2011). Training inhibitory control. A recipe for resisting sweet temptations. *Appetite* 56, 345–349. doi: 10.1016/j.appet.2010.12.017

Keller, C., and Hartmann, C. (2016). Not merely a question of self-control: the longitudinal effects of overeating behaviors, diet quality and physical activity on dieters' perceived diet success. *Appetite* 107, 213–221. doi: 10.1016/j.appet.2016.08.007

Laibson, D. (1997). Golden eggs and hyperbolic discounting. *Q. J. Econ.* 112, 443–478. doi: 10.1162/003355397555253

Liang, Z. Y., and Liu, H. (2011). Exploring the nature of intertemporal choice. *Adv. Psychol. Sci.* 19, 959–966. doi: 10.3724/SP.J.1042.2011.00959

Lopez, R. B., Milyavskaya, M., Hofmann, W., and Heatherton, T. F. (2016). Motivational and neural correlates of self-control of eating: a combined neuroimaging and experience sampling study in dieting female college students. *Appetite* 103, 192–199. doi: 10.1016/j.appet.2016.03.027

Lyu, Z., Zheng, P., and Jackson, T. (2016). Attention disengagement difficulties among average weight women who binge eat. *Eur. Eating Disord. Rev.* 24, 286–293. doi: 10.1002/erv.2438

Mazur, J. E. (1984). Tests of an equivalence rule for fixed and variable reinforcer delays. *J. Exp. Psychol. Anim. Behav. Process.* 10, 426–436. doi: 10.1037/0097-7403.10.4.426

Mazur, J. E. (1987). "An adjusting procedure for studying delayed reinforcement," in *Quantitative Analyses of Behavior: The Effect of Delay and of Intervening Events on Reinforcement Value* (Vol. 5), eds M. L. Commons, J. E. Mazur, J. A. Nevin and H. Rachlin (Hillsdale, NJ: Erlbaum), 55–73.

Mühlberg, C., Mathar, D., Villringer, A., Horstmann, A., and Neumann, J. (2016). Stopping at the sight of food'how gender and obesity impact on response inhibition. *Appetite* 107, 663–676. doi: 10.1016/j.appet.2016.08.121

Myerson, J., Green, L., and Warusawitharana, M. (2013). Area under the curve as a measure of discounting. *J. Exp. Anal. Behav.* 76, 235–243. doi: 10.1901/jeab.2001.76-235

Nederkoorn, C., Braet, C., Van Eijs, Y., Tanghe, A., and Jansen, A. (2006a). Why obese children cannot resist food: the role of impulsivity. *Eat. Behav.* 7, 315–322. doi: 10.1016/j.eatbeh.2005.11.005

Nederkoorn, C., Smulders, F. T. Y., Havermans, R. C., Roefs, A., and Jansen, A. (2006b). Impulsivity in obese women. *Appetite* 47, 253–256. doi: 10.1016/j.appet.2006.05.008

Nijs, I. M. T., Muris, P., Euser, A. S., and Franken, I. H. (2010). Differences in attention to food and food intake between overweight/obese and normal-weight females under conditions of hunger and satiety. *Appetite* 54, 243–254. doi: 10.1016/j.appet.2009.11.004

O'Donoghue, T., and Rabin, M. (1999). Doing it now or later. *Am. Econ. Rev.* 89, 103–124. doi: 10.1257/aer.89.1.103

Papies, E. K., Stroebe, W., and Aarts, H. (2008). The allure of forbidden food: on the role of attention in self-regulation. *J. Exp. Soc. Psychol.* 44, 1283–1292. doi: 10.1016/j.jesp.2008.04.008

Sayette, M. A., Shiffman, S., Tiffany, S. T., Niaura, R. S., Martin, C. S., and Shadel, W. G. (2000). The measurement of drug craving. *Addiction* 95, S189–S210. doi: 10.1046/j.1360-0443.95.8s2.8.x

Stunkard, A. (1959). Obesity and the denial of hunger. *Psychosom. Med.* 21, 281–290. doi: 10.1097/00006842-195907000-00004

Thaler, R. (1981). Some empirical evidence on dynamic inconsistency. *Econ. Lett.* 8, 201–207. doi: 10.1016/0165-1765(81)90067-7

van den Berg, L., Pieterse, K., Malik, J. A., Luman, M., Willems van Dijk, K., Oosterlaan, J., et al. (2011). Association between impulsivity, reward responsiveness and body mass index in children. *Int. J. Obes.* 35, 1301–1307. doi: 10.1038/ijo.2011.116

Veling, H., Aarts, H., and Papies, E. K. (2011a). Using stop signals to inhibit chronic dieters' responses toward palatable foods. *Behav. Res. Ther.* 49, 771–780. doi: 10.1016/j.brat.2011.08.005

Veling, H., Aarts, H., and Stroebe, W. (2011b). Fear signals inhibit impulsive behavior toward rewarding food objects. *Appetite* 56, 643–648. doi: 10.1016/j.appet.2011.02.018

Volkow, N., and Wise, R. (2005). How can drug addiction help us understand obesity? *Nat. Neurosci.* 8, 555–560. doi: 10.1038/nn1452

Weafer, J., and Fillmore, M. (2012). Alcohol-related stimuli reduce inhibitory control of behavior in drinkers. *Psychopharmacology* 222, 489–498. doi: 10.1007/s00213-012-2667-3

Werthmann, J., Roefs, A., Nederkoorn, C., Mogg, K., Bradley, B. P., and Jansen, A. (2011). Can(not) take my eyes off it: attention bias for food in overweight participants. *Health Psychol.* 30, 561–569. doi: 10.1037/a0024291

Wesley, M. J., and Bickel, W. K. (2014). Remember the future II: meta-analyses and functional overlap of working memory and delay discounting. *Biol. Psychiatry* 75, 435–448. doi: 10.1016/j.biopsych.2013.08.008

Weygandt, M., Mai, K., Dommes, E., Ritter, K., Leupelt, V., Spranger, J., et al. (2015). Impulse control in the dorsolateral prefrontal cortex counteracts post-diet weight regain in obesity. *Neuroimage* 109, 318–327. doi: 10.1016/j.neuroimage.2014.12.073

Wittmann, M., and Paulus, M. P. (2008). Decision making, impulsivity and time perception. *Trends Cogn. Sci.* 12, 7–12. doi: 10.1016/j.tics.2007.10.004

Yeomans, M. R., and Brace, A. (2015). Cued to act on impulse: more impulsive choice and risky decision making by women susceptible to overeating after exposure to food stimuli. *PLoS One* 10:e0137626. doi: 10.1371/journal.pone.0137626

Yoshikawa, T., Orita, K., Watanabe, Y., and Tanaka, M. (2012). Validation of the Japanese version of the power of food scale in a young adult population. *Psychol. Rep.* 111, 253–265. doi: 10.2466/08.02.06.15.pr0.111.4.253-265

Zauberman, G., Ratner, R. K., and Kim, B. K. (2009). Memories as assets: strategic memory protection in choice over time. *J. Consum. Res.* 35, 715–728. doi: 10.1086/592943

**Conflict of Interest Statement**: The authors declare that the research was conducted in the absence of any commercial or financial relationships that could be construed as a potential conflict of interest.

frontiers in Human Neuroscience

ORIGINAL RESEARCH
published: 24 September 2018
doi: 10.3389/fnhum.2018.00344

# Smoking Cessation With 20 Hz Repetitive Transcranial Magnetic Stimulation (rTMS) Applied to Two Brain Regions: A Pilot Study

*Da Chang[1], Jian Zhang[1], Wei Peng[1], Zhuowen Shen[1], Xin Gao[1], Youhong Du[1], Qiu Ge[1], Donghui Song[1], Yuanqi Shang[1] and Ze Wang[1,2]**

[1] Department of Psychology, Center for Cognition and Brain Disorders, Hangzhou Normal University, Hangzhou, China,
[2] Department of Radiology, Lewis Katz School of Medicine, Temple University, Philadelphia, PA, United States

Chronic smoking impairs brain functions in the prefrontal cortex and the projecting meso-cortical limbic system. The purpose of this pilot study is to examine whether modulating the frontal brain activity using high-frequency repetitive transcranial magnetic stimulation (rTMS) can improve smoking cessation and to explore the changing pattern of the brain activity after treatment. Fourteen treatment-seeking smokers were offered a program involving 10 days of rTMS treatment with a follow-up for another 25 days. A frequency of 20 Hz rTMS was sequentially applied on the left dorso-lateral prefrontal cortex (DLPFC) and the superior medial frontal cortex (SMFC). The carbon monoxide (CO) level, withdrawal, craving scales, and neuroimaging data were collected. Ten smokers completed the entire treatment program, and 90% of them did not smoke during the 25-day follow-up time. A significant smoking craving reduction and resting brain activity reduction measured by the cerebral blood flow (CBF) and brain entropy (BEN) were observed after 10 days of 20 Hz rTMS treatments compared to the baseline. Although limited by sample size, these pilot findings definitely showed a high potential of multiple-target high-frequency rTMS in smoking cessation and the utility of fMRI for objectively assessing the treatment effects.

**Keywords: smoking cessation, repetitive transcranial magnetic stimulation, brain entropy, cerebral blood flow, left dorso-lateral prefrontal cortex, superior medial frontal cortex**

OPEN ACCESS

***Edited by:***
*Xiaochu Zhang,*
*University of Science and Technology of China, China*

***Reviewed by:***
*Filippo Brighina,*
*Università degli Studi di Palermo, Italy*
*Reza Kazemi,*
*Atieh Clinical Neuroscience Center, Iran*

****Correspondence:***
*Ze Wang*
*zewangnew@163.com*

***Received:*** *28 May 2018*
***Accepted:*** *13 August 2018*
***Published:*** *24 September 2018*

***Citation:***
*Chang D, Zhang J, Peng W, Shen Z, Gao X, Du Y, Ge Q, Song D, Shang Y and Wang Z (2018) Smoking Cessation With 20 Hz Repetitive Transcranial Magnetic Stimulation (rTMS) Applied to Two Brain Regions: A Pilot Study. Front. Hum. Neurosci. 12:344. doi: 10.3389/fnhum.2018.00344*

## INTRODUCTION

Cigarette smoking is a leading cause of preventable disease and premature death (Benowitz, 2010). Long-term smoking cessation, however, is known to be difficult for most smokers because of nicotine dependence (Shiffman et al., 2008; Hughes et al., 2011; Stead et al., 2012). Nicotine affects the brain by binding to the endogenous nicotinic acetylcholine receptors (nAchRs) (Ries et al., 2014), and subsequently disturbs the various brain functions regulated by the nAchRs. Chronical exposure to nicotine will upregulate the nAchRs, especially the nicotine high affinitive α4β2 subtype (Dani et al., 2001; Placzek and Dani, 2008) which is more abundant on dopaminergic neurons in the ventral tegmental area (VTA) and the projecting areas including the ventral striatum, medial orbito-frontal cortex (MOFC), anterior cingulate cortex (ACC), insula, amygdala, and dorsal prefrontal cortex (Brody, 2006; Ries et al., 2014), inducing neuroadaptation associated

with abnormal dopaminergic activity in those areas (Hyman and Malenka, 2001; Robinson and Berridge, 2003; Volkow et al., 2003; Everitt et al., 2008; Kalivas and O'Brien, 2008). Due to the chronic nAchRs upregulation, abstinence from nicotine will dramatically increase the availability of unbound α4β2 nAchRs, which in turn leads to smoking craving (Staley et al., 2006) and the subsequent smoking relapse. Due to these neurobiological changes caused by chronic nicotine binding, treating smoking has proven to be highly difficult. The currently available effective methods, including medicines such as varenicline, bupropion, and nicotine replacement and psychotherapy, can still only provide around 25% abstinence rates at 6 months after the initial treatment (Hughes et al., 2011; Zwar et al., 2014).

At the macroscopic brain circuit level, the neurobiological effects of nicotine dependence converge to brain function disturbances. A potentially effective approach to treat nicotine dependence and smoking is to then revert the altered neural activity in the smokers' brain. Transcranial magnetic stimulation (TMS) is a non-invasive neuromodulational tool (Hallett, 2000) that can be applied for the treatment of chronic smoking because of the long-lasting neuromodulational effects on repetitive application of TMS (the so-called rTMS) (Thickbroom, 2007; Ziemann et al., 2008). TMS works through a varying magnetic field created by frequently charging and discharging a capacitor. The magnetic field can penetrate the scalp losslessly and create a varying electrical field in the superficial cerebral cortex, which subsequently modulates the postsynaptic potentials of neurons in the cortex (Trojak et al., 1900; Fregni and Pascualleone, 2007; Rossini and Rossi, 2007; Slotema et al., 2010; Machado et al., 2013; Lan et al., 2016). By controlling the frequency of the varying magnetic field, the TMS can exert either excitatory or inhibitory effects on the target site and remote brain areas (Hallett, 2007). High frequency rTMS (≥5 Hz) often causes excitatory effects and low-frequency rTMS (≤1 Hz) is often cited for its inhibitory effects (Pascual-Leone et al., 1994; Chen et al., 1997). The rTMS has been assessed in chronic smoking in several studies. In Eichhammer (2003), reported that 20-Hz rTMS on the left DLPFC significantly reduced the number of cigarettes smoked during an *ad libitum* smoking period but without significant change in cigarette craving. Several subsequent studies found that a high frequency rTMS over the DLPFC reduced cue-induced craving in nicotine and cocaine/methamphetamine dependence (Camprodon et al., 2007; Politi et al., 2008; Li et al., 2013a; Dinur-Klein et al., 2014; Pripfl et al., 2014; Shen et al., 2016), while low frequency rTMS over the left DLPFC increased the craving for the drug (Li et al., 2013b), which was inconsistent with the findings of a later study where a low frequency rTMS over the left DLPFC was found to decrease drug craving (Flores-Leal et al., 2015). In Dinur-Klein et al. (2014) performed a large size ($n$ = 77) rTMS-based cessation study by applying high frequency, low frequency, or sham stimulation for 13 days and then following up for 6 months. They reported a significant cigarette consumption reduction and nicotine dependence reduction on applying high- not low-frequency rTMS. Cigarette consumption reduction was further enhanced by combining the rTMS with smoking cue exposure. The 6 months abstinence rate was estimated to be 33%. Although very promising, their study was based on a customized deep stimulation coil, also called H coil, which has very limited availability due to the high cost and is nearly impossible to be applied to any other target brain site once the coil is designed. By contrast, the commonly used figure-of-eight-shaped coils can be readily applied to any superficial brain area and is available for any TMS system.

The purpose of this pilot study was to add to the early stage rTMS-based smoking cessation literature with new evidence. Two brain targets were chosen rather than one: the left DLPFC and the SMFC. The DLPFC is involved in inhibition control, which is known to be impaired in substance dependence. Exciting the DLPFC should then have the potential of enhancing the resistance capability for smoking. The SMFC has been shown to be activated while resisting drug craving (Hartwell et al., 2011) and is coupled with the orbitofrontal cortex, which is involved with impulsivity and is often implicated in drug-craving including smoking craving (Janes et al., 2014). Stimulating the SMFC should then provide a way to reduce smoking craving. Stimulating both the left DLPFC and the SMFC may increase the capability of inhibiting smoking and reducing the urge of smoking at the same time, leading to a more successful smoking cessation. To test this main hypothesis, both behavioral and neuroimaging data were collected to measure the treatment outcome. We previously showed that the chronic smokers had a more irregular resting state brain activity (Li et al., 2016), where the brain activity irregularity was measured by brain entropy (BEN). So one aim of this study was to test whether the rTMS can reduce BEN (Wang et al., 2014) in chronic smokers. Cerebral blood flow (CBF) is tightly coupled to the regional brain function and has been implicated in nicotine dependence (Franklin et al., 2006, 2011; Wang et al., 2007). In this study, we also collected the CBF data and aimed to test whether the rTMS treatment will alter the baseline CBF in smokers.

# MATERIALS AND METHODS

## Participants

This study was conducted at the Center for Cognition and Brain Disorders (CCBD) in the Affiliated Hospital of Hangzhou Normal University. All procedures were approved by the CCBD Institutional Review Board and adhered to the Declaration of Helsinki. Signed written consent forms were collected before any procedure. Fourteen treatment-seeking smokers (13 males/1 female, age: 43 ± 14.5 years) who smoked for more than 5 years (and more than 10 cigarettes each day) participated in the study. Subjects were excluded if they suffered from diabetes, alcoholism, and psychiatric disorders.

## Design

**Figure 1** illustrates the experimental paradigm used in this study. A total of 14 treatment-seeking smokers were offered a program involving 10 days rTMS treatment (T10) and 25 days follow-up (F25) after TMS and MRI safety screening. Subject exclusion criteria included: (1) metal in the brain or skull; (2) having pacemaker; (3) having medical implants such as

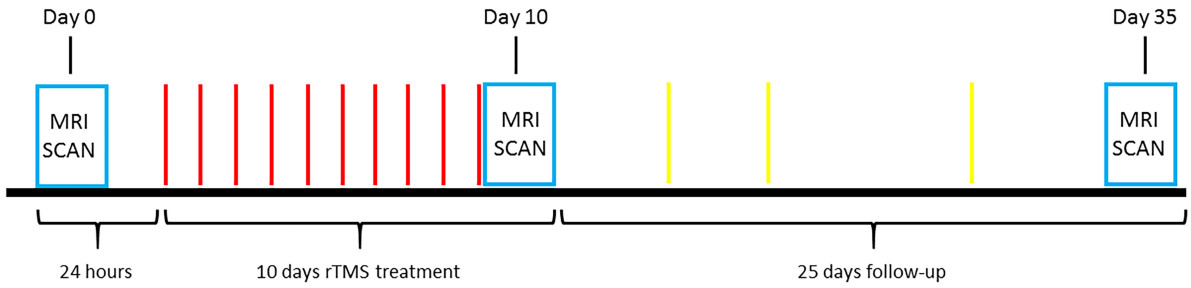


**FIGURE 1 |** The paradigm of the entire experiment. On Day 0, each smoker participated in an MRI scan session to collect the structural imagine, resting state fMRI, and ASL data. With a 24-h abstinence from smoking after the first MRI scan the 10 days treatment began. A 20 Hz rTMS was applied on the left dorso-lateral prefrontal cortex and the superior medial prefrontal cortex, sequentially. At each daily rTMS treatment session, each site received 1000 pulses with a magnitude adjusted to 90% of the resting motor threshold. The CO level, withdrawal, and craving scales were collected every day. After the last treatment (Day 10), the smokers had the MRI taken that was same as Day 0. In the following 25 days the CO level, withdrawal, and craving scales were collected randomly. Again, at the end of F25 (Day 35), the MRI data were collected.

intracardial lines or central venous catheter; (4) suffering from stroke, brain tumor or other brain trauma; (5) diagnosis of seizure or epilepsy; (6) undergone neurosurgery; (7) pregnancy; (8) having magnetic or electric implants in the body; (9) suffering from migraine; and (10) under medications. The rTMS treatment was started after a 24-h abstinence from smoking. A 20 Hz rTMS was applied on the left DLPFC and the SMFC. During each daily rTMS treatment session, 1000 TMS pulses with a magnitude adjusted to 90% of the resting motor threshold were applied to each of the two target sites, sequentially (LDLPFC followed by SMFC). Withdrawal, and craving scales were collected daily during T10 and several times on a random basis during F25 and at the end of F25, using the Minnesota Nicotine Withdrawal Scale (MNWS) (Cappelleri et al., 2005), together with the carbonmonoxide (CO) level. The CO level was used to monitor whether the subjects had smoked during the experiment. The research assistant was only explicitly asked to notice whether the subjects smoked based on a threshold value of CO $<$ 7ppm, and the actual CO values were not documented for most of the subjects. Neuroimaging data were collected at the baseline (24 h before the first treatment), after T10 and F25 (**Figure 1**).

## rTMS Parameters

The rTMS was performed using a Magstim TMS machine and a figure-of-eight coil (Magstim Inc., Sheffield, United Kingdom). The left DLPFC rTMS target was set to be the place with a coordinate of (x,y,z) = (−40, 26, 37) mm in the Montreal Neurological Institute (MNI) standard brain space and mapped to each individual subject's scalp using the BrainSight navigation system (Rogue Research Inc.). The SMFC rTMS target was located at one thumb width inferior to the midline of the left and right DLPFC according to the guidance of the probe placing rule in the electroencephalogram experiment. The coil was placed at an angle to the skull so that the magnetic field can act vertically on the cortex.

The rTMS was applied following the safety guidance provided by the International Workshop on the Safety of Repetitive Transcranial Magnetic Stimulator (Wassermann, 1998). For each site, the rTMS was administered in 20 successive pulse blocks interleaved with 28 s quitting time. Each block consisted of 50 pulses with 20 pulses per second (20 Hz) for 2.5 s. The magnitude of the pulse was set to be 90% of the resting motor threshold. The threshold was determined using the cycles of 10 single TMS pulses applied to the primary motor cortex. Beginning from low, the amplitude of the single pulse was gradually increased for each successive cycle until the thumb involuntarily moved five times within the same stimulation cycle. The amplitude of the final cycle was then used as the threshold.

## Imaging Parameters

Imaging experiments were performed on a 3.0T whole-body GE 750 MR scanner (GE, Milwaukee, WI, United States), using a standard 8-channel receive array. Structural images were acquired using a T1-weighted inversion prepared 3D spoiled gradient echo (IR-SPGR) sequence with FOV = 256 × 256 $mm^2$, inversion time = 450 ms, TR/TE = 7.2/2.1 ms, matrix = 256 × 256, and 176 sagittal slices with slice thickness = 1 mm. The resting-state fMRI (rsfMRI) data, i.e., the blood oxygen level-dependent (BOLD) signal, were acquired with a $T2^*$ weighted gradient-echo echo-planar imaging (EPI) sequence with the following parameters: matrix = 64 × 64, voxel size = 3 × 3 × 3 $mm^3$, and TR/TE = 2000/30 ms. A total of 37 axial slices were obtained in an interleaved order to cover the entire cerebrum and cerebellum from bottom to top. Arterial spin labeling (ASL) perfusion MRI was acquired with a GE product fast spin echo background suppressed 3D pseudo continuous ASL (pCASL) sequence with the following parameters: TR/TE = 4690/10.9 ms, 8 shots each with a spiral readout covering 512 k-space points, 40 axial slices, voxel size = 3.389 × 3.389 × 3.4 $mm^3$, number of repeat scan (NEX) = 3, labeling duration = 1500 ms, post-labeling delay = 1525 ms, and the duration of the ASL scan was 4 min 32 s.

## Data Processing

The rsfMRI images were preprocessed using SPM12[1] involving the following steps: (1) discarding the first 6 images to allow the

[1]http://www.fil.ion.ucl.ac.uk/spm

signal to reach stead state; (2) the origins of both structural and raw rsfMRI images were set to be the center of the image matrix; (3) slice-timing correction; (4) motion correction; (5) registering rsfMRI to the MNI standard brain space via each subject's T1 weighted anatomical image; (6) temporal nuisance correction using simple regression with the residual head motions, white matter signal, and cerebrospinal fluid (CSF) signal as the co-variants; (7) linearly detrending and temporal band-pass filtering (0.01–0.08 Hz) to eliminate high-frequency noise and low-frequency drift; and (8) spatial smoothing with an isotropic Gaussian kernel, full-width-at-half-maximum (FWHM) = 6 mm. Each subject's BEN map was calculated based on the preprocessed rsfMRI images with BENtbx[2] using an approximate entropy measurement, sample entropy (SampEn) with the parameters recommended in Wang et al. (2014); individual BEN maps were spatially normalized into the MNI space using the non-linear transform obtained by registering the structural MR image into the MNI space using SPM12.

Arterial spin labeling CBF images were processed using the SPM12-based batch scripts provided in ASLtbx (Wang et al., 2008). The following steps were included: (1) the origins of structural image, M0 map, and ASL images were set to be the center of the image matrix; (2) ASL CBF maps were calculated from the delta M and M0 maps and registered to the structural MR image for each subject; (3) CBF images were spatially normalized into the MNI using the similar procedure as mentioned above; and (4) CBF images were smoothed with an isotropic Gaussian filter with an FWHM = 6 mm.

Paired *t*-tests were performed on the preprocessed BEN maps and CBF maps to characterize the rTMS induced BEN and CBF changes, respectively. The statistical significance was defined by $p < = 0.01$ at the voxel level and a cluster size $> = 270$ [alpha $< 0.5$, corrected for multiple comparison using the Monte Carlo simulation-based correction approach provided in AFNI (the AlphaSim tool[3])].

## RESULTS

A total of 10 smokers completed the entire treatment program, of which 9 did not smoke during the entire period of 35 days. Complete MRI scans were only available for 8 subjects out of the 9 (all males, age: 47 ± 14.5). Withdrawal and craving at T10 and F25 were not significantly different; both were significantly reduced as compared to the baseline (**Figure 2**, $p < 0.05$).

**Figure 3** shows the T10 (after rTMS) vs. baseline BEN comparison results. After 10 days of rTMS treatment, a significant BEN reduction was found in the right OFC, right anterior insula, right dorsal striatum, and ACC.

**Figure 4** shows the results of CBF comparison between baseline and T10. The 10 days rTMS treatment induced a significant CBF reduction in a big portion of the cortical and sub-cortical areas in the right hemisphere including the right thalamus, right frontal and temporal cortex. The CBF reduction was also visible in the MOFC, ventral striatum, ACC, precuneus, left anterior insula, left PFC, and left DLPFC.

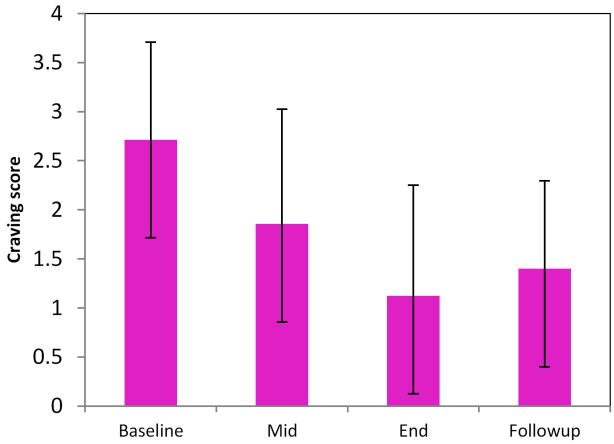


**FIGURE 2 |** Longitudinal changes of smoking craving during the pilot high-frequency rTMS-based smoking cessation therapy. Baseline, Mid, End, and Follow-up mean the data acquired at the time before smoking cessation (smoking as usual), 5 days of rTMS treatment, 10 days of rTMS treatment (T10), 25-day follow-up (F25).

## DISCUSSION AND CONCLUSION

This pilot study showed that a 20 Hz rTMS sequentially applied to the left DLPFC and the SMFC for 10 days produced a high smoking cessation rate, which was confirmed by both the behavioral measures and the fMRI data: rTMS caused smoking cessation for the entire 25-day follow-up time, reduced craving for smoking, reduced BEN in the prefrontal cortex as well as insula, and decreased CBF in the right hemisphere. The promising high smoking cessation rate (90% of the 10 participants) and craving reduction were consistent with the previous studies (Camprodon et al., 2007; Politi et al., 2008; Li et al., 2013a; Dinur-Klein et al., 2014; Pripfl et al., 2014; Shen et al., 2016), suggesting that high-frequency rTMS is a promising tool to treat chronic smoking.

These encouraging preliminary results supported our hypothesis of stimulating the left DLPFC to increase the capability of inhibiting smoking and stimulating the SMFC to reduce the urge of smoking, thereby resulting in the high cessation rate. Brain imaging was adopted as an objective measure to monitor the treatment effects. Both the dynamic and static property of brain activity were assessed – the former was with BEN and the latter was with CBF.

BEN is a relatively new brain activity metrics (Song et al., 2018). Different from other more widely used activity measures, BEN indicates the irregularity of brain activity, which is related to the brain information processing capacity. The reduced BEN by rTMS found in the current study was supported by our previous smoking-as-usual study where we found that the chronic smokers had a higher BEN in a big portion of the cortex, with the greatest BEN increases located in the lateral striatum, prefrontal cortex,

[2]https://cfn.upenn.edu/~zewang/BENtbx.php
[3]https://afni.nimh.nih.gov/

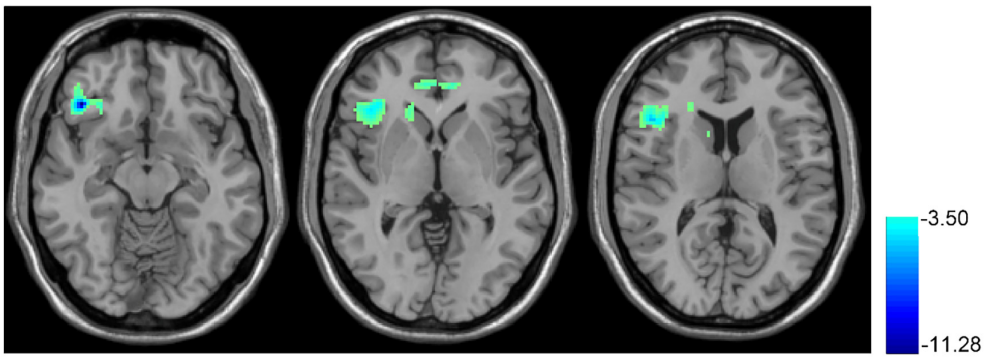


**FIGURE 3 |** rTMS-induced BEN decrease. Paired *t*-test, when compared with the baseline condition (no rTMS), showed the 10 days rTMS treatment-induced CBF decrease in the right orbital part of the inferior frontal gyrus and right insula. In the thresholded *t*-map, blue means lower after rTMS treatment, $p < 0.01$, AlphaSim corrected (cluster size >270).

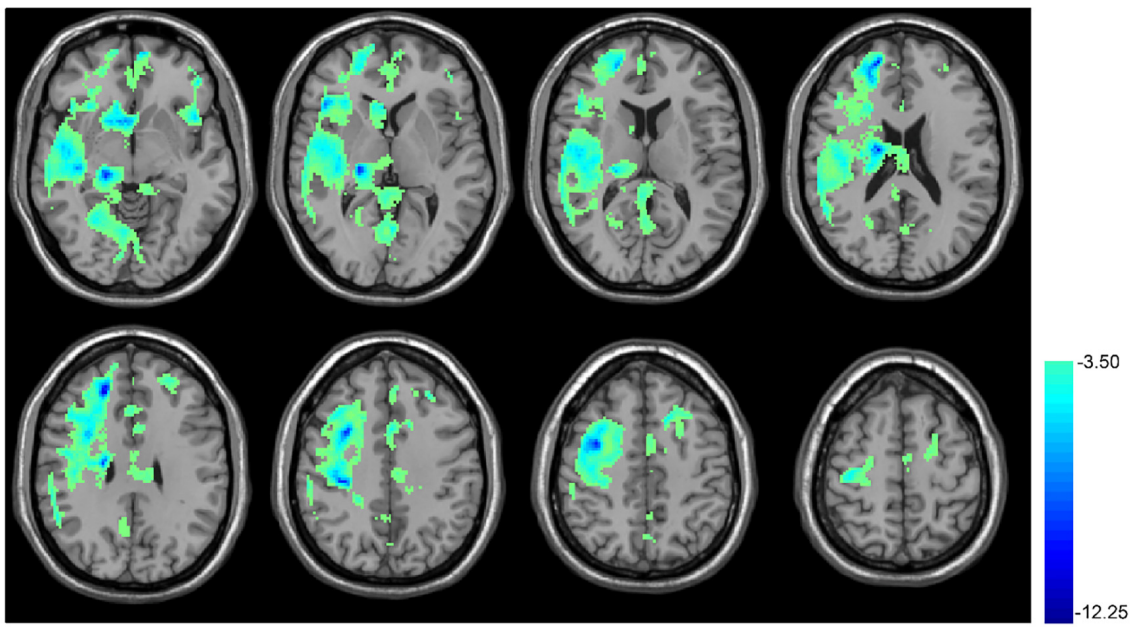


**FIGURE 4 |** rTMS-induced CBF decrease in cerebral cortex. Paired *t*-test, when compared with the baseline condition (no rTMS), showed the 10 days rTMS treatment-induced CBF decrease in the right temporal lobe cortex, the big portion of the frontal lobe, precentral gyrus, caudate, hippocampus, cuneus, and thalamus as well as both sides of the insula. In the thresholded *t*-map, blue means lower after rTMS treatment, $p < 0.01$, AlphaSim corrected (cluster size >270).

insula, middle and superior frontal cortex, and visual cortex (Li et al., 2016). Higher BEN in smokers might be a result of chronic psycho-stimulation by nicotine, similar to the increased BEN observed after taking psychedelic drugs (Carhart-Harris et al., 2014; Viol et al., 2017).

Smoking abstinence has been shown to cause regionally increased CBF (Boyajian and Otis, 2000; Zubieta et al., 2005; Wang et al., 2007), which was also related to abstinence-induced craving and withdrawal symptoms (Wang et al., 2007). The CBF reduction after 10 days of rTMS may then reflect a beneficiary brain effect of rTMS for smoking cessation, which was confirmed by the craving and withdrawal symptom reduction. Chronic smoking impairs the synthesis of nitric oxide and its regulatory role on CBF, resulting in a reduced CBF (Toda and Okamura, 2016). Accordingly, a full remission of nicotine dependence shall be accompanied with an increase of baseline CBF. This, however, could not be assessed in the current study due to the lack of MRI data acquired after the follow-up time.

As a preliminary study, there exist several limitations. The major limitation was the small sample size, which was mainly due to the difficulty of subject recruitment in Hangzhou. One possible reason is that smoking is still literally allowed in most public places. Another reason is the high work pressure and busy work schedule. Nevertheless, such a small sample size still yielded promising results, making it more valuable to perform

a full validation study in the future. Related to the difficulty of subject recruitment, the second limitation was that there was no control group for controlling the placebo effects of rTMS. All the subjects declined to participate in the study once they heard that they might be assigned to a control group and receive a SHAM stimulation. We then revised the protocol to a non-blind one. Even with that modification, we could only recruit 14 treatment-seeking smokers within a period of 2.5 years. Another limitation was that there was no control for the two-site stimulation and the order of the sites. This makes it impossible to find whether two sites are better than only one target and whether the order matters.

To sum up, the high-frequency rTMS sequentially applied to the left DLPFC and SMFC may potentially be an effective tool for improving the smoking cessation rate; BEN and CBF provide valuable means to monitor or quantify the treatment effects.

## AUTHOR CONTRIBUTIONS

All authors listed have made a substantial, direct and intellectual contribution to the work, and approved it for publication.

## FUNDING

This study was supported by the Natural Science Foundation of Zhejiang Province Grant LZ15H180001, and by the Youth 1000 Talent Program of China.

## ACKNOWLEDGMENTS

The authors thank Ying Jing, Zi-Yi Zhao, and Luo-Yu Wang for their contribution to the experiment.

## REFERENCES

Benowitz, N. L. (2010). Nicotine addiction. *N. Engl. J. Med.* 362, 2295–2303. doi: 10.1056/NEJMra0809890

Boyajian, R. A., and Otis, S. M. (2000). Acute effects of smoking on human cerebral blood flow: a transcranial Doppler ultrasonography study. *J. Neuroimaging* 10, 204–208. doi: 10.1111/jon2000104204

Brody, A. L. (2006). Functional brain imaging of tobacco use and dependence. *J. Psychiatr. Res.* 40, 404–418. doi: 10.1016/j.jpsychires.2005.04.012

Camprodon, J. A., Martínez-Raga, J., Alonso-Alonso, M., Shih, M. C., and Pascual-Leone, A. (2007). One session of high frequency repetitive transcranial magnetic stimulation (rTMS) to the right prefrontal cortex transiently reduces cocaine craving. *Drug Alcohol Depend.* 86, 91–94. doi: 10.1016/j.drugalcdep.2006.06.002

Cappelleri, J. C., Bushmakin, A. G., Baker, C. L., Merikle, E., Olufade, A. O., and Gilbert, D. G. (2005). Revealing the multidimensional framework of the Minnesota nicotine withdrawal scale. *Curr. Med. Res. Opin.* 21, 749–760. doi: 10.1185/030079905X43712

Carhart-Harris, R. L., Leech, R., Hellyer, P. J., Shanahan, M., Feilding, A., Tagliazucchi, E., et al. (2014). The entropic brain: a theory of conscious states informed by neuroimaging research with psychedelic drugs. *Front. Hum. Neurosci.* 8:20. doi: 10.3389/fnhum.2014.00020

Chen, R., Classen, J., Gerloff, C., Celnik, P., Wassermann, E. M., Hallett, M., et al. (1997). Depression of motor cortex excitability by low-frequency transcranial magnetic stimulation. *Neurology* 48, 1398–1403. doi: 10.1212/WNL.48.5.1398

Dani, J. A., Ji, D., and Zhou, F. M. (2001). Synaptic plasticity and nicotine addiction. *Neuron* 31, 349–352. doi: 10.1016/S0896-6273(01)00379-8

Dinur-Klein, L., Dannon, P., Hadar, A., Rosenberg, O., Roth, Y., Kotler, M., et al. (2014). Smoking cessation induced by deep repetitive transcranial magnetic stimulation of the prefrontal and insular cortices: a prospective, randomized controlled trial. *Biol. Psychiatry* 76, 742–749. doi: 10.1016/j.biopsych.2014.05.020

Eichhammer, P. (2003). High-Frequency repetitive transcranial magnetic stimulation decreases cigarette smoking. *J. Clin. Psychiatry* 64, 951–953. doi: 10.4088/JCP.v64n0815

Everitt, B. J., Belin, D., Economidou, D., Pelloux, Y., Dalley, J. W., and Robbins, T. W. (2008). Review. Neural mechanisms underlying the vulnerability to develop compulsive drug-seeking habits and addiction. *Philos. Trans. R Soc. Lond. B Biol. Sci.* 363, 3125–3135. doi: 10.1098/rstb.2008.0089

Flores-Leal, M., Sacristán-Rock, E., Jiménez-Angeles, L., and Azpiroz-Leehan, J. (2015). Low frequency repetitive transcranial magnetic stimulation effects over dorsolateral prefrontal cortex in moderate nicotine dependent subjects. *IFMBE Proc.* 49, 317–320. doi: 10.1007/978-3-319-13117-7_82

Franklin, T., Wang, Z., Sciortino, N., Derek, H., Hakun, J., Li, Y., et al. (2006). Perfusion fMRI of limbic activation to cigarette cues: male/female differences and blockade of brain's response with Baclofen treatment. *Neuropsychopharmacology* 31, S197–S197.

Franklin, T., Wang, Z., Suh, J. J., Hazan, R., Cruz, J., Li, Y., et al. (2011). Effects of varenicline on smoking cue-triggered neural and craving responses. *Arch. Gen. Psychiatry* 68, 516–526. doi: 10.1001/archgenpsychiatry.2010.190

Fregni, F., and Pascualleone, A. (2007). Technology insight: noninvasive brain stimulation in neurology-perspectives on the therapeutic potential of rTMS and tDCS. *Nat. Rev. Neurol.* 3, 383–393. doi: 10.1038/ncpneuro0530

Hallett, M. (2000). Transcranial magnetic stimulation. *Nature* 406, 147–150. doi: 10.1038/35018000

Hallett, M. (2007). Transcranial magnetic stimulation: a primer. *Neuron* 55, 187–199. doi: 10.1016/j.neuron.2007.06.026

Hartwell, K. J., Johnson, K. A., Li, X., Myrick, H., LeMatty, T., George, M. S., et al. (2011). Neural correlates of craving and resisting craving for tobacco in nicotine dependent smokers. *Addict. Biol.* 16, 654–666. doi: 10.1111/j.1369-1600.2011.00340.x

Hughes, J. R., Rennard, S. I., Fingar, J. R., Talbot, S. K., Callas, P. W., and Fagerstrom, K. O. (2011). Efficacy of varenicline to prompt quit attempts in smokers not currently trying to quit: a randomized placebo-controlled trial. *Nicot. Tobacco Res.* 13, 955–964. doi: 10.1093/ntr/ntr103

Hyman, S. E., and Malenka, R. C. (2001). Addiction and the brain: the neurobiology of compulsion and its persistence. *Nat. Rev. Neurosci.* 2, 695–703. doi: 10.1038/35094560

Janes, A. C., Farmer, S., Nickerson, L. D., and Lukas, S. E. (2014). An increase in tobacco craving is associated with enhanced medial prefrontal cortex network coupling. *PLoS One* 9:e88228. doi: 10.1371/journal.pone.0088228

Kalivas, P. W., and O'Brien, C. (2008). Drug addiction as a pathology of staged neuroplasticity. *Neuropsychopharmacology* 33, 166–180. doi: 10.1038/sj.npp.1301564

Lan, M. J., Chhetry, B. T., Liston, C., Mann, J. J., and Dubin, M. (2016). Transcranial magnetic stimulation of left dorsolateral prefrontal cortex induces brain morphological changes in regions associated with a treatment resistant major depressive episode: an exploratory analysis. *Brain Stimul.* 9, 577–583. doi: 10.1016/j.brs.2016.02.011

Li, X., Hartwell, K. J., Owens, M., Lematty, T., Borckardt, J. J., and Hanlon, C. A. (2013a). Repetitive transcranial magnetic stimulation of the dorsolateral prefrontal cortex reduces nicotine cue craving. *Biol. Psychiatry* 73, 714–720. doi: 10.1016/j.biopsych.2013.01.003

Li, X., Malcolm, R. J., Huebner, K., Hanlon, C. A., Taylor, J. J., and Brady, K. T. (2013b). Low frequency repetitive transcranial magnetic stimulation of the left dorsolateral prefrontal cortex transiently increases cue-induced craving for methamphetamine: a preliminary study. *Drug Alcohol Depend.* 133, 641–646. doi: 10.1016/j.drugalcdep.2013.08.012

Li, Z., Fang, Z., Hager, N., Rao, H., and Wang, Z. (2016). Hyper-resting brain entropy within chronic smokers and its moderation by Sex. *Sci. Rep.* 6:29435. doi: 10.1038/srep29435

Machado, S., Ariascarrión, O., Paes, F., Vieira, R. T., Caixeta, L., Novaes, F., et al. (2013). Repetitive transcranial magnetic stimulation for clinical applications in

neurological and psychiatric disorders: an overview. *Eur. J. Med.* 45, 191–206. doi: 10.5152/eajm.2013.39

Pascual-Leone, A., Valls-Solé, J., Wassermann, E. M., and Hallett, M. (1994). Responses to rapid-rate transcranial magnetic stimulation of the human motor cortex. *Brain* 117(Pt 4), 847–858. doi: 10.1093/brain/117.4.847

Placzek, A. N., and Dani, J. A. (2008). *Synaptic Plasticity within Midbrain Dopamine Centers Contributes to Nicotine Addiction, The Motivational Impact of Nicotine and its Role in Tobacco Use*. Berlin: Springer.

Politi, E., Fauci, E., Santoro, A., and Smeraldi, E. (2008). Daily sessions of transcranial magnetic stimulation to the left prefrontal cortex gradually reduce cocaine craving. *Am. J. Addict.* 17, 345–346. doi: 10.1080/10550490802139283

Pripfl, J., Tomova, L., Riecansky, I., and Lamm, C. (2014). Transcranial magnetic stimulation of the left dorsolateral prefrontal cortex decreases cue-induced nicotine craving and EEG delta power. *Brain Stimul.* 7, 226–233. doi: 10.1016/j.brs.2013.11.003

Ries, R. K., Fiellin, D. A., Miller, S. C., and Saitz, R. (2014). *The ASAM Principles of Addiction Medicine*. Philadelphia, PA: Lippincott Williams & Wilkins.

Robinson, T. E., and Berridge, K. C. (2003). Addiction. *Annu. Rev. Psychol.* 54, 25–53. doi: 10.1146/annurev.psych.54.101601.145237

Rossini, P. M., and Rossi, S. (2007). Transcranial magnetic stimulation: diagnostic, therapeutic, and research potential. *Neurology* 68, 484–488. doi: 10.1212/01.wnl.0000250268.13789.b2

Shen, Y., Cao, X., Tan, T., Shan, C., Wang, Y., Pan, J., et al. (2016). 10-Hz repetitive transcranial magnetic stimulation of the left dorsolateral prefrontal cortex reduces heroin cue craving in long-term addicts. *Biol. Psychiatry* 80, e13–e14. doi: 10.1016/j.biopsych.2016.02.006

Shiffman, S., Brockwell, S. E., Pillitteri, J. L., and Gitchell, J. G. (2008). Use of smoking-cessation treatments in the United States. *Am. J. Prev. Med.* 34, 102–111. doi: 10.1016/j.amepre.2007.09.033

Slotema, C. W., Blom, J. D., Hoek, H. W., and Sommer, I. E. (2010). Should we expand the toolbox of psychiatric treatment methods to include Repetitive Transcranial Magnetic Stimulation (rTMS)? A meta-analysis of the efficacy of rTMS in psychiatric disorders. *J. Clin. Psychiatry* 71, 873–884. doi: 10.4088/JCP.08m04872gre

Song, D., Chang, D., Zhang, J., Ge, Q., Zang, Y.-F., and Wang, Z. (2018). Associations of brain entropy (BEN) to cerebral blood flow and fractional Amplitude of low-frequency fluctuations in the resting brain. *Brain Imaging Behav.* (in press).

Staley, J. K., Krishnan-Sarin, S., Cosgrove, K. P., Krantzler, E., Frohlich, E., Perry, E., et al. (2006). Human tobacco smokers in early abstinence have higher levels of beta2* nicotinic acetylcholine receptors than nonsmokers. *J. Neurosci.* 26, 8707–8714. doi: 10.1523/JNEUROSCI.0546-06.2006

Stead, L. F., Perera, R., Bullen, C., Mant, D., Hartmann-Boyce, J., Cahill, K., et al. (2012). Nicotine replacement therapy for smoking cessation. *Cochrane Database Syst. Rev.* 11:CD000146. doi: 10.1002/14651858.CD000146.pub4

Thickbroom, G. W. (2007). Transcranial magnetic stimulation and synaptic plasticity: experimental framework and human models. *Exp. Brain Res.* 180, 583–593. doi: 10.1007/s00221-007-0991-3

Toda, N., and Okamura, T. (2016). Cigarette smoking impairs nitric oxide-mediated cerebral blood flow increase: implications for Alzheimer's disease. *J. Pharmacol. Sci.* 131, 223–232. doi: 10.1016/j.jphs.2016.07.001

Trojak, B., Meille, V., Achab, S., Lalanne, L., Poquet, H., Ponavoy, E., et al. (1900). Transcranial magnetic stimulation combined with nicotine replacement therapy for smoking cessation: a randomized controlled trial. *Brain Stimul.* 8, 1168–1174. doi: 10.1016/j.brs.2015.06.004

Viol, A., Palhano-Fontes, F., Onias, H., de Araujo, D. B., and Viswanathan, G. (2017). Shannon entropy of brain functional complex networks under the influence of the psychedelic Ayahuasca. *Sci. Rep.* 7:7388. doi: 10.1038/s41598-017-06854-0

Volkow, N. D., Fowler, J. S., and Wang, G. J. (2003). The addicted human brain: insights from imaging studies. *J. Clin. Invest.* 111, 1444–1451. doi: 10.1172/JCI18533

Wang, Z., Aguirre, G. K., Rao, H., Wang, J., Fernandez-Seara, M. A., Childress, A. R., et al. (2008). Empirical optimization of ASL data analysis using an ASL data processing toolbox: ASLtbx. *Magn. Reson. Imaging* 26, 261–269. doi: 10.1016/j.mri.2007.07.003

Wang, Z., Faith, M., Patterson, F., Tang, K., Kerrin, K., Wileyto, E. P., et al. (2007). Neural substrates of abstinence-induced cigarette cravings in chronic smokers. *J. Neurosci.* 1403:MC2153440. doi: 10.1523/JNEUROSCI.2966-07.2007

Wang, Z., Li, Y., Childress, A. R., and Detre, J. A. (2014). Brain entropy mapping using fMRI. *PLoS One* 9:e89948. doi: 10.1371/journal.pone.0089948

Wassermann, E. M. (1998). Risk and safety of repetitive transcranial magnetic stimulation: report and suggested guidelines from the International Workshop on the Safety of Repetitive Transcranial Magnetic Stimulation, June 5-7, 1996. *Electroencephalogr. Clin. Neurophysiol.* 108, 1–16. doi: 10.1016/S0168-5597(97)00096-8

Ziemann, U., Paulus, W., Nitsche, M. A., Pascual-Leone, A., Byblow, W. D., Berardelli, A., et al. (2008). Consensus: motor cortex plasticity protocols. *Brain Stimul.* 1, 164–182. doi: 10.1016/j.brs.2008.06.006

Zubieta, J. K., Heitzeg, M. M., Xu, Y., Koeppe, R. A., Ni, L., Guthrie, S., et al. (2005). Regional cerebral blood flow responses to smoking in tobacco smokers after overnight abstinence. *Am. J. Psychiatry* 162, 567–577. doi: 10.1176/appi.ajp.162.3.567

Zwar, N. A., Mendelsohn, C. P., and Richmond, R. L. (2014). Supporting smoking cessation. *BMJ* 348:f7535. doi: 10.1136/bmj.f7535

**Conflict of Interest Statement:** The authors declare that the research was conducted in the absence of any commercial or financial relationships that could be construed as a potential conflict of interest.

frontiers in Human Neuroscience

ORIGINAL RESEARCH
published: 28 September 2018
doi: 10.3389/fnhum.2018.00382

# Implicit Emotion Regulation Deficits in Trait Anxiety: An ERP Study

*Bingqian Liu*[1,2†], *Yi Wang*[1,2†] *and Xuebing Li*[1,2*]

[1]CAS Key Laboratory of Mental Health, Institute of Psychology, Chinese Academy of Sciences, Beijing, China, [2]University of Chinese Academy of Sciences, Beijing, China

According to the framework of emotion regulation (ER), both explicit and implicit forms are essential to our well-being. It is the interaction between these two processes that ensures adaptive emotional responses. Although many studies have focused on explicit ER deficits in anxiety, there is still a lack of awareness about the implicit form and its role in anxiety. To address this issue, we explored the time course of implicit ER processes in individuals with high and low trait anxiety (LTA). To do this, we employed the newly developed Priming-Identify (PI) paradigm, which includes a word-matching task (externally-generated implicit goals) and a facial expression identification task (emotion processing). We aimed to modulate the implicit ER goals of individuals through the application of different priming conditions (ER-related and -unrelated words). In addition to their behavioral effects, we recorded the influence of these priming conditions through event-related potentials (ERPs) during the facial expression identification task. Three ERP components were chosen as indexes of three stages of implicit ER processing: N170, early posterior negativity (EPN) and late positive potential (LPP). In individuals with LTA, the early N170 and the middle EPN were enlarged under the ER-related priming condition, while the LPP was not influenced. However, in individuals with high trait anxiety (HTA), we observed an absence of any significant differences between the ER-related and -unrelated priming conditions across all three ERP components. Furthermore, enlargements of N170 and EPN amplitudes were significantly correlated with a decrease in negative emotion experience scores. Our results suggest that HTA individuals experience implicit ER deficits during the early and middle stages of ER.

**Keywords: implicit emotion regulation, anxiety, trait anxiety, N170, EPN, LPP**

OPEN ACCESS

***Edited by:***
*Wenbo Luo,*
*Liaoning Normal University, China*

***Reviewed by:***
*Chunliang Feng,*
*Beijing Normal University, China*
*Wenfeng Feng,*
*Soochow University, China*

***Correspondence:**
*Xuebing Li*
*lixb@psych.ac.cn*

*†These authors have contributed equally to this work and should be considered co-first authors*

***Received:*** *24 April 2018*
***Accepted:*** *04 September 2018*
***Published:*** *28 September 2018*

***Citation:***
*Liu B, Wang Y and Li X (2018) Implicit Emotion Regulation Deficits in Trait Anxiety: An ERP Study. Front. Hum. Neurosci. 12:382. doi: 10.3389/fnhum.2018.00382*

## INTRODUCTION

With a global prevalence of 7.3%, anxiety disorders constitute the most prevalent class of mental disorder (American Psychiatric Association, 2013; Baxter et al., 2013). Although long considered disorders of emotion (Barlow, 1991; Beck and Emery, 2010), Kring (2010) noted that their most problematic and disruptive characteristic is not necessarily the content of the experienced negative emotion but rather its timing and intensity. This indicates the essential role played by emotion regulation (ER) in how individuals deal with anxiety. ER is generally defined as the application of abilities, methods or strategies "to influence which emotions we have, when we have them, and how these emotions are experienced or expressed" (Gross, 1998; Rottenberg and Gross, 2006). A growing body of research suggests that emotion dysregulation, the inability to regulate emotion, is heavily implicated in the etiology and maintenance of anxiety disorders

(Mennin, 2004; Kashdan et al., 2008; Cisler et al., 2010; Suveg et al., 2010; Hofmann et al., 2012). Given these considerations, further investigation into ER deficits and specifically their role in anxiety disorders would contribute to an improved understanding of this disruptive class of disorders.

According to the dual-process framework of ER (Gyurak et al., 2011), adaptive emotional responses depend on an interaction between both explicit and the implicit forms of processing. However, the majority of studies investigating ER have focused solely on deficits of explicit ER in anxiety, that is, processes that require conscious efforts. These have demonstrated a tendency for anxious individuals to overuse maladaptive strategies, such as suppression, in place of more adaptive ER strategies, such as reappraisal (Berking et al., 2008; McLaughlin et al., 2011; Ball et al., 2013; O'Toole et al., 2014; Schäfer et al., 2017). Implicit ER processes, on the other hand, are evoked automatically by stimuli and occur without awareness. It is unreasonable to assume that explicit ER could be employed at all times, given the conscious effort required. As a consequence, the efficient use of implicit ER strategies is regarded as crucial to well-being (Gyurak et al., 2011). Despite this, there are few studies examining the role of implicit ER in anxiety.

Two behavioral studies suggest the presence of deficits in implicit ER in anxious individuals. In one study performed by Jasper and Witthöft (2013), participants were asked to perform a character valence attribution task. As a result, a significant correlation was found between the affect misattribution procedure and trait anxiety scores in a threatening priming condition. This finding suggests the presence of an automatic misattribution of negative affect related to anxiety, which in turn might indicate a deficit of implicit ER within these individuals. Ma and Zhu (2012) employed a sentence unscrambling task to investigate implicit ER in trait anxiety. Reappraisal-related words as well as suppression-related words were included in this task to exogenously modulate the implicit ER goal. In the subsequent affective picture labeling task, they found that, compared with healthy controls, high trait anxiety (HTA) individuals showed a significantly higher level of arousal in response to pictures with emotional content for both negative emotion and neutral emotion pictures under suppression-related priming and non-priming conditions, but a non-significant difference under the reappraisal-related priming condition. In their study, they found that emotional experiences could be modulated by priming ER goals effectively and high trait anxious individuals probably had the deficit of implicit suppression strategy.

While these studies indicate that anxious individuals might present deficits of implicit ER at the behavioral level, other studies have explored their underlying neural mechanisms. In two studies employing event-related potential (ERP) techniques, by applying the Go/Nogo paradigm to children with anxiety, have observed an enlarged Nogo trial-related N2 (Lamm et al., 2011) as well as significantly larger posterior P1 and frontal N2 amplitudes (Hum et al., 2013). Since both P1 and N2 occur in the early stage, these results suggest a deficit in early implicit ER processing. One functional magnetic resonance imaging (fMRI) study showed that healthy adults were able to regulate emotional conflict without awareness, however, an absence of this ability was observed in patients who were suffering from generalized anxiety disorder (Etkin et al., 2010).

The above studies suggest the presence of implicit ER deficits in anxious individuals at both behavioral and neural levels. However, one may argue that some of the deficits described above are more related to the process of emotion generation rather than ER. Some researchers argue that these two types of processing are inextricably entwined, and the regulatory process is a durable aspect accompanying the development of emotion over time (Amstadter, 2008). Given its complexity, a methodology that reveals the time course of ER during processing might provide more insight into the underlying mechanism of implicit ER as well as associated anxiety-related deficits. ERP is a temporally sensitive technique that could potentially offer such an insight. Although existing studies of anxiety have revealed various relevant ERP components that occur during emotion processing (e.g., P1, N2), it is difficult to determine whether those elicited by the Go/Nogo paradigm or during passive viewing are truly related to ER rather than the process of emotion generation.

In the current study, we adopted the operational definition given by Mauss et al. (2007a) to investigate the deficits occurring during the process of nonconscious goal pursuit in anxiety. According to this definition automatic/implicit ER is a "goal-driven change to any aspect of one's emotions without making a conscious decision to do so, without paying attention to the process of regulating one's emotions, and without engaging in deliberate control." Thus, the mechanism underlying implicit ER is posited to be a nonconscious goal pursuit. Priming tasks, by their nature, offer the possibility of exogenously activating and manipulating the ER goals (e.g., emotion control and expression) of individuals without their conscious awareness. As a consequence, this can lead to the alteration of subsequent emotional experiences (Gallo et al., 2009; Williams et al., 2009; Yuan et al., 2015a).

Rather than evoking passive responses to specific emotional states, the recently developed Priming-Identify (PI) ERP paradigm (Wang and Li, 2017) was able to distinguish the emotional responses and ER processes. We adopted this method (Wang and Li, 2017) to explicitly alter implicit ER goals. We aimed to modulate them through two word-priming conditions in the word-matching component of the paradigm, namely ER-related and ER-unrelated priming. During this paradigm, after priming the ER goals, a facial expression identification task was used to investigate the alteration of emotional response processing, in which the electroencephalogram (EEG) signal was recorded. In order to ensure that this alteration was uniquely influenced by ER but not emotion generation, only threatening facial expressions (anger or fear) were presented during this task. In addition, an oral-based intention detection test was performed at the end of each testing session to ensure that the ER processing involved in this study was indeed implicit.

According to previous studies examining the time course of emotional facial processing (Frenkel and Bar-Haim, 2011;

Fruhholz et al., 2011; Leleu et al., 2015; Wieser and Moscovitch, 2015), three ERP components are important indexes during this process: N170, early posterior negativity (EPN) and late positive potential (LPP). N170 is a negative-going component that occurs over occipital-temporal regions (Hinojosa et al., 2015). It is considered to be a face-specific ERP component which reflects the early, automatic perceptual process of face encoding (Bentin et al., 1996; Eimer and Holmes, 2002; Walentowska and Wronka, 2012). EPN is an occipital-temporal negative-going wave, which has been found to be enlarged for negative compared to neutral facial expressions during both implicit and explicit tasks (Morel et al., 2014; Yoon et al., 2016). LPP is a centro-parietal positive component, which represents more strategic high-level processes such as enhanced encoding of emotional expressions (Schupp et al., 2004b; Yuan et al., 2015b). The early window of LPP is considered to be an index of the allocation of attentional resources (Dennis, 2010).

It has been suggested that responses to emotional faces could be detected by the early N170 and selected for further encoding by the middle EPN, which may lead to elaborate processing at the level of LPP (Fruhholz et al., 2011). Accordingly, it is possible that implicit ER processing of facial expression could also be indexed by these components. One study has investigated the alteration of these ERP components under conditions designed to prime implicit ER. By exploring the time course of implicit ER of healthy adults through the PI paradigm, Wang and Li (2017) observed a more negative N170 (i.e., enlargement of N170 amplitude) induced by implicit ER, while the middle EPN and the late LPP were not influenced. Based on these findings, they suggest that the enlarged N170 could be considered an effective index of implicit ER. In the current context, we suggest that deficits of implicit ER in anxiety occur during the early stage of emotional facial processing and be detectable through the absence of an enlarged N170 amplitude.

Based on the above rationale, the aim of the current study was to investigate potential implicit ER deficits in individuals with HTA, as compared with individuals with low trait anxiety (LTA). Two hypotheses were raised in view of the previous literature. First, we hypothesized that in individuals with LTA, the early N170 would be enlarged by ER-related priming, while the middle EPN and the late LPP would remain unaffected. Second, in individuals with HTA, these three ERP components would not show any significant difference between the ER-related and -unrelated priming conditions. That is, an ER-related deficit would be present in the early stage of emotional facial processing for those individuals with HTA.

# MATERIALS AND METHODS

## Participants

Thirty-six participants were selected from 570 college students in Beijing, China. The Spielberger Trait Anxiety Inventory (Spielberger et al., 1970) was applied during the pre-screening test. Participants with scores in the top 20% were allocated to the HTA group, and those with scores in the bottom 20% were allocated to the LTA group. Demographic information is presented in **Table 1**. All participants were right-handed, had normal or corrected-to-normal eyesight, and had no history of psychiatric or neurological disorders. All subjects gave written informed consent in accordance with the Declaration of Helsinki and were monetarily rewarded for their involvement. The research was approved by the local ethics committee (Institute of Psychology, Chinese Academy of Sciences).

**TABLE 1 |** Demographic information for high trait anxiety (HTA) and low trait anxiety (LTA) groups.

| Demographic information | HTA ($N$ = 18) | LTA ($N$ = 18) | $t$-value | $p$-value |
|---|---|---|---|---|
| Age ($M \pm$ SD) | 20.33 ± 2.09 | 20.55 ± 2.62 | −0.282 | 0.780 |
| Gender ($n$ male) | 13 | 9 | 1.365 | 0.181 |
| Years of education ($M \pm$ SD) | 14.06 ± 1.76 | 14.11 ± 2.14 | −0.085 | 0.933 |
| STAI-T ($M \pm$ SD) | 50.06 ± 3.61 | 29.11 ± 3.38 | 17.991 | < 0.001 |

## Stimulus Materials

In the current study, we used the same paradigm and stimulus materials as the study of Wang and Li (2017). First, for the word-matching task, two categories of priming words were selected for this study, namely ER-related (e.g., adjust, inhibit) and ER-unrelated (e.g., cancel, run) words. Priming words were evaluated and categorized by an independent group of Chinese students according to their meaning. The "ER-related" category corresponds to the "control" category in the previous study, whereby these words have been shown to effectively decrease negative emotion experience, that is, appropriate to induce implicit ER. "ER-unrelated" category corresponds to the previous "unrelated" category, all words within which has been shown to be not correlated with ER. The additional "expression" category in the prior study was not adopted in the present study because it has not been shown to effectively induce implicit ER. Second, for the facial expression identification task, all eighty face pictures were selected from the Chinese Facial Affective Picture System (CFAPS; Luo et al., 2010), including 40 fear faces and 40 anger faces. Male and female faces were equally presented in each condition. Differences in arousal between these two types of threatening facial expressions based on the CFAPS database was not significant ($t_{(78)} = -0.940$, $p = 0.351$). For more details, see Supplementary Information of the previous PI paradigm-based study (Wang and Li, 2017).

## Experiment Design and Procedure

The formal PI paradigm contained a word-matching task and a facial expression identification task. The word-matching task had two conditions according to the priming word categories (i.e., "ER-related" and "unrelated"). The facial expression identification task had two facial expressions, i.e., anger and fear. Participants were told that the aim of the study was to investigate the vocabulary processing and the emotional processing.

In the word-matching task, participants were asked to choose one word from a pair of words at the bottom of the screen that matched the meaning of the word presented at the top of the screen (i.e., find a synonym) by pressing the appropriate key. Participants were informed at the time of testing that

the aim of this task was to check their vocabulary ability. In the facial expression identification task, a fixation cross was presented at the center of the screen for 200–500 ms prior to a picture of a face. Participants were required to judge whether the expression on the face was one of anger or fear as quickly as possible during its presentation (1,000 ms). The corresponding relation between emotion and appropriate key was balanced across subjects. Once the facial expression had left the screen, a 1,000 ms blank page was presented before the beginning of the next trial. During and after the facial expression identification task, participants were required to rate their level of negative emotion experience using a 9-point scale, every 30 trials.

The order of the two priming conditions was completely randomized across participants with each condition divided into three successive blocks. In each block, participants were required to complete 10 word matching trials, followed by 66 facial identification trials and two ratings of negative emotional experience (see **Figure 1**). In order to minimize the task switching effect, the first six trials of the expression identification task in each block were excluded from data analysis. An intention detection test was performed at the end of each testing session, during which participants were asked to report whether they had noticed a relationship between the word matching task and the facial identification task.

## EEG Recording

The EEG was recorded from 64 scalp sites using tin electrodes placed on an elastic cap (NeuroScan Inc., Herndon, VA, USA) with a left mastoid reference electrode (online) and were re-referenced (offline) to the mean of bilateral mastoid electrodes. All electrode impedance was maintained below 5 KΩ. EEG signals were amplified using a 0.05–100 Hz band-pass and sampled at the rate of 500 Hz. During the offline analysis, the EEG data were filtered with a low-pass at 30 Hz (12 dB/oct). The ERP data were segmented from −200 ms to 1,000 ms relative to the face onset in the expression identification task, with a baseline correction of 200 ms pre-stimulus. Any trials in which the EEG voltages exceeded ±80 μV were excluded from analysis.

## Data Analysis

Negative emotion experience scores were analyzed for two ordinal positions (first and second) during facial identification task prior to both priming conditions (ER-related and ER-unrelated). Reaction times from the facial expression identification task were calculated for correct trials prior to two priming conditions (ER-related and ER-unrelated). Trials were excluded if the reaction time was <200 ms or >1500 ms.

For ERP data, average amplitudes were overlaid for correct trials prior to the two priming conditions. We combined these two types of threatening faces together for the ERP analysis

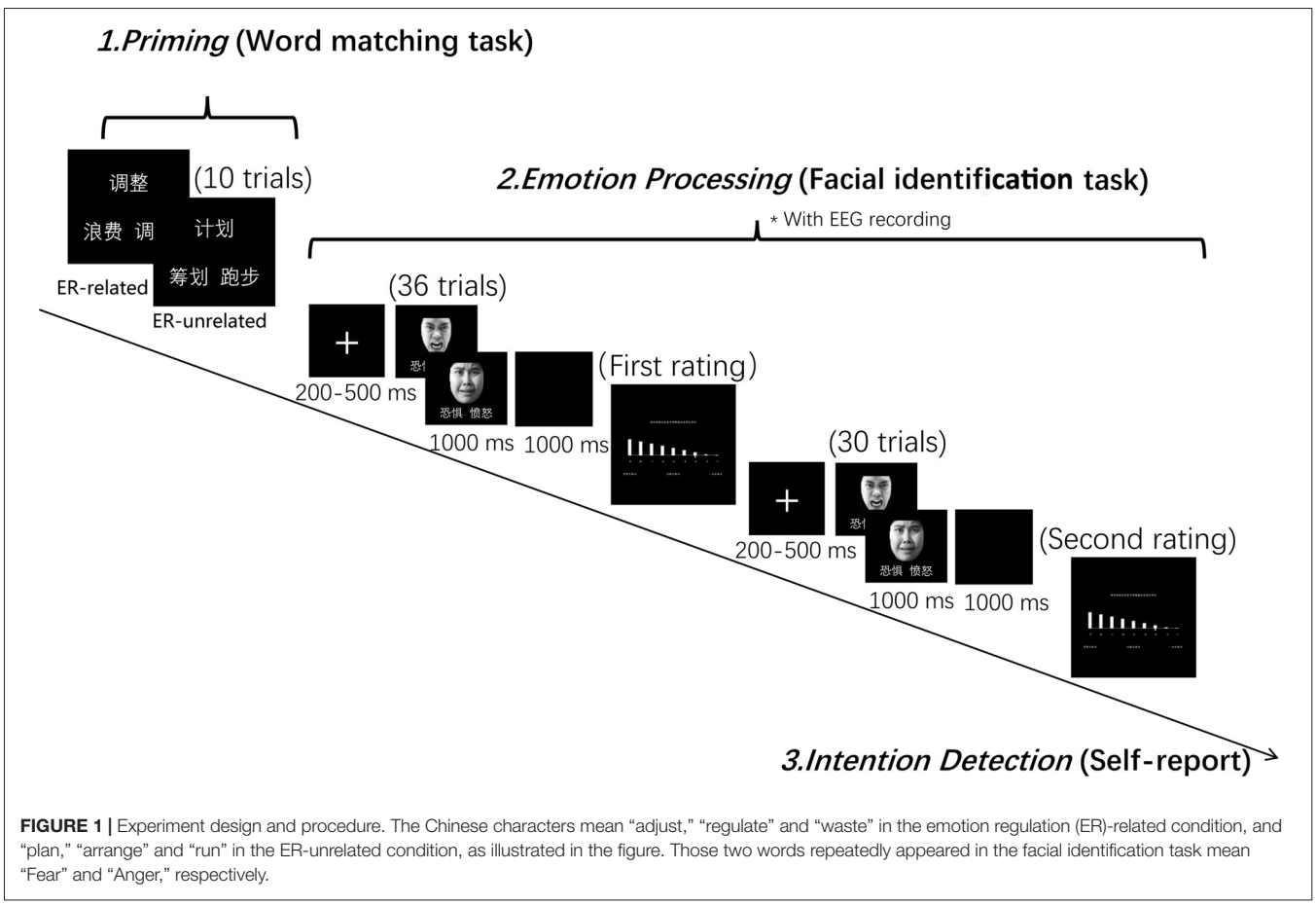


**FIGURE 1 |** Experiment design and procedure. The Chinese characters mean "adjust," "regulate" and "waste" in the emotion regulation (ER)-related condition, and "plan," "arrange" and "run" in the ER-unrelated condition, as illustrated in the figure. Those two words repeatedly appeared in the facial identification task mean "Fear" and "Anger," respectively.

as there were no significant priming effect differences between fear and anger face processing. In line with the previous study (Wang and Li, 2017), eight electrode sites (P7, P5, P6, P8, PO7, PO5, PO6, PO8) were selected for N170 (145–190 ms) and EPN (250–320 ms), and nine (C3, CZ, C4, CP3, CPZ, CP4, P3, PZ, P4) for the analysis of LPP (450–750 ms).

All statistical analyses were performed using SPSS (17.0; SPSS, Inc., Chicago, IL, USA) with a significance level set at 0.05. The Greenhouse-Geisser correction was used to compensate for sphericity violations. Partial eta-squared ($\eta_p^2$) were reported as an indicator of the effect size in ANOVA tests, where 0.06 represents a medium effect and 0.14 a large effect (Cohen, 1988).

# RESULTS

## Behavioral Results

### Negative Emotion Experience

Negative emotion experience rating scores were analyzed by a 2 (priming conditions: ER-related/ER-unrelated) × 2 (ordinal positions: first rating/second rating) × 2 (group: HTA/LTA) repeated measures ANOVA. We observed a significant main effect of priming condition ($F_{(1,34)}$ = 4.112, $p$ = 0.050, $\eta_p^2$ = 0.108). Specifically, the ER-related priming condition ($M$ = 4.115, SD = 0.286) was associated with a lower negative emotion experience score during the subsequent facial identification task than scores associated with the ER-unrelated priming ($M$ = 4.486, SD = 0.331). Results also revealed non-significant main effects for ordinal positions ($F_{(1,34)}$ = 0.243, $p$ = 0.625) and group ($F_{(1,34)}$ = 0.026, $p$ = 0.872). Although we found no significant interaction between priming conditions and group ($F_{(1,34)}$ = 1.315, $p$ = 0.259), descriptive statistics did reveal a larger difference of negative emotion experience scores between ER-related and ER-unrelated priming within the LTA group ($M$ = −0.581, SD = 1.263) than the HTA group ($M$ = −0.161, SD = 0.902; see **Figure 2**).

### Reaction Time

For the reaction time of facial identification task, a 2 (priming conditions: ER-related/ER-unrelated) × 2 (group: HTA/LTA) ANOVA indicated non-significant main effects of priming condition ($F_{(1,34)}$ = 0.129, $p$ = 0.721) and group effect ($F_{(1,34)}$ = 0.264, $p$ = 0.611). The interaction between priming and group was not significant ($F_{(1,34)}$ = 0.406, $p$ = 0.529; see **Figure 2**).

### Intention Detection

No participants realized that the word matching task was aimed at regulating negative emotion in the subsequent task, based on the oral self-report of all 36 participants.

## ERP Results

### N170 Amplitude

A 2 (priming conditions) × 2 (horizontal electrodes: P/PO) × 4 (vertical electrodes: 5/6/7/8) × 2 (group) repeated measures ANOVA was conducted for N170 amplitudes. We found a marginally significant main effect of priming condition ($F_{(1,34)}$ = 3.175, $p$ = 0.084, $\eta_p^2$ = 0.085), whereby ER-related priming elicited larger N170 ($M$ = 0.246, SD = 0.426) than the ER-unrelated priming ($M$ = 0.585, SD = 0.458). A significant main effect of vertical electrodes ($F_{(3,102)}$ = 20.207, $p$ < 0.001, $\eta_p^2$ = 0.373) was found, and the N170 at the right-side electrodes were significantly larger than left-side ones. We also observed a marginally significant interaction between priming condition and group ($F_{(1,34)}$ = 3.981, $p$ = 0.054, $\eta_p^2$ = 0.105). The main effects of horizontal electrodes ($F_{(1,34)}$ = 0.643, $p$ = 0.428) and group ($F_{(1,34)}$ = 2.163, $p$ = 0.151), however, were not significant.

Since the interaction between priming conditions and group was marginally significant, a further 2 (priming conditions) × 2 (horizontal electrodes: P/PO) × 4 (vertical electrodes: 5/6/7/8) repeated measures ANOVA was conducted separately within the HTA and the LTA group. In the HTA group, the main effect of priming was not significant ($F_{(1,17)}$ = 0.118, $p$ = 0.851), while in the LTA group, the analysis revealed a significant main effect of priming condition ($F_{(1,17)}$ = 5.177, $p$ = 0.036, $\eta_p^2$ = 0.233; see **Figure 3**).

### EPN Amplitude

For EPN amplitude, a 2 (priming conditions) × 2 (horizontal electrodes: P/PO) × 4 (vertical electrodes: 5/6/7/8) × 2 (group) repeated measures ANOVA revealed a significant main effect of priming ($F_{(1,34)}$ = 5.296, $p$ = 0.028, $\eta_p^2$ = 0.135). That is,

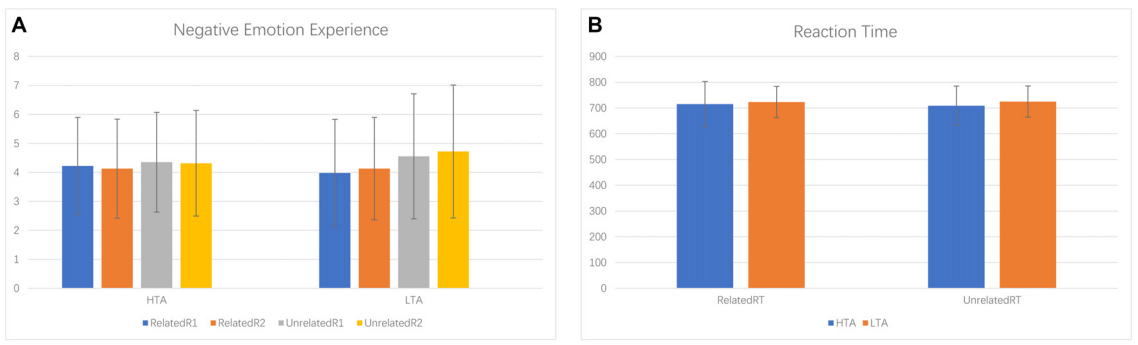


**FIGURE 2 |** Bar plots for negative emotion experience **(A)** and reaction time **(B)**.

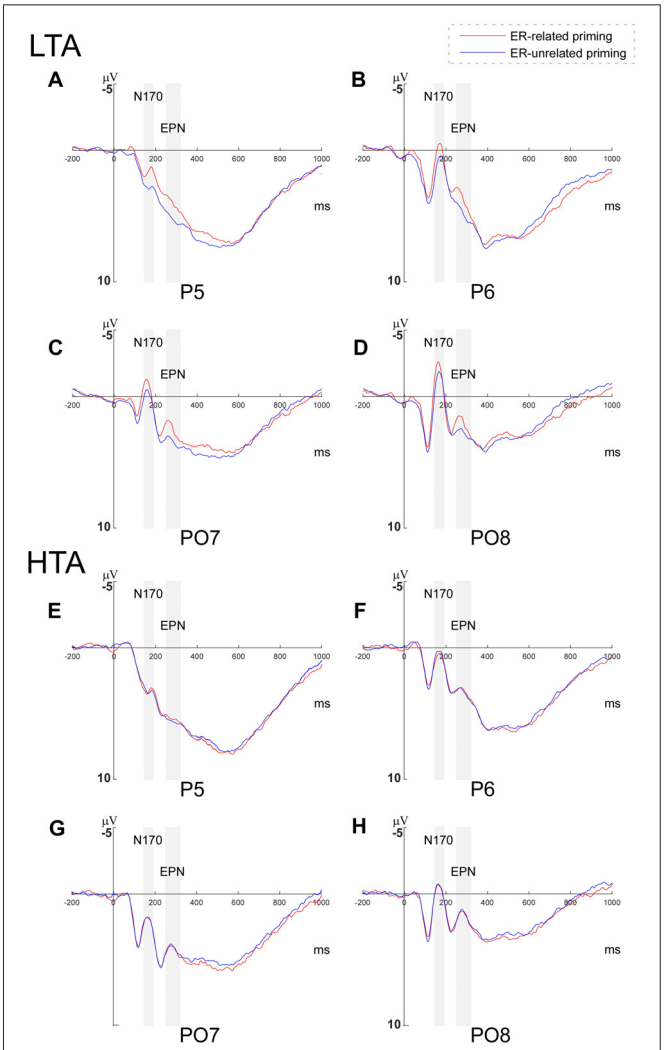


**FIGURE 3 |** Grand averages of N170 and early posterior negativity (EPN) amplitudes. Grand averages of N170 and EPN amplitudes evoked during the Priming-Identify (PI) task at P5, P6, PO7 and PO8 within **(A–D)** the low trait anxiety (LTA) and **(E–H)** the high trait anxiety (HTA) groups.

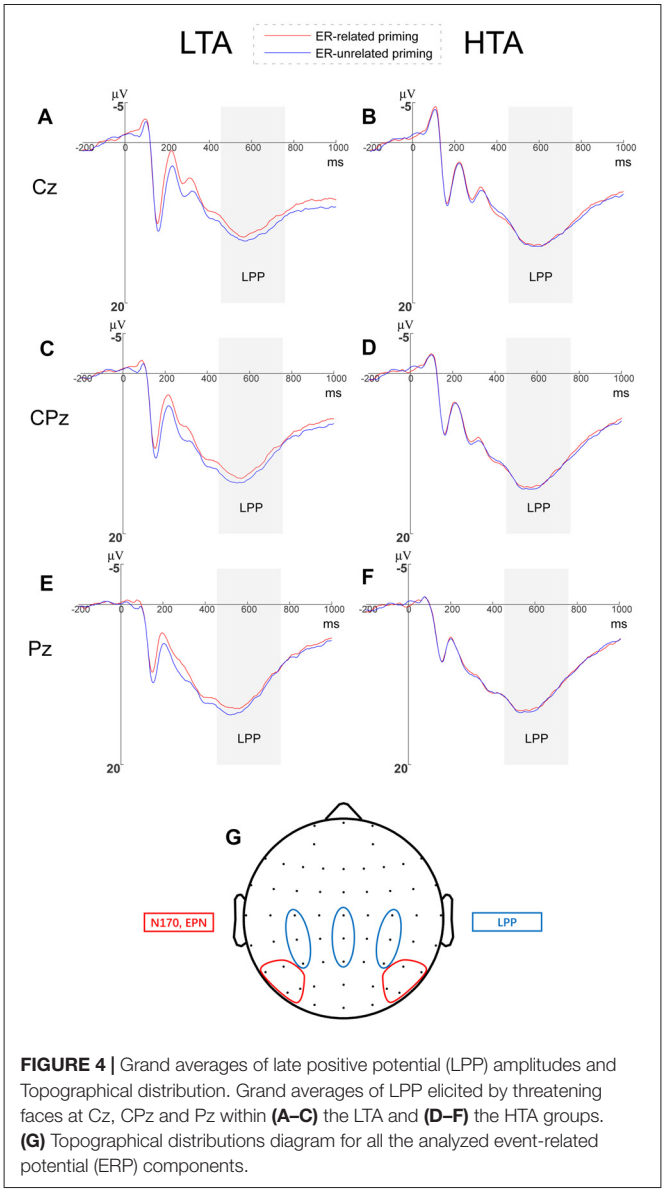


**FIGURE 4 |** Grand averages of late positive potential (LPP) amplitudes and Topographical distribution. Grand averages of LPP elicited by threatening faces at Cz, CPz and Pz within **(A–C)** the LTA and **(D–F)** the HTA groups. **(G)** Topographical distributions diagram for all the analyzed event-related potential (ERP) components.

ER-related priming ($M$ = 3.035, SD = 0.429) elicited larger EPN than ER-unrelated priming ($M$ = 3.510, SD = 0.470). A significant main effect of vertical electrodes ($F_{(3,102)}$ = 13.732, $p < 0.001$, $\eta_p^2$ = 0.288) was found, and the EPN at the right-side electrodes was larger than the left-side ones. The interaction between priming and group was marginally significant ($F_{(1, 34)}$ = 3.862, $p$ = 0.058, $\eta_p^2$ = 0.102). The main effects of horizontal electrodes ($F_{(1,34)}$ = 0.202, $p$ = 0.656) and group ($F_{(1,34)}$ = 0.007, $p$ = 0.935), however, were not significant.

To examine the interaction between priming and group, a further 2 (priming conditions) × 2 (horizontal electrodes: P/PO) × 4 (vertical electrodes: 5/6/7/8) repeated measures ANOVA was conducted within the HTA and the LTA group respectively. While the main effect of priming was not significant in the HTA group ($F_{(1,17)}$ = 0.091, $p$ = 0.767), it was significant in the LTA group ($F_{(1,17)}$ = 6.617, $p$ = 0.020, $\eta_p^2$ = 0.280; see **Figure 3**).

## LPP Amplitude

We analyzed LPP amplitudes by a 2 (priming conditions) × 3 (horizontal electrodes: C/CP/P) × 3 (vertical electrodes: 3/Z/4) × 2 (group) repeated measures ANOVA and found no significant main effects of horizontal electrodes ($F_{(2,68)}$ = 11.553, $p < 0.001$, $\eta_p^2$ = 0.254) and vertical electrodes ($F_{(2,68)}$ = 29.853, $p < 0.001$, $\eta_p^2$ = 0.468). We did observe that the LPP amplitude induced at central-parietal sites was larger than central and parietal sites (see **Figure 4**, a small topographical distribution diagram was presented in the **Figure 4** as well). The main effects of priming ($F_{(1,34)}$ = 0.013, $p$ = 0.910) and group ($F_{(1,34)}$ = 0.848, $p$ = 0.364) were not significant.

## Correlations

We found significantly different N170 and EPN amplitudes between the two priming conditions within the LTA group,

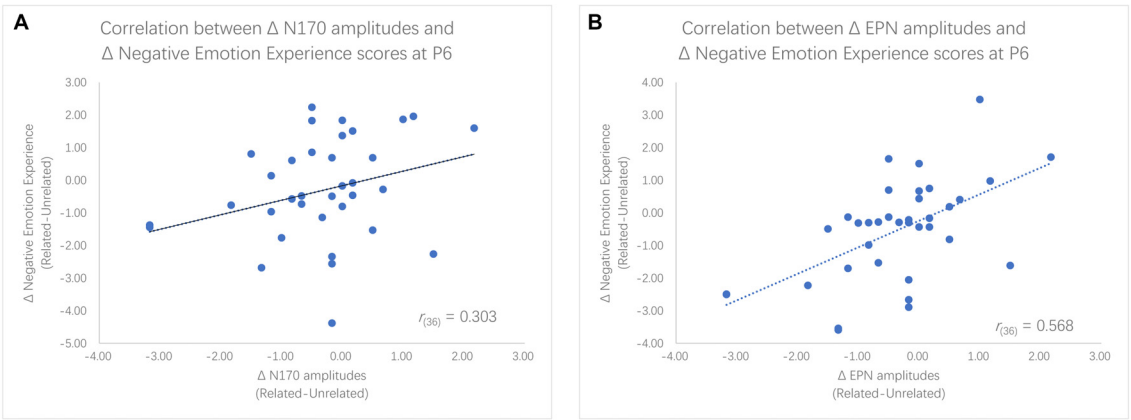


**FIGURE 5 |** Scatter plots for the correlation between enlargement of N170 amplitudes and decreases in Negative emotion experience rating scores **(A)** as well as the correlation between enlargement of EPN amplitudes and decreases in rating scores **(B)**.

but these differences were not significant within the HTA group. To further examine the relationship between ERP and behavior results, Pearson ($r$) correlation coefficients were computed between the negative emotion experience ratings and the N170 or EPN amplitudes. Given that the main effect of ordinal positions was not significant, we used the average of two ratings as the index of negative emotion experience. Results showed that decreases in negative emotion experience scores were significantly correlated with the enlargement of N170 amplitudes at P5 ($r_{(36)}$ = 0.346, $p$ = 0.039) and marginally significantly correlated with the enlargement of N170 amplitudes at P6 ($r_{(36)}$ = 0.303, $p$ = 0.072). Furthermore, decreases in negative emotion experience scores were significantly associated with greater EPN amplitudes at P6 ($r_{(36)}$ = 0.568, $p < 0.001$), P8 ($r_{(36)}$ = 0.436, $p$ = 0.008) and PO8 ($r_{(36)}$ = 0.615, $p < 0.001$; see **Figure 5**).

## DISCUSSION

The current study investigated the potential deficits in implicit ER in HTA and LTA individuals. First, at the behavioral level we showed that implicit ER processing, in the form of a decrease in negative emotion experience scores, was induced by an ER-related priming condition during a subsequent task. This effect was especially prominent in the LTA group. Second, findings from the intention detection test confirmed that participants were not explicitly aware of the fact that ER priming was being used to modulate subsequent emotional experience. In other words, all ER processing involved in this study did indeed take place at the implicit level. Third, we found a non-significant main effect of the ordinal position of negative emotion experience scores, demonstrating that the priming effect was not decreased with time. As, observed modulations in ERP components could be considered as effective indexes of ER. Fourth, decreases in negative emotion experience scores were associated with enlargements of N170 and EPN amplitudes, thus indicating that these components could effectively index implicit ER. Finally, early N170 amplitudes, as well as the middle EPN, were enlarged by ER-related priming words in the LTA group but not in the HTA group. That is, a lack of enlargement of N170 and EPN amplitudes was observed in anxious individuals during the implicit ER processing, while the late stage processing (LPP) was not modulated by implicit ER goals in either group. Our results suggest that anxious individuals show deficits in implicit ER occurring over the early and middle stages of emotion processing.

The present study focused on implicit ER processing in anxiety. Three ERP components were chosen for indexing the time course of implicit ER: N170, EPN and LPP. We observed an enlarged N170 amplitudes within the LTA group but not the HTA group, as well as a significant correlation of its enlargement with decreases in negative emotion experience scores. This finding in the LTA group supports our first hypothesis and confirms the notion that an enlarged N170 could be considered as an index of implicit ER during the early stage of face processing. The absence of an enlarged N170 within the HTA group suggests a deficit of implicit ER in anxiety, as put forward in our second hypothesis. N170 is a well-known face-specific component (Bentin et al., 1996; Carmel and Bentin, 2002), however, there is some inconsistencies regarding its role in emotional processing. Some studies report no significant N170 differences between emotional expressions and neutral ones, suggesting that it reflects the encoding of facial configuration but not signals relating to emotion (Eimer et al., 2003; Ashley et al., 2004). Contrary to this view, some other studies have reported that N170 is sensitive to facial expression, whereby threatening or joyful faces elicited larger N170 amplitude than neutral ones (Batty and Taylor, 2003; Blau et al., 2007; Luo et al., 2010). Our finding regarding its role in implicit ER may provide some insight into the source of this discrepancy. For instance, varying levels of engagement in implicit ER may explain much of the heterogeneity found across these studies. Regarding the role N170 plays in the emotional face processing, it was described in a well-known face processing

model that the facial structure encoding unit includes a view-center descriptions module and an expression-independent descriptions module, which might be isolated from each other (Bruce and Young, 1986). The view-center descriptions module provides information for the analysis of expression, and the expression-independent descriptions module provide information for the global configuration and of features. In the current study, facial expressions were homogeneous between both compared experimental conditions, and then the enhanced N170 could not reflect more elaborate emotion recognition processing. Consistent with both implicit ER (Mauss et al., 2007a) and face processing (Bruce and Young, 1986) models, we suggest that ER priming-induced enlargement of N170 observed in the present study represents attentional deployment. More specifically, ER goals facilitated facial structural encoding and deepened emotion-unrelated encoding (i.e., an implicit form of distraction). The absence of any enlargement of N170 amplitude within the HTA group might indicate a reduction in the ability to implicitly deploy attention (i.e., less efficient distraction) for individuals with anxiety.

In the present study, we were surprised to find a significant priming effect for the EPN amplitude within the LTA group, as well as a non-significant priming effect within the HTA group. Our hypothesis was formed on the basis of previous findings from a study using the PI paradigm (Wang and Li, 2017) and we expected the EPN to be unaffected during implicit ER processing within the LTA group. However, we also found that reductions in negative emotion experience scores were highly correlated with the enlargement of EPN amplitudes, which was not addressed in previous ER studies. The main difference of experimental task between in the current study and in the prior study is the amount of priming conditions. In the previous study (Wang and Li, 2017), healthy participants were primed with three conditions: control, Expression and Unrelated. Although the Expression priming condition was aimed at up-regulating the emotional response of participants, it failed to fulfill this intention and, consequently, only two priming conditions were included in the present study. We might speculate that the previously undiscovered priming effect of EPN might be due to the interference of the additional Expression priming condition on the statistical power.

Previous studies have observed a greater EPN induced by emotional stimuli than neutral stimuli during non-conscious processing (Schupp et al., 2004b; Pegna et al., 2008; Luo et al., 2010), regardless of whether the stimuli were scenes or faces (Junghöfer et al., 2001; Schupp et al., 2004a). Rellecke et al. (2012) found that angry expressions elicited a larger EPN than happy expressions, which was interpreted to show that the EPN amplitude reflects an automatic threat-privileged processing associated with affective stimuli evaluation. Conversely, other researchers have observed a more pronounced EPN for happy faces compared to angry ones (Bublatzky et al., 2014; Leleu et al., 2015). The existing results indicated that EPN could generally be regarded as a higher-level index of affective processing. However, only threatening expressions were included in the current study. These faces were homogeneous between both experimental conditions, so that the priming-induced enlargement of EPN amplitudes was more likely to reflect the cognitive representation instead of affective processing. Regarding its role in cognitive processing, previous study suggested that EPN reflects early selective attention in visual processing (Schupp et al., 2007), whereby the EPN amplitudes were observed by comparing emotional vs. neutral stimuli. In the present study, as shown by the statistically significant correlation, the EPN amplitudes were modulated by ER related priming words, suggesting another role EPN reflects in cognitive processing. Schupp et al. (2008) suggested that "EPN reflects a transitory processing period at which motivationally significant stimuli are 'tagged' for preferential processing in higher-order visual-associative brain areas." Based on previous literature regarding neural projections, Leleu et al. (2015) put forward an explanation for this transitory "tag" period at the neural level. They proposed that EPN may index an initial integration of the specific emotional meaning that the visual processing shares emotional content through connections between multiple locations (i.e., the visual system, the amygdala, the orbitofrontal cortex, the insula and the somatosensory cortices). This process of tagging emotional stimuli should be regarded as the implicit appraisal process in Gross's model of automatic emotional regulation (Mauss et al., 2007a; Mocaiber et al., 2010). Combined with our result, we can speculate that threatening stimuli could be "tagged" differently during implicit ER processing. Put another way, the observed enlargement of EPN amplitude may represent a change in appraisal at the implicit level. LTA individuals may have been able to efficiently "tag" the threatening expression as safe or non-dangerous when primed with ER-related words, thus leading to a decreased negative emotion experience. The lack of any EPN amplitude enlargement between the two priming conditions within the HTA group may indicate a deficit of implicit ER (a less effective change of implicit appraisal) in anxiety occurring during the middle stage of emotional processing.

In consistent with our hypothesis, the analysis of LPP amplitude revealed a non-significant main effect of priming with no anxiety-related impact. In addition, we found no correlation between LPP amplitudes and behavioral results. Our results seem contradictory to one from Mocaiber et al. (2010), which showed a reduced LPP within both HTA and LTA groups when individuals were given an "implicit reappraisal instruction" (i.e., "pictures do not correspond to real situations"). However, LPP has been considered by some researchers to represent the allocation of sustained resources of attention to emotional stimuli (Schupp et al., 2003, 2006; Yang et al., 2015; Yuan et al., 2015b), and hence, a frequently-used index in studies of explicit ER (Dennis, 2010). These results might involve conscious effort during ER processing, such that the fictitious condition could be considered an explicit "reappraisal" condition. Our result is consistent with the previous PI paradigm study in healthy adults (Wang and Li, 2017), which showed that LPP amplitudes were not influenced by any of the priming condition (e.g., control, expression). This suggests that implicit ER did not demand

cognitive resources at the late stage of emotion processing, and that no anxiety-related deficit of implicit ER was found at this stage.

The present study provides neural evidence for a deficit of implicit ER in anxiety, however, our results should be interpreted in the light of several limitations. First, in the present study, we used subjective rating scores of negative emotion experience to reflect the emotional response of participants after regulation came into effect. However, given the fact that implicit ER is by definition a process during which participants were without conscious, intention, awareness, or deliberate control (Mauss et al., 2007a), explicit behavioral level indicators might not be effective, stable, or sensitive enough as outcome measurements. Some studies have proposed that some physiological measurements, such as heart rate, mean arterial blood pressure, cardiac output, or total peripheral resistance, would represent more objective indexes of emotion responses (Jackson et al., 2003; Mauss et al., 2007b). In the future, more physiological indexes should be adopted to detect the effect of ER. Second, the present study does suffer from a small sample size, it has led to some marginally significant findings (e.g., interaction between priming and group on the ERP findings). Another possible reason for the findings could be that our participants were recruited from local colleges with a high or low level of trait anxiety. It would be more insightful to conduct our research on patients. Third, in the present study, enlarged N170 and EPN were found to be associated with implicit ER processing. However, future work could provide further insight through the addition of a non-priming condition, while still implicit, because one may compare results perceived from this condition with existing studies (Rossignol et al., 2005; Frenkel and Bar-Haim, 2011; Walentowska and Wronka, 2012; Otoole et al., 2013; Morel et al., 2014; Chronaki et al., 2018). A non-priming condition could be adopted to attain a "baseline level" state of emotional face processing. Such a state would be comparable with related studies and would, in turn, provide more insight into implicit ER in anxiety.

## CONCLUSION

To sum up, in the present study we observed an implicit ER deficit among anxious individuals occurring in the early and middle stages of emotion processing (emotion perception, emotion recognition). This deficit was expressed as an absence of enlargements in N170 and EPN amplitudes. Furthermore, we suggest that both N170 and EPN are effective indexes of implicit ER: N170 reflects implicit attention deployment and EPN reflects change of implicit appraisal.

## AUTHOR CONTRIBUTIONS

BL analyzed, interpreted the data and wrote the first draft of the manuscript. YW designed the study, collected and pretreated the data. XL generated the idea, designed the study, interpreted the data and wrote the first draft of the manuscript.

## FUNDING

This study was supported by National Nature Science Foundation of China supported this research (NSFC 31671136, 31530031) and CAS Key Laboratory of Mental Health, Institute of Psychology.

## REFERENCES

American Psychiatric Association. (2013). *Diagnostic and Statistical Manual of Mental Disorders.* 5th Edn. Washington, DC: American Psychiatric Association.

Amstadter, A. (2008). Emotion regulation and anxiety disorders. *J. Anxiety Disord.* 22, 211–221. doi: 10.1016/j.janxdis.2007.02.004

Ashley, V., Vuilleumier, P., and Swick, D. (2004). Time course and specificity of event-related potentials to emotional expressions. *Neuroreport* 15, 211–216. doi: 10.1097/00001756-200401190-00041

Ball, T. M., Ramsawh, H. J., Campbell-Sills, L., Paulus, M. P., and Stein, M. B. (2013). Prefrontal dysfunction during emotion regulation in generalized anxiety and panic disorders. *Psychol. Med.* 43, 1475–1486. doi: 10.1017/s0033291712002383

Barlow, D. H. (1991). Disorders of emotion. *Psychol. Inq.* 2, 58–71. doi: 10.1207/s15327965pli0201_15

Batty, M., and Taylor, M. J. (2003). Early processing of the six basic facial emotional expressions. *Cogn. Brain Res.* 17, 613–620. doi: 10.1016/s0926-6410(03)00174-5

Baxter, A., Scott, K. M., Vos, T., and Whiteford, H. (2013). Global prevalence of anxiety disorders: a systematic review and meta-regression. *Psychol. Med.* 43, 897–910. doi: 10.1017/s003329171200147x

Beck, A. T., and Emery, G. (2010). *Anxiety Disorders and Phobias: A Cognitive Perspective (20th Anniversary Edition).* Chongqing: Chongqing University Press.

Bentin, S., Allison, T., Puce, A., Perez, E., and McCarthy, G. (1996). Electrophysiological studies of face perception in humans. *J. Cogn. Neurosci.* 8, 551–565. doi: 10.1162/jocn.1996.8.6.551

Berking, M., Orth, U., Wupperman, P., Meier, L. L., and Caspar, F. (2008). Prospective effects of emotion-regulation skills on emotional adjustment. *J. Couns. Psychol.* 55, 485–494. doi: 10.1037/a0013589

Blau, V. C., Maurer, U., Tottenham, N., and McCandliss, B. D. (2007). The face-specific N170 component is modulated by emotional facial expression. *Behav. Brain Funct.* 3:7. doi: 10.1186/1744-9081-3-7

Bruce, V., and Young, A. (1986). Understanding face recognition. *Br. J. Psychol.* 77, 305–327. doi: 10.1111/j.2044-8295.1986.tb02199.x

Bublatzky, F., Gerdes, A. B., White, A. J., Riemer, M., and Alpers, G. W. (2014). Social and emotional relevance in face processing: happy faces of future interaction partners enhance the late positive potential. *Front. Hum. Neurosci.* 8:493. doi: 10.3389/fnhum.2014.00493

Carmel, D., and Bentin, S. (2002). Domain specificity versus expertise: factors influencing distinct processing of faces. *Cognition* 83, 1–29. doi: 10.1016/s0010-0277(01)00162-7

Chronaki, G., Broyd, S. J., Garner, M., Benikos, N., Thompson, M. J. J., Sonuga-Barke, E. J. S., et al. (2018). The moderating effect of self-reported state and trait anxiety on the late positive potential to emotional faces in 6–11-year-old children. *Front. Psychol.* 9:125. doi: 10.3389/fpsyg.2018.00125

Cisler, J. M., Olatunji, B. O., Feldner, M. T., and Forsyth, J. P. (2010). Emotion regulation and the anxiety disorders: an integrative review. *J. Psychopathol. Behav. Assess.* 32, 68–82. doi: 10.1007/s10862-009-9161-1

Cohen, J. (1988). *Statistical Power Analysis for the Behavioral Sciences.* 2nd Edn. Hillsdale, NJ: Lawrence Earlbaum Associates.

Dennis, T. A. (2010). Introduction to the special issue on neurophysiological markers for emotion and emotion regulation. *Dev. Neuropsychol.* 35, 125–128. doi: 10.1080/87565640903526496

Eimer, M., and Holmes, A. (2002). An ERP study on the time course of emotional face processing. *Neuroreport* 13, 427–431. doi: 10.1097/00001756-200203250-00013

Eimer, M., Holmes, A., and McGlone, F. P. (2003). The role of spatial attention in the processing of facial expression: an ERP study of rapid brain responses to six basic emotions. *Cogn. Affect. Behav. Neurosci.* 3, 97–110. doi: 10.3758/cabn.3.2.97

Etkin, A., Prater, K. E., Hoeft, F., Menon, V., and Schatzberg, A. F. (2010). Failure of anterior cingulate activation and connectivity with the amygdala during implicit regulation of emotional processing in generalized anxiety disorder. *Am. J. Psychiatry* 167, 545–554. doi: 10.1176/appi.ajp.2009.09070931

Frenkel, T. I., and Bar-Haim, Y. (2011). Neural activation during the processing of ambiguous fearful facial expressions: an ERP study in anxious and nonanxious individuals. *Biol. Psychol.* 88, 188–195. doi: 10.1016/j.biopsycho.2011.08.001

Fruhholz, S., Jellinghaus, A., and Herrmann, M. (2011). Time course of implicit processing and explicit processing of emotional faces and emotional words. *Biol. Psychol.* 87, 265–274. doi: 10.1016/j.biopsycho.2011.03.008

Gallo, I. S., Keil, A., McCulloch, K. C., Rockstroh, B., and Gollwitzer, P. M. (2009). Strategic automation of emotion regulation. *J. Pers. Soc. Psychol.* 96, 11–31. doi: 10.1037/a0013460

Gross, J. J. (1998). The emerging field of emotion regulation: an integrative review. *Rev. Gen. Psychol.* 2, 271–299. doi: 10.1037/1089-2680.2.3.271

Gyurak, A., Gross, J. J., and Etkin, A. (2011). Explicit and implicit emotion regulation: a dual-process framework. *Cogn. Emot.* 25, 400–412. doi: 10.1080/02699931.2010.544160

Hinojosa, J. A., Mercado, F., and Carretié, L. (2015). N170 sensitivity to facial expression: a meta-analysis. *Neurosci. Biobehav. Rev.* 55, 498–509. doi: 10.1016/j.neubiorev.2015.06.002

Hofmann, S. G., Sawyer, A. T., Fang, A., and Asnaani, A. (2012). Emotion dysregulation model of mood and anxiety disorders. *Depress. Anxiety* 29, 409–416. doi: 10.1002/da.21888

Hum, K. M., Manassis, K., and Lewis, M. D. (2013). Neural mechanisms of emotion regulation in childhood anxiety. *J. Child Psychol. Psychiatry* 54, 552–564. doi: 10.1111/j.1469-7610.2012.02609.x

Jackson, D. C., Mueller, C. J., Dolski, I., Dalton, K. M., Nitschke, J. B., Urry, H. L., et al. (2003). Now you feel it, now you don't: frontal brain electrical asymmetry and individual differences in emotion regulation. *Psychol. Sci.* 14, 612–617. doi: 10.1046/j.0956-7976.2003. psci_1473.x

Jasper, F., and Witthöft, M. (2013). Automatic evaluative processes in health anxiety and their relations to emotion regulation. *Cogn. Ther. Res.* 37, 521–533. doi: 10.1007/s10608-012-9484-1

Junghöfer, M., Bradley, M. M., Elbert, T., and Lang, P. J. (2001). Fleeting images: a new look at early emotion discrimination. *Psychophysiology* 38, 175–178. doi: 10.1111/1469-8986.3820175

Kashdan, T. B., Zvolensky, M. J., and McLeish, A. C. (2008). Anxiety sensitivity and affect regulatory strategies: individual and interactive risk factors for anxiety-related symptoms. *J. Anxiety Disord.* 22, 429–440. doi: 10.1016/j.janxdis.2007.03.011

Kring, A. M. (2010). The future of emotion research in the study of psychopathology. *Emot. Rev.* 2, 225–228. doi: 10.1177/1754073910361986

Lamm, C., Granic, I., Zelazo, P. D., and Lewis, M. D. (2011). Magnitude and chronometry of neural mechanisms of emotion regulation in subtypes of aggressive children. *Brain Cogn.* 77, 159–169. doi: 10.1016/j.bandc.2011.06.008

Leleu, A., Godard, O., Dollion, N., Durand, K., Schaal, B., and Baudouin, J. Y. (2015). Contextual odors modulate the visual processing of emotional facial expressions: an ERP study. *Neuropsychologia* 77, 366–379. doi: 10.1016/j.neuropsychologia.2015.09.014

Luo, W., Feng, W., He, W., Wang, N. Y., and Luo, Y. J. (2010). Three stages of facial expression processing: ERP study with rapid serial visual presentation. *Neuroimage* 49, 1857–1867. doi: 10.1016/j.neuroimage.2009.09.018

Ma, W., and Zhu, B. (2012). The effect on automatic emotion regulation of anxiety individuals in negative emotion. *Chin. J. Clin. Psychol.* 20, 510–513. doi: 10.16128/j.cnki.1005-3611.2012.04.006

Mauss, I. B., Bunge, S. A., and Gross, J. J. (2007a). Automatic emotion regulation. *Soc. Pers. Psychol. Comp.* 1, 146–167. doi: 10.1111/j.1751-9004.2007.00005.x

Mauss, I. B., Cook, C. L., and Gross, J. J. (2007b). Automatic emotion regulation during anger provocation. *J. Exp. Soc. Psychol.* 43, 698–711. doi: 10.1016/j.jesp.2006.07.003

McLaughlin, K. A., Hatzenbuehler, M. L., Mennin, D. S., and Nolen-Hoeksema, S. (2011). Emotion dysregulation and adolescent psychopathology: a prospective study. *Behav. Res. Ther.* 49, 544–554. doi: 10.1016/j.brat.2011.06.003

Mennin, D. S. (2004). Emotion regulation therapy for generalized anxiety disorder. *Clin. Psychol. Psychother.* 11, 17–29. doi: 10.1002/cpp.389

Mocaiber, I., Pereira, M. G., Erthal, F. S., Machado-Pinheiro, W., David, I. A., Cagy, M., et al. (2010). Fact or fiction? An event-related potential study of implicit emotion regulation. *Neurosci. Lett.* 476, 84–88. doi: 10.1016/j.neulet.2010.04.008

Morel, S., George, N., Foucher, A., Chammat, M., and Dubal, S. (2014). ERP evidence for an early emotional bias towards happy faces in trait anxiety. *Biol. Psychol.* 99, 183–192. doi: 10.1016/j.biopsycho.2014.03.011

O'Toole, M. S., Jensen, M. B., Fentz, H. N., Zachariae, R., and Hougaard, E. (2014). Emotion differentiation and emotion regulation in high and low socially anxious individuals: an experience-sampling study. *Cogn. Ther. Res.* 38, 428–438. doi: 10.1007/s10608-014-9611-2

Otoole, L. J., Decicco, J. M., Berthod, S., and Dennis, T. A. (2013). The N170 to angry faces predicts anxiety in typically developing children over a two-year period. *Dev. Neuropsychol.* 38, 352–363. doi: 10.1080/87565641.2013.802321

Pegna, A. J., Landis, T., and Khateb, A. (2008). Electrophysiological evidence for early non-conscious processing of fearful facial expressions. *Int. J. Psychophysiol.* 70, 127–136. doi: 10.1016/j.ijpsycho.2008.08.007

Rellecke, J., Sommer, W., and Schacht, A. (2012). Does processing of emotional facial expressions depend on intention? Time-resolved evidence from event-related brain potentials. *Biol. Psychol.* 90, 23–32. doi: 10.1016/j.biopsycho.2012.02.002

Rossignol, M., Philippot, P., Douilliez, C., Crommelinck, M., and Campanella, S. (2005). The perception of fearful and happy facial expression is modulated by anxiety: an event-related potential study. *Neurosci. Lett.* 377, 115–120. doi: 10.1016/j.neulet.2004.11.091

Rottenberg, J., and Gross, J. J. (2006). When emotion goes wrong: realizing the promise of affective science. *Clin. Psychol. Sci. Pract.* 10, 227–232. doi: 10.1093/clipsy/bpg012

Schäfer, J. Ö., Naumann, E., Holmes, E. A., Tuschen-Caffier, B., and Samson, A. C. (2017). Emotion regulation strategies in depressive and anxiety symptoms in youth: a meta-analytic review. *J. Youth Adolesc.* 46, 261–276. doi: 10.1007/s10964-016-0585-0

Schupp, H. T., Flaisch, T., Stockburger, J., and Junghöfer, M. (2006). Emotion and attention: event-related brain potential studies. *Prog. Brain Res.* 156, 31–51. doi: 10.1016/s0079-6123(06)56002-9

Schupp, H. T., Junghofer, M., Weike, A. I., and Hamm, A. O. (2003). Attention and emotion: an ERP analysis of facilitated emotional stimulus processing. *Neuroreport* 14, 1107–1110. doi: 10.1097/00001756-200306110-00002

Schupp, H. T., Junghöfer, M., Weike, A. I., and Hamm, A. O. (2004a). The selective processing of briefly presented affective pictures: an ERP analysis. *Psychophysiology* 41, 441–449. doi: 10.1111/j.1469-8986.2004.00174.x

Schupp, H. T., Ohman, A., Junghöfer, M., Weike, A. I., Stockburger, J., and Hamm, A. O. (2004b). The facilitated processing of threatening faces: an ERP analysis. *Emotion* 4, 189–200. doi: 10.1037/1528-3542.4.2.189

Schupp, H. T., Stockburger, J., Bublatzky, F., Junghöfer, M., Weike, A. I., and Hamm, A. O. (2007). Explicit attention interferes with selective emotion processing in human extrastriate cortex. *BMC Neurosci.* 8:16. doi: 10.1186/1471-2202-8-16

Schupp, H. T., Stockburger, J., Schmälzle, R., Bublatzky, F., Weike, A. I., and Hamm, A. O. (2008). Visual noise effects on emotion perception: brain potentials and stimulus identification. *Neuroreport* 19, 167–171. doi: 10.1097/wnr.0b013e3282f4aa42

Spielberger, C. D., Gorsuch, R. L., and Lushene, R. E. (1970). *Manual for The State-Trait Anxiety Inventory.* Palo Alto, CA: Consulting Psychologists Press.

Suveg, C., Morelen, D., Brewer, G. A., and Thomassin, K. (2010). The emotion dysregulation model of anxiety: a preliminary path analytic examination. *J. Anxiety Disord.* 24, 924–930. doi: 10.1016/j.janxdis.2010.06.018

Walentowska, W., and Wronka, E. (2012). Trait anxiety and involuntary processing of facial emotions. *Int. J. Psychophysiol.* 85, 27–36. doi: 10.1016/j.ijpsycho.2011.12.004

Wang, Y., and Li, X. (2017). Temporal course of implicit emotion regulation during a Priming-Identify task: an ERP study. *Sci. Rep.* 7:41941. doi: 10.1038/srep41941

Wieser, M. J., and Moscovitch, D. A. (2015). The effect of affective context on visuocortical processing of neutral faces in social anxiety. *Front. Psychol.* 6:1824. doi: 10.3389/fpsyg.2015.01824

Williams, L. E., Bargh, J. A., Nocera, C. C., and Gray, J. R. (2009). The unconscious regulation of emotion: nonconscious reappraisal goals modulate emotional reactivity. *Emotion* 9, 847–854. doi: 10.1037/a0017745

Yang, Q., Tang, P., Gu, R., Luo, W., and Luo, Y. J. (2015). Implicit emotion regulation affects outcome evaluation. *Soc. Cogn. Affect. Neurosci.* 10, 824–831. doi: 10.1093/scan/nsu124

Yoon, S., Shim, M., Kim, H. S., and Lee, S. H. (2016). Enhanced early posterior negativity to fearful faces in patients with anxiety disorder. *Brain Topogr.* 29, 262–272. doi: 10.1007/s10548-015-0456-0

Yuan, J., Ding, N., Liu, Y., and Yang, J. (2015a). Unconscious emotion regulation: nonconscious reappraisal decreases emotion-related physiological reactivity during frustration. *Cogn. Emot.* 29, 1042–1053. doi: 10.1080/02699931.2014.965663

Yuan, J., Ju, E., Meng, X., Chen, X., Zhu, S., Yang, J., et al. (2015b). Enhanced brain susceptibility to negative stimuli in adolescents: ERP evidences. *Front. Behav. Neurosci.* 9:98. doi: 10.3389/fnbeh.2015.00098

**Conflict of Interest Statement**: The authors declare that the research was conducted in the absence of any commercial or financial relationships that could be construed as a potential conflict of interest.

frontiers in Human Neuroscience

ORIGINAL RESEARCH
published: 01 October 2018
doi: 10.3389/fnhum.2018.00390

# Frontal Eye Field Involvement in Color and Motion Feature-Based Attention: Single-Pulse Transcranial Magnetic Stimulation

*Xi Chen*[1], *Jing-Na Jin*[1], *Fang Xiang*[1], *Zhi-Peng Liu*[1]* *and Tao Yin*[1,2]*

[1]*Institute of Biomedical Engineering, Chinese Academy of Medical Sciences & Peking Union Medical College, Tianjin, China,*
[2]*Neuroscience Center, Chinese Academy of Medical Sciences, Beijing, China*

An object can have multiple attributes, and visual feature-based attention (FBA) is the process of focusing on a specific one of them. During visual FBA, the frontal eye field (FEF) is considered to be an important brain area related to the choice of attribute. However, the study of the FEF in FBA remains inadequate. We applied single-pulse transcranial magnetic stimulation (TMS) to the right FEF (rFEF), and designed two independent experimental FBA tasks that each involved two attributes (color and motion), to explore the action time of FEF and the spatial transmission of the FEF signal, respectively. The results of the first experiment showed that when TMS was applied to the rFEF at 100 ms after the target image stimulus began, the subjects' response time increased significantly compared with the response time in the control trials (in which TMS was applied to the vertex). This indicated that inhibiting the rFEF influenced the progress of visual FBA. The results confirm that the FEF is involved in the early stage of visual attention (at ∼100 ms). In the second experiment, TMS was applied at 100 ms after the target image stimulus began. We analyzed the electroencephalogram (EEG) signal after TMS, and found that the electrode signal amplitudes for FC4 (which corresponded to the rFEF) were significantly correlated with the electrode signal amplitudes in the posterior regions. In addition, the amplitude rise of the posterior electrode signal lagged ∼50 ms behind that of the FC4. Furthermore, for color and motion, different areas in the posterior brain region were involved in signal transmission. In this study, the application of single-pulse TMS was shown to provide a direct and effective method for research on the FEF, and the combination of TMS and EEG recordings allows a high degree of time resolution, which can provide powerful evidence for research on neural signal transmission.

**Keywords: transcranial magnetic stimulation, frontal eye field, feature-based attention, color, motion**

OPEN ACCESS

***Edited by:***
*Xiaochu Zhang,*
*University of Science and Technology of China, China*

***Reviewed by:***
*Xiaoli Li,*
*Beijing Normal University, China*
*Wan Bai Kun,*
*Tianjin University, China*

***Correspondence:**
*Zhi-Peng Liu*
*lzpeng67@163.com*
*Tao Yin*
*bme500@163.com*

***Received:*** *04 July 2018*
***Accepted:*** *10 September 2018*
***Published:*** *01 October 2018*

***Citation:***
*Chen X, Jin J-N, Xiang F, Liu Z-P and Yin T (2018) Frontal Eye Field Involvement in Color and Motion Feature-Based Attention: Single-Pulse Transcranial Magnetic Stimulation. Front. Hum. Neurosci. 12:390. doi: 10.3389/fnhum.2018.00390*

## INTRODUCTION

The frontal eye field (FEF) is an area located near the junction between the anterior central sulcus and the posterior superior frontal sulcus (Paus, 1996), corresponding to Brodmann area 8. The FEF is an important brain area that has been reported to control eye movement (Bosch et al., 2013). Also, recent research has shown that the FEF is involved in visual attention, together with the posterior parietal cortex (PPC) and prefrontal ventral cortex (PFv; Lane et al., 2011).

Muggleton et al. (2011) conducted a comparative experiment on the FEF and PPC, and they found that the FEF was focused on the process of visual attention and accumulation of visual information, while PPC participated in the transformation of visual information to behavior. A similar result was obtained by Akaishi et al. (2013). The studies on the FEF can be divided into two main categories: exploring the action time of the FEF and exploring the function of the FEF with regard to the top-down signal from the frontal cortex.

Previous experiments (Kammer, 2007; Romei et al., 2007), have shown that the FEF plays a major role prior to initial processing in the primary visual cortex at the early stages of visual attention. More specifically, neurons in the FEF of monkeys have been shown to discriminate the target and interference stimuli since about 100 ms from visual stimulus began (Bichot and Schall, 1999). O'Shea et al. (2004) applied paired-pulse transcranial magnetic stimulation (TMS) to subjects at different time periods during visual attention, and they found that paired-pulse TMS at 40–80 ms after the beginning of the target stimulus suppressed the subjects' responses.

During visual attention, the transmission of visual information is thought to be controlled by a set of top-down signals from the frontal cortex, and the FEF is one of the important brain regions involved in the transmission. Recently, studies have demonstrated the transmission of the FEF signal to the posterior region of the brain, with the sequence of neural activity first involving the anterior and then the posterior brain regions (O'Shea et al., 2004; Brass et al., 2005). Further research has also shown that the correlation between the activities in the anterior and posterior brain regions demonstrates that the signal passes between them (Sakai and Passingham, 2003, 2006). In 2009, Morishima et al. proposed a single-pulse TMS method that involved the superposition of a nerve signal at the stimulation site and subsequently analyzing the transfer of this superimposed signal (Morishima et al., 2009). This allowed them to effectively prove that, when facial and motion information was being assessed, the signal transmission mechanism involved a top-down signal (Morishima et al., 2009). In 2014, Heinen et al. further proved this point using TMS combined with functional magnetic resonance imaging (fMRI; Heinen et al., 2014).

Both groups investigated the effect of the FEF during visual attention related to different tasks. However, regarding feature-based attention (FBA), attention is focused on a specific attribute of a single target, such as color, shape, or size (Treisman and Gelade, 1980; Tsujimoto and Tayama, 2004; Cavina-Pratesi et al., 2010), ignoring the other attributes. At present, there is not enough evidence on the function and action time of the FEF during FBA.

In visual FBA, the processing of different attributes is thought to correspond to different brain regions. In recent years, a large number of imaging and electrophysiological studies have provided evidence on the visual pathway involved in FBA. Studies have shown that the brain area corresponding to color information processing is located at V4/V8 in the occipital cortex (Pasupathy and Connor, 1999; Bichot et al., 2005; Zhou and Desimone, 2011). In contrast, the processing of motion information corresponds to the V5/MT region (Schoenfeld et al., 2007; Buracas and Albright, 2009; Alexander et al., 2018). However, whether this process is related to the FEF remains unknown.

Therefore, we designed two independent FBA experiments to explore the action time of the FEF and the spatial transmission of the FEF signal, respectively. The two experiments both involved applying single-pulse TMS to the right FEF (rFEF). The experiments only investigated the rFEF because research shows that rFEF has a hemispherical advantage over the left side (Marshall et al., 2015), i.e., the contribution of the right side to the attention process is greater than that of the left side.

In the first experiment, we set the stimulus interval between TMS and the beginning of the visual target stimulus to 0, 50, 100, 150 and 200 ms. Single-pulse TMS above the stimulation threshold was applied to the rFEF. Based on the experimental design used by Pourtois et al. (2001) for studying the PPC action time, the role of the FEF in FBA was explored by analyzing the response time of subjects as TMS was applied at different time points.

In the second experiment, we applied single-pulse TMS below the stimulation threshold at the time point associated with the maximum effect of the FEF (as shown in the first experiment) in order to facilitate an analysis of FEF signal transmission. The single-pulse TMS resulted in the superposition of a neural signal at the stimulated brain region (i.e., the FEF) that did not change the FEF's function, and then the FEF's function was studied by analyzing the subsequent spread of the superimposed signal.

# MATERIALS AND METHODS

## Subjects

Nine normal subjects (mean age: 26.3 ± 3.2 years) participated in the first experiment to explore the action time of the FEF. We excluded one subject's data as he could not concentrate on the visual FBA task for a sufficient length of time. In addition, 14 subjects (mean age: 26.1 ± 2.8 years) participated in the second experiment, which involved TMS combined with electroencephalogram (EEG) recording. The purpose of the second experiment was to explore the spatial transmission of the FEF signal. This study was carried out in accordance with the recommendations of TMS safety instructions, the ethics committee of the Institute of Biomedical Engineering, Chinese Academy of Medical Sciences & Peking Union Medical College. The protocol was approved by the ethics committee of the Institute of Biomedical Engineering, Chinese Academy of Medical Sciences. All subjects gave written informed consent in accordance with the Declaration of Helsinki.

## Task

The paradigms of the two experiments were the same. Subjects were presented with an FBA task that involved assessing a specific visual attribute depending on a specific cue letter (C for color or M for motion; **Figure 1**). The refresh rate of the liquid-crystal display (LCD) monitor was 60 Hz. The room was kept dark and quiet during the experiment, to ensure that the

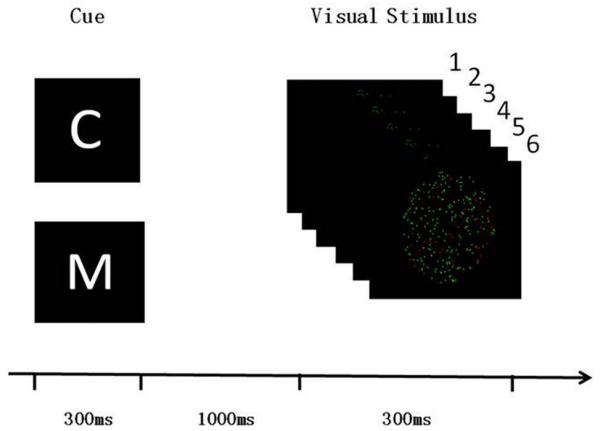


**FIGURE 1 |** Visual feature-based attention (FBA) task paradigm. Both of the experiment 1 and the experiment 2 used the same design paradigm. Subjects needed to discriminate either the color or the direction of moving for most of dots in the visual stimulus dynamic pictures. C and M cues indicated color and motion discrimination, respectively. The stimulus onset asynchrony between the cue and visual stimulus was 1,000 ms, and the screen kept black during this time.

subjects could focus on the FBA task. The task was written using E-prime software (E-prime2.0, Psychology Software Tools Inc., Sharpsburg, PA, USA). The subjects were required to assess the visual target information according to the cue letter. The visual target information was composed of six pictures, each of which were presented for 50 ms, making up a dynamic image stimulation. Two-hundred dots that were evenly distributed in the 6° of visual field located in the middle of the picture which was black background. The dots were randomly colored either red or green, which were set the same brightness and contrast, and they moved at 12°/s to the left or right. 20% of the dots were used as interference, i.e., they were different from the color or direction of motion of the other dots. The subjects were required to assess either the color or the direction of motion of most of the dots. That is, if the cue was C, subjects were required to assess the color of most of the dots, pushing button 1 for red and button 2 for green. If the cue was M, the subjects were required to assess the direction of motion, pushing button 1 when most dots move to the left and button 2 when they move to the right.

## TMS

For each subject, we first determined the TMS threshold intensity. Rest motor threshold (RMT) and active motor threshold (AMT) were measured individually for the first and second experiments. We defined RMT and AMT as the minimum TMS intensity that led to at least five electromyography signals being recorded in 10 successive TMS trials. For assessing the RMT, the subjects were seated on a chair with their right hand in a resting position, and for assessing the AMT, their right index finger was extended and lifted up. We delivered single-pulse TMS to the scalp position corresponding to the left primary motor cortex (the position was adjusted by moving the coil center in intervals of 0.5 cm) using an 8-shaped flat coil (Magstim, Whiteland, UK). A 70-mm coil was used for TMS, placing it tangentially over the scalp at 45° from the middle line.

## Site Localization

A structural MRI scan (T1) was obtained in advance for all subjects at Tianjin Medical University General Hospital. Stimulation sites for TMS were localized using the Brainsight system (Brainsight, Magstim, UK). This was used to match each subject to their MRI scan, on which the rFEF and vertex were marked before the experiments. The stimulation site in both the first and second experiments was set as the rFEF coordinates of Montreal Neurological Institute (MNI; $28 \pm 4$, $-5 \pm 5$, $49 \pm 4$), corresponding to the coordinates of the rFEF reported in previous study (Paus, 1996).

## Experiment 1

In the first experiment, single-pulse TMS (110% RMT) was applied, and the stimulation times were set to 0, 50, 100, 150 and 200 ms from the beginning of the first visual target stimulus (see **Figure 1**, each time point corresponds to the beginning of one of the pictures). TMS was applied to the rFEF and vertex in the experimental and control trials, respectively. The first experiment had 10 blocks, each containing 80 trials, leading to a total of 800 trials. Subjects rested for 5 min in the interval between each block. Regarding the 10 blocks, there was a $5 \times 2$ design (time points 0/50/100/150/200 ms and stimulation site FEF/vertex). The time point and stimulation site used for each block were both set randomly, and C/M were also set randomly in each block.

## Experiment 2

In the second experiment, single-pulse TMS (70% AMT) was applied, and the stimulation time was set to the time corresponding to the maximum FEF effect obtained in the first experiment. The experiment had 10 blocks, each containing 64 trials, leading to a total of 640 trials. The experiment had a $2 \times 2$ design (TMS/no TMS and C/M). The TMS and no TMS trials occurred randomly.

## EEG Recording and Data Analysis

Subject wore an EEG cap (Neuroscan, Compumedics, USA) and performed the color or motion FBA task while EEG recordings were obtained from 60 scalp electrodes. Two additional electrodes were used to record the electrooculographic (EOG) which used in removing the artifacts of eye movement and blinking for further EEG analysis. EEG signals were referenced to FCz and the ground electrode was at Afz, signals filtered at a frequency of 200 Hz DC and sampled at 20 kHz. To reduce the impact of artifacts resulting from the clicking sound of the TMS pulse, the subjects wore earplugs. After discarding the raw data from trials involving incorrect color/motion assessments, we used EEGLAB toolbox version 13.0 (EEGlab, SCCM, San Antonio, TX, USA) combined with Matlab version 10.0 (Matlab, Mathworks, Natick, MA, USA) to process the EEG data, resample the data at 1,000 Hz, and an interpolation method (Rogasch et al., 2014) was applied to remove the TMS pulse induced artifacts, during the time

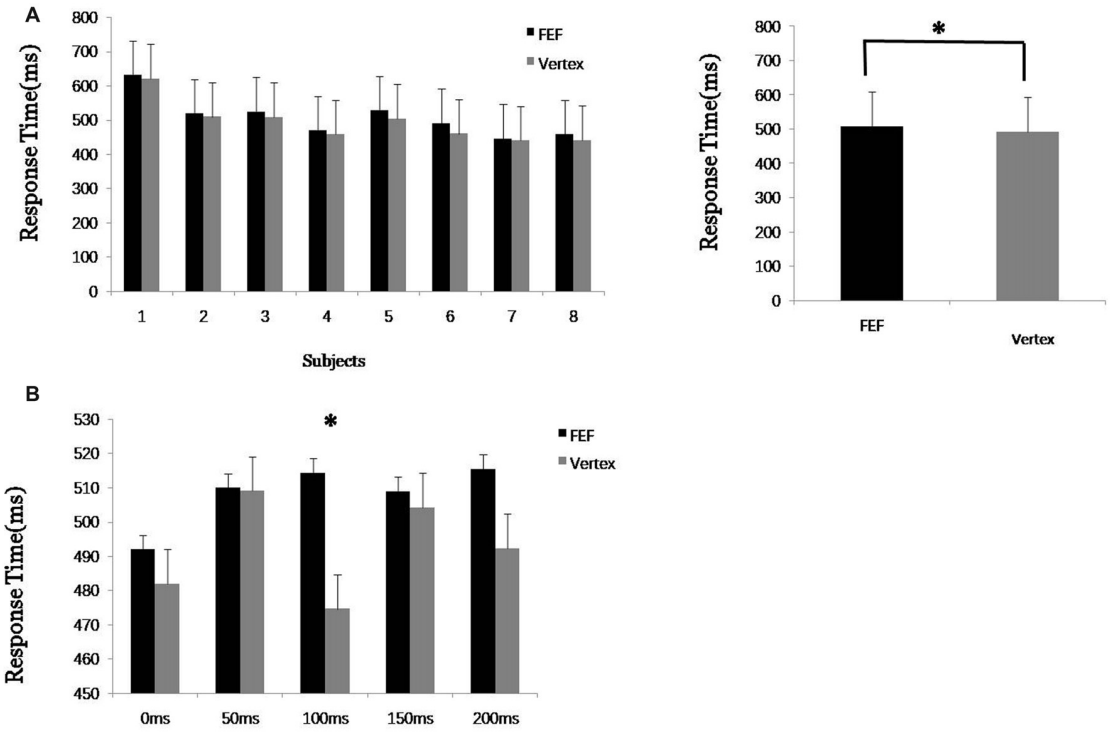


**FIGURE 2 |** Experiment 1 results. **(A)** Average response time of each eight subjects to transcranial magnetic stimulation (TMS) applied to the right frontal eye field (FEF) and vertex. **(B)** Response time after TMS at 0, 50, 100, 150 and 200 ms from the beginning of the first visual target stimulus. "*" means significantly different ($p < 0.05$).

interval of 40 ms before and after TMS (−20 ms to 20 ms). After interpolation algorithm, the EEG signals was filtered at 1–70 Hz and the reference was then changed to the average of the 60 electrodes, and the baseline was set to 20–40 ms before the TMS pulse was applied. Independent component analysis (ICA) was run two times to remove other artifacts, such as interpolation induced artifacts, TMS induced electromyogram (EMG) and blinking artifacts (Bai et al., 2016) during experiments. In the first ICA run, we identify the artifacts through components signal analysis combined with topographies, and further validate signals by statistical test after the second ICA run to remove the residual artifacts. After preprocessing the EEG data, the TMS-event-related potential (ERP) and no TMS-ERP signals were obtained separately for further analysis.

## Eye Movement Recording

In the second experiment, we used two additional electrodes to record horizontal and vertical eye movement signals. A Tobii (X1) eye tracker (Tobii, Sweden) was also used to record eye movement during the visual FBA task. The eye movement instrument was combined with the visual stimulation software (Eprime) to ensure synchronous measurements. The eye movement information was mainly recorded during visual target stimulation (∼300 ms) in both experiments, which included the binocular position coordinates and pupil diameter. The data were then analyzed to examine the subjects' attention.

## Analysis of Variance (ANOVA)

Analysis of variance (ANOVA) is a statistical procedure for summarizing a classical linear model which originally was developed by Fisher (1925). The classical idea of the ANOVA was to find out if there exists an influence of one or more factor variables (one factor in our experiment) over a normally distributed random variable. In the first experiment, we applied one factor variance analysis to explore the influence of two groups which included feature attributes (color and motion) and TMS stimulus sites (FEF and vertex) on the response time of subjects, individually, and the influence between the two groups.

## Pearson Correlation Coefficient Analysis

After data preprocessing, the difference in terms of TMS-ERP minus no TMS-ERP signal was used to calculate the Pearson correlations between the electrode signal of FC4 (near the rFEF) and the electrodes located in the parietal lobe and posterior region. The Pearson correlation coefficient was used to determine the degree of correlation between the electrode

**TABLE 1 |** Variance analysis results for response time in feature attributes (color/motion) and TMS stimulus sites (FEF/vertex).

| | FEF × vertex (color) | FEF × vertex (motion) | Feature × site |
|---|---|---|---|
| *p* value | 0.003* | 0.009* | 0.916 |

*"*" means significantly different ($p < 0.05$).*

signal amplitudes. Coefficients of −1 and 1 represent perfect correlation, and the closer each coefficient was near to −1/1, the correlation was stronger.

## Current Source Density Analysis

Standardized low-resolution brain electromagnetic tomography (sLORETA) is a source location method based on a mathematical model (Fuchs et al., 2002; Pascual-Marqui, 2002; Wagner et al., 2004; Jurcak et al., 2007). By assessing the EEG signal in order to locate the activity source in the cerebral cortex, neural activity and signal transmission can be analyzed spatially. sLORETA software is based on a probabilistic MNI brain volume scanned at a resolution of 5 mm. In our study, data were calculated point by point by sLORETA at 20–50 ms after TMS, and the data were then normalized after log conversion. The images in each section were then superimposed, one by one and averaged. To assess the difference between the color and motion attributes, sLORETA results for color and motion were analyzed using paired *t*-tests.

# RESULTS

## Behavioral Results

In the first experiment, data from eight subjects were analyzed (one subjects' data were excluded because he could not focus on the visual FBA task for a sufficiently long time). First, the response times when TMS was applied to the rFEF and vertex were statistically analyzed. To mitigate the effect of TMS being applied at different times, we averaged the response times of five groups of trials (TMS at 0, 50, 100, 150 and 200 ms from the beginning of the first visual target stimulus). The results showed that when TMS was applied to the rFEF, the response time was slightly longer than when TMS was applied to the vertex, and this difference was significant ($p < 0.05^*$, **Figure 2**). Thus, TMS applied to the FEF compared to TMS applied to the vertex led to interference in the behavioral response. This indicates that the FEF plays an important role in the process of visual FBA.

The reaction time when TMS was applied at different time points (0, 50, 100, 150 and 200 ms) was further analyzed. The

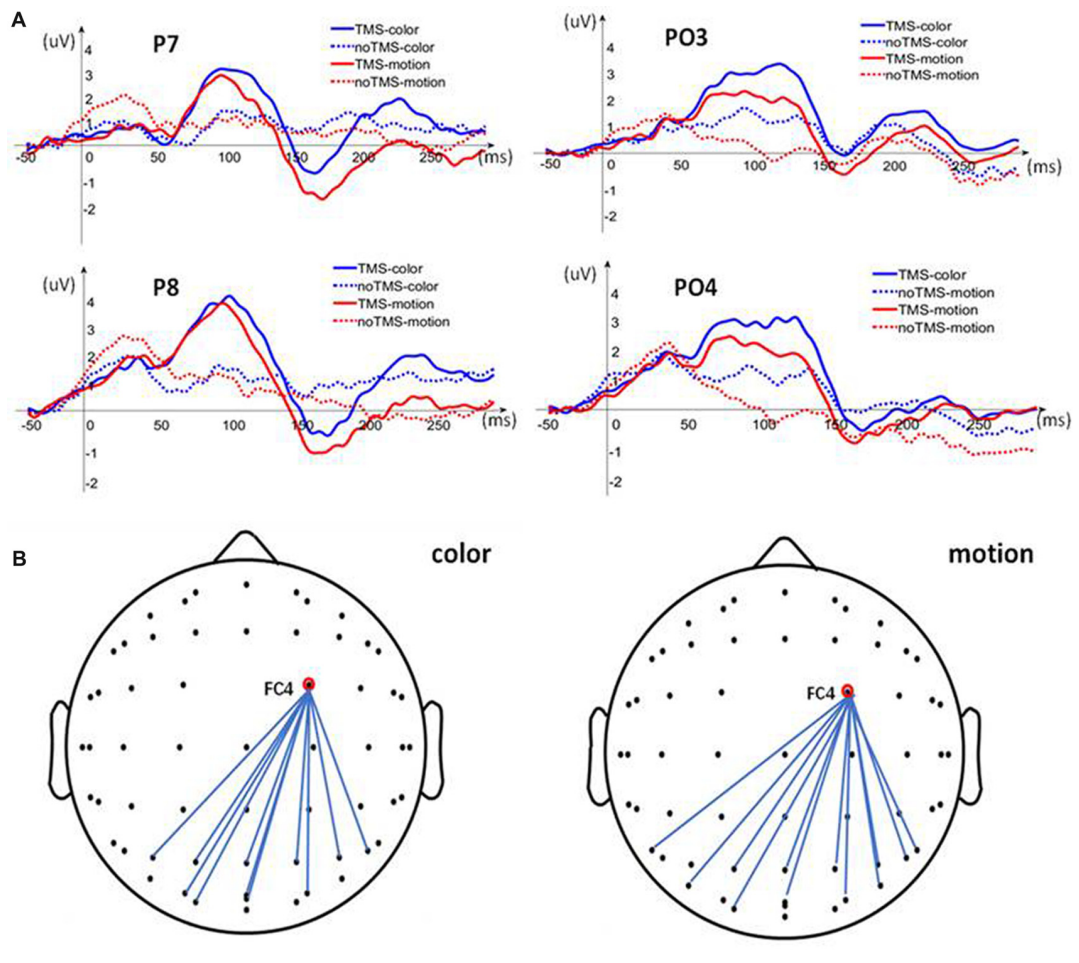


**FIGURE 3 |** Analysis of signal amplitudes. **(A)** Posterior electrode (P7, P8, PO3 and PO4) signal amplitude compared between the TMS-event-related potential (ERP) and no TMS-ERP trials for both color and motion. **(B)** Pearson correlation analysis between FC4 (corresponding to the rFEF) and electrodes in the parietal and posterior brain regions.

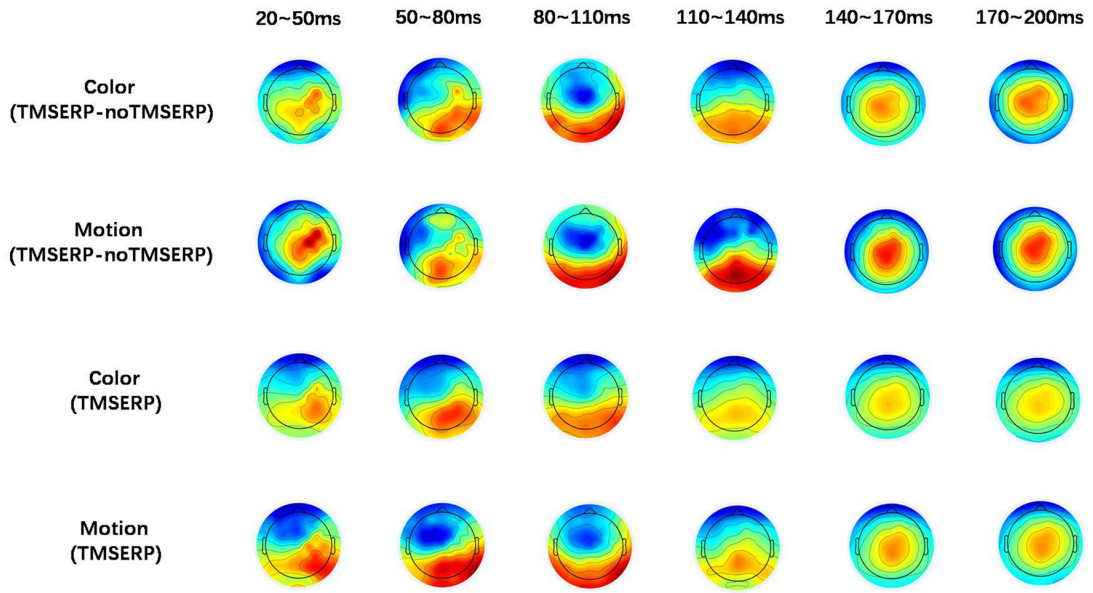


**FIGURE 4 |** Brain topographic maps. The upper two rows show brain topographic maps of the difference between TMS-ERP and no TMS-ERP during color and motion FBA tasks, respectively. The lower two rows show the brain topographic maps associated with TMS-ERP.

result showed that the response times when TMS was applied to the FEF at different time points were all longer than when TMS was applied to the vertex, but the difference was only significant (*) for the 100 ms time point. This shows that TMS

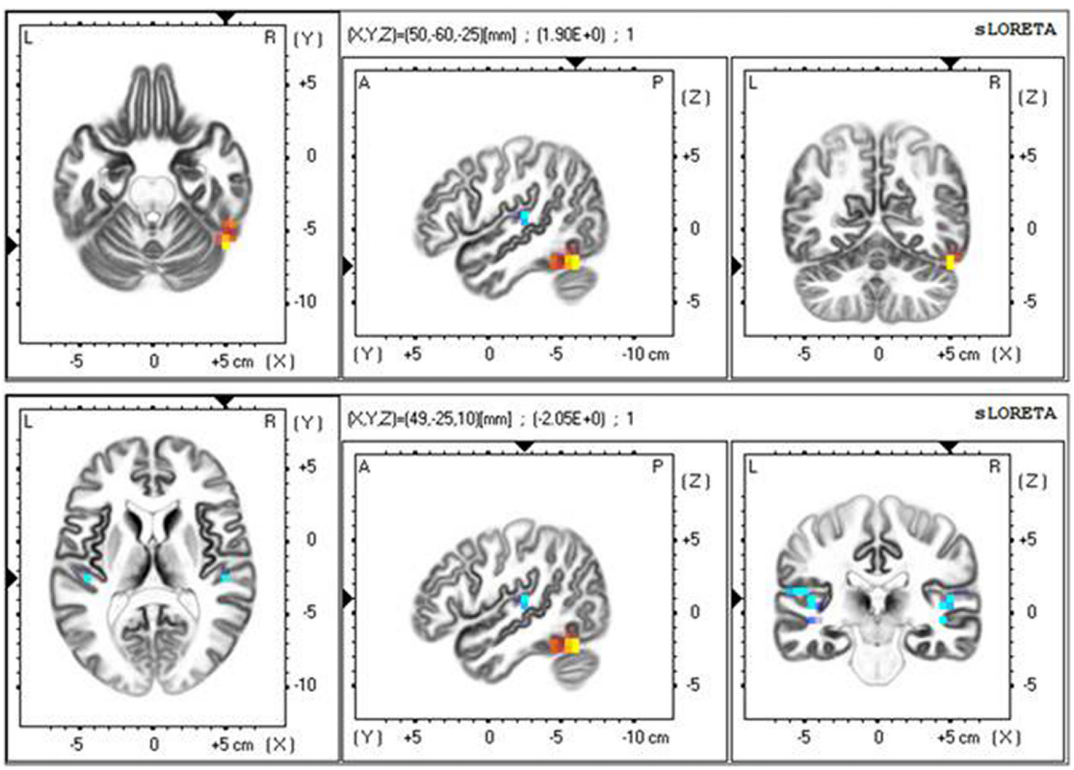


**FIGURE 5 |** Standardized low-resolution brain electromagnetic tomography (sLORETA) results at 20–50 ms after TMS.

leads to inhibition and the action time of the FEF regarding the visual FBA process occurs mainly at around 100 ms. This result also provided an important time parameter for TMS use in the second experiment. Thus, in the second experiment, single-pulse TMS was applied at 100 ms after the target image stimulus began, which maximized the effect on the FEF, making it more convenient to study the spatial transmission of the FEF signal. One-hundred milliseconds also corresponds to the beginning of the second visual stimulus picture (out of six pictures).

The results in **Table 1** show that, in the first experiment, when TMS was applied to the FEF at 100 ms, the response times (for both color and motion) were significantly changed ($p$ = 0.003 and 0.009, respectively) compared to the response times in the control trials (which involved TMS applied to the vertex). The results show that TMS significantly inhibited the FEF and thus inhibited the assessment of the two attributes (color and motion). The variance analysis between the two groups (color/motion × FEF/vertex), shown in the final column of **Table 1**, shows that there was no significantly difference between the feature attributes and the TMS stimulus sites. Furthermore, we cannot find the difference between color and motion through the response time of TMS on FEF and on vertex.

In the second experiment, TMS was applied at 100 ms after the target image stimulus began, and there was no significant difference in response time between the TMS and no TMS trials ($p > 0.05$). Thus, the effect of TMS only regard as an increase of the signal amplitude that could not change the neural function of the stimulus site (i.e., the FEF), to explore the spatial transmission of the FEF signal.

## TMS Combined With EEG Recordings

In the second experiment, after TMS applied to the rFEF, it was found that the amplitude of FC4 (corresponding to the rFEF) increased immediately during color and motion attention. The electrode signal amplitude in the posterior brain region also increased, but the rise in the amplitude lagged by ∼50 ms compared with that of FC4 (**Figure 3A**). To study the increase in the signal amplitude during the delayed time period, we further analyzed the Pearson correlation between the FC4 and the parietal and posterior brain regions at 20–50 ms after TMS, **Figure 3B**. We found that there was a strong correlation in the electrode signal amplitudes between many of the brain regions during both the color and motion FBA tasks. However, there were some differences regarding the electrodes for which there were significant Pearson correlations (color: P3, P4, 01, PZ, P1, P2, PO3, PO4, P6, POZ and OZ; motion: P4, O1, P7, P8, PZ, P1, P2, PO4, P6, PO7 and PO8 and POZ). These slight differences suggest that there are differences in neural signal transmission between color and motion FBA tasks, **Figure 4**.

To further explore the transmission direction of the signal from the rFEF after TMS, we divided the post-TMS EEG data (20–200 ms) into six periods containing 30 ms each. The effect of TMS was obtained by subtracting the no TMS-ERP recordings from the TMS-ERP recordings. The brain topographic maps associated with TMS, as shown in **Figure 4**, show that neural excitability was transferred from FC4 (near the stimulation point) to the posterior part of the brain at both 20–50 ms and 50–80 ms. At 80–140 ms, the neural excitability was transmitted to the posterior area, then back to the parietal lobe after 140 ms and it stayed in the parietal lobe until 200 ms. The brain topographic maps associated with TMS-ERP were also analyzed, and we found that the transfer effect was mainly associated with the initial time period (20–50 ms), which was consistent with the result regarding the TMS effect, but the neural excitability was transmitted more to the right hemisphere.

To further observe the spatial signal at 20–50 ms, we used a source location analysis method (sLORETA) to analyze the distribution of the current source density of the signal during the color and motion FBA tasks. We analyzed the difference between color and motion using paired $t$-tests in the statistical module of sLORETA. Current source density analyzed results at 20–50 ms after TMS are showed in **Figure 5**. The main positive distribution was in the fusiform gyrus (BA37), and the negative distribution was near the bilateral junction of the parietal and temporal lobes. The results show that the processing of different attributes in the posterior brain region is different, which concurs with previous researches showing that color processing is associated with V4 and motion processing is associated with MT/V5 (Zhou and Desimone, 2011; Alexander et al., 2018).

# DISCUSSION

In this study, we analyzed the action time of the FEF during visual FBA and the spatial transmission of the FEF signal. In the first experiment, we applied single-pulse TMS above the threshold (110% RMT). The response time of the subject was interfered when TMS was applied to the FEF compared with when TMS was applied to the vertex. Thus, we verified the important effect of the FEF in the visual FBA process. Additionally, we explored different TMS stimulus times and found that the effective action time of the FEF occurred during the early stage of attention, which was about 100 ms after the target image stimulus began. These results not only provide information regarding the action time of the FEF, but they also provided an important time parameter for the study of the spatial transmission of FEF signals in the second experiment. The duration of the effect of single-pulse TMS is shorter than that of paired-pulse TMS (O'Shea et al., 2004), which made our study of the FEF action time more accurate. This method (i.e., the use of single-pulse TMS) is of great significance to the study of visual attention and even to other neurocognitive studies.

The FEF signal, which is also called the top-down signal, has been thought to come from the prefrontal lobe and to be transferred to the posterior brain region. In our study, we applied single-pulse TMS below the stimulus threshold (70% AMT) without changing the function of the stimulus site (i.e., the FEF), as we consider the neural activity transfer as the superposition of a nerve signal in the stimulus brain region. By assessing the superimposed signal, the process of neural signal transmission can be accessed directly and effectively; this method was applied

and verified in a previous study (Johnson et al., 2012). This article provides evidence on FEF signal transmission during the assessment of different visual attributes. Single-pulse TMS combined with EEG recording has a high degree of time resolution, is quite effective for studying signal transmission processes, and is of great significance for research on the visual FBA mechanism.

Regarding the study of different attributes involved in visual FBA, there have been a large number of studies on color and motion. Different brain regions process color and motion information separately. V4, which is located near the fusiform gyrus, has mostly been shown to be responsible for processing color information. The V5/MT region, which is mainly located at the bilateral intersection of the parietal and temporal lobes, is mainly responsible for processing movement information (Lechak and Leber, 2012). In our study, we also found that there was a difference in the signal of the posterior brain area during the processing of different visual attributes. This result provides further support regarding the independance of color and motion information processing. At the same time, the difference of the signals in the posterior region was might closely related to the FEF during the process of visual FBA.

Our study not only analyzed the action time of the FEF from a behavioral perspective, but it also explored the spatial transmission of the FEF signal by combining single-pulse TMS with EEG recordings. The application of single-pulse TMS with different parameters in two experiments shows the various effects of TMS and indicates that TMS could be used to achieve different research objectives. The study also provides further evidence regarding the transmission of FEF signals. The study is of great importance for research on visual FBA, and it also provides details of an effective method for use in other neurocognitive studies.

## AUTHOR CONTRIBUTIONS

XC, J-NJ and FX were responsible for the design of the work, and completed the two experiments. XC and J-NJ completed the analysis and the interpretation of the data. XC, Z-PL and TY were responsible for drafting the manuscript.

## FUNDING

This research was supported by CAMS Initiative for Innovative Medicine (No. 2016-I2M-1004).

## ACKNOWLEDGMENTS

We thank all the volunteers and participants involved in this study, and thanks for the help during our experiments and data processing.

## REFERENCES

Akaishi, R., Ueda, N., and Sakai, K. (2013). Task-related modulation of effective connectivity during perceptual decision making: dissociation between dorsal and ventral prefrontal cortex. *Front. Hum. Neurosci.* 7:365. doi: 10.3389/fnhum.2013.00365

Alexander, B., Laycock, R., Crewther, D. P., and Crewther, S. G. (2018). An fMRI-neuronavigated chronometric TMS investigation of V5 and intraparietal cortex in motion driven attention. *Front. Hum. Neurosci.* 11:638. doi: 10.3389/fnhum.2017.00638

Bai, Y., Wan, X., Zeng, K., Ni, Y., Qiu, L., and Li, X. (2016). Reduction hybrid artifacts of EMG-EOG in electroencephalography evoked by prefrontal transcranial magnetic stimulation. *J. Neural Eng.* 13:066016. doi: 10.1088/1741-2560/13/6/066016

Bichot, N. P., and Schall, J. D. (1999). Effects of similarity and history on neural mechanisms of visual selection. *Nat. Neurosci.* 2, 549–554. doi: 10.1038/9205

Bichot, N. P., Rossi, A. F., and Desimone, R. (2005). Parallel and serial neural mechanisms for visual search in macaque area V4. *Science* 308, 529–534. doi: 10.1126/science.1109676

Bosch, S. E., Neggers, S. F. W., and Van der Stigchel, S. (2013). The role of the frontal eye fields in oculomotor competition: image-guided TMS enhances contralateral target selection. *Cereb. Cortex* 23, 824–832. doi: 10.1093/cercor/bhs075

Brass, M., Ullsperger, M., Knoesche, T. R., von Cramon, D., and Phillips, N. A. (2005). Who comes first? The role of the prefrontal and parietal cortex in cognitive control. *J. Cogn. Neurosci.* 17, 1367–1375. doi: 10.1162/0898929054985400

Buracas, G. T., and Albright, T. D. (2009). Modulation of neuronal responses during covert search for visual feature conjunctions. *Proc. Natl. Acad. Sci. U S A* 106, 16853–16858. doi: 10.1073/pnas.0908455106

Cavina-Pratesi, C., Kentridge, R. W., Heywood, C. A., and Milner, A. D. (2010). Separate channels for processing form, texture and color: evidence from fMRI adaptation and visual object agnosia. *Cereb. Cortex* 20, 2319–2332. doi: 10.1093/cercor/bhp298

Fisher, J. W. (1925). Some further experiments on the gyromagnetic effect. *Proc. R. Soc. Lond.* 109, 7–27. doi: 10.1098/rspa.1925.0104

Fuchs, M., Kastner, J., Wagner, M., Hawes, S., and Ebersole, J. S. (2002). A standardized boundary element method volume conductor model. *Clin. Neurophysiol.* 113, 702–712. doi: 10.1016/s1388-2457(02)00030-5

Heinen, K., Feredoes, E., Weiskopf, N., Ruff, C. C., and Driver, J. (2014). Direct evidence for attention-dependent influences of the frontal eye-fields on feature-responsive visual cortex. *Cereb. Cortex* 24, 2815–2821. doi: 10.1093/cercor/bht157

Johnson, J. S., Kundu, B., Casali, A. G., and Postle, B. R. (2012). Task-dependent changes in cortical excitability and effective connectivity: a combined TMS-EEG study. *J. Neurophysiol.* 107, 2383–2392. doi: 10.1152/jn.00707.2011

Jurcak, V., Tsuzuki, D., and Dan, I. (2007). 10/20, 10/10 and 10/5 systems revisited: their validity as relative head-surface-based positioning systems. *Neuroimage* 34, 1600–1611. doi: 10.1016/j.neuroimage.2006.09.024

Kammer, T. (2007). Visual masking by transcranial magnetic stimulation in the first 80 milliseconds. *Adv. Cogn. Psychol.* 3, 177–179. doi: 10.2478/v10053-008-0023-2

Lane, A. R., Smith, D. T., Schenk, T., and Ellison, A. (2011). The involvement of posterior parietal cortex in feature and conjunction visuomotor search. *J. Cogn. Neurosci.* 23, 1964–1972. doi: 10.1162/jocn.2010.21576

Lechak, J. R., and Leber, A. B. (2012). Individual differences in distraction by motion predicted by neural activity in MT/V5. *Front. Hum. Neurosci.* 6:12. doi: 10.3389/fnhum.2012.00012

Marshall, T. R., O'Shea, J., Jensen, O., and Bergmann, T. O. (2015). Frontal eye fields control attentional modulation of alpha and gamma oscillations in contralateral occipitoparietal cortex. *J. Neurosci.* 35, 1638–1647. doi: 10.1523/JNEUROSCI.3116-14.2015

Morishima, Y., Akaishi, R., Yamada, Y., Okuda, J., Toma, K., and Sakai, K. (2009). Task-specific signal transmission from prefrontal cortex in visual selective attention. *Nat. Neurosci.* 12, 85–91. doi: 10.1038/nn.2237

Muggleton, N. G., Kalla, R., Juan, C., and Walsh, V. (2011). Dissociating the contributions of human frontal eye fields and posterior parietal cortex

to visual search. *J. Neurophysiol.* 105, 2891–2896. doi: 10.1152/jn.01149.2009

O'Shea, J., Muggleton, N. G., Cowey, A., and Walsh, V. (2004). Timing of target discrimination in human frontal eye fields. *J. Cogn. Neurosci.* 16, 1060–1067. doi: 10.1162/0898929041502634

Pascual-Marqui, R. D. (2002). Standardized low resolution brain electromagnetic tomography (sLORETA): technical details. *Methods Find. Exp. Clin. Pharmacol.* 24, 5–12.

Pasupathy, A., and Connor, C. E. (1999). Responses to contour features in macaque area V4. *J. Neurophysiol.* 82, 2490–2502. doi: 10.1152/jn.1999.82.5.2490

Paus, T. (1996). Location and function of the human frontal eye-field: a selective review. *Neuropsychologia* 34, 475–483. doi: 10.1016/0028-3932(95)00134-4

Pourtois, G., Vandermeeren, Y., Olivier, E., and de Gelder, B. (2001). Event-related TMS over the right posterior parietal cortex induces ipsilateral visuo-spatial interference. *Neuroreport* 12, 2369–2374. doi: 10.1097/00001756-200108080-00017

Rogasch, N. C., Thomson, R. H., Farzan, F., Fitzgibbon, B. M., Bailey, N. W., Hernandez-Pavon, J. C., et al. (2014). Removing artefacts from TMS-EEG recordings using independent component analysis: importance for assessing prefrontal and motor cortex network properties. *Neuroimage* 101, 425–439. doi: 10.1016/j.neuroimage.2014.07.037

Romei, V., Murray, M. M., Merabet, L. B., and Thut, G. (2007). Occipital transcranial magnetic stimulation has opposing effects on visual and auditory stimulus detection: implications for multisensory interactions. *J. Neurosci.* 27, 11465–11472. doi: 10.1523/JNEUROSCI.2827-07.2007

Sakai, K., and Passingham, R. E. (2003). Prefrontal interactions reflect future task operations. *Nat. Neurosci.* 6, 75–81. doi: 10.1038/nn987

Sakai, K., and Passingham, R. E. (2006). Prefrontal set activity predicts rule-specific neural processing during subsequent cognitive performance. *J. Neurosci.* 26, 1211–1218. doi: 10.1523/JNEUROSCI.3887-05.2006

Schoenfeld, M. A., Hopf, J. M., Martinez, A., Mai, H. M., Sattler, C., Gasde, A., et al. (2007). Spatio-temporal analysis of feature-based attention. *Cereb. Cortex* 17, 2468–2477. doi: 10.1093/cercor/bhl154

Treisman, A. M., and Gelade, G. (1980). A feature-integration theory of attention. *Cogn. Psychol.* 12, 97–136. doi: 10.1016/0010-0285(80)90005-5

Tsujimoto, S., and Tayama, T. (2004). Independent mechanisms for dividing attention between the motion and the color of dynamic random dot patterns. *Psychol. Res* 68, 237–244. doi: 10.1007/s00426-003-0137-6

Wagner, M., Fuchs, M., and Kastner, J. (2004). Evaluation of sLORETA in the presence of noise and multiple sources. *Brain. Topogr.* 16, 277–280. doi: 10.1023/B:BRAT.0000032865.58382.62

Zhou, H., and Desimone, R. (2011). Feature-based attention in the frontal eye field and area V4 during visual search. *Neuron* 70, 1205–1217. doi: 10.1016/j.neuron.2011.04.032

**Conflict of Interest Statement**: The authors declare that the research was conducted in the absence of any commercial or financial relationships that could be construed as a potential conflict of interest.

frontiers in Human Neuroscience

ORIGINAL RESEARCH
published: 12 October 2018
doi: 10.3389/fnhum.2018.00417

# Environmental-friendly Eco-labeling Matters: Evidences From an ERPs Study

*Jia Jin*[1,2], *Xiaodong Dou*[3]*, *Liang Meng*[4] *and Haihong Yu*[5]

[1]Business School, Ningbo University, Ningbo, China, [2]Academy of Neuroeconomics and Neuromanagement, Ningbo University, Ningbo, China, [3]Law School, Ningbo University, Ningbo, China, [4]School of Business and Management, Shanghai International Studies University, Shanghai, China, [5]Faculty of Maritime and Transportation, Ningbo University, Ningbo, China

Nowadays, the international community is becoming increasingly concerned about the sustainable utilization of natural resources. In order to protect the environment and reward sustainable practices, eco-labeling that signifies the environmental friendliness of the labeled food is already widely promoted in many regions around the world. Thus, it is of great importance for researchers to study consumers' attitudes toward eco-labeled food as food is supposed to satisfy consumers' needs. This study employed the event-related potentials (ERPs) approach to investigate consumers' attitudes toward eco-labeled food by comparing their neural processing of visual stimuli depicting eco-labeled and non-labeled food. Our results showed that behaviorally, participants preferred to buy eco-labeled food rather than non-labeled one. At the neural level, we observed markedly smaller P2 and N2 amplitudes when pictures of eco-labeled food were presented. Furthermore, we also found that amplitudes of P2 were negatively correlated with participants' purchase intention. Therefore, our current findings suggest that, while the environmental-friendly eco-labeling was not to one's own interests, it might still be evocative, which induce consumers' positive emotion, bring less cognitive conflict to the purchase decision-making and then result in a greater purchasing intention. This effect might be the result of the delivered value of social desirability.

**Keywords: eco-labeling, ERPs, P2, N2, emotion, purchase intention**

OPEN ACCESS

***Edited by:***
*Xiaochu Zhang,*
*University of Science and Technology of China, China*

***Reviewed by:***
*Zhen Yuan,*
*University of Macau, Macau*
*Yujing Huang,*
*University of Cambridge, United Kingdom*

***Correspondence:**
*Xiaodong Dou*
*douxiaodong@nbu.edu.cn*

***Received:*** *04 April 2018*
***Accepted:*** *26 September 2018*
***Published:*** *12 October 2018*

***Citation:***
*Jin J, Dou X, Meng L and Yu H (2018) Environmental-friendly Eco-labeling Matters: Evidences From an ERPs Study. Front. Hum. Neurosci. 12:417. doi: 10.3389/fnhum.2018.00417*

## INTRODUCTION

Currently, environmental protection has become an important issue all over the world. As a result, the sustainable utilization of natural resources has claimed widespread attention from both researchers and practitioners. A series of policies and regulations have already been formulated for the protection of the environment and natural resources. Among the implemented policies, one of the most important and effective policies is the set-up of standards for environmental-friendly labels, which will help rectify order of the food market by recognizing and rewarding sustainable practices and influencing the choices people make when buying food products. Examples of existing programs and labels include Friends of the Sea, KRAV (Sweden), Label Rouge (France), Marine Eco-Label Japan, and Marine Stewardship Council's (MSC's) label.

As food products are supposed to satisfy consumers' needs, it is interesting and significant to promote eco-labeling by studying consumers' preference toward eco-labeled food. Previous studies have shown that consumers generally hold positive attitudes toward eco-labeled products. For

example, people tend to prefer the taste of a cup of coffee they believe to be "eco-friendly" over another cup that is believed to be "conventional," even if the two cups of coffee are actually identical (Sörqvist et al., 2013). Similar effects have been found across a range of products, including bread (Annett et al., 2008), bananas (Sörqvist et al., 2015), seafood (Wessells et al., 1999; Johnston et al., 2001) and clean energy (Nilsson et al., 2014). For instance, Johnston et al. (2001) compared consumers' preferences for eco-labeled seafood in the United States and Norway. They found that consumers preferred eco-labeled seafood in both countries. In China, Xu et al. (2012) found that Chinese consumers considered the seafood label as a more important information source compared with their own consumption experience, and they were willing to pay more for the eco-labeled seafood in order to protect societal benefits (Xu et al., 2012). While most of these studies examined consumers' preferences toward eco-labeled food on the behavioral level, few studies tried to explore the emotional experience and cognitive process underlying consumers' explicit preferences. As researchers suggested that capture of the emotional experience of consumers would help marketing professionals better understand consumers' preferences and then boost sales (Gountas and Gountas, 2007), this study aimed to examine the emotional experience and cognitive process underlying one's preferences for eco-labeled vs. non-labeled food. Specifically, we intended to explore whether there are discrepancies in both consumers' purchase intention and corresponding brain activities when they are exposed to eco-labeled vs. non-labeled food.

In recent years, with the development of non-invasive technologies, researchers began to measure one's cognitive and affective processes adopting neuroscientific methods such as event-related potentials (ERPs). These neuroscientific methods are believed to provide information that is not obtainable through conventional marketing method such as scales and interviews (Boksem and Smidts, 2015). Indeed, previous Consumer Neuroscience studies have made substantial contributions to the understanding of consumers' decision-making by investigating their cognitive and affective processes. For example, Wang et al. (2012) investigated consumers' affective responses to pendants by using ERPs. They reported that less beautiful pendants elicited larger P2 amplitudes than more beautiful ones. As more positive emotions were reported to give rise to a less pronounced P2, this finding suggested that beautiful pendants might induce more positive emotions (Wang et al., 2012). Thus, this study confirmed the involvement of the human emotional system in consumers' decision-making process.

When it comes to neuroscientific investigations of consumers' evaluation of food label, a pioneer study employed the functional magnetic resonance imaging (fMRI) technique to examine consumers' evaluation of the organic labeling, which found increased activities in the ventral striatum for foods labeled as "organic" in comparison to conventionally labeled food (Linder et al., 2010). Some follow-up studies have examined nutrition labels (Enax et al., 2015), health labels (Grabenhorst et al., 2013), as well as controversial food label (Lusk et al., 2015). It is worth noting that all these existing studies examined consumers' attitude toward self-beneficial label, which highlight the benefit for the consumers themselves. However, there also exist other kinds of labeling, which highlight that the main beneficiary of support is some other individual or organization. According to previous studies in marketing research (Fisher et al., 2008; White and Peloza, 2009), we refer this kind of labeling as "social-benefit."

Since previous neuroscience studies suggested that social rewards would activate the same reward circuitry (the striatum) as monetary rewards (Izuma et al., 2008), in this study we would like to examine whether the social-beneficial food label would also activate the same reward circuitry as the self-beneficial label. Compared with fMRI which has a high spatial resolution and a low temporal resolution, the ERPs technique is more affordable and can provide a high temporal resolution, which can reveal timing of brain activities (Friedman and Jonson, 2000). Therefore, in this study ERPs was adopted to examine consumers' evaluation of environmental-beneficial eco-labeling and to compare the neural differences between one's processing of self- and others-beneficial food labels.

Previous studies consistently suggested that ERPs is a valuable technique to illuminate consumers' decision-making process across multiple marketing-related domains, particularly those underlying emotions and preferences (Yoon et al., 2012; Smidts et al., 2014; Camerer and Yoon, 2015). Specifically, early ERP components, which refer to those appear at the first 300 ms after stimulus onset, were reported to reflect initial sensory encoding of emotionally significant stimuli (Junghöfer et al., 2001; Schupp et al., 2007). P2 is one of the most commonly examined early ERP components (e.g., Wang et al., 2012). Numerous ERPs studies have reported that the positive-going component P2 with a peak latency from 100 ms to 200 ms was sensitive to the emotional valence of presented stimuli (Paulmann and Kotz, 2008; Lai and Huettig, 2016). Furthermore, existing studies found that P2 typically showed a higher amplitude in response to negative stimuli than positive ones (Carretié et al., 2001; Huang and Luo, 2006; Lai and Huettig, 2016). That is, the P2 component was found to be modulated by the valence of one's emotion in response to affective stimuli.

N2 is another frequently studied ERP component in Consumer Neuroscience literatures. It typically peaks at approximately 250–350 ms after the onset of a stimulus (Folstein and Van Petten, 2008). Previous studies suggested that the N2 component is related to the cognitive control or conflict monitoring (Folstein and Van Petten, 2008). The typical N2 can be elicited by the go/no go paradigm and reaches its maximum in frontal areas. For example, in Eimer's (1993) work, the participants were asked to respond to a specific letter (go stimulus) but not to another one (non-go stimulus). Their results showed that a larger N2 amplitude was elicited by the non-go stimulus than the go stimulus (Eimer, 1993). In Consumer Neuroscience domain, the N2 was also found to reflect the cognitive control or conflict monitoring while evaluating the marketing-related stimuli (Ma et al., 2010; Jin et al., 2017; Shang et al., 2017). For example, Shang et al.'s (2017) work found that

a larger N2 amplitude was induced by perception of a social risk in contrast with the control condition during the evaluation of a product. This finding was explained that N2 may reflect the cognitive control or conflict monitoring as the participants have to regulate the cognitive conflict between an inherent desire to purchase the item and the discordant information they obtained from social interactions (Shang et al., 2017). Furthermore, in a more recent study, Jin et al. (2017) found the larger N2 amplitude can also be induced by negatively framed market information compared with positively framed one. Based on existing findings, we hypothesized that negative marketing stimuli will bring a greater cognitive control or enhanced conflict monitoring during consumption decision-making and thus elicit a larger N2 (negative polarity) compared with positive marketing related stimuli.

As has been introduced above, in the current study the ERPs was adopted to investigate consumers' attitudes toward eco-labeled food at the brain level. According to the aforementioned findings, we hypothesized that in the current study, eco-labeled and non-labeled seafood pictures may induce different brain activities, which would be manifested in discrepancies in P2 and N2 amplitudes. As the P2 can reflect the emotional valence of stimuli, we posited that eco-labeled seafood may elicit a smaller P2 amplitude than the non-labeled one, as participants would generally have more positive feelings toward eco-labeled seafood. In addition, as negative marketing related stimuli would elicit a larger N2 compared with positive marketing related stimuli, we also predicted the non-labeled seafood to elicit a larger N2 than the eco-labeled one.

# MATERIALS AND METHODS

## Participants

Twenty-one (M = 13, F = 8) right-handed healthy undergraduates and graduates from Ningbo University were recruited to participate in the current experiment. Their ages ranged from 19 to 25, with a mean age of 20.94 (SD = 1.39). All of the participants were native Chinese speakers without any history of neurological disorder or mental diseases. Their visual acuity was normal or corrected-to-normal. This study was carried out in accordance with the recommendations of Academy of Neuroeconomics and Neuromanagement at Ningbo University. The protocol was approved by the Academy of Neuroeconomics and Neuromanagement at Ningbo University. All subjects gave written informed consent in accordance with the Declaration of Helsinki. Data from two male participants were discarded because of excessive artifacts during electroencephalogram (EEG) recordings. Thus, data from 19 valid participants entered into the final analysis.

## Materials

This experiment has two experimental conditions (eco-labeled vs. non-labeled seafood), and there are 80 trials in each condition. Thus, the whole experiment involved 160 stimuli (80 seafood × 2 label categories). The 80 seafood pictures depict 20 fishes (e.g., *Pseudosciaena crocea*, pomfret, groupers, sierras, and squids), 20 shellfishes (e.g., oysters, razor clam, small clam, sea scallop and arctic shellfish), 20 crabs (e.g., shuttle crab, green crab, king crab, Dungeness crab, and tourteau) and 20 shrimps (e.g., prawn, lobster, squilla, greasyback shrimp, and *Penaeus orientolis*). To be standardized, all pictures were downloaded from the Internet and edited by Photoshop 7.0 (Adobe Systems Incorporated, San Jose, CA, USA).

The selected eco-labeling adopts the MSC label, which is certified by the most prominent eco-labeling certifier, the MSC. This Council is an international non-profit organization established to address the problem of unsustainable fishing and to safeguard seafood resources for the future. The blue MSC label makes it easier for everyone to find seafood that has been caught by fisheries that care for the environment. Because MSC is a label for seafood, only seafood pictures were selected to prepare the stimuli.

The standardization process takes the following steps: (1) the seafood image was tailored and processed to the size of 300*150 pixels and was located in a 270*360 pixel black background; and (2) consistent with Linder et al.'s (2010) work, each stimulus contained a food picture with a label. Seafood pictures were shown along with the original MSC label in the labeled condition, while the same food pictures were shown with an artificially created logo indicating production of that food in a conventional manner in the non-labeled condition. In other words, the food pictures used were identical in these two conditions, and the only difference lies in the label. The label was located in the top-right corner of the stimuli, the size of which was 70*100 pixel.

A pretest was conducted to ensure that subjects in the formal experiment can recognize most of the seafood demonstrated in the picture. Only when a participant candidate could recognize at least 75% of the seafood that would appear in the experiment could they pass the pretest and move on to the formal experimental. All the stimuli were randomly and evenly divided into four blocks in the formal experiment.

## Procedure

Participants were asked to sit in a sound-attenuated room 100 cm away from a computer-controlled monitor, on which the stimuli were presented. They were provided with a keypad to report their purchase intention of each product through a 4-point scale. Before the experiment started, the participant received a brochure introducing the meaning of the MSC label, including its certification authority, mission and so on.

As shown in **Figure 1**, each trial began with a fixation cross against a black background for 400–600 ms, which was followed by a blank screen lasting for 500 ms. Afterwards, a picture with a specific seafood and a label appeared for 2,000 ms. Then, the participants were asked to rate their purchase intention for the current item on a 4-point scale (1 means the lowest purchase intention, and 4 means the highest purchase intention). Stimuli, recording triggers and response data were presented and recorded using E-Prime 2.0 (Psychology Software Tools, Pittsburgh, PA, USA). The participants were asked to minimize blinks, eye movements, and muscle movements during the whole experiment. The formal experiment started after 10 practice trials.

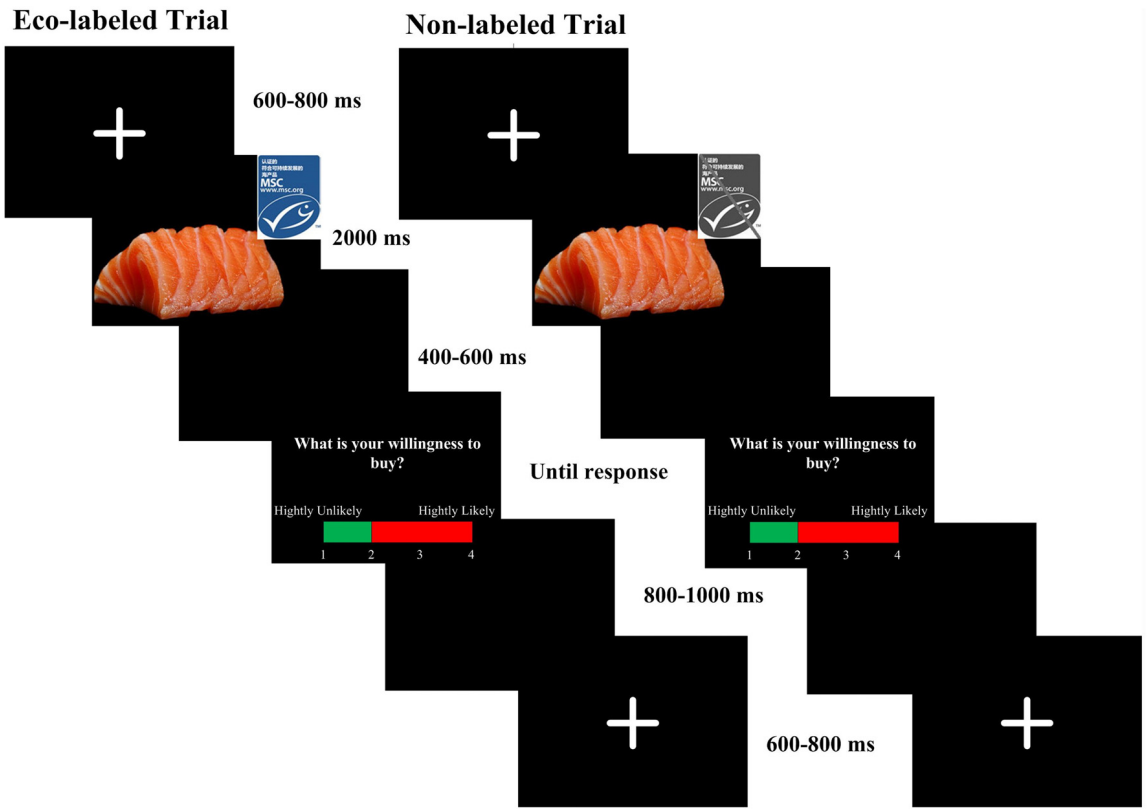


**FIGURE 1 |** Experimental task: participants were instructed to report their purchase intention toward two kinds of food (eco-labeled and non-labeled) on a 4-point scale. Electroencephalograms (EEGs) were recorded from the subjects throughout the experiment.

## Electroencephalogram (EEG) Recording and Analysis

EEGs were recorded with a cap containing 64 Ag/AgCl electrodes and a Neuroscan Synamp2 Amplifier (Scan 4.5, Neurosoft Labs, Inc). Its sampling rate was 500 Hz, and channel data were online band-pass-filtered from 0.05 Hz to 70 Hz. The experiment started only when electrode impedances were reduced to below 5 kΩ. A cephalic (forehead) location between FPz and Fz was used as the ground, and the left mastoid was used for reference. Electrooculograms (EOGs) were recorded from electrodes placed at 10 mm from the lateral canthi of both eyes (horizontal EOG) and above and below the left eye (vertical EOG), and EOG artifacts were off-line corrected for all subjects using the method proposed by Semlitsch et al. (1986).

EEG data were off-line transformed based on the average of the left and right mastoid references. EEG recordings were digitally filtered with a low-pass filter at 30 Hz (24 dB/Octave). For ERP analyses, the data were segmented for the epoch from 200 ms before the onset of stimulus on the video monitor to 800 ms after its onset, with the first 200 ms pre-target interval as a baseline. Trials containing amplifier clippings, bursts of electromyography activity, or peak-to-peak deflections exceeding ±100 μV were excluded. For each participant, EEG recordings were averaged for the two experimental conditions (eco-labeled vs. non-labeled) over each recording site.

The time window of 160–220 ms was chosen for the analysis of P2 based on visual observation and the guideline proposed by Picton et al. (2000). Ten electrodes (F3, F1, Fz, F2, F4, FC3, FC1, FCz, FC2 and FC4) in the frontal-central area were included into the statistical analysis. A 2 (Label: eco-labeled vs. non-labeled) × 10 (electrodes) ANOVA was conducted for the P2 analysis. Spearman correlation analysis was conducted between the P2 amplitude and participants' purchasing intention.

When it comes to the N2 component, from visual inspection of the grand averaged waveforms, it occurred to us that the waveform of N2 (300–400 ms) is superimposed on its preceding positive deflection (160–220 ms). Therefore, we used the peak-to-peak measure instead of the mean amplitude approach when analyzing the N2. As was suggested by Picton et al. (2000), the use of a peak-to-peak measure is justified in the following conditions: (1) a peak is superimposed on a slower wave or (2) an adjacent peak-trough ensemble is considered to reflect the same functional process. Within each averaged waveform, the amplitudes of the distinct peaks of the two conditions were measured as follows: first, a positive peak was identified as the

most positive peak within 160–220 ms after stimulus onset. Second, a negative peak (N2) was defined as the most negative peak observed within 300–400 ms after stimulus onset. The peak-to-peak amplitude of the N2 was obtained by subtracting amplitude of the positive peak amplitude from the negative peak. Then, a 2 (Label: eco-labeled vs. non-labeled) × 6 (electrode: F1, Fz, F2, FC1, FCz and FC2) ANOVA was performed for the N2 analysis.

The Greenhouse-Geisser (Greenhouse and Geisser, 1959) correction was applied for violation of the sphericity assumption in appropriate parts of the ANOVA (uncorrected *df*s were reported with ε and the corrected *p*-values). Effect sizes are provided as partial eta squared ($\eta_p^2$).

# RESULTS

## Behavioral Results

Behavioral data was shown in **Figure 2**. A pairwise *t*-test was conducted between purchase intention of eco-labeled and non-labeled food, which showed a significant main effect ($t_{(1,18)} = 6.730$, $p < 0.001$). This finding indicated that subjects had a greater willingness to buy eco-labeled food (M = 2.862, SD = 0.554) compared with non-labeled food (M = 1.780, SD = 0.523).

## ERP Results

### P2 Analysis

The two-way 2 (label) × 10 (electrodes) ANOVA for P2 amplitude in the time window of 160–220 ms suggested a significant main effect of label ($F_{(1,18)} = 8.632$, $p = 0.009$, $\eta_p^2 = 0.324$). As shown in **Figure 3A** the eco-labeled condition (M = 1.178 μV, SE = 0.911) elicited a smaller P2 amplitude (positive polarity: a larger voltage value means a larger amplitude) than the non-labeled condition (M = 1.923 μV, SE = 0.898).

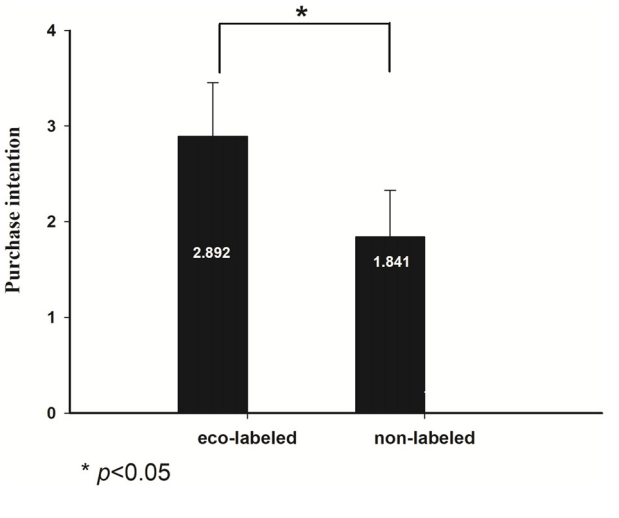


**FIGURE 2 |** Behavioral results of the purchasing intention: subjects' purchase intentions of the two kinds of food (eco-labeled and non-labeled) are provided.

We calculated the Spearman correlation between P2 amplitude on FCz and participants' purchase intention. Since the amplitude of P2 reached its peak on FCz in both conditions, we take FCz as an example. As shown in **Figure 3B**, the P2 amplitude in FCz was negatively correlated with participants' purchase intention of the seafood ($r = -0.416$, $p = 0.009$), which suggested that a larger P2 amplitude will be observed when participants have less willingness to buy the product. Magnitudes of all the 10 chosen electrodes as well as the average amplitude were significantly correlated with the purchase intention as well as shown in **Table 1**. The brain topography was shown in **Figure 3C**, which showed that the main difference between the two conditions was in the frontal part.

### N2 Analysis

The results of the two-way 2 (label) × 6 (electrodes) ANOVA for N2 amplitude are shown in **Figure 4**, which suggested that the non-labeled condition (M = −4.157 μV, SE = 0.633) elicited a significantly larger N2 amplitude compared to the eco-labeled condition (M = −3.376 μV, SE = 0.448; $F_{(1,18)} = 5.262$, $p = 0.034$, $\eta_p^2 = 0.226$).

# DISCUSSION

By adopting the ERPs approach, the present study explored neurocognitive processes associated with consumers' attitude and emotion toward eco-labeled food. Behaviorally, participants' purchase intention of eco-labeled food is significantly greater than non-labeled one. This finding is in accordance with the previous behavioral and empirical studies which suggested that participants preferred to buy eco-labeled food (e.g., Wessells et al., 1999; Xu et al., 2012).

A highlight of this study is that we explored consumers' evaluation of environmental-beneficial eco-labeling and compared the neural differences between one's processing of self- and others-beneficial food labels. Specifically, we observed a markedly smaller P2 when pictures of eco-labeled food were presented. We conjectured that it suggests that compared with non-labeled food, eco-labeled food would induce more positive emotions. Evidences from existing studies jointly provide rationale for our conjecture. First, as has been mentioned in the introduction, the P2 represents preliminary evaluation of the affective content of stimuli, and a decreased P2 amplitude is observed when displayed stimuli give rise to positive feelings (Carretié et al., 2001; Wang et al., 2012). Second, Previous studies on eco-labeling showed that it can successfully evoke one's positive emotions (Atkinson and Rosenthal, 2014). Third, the current behavioral results showed that participants' purchase intention of eco-labeled food is larger compared with non-labeled food. Subsequent analysis also showed that the P2 amplitude was negatively correlated with participants' purchase intention in this study. According to previous studies, positive emotions to marketing stimuli are positively related with behavioral intentions (White and Yu, 2005; Jang and Namkung, 2009; Kim and Lennon, 2013). Last but not least, the current paradigm is adapted

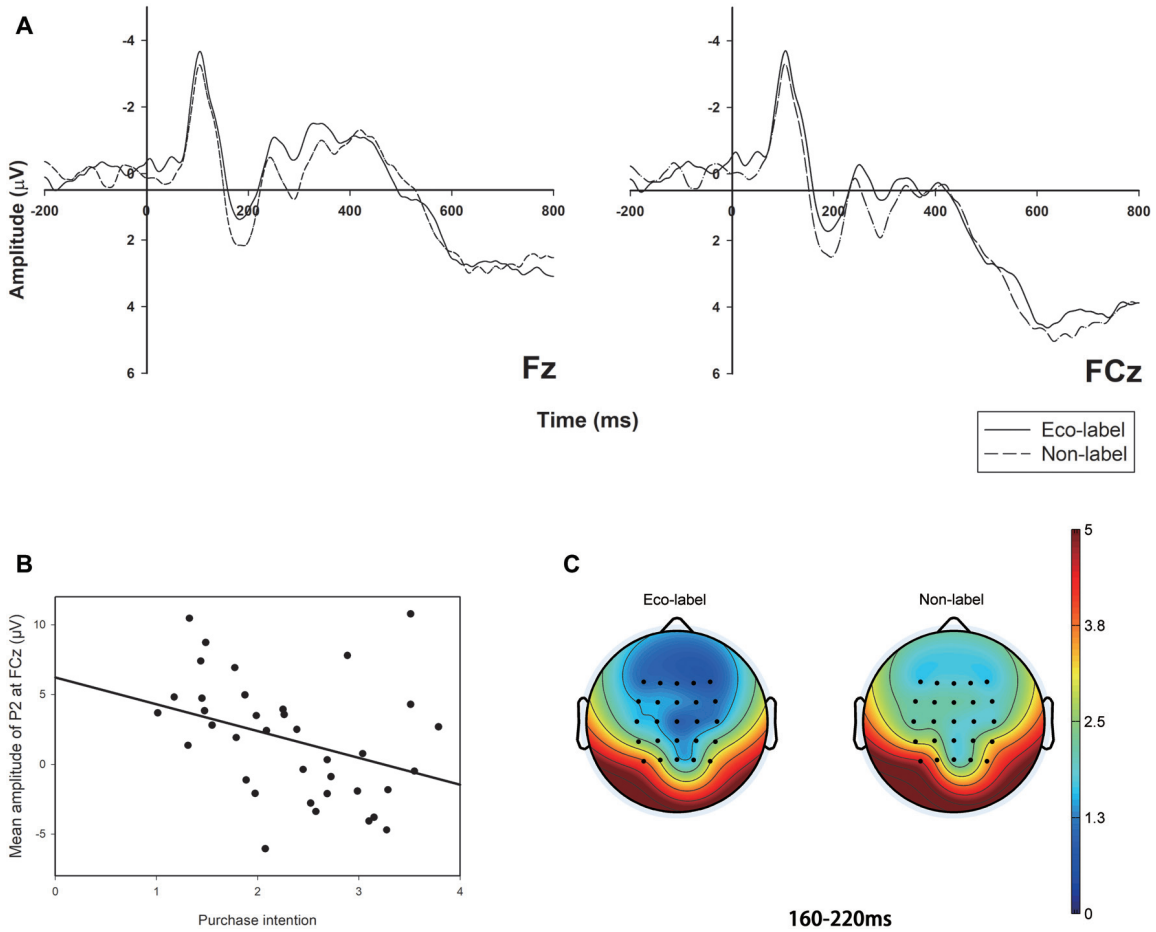


**FIGURE 3 |** P2 Grand-averaged event-related potential (ERP) waveforms in the frontal region with two electrodes, linear correlation between the amplitude of certain ERP components and behavioral results as well as the brain topography: **(A)** the comparison between eco-labeled and non-labeled food conditions in representative electrodes (Fz and FCz); the solid line represents eco-labeled food, whereas the dashed line represents the non-labeled food; **(B)** linear correlation between the amplitude of P2 and the participants' purchase intention; **(C)** the brain topography of the two conditions at the P2 time window of 160–220 ms.

from Linder et al.'s (2010) work. In their study, the fMRI was adopted. Processing of organic-labeled food information was found to increase activities of the ventral striatum, which is responsible for emotional processing, compared with that of conventionally labeled food info (Davidson and Irwin, 1999; Linder et al., 2010). To conclude, as both social and monetary rewards were found to activate the same striatum area (Izuma et al., 2008), our findings may support the hypothesis that consumers' preference can be reflected in brain activities, and specifically, the preferred eco-label can induce more positive emotions.

As a complementary finding, we also observed a significantly larger N2 in the non-labeled condition than in the eco-labeled one. As has been introduced in the introduction, N2 is a negative deflection which reflects the cognitive control or conflict monitoring brought by marketing stimuli. Therefore, the current results suggested that participants have to implement enhanced conflict monitoring while making the purchase intention of non-labeled food. This is consistent with the P2 and behavioral results, which suggested that eco-label food would induce more positive emotions and result in a higher purchase intention. Thus, we considered that consumers preferred the eco-labeled food emotionally and behaviorally and involved less cognitive conflicts.

**TABLE 1 |** Spearman correlation results between P2 amplitude and participants' purchase intention.

| | $R^2$ | *p* |
|---|---|---|
| F3 | −0.424 | 0.008 |
| F1 | −0.390 | 0.016 |
| Fz | −0.396 | 0.014 |
| F2 | −0.380 | 0.019 |
| F4 | −0.332 | 0.042 |
| FC3 | −0.498 | 0.001 |
| FC1 | −0.423 | 0.00 |
| FCz | −0.416 | 0.009 |
| FC2 | −0.415 | 0.010 |
| FC4 | −0.438 | 0.006 |
| Mean amplitudes | −0.407 | 0.011 |

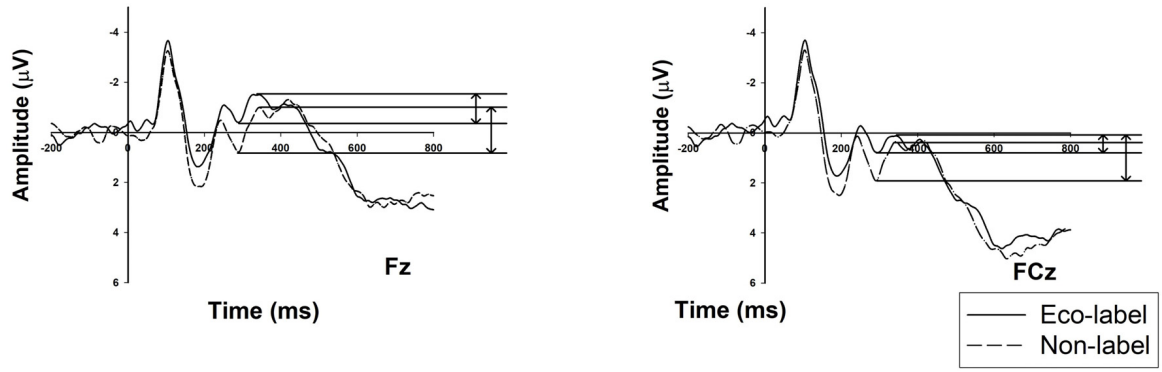


**FIGURE 4 |** N2 Grand-averaged ERP waveforms in the frontal region with two electrodes: the comparison between eco-labeled and non-labeled food conditions in representative electrodes (Fz and FCz); the solid line represents eco-labeled food, whereas the dashed line represents the non-labeled food.

Previous studies have reported similar results during the evaluation of organic-labeled food (Linder et al., 2010). However, the organic-labeled food pays more attention to the benefit of consumers themselves, while eco-labeled food focuses on its non-harm to the environment. Thus, as a complement to previous findings (Linder et al., 2010), our findings suggested that the environmental beneficial labeling can also induce consumers' positive emotions and lead to positive behavioral preferences. Another highlight of this study is that, different from previous studies, the high temporal resolution technique of ERPs was adopted. Both of the two ERP components being examined are at the stage of early automatic processing, which reflect preliminary sensory encoding of stimuli. Thus, our findings suggest that environmental-friendly eco-labeling can elicit one's positive emotions at early stage of cognitive processing.

Previous studies suggested that in addition to paying attention to one's own interest, one's thoughts and actions may also focus on activities that are evolutionary and adaptive, which contribute to the accumulation of enduring personal resources, such as development and maintenance of social relationships (Fredrickson, 1998; Fredrickson et al., 2008). Therefore, a potential mechanism underlying the observed effect in the current study might be social expectation, as to comply with the socially desirable act is beneficial to the development and maintenance of social relationships. Specifically, as behaving pro-environmentally is socially desirable and expected by members of the society as a whole (Milfont, 2009), the environmentally friendly behavior of eco-labeling can induce positive emotions and bring less cognitive conflict, which leads to the preference of environmentally beneficial eco-labeling.

We acknowledge some limitations in the current study. First, the sample size is relatively small. Only 19 valid participants were included in the final data analyses. Although the effect sizes of the current results are large enough according to previous studies, which stated that an effect size greater than 0.2 represents a large effect (Cohen, 1988), a greater sample size is always welcome to further verify the basic findings. Second, subjective preference for seafood was not measured in this study. When designing this experiment, we did not measure subjective preference for seafood, considering that this experiment has a within-subject design and the only difference between the two experimental conditions lies in the label. In other words, we examined the same participant's attitude to both labeled and non-labeled seafood. If one has (or does not have) a preference for seafood, his/her attitudes toward labeled and non-labeled seafood may still vary. However, after repeated deliberation, we deem that different evaluations of the seafood may further influence one's concern about the eco-label. This is what we neglected to consider when conducting this experiment, and follow-up studies that address our limitations are highly welcome.

To conclude, by employing the ERPs approach, the current study provided electrophysiological evidences for consumers' preference for and positive emotions toward eco-labeled food. Specifically, we found the environmental-friendly eco-labeling to arouse consumers' positive feelings and to bring less cognitive conflict, which were reflected in decreased P2 and N2 amplitudes, respectively. The current finding further suggests that, although the environmental-friendly eco-labeling was socially beneficial, which was not to the consumers' own interests, it would still induce their positive emotions to the product and then result in a greater purchasing intention. The socially desirable theory was adopted to give a tentative explanation to this phenomenon. Additionally, this study shows the value of neuroscientific methods in revealing consumers' (implicit) emotions as well as predicting their behavioral responses in studies of consumer behaviors.

## AUTHOR CONTRIBUTIONS

JJ, XD, LM and HY conceived the idea; wrote the article. JJ, LM and HY prepared the experimental stimuli. JJ collected the data and ran the data analysis. XD supervised the project. All authors made intellectual contributions to this project and gave approval to the final version of the manuscript for submission.

## FUNDING

This work was supported by grant 71603139 from the National Natural Science Foundation of China, grant 16YJC630049 from Humanities and Social Sciences Foundation of Ministry of Education of China, grant 17NDJC013Z from the Social Science Association of Zhejiang Province as a key project and sponsored by K.C. Wong Magna Fund in Ningbo University. The current work is the initial stage results of project "Research on the Regional Marine Environment Governance of the Yangtze River Delta under the Integration Strategy-Initiated from Ningbo" (16JDGH043) from key research center (Ocean Culture and Economics) of Philosophy and Social Sciences in Zhejiang Province. The funders had no role in study design; in the collection, analysis and interpretation of data; in the writing of the report; and in the decision to submit the article for publication.

## REFERENCES

Annett, L., Muralidharan, V., Boxall, P., Cash, S., and Wismer, W. (2008). Influence of health and environmental information on hedonic evaluation of organic and conventional bread. *J. Food Sci.* 73, H50–H57. doi: 10.1111/j.1750-3841.2008.00723.x

Atkinson, L., and Rosenthal, S. (2014). Signaling the Green sell: the influence of eco-label source, argument specificity and product involvement on consumer trust. *J. Advert.* 43, 33–45. doi: 10.1080/00913367.2013.834803

Boksem, M. A. S., and Smidts, A. (2015). Brain responses to movie trailers predict individual preferences for movies and their population-wide commercial success. *J. Mark. Res.* 52, 482–492. doi: 10.1509/jmr.13.0572

Camerer, C., and Yoon, C. (2015). Introduction to the journal of marketing research special issue on neuroscience and marketing. *J. Mark. Res.* 52, 423–426. doi: 10.1509/0022-2437-52.4.423

Carretié, L., Mercado, F., Tapia, M., and Hinojosa, J. A. (2001). Emotion, attention and the 'negativity bias', studied through event-related potentials. *Int. J. Psychophysiol.* 41, 75–85. doi: 10.1016/s0167-8760(00)00195-1

Cohen, J. (1988). *Statistical Power Analysis for the Behavioral Sciences.* 2nd Edn. Hillsdale, MI: Lawrence Erlbaum Associates.

Davidson, R. J., and Irwin, W. (1999). The functional neuroanatomy of emotion and affective style. *Trends Cogn. Sci.* 3, 11–21. doi: 10.1016/s1364-6613(98)01265-0

Eimer, M. (1993). Effects of attention and stimulus probability on ERPs in a Go/Nogo task. *Biol. Psychol.* 35, 123–138. doi: 10.1016/0301-0511(93)90009-w

Enax, L., Hu, Y., Trautner, P., and Weber, B. (2015). Nutrition labels influence value computation of food products in the ventromedial prefrontal cortex. *Obesity* 23, 786–792. doi: 10.1002/oby.21027

Fisher, R. J., Markvandenbosch, M., and Antia, K. D. (2008). An empathy-helping perspective on consumers' responses to fund-raising appeals. *J. Consum. Res.* 35, 519–531. doi: 10.1086/586909

Folstein, J. R., and Van Petten, C. V. (2008). Influence of cognitive control and mismatch on the N2 component of the ERP: a review. *Psychophysiology* 45, 152–170. doi: 10.1111/j.1469-8986.2007.00602.x

Fredrickson, B. L. (1998). What good are positive emotions? *Rev. Gen. Psychol.* 2, 300–319. doi: 10.1037/1089-2680.2.3.300

Fredrickson, B. L., Cohn, M. A., Coffey, K. A., Pek, J., and Finkel, S. M. (2008). Open hearts build lives: positive emotions, induced through loving-kindness meditation, build consequential personal resources. *J. Pers. Soc. Psychol.* 95, 1045–1062. doi: 10.1037/a0013262

Friedman, D., and Jonson, R. Jr. (2000). Event-related potential (ERP) studies of memory encoding and retrieval: a selective review. *Microsc. Res. Tech.* 51, 6–28. doi: 10.1002/1097-0029(20001001)51:1<6::aid-jemt2>3.0.co;2-r

Gountas, J., and Gountas, S. (2007). Personality orientations, emotional states, customer satisfaction and intention to repurchase. *Journal of Business Research* 60, 72–75. doi: 10.1016/j.jbusres.2006.08.007

Grabenhorst, F., Schulte, F. P., Maderwald, S., and Brand, M. (2013). Food labels promote healthy choices by a decision bias in the amygdala. *Neuroimage* 74, 152–163. doi: 10.1016/j.neuroimage.2013.02.012

Greenhouse, S. W., and Geisser, S. (1959). On methods in the analysis of profile data. *Psychometrika* 24, 95–112. doi: 10.1007/bf02289823

Huang, Y.-X., and Luo, Y.-J. (2006). Temporal course of emotional negativity bias: an ERP study. *Neurosci. Lett.* 398, 91–96. doi: 10.1016/j.neulet.2005.12.074

Izuma, K., Saito, D. N., and Sadato, N. (2008). Processing of social and monetary rewards in the human striatum. *Neuron* 58, 284–294. doi: 10.1016/j.neuron.2008.03.020

Jang, S. C., and Namkung, Y. (2009). Perceived quality, emotions and behavioral intentions: application of an extended Mehrabian-Russell model to restaurants. *J. Bus. Res.* 62, 451–460. doi: 10.1016/j.jbusres.2008.01.038

Jin, J., Zhang, W., and Chen, M. (2017). How consumers are affected by product descriptions in online shopping: event-related potentials evidence of the attribute framing effect. *Neurosci. Res.* 125, 21–28. doi: 10.1016/j.neures.2017.07.006

Johnston, R. J., Wessells, C. R., Donath, H., and Asche, F. (2001). A contingent choice analysis of ecolabelled seafood comparing consumer preferences in the United States and Norway. *J. Agric. Resour. Econ.* 26, 20–39.

Junghöfer, M., Bradley, M. M., Elbert, T. R., and Lang, P. J. (2001). Fleeting images: a new look at early emotion discrimination. *Psychophysiology* 38, 175–178. doi: 10.1111/1469-8986.3820175

Kim, J., and Lennon, S. J. (2013). Effects of reputation and website quality on online consumers' emotion, perceived risk and purchase intention. *J. Res. Interact. Mark.* 7, 33–56. doi: 10.1108/17505931311316734

Lai, V. T., and Huettig, F. (2016). When prediction is fulfilled: insight from emotion processing. *Neuropsychologia* 85, 110–117. doi: 10.1016/j.neuropsychologia.2016.03.014

Linder, N. S., Uhl, G., Fliessbach, K., Trautner, P., Elger, C. E., and Weber, B. (2010). Organic labeling influences food valuation and choice. *Neuroimage* 53, 215–220. doi: 10.1016/j.neuroimage.2010.05.077

Lusk, J. L., Crespi, J. M., Cherry, J. B. C., Mcfadden, B. R., Martin, L. E., and Bruce, A. S. (2015). An fMRI investigation of consumer choice regarding controversial food technologies. *Food Qual. Prefer.* 40, 209–220. doi: 10.1016/j.foodqual.2014.10.005

Ma, Q., Wang, K., Wang, X., Wang, C., and Wang, L. (2010). The influence of negative emotion on brand extension as reflected by the change of N2: a preliminary study. *Neurosci. Lett.* 485, 237–240. doi: 10.1016/j.neulet.2010.09.020

Milfont, T. L. (2009). The effects of social desirability on self-reported environmental attitudes and ecological behaviour. *Environmentalist* 29, 263–269. doi: 10.1007/s10669-008-9192-2

Nilsson, A., Hansla, A., and Biel, A. (2014). Feeling the green? Value orientation as a moderator of emotional response to green electricity. *J. Appl. Soc. Psychol.* 44, 672–680. doi: 10.1111/jasp.12258

Paulmann, S., and Kotz, S. A. (2008). Early emotional prosody perception based on different speaker voices. *Neuroreport* 19, 209–213. doi: 10.1097/wnr.0b013e3282f454db

Picton, T., Bentin, S., Berg, P., Donchin, E., Hillyard, S., Johnson, R., et al. (2000). Guidelines for using human event-related potentials to study cognition: recording standards and publication criteria. *Psychophysiology* 37, 127–152. doi: 10.1111/1469-8986.3720127

Schupp, H. T., Stockburger, J., Codispoti, M., Junghöfer, M., Weike, A. I., and Hamm, A. O. (2007). Selective visual attention to emotion. *J. Neurosci.* 27, 1082–1089. doi: 10.1523/JNEUROSCI.3223-06.2007

Semlitsch, H. V., Anderer, P., Schuster, P., and Presslich, O. (1986). A solution for reliable and valid reduction of ocular artifacts, applied to the P300 ERP. *Psychophysiology* 23, 695–703. doi: 10.1111/j.1469-8986.1986.tb00696.x

Shang, Q., Pei, G., and Jin, J. (2017). My friends have a word for it: event-related potentials evidence of how social risk inhibits purchase intention. *Neurosci. Lett.* 643, 70–75. doi: 10.1016/j.neulet.2017.02.023

Smidts, A., Hsu, M., Sanfey, A. G., Boksem, M. A., Ebstein, R. B., Huettel, S. A., et al. (2014). Advancing consumer neuroscience. *Mark. Lett.* 25, 257–267. doi: 10.1007/s11002-014-9306-1

Sörqvist, P., Haga, A., Langeborg, L., Holmgren, M., Wallinder, M., Nöstl, A., et al. (2015). The green halo: mechanisms and limits of the eco-label effect. *Food Qual. Prefer.* 43, 1–9. doi: 10.1016/j.foodqual.2015.02.001

Sörqvist, P., Hedblom, D., Holmgren, M., Haga, A., Langeborg, L., Nöstl, A., et al. (2013). Who needs cream and sugar when there is eco-labeling? Taste and willingness to pay for "eco-friendly" coffee. *PLoS One* 8:e80719. doi: 10.1371/journal.pone.0080719

Wang, X., Huang, Y., Ma, Q., and Li, N. (2012). Event-related potential P2 correlates of implicit aesthetic experience. *Neuroreport* 23, 862–866. doi: 10.1097/wnr.0b013e3283587161

Wessells, C. R., Johnston, R. J., and Donath, H. (1999). Assessing consumer preferences for ecolabeled seafood: the influence of species, certifier and household attributes. *Am. J. Agric. Econ.* 81, 1084–1089. doi: 10.2307/1244088

White, K., and Peloza, J. (2009). Self-benefit versus other-benefit marketing appeals: their effectiveness in generating charitable support. *J. Mark.* 73, 109–124. doi: 10.1509/jmkg.73.4.109

White, C., and Yu, Y. T. (2005). Satisfaction emotions and consumer behavioral intentions. *J. Serv. Mark.* 19, 411–420. doi: 10.1108/08876040510620184

Xu, P., Zeng, Y., Fong, Q., Lone, T., and Liu, Y. (2012). Chinese consumers' willingness to pay for green-and eco-labeled seafood. *Food Control* 28, 74–82. doi: 10.1016/j.foodcont.2012.04.008

Yoon, E. Y., Humphreys, G. W., Kumar, S., and Rotshtein, P. (2012). The neural selection and integration of actions and objects: an fMRI study. *J. Cogn. Neurosci.* 24, 2268–2279. doi: 10.1162/jocn_a_00256

**Conflict of Interest Statement**: The authors declare that the research was conducted in the absence of any commercial or financial relationships that could be construed as a potential conflict of interest.

frontiers in Human Neuroscience

ORIGINAL RESEARCH
published: 16 October 2018
doi: 10.3389/fnhum.2018.00412

# How the Dorsolateral Prefrontal Cortex Controls Affective Processing in Absence of Visual Awareness – Insights From a Combined EEG-rTMS Study

*Kati Keuper[1,2,3,4†], Esslin L. Terrighena[3,4†], Chetwyn C. H. Chan[5*], Markus Junghoefer[1,2*‡] and Tatia M. C. Lee[3,4,6,7*‡]*

[1] Institute of Biomagnetism and Biosignalanalysis, University Hospital Münster, University of Münster, Münster, Germany, [2] Otto Creutzfeldt Center for Cognitive and Behavioral Neuroscience, University of Münster, Münster, Germany, [3] Laboratory of Neuropsychology, The University of Hong Kong, Pokfulam, Hong Kong, [4] Laboratory of Social Cognitive Affective Neuroscience, The University of Hong Kong, Pokfulam, Hong Kong, [5] Applied Cognitive Neuroscience Laboratory, Department of Rehabilitation Sciences, The Hong Kong Polytechnic University, Kowloon, Hong Kong, [6] The State Key Laboratory of Brain and Cognitive Sciences, The University of Hong Kong, Pokfulam, Hong Kong, [7] Institute of Clinical Neuropsychology, The University of Hong Kong, Pokfulam, Hong Kong

OPEN ACCESS

**Edited by:**
*Xiaochu Zhang, University of Science and Technology of China, China*

**Reviewed by:**
*Lars Kuchinke, International Psychoanalytic University Berlin, Germany*
*Thomas Dresler, Universität Tübingen, Germany*

***Correspondence:**
*Chetwyn C. H. Chan*
*Chetwyn.chan@polyu.edu.hk*
*Markus Junghoefer*
*Markus.Junghoefer@uni-muenster.de*
*Tatia M. C. Lee*
*Tmclee@hku.hk*

*[†] These authors have contributed equally to this work*

*[‡] These authors are regarded as senior authors*

**Received:** 29 May 2018
**Accepted:** 24 September 2018
**Published:** 16 October 2018

**Citation:**
*Keuper K, Terrighena EL, Chan CCH, Junghoefer M and Lee TMC (2018) How the Dorsolateral Prefrontal Cortex Controls Affective Processing in Absence of Visual Awareness – Insights From a Combined EEG-rTMS Study. Front. Hum. Neurosci. 12:412. doi: 10.3389/fnhum.2018.00412*

The dorsolateral prefrontal cortex (DLPFC) plays a key role in the modulation of affective processing. However, its specific role in the regulation of neurocognitive processes underlying the interplay of affective perception and visual awareness has remained largely unclear. Using a mixed factorial design, this study investigated effects of inhibitory continuous theta-burst stimulation (cTBS) of the right DLPFC (rDLPFC) compared to an Active Control condition on behavioral ($N$ = 48) and electroencephalographic ($N$ = 38) correlates of affective processing in healthy Chinese participants. Event-related potentials (ERPs) in response to passively viewed subliminal and supraliminal negative and neutral natural scenes were recorded before and after cTBS application. We applied minimum-norm approaches to estimate the corresponding neuronal sources. On a behavioral level, we found evidence for reduced emotional interference by, and less negative and aroused ratings of negative supraliminal stimuli following rDLPFC inhibition. We found no evidence for stimulation effects on self-reported mood or the behavioral discrimination of subliminal stimuli. On a neurophysiological level, rDLPFC inhibition relatively enhanced occipito-parietal brain activity for both subliminal and supraliminal negative compared to neutral images (112–268 ms; 320–380 ms). The early onset and localization of these effects suggests that rDLPFC inhibition boosts automatic processes of "emotional attention" independently of visual awareness. Further, our study reveals the first available evidence for a differential influence of rDLPFC inhibition on subliminal versus supraliminal neural emotion processing. Explicitly, our findings indicate that rDLPFC inhibition selectively enhances late (292–360 ms) activity in response to supraliminal negative images. We tentatively suggest that this differential frontal activity likely reflects enhanced awareness-dependent down-regulation of negative scene processing, eventually leading to facilitated disengagement from and less negative and aroused evaluations of negative supraliminal stimuli.

**Keywords: EEG, rTMS, emotion perception, awareness, ERP, dlPFC**

## INTRODUCTION

The human brain preferentially processes negative information, even if this information is presented in absence of visual awareness (e.g., Bayle et al., 2009; for an fMRI meta-analysis, see Meneguzzo et al., 2014). This is reflected in faster detection and preferential processing of negative images, even if participants cannot report image contents above chance (i.e., subliminal exposure; Fazio, 2001; Spruyt et al., 2002; Winkielman and Berridge, 2004; Winkielman et al., 2005; Kiss and Eimer, 2008; Sabatini et al., 2009; Meneguzzo et al., 2014). A key brain structure that affects automatic and elaborate affective perception and modulates corresponding motivational responses is the dorsolateral prefrontal cortex (DLPFC) (Grisaru et al., 2001; Spielberg et al., 2008; De Raedt et al., 2010; Leyman et al., 2011). It plays a crucial role in top-down analysis and regulation of affective processing (Banks et al., 2007; Goldin et al., 2008; Notzon et al., 2017; Wager et al., 2008; Zwanzger et al., 2014). Valence-specific characteristics of such inhibitory control processes might be influenced by hemispheric asymmetries in prefrontal brain functioning (Grimshaw and Carmel, 2014). Such asymmetries likely modulate withdrawal and approach-related affect, whereby right hemispheric dominance has been linked to negative, withdrawal-related processing (for reviews, see Davidson, 1992a,b; Harmon-Jones et al., 2010; Grimshaw and Carmel, 2014).

In the current study, we investigated how the processing of subliminal and supraliminal negative, withdrawal-associated stimuli is affected by right DLPFC (rDLPFC) inhibition via transcranial magnetic stimulation (TMS). By combining TMS with electroencephalographic measures, we specifically investigate the spatiotemporal interplay of rDLPFC function and bottom-up emotion processing.

Electro- and magnetoencephalographic (EEG/MEG) studies have revealed that early (∼80–120 ms after stimulus onset) (Keil et al., 2002; Olofsson and Polich, 2007; Feng et al., 2014; Zhu et al., 2015) and mid-latency (∼120–300 ms) (Liddell et al., 2004; Williams et al., 2004; Balconi and Lucchiari, 2005b, 2007; Kiss and Eimer, 2008; Pegna et al., 2008; Kim et al., 2013; Nakajima et al., 2015) event-related potentials and fields (ERPs/ERFs) in response to both subliminal and supraliminal negative material differ from those to positive or neutral material. For example, Liddell et al. (2004) recorded ERPs in response to subliminally (10 ms) and supraliminally (170 ms) presented backward-masked fearful and neutral faces. This study reported main effects for emotion with enhanced frontal (FZ) amplitudes for fearful faces in mid-latency and late components. Further, findings revealed a double dissociation for subliminal and supraliminal fear processing whereby enhanced amplitudes were recorded at mid-latencies over central electrode sites (CZ) for subliminal fearful compared to neutral faces, while similar patterns for supraliminal fear faces were limited to late latencies and frontocentral sites (CZ, FZ). Studies employing source-reconstruction approaches have localized enhanced early and mid-latency responses to negative affective (vs. neutral) visual stimuli in occipital and temporal regions (Junghöfer et al., 2001, 2006; Olofsson et al., 2008; Bayle et al., 2009) and, less consistently, frontal brain regions (e.g., Bayle et al., 2009). These neural responses are thought to reflect mechanisms of "emotional attention," that is, enhanced automatic orientation to and ongoing preferential encoding of salient stimuli (Halgren and Marinkovic, 1995; Davidson, 2001; Liddell et al., 2004; Williams et al., 2004, 2006). Such mechanism may facilitate a fast feedforward transfer of motivationally relevant information from low- to high-level processing areas (Schupp et al., 2003a,b, 2004a,b; Carretié et al., 2004, 2006; Delplanque et al., 2006; Eimer et al., 2008; Olofsson et al., 2008). Conversely, enhanced late processing (∼300–600 ms) of negative compared to neutral material (Liddell et al., 2004; Kiss and Eimer, 2008; Nakajima et al., 2015) has mainly been found in response to supraliminal stimuli that are available to visual awareness (Liddell et al., 2004; Williams et al., 2004; Balconi and Lucchiari, 2005a,b, 2007; Pegna et al., 2008). Typically, negative–neutral dissociations at late processing stages are supported by distributed posterior and frontal brain networks (Olofsson et al., 2008). Functionally, they have been associated with elaborate processes, including ongoing (perceptual) stimulus evaluation (Leyman et al., 2009; Wessing et al., 2016; for review, see Schupp et al., 2006) and top-down emotion regulation (Kozel and George, 2002; Siegle et al., 2007; Poldrack et al., 2008; Guse et al., 2010; Ochsner et al., 2012; Ironside et al., 2016; Wessing et al., 2016).

The involvement of the prefrontal cortex in the regulation of affective processing is well-documented (Sarter et al., 2001; Bishop et al., 2004; Bressler et al., 2008; Bayle and Taylor, 2010). Despite a large corpus of studies investigating effects of right and left prefrontal rTMS on mood (e.g., Fitzgerald and Daskalakis, 2011) and affective processing (e.g., van Honk et al., 2002; Tupak et al., 2013), the *causal* role of the DLPFC in the modulation neurocognitive mechanisms associated with affective perception of negative, withdrawal-related stimuli has remained largely unclear. To date, only two TMS studies have explored effects of rDLPFC inhibition or excitation on the spatiotemporal dynamics of negative stimulus processing (Zwanzger et al., 2014; Notzon et al., 2017). Zwanzger et al. (2014) recorded magnetoencephalographic ERFs while individuals viewed supraliminal fearful and neutral facial expressions before and after inhibitory repetitive TMS (rTMS) to the rDLPFC or sham stimulation. Results showed that rDLPFC inhibition compared to sham increased early occipito-parietal and mid-latency temporal activations for fearful faces. Likewise, Notzon et al. (2017) reported increased neural activity to fearful faces in right occipital and right temporal regions, after inhibitory compared to excitatory rTMS was applied on the right rDLPFC. Given that such activity has been previously associated with automatic valence-specific feedforward processing of, and emotional attention to both subliminal and supraliminal negative images (Liddell et al., 2004; Williams et al., 2004; Balconi and Lucchiari, 2005a; Balconi, 2006; Balconi and Lucchiari, 2007; Eimer et al., 2008; Kiss and Eimer, 2008; Pegna et al., 2008; Smith, 2012; Kim et al., 2013; Nakajima et al., 2015), the modulatory influence of rDLPFC on early and mid-latency brain signatures of emotion perception might be independent of visual awareness. However, this remains to be tested experimentally, as all previous neurophysiological neurostimulation studies have employed supraliminal stimuli only.

The only behavioral study directly comparing effects of rDLPFC inhibition on subliminal and supraliminal negative processing investigated rTMS effects on top-town control in a modified emotional Stroop task (van Honk et al., 2002). Participants were asked to name the color of masked (subliminal) and unmasked (supraliminal) fearful vs. neutral faces. Findings revealed that inhibitory rDLPFC compared to sham stimulation decreased reaction times for color naming of supraliminal but not subliminal fearful faces. Such reduction of negativity biases following right-hemispheric prefrontal inhibition provides support to theories on hemispheric asymmetries of PFC function (for reviews, see Davidson, 1992a,b; Harmon-Jones et al., 2010; Grimshaw and Carmel, 2014). In this framework, rDLPFC inhibition should reduce right-hemispheric dominance and thereby attenuate negative, withdrawal-related responses. Importantly, van Honk et al. (2002) tentatively suggest that a reduction of negativity biases following rDLPFC inhibition might be limited to stimuli that enter participants' awareness.

Taken together, current literature indicates that rDLPFC inhibition may on the one hand enhance early bottom-up affect-related brain activation in early and mid-latency ERP/ERF components (Notzon et al., 2017; Zwanzger et al., 2014), which might be independent of stimulus awareness. On the other hand, in presence of visual awareness, rDLPFC inhibition may specifically facilitate elaborate emotion-regulatory behaviors (van Honk et al., 2002). In general, such elaborate mechanisms are reflected in relatively late components (Liddell et al., 2004; Williams et al., 2004; Kiss and Eimer, 2008; Nakajima et al., 2015). However, the spatiotemporal dynamics underpinning awareness-dependent effects of rDLPFC inhibition on affective processing have not yet been revealed.

This study investigated neural and behavioral effects of rDLPFC inhibition on negative scene processing with and without visual awareness. EEG recordings were taken while individuals viewed subliminal and supraliminal negative and neutral natural scenes before (Pre-cTBS) and after (Post-cTBS) inhibitory continuous Theta Burst Stimulation (cTBS, Huang et al., 2005) to the rDLPFC vs. the vertex (Cz, Active Control). Our study followed a 2 × 2 × 2 × 2 mixed factorial design with the between-subject factor Stimulation (rDLPFC inhibition vs. Active Control) and the within-subject factors Session (Pre-cTBS vs. Post-cTBS), Exposure (subliminal vs. supraliminal), and Valence (negative vs. neutral). After the passive viewing task, participants completed several behavioral tasks and self-report mood assessments. Based on these measures we set out to explore the impact of rDLPFC inhibition on (1) affective state, (2) attention mechanisms, (3) valence and arousal ratings, and (4) emotion discrimination in presence and absence of visual awareness.

First, before cTBS application (i.e., Pre-cTBS measurements), we expected enhanced processing of negative compared to neutral images for both subliminal and supraliminal exposure at early (80–120 ms) and mid-latency ERPs (120–300 ms) in occipito-temporal regions (Carretié et al., 2004; Liddell et al., 2004; Junghöfer et al., 2006). As predicted by a feedforward mechanism, such activity was hypothesized to progress toward parietal and frontal regions indexing increasing involvement of higher cortical networks in negative processing. Furthermore, exposure and valence were expected to interact at mid-latency (>120 ms) and/or late intervals (>300 ms) (Liddell et al., 2004; Williams et al., 2004; Kiss and Eimer, 2008; Nakajima et al., 2015). Due to a lack of previous ERP studies employing source localization, clear predictions regarding the underlying neuronal generators were not possible. Based on the above reviewed literature, an involvement of posterior and/or frontal brain regions seemed likely.

Second, and more importantly, we expected differential behavioral and neural effects of rDLPFC inhibition compared to Active Control. Based on van Honk et al. (2002), rDLPFC inhibition was expected to reduce negative processing biases at a behavioral level. On a neuronal level, rDLPFC inhibition was expected to result in increased early (80–120 ms) and mid-latency (120–300 ms) negative-neutral dissociations at occipito-parietal and temporal regions with enhanced activity for negative affective pictures (Zwanzger et al., 2014; Notzon et al., 2017). While these early effects were hypothesized to be independent from visual awareness, interactions of stimulation, exposure, and valence on neural activation differences (Post-cTBS *minus* Pre-cTBS) were predicted for late latencies (>300 ms). In accordance with top-down influences on elaborate processing of negative material (Bishop et al., 2004; Liddell et al., 2004; Kiss and Eimer, 2008; Pegna et al., 2008; Ochsner et al., 2009; Nakajima et al., 2015), an involvement of frontal structures was hypothesized.

# MATERIALS AND METHODS

## Participants

Forty-eight healthy participants (25 females, 23 males) between 18 and 37 years ($M$ = 21.46, $SD$ = 4.25) completed the behavioral tasks. EEG was recorded for a subset of 38 participants (22 females, 16 males) between 18 and 35 years ($M$ = 21.21, $SD$ = 3.81). Participants were recruited at two Hong Kong universities via advertisement and word-of-mouth. Participants received 250 HKD or course credits. In line with the Declaration of Helsinki, the study was approved by the Human Research Ethics Committee for Non-clinical Faculties, The University of Hong Kong, as well as the Human Subjects Ethics Sub-committee of the Hong Kong Polytechnic University. All participants were healthy Chinese Hong Kong locals, fluent in English and with normal or corrected-to-normal vision. Eligibility for receiving rTMS stimulation in accordance with TMS safety guidelines (Grossheinrich et al., 2009; Rossi et al., 2009) was determined using an extended version of the screening standard Transcranial Magnetic Stimulation Safety Questionnaire (TMS-SQ; Rossi et al., 2009). Individuals reporting current or past occurrence of epilepsy, strokes, head- or brain-related medical conditions, loss of consciousness, hearing problems, eye surgery, spinal cord injuries, mental health issues, medication intake, or mental implants were excluded from this study. Further exclusion criteria were pregnancy and family history of epilepsy. Participants were assigned one of two stimulation protocols (rDLPFC vs. Active Control) in a pseudorandom manner so that both groups were matched for gender, age,

and professional status. *Post hoc* statistical analyses further confirmed that groups were comparable regarding depression scores [Chinese Version of Beck's Depression Inventory – II (BDI-II); Beck et al., 1996; Byrne et al., 2004], state and trait anxiety [Chinese Version of State-Trait Anxiety Inventory (STAI); Spielberger et al., 1968; Spielberger, 1983; Shek, 1988, 1993], emotional regulation [Emotion Regulation Questionnaire (ERQ); Gross and John, 2003], and Pre-cTBS mood [Chinese Affect Scale (CAS); Hamid and Cheng, 1996, see **Table 1**].

## Procedure

Individuals filled in the TMS-SQ prior to the experimental session and only those eligible for safe rTMS administration were invited to attend. Individual sessions were conducted in a quiet room after participants had learned about the procedures and equipment and given written informed consent. Participants first completed BDI-II, STAI, ERQ, and CAS. Then, EEG cap and corresponding ocular electrodes were adjusted on the head of the participant and Pre-cTBS EEG activity was recorded while participants were exposed to the passive viewing presentation. No response was required during the presentation. In line with prior research (Liddell et al., 2004), participants were instructed to concentrate on the images and told they may need to answer questions about these images afterward. Subsequently, offline cTBS was administered on rDLPFC or vertex, the Active Control region, before participants viewed the Post-cTBS presentation accompanied by EEG recordings. Upon completion, participants again filled the CAS and then performed five behavioral tasks in the following order: facial

**TABLE 1 |** Description of the EEG and the Behavioral Samples.

| **Behavioral sample** | | | | | | |
|---|---|---|---|---|---|---|
| | | **Sample** | **rDLPFC inhibition** | **Active control** | | |
| Total *N* | | 48 | 24 | 24 | | |
| Gender *N* | Males | 23 | 11 | 12 | | |
| | Females | 25 | 13 | 12 | | |
| Profession *N* | Student | 46 | 23 | 23 | | |
| | Employed | 2 | 1 | 1 | | |
| | | ***M*(*SD*)** | ***M*(*SD*)** | ***M*(*SD*)** | ***F*(1,47)** | ***p*** |
| Age (years) | | 21.45 (4.25) | 21.08 (3.76) | 21.83 (4.74) | 0.368 | 0.547 |
| BDI | | 0.42 (0.31) | 0.36 (0.22) | 0.49 (0.38) | 1.986 | 0.166 |
| STAI (state) | | 36.94 (9.18) | 36.13 (9.40) | 37.75 (9.09) | 0.371 | 0.546 |
| STAI (trait) | | 45.13 (10.39) | 44.92 (10.24) | 45.33 (10.75) | 0.019 | 0.891 |
| ERQ (reappraisal) | | 5.33 (0.78) | 5.53 (0.74) | 5.13 (0.79) | 3.199 | 0.080 |
| ERQ (suppression) | | 4.51 (1.24) | 4.65 (1.09) | 4.38 (1.38) | 0.569 | 0.454 |
| CAS (pos) | | 2.24 (0.84) | 2.31 (0.81) | 2.16 (0.88) | 0.400 | 0.530 |
| CAS (neg) | | 1.09 (0.95) | 1.10 (0.94) | 1.08 (0.98) | 0.006 | 0.940 |
| **EEG sample (subgroup of behavioral sample)** | | | | | | |
| | | **Sample** | **rDLPFC inhibition** | **Active control** | | |
| Total *N* | | 38 | 19 | 19 | | |
| Gender *N* | Males | 16 | 8 | 8 | | |
| | Females | 22 | 11 | 11 | | |
| Profession *N* | Student | 36 | 18 | 18 | | |
| | Employed | 2 | 1 | 1 | | |
| | | ***M*(*SD*)** | ***M*(*SD*)** | ***M*(*SD*)** | ***F*(1,36)** | ***p*** |
| Age (years) | | 21.21 (3.81) | 20.42 (1.89) | 22.00 (5.00) | 1.657 | 0.206 |
| BDI | | 0.39 (0.32) | 0.35 (0.17) | 0.43 (0.41) | 0.771 | 0.386 |
| STAI (state) | | 1.91 (0.43) | 1.99 (0.30) | 1.93 (0.54) | 0.057 | 0.813 |
| STAI (trait) | | 2.22 (0.48) | 2.15 (0.34) | 2.30 (0.58) | 0.913 | 0.346 |
| ERQ (reappraisal) | | 5.35 (0.81) | 5.52 (0.68) | 5.19 (0.91) | 1.555 | 0.221 |
| ERQ (suppression) | | 4.51 (1.12) | 4.53 (0.83) | 4.47 (1.36) | 0.032 | 0.859 |
| CAS (pos) | | 2.20 (0.80) | 2.27 (0.19) | 2.13 (0.84) | 0.290 | 0.593 |
| CAS (neg) | | 1.04 (0.91) | 1.08 (0.83) | 0.99 (0.99) | 0.102 | 0.752 |

*BDI, Becks Depression Inventory; STAI, State-Trait-Anxiety-Inventory; ERQ, Emotion Regulation Questionnaire; reapp, reappraisal; sup, suppression; CAS, Chinese Affect Scale; pos, positive; neg, negative; M, mean, SD, standard deviation, rTMS, repetitive transcranial magnetic stimulation.*

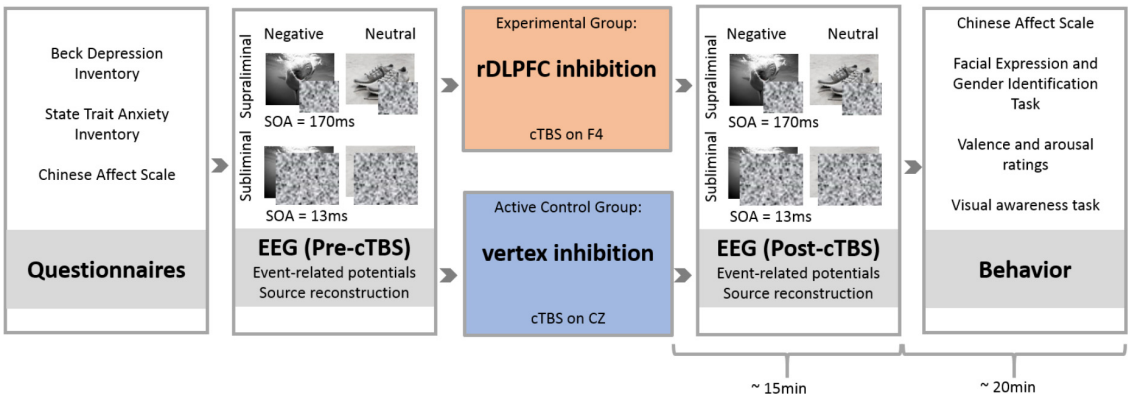


**FIGURE 1 |** Experimental paradigm. After completing questionnaires, participants were assigned to either the experimental or the Active Control group. In the experimental group (rDLPFC inhibition group), rDLPFC excitability was reduced by administration of inhibitory continuous Theta Burst Stimulation (cTBS) to electrode F4. The Active Control group received cTBS on CZ (vertex). Before and after cTBS-application (Pre-cTBS vs. Post-cTBS), participants viewed four blocks of backward-masked supraliminal (SOA = 170 ms) and subliminal (SOA = 13 ms) negative (e.g., shark) and neutral (e.g., shoes) scenes. Thereby, each of the overall eight blocks contained a different set of 50 images to avoid the emergence of familiarity effects or habituation through repetition of identical images across blocks. Within each block, each image was presented three times. The assignment of images to blocks was counterbalanced across subjects. Following EEG measurements, participants completed behavioral tasks in order to evaluate effects of cTBS stimulation on self-reported mood (CAS), on attention engagement to and disengagement from emotional stimuli (Facial Expression and Gender Identification Task), on valence and arousal ratings of images, and on discrimination of negative versus neutral images under supra- and subliminal viewing conditions (visual awareness task). All post-cTBS measurements were completed within 35 min after stimulation.

expression identification, facial gender identification (Nitsche et al., 2012; Zwanzger et al., 2014; Conson et al., 2015), valence and arousal evaluation of images (Feeser et al., 2014; Zwanzger et al., 2014; Balconi and Cobelli, 2015; Era et al., 2015), and detection and discrimination visual awareness tasks (Liddell et al., 2004; Williams et al., 2004). After conclusion of the experiment, participants were thoroughly debriefed and received contact details of the experimenter, supervisor, ethics committee, and university counseling services. The entire session took approximately 110 min (**Figure 1**).

## cTBS Protocol

To inhibit the rDLPFC, a continuous Theta-Burst Stimulation protocol (cTBS; Huang et al., 2005) was applied over the right F4 electrode using a Magstim stimulator (Magstim, Morrisville, NC, United States[1]) with a 70-mm figure-eight shaped double coil (Grossheinrich et al., 2009; Cho et al., 2010; Zwanzger et al., 2014). Explicitly, 200 bursts of three pulses at 50 Hz each were administered with a frequency of 5 Hz which resulted in a total of 600 pulses, i.e., train of three pulses was repeated every 200 ms for approximately 42 s (Cho et al., 2010; Oberman et al., 2011). Such brief cTBS has been associated with temporarily reduced cortical excitability for approximately 45 times stimulation length, i.e., around 30 min for 42 s stimulation (Klimesch, 1996; Oberman et al., 2011). The Active Control stimulation was administered on the vertex at electrode Cz, which is a region often targeted in control conditions (Kwan et al., 2007; Balconi and Ferrari, 2013) and which was shown to play a minor role in emotion processing, as revealed by a recent meta-analysis of 157 fMRI studies on emotional face and emotional scene processing (Sabatinelli et al., 2011). By choosing an active-controlled design, we intended to match the sensory experience of experimental and control group as closely as possible. Considering mixed empirical evidence for the assumption that individual motor or phosphene thresholds capture site-nonspecific factors of cortical excitability that will generalize to other brain areas (Boroojerdi et al., 2002; Gerwig et al., 2003; Antal et al., 2004; Stokes et al., 2012), we stimulated all participants with a fix intensity of 50% maximal stimulator output. All safety requirements regarding frequency, length, and stimulation intensity were adhered to (Wassermann, 1998; Machii et al., 2006; Rossi et al., 2009; Oberman et al., 2011). No side effects or discomfort were reported.

[1]http://www.magstim.com/

## Stimuli

For the passive viewing paradigm, we selected 200 negative and 200 neutral color images from well-established databases, including the International Affective Picture System (IAPS) (Lang et al., 1999, 2005; Gong and Wang, 2016), the Chinese Affective Picture Systems (CAPS) (Lu et al., 2005), and the Geneva Affective Picture Database (GAPED) (Dan-Glauser and Scherer, 2011). Pre-existing valence and arousal ratings for all images (Lang et al., 1999, 2005; Lu et al., 2005; Dan-Glauser and Scherer, 2011) were collapsed onto a nine-point scale in accordance with existing IAPS ratings. Valence and arousal ratings ranged from low to high, indicating negative-to-positive valence and low-to-high arousal, respectively. *T*-tests confirmed that negative images were rated as significantly lower in valence ($M = 2.44$, $SD = 0.93$) and higher in arousal ($M = 6.05$, $SD = 0.93$) than neutral images [valence: $M = 5.37$, $SD = 0.73$; arousal: $M = 3.29$, $SD = 1.40$; $t(398) = -34.982$, $p < 0.001$, $t(398) = 23.19$, $p < 0.001$, respectively].

All images were transformed into grayscale and luminance-matched via the SHINE toolbox (Willenbockel et al., 2010a,b) on Matlab 2008a (Mathworks, Natick, MA, United States[2]). This toolbox computes an average luminance histogram from the histograms of all images and matches all images to this reference [Negative: $M = 104.25$, $SD = 5.70$; Neutral: $M = 104.32$, $SD = 5.67$; $t(398) = -0.114$, $p = 0.909$]. Scrambled masks were made from each image, rendering its contents unrecognizable. The Matlab-based script calculated total pixels per image, and randomly changed the position of each pixel while keeping image width and height constant. Each negative and neutral image was followed by its corresponding scrambled mask.

## Experimental Task: Passive Viewing Paradigm

For the EEG recordings, participants sat in a quiet, dimly lit room. Visual images were presented centrally on a 13in SVGA monitor with a 1920 × 1080 resolution (refresh rate: 75 Hz), which was situated 60 cm from participants' eyes. Horizontal images were 195 × 260 px in size with a visual angle of 4 × 6° and vertical pictures were 142 × 195 px in size with a visual angle of 4 × 4.65°. As in previous EEG studies on subliminal emotion perception, backward-masked stimuli were presented in a block-design (Liddell et al., 2004; Williams et al., 2004) against a black background. Before and after cTBS application (Pre-cTBS vs. Post-cTBS), participants viewed four blocks of subliminal-neutral, supraliminal-neutral, subliminal-negative, and supraliminal-negative images. Thereby, each of the overall eight blocks contained a different set of 50 images to avoid the emergence of familiarity effects or habituation through frequent repetition of identical images. Stimuli were presented by means of E-Prime 2.0 Professional Software (Psychology Software Tools, Inc., Sharpsburg, PA, United States[3]). Within each block, 50 negative or neutral images were presented in random order and repeated three times. This resulted in 150 images per block and 600 images per presentation. Participants could choose to take a short break between blocks. To avoid confounding effects of order or stimulus sets, the order of blocks and the assignment of stimuli to experimental blocks were counterbalanced across participants using the Latin Square system.

Subliminal images were presented for 13 ms, supraliminal images for 170 ms. All images were preceded by a jittered inter-stimulus fixation cross (700–1000 ms) and succeeded by a scrambled mask (170 ms). Visual angles and exposure times were in accordance with those shown in previous subliminal research to ensure image content remains unreportable above chance (Liddell et al., 2004; Hsu et al., 2008; Japee et al., 2009; Ibáñez et al., 2011; Lee et al., 2011; Pegna et al., 2011; Li and Lu, 2014; Nakajima et al., 2015).

## EEG Recording and Analysis

Electroencephalographic signals were recorded in a sound-attenuated chamber with low lighting and electromagnetic shield, using a 64-channel TMS-compatible EEG cap (i.e., with non-magnetic electrodes and cables and flat electrodes to minimize TMS-coil to scalp distance; Easycap GmbH, Germany, Asian head shape) according to the International 10–20 system (Blom and Anneveldt, 1982). During recording, FCz was used as a reference point. Horizontal and vertical eye movement potentials were recorded via four ocular electrodes placed 1 cm from the outer canthus of each eye and 1 cm above and below the left eye. Following prior research (Smith, 2012; Hintze et al., 2014), all electronic impedances were kept at less than 10 kΩ and data were recorded continuously at a sampling rate of 1000 Hz. Signals were amplified via SynAmp2 and an online anti-aliasing low-pass filter was applied (Neuroscan Compumedics Ltd., Australia[4]).

Electroencephalographic data preprocessing was conducted via Curry 7 (Neuroscan Compumedics Ltd., Australia). Offline, the raw data were resampled to 250 Hz, and re-referenced to average reference. Data were filtered with a digital 0.1 Hz high-pass and a 35 Hz low-pass filter. ERP epochs from 200 ms pre-stimulus to 600 ms post-stimulus were computed separately for the four within-subject conditions (supraliminal-negative, supraliminal-neutral, subliminal-negative, subliminal-neutral) for rDLPFC inhibition and Active Control groups. The pre-stimulus interval from −200 ms to stimulus onset was used for baseline correction. Artifact rejection and eye blink correction were conducted and trials with amplitudes ±70 μV were rejected. This procedure led to rejection of an average of 14.3% of trials, equally distributed across all conditions [session × exposure × valence × stimulation; $F(1,36) = 0.255$, $p = 0.617$], which was deemed acceptable given prior research (Smith, 2012; Nomi et al., 2013; Hintze et al., 2014).

Separately for our experimental conditions, we then estimated the current sources for the averaged epochs using the L2-Minimum-Norm-Estimates approach (L2-MNE) (Hämäläinen and Ilmoniemi, 1994) and a spherical head model with evenly distributed 3 (radial, azimuthal, and polar direction) × 197 dipoles (see Hintze et al., 2014). The L2-MNE technique does not make prior assumptions regarding location of number of sources, but instead extracts generators based on the distribution of electric potential across the head sphere (Hämäläinen and Ilmoniemi, 1994; Hauk, 2004). Across all participants and conditions, the Tikhonov regularization parameter $k$ was set at 0.1.

Two main analyses were conducted. First, to replicate previous affective processing literature, a 2 × 2 factorial repeated measures ANOVA was conducted on Pre-cTBS data with the factors exposure (supraliminal vs. subliminal) and valence (negative vs. neutral). Second, to investigate the effects of rDLPFC inhibition on subliminal and supraliminal emotion processing, difference scores for neural responses were calculated by subtracting Pre-cTBS from Post-cTBS ERPs. These scores were submitted to a 2 × 2 × 2 mixed ANOVA with the factors exposure (supraliminal vs. subliminal), valence (negative vs. neutral), and stimulation (rDLPFC inhibition vs. Active Control).

A non-parametric statistical testing procedure that included correction for multiple comparisons (Maris and Oostenveld,

[2]http://www.mathworks.com/

[3]https://www.pstnet.com/

[4]compumedicsneuroscan.com

2007), similar to cluster-based permutation approaches used in hemodynamic imaging, was applied to reveal effects of interest. As part of this procedure, *F*-values of spatially neighboring (minimally five neighboring dipoles) and temporally consecutive (minimally five consecutive time points) test dipoles below a critical alpha level of $p = 0.05$ (sensor-level criterion) were summed up to so-called cluster masses. Based on prior research, the current study separately investigated time windows consistently reported to show affect-specific neural potentials during both supraliminal and subliminal negative facial expression processing. Correspondingly, the time windows of interest were defined as early from 80 to 120 ms (Carretié et al., 2004; Jiang et al., 2009; Keuper et al., 2013; Nomi et al., 2013; Li and Lu, 2014), mid-latency from 120 to 300 ms (Junghöfer et al., 2001; Carretié et al., 2004; Jiang et al., 2009; Kim et al., 2013) and late from 300 to 600 ms (Schupp et al., 2000, 2006; Olofsson et al., 2008; Pegna et al., 2011; Kim et al., 2013). To avoid latency biases toward late processes with much stronger and more sustained neural activations, cluster masses of relevant effects were calculated separately for the early (80–120 ms), mid-latency (120–300 ms), and late (300–600 ms) post-onset time intervals. They were tested against a random cluster-based permutation alpha level of $p = 0.05$, which was established via Monte Carlo simulations of identical analyses based on 1000 permuted drawings of experimental data sets (i.e., the *F* distributions for each time interval were built up by the 1000 clusters with the biggest masses within each time interval). Thus, only cluster masses exceeding an alpha level of $p = 0.05$ within each time interval were considered (cluster-level criterion). All significant spatiotemporal clusters with a minimum interval length of 10 ms and three neighboring source dipoles (Zwanzger et al., 2014) were further delineated in *post hoc* Bonferroni corrected paired and independent *t*-tests.

## Behavioral Tasks and Analyses

Participants completed behavioral tasks following the Post-cTBS EEG-measurement in order to evaluate behavioral effects of stimulation on self-reported mood (CAS, Hamid and Cheng, 1996), on attention engagement to and disengagement from facial stimuli with fearful and neutral expressions (Facial Expression and Gender Identification Task, Zwanzger et al., 2014), on valence and arousal ratings of negative and neutral images, and on discrimination of negative and neutral images under supra- and subliminal viewing conditions (visual awareness task; Liddell et al., 2004; Williams et al., 2004). All tasks were conducted within a time-window of 35 min after cTBS application.

### Chinese Affect Scale (CAS)

The CAS is a self-report scale measuring negative and positive affective mood states that has been specifically created for the Chinese population. It is reported to have high internal ($\alpha > 0.89$) and moderate re-test reliabilities ($r = 0.43$–$0.47$) (Hamid and Cheng, 1996). Importantly, it has been shown to adequately capture minor changes in momentary mood state (Hamid and Cheng, 1996). Using independent-sample *t*-tests, changes (Post-cTBS *minus* Pre-cTBS) in positive and negative affect ratings were compared between the rDLPFC inhibition group and the Active Control group.

### Facial Expression and Gender Identification Task

In the facial expression and gender identification task, participants were asked to either indicate the facial expression or the gender of 80 supraliminal gray-scale face images (40 males, 40 females) showing fearful (i.e., negative, 50%) and neutral (50%) facial expressions. The paradigm has been validated in a prior study exploring the impact of rTMS on affective processing (for details, please see Zwanzger et al., 2014). Reaction times and accuracy were recorded for both tasks and submitted to four separate 2 × 2-mixed ANOVAs with the within-subject factor valence (negative vs. neutral), the between-subjects factor stimulation (rDLPFC inhibition vs. Active Control). The Facial Expression and Gender Identification tasks were administered with the goal to identify between-group differences in negative biases due to enhanced attention orienting to and/or reduced attention disengagement from negative compared to neutral stimuli following rDLPFC inhibition. Preferential emotional attention orienting is typically reflected in the faster detection of negative compared to neutral stimuli. By contrast, tasks requiring disengagement of emotional attention toward non-emotional characteristics of stimuli (e.g., gender identification task) typically reveal slower reaction times for negative stimuli.

### Valence and Arousal Ratings

In the valence and arousal ratings, participants were exposed to 25 neutral and 25 negative images (195 × 260 px, visual angle 4 × 6°) that had been randomly chosen from the 400 images of the passive viewing paradigm. These images were presented against a white background and remained on the screen until participants had given their responses. For each image, participants rated valence and arousal on two separate computerized Visual Analogue Scales (VAS), which ranged from extremely negative to extremely positive (0–100), and not aroused to extremely aroused (0–100), respectively. Valence and arousal ratings were submitted to two separate 2 × 2-mixed ANOVAs with the within-subject factor valence (negative vs. neutral) and the between-subjects factor stimulation (rDLPFC inhibition vs. Active Control).

### Visual Awareness Task

In the visual awareness task (Liddell et al., 2004; Williams et al., 2004), we presented 96 negative and neutral images, randomly chosen from the passive viewing paradigm, in a subliminal or supraliminal block using E-prime 2.0 Professional. Images were preceded by a fixation cross of 500 ms, but otherwise followed the same parameters as the passive viewing paradigm. Participants were required to make a forced-choice decision after each image, indicating whether image contents were negative or neutral (discrimination task). This task was administered to confirm that subliminal images were not reportable above chance and to assess effects of rDLPFC inhibition on discrimination abilities. D-prime scores close to 0 ($d' = 0$) and greater than 1 ($d' > 1$), respectively, confirm that images did or did not remain subliminal below visual awareness (Green and Swets, 1966; Eimer et al., 2008;

Pegna et al., 2011; Smith, 2012; Zhang et al., 2012). In order to test for effects of stimulation on visual awareness, *d'* scores of the subliminal and the supraliminal block were submitted to two separate 2 × 2-way ANOVAs with the within-subject factors valence (negative vs. neutral) and the between-subjects factor stimulation (rDLPFC inhibition vs. Active Control).

# RESULTS

## Valence and Exposure Effects in Neurophysiological Pre-cTBS Measures

In order to replicate main effects of emotion and interactions of emotion and exposure, we separately investigated early (80–120 ms), mid-latency (120–300 ms), and late epochs (300–600 ms; e.g., Junghöfer et al., 2001; Schupp et al., 2006; Keuper et al., 2013) using 2 × 2 factorial repeated measures ANOVAs with the factors exposure (supraliminal vs. subliminal) and valence (negative vs. neutral). These revealed two significant clusters for the main effect of valence with greater amplitudes for negative than neutral images. First, in an early (96–116 ms) time window, effects were located in left occipital regions [$F(1,37) = 7.963$; $p = 0.008$; **Figure 2A**]. Second, at mid.latencies (160–228 ms) effects were found in left occipito-parietal and right temporo-parietal areas [$F(1,37) = 15.220$; $p < 0.001$; **Figure 2B**]. No late main effects were found for valence.

We further found a significant interaction between exposure and valence at late latencies (300–380 ms) in a frontal cluster with pronounced right hemisphere activation [$F(1,37) = 12.676$, $p = 0.001$; **Figure 2C**]. *Post hoc t*-tests demonstrated that this interaction was driven by increased amplitudes to subliminal negative compared to neutral images [$t(37) = 3.149$, $p = 0.003$]. Supraliminal compared to subliminal images elicited enhanced overall amplitudes in both valence conditions [negative: $t(37) = 8.320$, $p < 0.001$; neutral: $t(37) = 10.434$, $p < 0.001$]. No significant difference was found between amplitudes elicited by supraliminal negative compared to neutral images [$t(37) = -1.300$, $p = 0.202$].

## Effects of rDLPFC Inhibition on Behavioural Measures

### Chinese Affect Scale: No Effects of rDLPFC Inhibition on Self-Reported Mood

Independent-sample *t*-tests revealed no effects of stimulation on self-reported mood [negative affect: $t(46) = 0.768$, $p = 0.447$; positive affect: $t(46) = -0.514$, $p = 0.610$]. These findings suggest that rDLPFC inhibition did not affect the immediate affective state.

### Facial Expression and Gender Identification Task: Effects of rDLPFC Inhibition on Emotional Attention Engagement and Disengagement

To explore effects of stimulation on valence identification, we investigated response accuracies and reaction times of the Facial Expression Identification task using a 2 × 2-mixed ANOVAs with within-subjects factor valence and between-subjects factor stimulation (**Figures 3A,B**). Data revealed a significant main effect of valence on response accuracy [$F(1,46) = 11.559$, $p = 0.001$] with fewer correct responses for fearful ($M = 0.88$, $SD = 0.17$) compared to neutral faces ($M = 0.96$, $SD = 0.08$). There were neither a main effect of stimulation [$F(1,46) = 0.658$, $p = 0.421$] nor an interaction of valence and stimulation [$F(1,46) = 0.457$, $p = 0.503$] on response accuracy. Reaction times for facial expression identification were not affected by valence [$F(1,46) = 0.515$, $p = 0.477$], stimulation [$F(1,46) = 0.014$, $p = 0.907$], or their interaction [$F(1,46) = 0.051$, $p = 0.822$].

To explore stimulation effects on attentional disengagement from negative material, we investigated response accuracy and reaction times in the facial gender identification task. As rDLPFC inhibition was shown to facilitate attention disengagement (van Honk et al., 2002), we expected relatively higher response accuracies and/or faster reaction times specifically for the gender identification of negative faces following rDLPFC inhibition compared to Active Control. We found a significant main effect of valence on response accuracy [$F(1,46) = 11.806$, $p = 0.001$] with fewer correct responses for fearful ($M = 0.93$, $SD = 0.12$) compared to neutral faces ($M = 0.95$, $SD = 0.12$, **Figure 3C**). These findings are in line with research demonstrating emotional interference effects, which suggest that it is more difficult to disengage from emotional compared to neutral material, as emotional materials capture attention. Response accuracies were not affected by stimulation [$F(1,46) = 0.338$, $p = 0.564$] nor by the interaction between valence and stimulation [$F(1,46) = 0.041$, $p = 0.841$]. However, we found a significant interaction between stimulation and valence for reaction time [$F(1,46) = 4.073$, $p = 0.049$, **Figure 3D**]. While participants in the Active Control condition showed longer reaction times to fearful ($M = 681.16$ ms, $SD = 155.10$ ms) than to neutral facial expressions [$M = 611.19$ ms, $SD = 116.22$ ms, $\text{interference}_{\text{Neg}-\text{Neu}}$: $M = 69$ ms, $SD = 107.27$ ms; $t(23) = 3.194$, $p = 0.004$], this effect was absent in the rDLPFC inhibition group [$\text{interference}_{\text{Neg}-\text{Neu}}$: $M = -14.04$ ms, $SD = 173.41$ ms, $t(23) = -0.397$, $p = 0.695$]. Compared to the Active Control group, the rDLPFC inhibition group showed significantly shorter reaction times to fearful [$M = 583.94$ ms, $SD = 108.68$ ms; $t(46) = 2.515$, $p = 0.015$] and similar reaction times to neutral [$t(46) = 0.315$, $p = 0.754$] facial expressions. No significant main effects of stimulation [$F(1,46) = 2.558$, $p = 0.117$] or valence [$F(1,46) = 1.805$, $p = 0.186$] were found for reaction time. These findings indicate that rDLPFC inhibition by cTBS speeded up successful attentional disengagement from negative material, while interference effects in response accuracies remained unaffected.

### Valence and Arousal Ratings: Effects of rDLPFC Inhibition on Image Evaluations

To investigate effects of stimulation on explicit image evaluations, two 2 × 2-mixed ANOVAs with within-subjects factor valence and between-subjects factor stimulation were conducted for valence and arousal ratings of negative and neutral images.

For valence ratings (**Figure 3E**), there were significant main effects of valence [$F(1,46) = 671.52$, $p < 0.001$] and stimulation [$F(1,46) = 3.873$, $p = 0.05$] as well as a significant interaction

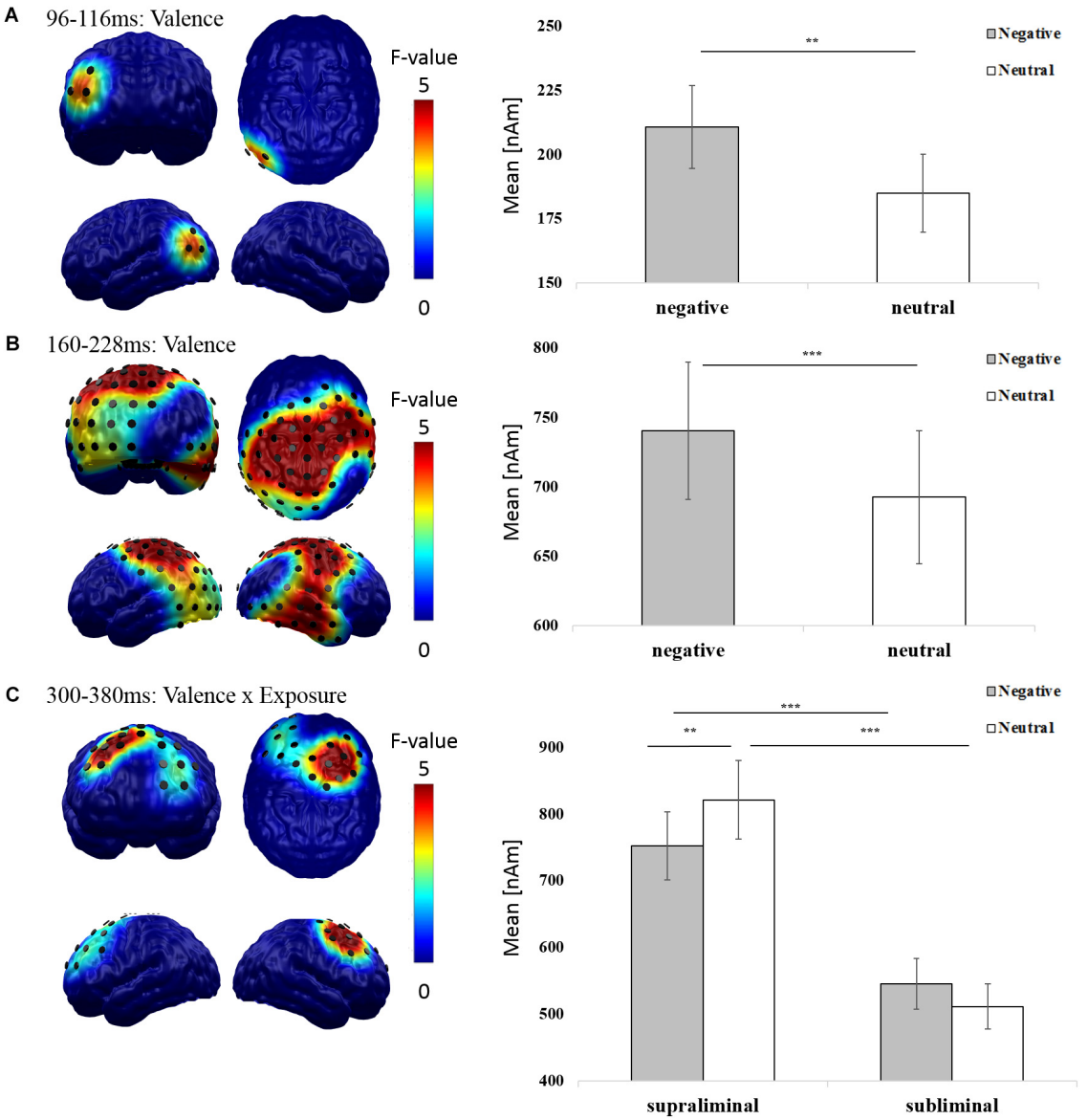


**FIGURE 2 |** Valence and exposure effects in neurophysiological Pre-cTBS data. The distribution of mean *F*-values for the **(A)** early (96–116 ms) and **(B)** mid-latency (160–228 ms) main effect of valence and the **(C)** late (300–380 ms) interaction of valence and exposure are displayed for all significant spatiotemporal clusters and masked at a significance level of $p < 0.05$ (sensor-criterion). Dipoles included in the spatiotemporal cluster ($p < 0.05$, corrected) are superimposed in black color. The bar plot depicts the regional mean neural activity in the respective spatiotemporal clusters in response to negative (gray) and neutral (white) images. Error bars indicate the standard errors of the means. Significant results of *post hoc t*-tests (Bonferroni corrected) are indicated (*$p < 0.05$, **$p < 0.01$, ***$p < 0.001$).

between valence and stimulation [$F(1,46) = 3.800$, $p = 0.05$]. Bonferroni-corrected *t*-tests showed that for both rDLPFC inhibition and Active Control group, negative images received lower valence ratings than neutral images [rDLPFC inhibition: Negative: $M = 18.54$, $SD = 5.39$, Neutral: $M = 43.94$, $SD = 5.97$, $t(46) = -14.599$, $p < 0.001$; Active Control: Negative: $M = 14.35$, $SD = 5.15$, Neutral: $M = 43.88$, $SD = 4.34$, $t(46) = -24.385$, $p < 0.001$]. Crucially, for negative images, individuals in the rDLPFC inhibition group gave significantly less negative (i.e., higher) valence ratings ($M = 18.54$, $SD = 5.39$) than those in the Active Control group [$M = 14.35$, $SD = 5.15$, $t(46) = -2.756$, $p = 0.008$]. No significant differences for neutral images were observed [$t(46) = -0.041$, $p = 0.968$].

For arousal ratings (**Figure 3F**), a significant main effect of valence [$F(1,46) = 264.463$, $p < 0.001$] and a significant interaction between valence and stimulation [$F(1,46) = 4.064$, $p = 0.05$] were observed. The main effect of stimulation was not significant [$F(1,46) = 1.829$, $p = 0.183$]. Not surprisingly, Bonferroni-corrected *t*-tests revealed that for both rDLPFC inhibition and Active Control conditions, negative images received higher arousal ratings than neutral images [rDLPFC inhibition: Negative: $M = 54.49$, $SD = 9.68$, Neutral: $M = 30.72$,

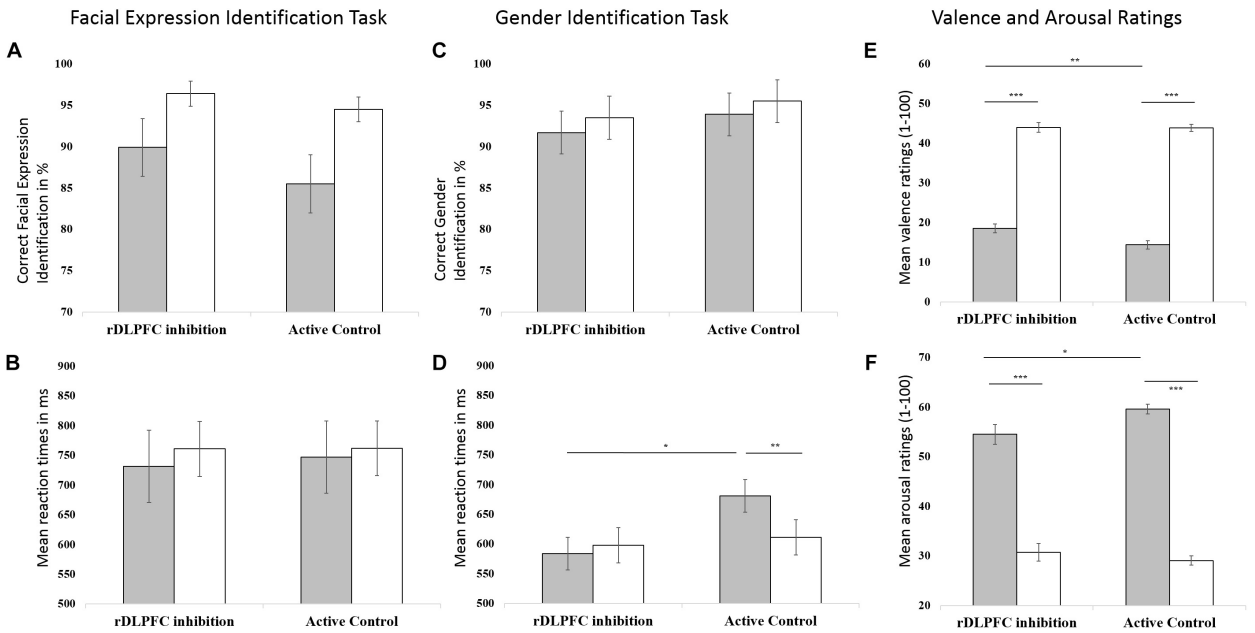


**FIGURE 3 |** Effects of stimulation (rDLPFC inhibition vs. Active Control) and valence (negative vs. neutral) on behavioral responses. Left column: **(A)** Mean response accuracies and **(B)** reaction times to negative (here: fearful; gray) and neutral (white) facial expressions in the Facial Expression Identification Task. Middle column: **(C)** Mean response accuracies and **(D)** reaction times to negative (here: fearful; gray) and neutral (white) facial expressions in the Gender Identification Task. Right Column: **(E)** Mean valence ratings and **(F)** arousal ratings in response to negative (gray) and neutral (white) images. Higher scores indicate more positive and higher arousal ratings, respectively. Error bars indicate the standard errors of the means. For significant interactions of valence and stimulation, results of *post hoc t*-tests (Bonferroni corrected) are indicated (*$p < 0.05$, **$p < 0.01$, ***$p < 0.001$).

$SD = 8.74$, $t(23) = -7.831$, $p < 0.001$; Active Control: Negative: $M = 59.60$, $SD = 4.70$, Neutral: $M = 29.04$, $SD = 4.55$, $t(23) = 20.951$, $p < 0.001$]. Importantly, for negative images, arousal ratings were significantly lower in the rDLPFC inhibition compared to the Active Control condition [$t(46) = 2.324$, $p = 0.025$] while no significant difference was detected for neutral images [$t(46) = -0.837$, $p = 0.407$].

### Visual Awareness Task: No Effects of rDLPFC Inhibition on Discrimination of Subliminal and Supraliminal Images

The visual awareness task at the end of the experimental session showed that participants were unable to report the emotional content of subliminally presented images above chance [$t(47) = 0.116$, $p = 0.908$; $d'$: $M = 0.22$, $SD = 0.51$]. In contrast, as expected, supraliminal stimuli could be discriminated above chance [$t(47) = 11.304$, $p < 0.001$, $d'$: $M = 1.89$, $SD = 0.98$]. Discrimination of both subliminal and supraliminal stimuli remained unaffected by the stimulation [$F(1,47) < 1$].

## Effects of rDLPFC Inhibition on Neurophysiological Measures

### Awareness-Independent Effects of rDLPFC Inhibition: Automatic Valence Processing

In a first step, to investigate stimulation–valence interactions that are independent of visual awareness, we calculated spatiotemporal clusters for the interaction of valence and stimulation. We found a significant cluster for the interaction between stimulation and valence within the mid-latency time window [120–268 ms; $F(1,36) = 22.299$, $p < 0.001$; **Figure 4A**] in an occipito-parietal brain area and within the late time window [320–380 ms; $F(1,36) = 9.759$, $p = 0.004$] in fronto-parietal areas (**Figure 4B**). *Post hoc* analyses for the mid-latency cluster revealed that, following rDLPFC inhibition, negative compared to neutral images elicited an increase in amplitude from Pre-cTBS to Post-cTBS [$F(1,36) = 10.730$, $p = 0.004$]. Conversely, in the Active Control condition, negative compared to neutral images elicited a relative decrease in amplitude from Pre-cTBS to Post-cTBS [$F(1,18) = 11.601$, $p = 0.003$]. In the late cluster, we observed effects in similar directions: While enhanced negative compared to neutral brain activity following rDLPFC inhibition failed to reach significance, negative images elicited reduced amplitudes from Pre-cTBS to Post-cTBS in the Active Control condition [$F(1,36) = 13.595$, $p = 0.002$].

As mid-latency effects started at the boundary between the early and mid-latency interval of interest, we conducted a follow-up analyses correcting for a merged time window between 80 and 300 ms. This analysis revealed that the interactive effect of valence and stimulation began to show significance at 112 ms. This early onset of the valence × stimulation interaction, which remains affected by the factor exposure, is in line with the claim that rDLPFC modulation enhances rather automatic neural processes reflecting motivated attention (e.g., Zwanzger et al., 2014).

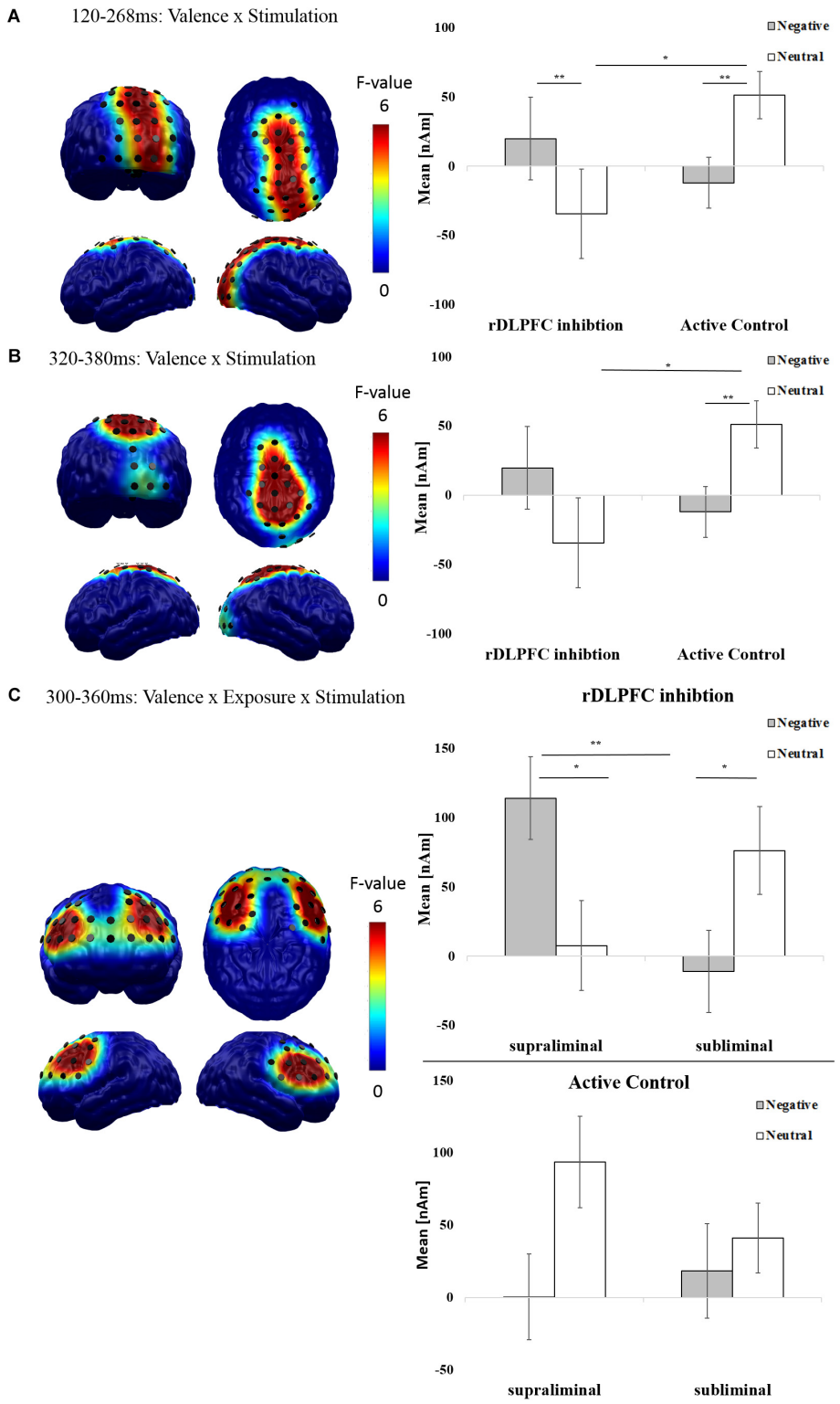


**FIGURE 4 |** Effects of rDLPFC inhibition on neurophysiological measures of affective processing: The spatial distribution of mean *F*-values for the **(A)** mid-latency (120–268 ms) and **(B)** late (320–380 ms) interaction of valence and stimulation, and **(C)** for the late (300–360 ms) interaction of valence, stimulation and exposure are displayed for all significant spatiotemporal clusters and masked at a significance level of $p < 0.05$ (sensor-criterion). Dipoles included in the spatiotemporal cluster ($p < 0.05$, corrected) are superimposed in black color. The bar plot depicts the regional mean neural difference activity (Post-cTBS *minus* Pre-cTBS, in nAm) in the respective spatiotemporal clusters in response to negative (gray) and neutral (white) scenes. Error bars indicate the standard errors of the means. Results of *post hoc* *t*-tests for significant interactions (Bonferroni corrected) are indicated (*$p < 0.05$, **$p < 0.01$, ***$p < 0.001$).

### Awareness-Dependent Effects of rDLPFC Inhibition: Elaborate Valence Processing

To reveal spatiotemporal clusters in which valence × stimulation interactions are modulated by visual awareness, we calculated cluster masses for the interaction between stimulation, valence, and exposure. While analyses in the early and mid-latency interval yielded no significant clusters, we found a significant cluster in the late time window (300–360 ms) at frontal sites [$F(1,37) = 11.527$, $p = 0.002$; **Figure 4C**]. As this late effect started at the boundary between the mid-latency and the late interval, we conducted follow-up tests for a merged time window (120–600 ms), which showed that the late activation began to show significance at 292 ms.

*Post hoc* 2 × 2 within-subjects ANOVAs with the factors valence and exposure for this late frontal spatio-temporal cluster were conducted separately for rDLPFC inhibition and Active Control groups. A significant interaction between exposure and valence was found for the rDLPFC inhibition condition [$F(1,18) = 28.474$, $p < 0.001$]. Bonferroni-corrected paired *t*-tests demonstrated that this interaction was driven by increased amplitudes for supraliminal negative images compared to neutral [$t(18) = 2.379$, $p = 0.029$] and compared to subliminal negative images [$t(18) = 3.569$, $p = 0.002$]. Crucially, a reverse pattern was noted for subliminal material, whereby subliminal neutral compared to negative images [$t(18) = -2.474$, $p = 0.024$] and supraliminal neutral images [trend toward significance; $t(18) = -1.933$, $p = 0.062$] elicited increased activity. By contrast a significant main effect of valence was found in the Active Control condition [$F(1,18) = 6.007$, $p = 0.025$] with increased amplitudes from Pre-cTBS to Post-cTBS for neutral compared to negative images.

These findings suggest that at later processing stages, rDLPFC inhibition results in enhanced affect-specific activation of dorsolateral brain structures only if negative images enter visual awareness. Based on the topography and the late onset of this awareness-dependent effect, it is plausible that it is linked to elaborate mechanisms such as emotion-regulation or attention disengagement (van Honk et al., 2002; Liddell et al., 2004).

## DISCUSSION

The rDLPFC plays a key role in the regulation of emotional processing (Ochsner et al., 2012). However, its specific role in the regulation of neurocognitive processes that underpin the interplay of affective perception and visual awareness is largely unknown. To address this research gap, the current study experimentally induced rDLPFC inhibition using inhibitory cTBS. In an active-controlled mixed factorial design, we studied the effects of this stimulation on subsequent behavioral and electroencephalographic responses to subliminally and supraliminally presented negative versus neutral scenes. We applied minimum-norm approaches to estimate the corresponding neuronal sources. In the following, we will first discuss findings of our EEG Pre-cTBS measurement and thereby consider how visual awareness affects the spatiotemporal dynamics of emotion processing under passive viewing conditions. Second, the key question of this study will be addressed: In which way does rDLPFC inhibition influence behavioral and neurophysiological correlates of emotional responses to supraliminal and subliminal visual stimuli? The discussion offers potential mechanisms and highlights areas of future investigation.

### Valence and Exposure Effects in Neurophysiological Pre-cTBS Measures

In our neurophysiological Pre-cTBS measures, we could replicate enhanced brain activation in response to negative images in an early (96–116 ms) left occipital cluster, which then extended to bilateral occipito-temporal and parietal regions in a mid-latency (160–228 ms) time interval (Schupp et al., 2003a, 2006, 2007; Carretié et al., 2004; Liddell et al., 2004; Balconi, 2006; Pegna et al., 2011; Qian et al., 2012). Importantly, and in line with previous research (Liddell et al., 2004), these rather early effects were not modulated by visual awareness. This finding supports the claim that early and mid-latency emotion effects are likely to reflect enhanced perceptual processing of and automatic attention orienting to highly motivationally relevant stimuli (Junghöfer et al., 2001; Olofsson et al., 2008; Carlson and Reinke, 2010; Keuper et al., 2013, 2014). The revealed neural patterns support a feedforward mechanism whereby enhanced automatic processing of negative stimuli begins early in the visual areas and is fed forward to higher cortical regions (Junghöfer et al., 2001, 2006; Olofsson et al., 2008; Pessoa and Adolphs, 2010). Moreover, as expected (Liddell et al., 2004; Williams et al., 2004; Kiss and Eimer, 2008; Nakajima et al., 2015) we found an interaction of exposure time and valence, which was most pronounced in the late time window (300–380 ms). Interestingly, this interaction was elicited by dorsolateral prefrontal structures and peaked in the same rDLPFC area, that was later stimulated – i.e., the region below electrode F4. In particular, this area was *less* activated in response to supraliminal negative compared to neutral stimuli, while such negative-neutral differentiation was absent in the subliminal condition. In their ERP study, Liddell et al. (2004) also reported a differentiation of amplitudes to negative compared to neutral supraliminal but not subliminal faces at similar latencies. Specifically, they found stronger positive amplitudes to negative supraliminal faces at frontocentral sites (Cz, Fz). Both, the topography and latency of this effect can nicely be reconciled with the literature of the so-called late positive potential (LPP), an emotion-sensitive ERP component indexing stronger evaluative processes in response to emotionally salient compared to neutral material (e.g., Schupp et al., 2006; Olofsson et al., 2008). However, as Liddell et al. (2004) did not employ source reconstruction approaches, the neuronal generators were not revealed in this particular study and thus remained speculative. Yet, there is ample evidence that distributed neuronal sources in visual processing areas and frontal regions contribute to the LPP (Olofsson et al., 2008; Wessing et al., 2016). Several authors have argued that stronger late-latency brain activation in visual processing areas reflects an ongoing, increasingly elaborate perceptual evaluation of emotional stimuli based on reentrant processing (Schupp et al., 2004a; Wessing et al., 2016). The strength of this

effect can be modulated by several factors including the use of voluntary regulatory strategies (e.g., reappraisal, Hajcak and Nieuwenhuis, 2006), as well as rDLPFC inhibition and excitation (Notzon et al., 2017). In passive viewing tasks, where an active regulation of emotional material via prefrontal structures is not instructed, stronger emotion effects in visual processing areas can temporally co-occur with *reduced* activation to emotional material in frontal regions (Wessing et al., 2016). Thus, overall, the direction and localization of the observed interaction of valence and exposure is in line with previous findings. The absence of a contribution of visual processing areas in this effect might be a consequence of the employed back-ward masking design, in which the masking stimulus may disrupt reentrant processing of the initial stimulus in perception-related brain regions (e.g., Fahrenfort et al., 2009).

Overall, our Pre-cTBS analyses on the one hand substantiate shared emotion-sensitive feedforward mechanisms for supraliminal and subliminal perception. On the other hand, they suggest differential late regulatory mechanisms for subliminal and supraliminal affective processing. These findings fit in well with two-stage models of stimulus perception (see Schupp et al., 2006), which link early and mid-latency emotion-sensitive components (<300 ms) to a large-capacity "perceptual scanning stage providing a more or less complete analysis of sensory information" (p. 47) and propose that a conscious representation of stimuli might depend on access to a capacity-limited second stage of processing, which is likely indexed by late components (>300 ms), especially the LPP.

The right dorsolateral prefrontal localization of the late interaction of exposure time and valence further stimulates the key question of this study: How does the rDLPFC control affective processing in presence versus absence of visual awareness?

## Effects of rDLPFC Inhibition on Behavioral Measures

In the following, we will discuss the results of our behavioral measures, which were designed to test the impact of rDLPFC inhibition via cTBS on (1) affective state, (2) attention orienting to and/or attention disengagement from negative compared to neutral stimuli, (3) valence and arousal ratings, and (4) emotion discrimination.

We found no effects of rDLPFC inhibition compared to Active Control on self-reported affective state. This supports previous literature, which failed to find mood effects following a single session of inhibitory cTBS on the rDLPFC (Tupak et al., 2013). Notably, changes in self-reported mood have been reported, when the left DLPFC was targeted (Tupak et al., 2013), although not consistently (Mosimann et al., 2000; Leyman et al., 2009). Importantly, there is ample evidence for antidepressant effects of rTMS after repeated sessions of prefrontal neurostimulation: In line with theories on hemispheric asymmetry (e.g., Davidson, 1992a,b), inhibitory rTMS to the rDLPFC as well as excitatory rTMS to the left DLPFC appear to improve depressive symptoms (e.g., Fitzgerald and Daskalakis, 2011).

Despite the lack of mood effects, our study found partial support for the hypothesis of reduced negative-processing biases following rDLPFC inhibition. First, in line with van Honk et al. (2002), our findings reveal reduced emotional interference by negative facial expressions in the Gender Identification Task. Specifically, we found fewer correct responses for fearful compared to neutral faces. Such effects of emotional interference are well documented (Phaf and Kan, 2007). They reveal that it is more difficult to ignore (task-irrelevant) emotional compared to neutral material, as emotional materials capture additional attentional resources (van Honk et al., 2002). Importantly, although rDLPFC inhibition compared to Active Control stimulation did not differentially modulate interference effects on the level of accuracy, individuals in the rDLPFC inhibition condition showed less emotional interference in the reaction times. Specifically, when identifying gender for faces with fearful expressions they showed faster responses than the Active Control group, while no group differences were found in response to neutral faces. This result is in line with the observation that individuals receiving inhibitory rTMS to the rDLPFC were quicker to identify the ink-color (green, blue, red, and yellow) of supraliminal fearful faces (van Honk et al., 2002, but see Tupak et al., 2013) than those receiving sham stimulation. Overall, relatively better task-performances in such implicit tasks are thought to result from more efficient processes of attention disengagement from the (task-irrelevant) negative content of stimuli (van Honk et al., 2002; Koster et al., 2005; Sagliano et al., 2016).

Second, in addition to more effective attentional disengagement from negative stimuli, the rDLPFC inhibition group rated negative scenes as less negative and less arousing. As predicted by theories of hemispheric asymmetries (for reviews, see Davidson, 1992a,b; Harmon-Jones et al., 2010; Grimshaw and Carmel, 2014), this finding further substantiates that rDLPFC inhibition may reduce withdrawal-related behaviors as indexed by the observed attenuation of negativity biases.

However, reductions of negativity biases following rDLPFC inhibition were not consistently observed in all tasks. We were not able to replicate effects of neurostimulation on the identification of fearful versus neutral faces following rDLPFC inhibition (Zwanzger et al., 2014). This lack of effect might result from several disparities between these two studies. First, we tested Chinese, not German participants, which may have affected task performance during the Identification of Facial Expressions of Caucasian faces in this task. Second, the frequent repetition of facial stimuli in the study by Zwanzger et al. (2014) may have influenced effects of rDLPFC inhibition on facial expression identification. In particular, Zwanzger et al. (2014) repeated the Facial Expression and Gender Identification Task before and after rTMS application, and used the same faces during the intermediate passive viewing task. By contrast, we administered the Facial Expression and Gender Identification Task only once and presented participants with subliminal and supraliminal negative and neutral scenes in the preceding passive viewing task. A third explanation for discrepancies in the findings may result from the use of different stimulation protocols [inhibitory low-frequency rTMS (1 Hz) vs. inhibitory cTBS] and control conditions (Sham vs. Active Control).

Further, the visual awareness task yielded no effects of cTBS stimulation. Neither in the subliminal nor in the supraliminal condition did we find evidence for an effect of rDLPFC inhibition. Thus, it seems unlikely that rDLPFC inhibition affected the identification and/or discrimination of negative and neutral stimuli. Importantly, this result confirms that in both groups, emotional contents of subliminal images were successfully rendered unrecognizable. This should be taken into consideration, when interpreting effects of rDLPFC inhibition on neurophysiological findings.

Taken together, our behavioral findings support the notion of a causal role of frontal structures in the regulation of negative stimulus processing (Phan et al., 2005). Yet, reductions of negativity biases following rDLPFC inhibition were observed in some tasks, while they were absent in others and did not readily translate into mood changes. In combination with inconsistent findings in the literature, this suggests that effects of rDLPFC inhibition on behavior might depend on various boundary conditions (e.g., rTMS protocol, frequency and site of stimulation, familiarity with stimulus material, etc.), that require further future investigation.

## Effects of rDLPFC Inhibition on Neurophysiological Measures

Importantly, observed reductions of behavioral negativity biases may result from different neuronal mechanisms. Theoretically, they may on the one hand be due to *reduced automatic encoding of negative material in the feedforward pathway*, contributing to less interference by and reduced negativity and arousal ratings of stimuli. On the other hand, they may be due to *increased speed and/or efficiency of encoding and projection of negative cues* to frontal regions and/or *enhanced prefrontal control at later processing stages*. In the following, we will closely evaluate these interpretations based on the time-course rTMS-driven emotion effects.

### Awareness-Independent Effects of rDLPFC Inhibition: Automatic Valence Processing

On a neurophysiological level, rDLPFC inhibition relatively enhanced occipito-parietal and centro-parietal brain activity for both subliminal and supraliminal negative images. These effects started in early intervals and were strongest at mid-latency and late processing stages (112–268 ms; 320–380 ms). The early onset of these effects (<120 ms) as well as their localization in perception-related brain areas substantiate previous reports of prefrontal modulatory influence on early brain signatures of emotional attention (also see Zwanzger et al., 2014; Notzon et al., 2017). Perception-related brain areas including occipito-parietal and also frontal regions have been previously implicated in stimulus-driven mechanisms of emotional attention (Olofsson et al., 2008) and the automatic feedforward sweep of negative information toward higher cortical regions (Schupp et al., 2006; Pessoa and Adolphs, 2010; Zwanzger et al., 2014). Importantly, these rather early interactions between stimulation site and valence were not affected by exposure time, which implies that even highly automatic stimulus-driven processes can be under prefrontal control. In line with this, Corbetta and Shulman (2002) proposed that interactions between (automatic) bottom-up processing and top-down control may work together to guide attention mechanisms. Specifically, it was proposed that "... task-relevant signals from the dorsal system 'filter' stimulus-driven signals in the ventral system, whereas stimulus-driven 'circuit-breaking' signals from the ventral system provide an interrupt to the dorsal system, reorienting it toward salient stimuli" (Fox et al., 2006). In line with our neurophysiological findings, this model predicts that inhibition of the rDLPFC as part of the dorsal system should reduce top-down control and thereby *enhance* bottom-up processing of salient (here: negative) stimuli in perception-associated brain areas (see also Zwanzger et al., 2014; Notzon et al., 2017).

However, previous research also suggests that strong stimulus-driven emotional responses are typically associated with *enhanced* interference effects on the behavioral level. Thus, predictions of the model by Corbetta and Shulman (2002) as well as our neurophysiological findings on cTBS effects on automatic valence processing seem to contradict our behavioral data, which – by contrast – suggest *reduced* interference by negative information. How can *boosted (early) brain activity reflecting enhanced emotional attention* be reconciled with *reduced behavioral negativity biases*? One possibility may be the initiation of *a (compensatory) top-down regulatory mechanism* that contributes to the ultimately observed behavioral effects. If such mechanism exists, one would expect the recruitment of frontal brain areas that support later, more elaborate awareness-dependent processes of emotion regulation (Kozel and George, 2002; van Honk et al., 2002; Bishop et al., 2004; Siegle et al., 2007; Poldrack et al., 2008; Guse et al., 2010; Ochsner et al., 2012; Ironside et al., 2016).

### Awareness-Dependent Effects of rDLPFC Inhibition: Elaborate Valence Processing

In fact, our findings indicate that rDLPFC inhibition enhances relatively late (292–360 ms) brain activity exclusively in response to negative images that are available to visual awareness, while reduced brain activity for negative compared to neutral images was found in the subliminal condition and in the Active Control group. Of note, to our knowledge, this is the first available evidence for a differential influence of rDLPFC inhibition on spatiotemporal neural correlates of subliminal vs. supraliminal negative processing. This interactive effect was found in bilateral dorsolateral prefrontal frontal regions. Compared to the interaction of valence and exposure in the Pre-cTBS data, which – interestingly – was found in the same brain region that was afterward stimulated (below electrode F4), this effect peaked in more ventral parts of the bilateral DLPFC.

Following Fox et al. (2006) this interactive effects might be the result of stronger bottom-up stimulus-driven "circuit-breaking" signals elicited by negative stimuli in the rDLPFC inhibition group, which then interrupt dorsal system functioning. Our findings indicate that this interruption and a reorientation of the dorsal system toward salient stimuli only takes place if stimuli enter visual awareness. In the light of our behavioral findings, which show a reduction of negative-processing biases following rDLPFC inhibition and previous studies associating inhibitory,

emotion-regulatory processes with DLPFC functioning (van Honk et al., 2002; Ochsner et al., 2012), one might speculate that this stronger prefrontal activation to negative supraliminal stimuli reflects an enhanced awareness-dependent down-regulation of negative scene processing. Such mechanism eventually leads to facilitated disengagement from and less negative and less arousing evaluations of negative stimuli.

Yet, although this idea aligns well with our behavioral findings and the previous literature, it appears surprising that such mechanism is seemingly underpinned by brain activity adjacent to and partly overlapping with the (inhibited!) rDLPFC. How can a brain region that was inhibited by means of cTBS effectively support emotion-regulatory functions? To account for this, it seems necessary to compare the exact localization of the stimulated brain region (i.e., those parts of the rDLPFC that are located directly under F4) with the observed cluster of the three-way interaction of valence, exposure, and stimulation. In fact, the stimulated area is localized slightly more dorsal than the observed effect. Although highly speculative, this might suggest that different parts of the rDLPFC serve different types of emotional control processes. First, the more dorsal part below F4 might control automatic bottom-up processes of emotional attention early in the processing stream and independently of visual awareness. Second, bilateral, more ventral parts of the DLPFC may support later more elaborate regulatory mechanisms that depend on visual awareness. Overall, our findings suggest that that behavioral responses to emotional stimuli depend on the flexible interplay of mechanisms that support fast automatic responses to emotional stimuli on the one hand and subsequent (compensatory?) regulatory strategies on the other.

## Limitations

Overall, our findings indicate that the spatiotemporal interplay between feedforward pathways in occipito-parietal areas and prefrontal regions, as well as interactions of different prefrontal brain regions underpin distinct aspects of affective processing. In the light of this complex interplay, the choice of the vertex (electrode Cz) as the Active Control stimulation site requires critical reflection. We based our decision for this use of Cz on several considerations: First, compared to passive-controlled designs using "Sham" stimulation (e.g., Zwanzger et al., 2014), active-controlled designs enable more specific conclusions regarding the specific contribution of the stimulated brain region to the observed effects. We were able to replicate early enhanced bottom-up processing of negative stimuli following rDLPFC inhibition (Zwanzger et al., 2014) when using Cz as an Active Control site. This strengthens the conclusion that emotion perception is in fact controlled by rDLPFC function. However, as an inherent disadvantage of active-controlled designs, an additional contribution of the Active Control site to this effect cannot be ruled out. Second, our aim to compare subliminal with supraliminal perceptual processing of emotional stimuli required an Active Control site with a minor role in earliest stages of visual feedforward-processing. Based on studies which localized early and also mid-latency responses to negative affective (vs. neutral) visual stimuli mainly in occipital and temporal regions (Junghöfer et al., 2001, 2006; Olofsson et al., 2008; Bayle et al., 2009), and also based on a recent meta-analysis of 157 fMRI studies on emotional face and emotional scene processing, which did not reveal significant affect-modulated activation of central structures (Sabatinelli et al., 2011), we selected Cz as a control site. However, as can be seen in **Figure 2**, our Pre-cTBS data clearly show a contribution of parietal brain regions (below electrode Cz) in mid-latency emotion effects. Further, especially late emotion-sensitive ERP components are often visible at centro-parietal midline electrodes (e.g., Schupp et al., 2004b). Although the estimated underlying sources of these late ERP components were mainly found at visual sensory and parietal and not central regions (Sabatinelli et al., 2006), we nevertheless cannot exclude the possibility that stimulation of Cz – e.g., by co-stimulation of parietal structures – influenced our results, in particular with regard to the awareness-dependent effects observed at later processing stages. Therefore, it would be of great interest to replicate this study under varying control conditions, e.g., passive "Sham" stimulation (e.g., Zwanzger et al., 2014). It would also be of interest to further investigate the hemispheric specificity of DLPFC inhibition on the interplay of valence processing and awareness, for example by targeting the left DLPFC. Future studies, which aim at elucidating the specific functional contribution of different brain regions and their functional connectivity may help to better understand how affective information is processed over time – with and without visual awareness.

Importantly, and in the light of these limitations, neuronal and behavioral findings of our study suggest that effective down-regulatory mechanisms following rDLPFC inhibition via cTBS may exclusively apply to negative stimuli that reach participants awareness. On the other hand, neurophysiological findings indicated that both supra- and subliminal negative stimuli received enhanced emotional attention following rDLPFC inhibition. Together, these findings imply that emotional stimuli that remain below awareness might still influence affective states in a subtler way. Such type of emotional reactivity might be difficult to capture by traditional behavioral tasks. Although we included several behavioral tasks to explore the direction that rTMS effects would take on different aspects of emotion processing, one additional limitation of our study regards the interpretability of our neuronal effects. As the neural data were collected during a passive viewing task, which required no responses from participants, the association between our electrophysiological and behavioral results remains partially speculative. Further, with exception of the visual awareness task, all behavioral measures used supraliminal images. This prevented firm conclusions on rTMS-induced mechanisms that are specific to subliminal affective processing. Therefore, future studies should employ active-response tasks to differentiate neurocognitive mechanisms involved in subliminal and supraliminal affective processing and their modulation by rDLPFC stimulation.

## Implications and Future Outlook

Overall, our study has provided important insights on the causal influence of rDLPFC function on affective processing

in presence and absence of visual awareness. In summary, we found evidence for reduced emotional interference by, and less negative and aroused ratings of negative supraliminal stimuli following rDLPFC inhibition. rDLPFC inhibition did not affect self-reported mood or the discrimination performance in the awareness task. Based on our finding of enhanced neurophysiological emotion effects at early and mid-latency processing stages, we suggested that rDLPFC inhibition boosts automatic processes of "emotional attention" independently of visual awareness. Further, our study revealed to our knowledge the first available evidence for a differential influence of rDLPFC inhibition on subliminal versus supraliminal neural emotion processing. We tentatively argued that this effect might reflect enhanced awareness-dependent down-regulation of negative scene processing, eventually leading to facilitated disengagement from and less negative and arousing evaluations of negative supraliminal stimuli. Future research is needed to understand in more detail how targeted non-invasive brain stimulation via rTMS may differentially influence subliminal and supraliminal emotional stimulus processing. A clearer picture of these mechanisms might have crucial implications for the understanding and treatment of mood and anxiety disorders, which are not only maintained and exacerbated by "conscious" negativity biases, but also by processes induced by subliminal emotional triggers. Bar-Haim et al. (2007) for instance revealed that for subliminally presented stimuli, anxiety patients showed a negativity bias but non-anxious individuals even revealed a bias away from threat. Therefore, studies combining neurostimulation techniques with neurophysiological and behavioral measures of conscious and preconscious affective processing not only in healthy controls, but also in mood- and anxiety-disordered patients may contribute important insights regarding the therapeutic use of rTMS to treat emotional dysfunctions and processing biases.

## AUTHOR CONTRIBUTIONS

KK, ET, and TL designed the experiment. ET conducted the study. KK and ET analyzed the data and wrote the manuscript. MJ and CC provided technical support during data collection and analysis, respectively. All authors read the manuscript and provided feedback.

## ACKNOWLEDGMENTS

We would like to acknowledge The University of Hong Kong May Endowed Professorship in Neuropsychology and the PPP Program for Project-Related Personal Exchange (supported by the German Academic Exchange Service and the Hong Kong Research Grants Council). Our gratitude further extends to Dr. K.H. Ting and Dr. Bolton Chau at The Hong Kong Polytechnic University for their support in the data collection process.

## REFERENCES

Antal, A., Nitsche, M. A., Kincses, T. Z., Lampe, C., and Paulus, W. (2004). No correlation between oving phosphene and motor thresholds: a transcranial magnetic stimulation study. *Neuroreport* 15, 297–302. doi: 10.1097/00001756-200402090-00017

Balconi, M. (2006). Exploring consciousness in emotional face decoding: an event-related potential analysis. *Genet. Soc. Gen. Psychol. Monogr.* 132, 129–150. doi: 10.1016/0013-4694(58)90053-1

Balconi, M., and Cobelli, C. (2015). rTMS on left prefrontal cortex contributes to memories for positive emotional cues: a comparison between pictures and words. *Neuroscience* 287, 93–103. doi: 10.1016/j.neuroscience.2014.12.015

Balconi, M., and Ferrari, C. (2013). Repeated transcranial magnetic stimulation on dorsolateral prefrontal cortex improves performance in emotional memory retrieval as a function of level of anxiety and stimulus valence. *Psychiatry Clin. Neurosci.* 67, 210–218. doi: 10.1111/pcn.12041

Balconi, M., and Lucchiari, C. (2005a). "Consciousness, emotion and face: an event-related potentials (ERP) study," in *Consciousness & Emotion: Agency, Conscious Choice, and Selective Perception*, eds R. D. Ellis and N. Newton (Amsterdam: John Benjamins Publishing Company), 121–135. doi: 10.1075/ceb.1.07bal

Balconi, M., and Lucchiari, C. (2005b). In the face of emotions: event-related potentials in supraliminal and subliminal facial expression recognition. *Genet. Soc. Gen. Psychol. Monogr.* 131, 41–69. doi: 10.1016/0013-4694(58)90053-1

Balconi, M., and Lucchiari, C. (2007). Consciousness and emotional facial expression recognition: subliminal/supraliminal stimulation effect on n200 and p300 ERPs. *J. Psychophysiol.* 21, 100–108. doi: 10.1027/0269-8803.21.2.100

Banks, S. J., Eddy, K. T., Angstadt, M., Nathan, P. J., and Phan, K. L. (2007). Amygdala–frontal connectivity during emotion regulation. *Soc. Cogn. Affect. Neurosci.* 2, 303–312. doi: 10.1093/scan/nsm029

Bar-Haim, Y., Lamy, D., Pergamin, L., Bakermans-Kranenburg, M. J., and Van Ijzendoorn, M. H. (2007). Threat-related attentional bias in anxious and nonanxious individuals: a meta-analytic study. *Psychol. Bull.* 133, 1–24. doi: 10.1037/0033-2909.133.1.1

Bayle, D. J., Henaff, M.-A., and Krolak-Salmon, P. (2009). Unconsciously perceived fear in peripheral vision alerts the limbic system: a MEG study. *PLoS One* 4:e8207. doi: 10.1371/journal.pone.0008207

Bayle, D. J., and Taylor, M. J. (2010). Attention inhibition of early cortical activation to fearful faces. *Brain Res.* 1313, 113–123. doi: 10.1016/j.brainres.2009.11.060

Beck, A. T., Steer, R. A., and Brown, G. K. (1996). *Beck Depression Inventory-II*. San Antonio, TX: Psychological Corporation.

Bishop, S., Duncan, J., Brett, M., and Lawrence, A. D. (2004). Prefrontal cortical function and anxiety: controlling attention to threat-related stimuli. *Nat. Neurosci.* 7, 184–188. doi: 10.1038/nn1173

Blom, J., and Anneveldt, M. (1982). An electrode cap tested. *Electroencephalogr. Clin. Neurophysiol.* 54, 591–594. doi: 10.1016/0013-4694(82)90046-3

Boroojerdi, B., Meister, I. G., Foltys, H., Sparing, R., Cohen, L. G., and Töpper, R. (2002). Visual and motor cortex excitability: a transcranial magnetic stimulation study. *Clin. Neurophysiol.* 113, 1501–1504. doi: 10.1016/S1388-2457(02)00198-0

Bressler, S. L., Tang, W., Sylvester, C. M., Shulman, G. L., and Corbetta, M. (2008). Top-down control of human visual cortex by frontal and parietal cortex in anticipatory visual spatial attention. *J. Neurosci.* 28, 10056–10061. doi: 10.1523/JNEUROSCI.1776-08.2008

Byrne, B. M., Stewart, S. M., and Lee, P. W. (2004). Validating the Beck depression inventory-II for Hong Kong community adolescents. *Int. J. Test.* 4, 199–216. doi: 10.1207/s15327574ijt0403_1

Carlson, J. M., and Reinke, K. S. (2010). Spatial attention-related modulation of the N170 by backward masked fearful faces. *Brain Cogn.* 73, 20–27. doi: 10.1016/j.bandc.2010.01.007

Carretié, L., Hinojosa, J. A., Albert, J., and Mercado, F. (2006). Neural response to sustained affective visual stimulation using an indirect task. *Exp. Brain Res.* 174, 630–637. doi: 10.1007/s00221-006-0510-y

Carretié, L., Hinojosa, J. A., Martín-Loeches, M., Mercado, F., and Tapia, M. (2004). Automatic attention to emotional stimuli: neural correlates. *Hum. Brain Mapp.* 22, 290–299. doi: 10.1002/hbm.20037

Cho, S. S., Ko, J. H., Pellecchia, G., Van Eimeren, T., Cilia, R., and Strafella, A. P. (2010). Continuous theta burst stimulation of right dorsolateral prefrontal cortex induces changes in impulsivity level. *Brain Stimul.* 3, 170–176. doi: 10.1016/j.brs.2009.10.002

Conson, M., Errico, D., Mazzarella, E., Giordano, M., Grossi, D., and Trojano, L. (2015). Transcranial electrical stimulation over dorsolateral prefrontal cortex modulates processing of social cognitive and affective information. *PLoS One* 10:e0126448. doi: 10.1371/journal.pone.0126448

Corbetta, M., and Shulman, G. L. (2002). Control of goal-directed and stimulus-driven attention in the brain. *Nat. Rev. Neurosci.* 3, 201–215. doi: 10.1038/nrn755

Dan-Glauser, E. S., and Scherer, K. R. (2011). The Geneva affective picture database (GAPED): a new 730-picture database focusing on valence and normative significance. *Behav. Res. Methods* 43, 468–477. doi: 10.3758/s13428-011-0064-1

Davidson, R. J. (1992a). Anterior cerebral asymmetry and the nature of emotion. *Brain Cogn.* 20, 125–151. doi: 10.1016/0278-2626(92)90065-T

Davidson, R. J. (1992b). Emotion and affective style: hemispheric substrates. *Psychol. Sci.* 3, 39–43. doi: 10.1111/j.1467-9280.1992.tb00254.x

Davidson, R. J. (2001). Toward a biology of personality and emotion. *Ann. N. Y. Acad. Sci.* 935, 191–207. doi: 10.1111/j.1749-6632.2001.tb03481.x

De Raedt, R., Leyman, L., Baeken, C., Van Schuerbeek, P., Luypaert, R., Vanderhasselt, M.-A., et al. (2010). Neurocognitive effects of HF-rTMS over the dorsolateral prefrontal cortex on the attentional processing of emotional information in healthy women: an event-related fMRI study. *Biol. Psychol.* 85, 487–495. doi: 10.1016/j.biopsycho.2010.09.015

Delplanque, S., Silvert, L., Hot, P., Rigoulot, S., and Sequeira, H. (2006). Arousal and valence effects on event-related P3a and P3b during emotional categorization. *Int. J. Psychophysiol.* 60, 315–322. doi: 10.1016/j.ijpsycho.2005.06.006

Eimer, M., Kiss, M., and Holmes, A. (2008). Links between rapid ERP responses to fearful faces and conscious awareness. *J. Neuropsychol.* 2, 165–181. doi: 10.1348/174866407X245411

Era, V., Candidi, M., and Aglioti, S. M. (2015). Subliminal presentation of emotionally negative vs. positive primes increases the perceived beauty of target stimuli. *Exp. Brain Res.* 233, 3271–3281. doi: 10.1007/s00221-015-4395-5

Fahrenfort, J. J., Scholte, H. S., and Lamme, V. A. F. (2009). Masking disrupts recurrent processing in human visual cortex. *J. Cogn. Neurosci.* 19, 1488–1497. doi: 10.1162/jocn.2007.19.9.1488

Fazio, R. H. (2001). On the automatic activation of associated evaluations: an overview. *Cogn. Emot.* 15, 115–141. doi: 10.1080/02699930125908

Feeser, M., Prehn, K., Kazzer, P., Mungee, A., and Bajbouj, M. (2014). Transcranial direct current stimulation enhances cognitive control during emotion regulation. *Brain Stimul.* 7, 105–112. doi: 10.1016/j.brs.2013.08.006

Feng, C., Li, W., Tian, T., Luo, Y., Gu, R., Zhou, C., et al. (2014). Arousal modulates valence effects on both early and late stages of affective picture processing in a passive viewing task. *Soc. Neurosci.* 9, 364–377. doi: 10.1080/17470919.2014.896827

Fitzgerald, P. B., and Daskalakis, Z. J. (2011). The effects of repetitive transcranial magnetic stimulation in the treatment of depression. *Exp. Rev. Med. Devices* 8, 85–95. doi: 10.1586/erd.10.57

Fox, M. D., Corbetta, M., Snyder, A. Z., Vincent, J. L., and Raichle, M. E. (2006). Spontaneous neuronal activity distinguishes human dorsal and ventral attention systems. *Proc. Natl. Acad. Sci. U.S.A.* 103, 10046–10051. doi: 10.1073/pnas.0604187103

Gerwig, M., Kastrup, O., Meyer, B. U., and Niehaus, L. (2003). Evaluation of cortical excitability by motor and phosphene thresholds in transcranial magnetic stimulation. *J. Neurol. Sci.* 215, 75–78. doi: 10.1016/S0022-510X(03)00228-4

Goldin, P. R., McRae, K., Ramel, W., and Gross, J. J. (2008). The neural bases of emotion regulation: reappraisal and suppression of negative emotion. *Biol. Psychiatry* 63, 577–586. doi: 10.1016/j.biopsych.2007.05.031

Gong, X., and Wang, D. (2016). Applicability of the international affective picture system in Chinese older adults: a validation study. *Psych J.* 5, 117–124. doi: 10.1002/pchj.131

Green, D., and Swets, J. (1966). *Signal Detection theory and Psychophysics*, Vol. 888. New York, NY: John Wiley, 889.

Grimshaw, G. M., and Carmel, D. (2014). An asymmetric inhibition model of hemispheric differences in emotional processing. *Front. Psychol.* 5:489. doi: 10.3389/fpsyg.2014.00489

Grisaru, N., Bruno, R., and Pridmore, S. (2001). Effect on the emotions of healthy individuals of slow repetitive transcranial magnetic stimulation applied to the prefrontal cortex. *J. ECT* 17, 184–189. doi: 10.1097/00124509-200109000-00007

Gross, J. J., and John, O. P. (2003). Individual differences in two emotion regulation processes: implications for affect, relationships, and well-being. *J. Pers. Soc. Psychol.* 85, 348–362. doi: 10.1037/0022-3514.85.2.348

Grossheinrich, N., Rau, A., Pogarell, O., Hennig-Fast, K., Reinl, M., Karch, S., et al. (2009). Theta burst stimulation of the prefrontal cortex: safety and impact on cognition, mood, and resting electroencephalogram. *Biol. Psychiatry* 65, 778–784. doi: 10.1016/j.biopsych.2008.10.029

Guse, B., Falkai, P., and Wobrock, T. (2010). Cognitive effects of high-frequency repetitive transcranial magnetic stimulation: a systematic review. *J. Neural. Transm.* 117, 105–122. doi: 10.1007/s00702-009-0333-7

Hajcak, G., and Nieuwenhuis, S. (2006). Reappraisal modulates the electrocortical response to unpleasant pictures. *Cogn. Affect. Behav. Neurosci.* 6, 291–297. doi: 10.3758/CABN.6.4.291

Halgren, E., and Marinkovic, K. (1995). "Neurophysiological networks integrating human emotions," in *The Cognitive Neurosciences*, ed. M. S. Gazzaniga (Cambridge, MA: The MIT Press), 1137–1151.

Hämäläinen, M. S., and Ilmoniemi, R. J. (1994). Interpreting magnetic fields of the brain: minimum norm estimates. *Med. Biol. Eng. Comput.* 32, 35–42. doi: 10.1007/BF02512476

Hamid, P. N., and Cheng, S.-T. (1996). The development and validation of an index of emotional disposition and mood state: the Chinese Affect Scale. *Educ. Psychol. Meas.* 56, 995–1014. doi: 10.1177/0013164496056006006

Harmon-Jones, E., Gable, P. A., and Peterson, C. K. (2010). The role of asymmetric frontal cortical activity in emotion-related phenomena: a review and update. *Biol. Psychol.* 84, 451–462. doi: 10.1016/j.biopsycho.2009.08.010

Hauk, O. (2004). Keep it simple: a case for using classical minimum norm estimation in the analysis of EEG and MEG data. *Neuroimage* 21, 1612–1621. doi: 10.1016/j.neuroimage.2003.12.018

Hintze, P., Junghöfer, M., and Bruchmann, M. (2014). Evidence for rapid prefrontal emotional evaluation from visual evoked responses to conditioned gratings. *Biol. Psychol.* 99, 125–136. doi: 10.1016/j.biopsycho.2014.03.010

Hsu, S.-M., Hetrick, W. P., and Pessoa, L. (2008). Depth of facial expression processing depends on stimulus visibility: behavioral and electrophysiological evidence of priming effects. *Cogn. Affect. Behav. Neurosci.* 8, 282–292. doi: 10.3758/CABN.8.3.282

Huang, Y.-Z., Edwards, M. J., Rounis, E., Bhatia, K. P., and Rothwell, J. C. (2005). Theta burst stimulation of the human motor cortex. *Neuron* 45, 201–206. doi: 10.1016/j.neuron.2004.12.033

Ibáñez, A., Hurtado, E., Lobos, A., Escobar, J., Trujillo, N., Baez, S., et al. (2011). Subliminal presentation of other faces (but not own face) primes behavioral and evoked cortical processing of empathy for pain. *Brain Res.* 1398, 72–85. doi: 10.1016/j.brainres.2011.05.014

Ironside, M., O'Shea, J., Cowen, P. J., and Harmer, C. J. (2016). Frontal cortex stimulation reduces vigilance to threat: implications for the treatment of depression and anxiety. *Biol. Psychiatry* 79, 823–830. doi: 10.1016/j.biopsych.2015.06.012

Japee, S., Crocker, L., Carver, F., Pessoa, L., and Ungerleider, L. G. (2009). Individual differences in valence modulation of face-selective M170 response. *Emotion* 9, 59–69. doi: 10.1037/a0014487

Jiang, Y., Shannon, R. W., Vizueta, N., Bernat, E. M., Patrick, C. J., and He, S. (2009). Dynamics of processing invisible faces in the brain: automatic neural encoding of facial expression information. *Neuroimage* 44, 1171–1177. doi: 10.1016/j.neuroimage.2008.09.038

Junghöfer, M., Bradley, M. M., Elbert, T. R., and Lang, P. J. (2001). Fleeting images: a new look at early emotion discrimination. *Psychophysiology* 38, 175–178. doi: 10.1111/1469-8986.3820175

Junghöfer, M., Sabatinelli, D., Bradley, M. M., Schupp, H. T., Elbert, T. R., and Lang, P. J. (2006). Fleeting images: rapid affect discrimination in the visual cortex. *Neuroreport* 17, 225–229. doi: 10.1097/01.wnr.0000198437.59883.bb

Keil, A., Bradley, M. M., Hauk, O., Rockstroh, B., Elbert, T., and Lang, P. J. (2002). Large-scale neural correlates of affective picture processing. *Psychophysiology* 39, 641–649. doi: 10.1111/1469-8986.3950641

Keuper, K., Zwanzger, P., Nordt, M., Eden, A., Laeger, I., Zwitserlood, P., et al. (2014). How 'love' and 'hate' differ from 'sleep': using combined electro/magnetoencephalographic data to reveal the sources of early cortical responses to emotional words. *Hum. Brain Mapp.* 35, 875–888. doi: 10.1002/hbm.22220

Keuper, K., Zwitserlood, P., Rehbein, M. A., Eden, A. S., Laeger, I., Junghöfer, M., et al. (2013). Early prefrontal brain responses to the hedonic quality of emotional words–A simultaneous EEG and MEG study. *PLoS One* 8:e70788. doi: 10.1371/journal.pone.0070788

Kim, E. Y., Lee, S.-H., Park, G., Kim, S., Kim, I., Chae, J.-H., et al. (2013). Gender difference in event related potentials to masked emotional stimuli in the oddball task. *Psychiatry Investig.* 10, 164–172. doi: 10.4306/pi.2013.10.2.164

Kiss, M., and Eimer, M. (2008). ERPs reveal subliminal processing of fearful faces. *Psychophysiology* 45, 318–326. doi: 10.1111/j.1469-8986.2007.00634.x

Klimesch, W. (1996). Memory processes, brain oscillations and EEG synchronization. *Int. J. Psychophysiol.* 24, 61–100. doi: 10.1016/S0167-8760(96)00057-8

Koster, E. H., De Raedt, R., Goeleven, E., Franck, E., and Crombez, G. (2005). Mood-congruent attentional bias in dysphoria: maintained attention to and impaired disengagement from negative information. *Emotion* 5, 446–455. doi: 10.1037/1528-3542.5.4.446

Kozel, F. A., and George, S. M. (2002). Meta-analysis of left prefrontal repetitive transcranial magnetic stimulation (rTMS) to treat depression. *J. Psychiatr. Pract.* 8, 270–275. doi: 10.1097/00131746-200209000-00003

Kwan, V. S., Barrios, V., Ganis, G., Gorman, J., Lange, C., Kumar, M., et al. (2007). Assessing the neural correlates of self-enhancement bias: a transcranial magnetic stimulation study. *Exp. Brain Res.* 182, 379–385. doi: 10.1007/s00221-007-0992-2

Lang, P. J., Bradley, M. M., and Cuthbert, B. N. (1999). *International Affective Picture System (IAPS): Instruction Manual and Affective Ratings*. Gainesville, FL: University of Florida.

Lang, P. J., Bradley, M. M., and Cuthbert, B. N. (2005). *International Affective Picture System (IAPS): Affective Ratings of Pictures and Instruction Manual*. Gainesville, FL: Center for the Study of Emotion & Attention.

Lee, S. Y., Kang, J. I., Lee, E., Namkoong, K., and An, S. K. (2011). Differential priming effect for subliminal fear and disgust facial expressions. *Attent. Percept. Psychophys.* 73, 473–481. doi: 10.3758/s13414-010-0032-3

Leyman, L., De Raedt, R., Vanderhasselt, M. A., and Baeken, C. (2009). Influence of high-frequency repetitive transcranial magnetic stimulation over the dorsolateral prefrontal cortex on the inhibition of emotional information in healthy volunteers. *Psychol. Med.* 39, 1019–1028. doi: 10.1017/S0033291708004431

Leyman, L., De Raedt, R., Vanderhasselt, M.-A., and Baeken, C. (2011). Effects of repetitive transcranial magnetic stimulation of the dorsolateral prefrontal cortex on the attentional processing of emotional information in major depression: a pilot study. *Psychiatry Res.* 185, 102–107. doi: 10.1016/j.psychres.2009.04.008

Li, T.-T., and Lu, Y. (2014). The subliminal affective priming effects of faces displaying various levels of arousal: an ERP study. *Neurosci. Lett.* 583, 148–153. doi: 10.1016/j.neulet.2014.09.027

Liddell, B. J., Williams, L. M., Rathjen, J., Shevrin, H., and Gordon, E. (2004). A temporal dissociation of subliminal versus supraliminal fear perception: an event-related potential study. *J. Cogn. Neurosci.* 16, 479–486. doi: 10.1162/089892904322926809

Lu, B., Hui, M., and Yu-Xia, H. (2005). The development of native Chinese affective picture system–a pretest in 46 college students. *Chin. Ment. Health J.* 19, 719–722.

Machii, K., Cohen, D., Ramos-Estebanez, C., and Pascual-Leone, A. (2006). Safety of rTMS to non-motor cortical areas in healthy participants and patients. *Clin. Neurophysiol.* 117, 455–471. doi: 10.1016/j.clinph.2005.10.014

Maris, E., and Oostenveld, R. (2007). Nonparametric statistical testing of EEG-and MEG-data. *J. Neurosci. Methods* 164, 177–190. doi: 10.1016/j.jneumeth.2007.03.024

Meneguzzo, P., Tsakiris, M., Schioth, H. B., Stein, D. J., and Brooks, S. J. (2014). Subliminal versus supraliminal stimuli activate neural responses in anterior cingulate cortex, fusiform gyrus and insula: a meta-analysis of fMRI studies. *BMC Psychol.* 2:52. doi: 10.1186/s40359-014-0052-1

Mosimann, U. P., Rihs, T. A., Engeler, J., Fisch, H.-U., and Schlaepfer, T. E. (2000). Mood effects of repetitive transcranial magnetic stimulation of left prefrontal cortex in healthy volunteers. *Psychiatry Res.* 94, 251–256. doi: 10.1016/S0165-1781(00)00146-3

Nakajima, K., Minami, T., and Nakauchi, S. (2015). Effects of facial color on the subliminal processing of fearful faces. *Neuroscience* 310, 472–485. doi: 10.1016/j.neuroscience.2015.09.059

Nitsche, M., Koschack, J., Pohlers, H., Hullemann, S., Paulus, W., and Happe, S. (2012). Effects of frontal transcranial direct current stimulation on emotional state and processing in healthy humans. *Front. Psychiatry* 3:58. doi: 10.3389/fpsyt.2012.00058

Nomi, J. S., Frances, C., Nguyen, M. T., Bastidas, S., and Troup, L. J. (2013). Interaction of threat expressions and eye gaze: an event-related potential study. *Neuroreport* 24, 813–817. doi: 10.1097/WNR.0b013e3283647682

Notzon, S., Steinberg, C., Zwanzger, P., and Junghöfer, M. (2017). Modulating emotion perception–Opposing effects of inhibitory and excitatory prefrontal cortex stimulation. *Biol. Psychiatry* 3, 329–336. doi: 10.1016/j.bpsc.2017.12.007

Oberman, L., Edwards, D., Eldaief, M., and Pascual-Leone, A. (2011). Safety of theta burst transcranial magnetic stimulation: a systematic review of the literature. *J. Clin. Neurophysiol.* 28, 67–74. doi: 10.1097/WNP.0b013e318205135f

Ochsner, K. N., Ray, R. R., Hughes, B., McRae, K., Cooper, J. C., Weber, J., et al. (2009). Bottom-up and top-down processes in emotion generation: common and distinct neural mechanisms. *Psychol. Sci.* 20, 1322–1331. doi: 10.1111/j.1467-9280.2009.02459.x

Ochsner, K. N., Silvers, J. A., and Buhle, J. T. (2012). Functional imaging studies of emotion regulation: a synthetic review and evolving model of the cognitive control of emotion. *Ann. N. Y. Acad. Sci.* 1251, E1–E24. doi: 10.1111/j.1749-6632.2012.06751.x

Olofsson, J. K., Nordin, S., Sequeira, H., and Polich, J. (2008). Affective picture processing: an integrative review of ERP findings. *Biol. Psychol.* 77, 247–265. doi: 10.1016/j.biopsycho.2007.11.006

Olofsson, J. K., and Polich, J. (2007). Affective visual event-related potentials: arousal, repetition, and time-on-task. *Biol. Psychol.* 75, 101–108. doi: 10.1016/j.biopsycho.2006.12.006

Pegna, A. J., Darque, A., Berrut, C., and Khateb, A. (2011). Early ERP modulation for task-irrelevant subliminal faces. *Front. Psychol.* 2:88. doi: 10.3389/fpsyg.2011.00088

Pegna, A. J., Landis, T., and Khateb, A. (2008). Electrophysiological evidence for early non-conscious processing of fearful facial expressions. *Int. J. Psychophysiol.* 70, 127–136. doi: 10.1016/j.ijpsycho.2008.08.007

Pessoa, L., and Adolphs, R. (2010). Emotion processing and the amygdala: from a 'low road' to 'many roads' of evaluating biological significance. *Nat. Rev. Neurosci.* 11, 773–783. doi: 10.1038/nrn2920

Phaf, R. H., and Kan, K. J. (2007). The automaticity of emotional Stroop: a meta-analysis. *J. Behav. Ther. Exp. Psychiatry* 38, 184–199. doi: 10.1016/j.jbtep.2006.10.008

Phan, K. L., Fitzgerald, D. A., Nathan, P. J., Moore, G. J., Uhde, T. W., and Tancer, M. E. (2005). Neural substrates for voluntary suppression of negative affect: a functional magnetic resonance imaging study. *Biol. Psychiatry* 57, 210–219. doi: 10.1016/j.biopsych.2004.10.030

Poldrack, R. A., Wagner, A. D., Ochsner, K. N., and Gross, J. J. (2008). Cognitive emotion regulation insights from social cognitive and affective neuroscience. *Curr. Dir. Psychol. Sci.* 17, 153–158. doi: 10.1111/j.1467-8721.2008.00566.x

Qian, C., Al-Aidroos, N., West, G., Abrams, R. A., and Pratt, J. (2012). The visual P2 is attenuated for attended objects near the hands. *Cogn. Neurosci.* 3, 98–104. doi: 10.1080/17588928.2012.658363

Rossi, S., Hallett, M., Rossini, P. M., Pascual-Leone, A., and Safety of TMS Consensus Group (2009). Safety, ethical considerations, and application guidelines for the use of transcranial magnetic stimulation in clinical practice and research. *Clin. Neurophysiol.* 120, 2008–2039. doi: 10.1016/j.clinph.2009.08.016

Sabatinelli, D., Fortune, E. E., Li, Q., Siddiqui, A., Krafft, C., Oliver, W. T., et al. (2011). Emotional perception: meta-analyses of face and natural scene processing. *Neuroimage* 54, 2524–2533. doi: 10.1016/j.neuroimage.2010.10.011

Sabatinelli, D., Lang, P. J., Keil, A., and Bradley, M. M. (2006). Emotional perception: correlation of functional MRI and event-related potentials. *Cereb. Cortex* 17, 1085–1091. doi: 10.1093/cercor/bhl017

Sabatini, E., Della Penna, S., Franciotti, R., Ferretti, A., Zoccolotti, P., Rossini, P. M., et al. (2009). Brain structures activated by overt and covert emotional visual stimuli. *Brain Res. Bull.* 79, 258–264. doi: 10.1016/j.brainresbull.2009.03.001

Sagliano, L., D'Olimpio, F., Panico, F., Gagliardi, S., and Trojano, L. (2016). The role of the dorsolateral prefrontal cortex in early threat processing: a TMS study. *Soc. Cogn. Affect. Neurosci.* 11, 1992–1998.

Sarter, M., Givens, B., and Bruno, J. P. (2001). The cognitive neuroscience of sustained attention: where top-down meets bottom-up. *Brain Res. Rev.* 35, 146–160. doi: 10.1016/S0165-0173(01)00044-3

Schupp, H. T., Cuthbert, B., Bradley, M., Hillman, C., Hamm, A., and Lang, P. (2004a). Brain processes in emotional perception: motivated attention. *Cogn. Emot.* 18, 593–611. doi: 10.1080/02699930341000239

Schupp, H. T., Cuthbert, B. N., Bradley, M. M., Cacioppo, J. T., Ito, T., and Lang, P. J. (2000). Affective picture processing: the late positive potential is modulated by motivational relevance. *Psychophysiology* 37, 257–261. doi: 10.1111/1469-8986.3720257

Schupp, H. T., Junghöfer, M., Weike, A. I., and Hamm, A. O. (2004b). The selective processing of briefly presented affective pictures: an ERP analysis. *Psychophysiology* 41, 441–449.

Schupp, H. T., Flaisch, T., Stockburger, J., and Junghöfer, M. (2006). Emotion and attention: event-related brain potential studies. *Prog. Brain Res.* 156, 31–51. doi: 10.1016/S0079-6123(06)56002-9

Schupp, H. T., Junghöfer, M., Weike, A. I., and Hamm, A. O. (2003a). Attention and emotion: an ERP analysis of facilitated emotional stimulus processing. *Neuroreport* 14, 1107–1110.

Schupp, H. T., Markus, J., Weike, A. I., and Hamm, A. O. (2003b). Emotional facilitation of sensory processing in the visual cortex. *Psychol. Sci.* 14, 7–13.

Schupp, H. T., Stockburger, J., Codispoti, M., Junghöfer, M., Weike, A. I., and Hamm, A. O. (2007). Selective visual attention to emotion. *J. Neurosci.* 27, 1082–1089. doi: 10.1523/JNEUROSCI.3223-06.2007

Shek, D. T. (1988). Reliability and factorial structure of the Chinese version of the State-Trait Anxiety Inventory. *J. Psychopathol. Behav. Assess.* 10, 303–317. doi: 10.1007/BF00960624

Shek, D. T. (1993). The Chinese version of the State-Trait Anxiety Inventory: its relationship to different measures of psychological well-being. *J. Clin. Psychol.* 49, 349–358. doi: 10.1002/1097-4679(199305)49:3<349::AID-JCLP2270490308>3.0.CO;2-J

Siegle, G. J., Thompson, W., Carter, C. S., Steinhauer, S. R., and Thase, M. E. (2007). Increased amygdala and decreased dorsolateral prefrontal BOLD responses in unipolar depression: related and independent features. *Biol. Psychiatry* 61, 198–209. doi: 10.1016/j.biopsych.2006.05.048

Smith, M. L. (2012). Rapid processing of emotional expressions without conscious awareness. *Cereb. Cortex* 22, 1748–1760. doi: 10.1093/cercor/bhr250

Spielberg, J. M., Stewart, J. L., Levin, R. L., Miller, G. A., and Heller, W. (2008). Prefrontal cortex, emotion, and approach/withdrawal motivation. *Soc. Pers. Psychol. Compass* 2, 135–153. doi: 10.1111/j.1751-9004.2007.00064.x

Spielberger, C. D. (1983). *Manual for the State-Trait Anxiety Inventory STAI (form Y)(" Self-Evaluation Questionnaire")*. Palo Alto, CA: Consulting Psychologists Press.

Spielberger, C. D., Lushene, R., and Gorsuch, R. (1968). *Self-Evaluation Questionnaire: STAI Form X-1*. Available at: http://hdl.handle.net/10477/1878

Spruyt, A., Hermans, D., Houwer, J. D., and Eelen, P. (2002). On the nature of the affective priming effect: affective priming of naming responses. *Soc. Cogn.* 20, 227–256. doi: 10.1521/soco.20.3.227.21106

Stokes, M. G., Barker, A. T., Dervinis, M., Verbruggen, F., Maizey, L., Adams, R. C., et al. (2012). Biophysical determinants of transcranial magnetic stimulation: effects of excitability and depth of targeted area. *J. Neurophysiol.* 109, 437–444. doi: 10.1152/jn.00510.2012

Tupak, S. V., Dresler, T., Badewien, M., Hahn, T., Ernst, L. H., Herrmann, M. J., et al. (2013). Inhibitory transcranial magnetic theta burst stimulation attenuates prefrontal cortex oxygenation. *Hum. Brain Mapp.* 34, 150–157. doi: 10.1002/hbm.21421

van Honk, J., Schutter, D. J., d'Alfonso, A. A., Kessels, R. P., and de Haan, E. H. (2002). 1 hz rTMS over the right prefrontal cortex reduces vigilant attention to unmasked but not to masked fearful faces. *Biol. Psychiatry* 52, 312–317. doi: 10.1016/S0006-3223(02)01346-X

Wager, T. D., Davidson, M. L., Hughes, B. L., Lindquist, M. A., and Ochsner, K. N. (2008). Prefrontal-subcortical pathways mediating successful emotion regulation. *Neuron* 59, 1037–1050. doi: 10.1016/j.neuron.2008.09.006

Wassermann, E. M. (1998). Risk and safety of repetitive transcranial magnetic stimulation: report and suggested guidelines from the International Workshop on the Safety of Repetitive Transcranial Magnetic Stimulation, June 5–7, 1996. *Electroencephalogr. Clin. Neurophysiol.* 108, 1–16.

Wessing, I., Romer, G., and Junghöfer, M. (2016). Hypervigilance-avoidance in children with anxiety disorders: magnetoencephalographic evidence. *J. Child Psychol. Psychiatry* 58, 103–112. doi: 10.1111/jcpp.12617

Willenbockel, V., Sadr, J., Fiset, D., Horne, G. O., Gosselin, F., and Tanaka, J. W. (2010a). Controlling low-level image properties: the SHINE toolbox. *Behav. Res. Methods* 42, 671–684. doi: 10.3758/BRM.42.3.671

Willenbockel, V., Sadr, J., Fiset, D., Horne, G. O., Gosselin, F., and Tanaka, J. W. (2010b). The SHINE toolbox for controlling low-level image properties. *J. Vis.* 10, 653, 653a. doi: 10.3758/BRM.42.3.671

Williams, L. M., Liddell, B. J., Kemp, A. H., Bryant, R. A., Meares, R. A., Peduto, A. S., et al. (2006). Amygdala–prefrontal dissociation of subliminal and supraliminal fear. *Hum. Brain Mapp.* 27, 652–661. doi: 10.1002/hbm.20208

Williams, L. M., Liddell, B. J., Rathjen, J., Brown, K. J., Gray, J., Phillips, M., et al. (2004). Mapping the time course of nonconscious and conscious perception of fear: an integration of central and peripheral measures. *Hum. Brain Mapp.* 21, 64–74. doi: 10.1002/hbm.10154

Winkielman, P., and Berridge, K. C. (2004). Unconscious emotion. *Curr. Dir. Psychol. Sci.* 13, 120–123. doi: 10.1111/j.0963-7214.2004.00288.x

Winkielman, P., Berridge, K. C., and Wilbarger, J. L. (2005). Unconscious affective reactions to masked happy versus angry faces influence consumption behavior and judgments of value. *Pers. Soc. Psychol. Bull.* 31, 121–135. doi: 10.1177/0146167204271309

Zhang, D., Wang, L., Luo, Y., and Luo, Y. (2012). Individual differences in detecting rapidly presented fearful faces. *PLoS One* 7:e49517. doi: 10.1371/journal.pone.0049517

Zhu, C., He, W., Qi, Z., Wang, L., Song, D., Zhan, L., et al. (2015). The time course of emotional picture processing: an event-related potential study using a rapid serial visual presentation paradigm. *Front. Psychol.* 6:954. doi: 10.3389/fpsyg.2015.00954

Zwanzger, P., Steinberg, C., Rehbein, M. A., Bröckelmann, A.-K., Dobel, C., Zavorotnyy, M., et al. (2014). Inhibitory repetitive transcranial magnetic stimulation (rTMS) of the dorsolateral prefrontal cortex modulates early affective processing. *Neuroimage* 101, 193–203. doi: 10.1016/j.neuroimage.2014.07.003

**Conflict of Interest Statement:** The authors declare that the research was conducted in the absence of any commercial or financial relationships that could be construed as a potential conflict of interest.

frontiers in Human Neuroscience

ORIGINAL RESEARCH
published: 18 October 2018
doi: 10.3389/fnhum.2018.00419

# Abstract Representations of Emotions Perceived From the Face, Body, and Whole-Person Expressions in the Left Postcentral Gyrus

*Linjing Cao[1], Junhai Xu[1]*, Xiaoli Yang[1], Xianglin Li[2] and Baolin Liu[1,3]**

*[1] School of Computer Science and Technology, Tianjin Key Laboratory of Cognitive Computing and Application, Tianjin University, Tianjin, China, [2] Medical Imaging Research Institute, Binzhou Medical University, Yantai, China, [3] State Key Laboratory of Intelligent Technology and Systems, Tsinghua National Laboratory for Information Science and Technology, Tsinghua University, Beijing, China*

Emotions can be perceived through the face, body, and whole-person, while previous studies on the abstract representations of emotions only focused on the emotions of the face and body. It remains unclear whether emotions can be represented at an abstract level regardless of all three sensory cues in specific brain regions. In this study, we used the representational similarity analysis (RSA) to explore the hypothesis that the emotion category is independent of all three stimulus types and can be decoded based on the activity patterns elicited by different emotions. Functional magnetic resonance imaging (fMRI) data were collected when participants classified emotions (angry, fearful, and happy) expressed by videos of faces, bodies, and whole-persons. An abstract emotion model was defined to estimate the neural representational structure in the whole-brain RSA, which assumed that the neural patterns were significantly correlated in within-emotion conditions ignoring the stimulus types but uncorrelated in between-emotion conditions. A neural representational dissimilarity matrix (RDM) for each voxel was then compared to the abstract emotion model to examine whether specific clusters could identify the abstract representation of emotions that generalized across stimulus types. The significantly positive correlations between neural RDMs and models suggested that the abstract representation of emotions could be successfully captured by the representational space of specific clusters. The whole-brain RSA revealed an emotion-specific but stimulus category-independent neural representation in the left postcentral gyrus, left inferior parietal lobe (IPL) and right superior temporal sulcus (STS). Further cluster-based MVPA revealed that only the left postcentral gyrus could successfully distinguish three types of emotions for the two stimulus type pairs (face-body and body-whole person) and happy versus angry/fearful, which could be considered as positive versus negative for three stimulus type pairs, when the cross-modal classification

OPEN ACCESS

**Edited by:**
*Wenbo Luo,*
*Liaoning Normal University, China*

**Reviewed by:**
*Renxin Chu,*
*Brigham and Women's Hospital, Harvard Medical School, United States*
*Xuntao Yin,*
*Army Medical University, China*

***Correspondence:**
*Junhai Xu*
*jhxu@tju.edu.cn*
*Baolin Liu*
*liubaolin@tsinghua.edu.cn*

**Received:** 09 April 2018
**Accepted:** 27 September 2018
**Published:** 18 October 2018

**Citation:**
*Cao L, Xu J, Yang X, Li X and Liu B (2018) Abstract Representations of Emotions Perceived From the Face, Body, and Whole-Person Expressions in the Left Postcentral Gyrus. Front. Hum. Neurosci. 12:419. doi: 10.3389/fnhum.2018.00419*

analysis was performed. Our study suggested that abstract representations of three emotions (angry, fearful, and happy) could extend from the face and body stimuli to whole-person stimuli and the findings of this study provide support for abstract representations of emotions in the left postcentral gyrus.

**Keywords: emotion, representational similarity analysis, fMRI, abstract representation, whole-brain searchlight**

## INTRODUCTION

The ability to understand the feelings of other people is part of successful social interactions in our daily life. Emotions can be perceived from various sensory cues, such as facial expressions, hand gestures, body movements, emotional whole-persons and vocal intonations (Gelder et al., 2006; Heberlein and Atkinson, 2009). These different sensory cues could elicit very similar emotions suggesting that the brain hosts "supramodal" or abstract representations of emotions regardless of the sensory cues. For example, fear can be recognized similarly from the eye region of faces, or postures and movements of body parts, suggesting that emotions might be represented at an abstract level. Numerous considerable efforts have been devoted to identify this kind of abstract representations that are invariant to the sensory cues (Peelen et al., 2010; Aube et al., 2015; Kim et al., 2015, 2017). Previous studies suggested that the medial prefrontal cortex (MPFC) contained representations of emotions that were invariant to perceptual modality (Peelen et al., 2010; Chikazoe et al., 2014) and generalized to emotions inferred in the absence of any overt display (Skerry and Saxe, 2014). And the neural representations in the MPFC and left superior temporal sulcus (STS) have been suggested to be modality-independent but emotion-specific (Peelen et al., 2010). By examining the neural representations of categorical valence (positive, neutral, and negative) elicited by visual and auditory modalities, modality-general representations were discovered in some specific regions, including the precuneus, bilateral MPFC, left STS/postcentral gyrus, right STS/middle frontal gyrus (MFG), inferior parietal lobe (IPL), and thalamus (Kim et al., 2017). Moreover, emotions were demonstrated to be indeed represented at an abstract level and the abstract representations could also be activated by the memories of an emotional event (Kim et al., 2015).

Although it has been demonstrated that facial and bodily emotions can be represented at an abstract level regardless of the sensory cue in specific brain regions (Peelen et al., 2010; Klasen et al., 2011; Chikazoe et al., 2014; Skerry and Saxe, 2014; Aube et al., 2015; Kim et al., 2017; Schirmer and Adolphs, 2017), the abstract representation is only elicited using one single face or body parts for the visual cue, suggesting that emotions could be similarly perceived by emotional faces or bodies. However, behavioral studies have suggested that the human brain can encode the whole-person expressions in a holistic rather than part-based manner (Soria Bauser and Suchan, 2013). Neuroimaging studies have also shown that body-selective areas preferred the whole-person to the sum of their parts (McKone et al., 2001; Maurer et al., 2002; Zhang et al., 2012). Another recent study found a preference of the whole-body to the sums of their scrambled parts in some body-sensitive areas (Brandman and Yovel, 2016), indicating a holistic representation of the whole-person expression. Therefore, the emotions of whole-person expressions should be explored individually rather than in an integrated way from the isolated emotional faces and bodies. Further, one of our latest study has found that in the extrastriate body area (EBA), the whole-person patterns were almost equally associated with weighted sums of face and body patterns, using different weights for happy expressions but equal weights for angry and fearful ones (Yang et al., 2018). So, it remains unclear how the whole-person's emotion is represented in the human brain and whether the representations of emotions of the face, body, and whole-person expressions can be abstractly formed in specific brain regions.

A series of previous neuroimaging studies have utilized traditional univariate analyses to explore the cognitive mechanism of emotions, such as the general linear model (GLM). The GLM is voxel-based by estimating the activation of each voxel from specific experimental conditions, and only the statistically significant voxels were reported, which led to the loss of the fine-grained pattern information (Haynes and Rees, 2006; Norman et al., 2006). At present, advanced approaches such as multivoxel pattern analysis (MVPA) or representational similarity analysis (RSA) (Nikolaus et al., 2008) allows us to decode the pattern information across the whole brain. As compared with the multivariate decoding method that extracted features from multidimensional space and resorted to categorical judgment, RSA can provide us richer information on neural representations, which provides a framework for characterizing representational structure and for testing computational models of that structure (Hajcak et al., 2007; Kriegeskorte and Kievit, 2013). And it decodes neural information from the perspective of multivariate patterns and bridges the gap between different regions, subjects and species. In RSA, neural activity patterns can be abstracted from specific brain regions and then the dissimilarities of neural activity patterns elicited by different stimuli or conditions are computed. The representational dissimilarity matrices (RDMs) of the conditions characterize the information carried by a given representation in the brain. The neural RDMs can then be compared to the dissimilarity space captured by a specific model to test whether specific brain regions could match the representation of the model successfully. The significant correlations between neural RDMs and models suggested that the model could decode neural information of specific brain regions. And RSA has also been used to go beyond classification to test specific alternative models of the dimensions that structure the representation of others' emotions, indicating that our knowledge of others' emotions is abstract

and high dimensional (Skerry and Saxe, 2015). Moreover, RSA could provide a novel method to investigate the representational structure down to the level of individual perspective rather than broad categorical information.

Although the representation of the human emotional expressions has been examined in many studies, it is not clear how the brain forms abstract emotional representations from whole-person's stimuli and whether specific brain regions could show emotion-specific but stimulus category-independent (body, face, and whole-person) representations. Hence, in this study, we hypothesized that the emotion category was independent of three different perceptual cues (body, face, and whole-person) and could be decoded based on the activity patterns from different emotions. Functional magnetic resonance imaging (fMRI) data were collected when participants classified emotions (angry, fearful, and happy) expressed by videos of faces, bodies and whole-persons. First, we conducted the RSA to examine whether some specific brain regions contained emotion-specific but stimulus category-independent representations of perceived emotions. One possible abstract representation of emotions is that the neural patterns are significantly correlated in within-emotion conditions across stimulus types but uncorrelated in between-emotion conditions. To test this hypothesis, the dissimilarity matrix was first established for the abstract emotion model and then the searchlight-based RSA was performed to calculate the correlations between the dissimilarity matrix capturing the model and the neural dissimilarity matrix of each voxel across the whole brain. Then the cross-modal MVPA was performed as the additional validation analysis on the data to verify whether the clusters identified by whole-brain RSA were truly informative to abstract representations of emotions. A further univariate analysis was finally conducted to explore the differences between the mean activation patterns of the significant clusters in different conditions.

# MATERIALS AND METHODS

## Participants

Twenty-four healthy volunteers were recruited in this study. All participants were right-handed, with normal or corrected-to-normal vision, and all declared having no history of neurological or psychiatric disorders. Four participants were excluded due to movement artifacts and twenty participants were finally included in the further analysis (10 females, mean age 21.8 $\pm$ 1.83 years, range from 19 to 25 years). This study was carried out in accordance with the recommendations of Institutional Review Board (IRB) of Tianjin Key Laboratory of Cognitive Computing and Application, Tianjin University with written informed consent from all subjects. All subjects gave written informed consent in accordance with the Declaration of Helsinki. The protocol was approved by the IRB of Tianjin Key Laboratory of Cognitive Computing and Application, Tianjin University. A separate group of volunteers ($n$ = 18) from the same community participated in a preliminary behavioral experiment to evaluate stimuli delivering emotional contents most effectively.

## Experiment Stimuli

Video clips with three emotions (happiness, anger and fear) (Grezes et al., 2007; de Gelder et al., 2012, de Gelder et al., 2015) were chosen from the GEMEP (GEneva Multimodal Emotion Portrayals) corpus (Banziger et al., 2012). Twenty-four video clips (four male and four female actors expressed each emotion) were selected and processed in grayscale using MATLAB (Kaiser et al., 2014; Soria Bauser and Suchan, 2015). Video clips of emotional facial expressions and bodily expressions were cropped using Adobe Premiere Pro CC 2014 by cutting out and masking the irrelevant aspect with Gaussian blur masks (Kret et al., 2011), so that non-facial body parts were not visible in clips of emotional facial expressions and facial features and expressions were not visible in clips of emotional bodily expressions. Also, the face clips were magnified when necessary. All videos clips were trimmed or combined to exactly fit the duration of 2000 ms (25 frame/s) by editing longer- or shorter-length clips, respectively. The generated clips were finally resized to 720 pixel $\times$ 576 pixel and presented on the center of the screen. Representative stimuli for the main experiment were presented in **Figure 1A**.

The experiment included a total of seventy-two video clips (3 emotions $\times$ 3 stimulus types $\times$ 8 videos per condition). In advance of the current study, a behavioral experiment had been conducted with another group of participants (8 females, mean age: 21.9 years; 10 males, mean age: 22.4 years) without any known difficulties in emotional processing for stimulus validation. Raters were asked to categorize the emotional materials with six labels (anger, surprise, happiness, sadness, fear, and disgust) and rated the perceived emotion intensity at a 9-point scale. For each condition, expressions were well recognized (happy whole-person: 95%, angry whole-person: 95%, fearful whole-person: 87%, happy face: 97%, angry face: 86%, fearful face: 74%, happy body: 75%, angry body: 93%, fearful body: 82%). There were no significant differences in the intensity rates between the selected videos for three emotional expressions [happiness versus anger: $t(17) = 0.73$, $p = 0.465$; happiness versus fear: $t(17) = 0.26$, $p = 0.796$; anger versus fear: $t(17) = 1.07$, $p = 0.285$].

In order to examine the quantitative differences in the amount of movement between videos, the movement per video was assessed by quantifying the variation for each pixel in the intensity of light (luminance) between two adjacent frames (Grezes et al., 2007; Peelen and Downing, 2007). For each frame, we averaged the score (on a scale reaching a maximum of 255) higher than 10 (10 corresponds to the noise level of the camera) across the pixels to estimate movements. Then, these scores were averaged for each video. No significant differences were observed between all three emotional expressions [happiness versus fear: $t(23) = 1.639$, $p = 0.108$; happiness versus anger: $t(23) = 0.833$, $p = 0.409$; anger versus fear: $t(23) = 2.045$, $p = 0.091$].

## Procedure

The procedure consisted of four runs (**Figure 1B**), each starting and ending with a 10 s fixation. Three emotions (happiness, anger, and fear) expressed by three stimulus types (face, body,

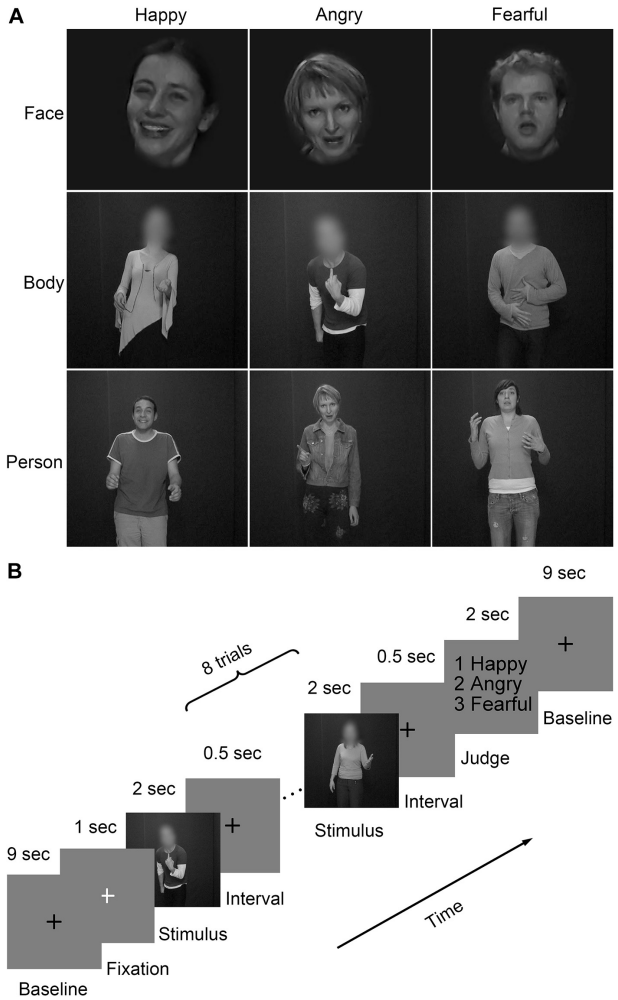


**FIGURE 1 |** Representative stimuli and paradigm of the experiment design. **(A)** Three stimulus types (face, body, and whole person) expressing three emotions (happy, angry, and fearful) were used in the experiment. The faces and bodies were masked with Gaussian blur masks; **(B)** A schematic overview of the presentation timing for emotion judgment task. Participants performed four fMRI runs, each starting and ending with a 10 s fixation baseline period. Emotions expressed by three stimulus types (face, body, and whole-person) were presented in each of the first three runs. The last run, only used emotions expressed by the whole-person. Within each run, 18 blocks of eight trials of the same category were pseudo-randomly presented. These blocks were separated by 10 s fixation interval (a black cross was presented for 9 s, followed by a white cross presented for 1 s to control subjects' attention). Each trial consisted of a 2 s video, followed by a 0.5 s interval. At the end of each block, participants were asked to make a choice between three emotions using a button press within a 2 s response window.

and whole-person) were presented in each of the first three runs. In the fourth run, only three kinds of the whole-person emotions (happiness, anger, and fear) expressed by the whole-person were presented. Within each run, eighteen blocks with eight trials were pseudo-randomly presented. These blocks were separated by a 10 s fixation interval (a black cross presented for 9 s and a white cross presented for 1 s to control subjects' attentions). Each trial consisted of a 2 s video, followed by a 0.5 s inter-stimulus interval (ISI). At the end of each block, participants were asked to make a choice between three emotions using a button press within a 2 s response window. One block-designed localizer run was also performed, in which the stimuli included 4 types of static or dynamic faces, bodies, whole-persons, and objects. This run contains a total of 16 blocks (4 types × dynamic/static × repeat 2 times), and these blocks including 8 trials (1.5 s each) were separated by 10 s fixation interval. Each trial consisted of a 1.4 s stimulus, followed by a 0.1 s ISI.

## Data Acquisition

Functional images were acquired using a 3.0 T Siemens scanner in Yantai Hospital Affiliated to Binzhou Medical University with a twenty-channel head coil. Foam pads and earplugs were used to reduce the head motion and scanner noise (Liang et al., 2017). For functional scans, an echo-planar imaging (EPI) sequence was used (T2* weighted, gradient echo sequence), with the following parameters: TR (repetition time) = 2000 ms, TE (echo time) = 30 ms, voxel size = 3.1 mm × 3.1 mm × 4.0 mm, matrix size = 64 × 64, 33 axial slices, 0.6 mm slices gap, FA = 90°. In addition, a high-resolution anatomical image was acquired using a three-dimensional magnetization-prepared rapid-acquisition gradient echo (3D MPRAGE) sequence (T1-weighted sequence), with the following parameters: TR = 1900 ms, TE = 2.52 ms, TI = 1100 ms, voxel size = 1 mm × 1 mm × 1 mm, matrix size = 256 × 256, FA = 9°. The stimuli were displayed by high-resolution stereo 3D glasses of VisualStim Digital MRI Compatible fMRI system.

## Data Analysis

### Behavioral Measures

For each participant, the response time and recognition accuracy of three kinds of emotions by three kinds of stimulus types were calculated. Then an analysis of variance (ANOVA) was performed on the accuracies to test the main effect and interactions between the factors Emotion and stimulus Category. Paired *t*-tests were further performed to examine the differences between all three emotions. The statistical analysis was performed using the SPSS 18 software.

### Data Preprocessing

Functional images were preprocessed and analyzed using the SPM8 software package[1] and MATLAB software (The Math Works). The first five volumes corresponding to the baseline of each run for all functional data were discarded to allow for equilibration effects. Slice-timing corrected and spatially realigned to the first volume for head-motion correction were performed for the remaining 283 volumes. Subsequently, the T1-weighted images were segmented into the gray matter, white matter and cerebrospinal fluid (CSF) for normalization after being co-registered to the mean functional images. Then the generated parameters were used to spatially normalize the functional images into the standard Montreal Neurological Institute (MNI) space at an isotropic voxel size of 3 mm × 3 mm × 3 mm. Especially, the images in the first four

[1]http://www.fil.ion.ucl.ac.uk/spm/software/spm8/

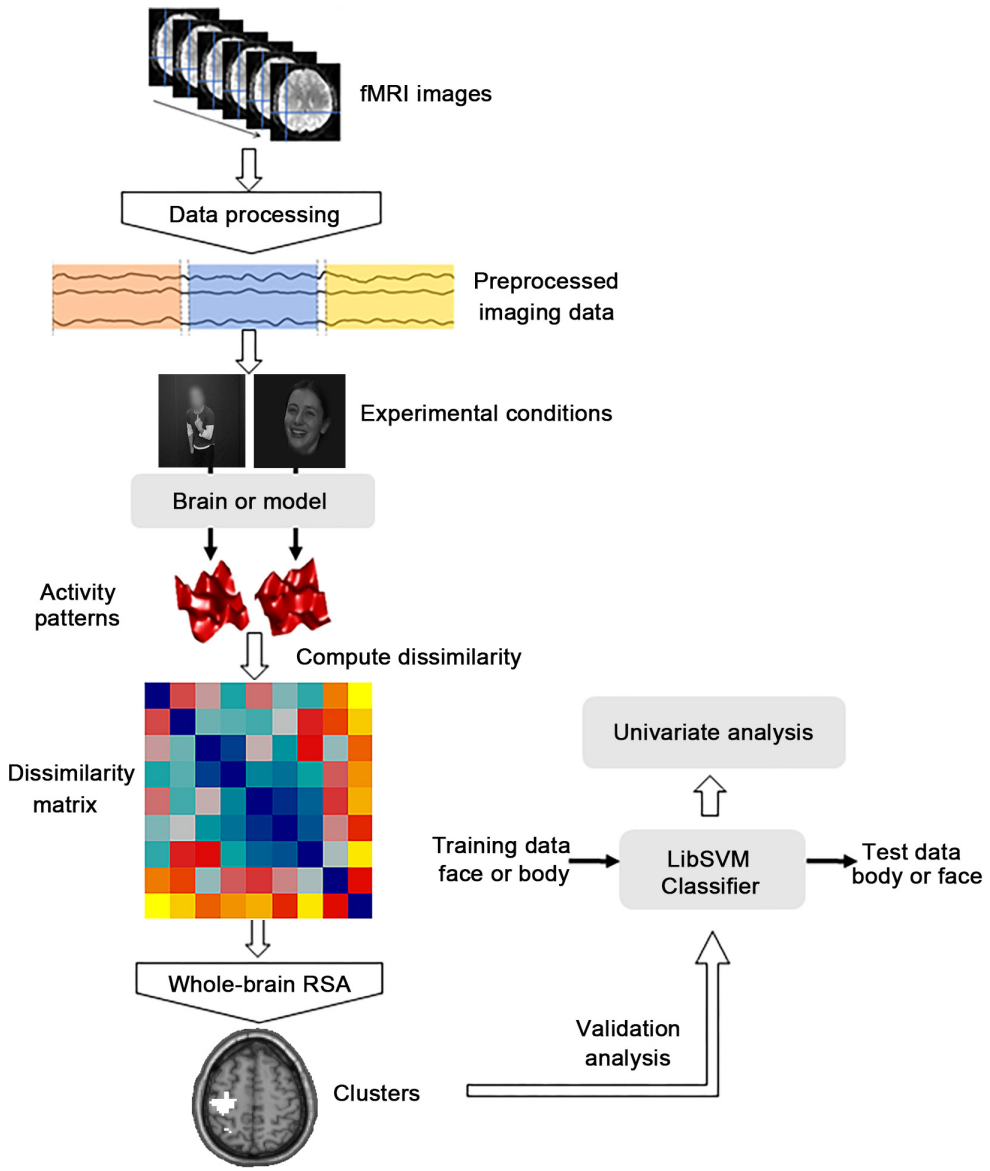


**FIGURE 2 |** Flow chart of the main analytical steps. There were three kinds of main procedures. The dissimilarity matrix was first established for the abstract emotion model and then the representational similarity analysis (RSA) was performed to calculate the correlations between the dissimilarity matrix capturing the model and the neural dissimilarity matrix of each voxel across the whole brain. Then the cross-modal multivoxel pattern analysis (MVPA) was performed as the additional validation analysis to verify whether the clusters identified by whole-brain RSA were truly informative to abstract representations of emotions. A further univariate analysis was then conducted to explore the differences between the mean activation patterns of the significant clusters identified from the MVPA procedure.

runs and the functional localization run were smoothed with a 4-mm full-width at half-maximum (FWHM) Gaussian filter (Zhang et al., 2016; Liang et al., 2018). Before the further analysis, fMRI data were fitted with a GLM to obtain regressors for all nine experimental conditions (happy face, angry face, fearful face, happy body, angry body, fearful body, happy whole-person, angry whole-person, and fearful whole-person). The GLM was constructed to model the data for each participant and the subsequent analysis was conducted on each of the first three runs, generating nine activation patterns in total. The sources of nuisance regressors along with their time derivatives were removed through the linear regression, including six head motion correction parameters, and averaged signals from the white matter and CSF (Xu et al., 2017; Geng et al., 2018). The main analytical steps included in this study were shown in **Figure 2**. In the searchlight analysis and cluster-based MVPA, only the data of the first three run were used.

## Representational Similarity Analysis

To localize regions that supported abstract representation of three emotions generalize across three stimulus types, the whole-brain RSA was performed, in which the RSA framework for the

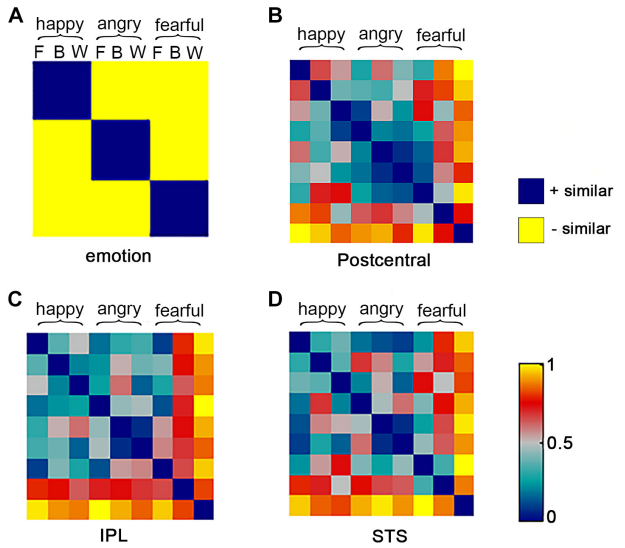


**FIGURE 3 |** Representational similarity analysis model and neural representational dissimilarity matrices (RDMs). For one abstract emotion model **(A)** and three neural representation of three clusters **(B–D)**, the representational dissimilarity matrices were calculated. The model is indexed at two levels in the order in which experimental conditions are rearranged: emotion (happy, angry, and fearful) and stimulus category (F: face B: body W: whole-person). The model dissimilarity matrix illustrates hypothetical correlations of different activity pattern, for example, significant similarity between pair of conditions that from the same emotion (happy–happy pair or angry–angry pair or fearful–fearful pair) should be observed in the abstract emotion model. The neural RDMs illustrate the actual representation of these three brain areas.

whole brain "searchlight" analysis was constructed using the RSA toolbox (Nili et al., 2014). To estimate the neural representational structure of the brain, a dissimilarity matrix was established for the abstract emotion model as follows: the model was established by setting 0 for all conditions of within-emotion across stimulus types (i.e., happy face-happy body pair or angry face-angry whole-person pair) and 1 anywhere else. In other words, setting 1 for all conditions of between-emotion (i.e., happy face-angry face pair or happy face-angry body pair), as shown in **Figure 3A**. Considering that the diagonal entries were not relevant to the hypothesis, they were set as NaNs for the model and excluded from the following analysis.

In whole-brain searchlight analysis, a spherical volume-based searchlight approach (Kriegeskorte et al., 2006) was used. For each participant and each voxel in the brain, we selected a searchlight of 9-mm radius and established the neural dissimilarity matrix for this sphere with the following procedures: for each of the nine stimulus conditions (3 emotions × 3 stimulus types), the neural activity patterns estimated by GLM were extracted from this sphere. Pair-wise dissimilarities were then computed between each of two different activity patterns using the correlation distance (1 minus the Pearson correlation) based on the pattern of GLM weights across conditions, resulting in a symmetrical 9 × 9 RDM for each participant. To examine whether the representations were independent of stimulus types and to what extent the abstract emotion model could account for neural pattern information, we then computed the Kendall's rank correlation coefficient (tau a) between the searchlight sphere and the abstract emotion model using the values derived from the upper triangles of neural RDMs and RDM of abstract emotion model. After that, the generated coefficients were assigned to the center voxel of the sphere in each searchlight analysis. This computational procedure was repeated across the whole brain for each individual, generating a whole-brain correlation map (r-map) for each participant (Nili et al., 2014). The group analysis was conducted based on the statistical r-maps, treating subjects as a random effect. One-side Wilcoxon sign-rank analysis was used to test in which voxel the correlation between the observed neural RDM and predicted model was significant by thresholding at $p < 0.01$ with a minimum cluster-size of 30 (resampled) contiguous voxels.

## Cluster-Based MVPA

In the cluster-based analysis, the cross-modal MVPA was performed as an additional validation analysis to verify whether the clusters identified by the searchlight analysis were truly informative to abstract representations of emotions, where the validation analysis is necessary because the identified significant searchlight clusters are not guaranteed to be informative (Etzel et al., 2013). There were two main functions in our verification analysis. First, Type I error was prevented which might falsely infer the existence of modal-generic voxels that is not existent by requiring this analysis to confirm the effect. Second, like the *posthoc* testing of a common effect, the specific nature of the representation of emotions was tested to better describe these effects. Crucially, this analysis did not introduce any new effects, but could rather clarify the nature of the observed effects and serve as a conservative criterion for identifying these effects. The MVPA method used in the current study is similar to those methods that have been successfully used in the previous exploration of affective space (Baucom et al., 2012; Shinkareva et al., 2014; Kim et al., 2017). A logical regression classifier was used for the cross-modal classification to examine the abstract representation of emotions at the group level (Bishop, 2006). In details, the data of the three stimulus types (face, body, and whole-person) were extracted separately, each of which contained the data of three emotional types. Then the logistic classifier was trained from the data of one stimulus type (i.e., face), and then the data of the other stimulus type (i.e., body or whole-person) was used as a test set. The logistic classifier was trained/tested separately for each cluster. We made a two-way classification analysis (happy versus angry/fearful, which could be considered as positive versus negative: P vs. N) and a three-way classification (happy versus angry versus fearful: H vs. A vs. F) analysis, which decomposed the data in an orthogonal manner. Classification accuracies were averaged across two cross-validation folds (i.e., face to body and vice versa) for each participant. For each participant, the significant cross-modal classification provides strong evidence of the structural validity of the classification, as the classification is unlikely to be driven by associated variables, such as lower-level features (e.g., motion, brightness, hue, etc.) between different stimulus types. For the

classification analysis between three emotional conditions, the one-sample *t*-test analysis was conducted to assess whether the group mean accuracy was significantly higher than the chance level (0.33). For the P vs. N classification analysis, half of the data for anger and fear conditions declined randomly, with each cross-validation equal to the baseline and therefore the chance level was 0.5. A one-sample *t*-test was also used to examine the significance of the group mean accuracy (the chance level was 0.5).

### Analysis of the Differences Between Mean Activation Patterns

A further univariate analysis was conducted to explore the differences between the mean activation patterns of the significant clusters identified from the MVPA procedure in different conditions. For each cluster, the beta values were averaged across voxels for each condition as described in previous studies (Peelen et al., 2010; Kim et al., 2015). The generated mean activation values for each cluster were input into a 3 emotions × 3 stimulus types ANOVA. To test whether there were significant differences between the emotion-specific activations across stimulus types, we examined whether the mean activations estimated by the beta values in these clusters were more similar for within-emotion response than between-emotion response. To this end, for each participant, the mean response magnitudes in three stimulus types (faces, bodies, and whole-persons) were subtracted from the data. Subsequently, we compared the absolute differences between the same emotion across different stimulus types (e.g., happy faces vs. happy bodies) and the absolute differences between different emotions across different stimulus types (e.g., happy faces vs. fearful bodies).

## RESULTS

## Behavior Analysis

The recognition accuracies of facial, bodily, and whole-person's emotions were at a relatively high level (mean accuracy = 98.0%, SD = 5.3) (happy faces: 100%, angry faces: 97.5%, fearful faces: 96.7%, happy bodies: 97.5%, angry bodies: 97.5%, fearful bodies: 96.7%, happy whole-persons: 100%, angry whole-persons: 98.8%, and fearful whole-persons: 97.1%). The 3 × 3 ANOVA was performed on the accuracies with the factors Emotion (happy, angry, and fearful) and stimulus Category (face, body, and whole-person), without significant main effect for Emotion [$F(2,38) = 2.98$, $p = 0.063$] and stimulus Category [$F(2,38) = 1.03$, $p = 0.367$], nor any significant interaction effect between these factors [$F(4,76) = 0.69$, $p = 0.599$]. The 3 × 3 ANOVA of the response time with the factors Emotion (happy, angry, and fearful) and stimulus Category (face, body, and whole-person) showed no significant main effect for stimulus Category [$F(2,38) = 1.91$, $p = 0.162$] but for Emotion [$F(2,38) = 20.53$, $p < 0.001$], nor any significant interaction between these factors was observed [$F(4,76) = 1.91$, $p = 0.118$]. Additionally, we performed paired comparisons among three emotions irrespective of the stimulus category. The results showed that the response time of the subjects to happy emotions was shorter than that to angry emotions [$t(19) = 3.98$, $p = 0.001$] or fearful emotions [$t(19) = 6.15$, $p < 0.001$]. In addition, they responded to angry emotions significantly faster than fearful ones [$t(19) = 2.75$, $p = 0.013$]. **Table 1** showed the statistical details of the group-level behavioral data. In the emotion identification task, the recognition accuracies and response times for the nine conditions of the subjects were shown in **Table 1**.

**TABLE 1 |** Mean emotion identification accuracies and corresponding response times.

| Emotion | Category | Recognition rate (%) | | Response time (ms) | |
|---|---|---|---|---|---|
| | | Mean | SD | Mean | SD |
| Happy | Face | 100 | 0 | 713.74 | 163.39 |
| | Body | 97.50 | 6.11 | 669.36 | 160.87 |
| | Whole-person | 100 | 0 | 675.25 | 155.35 |
| Angry | Face | 97.50 | 6.11 | 808.22 | 235.30 |
| | Body | 97.50 | 6.11 | 762.83 | 227.69 |
| | Whole-person | 98.75 | 3.05 | 767.05 | 224.22 |
| Fearful | Face | 96.67 | 6.84 | 809.54 | 234.73 |
| | Body | 96.67 | 6.84 | 825.16 | 220.20 |
| | Whole-person | 97.08 | 5.59 | 836.10 | 210.54 |

## Searchlight Similarity Analysis

In the searchlight similarity analysis, we compared the neural RDMs with the hypothetical abstract emotion model across the whole brain. The abstract emotion model was established by setting 0 for all conditions of within-emotion across stimulus types and 1 for all conditions of between-emotion, as shown in **Figure 3A**. The model RDM were indexed at two levels in the order where experimental conditions were rearranged: emotion (happy, angry, and fearful) and stimulus category (face, body, and whole-person). The model dissimilarity matrix illustrated the hypothetical correlations of different activity patterns for each condition, for example, the significant similarity between pair of conditions that from the same emotion (happy–happy pair or angry–angry pair or fearful–fearful pair) was observed in the abstract emotion model. Then the correlation map (r-map) for each participant was obtained and the random-effect group analysis ($N = 20$) was performed on the individual correlation map, revealing that all three clusters were significantly correlated with the abstract emotion model ($p < 0.01$, cluster size >30): left postcentral gyrus (−39, −21, 36), left IPL (−30, −54, 54), and right STS (51, −9, −24), as shown in **Figure 4**. The neural RDMs of the three clusters illustrated the actual representation of these brain areas. The neural RDMs, like the model, were also indexed at two levels) (**Figures 3B–D**). We discovered that the RDMs of specific brain regions were similar to the model to a certain extent. The correlations between within-emotions conditions were relatively high. For example, the correlations between three types of stimuli for the within-angry emotion conditions were relatively higher than the between-emotion conditions. The whole-brain searchlight analysis revealed that the abstract emotion model was positively related to the neural similarity in the left postcentral gyrus, left IPL, and right STS. The significantly positive correlations between the model and neural

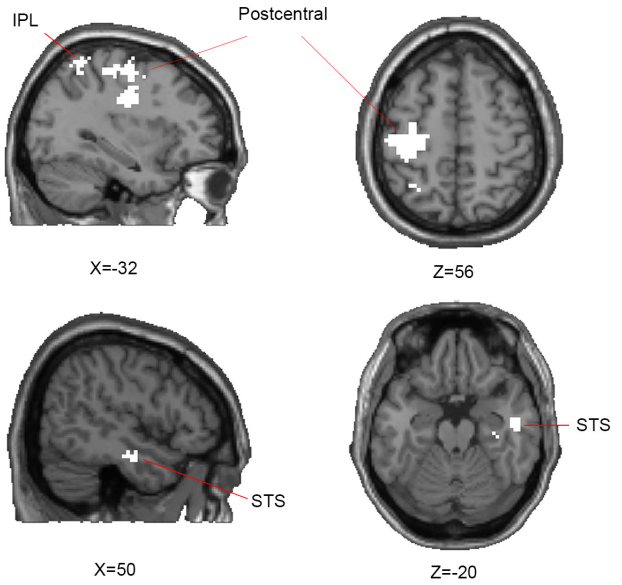


**FIGURE 4 |** Results of representational similarity analysis of whole-brain searchlight showing the significant clusters of abstract representation of emotion. For abstract representation of three emotions, three clusters are significantly correlated with the abstract emotion model: the left postcentral gyrus, inferior parietal lobe (IPL), and right superior temporal sulcus (STS) which are shown on axial and sagittal slices. One-side Wilcoxon sign-rank test was used in the second-level group analysis and p-map generated by thresholding at $p < 0.01$ with a minimum cluster-size of 30 contiguous voxels.

**TABLE 2 |** Significant clusters ($p < 0.01$, cluster size >30) correlated with the abstract emotion model from searchlight analysis.

| Anatomical region | Hemisphere | Cluster size | MNI coordinates | | | peak |
|---|---|---|---|---|---|---|
| | | | *x* | *y* | *z* | intensity |
| Postcentral gyrus | L | 323 | −39 | −21 | 36 | 28.99 |
| STS | R | 48 | 51 | −9 | −24 | 15.61 |
| IPL | L | 34 | −30 | −54 | 54 | 17.65 |

*The cluster size indicates number of voxels; STS, superior temporal sulcus; IPL, inferior parietal lobe; R, right; L, left.*

RDMs suggested an abstract representation of emotions in these three regions. **Table 2** depicted the detailed MNI coordinates of these clusters.

## Cluster-Based Cross-Modal MVPA

Cluster-based MVPA was conducted as a validation analysis to test whether clusters identified by the searchlight analysis contained information on the type of emotions, as proposed by Etzel et al.'s (2013) "Confirmation Test." The clearest evidence for an abstract representation of emotions is that the searchlight similarity analysis and MVPA converged on the same result, in other words, the clusters selected by the searchlight analysis could successfully distinguish either P vs. N or H vs. A vs. F for the cross-modal classification. Therefore, we only included those clusters that could distinguish either P vs. N or H vs. A vs. F using MVPA for any two or three of these three stimulus type pairs (face-body, face-whole person, and body-whole person). The clusters, which could not distinguish both P vs. N and H vs. A vs. F for all three pairs, were excluded from the further analysis. Classifying angry and fearful stimuli together versus happy stimuli (P vs. N) is important because the variation in this dimension clearly distinguishes bivalent representations and some brain regions may not be fine-grained to classify the three emotions, but can sort out different valences.

The cross-modal classification accuracies of three types of emotions for the three stimulus type pairs were higher than the baseline (0.33) for the left postcentral gyrus (face-body pair: 38.18, face-whole person pair: 34.29, body-whole person pair: 36.42) but lower for the STS and IPL. Similarly, the classification accuracies of P vs. N for three stimulus type pairs were higher than the chance level (0.5) for the left postcentral gyrus (face-body pair: 55.35, face-whole person pair: 52.92, body-whole person pair: 55.52) but not for the STS and IPL. Details were shown in **Table 3**. Additionally, one-sample *t*-tests in the left postcentral gyrus found that the classification accuracies for the face-body pair [$t(19) = 3.70$, $p = 0.002$] and body-whole person pair [$t(19) = 4.15$, $p = 0.001$] were significantly higher than 0.33 as distinguishing three types of emotions, and significantly higher than 0.5 as distinguishing P vs. N for the face-body pair [$t(19) = 4.14$, $p = 0.001$], face-whole person pair [$t(19) = 2.16$, $p = 0.044$] and body-whole person pair [$t(19) = 5.83$, $p < 0.001$], indicating that the left postcentral gyrus was informative on the type of emotions of all three stimulus types (face, body, and whole-person). The remaining two clusters could not distinguish the P vs. N or H vs. A vs. F significantly for any of the three pairs ($p > 0.05$).

### Mean Activation in the Identified Clusters by the Searchlight Analysis

The mean activation was extracted from the left postcentral gyrus by averaging the stimulus-related activations (as estimated from the GLMs) across all the voxels (**Figure 5**). The 3 × 3 ANOVA for parameter estimates of mean activation with the factors stimulus Category (face, body, and whole-person) and Emotion (happiness, anger, and fear) showed a main effect for Emotion

**TABLE 3 |** Classification accuracies from cross-modal MVPA for each searchlight cluster.

| Clusters | Hemisphere | H vs. A vs. F | | | P vs. N | | |
|---|---|---|---|---|---|---|---|
| | | F-B | F-W | B-W | F-B | F-W | B-W |
| Postcentral gyrus | L | 38.18* | 34.29 | 36.42* | 55.35* | 52.92* | 55.52* |
| STS | R | 33.04 | 31.17 | 32.85 | 52.02 | 50.46 | 49.15 |
| IPL | L | 33.06 | 31.29 | 32.21 | 51.56 | 48.25 | 48.69 |

*The cluster size indicates number of voxels; STS, superior temporal sulcus; IPL, inferior parietal lobe; *p < 0.05; R, right; L, left; H vs. A vs. F, happy versus angry versus fearful; P vs. N, happy versus angry/fearful which could be seen as positive versus negative; F-B, F-W, and B-W indicate the three stimulus type pairs (face-body, face-whole person, and body-whole person).*

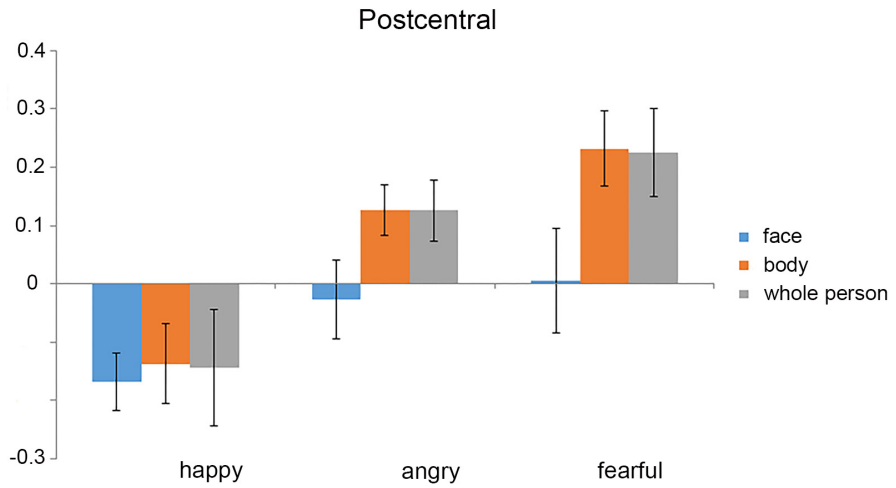


**FIGURE 5 |** Mean activation (parameter estimates) for each experimental condition in the left postcentral gyrus. The mean activation was extracted from the left postcentral gyrus by averaging the stimulus-related activations [as estimated from the general linear models (GLMs)] across all the voxels. We found that the mean activations in all of the stimulus conditions were below the baseline. Error bars show SEM.

[$F(2,38) = 7.34$, $p = 0.002$] and a weak trend towards main effect for stimulus Category [$F(2,38) = 3.07$, $p = 0.058$], and a weak trend towards interaction between these factors [$F(4,76) = 2.18$, $p = 0.079$] in the left postcentral gyrus, suggesting that the activation differences between the emotions differed in all three modalities. To further confirm whether there were the emotion-specific activation differences across stimulus types, we tested whether the average activations estimated by the beta values in the left postcentral gyrus were more similar for the within-emotion response than between-emotion response. If the mean activation values carried emotion-specific information, the mean within-emotion response difference should be smaller than the mean between-emotion response difference. However, the results showed that the mean within-emotion response difference was equivalent to the mean between-emotion response difference for all three stimulus type pairs in the postcentral gyrus ($p > 0.05$, for all tests). Thus, this confirmed that the mean response amplitude values might not provide emotion-specific information across different stimulus types.

## DISCUSSION

In this study, we used a searchlight-based RSA to investigate the regions that could represent emotions independent of the stimuli (body, face, and whole-person) mediating the emotions. The searchlight RSA with an abstract emotion model identified three clusters (left postcentral gyrus, left IPL, and right STS) that contained information about specific emotions regardless of the type of stimulus. Furthermore, the additional validation analysis found that the neural activity pattern in the left postcentral gyrus could successfully distinguish the happy versus angry/fearful conditions (positive versus negative, P vs. N) for all the three stimulus type pairs and three types of emotions (H vs. A vs. F) for two stimulus types pairs (body versus face and body versus whole-person), when the cross-modal classification analysis was performed. The other two clusters could not make a successful classification of the P vs. N or H vs. A vs. F for any of the three pairs. Therefore, the results further confirmed that the left postcentral gyrus played a crucial role in emotion representation at an abstract level. The univariate analysis showed that the mean within-emotion response difference was significantly smaller than that between-emotion response difference for all three stimulus type pairs in the left postcentral gyrus. This further confirmed that the left postcentral gyrus was truly informative of emotions of face, body and whole-person. Therefore, these findings provide evidence for emotion-specific representations in the left postcentral gyrus independent from the stimulus types (body, face, and whole-person) that conveyed the emotions.

### Representations of the Facial, Bodily, and Whole-Person's Emotions

The main goal of this study was to explore the regions that could represent emotions at an abstract level. Using a searchlight-based RSA, the left postcentral gyrus was identified to be capable of distinguishing three types of emotions for face-body pair and body-whole person pair and distinguishing happy versus angry/fearful (like positive versus negative) for all the three pairs. The left postcentral gyrus has often been shown to be involved in emotion processing (Viinikainen et al., 2010; Baucom et al., 2012; Kassam et al., 2013; Sarkheil et al., 2013; Flaisch et al., 2015; Kragel and LaBar, 2015). And it also has been found to be involved in emotional face and body processing (van de Riet et al., 2009) and the recognition of vocal expressions. One latest study confirmed the successful decoding of the affective category from perceived cues (facial and vocal expressions) by the activation patterns in the left postcentral gyrus, which was consistent with our study (Kragel and LaBar, 2016). Another recent research identified that the postcentral gyrus was critical for valence decoding. Furthermore, in the postcentral gyrus, the information

about valence (positive, neutral, and negative) was represented in activation patterns elicited by viewing photographs of different affective categories (Baucom et al., 2012), which was consistent with the present study. The postcentral gyrus also has been implicated in the perception of emotions based not just on facial expressions, but also on vocal prosody and whole-person's expressions, when subjects made emotion judgments (Heberlein and Atkinson, 2009). Consistent with our study, it indicated that the role of the postcentral gyrus in emotion recognition extended to recognizing whole-person emotional expressions. A previous finding revealed an interaction effect between emotion type and intensity corresponding to level of aversiveness in the postcentral gyrus when decoding dynamic facial expressions (Sarkheil et al., 2013). In contrast, our study only focused on the change in the emotion type, keeping the intensity unchanged. But we still found the abstract representation of face, body and whole-person in postcentral gyrus when the emotions were classified, suggesting that the extended cortical networks might be involved in processing the highly integrated information of face, body or whole-person stimuli. The postcentral gyrus also has been shown to make a consistent contribution to the cross-condition classification of four basic emotions induced by the video clips and imagery through emotion words. It indicated that the neural signatures were consistent within different emotions from video and imagery and suggested that the abstract representation of emotions was independent of the emotion induction procedure within the postcentral gyrus (Saarimaki et al., 2016). Consistent with this interpretation, our current results provide further evidence for the role of the left postcentral gyrus in abstract emotional processing by encoding emotional information regardless of the stimuli types (face, body, and whole-person). Furthermore, one recent study examined the neural representations of the categorical valence (positive, neutral, and negative) elicited by visual and auditory stimulus modalities, suggesting evidence for modality-general representations in the left postcentral gyrus (Kim et al., 2017). This finding directly compared different valence states, but specific emotional categories were not considered. Our study provided further evidence for the role of the left postcentral gyrus in abstract emotional processing by encoding three emotions (happiness, anger, and fear) expressed by different stimulus types. The searchlight-based RSA revealed an emotion-specific but stimulus category-independent neural representation in the left postcentral gurus. Our study suggested that abstract representations of emotions could extend from the face and body stimuli to whole-person stimuli. In summary, the findings of the current study provide support for the left postcentral gyrus for abstract representations of emotions.

The cross-modal classification of three emotions found that the mean accuracy was not significant for the face-whole person pair in the left postcentral gyrus. We speculated that as most of the low-level features (e.g., motion, brightness, hue, etc.) could not be shared between these two stimulus types, the effect of low-level features on a logical regression classifier trained from one stimulus type (face or whole-person) might not play a role in the testing of the other stimulus types (whole-person or face). In this study, only the construct of visual emotions were represented, which was easier to be influenced during the classification of three emotions. As previously demonstrated, this is because the encoding of the visual affect might be highly affected by the lower-level features in the visual modality (e.g., motion, brightness, hue, etc.) (Gabrielsson and Lindström, 2001; Lakens et al., 2013). Therefore, the differences between the stimuli of different emotional categories may be due to the accompanying differences of lower-level features rather than the emotional differences, which led to the classification performance for the face-whole person pair was not significant. Another possibility is that the left postcentral gyrus may not be fine-grained to classify the three emotions, but can sort out different valences (Peelen et al., 2010; Baucom et al., 2012; Kim et al., 2017). In recent researches, the postcentral gyrus was proved to be critical for valence decoding (Baucom et al., 2012; Kim et al., 2017), but insensitive to specific emotion categories, which could not successfully decode the specific affective categories from perceived cues (facial, bodily and vocal expressions) when the cross-modal classification analysis was performed (Peelen et al., 2010). In our present study, the left postcentral gyrus could still distinguish three types of emotions using MVPA for the two stimulus type pairs (face-body and body-whole person) and P vs. N for all the three stimulus type pairs, indicating that the left postcentral gyrus was informative to emotion representation of all three stimulus types (face, body, and whole-person) (Heberlein and Atkinson, 2009; Kragel and LaBar, 2016; Kim et al., 2017).

## Regions Where Emotions Could Not Be Represented

The searchlight-based RSA revealed that the neural RDMs of the IPL and rSTS were significantly correlated with the abstract emotion model. But both clusters could not make a significant classification between all three kinds of emotions and P vs. N for any of the three stimulus type pairs, suggesting that the significant correlations between neural RDMs of the IPL and rSTS and the abstract emotion model possibly arose from the overpowered nature of the searchlight analysis. Because the Type I error which might falsely infer the existence of modal-generic voxels that is not existent when the searchlight analysis was performed (Kim et al., 2017). And it might cause us to conclude that the hypothetical effects or relationships exist but in fact it doesn't. Therefore, our finding indicated that the IPL and rSTS might not contain enough information to make an abstract representation for facial, bodily, or whole-person's feelings.

The IPL and rSTS have been demonstrated that facial and bodily emotions can be coded at an abstract level regardless of the sensory cue in previous studies (Peelen et al., 2010; Watson et al., 2014; Jessen and Kotz, 2015; Kim et al., 2017), but these studies have focused only on the abstract representations elicited from single face or body parts. Furthermore, our study confirmed the unsuccessful cross-modal decoding of the affective category from perceived cues (facial, bodily, and whole-person's expressions) by the activation patterns in the IPL and rSTS, suggesting that the abstract representations of emotions might not extend from the face and body stimuli to whole-person stimuli in both clusters. However, the latest evidence

for modality-general representations in the IPL and rSTS has been confirmed by examining the neural representations of the categorical valence (positive, neutral, and negative) by visual and auditory stimulus modalities. Similarly, the inferior parietal cluster didn't show significant P vs. N (positive versus negative) or PN vs. 0 (positive/negative versus neutral) classification which was consistent with our study, but significant information from multidimensional scaling (MDS) (Kim et al., 2017) results for both P vs. N and PN vs. 0 representations. The confirmatory MDS analyses confirmed that this cluster is informative to valence representation, which might not be applicable to our results, because three kinds of visual stimuli were used in our experiment without auditory stimuli. Similarly, future work is needed to model the similarity structure dimensionally using a MDS method for our two clusters to reveal the underlying mechanisms when perceiving the emotions of face, body and whole-person, and to explore whether both clusters could represent all three stimulus types' emotions at an abstract level.

Behavioral and neuroimaging studies have suggested that the human brain could encode whole-persons in a holistic rather than part-based manner (McKone et al., 2001; Maurer et al., 2002; Zhang et al., 2012; Soria Bauser and Suchan, 2013), indicating that the whole-person's emotional expression might not be integrated from the isolated emotional faces and bodies. Our latest study has found that in the EBA, the whole-person patterns were almost equally associated with weighted sums of face and body patterns, using different weights for happy expressions but equal weights for angry and fearful ones (Yang et al., 2018), but this was not established for the other regions. Although some other regions like MPFC, left STS and precuneus have been demonstrated to be capable of coding the facial and bodily emotions at an abstract level regardless of the sensory cue (Peelen et al., 2010; Klasen et al., 2011; Chikazoe et al., 2014; Skerry and Saxe, 2014; Aube et al., 2015; Kim et al., 2017; Schirmer and Adolphs, 2017), these regions that were not sensitive to whole-person stimuli might not be able to represent the emotions of whole-person stimuli (Tsao et al., 2003; Pinsk et al., 2005; Heberlein and Atkinson, 2009). A recent study found that there existed a cross-modal adaptation in the right pSTS using dynamic face-to-voice stimuli, suggesting the presence of integrative, multisensory neurons in this area (Watson et al., 2014). Similar results were observed when body-to-voice stimuli were used (Jessen and Kotz, 2015). It indicated that the integration of different stimulus types might attribute to interleaved populations of unisensory neurons responding to face, body or voice or rather by multimodal neurons receiving input from different stimulus types. By examining the adaptation to facial, vocal and face-voice emotional stimuli, the multisensory STS showed equally adaptive responses to faces and voices, while the modality-specific cortices, such as face-sensitive and voice-sensitive cortices in STS, showed a stronger response to their respective preferred stimuli (Ethofer et al., 2013). Hence, the IPL and rSTS that have been demonstrated to be capable of representing facial and bodily emotions at an abstract level might not had the integrative, multisensory neurons which can adapt to whole-persons' emotion. Therefore, the IPL and rSTS might not be able to represent the emotions extending beyond face and body stimuli to whole-person stimuli.

## Limitation

There are several limitations to be addressed in this study. The first one is that the emotional state was expressed only via the visual modality. Therefore, our results may not be generalized to other modalities, such as auditory or tactile emotional stimuli. The purpose of our study was to investigate whether there were specific regions that could represent whole-person's emotions with facial and bodily emotion expressions abstractly. Three types of emotional stimuli of visual modality were used in our study. However, as there is no auditory or tactile condition, our research is limited to a certain extent. Future work is needed to explore the cross-modal representation of emotions. Another limitation is that the generality of our findings may be influenced by the relatively small sample size ($N$ = 20) for functional MRI studies on healthy participants. To verify whether the number of participants was valid, the pre-determined sample size was computed with a priori power analysis which was conducted using the statistical software G*Power[2]. The analysis showed that the sample size of this study was moderate and our results remained valid and efficient. Although many studies on the emotional expressions had comparative sample size (Peelen et al., 2010; Kim et al., 2015, 2016, 2017), a larger sample size could better prove the effectiveness of our findings and a bigger statistical power can be obtained. So, replicating this study with a larger number of participants appears considerable in the future work. In addition, examining the potential of age-related differences between different age groups is also an issue worthy of study in the future.

# CONCLUSION

We found emotions can be represented at an abstract level using three emotional stimuli in the left postcentral gyrus, left IPL and rSTS by using a whole-brain RSA. These three clusters probably contain emotion-specific but stimulus category-independent representations of perceived emotions (happy, angry, and fearful). Further cluster-based MVPA revealed that only the left postcentral gyrus could distinguish three types of emotions and happy versus angry/fearful which could be considered as positive versus negative for the two or three stimulus type pairs. Future research will be needed to model the similarity structure dimensionally using a MDS method for the IPL and right STS to reveal the underlying mechanisms when the face, body and whole-person expressions are perceived.

# AUTHOR CONTRIBUTIONS

BL and XY designed the experiments. JX, XY, and XL performed the experiments. LC and JX analyzed the results. LC wrote the manuscript. JX, BL, and XL contributed to manuscript revision. All authors contributed to discuss the results and have approved the final manuscript.

[2]http://www.gpower.hhu.de/

## FUNDING

This work was supported by the National Natural Science Foundation of China (Nos. 61860206010, U1736219, 61571327, and 61703302).

## ACKNOWLEDGMENTS

We would like to thank Prof. Irene Rotondi (Campus Biotech, University of Geneva, Switzerland) for supplying the GEMEP Corpus.

## REFERENCES

Aube, W., Angulo-Perkins, A., Peretz, I., Concha, L., and Armony, J. L. (2015). Fear across the senses: brain responses to music, vocalizations and facial expressions. *Soc. Cogn. Affect. Neurosci.* 10, 399–407. doi: 10.1093/scan/nsu067

Banziger, T., Mortillaro, M., and Scherer, K. R. (2012). Introducing the Geneva multimodal expression corpus for experimental research on emotion perception. *Emotion* 12, 1161–1179. doi: 10.1037/a0025827

Baucom, L. B., Wedell, D. H., Wang, J., Blitzer, D. N., and Shinkareva, S. V. (2012). Decoding the neural representation of affective states. *Neuroimage* 59, 718–727. doi: 10.1016/j.neuroimage.2011.07.037

Bishop, C. M. (2006). *Pattern Recognition and Machine Learning (Information Science and Statistics)*. New York, NY: Springer-Verlag Inc.

Brandman, T., and Yovel, G. (2016). Bodies are represented as wholes rather than their sum of parts in the occipital-temporal cortex. *Cereb. Cortex* 26, 530–543. doi: 10.1093/cercor/bhu205

Chikazoe, J., Lee, D. H., Kriegeskorte, N., and Anderson, A. K. (2014). Population coding of affect across stimuli, modalities and individuals. *Nat. Neurosci.* 17, 1114–1122. doi: 10.1038/nn.3749

de Gelder, B., De Borst, A. W., and Watson, R. (2015). The perception of emotion in body expressions. *Wiley Interdiscip. Rev. Cogn. Sci.* 6, 149–158. doi: 10.1002/wcs.1335

de Gelder, B., Hortensius, R., and Tamietto, M. (2012). Attention and awareness each influence amygdala activity for dynamic bodily expressions-a short review. *Front. Integr. Neurosci.* 6:54. doi: 10.3389/fnint.2012.00054

Ethofer, T., Bretscher, J., Wiethoff, S., Bisch, J., Schlipf, S., Wildgruber, D., et al. (2013). Functional responses and structural connections of cortical areas for processing faces and voices in the superior temporal sulcus. *Neuroimage* 76, 45–56. doi: 10.1016/j.neuroimage.2013.02.064

Etzel, J. A., Zacks, J. M., and Braver, T. S. (2013). Searchlight analysis: promise, pitfalls, and potential. *Neuroimage* 78, 261–269. doi: 10.1016/j.neuroimage.2013.03.041

Flaisch, T., Imhof, M., Schmalzle, R., Wentz, K. U., Ibach, B., and Schupp, H. T. (2015). Implicit and explicit attention to pictures and words: an FMRI-study of concurrent emotional stimulus processing. *Front. Psychol.* 6:1861. doi: 10.3389/fpsyg.2015.01861

Gabrielsson, A., and Lindström, E. (2001). "The influence of musical structure on emotional expression," in *Music and Emotion: Theory and Research*, eds P. N. Juslin and J. A. Sloboda (Oxford: Oxford University Press), 235–239.

Gelder, B. D., Meeren, H. K. M., Righart, R., Stock, J. V. D., Van De Riet, W. A. C., and Tamietto, M. (2006). Beyond the face: exploring rapid influences of context on face processing. *Prog. Brain. Res.* 155, 37–48. doi: 10.1016/S0079-6123(06)55003-4

Geng, X., Xu, J., Liu, B., and Shi, Y. (2018). Multivariate classification of major depressive disorder using the effective connectivity and functional connectivity. *Front. Neurosci.* 12:38. doi: 10.3389/fnins.2018.00038

Grezes, J., Pichon, S., and De Gelder, B. (2007). Perceiving fear in dynamic body expressions. *Neuroimage* 35, 959–967. doi: 10.1016/j.neuroimage.2006.11.030

Hajcak, G., Molnar, C., George, M. S., Bolger, K., Koola, J., and Nahas, Z. (2007). Emotion facilitates action: a transcranial magnetic stimulation study of motor cortex excitability during picture viewing. *Psychophysiology* 44, 91–97. doi: 10.1111/j.1469-8986.2006.00487.x

Haynes, J. D., and Rees, G. (2006). Decoding mental states from brain activity in humans. *Nat. Rev. Neurosci.* 7, 523–534. doi: 10.1038/nrn1931

Heberlein, A. S., and Atkinson, A. P. (2009). Neuroscientific evidence for simulation and shared substrates in emotion recognition: beyond faces. *Emot. Rev.* 1, 162–177. doi: 10.1177/1754073908100441

Jessen, S., and Kotz, S. A. (2015). Affect differentially modulates brain activation in uni- and multisensory body-voice perception. *Neuropsychologia* 66, 134–143. doi: 10.1016/j.neuropsychologia.2014.10.038

Kaiser, D., Strnad, L., Seidl, K. N., Kastner, S., and Peelen, M. V. (2014). Whole person-evoked fMRI activity patterns in human fusiform gyrus are accurately modeled by a linear combination of face- and body-evoked activity patterns. *J. Neurophysiol.* 111, 82–90. doi: 10.1152/jn.00371.2013

Kassam, K. S., Markey, A. R., Cherkassky, V. L., Loewenstein, G., and Just, M. A. (2013). Identifying emotions on the basis of neural activation. *PLoS One* 8:e66032. doi: 10.1371/journal.pone.0066032

Kim, J., Schultz, J., Rohe, T., Wallraven, C., Lee, S. W., and Bulthoff, H. H. (2015). Abstract representations of associated emotions in the human brain. *J. Neurosci.* 35, 5655–5663. doi: 10.1523/JNEUROSCI.4059-14.2015

Kim, J., Shinkareva, S. V., and Wedell, D. H. (2017). Representations of modality-general valence for videos and music derived from fMRI data. *Neuroimage* 148, 42–54. doi: 10.1016/j.neuroimage.2017.01.002

Kim, J., Wang, J., Wedell, D. H., and Shinkareva, S. V. (2016). Identifying core affect in individuals from fMRI responses to dynamic naturalistic audiovisual stimuli. *PLoS One* 11:e0161589. doi: 10.1371/journal.pone.0161589

Klasen, M., Kenworthy, C. A., Mathiak, K. A., Kircher, T. T., and Mathiak, K. (2011). Supramodal representation of emotions. *J. Neurosci.* 31, 13635–13643. doi: 10.1523/JNEUROSCI.2833-11.2011

Kragel, P. A., and LaBar, K. S. (2015). Multivariate neural biomarkers of emotional states are categorically distinct. *Soc. Cogn. Affect. Neurosci.* 10, 1437–1448. doi: 10.1093/scan/nsv032

Kragel, P. A., and LaBar, K. S. (2016). Somatosensory representations link the perception of emotional expressions and sensory experience. *eNeuro* 3, ENEURO.0090-15.2016. doi: 10.1523/ENEURO.0090-15.2016

Kret, M. E., Pichon, S., Grezes, J., and De Gelder, B. (2011). Similarities and differences in perceiving threat from dynamic faces and bodies. An fMRI study. *Neuroimage* 54, 1755–1762. doi: 10.1016/j.neuroimage.2010.08.012

Kriegeskorte, N., Goebel, R., and Bandettini, P. (2006). Information-based functional brain mapping. *Proc. Natl. Acad. Sci. U.S.A.* 103, 3863–3868. doi: 10.1073/pnas.0600244103

Kriegeskorte, N., and Kievit, R. A. (2013). Representational geometry: integrating cognition, computation, and the brain. *Trends Cogn. Sci.* 17, 401–412. doi: 10.1016/j.tics.2013.06.007

Lakens, D., Fockenberg, D. A., Lemmens, K. P. H., Ham, J., and Midden, C. J. H. (2013). Brightness differences influence the evaluation of affective pictures. *Cogn. Emot.* 27, 1225–1246. doi: 10.1080/02699931.2013.781501

Liang, Y., Liu, B., Li, X., and Wang, P. (2018). Multivariate pattern classification of facial expressions based on large-scale functional connectivity. *Front. Hum. Neurosci.* 12:94. doi: 10.3389/fnhum.2018.00094

Liang, Y., Liu, B., Xu, J., Zhang, G., Li, X., Wang, P., et al. (2017). Decoding facial expressions based on face-selective and motion-sensitive areas. *Hum. Brain Mapp.* 38, 3113–3125. doi: 10.1002/hbm.23578

Maurer, D., Grand, R. L., and Mondloch, C. J. (2002). The many faces of configural processing. *Trends Cogn. Sci.* 6, 255–260. doi: 10.1016/S1364-6613(02)01903-4

McKone, E., Martini, P., and Nakayama, K. (2001). Categorical perception of face identity in noise isolates configural processing. *J. Exp. Psychol. Hum. Percept. Perform.* 27, 573–599. doi: 10.1037/0096-1523.27.3.573

Nikolaus, K., Marieke, M., and Peter, B. (2008). Representational similarity analysis – connecting the branches of systems neuroscience. *Front. Syst. Neurosci.* 2:4. doi: 10.3389/neuro.06.004.2008

Nili, H., Wingfield, C., Walther, A., Su, L., Marslenwilson, W., and Kriegeskorte, N. (2014). A toolbox for representational similarity analysis. *PLoS Comput. Biol.* 10:e1003553. doi: 10.1371/journal.pcbi.1003553

Norman, K. A., Polyn, S. M., Detre, G. J., and Haxby, J. V. (2006). Beyond mind-reading: multi-voxel pattern analysis of fMRI data. *Trends Cogn. Sci.* 10, 424–430. doi: 10.1016/j.tics.2006.07.005

Peelen, M. V., Atkinson, A. P., and Vuilleumier, P. (2010). Supramodal representations of perceived emotions in the human brain. *J. Neurosci.* 30, 10127–10134. doi: 10.1523/JNEUROSCI.2161-10.2010

Peelen, M. V., and Downing, P. E. (2007). The neural basis of visual body perception. *Nat. Rev. Neurosci.* 8, 636–648. doi: 10.1038/nrn2195

Pinsk, M. A., Desimone, K., Moore, T., Gross, C. G., and Kastner, S. (2005). Representations of faces and body parts in macaque temporal cortex: a functional MRI study. *Proc. Natl. Acad. Sci. U.S.A.* 102, 6996–7001. doi: 10.1073/pnas.0502605102

Saarimaki, H., Gotsopoulos, A., Jaaskelainen, I. P., Lampinen, J., Vuilleumier, P., Hari, R., et al. (2016). Discrete neural signatures of basic emotions. *Cereb. Cortex* 26, 2563–2573. doi: 10.1093/cercor/bhv086

Sarkheil, P., Goebel, R., Schneider, F., and Mathiak, K. (2013). Emotion unfolded by motion: a role for parietal lobe in decoding dynamic facial expressions. *Soc. Cogn. Affect. Neurosci.* 8, 950–957. doi: 10.1093/scan/nss092

Schirmer, A., and Adolphs, R. (2017). Emotion perception from face, voice, and touch: comparisons and convergence. *Trends Cogn. Sci.* 21, 216–228. doi: 10.1016/j.tics.2017.01.001

Shinkareva, S. V., Wang, J., Kim, J., Facciani, M. J., Baucom, L. B., and Wedell, D. H. (2014). Representations of modality-specific affective processing for visual and auditory stimuli derived from functional magnetic resonance imaging data. *Hum. Brain Mapp.* 35, 3558–3568. doi: 10.1002/hbm.22421

Skerry, A. E., and Saxe, R. (2014). A common neural code for perceived and inferred emotion. *J. Neurosci.* 34, 15997–16008. doi: 10.1523/JNEUROSCI.1676-14.2014

Skerry, A. E., and Saxe, R. (2015). Neural representations of emotion are organized around abstract event features. *Curr. Biol.* 25, 1945–1954. doi: 10.1016/j.cub.2015.06.009

Soria Bauser, D., and Suchan, B. (2015). Is the whole the sum of its parts? *Behav. Brain Res.* 281, 102–110. doi: 10.1016/j.bbr.2014.12.015

Soria Bauser, D. A., and Suchan, B. (2013). Behavioral and electrophysiological correlates of intact and scrambled body perception. *Clin. Neurophysiol.* 124, 686–696. doi: 10.1016/j.clinph.2012.09.030

Tsao, D. Y., Freiwald, W. A., Knutsen, T. A., Mandeville, J. B., and Tootell, R. B. (2003). Faces and objects in macaque cerebral cortex. *Nat. Neurosci.* 6, 989–995. doi: 10.1038/nn1111

van de Riet, W. A., Grezes, J., and De Gelder, B. (2009). Specific and common brain regions involved in the perception of faces and bodies and the representation of their emotional expressions. *Soc. Neurosci.* 4, 101–120. doi: 10.1080/17470910701865367

Viinikainen, M., Jaaskelainen, I. P., Alexandrov, Y., Balk, M. H., Autti, T., and Sams, M. (2010). Nonlinear relationship between emotional valence and brain activity: evidence of separate negative and positive valence dimensions. *Hum. Brain Mapp.* 31, 1030–1040. doi: 10.1002/hbm.20915

Watson, R., Latinus, M., Noguchi, T., Garrod, O., Crabbe, F., and Belin, P. (2014). Crossmodal adaptation in right posterior superior temporal sulcus during face-voice emotional integration. *J. Neurosci.* 34, 6813–6821. doi: 10.1523/JNEUROSCI.4478-13.2014

Xu, J., Yin, X., Ge, H., Han, Y., Pang, Z., Liu, B., et al. (2017). Heritability of the effective connectivity in the resting-state default mode network. *Cereb. Cortex* 27, 5626–5634. doi: 10.1093/cercor/bhw332

Yang, X., Xu, J., Cao, L., Li, X., Wang, P., Wang, B., et al. (2018). Linear representation of emotions in whole persons by combining facial and bodily expressions in the extrastriate body area. *Front. Hum. Neurosci.* 11:653. doi: 10.3389/fnhum.2017.00653

Zhang, G., Cheng, Y., and Liu, B. (2016). Abnormalities of voxel-based whole-brain functional connectivity patterns predict the progression of hepatic encephalopathy. *Brain Imaging Behav.* 11, 784–796. doi: 10.1007/s11682-016-9553-2

Zhang, J., Li, X., Song, Y., and Liu, J. (2012). The fusiform face area is engaged in holistic, not parts-based, representation of faces. *PLoS One* 7:e40390. doi: 10.1371/journal.pone.0040390

**Conflict of Interest Statement:** The authors declare that the research was conducted in the absence of any commercial or financial relationships that could be construed as a potential conflict of interest.

frontiers in Human Neuroscience

ORIGINAL RESEARCH
published: 12 November 2018
doi: 10.3389/fnhum.2018.00446

# The Effect of High-Definition Transcranial Direct Current Stimulation of the Right Inferior Frontal Gyrus on Empathy in Healthy Individuals

*Xiaoling Wu[1,2,3†], Feifei Xu[1,2,3†], Xingui Chen[2,3,4], Lu Wang[4], Wanling Huang[4], Ke Wan[4], Gong-Jun Ji[1,2,3], Guixian Xiao[4], Sheng Xu[1], Fengqiong Yu[1,2,3], Chunyan Zhu[1,2,3], Chunhua Xi[2,3,5]* and Kai Wang[1,2,3,4]**

[1]Department of Medical Psychology, Chaohu Clinical Medical College, Anhui Medical University, Hefei, China , [2]Anhui Province Key Laboratory of Cognition and Neuropsychiatric Disorders, Hefei, China, [3]Collaborative Innovation Center for Neuropsychiatric Disorders and Mental Health, Anhui, China, [4]Department of Neurology, The First Affiliated Hospital of Anhui Medical University, Hefei, China, [5]Department of Neurology, The Third Affiliated Hospital of Anhui Medical University, Hefei, China

Empathy, including cognitive and emotional empathy, refers to the ability to infer the mental states of others and to the capacity to share emotions. The neural mechanisms involved in empathy are complex and not yet fully understood, and previous studies have shown that both cognitive and emotional empathy are closely associated with the inferior frontal gyrus (IFG). In this study, we examined whether empathy can be modulated by high-definition transcranial direct current stimulation (HD-tDCS) of the right IFG. Twenty-three healthy participants took part in all three experimental conditions (i.e., anodal, cathodal and sham stimulation) in a randomized order. Participants then completed the Chinese version of the Multifaceted Empathy Test (MET), which assesses both cognitive and emotional empathy. The results show that scores obtained for cognitive empathy following cathodal stimulation are significantly lower than those obtained following sham stimulation. In addition, scores obtained for cognitive empathy following anodal stimulation are higher than those obtained following sham stimulation, though the difference is only marginally significant. However, the results fail to show whether the stimulation of the right IFG via HD-tDCS plays a role in emotional empathy. Our results suggest that the right IFG plays a key role in cognitive empathy and indicate that HD-tDCS can regulate cognitive empathy by inducing excitability changes in the right IFG.

**Keywords: cognitive empathy, emotional empathy, high-definition transcranial direct current stimulation, inferior frontal gyrus, Multifaceted Empathy Test**

OPEN ACCESS

***Edited by:***
*Wenbo Luo,*
*Liaoning Normal University, China*

***Reviewed by:***
*Hongbo Yu,*
*Yale University, United States*
*Ke Zhou,*
*Shenzhen University, China*

****Correspondence:***
*Chunhua Xi*
*xch3149@126.com*
*Kai Wang*
*wangkai1964@126.com*

*[†]These authors have contributed equally to this work*

***Received:*** *23 May 2018*
***Accepted:*** *17 October 2018*
***Published:*** *12 November 2018*

***Citation:***
*Wu X, Xu F, Chen X, Wang L, Huang W, Wan K, Ji G-J, Xiao G, Xu S, Yu F, Zhu C, Xi C and Wang K (2018) The Effect of High-Definition Transcranial Direct Current Stimulation of the Right Inferior Frontal Gyrus on Empathy in Healthy Individuals. Front. Hum. Neurosci. 12:446. doi: 10.3389/fnhum.2018.00446*

## INTRODUCTION

As a sociocognitive ability, empathy plays a very important role in our interpersonal interactions (Decety and Cowell, 2014). Empathy involves both cognitive and emotional components that correspond to two abilities, the first of which is the ability to infer the mental states of another (i.e., "I understand what you feel") and is described as cognitive empathy

(Decety and Lamm, 2006; Harvey et al., 2013). The second is the ability to respond to the observed emotions of others or to share a "fellow feeling" (i.e., "I feel what you feel") and is known as emotional empathy, which includes emotional recognition, emotional contagion, and the sharing of pain (Shamay-Tsoory et al., 2009; Shamay-Tsoory, 2011). Current evolutionary evidence supports the theory that emotional empathy develops earlier than cognitive empathy, the latter of which involves higher levels of cognitive functioning (Shamay-Tsoory et al., 2009; Shamay-Tsoory, 2011). There is still controversy regarding the role of empathy in our daily lives and such debate mainly focuses on the relationship between empathy and morality. Bloom believed that empathy can produce moral prejudice, which can cause individuals to experience personal biases toward those whom they are close to or familiar with when making moral decisions (Bloom, 2016, 2017). However, some researchers have opposed this view by arguing that empathy is a moral force that can motivate engagement in prosocial behavior (Zaki, 2016, 2017). Zaki (2016), for example, argued that prejudice resulting from processes of empathy described in Bloom is not the cause of empathy itself but rather reflects the motivations of the individual. Despite this controversy, most current studies have supported the important role of empathy in our lives in enabling us to accurately recognize the emotions and behaviors of others and to respond appropriately (Fan et al., 2011). Empathic impairment not only seriously affects the daily lives of people but also leads to many serious social problems (Zaki, 2016). Therefore, the study of empathic impairment is crucial to the study of empathy.

The neural mechanisms involved in empathy are complex and not yet fully understood. In recent years brain lesion and imaging studies have been widely used to explore the neural mechanisms that underlie empathy. Research has shown that cognitive empathy is generally supported by the activation of the medial prefrontal cortex (MPFC), right temporoparietal junction (TPJ), inferior frontal gyrus (IFG), supplementary motor area and anterior midcingulate cortex (aMCC; Völlm et al., 2006; Schulte-Rüther et al., 2007, 2008; Hooker et al., 2008, 2010; Massey et al., 2017) while emotional empathy involves the activation of brain regions such as the IFC, anterior insula (INS), anterior cingulate cortex (ACC) and superior temporal sulci (STS; Schulte-Rüther et al., 2008; Shamay-Tsoory et al., 2009; Shamay-Tsoory, 2011; Leigh et al., 2013; Oishi et al., 2015). Shamay-Tsoory et al. (2009) found that patients who have suffered damage to the ventral MPFC experience low levels of cognitive empathy and that those who have sustained damage to the IFC exhibit low levels of emotional empathy. Moreover, magnetic resonance imaging (MRI) studies of the neural mechanisms underlying empathy are extensive. Massey et al. (2017) found that the cortical thickness of the mPFC, right IFG, aMCC, INS and left TPJ in healthy subjects is significantly associated with cognitive empathy. Pfeifer et al. (2008) found the significant activation of the right IFG, right INS and right amygdala in children during engagement in empathic behavior and showed that the activation of the right IFG is significantly associated with the Interpersonal Reactivity Index (IRI), a self-reported empathy questionnaire. Schulte-Rüther et al. (2007) also found that the mPFC, bilateral IFG and STS are clearly activated during an empathic interpersonal face-to-face interaction task and that the activation of the right IFG and left STS is significantly correlated with scores obtained from participants using two self-reported emotional empathy scales. These studies show that the IFG plays a highly significant role in the brain mechanisms that underlie empathy.

As far as we know, measurements of empathy used in past studies have mainly included self-reported scale and behavioral task measurements. The most widely used self-reported scale is the IRI scale (Davis, 1980), which measures both cognitive and emotional empathy. However, during engagement in empathic behavioral tasks, most tasks cannot measure cognitive and emotional empathy simultaneously, as they typically measured a single form of empathy like cognitive empathy (Baron-Cohen et al., 2001; Smith et al., 2015; Mai et al., 2016; Massey et al., 2017; Oliver et al., 2018) and emotional empathy (Derntl et al., 2012; Smith et al., 2014). To address this limitation, Dziobek et al. (2008) developed a new measure of empathy, the Multifaceted Empathy Test (MET), which is designed to measure both cognitive and emotional empathy. The MET is a well-established task that has been widely used in the study of healthy subjects (Hysek et al., 2014; Ze et al., 2014; Kuypers et al., 2017) and of those with various psychiatric disorders, including patients diagnosed with schizophrenia (Lehmann et al., 2014), depressive disorder (Wingenfeld et al., 2016), autism spectrum disorder (Dziobek et al., 2008; Mazza et al., 2014), and borderline personality disorder (Harari et al., 2010; Dziobek et al., 2011; Wingenfeld et al., 2014). The present study uses the Chinese version of the Multifaceted Empathy Test (MET-C) revised by Zhu et al. (2018), which is highly internally reliable and valid. The MET-C is stronger in ecological validity than self-report questionnaires that measure empathy, as the test measures several photorealistic stimuli (Dziobek et al., 2008). Therefore, the MET-C serves as a better behavioral paradigm for measuring empathy.

Studies have shown that empathic impairment affects people's social interactions, and studies of psychiatric patients have found that empathic impairment is a core deficit observed in psychiatric disorders that directly leads to the severe impairment of their social functions (Dapretto et al., 2006; Derntl et al., 2009; Smith et al., 2015). Thus, the present study considered neuromodulatory technologies are used to enhance empathic abilities. Transcranial direct current stimulation (tDCS) is a noninvasive neurostimulation technique that involves applying a weak direct current (usually 1–2 mA) through electrodes placed on the scalp that can alter the activity and excitability of cortical neurons, thereby inducing changes in neural functioning. Stimulation polarity determines the direction of cortical excitability changes, and anodal stimulation can generally increase the excitability of the cortex while cathodal stimulation has the opposite effect. Conventional tDCS involves the placement of two large sponge electrodes (25–35 $cm^2$; one anode and one cathode electrode) onto two different areas of the scalp such that the current flows from the anode to the cathode (Nitsche and Paulus, 2001;

Nitsche et al., 2003; Hogeveen et al., 2016; Godinho et al., 2017). However, studies have shown that conventional tDCS currents are relatively diffuse and cannot focus currents on the target area of interest due to their weak levels of spatial focality (Antal et al., 2014; Meinzer et al., 2014). However, more recent developments in high-definition tDCS (HD-tDCS) have sought to address this shortcoming (Datta et al., 2008, 2009). HD-tDCS uses arrays of five small circular electrodes (1 cm diameter) rather than traditional large sponge electrodes and applies a 4 × 1 ring electrode configuration with a central electrode positioned over the target brain region and with four return electrodes (each receiving 25% of the return current) positioned around it, thus allowing currents to enhance brain targeting in the area surrounded by return electrodes (Datta et al., 2009; Minhas et al., 2010; Hogeveen et al., 2016). In short, HD-tDCS ensures higher levels of spatial focality than conventional tDCS, which can offer a better understanding of the causal relationship between changes in brain excitability and subsequent changes in behavioral or cognitive ability (Hogeveen et al., 2016).

In recent years, tDCS has been widely used in research studies to investigate the social cognitive abilities of healthy subjects (Nitsche et al., 2012; Willis et al., 2015; Mai et al., 2016; Adenzato et al., 2017; Martin et al., 2017) and of psychiatric patients (Brennan et al., 2017; Philip et al., 2017). Studies have shown that anodal stimulation can typically enhance certain social cognitive abilities while cathodal stimulation has the opposite effect. Until now only a few research studies have employed tDCS to investigate empathy in healthy subjects (Wang et al., 2014; Rêgo et al., 2015; Mai et al., 2016; Coll et al., 2017; Nobusako et al., 2017). Mai et al. (2016) found that the cathodal tDCS stimulation of the right TPJ inhibits the capacity for cognitive empathy. Furthermore, Nobusako et al. (2017) found that the anodal tDCS of the right IFC enhances capacities for perspective-taking (PT), which is used to evaluate cognitive empathy. However, no studies have applied tDCS to examine emotional empathy. In short, the above findings suggest that tDCS-induced cortical excitability can modify cognitive functioning.

From the above studies we know that the IFG (particularly the right IFG) plays an important role in empathy (Lawrence et al., 2006; Schulte-Rüther et al., 2007, 2008; Pfeifer et al., 2008; Massey et al., 2017; Nobusako et al., 2017). Thus, we can explore the relationship between changes in IFG activity and empathic ability through HD-tDCS, and changes in empathy as a result of HD-tDCS may be further assessed by using the MET-C. Accordingly, our hypothesis suggests that the anodal HD-tDCS stimulation of the right IFG may enhance cognitive and emotional empathy while the cathodal stimulation may have the opposite effect.

# MATERIALS AND METHODS

## Participants

Twenty-four healthy right-handed adults (mean age 24.39 ± 3.47 years; 16.65 ± 1.66 years of education; 17 females) participated in the study. One of the male participants withdrew from the study after the first stimulation. As such, complete and reliable data were obtained for 23 participants. All participants had normal vision and none were colorblind. None of the participants had a history of neurological or psychiatric illness, head injury, alcohol dependance, or drug dependance. Participants took no psychoactive drugs, experienced no illnesses or major life events that caused significant changes in their mood, and did not smoke or drink for the duration of the experiment. The study was approved by the Medical Ethics Committee of Anhui Medical University, Hefei, China. Each participant provided their written informed consent prior to the study.

## Measures

### Neuropsychological Assessment

The basic cognitive functioning and emotional conditions of the participants were assessed by administering standardized neuropsychological tests. The IRI was used to measure the cognitive and emotional empathic traits of the participants such that cognitive empathy was assessed using PT and Fantasy (F) subscales while emotional empathy was measured using subscales for empathic concern (EC) and personal distress (PD; Davis, 1980). The Hamilton Anxiety Scale (HAMA) and Hamilton Depression Scale (HAMD) were used to evaluate potential anxiety and depressive symptoms experienced by the participants. Finally, overall cognitive functioning was measured through a Montreal Cognitive Assessment (MoCA) test.

### Behavioral Measurement

The MET-C was administered to assess the two components of empathy, cognitive and emotional empathy. The task involved the presentation of 40 emotional pictures of adults and children of both genders. The images included 20 positive and 20 negative pictures (valence) and most portrayed a particular social context (see **Figure 1**). Measurements of both cognitive and emotional empathy were taken in four blocks, producing a total of eight blocks. Each block involved 10 trials, resulting in a total of 80 trials. Participants were asked to answer two questions. For the cognitive empathy assessment, participants were asked to judge the emotional states of the individuals shown in the pictures based on the given social context (social clues) and the facial expressions of the individuals (facial clues) and to select the most appropriate answer from four emotional state descriptors. Scores for correctly answered questions ranged from 0 to 40 and accuracy and response times (RTs) were recorded for each trial that assessed cognitive empathy. For the emotional empathy assessment, participants were asked to evaluate how much they experienced the emotions of the individuals shown in the pictures on a scale of 0–9 (0 = not at all, 9 = very much). The average rating was calculated to produce a score for emotional empathy. Prior to completing the formal experiment, all participants received brief training to ensure that they had a thorough understanding of the task requirements.

## HD-tDCS Stimulation

HD-tDCS was administered through a battery-driven constant-current stimulator (Neuroelectrics, Barcelona, Spain). Based on

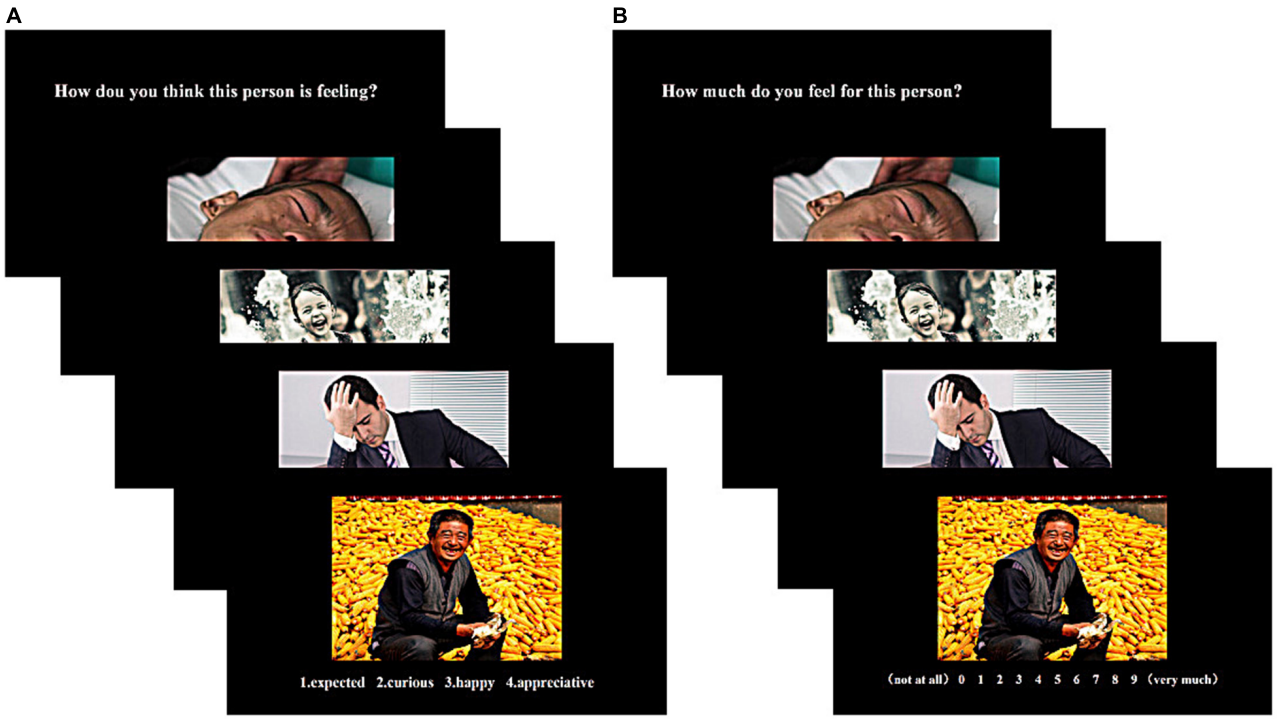


**FIGURE 1 |** Tasks for measuring cognitive empathy **(A)** and emotional empathy **(B)**. Stimuli were presented in blocks of 10. Each block was introduced with a question indicating the block type.

previous studies and the International 10/20 EEG System, as the target region (anode or cathode electrode) for stimulation we selected FC6 (Hogeveen et al., 2015, 2016; Nobusako et al., 2017) and return electrodes were placed in four locations around the central electrode corresponding to F10, CP2, TP8 and F2 (**Figure 2A**; Hogeveen et al., 2016). The distance between each return electrode and central electrode was measured as ∼6 cm. Under the active HD-tDCS condition, a relatively weak current (1.5 mA) was delivered for 20 min. For sham stimulation, a 1.5 mA current stimulus was delivered and lasted only 30 s consistent with previous research (Civai et al., 2015; Mai et al., 2016; Tang et al., 2017). For all three stimulation conditions, the stimulation commenced with the delivery of a current that slowly increased from 0 mA to 1.5 mA (ramp-up duration of 15 s) and that slowly dropped from 1.5 mA to 0 mA at the end of the stimulation (ramp-down duration of 15 s; Cerruti and Schlaug, 2008; Holland et al., 2011). The slow rise and fall in current allowed the participants to adapt gradually to the stimulation, thereby avoiding experiencing a tingling sensation from the current (Zito et al., 2015).

**Figure 2B** shows the distribution of the electrical field across cortical gray matter for the selected montage. The distribution of the electrical field produced by HD-tDCS is concentrated in the right prefrontal region, and the maximal intensity of 0.63 V/m occurs around the central electrode while the current flow is largely limited to the area defined by return electrodes. These findings are consistent with previous HD-tDCS studies showing that HD-tDCS offers enhanced levels of spatial focality.

## Experimental Design

We employed a single-blind, sham-controlled, within-subject study design. Each participant underwent all three experimental conditions (i.e., anodal, cathodal, and sham stimulation) in a randomized order. Prior to the first stimulation, all participants provided basic demographic information and underwent neuropsychological tests. They then randomly received HD-tDCS stimulation (anodal, cathodal and sham stimulation). During stimulation, participants were asked to sit alone in a quiet room to prevent the external environment from affecting the experimental results. After the stimulation, the MET-C test was immediately performed. During the test, every participant maintained a good sitting posture to ensure that his or her finger could easily touch the computer keyboard to select a choice. All participants completed a total of three stimulation periods which were held at least 7 days apart to discourage practice and memory effects. Each experiment lasted ∼40 min including 10 min of preparation, 20 min of stimulation, and 10 min designated for the behavioral task. **Figure 3** illustrates this experimental design.

## Data Analysis

A data analysis was performed using SPSS 18.0 (IBM, Armonk, NY, USA). Data on behavioral measures of accuracy, RTs for the cognitive empathy task and average ratings for the emotional empathy task were analyzed through a repeated-measures analysis of variance (ANOVA) with two independent within-subject factors (stimulation conditions, 3; valence, 2). When

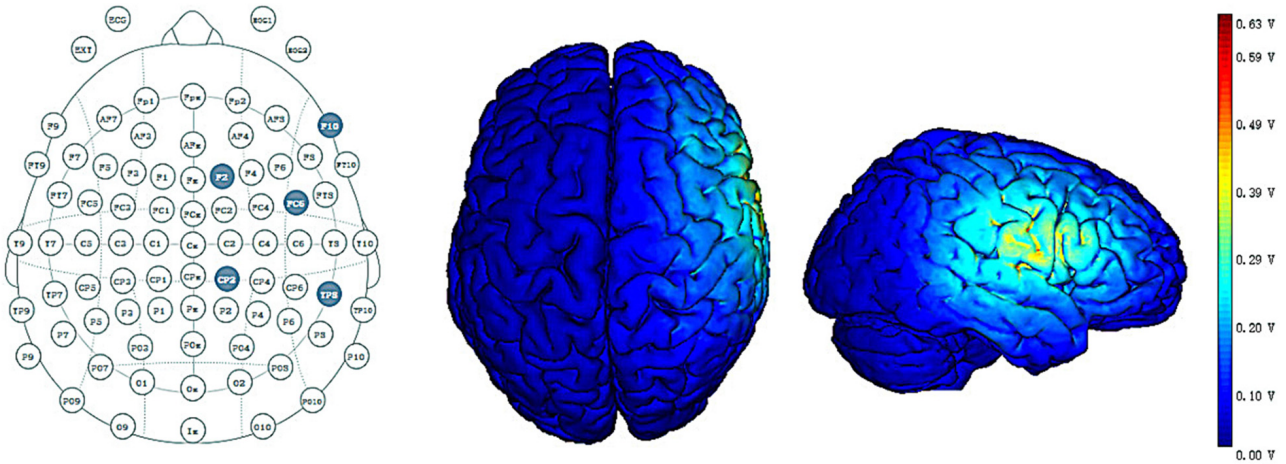


**FIGURE 2 | (A)** High-definition transcranial direct current stimulation (HD-tDCS) electrode position. FC6 represents the central electrode, and F2, F10, CP2 and TP8 represent return electrodes. **(B)** Stimulated distribution of the electric field in cortical gray matter with the selected montage.

sphericity violation occurred, Greenhouse-Geisser corrections were performed. Further *post hoc* analyses were carried out using Fisher's Least Significant Difference test where appropriate. A Pearson correlation coefficient ($r$) was used to assess the correlation between the personality measures and HD-tDCS effects on cognitive and emotional empathy. For all of the statistical tests, the alpha level was defined as $p < 0.05$.

# RESULTS

## Demographic Data and Neuropsychological Tests

This section presents a summary of the participants' demographic information and the results of neuropsychological assessments (age 24.39 ± 3.55, years of education 16.64 ± 1.73,

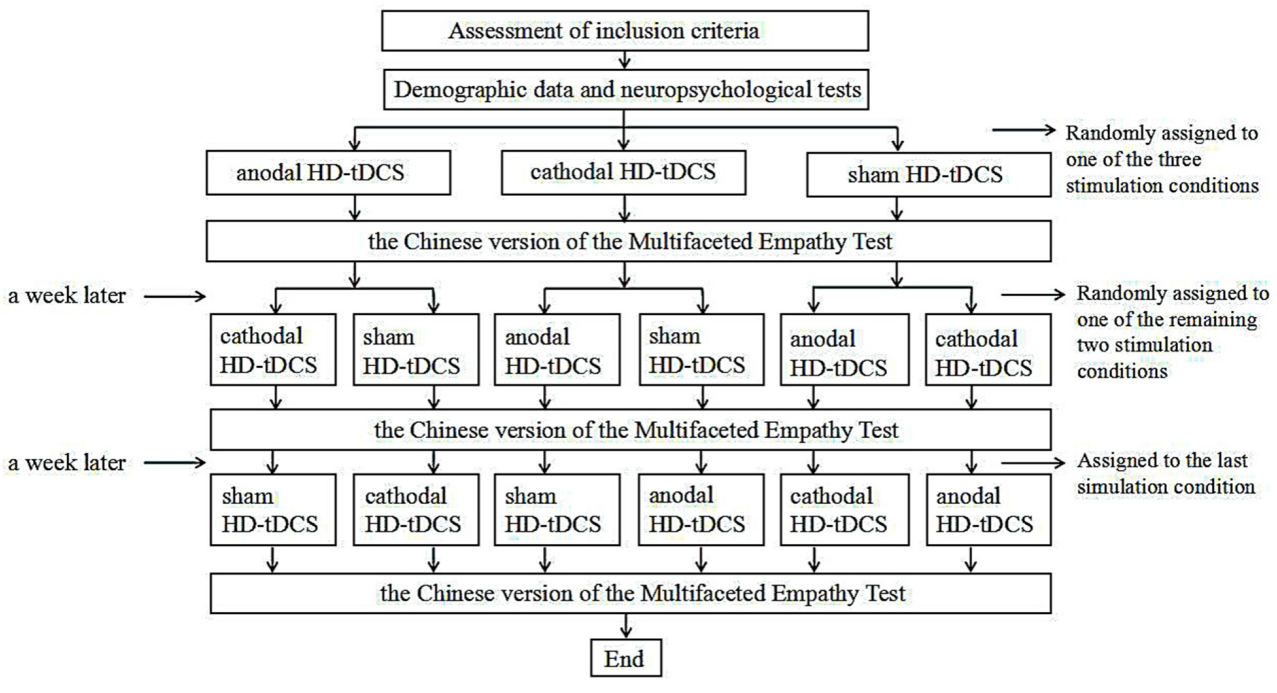


**FIGURE 3 |** Experimental design of the single-blind, within-subject and sham control trial.

HAMA 3.48 ± 2.11, HAMD 2.65 ± 2.60, MoCA 28.17 ± 1.53, IRI total score 51.13 ± 8.85, PT 11.13 ± 3.09, F 15.48 ± 2.91, EC 16.52 ± 3.87, PD 8.00 ± 3.71). It took all participants ∼30 min to complete the assessment.

## Behavioral Results

**Table 1** shows descriptive statistics for cognitive and emotional empathy with two valences for participants who completed all three stimulations. A violin plot (see **Figure 4**) shows the data distribution and probability density. It combines characteristics of the box plots and histograms due illustrate the distribution of the data. **Figure 4** shows the distribution of accuracy levels and RTs for cognitive empathy and average ratings for emotional empathy of all of the participants for all three stimulation conditions.

## Cognitive Empathy

### Accuracy

A repeated-measures ANOVA shows a reliable main effect of the stimulation conditions (anodal vs. sham vs. cathodal; $F_{(2,68)} = 8.779$, $p = 0.001$, $\eta^2 = 0.285$) for accuracy in cognitive empathy. *Post hoc* analyses further reveal a significant difference between the anodal and cathodal stimulation conditions ($p < 0.001$) and between the cathodal and sham stimulation conditions ($p = 0.038$) and show a marginally significant difference between the anodal and sham stimulation conditions ($p = 0.077$; **Table 2**, **Figure 5**). Relative to the sham stimulation, the cathodal stimulation generated a lower score for cognitive empathy while the anodal stimulation generated a higher score (**Table 1**), indicating that the active HD-tDCS stimulation of the right IFC can regulate the accuracy of cognitive empathy. However, the main effect of valence and the interaction effect of stimulation condition × valence were not found to affect accuracy in cognitive empathy.

### RTs

A repeated-measures ANOVA reveals a reliable main effect of valence (positive vs. negative; $F_{(1,68)} = 44.752$, $p < 0.001$, $\eta^2 = 0.670$, Greenhouse-Geisser corrected) for RTs in cognitive empathy (**Table 2**, **Figure 5**). Relative to the positive valence, we find slower RTs for stimuli with a negative valence (**Table 1**). However, the main effect of stimulation conditions and the interaction effect of stimulation conditions × valence were not found for RTs in terms of cognitive empathy, showing that the active HD-tDCS stimulation of the right IFC had no significant effect on RTs in terms of cognitive empathy.

## Emotional Empathy

The results of the repeated-measures ANOVA do not reveal the main effects of stimulation conditions and valence or interaction effects of stimulation conditions × valence on emotional empathy, indicating that the active tDCS stimulation of the right IFC might have no significant modulatory effect on emotional empathy (**Table 2**, **Figure 5**).

## Correlation Analyses

We also analyzed the correlation between the personality measures and HD-tDCS effects (**Table 3**). Pearson correlation analyses (two-tailed) show that Fantasy subscale scores present a significantly negative correlation with anodal ($r = -0.420$, $p = 0.046$, **Figure 6A**) and cathodal ($r = -0.468$, $p = 0.024$, **Figure 6B**) HD-tDCS effects in terms of accuracy in cognitive empathy but that the other personality measures are not significantly associated with HD-tDCS effects whether in terms of cognitive or emotional empathy. The results show lower Fantasy subscale scores and higher anodal and cathodal HD-tDCS effects of accuracy on cognitive empathy, showing that the Fantasy subscale score may play a predictive role in HD-tDCS effects on cognitive empathy.

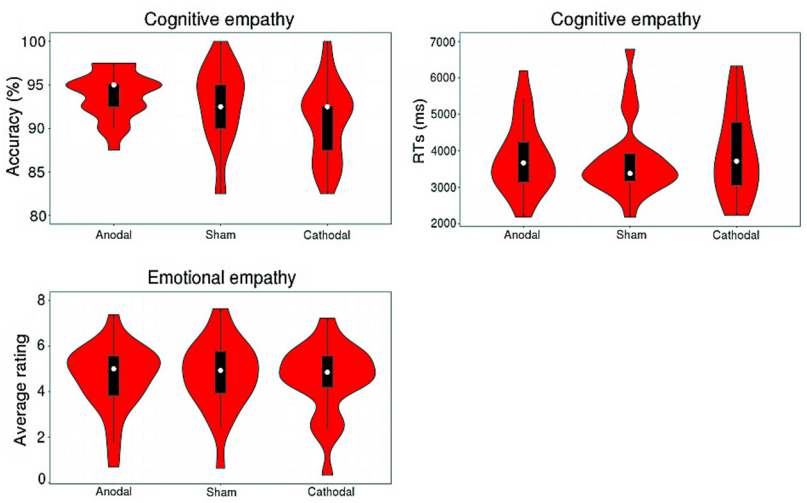


**FIGURE 4 |** Distribution of the accuracy and response times (RTs) of cognitive empathy and the average rating for emotional empathy for all participants of three stimulations.

**TABLE 1 |** Means, standard deviations (SDs) and 95% confidence intervals of Chinese version of the Multifaceted Empathy Test (MET-C) scores for the three stimulation conditions.

| Stimulation conditions | Empathy (MET-C) | Valence | Mean | SD | 95% Confidence interval | |
|---|---|---|---|---|---|---|
| | | | | | Lower | Upper |
| Anodal | Cognitive empathy | | | | | |
| (*n*=23) | Accuracy (%) | Positive | 94.13 | 5.15 | 91.91 | 96.36 |
| | | Negative | 93.48 | 4.63 | 91.48 | 95.48 |
| | | Total | 93.80 | 2.70 | 92.63 | 94.97 |
| | RTs (ms) | Positive | 3,415 | 727 | 3,101 | 3,729 |
| | | Negative | 4,193 | 1,329 | 3,618 | 4,768 |
| | | Total | 3,804 | 999 | 3,372 | 4,236 |
| | Emotional empathy | Positive | 4.62 | 1.63 | 3.91 | 5.33 |
| | | Negative | 4.54 | 1.68 | 3.81 | 5.27 |
| | | Total | 4.58 | 1.49 | 3.94 | 5.23 |
| Sham | Cognitive empathy | | | | | |
| (*n*=23) | Accuracy (%) | Positive | 93.04 | 6.17 | 90.38 | 95.71 |
| | | Negative | 92.17 | 6.00 | 89.58 | 94.77 |
| | | Total | 92.61 | 4.62 | 90.61 | 94.60 |
| | RTs (ms) | Positive | 3,472 | 960 | 3,057 | 3,886 |
| | | Negative | 4,040 | 1,190 | 3,525 | 4,555 |
| | | Total | 3,756 | 1,061 | 3,297 | 4,214 |
| | Emotional empathy | Positive | 4.81 | 1.71 | 4.07 | 5.55 |
| | | Negative | 4.61 | 1.77 | 3.84 | 5.37 |
| | | Total | 4.71 | 1.57 | 4.03 | 5.39 |
| Cathodal | Cognitive empathy | | | | | |
| (*n*=23) | Accuracy (%) | Positive | 92.17 | 6.54 | 89.35 | 95.00 |
| | | Negative | 89.35 | 5.70 | 86.88 | 91.81 |
| | | Total | 90.76 | 4.49 | 88.82 | 92.70 |
| | RTs (ms) | Positive | 3,550 | 1,015 | 3,111 | 3,989 |
| | | Negative | 4,273 | 1,388 | 3,673 | 4,873 |
| | | Total | 3,912 | 1,181 | 3,401 | 4,422 |
| | Emotional empathy | Positive | 4.65 | 1.54 | 3.99 | 5.32 |
| | | Negative | 4.40 | 1.76 | 3.64 | 5.16 |
| | | Total | 4.53 | 1.58 | 3.85 | 5.21 |

## DISCUSSION

The purpose of this study was to assess the impact of HD-tDCS on cognitive and emotional empathy in healthy participants. HD-tDCS targeting the right IFC was shown to regulate accuracy but with no effect on RTs for cognitive empathy. The accuracy of cognitive empathy for participants of the anodal stimulation test was higher than those of the sham stimulation, though the difference is only marginally significant. The accuracy of cognitive empathy for participants of the cathodal stimulation is significantly lower than that of participants of the sham stimulation. However, the active

**TABLE 2 |** Repeated-measures ANOVA on the accuracy and response times (RTs) of cognitive empathy and average ratings of emotional empathy derived from different stimulation conditions and valences.

| Factor | *F* | *P* | $\eta^2$ | 95% Confidence interval for difference | |
|---|---|---|---|---|---|
| | | | | Lower | Upper |
| Cognitive empathy | | | | | |
| Accuracy (%) | | | | | |
| Stimulation condition (Anodal vs. Sham vs. Cathodal) | 8.779** | 0.001 | 0.285 | | |
| Anodal vs. Cathodal | | <0.001 | | 1.587 | 4.500 |
| Anodal vs. Sham | | 0.077 | | −0.143 | 2.534 |
| Cathodal vs. Sham | | 0.038 | | 0.116 | 3.579 |
| Valence (positive vs. negative) | 1.256 | 0.274 | 0.054 | | |
| Stimulation condition × valence | 0.784 | 0.463 | 0.034 | | |
| RTs (ms) | | | | | |
| Stimulation condition (Anodal vs. Sham vs. Cathodal) | 0.429 | 0.654 | 0.019 | | |
| Valence (positive vs. negative) | 44.752** | <0.001 | 0.670 | −903.528 | −475.892 |
| Stimulation condition × valence | 1.480 | 0.239 | 0.063 | | |
| Emotional empathy (max. 9) | | | | | |
| Stimulation condition (Anodal vs. Sham vs. Cathodal) | 0.858 | 0.431 | 0.038 | | |
| Valence (positive vs. negative) | 0.504 | 0.485 | 0.022 | | |
| Stimulation condition × valence | 0.362 | 0.698 | 0.016 | | |

**$p < 0.01$.

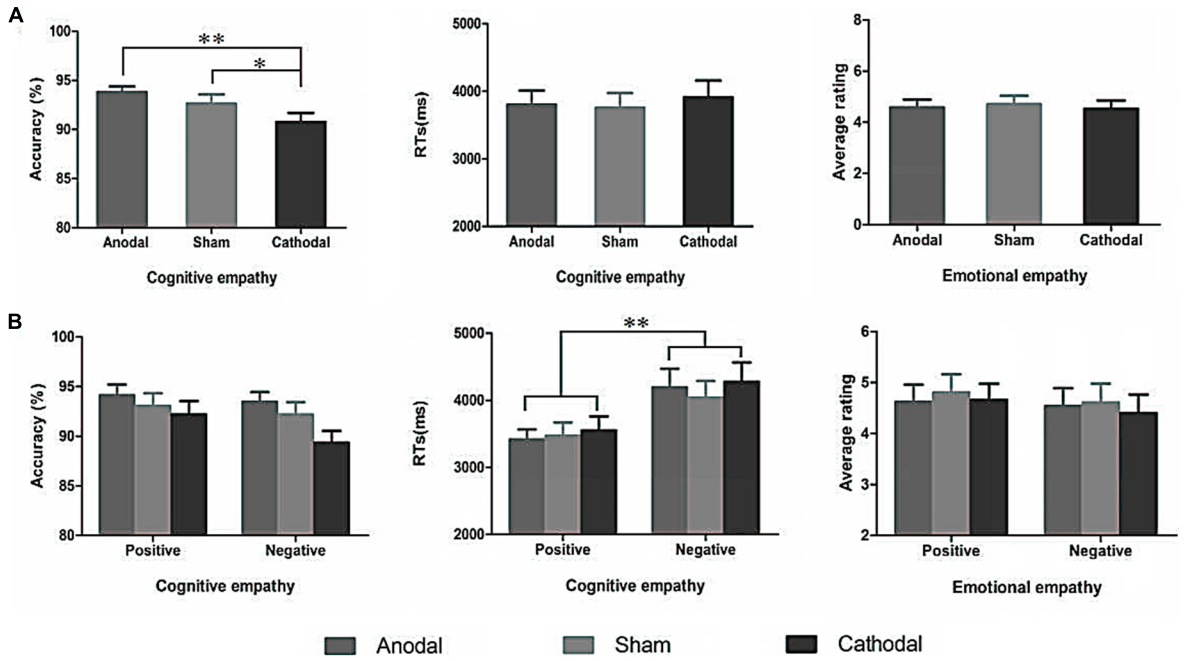


**FIGURE 5 |** The accuracy and RTs of cognitive empathy, and average ratings of emotional empathy derived from the three stimulation conditions **(A)** and two valences **(B)**. Error bars indicate SEM (standard error of the mean) values, $^{*}p < 0.05$, $^{**}p < 0.01$.

HD-tDCS of the right IFC had no effect on emotional empathy.

Brain injury and neuroimaging studies of healthy subjects support the important role of the IFG in empathy (Shamay-Tsoory et al., 2003, 2009; Lawrence et al., 2006; Schulte-Rüther et al., 2007, 2008; Pfeifer et al., 2008; Massey et al., 2017). In addition, functional MRI studies of patients with empathic injuries confirm the important role of the IFG in empathy (Dapretto et al., 2006; Smith et al., 2015). Smith et al. (2015) utilized an emotional PT task that assessed cognitive empathy to study the neural mechanisms of empathy in schizophrenia and found that compared to healthy subjects, bilateral IFG activation in the patient group was significantly reduced during the performance of cognitive empathic tasks. Relative to typically developing children, Dapretto et al. (2006) found that the bilateral IFG is not activated in children with autism. The role of the IFG in empathy is also supported by the human mirror neuron system (hMNS). The hMNS is thought to serve as a neural mechanism for understanding others' intentions, thoughts, actions, and emotions (Fogassi et al., 2005). In addition, the involvement of the hMNS can allow the brain to activate the characterization of observed emotions, thus allowing us to feel the same emotions that we observe in others (Wicker et al., 2003; Jackson et al., 2005). As a core component of the hMNS, the IFG is closely associated with human cognitive and emotional empathy.

Our results indicate that the HD-tDCS of the right IFG has a modulatory effect on the accuracy of cognitive empathy but has no significant effect on RTs. The findings show that the cognitive empathy accuracy of participants receiving cathodal stimulation is significantly lower than that of participants

**TABLE 3 |** Correlation between the personality measures and high-definition transcranial direct current stimulation (HD-tDCS) effects on cognitive and emotional empathy.

| Pearson correlation | IRI | PT | *F* | EC | PD | MoCA | HAMA | HAMD |
|---|---|---|---|---|---|---|---|---|
| Cognitive empathy | | | | | | | | |
| Accuracy (%) | | | | | | | | |
| Anodal-Sham | −0.097 | 0.078 | −0.420* | 0.173 | −0.149 | −0.214 | −0.266 | −0.383 |
| Cathodal-Sham | −0.204 | 0.103 | −0.468* | −0.045 | −0.161 | −0.112 | −0.227 | −0.261 |
| RTs (ms) | | | | | | | | |
| Anodal-Sham | −0.121 | −0.361 | 0.261 | −0.304 | 0.126 | −0.027 | −0.237 | −0.027 |
| Cathodal-Sham | 0.017 | −0.067 | 0.216 | −0.200 | 0.136 | −0.187 | 0.146 | 0.269 |
| Emotional empathy | | | | | | | | |
| Anodal-Sham | 0.052 | 0.052 | 0.184 | −0.130 | 0.073 | 0.042 | 0.141 | −0.246 |
| Cathodal-Sham | 0.017 | 0.400 | −0.111 | −0.062 | −0.141 | −0.195 | 0.290 | −0.025 |

*$p < 0.05$.

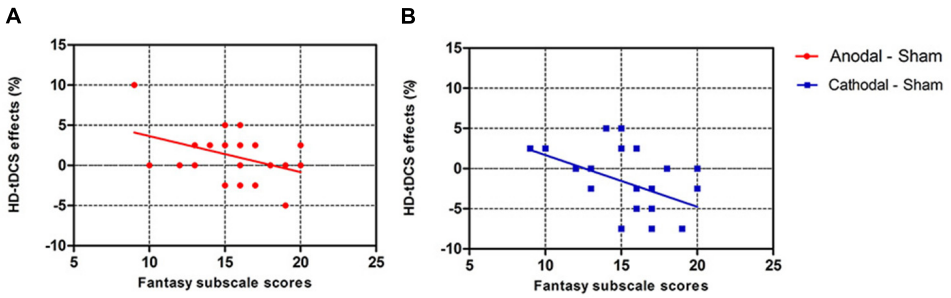


**FIGURE 6 |** Scatter diagram showing correlations between scores of the Fantasy subscale and HD-tDCS effects for accuracy in cognitive empathy (**A**, anodal $r = -0.420$, $p = 0.046$; **B**, cathodal $r = -0.468$, $p = 0.024$). Note that equal HD-tDCS effects of participants sometimes might be covered by only one data point.

receiving sham stimulation consistent with previous studies employing tDCS (Mai et al., 2016; Coll et al., 2017). Furthermore, cognitive empathy accuracy following anodal stimulation is higher than it is after sham stimulation, though the difference is only marginally significant. This may be the case because MET-C cognitive empathy tasks are easy for healthy subjects to complete. As such, it is difficult to elicit a substantial improvement from HD-tDCS stimulation. In spite of this, the result also implies a potential improvement resulting from anodal stimulation. In short, our study is consistent with previous neuroimaging and brain injury studies (Shamay-Tsoory et al., 2003, 2009; Lawrence et al., 2006; Schulte-Rüther et al., 2007, 2008; Pfeifer et al., 2008; Smith et al., 2015; Massey et al., 2017) and confirms the important role of the IFG in cognitive empathy and the effective role of HD-tDCS in regulating social cognitive functioning. Notably, our results also show that participants responded to negative emotional pictures longer than positive emotional pictures during cognitive empathic tasks consistent with previous studies (Leppänen and Hietanen, 2004; Song et al., 2017; Aldunate et al., 2018). Earlier findings have shown that during emotional recognition, happiness is recognized faster than sadness (Crews and Harrison, 1994; Leppänen and Hietanen, 2004), anger (Hugdahl et al., 1993) and disgust (Stalans and Wedding, 1985). The advantage inherent in responding to positive emotions may result from low levels of physical difference, rendering happy emotions visually more unique and thus easier to identify than others (Leppänen and Hietanen, 2004).

With respect to emotional empathy, the findings are in conflict with the hypotheses of this study, which failed to show that different types of stimulation like HD-tDCS have a significant modulatory effect on emotional empathy. This result may be attributed to the following. First, our task measured emotional empathy in terms of the intensity of emotional mirroring, which reflects only one component of emotional empathy (Oliver et al., 2015), thereby disregarding other measurement components such as EC. Thus, emotional empathy as measured using the MET-C cannot reflect emotional empathy in its entirety. Second, in comparison to cognitive empathy, the measurement of emotional empathy is more subjective. As such, both the external environment and bodily states of the participants had a substantial influence on their responses during the task (e.g., emotional states on the day of the experiment), and due to the small number of participants tested, random error effects were difficult to control, potentially affecting the results of the study. Furthermore, a rating scale of 0–9 was used for the emotional empathy task, which may not have been sensitive enough to evaluate the effects of HD-tDCS on emotional empathy. Finally, our results may simply show that the active stimulation of the right IFG by HD-tDCS has no or little effect on emotional empathy.

Despite these limitations our findings assist us in understanding the relationship between the IFG and empathy and offer evidence of the potential contributions of HD-tDCS in the realm of social cognition. As far as we know this is the first study to explore the role of the right IFG in empathy via HD-tDCS. Future studies may use larger samples or different empathy tasks to validate our findings. In addition, many studies suggest that the left IFG plays an important role in empathy (Lawrence et al., 2006; Jabbi et al., 2007; Hooker et al., 2008, 2010; Greimel et al., 2010; Sassa et al., 2012) and future research can explore the modulatory effects of HD-tDCS on empathy by targeting the left IFG to further examine the relationship between the IFG and empathy. Finally, studies have shown that many psychiatric patients and particularly patients with schizophrenia suffer from a serious empathy disorder and that cognitive empathy is more severely impaired in psychiatric patients (Dapretto et al., 2006; Derntl et al., 2009; Smith et al., 2015). Future studies can elaborate upon our research by investigating empathy in such patients and the role of anodal stimulation while further exploring the clinical significance of HD-tDCS in improving social cognitive abilities.

## CONCLUSION

Our findings confirm that the cathodal HD-tDCS of the right IFC can lead to an impairment of cognitive empathy while anodal stimulation can spur an improvement. However, the active HD-tDCS of the right IFC has no effect on emotional empathy. In summary, we believe that the IFG plays an important role in cognitive empathy and that

HD-tDCS can be effective in modulating social cognitive abilities.

## AUTHOR CONTRIBUTIONS

The experiment was designed by XW, FX, CX and KWang. WH, KWan, XC, SX and GX performed data collection and analysis. XW wrote the article. LW, G-JJ, FY and CZ were responsible for modifying the article. All of the authors made their own contributions to the final article and all have agreed to the submission of this version.

## FUNDING

This research was supported by the National Natural Science Foundation of China (Grant nos. 31571149, 81171273, 91232717 and 91432301) and the National Basic Research Program of China (No. 973 Program, 2012CB720704 and 2015CB856405).

## REFERENCES

Adenzato, M., Brambilla, M., Manenti, R., De Lucia, L., Trojano, L., Garofalo, S., et al. (2017). Gender differences in cognitive Theory of Mind revealed by transcranial direct current stimulation on medial prefrontal cortex. *Sci. Rep.* 7:41219. doi: 10.1038/srep41219

Aldunate, N., Villena-González, M., Rojas-Thomas, F., López, V., and Bosman, C. A. (2018). Mood detection in ambiguous messages: the interaction between text and emoticons. *Front. Psychol.* 9:423. doi: 10.3389/fpsyg.2018.00423

Antal, A., Bikson, M., Datta, A., Lafon, B., Dechent, P., Parra, L. C., et al. (2014). Imaging artifacts induced by electrical stimulation during conventional fMRI of the brain. *Neuroimage* 85, 1040–1047. doi: 10.1016/j.neuroimage.2012.10.026

Baron-Cohen, S., Wheelwright, S., Hill, J., Raste, Y., and Plumb, I. (2001). The "Reading the Mind in the Eyes" Test revised version: a study with normal adults, and adults with Asperger syndrome or high-functioning autism. *J. Child. Psychol. Psychiatry* 42, 241–251. doi: 10.1017/s0021963001006643

Bloom, P. (2016). *Against Empathy: The Case for Rational Compassion.* New York, NY: HarperCollins.

Bloom, P. (2017). Empathy and its discontents. *Trends Cogn. Sci.* 21, 24–31. doi: 10.1016/j.tics.2016.11.004

Brennan, S., McLoughlin, D. M., O'Connell, R., Bogue, J., O'Connor, S., McHugh, C., et al. (2017). Anodal transcranial direct current stimulation of the left dorsolateral prefrontal cortex enhances emotion recognition in depressed patients and controls. *J. Clin. Exp. Neuropsychol.* 39, 384–395. doi: 10.1080/13803395.2016.1230595

Cerruti, C., and Schlaug, G. (2008). Anodal transcranial direct current stimulation of the prefrontal cortex enhances complex verbal associative thought. *J. Cogn. Neurosci.* 21, 1980–1987. doi: 10.1162/jocn.2008.21143

Civai, C., Miniussi, C., and Rumiati, R. I. (2015). Medial prefrontal cortex reacts to unfairness if this damages the self: a tDCS study. *Soc. Cogn. Affect. Neurosci.* 10, 1054–1060. doi: 10.1093/scan/nsu154

Coll, M. P., Tremblay, M. B., and Jackson, P. L. (2017). The effect of tDCS over the right temporo-parietal junction on pain empathy. *Neuropsychologia* 100, 110–119. doi: 10.1016/j.neuropsychologia.2017.04.021

Crews, W. D. Jr., and Harrison, D. W. (1994). Cerebral asymmetry in facial affect perception by women: neuropsychological effects of depressed mood. *Percept. Mot. Skills* 79, 1667–1679. doi: 10.2466/pms.1994.79.3f.1667

Dapretto, M., Davies, M. S., Pfeifer, J. H., Scott, A. A., Sigman, M., Bookheimer, S. Y., et al. (2006). Understanding emotions in others: mirror neuron dysfunction in children with autism spectrum disorders. *Nat. Neurosci.* 9, 28–30. doi: 10.1038/nn1611

Datta, A., Bansal, V., Diaz, J., Patel, J., Reato, D., and Bikson, M. (2009). Gyri-precise head model of transcranial direct current stimulation: improved spatial focality using a ring electrode versus conventional rectangular pad. *Brain Stimul.* 2, 201.e1–207.e1. doi: 10.1016/j.brs.2009.03.005

Datta, A., Elwassif, M., Battaglia, F., and Bikson, M. (2008). Transcranial current stimulation focality using disc and ring electrode configurations: FEM analysis. *J. Neural Eng.* 5, 163–174. doi: 10.1088/1741-2560/5/2/007

Davis, M. H. (1980). A multidimensional approach to individual differences in empathy. *JSAS Catalog Sel. Doc. Psychol.* 10:85 .

Decety, J., and Cowell, J. M. (2014). Friends or foes: is empathy necessary for moral behavior? *Perspect. Psychol. Sci* 9, 525–537. doi: 10.1177/1745691614545130

Decety, J., and Lamm, C. (2006). Human empathy through the lens of social neuroscience. *ScientificWorldJournal* 6, 1146–1163. doi: 10.1100/tsw.2006.221

Derntl, B., Finkelmeyer, A., Toygar, T. K., Hülsmann, A., Schneider, F., Falkenberg, D. I., et al. (2009). Generalized deficit in all core components of empathy in schizophrenia. *Schizophr. Res.* 108, 197–206. doi: 10.1016/j.schres.2008.11.009

Derntl, B., Finkelmeyer, A., Voss, B., Eickhoff, S. B., Kellermann, T., and Schneider, F. (2012). Neural correlates of the core facets of empathy in schizophrenia. *Schizophr. Res.* 136, 70–81. doi: 10.1016/j.schres.2011.12.018

Dziobek, I., Preissler, S., Grozdanovic, Z., Heuser, I., Heekeren, H. R., and Roepke, S. (2011). Neuronal correlates of altered empathy and social cognition in borderline personality disorder. *Neuroimage* 57, 539–548. doi: 10.1016/j.neuroimage.2011.05.005

Dziobek, I., Rogers, K., Fleck, S., Bahnemann, M., Heekeren, H. R., Wolf, O. T., et al. (2008). Dissociation of cognitive and emotional empathy in adults with Asperger syndrome using the Multifaceted Empathy Test (MET). *J. Autism Dev. Disord.* 38, 464–473. doi: 10.1007/s10803-007-0486-x

Fan, Y., Duncan, N. W., de Greck, M., and Northoff, G. (2011). Is there a core neural network in empathy? An fMRI based quantitative meta-analysis. *Neurosci. Biobehav. Rev.* 35, 903–911. doi: 10.1016/j.neubiorev.2010.10.009

Fogassi, L., Ferrari, P. F., Gesierich, B., Rozzi, S., Chersi, F., and Rizzolatti, G. (2005). Parietal lobe: from action organization to intention understanding. *Science* 308, 662–667. doi: 10.1126/science.1106138

Godinho, M. M., Junqueira, D. R., Castro, M. L., Loke, Y., Golder, S., and Neto, H. P. (2017). Safety of transcranial direct current stimulation: evidence based update 2016. *Brain Stimul.* 10, 983–985. doi: 10.1016/j.brs.2017.07.001

Greimel, E., Schulte-Rüther, M., Fink, G. R., Piefke, M., Herpertz-Dahlmann, B., and Konrad, K. (2010). Development of neural correlates of empathy from childhood to early adulthood: an fMRI study in boys and adult men. *J. Neural Transm.* 117, 781–791. doi: 10.1007/s00702-010-0404-9

Harari, H., Shamay-Tsoory, S. G., Ravid, M., and Levkovitz, Y. (2010). Double dissociation between cognitive and affective empathy in borderline personality disorder. *Psychiatry Res.* 175, 277–279. doi: 10.1016/j.psychres.2009.03.002

Harvey, P. O., Zaki, J., Lee, J., Ochsner, K., and Green, M. F. (2013). Neural substrates of empathic accuracy in people with schizophrenia. *Schizophr. Bull.* 39, 617–628. doi: 10.1093/schbul/sbs042

Hogeveen, J., Grafman, J., Aboseria, M., David, A., Bikson, M., and Hauner, K. K. (2016). Effects of high-definition and conventional tDCS on response inhibition. *Brain Stimul.* 9, 720–729. doi: 10.1016/j.brs.2016.04.015

Hogeveen, J., Obhi, S. S., Banissy, M. J., Santiesteban, I., Press, C., Catmur, C., et al. (2015). Task-dependent and distinct roles of the temporoparietal junction and inferior frontal cortex in the control of imitation. *Soc. Cogn. Affect. Neurosci.* 10, 1003–1009. doi: 10.1093/scan/nsu148

Holland, R., Leff, A. P., Josephs, O., Galea, J. M., Desikan, M., Price, C. J., et al. (2011). Speech facilitation by left inferior frontal cortex stimulation. *Curr. Biol.* 21, 1403–1407. doi: 10.1016/j.cub.2011.07.021

Hooker, C. I., Verosky, S. C., Germine, L. T., Knight, R. T., and D'Esposito, M. (2008). Mentalizing about emotion and its relationship to empathy. *Soc. Cogn. Affect. Neurosci.* 3, 204–217. doi: 10.1093/scan/nsn019

Hooker, C. I., Verosky, S. C., Germine, L. T., Knight, R. T., and D'Esposito, M. (2010). Neural activity during social signal perception correlates with self-reported empathy. *Brain Res.* 1308, 100–113. doi: 10.1016/j.brainres.2009.10.006

Hugdahl, K., Iversen, P. M., and Johnsen, B. H. (1993). Laterality for facial expressions: does the sex of the subject interact with the sex of the stimulus face? *Cortex* 29, 325–331. doi: 10.1016/s0010-9452(13)80185-2

Hysek, C. M., Schmid, Y., Simmler, L. D., Domes, G., Heinrichs, M., Eisenegger, C., et al. (2014). MDMA enhances emotional empathy and prosocial behavior. *Soc. Cogn. Affect. Neurosci.* 9, 1645–1652. doi: 10.1093/scan/nst161

Jabbi, M., Swart, M., and Keysers, C. (2007). Empathy for positive and negative emotions in the gustatory cortex. *Neuroimage* 34, 1744–1753. doi: 10.1016/j.neuroimage.2006.10.032

Jackson, P. L., Meltzoff, A. N., and Decety, J. (2005). How do we perceive the pain of others? A window into the neural processes involved in empathy. *Neuroimage* 24, 771–779. doi: 10.1016/j.neuroimage.2004.09.006

Kuypers, K. P., Dolder, P. C., Ramaekers, J. G., and Liechti, M. E. (2017). Multifaceted empathy of healthy volunteers after single doses of MDMA: a pooled sample of placebo-controlled studies. *J. Psychopharmacol.* 31, 589–598. doi: 10.1177/0269881117699617

Lawrence, E. J., Shaw, P., Giampietro, V. P., Surguladze, S., Brammer, M. J., and David, A. S. (2006). The role of 'shared representations' in social perception and empathy: an fMRI study. *Neuroimage* 29, 1173–1184. doi: 10.1016/j.neuroimage.2005.09.001

Lehmann, A., Bahcesular, K., Brockmann, E. M., Biederbick, S. E., Dziobek, I., Gallinat, J., et al. (2014). Subjective experience of emotions and emotional empathy in paranoid schizophrenia. *Psychiatry Res.* 220, 825–833. doi: 10.1016/j.psychres.2014.09.009

Leigh, R., Oishi, K., Hsu, J., Lindquist, M., Gottesman, R. F., Jarso, S., et al. (2013). Acute lesions that impair affective empathy. *Brain* 136, 2539–2549. doi: 10.1093/brain/awt177

Leppänen, J. M., and Hietanen, J. K. (2004). Positive facial expressions are recognized faster than negative facial expressions, but why? *Psychol. Res.* 69, 22–29. doi: 10.1007/s00426-003-0157-2

Mai, X., Zhang, W., Hu, X., Zhen, Z., Xu, Z., Zhang, J., et al. (2016). Using tDCS to explore the role of the right temporo-parietal junction in theory of mind and cognitive empathy. *Front. Psychol.* 7:380. doi: 10.3389/fpsyg.2016.00380

Martin, A. K., Huang, J., Hunold, A., and Meinzer, M. (2017). Sex mediates the effects of high-definition transcranial direct current stimulation on "mind-reading". *Neuroscience* 366, 84–94. doi: 10.1016/j.neuroscience.2017.10.005

Massey, S. H., Stern, D., Alden, E. C., Petersen, J. E., Cobia, D. J., Wang, L., et al. (2017). Cortical thickness of neural substrates supporting cognitive empathy in individuals with schizophrenia. *Schizophr. Res.* 179, 119–124. doi: 10.1016/j.schres.2016.09.025

Mazza, M., Pino, M. C., Mariano, M., Tempesta, D., Ferrara, M., De Berardis, D., et al. (2014). Affective and cognitive empathy in adolescents with autism spectrum disorder. *Front. Hum. Neurosci.* 8:791. doi: 10.3389/fnhum.2014.00791

Meinzer, M., Lindenberg, R., Darkow, R., Ulm, L., Copland, D., and Floel, A. (2014). Transcranial direct current stimulation and simultaneous functional magnetic resonance imaging. *J. Vis. Exp.* 86:e51730. doi: 10.3791/51730

Minhas, P., Bansal, V., Patel, J., Ho, J. S., Diaz, J., Datta, A., et al. (2010). Electrodes for high-definition transcutaneous DC stimulation for applications in drug delivery and electrotherapy, including tDCS. *J. Neurosci. Methods* 190, 188–197. doi: 10.1016/j.jneumeth.2010.05.007

Nitsche, M. A., Fricke, K., Henschke, U., Schlitterlau, A., Liebetanz, D., Lang, N., et al. (2003). Pharmacological modulation of cortical excitability shifts induced by transcranial direct current stimulation in humans. *J. Physiol.* 553, 293–301. doi: 10.1113/jphysiol.2003.049916

Nitsche, M. A., Koschack, J., Pohlers, H., Hullemann, S., Paulus, W., and Happe, S. (2012). Effects of frontal transcranial direct current stimulation on emotional state and processing in healthy humans. *Front. Psychiatry* 3:58. doi: 10.3389/fpsyt.2012.00058

Nitsche, M. A., and Paulus, W. (2001). Sustained excitability elevations induced by transcranial DC motor cortex stimulation in humans. *Neurology* 57, 1899–1901. doi: 10.1212/wnl.57.10.1899

Nobusako, S., Nishi, Y., Nishi, Y., Shuto, T., Asano, D., Osumi, M., et al. (2017). Transcranial direct current stimulation of the temporoparietal junction and inferior frontal cortex improves imitation-inhibition and perspective-taking with no effect on the autism-spectrum quotient score. *Front. Behav. Neurosci.* 11:84. doi: 10.3389/fnbeh.2017.00084

Oishi, K., Faria, A. V., Hsu, J., Tippett, D., Mori, S., and Hillis, A. E. (2015). Critical role of the right uncinate fasciculus in emotional empathy. *Ann. Neurol.* 77, 68–74. doi: 10.1002/ana.24300

Oliver, L. D., Mitchell, D. G., Dziobek, I., MacKinley, J., Coleman, K., Rankin, K. P., et al. (2015). Parsing cognitive and emotional empathy deficits for negative and positive stimuli in frontotemporal dementia. *Neuropsychologia* 67, 14–26. doi: 10.1016/j.neuropsychologia.2014.11.022

Oliver, L. D., Vieira, J. B., Neufeld, R. W. J., Dziobek, I., and Mitchell, D. G. V. (2018). Greater involvement of action simulation mechanisms in emotional versus cognitive empathy. *Soc. Cogn. Affect. Neurosci.* 13, 367–380. doi: 10.1093/scan/nsy013

Pfeifer, J. H., Iacoboni, M., Mazziotta, J. C., and Dapretto, M. (2008). Mirroring others' emotions relates to empathy and interpersonal competence in children. *Neuroimage* 39, 2076–2085. doi: 10.1016/j.neuroimage.2007.10.032

Philip, N. S., Nelson, B. G., Frohlich, F., Lim, K. O., Widge, A. S., and Carpenter, L. L. (2017). Low-intensity transcranial current stimulation in psychiatry. *Am. J. Psychiatry* 174, 628–639. doi: 10.1176/appi.ajp.2017.16090996

Rêgo, G. G., Lapenta, O. M., Marques, L. M., Costa, T. L., Leite, J., Carvalho, S., et al. (2015). Hemispheric dorsolateral prefrontal cortex lateralization in the regulation of empathy for pain. *Neurosci. Lett.* 594, 12–16. doi: 10.1016/j.neulet.2015.03.042

Sassa, Y., Taki, Y., Takeuchi, H., Hashizume, H., Asano, M., Asano, K., et al. (2012). The correlation between brain gray matter volume and empathizing and systemizing quotients in healthy children. *Neuroimage* 60, 2035–2041. doi: 10.1016/j.neuroimage.2012.02.021

Schulte-Rüther, M., Markowitsch, H. J., Fink, G. R., and Piefke, M. (2007). Mirror neuron and theory of mind mechanisms involved in face-to-face interactions: a functional magnetic resonance imaging approach to empathy. *J. Cogn. Neurosci.* 19, 1354–1372. doi: 10.1162/jocn.2007.19.8.1354

Schulte-Rüther, M., Markowitsch, H. J., Shah, N. J., Fink, G. R., and Piefke, M. (2008). Gender differences in brain networks supporting empathy. *Neuroimage* 42, 393–403. doi: 10.1016/j.neuroimage.2008.04.180

Shamay-Tsoory, S. G. (2011). The neural bases for empathy. *Neuroscientist* 17, 18–24. doi: 10.1177/1073858410379268

Shamay-Tsoory, S. G., Aharon-Peretz, J., and Perry, D. (2009). Two systems for empathy: a double dissociation between emotional and cognitive empathy in inferior frontal gyrus versus ventromedial prefrontal lesions. *Brain* 132, 617–627. doi: 10.1093/brain/awn279

Shamay-Tsoory, S. G., Tomer, R., Berger, B. D., and Aharon-Peretz, J. (2003). Characterization of empathy deficits following prefrontal brain damage: the role of the right ventromedial prefrontal cortex. *J. Cogn. Neurosci.* 15, 324–337. doi: 10.1162/089892903321593063

Smith, M. J., Horan, W. P., Cobia, D. J., Karpouzian, T. M., Fox, J. M., and Reilly, J. L. (2014). Performance-based empathy mediates the influence of working memory on social competence in schizophrenia. *Schizophr. Bull.* 40, 824–834. doi: 10.1093/schbul/sbt084

Smith, M. J., Schroeder, M. P., Abram, S. V., Goldman, M. B., Parrish, T. B., Wang, X., et al. (2015). Alterations in brain activation during cognitive empathy are related to social functioning in schizophrenia. *Schizophr. Bull.* 41, 211–222. doi: 10.1093/schbul/sbu023

Song, J., Liu, M., Yao, S., Yan, Y., Ding, H., and Yan, T. (2017). Classification of emotional expressions is affected by inversion: behavioral and electrophysiological evidence. *Front. Behav. Neurosci.* 11:21. doi: 10.3389/fnbeh.2017.00021

Stalans, L., and Wedding, D. (1985). Superiority of the left hemisphere in the recognition of emotional faces. *Int. J. Neurosci.* 25, 219–223. doi: 10.3109/00207458508985373

Tang, H., Ye, P., Wang, S., Zhu, R., Su, S., Tong, L., et al. (2017). Stimulating the right temporoparietal junction with tDCS decreases deception in moral hypocrisy and unfairness. *Front. Psychol.* 8:2033. doi: 10.3389/fpsyg.2017.02033

Völlm, B. A., Taylor, A. N., Richardson, P., Corcoran, R., Stirling, J., McKie, S., et al. (2006). Neuronal correlates of theory of mind and empathy: a functional magnetic resonance imaging study in a nonverbal task. *Neuroimage* 29, 90–98. doi: 10.1016/j.neuroimage.2005.07.022

Wang, J., Wang, Y., Hu, Z., and Li, X. (2014). Transcranial direct current stimulation of the dorsolateral prefrontal cortex increased pain empathy. *Neuroscience* 281, 202–207. doi: 10.1016/j.neuroscience.2014.09.044

Wicker, B., Keysers, C., Plailly, J., Royet, J. P., Gallese, V., and Rizzolatti, G. (2003). Both of us disgusted in My insula: the common neural basis of seeing and feeling disgust. *Neuron* 40, 655–664. doi: 10.1016/S0896-6273(03)00679-2

Willis, M. L., Murphy, J. M., Ridley, N. J., and Vercammen, A. (2015). Anodal tDCS targeting the right orbitofrontal cortex enhances facial expression recognition. *Soc. Cogn. Affect. Neurosci.* 10, 1677–1683. doi: 10.1093/scan/nsv057

Wingenfeld, K., Kuehl, L. K., Dziobek, I., Roepke, S., Otte, C., and Hinkelmann, K. (2016). Effects of mineralocorticoid receptor blockade on empathy in patients with major depressive disorder. *Cogn. Affect. Behav. Neurosci.* 16, 902–910. doi: 10.3758/s13415-016-0441-4

Wingenfeld, K., Kuehl, L. K., Janke, K., Hinkelmann, K., Dziobek, I., Fleischer, J., et al. (2014). Enhanced emotional empathy after mineralocorticoid receptor stimulation in women with borderline personality disorder and healthy women. *Neuropsychopharmacology* 39, 1799–1804. doi: 10.1038/npp.2014.36

Zaki, J. (2016). "Empathy is a moral force," in *The Atlas of Moral Psychology*, eds K. Gray and J. Graham (New York, NY: Guilford Press), 49–58.

Zaki, J. (2017). Moving beyond stereotypes of empathy. *Trends Cogn. Sci.* 21, 59–60. doi: 10.1016/j.tics.2016.12.004

Ze, O., Thoma, P., and Suchan, B. (2014). Cognitive and affective empathy in younger and older individuals. *Aging. Ment. Health.* 18, 929–935. doi: 10.1080/13607863.2014.899973

Zhu, Y., Chen, X., Wu, X., Xu, S., Cao, Z., Wang, K., et al. (2018). The multifaceted empathy test scale: development, reliability and validity. *Acta Univers. Med. Anhui.* 53:7. doi: 10.19405/j.cnki.issn1000-1492.2018.07.023

Zito, G. A., Senti, T., Cazzoli, D., Müri, R. M., Mosimann, U. P., Nyffeler, T., et al. (2015). Cathodal HD-tDCS on the right V5 improves motion perception in humans. *Front. Behav. Neurosci.* 9:257. doi: 10.3389/fnbeh.2015.00257

**Conflict of Interest Statement**: The authors declare that the research was conducted in the absence of any commercial or financial relationships that could be construed as a potential conflict of interest.

frontiers in Human Neuroscience

ORIGINAL RESEARCH
published: 15 November 2018
doi: 10.3389/fnhum.2018.00453

# Test–Retest Reliability of Mismatch Negativity (MMN) to Emotional Voices

*Chenyi Chen[1,2,3,4], Chia-Wen Chan[2] and Yawei Cheng[1,5,6]**

[1] Department of Physical Medicine and Rehabilitation, National Yang-Ming University Hospital, Yilan, Taiwan, [2] Graduate Institute of Injury Prevention and Control, Taipei Medical University, Taipei, Taiwan, [3] Institute of Humanities in Medicine, Taipei Medical University, Taipei, Taiwan, [4] Research Center of Brain and Consciousness, Shuang Ho Hospital, Taipei Medical University, Taipei, Taiwan, [5] Institute of Neuroscience and Brain Research Center, National Yang-Ming University, Taipei, Taiwan, [6] Department of Research and Education, Taipei City Hospital, Taipei, Taiwan

A voice from kin species conveys indispensable social and affective signals with uniquely phylogenetic and ontogenetic standpoints. However, the neural underpinning of emotional voices, beyond low-level acoustic features, activates a processing chain that proceeds from the auditory pathway to the brain structures implicated in cognition and emotion. By using a passive auditory oddball paradigm, which employs emotional voices, this study investigates the test–retest reliability of emotional mismatch negativity (MMN), indicating that the deviants of positively (happily)- and negatively (angrily)-spoken syllables, as compared to neutral standards, can trigger MMN as a response to an automatic discrimination of emotional salience. The neurophysiological estimates of MMN to positive and negative deviants appear to be highly reproducible, irrespective of the subject's attentional disposition: whether the subjects are set to a condition that involves watching a silent movie or do a working memory task. Specifically, negativity bias is evinced as threatening, relative to positive vocalizations, consistently inducing larger MMN amplitudes, regardless of the day and the time of a day. The present findings provide evidence to support the fact that emotional MMN offers a stable platform to detect subtle changes in current emotional shifts.

**Keywords: emotional voice, mismatch negativity, test–retest reliability, attention disposition, circadian sessions**

OPEN ACCESS

***Edited by:***
*Delin Sun,*
*Duke University, United States*

***Reviewed by:***
*Junling Gao,*
*University of Hong Kong, Hong Kong*
*Jiushu Xie,*
*Nanjing Normal University, China*

***Correspondence:**
*Yawei Cheng*
*ywcheng2@ym.edu.tw*

***Received:*** *13 July 2018*
***Accepted:*** *24 October 2018*
***Published:*** *15 November 2018*

***Citation:***
*Chen C, Chan C-W and Cheng Y (2018) Test–Retest Reliability of Mismatch Negativity (MMN) to Emotional Voices. Front. Hum. Neurosci. 12:453. doi: 10.3389/fnhum.2018.00453*

## INTRODUCTION

Mismatch Negativity (MMN) is a differential wave obtained by subtracting the auditory event-related potential (ERP) component evoked by frequent, repetitive "standard" sounds from the ERP component evoked in response to the infrequent deviants that are interspersed within a constant auditory stream. It is defined as a negative ERP displacement, particularly, at the frontocentral and central scalp electrodes relative to a mastoid or nose reference electrode (Naatanen et al., 2007). The MMN reflects the early saliency detection of auditory stimuli that is generated in a hierarchical network involving primary and secondary auditory regions as well as specific brain regions regarding stimulus discrimination, based on the perceptual processes of physical features (Rinne et al., 2000; Doeller et al., 2003; Pulvermuller and Shtyrov, 2006; Garrido et al., 2008; Thonnessen et al., 2010). The "model-adjustment hypothesis" of MMN indicates that the MMN is evinced

from the comparison process between a sensory input and a "memory-based" perceptual model (Naatanen and Winkler, 1999; Naatanen et al., 2005).

In the same vein, previous studies suggested that, in addition to many basic features of sounds such as frequency, duration, intensity, or even sound omissions, the MMN could also be utilized as an index of the salience of emotional voice processing (Schirmer and Kotz, 2006; Schirmer et al., 2008; Schirmer and Escoffier, 2010; Thonnessen et al., 2010). When meaningless syllables "dada" are spoken with emotionally neutral, happy, or disgusted prosodies, administered by way of a passive oddball paradigm, disgusted deviants in comparison with happy deviants have been seen to elicit stronger magnetoencephalographic counterparts of MMN (MMNm) and MMNm-related cortical activities in the right anterior insular cortex, a region that has been previously demonstrated as critical in the processing of negative emotions, such as disgusted facial expressions (Chen et al., 2014). This procedure has also been employed to measure voice and emotional processing in infants (Cheng et al., 2012; Zhang et al., 2014). Newborns have been found to be sensitive to emotional voices beyond specific language and exhibit the comparable ability with adults to process the affective information in voices (Fan et al., 2013; Hung and Cheng, 2014; Chen et al., 2015). Voices with affective information are supposed to elicit higher recruitment of associated resources than those with non-affective information.

Given the fact that MMN can be generated without the need of the subjects' explicit attention toward the sound stimuli, it proves to be beneficial in investigations regarding populations with potential attention deficit comorbidities. It is noteworthy that even though attention is not necessary to evoke MMN, it has been observed that MMN is sensitive to attention. When the subject's attention is directed elsewhere, the MMN is usually elicited quite similarly to when the sequence of standard and deviant sounds is attended. Nevertheless, MMN amplitude may be somewhat attenuated under certain conditions with highly focused attention elsewhere (Naatanen et al., 2007). In accordance with the most important implication of MMN serving as a valid tool to detect and assess neurological, neuropsychiatric, and neurodevelopmental disorders (Naatanen et al., 2015), as well as healthy aging (Naatanen et al., 2012), emotional MMN has also been linked with potential clinical ERP biomarkers, especially in detecting abnormalities in emotional processing, such as those observed in delinquents with conduct disorder symptoms, people with autism spectrum conditions, and positive symptoms in schizophrenia (Hung et al., 2013; Fan and Cheng, 2014; Chen et al., 2016a). Previous electroencephalography (EEG) studies have evaluated the reliability of MMN dependent on duration, frequency, and intensity changes in stimulus and provided its detectability and essentiality for potential ERP biomarkers in clinical research. Moderate to robust reliability for ERPs, ranging between 0.37 and 0.87, have been identified (Frodl-Bauch et al., 1997; Kathmann et al., 1999; Tervaniemi et al., 1999; Schroger et al., 2000; Light and Braff, 2005; Hall et al., 2006; Light et al., 2012). The replicability of MMNm has also been assessed, with reports stating high intraclass correlation coefficients (ICC) for duration (0.89), frequency (0.86), and omission (0.63∼0.9) deviants (Tervaniemi et al., 2005; Recasens and Uhlhaas, 2017).

It is noteworthy that while anxious states were purposely elicited in healthy participants by exposure to unpredictable aversive shocks, threat-induced anxiety was observed to induce anxious hypervigilance and produce an enlargement of the MMNm to pure tone deviants (Cornwell et al., 2017). Considering the emotional salience inherited in vocal expression, emotional MMN can help in identifying the comprehension of vocal emotionality as a special domain, beyond general processing and vigilance to mechanically stabilize environmental changes (Schirmer and Kotz, 2006). For instance, emotional MMN may serve as a proxy to access the ERP correlates of trait and state anxiety and the automatic emotional salience processing in the sleeping brain (Cheng et al., 2012; Chen et al., 2016b, 2017). While several studies have assessed the stability of MMN to non-vocal and pure tone deviants, test–retest reliability of emotional MMN is currently unclear. Given the use of emotional MMN as a potential proxy for approaching the automatic emotional saliency in individuals with aberrant emotional processing and attention deficit comorbidities, we evaluated the stability of emotional MMN under various attentional conditions as well as on different days and on different times of a day.

The test–retest reliability for different times of day was assessed by recording the ERPs in the mid-morning (10:30 AM) and in the mid-afternoon (15:30 PM) of the same day. Then, two weeks later, the same two sessions were recorded again, this time in order to examine the test–retest reliability of emotional MMN on different days. In order to assess the reliability under different attentional conditions, the participants were subjected to two different tasks (that were later used for comparison). In one task, they were required to direct their attention to a working memory task: first, they evaluated the position of an undergoing visual stimulus, and then they compared the position of the undergoing stimulus with that of the two trials before (*2*-back); in the other task, the subjects were asked to watch a silent movie.

For the end of this study, we hypothesize that the deviant stimuli embedded in the oddball paradigm (whether they are of positively or negatively spoken syllables), when compared to neutral standards, can evoke MMN as an outcome of the automatic discrimination of emotional salience. We further hypothesize that the neurophysiological estimates of MMN to positive and negative deviants will appear to be highly reproducible, irrespective of the attentional disposition generated in the participants by means of the tasks they are set to perform, namely watching a silent movie or engaging in a working memory task, thus providing evidence of emotional MMN as a stable platform to detect subtle changes in current emotional shifts.

# MATERIALS AND METHODS

## Subjects

Twenty healthy volunteers (10 males), aged between 20 and 26 years, participated in this study after providing written informed consent and receiving monetary compensation for their

participation. All participants had normal bilateral peripheral hearing (pure tone average thresholds <15 dB HL) and normal middle ear function at the time of testing. None of them had a history of neurological, endocrinal, and/or psychiatric disorders; no subjects were taking any medication at the time of testing. This study was approved by the ethics committee at National Yang-Ming University and conducted in accordance with the Declaration of Helsinki.

## Auditory Stimuli

Three emotional syllables were used to elicit auditory ERPs. A female speaker from a performing arts school produced meaningless syllables "dada" with three sets of emotional (happy, angry, and neutral) prosodies (Cheng et al., 2012; Hung et al., 2013; Chen et al., 2014). Compared to fearful prosody, angry prosody showed more similarity in physical attribute with happy prosody (**Supplementary Figure 3**). On the other hand, both anger and happiness are approach-related affects, whereas fear reflects the opposing direction of motivational engagement (withdrawal or avoidance). Therefore, we selected happy voices to stand for the positive emotion and angry voices for the negative one. Emotional syllables were edited to become equally long (550-ms) and loud (min: 57 dB; max: 62 dB; mean 59 dB) using Cool Edit Pro 2.0 and Sound Forge 9.0 (**Figure 1**). Each syllable set was rated for emotionality on a 5-point Likert-scale by a total of 120 listeners (60 men). For the angry set, listeners classified each angry prosody on a scale of extremely angry to not angry at all. For the happy set, listeners classified each happy prosodies on a scale of extremely happy to not happy at all. For the neutral set, listeners classified the neutral prosodies on a scale of extremely emotional to not emotional at all. Emotional syllables that were consistently identified as extremely angry and extremely happy (i.e., the highest ratings), as well as the most emotionally neutral (i.e., the lowest rating), were used as the stimuli. The Likert-scale (mean ± SD) of happy, angry, and neutral syllables were 4.34 ± 0.65, 4.26 ± 0.85, and 2.47 ± 0.87, respectively. Neutral syllables were employed as standard (S), and happy and angry syllables designed as two isometric deviants (D1 and D2) followed the oddball paradigm. Each session consisted of 800 standards, 100 D1 s, and 100 D2 s. A minimum of two standards was presented between any two deviants. The successive deviants were always diverse. The stimulus onset asynchrony was 1200 ms.

## Procedures

The experiment consisted of four sessions. The first two sessions were recorded in the mid-morning (10:30 AM) and mid-afternoon (15:30 PM) to examine the test–retest reliability of emotional MMN at different times of the day. Then, two weeks later, the same two sessions were recorded again to examine the test–retest reliability of emotional MMN on different days. The procedures and the order of the experiments were identical on the two different days. Half of the participants ($n$ = 10, 5 males) were asked to evaluate the position of a visual stimulus; then, they were asked to compare the position of an undergoing stimulus with that of the previous two trials (*2*-back), and during all these sessions, the auditory ERPs to irrelevant emotionally spoken syllables "dada" were being recorded. The other half of the subjects ($n$ = 10, 5 males) watched a silent movie without paying attention to the sounds during the passive auditory oddball paradigm. The factor of attention on emotional MMN was employed by manipulating the task load on irrelevant working memory processing (*2*-back).

## *2*-Back Working Memory Task

The software for the *2*-back task, developed by Paul Hoskinson, comes from an online website (Brain Workshop[1]). In every trial, each blue square was displayed in a 3 × 3 matrix and the stimulus onset asynchrony was varied (max: 3 s). During the *2*-back task, participants were requested to decide whether the undergoing stimulus was at the same location as the stimulus of the previous two trials by pressing the "A" button on a keyboard. The subjects were able to practice the *2*-back task, immediately before the EEG recording, in order to get familiar with it beforehand.

## Electroencephalogram Apparatus and Recording

The EEG experiment was conducted in a sound-attenuated, dimly lit and electrically shielded room. Stimuli were presented binaurally via two loudspeakers placed at approximately 30 cm on the right and left sides of the subject's head. The sound-pressure level (SPL) peaks of different types of stimuli were equalized to eliminate the effect of the substantially greater energy of the angry stimuli. The mean background noise level was around 35 dB SPL. The EEG was continuously recorded from 32 scalp sites using electrodes mounted on an elastic cap and positioned according to the modified International 10–20 system, with the addition of two mastoid electrodes. The electrode at the right mastoid (A2) was used as an online reference. Eye blinks and vertical eye movements were monitored with electrodes located above and below the left eye. The horizontal electrooculogram (EOG) was recorded from electrodes placed laterally 1.5 cm to the left and right external canthi. A ground electrode was placed on the forehead. Electrode/skin impedance was kept to < 5 kΩ. Channels were re-referenced off-line to the average of the left and right mastoid recordings [(A1 + A2)/2]. Signals were sampled at 500 Hz, band-pass filtered at 0.1–100 Hz, and epoched over an analysis time of 600 ms, including the prestimulus time of 100 ms used for baseline correction. An automatic artifact rejection system excluded from the average of all trials containing transients exceeding ± 70 μV at recording electrodes and ± 100 μV at the horizontal EOG channel. Furthermore, the quality of ERP traces was ensured by careful visual inspection in every subject and trial by applying appropriate digital, zero-phase shift band-pass filters (0.1–50 Hz, 24 dB/octave). Gratton-Coles ocular artifact correction was performed on the EEG data to identify and correct ocular movements, with seeded off electrode Fp1 (Gratton et al., 1983). The first ten epochs of each sequence were omitted from the averaging in order to exclude unexpected large responses elicited by the initiation of the sequences.

[1] http://brainworkshop.sourceforge.net/

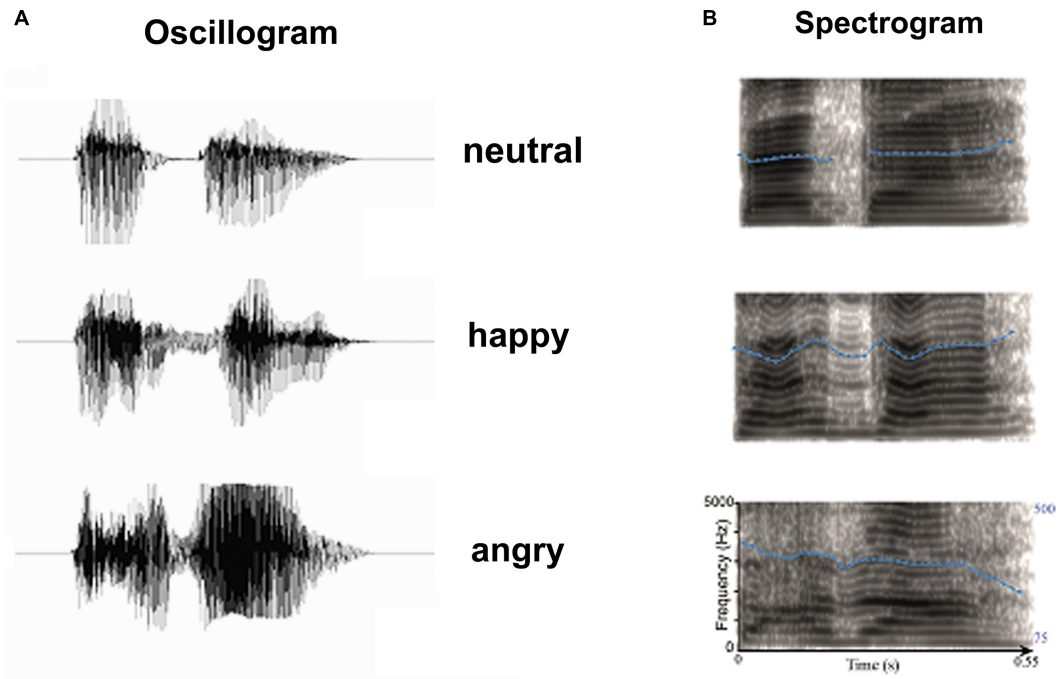


**FIGURE 1 |** Acoustic properties of stimulus materials: **(A)** Oscillogram and **(B)** Spectrogram of auditory stimulus. Blue dot lines in the spectrum denote the flow of fundamental frequency at each time point, which represents the pitch flow of emotional syllables.

## Data Analysis

The amplitudes of emotional MMN were analyzed as an average within a 50-ms time window surrounding the peak latency at the electrode sites F3, Fz, F4, C3, Cz, and C4. The MMN peak was defined as the largest negativity in the subtraction between the deviant and standard ERPs, during a period of 150–250 ms after sound onset. Only the standards presented before the deviants were included in the analysis. To avoid the order effect that might carry over within a short range of interval in the same day, statistical analyses on emotional MMN were conducted separately for morning and afternoon period, using a four-way analysis of variance (ANOVA) comprising the group factor Attention (silent movie vs. *2*-back), and the repeated-measures factors Deviant Type (angry vs. happy), Session (day 1 vs. day 2), and Electrode (F3, Fz, F4, C3, Cz, and C4). The dependent variables were the mean amplitudes and peak latencies of the MMN at the selected electrode sites. Degrees of freedom were corrected using the Greenhouse-Geisser method. The *post hoc* comparison was conducted only when preceded by significant main effects. Statistical power (1 – β) was estimated by G*Power 3.1 software (Faul et al., 2009).

Test–retest reliability was calculated and estimated by the values of the ICC (Shrout and Fleiss, 1979). The ICC could assess the degree of relative consistency among various measures across different sessions. It was calculated as the ratio between the between-subject variance and the total variance across all measures and participants. Unlike Pearson's correlation coefficient, which measures the strength of the linear association between two measures, the ICC takes into account the variability of the total sample and reflects the agreement of the measures obtained across sessions. An ICC value of 1 indicates perfect within-subject reliability, whereas an ICC of 0 indicates no reliability. The ICC was assessed for both amplitude and latency signals between different days and circadian sessions. Step-down Holm–Bonferroni correction was used to control the familywise error to counteract the problem of multiple comparisons in all reported results (both the main manuscript and the supporting materials).

# RESULTS

## MMN Amplitude and Peak Latency

In general, morphology and amplitudes of the grand average curves are quite similar in the morning and afternoon periods of day 1 and day 2. This was confirmed by the statistical analysis conducted on MMN amplitudes (**Figures 2, 3** and **Supplementary Figures 1**, **2**). In the morning period, none of the Session effect was found either as a main effect [$F(1,18) = 1.88$, $p = 0.19$, $\eta^2 = 0.094$, (1-β) = 13%] or when interacting with other variables (all $p > 0.2$). This was also true for the afternoon period [main effect of Session: $F(1,18) = 1.13$, $p = 0.3$, $\eta^2 = 0.059$, (1-β) = 6%; interactions between Session and other variables: all $p > 0.2$]. Both morning and afternoon periods showed main effects of the Deviant Type [morning: $F(1,18) = 30.44$, $p < 0.001$, $\eta^2 = 0.628$, (1-β) = 96%; afternoon: $F(1,18) = 46.4$, $p < 0.001$, $\eta^2 = 0.72$, (1-β) = 99%] and the Electrode [morning: $F(5,90) = 4.48$, $p = 0.01$, $\eta^2 = 0.199$, (1-β) = 33%; afternoon:

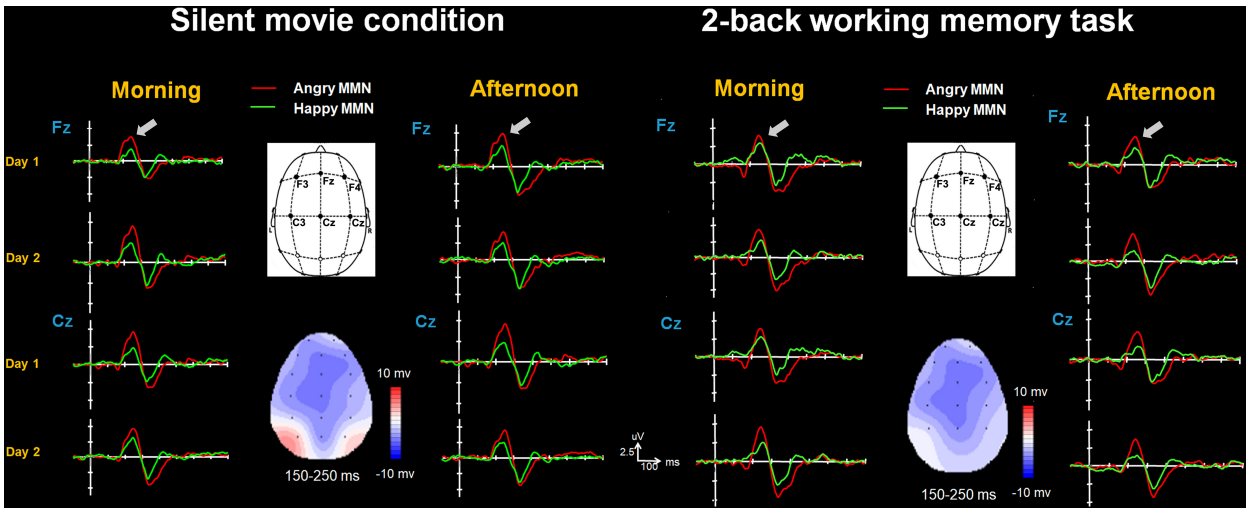


**FIGURE 2 |** The happy MMN (green lines) and angry MMN (red lines) recorded from F3 to C4 electrodes, averaged across all subjects when watching the silent movie and performing the *2*-back working memory task. The gray arrows indicate the time window of MMN.

$F(5,90) = 2.83$, $p = 0.02$, $\eta^2 = 0.136$, $(1\text{-}\beta) = 16\%$]. Angry MMN (morning: 3.99 ± 0.28; afternoon: 3.39 ± 0.25) was significantly stronger than happy MMN (morning: 2.35 ± 0.16; afternoon: 1.82 ± 0.18) irrespective of the session or the attention. The MMN had the strongest amplitudes at electrode Fz (morning: 3.49 ± 0.22, afternoon: 2.77 ± 0.26) and Cz (morning: 3.43 ± 0.19, afternoon: 2.74 ± 0.18) as compared to F3 (morning: 2.97 ± 0.25, afternoon: 2.52 ± 0.22), F4 (morning: 3.18 ± 0.21, afternoon: 2.74 ± 0.22), C3 (morning: 2.98 ± 0.18, afternoon: 2.43 ± 0.17), or C4 (morning: 2.97 ± 0.17, afternoon: 2.44 ± 0.16) irrespective of the session or the attention [Fz vs. F3: mean difference −0.387, $p < 0.001$; Fz vs. C3: mean difference −0.426, $p = 0.021$; Fz vs. C4: mean difference −0.427, $p = 0.001$; Cz vs. F3: mean difference −0.339, $p = 0.015$; Cz vs. C3: mean difference −0.378, $p = 0.001$; Cz vs. C4: mean difference −0.379, $p < 0.001$]. Attention did not affect emotional MMN amplitudes, as shown by testing the group factor and its interaction with the repeated measures of Session, Deviant Type, and Electrodes factors. Neither a main effect was found [morning: $F(1,18) = 0.4$, $p = 0.54$, $\eta^2 = 0.022$, $(1\text{-}\beta) = 5\%$; afternoon: $F(1,18) = 0.5$, $p = 0.49$, $\eta^2 = 0.027$, $(1\text{-}\beta) = 5\%$] nor was there any significant interaction [Attention × Session/morning: $F(1,18) = 0.22$, $p = 0.65$, $\eta^2 = 0.012$, $(1\text{-}\beta) = 5\%$; Attention × Session/afternoon: $F(1,18) = 1.19$, $p = 0.29$, $\eta^2 = 0.062$, $(1\text{-}\beta) = 6\%$; Attention × Deviant Type/morning: $F(1,18) = 0.7$, $p = 0.41$, $\eta^2 = 0.037$, $(1\text{-}\beta) = 5\%$; afternoon: $F(1,18) = 1.59$, $p = 0.22$, $\eta^2 = 0.081$, $(1\text{-}\beta) = 7\%$; Attention × Session × Deviant Type × Electrode/morning: $F(5,90) = 1.61$, $p = 0.22$, $\eta^2 = 0.082$, $(1\text{-}\beta) = 13\%$; Attention × Session × Deviant Type × Electrode/afternoon: $F(5,90) = 1.22$, $p = 0.31$, $\eta^2 = 0.063$, $(1\text{-}\beta) = 9\%$].

The repeated-measures ANOVA conducted on the MMN peak latencies also revealed that none of Session effect was found either as a main effect [morning: $F(1,18) = 1.55$, $p = 0.23$, $\eta^2 = 0.079$, $(1\text{-}\beta) = 10\%$; afternoon: $F(1,18) = 1.86$, $p = 0.19$, $\eta^2 = 0.094$, $(1\text{-}\beta) = 13\%$] or interacting with other variables (all $p > 0.3$). Attention did not affect the emotional MMN peak latencies, as shown by testing the group factor and its interaction with the Session, Deviant Type, and Electrodes factors. Neither a main effect was not found [morning: $F(1,18) = 2.27$, $p = 0.15$, $\eta^2 = 0.112$, $(1\text{-}\beta) = 9\%$; afternoon: $F(1,18) = 2.41$, $p = 0.14$, $\eta^2 = 0.118$, $(1\text{-}\beta) = 9\%$] nor was there any significant interaction [Attention × Session/morning: $F(1,18) = 0.94$, $p = 0.35$, $\eta^2 = 0.049$, $(1\text{-}\beta) = 6\%$; Attention × Session/afternoon: $F(1,18) = 0.03$, $p = 0.86$, $\eta^2 = 0.002$, $(1\text{-}\beta) = 5\%$; Attention × Deviant Type/morning: $F(1,18) = 0.005$, $p = 0.94$, $\eta^2 < 0.001$, $(1\text{-}\beta) < 5\%$; Attention × Deviant Type/afternoon: $F(1,18) = 0.005$, $p = 0.94$, $\eta^2 < 0.001$, $(1\text{-}\beta) < 5\%$; Attention × Session × Deviant Type × Electrode/morning: $F(5,90) = 0.56$, $p = 0.73$, $\eta^2 = 0.03$, $(1\text{-}\beta) = 6\%$; Attention × Session × Deviant Type × Electrode/afternoon: $F(5,90) = 0.43$, $p = 0.69$, $\eta^2 = 0.023$, $(1\text{-}\beta) = 6\%$].

## Test–Retest Reliability

The ICC for angry MMN amplitudes were robust on different days and at different times of a day (Circadian: morning vs. afternoon) during the silent movie condition (Day: ICC = 0.71, $p = 0.004$; Circadian: ICC = 0.674, $p = 0.01$) (**Figure 3A** and **Table 1**). In the *2*-back working memory condition, the ICC for angry MMN amplitudes showed moderate reliability on different days and at different times of a day (Day: ICC = 0.449, $p = 0.097$; Circadian: ICC = 0.575, $p = 0.038$) (**Figure 3B** and **Table 1**). The ICC indicated overall strong values for the angry MMN peak latencies, both in the silent movie (Day: ICC = 0.792, $p < 0.001$; Circadian: ICC = 0.908, $p < 0.001$) and *2*-back conditions (Day: ICC = 0.85, $p < 0.001$;

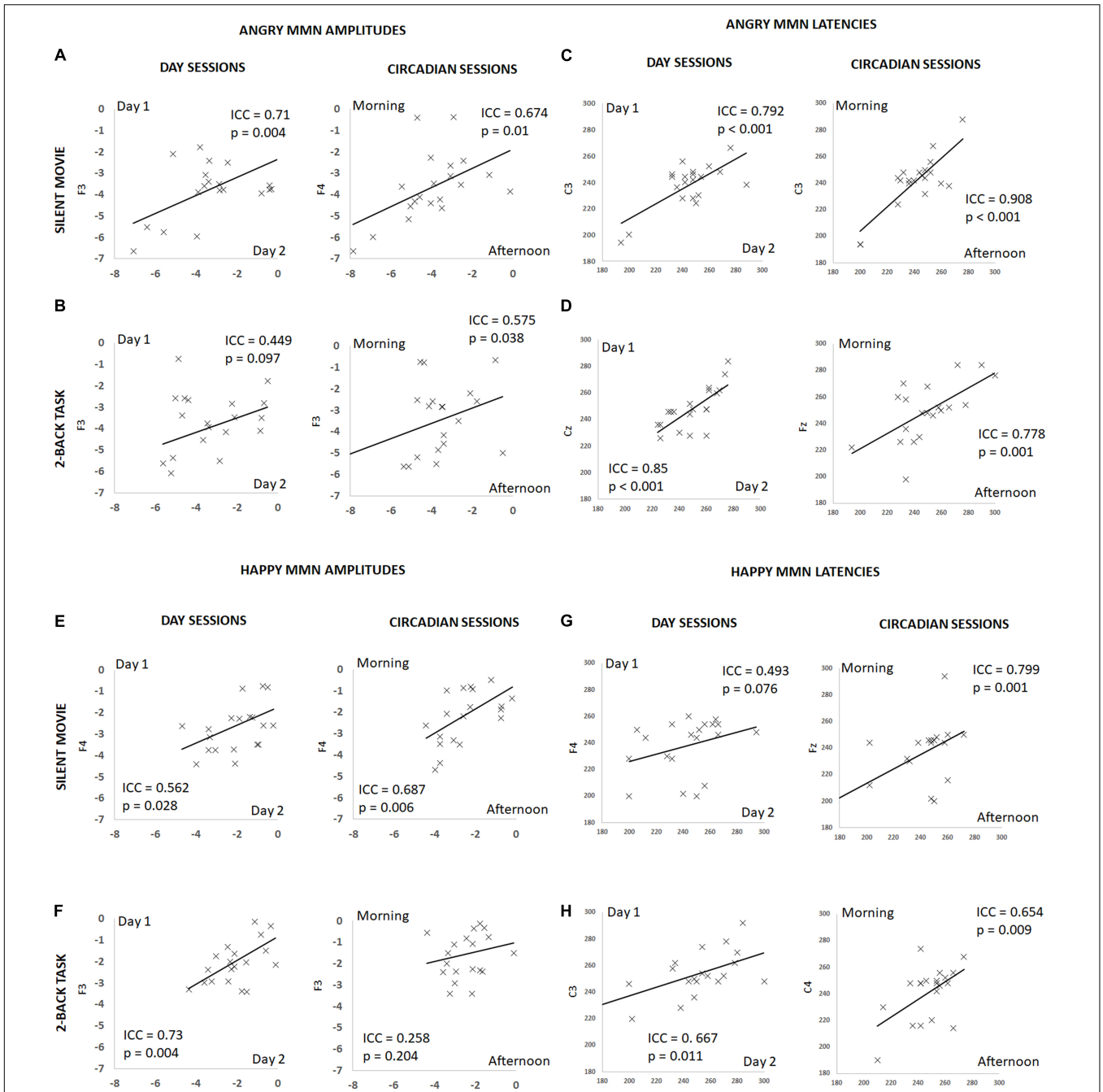


**FIGURE 3 |** Summary of individual estimates for intraclass correlation coefficient (ICC) in amplitude and latency, for angry and happy MMN, on different days and at different times of a day, during the silent movie and *2*-back working memory task conditions. *X*-axis denotes individual values in day 2 or afternoon session and *Y*-axis in day 1 or morning session. Plots show test–retest angry MMN amplitudes in the silent movie condition **(A)** and in the *2*-back condition **(B)**, test–retest angry MMN peak latencies in the silent movie condition **(C)** and in the *2*-back condition **(D)**, test–retest happy MMN amplitudes in the silent movie condition **(E)** and in the *2*-back condition **(F)**, and test–retest happy MMN peak latencies in the silent movie condition **(G)** and in the *2*-back condition **(H)**.

Circadian: ICC = 0.778, $p$ = 0.001) (**Figures 3C,D** and **Table 1**).

Similarly, the ICC values for happy MMN amplitudes indicated fair to good reliability on different days and at different times of a day during the silent movie condition (Day: ICC = 0.562, $p$ = 0.028; Circadian: ICC = 0.687, $p$ = 0.006) (**Figure 3E** and **Table 1**). The ICC for happy MMN amplitudes in the *2*-back condition evidenced a good reliability on different days, but a weak reliability at different times of a day (Day: ICC = 0.73, $p$ = 0.004; Circadian: ICC = 0.258, $p$ = 0.204) (**Figure 3F** and **Table 1**). Happy MMN peak latencies obtained during silent movie (Day: ICC = 0.493, $p$ = 0.076; Circadian:

ICC = 0.799, $p = 0.001$) and 2-back conditions (Day: ICC = 0.667; $p = 0.011$; Circadian: ICC = 0.654, $p = 0.009$) showed less robust ICC values when compared to its values for angry MMN peak latencies (**Figures 3G,H** and **Table 1**).

Fisher r-to-z transformation was conducted on the highest ICC values of each category to examine whether there were significant ICC differences between amplitudes and latencies, *2*-back memory tasks and silent movie condition, as well as happy and angry emotion. The ICC of angry MMN was higher than that of happy MMN in both the silent movie (Day: ICC angry MMN latency = 0.792 vs. ICC happy MMN latency = 0.075, $p = 0.004$; Circadian: ICC angry MMN latency = 0.908 vs. ICC happy MMN latency = 0.661, $p = 0.04$) and the working memory condition (Day: ICC angry MMN latency = 0.85 vs. ICC happy MMN latency = −0.075, $p < 0.001$). The ICC for latency was higher than the ICC for amplitude in both happy (Circadian: ICC amplitude = 0.39 vs. ICC latency = 0.799, $p = 0.046$) and angry MMN (Day: ICC amplitude = 0.156 vs. ICC latency = 0.85, $p = 0.001$; Circadian: ICC amplitude = 0.332 vs. ICC latency = 0.908, $p < 0.001$). The ICC in the silent movie condition was found to be higher than that of in the working memory condition (Happy MMN amplitudes: ICC movie = 0.687 vs. ICC memory = 0.032, $p = 0.018$).

## DISCUSSION

In this study, we investigated the test–retest reliability of emotional MMN that was elicited by vocal emotional expressions. The results demonstrated that both deviants of positively (happily)- and negatively (angrily)-spoken syllables when compared with neutral standards could reliably trigger MMN in response to emotional salience processing. Specifically, the neurophysiological estimates of MMN to both angry and happy deviants appeared to be highly reproducible, irrespective of whether a passive auditory oddball paradigm was incorporated during the silent

**TABLE 1 |** Test–retest intraclass correlation coefficients (ICC) for emotional MMN amplitudes and latencies, separately for angry- and happy-syllable deviants, in each group watching the silent movie ($n = 10$) or performing the *2*-back working memory task ($n = 10$), on different days (day 1 vs. day 2) and at different times of the day (Circadian: morning vs. afternoon).

| Electrode | Happy MMN amplitude | | Angry MMN amplitude | |
|---|---|---|---|---|
| | Day | Circadian | Day | Circadian |
| Silent movie | | | | |
| F3 | 0.465 | 0.56 | 0.71** | 0.397 |
| Fz | 0.34 | 0.39 | 0.216 | −0.343 |
| F4 | 0.562 | 0.687** | 0.57 | 0.674** |
| C3 | 0.163 | 0.058 | 0.591 | 0.332 |
| Cz | 0.444 | 0.191 | 0.554 | 0.319 |
| C4 | 0.452 | 0.573 | 0.321 | 0.358 |
| *2*-back working memory task | | | | |
| F3 | 0.73** | 0.258 | 0.449 | 0.575 |
| Fz | 0.421 | 0.101 | 0.268 | 0.555 |
| F4 | 0.565 | 0.032 | 0.06 | 0.543 |
| C3 | 0.62 | 0.178 | 0.375 | 0.418 |
| Cz | 0.377 | −0.028 | 0.156 | 0.484 |
| C4 | 0.512 | 0.091 | 0.152 | 0.326 |
| | **Happy MMN peak latency** | | **Angry MMN peak latency** | |
| Silent movie | | | | |
| F3 | 0.477 | 0.762*** | 0.649* | 0.448 |
| Fz | 0.41 | 0.799*** | 0.29 | 0.394 |
| F4 | 0.493 | 0.257 | 0.722** | 0.798*** |
| C3 | 0.075 | 0.661** | 0.792*** | 0.908*** |
| Cz | 0.311 | 0.337 | 0.712** | 0.795*** |
| C4 | 0.458 | 0.214 | 0.705** | 0.689** |
| *2*-back working memory | | | | |
| F3 | 0.483 | 0.499 | 0.593 | 0.645* |
| Fz | 0.558 | 0.594 | 0.768*** | 0.778*** |
| F4 | 0.272 | 0.458 | 0.697** | 0.751** |
| C3 | 0.667 | 0.638 | 0.47 | 0.726** |
| Cz | −0.075 | 0.424 | 0.85*** | 0.594 |
| C4 | 0.534 | 0.654 | 0.255 | 0.556 |

*$P < 0.05$; **$P < 0.01$; ***$P < 0.001$; corrected for multiple comparisons.*

movie observation or a working memory performance task (**Table 1**).

Emotional MMN amplitudes and latencies were neither significantly affected by the different sessions (day 1 vs. day 2) and the attentional loadings (silent movie vs. *2*-back task) nor by any other significant interactions between these two variables in both morning and afternoon sessions, respectively. In accordance with our previous findings, angry MMN elicited stronger amplitudes than happy MMN (Fan et al., 2013; Fan and Cheng, 2014; Chen et al., 2016a). Angry MMN, rather than neutral or non-vocal MMN amplitudes, was associated with the severity of autistic traits, indicating atypical emotional voice processing at the early automatic stage (Fan and Cheng, 2014). Higher state anxiety and ensuing heart rate acceleration was also found to be associated with larger angry MMN amplitudes but not neutral MMN amplitudes (Schirmer and Escoffier, 2010). Acute testosterone administration modulated neural dynamics of voice perception and emotional MMN, but not of non-vocal MMN, indicating the role o neural dynamics on modulating pre-attentive sensory processing and involuntary attention switches in response to emotional voices (Chen et al., 2015). Taken together, voice- and emotion-dependent modulation specifically found in vocal MMN, rather than non-vocal MMN, is difficult to synthesize with bottom-up neural adaptation or oscillatory rebound accounts (May and Tiitinen, 2010). Thus, it may instead support the involvement of predictive top-down mechanisms and memory-based model-adjustment hypothesis (Naatanen et al., 2005; Garrido et al., 2008; Wacongne et al., 2012; Lieder et al., 2013). With a five-way ANOVA comprising the group factor Attention (silent movie vs. 2-back), and the repeated-measures factors Deviant Type (angry vs. happy), Session (day 1 vs. day 2), Electrode (F3, Fz, F4, C3, Cz, and C4), and an additional variable of Time (morning vs. afternoon), we identified a main effect of Time besides the effect uncovered in the main text (**Supplementary Results**). The MMN had larger amplitudes in the morning ($3.17 \pm 0.177$) compared to afternoon session ($2.62 \pm 0.18$) as a manifesto of practice/order effect in which the subjects do exactly the same tasks within hours.

Angry MMN amplitudes and latencies showed robust ICC test–retest reliability, whereas happy MMN amplitudes and latencies showed fair to good ICC values, over day and circadian sessions during the silent movie condition. Negative emotionality, which has a greater effect on one's psychological state and processes than neutral or positive ones, have been reported and largely converged with factors previously shown to impact the processing of emotional facial expressions, unpleasant thoughts, or social interactions, suggesting a modality-independent impact of negativity bias (Kanouse and Hanson, 1972; Baumeister et al., 2001; Rozin and Royzman, 2001; Young et al., 2017). Threatening voices, such as angry vocalizations that could consistently trigger an alert response across different environmental conditions, served as the origin for evolving a specialized signal processing that facilitates survival.

During the silent movie condition, the ICC for both angry and happy MMN amplitudes indicated robust and fair reliabilities on different days and at different times of a day. However, during the *2*-back working memory task condition, the ICC values showed moderate reliabilities for angry MMN amplitudes and weak reliabilities for happy MMN amplitudes (**Figure 3B** and **Table 1**). Emotional processing is closely intertwined with the attention control system, such that emotionally salient and threatening stimuli will automatically capture attention (Taylor and Fragopanagos, 2005; Carlson et al., 2009; Yamaguchi and Onoda, 2012). Meanwhile, diverting attention is also found to suppress emotional influences in human amygdala responses (Morawetz et al., 2010; Pourtois et al., 2013). While the neural processing of emotional voices, beyond low-level acoustic features, recruits a processing chain that proceeds from the auditory pathway to brain structures implicated in social cognition, the heavy demand for cognitive resources and high load of task-irrelevant streams result in reduced emotional MMN amplitudes during the *2*-back working memory task (Schirmer and Kotz, 2006; Fan et al., 2013). Given that we have neither found a significant main effect nor any other interaction of attention, the high load of cognitive demand does not affect emotional MMN amplitudes in this cohort. The neural response to emotional salience that varied with high competition between automatic emotional processing and task-irrelevant loading may possibly manifest the fact that emotional MMN is sensitive and prone to capture the subtle individual differences in trait anxiety, as well as current emotional states, where present anxiety shifts from current vigilance to threatening signals and overcomes the competition of cognitive resources (Schirmer and Escoffier, 2010; Chen et al., 2015, 2017). Despite the fact that we did not find significant differences in emotional MMN during the *2*-back working memory task and the silent movie conditions, the limitation of the small group size and the variance in attentional load (e.g., n-back) should be taken into account (Fan et al., 2013). Future studies to examine task difficulty and test–retest reliability of (emotional) MMN are warranted.

Notably, when extremely high anxiety was deliberately induced by an unpredictable electrical shock, the enlarged pure-tone-MMNm was found to reflect an anxious hypervigilance state. Importantly, this heightened neurophysiological index of anxious hypervigilance could be reversed by an inhibitory gamma-aminobutyric acidergic action with alprazolam (Cornwell et al., 2017). Given the fact that voice processing the sounds of kin species has its unique phylogenetic and ontogenetic significance, an oddball paradigm deployed with emotional voices offers a platform to detect the subtle changes in current emotional shifts (Belin et al., 2000; Belin and Grosbras, 2010; Schirmer and Escoffier, 2010).

Our findings suggest that emotional MMN responses could be reliably obtained in conditions without task demands. However, whether the variation of test–retest emotional MMN in the individual level reflects a moment-to-moment emotional state shift remains as an important and promising inquiry. Our study underscores and sheds light on the need to take into account the instant, current emotional state at the individual level while trying to utilize MMN as a biomarker for diagnosis and translational medicine.

## AUTHOR CONTRIBUTIONS

YC designed the study. CC and C-WC organized the database and performed the statistical analysis. CC wrote the first draft of the manuscript. CC, C-WC, and YC wrote sections of the manuscript. All authors contributed to manuscript revision, read, and approved the submitted version.

## FUNDING

The study was funded by the Ministry of Science and Technology (MOST 106-2420-H-010-004-MY2, 106-2410-H-010-002-MY2, and 107-2314-B-038-012), National Yang-Ming University Hospital (RD2017-005), Taipei Medical University (TMU106-AE1-B32 and DP2-107-21121-01-N-03), and the Brain Research Center from The Featured Areas Research Center Program within the framework of the Higher Education Sprout Project by the Ministry of Education (MOE) in Taiwan.

## ACKNOWLEDGMENTS

We thank Pin-Chia Huang for assisting with data collection.

## SUPPLEMENTARY MATERIAL

The Supplementary Material for this article can be found online at: https://www.frontiersin.org/articles/10.3389/fnhum.2018.00453/full#supplementary-material

## REFERENCES

Baumeister, R. F., Finkenauer, C., and Vohs, K. D. (2001). Bad is stronger than good. *Rev. Gen. Psychol.* 5, 323–370. doi: 10.1037/1089-2680.5.4.323

Belin, P., and Grosbras, M. H. (2010). Before speech: cerebral voice processing in infants. *Neuron* 65, 733–735. doi: 10.1016/j.neuron.2010.03.018

Belin, P., Zatorre, R. J., Lafaille, P., Ahad, P., and Pike, B. (2000). Voice-selective areas in human auditory cortex. *Nature* 403, 309–312. doi: 10.1038/35002078

Carlson, J. M., Reinke, K. S., and Habib, R. (2009). A left amygdala mediated network for rapid orienting to masked fearful faces. *Neuropsychologia* 47, 1386–1389. doi: 10.1016/j.neuropsychologia.2009.01.026

Chen, C., Chen, C. Y., Yang, C. Y., Lin, C. H., and Cheng, Y. (2015). Testosterone modulates preattentive sensory processing and involuntary attention switches to emotional voices. *J. Neurophysiol.* 113, 1842–1849. doi: 10.1152/jn.00587.2014

Chen, C., Hu, C. H., and Cheng, Y. (2017). Mismatch negativity (MMN) stands at the crossroads between explicit and implicit emotional processing. *Hum. Brain Mapp.* 38, 140–150. doi: 10.1002/hbm.23349

Chen, C., Lee, Y. H., and Cheng, Y. (2014). Anterior insular cortex activity to emotional salience of voices in a passive oddball paradigm. *Front. Hum. Neurosci.* 8:743. doi: 10.3389/fnhum.2014.00743

Chen, C., Liu, C. C., Weng, P. Y., and Cheng, Y. (2016a). Mismatch negativity to threatening voices associated with positive symptoms in schizophrenia. *Front. Hum. Neurosci.* 10:362. doi: 10.3389/fnhum.2016.00362

Chen, C., Sung, J. Y., and Cheng, Y. (2016b). Neural dynamics of emotional salience processing in response to voices during the stages of sleep. *Front. Behav. Neurosci.* 10:117. doi: 10.3389/fnbeh.2016.00117

Cheng, Y., Lee, S. Y., Chen, H. Y., Wang, P. Y., and Decety, J. (2012). Voice and emotion processing in the human neonatal brain. *J. Cogn. Neurosci.* 24, 1411–1419. doi: 10.1162/jocn_a_00214

Cornwell, B. R., Garrido, M. I., Overstreet, C., Pine, D. S., and Grillon, C. (2017). The unpredictive brain under threat: a neurocomputational account of anxious hypervigilance. *Biol. Psychiatry* 82, 447–454. doi: 10.1016/j.biopsych.2017.06.031

Doeller, C. F., Opitz, B., Mecklinger, A., Krick, C., Reith, W., and Schroger, E. (2003). Prefrontal cortex involvement in preattentive auditory deviance detection: neuroimaging and electrophysiological evidence. *Neuroimage* 20, 1270–1282. doi: 10.1016/S1053-8119(03)00389-6

Fan, Y. T., and Cheng, Y. (2014). Atypical mismatch negativity in response to emotional voices in people with autism spectrum conditions. *PLoS One* 9:e102471. doi: 10.1371/journal.pone.0102471

Fan, Y. T., Hsu, Y. Y., and Cheng, Y. (2013). Sex matters: n-back modulates emotional mismatch negativity. *Neuroreport* 24, 457–463. doi: 10.1097/WNR.0b013e32836169b9

Faul, F., Erdfelder, E., Buchner, A., Lang, A. G. (2009). Statistical power analyses using G*Power 3.1: tests for correlation and regression analyses. *Behav. Res. Methods* 41, 1149–1160. doi: 10.3758/BRM.41.4.1149

Frodl-Bauch, T., Kathmann, N., Moller, H. J., and Hegerl, U. (1997). Dipole localization and test-retest reliability of frequency and duration mismatch negativity generator processes. *Brain Topogr.* 10, 3–8. doi: 10.1023/A:1022214905452

Garrido, M. I., Friston, K. J., Kiebel, S. J., Stephan, K. E., Baldeweg, T., and Kilner, J. M. (2008). The functional anatomy of the MMN: a DCM study of the roving paradigm. *Neuroimage* 42, 936–944. doi: 10.1016/j.neuroimage.2008.05.018

Gratton, G., Coles, M. G. H., and Donchin, E. (1983). A new method for off-line removal of ocular artifact. *Electroencephalogr. Clin. Neurophysiol.* 55, 468–484. doi: 10.1016/0013-4694(83)90135-9

Hall, M. H., Schulze, K., Rijsdijk, F., Picchioni, M., Ettinger, U., Bramon, E., et al. (2006). Heritability and reliability of P300, P50 and duration mismatch negativity. *Behav. Genet.* 36, 845–857. doi: 10.1007/s10519-006-9091-6

Hung, A. Y., Ahveninen, J., and Cheng, Y. (2013). Atypical mismatch negativity to distressful voices associated with conduct disorder symptoms. *J. Child Psychol. Psychiatry* 54, 1016–1027. doi: 10.1111/jcpp.12076

Hung, A. Y., and Cheng, Y. (2014). Sex differences in preattentive perception of emotional voices and acoustic attributes. *Neuroreport* 25, 464–469. doi: 10.1097/WNR.0000000000000115

Kanouse, D. E., and Hanson, L. (1972). *Negativity in Evaluations*. Morristown, NJ: General Learning Press.

Kathmann, N., Frodl-Bauch, T., and Hegerl, U. (1999). Stability of the mismatch negativity under different stimulus and attention conditions. *Clin. Neurophysiol.* 110, 317–323. doi: 10.1016/S1388-2457(98)00011-X

Lieder, F., Stephan, K. E., Daunizeau, J., Garrido, M. I., and Friston, K. J. (2013). A neurocomputational model of the mismatch negativity. *PLoS Comput. Biol.* 9:e1003288. doi: 10.1371/journal.pcbi.1003288

Light, G. A., and Braff, D. L. (2005). Stability of mismatch negativity deficits and their relationship to functional impairments in chronic schizophrenia. *Am. J. Psychiatry* 162, 1741–1743. doi: 10.1176/appi.ajp.162.9.1741

Light, G. A., Swerdlow, N. R., Rissling, A. J., Radant, A., Sugar, C. A., Sprock, J., et al. (2012). Characterization of neurophysiologic and neurocognitive biomarkers for use in genomic and clinical outcome studies of schizophrenia. *PLoS One* 7:e39434. doi: 10.1371/journal.pone.0039434

May, P. J., and Tiitinen, H. (2010). Mismatch negativity (MMN), the deviance-elicited auditory deflection, explained. *Psychophysiology* 47, 66–122. doi: 10.1111/j.1469-8986.2009.00856.x

Morawetz, C., Baudewig, J., Treue, S., and Dechent, P. (2010). Diverting attention suppresses human amygdala responses to faces. *Front. Hum. Neurosci.* 4:226. doi: 10.3389/fnhum.2010.00226

Naatanen, R., Jacobsen, T., and Winkler, I. (2005). Memory-based or afferent processes in mismatch negativity (MMN): a review of the evidence. *Psychophysiology* 42, 25–32. doi: 10.1111/j.1469-8986.2005.00256.x

Naatanen, R., Kujala, T., Escera, C., Baldeweg, T., Kreegipuu, K., Carlson, S., et al. (2012). The mismatch negativity (MMN)–a unique window to disturbed

central auditory processing in ageing and different clinical conditions. *Clin. Neurophysiol.* 123, 424–458. doi: 10.1016/j.clinph.2011.09.020

Naatanen, R., Paavilainen, P., Rinne, T., and Alho, K. (2007). The mismatch negativity (MMN) in basic research of central auditory processing: a review. *Clin. Neurophysiol.* 118, 2544–2590. doi: 10.1016/j.clinph.2007.04.026

Naatanen, R., Shiga, T., Asano, S., and Yabe, H. (2015). Mismatch negativity (MMN) deficiency: a break-through biomarker in predicting psychosis onset. *Int. J. Psychophysiol.* 95, 338–344. doi: 10.1016/j.ijpsycho.2014.12.012

Naatanen, R., and Winkler, I. (1999). The concept of auditory stimulus representation in cognitive neuroscience. *Psychol. Bull.* 125, 826–859. doi: 10.1037/0033-2909.125.6.826

Pourtois, G., Schettino, A., and Vuilleumier, P. (2013). Brain mechanisms for emotional influences on perception and attention: what is magic and what is not. *Biol. Psychol.* 92, 492–512. doi: 10.1016/j.biopsycho.2012.02.007

Pulvermuller, F., and Shtyrov, Y. (2006). Language outside the focus of attention: the mismatch negativity as a tool for studying higher cognitive processes. *Prog. Neurobiol.* 79, 49–71. doi: 10.1016/j.pneurobio.2006.04.004

Recasens, M., and Uhlhaas, P. J. (2017). Test-retest reliability of the magnetic mismatch negativity response to sound duration and omission deviants. *Neuroimage* 157, 184–195. doi: 10.1016/j.neuroimage.2017.05.064

Rinne, T., Alho, K., Ilmoniemi, R. J., Virtanen, J., and Naatanen, R. (2000). Separate time behaviors of the temporal and frontal mismatch negativity sources. *Neuroimage* 12, 14–19. doi: 10.1006/nimg.2000.0591

Rozin, P., and Royzman, E. B. (2001). Negativity bias, negativity dominance, and contagion. *Pers. Soc. Psychol. Rev.* 5, 296–320. doi: 10.1207/S15327957PSPR0504_2

Schirmer, A., and Escoffier, N. (2010). Emotional MMN: anxiety and heart rate correlate with the ERP signature for auditory change detection. *Clin. Neurophysiol.* 121, 53–59. doi: 10.1016/j.clinph.2009.09.029

Schirmer, A., Escoffier, N., Li, Q. Y., Li, H., Strafford-Wilson, J., and Li, W. I. (2008). What grabs his attention but not hers? Estrogen correlates with neurophysiological measures of vocal change detection. *Psychoneuroendocrinology* 33, 718–727. doi: 10.1016/j.psyneuen.2008.02.010

Schirmer, A., and Kotz, S. A. (2006). Beyond the right hemisphere: brain mechanisms mediating vocal emotional processing. *Trends Cogn. Sci.* 10, 24–30. doi: 10.1016/j.tics.2005.11.009

Schroger, E., Giard, M. H., and Wolff, C. (2000). Auditory distraction: event-related potential and behavioral indices. *Clin. Neurophysiol.* 111, 1450–1460. doi: 10.1016/S1388-2457(00)00337-0

Shrout, P. E., and Fleiss, J. L. (1979). Intraclass correlations: uses in assessing rater reliability. *Psychol. Bull.* 86, 420–428. doi: 10.1037/0033-2909.86.2.420

Taylor, J. G., and Fragopanagos, N. F. (2005). The interaction of attention and emotion. *Neural Netw.* 18, 353–369. doi: 10.1016/j.neunet.2005.03.005

Tervaniemi, M., Lehtokoski, A., Sinkkonen, J., Virtanen, J., Ilmoniemi, R. J., and Naatanen, R. (1999). Test-retest reliability of mismatch negativity for duration, frequency and intensity changes. *Clin. Neurophysiol.* 110, 1388–1393. doi: 10.1016/S1388-2457(99)00108-X

Tervaniemi, M., Sinkkonen, J., Virtanen, J., Kallio, J., Ilmoniemi, R. J., Salonen, O., et al. (2005). Test-retest stability of the magnetic mismatch response (MMNm). *Clin. Neurophysiol.* 116, 1897–1905. doi: 10.1016/j.clinph.2005.03.025

Thonnessen, H., Boers, F., Dammers, J., Chen, Y. H., Norra, C., and Mathiak, K. (2010). Early sensory encoding of affective prosody: neuromagnetic tomography of emotional category changes. *Neuroimage* 50, 250–259. doi: 10.1016/j.neuroimage.2009.11.082

Wacongne, C., Changeux, J. P., and Dehaene, S. (2012). A neuronal model of predictive coding accounting for the mismatch negativity. *J. Neurosci.* 32, 3665–3678. doi: 10.1523/JNEUROSCI.5003-11.2012

Yamaguchi, S., and Onoda, K. (2012). Interaction between emotion and attention systems. *Front. Neurosci.* 6:139. doi: 10.3389/fnins.2012.00139

Young, K. S., Parsons, C. E., LeBeau, R. T., Tabak, B. A., Sewart, A. R., Stein, A., et al. (2017). Sensing emotion in voices: negativity bias and gender differences in a validation study of the Oxford Vocal ('OxVoc') sounds database. *Psychol. Assess.* 29, 967–977. doi: 10.1037/pas0000382

Zhang, D., Liu, Y., Hou, X., Sun, G., Cheng, Y., and Luo, Y. (2014). Discrimination of fearful and angry emotional voices in sleeping human neonates: a study of the mismatch brain responses. *Front. Behav. Neurosci.* 8:422. doi: 10.3389/fnbeh.2014.00422

**Conflict of Interest Statement:** The authors declare that the research was conducted in the absence of any commercial or financial relationships that could be construed as a potential conflict of interest.

frontiers in Human Neuroscience

ORIGINAL RESEARCH
published: 20 November 2018
doi: 10.3389/fnhum.2018.00432

# Effect of Neuromuscular Electrical Stimulation Training on the Finger Extensor Muscles for the Contralateral Corticospinal Tract in Normal Subjects: A Diffusion Tensor Tractography Study

*Sung Ho Jang and You Sung Seo* *

*Department of Physical Medicine and Rehabilitation, College of Medicine, Yeungnam University, Daegu, South Korea*

**Objectives**: Neuromuscular electrical stimulation (NMES) is a popular rehabilitative modality to improve motor function of the extremities and trunk. In this study, we investigated changes of hand function and the contralateral corticospinal tract (CST) with treatment by NMES on the finger extensor muscles for 2 weeks, using serial diffusion tensor tractography (DTT).

**Methods**: Thirteen right handed normal subjects were recruited. Treatment was applied to the left hand (the NMES side), and the right hand was the control side. NMES was applied for 30 min/day, 7 days per week, for 2 weeks. Hand motor function was evaluated twice at pre-NMES and post-NMES training using grip strength (GS), Purdue pegboard test (PPT) and tip pinch. The fractional anisotropy (FA), mean diffusivity (MD) and tract volume (TV) of the CST in both hemispheres were measured using DTT.

**Results**: On the control side, the clinical scores did not differ significantly between pre- and post-NMES training ($p > 0.05$). However, on the NMES side, PPT and tip pinch improved significantly ($p < 0.05$), although GS did not. TV of the right CST increased significantly at post-NMES training ($p < 0.05$) whereas FA and MD did not differ significantly ($p > 0.05$). By contrast, FA, MD and TV on the left CST did not change significantly ($p > 0.05$).

**Conclusion**: We demonstrated facilitation of the contralateral CST with improvement of fine motor activity by 2 weeks of NMES training of peripheral muscles in normal subjects. We think our results can be applied to the normal subjects and patients with brain injury to improve the fine motor function of the hand and facilitate the normal CST or healing of the injured CST.

**Keywords: neuromuscular electrical stimulation, diffusion tensor tractography, corticospinal tract, hand function, finger extensor**

OPEN ACCESS

***Edited by:***
*Delin Sun,*
*Duke University, United States*

***Reviewed by:***
*Dong-Hoon Lee,*
*University of Sydney, Australia*
*Ying Wang,*
*University of Science and Technology of China, China*
*Junling Gao,*
*University of Hong Kong, Hong Kong*

***Correspondence:**
*You Sung Seo*
*yousung1008@hanmail.net*

***Received:*** *31 March 2018*
***Accepted:*** *02 October 2018*
***Published:*** *20 November 2018*

***Citation:***
*Jang SH and Seo YS (2018) Effect of Neuromuscular Electrical Stimulation Training on the Finger Extensor Muscles for the Contralateral Corticospinal Tract in Normal Subjects: A Diffusion Tensor Tractography Study. Front. Hum. Neurosci. 12:432. doi: 10.3389/fnhum.2018.00432*

## INTRODUCTION

Neuromuscular electrical stimulation (NMES), a popular rehabilitative modality, induces contraction of neuromuscular system by applying electrical current (Rushton, 1997; Powell et al., 1999; Chae and Yu, 2000; Daly and Ruff, 2007; Kim et al., 2010; Doucet et al., 2012; Maddocks et al., 2013; de Oliveira Melo et al., 2013). In the field of rehabilitation, NMES has long been used to improve motor function of the muscles of extremities and trunk, and the working mechanisms have been suggested as improvement of muscle strength, decrease of spasticity of antagonist muscles, increased range of motion, improvement of voluntary motor control and recovery of functional movement (Rushton, 1997; Powell et al., 1999; Chae and Yu, 2000; Daly and Ruff, 2007; Kim et al., 2010; Doucet et al., 2012; Maddocks et al., 2013; de Oliveira Melo et al., 2013). Furthermore, several studies have reported that NMES facilitates healing of the corticospinal tract (CST) directly (Han et al., 2003; Mang et al., 2010, 2011; Wei et al., 2013; Chen et al., 2014).

The CST is the most important neural tract for motor function in the human brain, and is associated with voluntary movements of proximal and distal musculature, especially fine motor activity of the hand (York, 1987; Davidoff, 1990; Jang, 2014; Jang et al., 2014b). To improve motor function, it is important to facilitate the CST in both normal subjects and patients with brain injury. Many studies have demonstrated CST healing using repetitive transcranial magnetic stimulation (rTMS), hand-arm bimanual intensive therapy or NMES (Han et al., 2003; Kim et al., 2006; Khedr et al., 2010; Mang et al., 2010, 2011; Wei et al., 2013; Chen et al., 2014; Weinstein et al., 2015; Chang et al., 2016). These studies evaluated their effect using functional magnetic resonance imaging (fMRI) and diffusion tensor imaging (DTI), although these methods have limited precision to evaluate change of the entire CST (Han et al., 2003; Kim et al., 2006; Khedr et al., 2010; Mang et al., 2010, 2011; Wei et al., 2013; Chen et al., 2014; Weinstein et al., 2015; Chang et al., 2016).

DTI has a unique advantage in identification and estimation of subcortical white matter by virtue of their ability to visualize water diffusion characteristics. However, it is difficult to get objective results because the results could be subjective depending on the location of the region of interest (ROI) which is applied by a data analyzer. By contrast, diffusion tensor tractography (DTT) for reconstruction of the neural tracts usually employs a combined ROI method that reconstructs only neural fibers passing more than two ROI areas. The ROI areas and reconstruction conditions for the neural tracts are well-defined for each neural tract (Mori et al., 1999; Wakana et al., 2007; Malykhin et al., 2008; Wang et al., 2012; Lee and Jang, 2015; Brandstack et al., 2016; Jang, 2016). High repeatability and reliability of DTT method for the neural tracts have been demonstrated in many studies (Mori et al., 1999; Wakana et al., 2007; Malykhin et al., 2008; Danielian et al., 2010; Wang et al., 2012; Seo and Jang, 2014; Lee and Jang, 2015; Brandstack et al., 2016; Jang, 2016). Therefore, experienced analyzers can reconstruct the neural tracts without significant inter- and intra-analyzer variation. The main advantage of DTT over DTI is that the entire neural tract can be evaluated in terms of DTT parameters, including fractional anisotropy (FA), mean diffusivity (MD) and tract volume (TV) and configurational analysis. DTT enables three-dimensional reconstruction and estimation of the CST in the human brain (Mori et al., 1999; Yamada et al., 2003; Puig et al., 2010). Therefore, we think that DTT would be more appropriate than fMRI or DTI to detect change of the entire CST. We hypothesized that application of the NMES on the finger extensor muscles could facilitate the contralateral CST that can be evaluated precisely with serial DTTs.

In the current study, we investigated changes of hand function and the contralateral CST with application NMES on the finger extensor muscles for 2 weeks, using serial DTTs.

## MATERIALS AND METHODS

### Subjects

Thirteen right-handed healthy subjects (five males, eight females; 23.23 ± 3.59, range 21–33) were recruited according to the following criteria: (1) no previous history of psychiatric, neurological, or physical illness; (2) no brain lesion on conventional MRI, confirmed by a neuroradiologist; and (3) right handed, confirmed by the Edinburgh Handedness Inventory (Oldfield, 1971). Treatment was applied to the left hand (the NMES side), and the right hand was the control side. All subjects provided written informed consent prior to the start of the study, and the study protocol was approved by the Institutional Review Board of a Yeungnam University hospital.

### Neuromuscular Electrical Stimulation (NMES) Training

NMES was applied through a two-channel electrical simulator (EMGFES 1,000, Cyber Medic, South Korea). Monophasic square wave pulses were used at the rate of 30 Hz with a pulse width of 200 μs, pulsed 3 s on and 2 s off. Square surface stimulation electrodes were used to activate finger extensor muscles of the left hand (fixed to the skin with adhesive gel). The electrodes were positioned with a cathode over the left extensor digitorum communis and an anode on the left forearm near the wrist. The stimulation intensity was adjusted to produce the maximum extension of the finger within the limit that the subject did not feel any discomfort (range of stimulation intensity: 8 ∼ 13 mA; Shin et al., 2008; Jang et al., 2014a). The subjects were given NMES training as follows: 30 min/day, 7 days per week for 2 weeks.

### Clinical Evaluation

Grip strength (GS), Purdue pegboard test (PPT) and tip pinch were used evaluate hand function at pre- and post-NMES training. There are several clinical evaluation tools for these parameters. For GS, the subjects were asked to sit on a chair with their hip joint flexed at 90°, and shoulder joint in a

neutral position, elbow fixed at 90° flexion, forearm in a neutral position, and wrist at 0° to 15° radial deviation. The Jamar dynamometer (Jamar Hydraulic Hand Dynamometer, model-5030J1) was used to evaluate GS. For PPT (Lafayette instruments, model 32020), the subjects were required to place as many pegs as possible in 30-s periods using the right hand and left hand. For tip pinch, the subjects push the tip of index finger and hold the pinch gauge with thumb. A hydraulic pinch gauge measured the force between index finger and thumb, parameters indicate the strength of the two fingers (Tiffin and Asher, 1948; Smith and Benge, 1985; Reddon et al., 1988; Kim et al., 1994; Kong et al., 2014). All of the clinical evaluations were performed three times and average value was calculated.

## Fiber Tracking

Using a six-channel head coil with single-shot echo planar imaging on 1.5 T (Philips Ltd., Best, Netherlands), DTI was acquired at pre- and post-NMES training (2 weeks after pre-NMES-training). For each of the 32 non-collinear diffusion sensitizing gradients, 70 contiguous slices (number of excitations: 1, imaging reduction factor (sensitivity encoding (SENSE) factor): 2, field of view: 240 × 240 $mm^2$, reconstructed to matrix: 192 × 192, acquisition matrix: 96 × 96, parallel echo planar imaging factor: 59, TE: 72 ms, TR: 10, 398 ms, b: 1,000 $s/mm^2$, and a slice thickness of 2.5 mm) were acquired. To analyze the CST, the single-tensor model was used within the DTI task card software (Philips Extended MR Workspace 2.6.3). Each DTI replication was intra-registered to the baseline "b0" images to correct for residual eddy-current image distortions and head motion effect, using a diffusion registration package (Philips Medical Systems). DTI-Studio software (CMRM, Johns Hopkins Medical Institute, Baltimore, MD, USA) was used for reconstruction of the CST. DTI-Studio is one of the most popular and commonly used the program for analysis of DTI data. Furthermore, it has an advantage of applying to the various sources of data and the efficient fiber tracking. In detail, for the fiber tracking, two thresholds (FA and tract turning-angle) was used and tracking is performed from all pixels, in which FA values and turning-angle are higher and lower than thresholds. Fiber tracking was based on the fiber assignment continuous tracking algorithm and a multiple ROIs approach. For reconstruction of the CST, ROI was placed on the upper pons (portion of anterior blue color) on the color map with an axial image. The second ROI was placed on the mid pons (portion of anterior blue color) on the color map with an axial image. The termination criteria used default value FA <0.2, angle <60° (Kunimatsu et al., 2004).

## Statistical Analysis

SPSS software (SPSS Inc. Released 2006. SPSS for Windows, Version 15.0. Chicago) was used for data analysis. The paired *t*-test was used for determination of differences in values of clinical scores and DTT parameters of the subjects between the NMES and control sides. Pearson correlation coefficients were calculated to assess the strength of association between clinical scores (GS, PPT and tip pinch) and DTT parameters of the CST.

**TABLE 1 |** Clinical scores at pre- and post-neuromuscular electrical stimulation training.

| | | Pre-NMES training | Post-NMES training | *p*-value |
|---|---|---|---|---|
| GS | Control | 32.1 ± 8.8 | 32.2 ± 7.6 | 0.127 |
| | NMES | 33.2 ± 9.1 | 33.2 ± 9.7 | 0.387 |
| PPT | Control | 14.8 ± 1.7 | 14.7 ± 1.9 | 0.144 |
| | NMES | 16.3 ± 1.9 | 16.8 ± 1.7 | 0.018* |
| Tip pinch | Control | 3.2 ± 1.5 | 3.2 ± 1.8 | 0.377 |
| | NMES | 3.5 ± 1.3 | 3.8 ± 1.4 | 0.003* |

*NMES, neuromuscular electrical stimulation; GS, grip strength; PPT, Purdue pegboard test. Values mean ± standard deviation. *Significant differences between pre- and post-NMES trainings, p < 0.05.*

Null hypotheses of no difference were rejected if *p*-values were less than 0.05.

# RESULTS

**Table 1** shows average scores of GS, PPT and tip pinch between the NMES and control sides in pre- and post-NMES training. On the control side, no clinical scores (GS, PPT and tip pinch) differed significantly between pre- and post-NMES training ($p > 0.05$). On the NMES side, PPT and tip pinch improved significantly ($p < 0.05$) with the NMES training, although GS did not.

A summary of comparison of the DTT parameters between the right and left CSTs is shown **Table 2**. Regarding the configuration, the TV of the right CST shows more thicker at post-NMES training compared with pre-NMES training (**Figure 1**); and TV of the right CST increased significantly at post-NMES training compared with pre-NMES training ($p < 0.05$) whereas FA and MD did not change significantly ($p > 0.05$; **Figure 2**). In contrast, FA, MD and TV did not change in the left CST between pre-NMES and post-NMES trainings ($p > 0.05$).

Correlation coefficients did not differ significantly between clinical scores (GS, PPT and tip pinch) and DTT parameters (FA (GS: $r = 0.263$, $p > 0.05$; PPT: $r = 0.325$, $p > 0.05$; tip pinch: $r = 0.442$, $p > 0.05$), MD (GS: $r = 0.342$, $p > 0.05$; PPT: $r = 0.441$, $p > 0.05$ ; tip pinch: $r = 0.612$, $p > 0.05$) and TV (GS: $r = 0.658$, $p > 0.05$; PPT: $r = 0.335$, $p > 0.05$; tip pinch: $r = 0.741$, $p > 0.05$)) in the NMES and control sides ($p > 0.05$).

**TABLE 2 |** Diffusion tensor tractography (DTT) parameters at pre- and post-neuromuscular electrical stimulation training.

| | | Pre-NMES training | Post-NMES training | *p*-value |
|---|---|---|---|---|
| FA | NMES | 0.47 ± 0.13 | 0.51 ± 0.02 | 0.374 |
| | Control | 0.51 ± 0.02 | 0.51 ± 0.03 | 0.391 |
| MD | NMES | 0.84 ± 0.05 | 0.84 ± 0.05 | 0.635 |
| | Control | 0.83 ± 0.05 | 0.83 ± 0.05 | 0.528 |
| TV | NMES | 1696.85 ± 559.88 | 2017.23 ± 490.48 | 0.001* |
| | Control | 1857.23 ± 712.22 | 1986.62 ± 657.27 | 0.399 |

*NMES, neuromuscular electrical stimulation; FA, fractional anisotropy; MD, mean diffusivity; TV, tract volume. Values: mean ± standard deviation *Significant differences between pre- and post-NMES trainings, p < 0.05.*

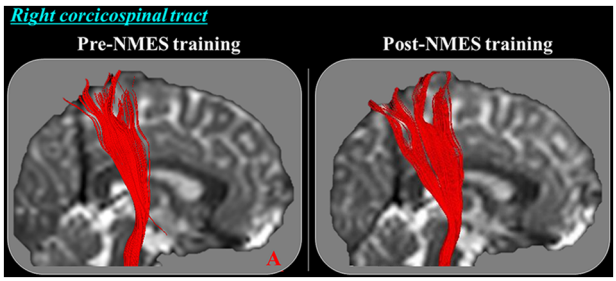


**FIGURE 1 |** Diffusion tensor tractography (DTT) for the right corticospinal tract (CST) in a representative subject (21-year old female). The right CST on post-neuromuscular electrical stimulation (NMES) training become thicker compared with pre-NMES training in this subject.

## DISCUSSION

In the current study, using DTT, we investigated change of the CST between pre- and post-NMES training with application of NMES on the finger extensor muscles for 2 weeks. Our results can be summarized as follows. First, PPT and tip pinch improved on the NMES (left hand) side without change of GS. Second, TV of the right CST that innervates the left finger extensor muscles, increased after NMES training without change of FA and MD value.

In neuro-rehabilitaion, NMES is commonly applied to the finger extensor muscles of the affected hand because the affected hand usually shows flexor spasticity in hemiparetic patients with brain injury (Nakipğlu Yuzer et al., 2017; Pundik et al., 2018). Therefore, NMES was applied to the finger extensor muscles in this study. NMES training produced improvements in PPT and tip pinch, although not in GS. PPT and tip pinch represent finer motor function of hand than GS. This suggests that NMES treatment of the finger extensor muscles might be more effective in improving finer motor activity than gross muscle power. This appears consistent with studies showing that the CST is important in fine motor activity and strength (Kim et al., 2006; Khedr et al., 2010; Mang et al., 2010, 2011; Weinstein et al., 2015; Chang et al., 2016). In addition, NMES training which was applied to extend the finger extensors maximally appeared to facilitate the function of the finger extensors which are needed to perform finer motor function of the hand.

Among DTT parameters, FA, MD and TV have most commonly been used to evaluate the state of a neural tract (Assaf and Pasternak, 2008; Neil, 2008; Pagani et al., 2008). FA value indicates the degree of directionality of water diffusion and the white matter organization; in detail, the degree of directionality and integrity of white matter microstructures such as axon, myelin, and microtubule (Assaf and Pasternak, 2008; Neil, 2008; Pagani et al., 2008). The MD value indicates the magnitude of water diffusion in tissue, and TV is determined by the number of voxels included in a neural tract, thereby suggesting the total number of fibers of a neural tract (Pagani et al., 2008). Therefore, increased values of TV in the CST indicate increment in fiber number of the CST compared with post-NMES training (Pagani et al., 2008; Jang et al., 2013). This result agrees with studies that report association between improvement of motor function and increment of TV of the CST (Schaechter et al., 2009; Jang et al., 2014b; Seo and Jang, 2015).

Many studies have tried to facilitate healing of the CST using rehabilitative interventions including rTMS, hand-arm bimanual intensive therapy, and NMES (Han et al., 2003; Kim et al., 2006; Khedr et al., 2010; Mang et al., 2010, 2011; Wei et al., 2013; Chen et al., 2014; Weinstein et al., 2015; Chang et al., 2016). Several studies demonstrated an activating or facilitating effect of NMES on the CST (Kim et al., 2006; Khedr et al., 2010; Mang et al., 2010, 2011; Weinstein et al., 2015; Chang et al., 2016). In 2003, Han et al. reported activation of the primary motor cortex by application of NMES on the wrist extensor muscles in eight normal subjects using fMRI (Han et al., 2003). In 2010, Mang et al. demonstrated that applying 100 Hz on the common peroneal nerve is the most appropriate frequency of NMES to facilitate the CST in eight normal subjects using motor-evoked potential (MEP) on transcranial magnetic stimulation (TMS; Mang et al., 2010). The next year, Mang et al. (2011) studied the effect of NMES on target muscle for 40 min in 14 normal subjects and found the facilitation of the CST using MEP on TMS. Using DTI, two studies reported the facilitation of the CST using NMES (Wei et al., 2013; Chen et al., 2014). In 2013, Wei et al. investigated the effect of NMES on the wrist extensor muscles for 20 days in 12 stroke patients at the subacute stage and demonstrated that hand function was improved, and FA value of the CST in the posterior limb of the internal capsule was increased (Wei et al., 2013). Subsequently,

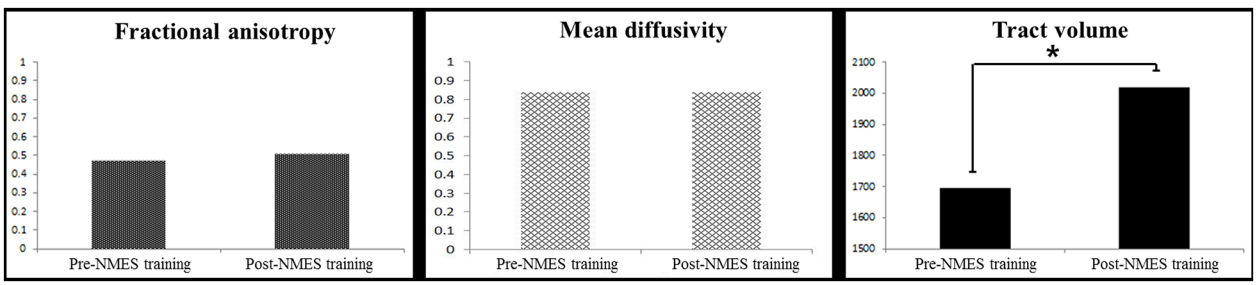


**FIGURE 2 |** Comparison of group analysis of DTT parameters for the right CST of pre- and post-NMES training (*$p < 0.05$).

Chen et al. (2014) investigated the effect of NMES for 3 weeks in 48 stroke patients at the early stage, and they found that NMES improved motor function and increment of FA value of the CST around the lesion area. Although results of the above two DTI studies appeared to demonstrate an effect of NMES on the CST using DTI, these studies investigated the effects only in a specific area of the CST pathway. Therefore, to the best of our knowledge, this is the first study to demonstrate an effect of NMES for the entire CST by NMES training on the finger extensor muscles, evaluated by DTT in normal subjects.

However, the limitations of this study should be considered. First, DTT can produce false negative results throughout the white matter of the brain because of crossing fiber or partial volume effect (Parker and Alexander, 2005). Second, we investigated the effect of the NMES training for 2 weeks and could not evaluate the long-term effect of NMES training. Third, there might be a ceiling effect in the evaluation of clinical data of the right hand in the right-handed subjects. As a result, alternative assign of the right hand or the left hand as a training side could have ruled out the possibility of a ceiling effect. Fourth, this study included a small number of subjects. Fifth, we did not rule out the possibility by the sensory stimulation which was applied by electrical current during NMES training in improvement of the hand function. Last, we used the opposite side of the NMES application as the control side instead of recruiting a control group. Two times scanning of DTI was not easy in terms of cost and the compliance of the subjects. In addition, sham stimulation for the control side was not applicable because NMES training is not passive stimulation, but active stimulation. The fact that sham stimulation was not applied for the control side might induce placebo effect. However, we think that the placebo effect could be ruled out to a certain degree because the CST on DTT has anatomical characteristics instead of functional characteristics.

In conclusion, we demonstrated the facilitation of the contralateral CST with improvement of fine motor activity by 2 weeks of NMES training on peripheral muscles in normal subjects. We think our results can be applied to the sports training for normal subjects including athletes and the patients with brain injury to improve the fine motor function of the hand and facilitate the normal subjects or healing of the injured CST. Further long-term follow up studies involving larger numbers of normal subjects and patients with brain injury should be encouraged.

## AUTHOR CONTRIBUTIONS

SH: study concept and design, manuscript development and writing. YS: study concept and design, acquisition and analysis of data, manuscript authorization.

## FUNDING

This work was supported by the Medical Research Center Program (2015R1A5A2009124) through the National Research Foundation of Korea (NRF) funded by the Ministry of Science, ICT and Future Planning.

## REFERENCES

Assaf, Y., and Pasternak, O. (2008). Diffusion tensor imaging (DTI)-based white matter mapping in brain research: a review. *J. Mol. Neurosci.* 34, 51–61. doi: 10.1007/s12031-007-0029-0

Brandstack, N., Kurki, T., Laalo, J., Kauko, T., and Tenovuo, O. (2016). Reproducibility of tract-based and region-of-interest DTI analysis of long association tracts. *Clinl. Neuroradiol.* 26, 199–208. doi: 10.1007/s00062-014-0349-8

Chae, J., and Yu, D. (2000). A critical review of neuromuscular electrical stimulation for treatment of motor dysfunction in hemiplegia. *Assist. Technol.* 12, 33–49. doi: 10.1080/10400435.2000.10132008

Chang, W. H., Uhm, K. E., Shin, Y. I., Pascual-Leone, A., and Kim, Y. H. (2016). Factors influencing the response to high-frequency repetitive transcranial magnetic stimulation in patients with subacute stroke. *Restor. Neurol. Neurosci.* 34, 747–755. doi: 10.3233/rnn-150634

Chen, D., Yan, T., Li, G., Li, F., and Liang, Q. (2014). Functional electrical stimulation based on a working pattern influences function of lower extremity in subjects with early stroke and effects on diffusion tensor imaging: a randomized controlled trial. *Zhonghua Yi Xue Za Zhi* 94, 2886–2892. doi: 10.3760/cma.j.issn.0376-2491.2014.37.003

Daly, J. J., and Ruff, R. L. (2007). Construction of efficacious gait and upper limb functional interventions based on brain plasticity evidence and model-based measures for stroke patients. *ScientificWorldJournal* 7, 2031–2045. doi: 10.1100/tsw.2007.299

Danielian, L. E., Iwata, N. K., Thomasson, D. M., and Floeter, M. K. (2010). Reliability of fiber tracking measurements in diffusion tensor imaging for longitudinal study. *Neuroimage* 49, 1572–1580. doi: 10.1016/j.neuroimage.2009.08.062

Davidoff, R. A. (1990). The pyramidal tract. *Neurology* 40, 332–339. doi: 10.1212/WNL.40.2.332

de Oliveira Melo, M., Aragao, F. A., and Vaz, M. A. (2013). Neuromuscular electrical stimulation for muscle strengthening in elderly with knee osteoarthritis–a systematic review. *Complement. Ther. Clin. Pract.* 19, 27–31. doi: 10.1016/j.ctcp.2012.09.002

Doucet, B. M., Lam, A., and Griffin, L. (2012). Neuromuscular electrical stimulation for skeletal muscle function. *Yale J. Biol. Med.* 85, 201–215.

Han, B. S., Jang, S. H., Chang, Y. M., Byun, W. M., Lim, S. K., and Kang, D. S. (2003). Functional magnetic resonance image finding of cortical activation by neuromuscular electrical stimulation on wrist extensor muscles. *Am. J. Phys. Med. Rehabil.* 82, 17–20. doi: 10.1097/00002060-200301000-00003

Jang, S. H. (2014). The corticospinal tract from the viewpoint of brain rehabilitation. *J. Rehabil. Med.* 46, 193–199. doi: 10.2340/16501977-1782

Jang, S. H. (2016). Dignostic history of traumatic axonal injury in patients with cerebral concussion and mild traumatic brain injury. *Brain Neurorehabil.* 9, 1–8. doi: 10.12786/bn.2016.9.e1

Jang, S. H., Chang, C. H., Lee, J., Kim, C. S., Seo, J. P., and Yeo, S. S. (2013). Functional role of the corticoreticular pathway in chronic stroke patients. *Stroke* 44, 1099–1104. doi: 10.1161/strokeaha.111.000269

Jang, S. H., Jang, W. H., Chang, P. H., Lee, S.-H., Jin, S.-H., Kim, Y. G., et al. (2014a). Cortical activation change induced by neuromuscular electrical stimulation during hand movements: a functional NIRS study. *J. Neuroeng. Rehabil.* 11:29. doi: 10.1186/1743-0003-11-29

Jang, S. H., Kim, K., Kim, S. H., Son, S. M., Jang, W. H., and Kwon, H. G. (2014b). The relation between motor function of stroke patients and diffusion tensor imaging findings for the corticospinal tract. *Neurosci. Lett.* 572, 1–6. doi: 10.1016/j.neulet.2014.04.044

Khedr, E. M., Etraby, A. E., Hemeda, M., Nasef, A. M., and Razek, A. A. (2010). Long-term effect of repetitive transcranial magnetic stimulation on motor function recovery after acute ischemic stroke. *Acta Neurol. Scand.* 121, 30–37. doi: 10.1111/j.1600-0404.2009.01195.x

Kim, K. M., Croy, T., Hertel, J., and Saliba, S. (2010). Effects of neuromuscular electrical stimulation after anterior cruciate ligament reconstruction on quadriceps strength, function and patient-oriented outcomes: a systematic review. *J. Orthop. Sports. Phys. Ther.* 40, 383–391. doi: 10.2519/jospt.2010.3184

Kim, Y. T., Kang, S. Y., Kim, H. S., and Shin, B. S. (1994). Hand strength and dextricity evaluation with age. *J. Kor. Acad. Rehabil. Med.* 18, 780–788.

Kim, Y.-H., You, S.-H., Ko, M.-H., Park, J.-W., Lee, K. H., Jang, S. H., et al. (2006). Repetitive transcranial magnetic stimulation-induced corticomotor excitability and associated motor skill acquisition in chronic stroke. *Stroke* 37, 1471–1476. doi: 10.1161/01.str.0000221233.55497.51

Kong, S., Lee, K. S., Kim, J., and Jang, S. H. (2014). The effect of two different hand exercises on grip strength, forearm circumference and vascular maturation in patients who underwent arteriovenous fistula surgery. *Ann. Rehabil. Med.* 38, 648–657. doi: 10.5535/arm.2014.38.5.648

Kunimatsu, A., Aoki, S., Masutani, Y., Abe, O., Hayashi, N., Mori, H., et al. (2004). The optimal trackability threshold of fractional anisotropy for diffusion tensor tractography of the corticospinal tract. *Magn. Reson. Med. Sci.* 3, 11–17. doi: 10.2463/mrms.3.11

Lee, H. D., and Jang, S. H. (2015). Injury of the corticoreticular pathway in patients with mild traumatic brain injury: a diffusion tensor tractography study. *Brain Inj.* doi: 10.3109/02699052.2015.1045028 [Epub ahead of print].

Maddocks, M., Gao, W., Higginson, I. J., and Wilcock, A. (2013). Neuromuscular electrical stimulation for muscle weakness in adults with advanced disease. *Cochrane Database Syst. Rev.* 1:CD009419. doi: 10.1002/14651858.CD009419.pub2

Malykhin, N., Concha, L., Seres, P., Beaulieu, C., and Coupland, N. J. (2008). Diffusion tensor imaging tractography and reliability analysis for limbic and paralimbic white matter tracts. *Psychiatry Res.* 164, 132–142. doi: 10.1016/j.pscychresns.2007.11.007

Mang, C. S., Clair, J. M., and Collins, D. F. (2011). Neuromuscular electrical stimulation has a global effect on corticospinal excitability for leg muscles and a focused effect for hand muscles. *Exp. Brain Res.* 209, 355–363. doi: 10.1007/s00221-011-2556-8

Mang, C. S., Lagerquist, O., and Collins, D. F. (2010). Changes in corticospinal excitability evoked by common peroneal nerve stimulation depend on stimulation frequency. *Exp. Brain Res.* 203, 11–20. doi: 10.1007/s00221-010-2202-x

Mori, S., Crain, B. J., Chacko, V. P., and van Zijl, P. C. (1999). Three-dimensional tracking of axonal projections in the brain by magnetic resonance imaging. *Ann. Neurol.* 45, 265–269. doi: 10.1002/1531-8249(199902)45:2<265::aid-ana21>3.0.co;2-3

Nakipğlu Yuzer, G. F., Köse dönmez, B., and Ozgirgin, N. (2017). A randomized controlled study: effectiveness of functional electrical stimulation on wrist and finger flexor spasticity in hemiplegia. *J. Stroke Cerebrovasc. Dis.* 26, 1467–1471. doi: 10.1016/j.jstrokecerebrovasdis.2017.03.011

Neil, J. J. (2008). Diffusion imaging concepts for clinicians. *J. Magn. Reson. Imaging* 27, 1–7. doi: 10.1002/jmri.21087

Oldfield, R. C. (1971). The assessment and analysis of handedness: the edinburgh inventory. *Neuropsychologia* 9, 97–113. doi: 10.1016/0028-3932(71)90067-4

Pagani, E., Agosta, F., Rocca, M. A., Caputo, D., and Filippi, M. (2008). Voxel-based analysis derived from fractional anisotropy images of white matter volume changes with aging. *Neuroimage* 41, 657–667. doi: 10.1016/j.neuroimage.2008.03.021

Parker, G. J. M., and Alexander, D. C. (2005). Probabilistic anatomical connectivity derived from the microscopic persistent angular structure of cerebral tissue. *Philos. Trans. R. Soc. Lond. B Biol. Sci.* 360, 893–902. doi: 10.1098/rstb.2005.1639

Powell, J., Pandyan, A. D., Granat, M., Cameron, M., and Stott, D. J. (1999). Electrical stimulation of wrist extensors in poststroke hemiplegia. *Stroke* 30, 1384–1389. doi: 10.1161/01.str.30.7.1384

Puig, J., Pedraza, S., Blasco, G., Daunis-i-Estadella, A., Prats, A., Prados, F., et al. (2010). Wallerian degeneration in the corticospinal tract evaluated by diffusion tensor imaging correlates with motor deficit 30 days after middle cerebral artery ischemic stroke. *Am. J. Neuroradiol.* 31, 1324–1330. doi: 10.3174/ajnr.a2038

Pundik, S., McCabe, J., Skelly, M., Tatsuoka, C., and Daly, J. J. (2018). Association of spasticity and motor dysfunction in chronic stroke. *Ann. Phys. Rehabil. Med.* doi: 10.1016/j.rehab.2018.07.006 [Epub ahead of print].

Reddon, J. R., Gill, D. M., Gauk, S. E., and Maerz, M. D. (1988). Purdue pegboard: test-retest estimates. *Percept. Mot. Skills* 66, 503–506. doi: 10.2466/pms.1988.66.2.503

Rushton, D. N. (1997). Functional electrical stimulation. *Physiol. Meas.* 18, 241–275. doi: 10.1088/0967-3334/18/4/001

Schaechter, J. D., Fricker, Z. P., Perdue, K. L., Helmer, K. G., Vangel, M. G., Greve, D. N., et al. (2009). Microstructural status of ipsilesional and contralesional corticospinal tract correlates with motor skill in chronic stroke patients. *Hum. Brain Mapp.* 30, 3461–3474. doi: 10.1002/hbm.20770

Seo, J. P., and Jang, S. H. (2014). Injury of the spinothalamic tract in a patient with mild traumatic brain injury: diffusion tensor tractography study. *J. Rehabil. Med.* 46, 374–377. doi: 10.2340/16501977-1783

Seo, J. P., and Jang, S. H. (2015). Traumatic axonal injury of the corticospinal tract in the subcortical white matter in patients with mild traumatic brain injury. *Brain Inj.* 29, 110–114. doi: 10.3109/02699052.2014.973447

Shin, H. K., Cho, S. H., Jeon, H.-S., Lee, Y. H., Song, J. C., Jang, S. H., et al. (2008). Cortical effect and functional recovery by the electromyography-triggered neuromuscular stimulation in chronic stroke patients. *Neurosci. Lett.* 442, 174–179. doi: 10.1016/j.neulet.2008.07.026

Smith, R. O., and Benge, M. W. (1985). Pinch and grasp strength: standardization of terminology and protocol. *Am. J. Occup. Ther.* 39, 531–535. doi: 10.5014/ajot.39.8.531

Tiffin, J., and Asher, E. J. (1948). The purdue pegboard; norms and studies of reliability and validity. *J. Appl. Psychol.* 32, 234–247. doi: 10.1037/h0061266

Wakana, S., Caprihan, A., Panzenboeck, M. M., Fallon, J. H., Perry, M., Gollub, R. L., et al. (2007). Reproducibility of quantitative tractography methods applied to cerebral white matter. *Neuroimage* 36, 630–644. doi: 10.1016/j.neuroimage.2007.02.049

Wang, J. Y., Abdi, H., Bakhadirov, K., Diaz-Arrastia, R., and Devous, M. D. (2012). A comprehensive reliability assessment of quantitative diffusion tensor tractography. *Neuroimage* 60, 1127–1138. doi: 10.1016/j.neuroimage.2011.12.062

Wei, W. J., Bai, L. J., Wang, J., Dai, R. W., Tong, R. K. Y., Zhang, Y. M., et al. (2013). A longitudinal study of h and motor recovery after sub-acute stroke: a study combined fMRI with diffusion tensor imaging. *PLOs One* 8:e64154. doi: 10.1371/journal.pone.0064154

Weinstein, M., Myers, V., Green, D., Schertz, M., Shiran, S. I., Geva, R., et al. (2015). Brain plasticity following intensive bimanual therapy in children with hemiparesis: preliminary evidence. *Neural Plast.* 2015:798481. doi: 10.1155/2015/798481

Yamada, K., Mori, S., Nakamura, H., Ito, H., Kizu, O., Shiga, K., et al. (2003). Fiber-tracking method reveals sensorimotor pathway involvement in stroke patients. *Stroke* 34, E159–E162. doi: 10.1161/01.str.0000085827.54986.89

York, D. H. (1987). Review of descending motor pathways involved with transcranial stimulation. *Neurosurgery* 20, 70–73. doi: 10.1097/00006123-198701000-00021

**Conflict of Interest Statement**: The authors declare that the research was conducted in the absence of any commercial or financial relationships that could be construed as a potential conflict of interest.

frontiers in Human Neuroscience

ORIGINAL RESEARCH
published: 28 November 2018
doi: 10.3389/fnhum.2018.00476

# Taking Others as a Mirror: Contingent Social Comparison Promotes Task Engagement

*Lei Wang*[1,2], *Xiaoshuang Zhang*[1,2], *Lu Li*[1,2] *and Liang Meng*[3,4]*

[1]School of Management, Zhejiang University, Hangzhou, China, [2]Neuromanagement Lab, Zhejiang University, Hangzhou, China, [3]School of Business and Management, Shanghai International Studies University, Shanghai, China, [4]Laboratory of Applied Brain and Cognitive Sciences, Shanghai International Studies University, Shanghai, China

Social comparison implemented in an informational while not controlling manner can be motivating. In order to directly examine the effect of contingent social comparison on one's task engagement, we manipulated social comparison in an experimental study and adopted an electrophysiological approach to measure one' task engagement. In this experiment, we engaged the participants in a modified stop-watch (SW) task which requires a button press to stop the watch within a given time interval and instructed the participants to either play alone or simultaneously play with a same-sex counterpart. In the latter case, they could freely solicit feedback on their counterparts' performance besides their own. Enlarged stimulus-preceding negativity (SPN) and error-related negativity (ERN) were observed in the two-player condition, indicating strengthened anticipatory attention toward the task-onset stimulus at the pre-task stage and enhanced performance surveillance during task execution. As a complement, self-report data suggested that the participants were more intrinsically motivated to engage in the SW task when contingent social comparison was present. Thus, converging electrophysiological and behavioral evidences suggested the pivotal role of contingent social comparison in promoting self-directed task engagement.

**Keywords: social comparison, task engagement, stimulus-preceding negativity, error-related negativity, event-related potentials**

OPEN ACCESS

***Edited by:***
*Xiaochu Zhang,*
*University of Science and Technology of China, China*

***Reviewed by:***
*Cuicui Wang,*
*Hefei University of Technology, China*
*Yin Wu,*
*Shenzhen University, China*

***Correspondence:**
*Liang Meng*
*promise_land@shisu.edu.cn*

***Received:*** *26 September 2018*
***Accepted:*** *14 November 2018*
***Published:*** *28 November 2018*

***Citation:***
*Wang L, Zhang X, Li L and Meng L (2018) Taking Others as a Mirror: Contingent Social Comparison Promotes Task Engagement. Front. Hum. Neurosci. 12:476. doi: 10.3389/fnhum.2018.00476*

## INTRODUCTION

In our daily life, individuals frequently encounter social comparison, a core feature and shared characteristic of social groups. Social comparison refers to a central mental process, through which people get to compare their own abilities and opinions with those of others for self-improvement and/or subjective well-being (Festinger, 1954; Wills, 1981). A series of studies suggested that self-improvement can be prompted by social comparison, which would subsequently increase the intrinsic reward when performing the original task (Wayment and Taylor, 1995; Suls and Wheeler, 2000). In support of this argument, several functional Magnetic Resonance Imaging (fMRI) studies reported that ventral striatum, which is responsible for reward processing, would show enhanced activation when social comparison information was provided (Fliessbach et al., 2007; Dvash et al., 2010; Bault et al., 2011; Lindner et al., 2014; Simon et al., 2014). While these studies suggested social comparison to be beneficial, some classical behavioral experiments consistently reported the

withering effect of social comparison on one's motivation to perform subsequent tasks (Deci et al., 1981; Vallerand et al., 1986; Jagacinski and Nicholls, 1987; Clinkenbeard, 1989). Based on these conflicting results, we can see that although information provided by social comparison can be beneficial, it is not always conductive to one's (autonomous) motivation. Thus, a sound theoretical framework is needed to integrate these seemingly contradictory findings.

According to self-determination theory (SDT), one of the most predominant theories on human motivation, there exists three basic psychological needs, which are autonomy, competence and relatedness, respectively (Deci and Ryan, 1985). Once these basic needs are satisfied, people would be more autonomously motivated and then proactively engage themselves in tasks (Deci et al., 2001; Gagné and Deci, 2005; Stone et al., 2008). Compared with intrinsic motivation which serves as a psychological factor in regulating human beings' behaviors, task engagement is more externally visible and can be measured in a more objective manner (Ainley, 2012; Reeve, 2012). Much previous research has found that intrinsically motivated employees inclined to exhibit higher degrees of work engagement (Gagné and Deci, 2005; Rich, 2006; Thomas, 2009; Haivas et al., 2013; Stoeber et al., 2013). If the fundamental psychological needs mentioned in SDT were satisfied, employees would be more autonomously motivated and then proactively engage themselves in their work (Stone et al., 2008). When it comes to social comparison, information provided by social comparison may serve to facilitate one's perceived competence and can be beneficial (Ryan and Deci, 2017), but the way that social comparison is implemented may undermine one's perceived autonomy and counteract its own positive effect. For instance, when interpersonal context is pressured, autonomy would be threatened, which is detrimental to one's intrinsic motivation (Reeve and Deci, 1996). Thus, social comparison that is implemented in an informational while not controlling manner would be motivating. In this study, we explore the positive effect of contingent social comparison on one's task engagement, wherein social comparison is encouraged rather than enforced. With contingent social comparison, the information about how well one has performed and the opportunity to compare oneself with others can be provided upon request, which means that the social comparison information is provided only in a voluntary manner. Thus, the participants are not forced to compared with others if they are not willing to. In this study, we pay special attention to the extent to which the participants would proactively engage in the stop-watch (SW) task and the degree of cognitive effort they would voluntarily expend during task execution, that is, one's self-directed task engagement under contingent social comparison.

In order to measure one's task engagement, we modified a classical SW task widely adopted by previous studies (Murayama et al., 2010; Ma et al., 2014; Jin et al., 2015; Fang et al., 2018). In a pioneering study, Murayama and co-authors found the game-like SW task, a both challenging and attractive task, was applicable to the measurement of one's intrinsic motivation (Murayama et al., 2010). Since intrinsic motivation has been suggested to be a driving force of task engagement (Thomas, 2009), we deemed that the SW task would also be appropriate for the purpose of this study. In order to engage participants in social interactions, we employed a two-player online version of the SW task, which was developed in one of our recent studies (Meng et al., 2016). To make sure that the participants were autonomously engaged in the tasks rather than externally driven, they received fixed payments irrelevant to their task performances. Two experimental conditions were set up for each participant, wherein one either completed the SW task alone and only got his/her own task performance (single-player SW task) or played along with a same-sex participant (two-player SW task). In the latter case, one could freely choose whether to solicit feedback on his/her counterpart's task performance or not after completing the task. In order to objectively measure one's task engagement during the SW task, we adopted the electroencephalogram (EEG) with high temporal precision. Electrophysiological responses of the paired participants were recorded throughout the experiment.

With the development of cognitive neuroscience, researchers embarked on exploring the neural correlates of intrinsic motivation (Jin et al., 2015). Pioneering electrophysiological studies adopted magnitudes of feedback-related negativity (FRN) loss-win difference wave (d-FRN) upon feedback (Ma et al., 2014; Meng and Ma, 2015) and stimulus-preceding negativity (SPN) toward feedback (Meng and Ma, 2015; Meng et al., 2016; Ma et al., 2017) to measure one's intrinsic motivation, both of which were agreed on to be sensitive to one's motivation level (San Martín, 2012; Wang et al., 2017, 2018). Although these pioneering findings are illuminating, engagement during the task was not measured. One motivational stage that interested us was task preparation. Since completion of the SW task naturally requires concentration, the participants have to be well prepared during the pre-task stage and stay focused in order to win. In addition, as our previous studies showed (Ma et al., 2014, 2017; Meng et al., 2016), the participants generally learnt about their task performances immediately upon button press in the SW task, which made it possible for us to measure one's performance monitoring during the task. Thus, in this study, we focused on cognitive preparation and performance monitoring of the SW task and examined the SPN elicited by the anticipation of task onset stimuli and error-related negativity (ERN) observed around behavioral responses during task execution.

SPN is an event-related potential (ERP) component that reflects processes related to anticipatory attention (Böcker et al., 2001; van Boxtel and Böcker, 2004; Brunia et al., 2012; Meng and Ma, 2015; Meng et al., 2016; Ma et al., 2017; Wang et al., 2017, 2018), which is generally a sustained, negative shift that occurs when a person actively anticipates the onset of certain task-relevant stimuli (van Boxtel and Böcker, 2004). Previous studies have found that task engagement was associated with attention resource availability and that enhanced task engagement could increase participants' attention level (Matthews et al., 2010a,b). Thus, we adopted the magnitude of SPN to measure one's task engagement. While most studies focused on the SPN toward feedback stimuli (Meng and Ma, 2015; Meng et al., 2016; Ma et al., 2017), few studies paid

attention to the anticipation of task-onset stimuli. According to recent literatures, the SPN can also be observed prior to stimuli that convey instructions for the impending task, whose amplitude would be relatively small (around 1 μV). During this period, the participants should be cognitively preparing for the upcoming task, and magnitude of the SPN can reflect their concentration level (Böcker et al., 2001; van Boxtel and Böcker, 2004; Brunia et al., 2012). In this study, we focused on the SPN elicited during the task preparation stage, a stage before the display of the stopwatch icon. As an effort-requiring task, SW requires millisecond-level precision. Thus, the participants have to be mentally prepared for the task-onset cue in order to better complete it. If contingent social comparison (the opportunity to check one's counterpart's task performance in a voluntary manner) is indeed beneficial, we predicted the participants to be more focused when preparing for the upcoming SW task and pay more sustained anticipatory attention toward onset of the task, eliciting a more pronounced SPN at the pre-task stage of the two-player SW task condition (Böcker et al., 2001; Kotani et al., 2015; Meng and Yang, 2018).

ERN is generally elicited within 100 ms of one's incorrect responses, which directly reflects the level of performance surveillance during the task and helps individuals to improve subsequent behaviors and get better outcomes (Ullsperger et al., 2014). In addition to SPN, previous studies also suggested ERN to reflect the level of task engagement and/or concern about the outcome of a certain task (Tops et al., 2006; Meng and Yang, 2018). It was found that, when people were engaged in certain tasks to a greater extent, they would care more about the commission of errors and react more intensely once they missed a certain goal (Santesso et al., 2005; Tops et al., 2006; Meng and Yang, 2018). In this study, the participants could learn about their task performances when working on the SW task, as they could observe the time point they responded and compare it with the target. It is worth noting that, although we had predefined a success time interval (2.95 s–3.05 s), the participants would naturally compare their performances with the target time point (3.00 s). As most responses would deviate from the target time point to a certain extent, we predicted to observe the ERN despite the objective correctness of the response. According to our hypothesis, if contingent social comparison indeed has positive effects on task engagement, the participants should care more about committing errors or underperforming in the two-player condition, which leads to a more negative ERN during task execution.

# MATERIALS AND METHODS

## Participants

This study was approved by the internal review board of Zhejiang University Neuromanagement Lab. In order to obtain a representative sample, the participants were randomly selected from students who voluntarily registered for this experiment in response to our message posted on the internal Bulletin Board System (BBS) of Zhejiang University. For each experimental session, two same-sex participants, who were unknown to each other, were recruited and paired. In total, 24 healthy registered graduate and undergraduate students (14 males) in varied majors were enrolled. Data from three participants were excluded due to insufficient valid trials, and ages of the remaining subjects were between 19 and 25 (21.62 years ± 1.50 SD). According to self-reports acquired before the experiment, all of them had either normal or corrected-to-normal vision and no history of neurological disorder or mental diseases. A written informed consent statement was acquired from each participant prior to the experiment.

## Experiment Stimuli and Procedure

Before the experiment, the paired participants met and were briefly introduced to each other at the laboratory. They were then led to take seats in separate rooms and read the instruction printed on paper handouts. The room was dimly lit, sound-attenuated and electrically shielded. Stimuli were presented at the center of a computer monitor with 1-m distance away from the participant and with a visual angle of 2.89° × 3.04°. Each participant should accomplish SW tasks of two different versions, namely, a single-player task and a two-player online task. The former task was a modification of Murayama et al.'s (2010) paradigm, while the latter task was originally developed by Meng et al. (2016). There were two blocks for each version of the SW task and each block contained 40 trials. In order to eliminate the sequence effect, experimental conditions were counter-balanced across the participants. Half of the participants completed the single-player SW task at first and then the two-player version, while the rest participants completed them in a reversed sequence. All the participants were instructed to use a keypad to respond throughout the experiment.

At the beginning of each trial, a fixation cross was displayed for 500 ms at the center of the screen, followed by a 1,000 ms blank screen. Afterwards, the stopwatch icon would appear and automatically start running from 0.00 s. The participants were informed to respond with their dominant hand to stop the watch around 3.00 s by pressing any button on the keypad. They were encouraged to respond as accurate as possible, and the success interval was predefined as 2.95 s to 3.05 s. During feedback, if the participant succeeded, his/her performance would appear in green. If not, in red. The target stopwatch stimulus was displayed for a maximum of 5,000 ms. If the participant did not respond within the given interval, the watch would automatically stop at 5.00 s.

Just as what **Figure 1A** illustrated, during the single-player SW task, the participant's response (or the stop of the watch) was followed by the feedback of his/her own task performance. The major difference between the single-player and the two-player SW task lies in the choosing phase (see **Figure 1B**). As the procedure of the experiment has to be balanced between the two participants during the two-player online SW task, only after both participants responded would they be directed to the choosing phase of the task. Otherwise, the one who responded earlier had to wait for the counterpart. After both participants responded (or the watch stopped automatically), a probe stimulus "*YES*?" colored in red would appear on the screen. At this stage, each participant could freely choose whether to view the counterpart's outcome or not. They were assured

that the choice was independently made, and neither of them would know their counterpart's choice. It is worth noting that the decision of a certain player did not influence the feedback information that the other player would receive. For instance, if a player solicited feedback on his/her counterpart's performance while the counterpart did not do so, only the former player would receive feedback on the task performances of both players in that trial. Compared with previous studies involving some players actually played by the experimenters (Meng et al., 2016; Ma et al., 2017), this study allowed the participants to complete tasks simultaneously with an actual same-sex counterpart and to interact with each other during the tasks. Besides, we did not manipulate feedback information, and the displayed outcomes reflected actual task performances.

In order to match the single-player SW condition, the default option of the two-player SW condition was not to check the counterpart's task performance. If a participant decided to solicit the counterpart's outcome, he/she should press button "1" on the keypad within 1,000 ms after onset of "*YES?*." Upon button press, the stimulus would turn to a green "*YES!*," and then task performances of both players would be provided for this player. If a participant did not take an active action within 1,000 ms, only his/her own outcome would be presented, as was the case in the single-player SW condition. For both single-player and two-player SW tasks, the feedback stage would last for 1,500 ms. Besides, there was a between-trial interval that lasted for 800–1,000 ms before the next trial started. During the whole experiment, stimuli, recording triggers and behavioral responses were presented and recorded by E-Prime 2.0 (Psychology Software Tools, Pittsburgh, PA, USA).

Before the formal experiment started, each participant was required to practice the single-player SW task for at least 10 trials until he/she thought that it was ready for him/her to start. Also, all the participants were confirmed that they would receive a 40 RMB reimbursement for their attendance, and that their task performances had nothing to do with their payoffs. They were encouraged to stop the watch at 3.00 s as accurate as possible and to enjoy the game. After the experiment, they were debriefed and paid accordingly. Besides, they were instructed to rate their interests in both the single-player and the two-player SW task using a six-point, semantic differential scale (0 = the least interesting, and 5 = the most interesting). Their motivation to win (0 = the weakest motivation, and 5 = the strongest motivation) and the effort they had made (0 = the least effort having made, and 5 = the greatest effort having made) were also measured.

## EEG Recording

EEGs were recorded (band-pass 0.05 Hz to 70 Hz, sampling rate 500 Hz) from 64 scalp sites with the Neuroscan Synamp2 Amplifier (Scan 4.5, Neurosoft Labs, Inc., Sterling, VA, USA). An electrode located between FPz and Fz on the forehead was used as a ground electrode. The left mastoid was selected for the online reference and data of the average of left and right mastoids served as the offline re-reference. Vertical electrooculogram (EOG) was recorded from the electrodes above and below the left eye, and the horizontal EOG was recorded at the left and right orbital rim. The experimenters made sure that electrode impedance was reduced to less than 5 kΩ before the experiment formally started, which was maintained during the whole experiment.

During the offline EEG analysis, the re-reference was conducted by Neuroscan 4.5 while the rest analyses were conducted by Letswave toolbox (Mouraux, Brussels, Belgium[1]) embedded in Matlab (MathWorks, Natick, MA, USA). The vertical EOG artifacts were removed, which was followed by band-pass filtering (0.1–30 Hz for the SPN, and 0.5–30 Hz for the ERN; 24 dB/octave). In terms of the SPN, we segmented the time window of 800 ms prior to stopwatch stimulus onset, with the activity from −800 ms to −600 ms serving as the baseline. For the ERN, the time window of 400 ms before and 400 ms after button press (which would stop the watch) of the participants was segmented and the whole epoch was corrected relative to the baseline, that is, 400–200 ms before button press. Trials containing amplifier clipping or bursts of electromyography activity, as well as whose peak-to-peak deflection exceeded ±100 μV were all excluded. For each participant, the recorded EEGs were separately averaged over each recording site under each condition. For the SPN, the EEG epochs were averaged for single-player (no social comparison) and two-player (contingent social comparison) conditions. For the ERN, there was another within-subject factor, and the epochs were averaged for outcome (success vs. failure) in addition to social comparison (single-player vs. two-player) conditions.

## Data Analysis

Most studies on the SPN reported a right hemisphere dominance (Brunia et al., 2000, 2011; van Boxtel and Böcker, 2004; Kotani et al., 2015; Meng et al., 2016; Ma et al., 2017), which means that the most pronounced SPNs were typically observed from the anterior electrodes on the right side. According to these literatures as well as the topographic map of this study, we analyzed the SPN amplitudes from the electrodes F4, F6, F8, FC4, FC6 and FT8 and then used the mean amplitudes within the time window of 200 ms to 0 ms before onset of the stopwatch stimulus to conduct an ANOVA with within-subject factors of social comparison and electrode. In terms of the ERN, in accordance with previous literatures (Gehring et al., 1993; Riesel et al., 2013) and the topographic map of this study, data from six frontocentral electrodes (F1, Fz, F2, FC1, FCz and FC2) went into the statistical analysis. A 2 (social comparison) × 2 (outcome) × 6 (electrode) repeated measures ANOVA was performed on the ERN within the time window of −50 ms to 50 ms around button press. For both the SPN and the ERN, simple effect analyses were conducted if the interaction effect was significant and the Greenhouse-Geisser correction was applied in all statistical analyses when necessary. For behavioral data, average absolute deviations around the target (the absolute value of the difference between the stopping time and the target time point, that is, 3.00 s) were calculated, and paired *t*-test was adopted for statistical within-subject comparisons.

[1] http://www.letswave.org

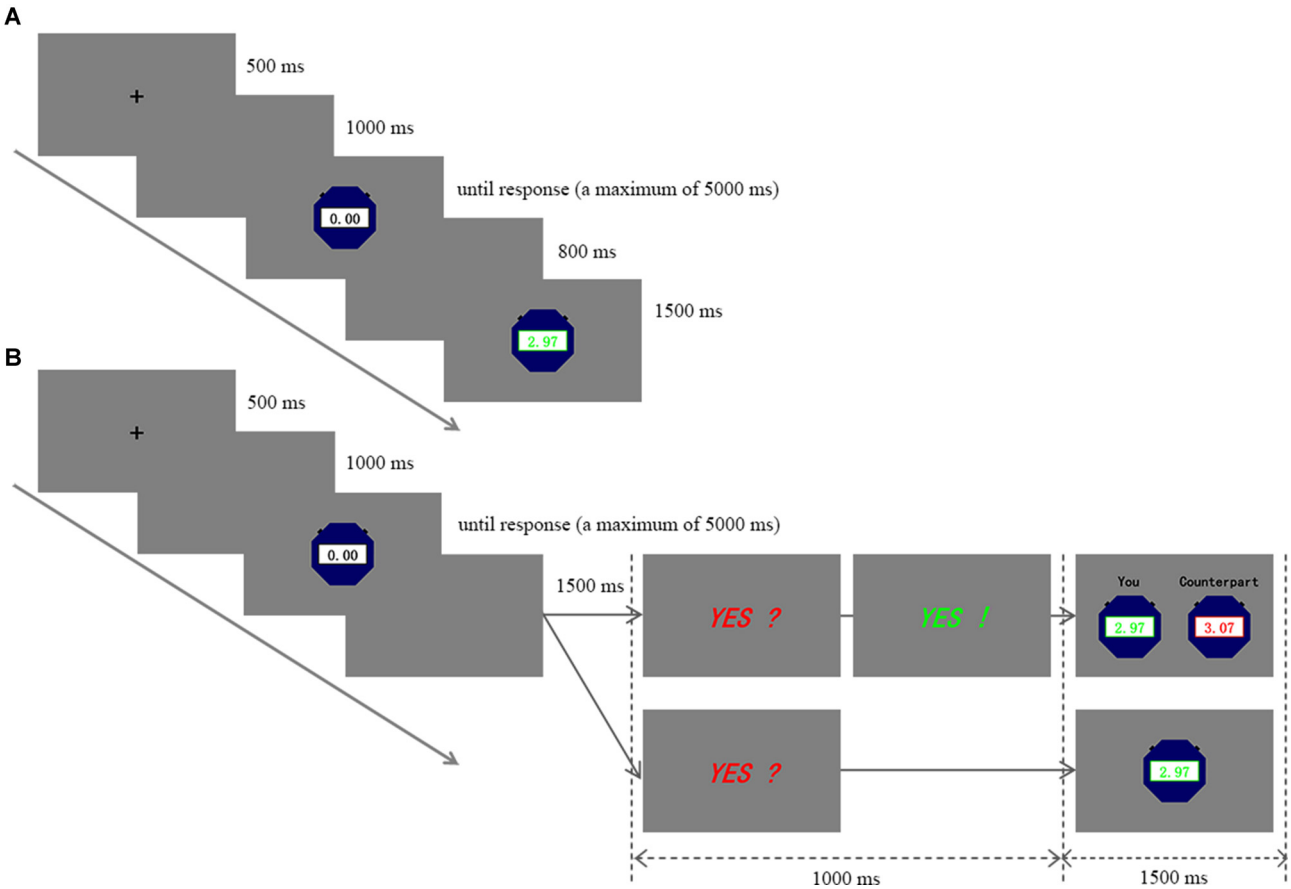


**FIGURE 1 |** Experimental procedure. The participants were instructed to accomplish the single-player stop-watch (SW) task and the two-player online SW task respectively in two different experimental sessions. For each trial, "+" cue was followed by a 1,000 blank screen. Afterwards, the task-onset cue, namely, the SW icon would appear. Regardless of the experimental condition, the participants were instructed to press any single button on the keypad with their dominant hand to stop the watch around 3.00 s as accurate as possible. **(A)** During the single-player SW task, only the participant's own performance was displayed after a short delay. **(B)** There was an additional choosing phase following the button response during the two-player online SW task. After both participants responded or the watch stopped automatically, the probe "*YES?*" colored in red appeared. If the participant solicited to view his/her counterpart's outcome, he/she should respond with button "1" within 1,000 ms, and then the probe would turn into a green "*YES!*" and performance of both players would be displayed. The default option was not to view the counterpart's performance. If the participant did not respond in time, then only his/her own performance would be shown. For both tasks, the feedback stage would last for 1,500 ms and the between-trial interval would last for 800–1,000 ms.

# RESULTS

## Behavioral Results

Results of paired *t*-tests showed that success rates of the two conditions were not significantly different from each other ($M_{\text{single-player}}$ = 0.3679, SD = 0.1231; $M_{\text{two-player}}$ = 0.3976, SD = 0.1183; $t_{(20)} = -1.618$, $p = 0.121$). When feedback on the counterpart's task performance was available, the participants checked their counterpart's task performance in 56.13 ± 29.07% trials. However, the percentage of feedback solicitation was not significantly different between success and failure conditions ($M_{\text{success}}$ = 0.5985, SD = 0.3381; $M_{\text{failure}}$ = 0.5218, SD = 0.2946; $t_{(20)} = 1.527$, $p = 0.143$).

Results from subjective ratings indicated that the participants deemed the two-player SW task as more interesting than the single-player version, and that they enjoyed the former task to a greater extent ($M_{\text{single-player}}$ = 2.76, SD = 1.136; $M_{\text{two-player}}$ = 3.71, SD = 1.007; $t_{(20)} = -8.771$, $p < 0.001$). Moreover, they held a stronger motivation to win during the two-player game ($M_{\text{single-player}}$ = 3.00, SD = 0.837; $M_{\text{two-player}}$ = 3.86, SD = 0.964; $t_{(20)} = -4.954$, $p < 0.001$) and thus paid more effort to complete it ($M_{\text{single-player}}$ = 3.71, SD = 0.902; $M_{\text{two-player}}$ = 4.05, SD = 0.805; $t_{(20)} = -2.646$, $p = 0.016$).

## ERPs

As shown in **Figure 2**, the mean SPN amplitude in the single-player condition was 1.0053 μV, while it was −1.3742 μV (negative polarity: smaller voltage value means larger amplitude) under the two-player condition. ANOVA results illustrated a significant main effect of social comparison ($F_{(1,20)} = 4.570$; $p = 0.045$). In spite of this, neither the main effect of electrode ($F_{(2.13,42.55)} = 1.137$; $p = 0.333$), nor the interaction between social comparison and electrode ($F_{(2.88,57.68)} = 0.620$; $p = 0.599$) were significant. For the ERN (see **Figure 3**), the

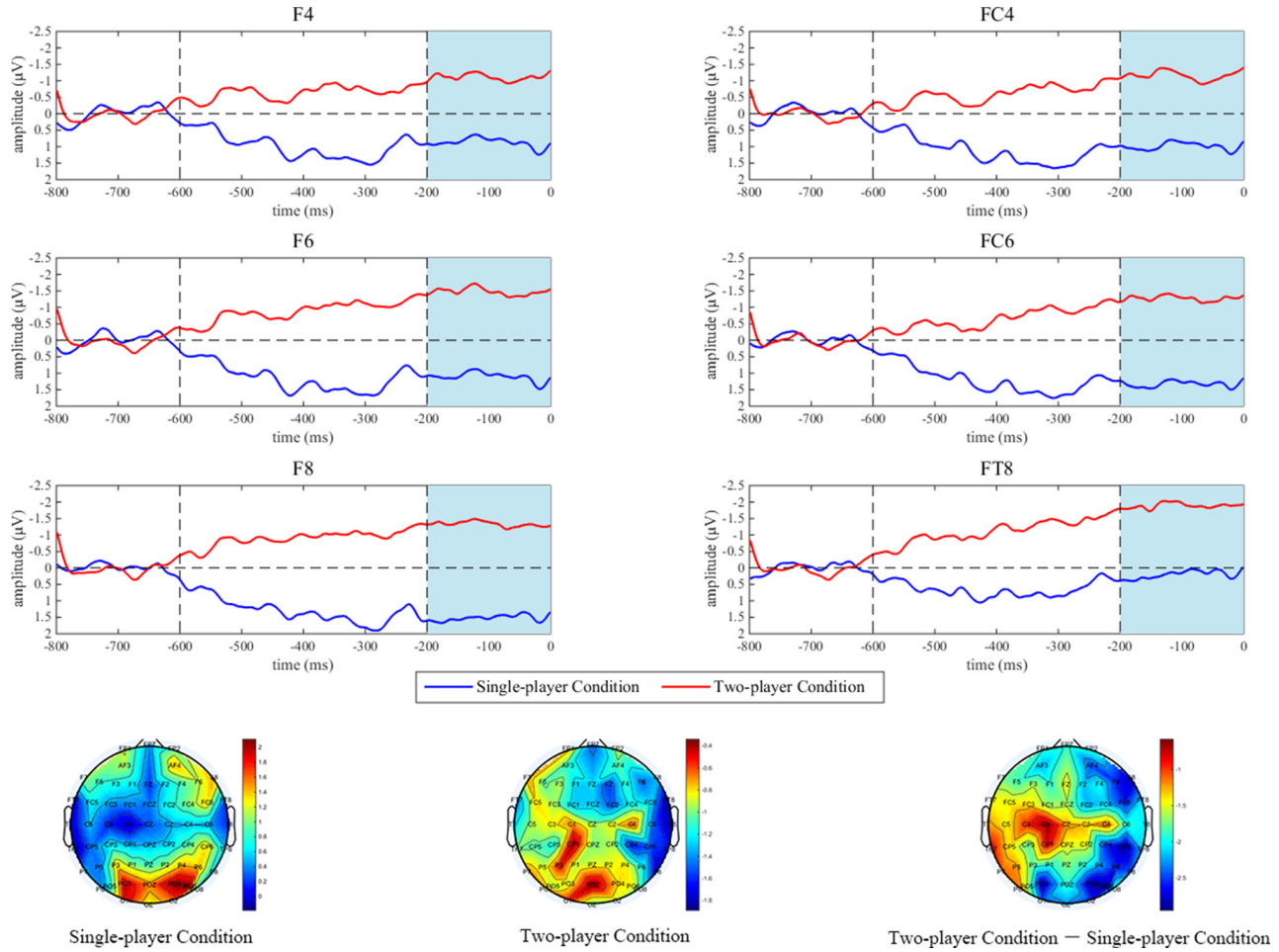


**FIGURE 2 |** The stimulus-proceeding negativity (SPN) results prior to task onset. Grand-averaged event-related potential (ERP) waveforms of SPN from six anterior electrodes on the right side (F4, F6, F8, FC4, FC6 and FT8) are shown for single-player (marked in the blue line) and two-player conditions (marked in the red line) respectively. The time window of interest is marked in shades of light blue. The scalp topographic distributions of the SPN are provided for the single-player condition (the bar ranges from (−0.20 μV to 2.12 μV), the two-player condition (−2.00 μV to −0.30 μV), and the two-player condition minus the single-player condition (−3.00 μV to −0.55 μV), respectively.

main effect of social comparison ($F_{(1,20)}$ = 7.597; $p$ = 0.012) and electrode ($F_{(2.31,46.10)}$ = 17.090; $p$ < 0.001) were both significant, and the mean amplitudes were greater in the two-player condition (−4.8228 μV) compared with the single-player condition (−3.9734 μV). However, the main effect of outcome was not significant ($F_{(1,20)}$ = 0.007; $p$ = 0.933). Interaction effects between social comparison and outcome ($F_{(1,20)}$ = 0.218; $p$ = 0.646), social comparison and electrode ($F_{(3.28,65.57)}$ = 0.491; $p$ = 0.706), as well as outcome and electrode ($F_{(2.55,51.08)}$ = 1.554; $p$ = 0.216) were all non-significant. The interaction effect between social comparison, outcome and electrode reached marginal significance ($F_{(3.43,68.53)}$ = 2.325; $p$ = 0.074).

## DISCUSSION

In our daily life, people are frequently engaged in social comparisons. Through comparing their own beliefs, attitudes, abilities as well as achievements with those of others, people get to understand and evaluate themselves in a better way (Wood, 1996). While the phenomenon of social comparison is frequently observed, it can take place in different forms. Under certain circumstances, social comparison is explicit and may serve as a formal mechanism. For instance, in the work setting, typically the salary of employees is based not only on their objective work performances, but also their performances compared to others. However, in other situations, social comparison may be implicit and contingent, such as the case in the two-player condition of this study. While we emphasized to the participants that their final payoffs were not related with their task performances, they were still confronted with contingent social comparison since information on the counterpart's performance was available once requested. On the one hand, one can freely choose to learn about the counterpart's performance at one's own discretion. On the other hand, without being told, his/her own performance can be

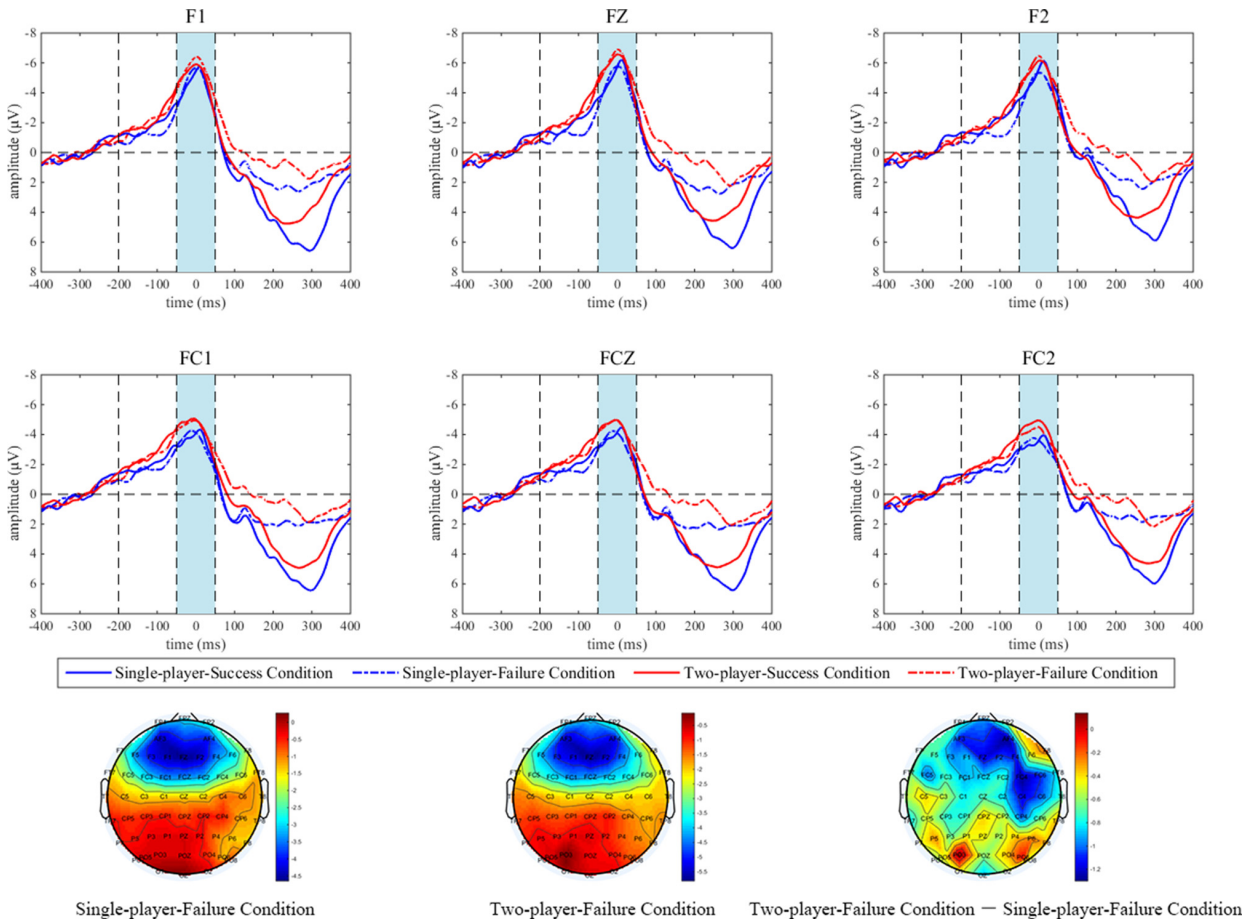


**FIGURE 3 |** The results of error-related negativity (ERN) around behavioral responses. Grand-averaged ERP waveforms of ERN from six frontocentral electrodes (F1, FZ, F2, FC1, FCZ and FC2) are shown in relation to social comparison (single-player condition vs. two-player condition) and outcome (success vs. failure). Results in the single-player condition and the two-player condition are shown in blue and red lines respectively. In addition, solid vs. dotted lines display outcomes of successes vs. failures. The time window of interest is marked in shades of light blue. The scalp topographic distributions of the ERN are provided for the single-player-failure condition (the bar ranges from −4.65 μV to 0.30 μV), the two-player-failure condition (−5.85 μV to 0 μV), and the two-player-failure condition minus the single-player-failure condition (−1.30 μV to 0.15 μV), respectively.

solicited by the counterpart at any time during the experiment as well.

Behavioral results of this study suggested that the participants were indeed quite curious about their counterparts' task performances when contingent social comparison was present, as feedback was requested on 56.13% of the two-player SW trials. According to self-report, the participants were more (intrinsically) motivated to win the game, enjoyed the two-player online SW task to a greater extent, and made greater efforts to complete the task. Since effort provision is closely related to task engagement (Matthews et al., 2002, 2010a), and the participants were not awarded by performance-based rewards, these results jointly indicated that contingent social comparison is beneficial. In line with the behavioral results, the electrophysiological results exhibited that the SPN upon the task onset stimulus loomed larger when contingent social comparison was present (two-player SW task) than when it was absent (single-player SW task). Meanwhile, a similar effect was observed on the ERN. These findings suggested that the participants made a good cognitive preparation and might implement enhanced performance surveillance, which further supported the pivotal role of contingent social comparison in promoting one's task engagement.

Several mainstream theories on intrinsic motivation and/or social comparison may help explain the current findings from diverse perspectives. According to SDT, external information that is informational while not controlling could effectively enhance one's intrinsic motivation on a given task through the fulfillment of basic psychological needs (Pittman et al., 1980; Ryan, 1982; Ryan et al., 1983; Koestner et al., 1984; Deci and Ryan, 1985), which may further enhance one's task engagement (Deci et al., 2001; Gagné and Deci, 2005; Stone et al., 2008). For instance, in the experiment conducted by Koestner et al. (1984), children were randomly distributed into three groups to paint a picture with informational-limits, controlling-limits, or non-limits instructions. Relative to the

controlling-limits group, children in the informational-limits group spent more time painting in their spare time and showed greater intrinsic motivation in painting. In this study, feedback on one's counterpart's task performance is informational, as it provided information on how well the counterpart was completing the task. This served as a reference and helped one to understand how well he/she was completing the task, which enhanced one's perceived competence. Besides, this feedback was not implemented in a controlling manner, which reinforced one's autonomy. For one thing, the participants received fixed payoffs regardless of their task performances. For another, they could choose to receive this additional feedback at their own discretions. Given the informational and non-controlling nature of additional feedback upon request, one's intrinsic motivation was effectively facilitated, which led to greater engagement in the task (Deci and Ryan, 1985; Stone et al., 2008). According to another argument on social comparison, one's inclination to compare with others stems from the pursuit of self-improvement, as one may engage in social comparisons to motivate himself/herself to perform better (Suls and Wheeler, 2000). Through social comparison, people get to learn better about their own strengths and weaknesses and thus can actively improve themselves, which brings greater satisfaction and a sense of achievement. Consequently, they will proactively engage themselves in tasks and sustain an optimal status (Wayment and Taylor, 1995). Taken together, as the two-player condition of this study offered an avenue for contingent social comparison, one's task engagement got enhanced as a result.

Besides verifying the beneficial effect of contingent social comparison on self-directed task engagement, one of the theoretical contributions of this study is the exploration of the neural correlates underlying one's task engagement during social interactions. In this study, we adopted EEGs with high temporal precision and manipulated the presence of contingent social comparison (the single-player condition vs. the two-player condition). While task engagement has been closely associated with intrinsic motivation (Rich, 2006; Haivas et al., 2013; Stoeber et al., 2013; Reeve and Lee, 2014), existing electrophysiological studies focused on the latter construct, while the neural correlates underlying task engagement were less examined. For instance, in a series of studies, we have applied EEGs to track one's intrinsic motivation level during effort-requiring tasks and examined various influencing factors of it (Ma et al., 2014, 2017; Meng and Ma, 2015; Meng et al., 2016; Fang et al., 2018). These studies mainly focused on feedback-related cognitive processing, and we adopted either SPN during feedback anticipation or d-FRN during feedback evaluation to measure one's intrinsic motivation. While these pioneering investigations are inspiring, none of them directly examined proactive task engagement, which could be evidenced by amounts of attention paid to experimental stimuli and the way a participant completed the experimental task (Reeve, 2012). Since cognitive preparation and performance surveillance levels reflect one's task engagement, through measuring the SPN toward initiation of SW tasks during the pre-task stage and the ERN observed around behavioral responses during task execution, in this study we get to gauge task engagement in a more direct manner.

While these findings are illuminating, we have to recognize that this study is exploratory in nature. While most studies examined the SPN toward feedback or rewards, we focused on the SPN elicited during the anticipation of task-onset stimuli. Given that a few pioneering studies reported to observe the SPN (although relatively small in magnitude) when the participants are cognitively preparing for the upcoming task (Böcker et al., 2001; van Boxtel and Böcker, 2004; Brunia et al., 2012; Meng and Yang, 2018) as is the case in this study, follow-up studies on the SPN observed on the pre-task stage are needed to provide additional support for our current findings. In addition, although online performance surveillance can be implemented, compared with speeded response tasks such as the Stroop task and the Flanker task, the SW is not an optimal task to elicit the ERN. As reported in previous studies, a correct while relative slow response in speeded response tasks would be accompanied by an ERN pattern, which is similar with that elicited by failures (Vidal et al., 2003; Gehring et al., 2012). As a successful attempt in the SW (such as stopping the watch at 3.04 s) still deviates from the target time point (3.00 s) to a certain extent, this might help explain the null outcome/valence effect on ERN in this study. Another limitation of this study is that, while we measured the intrinsic motivation level through self-report, we neglected to include subjective ratings of task engagement in our questionnaire, which might give further support to the electrophysiological findings of this study.

## CONCLUSION

In order to directly examine the effect of contingent social comparison on task engagement, we modified the classical SW task and instructed the participants to either play alone or simultaneously play with a same-sex counterpart. In the latter case, they have the discretion in deciding whether to view their counterparts' outcomes in addition to their own or not. The participants reported to enjoy the two-player SW game more and worked harder on it. In addition, compared with the single-player condition, more pronounced SPNs and ERNs were respectively observed at the pre-task stage and around behavioral responses in the two-player condition. Thus, converging evidences suggested that contingent social comparison would effectively promote one's autonomous task engagement.

## ETHICS STATEMENT

This study was carried out in accordance with the requirements of the Neuromanagement Lab Ethics Committee at Zhejiang University. All the participants gave a written informed consent according to the Declaration of Helsinki. All the participants had normal or corrected-to-normal vision. None of them reported any history of psychiatric or neurological disorders.

## AUTHOR CONTRIBUTIONS

LM, LW and XZ conceived and designed the study. XZ and LL collected and analyzed the data. XZ and LM interpreted the data

and drafted the manuscript. LM, LW, XZ and LL reviewed and edited the manuscript. LM and LW administered the project.

## FUNDING

This work was funded by the National Natural Science Foundation of China (71701131, 71871199, 71471163), Humanities and Social Sciences Research Fund supported by Ministry of Education of China (17YJC630104), Chinese Academy of Engineering (2018-XY-45), "Chen Guang" project (16CG36) supported by Shanghai Municipal Education Commission and Shanghai Education Development Foundation, and the Planning Fund of Shanghai International Studies University (20161140012).

## REFERENCES

Ainley, M. D. (2012). "Students' interest and engagement in classroom activities," in *Handbook of Research on Student Engagement*, eds S. L. Christenson, A. L. Reschly and C. Wylie (New York, NY: Springer), 283–302.

Bault, N., Joffly, M., Rustichini, A., and Coricelli, G. (2011). Medial prefrontal cortex and striatum mediate the influence of social comparison on the decision process. *Proc. Natl. Acad. Sci. U S A* 108, 16044–16049. doi: 10.1073/pnas.1100892108

Böcker, K. B. E., Baas, J. M. P., Kenemans, J. L., and Verbaten, M. N. (2001). Stimulus-preceding negativity induced by fear: a manifestation of affective anticipation. *Int. J. Psychophysiol.* 43, 77–90. doi: 10.1016/s0167-8760(01)00180-5

Brunia, C. H. M., de Jong, B. M., van den Berg-Lenssen, M. M. C., and Paans, A. M. J. (2000). Visual feedback about time estimation is related to a right hemisphere activation measured by PET. *Exp. Brain Res.* 130, 328–337. doi: 10.1007/s002219900293

Brunia, C. H. M., Hackley, S. A., van Boxtel, G. J. M., Kotani, Y., and Ohgami, Y. (2011). Waiting to perceive: reward or punishment? *Clin. Neurophysiol.* 122, 858–868. doi: 10.1016/j.clinph.2010.12.039

Brunia, C. H. M., van Boxtel, G. J. M., and Böcker, K. B. E. (2012). "Negative slow waves as indices of anticipation: the bereitschaftspotential, the contingent negative variation and the stimulus-preceding negativity," in *The Oxford Handbook of Event-Related Potential Components*, eds S. J. Luck and E. S. Kappenman (New York, NY: Oxford University Press), 189–207.

Clinkenbeard, P. R. (1989). The motivation to win negative aspects of success at competition. *J. Educ. Gift.* 12, 293–305. doi: 10.1177/016235328901200405

Deci, E. L., Betley, G., Kahle, J., Abrams, L., and Porac, J. (1981). When trying to win: competition and intrinsic motivation. *Pers. Soc. Psychol. Bull.* 7, 79–83. doi: 10.1177/014616728171012

Deci, E. L., and Ryan, R. M. (1985). *Intrinsic Motivation and Self-Determination in Human Behavior*. New York, NY: Plenum.

Deci, E. L., Ryan, R. M., Gagné, M., Leone, D. R., Usunov, J., and Kornazheva, B. P. (2001). Need satisfaction, motivation and well-being in the work organizations of a former eastern bloc country: a cross-cultural study of self-determination. *Pers. Soc. Psychol. Bull.* 27, 930–942. doi: 10.1177/01461672012778002

Dvash, J., Gilam, G., Ben-Ze'Ev, A., Hendler, T., and Shamay-Tsoory, S. G. (2010). The envious brain: the neural basis of social comparison. *Hum. Brain Mapp.* 31, 1741–1750. doi: 10.1002/hbm.20972

Fang, H., He, B., Fu, H., Zhang, H., Mo, Z., and Meng, L. (2018). A surprising source of self-motivation: prior competence frustration strengthens one's motivation to win in another competence-supportive activity. *Front. Hum. Neurosci.* 12:314. doi: 10.3389/fnhum.2018.00314

Festinger, L. (1954). A theory of social comparison processes. *Hum. Relat.* 7, 117–140. doi: 10.1177/001872675400700202

Fliessbach, K., Weber, B., Trautner, P., Dohmen, T., Sunde, U., Elger, C. E., et al. (2007). Activity in the human ventral striatum social comparison affects reward-related brain. *Science* 318, 1305–1308. doi: 10.1126/science.1145876

Gagné, M., and Deci, E. L. (2005). Self-determination theory and work motivation. *J. Organ. Behav.* 26, 331–362. doi: 10.1002/job.322

Gehring, W. J., Goss, B., Coles, M. G. H., Meyer, D. E., and Donchin, E. (1993). A neural system for error detection and compensation. *Psychol. Sci.* 4, 385–390. doi: 10.1111/j.1467-9280.1993.tb00586.x

Gehring, W. J., Liu, Y., Orr, J. M., and Carp, J. (2012). "The error-related negativity (ERN/Ne)," in *The Oxford Handbook of Event-Related Potential Components*, eds S. J. Luck and E. S. Kappenman (New York, NY: Oxford University Press), 231–291.

Haivas, S., Hofmans, J., and Pepermans, R. (2013). Volunteer engagement and intention to quit from a self-determination theory perspective. *J. Appl. Soc. Psychol.* 43, 1869–1880. doi: 10.1111/jasp.12149

Jagacinski, C. M., and Nicholls, J. G. (1987). Competence and affect in task involvement and ego involvement: the impact of social comparison information. *J. Educ. Psychol.* 79, 107–114. doi: 10.1037/0022-0663.79.2.107

Jin, J., Yu, L., and Ma, Q. (2015). Neural basis of intrinsic motivation: evidence from event-related potentials. *Comput. Intell. Neurosci.* 2015:698725. doi: 10.1155/2015/698725

Koestner, R., Ryan, R. M., Bernieri, F., and Holt, K. (1984). Setting limits on children's behavior: the differential effects of controlling vs. informational styles on intrinsic motivation and creativity. *J. Pers.* 52, 233–248. doi: 10.1111/j.1467-6494.1984.tb00879.x

Kotani, Y., Ohgami, Y., Ishiwata, T., Arai, J., Kiryu, S., and Inoue, Y. (2015). Source analysis of stimulus-preceding negativity constrained by functional magnetic resonance imaging. *Biol. Psychol.* 111, 53–64. doi: 10.1016/j.biopsycho.2015.08.005

Lindner, M., Rudorf, S., Birg, R., Falk, A., Weber, B., and Fliessbach, K. (2014). Neural patterns underlying social comparisons of personal performance. *Soc. Cogn. Affect. Neurosci.* 10, 569–576. doi: 10.1093/scan/nsu087

Ma, Q., Jin, J., Meng, L., and Shen, Q. (2014). The dark side of monetary incentive: how does extrinsic reward crowd out intrinsic motivation. *Neuroreport* 25, 194–198. doi: 10.1097/WNR.0000000000000113

Ma, Q., Pei, G., and Meng, L. (2017). Inverted u-shaped curvilinear relationship between challenge and one's intrinsic motivation: evidence from event-related potentials. *Front. Neurosci.* 11:131. doi: 10.3389/fnins.2017.00131

Matthews, G., Campbell, S. E., Falconer, S., Joyner, L. A., Huggins, J., Gilliland, K., et al. (2002). Fundamental dimensions of subjective state in performance settings: task engagement, distress and worry. *Emotion* 2, 315–340. doi: 10.1037/1528-3542.2.4.315

Matthews, G., Warm, J. S., Reinerman, L. E., Langheim, L. K., and Saxby, D. J. (2010a). "Task engagement, attention and executive control," in *Handbook of Individual Differences in Cognition: Attention, Memory and Executive Control*, eds A. Gruszka, G. Matthews and B. Szymura (New York, NY: Springer), 205–230.

Matthews, G., Warm, J. S., Reinerman-Jones, L. E., Langheim, L. K., Washburn, D. A., and Tripp, L. (2010b). Task engagement, cerebral blood flow velocity and diagnostic monitoring for sustained attention. *J. Exp. Psychol. Appl.* 16, 187–203. doi: 10.1037/a0019572

Meng, L., and Ma, Q. (2015). Live as we choose: the role of autonomy support in facilitating intrinsic motivation. *Int. J. Psychophysiol.* 98, 441–447. doi: 10.1016/j.ijpsycho.2015.08.009

Meng, L., and Yang, Z. (2018). Feedback is the breakfast of champions: the significance of self-controlled formal feedback for autonomous task engagement. *Neuroreport* 29, 13–18. doi: 10.1097/WNR.0000000000000921

Meng, L., Pei, G., Zheng, J., and Ma, Q. (2016). Close games versus blowouts: optimal challenge reinforces one's intrinsic motivation to win. *Int. J. Psychophysiol.* 110, 102–108. doi: 10.1016/j.ijpsycho.2016.11.001

Murayama, K., Matsumoto, M., Izuma, K., and Matsumoto, K. (2010). Neural basis of the undermining effect of monetary reward on intrinsic motivation. *Proc. Natl. Acad. Sci. U S A* 107, 20911–20916. doi: 10.1073/pnas.1013305107

Pittman, T. S., Davey, M. E., Alafat, K. A., Wetherill, K. V., and Kramer, N. A. (1980). Informational versus controlling verbal rewards. *Pers. Soc. Psychol. Bull.* 6, 228–233. doi: 10.1177/014616728062007

Reeve, J. (2012). "A self-determination theory perspective on student engagement," in *Handbook of Research on Student Engagement*, eds S. L. Christenson, A. L. Reschly and C. Wylie (New York, NY: Springer), 149–172.

Reeve, J., and Deci, E. L. (1996). Elements of the competitive situation that affect intrinsic motivation. *Pers. Soc. Psychol. Bull.* 22, 24–33. doi: 10.1177/0146167296221003

Reeve, J., and Lee, W. (2014). Students' classroom engagement produces longitudinal changes in classroom motivation. *J. Educ. Psychol.* 106, 527–540. doi: 10.1037/a0034934

Rich, B. L. (2006). *Job Engagement: Construct Validation and Relationships with Job Satisfaction, Job Involvement and Intrinsic Motivation.* (Unpublished doctoral dissertation) Gainesville, FL: University of Florida.

Riesel, A., Weinberg, A., Endrass, T., Meyer, A., and Hajcak, G. (2013). The ERN is the ERN is the ERN? Convergent validity of error-related brain activity across different tasks. *Biol. Psychol.* 93, 377–385. doi: 10.1016/j.biopsycho.2013.04.007

Ryan, R. M. (1982). Control and information in the intrapersonal sphere: an extension of cognitive evaluation theory. *J. Pers. Soc. Psychol.* 43, 450–461. doi: 10.1037/0022-3514.43.3.450

Ryan, R. M., and Deci, E. L. (2017). *Self-Determination Theory: Basic Psychological Needs in Motivation, Development and Wellness.* New York, NY: Guilford Publications.

Ryan, R. M., Mims, V., and Koestner, R. (1983). Relation of reward contingency and interpersonal context to intrinsic motivation: a review and test using. *J. Pers. Soc. Psychol.* 45, 736–750. doi: 10.1037/0022-3514.45.4.736

San Martín, R. (2012). Event-related potential studies of outcome processing and feedback-guided learning. *Front. Hum. Neurosci.* 6:304. doi: 10.3389/fnhum.2012.00304

Santesso, D. L., Segalowitz, S. J., and Schmidt, L. A. (2005). ERP correlates of error monitoring in 10-year olds are related to socialization. *Biol. Psychol.* 70, 79–87. doi: 10.1016/j.biopsycho.2004.12.004

Simon, D., Becker, M. P. I., Mothes-Lasch, M., Miltner, W. H. R., and Straube, T. (2014). Effects of social context on feedback-related activity in the human ventral striatum. *NeuroImage* 99, 1–6. doi: 10.1016/j.neuroimage.2014.05.071

Stoeber, J., Davis, C. R., and Townley, J. (2013). Perfectionism and workaholism in employees: the role of work motivation. *Pers. Individ. Dif.* 55, 733–738. doi: 10.1016/j.paid.2013.06.001

Stone, D. N., Deci, E. L., and Ryan, R. M. (2008). Beyond talk: creating autonomous motivation through self-determination theory. *J. Gen. Manage.* 33, 1867–1876. doi: 10.1177/030630700903400305

Suls, J., and Wheeler, L. (2000). *Handbook of Social Comparison: Theory and Research.* Dordrecht: Kluwer.

Thomas, K. W. (2009). *Intrinsic Motivation at Work: What Really Drives Employee Engagement?* San Francisco: Berrett-Koehler Publishers.

Tops, M., Boksem, M. A., Wester, A. E., Lorist, M. M., and Meijman, T. F. (2006). Task engagement and the relationships between the error-related negativity, agreeableness, behavioral shame proneness and cortisol. *Psychoneuroendocrinology* 31, 847–858. doi: 10.1016/j.psyneuen.2006.04.001

Ullsperger, M., Danielmeier, C., and Jocham, G. (2014). Neurophysiology of performance monitoring and adaptive behavior. *Physiol. Rev.* 94, 35–79. doi: 10.1152/physrev.00041.2012

Vallerand, R. J., Gauvin, L. I., and Halliwell, W. R. (1986). Negative effects of competition on children's intrinsic motivation. *J. Soc. Psychol.* 126, 649–656. doi: 10.1080/00224545.1986.9713638

van Boxtel, G. J. M., and Böcker, K. B. E. (2004). Cortical measures of anticipation. *J. Psychophysiol.* 18, 61–76. doi: 10.1027/0269-8803.18.23.61

Vidal, F., Burle, B., Bonnet, M., Grapperon, J., and Hasbroucq, T. (2003). Error negativity on correct trials: a reexamination of available data. *Biol. Psychol.* 64, 265–282. doi: 10.1016/s0301-0511(03)00097-8

Wang, L., Sun, H., Li, L., and Meng, L. (2018). Hey, what is your choice? uncertainty and inconsistency enhance subjective anticipation of upcoming information in a social context. *Exp. Brain Res.* 236, 2797–2810. doi: 10.1007/s00221-018-5336-x

Wang, L., Zheng, J., and Meng, L. (2017). Effort provides its own reward: endeavors reinforce subjective expectation and evaluation of task performance. *Exp. Brain Res.* 235, 1107–1118. doi: 10.1007/s00221-017-4873-z

Wayment, H. A., and Taylor, S. E. (1995). Self-evaluation processes: motives, information use and self-esteem. *J. Pers.* 63, 729–757. doi: 10.1111/j.1467-6494.1995.tb00315.x

Wills, T. A. (1981). Downward comparison principles in social psychology. *Psychol. Bull.* 90, 245–271. doi: 10.1037/0033-2909.90.2.245

Wood, J. V. (1996). What is social comparison and how should we study it? *Pers. Soc. Psychol. Bull.* 22, 520–537. doi: 10.1177/0146167296225009

**Conflict of Interest Statement**: The authors declare that the research was conducted in the absence of any commercial or financial relationships that could be construed as a potential conflict of interest.

frontiers in Human Neuroscience

GENERAL COMMENTARY
published: 03 December 2018
doi: 10.3389/fnhum.2018.00480

# Commentary: Efficacy and Safety of Transcranial Direct Current Stimulation as an Add-on Treatment for Bipolar Depression: A Randomized Clinical Trial

*Zhen-Yu Hu†, Xiaoli Liu†, Hong Zheng† and Dong-Sheng Zhou**

*Ningbo Kangning Hospital, Ningbo, China*

**Keywords: transcranial direct current stimulation (tDCS), bipolar depression, dorsolateral prefrontal cortex, Hamilton depression rating scale (HAMD), randomizad controlled trial**

**A commentary on**

**Efficacy and Safety of Transcranial Direct Current Stimulation as an Add-on Treatment for Bipolar Depression: A Randomized Clinical Trial**
*by Sampaio-Junior, B., Tortella, G., Borrione, L., Moffa, A. H., Machado-Vieira, R., Cretaz, E., et al. (2018). JAMA Psychiatry 75, 158–166. doi: 10.1001/jamapsychiatry.2017.4040*

OPEN ACCESS

***Edited by:***
*Wenbo Luo,*
*Liaoning Normal University, China*

***Reviewed by:***
*Andrea De Bartolomeis,*
*Università degli Studi di Napoli Federico II, Italy*
*Dandan Zhang,*
*Shenzhen University, China*

***Correspondence:**
*Dong-Sheng Zhou*
*wyzhouds@sina.com*

*†These authors have contributed equally to this work*

***Received:*** *12 July 2018*
***Accepted:*** *16 November 2018*
***Published:*** *03 December 2018*

***Citation:***
*Hu Z-Y, Liu X, Zheng H and Zhou D-S (2018) Commentary: Efficacy and Safety of Transcranial Direct Current Stimulation as an Add-on Treatment for Bipolar Depression: A Randomized Clinical Trial. Front. Hum. Neurosci. 12:480. doi: 10.3389/fnhum.2018.00480*

Bipolar disorder is a severe, recurrent psychiatric disorder, characterized by repeated remission and deterioration (Soares-Weiser et al., 2007). Bipolar disorder causes a high burden medical care for the individuals and society (Ferrari et al., 2016). Compared to manic episode, depressive one is much more frequent and prolonged in bipolar disorder patients (Suppes et al., 2005). Currently there are several therapeutic approaches for bipolar depression (BD), including pharmacological treatment, electroconvulsive therapy (ECT), cognitive behavioral therapy (CBT) and repetitive transcranial magnetic stimulation (rTMS) (Judd et al., 2002; Okumura and Ichikura, 2014; Blumberger et al., 2018).

Transcranial direct current stimulation (tDCS) is a non-invasive brain stimulation (NIBS) method with proven efficacy for neuropsychiatric disorders. It is also easily portable, with low cost and simple for manipulation. It delivers a weak current to the cortex through scalp electrodes and then induces changes in cortical excitability (Chang et al., 2015). Anodal stimulation facilitates depolarization of neurons, which enhances the cortex excitability, cathodal stimulation leads to hyperpolarization of neurons, which inhibits the cortex function (Nitsche et al., 2003; Hasan et al., 2011). tDCS stimulation leads to changes in connected cortical and subcortical regions as well (Stagg et al., 2010; Lang et al., 2015). Previous studies demonstrated the prospective potential of tDCS in unipolar depression (Shiozawa et al., 2014; Brunoni et al., 2016). However, few studies have been conducted on the treatment effectiveness of tDCS in BD.

Recently, Sampaio-Junior et al. conducted the first randomized sham-control clinical trial on 59 subjects, which intended to determine the efficacy and safety of tDCS for BD (Sampaio-Junior et al., 2018). Requirements for the participants are between the ages of 18 and 65, diagnosed BD, Hamilton Depression Rating Scale (HDRS-17) scored higher than 17, low suicide risk (evaluated by Mini-International Neuropsychiatric Interview questionnaire), in stable condition after 4-week pharmacologic treatment. The connections to the stimulator were concealed so that neither experimenter nor participant could determine the polarity of stimulation. HDRS-17, Montgomery-Åsberg Depression Rating Scale, Clinical Global Impression(CGI) depression scale, cumulative

responses (defined as from baseline, HDRS-17 scores reduced >50% at week 2, 4, 6), remission rates were totally assessed at baseline, week 2, week 4, and week 6. In addition, rates of adverse events were recorded at week 2, 6.

Similar to many tDCS and rTMS studies, the clinical trial was administered to dorsolateral prefrontal cortex (DLPFC), which is a core region involves in cognitive control and emotion modulation. The location of DLPFC was determined by EASYstrap, a better positioning method compared to other methods. The anode (left) and cathode (right) electrode were placed on the bilateral DLPFC, respectively. 12 sessions of 2 mA (30 min) tDCS were performed, ten of which applied daily from Monday to Friday, with weekends off, two of which were performed at week 4 and 6 (study end point). The treatment schedule was same to previous studies, which made the results comparable (Brunoni et al., 2013).

The randomized sham-control trial continued for nearly 2 years. In active tDCS group, HDRS-17 score declined significantly when compared to the baseline. Through Kaplan-Meier analysis, the add-on intervention group shown to be more efficacious than sham group, showing higher cumulative response rate and remission rate. In addition, the change of Montgomery-Åsberg Depression Rating Scale indicated that active tDCS group had significant improvements than sham group ($P < 0.05$, but not significant in CGI). Besides skin redness, other adverse event rates were insignificantly different between active and sham group at each time point.

Previous studies only conducted small sample sized open-label protocol in mixed population of unipolar-bipolar subjects (Brunoni et al., 2012; Palm et al., 2012). The study was the first randomized double-blind sham-control trial to confirm the efficacy and safety of prefrontal tDCS applied to BD. The study would provide insights for further large multi-center studies. In addition, as we all know the BD patients suffered cognitive impairment (Wingo et al., 2009), it raises a concern whether tDCS treatment would enhance BD cognitive behaviors such as working memory, emotion process, attention bias and so on.

There are still some limitations in the present study. First, it is unknown if active tDCS was superior than sham in sustained remission. Perhaps this is due to the fact that remission analysis or tDCS design was not optimal? Second, CGI depression scale might not be sensitive for current sample population—given the less severity. Third, though utilizing proper randomization methods, the random distributions of baseline variables of the small sample were imbalanced. Forth, in integrity of blinding, as nearly three-fifths participants of each group identified correctly the allocation group, which might cause guinea pig effect.

In conclusion, the trial based on small sample presented the effectiveness, tolerance and safety of tDCS in bipolar depression patients. The promising result also inspires further research to demonstrate the efficacy of tDCS on BD in a large sample. Neuroscience studies indicated that individuals with BD displays cognitive deficits (Depp et al., 2016), so whether add-on tDCS intervention showing positive impacts on cognition requires more explorations.

The underlying neural mechanism of why tDCS can treat BD is yet unknown. Neuroplasticity as a neurophysiologic condition for depression is well recognized (Henn and Vollmayr, 2004), which is unclear if this is the case for BD patients. It is possible that tDCS induced neuroplasticity might contribute to alleviation of unipolar depression symptoms (Nitsche et al., 2009), which warrants further investigation.

## AUTHOR CONTRIBUTIONS

D-SZ designed the study. Z-YH, XL performed and write the study. HZ contributed to revised work. All authors have read and approved the final version of the manuscript.

## FUNDING

The study was supported by the Medical Science and Technology Project in Ningbo (2016A37, 2017A10) and the Major Science and Technology Projects in Ningbo, Zhejiang Province, China (2017C510012).

## ACKNOWLEDGMENTS

The authors thank their department for supports.

## REFERENCES

Blumberger, D. M., Vila-Rodriguez, F., Thorpe, K. E., Feffer, K., Noda, Y., Giacobbe, P., et al. (2018). Effectiveness of theta burst versus high-frequency repetitive transcranial magnetic stimulation in patients with depression (THREE-D): a randomised non-inferiority trial. *Lancet* 391, 1683–1692. doi: 10.1016/S0140-6736(18)30295-2

Brunoni, A. R., Ferrucci, R., Bortolomasi, M., Scelzo, E., Boggio, P. S., Fregni, F., et al. (2012). Interactions between transcranial direct current stimulation (tDCS) and pharmacological interventions in the Major Depressive Episode: findings from a naturalistic study. *Eur. Psychiatry* 28, 356–361. doi: 10.1016/j.eurpsy.2012.09.001

Brunoni, A. R., Moffa, A. H., Fregni, F., Palm, U., Padberg, F., Blumberger, D. M., et al. (2016). Transcranial direct current stimulation for acute major depressive episodes: meta-analysis of individual patient data. *Br. J. Psychiatry J. Ment. Sci.* 208:522. doi: 10.1192/bjp.bp.115.164715

Brunoni, A. R., Valiengo, L., Baccaro, A., Zanão, T. A., de Oliveira, J. F., Goulart, A., et al. (2013). The sertraline vs. electrical current therapy for treating depression clinical study: results from a factorial, randomized, controlled trial. *JAMA Psychiatry* 70, 383–391. doi: 10.1001/2013.jamapsychiatry.32

Chang, M. C., Kim, D. Y., and Park, D. H. (2015). Enhancement of cortical excitability and lower limb motor function in patients with stroke by transcranial direct current stimulation. *Brain Stimulat.* 8, 561–566. doi: 10.1016/j.brs.2015.01.411

Depp, C. A., Dev, S., and Eyler, L. T. (2016). Bipolar depression and cognitive impairment: shared mechanisms and new treatment avenues. *Psychiatr. Clin. North Am.* 39, 95–109. doi: 10.1016/j.psc.2015.09.004

Ferrari, A. J., Stockings, E., Khoo, J. P., Erskine, H. E., Degenhardt, L., Vos, T., et al. (2016). The prevalence and burden of bipolar disorder: findings from the Global Burden of Disease Study 2013. *Bipolar Disord.* 18, 440–450. doi: 10.1111/bdi.12423

Hasan, A., Nitsche, M. A., Rein, B., Schneider-Axmann, T., Guse, B., Gruber, O., et al. (2011). Dysfunctional long-term potentiation-like plasticity in schizophrenia revealed by transcranial direct current stimulation. *Behav. Brain Res.* 224, 15–22. doi: 10.1016/j.bbr.2011.05.017

Henn, F. A., and Vollmayr, B. (2004). Basic pathophysiological mechanisms in depression: what are they and how might they affect the course of the illness? *Pharmacopsychiatry* 37, 152–156. doi: 10.1055/s-2004-832670

Judd, L. L., Akiskal, H. S., Schettler, P. J., Endicott, J., Maser, J., Solomon, D. A., et al. (2002). The long-term natural history of the weekly symptomatic status of bipolar I disorder. *Arch. Gen. Psychiatry* 59, 530–537. doi: 10.1001/archpsyc.59.6.530

Lang, N., Siebner, H. R., Ward, N. S., Lee, L., Nitsche, M. A., Paulus, W., et al. (2015). How does transcranial DC stimulation of the primary motor cortex alter regional neuronal activity in the human brain? *Eur. J. Neurosci.* 22, 495–504. doi: 10.1111/j.1460-9568.2005.04233.x

Nitsche, M. A., Kuo, M. F., Karrasch, R., Wächter, B., Liebetanz, D., and Paulus, W. (2009). Serotonin affects transcranial direct current-induced neuroplasticity in humans. *Aktuelle Neurologie* 66:503. doi: 10.1016/j.biopsych.2009.03.022

Nitsche, M. A., Liebetanz, D., Lang, N., Antal, A., Tergau, F., and Paulus, W. (2003). Safety criteria for transcranial direct current stimulation (tDCS) in humans. *Clin. Neurophysiol.* 114, 2220–2222. doi: 10.1016/S1388-2457(03)00235-9

Okumura, Y., and Ichikura, K. (2014). Efficacy and acceptability of group cognitive behavioral therapy for depression: a systematic review and meta-analysis. *J. Affect. Disord.* 164, 155–164. doi: 10.1016/j.jad.2014.04.023

Palm, U., Schiller, C., Fintescu, Z., Obermeier, M., Keeser, D., Reisinger, E., et al. (2012). Transcranial direct current stimulation in treatment resistant depression: a randomized double-blind, placebo-controlled study. *Brain Stimulat.* 5, 242–251. doi: 10.1016/j.brs.2011.08.005

Sampaio-Junior, B., Tortella, G., Borrione, L., Moffa, A. H., Machado-Vieira, R., Cretaz, E., et al. (2018). Efficacy and safety of transcranialdirect current stimulation as an add-on treatment for bipolar depression: a randomized clinical trial. *JAMA Psychiatry* 75, 158–166. doi: 10.1001/jamapsychiatry.2017.4040

Shiozawa, P., Fregni, F., Benseñor, I. M., Lotufo, P. A., Berlim, M. T., Daskalakis, J. Z., et al. (2014). Transcranial direct current stimulation for major depression: an updated systematic review and meta-analysis. *Int. J. Neuropsychopharmacol.* 17, 1443–1452. doi: 10.1017/S1461145714000418

Soares-Weiser, K., Bravo Vergel, Y., Beynon, S., Dunn, G., Barbieri, M., Duffy, S., et al. (2007). A systematic review and economic model of the clinical effectiveness and cost-effectiveness of interventions for preventing relapse in people with bipolar disorder. *Health Technol. Assess* 11, iii-iv, ix-206. doi: 10.3310/hta11390

Stagg, C. J., O'Shea, J., Kincses, Z. T., Woolrich, M., Matthews, P. M., and Johansen-Berg, H. (2010). Modulation of movement-associated cortical activation by transcranial direct current stimulation. *Eur. J. Neurosci.* 30, 1412–1423. doi: 10.1111/j.1460-9568.2009.06937.x

Suppes, T., Kelly, D. I., and Perla, J. M. (2005). Challenges in the management of bipolar depression. *J. Clin. Psychiatry* 66, 11–16.

Wingo, A. P., Harvey, P. D., and Baldessarini, R. J. (2009). Neurocognitive impairment in bipolar disorder patients: functional implications. *Bipolar Disord.* 11, 113–125. doi: 10.1111/j.1399-5618.2009.00665.x

**Conflict of Interest Statement:** The authors declare that the research was conducted in the absence of any commercial or financial relationships that could be construed as a potential conflict of interest.

frontiers in Human Neuroscience

ORIGINAL RESEARCH
published: 28 January 2019
doi: 10.3389/fnhum.2018.00541

# Mindfulness Improves Emotion Regulation and Executive Control on Bereaved Individuals: An fMRI Study

*Feng-Ying Huang[1], Ai-Ling Hsu[2], Li-Ming Hsu[3], Jaw-Shiun Tsai[4,5], Chih-Mao Huang[6], Yi-Ping Chao[7], Tzung-Jeng Hwang[8] and Changwei W. Wu[9,10]**

[1] Department of Education, College of Education, National Taipei University of Education, Taipei, Taiwan, [2] Department of Radiology, Wan Fang Hospital, Taipei Medical University, Taipei, Taiwan, [3] Department of Radiology and Biomedical Research Imaging Center, School of Medicine, University of North Carolina at Chapel Hill, Chapel Hill, NC, United States, [4] Department of Family Medicine, College of Medicine and Hospital, National Taiwan University, Taipei, Taiwan, [5] Center for Complementary and Integrated Medicine, National Taiwan University Hospital, Taipei, Taiwan, [6] Department of Biological Science and Technology, College of Biological Science and Technology, National Chiao Tung University, Hsinchu, Taiwan, [7] Graduate Institute of Medical Mechatronics, Chang Gung University, Taoyuan, Taiwan, [8] Department of Psychiatry, National Taiwan University Hospital and College of Medicine, Taipei, Taiwan, [9] Graduate Institute of Mind, Brain and Consciousness, Taipei Medical University, Taipei, Taiwan, [10] Research Center of Brain and Consciousness, Shuang Ho Hospital, New Taipei, Taiwan

The grief of bereavement is recognized as a severe psychosocial stressor that can trigger a variety of mental and physical disorders, and the long-lasting unresolved grief has a detrimental effect on brain functionality. Literature has documented mindfulness-based cognitive therapy (MBCT) as an efficient treatment for improving well-being, specifically related to the mood and cognition, in a variety of populations. However, little attention has been devoted to neural mechanisms with regard to bereaved individuals' cognition after MBCT intervention. In this study, we recruited 23 bereaved participants who lost a significant relative within 6 months to 4 years to attend 8-week MBCT course. We used self-reporting questionnaires to measure emotion regulation and functional magnetic resonance imaging (fMRI) with the numerical Stroop task to evaluate the MBCT effect on executive control among the bereaved participants. The self-reported questionnaires showed improvements on mindfulness and reductions in grief, difficulties in emotion regulation, anxiety, and depression after the MBCT intervention. The fMRI analysis demonstrated two scenarios: (1) the activity of the fronto-parietal network slightly declined accompanied with significant improvements in the reaction time of incongruent trials; (2) the activities in the posterior cingulate cortex and thalamus were positively associated with the Texas Revised Inventory of Grief, implying emotional interferences on cognitive functions. Results indicated that MBCT facilitated the executive control function by alleviating the emotional interferences over the cognitive functions and suggested that the 8-week MBCT intervention significantly improved both executive control and emotion regulation in bereaved individuals.

**Keywords: bereavement grief, mindfulness-based cognitive therapy (MBCT), emotion regulation, executive control, functional magnetic resonance imaging (fMRI)**

OPEN ACCESS

***Edited by:***
*Xiaochu Zhang,*
*University of Science and Technology of China, China*

***Reviewed by:***
*Der-Yow Chen,*
*National Cheng Kung University, Taiwan*
*Qihong Zou,*
*Peking University, China*

****Correspondence:***
*Changwei W. Wu*
*sleepbrain@tmu.edu.tw*

***Received:*** *15 October 2018*
***Accepted:*** *31 December 2018*
***Published:*** *28 January 2019*

***Citation:***
*Huang F-Y, Hsu A-L, Hsu L-M, Tsai J-S, Huang C-M, Chao Y-P, Hwang T-J and Wu CW (2019) Mindfulness Improves Emotion Regulation and Executive Control on Bereaved Individuals: An fMRI Study. Front. Hum. Neurosci. 12:541. doi: 10.3389/fnhum.2018.00541*

## INTRODUCTION

Suffering the death of a loved one is recognized as a severe psychological stressor that results in a time of excessive risk of mental and physical problems (Stroebe et al., 2007; Buckley et al., 2010). The emotional response to bereavement, mainly referred to as grief, incorporates diverse biological, psychological, and behavioral symptoms. Bereavement grief has been associated with symptoms of depression, distress, and anxiety (Byrne and Raphael, 1997; Zisook et al., 1997; Taylor et al., 1999). These negative impacts thus complicated bereaved individuals' heath problems (Beem et al., 2000; Buckley et al., 2010; Assareh et al., 2015) and potentially cause a reduction in cognitive functions (Clayton et al., 1971; Gündel et al., 2003; Rosnick et al., 2010). Furthermore, considerable evidence has also shown increased mortality and morbidity rates in the early months of bereavement (Young et al., 1963; Lichtenstein et al., 1998; Christakis and Iwashyna, 2003; Hart et al., 2007), although widowers have been identified as possibly most at risk (Kaprio et al., 1987; Buckley et al., 2010).

Mindfulness is commonly defined as paying attention to the internal and external experiences occurring in the present moment, without judgment or reaction (Kabat-Zinn, 1994). Fostering the ability to be focused on the present moment and detached observers of our inner cognition or emotions that are adopted during mindfulness training is thought to promote cognitive function and to enhance objective and adaptive strategies of responding to emotional or cognitive triggers (Bishop, 2004; Kang et al., 2013). Neuroimaging research of mindfulness also demonstrated that mindfulness can reduce the activity of the amygdala and increases the thickness of the cerebral cortex (Hölzel et al., 2011; Kral et al., 2018). Several key elements such as attention regulation, body awareness, emotion regulation, acceptance, self-transcendence, and cognitive flexibility are considered to be developed effectively by mindfulness training (Shapiro et al., 2006; Moore and Malinowski, 2009; Hölzel et al., 2011; Vago and Silbersweig, 2012). Research on mindfulness has been well documented to be beneficial for people's emotional regulation (Hölzel et al., 2011; Teper and Inzlicht, 2013; Roemer et al., 2015), such as in psychotherapy for Major Depressive Disorder (Ma and Teasdale, 2004), Anxiety Disorder (Goldin and Gross, 2010). The mindfulness-based intervention has been found to decrease relapse or recurrence of depression (Teasdale et al., 2000), with equivalent effectiveness to antidepressant treatment (Kuyken et al., 2015), to strengthen the ability of emotion regulation, such as the management of anxiety symptoms (Hoge et al., 2013) and stress (Shapiro et al., 2005). Remarkably, mindfulness interventions have been reported to improve executive functions (Teper and Inzlicht, 2013), such as working memory and sustained attention and attention switching (Chambers et al., 2007; Jha et al., 2007; Zeidan et al., 2010). In addition, based on a review paper conducted by Gallant (2016), the benefit of mindfulness on inhibition is more consistently identified than other executive functions.

Given the reviewed literature on beneficial effects of mindfulness, mindfulness-based cognitive therapy (MBCT) is developed accordingly as a group-based intervention that teaches participants (1) keeping awareness without fusion with contents of cognition or psychophysical experiences; (2) observing the emotional arousals corresponding to the stressful events, such as grief and negative thought specifically evoked by the death of relative one; (3) accepting the emotion without judgments and then switching attention to a neutral object (e.g., the body sensations or breath) (Teasdale et al., 2000; Segal et al., 2002, 2013). MBCT has been proven a great success in assisting patients with depressive and bipolar disorders for exercising mood regulation, and broad attention and inhibitory control (Kuyken et al., 2015; Lovas and Schuman-Olivier, 2018). Although MBCT provides a positive impact on bereaved individuals, the remaining issues are whether emotional disentanglements improve cognitive functions and what the underlying neurophysiological basis is. Henceforth, we examined MBCT modulations on bereaved individuals in terms of their neural activities using a cognitive-fMRI experiment with the numerical Stroop task, and emotion regulation abilities using a series of self-reported questionnaires. We therefore hypothesized that the cognitive function in bereaved participants would be improved following the MBCT training, where the same participants were evaluated before and after the MBCT intervention.

## MATERIALS AND METHODS

We used the experimental design with both self-reported questionnaires and fMRI sessions before the 8-week MBCT training (***Pre***) and after MBCT intervention (***Post***), respectively. A within-subject design was employed to compare the cognitive performance and fMRI activation changes related to 8-week MBCT intervention.

### Participants

Twenty-three bereaved subjects (21 females and 2 males) aged between 25 and 66 (mean = 48.35, *SD* = 11.14) having lost at least one significant relative within 6 months to 4 years and having self-reported unresolved grief participated in the study. The participants were recruited by flyers distributed throughout the Taipei city and by advertising in National Taipei University in Education's Internet forums. All Participants were native Mandarin speakers. Participants would receive a free 8-week MBCT course. Exclusion criteria were: previous mindfulness meditation experience, history of psychological/psychiatric disease, use of prescription drugs, and MR incompatibility. Four of these were excluded for the following reasons: two moved out of city before the MBCT intervention; one dropped out in the middle of intervention; another one could not make it to the MRI scan after intervention. Complete data sets were thus available from 19 and 20 participants for fMRI scanning and questionnaire analysis, respectively. Written informed consent was obtained from each participant in accordance with the guidelines and the study protocol approved by the Research Ethics Office of National Taiwan University.

## Self-Reported Questionnaires

The severity of grief was assessed by Texas Revised Inventory of Grief (TRIG) (Faschingbauer et al., 1987), which is composed of the parts of past behaviors and present feelings. Since the aim of this study is to evaluate the effects of MBCT intervention on the present cognitive and emotion reactions, only present grief part of the inventory was used in the present study. In testing the tendency of anxiety level and the severity of depressive symptoms, the Generalized Anxiety Disorder-7 (GAD-7) (Spitzer et al., 2006) and the 18-item Taiwan Depression Scale (Lee et al., 2000) were adopted, respectively. To further evaluate the degree of difficulty of emotion regulation, Difficulties in Emotion Regulation Scale (DERS) (Gratz and Roemer, 2004) was employed.

The Five Facet Mindfulness Questionnaire (FFMQ) is a widely used 39-item questionnaire sensitively assessing the traits that are cultivated by mindfulness (Baer et al., 2008). Since the validity and reliability of the Taiwanese version of FFMQ has been verified elsewhere (Huang et al., 2015), we directly employed the T-FFMQ and reported the total scores in this study.

## Mindfulness-Based Cognitive Therapy (MBCT)

The intervention followed the group-based MBCT program (Segal et al., 2013), which consists of once-weekly meetings (with a duration of 2.5 h) plus daily home practice (30–40 min a day) in the 8 weeks of the course. During the group sessions, participants were led by a group therapist with skills training and in-class practice in (1) guided meditation, (2) experiential exercises, and (3) discussions of the participants' daily practices. The group therapist, the first author of this study, is a certificated grief therapist and has more than 3,200 h of experience in facilitating mindfulness group interventions. Specific in-class guided meditation included body scans, sitting meditation, compassion meditation, and yoga. In addition to the group sessions, participants were instructed to practice mindfulness exercises aided by standard audio-recordings throughout the day, and to record their daily practice times at home, which were evaluated in the weekly course session. Furthermore, an extra 2-h introduction session of "acknowledgment of grief and theory of psycho-physical reactions to loss" specifically designed for bereaved individuals was added before the standard MBCT program.

## Experimental Tasks

The fMRI session was divided into three sessions with two sessions of numerical Stroop tasks. Stimuli were presented via E-prime (Psychology Software Tools, Pittsburgh, PA, United States) with a back-projection system. The visual stimuli were presented in 800 × 600 resolution. Participants viewed the stimuli using a mirror mounted on the head-coil and the viewing field was 8.4° (H) by 6.3° (V) at a viewing distance of 420 cm. Participants were instructed to respond with a button press using the index and middle fingers of their right hand (Lumina response pad; Cedrus, San Pedro, CA, United States).

We conducted the numerical Stroop tasks in the current study to assess the executive control function for bereaved participants. Two types of magnitude judgments were included in this task: a physical size task and a numerical magnitude task. In the physical size task, participants were presented with a pair of digits and were instructed to judge which digit was physically larger while ignoring the numerical magnitude of the digits. On the other hand, in the numerical magnitude task, participants were viewing a pair of digits and were asked to indicate which was numerically larger while ignoring their physical size. In both tasks, the individual digits between 1 and 9 excluding 5 were used to create the digit pairs, and digit pairs were presented in Arial font with two different font sizes (55 and 73) to manipulate the physical size of the items. For each session in numerical Stroop task, four blocks were designed with two blocks of congruent condition and two blocks of incongruent condition, and the presentation sequence was randomized to minimize the fatigue effects. Each block started with a 30-s fixation-cross resting period and 36-s presentation of digit-pair trials, with each trial consisting of a 1-s fixation and 1-s presentation of stimulus. The participants were asked to make judgments by pressing buttons within the 1-s stimuli presentation periods. In congruent blocks, the digit that was larger in magnitude was also larger in physical size. In incongruent trials, the digit that was larger in magnitude was smaller in the physical size. The total acquisition time for the numerical Stroop task was 264 s.

## MRI Data Acquisition

The MRI experiments were conducted at a 3T PRISMA scanner (Siemens, Erlangen, Germany) at the National Taiwan University. All visual stimuli were given by a projector with E-Prime software, reflected by mirror settings. To alleviate the motion artifact due to the speaking, the head position of participants was immobilized using the thermoset plastics. The scanning protocol included one high-resolution $T_1$-weighted anatomical image using 3D-MPRAGE sequence and two functional sessions of numerical Stroop tasks using a single-shot, gradient-echo-based echo-planar imaging (GE-EPI) sequence. The detailed parameters for 3D-MPRAGE sequence was listed below: 192 × 192 × 176 matrix size; 1 mm × 1 mm × 1 mm in-plane resolution; 900 ms inversion time; repetition time (TR) = 1,900 ms, echo time (TE) = 2.28 ms; flip angle (FA) = 9°; bandwidth = 200 Hz/pixel; NEX = 1. Total scan time is 5 min 21 s. Subsequently, the functional sessions shared the same geometry settings: 37 axial slices (FOV = 220 × 220 $mm^2$, 64 × 64 in-plane matrix size, and 3.4 mm thickness) acquired in an interleaved manner, aligned along the anterior commissure–posterior commissure (AC-PC) line with whole-brain coverage. The GE-EPI scan protocol was using imaging parameters as follows: TR = 2 s, TE = 35 ms, FA = 84°, bandwidth = 2368 Hz/pixel and total acquisition time for each session was 264 s.

## Data Analysis

All MRI data processing were analyzed by using Analysis of Functional Neuroimaging (AFNI) software package (Cox, 1996) and FMRIB Software Library (FSL) (Jenkinson et al., 2012).

**TABLE 1 |** Descriptive and statistical overview of self-reported questionnaires between pre- and post-MBCT on grief bereavement (means and standard deviations).

| Source | Pre-MBCT | | Post-MBCT | | *t*-test | | |
|---|---|---|---|---|---|---|---|
| | *Mean* | *SD* | *Mean* | *SD* | *t*-value | *p*-value | Cohen's *d* |
| TRIG | 49.80 | 13.47 | 37.95 | 12.58 | −3.98 | 0.001** | −0.89 |
| GAD-7 | 10.30 | 5.32 | 6.50 | 5.31 | −2.89 | 0.009** | −0.65 |
| Depression | 23.35 | 11.41 | 12.90 | 11.74 | −5.23 | 0.000** | −1.17 |
| DERS | 103.10 | 19.16 | 88.95 | 19.07 | −3.39 | 0.003** | −0.76 |
| T-FFMQ | 111.10 | 17.18 | 127.45 | 23.94 | 3.57 | 0.002** | 0.80 |

**$p < 0.01$.

The task-fMRI data sets were preprocessed including slice-timing correction, motion correction, spatial normalization into the Montreal Neurological Institute (MNI) template space, 6-mm FWHM spatial smoothing. After preprocessing, task-fMRI responses for the congruent and incongruent conditions were separately modeled by convolving a canonical hemodynamic response function (HRF) with the task paradigm and retrieved the beta value as the effect size. The design matrix in a first-level fixed-effects analysis comprises two regressors of main interest: one for intervention (pre- vs. post-MBCT) and another for condition (congruent or incongruent) contrasts. Furthermore, six additional regressors modeled the head motion in preprocessing were set as the covariates of no interest. Parameter estimates from the resulting contrast maps were then entered into a second-level random-effects analysis to identify brain regions that were significantly activated by a contrast across participants. Voxel-wise one-sample *t*-tests were conducted to detect the activated voxels associated with task conditions under both before and after the MBCT intervention. As the correction for multiple comparisons, the significance level of corrected $p < 0.01$ was set with a combination of uncorrected threshold of $p < 0.001$ and individual cluster size of 90 contiguous voxels. To further interpret the 8-week MBCT effect, we performed the voxel-wise paired sample *t*-test for each task condition. Considering the reduction of statistical sensitivity on intervention effect due to the noise amplification of substation method, the multiple comparison was conducted with an explicit brain mask, and the overall significance level of $p < 0.05$ was controlled in combination of uncorrected threshold of $p < 0.005$ and individual cluster size of 103 contiguous voxels. The group-level activation areas were served as prior knowledge for the following region-of-interest (ROI) analysis. To avoid the double-dipping problem, we extracted the ROI values based on the automated anatomical labeling (AAL) template (Tzourio-Mazoyer et al., 2002) and performed the brain-behavior correlation analysis with questionnaire scores. Furthermore, since the thalamus is generally involved in the emotion regulation (Greicius et al., 2007; Peng et al., 2012), the thalamic ROI was hypothetically selected for the correlation analysis in this study.

The primary behavioral outcome was computed as the percent increase in RT to incongruent stimuli over and above the average RT to congruent stimuli ([(incongruent-congruent)/congruent] × 100) (Colcombe et al., 2005). The percent increase measure was derived to reflect interference unbiased by differences in base RT. Only correct responses were included in the outcome measure. Paired *t*-test was conducted between the MBCT interventions in general. However, if the data distribution violated the normality assumption by Shapiro–Wilk test, the non-parametric Mann–Whitney test was used instead. In addition, a two-way repeated-measure analysis of variance (ANOVA) was performed on within-subject factors of time (pre-MBCT, post-MBCT) and conditions (congruent, incongruent).

# RESULTS

## Results of Self-Reported Questionnaires

To examine self-reported questionnaires with regards to the effectiveness of the MBCT intervention, participants' post-MBCT scores were compared with their pre-MBCT scores on FFMQ, TRIG, DERS, Depression and Anxiety scores by using repeat measure of *t*-test. All scores of mindfulness and psychological variables were significant at $p < 0.01$. For instance, effect of TRIG was significant at $t(19) = -3.98$, $p < 0.001$, $d = -0.89$. Similarly, T-FFMQ was significant at $t(19) = 3.57$, $p < 0.01$, $d = 0.80$. The MBCT intervention was associated with effect sizes (Cohen's *d*) of −0.89, −0.65, −1.17, and −0.76 for alleviating grief, anxiety, depression and difficulty of emotion regulation, respectively, whereas the effect size was 0.80 for improving the mindfulness level. These robust effect sizes indicated that MBCT greatly reduced negative emotions, and increased the mindfulness level among bereaved participants. Summary of the results for each psychological variable were shown in **Table 1**.

**TABLE 2 |** Comparison of reaction time and percentage interference between pre- and post-MBCT on grief bereavement.

| Source | Congruent | | Incongruent | | *% Interference* | |
|---|---|---|---|---|---|---|
| | *Mean* | *SE* | *Mean* | *SE* | *Mean* | *SE* |
| Pre-MBCT | 549.8 | 11.4 | 623.8 | 13.9 | 13.1 | 1.4 |
| Post-MBCT | 564.5 | 10.6 | 608.0 | 11.7 | 8.7 | 1.8 |
| Significance | Interaction: | | | | Mann–Whitney† | |
| | $F(1,18) = 6.73$, $p = 0.018$* | | | | $z = -2.33$, $p = 0.002$** | |

†*Mann–Whitney test was used instead of paired t-test because of the normality violation.* *$p < 0.05$; **$p < 0.01$.

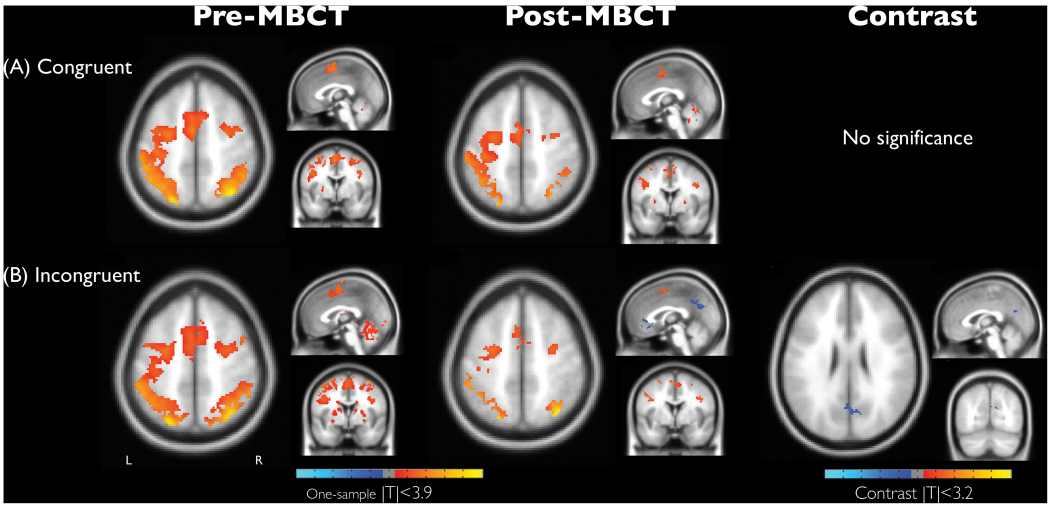


**FIGURE 1 |** Brain activation maps associated with condition effect of **(A)** congruency and **(B)** incongruency and its difference and the intervention effect (before and after MBCT) in the numerical Stroop task on grief bereavement (AlphaSim corrected $p < 0.05$). Anatomical images were shown with coordinate location = [0, 0, 52] for one-sample t maps and [–2, –70, 26] for contrast maps. L, the left hemisphere.

**TABLE 3 |** Peak locations of brain activities associated with congruent condition during the numerical Stroop task, including before and after the MBCT intervention (AlphaSim corrected $p < 0.05$).

| Brain regions | | L/R | AAL | *x* | *y* | *z* | *t*-value |
|---|---|---|---|---|---|---|---|
| ***Pre-MBCT (congruent condition)*** | | | | | | | |
| Frontal | Supplementary motor area | L | 19 | −4 | −4 | 58 | 8.421 |
| | Middle frontal gyrus | R | 8 | 46 | 0 | 56 | 6.288 |
| | Inferior frontal gyrus | R | 12 | 56 | 14 | 20 | 7.161 |
| | | R | 14 | 38 | 28 | 30 | 5.767 |
| Parietal | Inferior parietal lobule | L | 61 | −28 | −56 | 44 | 9.687 |
| | Angular gyrus | R | 66 | 30 | −54 | 46 | 8.515 |
| Occipital | Inferior occipital cortex | L | 53 | −18 | −90 | −8 | 8.131 |
| Cerebellum | | R | 98 | 16 | −50 | −20 | 9.417 |
| | | L | 99 | −24 | −64 | −28 | 7.738 |
| | | R | 104 | 18 | −60 | −46 | 7.11 |
| | | L | 91 | −8 | −76 | −24 | 6.67 |
| Subcortical | Thalamus | L | 77 | −16 | −12 | 10 | 6.117 |
| ***Post-MBCT (congruent condition)*** | | | | | | | |
| Frontal | Precentral gyrus | L | 1 | −30 | −28 | 56 | 9.066 |
| | | R | 2 | 56 | 12 | 36 | 6.216 |
| | | R | 2 | 22 | −6 | 54 | 5.211 |
| | Supplementary motor area | L | 19 | −4 | −4 | 56 | 6.113 |
| Parietal | Angular gyrus | R | 66 | 28 | −58 | 42 | 6.154 |
| | Inferior parietal lobule | R | 62 | 38 | −44 | 56 | 5.584 |
| Occipital | Lingual gyrus | R | 48 | 24 | −88 | −6 | 8.097 |
| | Middle occipital gyrus | L | 51 | −40 | −86 | −4 | 7.599 |
| Temporal | Superior temporal gyrus | L | 81 | −50 | −40 | 24 | 6.676 |
| | Inferior temporal gyrus | R | 90 | 52 | −44 | −10 | 5.633 |
| Cerebellum | | R | 98 | 20 | −48 | −22 | 8.313 |
| | | L | 99 | −20 | −60 | −30 | 6.959 |
| Subcortical | Thalamus | L | 77 | −14 | −22 | 6 | 6.27 |
| | Caudate nucleus | R | 72 | 18 | −8 | 26 | 4.793 |
| | Putamen | R | 74 | 26 | 2 | 16 | 4.781 |

**TABLE 4 |** Peak locations of brain activities associated with incongruent condition during the numerical Stroop task, including before and after the MBCT intervention (AlphaSim corrected $p < 0.05$).

| Brain regions | | L/R | AAL | *x* | *y* | *z* | *t*-value |
|---|---|---|---|---|---|---|---|
| ***Pre-MBCT (incongruent condition)*** | | | | | | | |
| Parietal | Inferior parietal lobule | L | 61 | −40 | −50 | 50 | 9.243 |
| | Postcentral gyrus | R | 58 | 58 | −20 | 32 | 8.198 |
| Occipital | Inferior occipital cortex | R | 54 | 28 | −88 | −2 | 10.584 |
| Cerebellum | | R | 104 | 32 | −52 | −56 | 8.916 |
| | | R | 104 | 20 | −66 | −46 | 6.613 |
| ***Post-MBCT (incongruent condition)*** | | | | | | | |
| Frontal | Supplementary motor area | R | 20 | 6 | 0 | 56 | 6.228 |
| | Anterior cingulate gyrus | L | 31 | −2 | 38 | 0 | −7.867 |
| | Precentral gyrus | L | 1 | −34 | −26 | 56 | 7.031 |
| | | R | 2 | 44 | 6 | 28 | 6.268 |
| | | L | 1 | −32 | −4 | 56 | 5.785 |
| | | R | 2 | 28 | −8 | 52 | 5.619 |
| | | L | 1 | −48 | 0 | 38 | 5.382 |
| | Insula | R | 30 | 32 | 16 | 12 | 6.831 |
| | | L | 29 | −36 | 10 | 10 | 6.269 |
| Parietal | Superior parietal lobule | L | 59 | −24 | −62 | 42 | 6.808 |
| | Rolandic operculum | R | 18 | 40 | −20 | 22 | −6.73 |
| | Angular gyrus | R | 66 | 30 | −54 | 44 | 6.209 |
| | Precuneus | L | 67 | −4 | −62 | 28 | −9.153 |
| | | R | 68 | 6 | −52 | 30 | −7.538 |
| Occipital | Inferior occipital cortex | L | 53 | −22 | −94 | −8 | 6.681 |
| Cerebellum | | R | 100 | 28 | −64 | −26 | 6.227 |
| Subcortical | Caudate nucleus | L | 71 | −18 | −18 | 22 | 6.984 |

This finding indicated that the mindfulness intervention has positive effects on bereaved emotion regulation, grief alleviation, and increase of mindfulness score as significant differences were observed for the comparisons of scores between post-MBCT and pre-MBCT. Furthermore, in order to examine the relationship between mindfulness and affective reactivity, correlation analyses were conducted between the FFMQ scale and post-MBCT intervention negative emotion state, which includes TRIG-Present, GAD-7, Depression, DERS scales. The results indicate that the mindfulness state of post was highly negatively correlated with all negative emotion state, TRIG-Present $r = -0.52$, $p < 0.05$; GAD-7 $r = -0.70$, $p < 0.001$; Depression $r = -0.59$, $p < 0.01$; DERS $r = -0.91$, $p < 0.001$.

## Behavioral Results

Accuracy and RT of all participants were recorded while they performed the Stroop task in the scanner. The accuracy did not present significant difference across MBCT by Mann–Whitney test, *ns* (pre-MBCT accuracy = 86.2% and post-MBCT accuracy = 86.8%). We found that RT to congruent trials (in both numerical magnitude and physical size) was not reliably different between pre- and post-MBCT, $t(37) = 0.59$, *ns*, whereas a significant reduction in RT to incongruent trials, $t(37) = -2.4$, $p < 0.05$. Significant interaction effect of RT was found in intervention × condition, $F(1,18) = 6.73$, $p < 0.018$. Furthermore, an additional comparison of the proportional interference scores, unbiased by differences in base RT, showed significant reduction after MBCT intervention (from 13.1 to 8.7%), $p = 0.002$. Details were listed in **Table 2**.

## Neuroimage Results on Numerical Stroop Task

**Figure 1** demonstrates the significant recruitment of the dorsal attention network (DAN) in a single session of performing the numerical Stroop task, and the detailed information of brain regions were shown in **Tables 3–5**. The DAN activation level was generally reduced after MBCT while preserving the accuracy, but the results of incongruent trials, involving in the higher cognitive-load of inhibition, disclosed significant deactivation in both anterior cingulate cortex (ACC) and posterior cingulate cortex (PCC). Similar to the RT results, the congruent trials did not present MBCT effects in brain recruitments, whereas the brain recruitment to incongruent trials after MBCT only showed significant reduction in right PCC/precuneus under AlphaSim $p < 0.05$. The interaction effect of fMRI results

**TABLE 5 |** Peak locations of brain regions showing intervention differences in brain activity during incongruent condition of numerical Stroop task (AlphaSim corrected $p < 0.05$).

| Brain regions | | L/R | AAL | *x* | *y* | *z* | *t*-value |
|---|---|---|---|---|---|---|---|
| ***Pre-MBCT > Post-MBCT (incongruent condition)*** | | | | | | | |
| Parietal | Precuneus/Cuneus | R | 68/46 | 10 | −62 | 22 | 4.256 |

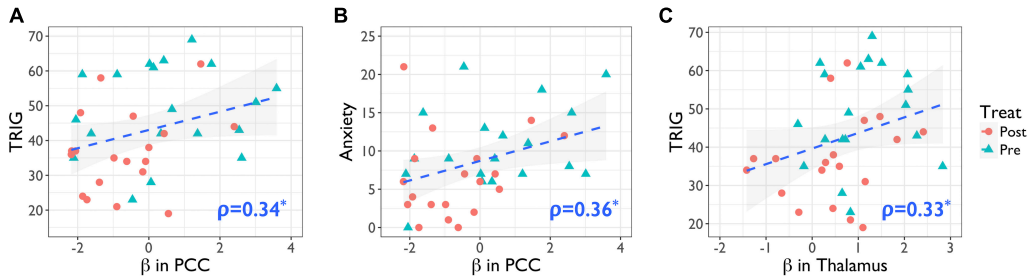


**FIGURE 2 |** Positive associations of neuropsychological tests and the brain activity (beta value) in the incongruent condition of numerical Stroop task. **(A)** PCC activity in numerical Stroop associated with the TRIG score, $r = 0.34$, $p < 0.04$; **(B)** PCC activity in numerical Stroop associated with the Anxiety score, $r = 0.36$, $p < 0.03$; **(C)** thalamus activity in numerical Stroop associated with the TRIG score, $r = 0.33$, $p < 0.05$. Statistical significance was based on Spearman's ρ. PCC, posterior cingulate cortex; TRIG, Texas Revised Inventory of Grief; Anxiety, Becker Anxiety Inventory.

(intervention × condition) showed single negative activation located at PCC, similar as the incongruency outcome. We further evaluated the associations between the neuropsychological assessment and the brain regional activity (PCC and hypothetical thalamus) involved in the incongruent condition of the numerical Stroop task. **Figure 2** shows significant correlations (a) between TRIG and PCC; (b) between Anxiety and PCC; and (c) TRIG and thalamus, Spearman's $\rho > 0.33$, $p < 0.05$. **Figure 2** demonstrates that less grief and anxiety were associated with reduced brain activations of PCC or thalamus involved in the numerical Stroop task.

## DISCUSSION

The purpose of the current study was to investigate the facilitative effect of an 8-week MBCT on emotion regulation and executive function in bereavement grief. As being taught to acknowledge all emotion, thoughts, and body sensations with non-judgmental acceptance, the bereaved participants attempted to avoid being engulfed by the catastrophic stories of what these cognition associated with them (Kabat-Zinn, 1994). As predicted, the bereaved participants after MBCT intervention reported a significant decrease in grief, anxiety, depression, and difficulties in emotion regulation, as well as increases in the mindfulness state. These positive changes may arise from the fact that bereaved participants foster a monitoring ability on their grief reactions with emotional acceptance, non-judgmental attitude and switching attention back to the present moment. Such practices over time may sharpen the participants' skills of emotion regulation in their daily life, allowing them to relax physically. From the group discussion, many bereaved reported they have had better sleep and felt more vitality in their daily life after the MBCT intervention.

Our first aim is to study the cognitive improvements following the grief mitigation following the MBCT intervention. The Stroop task is a cognitive measure to probe the executive control function, which allows people to overcome impulses and override automatic behavior. In this work, we replaced the traditional color-word Stroop task with the numerical Stroop task for the bereaved participants considering their inability to handle high cognitive load in the beginning phase (Huang et al., 2012). Following the mindfulness training, we noticed the reduced interference RT score when performing the numerical Stroop task in the bereaved participants, indicating the improved cognitive control performances (Colcombe et al., 2005) associated with the declined grief level following the MBCT. Previously, Teper and Inzlicht (2013) and Teper et al. (2013) demonstrated higher emotional acceptance and better performance in the EEG-based Stroop task among mindfulness meditators, suggesting mindfulness trainings such as meditative practices facilitate the executive control. Gallant (2016) also supported this statement in their review article (Gallant, 2016). Furthermore, even though Teper and Inzlicht (2013) conjectured that mindfulness practices promoted executive control preceding the emotion-regulation improvements. However, we could not verify the conjecture based on our observations in bereaved population. Further experimental design is warranted to prove this notion.

Secondly, practicing mindfulness allowed the bereaved individuals to stop overwhelming spontaneous ruminations and decrease the emotional interferences over the cognitive functions. Therefore, we used the fMRI experiment to disclose the underlying neurophysiological basis of MBCT-based cognitive improvements in bereavement grief. Results showed the numerical Stroop activation of bilateral DAN, encompassing the middle frontal gyrus and superior parietal gyrus, similar to the previous report (Huang et al., 2012). Overall, after the MBCT intervention, the reduced DAN activity implied the less cognitive loads involved in the numerical Stroop task. Meanwhile, the deactivations of ACC and PCC in the bereaved participants became prominent when dealing with the incongruent trials, indicating a cross-network interaction in the task. Interestingly, the default-mode network (DMN) deactivation was previously noticed in coping with high cognitive loads of working memory tasks (Liang et al., 2016). We conjectured that the mismatches originate from a hyper-activity of DMN with excessive internal thoughts in the bereaved population, thereby intervening their normal functions in cognitive performances. Similarly, Gündel et al. (2003) reported the activities of PCC and medial frontal gyrus among the bereaved women responding to grief-related words, indicating these regions are involved in the affective

processing. Christoff et al. (2016) in her review elaborated the role of DMN core in internal and spontaneous thoughts, impacting the conceptual and emotional processing. In our report, the PCC activity in the numerical Stroop task had significant positive correlation with TRIG and Anxiety, revealing that strong grief level associates with the positive beta value of PCC performing the numerical Stroop task. At last, we did not find the hypothetical correlation between T-FFMQ and PCC/thalamus activity. One possibility is that DMN-related regions can be more involved in the spontaneous activities of emotional arousal, rather than participating in the mindfulness directly. The other possibility is that the mindfulness dosage of the conventional 8-week MBCT protocol may be insufficient for relieving emotion disentanglements in bereavement grief. Further MBCT-based studies are warranted to verify the speculation on the bereaved population.

Though the current results suggest that MBCT practices leads to enhanced emotion regulation in subjective assessments and executive control in fMRI environment, we did not probe the brain activity involved in the emotion arousal. To the humanity concerns, we attempt to avoid raising extra affective arousal to the bereaved participants. Since our study did not employ a direct measure of emotional sensitivity, it is difficult to say whether DMN and thalamus were directly involved in affective processing; however, the literature gave strong support on the emotional involvement of both PCC, ACC and thalamus in major depressive disorder, insomnia and anxiety disorders (Greicius et al., 2007; Bastien, 2011; Christoff et al., 2016). Secondly, due to the individual differences of participation timing, initial sadness degree and comprehension ability on mindfulness, the learning curve to achieve the expected mindfulness was diverse. For example, some of them had reported being able to relate their situations in a mindful way in the final session of the MBCT course, but some reported that they felt better only when they were inside of the group. Therefore, the emotional stability in the same MBCT group exhibited strong inter-subject variability, imposing one of the confounding factors on the final assessments. Third, Huang et al. (2012) used the numerical magnitude and physical size of the numerical Stroop task to differentiate the hemispheric laterality between the elderly and youth; however, we did not notice the laterality changes in the current work.

Additionally, one practical challenge in this study was the recruitment of a control group without treatments, due to the fact that none of the recruited bereaved participants was willing to be enrolled in the control group. Nevertheless, the enrollment of the active control might be bypassed, because literature disclosed that the grief perception measured by TRIG after the bereavement point took multiple years to recover back to a normal status, far from 8 weeks of MBCT (Zisook et al., 1982). Similarly, Tseng et al. (2017) reported Taiwanese bereavements took approximately 4 years to restore the depression scale to the level prior to the bereavement. The evidence demonstrated that the grief bereavements have long-term impacts without treatments and are not easily alleviated within 8 weeks. Further investigations are warranted to support the statements on the topic of grief bereavements.

Conclusively, practicing the 8-week mindfulness training allowed significant alleviation of grief, anxiety, depression, and elevated their mindfulness state in bereaved individuals. The mindfulness training not only benefited emotion regulation, but also reduced the emotional interferences over cognitive functions. Results revealed the reduced interference RT score in the numerical Stroop task among the bereaved participants, indicating improved executive control function. Furthermore, the positive brain activities of PCC and thalamus showed the intervening effect on the Stroop task, but the intervening effects of PCC and thalamus were reduced following the MBCT intervention, associated with the reduced bereavement grief. Based on the beneficial effects of MBCT intervention, we encourage the bereaved population to practice mindfulness training to avoid overwhelming emotional arousal and to preserve the quality of daily life.

## AUTHOR CONTRIBUTIONS

F-YH, CW, Y-PC, and C-MH contributed to the conception and experiment design. F-YH, A-LH, and CW contributed to preparation and revision of the manuscript. CW and L-MH contributed to data analysis. J-ST and T-JH contributed to clinical evaluation of mental health. All authors reviewed and approved the manuscript.

## FUNDING

This study was supported by the Taiwan Ministry of Science and Technology under grant number MOST 106-2420-H-152-001 and MOST 106-2420-H-038-005-MY2.

## ACKNOWLEDGMENTS

We would like to thank all bereaved participants and the Imaging Center for Integrated Body, Mind and Culture Research, National Taiwan University and Taiwan Ministry of Science and Technology in support of MRI facilities.

## REFERENCES

Assareh, A. A., Sharpley, C. F., McFarlane, J. R., and Sachdev, P. S. (2015). Biological determinants of depression following bereavement. *Neurosci. Biobehav. Rev.* 49, 171–181. doi: 10.1016/j.neubiorev.2014.12.013

Baer, R. A., Smith, G. T., Lykins, E., Button, D., Krietemeyer, J., Sauer, S., et al. (2008). Construct validity of the five facet mindfulness questionnaire in meditating and nonmeditating samples. *Assessment* 15, 329–342. doi: 10.1177/1073191107313003

Bastien, C. H. (2011). Insomnia: neurophysiological and neuropsychological approaches. *Neuropsychol. Rev.* 21, 22–40. doi: 10.1007/s11065-011-9160-3

Beem, E. E., Maes, S., Cleiren, M., Schut, H. A., and Garssen, B. (2000). Psychological functioning of recently bereaved, middle-aged women: the first 13 months. *Psychol. Rep.* 87, 243–254. doi: 10.2466/pr0.2000.87.1.243

Bishop, S. R. (2004). Mindfulness: a proposed operational definition. *Clin. Psychol.* 11, 230–241. doi: 10.1093/clipsy/bph077

Buckley, T., McKinley, S., Tofler, G., and Bartrop, R. (2010). Cardiovascular risk in early bereavement: a literature review and proposed mechanisms. *Int. J. Nurs. Stud.* 47, 229–238. doi: 10.1016/j.ijnurstu.2009.06.010

Byrne, G. J., and Raphael, B. (1997). The psychological symptoms of conjugal bereavement in elderly men over the first 13 months. *Int. J. Geriatr. Psychiatry* 12, 241–251. doi: 10.1002/(SICI)1099-1166(199702)12:2<241::AID-GPS590>3.0.CO;2-0

Chambers, R., Lo, B. C. Y., and Allen, N. B. (2007). The impact of intensive mindfulness training on attentional control, cognitive style, and affect. *Cogn. Ther. Res.* 32, 303–322. doi: 10.1176/ajp.149.7.936

Christakis, N. A., and Iwashyna, T. J. (2003). The health impact of health care on families: a matched cohort study of hospice use by decedents and mortality outcomes in surviving, widowed spouses. *Soc. Sci. Med.* 57, 465–475. doi: 10.1016/S0277-9536(02)00370-2

Christoff, K., Irving, Z. C., Fox, K. C. R., Spreng, R. N., and Andrews-Hanna, J. R. (2016). Mind-wandering as spontaneous thought: a dynamic framework. *Nat. Rev. Neurosci.* 17, 718–731. doi: 10.1016/j.conb.2014.12.006

Clayton, P. J., Halikes, J. A., and Maurice, W. L. (1971). The bereavement of the widowed. *Dis. Nerv. Syst.* 32, 597–604.

Colcombe, S. J., Kramer, A. F., Erickson, K. I., and Scalf, P. (2005). The implications of cortical recruitment and brain morphology for individual differences in inhibitory function in aging humans. *Psychol. Aging* 20, 363–375. doi: 10.1037/0882-7974.20.3.363

Cox, R. W. (1996). AFNI: software for analysis and visualization of functional magnetic resonance neuroimages. *Comput. Biomed. Res.* 29, 162–173. doi: 10.1006/cbmr.1996.0014

Faschingbauer, T. R., Zisook, S., and DeVaul, R. A. (1987). "The texas revised inventory of grief," in *Biopsychosocial Aspects of Bereavement*, ed. S. Zisook (Washington, DC: American Psychiatric Press), 111–124.

Gallant, S. N. (2016). Mindfulness meditation practice and executive functioning: breaking down the benefit. *Conscious. Cogn.* 40, 116–130. doi: 10.1016/j.concog.2016.01.005

Goldin, P. R., and Gross, J. J. (2010). Effects of mindfulness-based stress reduction (MBSR) on emotion regulation in social anxiety disorder. *Emotion* 10, 83–91. doi: 10.1037/a0018441

Gratz, K. L., and Roemer, L. (2004). Multidimensional assessment of emotion regulation and dysregulation: development, factor structure, and initial validation of the difficulties in emotion regulation scale. *J. Psychopathol. Behav. Assess.* 26, 41–54. doi: 10.1023/B:JOBA.0000007455.08539.94

Greicius, M. D., Flores, B. H., Menon, V., Glover, G. H., Solvason, H. B., Kenna, H., et al. (2007). Resting-state functional connectivity in major depression: abnormally increased contributions from subgenual cingulate cortex and thalamus. *Biol. Psychiatry* 62, 429–437. doi: 10.1016/j.biopsych.2006.09.020

Gündel, H., O'Connor, M.-F., Littrell, L., Fort, C., and Lane, R. D. (2003). Functional neuroanatomy of grief: an FMRI study. *Am. J. Psychiatry* 160, 1946–1953. doi: 10.1176/appi.ajp.160.11.1946

Hart, C. L., Hole, D. J., Lawlor, D. A., Smith, G. D., and Lever, T. F. (2007). Effect of conjugal bereavement on mortality of the bereaved spouse in participants of the Renfrew/Paisley Study. *J. Epidemiol. Community Health* 61, 455–460. doi: 10.1136/jech.2006.052043

Hoge, E. A., Bui, E., Marques, L., Metcalf, C. A., Morris, L. K., Robinaugh, D. J., et al. (2013). Randomized controlled trial of mindfulness meditation for generalized anxiety disorder: effects on anxiety and stress reactivity. *J. Clin. Psychiatry* 74, 786–792. doi: 10.4088/JCP.12m08083

Hölzel, B. K., Lazar, S. W., Gard, T., Schuman-Olivier, Z., Vago, D. R., and Ott, U. (2011). How does mindfulness meditation work? proposing mechanisms of action from a conceptual and neural perspective. *Perspect. Psychol. Sci.* 6, 537–559. doi: 10.1177/1745691611419671

Huang, C.-M., Polk, T. A., Goh, J. O., and Park, D. C. (2012). Both left and right posterior parietal activations contribute to compensatory processes in normal aging. *Neuropsychologia* 50, 55–66. doi: 10.1016/j.neuropsychologia.2011.10.022

Huang, F.-Y., Wu, C.-W., Bhikshu, H.-M., Shih, G.-H., Chao, Y.-P., and Dai, C.-T. (2015). Validation of the Taiwanese Version of the Five Facet Mindfulness Questionnaire (T-FFMQ). *Psychol. Test.* 62, 231–260.

Jenkinson, M., Beckmann, C. F., Behrens, T. E. J., Woolrich, M. W., and Smith, S. M. (2012). FSL. *Neuroimage* 62, 782–790. doi: 10.1016/j.neuroimage.2011.09.015

Jha, A. P., Krompinger, J., and Baime, M. J. (2007). Mindfulness training modifies subsystems of attention. *Cogn. Affect. Behav. Neurosci.* 7, 109–119. doi: 10.3758/CABN.7.2.109

Kabat-Zinn, J. (1994). *Mindfulness Meditation for Everyday Life*. Totnes: Piatkus Books.

Kang, Y., Gruber, J., and Gray, J. R. (2013). Mindfulness and De-Automatization. *Emot. Rev.* 5, 192–201. doi: 10.1126/science.1162548

Kaprio, J., Koskenvuo, M., and Rita, H. (1987). Mortality after bereavement: a prospective study of 95,647 widowed persons. *Am. J. Public Health* 77, 283–287. doi: 10.2105/AJPH.77.3.283

Kral, T. R. A., Schuyler, B. S., Mumford, J. A., Rosenkranz, M. A., Lutz, A., and Davidson, R. J. (2018). Impact of short- and long-term mindfulness meditation training on amygdala reactivity to emotional stimuli. *Neuroimage* 181, 301–313. doi: 10.1016/j.neuroimage.2018.07.013

Kuyken, W., Hayes, R., Barrett, B., Byng, R., Dalgleish, T., Kessler, D., et al. (2015). The effectiveness and cost-effectiveness of mindfulness-based cognitive therapy compared with maintenance antidepressant treatment in the prevention of depressive relapse/recurrence: results of a randomised controlled trial (the PREVENT study). *Health Technol. Assess.* 19, 1–124. doi: 10.3310/hta19730

Lee, Y., Yang, M.-J., Lai, T.-J., Chiu, N.-M., and Chau, T.-T. (2000). Development of the Taiwanese depression questionnaire. *Chang Gung Med. J.* 23, 688–694.

Liang, X., Zou, Q., He, Y., and Yang, Y. (2016). Topologically reorganized connectivity architecture of default-mode, executive-control, and salience networks across working memory task loads. *Cereb. Cortex* 26, 1501–1511. doi: 10.1093/cercor/bhu316

Lichtenstein, P., Gatz, M., and Berg, S. (1998). A twin study of mortality after spousal bereavement. *Psychol. Med.* 28, 635–643. doi: 10.1017/S0033291798006692

Lovas, D. A., and Schuman-Olivier, Z. (2018). Mindfulness-based cognitive therapy for bipolar disorder: a systematic review. *J. Affect. Disord.* 240, 247–261. doi: 10.1016/j.jad.2018.06.017

Ma, S. H., and Teasdale, J. D. (2004). Mindfulness-based cognitive therapy for depression: replication and exploration of differential relapse prevention effects. *J. Consult. Clin. Psychol.* 72, 31–40. doi: 10.1037/0022-006X.72.1.31

Moore, A., and Malinowski, P. (2009). Meditation, mindfulness and cognitive flexibility. *Conscious. Cogn.* 18, 176–186. doi: 10.1016/j.concog.2008.12.008

Peng, D.-H., Shen, T., Zhang, J., Huang, J., Liu, J., Liu, S.-Y., et al. (2012). Abnormal functional connectivity with mood regulating circuit in unmedicated individual with major depression: a resting-state functional magnetic resonance study. *Chin. Med. J.* 125, 3701–3706.

Roemer, L., Williston, S. K., and Rollins, L. G. (2015). Mindfulness and emotion regulation. *Curr. Opin. Psychol.* 3, 52–57. doi: 10.1016/j.copsyc.2015.02.006

Rosnick, C. B., Small, B. J., and Burton, A. M. (2010). The effect of spousal bereavement on cognitive functioning in a sample of older adults. *Neuropsychol. Dev. Cogn. B Aging Neuropsychol. Cogn.* 17, 257–269. doi: 10.1080/13825580903042692

Segal, J. V., Williams, J. M. G., and Teasdale, J. D. (2002). *Mindfulness-based Cognitive Therapy for Depression*. New York, NY: Guilford Press.

Segal, Z. V., Williams, J. M. G., and Teasdale, J. D. (2013). *Mindfulness-Based Cognitive Therapy for Depression*, Second Edn. New York, NY: Guilford Press.

Shapiro, S. L., Astin, J. A., Bishop, S. R., and Cordova, M. (2005). Mindfulness-based stress reduction for health care professionals: results from a randomized trial. *Int. J. Stress Manag.* 12, 164–176. doi: 10.1037/1072-5245.12.2.164

Shapiro, S. L., Carlson, L. E., Astin, J. A., and Freedman, B. (2006). Mechanisms of mindfulness. *J. Clin. Psychol.* 62, 373–386. doi: 10.1002/jclp.20237

Spitzer, R. L., Kroenke, K., Williams, J. B. W., and Löwe, B. (2006). A brief measure for assessing generalized anxiety disorder: the GAD-7. *Arch. Intern. Med.* 166, 1092–1097. doi: 10.1001/archinte.166.10.1092

Stroebe, M., Schut, H., and Stroebe, W. (2007). Health outcomes of bereavement. *Lancet* 370, 1960–1973. doi: 10.1016/S0140-6736(07)61816-9

Taylor, M. P., Reynolds, C. F., Frank, E., Dew, M. A., Mazumdar, S., Houck, P. R., et al. (1999). EEG sleep measures in later-life bereavement depression. A randomized, double-blind, placebo-controlled evaluation of nortriptyline. *Am. J. Geriatr. Psychiatry* 7, 41–47. doi: 10.1097/00019442-199902000-00006

Teasdale, J. D., Segal, Z. V., Williams, J. M., Ridgeway, V. A., Soulsby, J. M., and Lau, M. A. (2000). Prevention of relapse/recurrence in major depression by mindfulness-based cognitive therapy. *J. Consult. Clin. Psychol.* 68, 615–623. doi: 10.1037/0022-006X.68.4.615

Teper, R., and Inzlicht, M. (2013). Meditation, mindfulness and executive control: the importance of emotional acceptance and brain-based performance monitoring. *Soc. Cogn. Affect. Neurosci.* 8, 85–92. doi: 10.1037/0033-295X.111.4.939

Teper, R., Segal, Z. V., and Inzlicht, M. (2013). Inside the mindful mind. *Curr. Dir. Psychol. Sci.* 22, 449–454. doi: 10.1177/0963721413495869

Tseng, F.-M., Petrie, D., and Leon-Gonzalez, R. (2017). The impact of spousal bereavement on subjective wellbeing: evidence from the Taiwanese elderly population. *Econ. Hum. Biol.* 26, 1–12. doi: 10.1016/j.ehb.2017.01.003

Tzourio-Mazoyer, N., Landeau, B., Papathanassiou, D., Crivello, F., Etard, O., Delcroix, N., et al. (2002). Automated anatomical labeling of activations in SPM using a macroscopic anatomical parcellation of the MNI MRI single-subject brain. *Neuroimage* 15, 273–289. doi: 10.1006/nimg.2001.0978

Vago, D. R., and Silbersweig, D. A. (2012). Self-awareness, self-regulation, and self-transcendence (S-ART): a framework for understanding the neurobiological mechanisms of mindfulness. *Front. Hum. Neurosci.* 6:296. doi: 10.3389/fnhum.2012.00296

Young, M., Benjamin, B., and Wallis, C. (1963). The Mortality of Widowers. *Lancet* 2, 454–456. doi: 10.1016/S0140-6736(63)92193-7

Zeidan, F., Johnson, S. K., Diamond, B. J., David, Z., and Goolkasian, P. (2010). Mindfulness meditation improves cognition: evidence of brief mental training. *Conscious. Cogn.* 19, 597–605. doi: 10.1016/j.concog.2010.03.014

Zisook, S., DeVaul, R. A., and Click, M. A. (1982). Measuring symptoms of grief and bereavement. *Am. J. Psychiatry* 139, 1590–1593. doi: 10.1176/ajp.139.12.1590

Zisook, S., Paulus, M., Shuchter, S. R., and Judd, L. L. (1997). The many faces of depression following spousal bereavement. *J. Affect. Disord.* 45, 85–94; discussion 94–95. doi: 10.1016/S0165-0327(97)00062-1

**Conflict of Interest Statement:** The authors declare that the research was conducted in the absence of any commercial or financial relationships that could be construed as a potential conflict of interest.

frontiers in Human Neuroscience

ORIGINAL RESEARCH
published: 30 April 2019
doi: 10.3389/fnhum.2019.00132

# Facial Attractiveness of Chinese College Students With Different Sexual Orientation and Sex Roles

*Juan Hou[1]*, Lumeng Sui[1], Xinxin Jiang[1], Chengyang Han[2] and Qiang Chen[1]**

[1] Department of Philosophy, Anhui University, Hefei, China, [2] College of Education, Zhejiang University, Hangzhou, China

Facial attractiveness refers to a positive and joyful emotional experience induced by the face of a target person and the extent to which other people are driven to be close to their wishes. Since the 1970s, face attractiveness has gradually emerged in western psychological research, but most of the studies were confined to heterosexuals. More recently, some scholars have pointed out that sexual orientation may affect the judgment of facial attractiveness of individuals. Based on previous literature, this study proposed to explore the different facial attractiveness of individuals with different sexual orientations and sexual roles. Participants in this study were divided into two types (according to sexual orientation and sexual role) by the Sex Role Inventory for College Students (CSRI). Also, the eye-tracking technique was used to record the path of eye movements, where face images were manipulated by sexual dimorphism clues. The results showed that (1) compared to heterosexual men, homosexual men were significantly more likely to choose masculine faces as more attractive faces in paired faces; (2) male homosexuals are likely to have the feminization bias, and female homosexuals are likely to have the masculinization bias; and (3) the masculine faces are more attractive than feminine faces to participants whose sex role is feminine type and androgynous type.

**Keywords: facial attractiveness, sexual dimorphism, homosexuality, sex role, eye tracking**

OPEN ACCESS

***Edited by:***
*Delin Sun,*
*Duke University, United States*

***Reviewed by:***
*Huijun Zhang,*
*Guangdong University of Technology, China*
*Peilian Chi,*
*University of Macau, China*

****Correspondence:***
*Juan Hou*
*daisyhoujuan@gmail.com*
*Qiang Chen*
*Qiang.chen@warwick.ac.uk*

***Received:*** *07 September 2018*
***Accepted:*** *01 April 2019*
***Published:*** *30 April 2019*

***Citation:***
*Hou J, Sui L, Jiang X, Han C and Chen Q (2019) Facial Attractiveness of Chinese College Students With Different Sexual Orientation and Sex Roles. Front. Hum. Neurosci. 13:132. doi: 10.3389/fnhum.2019.00132*

## INTRODUCTION

Facial attractiveness refers to the greatest degree of pleasure given to the senses (Li and Chen, 2010). Previous studies have investigated that faces were identified by averageness, symmetry, and sexual dimorphism. All of the three elements are regarded to contribute to the attractiveness of an individual's face (Grammer and Thornhill, 1994; Perrett et al., 1999; Rhodes, 2006; Rennels et al., 2008). Also, studies relying on attractiveness assessments of static facial images are ecologically valid (Kościński, 2013).

However, what are the factors that would influence people's judgments of facial attractiveness? Chen et al. (1997) classified the factors affecting facial attractiveness into two hypotheses: the observer hypothesis and the owner hypothesis.

The observer hypothesis refers to the observer's characteristics (such as the observer's physiological, cognitive, and sociocultural factors), which play an important role when judging facial attractiveness (Kou et al., 2013). For example, according to Zhang and Zheng (2016), the degree of angled faces (angle effect) is an essential factor in the assessment of facial attractiveness.

Their results indicated that vertical faces were more attractive than other faces and that left-leaning faces were more attractive than right-leaning faces.

Nevertheless, the owner hypothesis focuses on features inherent in the physiognomy of the owner's face, which would affect their judgment of face attractiveness (Little and Perrett, 2002). Hence, this hypothesis believes that face attractiveness is a stable trait of people (Jones et al., 2004). The research mainly uses the facial metric method to measure the faces. The primary method is to quantify every landmark point of a face by using Morph to change the position, distance, arrangement, and proportion of the landmark points, determining the geometric characteristics of the face. This method affects the judgment of facial attractiveness, such as averageness, symmetry, and sexual dimorphism (Kou et al., 2013).

Among them, sexual dimorphism refers to mature men and women after the development of adolescence; their secondary sexual characteristics gradually develop the body of sexual dimorphism, that is, masculine and feminine (Perrett et al., 1998). Sexual dimorphism not only is an essential indicator of facial attractiveness but also plays an important role in mate selection (Wen and Zuo, 2012). More precisely, according to Conroy-Beam et al. (2015), sexual dimorphism in mate selection "has cascading sex-specific consequences for important human endeavors such as marriage, child rearing, and divorce, all which suggest that sexes face are importantly different evolutionary histories and trajectories."

Studies on sexual dimorphism have found that feminized female faces are considered attractive (Rhodes, 2006). However, there is no consistent conclusion in preference for male faces. Some researchers have found that women prefer masculine male faces (Miller and Todd, 1998; Gangestad and Scheyd, 2005). However, other studies argued that women have a weak preference for masculinized male faces, but a stronger preference for feminized male faces (Rhodes et al., 2003; DeBruine et al., 2006; Welling et al., 2007; Little et al., 2008). Wen and Zuo (2012) evaluated women's judgments of the attractiveness of men's faces under the condition of sexual dimorphism and found that female participants preferred masculinized male faces. Also, the mean pupil dilation and the mean fixation count on male faces were significantly higher than that on female faces. Yang (2015) had used synthetic face images as his experimental materials and adopted eye-track technology as well as questionnaires to explore male and female preferences. They observed that compared with androgynous faces, both male and female participants preferred masculine male faces. Meanwhile, the eye movement data showed that although longer gaze duration and a greater number of fixations were found when males and females were watching masculine male faces, no significant differences appeared. Moreover, in their study, they also discovered that compared to androgynous faces, the behavior data showed that both males and females prefer feminine female faces. Besides, they noted that when viewing feminine female faces, males, and females had a longer fixation duration and a greater number of fixations.

Nonetheless, previous studies mostly focused on sexual dimorphism in heterosexual groups and seldom considered different sexual orientation. Also, as the number of homosexuals increases, some researchers have pointed out that sexual orientation may affect the individual's judgment of facial attractiveness (Steffens et al., 2013). For heterosexual groups, attractive opposite-sex faces are more rewarding, while homosexual groups think attractive same-sex faces are more satisfying (Kranz and Ishai, 2006). Glassenberg et al. (2010) used four types of face pictures (masculinized and feminized male and female faces) to examine the preference of different sexual orientations for masculinity–femininity. They noted that homosexual men had stronger preferences for masculinized male faces, whereas homosexual women had stronger preferences for masculinized female faces than heterosexual women. Other research studies noticed that homosexual men were able to identify more male faces than female faces, whereas heterosexual men can recognize more female faces than male faces (Beres et al., 2014; Li, 2016, unpublished). These findings further confirmed the importance of sexual orientation in the field of facial attractiveness.

Through prior studies on sexual dimorphism and sexual orientation, we know that differences in sex and sexual orientation would influence individuals' face preferences. But what about individuals' psychological sex differences? Does an individual's psychological awareness of their gender affect their face preferences?

Qian et al. (2000) compiled the Sex Role Inventory for College Students (CSRI), which divides college students into four sex roles: masculine, feminine, androgynous, and undifferentiated, accounting for 24.7, 15.4, 31.5, and 28.4% of males and 22.5, 28.0, 25.0, and 24.5% of females, respectively. However, her study did not divide participants according to sexual orientation; therefore, when the participants were divided into different sexual orientation groups, would the proportion of their sex roles be different? Do the different sex role types affect their face preferences? These questions are worth studying.

According to previous studies, there is no consensus among researchers on face preferences of homosexuals. Bailey et al. (1997) have suggested that homosexual men prefer masculine male faces, while homosexual women have no preference for either masculinity or femininity in women. Echoing to this, Glassenberg et al. (2010) discovered that homosexual males showed stronger preferences for masculinity in male faces than did all of the other groups (homosexual women and heterosexual men and women). Also, homosexual women demonstrated stronger preferences for masculinity in female faces than did heterosexual women. Therefore, the first hypothesis we examined was that homosexual men might prefer masculinized faces, while homosexual women have no significant preference. Turning to the question of the relationship between participants and their sex roles, Qian et al. (2000) found that the sex roles of most men were the androgynous type and that for women were the feminine type. Thus, we speculated that the proportion of sex roles in our study would change, and we hypothesized that most homosexual men sex roles would be a feminine type and most homosexual women sex roles would be a masculine type. Finally, we also want to observe if a particular connection exists between participants' sex role and their facial preference. In the Johnston et al. (2001) study, they found that different Bem Sex Role Inventory (BSRI) sex role groups exhibit different

face preferences. Combined with prior hypotheses of this study, therefore, we hypothesized that participants with masculine sex roles preferred feminized faces, while participants with feminine sex roles preferred masculinized faces.

Besides, we found that previous studies mostly invited participants to evaluate the paired stimuli subjectively; for example, Sun et al. (2012) used forced choice to investigate the influence of the position of the left-side and the right-side face to facial attractiveness. However, other studies argue that the eye-tracking technique is a more efficient way to collect data on participants' attention, which could shed light on the relative traits when people are making attractiveness judgments. Eye tracking is a method based on using computer equipment to record eye movements and the corresponding pupillary–corneal reflection (Richards et al., 2015). In the Corbetta et al. (1998) study, they pointed out that the brain captures information throughout the fixations of eye movement. Meanwhile, through recording the duration and the location of fixations of eye movement, it is conceivable to learn what characteristics a participant would consider most relevant. If the participant has an interest in a feature, his or her eyes will be attracted to this specific feature (Berlyne, 1958). Furthermore, in eye-tracking experiments, regardless of participants' attention, whether it be endogenous or exogenous, the eye-tracking technique can quickly capture and transfer results to an intuitionistic data to achieve a goal (Ruz and Lupiáñez, 2002; Dixson et al., 2011). For example, Zhang et al. (2016) used the eye-tracking technique to explore the effect of smiling on the cognitive processing of facial attractiveness. The results showed that smiling influences face attractiveness. The mouth and the eyes are crucial for individuals' judgment of facial attractiveness. As a new and fundamental cognitive method, the eye-tracking technique can provide immediate and objective eye movement indicators for cognitive processing. In this study, the eye-movement technique was used to discover the unintentional attention of participants with different sexual orientations when they were viewing different kinds of faces. Meanwhile, adopting questionnaires and the combination of subjective and objective methods could give us a more precise and more comprehensive understanding of data.

In conclusion, on the basis of previous studies to explore whether there are differences in their face preferences for sexual dimorphism clues, the current study proposes to use the CSRI and Kinsey Scale to classify participants into two types: sexual orientation and sex roles. From a more objective point of view, this study was undertaken to provide unbiased eye movement indicators for sexual dimorphism on the impact of facial attractiveness. Meanwhile, in this study, we examine the following hypotheses on facial attractiveness, which arise from these considerations: (a) homosexual men might prefer masculinized faces, while homosexual women have no significant preference; (b) most homosexual men's sex roles would be a feminine type and most homosexual women's sex roles would be a masculine type; and (c) participants' sex roles in masculine type prefer feminized faces, while participants with feminine sex role type prefer masculinized faces.

# MATERIALS AND METHODS

## Ethics Statement

The study was approved by the Human Research Ethics Committee of Anhui University. All participants gave consent to participate in the study and principles expressed in the Declaration of Helsinki were strictly followed. Participants were undergraduate students. Informed consent was obtained in written form from all participants.

The youngest participant was 18 years old. We did not obtain informed consent from the next of kin, caretakers, or guardians on behalf of the minors/children enrolled in our study. These college students were considered to have comparable intelligence and ability, and able to take charge of their behaviors.

## Participants

A total of 95 participants came from a number of online sources (including Chinese homosexual app, Tencent homosexual online groups, QQ, and WeChat) where we posted advertisements asking for men and women who were interested in helping with a 40-min eye-tracking study on facial attractiveness (mean age = 20.06, *SD* = 1.47). All participants were between the ages of 18 and 24 years. Of them, 22 men and 23 women identified themselves as heterosexual, and 25 men and 25 women identified themselves as homosexual. Sexual orientation was determined by asking participants to select one of seven statements that best described their sexual orientation. The eight statements provided in the survey were taken from the Kinsey scale (Kinsey et al., 1949). All participants were right-handed and had normal or corrected-to-normal vision. Before the experiment, participants were informed about the study's purpose and procedure, and they were paid 30 RMB after the experiment.

To separate our participants into four groups (homosexual and heterosexual male and female), individuals who rated themselves as "exclusively homosexual," "predominantly homosexual, only incidentally heterosexual," and "predominantly homosexual, but more than incidentally heterosexual" were classified as homosexual, whereas individuals who rated themselves as "exclusively heterosexual," "predominantly heterosexual, only incidentally homosexual," and "predominantly heterosexual, but more than incidentally homosexual" were classified as heterosexual. Bisexual people were not the focus of this study, so they were not brought into our data analysis.

## Questionnaire Measures

### The Kinsey Scale

The Kinsey Scale only has one item, which is used as a criterion for judging the sexual orientation of the participants. The scale is rated on an eight-point Likert scale (ranging from "1 = Exclusively heterosexual" to "8 = No socio-sexual contacts or reactions").

### The Sex Role Inventory for College Students (CSRI)

The Sex Role Inventory for College Students (CSRI; Qian et al., 2000) has five categories, including Masculine Positive Category (strong, capable, etc)., Masculine Negative Category (reckless, impatient, etc)., Feminine Positive Category (tender, virtuous,

etc)., Feminine Negative Category (lachrymose, hesitating, etc)., and Neutral Category (dedicated, impatient, complacent, etc). Each category is formatted with 20 different personality traits that participants rate themselves based on a five-point Likert scale ranging from "−2 = Totally different" to "+2 = Exactly the same." Also, the participants could be classified into four sex role types, masculine, feminine, androgynous, and undifferentiated, according to Qian et al. (2000). Its Cronbach's alpha in the present study was 0.88.

## Preparation of Composite Facial Images

Three composite versions (masculine, average, and feminine) of male and female face stimuli were collected by sexual dimorphism. All the faces (students at Anhui University; 32 males, 32 females) were photographed under standard lighting conditions with neutral facial expression. Also, all of the participants signed a consent form and allowed their photographs to be used in this study and publishing.

To manipulate these photos of faces into our stimuli, we first conducted all the pictures into uniform size (27.09 × 27.09 cm) and the same pixel (1024 × 1024) by PS technology and all the pictures were processed into black and white. Next, we randomly selected 16 male and female faces, respectively, from 64 photographed faces to synthesize male and female average face prototypes by using Fanta Morph 5.9 software. Then, we created the landmark points in each face that identified the shapes, positions, and outlines of these faces. Furthermore, we slightly tweaked the locations of the landmark points in each picture.

To produce an image composed of the two faces, we equated the numeric (pixels) of the landmark points in two pictures. Then, by using the same method, the composite images of the two faces were further synthesized with the other composite images composed of two faces, resulting in an image made of four faces. In this way, we eventually gained two prototype faces that formed of 16 faces.

After that, we manipulated the sexual dimorphism in facial images by using the website https://webmorph.org//, created by DeBruine and others at the School of Psychology (DeBruine, 2017), University of Glasgow. We uploaded the average male and female face prototypes to the website for processing. Lastly, the feminized and masculinized facial stimuli were obtained (see **Figures 1**, **2**). The images of three pairs of female face prototypes were received by the same method.

Then, we randomly selected 40 photographs from the remaining 43 male and 41 female faces, and by manipulating the sexual dimorphism in these facial images, we finally had 46 pairs of masculinized and feminized faces. After that, we invited 80 undergraduates (41 male, 39 female, mean age = 19.12, *SD* = 0.663, ranging from 18 to 21 years) to select which one seemed more masculine (see **Table 1**). Binomial statistical analysis of the results showed that the masculinization of all the matched control groups was significant. Finally, we randomly selected 20 pairs of faces (half male and half female) as the experimental materials.

**FIGURE 1 |** Facial images of a female that were "feminized" and "masculinized" 50% in shape. Left, Chinese female, feminized; right, Chinese female, masculinized.

**FIGURE 2 |** Facial images of a male that were "feminized" and "masculinized" 50% in shape. Left, Chinese male, feminized; right, Chinese male, masculinized.

## Apparatus

Stimuli were presented on an 18.5-in. monitor at a resolution of 1,024 × 768 pixels and with a refresh rate of 60 Hz. Eye movements were captured and recorded by an EyeLink 1000 Desktop Eye Tracking System (SR Research Ltd., Mississauga, ON, Canada). The system has a sampling rate of 1,000 Hz. The distance between monitor and chin rest was 60 cm. To ensure participants were at ease and to minimize unnecessary head movements, a chin rest was used. The experiment program was created using SR Research Experiment Builder software (version 1.10.165), which is compatible with the EyeLink 1000 eye tracker. Participants viewed the stimuli using both eyes, but only the

**TABLE 1 |** Evaluation of experimental facial stimuli.

| Picture number | 5 | 7 | 8 | 9 | 12 | 13 | 14 | 19 | 20 | 23 | 24 | 25 | 26 | 28 | 37 | 39 | 41 | 42 | 45 | 46 |
|---|---|---|---|---|---|---|---|---|---|---|---|---|---|---|---|---|---|---|---|---|
| Sex | M | F | F | F | M | F | M | M | M | F | F | F | M | M | F | F | M | F | M | M |
| Masculine selection | 78 | 77 | 77 | 80 | 78 | 77 | 78 | 76 | 76 | 79 | 75 | 71 | 75 | 70 | 78 | 79 | 77 | 78 | 74 | 73 |
| Feminine selection | 2 | 3 | 3 | 0 | 2 | 3 | 2 | 4 | 4 | 1 | 5 | 9 | 5 | 10 | 2 | 1 | 3 | 2 | 6 | 7 |

position of the left eye was tracked and recorded. The eye tracker was calibrated using a series of nine fixed targets distributed around the display, followed by a nine-point accuracy test.

## Procedure

The experiment was conducted in a psychological eye movement laboratory, which is a quiet and undisturbed setting. Psychology students were selected as experimenters and individually tested participants. On arrival, participants read and signed an informed consent form that briefly described the content and procedure of this study. Later, participants were asked to answer the Kinsey Scale. To exclude the bisexuals and asexuals, participants who chose 4 and 8 on the Kinsey Scale were eliminated. After that, participants completed the College Students' Gender Role Scale for self-evaluation and entered the eye movement experiment.

The eye-tracking session was divided into two stages – (a) Preparation stage: the participant sat in a chair that was 65 cm away from the display device. To ensure the accuracy of experimental data, participants' heads were fixated, and their lower foreheads were placed on a U-shaped bracket. (b) Experiment stage: The following instructions were presented on the screen – "Hello, welcome to participate in this experiment! This experiment consists of two parts: the calibration part and the experiment part. Please strictly follow the instructions and the hints of the experimenter. Next, we will enter the calibration section. If you are ready, press the Q on the keyboard." Subsequently, the eye movement instrument was adjusted. The first step consisted of calibrating the eye-tracking system with nine points, and the second step involved validation of errors of the process in which the machine tracked the eyes. After calibration, the screen presented the experimental instruction: "After a while, please look at the gaze points on the screen. Face images will appear on the screen in pairs, which are very similar to each other, with very subtle differences. After they disappear, you need to choose the one which you believe is more attractive. If you think that the left face is more attractive, please press C on the keyboard; if you think the right face is more attractive, please press M on the keyboard. If you have understood the above instructions, please press Y to start." Twenty-six pairs of male and female faces appeared randomly, each pair consisting of a masculinized and feminized version of the same individual. The order of pairs and the side of the screen on which a given image was shown were both randomized among participants. Participants were instructed to choose which face they thought was more attractive for each pair. The experimental process is shown in **Figure 3**.

## Data Analysis

Before all analyses, we processed initial eye movement data through the EyeLink Data Viewer analysis software (SR Research). Also, the statistics software package SPSS 16.0 was used for further data analysis. We calculated three eye movement variables: (a) mean number of fixations, which refers to the sum of all fixations in a stimulus; (b) mean first fixation duration, which refers to the average duration (in milliseconds) of the first fixations in a stimulus; and (c) mean pupil size, which refers to the average size (in arbitrary units) of pupil dilation or contraction when viewing stimuli.

The collected data were analyzed in the following ways: first, based on the Kinsey scale, 0–3 were heterosexuals, 5–7 were homosexuals, and 4 (bisexuals), and 8 (asexuals) were excluded from the data. Then, to explore the visual attention patterns of different sexual orientation in watching two different faces (masculinized and feminized), we conducted a 2 (sexual dimorphism: masculine, feminine) × 4 (sexual orientation: homosexual and heterosexual, male and female) mixed analysis of variance (ANOVA). Next, each participant was assigned to four levels (A = masculine, B = feminine, C = androgynous, D = undifferentiated) according to his/her self-rating on the CSRI. To explore the visual attention patterns of participants with different sex roles in watching two different sexual dimorphism stimulations, we conducted a 2 (sexual dimorphism: masculine, feminine) × 4 (sex role: A, B, C, D) mixed ANOVA. Finally, in order to find out the relationship between eye-tracking indicators and the scores of CSRI, we adopted a hierarchical multiple regression analysis.

# RESULTS

The experimental results included behavioral data and eye movement data. The behavioral data were as follows: the probability of choosing masculine faces as more attractive faces in paired faces and the classification of four sex roles. Eye movement data were as follows: the mean number of fixations, the mean duration of the first fixation duration, and the mean pupil size.

In experiment 1, after eliminating the questionnaires with missing data, the data of CSRI were analyzed and excluded from the data of 14 participants. The data of 81 participants (21 homosexual men, 19 heterosexual men, 21 homosexual women, and 20 heterosexual women) were entered into the classification of sex role process. In eye movement data analysis, because of eye fatigue or head movement, the eye movement instrument was unable to record some participants' data or recorded data inaccurately. Therefore, the data of seven participants were deleted from the eye movement experiment data analysis. Finally, 88 participants (21 homosexual men, 22 heterosexual men, 22 homosexual women, and 23 heterosexual women) entered the eye movement data analysis. Data analysis used SPSS16.0.

At the onset of data analysis, we analyzed if eye moment indicator differences exist within gender. A significant difference was found between gender and the number of fixations ($t = 2.039$, $p = 0.042$, Cohen's $d = 0.096$). But the results showed no differences between gender and pupil size ($t = 0.155$, $p = 0.877$) as well as the first fixation duration ($t = 1.758$, $p = 0.079$).

## Sexual Orientation and Sexual Dimorphism on Facial Attractiveness

### The Proportion of Masculinized Faces Chosen as More Attractive Faces

To find the proportion of choosing masculinized faces as more attractive in paired faces, a 2 (gender) × 2 (sexual orientation: homosexuals and heterosexuals) ANOVA was conducted. Data

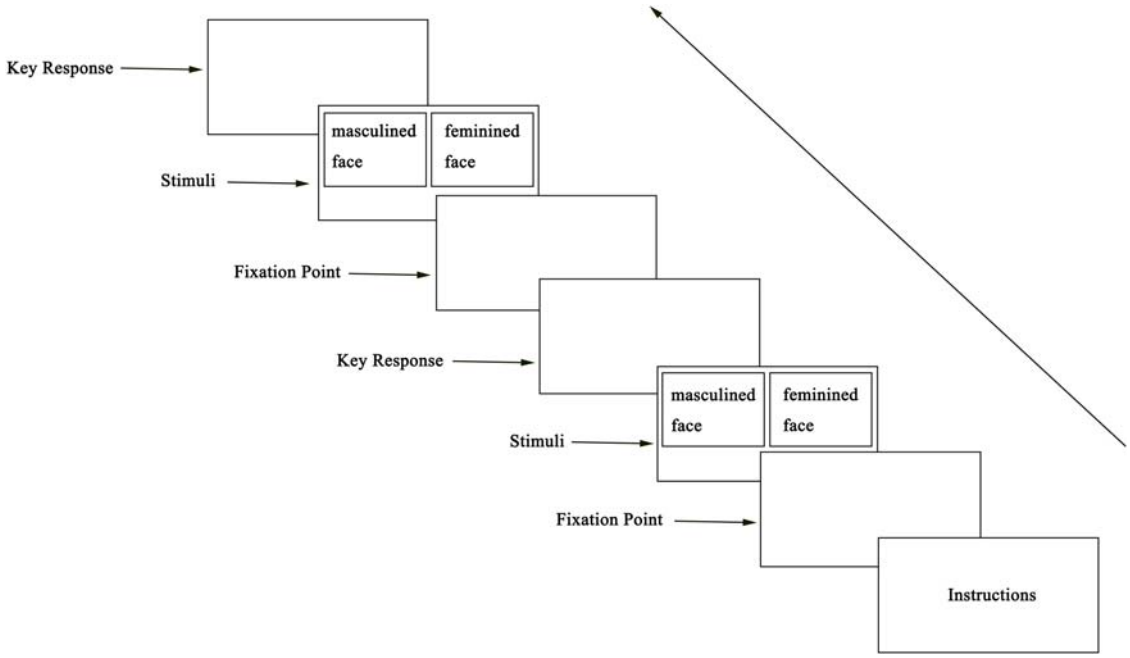


**FIGURE 3 |** Experiment flowchart.

**TABLE 2 |** The probability of choosing masculine faces as more attractive faces in different types of subjects (M ± SD).

| Types | Sexual dimorphism | M ± SD |
|---|---|---|
| Homosexual men | Masculinized | 0.52 ± 0.14 |
| Heterosexual men | Masculinized | 0.37 ± 0.15 |
| Homosexual women | Masculinized | 0.48 ± 0.21 |
| Heterosexual women | Masculinized | 0.46 ± 0.17 |

are presented in **Table 2**. The results indicated that there was a significant main effect of sexual orientation, $F(1,84) = 6.219$, $p < 0.05$, $\eta_p^2 = 0.069$. Homosexuals ($ME = 0.504$, $SD = 0.181$) have a higher fluency in choosing masculinized faces as more attractive faces in paired faces than heterosexuals ($ME = 0.414$, $SD = 0.161$). Analysis revealed neither a significant main effect of gender, $F(1,84) = 0.332$, $p = 0.566$, $\eta_p^2 = 0.004$, nor the interaction effect between sexual orientation and gender, $F(1,84) = 2.968$, $p = 0.089$, $\eta_p^2 = 0.034$.

## Sexual Orientation Difference in Viewing Patterns to Different Sexual Dimorphism Faces

A 2 (sexual dimorphism: masculine, feminine) × 4 (sexual orientation: homosexual and heterosexual, male and female) mixed ANOVA was conducted. Means and standard errors for participants gazing at faces are shown in **Table 3** and **Figure 4**.

For mean pupil size, analyses did not show a significant effect of group, $F(3,84) = 1.065$, $p = 0.369$, $\eta_p^2 = 0.037$, or the main effect by sexual dimorphism, $F(1,84) = 1.104$, $p = 0.296$, $\eta_p^2 = 0.013$. There was a significant interaction effect between sexual dimorphism and subjects' types, $F(3,84) = 2.708$, $p < 0.05$, $\eta_p^2 = 0.088$. Simple effect analysis showed that when participants viewed masculine or feminine faces, there was no difference in their pupil size. However, for homosexual men, when viewing masculine faces, their pupil sizes were significantly smaller than when they viewed the feminine faces, $F(1,20) = 8.409$, $p < 0.01$, $\eta_p^2 = 0.091$.

For the first fixation duration, analyses did not reveal a significant effect of group, $F(3,84) = 1.937$, $p = 0.130$, $\eta_p^2 = 0.065$. There was a significant main effect of sexual dimorphism, $F(1,84) = 5.152$, $p < 0.05$, $\eta_p^2 = 0.058$, and a significant interaction effect between sexual dimorphism and sexual orientation, $F(3,84) = 5.973$, $p < 0.01$, $\eta_p^2 = 0.176$. Simple effect analysis showed that the first fixation duration of homosexual men was significantly shorter than that of heterosexual men ($p < 0.01$), homosexual women ($p < 0.05$), and heterosexual women ($p < 0.05$). When homosexual men were viewing feminine faces, their first fixation duration was significantly longer than that of the other three types ($p < 0.05$). Moreover, for homosexual men, when they were observing masculine faces, their first fixation duration was significantly shorter than their observation of feminine faces, $F(1,20) = 22.512$, $p < 0.01$, $\eta_p^2 = 0.211$, while for the other three types of subjects, no differences were found.

For the number of fixations, analyses revealed a significant effect of group, $F(3,84) = 4.382$, $p < 0.01$, $\eta_p^2 = 0.135$, as well as a significant main effect of sexual dimorphism, $F(1,84) = 5.075$, $p < 0.05$, $\eta_p^2 = 0.057$, and a significant interaction effect between sexual dimorphism and sexual orientation, $F(3,84) = 4.651$, $p < 0.01$, $\eta_p^2 = 0.142$. Simple effect analysis showed that when participants observed masculine faces in all four types,

**TABLE 3 |** Eye movement indicators of subjects with different sexual orientations (M ± SD).

| Types | Sexual dimorphism | Mean pupil size (mm) | The first fixation duration (ms) | The number of fixations |
|---|---|---|---|---|
| Homosexual men | Masculinized | 1966.38 ± 662.85 | 207.67 ± 51.87 | 9.30 ± 1.63 |
| | Feminized | 2056.71 ± 533.89 | 379.27 ± 306.88 | 29.55 ± 44.98 |
| Heterosexual men | Masculinized | 2229.70 ± 554.57 | 257.29 ± 40.93 | 8.82 ± 1.52 |
| | Feminized | 2234.53 ± 560.45 | 250.96 ± 38.15 | 9.12 ± 1.30 |
| Homosexual women | Masculinized | 2072.96 ± 467.30 | 248.08 ± 32.22 | 9.32 ± 1.32 |
| | Feminized | 2049.95 ± 465.15 | 248.92 ± 35.31 | 9.15 ± 1.44 |
| Heterosexual women | Masculinized | 1971.27 ± 502.60 | 245.48 ± 48.60 | 9.27 ± 1.69 |
| | Feminized | 1963.13 ± 506.99 | 239.87 ± 39.40 | 9.58 ± 1.19 |

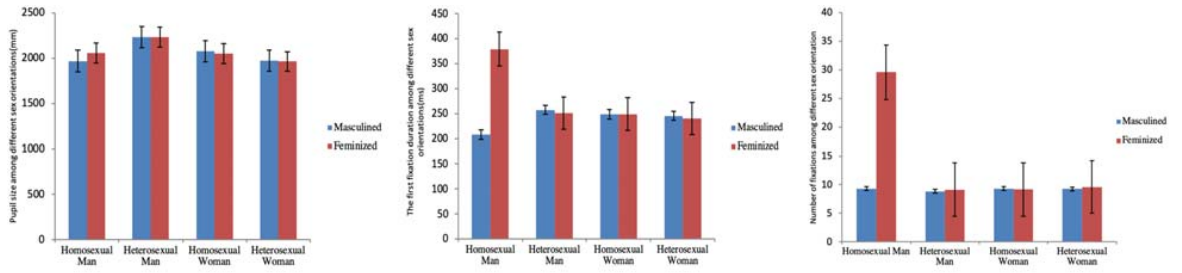


**FIGURE 4 |** Eye movement indicators among sexual orientations. Left, pupil size among different sexual orientations (mm); middle, the first fixation duration among different sexual orientations (ms); right, number of fixations among different sexual orientations. Error bars represent ± 1 standard error.

there was no significant difference in the number of fixations. Conversely, compared to feminine faces, the number of fixations of homosexual men was significantly more than that of the other types ($p < 0.05$). Concerning homosexual men themselves, the number of fixations in viewing masculine faces was significantly less than watching feminine faces, $F(1,20) = 18.587$, $p < 0.01$, $\eta_p^2 = 0.181$. For the other three types of subjects, no differences were found.

Next, we considered the gender of pictures. Thus, we conducted a 2 (sex of pictures) × 2 (sexual dimorphism) × 4 (sexual orientations) ANOVA. The ANOVA reported a significant main effect of the gender of pictures, $F(1,84) = 10.48$, $p < 0.005$, $\eta_p^2 = 0.111$. There was a significant interaction effect between the gender of pictures and sexual orientations, $F(3,84) = 4.424$, $p < 0.005$, $\eta_p^2 = 0.136$, and a significant interaction effect between the gender of pictures and sexual dimorphism, $F(1,84) = 13.211$, $p < 0.001$, $\eta_p^2 = 0.136$.

## Sex Role and Sexual Dimorphism on Facial Attractiveness

### Classification of Sex Role

Based on the scores of the two positive scales, each participant was grouped into four sex role types by Spence's median classification, which calculated the median scores of the Masculine Positive Category (M) and the Feminine Positive Category (F). According to this criterion, the participants were grouped into four types: high M and low F participants were considered a masculine type, low M and high F participants were a feminine type, high M and high F participants were an androgynous type, and low M and low F participants were an undifferentiated type. The results are shown in **Table 4**.

We analyzed the frequency of choosing masculinized faces as more attractive faces by ANOVA. The results showed that there was no difference among different sex role types, $F(3,80) = 0.182$, $p > 0.05$. The results are shown in **Table 5**.

### Sex Role Difference in Viewing Patterns to Different Sexual Dimorphism Faces

A 2 (sexual dimorphism: masculinized, feminized) × 4 (sex role: masculine, feminine, androgynous, and undifferentiated) mixed ANOVA was conducted. Means and standard errors for participants gazing at faces are shown in **Table 6** and **Figure 5**.

For mean pupil size, analyses did not show a significant interaction effect, $F(3,77) = 1.740$, $p = 0.166$, or the main effect by sexual dimorphism, $F(1,77) = 2.227$, $p = 0.140$. There was a significant effect by group, $F(3,77) = 2.787$, $p < 0.05$, $\eta_p^2 = 0.098$. The *post hoc* results showed that when watching masculine faces, the pupil size of the androgynous type was significantly smaller than that of the undifferentiated type ($p < 0.05$). When viewing feminine faces, a marginal difference ($p = 0.051$) was found for the pupil size of androgynous and undifferentiated subjects, and the pupil size of androgynous subjects was smaller than that of undifferentiated subjects.

For the first fixation duration, analyses did not reveal a significant interaction effect, $F(3,77) = 1.999$, $p = 0.121$, or the effect of group, $F(3,77) = 0.861$, $p = 0.465$. There was a significant main effect of sexual dimorphism, $F(1,77) = 6.400$, $p < 0.05$, $\eta_p^2 = 0.077$. The *post hoc* test showed that when participants were looking at masculine faces, the first fixation

**TABLE 4 |** Distribution of four sex role types.

| | Masculine | Feminine | Androgynous | Undifferentiated | Total |
|---|---|---|---|---|---|
| Homosexual men | 4 (19.0%) | 9 (38.0%) | 3 (19.0%) | 5 (23.8%) | 21 |
| Homosexual women | 6 (28.5%) | 0 (0%) | 10 (47.6%) | 5 (23.8%) | 21 |
| Heterosexual men | 3 (19.0%) | 3 (19.0%) | 10 (52.3%) | 3 (9.5%) | 19 |
| Heterosexual women | 5 (23.8%) | 4 (19.0%) | 8 (38.0%) | 3 (19.0%) | 20 |
| Total | 18 (22.6%) | 16 (19.0%) | 31 (40.4%) | 16 (19.0%) | 81 |

**TABLE 5 |** The probability of choosing masculine faces as more attractive faces in different sex role types of subjects (M ± SD).

| Sex role types | Sexual dimorphism | M ± SD |
|---|---|---|
| Masculine | Masculinized | 0.48 ± 0.18 |
| Feminine | Masculinized | 0.44 ± 0.15 |
| Androgynous | Masculinized | 0.45 ± 0.17 |
| Undifferentiated | Masculinized | 0.47 ± 0.19 |

duration of feminine subjects was significantly shorter than that of undifferentiated subjects ($p < 0.05$), whereas when they were watching feminine faces, there were no differences among all the four group types. For feminine subjects, their first fixation duration on masculine faces was significantly shorter compared to feminine faces, $F(1,15) = 5.333$, $p < 0.05$, $\eta_p^2 = 0.065$. Identical results were also found in androgynous subjects, $F(1,15) = 4.936$, $p < 0.05$, $\eta_p^2 = 0.060$.

For the number of fixations, analyses revealed a significant main effect of sexual dimorphism, $F(1,77) = 6.346$, $p < 0.05$, $\eta_p^2 = 0.076$. There was no significant interaction effect between sexual dimorphism and subjects' sex roles, $F(3,77) = 2.110$, $p = 0.106$, or a significant main effect of sex role, $F(3,77) = 2.390$, $p = 0.075$. The *post hoc* test showed that when viewing masculine faces, the number of fixations made by feminine subjects was significantly less than the observation of feminine faces, $F(1,15) = 6.420$, $p < 0.05$, $\eta_p^2 = 0.077$. Identical results were again found in the androgynous group, $F(1,15) = 4.203$, $p < 0.05$, $\eta_p^2 = 0.052$.

A 2 (sex of pictures) × 2 (sexual dimorphism) × 4 (sexual orientations) ANOVA was then carried out. The ANOVA reported a significant main effect of the gender of pictures, $F(1,77) = 10.40$, $p < 0.005$, $\eta_p^2 = 0.119$, and a significant interaction effect between the gender of pictures and sexual orientations, $F(1,77) = 14.55$, $p < 0.001$, $\eta_p^2 = 0.159$.

## The Effect of Sexual Orientation and Sexual Roles on Eye Movement Indicators

As the 2 × 2 × 4 ANOVA indicated that the interaction effect of sexual orientation and sex role was not significant, we conducted a hierarchical multiple regression analysis in order to consider the effect of sexual orientation and sex role in the first fixation duration and the number of fixations.

The hierarchical multiple regression was conducted with the first fixation duration of participants viewing the masculine faces (the dependent variable). Sexual orientation was entered at stage 1 of the regression and sex role was added at stage 2. The results revealed that at stage 1, sexual orientation contributed significantly to the regression model, $F(1,79) = 4.361$, $p < 0.05$, adjusted $R^2 = 0.040$, $R^2$ change = 0.052, $\beta = 0.229$. As the variable sex role was entered, it explained an additional 7.4% of the variation in the first fixation duration of watching masculine faces, $F(2,78) = 4.214$, $p < 0.05$. The first fixation duration of participants observing the feminine faces (the dependent variable) was then entered at the sexual orientation, at stage 1, and sex role, at stage 2. Model 1, with the sexual orientation, was the only predictor that explained 7.7% of variance and was considered to be significant, $F(1,79) = 7.647$, $p < 0.01$. Model 2, in which sex role was added, did not explain further variance and was not significant, $F(1,78) = 0.064$, $p = 0.80$, adjusted $R^2 = 0.066$, $R^2$ change = 0.001. Furthermore, the number of fixation of participants when observing the feminine face was used as the dependent variable. The independent variable at stage 1 was the sexual orientation. Sex role was put in at stage 2. The results at stage 1 indicated that sexual orientation contributed significantly, $F(1,79) = 7.020$, $p < 0.05$, adjusted $R^2 = 0.070$, $R^2$ change = 0.082, $\beta = -0.286$. At stage 2, sex role was not significant, $F(1,78) = 0.120$, $p = 0.730$, adjusted $R^2 = 0.060$, $R^2$ change = 0.001. Generally speaking, the prediction and function of sexual orientation are more significant than the prediction of sex role.

# DISCUSSION

## General Discussion

Using an eye-tracking task, the present study investigated whether preference differences exist in subjects with different sexual orientations and sex roles from different sexual dimorphism stimuli. Findings from the Bailey et al. (1997) study revealed that compared to heterosexual men, homosexual men preferred masculinized faces, while no significant differences were found between homosexual women and heterosexual women. Most gay males prefer partners who described themselves as masculine (Valentova et al., 2014). In our study, we replicated this finding. Homosexual subjects had a higher fluency in choosing masculine faces as more attractive faces in paired faces than heterosexual groups. In particular, we certainly found that masculine faces are more attractive to homosexual men than heterosexual men. However, no significant differences existed in heterosexual and homosexual female groups. Hence, this supported our hypothesis 1.

**TABLE 6 |** Eye movement indicators of subjects with different sexual role types (M ± SD).

| Types | Sexual dimorphism | Mean pupil size (mm) | The first fixation duration (ms) | The number of fixations |
|---|---|---|---|---|
| Masculine | Masculinized | 2094.12 ± 646.80 | 233.76 ± 29.99 | 9.04 ± 1.68 |
| | Feminized | 2082.21 ± 629.45 | 241.10 ± 42.39 | 9.36 ± 1.74 |
| Feminine | Masculinized | 2072.62 ± 617.94 | 218.26 ± 46.43 | 10.11 ± 1.39 |
| | Feminized | 2140.97 ± 526.39 | 323.88 ± 260.90 | 24.86 ± 41.91 |
| Androgynous | Masculinized | 1731.89 ± 403.70 | 227.83 ± 50.01 | 9.00 ± 1.66 |
| | Feminized | 1792.69 ± 327.27 | 329.44 ± 262.89 | 20.93 ± 33.38 |
| Undifferentiated | Masculinized | 2233.59 ± 500.77 | 257.38 ± 52.80 | 8.95 ± 1.32 |
| | Feminized | 2219.65 ± 510.55 | 256.32 ± 38.39 | 9.00 ± 1.04 |

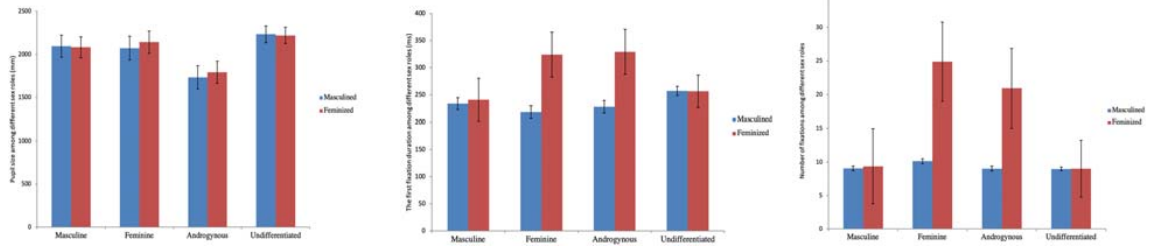


**FIGURE 5 |** Eye movement indicators among sex roles. Left, pupil size among different sex roles (mm); middle, the first fixation duration among different sex roles (ms); right, number of fixations among different sex roles. Error bars represent ± 1 standard error.

Furthermore, Bailey et al. (1997) hypothesized that homosexual men might seek and have similar face preferences to heterosexual women, whereas homosexual women may have similar face preferences to heterosexual men. According to the CSRI questionnaire, the current findings show little evidence of homosexual men treating themselves into a feminine group, and homosexual women treating themselves into a masculine group, hence potentially supporting our hypothesis 2.

Moreover, from findings in sex roles, we also found that compared to feminine faces, masculine faces are more attractive to subjects within feminine type and androgynous type. This partly supported our hypothesis 3, that masculinized faces are more attractive to participants within feminine sex roles. However, no significant differences were detected in the masculine group.

## Sexual Orientation and Sex Role Difference in Viewing Patterns

Pupil size reflects emotional arousal and autonomic activation during affective picture viewing (Partala and Surakka, 2003; Laeng and Falkenberg, 2007; Han and Yan, 2010), and increasing mental load and difficulty of tasks can lead to enlargement of pupil dilation in cognitive tasks (Zhou and Liu, 2009). When viewing masculinized and feminized faces, the average pupil size of the subjects with different sexual orientations was different.

The first fixation duration reflects the early recognition process as well as the sensitivity to materials (Ding et al., 2007). We found that the first fixation duration of homosexual men was significantly shorter than the other three types when viewing masculinized faces, and the first fixation duration of homosexual men was significantly longer than the other three groups when viewing feminine faces. This finding could be explained as in the early recognition process of face images, the sensitivity to the difficulty of processing feminized faces is higher than that of masculinized faces. Further, it also proves that subjects for masculine faces will have a higher level of processing and load. In other words, compared to feminized faces, homosexual men would first take notice of masculinized faces.

The number of fixations reflects the ability of the subjects to deal with stimuli as well as the difficulty of the stimulations (Wen and Zuo, 2012). In our study, we found that the number of fixations of homosexual male watched feminized faces significantly more than masculinized faces. The number of fixations reflected the difficulty of processing, indicating that compared to masculinized faces, homosexual men judged feminized faces as more difficult and consequently processed more deeply. This result is similar to research of Sulikowski et al. (2013) where homosexual men showed less sensitivity than heterosexual men in terms of attractiveness to female faces. The results were consistent with the data of pupil dilation and first fixation duration, suggesting that sexual orientation was one of the factors affecting face attractiveness.

Our study further revealed that when watching masculinized faces, the pupil size of androgynous subjects was significantly smaller than that of undifferentiated subjects. Moreover, when viewing masculine faces, the first fixation duration of participants in the feminine group was significantly shorter than that in the undifferentiated group. Moreover, compared to the viewing of feminine faces, the first fixation duration and the number

of fixations of the feminine and the androgynous group were shorter. These results may indicate that sex role type is one of the factors influencing the face attractiveness of different sexual orientation subjects.

## The Feminization and Masculinization Bias of Homosexuals

Besides, we speculated that under the condition of dividing participants by their sexual orientation, the proportion of sex roles would change compared to Qian et al. (2000). In our study, 40.4% of the subjects were found to be undifferentiated. This may relate to the average age of the participants. We mainly studied college students, aged between 18 and 24 years old; at this age, young people are mostly in the "psychological weaning period." Their concept of psychological gender is not perfect enough to support them to affirm their sex role. After classifying homosexual men according to their sexual orientation, we found that most of the male homosexual's sex role was a feminine type, but no female homosexual's sex role types were feminine. This is partly consistent with the findings of Zheng and Zheng (2009); that is, homosexual men have a feminized inclination to a certain extent. We believe that this may be related to the sex role type of subjects. Chinese gay men mostly use "1," "0," and "both" to distinguish their identity in their partnership, which is equal to "tops," "bottoms," and "versatile." In the social and cultural context, "1" is given more meaning (i.e., virile, strong, and so forth), and "0" is considered to be a sissy or womanish (Bai et al., 2013). Previous studies found that compared to the masculinized male faces, the "1" prefer feminized male faces, and the "0" prefer partners with masculinized faces (Zheng and Zheng, 2015; Zhang et al., 2018). Therefore, we suggest that the feminization bias of homosexual men may be partly due to the differences in individual identities in their partnerships.

## Sexual Orientation and Sex Role

The data of regression analysis suggested that the predicted function of sexual orientation is more significant than the prediction of sex role. This is consistent with the previous study, which proposed that the preference for faces may differ between heterosexuals and homosexuals (Glassenberg et al., 2010). Further, sexual orientation plays an important role in judgment (Ishai, 2007; Lippa, 2007), which could highlight that it is a predicted function in this study. However, considering the sex role, the current study was not powerful enough to prove the significance of facial attractiveness. Hence, the research of sex role still needs to be carried out.

## Limitations and Future Directions

This study is a preliminary exploration of different sexual orientations and sex role preferences in facial attractiveness. However, several limitations of this study should be taken into consideration when making future comparisons.

Initially, it is necessary to increase the sample size since the power is directly based on it. Meanwhile, the participants selected in this study are college students, whose sample representativeness has certain limitations. Thus, in future studies, we not only need to expand the sample size but also further investigate the different ages and occupations of homosexuals and heterosexuals.

Secondly, this study did not put the menstrual cycle into consideration. Several studies have found that the menstrual cycle may have effects on women's judgements for various traits (Penton-Voak et al., 1999; Little et al., 2007; Jones et al., 2008; Little and Jones, 2012); besides, Roberts et al. (2004) have discovered that female faces were more attractive at peak fertility in the menstrual cycle. Therefore, it is recommended for future studies to classify the influence of menstrual cycle.

Third, the role of homosexuals in their partnership should also be considered. Thus, in future studies, we can recruit subjects according to their roles in a homosexual partnership. Lastly, in terms of the evaluation of indicators, we can further combine functional magnetic resonance imaging (fMRI), event-related potential (ERP), and other cognitive neuroscience and technology equipment to provide more objective and scientific indicators for face preference.

# ETHICS STATEMENT

The study was approved by the Human Research Ethics Committee of Anhui University. All participants gave consent to participate in the study and principles expressed in the Declaration of Helsinki were closely followed. Participants were undergraduate students. Informed consent was obtained in written form from all participants. The youngest participant was 18 years old. We did not obtain informed consent from the next of kin, caretakers, or guardians on behalf of the minors/children enrolled in our study. These college students were considered to have comparable intelligence and ability, and able to take charge of their behaviors.

# AUTHOR CONTRIBUTIONS

JH, QC, LS, and XJ conceived and designed the experiments. QC, LS, and XJ performed the experiments. QC and XJ analyzed the data. QC, LS, and CH contributed to the materials and analysis tools. JH, QC, XJ, LS, and CH wrote the manuscript. JH, QC, and LS discussed the result. JH, QC, and CH gave the final approval of the version to be published.

# FUNDING

This study was supported by a Chinese Provincial Undergraduate Innovative Program of Anhui University (No. 201710357393).

# ACKNOWLEDGMENTS

We thank the native English speaker Nileema Ali from the University of Warwick and Dr. G. P. Sharpling from the University of Warwick for helping us revise the language. We also thank Yuanyuan Li from Anhui University for assisting in this study.

## REFERENCES


Bai, L., Xu, Z. L., and Tang, H. M. (2013). Gender norm and male homosexual identity. *Chin. J. Hum. Sex.* 22, 78–83.

Bailey, J. M., Kim, P. Y., Hills, A., and Linsenmeier, J. A. (1997). Butch, femme, or straight acting? Partner preferences of gay men and lesbians. *J. Pers. Soc. Psychol.* 73, 960–973. doi: 10.1037/0022-3514.73.5.960

Beres, M. A., Senn, C. Y., and McCaw, J. (2014). Navigating ambivalence: how heterosexual young adults make sense of desire differences. *J. Sex Res.* 51, 765–776. doi: 10.1080/00224499.2013.792327

Berlyne, D. E. (1958). The influence of complexity and novelty in visual figures on orienting responses. *J. Exp. Psychol.* 55, 289–296. doi: 10.1037/h0043555

Chen, A. C., German, C., and Zaidel, D. W. (1997). Brain asymmetry and facial attractiveness: facial beauty is not simply in the eye of the beholder. *Neuropsychologia* 35, 471–476. doi: 10.1016/S0028-3932(96)00065-6

Conroy-Beam, D., Buss, D. M., Pham, M. N., and Shackelford, T. K. (2015). How sexually dimorphic are human mate preferences? *Pers. Soc. Psychol. Bull.* 41, 1082–1093. doi: 10.1177/0146167215590987

Corbetta, M., Akbudak, E., Conturo, T. E., Snyder, A. Z., Ollinger, J. M., Drury, H. A., et al. (1998). A common network of functional areas for attention and eye movements. *Neuron* 21, 761–773. doi: 10.1016/S0896-6273(00)80593-0

DeBruine, L. (2017). *Webmorph (Version v0.0.0.9001)*.

DeBruine, L. M., Jones, B. C., Little, A. C., Boothroyd, L. G., Perrett, D. I., Penton-Voak, I. S., et al. (2006). Correlated preferences for facial masculinity and ideal or actual partner's masculinity. *Proc. R. Soc. London, Ser. B* 273, 1355–1360. doi: 10.1098/rspb.2005.3445

Ding, X. Y., Kong, K. Q., and Wang, X. F. (2007). The relationship between eye movements and reading achievements in English fast reading. *Psychol. Sci.* 30, 535–539.

Dixson, B. J., Grimshaw, G. M., Linklater, W. L., and Dixson, A. F. (2011). Eye tracking of men's preferences for female breast size and areola pigmentation. *Arch. Sex. Behav.* 40, 51–58. doi: 10.1007/s10508-010-9601-8

Gangestad, S. W., and Scheyd, G. J. (2005). The evolution of human physical attractiveness. *Annu. Rev. Anthropol.* 34, 523–548. doi: 10.1146/annurev.anthro.33.070203.143733

Glassenberg, A. N., Feinberg, D. R., Jones, B. C., Little, A. C., and DeBruine, L. M. (2010). Sex-dimorphic face shape preference in heterosexual and homosexual men and women. *Arch. Sex. Behav.* 39, 1289–1296. doi: 10.1007/s10508-009-9559-6

Grammer, K., and Thornhill, R. (1994). Human (*Homo sapiens*) facial attractiveness and sexual selection: the role of symmetry and averageness. *J. Comp. Psychol.* 108, 233–242. doi: 10.1037/0735-7036.108.3.233

Han, Y. H., and Yan, G. L. (2010). The application of the method of eye movement analysis in preschoolers' cognitive research. *Psychol. Sci.* 1, 191–193.

Ishai, A. (2007). Sex, beauty and the orbitofrontal cortex. *Int. J. Psychophysiol.* 63, 181–185. doi: 10.1016/j.ijpsycho.2006.03.010

Johnston, V. S., Hagel, R., Franklin, M., Fink, B., and Grammer, K. (2001). Male facial attractiveness: evidence for hormone-mediated adaptive design. *Evol. Hum. Behav.* 22, 251–267. doi: 10.1016/S1090-5138(01)00066-6

Jones, B. C., DeBruine, L. M., Perrett, D. I., Little, A. C., Feinberg, D. R., and Smith, M. J. L. (2008). Effects of menstrual cycle phase on face preferences. *Arch. Sex. Behav.* 37, 78–84. doi: 10.1007/s10508-007-9268-y

Jones, B. C., Little, A. C., Burt, D. M., and Perrett, D. I. (2004). When facial attractiveness is only skin deep. *Perception* 33, 569–576. doi: 10.1068/p3463

Kinsey, A. C., Pomeroy, W. P., and Martin, C. E. (1949). Sexual behaviour in the human male. *J. Neuropathol. Exp. Neurol.* 8, 272–275.

Kościński, K. (2013). Perception of facial attractiveness from static and dynamic stimuli. *Perception* 42, 163–175. doi: 10.1068/p7378

Kou, H., Su, Y., Zhang, Y., Kong, F., Hu, Y., Wang, Y., et al. (2013). Influential factors of facial attractiveness: the observer hypothesis. *Adv. Psychol. Sci.* 21, 2144–2153. doi: 10.3724/SP.J.1042.2013.02144

Kranz, F., and Ishai, A. (2006). Face perception is modulated by sexual preference. *Curr. Biol.* 16, 63–68. doi: 10.1016/j.cub.2005.10.070

Laeng, B., and Falkenberg, L. (2007). Women's pupillary responses to sexually significant others during the hormonal cycle. *Horm. Behav.* 52, 520–530. doi: 10.1016/j.yhbeh.2007.07.013

Li, O., and Chen, H. (2010). The retrospect and prospect of facial attractiveness. *Adv. Psychol. Sci.* 18, 472–479.

Lippa, R. A. (2007). The preferred traits of mates in a cross-national study of heterosexual and homosexual men and women: an examination of biological and cultural influences. *Arch. Sex. Behav.* 36, 193–208. doi: 10.1007/s10508-006-9151-2

Little, A. C., and Jones, B. C. (2012). Variation in facial masculinity and symmetry preferences across the menstrual cycle is moderated by relationship context. *Psychoneuroendocrinology* 37, 999–1008. doi: 10.1016/j.psyneuen.2011.11.007

Little, A. C., Jones, B. C., Burt, D. M., and Perrett, D. I. (2007). preferences for symmetry in faces change across the menstrual cycle. *Biol. Psychol.* 76, 209–216. doi: 10.1016/j.biopsycho.2007.08.003

Little, A. C., Jones, B. C., Waitt, C., Tiddeman, B. P., Feinberg, D. R., Perrett, D. I., et al. (2008). Symmetry is related to sexual dimorphism in faces: data across culture and species. *PloS One* 3:e2106. doi: 10.1371/journal.pone.0002106

Little, A. C., and Perrett, D. I. (2002). Putting beauty back in the eye of the beholder. *Psychologist* 15, 28–32.

Miller, G. F., and Todd, P. M. (1998). Mate choice turns cognitive. *Trends Cogn. Sci.* 2, 190–198. doi: 10.1016/S1364-6613(98)01169-3

Partala, T., and Surakka, V. (2003). Pupil size variation as an indication of affective processing. *Int. J. Hum. Comput. Stud.* 59, 185–198. doi: 10.1016/S1071-5819(03)00017-X

Penton-Voak, I. S., Perrett, D. I., Castles, D. L., Kobayashi, T., Burt, D. M., Murray, L. K., et al. (1999). Menstrual cycle alters face preference. *Nature* 399, 741–742. doi: 10.1038/21557

Perrett, D. I., Burt, D. M., Penton-Voak, I. S., Lee, K. J., Rowland, D. A., and Edwards, R. (1999). Symmetry and human facial attractiveness. *Evol. Hum. Behav.* 20, 295–307. doi: 10.1016/S1090-5138(99)00014-8

Perrett, D. I., Lee, K. J., Penton-Voak, I., Rowland, D., Yoshikawa, S., Burt, D. M., et al. (1998). Effects of sexual dimorphism on facial attractiveness. *Nature* 394:884. doi: 10.1038/29772

Qian, M., Zhang, G., Luo, S., and Zhang, S. (2000). Sex role inventory for college students (CSRI). *Acta Psychol. Sin.* 32, 99–104.

Rennels, J. L., Bronstad, P. M., and Langlois, J. H. (2008). Are attractive men's faces masculine or feminine? The importance of type of facial stimuli. *J. Exp. Psychol. Hum. Percept. Perform.* 34, 884–893. doi: 10.1037/0096-1523.34.4.884

Rhodes, G. (2006). The evolutionary psychology of facial beauty. *Annu. Rev. Psychol.* 57, 199–226. doi: 10.1146/annurev.psych.57.102904.190208

Rhodes, G., Chan, J., Zebrowitz, L. A., and Simmons, L. W. (2003). Does sexual dimorphism in human faces signal health? *Proc. R. Soc. Lond. Ser. B* 270(Suppl. 1), S93–S95. doi: 10.1098/rsbl.2003.0023

Richards, M. R., Fields, H. W. Jr, Beck, F. M., Firestone, A. R., Walther, D. B., Rosenstiel, S., et al. (2015). Contribution of malocclusion and female facial attractiveness to smile esthetics evaluated by eye tracking. *Am. J. Orthod. Dentofacial Orthop.* 147, 472–482. doi: 10.1016/j.ajodo.2014.12.016

Roberts, S. C., Havlicek, J., Flegr, J., Hruskova, M., Little, A. C., Jones, B. C., et al. (2004). Female facial attractiveness increases during the fertile phase of the menstrual cycle. *Proc. R. Soc. Lond. Ser. B* 271(Suppl. 5), S270–S272. doi: 10.1098/rsbl.2004.0174

Ruz, M., and Lupiáñez, J. (2002). A review of attentional capture: on its automaticity and sensitivity to endogenous control. *Psicológica* 23, 283–309.

Steffens, M. C., Landmann, S., and Mecklenbräuker, S. (2013). Participant sexual orientation matters: new evidence on the gender bias in face recognition. *Exp. Psychol.* 60, 362–367. doi: 10.1027/1618-3169/a000209

Sulikowski, D., Iannelli, T., Barron, A., and Burke, D. (2013). "Homosexual men show reduced sensitivity to cues of attractiveness in female faces," in *Proceedings of the 8th Biannual Meeting of the Australasian Evolution Society30*, (Geelong, VIC).

Sun, Y. H., Shi, H. M., Liu, F., Wang, Z., and Li, H. D. (2012). Effect of hale-faces and their locations on face attractiveness. *Chin. J. Appl. Psychol.* 18, 139–145.

Valentova, J. V., Stulp, G., Třebický, V., and Havlíček, J. (2014). Preferred and actual relative height among homosexual male partners vary with preferred dominance and sex role. *PloS One* 9:e86534. doi: 10.1371/journal.pone.0086534

Welling, L. L., Jones, B. C., DeBruine, L. M., Conway, C. A., Smith, M. L., Little, A., et al. (2007). Raised salivary testosterone in women is associated with increased attraction to masculine faces. *Horm. Behav.* 52, 156–161. doi: 10.1016/j.yhbeh.2007.01.010

Wen, F.-F., and Zuo, B. (2012). The effects of transformed gender facial features on face preference of college students: based on the test of computer graphics and eye movement tracks. *Acta Psychol. Sin.* 44, 14–29. doi: 10.3724/SP.J.1041.2012.00014

Yang, T. (2015). *Effect of sexually dimorphic cues on face preference: an eye-tracking study*. Doctoral dissertation. Chongqing: Xinan University.

Zhang, J., Zheng, L., and Zheng, Y. (2018). Consistency in preferences for masculinity in faces, bodies, voices, and personality characteristics among homosexual men in China. *Pers. Individ. Dif.* 134, 137–142. doi: 10.1016/j.paid.2018.06.009

Zhang, L. L., Wei, B., and Zhang, Y. (2016). Smile modulates the effect of facial attractiveness: an eye movement study. *Psychol. Explor.* 36, 13–17.

Zhang, Y., and Zheng, M. X. (2016). Facial attractiveness in the eye of the beholder: one eye movement research of the angle effect. *Stud. Psychol. Behav.* 14, 459–464.

Zheng, L., and Zheng, Y. (2015). Preferences for masculinity across faces, bodies, and personality traits in homosexual and bisexual Chinese men: relationship to sexual self-labels and attitudes toward masculinity. *Arch. Sex. Behav.* 45, 725–733. doi: 10.1007/s10508-015-0543-z

Zheng, L. J., and Zheng, Y. (2009). Research on heterosexual tendency of homosexual subjects in China. *Chin. Public Health* 25, 499–500.

Zhou, Y., and Liu, J. S. (2009). Using eye-movement to study implicit aggressiveness. *Psychol. Sci.* 32, 858–860.

**Conflict of Interest Statement:** The authors declare that the research was conducted in the absence of any commercial or financial relationships that could be construed as a potential conflict of interest.

frontiers in Human Neuroscience

ORIGINAL RESEARCH
published: 21 May 2019
doi: 10.3389/fnhum.2019.00108

# TFEB Probably Involved in Midazolam-Disturbed Lysosomal Homeostasis and Its Induced β-Amyloid Accumulation

*Dan Cheng[1†], Qilian Tan[1†], Qianyun Zhu[1], Jiqian Zhang[1], Xiaoyu Han[1], Panpan Fang[1], Weilin Jin[2] and Xuesheng Liu[1]**

[1]*Department of Anesthesiology, First Affiliated Hospital of Anhui Medical University, Hefei, China,* [2]*Key Laboratory for Thin Film and Microfabrication Technology of Ministry of Education, Institute of Nano Biomedicine and Engineering, Department of Instrument Science and Engineering, School of Electronic Information and Electronic Engineering, Shanghai Jiao Tong University, Shanghai, China*

OPEN ACCESS

**Edited by:**
*Xiaochu Zhang, University of Science and Technology of China, China*

**Reviewed by:**
*Gabriel Gonzalez-Escamilla, University Medical Centre, Johannes Gutenberg University Mainz, Germany*
*Yan Wang, University of North Carolina at Chapel Hill, United States*

***Correspondence:**
*Xuesheng Liu*
*liuxuesheng@ahmu.edu.cn*

*†These authors have contributed equally to this work and are co-first authors*

**Received:** *16 October 2018*
**Accepted:** *11 March 2019*
**Published:** *21 May 2019*

**Citation:**
*Cheng D, Tan Q, Zhu Q, Zhang J, Han X, Fang P, Jin W and Liu X (2019) TFEB Probably Involved in Midazolam-Disturbed Lysosomal Homeostasis and Its Induced β-Amyloid Accumulation. Front. Hum. Neurosci. 13:108. doi: 10.3389/fnhum.2019.00108*

Alzheimer's disease (AD) is one of the most common neurodegenerative diseases, and β-amyloid (Aβ) plays a leading role in the pathogenesis of AD. The transcription factor EB (TFEB), a main regulating factor of autophagy and lysosome biosynthesis, is involved in the pathogenesis of AD by regulating autophagy-lysosomal pathways. To date, the choice of anesthetics during surgery in patients with neurodegenerative diseases and evaluation of the effects and underlying mechanisms in these patients have rarely been reported. In this study, the HEK293-APP cells overexpressing APP and Hela cells were used. The cells were treated with midazolam at different concentrations and at different times, then lysosomes were stained by lysotracker and their morphology was observed under a fluorescence microscope. The number and size of lysosomes were analyzed using the ImageJ software. The levels of TFEB in the nucleus and APP-cleaved intracellular proteins were detected by nuclear separation and Western Blot. Finally, ELISA was used to detect the levels of Aβ40 and Aβ42 in the cells after drug treatment. We found that 30 μM midazolam decreased the number of lysosomes and increased its size in HEK293 and HeLa cells. However, 15 μM midazolam transiently disturbed lysosomal homeostasis at 24 h and recovered it at 36 h. Notably, there was no significant difference in the extent to which lysosomal homeostasis was disturbed between treatments of different concentrations of midazolam at 24 h. In addition, 30 μM midazolam prevents the transport of TFEB to the nucleus in either normal or starved cells. Finally, the intracellular C-terminal fragment β (CTFβ), CTFα, Aβ40 and Aβ42 levels were all significantly elevated in 30 μM midazolam-treated HKE293-APP cells. Collectively, the inhibition of TFEB transport to the nucleus may be involved in midazolam-disturbed lysosomal homeostasis and its induced Aβ accumulation *in vitro*. The results indicated the risk of accelerating the pathogenesis of AD by midazolam and suggested that TFEB might be a candidate target for reduction of midazolam-dependent neurotoxicity.

**Keywords: emotion, β-amyloid, lysosome, TFEB, midazolam**

## INTRODUCTION

Alzheimer's disease (AD) is one of the most common neurodegenerative diseases, mainly characterized by progressive learning and memory dysfunction, and many of the patients with AD exhibit abnormal emotions (Mirakhur et al., 2004; Potter and Steffens, 2007). Extracellular β-amyloid (Aβ) deposition, intracellular neurofibrillary tangles and a decreased number of synapses and neurons are the dominant pathological features (Laferla et al., 2007; Ubhi and Masliah, 2013) and among them, Aβ received particular attention. The amyloid precursor protein APP is first hydrolyzed by β-secretase and α-secretase to produce the corresponding C-terminal fragment β (CTFβ) C99 and shorter C83 (CTFα), and then CTFβ is further cleaved by γ-secretase to produce Aβ and other fragments (Vassar et al., 2009; De Strooper and Annaert, 2010). Aβ40 and Aβ42 are the main components of long-chain Aβ *in vivo* (Tahmasebinia and Emadi, 2017). Multiple studies have shown that Aβ is closely related to apathy-like behavior, anxiety-like behavior and depression (Wu et al., 2015; Zare et al., 2015; Souza et al., 2016). There are many clinical studies showing that anesthetics can induce postoperative delirium and postoperative cognitive dysfunction in surgical patients (Bilotta et al., 2010; Hussain et al., 2014). Numerous laboratory studies have revealed that inhaled anesthetic sevoflurane and isoflurane could promote the processing of APP, Aβ production and accelerate the progression of AD-related pathological development (Dong et al., 2009; Xie and Xu, 2013; Zhang et al., 2017). However, the effects and mechanisms of intravenous anesthetics on AD are rare.

As an important organelle for intracellular constituent degradation, signal transduction, cellular secretion, plasma membrane repair and energy metabolism, lysosomes are closely associated with neurodegenerative diseases *via* clearance of damaged organelles or aggregated proteins that can cause disease (Settembre et al., 2013b). Lysosomal dysfunction can lead to abnormal protein degradation disorders and deposition, which may cause neurodegenerative diseases (Nixon et al., 2000; Zhang et al., 2009). Abnormal lysosome accumulation is one early histological change in AD patients (Cataldo et al., 1994, 2000; Nixon et al., 2000), and enhancement of lysosomal function can reduce the amyloid deposition and improve the cognitive function in the mouse model of AD (Kawarabayashi et al., 1997; Shie et al., 2003; Langui et al., 2004). Besides, our previous study revealed that inhaled anesthetic sevoflurane could impair autophagic degradation, which depends on lysosomal function, and accelerates the pathological progress of AD in APP/PS1 mouse (Geng et al., 2018). Our published research has showed that midazolam could increase mutant huntingtin protein levels (Zhang et al., 2018). However, the underlying mechanisms of how anesthetics impact on lysosome function is unknown.

The transcription factor EB (TFEB) is a major regulator of lysosomal biosynthesis, which is coordinated by driving autophagy and expression of lysosomal genes (Settembre et al., 2011). TFEB exists in the cytoplasm in the form of inactive phosphorylation under the physiological condition (Kim et al., 2016). In the case of lysosomal abnormalities or starvation, TFEB translocates from the cytoplasm to the nucleus and performs its function as a transcription factor (Settembre et al., 2013a). Xiao and Zhang's study has demonstrated that TFEB can regulate production of autophagosomes and degradation of lysosomes by the autophagy-lysosomal pathway in the mouse model of AD, which accelerates Aβ and amyloid plaques clearance (Xiao et al., 2014, 2015; Zhang and Zhao, 2015) and improves the cognitive function of mouse (Zhang and Zhao, 2015). Increasing evidence has revealed that some drugs attenuate amyloid plaque pathology by regulating TFEB (Bao et al., 2016; Chandra et al., 2018), but there are few studies on the regulation of TFEB by anesthetics.

Midazolam is a commonly used intravenous anesthetic for sedation and balanced general anesthesia during surgery. Our previous study has shown that midazolam could impair the autophagic degradation by downregulating the lysosomal aspartyl protease cathepsin D levels. In this work, we found that 30 μM midazolam decreased the number of lysosomes and increased its size in HEK293 and HeLa cells. Midazolam could also prevent TFEB transport to the nucleus, which may account for the impaired lysosomal homeostasis. Finally, the intracellular Aβ levels were elevated in midazolam treated HKE293-APP cells. These results revealed the risk of accelerating the pathogenesis of AD by midazolam and implied the probable mechanism of anaesthetic-induced abnormal emotion in surgery patients.

## MATERIALS AND METHODS

### Antibodies and Agents

Lyso-Tracker Red (1:10,000; DND-99) was purchased from invitrogen; anti-TFEB antibody (1:800; 13,372-1-AP) was purchased from proteintech; anti-H3 antibody (1:1,500; 17,168-1-AP) was purchased from Abcam, USA; mouse anti-Aβ antibody (1:1,000 dilution) was purchased from Abcam, USA; mouse anti-β-actin antibody (1:1,000 dilution) was purchased from Abcam, USA; mouse monoclonal antibodies used were agonist Aβ (1:10,000) and β-actin (1:10,000); rabbit monoclonal antibodies used were against TFEB (1:5,000) and H3 (1:10,000); BCA protein quantification kit was purchased from China Biyuntian Biotechnology Co., Ltd.; Aβ40 and Aβ42 ELISA kits were purchased from CUSABIO, China.

### Cell Culture

Cells were cultured at 37°C with 5% $CO_2$ in Dulbecco's modified Eagle's medium supplemented with 10% fetal bovine serum (FBS). HEK293 cells are primary embryonic human kidney cells, HEK293-APP are APP-overexpressed HEK293B cells, and these cells were kindly provided by WJ in Shanghai Jiao Tong University. HeLa cells are human cervical cancer cell lines, and they were kindly provided by Professor Longping Wen in the University of Science and Technology of China. Nutrient starvation assays were performed in the presence of Earle's Balanced Salt Solution (EBSS).

### Lysosomal Staining

For LysoTracker Red DND-99 assay, Cells were seeded in a 24-well culture plate at a density of $5 \times 10^4$ cells per

well, incubated in 37°C, 5% $CO_2$ for 24 h and then treated with midazolam for different times and washed twice in PBS. Next, the cells were incubated in medium containing 1 μM LysoTracker Red DND-99 (Invitrogen, L-7528) dye for 10 min. Cells were washed twice in PBS and observed under an LSM 710 confocal microscope (Carl Zeiss AG, Oberkochen Germany). The size and number of lysosomes were measured by ImageJ software using its "analyze particle" analysis tool with default image/adjust/threshold settings. For lysosomal morphology and size, as well as the effect size between the two groups were calculated using Ellis (2010), "Effect Size FAQs," website.

## Co-location Detection

To explore the relationship between midazolam and TFEB translocation, the live cell imaging analysis was carried out. After being treated with or without 30 μM midazolam for 24 h and starved for 4 h, EGFP-TFEB/HeLa Cells were washed twice in PBS, then incubated with DAPI (blue) for 10 min, the cellular fluorescence was observed by confocal microscopy (Carl Zeiss AG, Oberkochen Germany). The HeLa EGFP-TFEB cell lines were kindly provided by professor Wen Longping, which expressed strong green fluorescence under a fluorescence microscope.

## Nuclear and Cytoplasm Separation

The sucrose buffer [1 M sucrose, 0.1 M $CaCl_2$, 1 m magnesium acetate, $250 \times 10^{-3}$ M ethylenediaminetetraacetic acid (EDTA), $100 \times 10^{-3}$ M dithiothreitol (DTT), and $100 \times 10^{-3}$ M phenylmethylsulfonyl fluoride (PMSF)] was used to separate nuclear and cytoplasm fraction. Briefly, cells were collected from a 24-well cell culture plate after treatment and washed by PBS, and then 100–200 μL sucrose NP-40 (0.5% NP-40 in sucrose buffer) buffer was added. Those samples were put on ice for 15 min and centrifuged for 10 min at 1,000× *g*. The supernatant was the cytoplasm fraction. In contrast, the precipitation was the nuclear fraction and washed by sucrose buffer before adding cell lysis buffer and boiling.

## Western Blot Analysis

Cells were lysed with sample buffer and boiled for 10 min. Proteins were separated by sodium dodecyl sulfate polyacrylamide gel electrophoresis and were transferred onto nitrocellulose membranes. The membranes were incubated with the primary antibody at 4°C overnight and the second antibody for 1 h at 37°C. Membranes were incubated with the ECL kit and visualized using a chemiluminescence instrument (ImageQuant LAS 4000, GE Healthcare, Little Chalfont, UK).

## Enzyme-Linked Immunosorbent Assay

The cells were homogenized in PBS followed by RIPA buffer [50 mM Tris-HCl, 150 mM NaCl, 1% Triton X-100, 0.1% SDS, and 1× protease inhibitor (Xiao et al., 2014)]. The concentrations of Aβ40 and Aβ42 intracellular were detected by a human-specific ELISA kit (CUSABIO, China), according to the manufacturer's instructions.

## Experimental Grouping

(1) For lysosomal homeostasis detection, HEK293 and Hela cells were divided into two groups: 15 μM and 30 μM midazolam treatment groups. At 0, 24 h and 36 h, the size and morphology of the lysosomes were observed; (2) for TFEB levels detection, HEK293 and Hela cells were divided into two groups: 15 μM and 30 μM midazolam treatment groups. Detect the levels of TFEB at different times (0 h, 24 h, 36 h) in the nucleus; (3) for TFEB levels detection in the case of starvation with or without 30 μM midazolam, HEK293 and Hela cells were divided into four groups: control, midazolam, starvation and midazolam+starvation. Detect the level of TFEB in the nucleus; and (4) for Aβ levels detection, HEK293 cells were divided into control and 30 μM midazolam treatment group. Detect the C83, C99 levels.

## Statistical Analysis

All data are shown as Mean ± SEM. Data were analyzed by two-tailed Student's *t*-test for detecting significant differences between two groups. For lysosomal homeostasis detection, the lysosomal size and number were analyzed by one-way ANOVA followed by *post hoc* Tukey's test. The Western Blot results were analyzed by one-way ANOVA, followed by Tukey's *Post hoc* test or two-tailed Student's *t*-test. For Aβ40 and Aβ42 detection using ELISA, the results were analyzed by two-tailed Student's *t*-test. Differences were considered statistically significant at $^{*}p < 0.05$ and $^{**}p < 0.01$, $^{***}p < 0.001$.

# RESULTS

## Midazolam Impair Lysosomal Homeostasis

To evaluate the effect of midazolam on lysosomes, HEK293 and HeLa cells were treated with different concentrations of midazolam for 24 h or 36 h. After 15 μM midazolam treatment, the number ($p < 0.001$, effect sizes: 2.820) and size ($p < 0.001$, effect sizes: 6.586) of lysosomes were transiently decreased and became larger at 24 h compared with 0 h, respectively. The above changes were counteracted at 36 h ($p > 0.5$, effect sizes: 0.036; 0.824; **Figures 1A–C**). However, 30 μM midazolam continuously decreased lysosome number ($p < 0.001$, effect sizes: 4.480) and swelled lysosomes ($p < 0.001$, effect sizes: 2.890) until 36 h (**Figures 1A–C**). What's more, the same experiment was carried out in Hela cells, and the results were similar to those of HEK293 cells (**Figures 1D–F**), at 15 μM midazolam, the number ($p < 0.001$, effect sizes: 3.115) and size ($p < 0.001$, effect sizes: 2.035) of lysosomes temporarily decreased and became larger at 24 h, and these changes were offset at 36 h ($p > 0.5$, effect sizes: 0.017; 0.896), but 30 μM midazolam continued to reduce the number of lysosomes ($p < 0.001$, effect sizes: 3.70) and lysosomes expand ($p < 0.001$, effect sizes: 3.71) until 36 h. Notably, the size and number of lysosomes had no significant difference under different concentrations of midazolam treatment at 24 h, indicating the similar extent of damage to the lysosomal homeostasis by midazolam (**Supplementary Figure S1**).

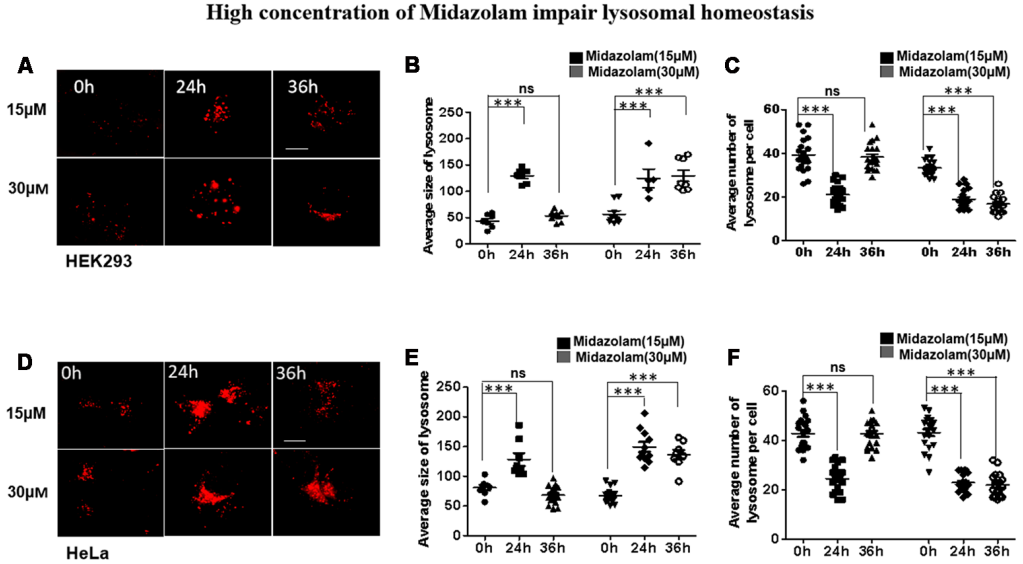


**FIGURE 1 |** Midazolam disturbs lysosomal homeostasis. HEK293 and Hela cells were treated with 15 μM or 30 μM midazolam for 0–36 h. The size and morphology of the lysosomes were observed under a microscope. **(A,D)** Lysosomal staining pattern of HEK293 cells and HeLa cells treated with 15 μM or 30 μM midazolam at 0 h, 24 h, and 36 h, respectively. **(B,E)** Statistical results of the average size of lysosomes in HEK293 cells and HeLa cells, respectively. **(C,F)** Statistical results of the average number of lysosomes per HEK293 and HeLa cell, respectively. For lysosomal number and lysosomal size statistics, at least 30 cells per group were counted. Scale bar = 2 μM (Mean ± SEM. ***$p < 0.001$, ns, no significant).

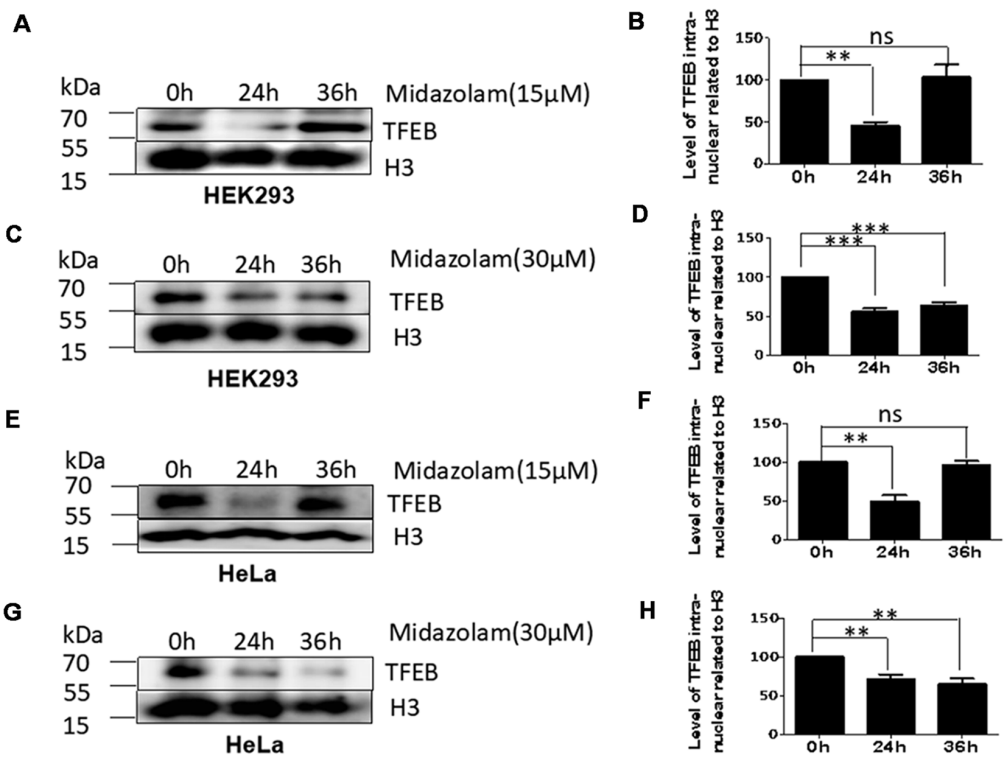


**FIGURE 2 |** Lysosome homeostasis disruption accompanied by TFEB fails to transport to the nucleus. After treatment with 15 μM or 30 μM midazolam, the levels of TFEB at different times in the nucleus were examined. **(A,C)** Western Blot results of nuclear TFEB level in HEK293 cells. **(B,D)** Statistical results of **(A,C)**, respectively. **(E,G)** Western Blot results of nuclear TFEB level in HeLa cells. **(F,H)** Statistical results of **(B,D)**, respectively (Mean ± SEM. $N = 3$. **$p < 0.01$, ***$p < 0.001$, ns: no significant).

## Lysosome Homeostasis Disruption Accompanied by Failed Transportation of TFEB

As TFEB is the major regulator of lysosome biosynthesis, the levels of TFEB in the nucleus was detected in midazolam-treated cells. The results showed that nuclear TFEB levels were reduced at 24 h in both HKK293 and HeLa cells treated with 15 μM midazolam compared with 0 h, but it was recovered at 36 h (**Figures 2A,B,E,F**). However, the nuclear TFEB continued to decrease until 36 h after 30 μM midazolam treatment (**Figures 2C,D,G,H**). These data were consistent with changes in the size and number of lysosomes previously found (**Figures 1B,C,E,F**), indicating a relationship between lysosomal homeostasis disruption and TFEB transportation failure.

## Midazolam Prevents TFEB From Transport to the Nucleus

In starvation condition, TFEB will transport from cytoplasm to nucleus to upregulate lysosomal function and autophagy, and then provide enough nutrients for the cells to survive (Settembre et al., 2011). To further verify whether midazolam could prevent TFEB transportation, nuclear TFEB levels were tested in starved cells with or without 30 μM midazolam treatment. Indeed, the TFEB levels were elevated in starved HEK293 cells. To the contrary, it was reduced in starved cells that were pretreated with midazolam (**Figures 3A,C**). Besides, the same results were observed in HeLa cells (**Figures 3B,D**), the levels of TFEB increased in HeLa cells for the treatment of starvation. Conversely, it was decreased in starved cells pretreated with midazolam. Furthermore, HeLa cells overexpressing GFP-TFEB were used to confirm the inhibition of TFEB translocation by midazolam. In starved HeLa cells, most of the GFP-tagged TFEB entered the nucleus, however, it was few in midazolam pre-treated starved cells (**Figure 3E**). These results demonstrated that 30 μM midazolam could indeed block TFEB from entering the nucleus. In this case, once lysosomes were disrupted by midazolam, it would not be repaired.

## Midazolam Induces Aβ Accumulation

Aβ has been shown to be neurotoxic and plays a leading role in the pathogenesis of AD. The lysosome is an important organ required for Aβ degradation (Xiao et al., 2014; Aguzzi and Haass, 2003; De Kimpe et al., 2013). However, 30 μM midazolam not only impaired lysosomal homeostasis but also had an impact on lysosome biogenesis regulator TFEB, thus, we assume that midazolam might change the metabolism of Aβ. Therefore, the level of APP cleavage products C83, C99, Aβ40 and Aβ42 were further detected in APP-overexpressed HEK293 cells. Indeed, the results showed that the contents of C83, C99 (**Figures 4A,B**), intracellular Aβ40 and Aβ42 (**Figures 4C,D**) were all elevated after midazolam treatment.

# DISCUSSION

In this study, we found that the clinically used anesthetic sedative midazolam increased intracellular Aβ levels, suggesting that midazolam may promote the pathological process of AD. Additionally, our previous studies have also shown that midazolam increases intracellular mutant huntingtin protein, revealing its risk of accelerating the pathogenesis

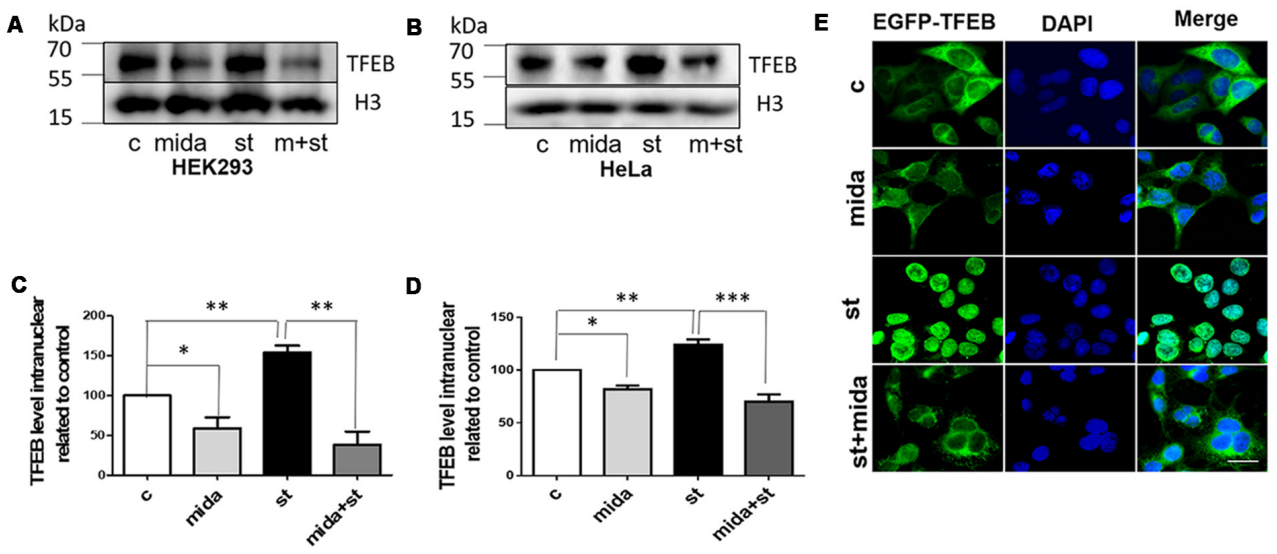


**FIGURE 3 |** Midazolam prevents TFEB transport to the nucleus in the starved cell. Starvation 4 h as a positive control, is known to facilitate the intervention of TFEB into the nucleus. Before starved for 4 h, cells were pretreated with or without 30 μM midazolam for 24 h. **(A,B)** Western Blot results of nuclear TFEB levels in HEK293 cells and HeLa cells, respectively. **(C,D)** Statistical results of nuclear TFEB levels related to H3 levels in HEK293 cells and HeLa cells, respectively. **(E)** Representative fluorescent pictures of GFP-TFEB/HeLa cells nucleus translocation. The nucleus was stained by DAPI. Scale bar = 20 μM. C Control, Mida: Midazolam, St: Starvation (Mean ± SEM. $N = 3$. $^{*}p < 0.05$, $^{**}p < 0.01$, $^{***}p < 0.001$, ns, no significant).

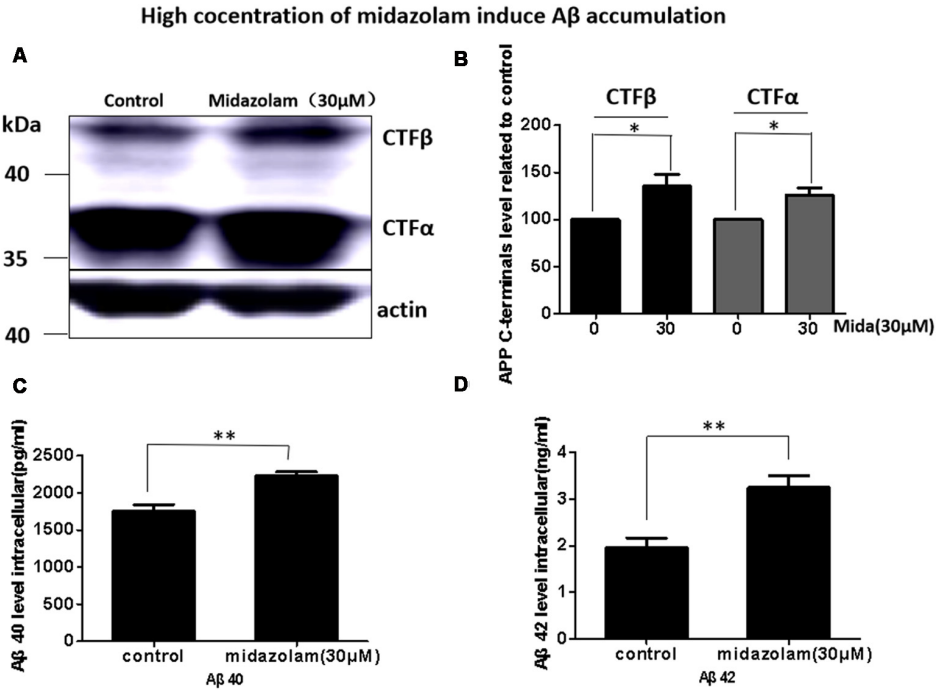


**FIGURE 4 |** Midazolam triggers the accumulation of Aβ. HEK293-APP cells were treated with 30 μM midazolam for 36 h. **(A)** Western Blot results of C83, C99 levels. **(B)** Statistical results of **(A)**. **(C,D)** ELISA results of intracellular Aβ40 and Aβ42 levels (Mean ± SEM. $N = 3$. $^{*}p < 0.05$, $^{**}p < 0.01$).

of polyglutamine diseases (Zhang et al., 2018). These results suggested that midazolam might have the ability to trigger the aggregation of neurotoxic proteins, and therefore, midazolam may not be the anesthetic of choice for use in patients with neurodegenerative disease.

Notably, midazolam-induced accumulation of neurotoxic protein aggregates was always accompanied by impaired lysosomes/autolysosomes function. In this article, we demonstrate that midazolam destroys lysosomal homeostasis primarily in HEK293 cells which is commonly used instrumental cells with high transfection efficiency and convenient operation in the study of molecular mechanism. They are also often used to study the pathogenesis of Alzheimer's disease. HT22 is hippocampal neuronal cell lines of mouse. And we further test the inhibitory effect of midazolam on lysosomal homeostasis in HT22 cells, the result is the same as HEK293 cells (**Supplementary Figure S2**). Some other intravenous anesthetics have also been reported to impair lysosomes. Ren found that prolonged use of the anesthetic propofol increased the pH of the lysosome and destroyed the lysosomal function (Ren et al., 2017). Propofol could also induce lysosomal membrane permeabilization (LMP), loss of mitochondrial transmembrane potential (MTP) and caspase-dependent apoptosis (Hsing et al., 2012). Although our previous work had also shown that midazolam could disrupt the autophagic degradation pathway and impair the lysosomal homeostasis by downregulating Cathepsin D (Zhang et al., 2018), the reason why damaged lysosomes could not be regenerated was still unknown before this work.

The TFEB, a major regulator of lysosomal biosynthesis, is coordinated by driving autophagy and expression of lysosomal genes (Settembre et al., 2011). However, in this work, we found that a high concentration of midazolam-disturbed lysosomal homeostasis was accompanied by TFEB nuclear translocation failure. Furthermore, we proved that midazolam could also prevent starvation-triggered TFEB transportation. And in this case, damaged lysosome could not have been cleared and regenerated (Nixon and Cataldo, 2006; Settembre et al., 2012), which may account for the irreparability of lysosomal homeostasis. However, the exact relationship between TFEB and disturbed lysosomal homeostasis needs to be further explored.

The impaired autolysosomal function has been reported in sevoflurane-exposed AD mice, and it may be involved in the acceleration of the AD pathological process by sevoflurane (Geng et al., 2018). In this work, midazolam disturbed the lysosomal homeostasis and increased the levels of AD-related proteins, C83, C99 and Aβ40 and Aβ42. Although lysosome is the important organ for Aβ degradation, and enhanced lysosomal function could alleviate AD pathology and improve cognitive function of AD mouse (Nixon et al., 2000; Zhang et al., 2009), whether disturbed lysosomal homeostasis accounts for midazolam-induced accumulation of Aβ still requires verification. In addition, this work is carried out *in vitro* since *in vitro* cell experiments are unilateral and the pathological process cannot be completely simulated *in vivo*. Thus, the effect and mechanism of action of midazolam in AD should be further investigated *in vivo*. Studies have shown that TFEB

enhances flux through lysosomal degradative pathways to induce APP degradation and reduce Aβ generation. Activation of TFEB in neurons is an effective strategy to attenuate Aβ generation and attenuate amyloid plaque deposition in AD (Xiao et al., 2015). In this work, we found that midazolam disrupted the lysosomal homeostasis, prevented TFEB from entering the nucleus, and increased accumulation of Aβ in the cells. Therefore, overexpression of TFEB probably reduced the accumulation of Aβ by midazolam, which needs further study. In summary, midazolam disturbed the homeostasis of lysosomes and prevented the TFEB transport to the nucleus. Midazolam also enhanced the accumulation of AD-related proteins C83, C99, Aβ40 and Aβ42. The results indicated the risk of accelerating the pathogenesis of AD by midazolam and suggested that TFEB might be a candidate target for reduction of midazolam-dependent neurotoxicity.

## AUTHOR CONTRIBUTIONS

DC and QT designed and conducted the study, analyzed and interpreted the data and wrote the manuscript. QZ participated in the work of additional figures 1 and 2 in the later period and participated in the revision of the article. JZ, XH and PF helped conduct the study. WJ provided us with a strain of cells. XL conceived and designed the study, analyzed and interpreted the data, and drafted and critically revised the manuscript.

## FUNDING

This work was supported by grants from the National Natural Science Foundation of China (81571039, 81870841, 81701073, 81171031); Key Projects of Natural Science Research in Anhui Colleges and Universities (KJ2017A193).

## ACKNOWLEDGMENTS

We would like to thank the participants for participating in the study. HEK293 cells were kindly provided by WJ in Shanghai Jiao Tong University. HeLa cells and HeLa EGFP-TFEB cell lines were kindly provided by Prof. Longping Wen in the University of Science and Technology of China.

## SUPPLEMENTARY MATERIAL

The Supplementary Material for this article can be found online at: https://www.frontiersin.org/articles/10.3389/fnhum.2019.00108/full#supplementary-material

## REFERENCES

Aguzzi, A., and Haass, C. (2003). Games played by rogue proteins in prion disorders and Alzheimer's disease. *Science* 302, 814–818. doi: 10.1126/science.1087348

Bao, J., Zheng, L., Zhang, Q., Li, X., Zhang, X., Li, Z., et al. (2016). Deacetylation of TFEB promotes fibrillar Aβ degradation by upregulating lysosomal biogenesis in microglia. *Protein Cell* 7, 417–433. doi: 10.1007/s13238-016-0269-2

Bilotta, F., Doronzio, A., Stazi, E., Titi, L., Fodale, V., Di Nino, G., et al. (2010). Postoperative cognitive dysfunction: toward the Alzheimer's disease pathomechanism hypothesis. *J. Alzheimers. Dis.* 22, 81–89. doi: 10.3233/jad-2010-100825

Cataldo, A. M., Hamilton, D. J., and Nixon, R. A. (1994). Lysosomal abnormalities in degenerating neurons link neuronal compromise to senile plaque development in Alzheimer disease. *Brain Res.* 640, 68–80. doi: 10.1016/0006-8993(94)91858-9

Cataldo, A. M., Peterhoff, C. M., Troncoso, J. C., Gomez-Isla, T., Hyman, B. T., and Nixon, R. A. (2000). Endocytic pathway abnormalities precede amyloid β deposition in sporadic Alzheimer's disease and down syndrome. *Am. J. Pathol.* 157, 277–286 doi: 10.1016/s0002-9440(10)64538-5

Chandra, S., Jana, M., and Pahan, K. (2018). Aspirin induces lysosomal biogenesis and attenuates amyloid plaque pathology in a mouse model of Alzheimer's disease via PPARα. *J. Neurosci.* 38, 6682–6699. doi: 10.1523/JNEUROSCI.0054-18.2018

De Kimpe, L., Van Haastert, E. S., Kaminari, A., Zwart, R., Rutjes, H., Hoozemans, J. J., et al. (2013). Intracellular accumulation of aggregated pyroglutamate amyloid β: convergence of aging and Aβ pathology at the lysosome. *Age* 35, 673–687. doi: 10.1007/s11357-012-9403-0

De Strooper, B., and Annaert, W. (2010). Novel research horizons for presenilins and γ-secretases in cell biology and disease. *Annu. Rev. Cell Dev. Biol.* 26, 235–260. doi: 10.1146/annurev-cellbio-100109-104117

Dong, Y., Zhang, G., Zhang, B., Moir, R. D., Xia, W., Marcantonio, E. R., et al. (2009). The common inhalational anesthetic sevoflurane induces apoptosis and increases β-amyloid protein levels. *Arch. Neurol.* 66, 620–631. doi: 10.1001/archneurol.2009.48

Ellis, P. D. (2010). *The Essential Guide to Effect Sizes: Statistical Power, Meta-Analysis, and the Interpretation of Research Results*. Cambridge: Cambridge University Press.

Geng, P., Zhang, J., Dai, W., Han, X., Tan, Q., Cheng, D., et al. (2018). Autophagic degradation deficit involved in sevoflurane-induced amyloid pathology and spatial learning impairment in APP/PS1 transgenic mice. *Front. Cell. Neurosci.* 12:185. doi: 10.3389/fncel.2018.00185

Hsing, C. H., Chen, Y. H., Chen, C. L., Huang, W. C., Lin, M. C., Tseng, P. C., et al. (2012). Anesthetic propofol causes glycogen synthase kinase-3β-regulated lysosomal/mitochondrial apoptosis in macrophages. *Anesthesiology* 116, 868–881. doi: 10.1097/aln.0b013e31824af68a

Hussain, M., Berger, M., Eckenhoff, R. G., and Seitz, D. P. (2014). General anesthetic and the risk of dementia in elderly patients: current insights. *Clin. Interv. Aging* 9, 1619–1628. doi: 10.2147/cia.s49680

Kawarabayashi, T., Igeta, Y., Sato, M., Sasaki, A., Matsubara, E., Kanai, M., et al. (1997). Lysosomal generation of amyloid β protein species in transgenic mice. *Brain Res.* 765, 343–348. doi: 10.1016/S0006-8993(97)00695-1

Kim, S., Choi, K. J., Cho, S. J., Yun, S. M., Jeon, J. P., Koh, Y. H., et al. (2016). Fisetin stimulates autophagic degradation of phosphorylated tau via the activation of TFEB and Nrf2 transcription factors. *Sci. Rep.* 6:24933. doi: 10.1038/srep24933

Laferla, F. M., Green, K. N., and Oddo, S. (2007). Intracellular amyloid-β in Alzheimer's disease. *Nat. Rev. Neurosci.* 8, 499–509. doi: 10.1038/nrn2168

Langui, D., Girardot, N., El Hachimi, K. H., Allinquant, B., Blanchard, V., Pradier, L., et al. (2004). Subcellular topography of neuronal Aβ peptide in APPxPS1 transgenic mice. *Am. J. Pathol.* 165, 1465–1477. doi: 10.1016/s0002-9440(10)63405-0

Mirakhur, A., Craig, D., Hart, D. J., Mcllroy, S. P., and Passmore, A. P. (2004). Behavioural and psychological syndromes in Alzheimer's disease. *Int. J. Geriatr. Psychiatry* 19, 1035–1039. doi: 10.1002/gps.1203

Nixon, R. A., and Cataldo, A. M. (2006). Lysosomal system pathways: genes to neurodegeneration in Alzheimer's disease. *J. Alzheimers. Dis.* 9, 277–289. doi: 10.3233/jad-2006-9s331

Nixon, R. A., Cataldo, A. M., and Mathews, P. M. (2000). The endosomal-lysosomal system of neurons in Alzheimer's disease pathogenesis: a review. *Neurochem. Res.* 25, 1161–1172. doi: 10.1023/A:1007675508413

Potter, G. G., and Steffens, D. C. (2007). Contribution of depression to cognitive impairment and dementia in older adults. *Neurologist* 13, 105–117. doi: 10.1097/01.nrl.0000252947.15389.a9

Ren, G., Zhou, Y., Liang, G., Yang, B., Yang, M., King, A., et al. (2017). General anesthetics regulate autophagy via modulating the inositol 1,4,5-trisphosphate receptor: implications for dual effects of cytoprotection and cytotoxicity. *Sci. Rep.* 7:12378. doi: 10.1038/s41598-017-11607-0

Settembre, C., De Cegli, R., Mansueto, G., Saha, P. K., Vetrini, F., Visvikis, O., et al. (2013a). TFEB controls cellular lipid metabolism through a starvation-induced autoregulatory loop. *Nat. Cell Biol.* 15, 647–658. doi: 10.1038/ncb2718

Settembre, C., Di Malta, C., Polito, V. A., Garcia Arencibia, M., Vetrini, F., Erdin, S., et al. (2011). TFEB links autophagy to lysosomal biogenesis. *Science* 332, 1429–1433. doi: 10.1126/science.1204592

Settembre, C., Fraldi, A., Medina, D. L., and Ballabio, A. (2013b). Signals from the lysosome: a control centre for cellular clearance and energy metabolism. *Nat. Rev. Mol. Cell Biol.* 14, 283–296. doi: 10.1038/nrm3565

Settembre, C., Zoncu, R., Medina, D. L., Vetrini, F., Erdin, S., Erdin, S., et al. (2012). A lysosome-to-nucleus signalling mechanism senses and regulates the lysosome via mTOR and TFEB. *EMBO J.* 31, 1095–1108. doi: 10.1038/emboj.2012.32

Shie, F. S., Leboeuf, R. C., and Jin, L. W. (2003). Early intraneuronal Abeta deposition in the hippocampus of APP transgenic mice. *Neuroreport* 14, 123–129. doi: 10.1097/01.wnr.0000051151.87269.7d

Souza, L. C., Jesse, C. R., Antunes, M. S., Ruff, J. R., De Oliveira Espinosa, D., Gomes, N. S., et al. (2016). Indoleamine-2,3-dioxygenase mediates neurobehavioral alterations induced by an intracerebroventricular injection of amyloid-β1–42 peptide in mice. *Brain Behav. Immun.* 56, 363–377. doi: 10.1016/j.bbi.2016.03.002

Tahmasebinia, F., and Emadi, S. (2017). Effect of metal chelators on the aggregation of β-amyloid peptides in the presence of copper and iron. *Biometals* 30, 285–293. doi: 10.1007/s10534-017-0005-2

Ubhi, K., and Masliah, E. (2013). Alzheimer's disease: recent advances and future perspectives. *J. Alzheimers. Dis.* 33, S185–194. doi: 10.3233/JAD-2012-129028

Vassar, R., Kovacs, D. M., Yan, R., and Wong, P. C. (2009). The beta-secretase enzyme BACE in health and Alzheimer's disease: regulation, cell biology, function and therapeutic potential. *J. Neurosci.* 29, 12787–12794. doi: 10.1523/JNEUROSCI.3657-09.2009

Wu, B., Wei, Y., Wang, Y., Su, T., Zhou, L., Liu, Y., et al. (2015). Gavage of D-Ribose induces Aβ-like deposits, Tau hyperphosphorylation as well as memory loss and anxiety-like behavior in mice. *Oncotarget* 6, 34128–34142. doi: 10.18632/oncotarget.6021

Xiao, Q., Yan, P., Ma, X., Liu, H., Perez, R., Zhu, A., et al. (2014). Enhancing astrocytic lysosome biogenesis facilitates Aβ clearance and attenuates amyloid plaque pathogenesis. *J. Neurosci.* 34, 9607–9620. doi: 10.1523/jneurosci.3788-13.2014

Xiao, Q., Yan, P., Ma, X., Liu, H., Perez, R., Zhu, A., et al. (2015). Neuronal-targeted TFEB accelerates lysosomal degradation of APP, reducing Aβ generation and amyloid plaque pathogenesis. *J. Neurosci.* 35, 12137–12151. doi: 10.1523/JNEUROSCI.0705-15.2015

Xie, Z., and Xu, Z. (2013). General anesthetics and β-amyloid protein. *Prog. Neuropsychopharmacol. Biol. Psychiatry* 47, 140–146. doi: 10.1016/j.pnpbp.2012.08.002

Zare, N., Khalifeh, S., Khodagholi, F., Shahamati, S. Z., Motamedi, F., and Maghsoudi, N. (2015). Geldanamycin reduces Aβ-associated anxiety and depression, concurrent with autophagy provocation. *J. Mol. Neurosci.* 57, 317–324. doi: 10.1007/s12031-015-0619-1

Zhang, J., Dai, W., Geng, P., Zhang, L., Tan, Q., Cheng, D., et al. (2018). Midazolam enhances mutant huntingtin protein accumulation via impairment of autophagic degradation *in vitro*. *Cell Physiol. Biochem.* 48, 683–691. doi: 10.1159/000491895

Zhang, L., Sheng, R., and Qin, Z. (2009). The lysosome and neurodegenerative diseases. *Acta Biochim. Biophys. Sin. Shanghai.* 41, 437–445. doi: 10.1093/abbs/gmp031

Zhang, S., Hu, X., Guan, W., Luan, L., Li, B., Tang, Q., et al. (2017). Isoflurane anesthesia promotes cognitive impairment by inducing expression of β-amyloid protein-related factors in the hippocampus of aged rats. *PLoS One* 12:e0175654. doi: 10.1371/journal.pone.0175654

Zhang, Y. D., and Zhao, J. J. (2015). TFEB participates in the Aβ-induced pathogenesis of Alzheimer's disease by regulating the autophagy-lysosome pathway. *DNA Cell Biol.* 34, 661–668. doi: 10.1089/dna.2014.2738

**Conflict of Interest Statement**: The authors declare that the research was conducted in the absence of any commercial or financial relationships that could be construed as a potential conflict of interest.

frontiers in Human Neuroscience

ORIGINAL RESEARCH
published: 31 May 2019
doi: 10.3389/fnhum.2019.00175

# Affective and Cognitive Empathy in Pre-teachers With Strong or Weak Professional Identity: An ERP Study

*Juncheng Zhu[1]*†, Xin Qiang Wang[1]*†, Xiaoxin He[2], Yuan-Yan Hu[3], Fuhong Li[1], Ming-Fan Liu[1] and Baojuan Ye[1]*

[1]School of Psychology, Jiangxi Key Laboratory of Psychology and Cognition Science, Center for Mental Health Education and Research, Jiangxi Normal University, Nanchang, China, [2]Jiangxi College of Foreign Studies, Nanchang, China, [3]Chongqing University of Arts and Sciences, Chongqing, China

Pain empathy is influenced by a number of factors. However, few studies have examined the effects of strength of professional identity on pain empathy in pre-service teachers. This study used the event-related potential (ERP) technique, which offers a high temporal resolution, to investigate the neurocognitive mechanisms of pain empathy in pre-teachers with strong or weak professional identity. The N110 and P300 components have been shown to reflect an individual's emotional sharing and cognitive evaluation in pain empathy, respectively. The results of the current study show that pre-teachers with strong professional identity showed a significant difference in N110 amplitudes evoked towards painful and non-painful stimuli; whereas pre-teachers with weak professional identity did not show a significant difference in the amplitudes evoked by the two stimulus types. For the P300 component, pre-teachers with weak professional identity showed a significant difference in the amplitudes evoked towards painful and non-painful stimuli; whereas pre-teachers with strong professional identity did not show a significant difference in the amplitudes evoked by the two stimulus types. Our results indicate that pre-teachers with strong professional identity show a higher level of pain empathy than those with weak professional identity.

**Keywords: ERP, N110, P300, pain empathy, pre-teachers, professional identity**

OPEN ACCESS

***Edited by:***
*Delin Sun,*
*Duke University, United States*

***Reviewed by:***
*Xiangru Zhu,*
*Henan University, China*
*Tifei Yuan,*
*Shanghai Mental Health Center (SMHC), China*

***Correspondence:**
*Juncheng Zhu*
*zhujcpsy@126.com*
*Xin Qiang Wang*
*xinqiangw101@163.com*

*†These authors have contributed equally to this work and are co-first authors*

***Received:*** *17 July 2018*
***Accepted:*** *14 May 2019*
***Published:*** *31 May 2019*

***Citation:***
*Zhu J, Wang XQ, He X, Hu Y-Y, Li F, Liu M-F and Ye B (2019) Affective and Cognitive Empathy in Pre-teachers With Strong or Weak Professional Identity: An ERP Study. Front. Hum. Neurosci. 13:175. doi: 10.3389/fnhum.2019.00175*

## INTRODUCTION

Teacher empathy is a teacher's ability to genuinely consider issues from a student's point of view. It is the ability to see from a student's perspective and to empathize with the student's thoughts and feelings, thereby gaining the ability to choose suitable teaching methods and more effectively guide students in their academic and emotional growth (Peart and Campbell, 1999; Li et al., 2015). Teacher empathy is a key personal competency and an important criterion for successful vocational teaching. Studies have shown that success in vocational teaching requires the joint effects of cognitive and affective empathy (Stojiljković et al., 2012). Affective empathy enables individuals to exhibit more altruistic behaviors, whereas cognitive empathy allows individuals to rationally select the best way to help others (Smith, 2006). Teacher empathy is a key feature of teachers who have strong professional identity, allowing them to effectively establish good teacher-student relationships and a relaxed teaching environment (Stojiljković et al., 2011). It can also promote students' academic achievement and teachers' professional growth (Li et al., 2015; Peck et al., 2015).

It is unknown whether professional identity plays a role in teacher empathy, and we thus sought to examine the effects of professional identity on teacher empathy in this study.

Pain empathy is the perception, judgment and emotional response to pain in others (Danziger et al., 2006; Meng et al., 2012) and has been shown to be one of the main manifestations of empathy in teachers (McAllister and Irvine, 2002). Studies have found that individuals may feel pain when observing pain in others, leading to greater compassion and concern (Singer et al., 2004; Gao et al., 2015). Event-related potential (ERP) studies have shown that viewing pictures of others in painful and non-painful situations leads to significant differences in the amplitudes of N110 and P300 components, with painful images evoking higher positive amplitudes (Fan and Han, 2008; Decety et al., 2010). The N110 and P300 components, which are important ERP indicators of pain empathy, have been shown to reflect an individual's emotional sharing and cognitive evaluation in pain empathy, respectively (Fan and Han, 2008; Decety et al., 2010; Meng et al., 2013). In this study, N110 and P300 were used as key reference indicators to evaluate the differences in emotional sharing and cognitive evaluation in pre-teachers with differing levels of professional identity.

Pain empathy is influenced by a number of factors, such as attention (Gu and Han, 2007; Fan and Han, 2008), personal characteristics (Singer et al., 2006; Singer and Lamm, 2009), gender (Han et al., 2008), and attitude (Decety et al., 2009). Researchers have found that prosocial characteristics can also influence pain empathy. For example, one study in nurses found that burnout and empathy were negatively correlated in the nursing profession (Yuguero et al., 2017), suggesting that weak professional identity affects empathic abilities in nurses. Several surveys have reported that both pre-service and in-service nurses and doctors show significant positive correlations between professional identity and empathy and its components (such as perspective taking; Zhang, 2014; Mao, 2017; Visser et al., 2018). In a 10-week empathy training experiment in secondary vocational nursing students, Zhu (2017) showed that combining both traditional teaching and an experiential training model resulted in significantly improved professional identity following empathy training, particularly in the fields of professional emotion and professional expectations.

Similarly, empathy plays an important role in the teachers' professional identity and professional development (McAllister and Irvine, 2002; Kitchen, 2005). Strong professional identity in pre-teachers enables greater empathy towards students, and hence pre-teachers with a strong professional identity are better able to adopt more suitable methods to understand and care for their students (Barr, 2011). In contrast, weak professional identity in pre-teachers may possibly lead to greater burnout, which may also significantly impact the ability of pre-teachers to empathize with their students (Kremer and Hofman, 1985; Chen, 2007). This, in turn, may hinder the healthy development of students. One narrative research study reported that empathy has a positive influence on the professional identity of teachers (Glazzard and Dale, 2013). Another survey study found that teacher professional identity is closely related to empathy and that there is an especially close relationship between professional efficacy and empathy (Goroshit and Hen, 2016). According to a core two-factor model of professional identity, professional efficacy is the core component of professional identity in teachers (Wang et al., 2011). In addition, qualitative research has found that the cultivation of strong professional identity is an important personal factor in the formation of teacher empathy (Guo, 2015). Therefore, the following hypothesis was examined in the current study: pre-teachers with stronger professional identities will show better empathic abilities, while pre-teachers with weak professional identities will show a lower level of empathy towards students.

Thus far, most previous studies on empathy have employed questionnaire surveys and behavioral methods, but few have used the ERP technique, with its high temporal resolution, to explore the neurocognitive mechanisms underlying the empathy of pre-teachers with different levels of professional identity. Investigating the neurocognitive mechanisms of pain empathy responses in pre-teachers with different levels of professional identity will help to further our understanding of the cognitive processing and neurocognitive basis of pain empathy in this group. More complete knowledge of the mechanisms of pain empathy can also provide insight into the neurocognitive mechanisms underlying the relationship between teacher professional identity and empathy. It is possible that the empathic ability of pre-teachers can be enhanced by increasing professional identity or, conversely, that developing teacher empathy can promote professional identity.

# MATERIALS AND METHODS

## Participants

In China, pre-service teachers are university students who are majoring in normal education, usually at a normal university (teachers' university) oriented to the teaching profession. These students are trained in teaching skills and participate in school-based field experiences. The Professional Identification Scale for Normal Students (PISNS; Wang et al., 2010, 2017) was administered to 395 pre-service teachers from a normal university in Jiangxi, China. Each participant was a second-semester sophomore. Pre-service teachers who scored in the top and bottom 27% were classified as belonging to the strong and weak professional identity groups, respectively. Of these, pre-service teachers were selected for inclusion in this study if they met the other inclusion criteria (e.g., voluntary participation, no previous participation in similar experiments, etc.). Women are known to occupy a larger proportion of the new generation of teachers (i.e., those who are less than 30 years of age). Especially in the lower grades, the vast majority of teachers are female (OECD, 2017). In normal universities in China, female students account for more than two-thirds of pre-service teachers (Zhu and Wang, 2017). In Chinese society and culture, it is more common for women to become teachers as this career conforms to both societal and family expectations of women. Studies have found that teachers also conform to the requirements of female students in their own professional orientation (Wang et al., 2014; Wu, 2018). Therefore, female pre-service teachers

are more suitable for random samples, and the current study selected female pre-service teachers for inclusion in our sample. Of the 26 female pre-service teachers who met the inclusion criteria, two were excluded due to too many artifacts. Thus, a total of 24 female pre-service teachers were included in this study: 12 in the strong professional identity group (questionnaire total score ≥53 points, mean score: 51.33 ± 1.87) and 12 in the weak professional identity group (questionnaire total score ≤34 points, mean score: 33.33 ± 2.15). The *PISNS* total scores of the two groups were analyzed using an independent samples *t*-test, with the results showing that $t_{(22)} = 21.88$, $p < 0.001$, and *Cohen's d* = 9.32. This implies that participant screening was effective. The participants were between the ages of 19 and 21 years, with a mean age of 19.9 years and standard deviation of 0.65 years. There was no significant difference in the mean ages of the two study groups (strong professional identity group: 19.83 ± 0.72, weak professional identity group: 20.0 ± 0.60, $t_{(22)} = 0.62$, $p = 0.54$). All participants were right-handed, had normal vision or normal corrected vision, no partial or total color blindness, no major physical or psychological diseases, and had never participated in similar experiments. The participants were informed of the purpose of the study prior to the experiment, and written informed consent was obtained. This study was approved by the ethics committee at our institution. Before the experiment, the participants did not know the reward when they finished the experiment. Participants were given a reward (15RMB and extra credit) following completion of this experiment.

## Materials

### Professional Identification Scale for Normal Students (PISNS)

The *PISNS*, compiled by Wang et al. (2010) was used to measure the professional identity of student teachers. This scale has been used in previous studies (Wang et al., 2017; Zhu and Wang, 2017) and includes four dimensions: professional willingness and expectations, professional volition, professional values, and professional efficacy. A total of 12 items are scored on a five-point scale from 1 (strongly disagree) to 5 (strongly agree). A higher score indicates that the student teacher has a stronger professional identity. In this study, the internal consistency reliability of the scale was 0.84. Confirmatory factor analysis showed that $\chi^2/df = 5.39$, RMSEA = 0.08; and that model IFI, NFI, TLI, CFI and other relative fit indices all fell within an acceptable range, between 0.91 and 0.94. Thus, the overall quality of this scale is good, and it has high reliability and validity.

### Experimental Materials in the Pain Empathy Task

The participants viewed 120 pictures, 60 of which were painful and 60 of which were non-painful. These stimuli have been used in previous ERP studies (Meng et al., 2013; Wang et al., 2014). The stimuli were all based on events in everyday life. Painful pictures showed events such as accidentally cutting one's hand with a knife, while non-painful pictures showed events such as cutting a watermelon. The size and pixel resolution of all pictures were 9 × 6.76 cm (width × height) and 100 pixels. During the task, the pictures were presented in the center of the screen, and the size of the pictures presented was 22.5 × 16.9 cm (width × height). The distance between the pictures and the participants was 100 cm, and the viewing angle was 12.8° × 7.7°.

## Experimental Design

A 2 (professional identity: strong vs. weak) × 2 (stimulus: pain vs. no-pain) mixed factorial design was employed in this experiment, where professional identity was the between-group factor and stimulus type was the within-subjects factor. The dependent variables were the behavioral reaction time (RT) and the electroencephalography (EEG) results.

## Experimental Procedure

The experimental stimuli were presented using E-Prime 2.0. The background color of the stimulus presentation was gray. The participants' RT and correct response rate (CRR) was automatically recorded by a computer. The experiment had a total of four blocks, with 60 trials per block and a break between each block. The subjects were given the following instructions in their native language: "Please imagine that the hands and feet in the pictures are the hands and feet of your students when perceiving the following pictures." The participants were given a practice stage prior to the start of the experiment, which allowed them to familiarize themselves with the experimental task and keypress response. First, the participants were asked to focus on the fixation cross "+" on the screen, which was followed by the stimulus pictures. If the participants perceived that pain was felt in the pictures, they were asked to press "1" on the keyboard; if not, they were asked to press "2." Painful and non-painful pictures were presented in a random order. The fixation cross was presented for a random duration between 400 ms and 600 ms. The stimulus was then presented for a maximum duration of 2,500 ms, followed by a blank screen for 1,000 ms. The participants were required to respond as quickly and

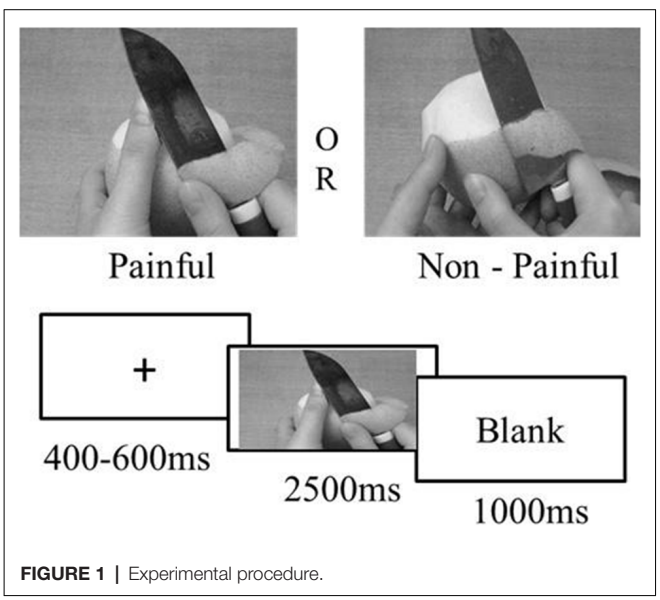


**FIGURE 1** | Experimental procedure.

as accurately as possible. The experimental procedure is shown in **Figure 1**.

## Data Collection

BrainVision EEG recording and analysis software (Germany) was employed. EEG was performed using a 64-channel EEG cap, and the electrodes were distributed according to the International 10-20 system. The bilateral mastoids were used as a reference for recording. The electrodes placed on the bilateral outer canthi were used to measure horizontal electrooculography, and the electrodes placed above and below the right eye were used to measure vertical electrooculography. The impedance of all electrodes was below 5 kΩ, the bandpass filter was 0.1–30 Hz, and all EEG signals with electrode voltage greater than ±80 μv were automatically discarded (Xie et al., 2017). Fifty-two trials were discarded under each condition.

## Data Processing and Analysis

BrainVision Analyzer 2.1 was used to perform offline referencing, filtering (criteria: 0.01–30 Hz), removal of ocular interference, segmentation (−200 to 1,000 ms), baseline correction (criteria: −200 to 0 ms), artifact removal (criteria: ±80 μv), and overlaying of ERPs produced by correct responses to the target stimuli. Based on the aims of this study and previous findings on empathy, we processed and analyzed the mean amplitudes of N110 (90–160 ms) and P300 (300–460 ms). According to previous studies (Fan and Han, 2008; Han et al., 2008; Decety et al., 2010; Gao et al., 2015; Cui et al., 2016), data analysis was performed using the F3, F4, FZ, FC3, FC4 and FCZ electrodes for the N110 component and the P3, P4, PZ, PO3, PO4 and POZ electrodes for the P300 component. A 2 (professional identity: strong vs. weak) × 2 (stimulus type: pain vs. no-pain) × (electrode position) three-way repeated measures analysis of variance (ANOVA) was performed, and a Greenhouse-Geisser correction was performed on the resulting $p$ values. The raw data supporting the conclusions of this manuscript will be made available by the authors, without undue reservation, to any qualified researcher.

# RESULTS

## Behavioral Results

The mean RT and CRR of participants with strong and weak professional identities are shown in **Table 1**. Two-way repeated measures ANOVA was performed on the RT and CRR. For RT, the main effect of stimulus types was not significant ($F_{(1,22)} = 1.16$, $p > 0.05$); the main effect of professional identity was not significant ($F_{(1,22)} = 1.70$, $p > 0.05$); and the interaction effect of stimulus type and professional identity was not significant ($F_{(1,22)} = 1.59$, $p > 0.05$). Likewise, for CRR, the main effect of stimulus types was not significant ($F_{(1,22)} = 2.58$, $p > 0.05$); the main effect of professional identity was not significant ($F_{(1,22)} = 0.51$, $p > 0.05$); and the interaction effect of stimulus type and professional identity was not significant ($F_{(1,22)} = 0.19$, $p > 0.05$).

## ERP Results

For the N110 component, the main effect of N110 component amplitude was significant ($F_{(1,22)} = 3.64$, $p = 0.02$, $\eta_p^2 = 0.50$); the main effect of stimulus type was significant ($F_{(1,22)} = 8.63$, $p = 0.008$, $\eta_p^2 = 0.28$); the main effect of professional identity was not significant ($F_{(1,22)} = 0.26$, $p = 0.61$); the interaction effect of the amplitude and stimulus type was not significant ($F_{(1,22)} = 0.84$, $p = 0.54$); the interaction effect of the amplitude and stimulus type and professional identity was not significant ($F_{(1,22)} = 0.76$, $p = 0.59$); and the interaction effect of stimulus type and professional identity was marginally significant ($F_{(1,22)} = 3.94$, $p = 0.06$, $\eta_p^2 = 0.15$). $P < 0.05$ is not an absolute threshold of rejecting or accepting the hypothesis, and to ignore marginally significant findings may overlook the important results tightly associated with research questions. We have a clearly defined research hypothesis about the association between professional identity and stimulus type, and it is thus worthy to fully investigate the simple main effects even if the ANOVA interaction is only marginally significant. Simple effects testing of the interaction effect between stimulus type and professional identity showed that in the strong professional identity group there was a significant difference between painful and non-painful stimuli ($p = 0.001$; **Figure 2**; for FZ in **Figure 4**). Further, painful stimuli evoked a less negative N110 amplitude than did non-painful stimuli. In the weak professional identity

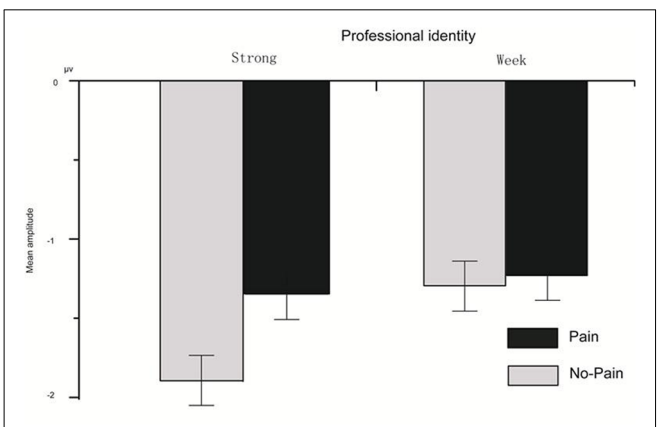


**FIGURE 2 |** Interaction effect of professional identity and pain empathy for the N110 component.

**TABLE 1 |** Mean reaction time (RT) and correct response rate (CRR) of the pain empathy task (M ± SD).

| | Strong professional identity ($n$ = 12) | | Weak professional identity ($n$ = 12) | |
|---|---|---|---|---|
| | Pain | No-pain | Pain | No-pain |
| RT (ms) | 970.22 ± 138.61 | 873.95 ± 139.17 | 920.54 ± 127.82 | 877.82 ± 155.15 |
| CRR (%) | 0.91 ± 0.08 | 0.93 ± 0.04 | 0.92 ± 0.09 | 0.96 ± 0.07 |

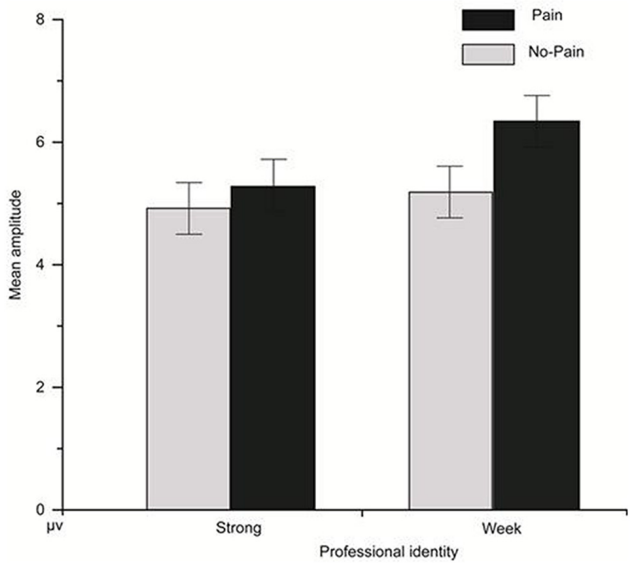


**FIGURE 3 |** Interaction effect of professional identity and pain empathy for the P300 component.

group, there was no significant difference between painful and non-painful stimuli ($p = 0.52$).

For the P300 component, the main effect of P300 component amplitude was significant ($F_{(1,22)} = 6.60$, $p = 0.001$, $\eta_p^2 = 0.65$); the main effect of stimulus type was significant ($F_{(1,22)} = 10.07$, $p = 0.004$, $\eta_p^2 = 0.31$); the interaction effect of the amplitude and stimulus type was significant ($F_{(1,22)} = 9.25$, $p = 0.001$, $\eta_p^2 = 0.72$); the interaction effect of the amplitude and stimulus type and professional identity was not significant ($F_{(1,22)} = 0.63$, $p = 0.68$); the main effect of professional identity was not significant ($F_{(1,22)} = 0.73$, $p = 0.40$); and the interaction effect of stimulus type and professional identity was marginally significant ($F_{(1,22)} = 3.66$, $p = 0.07$, $\eta_p^2 = 0.14$). $P<0.05$ is not an absolute threshold of rejecting or accepting the hypothesis, and to ignore marginally significant findings may overlook the important results tightly associated with research questions. We have a clearly defined research hypothesis about the association between professional identity and stimulus type, and it is thus worthy to fully investigate the simple main effects even if the ANOVA interaction is only marginally significant. Simple effects testing of the interaction effect between stimulus type and professional identity showed that, in the strong professional identity group, there was no significant difference between painful and non-painful stimuli ($p = 0.36$). In the weak professional identity group, there was a significant difference between painful and non-painful stimuli ($p = 0.002$), with painful stimuli evoking a more positive P300 amplitude than non-painful stimuli shown in **Figure 3**; for PZ in **Figure 4**.

For the frontal section of the brain, we chose four electrodes (F3, F4, FC3, and FC4) and analyzed 2 hemispheres (left, right) × 2 groups (professional identity: strong vs. weak) × 2 experimental conditions (stimulus type: pain vs. no-pain). According to the results of the repeated measures ANOVA, the main effect of hemisphere was not significant ($F_{(1,22)} = 0.43$, $p = 0.52$); the interaction effect of hemisphere and professional identity was not significant ($F_{(1,22)} = 0.003$, $p = 0.96$); and the interaction effect of hemisphere and stimulus type and professional identity was not significant ($F_{(1,22)} = 1.86$, $p = 0.19$).

For the parietal section of the brain, we chose four electrodes (P3, P4, PO3, PO4) and analyzed 2 hemispheres (left, right) × 2 groups (professional identity: strong vs. weak) × 2 experimental conditions (stimulus type: pain vs. no-pain). According to the results of the repeated measures ANOVA, the main effect of hemisphere was not significant ($F_{(1,22)} = 0.27$, $p = 0.61$); the interaction effect of hemisphere and professional identity was not significant ($F_{(1,22)} = 0.08$, $p = 0.78$); and the interaction effect of hemisphere and stimulus type and professional identity was not significant ($F_{(1,22)} = 0.50$, $p = 0.49$).

## DISCUSSION

To the best of our knowledge, this is the first ERP study to examine the effects of strength of professional identity on pain empathy in pre-service teachers. This study examined the cognitive processing features of pain empathy in pre-service teachers with strong and weak professional identities using the ERP technique, which has a high temporal resolution. Our results revealed that, although behavioral indicators showed no significant differences in the pain empathy between pre-teachers with strong professional identity and those with weak professional identity, painful pictures evoked less negative amplitudes for the N110 and P300 components in both groups. This finding is consistent with past studies (Fan and Han, 2008; Meng et al., 2012, 2013), indicating that the experimental manipulation of this study was valid. The results of the current study also demonstrate that pre-teachers with strong professional identity showed a significant difference in the N110 component when shown painful vs. non-painful stimuli, whereas pre-teachers with weak professional identity did not show a significant difference. In contrast, pre-teachers with weak professional identity showed a significant difference in the P300 component when shown painful vs. non-painful stimuli, whereas pre-teachers with strong professional identity did not show a significant difference.

The N110 component reflects an individual's early perceptual processing and is a key indicator for the mechanisms of emotional sharing in pain empathy (Fan and Han, 2008; Han et al., 2008; Decety et al., 2010). Our results indicate that there is a significant difference in the N110 component evoked by painful vs. non-painful stimuli in pre-teachers with strong professional identity, but not in those with weak professional identity. According to the theory of emotional sharing, the basis of empathy is the emotional sharing between individuals (Jeannerod, 1999; Decety and Sommerville, 2003). Individuals with stronger empathic abilities will thus also show greater emotional sharing (Decety and Lamm, 2006). Two key features of pre-teachers with strong professional identity are their strong identification with the teaching profession and their high enthusiasm towards their students. Pre-teachers with

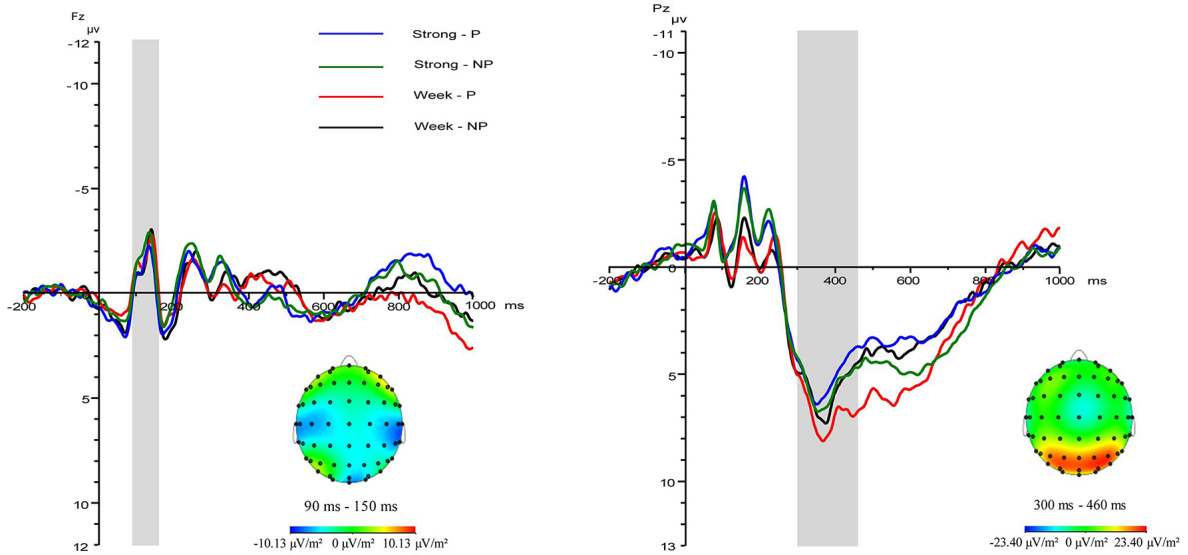


**FIGURE 4 |** Grand mean waveforms of event-related potential (ERP) evoked by painful and non-painful stimuli in pre-teachers with different levels of professional identity. Strong-P/NP represent painful and non-painful stimulus, respectively, in participants with strong professional identity; Weak-P/NP represent painful and non-painful stimulus, respectively, in participants with weak professional identity.

strong professional identity were able to engage in different levels of emotional sharing when faced with painful and non-painful stimuli. This implies that they are more easily affected by painful stimuli experienced by students, which evokes similar perceptions of pain. Conversely, pre-teachers with weak professional identity would be expected to show low identification with the teaching profession and low enthusiasm towards their students. As expected, the results of the current study demonstrate that pre-teachers with weak professional identity did not show significant differences in emotional sharing between painful and non-painful stimuli. Taken together, these results imply that pre-teachers with different levels of professional identity have different thresholds of empathy for student pain.

The P300 component reflects an individual's cognitive evaluation and regulatory processing of pain empathy. It occurs after the N110 component and involves the conscious cognitive evaluation of stimuli (Fan and Han, 2008; Han et al., 2008; Song et al., 2016). Decety et al. (2010) compared the differences in pain empathy between doctors and ordinary individuals and found no significant difference in the P300 components induced by doctors' observations of pain vs. non-pain pictures. This reflects the importance of doctors being trained to reduce and ignore the disturbance and inner impact caused by the perception of pain in order to maintain professional behavior. That is to say, doctors should adjust and suppress negative emotions induced by pain stimuli in order to focus their cognitive resources on helping others. Our results demonstrate that pre-teachers with weak professional identity show significant differences in the P300 amplitudes evoked by painful and non-painful stimuli, whereas this difference was not significant in pre-teachers with strong professional identity. Empathy can be subdivided into affective and cognitive empathy (Stojiljković et al., 2012). Although teachers are as helpful as doctors, teachers should not ignore the suffering of students, but should always care about the suffering of students, and show empathy. The N110 component reflects early perception processing and is an important indicator of emotional sharing in pain empathy. This study found that there were significant differences in the N110 component between pre-service teachers with strong professional identity under pain and non-pain stimuli. This result suggests that pre-teachers with strong professional identity show greater abilities in emotional sharing and that these same pre-teachers are better able both to recognize the reasons for empathizing with their students and to attenuate the arousal level elicited by painful stimuli, leading to a lowered amplitude of the P300 component. Pre-teachers with strong professional identity show emotional sharing in pain empathy at an earlier point in perceptual processing, which may facilitate the regulation and alleviation of emotional exhaustion. As for pre-teachers with weak professional identity, the significant difference in the P300 component when shown painful vs. non-painful stimuli is due to their lower emotional sharing abilities towards their students and the activation of the internal aversive motivational system by the negative stimuli (Bartholow et al., 2006). This in turn led to higher arousal levels towards painful stimuli. In conclusion, pre-teachers with stronger professional identities showed better empathic abilities, as measured by ERP, while pre-teachers with weak professional identities showed a lower level of pain empathy. Studies have found that empathy in teachers can be significantly improved through training (Warner, 1984). Therefore, in the future, researchers may consider improving professional identity and alleviating job burnout by training

teachers in empathy. The results of this study support the results of previous qualitative and investigative studies that have reported a close correlation between teacher professional identity and empathy (Glazzard and Dale, 2013; Li et al., 2015; Goroshit and Hen, 2016). However, because relatively few participants volunteered and met the inclusion criteria for the present study, our results need to be confirmed in future studies using larger samples. In addition, this research also has some limitation, such as simple effects testing after the interaction effect of stimulus type and professional identity was marginally significant. Some studies have suggested that social relationships and interpersonal distance affect pain empathy (Song et al., 2016; Cross et al., 2019). However, participants are a second-semester sophomore in present study, who are mainly in the learning stage of theoretical knowledge and skills of education and teaching, and have a low degree of real involvement in education and teaching and contact with students, which may be the potential causes of the marginal significance. In the future, senior or in-service teachers with deeper socialization of teacher-student relationship could be chosen to further explore the interaction effect of stimulus type and professional identity.

## ETHICS STATEMENT

This study was carried out in accordance with the recommendations of the ethics committee of School of Psychology, Jiangxi Normal University. The protocol was approved by the ethics committee of School of Psychology, Jiangxi Normal University.

## AUTHOR CONTRIBUTIONS

XW was responsible for the design of the study, data collection, interpretation of data for the work, article writing and revising. JZ contributed to the design of the study, data collection, data analysis, article writing and revising. XH contributed towards data collection. YH, FL, ML, and BY all contributed towards the revision of the article.

## FUNDING

This work was supported by the key Project of the Thirteenth Five-Year Plan of Jiangxi Education Science in 2018 (18ZD012).

## REFERENCES

Barr, J. J. (2011). The relationship between teachers' empathy and perceptions of school culture. *Educ. Stud.* 37, 365–369. doi: 10.1080/03055698.2010.506342

Bartholow, B. D., Bushman, B. J., and Sestir, M. A. (2006). Chronic violent video game exposure and desensitization to violence: behavioral and event-related brain potential data. *J. Exp. Soc. Psychol.* 42, 532–539. doi: 10.1016/j.jesp.2005.08.006

Chen, Y. (2007). *Exploring Teacher Burnout and Teacher Identity in a Professional Technical School: A Survey on Teacher Burnout*. Jinhua: Zhejiang Normal University. Unpublished Master degree thesis.

Cross, E. S., Riddoch, K. A., Pratts, J., Titone, S., Chaudhury, B., and Hortensius, R. (2019). A neurocognitive investigation of the impact of socializing with a robot on empathy for pain. *Philos. Trans. R. Soc. Lond. B Biol. Sci.* 374:20180034. doi: 10.1098/rstb.2018.0034

Cui, F., Ma, N., and Luo, Y. J. (2016). Moral judgment modulates neural responses to the perception of other's pain: an ERP study. *Sci. Rep.* 6:20851. doi: 10.1038/srep20851

Danziger, N., Prkachin, K. M., and Willer, J. C. (2006). Is pain the price of empathy? The perception of others' pain in patients with congenital insensitivity to pain. *Brain* 129, 2494–2507. doi: 10.1093/brain/awl155

Decety, J., Echols, S., and Correll, J. (2009). The blame game: the effect of responsibility and social stigma on empathy for pain. *J. Cogn. Neurosci.* 22, 985–997. doi: 10.1162/jocn.2009.21266

Decety, J., and Lamm, C. (2006). Human empathy through the lens of social neuroscience. *ScienceWorldJournal* 6, 1146–1163. doi: 10.1100/tsw.2006.221

Decety, J., and Sommerville, J. (2003). A Shared representation between self and others: a social cognitive neuroscience view. *Trends Cogn. Sci.* 7, 527–533. doi: 10.1016/j.tics.2003.10.004

Decety, J., Yang, C. Y., and Cheng, Y. W. (2010). Physicians down-regulate their pain empathy response: an event-related brain potential study. *Neuroimage* 50, 1676–1682. doi: 10.1016/j.neuroimage.2010.01.025

Fan, Y., and Han, S. H. (2008). Temporal dynamic of neural mechanisms involved in empathy for pain: an event-related brain potential study. *Neuropsychologia* 46, 160–173. doi: 10.1016/j.neuropsychologia.2007.07.023

Gao, X. M., Weng, L., Zhou, Q., Zhao, C., and Li, F. (2015). Dose violent offenders have lower capacity of empathy for pain: evidence from ERPs. *Acta Psychol. Sin.* 47, 478–487. doi: 10.3724/sp.j.1041.2015.00478

Glazzard, J., and Dale, K. (2013). Trainee teachers with dyslexia: personal narratives of resilience. *J. Res. Spec. Educ. Needs* 13, 26–37. doi: 10.1111/j.1471-3802.2012.01254.x

Goroshit, M., and Hen, M. (2016). Teachers' empathy: can it be predicted by self-efficacy? *Teach. Teach.* 22, 805–818. doi: 10.1080/13540602.2016.1185818

Guo, B. Y. (2015). *Understanding Instead of Teaching: A Narrative Research on the Teaching Empathy of a High School Teacher*. Jinhua: Zhejiang Normal University. Unpublished Master degree thesis.

Gu, X. S., and Han, S. H. (2007). Attention and reality constraints on the neural processes of empathy for pain. *Neuroimage* 36, 256–267. doi: 10.1016/j.neuroimage.2007.02.025

Han, S. H., Fan, Y., and Mao, L. H. (2008). Gender difference in empathy for pain: an electrophysiological investigation. *Brain Res.* 1196, 85–93. doi: 10.1016/j.brainres.2007.12.062

Jeannerod, M. (1999). The 25th bartlett lecture. To act or not to act: perspective on the representation of actions. *Q. J. Exp. Psychol. A* 52A, 1–29. doi: 10.1080/713755803

Kitchen, J. (2005). Conveying respect and empathy: becoming a relational teacher educator. *Stud. Teach. Educ.* 1, 195–207. doi: 10.1080/17425960500288374

Kremer, L., and Hofman, J. E. (1985). Teachers' professional identity and burn-out. *Res. Educ.* 34, 89–95. doi: 10.1177/003452378503400106

Li, W. J., Ding, W., Sun, B. H., and Yu, L. L. (2015). The effects of teachers' empathy on students' academic achievement: a hierarchical linear analysis based on the measurement of animated narrative vignettes simulations. *Psychol. Dev. Educ.* 31, 719–727. doi: 10.16187/j.cnki.issn1001-4918.2015.06.11

Mao, Z. Z. (2017). *Research on the Status Quo of Nursing Students' Empathy and Career Identity and the Relations Between the Two in the Context of Tense Doctor-patient Relationship*. Kunming: Yunnan Normal University. Unpublished Master degree thesis.

McAllister, G., and Irvine, J. J. (2002). The role of empathy in teaching culturally diverse students: a qualitative study of teachers' beliefs. *J. Teach. Educ.* 53, 433–443. doi: 10.1177/002248702237397

Meng, J., Hu, L., Shen, L., Yang, Z., Chen, H., Huang, X. T., et al. (2012). Emotional primes modulate the responses to others' pain: an ERP study. *Exp. Brain Res.* 220, 277–286. doi: 10.1007/s00221-012-3136-2

Meng, J., Jackson, T., Chen, H., Hu, L., Yang, Z., Su, Y. H., et al. (2013). Pain perception in the self and observation of others: an ERP investigation. *Neuroimage* 72, 164–173. doi: 10.1016/j.neuroimage.2013.01.024

OECD. (2017). "Gender imbalances in the teaching profession," in *Education Indicators in Focus (No.49)*. Paris: OECD Publishing. doi: 10.1787/54f0ef95-en

Peart, N. A., and Campbell, F. A. (1999). At-risk students' perceptions of teacher effectiveness. *J. Just Caring Educ.* 5, 269–284.

Peck, N. F., Maude, S. P., and Brotherson, M. J. (2015). Understanding preschool teachers' perspectives on empathy: a qualitative inquiry. *Early Child. Educ. J.* 43, 169–179. doi: 10.1007/s10643-014-0648-3

Singer, T., and Lamm, C. (2009). The social neuroscience of empathy. *Ann. N Y Acad. Sci.* 1156, 81–96. doi: 10.1111/j.1749-6632.2009.04418.x

Singer, T., Seymour, B., O'Doherty, J., Kaube, H., Dolan, R. J., and Frith, C. D. (2004). Empathy for pain involves the affective but not sensory components of pain. *Science* 303, 1157–1162. doi: 10.1126/science.1093535

Singer, T., Seymour, B., O'Doherty, J. P., Stephan, K. E., Dolan, R. J., and Frith, C. D. (2006). Empathic neural responses are modulated by the perceived fairness of others. *Nature* 439, 466–469. doi: 10.1038/nature04271

Smith, A. (2006). Cognitive empathy and emotional empathy in human behavior and evolution. *Psychol. Rec.* 56, 3–21. doi: 10.1007/bf03395534

Song, J., Guo, F. B., Zhang, Z., Yuan, S., Jin, H., and Wang, Y. W. (2016). Interpersonal distance influences on pain empathy: friends priming effect. *Acta Psychol. Sin.* 48, 833–844. doi: 10.3724/sp.j.1041.2016.00833

Stojiljković, S., Djigić, G., and Zlatković, B. (2012). Empathy and teachers' roles. *Proc. Soc. Behav. Sci.* 69, 960–966. doi: 10.1016/j.sbspro.2012.12.021

Stojiljković, S., Stojanović, A., and Dosković, Z. (2011). "Moral reasoning and empathy in Serbian teachers," in *Oral-Presentation Submitted on International Conference on Education and Educational Psychology ICEEPSY 2011*, Istanbul Turkey), 133–134. Abstracts.

Visser, C. L. F., Wilschut, J. A., Isik, U., van der Burgt, S. M. E., Croiset, G., and Kusurkar, R. A. (2018). The association of readiness for interprofessional learning with empathy, motivation and professional identity development in medical students. *BMC Med. Educ.* 18:125. doi: 10.1186/s12909-018-1248-5

Wang, T., Ge, Y., Zhang, J., Liu, J., and Luo, W. (2014). The capacity for pain empathy among urban Internet-addicted left-behind children in China: an event-related potential study. *Comput. Hum. Behav.* 33, 56–62. doi: 10.1016/j.chb.2013.12.020

Wang, X. Q., Zeng, L. H., Zhang, D. J., and Sen, L. I. (2010). An initial research on the professional identification scale for normal students. *J. South. Univ.* 36, 152–157. doi: 10.13718/j.cnki.xdsk.2010.05.020

Wang, X. Q., Zhang, D. J., and Zeng, L. H. (2011). Professional value and professional efficacy: the dual core factor model of professional identity in normal students. *Psychol. Dev. Educ.* 6, 662–669. doi: 10.16187/j.cnki.issn1001-4918.2011.06.005

Wang, X. Q., Zhu, J. C., Liu, L., and Chen, X. Y. (2017). Cognitive-processing bias in Chinese student teachers with strong and weak professional identity. *Front. Psychol.* 8:784. doi: 10.3389/fpsyg.2017.00784

Warner, R. E. (1984). Can teachers learn empathy? *Educ. Can.* 24, 39–41.

Wu, X. W. (2018). The gender structural change of rural teachers in china—a study based on Q county in heibei province. *J. China Womens Univ.* 6, 51–58. doi: 10.13277/j.cnki.jcwu.2018.06.011

Xie, L., Ren, M., Cao, B., and Li, F. (2017). Distinct brain responses to different inhibitions: evidence from a modified flanker task. *Sci. Rep.* 7:6657. doi: 10.1038/s41598-017-04907-y

Yuguero, O., Ramon Marsal, J., Esquerda, M., Vivanco, L., and Soler-González, J. (2017). Association between low empathy and high burnout among primary care physicians and nurses in Lleida, Spain. *Eur. J. Gen. Pract.* 23, 4–10. doi: 10.1080/13814788.2016.1233173

Zhang, H. (2014). *Study on the Relationship between Compassion Fatigue and Professional Identity in Critical Care Nurse*. Jinan: Shandong University. Unpublished Master degree thesis.

Zhu, Y. B. (2017). An empirical study on the influence of empathy cultivation on professional identity of secondary vocational nursing students. *Health Vocat. Educ.* 35, 110–111.

Zhu, J. C., and Wang, X. Q. (2017). The relationship between professional identity and suicide ideation among pre-teachers: the mediating role of depression and its gender difference. *Psychol. Dev. Educ.* 33, 614–621. doi: 10.16187/j.cnki.issn1001-4918.2017.05.12

**Conflict of Interest Statement**: The authors declare that the research was conducted in the absence of any commercial or financial relationships that could be construed as a potential conflict of interest.

frontiers in Human Neuroscience

GENERAL COMMENTARY
published: 02 July 2019
doi: 10.3389/fnhum.2019.00218

# Response to Commentary: Efficacy and Safety of Transcranial Direct Current Stimulation as an Add-on Treatment for Bipolar Depression: A Randomized Clinical Trial

*Andre R. Brunoni*[1,2]* *and Bernardo Sampaio-Junior*[2]

[1] Department of Internal Medicine, Faculdade de Medicina da Universidade de São Paulo, São Paulo, Brazil, [2] Laboratory of Neurosciences (LIM-27), Department and Institute of Psychiatry, Faculdade de Medicina da Universidade de São Paulo, São Paulo, Brazil

**Keywords: bipolar depression, non-invasive brain electrical stimulation, clinical trial (RCT), blinding (masking), transcranial direct current electrical stimulation**

**A Commentary on**

**Commentary: Efficacy and Safety of Transcranial Direct Current Stimulation as an Add-on Treatment for Bipolar Depression: A Randomized Clinical Trial**
*by Hu, Z.-Y., Liu, X., Zheng, H., and Zhou, D.-S. (2018). Front. Hum. Neurosci. 12:480. doi: 10.3389/fnhum.2018.00480*

OPEN ACCESS

***Edited by:***
*Delin Sun,*
*Duke University, United States*

***Reviewed by:***
*Reza Kazemi,*
*Atieh Clinical Neuroscience Center, Iran*
*Junling Gao,*
*The University of Hong Kong, Hong Kong*

***Correspondence:**
*Andre R. Brunoni*
*brunoni@usp.br*

***Received:*** *23 February 2019*
***Accepted:*** *14 June 2019*
***Published:*** *02 July 2019*

***Citation:***
*Brunoni AR and Sampaio-Junior B (2019) Response to Commentary: Efficacy and Safety of Transcranial Direct Current Stimulation as an Add-on Treatment for Bipolar Depression: A Randomized Clinical Trial. Front. Hum. Neurosci. 13:218. doi: 10.3389/fnhum.2019.00218*

We read the letter of Hu et al. (2018) commenting on our randomized clinical trial that examined the efficacy and safety of transcranial direct current stimulation (tDCS) in bipolar depression (Sampaio-Junior et al., 2018) with great interest. We believe that the authors have performed an adequate summary of our main study findings and limitations. Nonetheless, there are some issues that deserve further clarification.

First, the authors stated that the "*connections of the stimulator were concealed (...) [as to not] determine the polarity of stimulation.*" This is imprecise. We employed tDCS devices that automatically deliver active or sham stimulation according to a code that is inserted in the device's keypad, as done in our previous studies (Brunoni et al., 2013b, 2014, 2017; Valiengo et al., 2016). Therefore, there is no concealment of connections, nor blinding of the stimulation polarity.

Second, the authors suggested that sustained remission was not proven because "remission analysis" or "tDCS design" was not optimal. The most likely explanation for lack of statistically significant differences in remission is due to a low sample size and, hence, an underpowered analysis. We agree that a larger sample size would demonstrate more meaningful results. Nonetheless, the study design was a randomized clinical trial, which is considered the "gold standard" to prove causality associated with an intervention, and the remission analysis was based on cumulative (sustained) remission, a more robust and clinically meaningful outcome than remission at any given time point.

Third, the authors said that a "*guinea pig effect*" was caused "*as nearly three-fifths participants of each group identified the allocation group.*" It is unclear what the authors mean for "guinea pig effect," as this term is not often used (and the authors provided no references for such term). From a sociology book (Brinkerhoff et al., 2007), such effect would occur "*when subjects' knowledge that they are participating in an experiment affects their response*" and would relate to social desirability, as subjects would behave as they think it would be

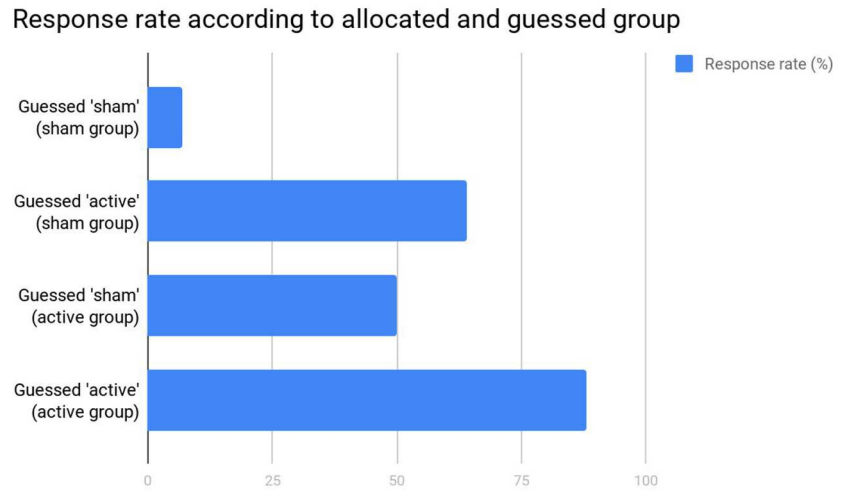


**FIGURE 1 |** Response rates in the original study (Sampaio-Junior et al., 2018).

expected by the examiners. According to this definition (the only one we were able to find), such effect occurs in *all* randomized clinical trials, regardless of intervention or blinding. Therefore, the author's association between a guinea pig effect and (supposedly) a lack of blinding is a *non-sequitur*. We highlight that the sham method used in our study was proven to be as reliable as the gold standard placebo-pill (Brunoni et al., 2013a). Although an active control (e.g., stimulation of another brain region) could be implemented in design, this would add additional difficulties in staff blinding who would identify the allocation group based on electrode positioning.

Fourth, the authors critically omitted that correct group guessing was not above chance. Importantly, although we indeed used group guessing as a proxy for blinding integrity, it is important to mention that correct guessing can occur due to (lack of) improvement. Such effect can be observed in **Figure 1**. In patients allocated to sham group, there was a statistically significant difference in terms of response ($p < 0.001$) between those who correctly guessed that they were in sham group (6.7%) and those who incorrectly guessed that they were in active group (63.6%). Likewise, in patients allocated to active group, there was a statistically significant difference in terms of response ($p = 0.04$) between those who incorrectly guessed they were in sham group (50%) and those who correctly guessed they were in active group (87.5%). Therefore, participants tended to guess they were in the active group if they presented response, and that they were in the sham group if they did not present response. Reverse causality is unlikely as, overall, patients in the active group responded twice as more than in sham group, guessing was not beyond chance, and tDCS blinding seems to be as effective as the gold-standard placebo pill (Brunoni et al., 2013a). For these reasons, routine blinding checking is not anymore recommended in randomized clinical trials (Schulz et al., 2010).

Fifth, the authors made some comments regarding the scales and randomization methods we adopted. It is important to underscore that the study methodology was published a priori (Pereira Junior Bde et al., 2015) and that it abides to the state-of-the-art methodology in clinical trial design. In hindsight, we agree that the Clinical Global Impression (CGI) was not the optimal choice for our sample and that other scales could have been used, such as the Bipolar Depression Rating Scale (Berk et al., 2007).

Finally, tDCS was well-tolerated, as only skin redness was statistically higher in the active vs. sham group. Moreover, although the rate of treatment-emergent affective switch (TEAS) was high, rates were similar in both groups. Importantly, TEAS was based on a Young Mania Rating Scale score >8. Clinically, these episodes did not meet the criteria for a major depressive episode with mixed features, hypomania, or mania and required no hospitalization, trial discontinuation, or specific treatment.

We agree that our trial presents limitations that demand further investigations of tDCS efficacy in bipolar depression. Considering the burden of disease, and the advantages of tDCS regarding portability and safety (Brunoni et al., 2018), showing that tDCS is effective for this condition would bring enormous clinical gains.

## AUTHOR CONTRIBUTIONS

All authors listed have made a substantial, direct and intellectual contribution to the work, and approved it for publication.

## ACKNOWLEDGMENTS

This work was supported by a 2013 NARSAD Young Investigator from the Brain & Behavior Research Foundation (Grant Number 20493). AB is recipient of a research fellowship award from CNPq (303197) and is a CAPES - Humboldt experienced researcher alumni.

## REFERENCES


Berk, M., Malhi, G. S., Cahill, C., Carman, A. C., Hadzi-Pavlovic, D., Hawkins, M. T., et al. (2007). The Bipolar Depression Rating Scale (BDRS): its development, validation and utility. *Bipolar Disord*. 9, 571–579. doi: 10.1111/j.1399-5618.2007.00536.x

Brinkerhoff, D., White, L. K., Ortega, S., and Weitz, R. (2007). *Essentials of Sociology*. Toronto, ON: Cengage Learning.

Brunoni, A. R., Boggio, P. S., De Raedt, R., Benseñor, I. M., Lotufo, P. A., Namur, V., et al. (2014). Cognitive control therapy and transcranial direct current stimulation for depression: a randomized, double-blinded, controlled trial. *J. Affect. Disord*. 162, 43–49. doi: 10.1016/j.jad.2014.03.026

Brunoni, A. R., Moffa, A. H., Sampaio-Junior, B., Borrione, L., Moreno, M. L., Fernandes, R. A., et al. (2017). Trial of electrical direct-current therapy versus escitalopram for depression. *N. Engl. J. Med*. 376, 2523–2533. doi: 10.1056/NEJMoa1612999

Brunoni, A. R., Sampaio-Junior, B., Moffa, A. H., Aparício, L. V., Gordon, P., Klein, I., et al. (2018). Noninvasive brain stimulation in psychiatric disorders: a primer. *Braz. J. Psychiatr*. 41, 70–81. doi: 10.1590/1516-4446-2017-0018

Brunoni, A. R., Schestatsky, P., Lotufo, P. A., Benseñor, I. M., and Fregni, F. (2013a). Comparison of blinding effectiveness between sham tDCS and placebo sertraline in a 6-week major depression randomized clinical trial. *Clin Neurophysiol*. 125, 298–305. doi: 10.1016/j.clinph.2013.07.020

Brunoni, A. R., Valiengo, L., Baccaro, A., Zanão, T. A., de Oliveira, J. F., Goulart, A., et al. (2013b). The sertraline vs. electrical current therapy for treating depression clinical study: results from a factorial, randomized, controlled trial. *JAMA Psychiatry* 70, 383–391. doi: 10.1001/2013.jamapsychiatry.32

Hu, Z. Y., Liu, X., Zheng, H., and Zhou, D. S. (2018). Commentary: efficacy and safety of transcranial direct current stimulation as an add-on treatment for bipolar depression: a randomized clinical trial. *Front. Hum. Neurosci*. 12:480. doi: 10.3389/fnhum.2018.00480

Pereira Junior Bde, S., Tortella, G., Lafer, B., Nunes, P., Benseñor, I. M., Lotufo, P. A., et al. (2015). The Bipolar Depression Electrical Treatment Trial (BETTER): design, rationale, and objectives of a randomized, sham-controlled trial and data from the pilot study phase. *Neural Plast*. 2015:684025. doi: 10.1155/2015/684025

Sampaio-Junior, B., Tortella, G., Borrione, L., Moffa, A. H., Machado-Vieira, R., Cretaz, E., et al. (2018). Efficacy and safety of transcranial direct current stimulation as an add-on treatment for bipolar depression: a randomized clinical trial. *JAMA Psychiatry* 75, 158–166. doi: 10.1001/jamapsychiatry.2017.4040

Schulz, K. F., Altman, D. G., and Moher, D. (2010). CONSORT 2010 statement: updated guidelines for reporting parallel group randomised trials. *BMJ*. 340:c332. doi: 10.1136/bmj.c332

Valiengo, L. C., Goulart, A. C., de Oliveira, J. F., Benseñor, I. M., Lotufo, P. A., and Brunoni, A. R. (2016). Transcranial direct current stimulation for the treatment of post-stroke depression: results from a randomised, sham-controlled, double-blinded trial. *J. Neurol. Neurosurg. Psychiatry* 88, 170–175. doi: 10.1136/jnnp-2016-314075


**Conflict of Interest Statement:** The authors declare that the research was conducted in the absence of any commercial or financial relationships that could be construed as a potential conflict of interest.

frontiers in Human Neuroscience

MINI REVIEW
published: 07 April 2020
doi: 10.3389/fnhum.2020.00021

# Recent Progress in Sleep Quality Monitoring and Non-drug Sleep Improvement

*Jing Chi*[1*†], *Wei Cao*[1*†] *and Yan Gu*[2]

[1] Shenzhen Qianhai Icecold IT Co., Ltd., Shenzhen, China, [2] Center for Stem Cells and Regenerative Medicine, Key Laboratory of Tissue Engineering and Regenerative Medicine of Zhejiang Province, Zhejiang University School of Medicine, Hangzhou, China

Insomnia is one of the most common health risk factors in the population as well as in clinical practice, which is associated with genes, neuron, environment, behavior, and physiology, etc. This review summarizes the recent progress in sleep quality monitoring and non-drug sleep improvement. The innovation of wearable and effective invention suggests a new approach and have deep implications toward sleep improvement and yet, the health care innovation system is also facing the challenge to foster the progress.

**Keywords: insomnia, sleep disorders, sleep quality, sleep monitoring, polysomnography, light pollution**

OPEN ACCESS

***Edited by:***
*Xiaochu Zhang,*
*University of Science and Technology of China, China*

***Reviewed by:***
*Li-Zhuang Yang,*
*Hefei Institutes of Physical Science (CAS), China*
*Xiaosong He,*
*University of Pennsylvania, United States*

****Correspondence:***
*Jing Chi*
*jchi@pegasiglass.com*
*Wei Cao*
*u3001393@connect.hku.hk*

*† These authors have contributed equally to this work*

***Specialty section:***
*This article was submitted to Health, a section of the journal Frontiers in Human Neuroscience*

***Received:*** *16 October 2018*
***Accepted:*** *17 January 2020*
***Published:*** *07 April 2020*

***Citation:***
*Chi J, Cao W and Gu Y (2020) Recent Progress in Sleep Quality Monitoring and Non-drug Sleep Improvement. Front. Hum. Neurosci. 14:21. doi: 10.3389/fnhum.2020.00021*

## INTRODUCTION

Insomnia is one of the most common health risk factors in the population as well as in clinical practice, which is associated with genes, neurons, environment, behavior, physiology, etc. (Buysse, 2013; Harvey et al., 2014). Insomnia is defined as the subjective perception of difficulty with sleep initiation (over 30 min of sleep latency), duration, and consolidation, resulting in dissatisfied sleep quality despite adequate opportunity for sleep (Schutte-Rodin et al., 2008). The understanding of the whole dynamics of the sleep–wake cycle could lead us to a better solution on insomnia, which is controlled by interactive neurochemical processes among multiple neural structures (Espana and Scammell, 2004; Brown et al., 2012).

Insomnia has gradually become a prevalent phenomenon in fast-paced urban life. Insomnia occurs among individuals of different ages (Johnson et al., 2006; Kryger, 2006), and symptoms occur in approximately 33–50% of the adult population (Ancoli-Israel and Roth, 1999). Insomnia is the most prevalent and accounts for almost half of all sleep disorders (15% of the whole population) (Cao et al., 2017). Due to the complexity of the neural system that controls sleep, it is a great challenge to accurately diagnose and treat insomnia.

During the past few years, a wide range of hardware including wearable devices has enabled us to access more personal health performance via mobile applications and help improved our health. However, the reliability and validation vary among different applications (Peake et al., 2018). For insomnia management and improvement, it is critical to develop a set of comprehensive sleep valuation as well as following therapies (Kapur et al., 2017).

This review summarizes the recent progress in sleep quality monitoring and non-drug sleep improvement, with a comprehensive analysis on the related advantages and limitations, trying to conclude effective suggestions for sleep problems improvement in general.

## SLEEP QUALITY MONITORING

Insomnia should be properly diagnosed before treatment. Subjective sleep quality assessment is mainly through subtly developed questionnaires. The most commonly used forms are the *Morning Evening Questionnaire (MEQ)*, *Pittsburgh Sleep Quality Index (PSQI)*, *the Hamilton scale*, etc. (Schwab et al., 1967; Horne and Ostberg, 1976; Buysse et al., 1989). PSQI sleep quality assessment was invented by the University of Pittsburgh and was most frequently used. It contains nine questions with each answer scoring between 0 and 3. The PSQI index is calculated as the sum of all the scores. The lower the score is, the better the sleep quality. Clinical studies have shown that the PSQI demonstrates high reliability and validity to analyze sleep problems under many circumstances, but just like other self-report inventories, its scores can be easily affected by the testee (Grandner et al., 2006; Mollayeva et al., 2016).

Sleep doctors routinely use a device called polysomnography recorder (PSG) for sleep quality monitoring (Jafari and Mohsenin, 2010). The PSG records electroencephalogram (EEG), electromyogram (EMG), electrocardiogram (ECG), respiration, and body movements along with other vital signs. Polysomnography is commonly used for sleep quality assessment, therapy, and sleep disorders (Gregorio et al., 2011). There are several limitations to obtain high quality of PSG data, including the first night effect in decreased sleep efficiency due to the unfamiliar environment and lack of comfort brought by the test, the difference in PSG variables by sex and different age groups, the control subjects, research angles and environments of different lab groups, and so on, thus making PSG hard for normalization (Newell et al., 2012; Boulos et al., 2019).

Presently, new technologies and innovations on *wearables* have made sleep monitoring easy to use and enable us to access sleep data in a real-world environment, compared to PSG (Kelly et al., 2012). Recent systematic reviews on the sleep monitoring methods have been introduced to value sleep quality, emphasizing the powerful innovation of wearables and the application on athletes, which allows complementary access with respect to classical sleep quality valuation and diagnose insomnia and its severity level (Peake et al., 2018; Claudino et al., 2019). Comparison on the result between PSG and wearables has shown consistency but needs further refinement for reliability (Lee et al., 2019).

The new Apple watch not only has a sleep monitoring function but also achieved CFDA approval for early warning of atrial fibrillation. A small electrocardiographic device developed by Harvard University infers sleep quality by cardiopulmonary coupling (CPC) monitoring (Thomas et al., 2005). These products are relatively simple in structure when compared to the PSG and are much more comfortable to wear. Most sleep monitoring devices in the consumer market refer to actigraph (body movement), heart rate, and heart rate variability (HRV) to predict sleep structure, to evaluate the quality of sleep (Kosmadopoulos et al., 2014). Other products with comparable functions include wrist bands, sleep monitoring belts, and radar beam trackers. One of such examples is the sleep monitoring belt based on piezoelectric sensing technology developed by an Israeli company named EarlySense and a Finlandizei company called Beddit recently acquired by Apple.

The accuracy of these consumable products, however, has been challenged by medical doctors, and whether they could replace the PSG device for clinical use is yet to be determined. However, a recent trend on the cooperation between the pharmaceutical and wearable companies has been shaping. For instance, Eli Lily and Apple have started large-scale clinical trials on Alzheimer's disease, with the help of iPhones, watches, and sleep monitor belt.

## NON-DRUG THERAPY AND SLEEP IMPROVEMENT TECHNIQUES FOR INSOMNIA

Currently, most insomnia patients take hypnotic drugs for treatment. However, a large percentage of the population feel reluctant to take sleeping pills, and this led to the development of non-drug insomnia therapeutics. Non-drug treatment of insomnia is divided into two major categories: cognitive behavioral therapy for insomnia (CBT-I), which is performed in the absence of auxiliary devices (Morin, 2004), and physiotherapy through repetitive transcranial magnetic resonance (rTMS), white noise and music, aromatherapy, and light therapy devices.

*Cognitive behavioral therapy (CBT)* is a fairly simple and easy way to treat insomnia. It can relieve insomnia through such behavioral interventions as sleep restriction, stimulus control, and paradoxical intervention. For example, sleep restriction allows a subject to stay in bed only when he or she feels sleepy and this gradually improves sleep quality by increasing sleep efficiency (Miller et al., 2014). Stimulus control improves sleep quality by limiting non-sleep behaviors in the bed and establishing good bed-sleep conditioned reflexes (Hood et al., 2014). No auxiliary devices are needed for CBT-I, but the drawback of this tool is its low compliance rate.

*Repetitive transcranial magnetic stimulation (rTMS)* relieves insomnia by lowering the level of arousal for the targeted cerebral cortex (Jiang et al., 2013). Low-frequency (<1 Hz) repetitive transcranial stimulation inhibits the excitement of the cerebral cortex and can induce slow waves, a brain wave that mostly appears as a subject enters deep sleep. Although this method is effective, the equipment is too large for consumable commercialization.

*White noise* refers to the combination of sound of multiple frequencies. White noise diminishes the excessive concentration of attention to relax the mood and alleviate insomnia (Messineo et al., 2017). Most natural sounds such as wind, rain, water flow, and other natural sounds all belong to the white noise family. White noise is often used in conjunction with soothing music to regulate mood and help with sleep.

*Aromatherapy* and *meditation* are commonly used together. Both methods are considered to be effective in reducing psychological stress. The fragrance of natural flowers and plants has been accompanying human beings into dreams throughout the 2 million years of evolution. We used to

live in the jungle, mountains, or grasslands. It is thought that the awakened memories in ancient times help us fall into sleep faster. Meditation helps people relax and rapidly fall asleep by distracting attention and reducing anxiety (Martires and Zeidler, 2015).

*Light therapy* is gaining increasing attention from doctors and hospitals. The principle of light therapy is to adjust the phase and amplitude of biological clock oscillation through specific light stimulation, so as to establish and consolidate a regular sleep–wake cycle and improve the quality of sleep (van Maanen et al., 2016). Light therapy products have been developed in the form of large light boards and small desktop lightboxes. Recently, head-mounted light therapy glasses have been invented to improve portability and ease of use. The innovation has dramatically increased the patients' compliance with light therapy.

## DISCUSSION AND CONCLUSION

Having a better knowledge on sleep physiology and insomnia is important for both health and medical reasons. Although we lack further understanding of the nerve system controlling the sleep–wake cycle, it doesn't stop us from seeking better monitoring and treatment on insomnia.

The pre-programmed passive wearables provide us a new angle to understand sleep, together with the classical evaluation form and PSG, shaping a comprehensive monitoring ecosphere and potential synergistic effect for clinical, post-hospital, and daily needs.

On the other hand, we need a better solution to improve sleep disorder, and there has been progress showing that, besides sleep medications, we do have more effective choices owing to the development of non-drug insomnia therapeutic.

The availability of digitized data in clinical and daily scenarios, combined with the arrival of powerful artificial intelligence (AI) algorithms, could bring deeper implications for health and medicine industry. New medicine or non-drug equipment like light therapy will speed up the upgrade.

The health innovation system should promote such progress by working closely with hospitals, pharmaceutical companies, and academic institutes. Proper guidance should be given to educate the public on the limitations along with the promotion of health technologies.

## AUTHOR CONTRIBUTIONS

WC and JC: first draft. WC: literature. YG: modified. JC: proofreading.

## REFERENCES


Ancoli-Israel, S., and Roth, T. (1999). Characteristics of insomnia in the United States: results of the 1991 national sleep foundation survey. I. *Sleep* 22(Suppl. 2), S347–S353.

Boulos, M. I., Jairam, T., Kendzerska, T., Im, J., Mekhael, A., and Murray, B. J. (2019). Normal polysomnography parameters in healthy adults: a systematic review and meta-analysis. *Lancet Respir. Med.* 7, 533–543. doi: 10.1016/S2213-2600(19)30057-8

Brown, R. E., Basheer, R., McKenna, J. T., Strecker, R. E., and McCarley, R. W. (2012). Control of sleep and wakefulness. *Physiol. Rev.* 92, 1087–1187. doi: 10.1152/physrev.00032.2011

Buysse, D. J. (2013). Insomnia. *JAMA* 309, 706–716. doi: 10.1001/jama.2013.193

Buysse, D. J., Reynolds, C. F. III, Monk, T. H., Berman, S. R., and Kupfer, D. J. (1989). The Pittsburgh Sleep Quality Index: a new instrument for psychiatric practice and research. *Psychiatry Res.* 28, 193–213. doi: 10.1016/0165-1781(89)90047-4

Cao, X. L., Wang, S. B., Zhong, B. L., Zhang, L., Ungvari, G. S., Ng, C. H., et al. (2017). The prevalence of insomnia in the general population in China: a meta-analysis. *PLoS One* 12:e0170772. doi: 10.1371/journal.pone.0170772

Claudino, J. G., de Sa Souza, H., Simim, M., Fowler, P., de Alcantara Borba, D., Melo, M., et al. (2019). Which parameters to use for sleep quality monitoring in team sport athletes? A systematic review and meta-analysis. *BMJ Open Sport Exerc. Med.* 5:e000475. doi: 10.1136/bmjsem-2018-000475

Espana, R. A., and Scammell, T. E. (2004). Sleep neurobiology for the clinician. *Sleep* 27, 811–820.

Grandner, M. A., Kripke, D. F., Yoon, I. Y., and Youngstedt, S. D. (2006). Criterion validity of the pittsburgh sleep quality index: investigation in a non-clinical sample. *Sleep Biol. Rhythms* 4, 129–139.

Gregorio, M. G., Jacomelli, M., Inoue, D., Genta, P. R., de Figueiredo, A. C., and Lorenzi-Filho, G. (2011). Comparison of full versus short induced-sleep polysomnography for the diagnosis of sleep apnea. *Laryngoscope* 121, 1098–1103. doi: 10.1002/lary.21658

Harvey, C. J., Gehrman, P., and Espie, C. A. (2014). Who is predisposed to insomnia: a review of familial aggregation, stress-reactivity, personality and coping style. *Sleep Med. Rev.* 18, 237–247. doi: 10.1016/j.smrv.2013.11.004

Hood, H. K., Rogojanski, J., and Moss, T. G. (2014). Cognitive-behavioral therapy for chronic insomnia. *Curr. Treat. Options Neurol.* 16:321. doi: 10.1007/s11940-014-0321-6

Horne, J. A., and Ostberg, O. (1976). A self-assessment questionnaire to determine morningness-eveningness in human circadian rhythms. *Int. J. Chronobiol.* 4, 97–110.

Jafari, B., and Mohsenin, V. (2010). Polysomnography. *Clin. Chest. Med.* 31, 287–297. doi: 10.1016/j.ccm.2010.02.005

Jiang, C. G., Zhang, T., Yue, F. G., Yi, M. L., and Gao, D. (2013). Efficacy of repetitive transcranial magnetic stimulation in the treatment of patients with chronic primary insomnia. *Cell Biochem. Biophys.* 67, 169–173. doi: 10.1007/s12013-013-9529-4

Johnson, E. O., Roth, T., Schultz, L., and Breslau, N. (2006). Epidemiology of DSM-IV insomnia in adolescence: lifetime prevalence, chronicity, and an emergent gender difference. *Pediatrics* 117:e00247-56.

Kapur, V. K., Auckley, D. H., Chowdhuri, S., Kuhlmann, D. C., Mehra, R., Ramar, K., et al. (2017). Clinical practice guideline for diagnostic testing for adult obstructive sleep apnea: an american academy of sleep medicine clinical practice guideline. *J. Clin. Sleep Med.* 13, 479–504. doi: 10.5664/jcsm.6506

Kelly, J. M., Strecker, R. E., and Bianchi, M. T. (2012). Recent developments in home sleep-monitoring devices. *ISRN Neurol.* 2012:768794. doi: 10.5402/2012/768794

Kosmadopoulos, A., Sargent, C., Darwent, D., Zhou, X., and Roach, G. D. (2014). Alternatives to polysomnography (PSG): a validation of wrist actigraphy and a partial-PSG system. *Behav. Res. Methods* 46, 1032–1041. doi: 10.3758/s13428-013-0438-7

Kryger, M. H. (2006). The burden of chronic insomnia on society. *Manag. Care* 15(9 Suppl. 6), 1–5.

Lee, X. K., Chee, N., Ong, J. L., Teo, T. B., van Rijn, E., Lo, J. C., et al. (2019). Validation of a consumer sleep wearable device with actigraphy and polysomnography in adolescents across sleep opportunity manipulations. *J. Clin. Sleep Med.* 15, 1337–1346. doi: 10.5664/jcsm.7932

Martires, J., and Zeidler, M. (2015). The value of mindfulness meditation in the treatment of insomnia. *Curr. Opin. Pulm. Med.* 21, 547–552. doi: 10.1097/MCP.0000000000000207

Messineo, L., Taranto-Montemurro, L., Sands, S. A., Oliveira Marques, M. D., Azabarzin, A., and Wellman, D. A. (2017). Broadband sound administration improves sleep onset latency in healthy subjects in a model of transient insomnia. *Front. Neurol.* 8:718. doi: 10.3389/fneur.2017.00718

Miller, C. B., Espie, C. A., Epstein, D. R., Friedman, L., Morin, C. M., Pigeon, W. R., et al. (2014). The evidence base of sleep restriction therapy for treating insomnia disorder. *Sleep Med. Rev.* 18, 415–424. doi: 10.1016/j.smrv.2014.01.006

Mollayeva, T., Thurairajah, P., Burton, K., Mollayeva, S., Shapiro, C. M., and Colantonio, A. (2016). The Pittsburgh sleep quality index as a screening tool for sleep dysfunction in clinical and non-clinical samples: a systematic review and meta-analysis. *Sleep Med. Rev.* 25, 52–73. doi: 10.1016/j.smrv.2015.01.009

Morin, C. M. (2004). Cognitive-behavioral approaches to the treatment of insomnia. *J. Clin. Psychiatry* 65(Suppl. 16), 33–40.

Newell, J., Mairesse, O., Verbanck, P., and Neu, D. (2012). Is a one-night stay in the lab really enough to conclude? First-night effect and night-to-night variability in polysomnographic recordings among different clinical population samples. *Psychiatry Res.* 200, 795–801. doi: 10.1016/j.psychres.2012.07.045

Peake, J. M., Kerr, G., and Sullivan, J. P. (2018). A critical review of consumer wearables, mobile applications, and equipment for providing biofeedback, monitoring stress, and sleep in physically active populations. *Front. Physiol.* 9:743. doi: 10.3389/fphys.2018.00743

Schutte-Rodin, S., Broch, L., Buysse, D., Dorsey, C., and Sateia, M. (2008). Clinical guideline for the evaluation and management of chronic insomnia in adults. *J. Clin. Sleep Med.* 4, 487–504. doi: 10.5664/jcsm.27286

Schwab, J. J., Bialow, M. R., Clemmons, R. S., and Holzer, C. E. (1967). Hamilton rating scale for depression with medical in-patients. *Br. J. Psychiatry* 113, 83–88.

Thomas, R. J., Mietus, J. E., Peng, C. K., and Goldberger, A. L. (2005). An electrocardiogram-based technique to assess cardiopulmonary coupling during sleep. *Sleep* 28, 1151–1161. doi: 10.1093/sleep/28.9.1151

van Maanen, A., Meijer, A. M., van der Heijden, K. B., and Oort, F. J. (2016). The effects of light therapy on sleep problems: a systematic review and meta-analysis. *Sleep Med. Rev.* 29, 52–62. doi: 10.1016/j.smrv.2015.08.009

**Conflict of Interest:** WC and JC were employed by the company Shenzhen Qianhai Icecold IT Co., Ltd.

The remaining author declares that the research was conducted in the absence of any commercial or financial relationships that could be construed as a potential conflict of interest.

# Advantages of publishing in Frontiers

**OPEN ACCESS**
Articles are free to read for greatest visibility and readership

**FAST PUBLICATION**
Around 90 days from submission to decision

**HIGH QUALITY PEER-REVIEW**
Rigorous, collaborative, and constructive peer-review

**TRANSPARENT PEER-REVIEW**
Editors and reviewers acknowledged by name on published articles

**Frontiers**
Avenue du Tribunal-Fédéral 34
1005 Lausanne | Switzerland

**Visit us:** www.frontiersin.org
**Contact us:** frontiersin.org/about/contact

**REPRODUCIBILITY OF RESEARCH**
Support open data and methods to enhance research reproducibility

**DIGITAL PUBLISHING**
Articles designed for optimal readership across devices

**FOLLOW US**
@frontiersin

**IMPACT METRICS**
Advanced article metrics track visibility across digital media

**EXTENSIVE PROMOTION**
Marketing and promotion of impactful research

**LOOP RESEARCH NETWORK**
Our network increases your article's readership